Level 1 and Level 2 Hydrogeological and Hydrological Impact Assessment Report of the Proposed Burlington Quarry Extension, Nelson Aggregates Co.

Prepared for:

Nelson Aggregates Company
P.O. Box 1070
Burlington, Ontario L7P 0G8

Prepared by:

3363 Yonge Street
Toronto, Ontario M4N 2M6

April 2020

Earthfx Incorporated

Earth Science Information Systems

April 28, 2020

Nelson Aggregates Co.
P.O. Box 1070
Burlington, Ontario
L7P 0G8

Attention: Mr. Quinn Moyer, President

RE: Level 1 and Level 2 Hydrogeological and Hydrological Impact Assessment Report of the Proposed Burlington Quarry Extension

Dear Mr. Moyer:

Earthfx Incorporated is pleased to submit the following Hydrogeological and Hydrological Assessment of the proposed Burlington Quarry Extension. This report describes the physical setting of the area surrounding the Burlington Quarry, the geologic and hydrogeologic conditions, and the integrated numerical model developed to simulate the effects of the quarry extension on the surface water and groundwater systems in the quarry vicinity.

If you have any questions, please do not hesitate to call.

Yours truly
Earthfx Incorporated

Dirk Kassenaar, M.Sc., P.Eng.
President

E.J. Wexler, M.Sc., M.S.E., P.Eng.
Director of Modelling Services

LICENSED PROFESSIONAL ENGINEER
J.D.C. KASSENAAR
PROVINCE OF ONTARIO

LICENSED PROFESSIONAL ENGINEER
E.J. WEXLER
100132311
PROVINCE OF ONTARIO

3363 Yonge St., Toronto, Ontario, Canada M4N 2M6
T: 416.410.4260 F: 416.481.6026
www.earthfx.com

Table of Contents

EXECUTIVE SUMMARY 22

1 INTRODUCTION 27

1.1 OBJECTIVES 27
1.2 STUDY APPROACH 30
1.3 LEVEL 1/LEVEL 2 STUDY COMPONENTS AND METHODOLOGY 30
1.3.1 Field Investigations 30
1.3.2 Site Characterization and Baseline Conditions Analysis 31
1.3.3 Level 2 Development Impact Assessment and Mitigation Measures 32
1.3.4 Stream, Wetland, Pond and Lake Model Representations 32
1.3.5 Surface Water Effects Analysis, Water Management, and Water Budgets 33
1.3.6 Adaptive Management Plan (AMP) 33
1.3.7 Level 1/Level 2 Methodology Summary 33
1.4 STUDY AREA EXTENTS 33
1.4.1 Model Extraction Area Extents 34

2 BACKGROUND 36

2.1 PREVIOUS STUDIES 36
2.2 LONG TERM MONITORING NETWORK 36
2.3 BACKGROUND ANALYSIS AND UPDATES 39
2.4 INTEGRATED MODELLING STUDIES 39

3 PHYSICAL SETTING 40

3.1 TOPOGRAPHY 40
3.2 PHYSIOGRAPHY 40
3.3 DRILLING AND FIELD INVESTIGATION PROGRAM OVERVIEW 44
3.3.1 Golder 2004 Drilling and Monitoring Program 44
3.3.2 Azimuth Environmental 2018 - 2019 Drilling and Monitoring Program 45
3.3.3 Site Development History 45
3.4 PALEOZOIC GEOLOGY 52
3.4.1 Queenston Formation 54
3.4.2 Whirlpool Formation 54
3.4.3 Cabot Head Formation 54
3.4.4 Silurian Units 57
3.4.5 Amabel Formation 67
3.5 QUATERNARY GEOLOGY 71
3.5.1 Halton Till 71
3.5.2 Mackinaw Interstadial Sediments 71
3.5.3 Postglacial lacustrine sands 72
3.6 STRATIGRAPHIC INTERPRETATION - CONCLUSIONS 72

4 HYDROLOGIC SETTING 76

4.1 CLIMATE 76
4.1.1 Precipitation and Temperature 76
4.1.2 Solar radiation 82
4.2 LAND USE AND SOIL PROPERTIES 82
4.3 SURFACE WATER RESOURCES 82
4.3.1 Stream Network and Streamflow 86
4.3.2 Karst Sinks and Springs 86

4.3.3 Lakes and Ponds *87*
4.3.4 Wetlands *89*
4.3.5 Surface Water Takings and Diversions *89*
4.4 SURFACE WATER INVESTIGATIONS: OVERVIEW 89

5 HYDROGEOLOGIC SETTING 92

5.1 INTRODUCTION 92
5.2 HYDROSTRATIGRAPHIC MODEL LAYERS 92
5.2.1 Layer 1: Post-Glacial (Surficial) Deposits *93*
5.2.2 Layer 2: Halton Till Aquitard *93*
5.2.3 Layer 3: Mackinaw Interstadial Sediments (MIS) *93*
5.2.4 Layer 4: Weathered Bedrock/Overburden Interface Aquifer *103*
5.2.5 Layer 5: Upper Bulk Amabel Aquifer *103*
5.2.5.1 Amabel Formation Hydraulic Conductivity 104
5.2.5.2 Anisotropy and Vertical Flow Patterns 104
5.2.6 Layer 6: Middle Amabel Fracture Zone *105*
5.2.7 Layer 7: Lower Bulk Amabel Aquifer *105*
5.2.8 Layer 8: Lower Fracture Zone *106*
5.2.9 Layer 9: Lower Aquitard *108*
5.2.10 Summary *108*
5.3 GROUNDWATER LEVELS 108
5.3.1 Water Level Data Sources and Monitoring Record *108*
5.3.1.1 Static Water Level Data 109
5.3.1.2 Transient Water Level Data 109
5.3.2 Regional Water Level Patterns *109*
5.3.2.1 Vertical Head Differences 110
5.3.3 Water Level Fluctuations *114*
5.3.3.1 Seasonal and Inter-annual Patterns 114
5.3.3.2 Quarry Water Level Patterns 115
5.4 GROUNDWATER USE 117
5.4.1 Private Water Wells *118*
5.5 CONCLUSIONS 118

6 INTEGRATED MODEL DEVELOPMENT AND CALIBRATION 120

6.1 INTRODUCTION 120
6.2 INTEGRATED MODELLING - OVERVIEW 120
6.2.1 Integrated Modelling *120*
6.3 USGS GSFLOW OVERVIEW 121
6.3.1 Spatial Representation *122*
6.3.2 PRMS Submodel Soil Zone Processes *124*
6.3.3 GSFLOW Process and Region Integration *125*
6.3.4 Groundwater/Surface Water Feedback *125*
6.3.5 Temporal Discretization and Submodel Coupling *127*
6.4 GSFLOW MODEL DEVELOPMENT PROCESS 127
6.5 PRMS SUBMODEL DEVELOPMENT OVERVIEW 128
6.6 PARAMETER ASSIGNMENT 129
6.7 CLIMATE DATA 132
6.8 PRMS MODEL CALIBRATION RESULTS 132
6.9 PRMS SUBMODEL OUTPUTS 135
6.10 MODFLOW SUBMODEL DEVELOPMENT OVERVIEW 140
6.10.1 Model Construction *140*
6.11 GSFLOW MODEL CALIBRATION 142
6.11.1 GSFLOW Surface Water Streamflow Calibration *143*

6.11.2 Regional GSFLOW Calibration 145
6.11.3 Calibration to Local Transient Water Level Data 145
6.11.3.1 Wells within 100 m of the Quarry Face 149
6.11.3.2 Wells between 100 m and 800 m of the Quarry Face 149
6.11.3.3 Wells greater than 800 m from the Quarry Face 150
6.11.3.4 Quarry Effects Calibration: Conclusions 152
6.11.4 Shallow Groundwater Calibration 152
6.11.5 Wetland and Pond Calibration 155
6.11.6 Perched Wetland Ponds 155
6.11.6.1 MNRF Wetland 13025 156
6.11.6.2 MNRF Wetland 13031 157
6.11.6.3 MNRF Wetland 13032 (Earthfx Wetland Number 19) 158
6.11.6.4 Perched Wetland Conclusions 160
6.11.7 GSFLOW Outputs 160
6.11.8 GSFLOW Calibration Conclusions 161

7 BASELINE CONDITIONS ANALYSIS 165

7.1 INTRODUCTION 165
7.2 BASELINE ASSESSMENT 165
7.2.1 Time Period 165
7.2.2 Scenario Summary and Nomenclature 166
7.2.3 Surface Water Flows 166
7.2.4 Seasonal and Inter-annual Groundwater Levels 167
7.2.5 Surface Water/Groundwater Interaction 178
7.2.5.1 Recharge 178
7.2.5.2 Groundwater ET 178
7.2.5.3 Surface Discharge 178
7.2.5.4 Stream Leakage (Hyporheic Exchange) 179
7.2.6 Wetland Water Budgets 179
7.3 BASELINE CONCLUSIONS 190

8 LEVEL 2 FUTURE CONDITIONS EVALUATION 191

8.1 PROPOSED EXTRACTION 191
8.2 LEVEL 2 EVALUATION REQUIREMENTS 191
8.3 LEVEL 2 ASSESSMENT OVERVIEW 191
8.4 MODEL EVALUATION OF EXTRACTION PHASES 193
8.4.1 Scenario Summary 193
8.5 SCENARIO P12 196
8.5.1 P12 Drawdowns and Surface Water Flows 198
8.5.2 P12 Seasonal and Inter-Annual Groundwater Levels 204
8.5.3 P12 Surface Water/Groundwater Interaction 211
8.5.4 P12 Wetland Water Budgets 211
8.5.5 P12 Level 2 Conclusions 225
8.6 SCENARIO P34 225
8.6.1 Infiltration Pond 226
8.6.2 P34 Drawdowns and Surface Water Flows 226
8.6.3 P12 Recovery 226
8.7 SCENARIO P3456 230
8.7.1 P3456 Drawdowns and Surface Water Flows 230
8.7.2 P3456 Seasonal and Inter-annual Groundwater Levels 234
8.7.3 P3456 Surface Water/Groundwater Interaction 242
8.7.4 P3456 Wetland Water Budgets 242
8.7.5 P3456 North Quarry Discharge and Infiltration Pond 243

8.7.6 P3456 Effects on Medad Valley 252
8.7.7 P3456 Level 2 Conclusions 256
8.8 SCENARIO RHB1 260
8.8.1 RHB1 Drawdowns and Surface Water Flows 260
8.8.2 RHB1 Seasonal and Inter-annual Groundwater Levels 264
8.8.3 RHB1 Surface Water/Groundwater Interaction 272
8.8.4 RHB1 Wetland Water Budgets 272
8.8.5 RHB1 Level 2 Conclusions 280
8.9 SCENARIO RHB2 280
8.9.1 RHB2 Drawdowns and Surface Water Flows 280
8.9.2 RHB2 Seasonal and Inter-annual Groundwater Levels 285
8.9.3 RHB2 Surface Water/Groundwater Interaction 293
8.9.4 RHB2 Wetland Water Budgets 293
8.9.5 RHB2 Level 2 Conclusions 293
8.10 LEVEL 2 IMPACT ASSESSMENT CONCLUSIONS 301
8.10.1 System Understanding 301
8.10.2 Drawdowns 301
8.10.3 Water Supply 301
8.10.4 Stream and Wetland Function 302

9 DEVELOPMENT OF THE GROUNDWATER MONITORING PROGRAM 303

9.1 OBJECTIVES 303
9.2 ON-SITE MONITORING WELLS 303
9.3 OFF-SITE DOMESTIC WATER WELLS 303
9.4 GROUNDWATER IMPACT ASSESSMENT METHODOLOGY 304
9.4.1 Monitoring of Background Groundwater Conditions 305
9.4.2 Comprehensive Groundwater Elevation Trend Analysis 305
9.4.3 Proposed Groundwater Threshold Levels 307
9.4.4 Proposed Groundwater Mitigation Measures 307
9.5 GROUNDWATER MONITORING NETWORK AND THRESHOLDS (PHASE 1 AND 2: SOUTHERN EXTRACTION AREA) 308
9.5.1 Groundwater Monitoring Program 308
9.5.2 Groundwater Thresholds 313
9.6 GROUNDWATER MONITORING NETWORK AND THRESHOLDS (WESTERN EXTENSION) 314
9.6.1 Drilling of Groundwater Sentry Wells 314
9.6.2 Groundwater Monitoring Program 314
9.6.3 Groundwater Thresholds 315
9.7 WATER WELL INTERFERENCE COMPLAINT PROTOCOL 318

10 COMPLIANCE MONITORING AND ASSESSMENT 319

10.1 GROUNDWATER MONITORING PROGRAM 319
10.1.1 On-Site Groundwater Monitoring Program 319
10.1.2 Private Water Well Monitoring 322

11 SUMMARY AND CONCLUSIONS 323

11.1 INTRODUCTION 323
11.2 HYDROGEOLOGIC AND HYDROLOGIC SYSTEM SUMMARY 323
11.3 LEVEL 2 IMPACT ASSESSMENT 324
11.3.1 Baseline Conditions 324
11.3.2 Summary of South Extension Area Effects 324
11.3.2.1 Area of Influence 324
11.3.2.2 Wetlands and Surface Water Features 325
11.3.2.3 Domestic Water Wells 325

11.3.3 Summary of West Extension Area Effects *325*
11.3.3.1 Area of Influence 325
11.3.3.2 Wetlands and Surface Water Features 325
11.3.3.3 Domestic Water Wells 326
11.3.4 Rehabilitation and Closure *326*
11.4 CONCLUSIONS 326

12 RECOMMENDATIONS 328

13 LIMITATIONS 329

14 REFERENCES CITED 330

15 APPENDIX A: HYDROGEOLOGIC FIELD INVESTIGATIONS 333

15.1 DRILLING PROGRAM 334
15.2 HYDRAULIC TESTING PROGRAM 366
15.2.1 Downhole Packer Testing *366*
15.2.1.1 BS-01 Packer Test Interpretation 367
15.2.1.2 BS-02 Packer Test Interpretation 368
15.2.1.3 BS-04 Packer Test Interpretation 368
15.2.1.4 BS-05 Packer Test Interpretation 368
15.2.2 Pumping Test *369*
15.2.2.1 Monitoring Program 369
15.2.2.2 Pumping Test Interpretation 370
15.3 MONITORING WELL CONSTRUCTION 378
15.4 GEOPHYSICAL LOGGING 379
15.5 GROUNDWATER MONITORING PROGRAM 389
15.6 HYDROGEOCHEMICAL TESTING 397
15.7 RESIDENTIAL WELL SURVEY 400

16 APPENDIX B: KARST INVESTIGATION 401

16.1 INTRODUCTION 402
16.2 SURFICIAL KARST FEATURES 403
16.3 TESTS USING WELLS 405
16.4 CONCEPTUAL MODEL OF THE DOLOSTONE AQUIFER 406
16.5 REFERENCES 408
16.6 TABLES AND FIGURES 409
16.7 APPENDIX A: TRACER TESTING 420

17 APPENDIX C: HYDROLOGIC SUB-MODEL DEVELOPMENT 441

17.1 INTRODUCTION 441
17.2 MODEL DESCRIPTION 441
17.3 PRMS SUB-MODEL CONSTRUCTION 444
17.4 PARAMETER ASSIGNMENT 445
17.4.1 Topography-related Properties *445*
17.4.2 Soil Properties *446*
17.4.3 Land Use-related Properties *446*
17.4.4 Hydrological Processes Parameters *447*
17.5 CLIMATE DATA SETS 447
17.5.1 Precipitation and Temperature *447*
17.5.2 Solar radiation *448*
17.6 PRMS SUBMODEL RESULTS 448
17.6.1 PRMS Calibration Results and Discussion *448*
17.6.2 Baseline Conditions Simulation Results *448*
17.6.3 Surface Water Calibration Results *450*

17.6.4 Daily Grindstone Creek Inflows 450
17.7 TABLES 452
17.8 FIGURES 454

18 APPENDIX D: GROUNDWATER SUB-MODEL DEVELOPMENT 479

18.1 INTRODUCTION 479
18.1.1 Groundwater Flow Equation 479
18.1.2 Model Description 480
18.1 MODEL DISCRETIZATION 480
18.1.1 Model Grid 481
18.1.2 Model Layers 481
18.2 MODEL BOUNDARY CONDITIONS 482
18.2.1 Constant-Head and No-Flow Boundary Conditions 483
18.2.2 Head-Dependent Discharge 483
18.2.3 Top of Model Flux Boundary 484
18.3 SURFACE WATER FEATURES 484
18.3.1 Stream Network 484
18.3.2 Lake and Wetland Representation 486
18.4 GROUNDWATER RECHARGE 486
18.5 GROUNDWATER TAKINGS 486
18.6 GROUNDWATER MODEL PARAMETERS 487
18.7 GROUNDWATER MODEL PRE-CALIBRATION 487
18.8 TABLES 491
18.9 FIGURES 493

19 APPENDIX E: INTEGRATED GSFLOW MODEL CALIBRATION 512

19.1 CALIBRATION STRATEGY 512
19.2 REGIONAL SCALE STREAM FLOW CALIBRATION 512
19.3 REGIONAL SCALE GROUNDWATER CALIBRATION 513
19.4 LOCAL SURFACE WATER CALIBRATION 516
19.4.1 SW1: Main Quarry Discharge 520
19.4.2 SW6: South Quarry Discharge 521
19.4.3 Medad Valley Stream Gauges 523
19.5 LOCAL GROUNDWATER CALIBRATION 525
19.5.1 Calibration Cross Sections 525
19.5.2 Calibration and Transient Water Level Overview 525
19.5.3 Wells within 100 m of the Quarry Face 532
19.5.4 Wells between 100 m and 800 m of the Quarry Face 533
19.5.5 Wells greater than 800 m from the Quarry Face 538
19.5.6 Shallow System Calibration (Mini-piezometers) 540
19.5.7 Groundwater Calibration Conclusions 546
19.6 CALIBRATION TO SURFACE WATER POND STAFF GAUGES 546
19.6.1 Wetland Calibration Conclusions 550
19.7 GSFLOW OUTPUTS 550
19.8 WATER BUDGET ASSESSMENT 553
19.8.1 GSFLOW Water Budgets 553

20 APPENDIX F: CURRICULA VITAE OF REPORT AUTHORS 559

List of Tables

Table 5.1: Summary of hydrogeologic properties of the Amabel Formation. 104
Table 5.2: Groundwater PTTW (within 5 km) 117
Table 5.3: Private wells located within 500 m of extraction boundary and have less than 10 m of available drawdown. 119
Table 6.1: Processes and GSFLOW submodels. 121
Table 6.2: Mapping of model layers to hydrostratigraphic units. 141
Table 6.3: Wetland 13032 pond and drive point water levels. (Source: Ray Blackport, provided by David Donnelly via email July 8, 2010) 158
Table 7.1: Scenario summary. 166
Table 7.2: MNRF Wetland ID Numbers vs Earthfx ID Numbers. 179
Table 7.3: Summary of groundwater-wetland interactions. 180
Table 8.1: Evaluation of need for Level 2 Hydrogeological Assessment 192
Table 8.2: Summary of changes relative to Baseline Conditions for each future scenario 195
Table 8.3: Scenario Summary 196
Table 8.4: Numerical model layers and corresponding hydrostratigraphic layers 196
Table 8.5: Water budget comparison between Baseline and P12 conditions. 212
Table 8.6: P3456 wetland water budget comparison. 243
Table 9.1: Monitoring Well Details (Southern Extension) 311
Table 9.2: Groundwater Threshold Values 313
Table 9.3: Monitoring Well Details (Western Extension) 315
Table 10.1: On-Site Groundwater Monitoring and Evaluation Program 319
Table 10.2: Groundwater Quality Parameters 320
Table 10.3: Private Monitoring Well Locations 322
Table 17.1: Surficial soil property lookup table. 452
Table 17.2: SOLRIS land use lookup table. 453
Table 18.1 Numerical model layers and corresponding hydrostratigraphic layers. 491
Table 18.2: Summary of stream properties organized by type. 491
Table 18.3: Summary of outlet structure properties 491
Table 18.4: Final calibrated model parameter values. 492
Table 19.1: Groundwater budget for the GSFLOW model area for WY2010 to WY2014. 554
Table 19.2: MNRF Wetland vs Earthfx ID number 555

List of Figures

Figure 1.1: Site location. 28
Figure 1.2: Burlington Quarry showing South and West extension areas. 29
Figure 1.3: Study area and integrated model extents. 35
Figure 2.1: Groundwater monitoring locations....37
Figure 2.2: Surface water monitoring locations. 38
Figure 3.1: Land surface topography from the 5-m digital elevation model. 41
Figure 3.2: Local topography in the vicinity of the Burlington Quarry. 42
Figure 3.3: Physiographic units and features (from Chapman and Putnam, 2007). 43
Figure 3.4: Well locations - South Extension area. 46
Figure 3.5: Sample borehole log from the South Extension area. 47
Figure 3.6: Well locations: West Extension area. 48
Figure 3.7: Sample borehole log from the West Extension area (BS-04). 49
Figure 3.8: Site development conditions in 2005. 50
Figure 3.9: Site development conditions in 2019. 51
Figure 3.10: Stratigraphic relationships and comparison of stratigraphic nomenclature. 52
Figure 3.11: Bedrock geology for the study area (from Armstrong and Dodge, 2007). 53
Figure 3.12: Conceptual stratigraphic cross section. 54
Figure 3.13: Top of the Cabot Head Formation (masl). 55
Figure 3.14: Thickness of the Cabot Head Formation (m). 56
Figure 3.15: Top of the Reynales Formation (masl). 59
Figure 3.16: Thickness of the Reynales Formation (m). 60
Figure 3.17: Cross section locations....61
Figure 3.18: Guelph Line cross section. 62
Figure 3.19: Blind Line cross section. 63
Figure 3.20: Cedar Springs Road cross section. 64
Figure 3.21: 2nd Side Road cross section....65
Figure 3.22: West-East quarry cross section....66
Figure 3.23: Top of bedrock (top of Amabel above the Niagara Escarpment), in masl. 68
Figure 3.24: Thickness of the Amabel Formation (m). 69
Figure 3.25: BS-01 Borehole log showing the Goat Island Formation. 70
Figure 3.26: Surficial geology (data from OGS, 2010). 73
Figure 3.27: Thickness of the Halton Till (m). 74
Figure 3.28: Thickness of MIS sands above the Niagara Escarpment and ORAC sands below (m). 75
Figure 4.1: Environment Canada climate stations within about 25 km of the Burlington Quarry....77
Figure 4.2: Period of record of climate stations proximal to the study area. 78
Figure 4.3: Average annual precipitation from WY1951 to WY2019 with the total number of reporting stations....79
Figure 4.4: Average annual rain and snow from WY1951 to WY2019. 79
Figure 4.5: Average annual temperature from WY1951 to WY2019 with the total number of reporting stations....79
Figure 4.6: Interpolated average annual precipitation WY1951 – WY2019. 80
Figure 4.7: Interpolated annual average temperature WY1951 – WY2019. 81
Figure 4.8: SOLRIS v3 (after MNRF, 2019) land use classification. 83
Figure 4.9: Surficial soil complex mapping (after MNR, 2013). 84
Figure 4.10: Streams, lakes, and wetlands in the study area. 85
Figure 4.11: Daily measured streamflow at Grindstone Creek near Aldershot (02HB012) and Grindstone Creek near Millgrove (02HB028). 87
Figure 4.12: Daily measured log-streamflow at Grindstone Creek near Aldershot (02HB012) and Grindstone Creek near Millgrove (02HB028). 88
Figure 4.13: Permitted water takings in the study area. 90

Figure 4.14: Locations of wetland and streamflow monitoring locations and karst features. 91
Figure 5.1: Hydrostratigraphic cross section locations. 94
Figure 5.2: 2nd Side Road section. 95
Figure 5.3: Colling Road hydrostratigraphic cross section. 96
Figure 5.4: Cedar Springs Road section. 97
Figure 5.5: Televiewer cross section through the West Extension Area. 98
Figure 5.6: West Extension packer test section. 99
Figure 5.7: South Extension packer test Section 1. 100
Figure 5.8: South Extension packer test Section 2. 101
Figure 5.9: Burlington Quarry Amabel outcrop profile (from Golder 2004, Plate 1). 102
Figure 5.10: Lower zone quarry discharge near OW03-15 (Worthington Groundwater, 2006). 106
Figure 5.11: Water levels recorded in Monitoring Well OW03-15 (50 m from Quarry face). 107
Figure 5.12: Water levels recorded in Monitoring Well OW03-14 (175 m to 40 m from Quarry face). 108
Figure 5.13: Groundwater levels (m) from wells less than 15 m deep. 111
Figure 5.14: Groundwater levels (m) from wells greater than 15 m deep. 112
Figure 5.15: Vertical head differences (shallow minus deep groundwater levels, in m). 113
Figure 5.16: Transient groundwater response to precipitation and (simulated) snowmelt events. 114
Figure 5.17: Inter-annual variation in groundwater levels at PGMN Well W000005-1 versus monthly average precipitation and snowmelt. 115
Figure 5.18: Monitor OW03-21, located 300 m from quarry face 116
Figure 5.19: Monitor MW03-09, located 650 m from the quarry face. 116
Figure 5.20: Monitor OW03-17, located 1050 m from the quarry face. 117
Figure 6.1: Integrated numerical representation of the surface and subsurface using a cell based approach (USGS Image). 120
Figure 6.2: Schematic diagram of the GSFLOW process regions. 122
Figure 6.3: Different grid resolutions are available for each process region within GSFLOW. 123
Figure 6.4: PRMS Soil Zone Processes 124
Figure 6.5: Processes moving water between GSFLOW regions. 125
Figure 6.6: Changes in the spring and summer position of the water table increasing Dunnian runoff and the size of the "Contributing Area" (from Markstrom *et al.*, 2008). 126
Figure 6.7: Head-dependant groundwater discharge to streams (l) and leakage from streams (r). 127
Figure 6.8: Computational sequence for an integrated PRMS/MODFLOW simulation in GSFLOW (modified from Markstrom *et al.* (2008)). 128
Figure 6.9: Portion of the PRMS model grid in the quarry vicinity. 130
Figure 6.10: Surficial soil hydraulic conductivity. 131
Figure 6.11: Percent impervious cover per cell assigned based on SOLRIS v.3 land cover. 133
Figure 6.12: Simulated and observed streamflow (in m^3s) at the Grindstone Creek near Millgrove gauge along with precipitation and snowmelt. 134
Figure 6.13: Simulated and observed streamflow (in m^3s) at the Grindstone Creek near Aldershot gauge along with precipitation and snowmelt. 134
Figure 6.14: Simulated annual average precipitation in the PRMS submodel in mm/yr. 136
Figure 6.15: Simulated annual average cascading runoff (Hortonian, Dunnian, and interflow) passing through each cell in m^3/d. 137
Figure 6.16: Simulated annual average actual evapotranspiration (soil zone ET, canopy losses and sublimation) in mm/yr. 138
Figure 6.17: Simulated annual net average groundwater recharge in mm/yr. 139
Figure 6.18: Simulated (red) and observed streamflow (blue, in m^3s) at the Grindstone Creek near Aldershot gauge. 143
Figure 6.19: Simulated and observed flow at SW10B for WY2019. 144
Figure 6.20: Simulated SW9 Streamflow in 2019 (blue) very closely matches the observed values. 144
Figure 6.21: Well locations and calibration cross sections. 146

Figure 6.22: West calibration section.....147
Figure 6.23: East calibration section.....148
Figure 6.24: Comparison of simulated (thick line) and observed (thin line) potentials in Layers 4 (red) and 8 (blue) at wells OW03-15A and OW03-15C. 149
Figure 6.25: Comparison of Observed and Predicted water levels at Monitor OW03-21 150
Figure 6.26: Comparison of observed and simulated water levels at monitor OW03-31 (Note: deep monitor in layer 6, shallow monitor in Layer 4-5). 151
Figure 6.27: Comparison of observed and simulated water levels at monitor OW03-29. 151
Figure 6.28: Mini-piezometer and pond staff gauge locations. 153
Figure 6.29: Observed and simulated pond elevation at MP16. 154
Figure 6.30: Observed and simulated shallow water levels at MP6.....154
Figure 6.31: Observed and simulated pond and mini-piezometer elevation at Golder SG2 and MP5. 155
Figure 6.32: Perched Wetland Cross Section 156
Figure 6.33: Wetland 13025 simulated pond water levels compared to MP-33 measurements 157
Figure 6.34: Wetland 13031 water levels compared to water table monitor OW03-19C.....158
Figure 6.35: Wetland 13032 water level recession. Purple symbols mark the water level recession between the May 17 and July 11 time period.....159
Figure 6.36: Wetland 13032 simulated water level showing similar spring recession patterns.....159
Figure 6.37: Average monthly simulated heads (in masl) and streamflow (in m^3/d) for March. 162
Figure 6.38: Average monthly simulated heads (in masl) and streamflow (in m^3/d) for September.163
Figure 6.39: Average monthly groundwater budget for the study area (all flows in m^3/d). 164
Figure 7.1: Locations selected for comparative analyses of streamflow and groundwater levels. ...168
Figure 7.2: Average simulated heads in Model Layer 6 (masl) and streamflow (m^3/s) for WY2010 to WY2014. 169
Figure 7.3: Available Drawdown in Layer 8 - Baseline Conditions.....170
Figure 7.4: Simulated streamflow at SW09 for WY2010 to WY2014 - Baseline Conditions. 171
Figure 7.5: Simulated streamflow at SW09 for WY2015 toWY2019 - Baseline Conditions. 171
Figure 7.6: Simulated streamflow at SW29 for WY2010 to WY2014 - Baseline Conditions. 172
Figure 7.7: Simulated streamflow at SW29 for WY2015 to WY2019 - Baseline Conditions. 172
Figure 7.8: Simulated streamflow at SW36A for WY2010 to WY2014 - Baseline Conditions. 173
Figure 7.9: Simulated streamflow at SW36A for WY2015 to WY2019 - Baseline Conditions. 173
Figure 7.10: Simulated streamflow at SW28 for WY2010 to WY2014 - Baseline Conditions. 174
Figure 7.11: Simulated streamflow at SW28 for WY2015 to WY2019 - Baseline Conditions. 174
Figure 7.12: Simulated streamflow at SW10B for WY2010 to WY2014 - Baseline Conditions. 175
Figure 7.13: Simulated precipitation and streamflow at SW10B for WY2015 to WY2019 - Baseline Conditions. 175
Figure 7.14: Simulated streamflow at SW07 for WY2010 to WY2014 - Baseline Conditions. 176
Figure 7.15: Simulated streamflow at SW07 for WY2015 to WY2019 - Baseline Conditions. 176
Figure 7.16: Simulated heads in Model Layers 6 at groundwater assessment locations GW1 to GW-8 for WY2010 to WY 2014 - Baseline Conditions. 177
Figure 7.17: Simulated heads in Model Layers 6 at groundwater assessment locations GW1 to GW-8 for WY2015 to WY2019 - Baseline Conditions. 177
Figure 7.18: Average simulated groundwater recharge (mm/yr) under Baseline Conditions. 181
Figure 7.19: Average simulated groundwater ET (mm/yr) under Baseline Conditions.....182
Figure 7.20: Average simulated groundwater discharge to the soil zone (m^3/d) under Baseline Conditions. 183
Figure 7.21: Average simulated streamflow loss to groundwater (blue) or groundwater discharge to streams (red) (m^3/d) under Baseline Conditions. 184
Figure 7.22: Significant wetland features selected for water budget analysis 185
Figure 7.23: Detailed water budget for Wetland 9 averaged over WY2010 to WY2014 under Baseline Conditions. 186

Figure 7.24: Detailed water budget for Wetland 16 averaged over WY2010 to WY2014 under Baseline Conditions. 186
Figure 7.25: Detailed water budget for Wetland 17 averaged over WY2010 to WY2014 under Baseline Conditions. 187
Figure 7.26: Detailed water budget for Wetland 18 averaged over WY2010 to WY2014 under Baseline Conditions. 187
Figure 7.27: Detailed water budget for Wetland 19 averaged over WY2010 to WY2014 under Baseline Conditions. 188
Figure 7.28: Detailed water budget for Wetland 20 averaged over WY2010 to WY2014 under Baseline Conditions. 188
Figure 7.29: Detailed water budget for Wetland 21 averaged over WY2010 to WY2014 under Baseline Conditions. 189
Figure 7.30: Detailed water budget for Wetland 22 averaged over WY2010 to WY2014 under Baseline Conditions. 189
Figure 8.1: Comparison of water level fluctuations at Location GW1 (near the Medad) versus GW7 indicates that the Medad location is no drought sensitive....193
Figure 8.2: Proposed extraction phases. 194
Figure 8.3: Scenario P12 configuration. 197
Figure 8.4: Average simulated heads in Model Layer 6 (masl) and streamflow (m^3/s) for WY2014 to WY2019 under Scenario P12. 199
Figure 8.5: Average simulated drawdown in Model Layer 6 (m) and increase/decrease in streamflow (m^3/s) for WY2014 to WY2019 under Scenario P12. 200
Figure 8.6: Simulated streamflow at SW09 for WY2014 to WY2019 – P12 and Baseline Conditions. 201
Figure 8.7: Simulated streamflow at SW29 for WY2014 to WY2019 – P12 and Baseline Conditions. 201
Figure 8.8: Simulated streamflow at SW36A for WY2014 to WY2019 – P12 and Baseline Conditions. 202
Figure 8.9: Simulated streamflow at SW28 for WY2014 to WY2019 – P12 and Baseline Conditions. 202
Figure 8.10: Simulated streamflow at SW10B for WY2014 to WY2019 – P12 and Baseline Conditions. 203
Figure 8.11: Simulated streamflow at SW07 for WY2014 to WY2019 – P12 and Baseline Conditions. 203
Figure 8.12: Simulated heads and drawdowns in Model Layers 6 at GW1 for WY2014 to WY2019 - P12 and Baseline Conditions. 205
Figure 8.13: Simulated heads and drawdowns in Model Layers 6 at GW2 for WY2014 to WY2019 - P12 and Baseline Conditions. 205
Figure 8.14: Simulated heads and drawdowns in Model Layers 6 at GW3 for WY2014 to WY2019 - P12 and Baseline Conditions. 206
Figure 8.15: Simulated heads and drawdowns in Model Layers 6 at GW4 for WY2014 to WY2019 - P12 and Baseline Conditions. 206
Figure 8.16: Simulated heads and drawdowns in Model Layers 6 at GW5 for WY2014 to WY2019 - P12 and Baseline Conditions. 207
Figure 8.17: Simulated heads and drawdowns in Model Layers 6 at GW6 for WY2014 to WY2019 - P12 and Baseline Conditions. 207
Figure 8.18: Simulated heads and drawdowns in Model Layers 6 at GW7 for WY2014 to WY2019 - P12 and Baseline Conditions. 208
Figure 8.19: Simulated heads and drawdowns in Model Layers 6 at GW8 for WY2014 to WY2019 - P12 and Baseline Conditions. 208
Figure 8.20: Average available drawdown under P12 conditions. 209
Figure 8.21: Minimum available drawdown under P12 Drought conditions. 210

Figure 8.22: Average simulated groundwater recharge (mm/yr) for WY2014 to WY2019 – Scenario P12. 213
Figure 8.23: Average simulated groundwater ET (mm/yr) for WY2014 to WY2019 – Scenario P12. 214
Figure 8.24: Average simulated streamflow loss (blue) to groundwater or groundwater discharge to streams (red) (m^3/d) for WY2014 to WY2019 – Scenario P12. 215
Figure 8.25: Average simulated groundwater discharge to the soil zone (m^3/d) for WY2014 to WY2019 – Scenario P12. 216
Figure 8.26: Wetland cross section location. 217
Figure 8.27: Wetland cross section. 218
Figure 8.28: Comparison of pond water levels in Wetland 19 (MNRF 13032) under baseline (blue) and P12 conditions (red). Purple symbols show spring recession period. 219
Figure 8.29: Comparison of leakage from Wetland 19 to groundwater under Baseline and P12 conditions. 220
Figure 8.30: Detailed water budget for Wetland 9 averaged over WY2010 and WY2011 under Scenario P12. 221
Figure 8.31: Detailed water budget for Wetland 16 averaged over WY2010 and WY2011 under Scenario P12. 221
Figure 8.32: Detailed water budget for Wetland 17 averaged over WY2010 and WY2011 under Scenario P12. 222
Figure 8.33: Detailed water budget for Wetland 18 averaged over WY2010 and WY2011 under Scenario P12. 222
Figure 8.34: Detailed water budget for Wetland 19 averaged over WY2010 and WY2011 under Scenario P12. 223
Figure 8.35: Detailed water budget for Wetland 20 averaged over WY2010 and WY2011 under Scenario P12. 223
Figure 8.36: Detailed water budget for Wetland 21 averaged over WY2010 and WY2011 under Scenario P12. 224
Figure 8.37: Detailed water budget for Wetland 22 averaged over WY2010 and WY2011 under Scenario P12. 224
Figure 8.38: Scenario P34 configuration. 227
Figure 8.39: Average simulated heads in Model Layer 6 (masl) and streamflow (m^3/s) for WY2010 to WY2014 under Scenario P34. 228
Figure 8.40: Average simulated drawdown in Model Layer 6 (m) and increase/decrease in streamflow (m^3/s) for WY2010 to WY2015 under Scenario P34. 229
Figure 8.41: Scenario P3456 configuration. 231
Figure 8.42: Average simulated heads in Model Layer 6 (masl) and streamflow (m^3/s) for WY2010 to WY2014 under Scenario P3456. 232
Figure 8.43: Average simulated drawdown in Model Layer 6 (m) and increase/decrease in streamflow (m^3/s) for WY2010 to WY2014 under Scenario P3456. 233
Figure 8.44: Simulated streamflow at SW09 for WY 2014-2019 – P3456 and Baseline Conditions. 235
Figure 8.45: Simulated streamflow at SW29 for WY 2014-2019 – P3456 and Baseline Conditions. 235
Figure 8.46: Simulated streamflow at SW36A for WY 2014-2019 – P3456 and Baseline Conditions. 236
Figure 8.47: Simulated streamflow at SW28 for WY 2014-2019 – P3456 and Baseline Conditions. 236
Figure 8.48: Simulated streamflow at SW10B for WY 2014-2019 – P3456 and Baseline Conditions. 237
Figure 8.49: Simulated streamflow at SW07 for WY 2014-2019 – P3456 and Baseline Conditions. 237

Figure 8.50: Simulated heads and drawdowns in Model Layers 6 at GW1 for WY 2014-2019 - P3456 and Baseline Conditions. 238
Figure 8.51: Simulated heads and drawdowns in Model Layers 6 at GW2 for WY 2014-2019 - P3456 and Baseline Conditions. 238
Figure 8.52: Simulated heads and drawdowns in Model Layers 6 at GW3 for WY 2014-2019 - P3456 and Baseline Conditions. 239
Figure 8.53: Simulated heads and drawdowns in Model Layers 6 at GW4 for WY 2014-2019 - P3456 and Baseline Conditions. 239
Figure 8.54: Simulated heads and drawdowns in Model Layers 6 at GW5 for WY 2014-2019 - P3456 and Baseline Conditions. 240
Figure 8.55: Simulated heads and drawdowns in Model Layers 6 at GW6 for WY 2014-2019 - P3456 and Baseline Conditions. 240
Figure 8.56: Simulated heads and drawdowns in Model Layers 6 at GW7 for WY 2014-2019 - P3456 and Baseline Conditions. 241
Figure 8.57: Simulated heads and drawdowns in Model Layers 6 at GW8 for WY 2014-2019 - P3456 and Baseline Conditions. 241
Figure 8.58: Average simulated groundwater recharge (mm/yr) for WY 2010-2014 – Scenario P3456. 244
Figure 8.59: Average simulated groundwater ET (mm/yr) for WY 2010-2014 – Scenario P3456. 245
Figure 8.60: Average simulated streamflow loss to groundwater or groundwater discharge to streams (m^3/d) for WY 2010-2014 – Scenario P3456. 246
Figure 8.61: Average simulated groundwater discharge to the soil zone (m^3/d) for WY 2010-2014 – Scenario P3456. 247
Figure 8.62: Detailed water budget for Wetland 9 averaged over WY2010 and WY2011 under Scenario P3456. 248
Figure 8.63: Detailed water budget for Wetland 16 averaged over WY2010 and WY2011 under Scenario P3456. 248
Figure 8.64: Detailed water budget for Wetland 17 averaged over WY2010 and WY2011 under Scenario P3456. 249
Figure 8.65: Detailed water budget for Wetland 18 averaged over WY2010 and WY2011 under Scenario P3456. 249
Figure 8.66: Detailed water budget for Wetland 19 averaged over WY2010 and WY2011 under Scenario P3456. 250
Figure 8.67: Detailed water budget for Wetland 20 averaged over WY2010 and WY2011 under Scenario P3456. 250
Figure 8.68: Detailed water budget for Wetland 21 averaged over WY2010 and WY2011 under Scenario P3456. 251
Figure 8.69: Detailed water budget for Wetland 22 averaged over WY2010 and WY2011 under Scenario P3456. 251
Figure 8.70: Change in groundwater discharge to the soil zone between Baseline and P3456. 253
Figure 8.71: Change in streamflow between Baseline and P3456 254
Figure 8.72: Hydrograph showing stream flow 250 m upstream of SW07 for WY2010 to WY2014 255
Figure 8.73: Hydrograph showing stream flow 250 m upstream of SW07 for WY2012 (enlargement to show detail) 255
Figure 8.74: Baseline vs P3456 Change in flow at SW14 256
Figure 8.75: Average available drawdown under P3456 conditions. 258
Figure 8.76: Minimum available drawdown under P3456 drought conditions. 259
Figure 8.77: Scenario RHB1 configuration. 261
Figure 8.78: Average simulated heads in Model Layer 6 (masl) and streamflow (m^3/s) for WY2010 to WY2012 under Scenario RHB1. 262
Figure 8.79: Average simulated drawdown in Model Layer 6 (m) and increase/decrease in streamflow (m^3/s) for WY2010 to WY2012 under Scenario RHB1. 263
Figure 8.80: Simulated streamflow at SW09 for WY 2010-2012 – RHB1 and Baseline Conditions. 265

Figure 8.81: Simulated streamflow at SW29 for WY2010-WY2012 – RHB1 and Baseline Conditions. 265
Figure 8.82: Simulated streamflow at SW36A for WY2010-WY2012 – RHB1 and Baseline Conditions. 266
Figure 8.83: Simulated streamflow at SW28 for WY2010-WY2012 – RHB1 and Baseline Conditions. 266
Figure 8.84: Simulated streamflow at SW10B for WY2010-WY2012 – RHB1 and Baseline Conditions. 267
Figure 8.85: Simulated streamflow at SW07 for WY2010-WY2012 – RHB1 and Baseline Conditions. 267
Figure 8.86: Simulated heads and drawdowns in Model Layers 6 at GW1 for WY2010-WY2012 – RHB1 and Baseline Conditions. 268
Figure 8.87: Simulated heads and drawdowns in Model Layers 6 at GW2 for WY2010-WY2012 – RHB1 and Baseline Conditions. 268
Figure 8.88: Simulated heads and drawdowns in Model Layers 6 at GW3 for WY2010-WY2012 – RHB1 and Baseline Conditions. 269
Figure 8.89: Simulated heads and drawdowns in Model Layers 6 at GW4 for WY2010-WY2012 – RHB1 and Baseline Conditions. 269
Figure 8.90: Simulated heads and drawdowns in Model Layers 6 at GW5 for WY2010-WY2012 – RHB1 and Baseline Conditions. 270
Figure 8.91: Simulated heads and drawdowns in Model Layers 6 at GW6 for WY2010-WY2012 – RHB1 and Baseline Conditions. 270
Figure 8.92: Simulated heads and drawdowns in Model Layers 6 at GW7 for WY2010-WY2012 – RHB1 and Baseline Conditions. 271
Figure 8.93: Simulated heads and drawdowns in Model Layers 6 at GW8 for WY2010-WY2012 – RHB1 and Baseline Conditions. 271
Figure 8.94: Average simulated groundwater recharge (mm/yr) for WY2010-WY2012 – Scenario RHB1. 273
Figure 8.95: Average simulated groundwater ET (mm/yr) for WY2010-WY2012 – Scenario RHB1. 274
Figure 8.96: Average simulated streamflow loss to groundwater or groundwater discharge to streams (m^3/d) for WY2010-WY2012 – Scenario RHB1. 275
Figure 8.97: Average simulated groundwater discharge to the soil zone (m^3/d) for WY2010-WY2012 – Scenario RHB1. 276
Figure 8.98: Detailed water budget for Wetland 9 averaged over WY2010 to WY2012 under Scenario RHB1. 277
Figure 8.99: Detailed water budget for Wetland 16 averaged over WY2010 to WY2012 under Scenario RHB1. 277
Figure 8.100: Detailed water budget for Wetland 17 averaged over WY2010 to WY2012 under Scenario RHB1. 278
Figure 8.101: Detailed water budget for Wetland 18 averaged over WY2010 to WY2012 under Scenario RHB1. 278
Figure 8.102: Detailed water budget for Wetland 20 averaged over WY2010 to WY2012 under Scenario RHB1. 279
Figure 8.103: Detailed water budget for Wetland 22 averaged over WY2010 to WY2012 under Scenario RHB1. 279
Figure 8.104: Scenario RHB2 configuration. 282
Figure 8.105: Average simulated heads in Model Layer 6 (masl) and streamflow (m^3/s) for WY2010 to WY2014 under Scenario RHB2. 283
Figure 8.106: Average simulated change in head in Model Layer 6 (m) and increase/decrease in streamflow (m^3/s) for WY2010 to WY2014 under Scenario RHB2. 284
Figure 8.107: Simulated streamflow at SW09 for WY 2010-2014 – RHB2 and Baseline Conditions. 286

Figure 8.108: Simulated streamflow at SW29 for WY2010-WY2014 – RHB2 and Baseline Conditions. 286
Figure 8.109: Simulated streamflow at SW36A for WY2010-WY2014 – RHB2 and Baseline Conditions. 287
Figure 8.110: Simulated streamflow at SW28 for WY2010-WY2014 – RHB2 and Baseline Conditions. 287
Figure 8.111: Simulated streamflow at SW10B for WY2010-WY20142 – RHB2 and Baseline Conditions. 288
Figure 8.112: Simulated streamflow at SW07 for WY2010-WY2014 – RHB2 and Baseline Conditions. 288
Figure 8.113: Simulated heads and drawdowns in Model Layers 6 at GW1 for WY2010-WY2014 – RHB2 and Baseline Conditions. 289
Figure 8.114: Simulated heads and drawdowns in Model Layers 6 at GW2 for WY2010-WY2014 – RHB2 and Baseline Conditions. 289
Figure 8.115: Simulated heads and drawdowns in Model Layers 6 at GW3 for WY2010-WY2014 – RHB2 and Baseline Conditions. 290
Figure 8.116: Simulated heads and drawdowns in Model Layers 6 at GW4 for WY2010-WY2014 – RHB2 and Baseline Conditions. 290
Figure 8.117: Simulated heads and drawdowns in Model Layers 6 at GW5 for WY2010-WY2014 – RHB2 and Baseline Conditions. 291
Figure 8.118: Simulated heads and drawdowns in Model Layers 6 at GW6 for WY2010-WY2014 – RHB2 and Baseline Conditions. 291
Figure 8.119: Simulated heads and drawdowns in Model Layers 6 at GW7 for WY2010-WY2014 – RHB2 and Baseline Conditions. 292
Figure 8.120: Simulated heads and drawdowns in Model Layers 6 at GW8 for WY2010-WY2014 – RHB2 and Baseline Conditions. 292
Figure 8.121: Average simulated groundwater recharge (mm/yr) for WY2010-WY2014 – Scenario RHB2. 294
Figure 8.122: Average simulated groundwater ET (mm/yr) for WY2010-WY2014 – Scenario RHB2. 295
Figure 8.123: Average simulated streamflow loss to groundwater or groundwater discharge to streams (m^3/d) for WY2010-WY2014 – Scenario RHB2. 296
Figure 8.124: Average simulated groundwater discharge to the soil zone (m^3/d) for WY2010-WY2014 – Scenario RHB2. 297
Figure 8.125: Detailed water budget for Wetland 9 averaged over WY2010 to WY2014 under Scenario RHB2. 298
Figure 8.126: Detailed water budget for Wetland 16 averaged over WY2010 to WY2014 under Scenario RHB2. 298
Figure 8.127: Detailed water budget for Wetland 17 averaged over WY2010 to WY2014 under Scenario RHB2. 299
Figure 8.128: Detailed water budget for Wetland 18 averaged over WY2010 to WY2014 under Scenario RHB2. 299
Figure 8.129: Detailed water budget for Wetland 20 averaged over WY2010 to WY2014 under Scenario RHB2. 300
Figure 8.130: Detailed water budget for Wetland 22 averaged over WY2010 to WY2014 under Scenario RHB2. 300
Figure 9.1: Location of Well DW2 306
Figure 9.2: Groundwater Monitoring Network (Southern Extension) 310
Figure 9.3: Available Drawdown (Southern Extension) 312
Figure 9.4: Groundwater Monitoring Locations (West Extension) 316
Figure 9.5: Available Drawdown (West Extension) 317
Figure 10.1: AMP Groundwater Monitoring Locations 321
Figure 17.1: PRMS hydrologic processes 441

Figure 17.2: PRMS two-layer snowpack conceptualization and components of the snowpack energy balance, accumulation, snowmelt, and sublimation algorithms (from Markstrom *et al.*, 2015). 442
Figure 17.3: Influence of soil zone moisture on recharge, interflow, and runoff processes.....444
Figure 17.4: PRMS extended model boundary for Grindstone Creek. 454
Figure 17.5: Portion of the PRMS model grid in the quarry vicinity.....455
Figure 17.6: PRMS subbasins for the extended PRMS model. 456
Figure 17.7: PRMS model topography. 457
Figure 17.8: PRMS model cell slope. 458
Figure 17.9: Cascade network near the Nelson Burlington Quarry.....459
Figure 17.10: Surficial soil index (MNR, 2013). 460
Figure 17.11: Surficial soil hydraulic conductivity. 461
Figure 17.12: SOLRIS v3 (MNRF, 2019) land use index. 462
Figure 17.13: Percent impervious cover per cell assigned based on SOLRIS v.3 land cover. 463
Figure 17.14: Environment Canada AES climate stations within 25 km of the study area. 464
Figure 17.15: Interpolated average annual precipitation (data from WY1951 to WY2019). 465
Figure 17.16: Interpolated annual average temperature (data from WY1951 to WY2019). 466
Figure 17.17: Simulated annual average precipitation in the PRMS submodel in mm/yr. 467
Figure 17.18: Simulated annual average net precipitation (after canopy interception and sublimation) in mm/yr. 468
Figure 17.19: Simulated annual average evaporation from canopy interception and sublimation in mm/yr. 469
Figure 17.20: Simulated annual average Hortonian overland runoff in mm/yr. 470
Figure 17.21: Simulated annual average cascading runoff (Hortonian, Dunnian, and interflow) passing through each cell in m^3/d. 471
Figure 17.22: Simulated annual average runoff (Hortonian and Dunnian) and Interflow to streams in m^3/d. 472
Figure 17.23: Simulated annual average infiltration to the soil zone in mm/yr.....473
Figure 17.24: Simulated annual average actual evapotranspiration (soil zone ET, canopy losses and sublimation) in mm/yr.....474
Figure 17.25: Simulated annual net average groundwater recharge in mm/yr. 475
Figure 17.26: Simulated and observed streamflow (in m^3s) at the Grindstone Creek near Millgrove gauge along with precipitation and snowmelt. 476
Figure 17.27: Simulated and observed streamflow (in m^3s) at the Grindstone Creek near Aldershot gauge along with precipitation and snowmelt. 476
Figure 17.28: Observed streamflow at Grindstone Creek near Millgrove (WSC Station No. 02HB028) 477
Figure 17.29: Incremental and cumulative simulated streamflow in PRMS subbasin 2 and 3. 477
Figure 17.30: Partial synthetic hydrograph of Grindstone Creek inflows to be applied to the integrated GSFLOW model. 478
Figure 18.1: Stream network and lake representation in the SFR2 and LAK3 modules (modified from Markstrom, *et al.*, 2008).....484
Figure 18.2: Simulated stream channel geometry.....485
Figure 18.3: Steady State Model Calibration.....490
Figure 18.4: Finite-difference grid for the MODFLOW submodel in GSFLOW. 493
Figure 18.5: MODFLOW Model Layers showing layer continuity. 494
Figure 18.6: MODFLOW layer hydraulic conductivity. 495
Figure 18.7: MODFLOW layer anisotropy, showing vertical connectivity in the bulk Amabel. 496
Figure 18.8: Model boundary conditions for the calibration/baseline scenario. 497
Figure 18.9: Simulated stream and lakes by type. 498
Figure 18.10: Simulated average groundwater recharge in the GSFLOW model under baseline conditions. 499

Figure 18.11: Final calibrated hydraulic conductivity values for Layer 1, in m/s, based on surficial geology. 500
Figure 18.12: Final calibrated hydraulic conductivity values for Layer 2 (mainly Halton Till), in m/s. 501
Figure 18.13: Final calibrated hydraulic conductivity values for Layer 3, mainly MIS Fm. and ORAC, in m/s. 502
Figure 18.14: Final calibrated hydraulic conductivity values for Layer 4, mainly weathered Goat Island/Gasport Fm. above the Niagara Escarpment, in m/s. 503
Figure 18.15: Final calibrated hydraulic conductivity values for Layer 5, mainly upper bulk Goat Island/Gasport Fm. above the Niagara Escarpment, in m/s. 504
Figure 18.16: Final calibrated hydraulic conductivity values for Layer 6, mainly middle fracture zone in the Goat Island/Gasport Fm. above the Niagara Escarpment, in m/s. 505
Figure 18.17: Final calibrated hydraulic conductivity values for Layer 7, mainly lower bulk Goat Island/Gasport Fm. above the Niagara Escarpment, in m/s. 506
Figure 18.18: Final calibrated hydraulic conductivity values for Layer 8, mainly lower fracture zone in the Goat Island/Gasport Fm. above the Niagara Escarpment, in m/s. 507
Figure 18.19: Final calibrated hydraulic conductivity values for Layer 9, mainly lower aquitards above the Niagara Escarpment, in m/s. 508
Figure 18.20: Final calibrated vertical hydraulic conductivity values for Layer 5, mainly upper bulk Goat Island/Gasport Fm. above the Niagara Escarpment, in m/s. 509
Figure 18.21: Final calibrated hydraulic conductivity values for Layer 7, mainly lower bulk Goat Island/Gasport Fm. above the Niagara Escarpment, in m/s. 510
Figure 18.22: Simulated steady state heads in Model Layer 6 (representing the middle fracture zone) versus average water levels in wells (in masl). 511
Figure 19.1: Simulated (red) and observed streamflow (blue, in m3s) at the Grindstone Creek near Aldershot gauge. 512
Figure 19.2: Average GSFLOW simulated water levels in Model Layer 6 (representing the middle fracture zone) versus static water levels in wells (in masl). 514
Figure 19.3: Predicted average water level (masl) versus Observed MECP water well measurements 515
Figure 19.4: Flow monitoring stations used in the local streamflow calibration. 517
Figure 19.5: Simulated and observed streamflow at SW-10B for WY2017 to WY2019. 518
Figure 19.6: SW10B Comparison of observed (red) and simulated (blue) streamflow for 2019. 518
Figure 19.7: Simulated and observed streamflow at SW-09 for WY2017 to WY2019. 519
Figure 19.8: Simulated SW9 streamflow in 2019 (blue) very closely matches the observed values. 519
Figure 19.9: Simulated and observed streamflow at SW-29 for WY2017 to WY2019. 520
Figure 19.10: Comparison of simulated (red) and observed flows at the North Quarry discharge. 521
Figure 19.11: Simulated (red) and observed flows at the South Quarry discharge. 522
Figure 19.12: Simulated (red) and observed (blue) 2017 South Quarry discharge. 522
Figure 19.13: Simulated (red) and observed Medad Valley streamflow at SW2. 523
Figure 19.14: Simulated (red) and observed Medad Valley streamflow at SW2 in 2017. 524
Figure 19.15: Simulated (red) and observed Medad Valley streamflow at SW2 in 2018. 524
Figure 19.16: Wells in the South Extension area. 526
Figure 19.17: Location of calibration cross sections. 527
Figure 19.18: West calibration section. 528
Figure 19.19: Central calibration section. 529
Figure 19.20: East calibration section. 530
Figure 19.21: South calibration section. 531
Figure 19.22: Comparison of observed and simulated water levels at monitor OW03-15. 532
Figure 19.23: Comparison of observed and simulated water levels at monitor OW03-14. 533
Figure 19.24: Comparison of observed and simulated water levels at monitor OW03-21. 534

Figure 19.25: Comparison of observed and simulated water levels at monitor MW03-09 (Note: deep monitor is above layer 8). 535
Figure 19.26: Comparison of observed and simulated water levels at monitor OW03-30 (Note: deep monitor is in layer 7). 535
Figure 19.27: Comparison of observed and simulated water levels at monitor OW03-31 (Note: deep monitor in layer 6, shallow monitor in Layer 4-5). 536
Figure 19.28: Comparison of observed and simulated water levels at monitor MW03-02. 537
Figure 19.29: Comparison of observed and simulated water levels at monitor MW03-01 537
Figure 19.30: Comparison of observed and simulated water levels at monitor OW03-17. 538
Figure 19.31: Comparison of observed and simulated water levels at monitor OW03-18. 539
Figure 19.32: Comparison of observed and simulated water levels at monitor OW03-29. 539
Figure 19.33: Comparison of observed and simulated water levels at monitor OW03-19. 540
Figure 19.34: Mini-piezometer and pond staff gauge locations. 542
Figure 19.35: Observed and simulated shallow water levels at GP03-37. 543
Figure 19.36: Observed and simulated shallow water levels at MP17. 543
Figure 19.37: Observed and simulated shallow water levels at MP13. 544
Figure 19.38: Observed and simulated shallow water levels at MP11. 544
Figure 19.39: Observed and simulated shallow water levels at MP29. 545
Figure 19.40: Observed and simulated shallow water levels at MP6 (near Pond H). 545
Figure 19.41: Observed and simulated pond elevation at SW13A-SG (Wetland 11). 547
Figure 19.42: Observed and simulated pond elevation at Golder SG-3 (in Wetland 17). 547
Figure 19.43: Observed and simulated pond and mini-piezometer elevation at Golder SG2 and MP5. 548
Figure 19.44: Observed and simulated pond elevation at MP16. 549
Figure 19.45: Observed and simulated pond elevation at SW16A-SG (note: range of measurements is less than 6 cm). 549
Figure 19.46: Average monthly simulated heads (in masl) and streamflow (in m^3/d) for March. 551
Figure 19.47: Average monthly simulated heads (in masl) and streamflow (in m^3/d) for September. 552
Figure 19.48: Average monthly groundwater budget for the study area (all flows in m^3/d). 555
Figure 19.49: Significant wetland features selected for water budget analysis. 556
Figure 19.50: MNRF versus Earthfx Wetland ID numbers. 557
Figure 19.51: Detailed water budget for Wetland 9 averaged over WY2010 to WY2014 under baseline conditions. 558
Figure 19.52: Detailed water budget for Wetland 17 averaged over WY2010 to WY2014 under baseline conditions. 558

Level 1 and Level 2 Hydrogeological and Hydrological Impact Assessment of the Proposed Burlington Quarry Extension

Executive Summary

Nelson Aggregates Co. (Nelson) operates the Burlington Quarry near the intersection of Side Road 2 and Guelph Line, in the City of Burlington, Region of Halton. The quarry is 218.7 hectares (ha) in size and is located on the watershed divide between Bronte Creek and Grindstone Creek near Mount Nemo. The quarry has been in existence since 1953 and has been operated by Nelson since 1983. The primary source of aggregate is the Amabel Formation dolostone, which is a provincially-significant aggregate resource.

The Nelson proposal includes the extension of the existing quarry to the west and south. The proposed South Extension covers approximately 18 hectares (ha), with 14.5 ha of extraction, and the proposed West Extension covers approximately 60 ha, with 35.7 ha of extraction.

The objective of this Level 2 ARA investigation is to characterize the existing conditions at the Burlington quarry site, describe the development of an integrated groundwater/surface water assessment model, and predict any likely changes to the hydrologic and hydrogeologic conditions at different phases of extraction and final rehabilitation.

Methodology

The assessment methodology used in this study is the same as that used by Earthfx for multiple Source Water Protection Tier 3 Water Budget and Wellhead Protection studies conducted for the Province of Ontario. The same model and methodology were used, and the key aspects of the approach include:

1. Fully integrated analysis and simulation of all surface water and groundwater processes
2. Fully transient assessment of system behaviour on a daily basis for a period of years; including significant drought and wet year conditions.
3. Detailed daily comparative assessment including evaluation of the minimum, average and maximum impact of development
4. Full water budget accounting on a daily basis.

Earthfx has used the same advanced methodology for Source Water Protection studies for the Region of Halton, Conservation Halton, City of Hamilton, Region of York, Region of Peel, Toronto and Region Conservation Authority, Lake Simcoe Conservation Authority, Grand River Conservation Authority, City of Toronto and other water management agencies across Canada and the USA.

Site Setting

The study area is predominantly covered by the low permeability Halton Till, a fine grained silty to clayey till that was deposited approximately 13,000 years ago by a glacial lobe that advanced out of the Lake Ontario basin. Beneath the Halton Till are occasional deposits of sands on the bedrock surface. These sands and the upper weathered bedrock form an upper water table aquifer.

The upper most bedrock unit is commonly referred to as the Amabel Formation, but in recent literature it has been subdivided into the Goat Island and Gasport Formations. The Amabel is a massive, fine

grained dolostone with an average thickness of 25 m. The Amabel includes occasional vertical fractures and there is good evidence of an intermediate and lower fracture zone. Beneath the Amabel are thin interbedded shale and limestone units and the thick, low permeability Cabot Head Shale.

The highest measured ground water elevations are located near the crest of Mt. Nemo, northwest of the existing quarry. There is radial flow in all directions from this regional high, but, in general, the predominant groundwater flow direction follows the dipping topography and bedrock layers to the south and west. The Medad Valley is incised into the Cabot Head shale aquitard and receives groundwater discharge from the overlying dolostones.

Water supply wells in the area are typically constructed as open boreholes drilled 10 to 15 m into the Amabel formation. Wells are drilled sufficiently deep to encounter one or more bedrock fractures with adequate flow for domestic use. Static water levels in these wells are highly variable, depending on local fracture conditions and seasonal recharge.

In general, there is limited interaction between the local streams and groundwater system because of the low permeability of the surficial Halton Till aquitard. The water table is generally found in the shallow bedrock, but in low lying areas in the spring it can rise into the overburden and discharge to the streams and wetlands. There are two karstic streams to the south and north of the quarry where streamflow disappears into the shallow bedrock and reappears a few hundred metres downslope as small groundwater springs. There are other groundwater springs (and karst discharge features) in the Medad Valley, but these are masked by the wetlands that fill the valley.

Groundwater monitoring since 2003 has delineated the effects of quarry development on water levels in and around the active quarry. A distinctive pattern of water level changes in the Amabel layers are observed as the quarry advances, with enhanced water level variability observed up to 650 m from the quarry face during the late summer. Baseline (current condition) numerical model simulations closely replicate this pattern and illustrate how groundwater recharge in the spring replenishes the system through downward in the vertical fractures.

The numerical simulations confirm that the majority of the wetlands and streams are isolated from the water table by the low permeability Halton Till. A total of 5 of the 22 mapped wetlands in and around the quarry receive groundwater upwelling in the spring, however groundwater is in every case a very small percentage (less than 3%) of the overall inflows into the wetland.

Baseline Conditions

The system behaviour in and around the existing quarry is extremely well understood. The long-term monitoring (including the monitoring of the 2005-2019 advancement of the south extraction face) provides a clear groundwater response that has been accurately simulated by the transient integrated model. The detailed field investigations, together with the simulation of this large-scale response, provides significant confidence in the numerical model and the resulting impact assessment. The baseline conditions are very well understood.

The local conditions around each extension phase result in somewhat different drawdown patterns for each expansion scenario, however the overall conclusions and general patterns are consistent with the existing quarry. The configuration of the excavation, local recharge, hydrogeologic setting and proximity to the existing quarry affect the area of influence.

Level 2 Assessment Scenarios

The Level 2 impact assessment scenarios present a detailed and exhaustive comparison of the proposed developments to the baseline conditions. All pertinent aspects of the surface water and

ground water system have been compared across a wide range of climate conditions. The integrated approach ensures that surface and groundwater functions and water budgets are fully reconciled. Many wells in the upland area exhibit more than 2 m of seasonal and inter-annual variation, so distinguishing quarry influence below this level would be difficult.

South Extension Effects

The predicted drawdowns associated with the South Extension diminish rapidly with distance from the excavation. The 2.0 m drawdown cone extends up to 1000 m from the excavation in the middle Amabel aquifer, but the 2.0 m drawdown is much more limited in the springtime, extending less than 700 m, because of the higher recharge and water levels associated with the spring snowmelt.

The majority of the wetlands in the vicinity of the South Extension are perched above the water table in the low permeability Halton Till. As noted, a total of 5 of the 22 wetlands evaluated do receive groundwater inflow in the spring, but the percentage of groundwater inflows relative to the total inflows is less than 3%. During South Quarry extraction, the drawdown in the water table will limit groundwater upwelling into those five wetlands that do normally receive groundwater inflow. The effects of this change, a loss of 3% of the inflow, will be so small that it cannot be measured in the field. This reduction in upwelling occurs in the springtime when the wetlands are already relatively wet, further minimizing the hydrologic effects.

From a water supply perspective, the South Extension is optimally located, as it is in an area with up to 22 m of available drawdown in the Amabel Aquifer. The excavation is also relatively distant and isolated from private wells along Cedar Springs Road, Sideroad 1 and Guelph Line, so it is unlikely to impact those wells.

Existing private water supply wells generally draw from the middle to lower portions of the Amabel, with a few tapping into the deep fracture zone at base of Amabel. There is extensive additional available drawdown for all wells, should they require increased supply, as they could be extended the full depth and into the lower Amabel fracture zone.

West Extension Effects

The 2.0 m drawdown cone associated with the West Extension extends up to 500 m from the excavation in the middle Amabel aquifer. The West Extension is next to a locally significant groundwater discharge area, so water levels are less subject to drought and seasonal fluctuations. The proximity to the discharge area helps to mitigate the local effects of the excavation.

There are two perched wetlands in the immediate vicinity of the West Extension. Neither of these receive groundwater inflows, so lowering the water table will not affect their hydrogeologic interactions and function.

The Medad Valley is a locally significant groundwater discharge area that receives the majority of the groundwater that flows in and around the existing and proposed quarry. The development of the West Extension will shift some of the groundwater discharge to the north, through the North Discharge pond, but ultimately all of this discharge simply enters the Medad Valley in a similar manner to the current discharge.

The central ditch and pond system in the existing golf course extraction area will be removed during excavation. This system is currently supplied by the diversion of discharge from the existing quarry. To help preserve the current groundwater and surface water flow conditions created by this ditch and pond system, a new infiltration pond will be constructed between the West Extension and Cedar Springs Road.

The private wells in the vicinity of the West Extension will see a decline of approximately 2 m in available drawdown, however the majority of the wells have between 10 and 16 m of Amabel Aquifer drawdown after excavation, so deepening a well is a viable mitigation measure. Near the intersection of Colling Road and Cedar Springs Road there are a few wells that will have between 5 and 10 m of available drawdown, however these are in a significant discharge area so it is likely that there will be sufficient flow to meet their private supply needs.

Rehabilitation and Closure

Two rehabilitation options were evaluated. Under both scenarios the South Extension will be allowed to re-fill and become a natural lake. This lake will return groundwater water levels to current conditions, with some minor flattening of the water table around the lake. Surface water interactions and private well levels will return to current conditions.

Under Rehabilitation Scenario 1, the main quarry and West Extension will be rehabilitated, including regrading and consolidation of the quarry lakes. The overall hydrogeologic and hydrologic conditions will be similar to the final excavation phase, with some recovery in water levels due to the consolidation of the quarry lakes.

Under Rehabilitation Scenario 2, the quarry floor will be regraded, pumping will cease, and the entire quarry will be allowed to fill to become a single large lake. Groundwater levels will rise, except near the stream segments that currently carry the discharge, where they will fall due to the reduction in stream leakage. Under this scenario, quarry discharge to a tributary of Willoughby Creek north of Colling Road and to the upstream end of the West Arm of the West Branch of Mount Nemo Creek will cease causing long-term impacts to downstream fish habitat compared to the existing approved post-extraction water management plan (See Savanta, 2020 and Tatham, 2020 for details).

Conclusions

This Level 2 ARA Impact Assessment presents a detailed comparative evaluation of the effects of the proposed extension of the Nelson Burlington Quarry. The existing (baseline) site conditions are fully characterized and the numerical model closely replicates the observed surface water and groundwater processes and water budget. The predicted effects of the South and West Extension have been systematically evaluated on a daily basis across a range of seasonal and inter-annual (wet and dry year) climate conditions. The predicted effects on groundwater levels are consistent with the existing quarry, and significant available groundwater resources remain through the development and closure phases. The streams and wetlands in the study area are relatively isolated from the predicted changes in the groundwater system by the low permeability Halton Till, and no measurable change will occur in the nearby wetland water budgets.

At the subwatershed scale, the proposed extension will not change the overall surface water and groundwater flow system. There will be no cross-watershed impacts, groundwater recharge rates will be preserved, and groundwater and surface water in and around the quarry will continue to flow toward the Medad Valley. The quality and quantity of groundwater needed for the natural environment and wells will be protected, and no municipal wellhead protection areas will be impacted.

Rehabilitation Scenario 1 will preserve the current surface water conditions, where quarry discharge has provided fish habitat for both the tributary of Willoughby Creek north of Colling Road and to the upstream end of the West Arm of the West Branch of Mount Nemo Creek (See Savanta, 2020 and Tatham, 2020 for details). Rehabilitation Scenario 2 would result in adverse impacts to the surface water system compared to baseline conditions. A comprehensive monitoring and response plan has been developed based on the statistical percentile methodology as defined in the Ontario Low Water

Response Program. The additional available groundwater resources have been quantified, and a well mitigation program has been proposed.

1 Introduction

1.1 Objectives

Nelson Aggregates Co. (Nelson) operates the Burlington Quarry near the intersection of Side Road 2 and Guelph Line, in the City of Burlington, Region of Halton (Figure 1.1). The quarry is 218.7 hectares (ha) in size and is located on the watershed divide between Bronte Creek and Grindstone Creek near Mount Nemo. The quarry has been in existence since 1953 and has been operated by Nelson since 1983. The primary source of aggregate is the Amabel Formation dolostone, which is a provincially-significant aggregate resource.

Nelson owns additional lands adjacent to the southeast and southwest sides of the existing quarry and proposes to extend quarrying operations into these areas (Figure 1.2). Please note that in this report, the proposed southeast extension lands are referred to as the "South Lands" and the proposed southwest extension lands are referred to as the "West Lands". The proposed extension in the South Lands covers approximately 18 hectares (ha) (with 14.5 ha of extraction) and the West Lands extension covers approximately 60 ha (with 35.7 ha of extraction).

This investigation is being conducted in support of applications under the Aggregate Resources Act (ARA), the Planning Act, and the Niagara Escarpment Planning and Development Act. The Application is for a Category 2 - Class “A” Quarry below Water. The purpose of this investigation is to meet the requirements of the Ontario Ministry of Natural Resources and Forestry (MNRF) Level 1/Level 2 Hydrogeological Investigation. This includes:

- Field characterization of the current hydrogeologic conditions at the quarry site; (Please note that current and previous field investigation are discussed further on.)
- Quantitative evaluation of the current hydrogeologic and hydrologic conditions through the development of an integrated groundwater/surface water model of the site and extension areas; (Feld investigations and additional hydrologic analyses conducted by Tatham Engineering are discussed further on.)
- Simulation and analysis of the likely changes to groundwater and surface water flows and levels under different phases of the proposed quarry extension and closure;
- Simulation and evaluation of measures to minimize the effects of quarry extension on nearby private wells;
- Simulation of site conditions under a range of climate conditions (including recent drought and wet years) to identify monitoring threshold levels based on the same technical approach used in the Ontario Low Water Response program;
- Quantitative evaluation of the hydrologic and hydrogeologic water budget under current and future extension and rehabilitation scenarios. This includes simulation of all quarry inflows and outflows, and detailed, feature-based wetland water budgets that quantify surface water and groundwater interactions.

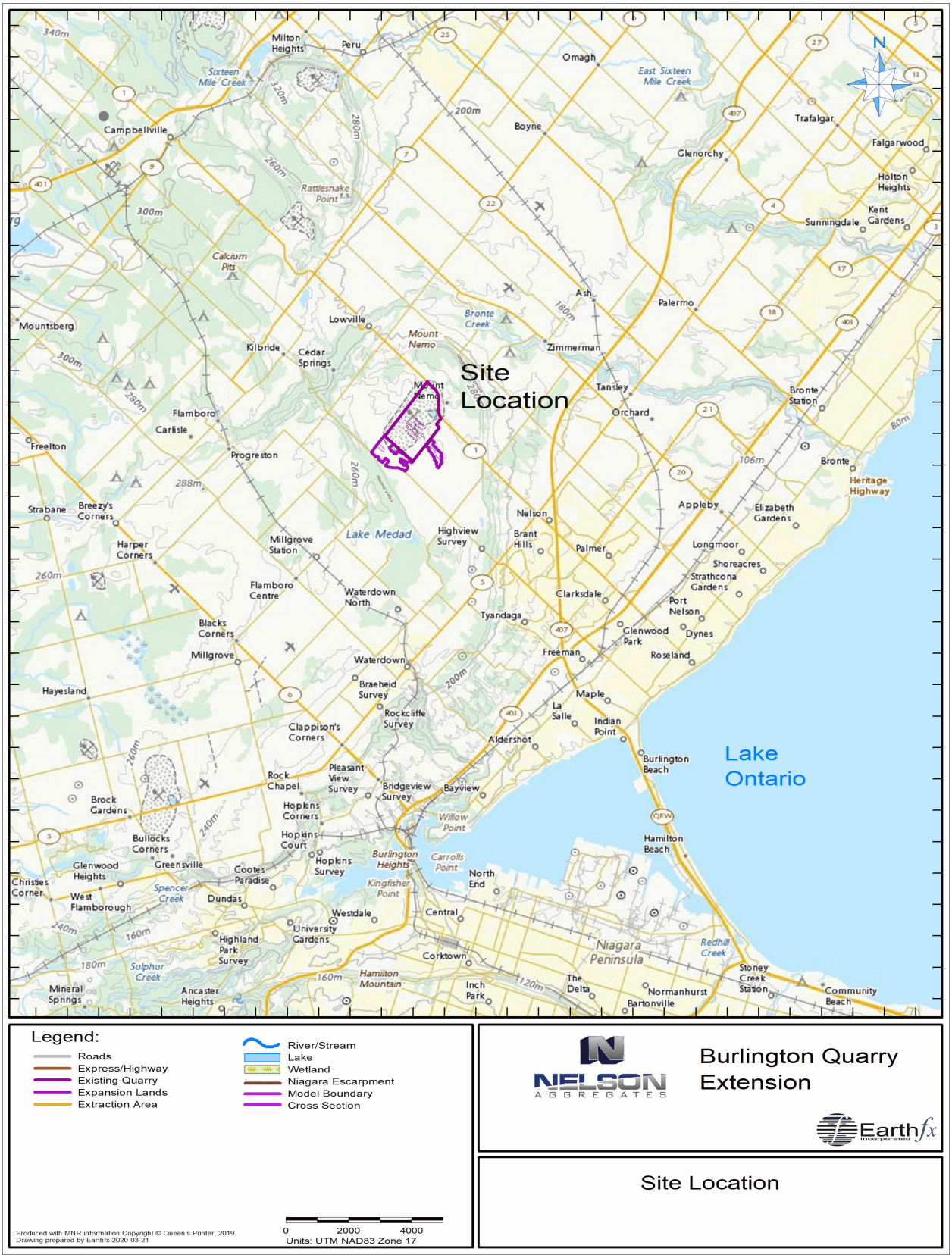

Figure 1.1: Site location.

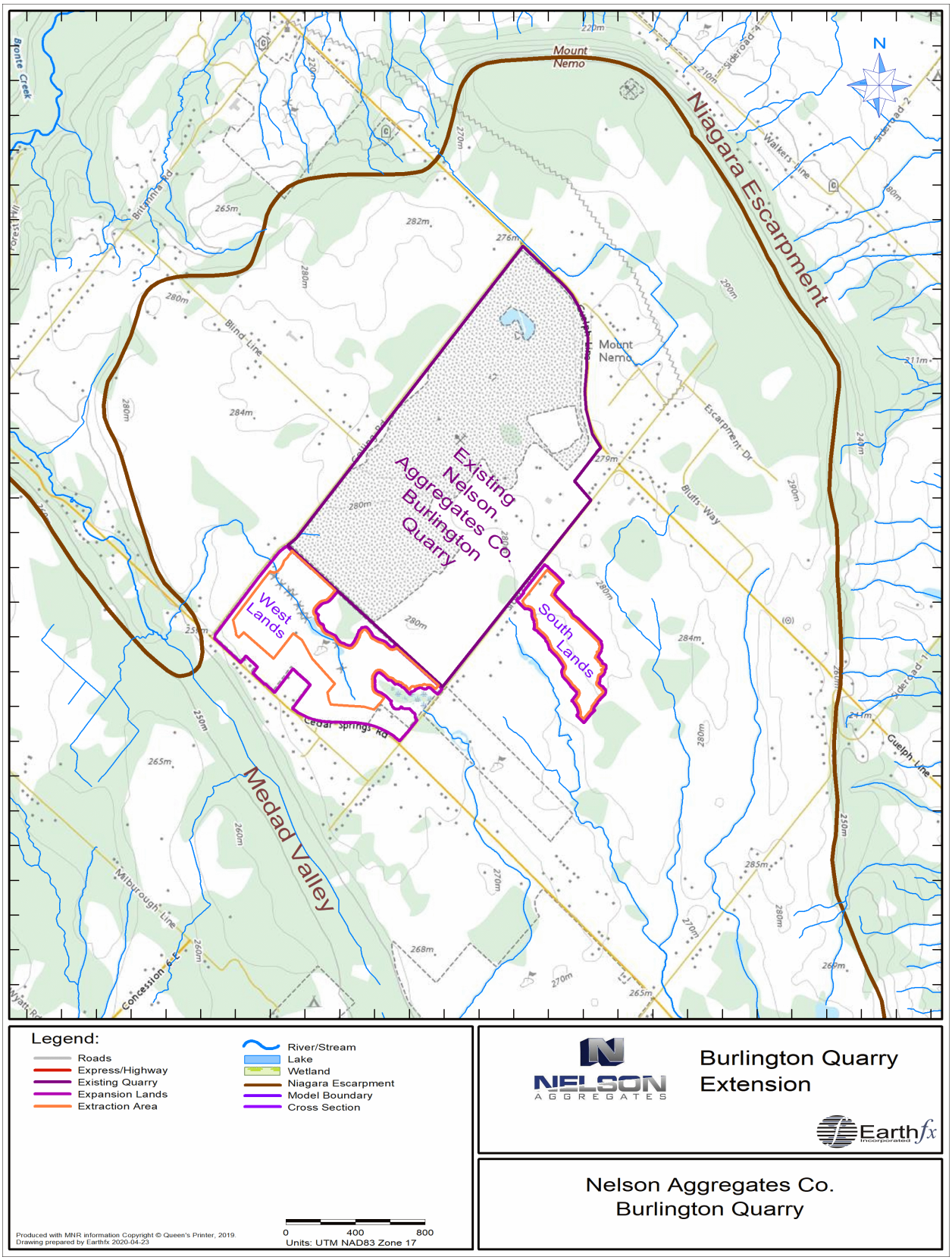

Figure 1.2: Burlington Quarry showing South and West extension areas.

1.2 Study Approach

The study approach is based on the use of an integrated surface water and groundwater model to evaluate all water resources issues in a comprehensive and consistent manner. This approach addresses the entire hydrologic cycle, with 100% water budget accounting. Measured precipitation rates are added to the top of the model, and the model is evaluated against observed streamflow and quarry water management records.

A key aspect of this integrated model approach is that it evaluates the effects of the quarry extension on continuous multi-year basis, spanning a range of climate conditions. This is a significant improvement over a simple comparison of average before and after conditions. In this study, the effects of development are compared on a daily basis across both wet years and dry years. The effects of surface water and groundwater storage, including wetlands, ponds, aquifer storage, quarry water management and even snowpack and snowmelt are fully quantified.

The Adaptive Management Plan thresholds and mitigation (supplied under separate cover) are also based on simulations of future development under a range of inter-annual climate conditions, including drought. The selection of the threshold levels is based on the same statistical percentile methodology as defined for the Ontario Low Water Response Program. The model has also been used to evaluate future total available drawdown, so the potential for mitigation (for example, deepening of wells) is clearly addressed.

As well, the numerical modelling approach used in this study is the identical to that introduced by Earthfx Inc. for recent Tier 3 Source Water Protection (SWP) studies in Hamilton and Halton Region. The Tier 3 studies represent the highest level of provincial water budget analysis and risk assessment, and this study meets (or exceeds) that level of analysis.

1.3 Level 1/Level 2 Study Components and Methodology

This Level 1 and 2 Hydrogeological and Hydrological Impact Assessment Report has been undertaken in accordance with the requirements of the Aggregate Resources Act, 1997. In addition, this hydrogeological assessment has been completed in accordance with the Terms of Reference for the Level 1 and 2 Hydrogeological and Hydrologic Impact Assessment of the Proposed Burlington Quarry Extension (February 2020). The Terms of Reference were prepared in consultation with Halton Region and Halton Conservation following the Halton Region Aggregate Resources Reference Manual.

The following is an overview of the studies and companion documents to this report that together meet this requirement.

1.3.1 Field Investigations

Data Compilation: An extensive program of field investigations and monitoring was initiated at this site in 2003. This included field drilling, aquifer testing, and long-term water level and streamflow monitoring programs. This information was compiled into a comprehensive database and in integrated throughout this report. A more detailed overview of previous field investigations is described in Section 3.3.1.

Hydrogeologic Field Data Collection: In 2018 and 2019, Azimuth Environmental Consulting, Inc. (Azimuth Environmental) and Worthington Groundwater conducted the following field investigations:

- Borehole drilling, geophysical and televiewer logging program
- Aquifer testing:
    - Pumping tests
    - Borehole packer test program
    - Borehole flowmeter logging program
- Groundwater monitor installation and continuous water level monitoring
- Groundwater quality and surface water quality testing
- Aerial drone elevation survey
- Private well survey
- Karst investigation (Worthington)

The results of these investigations are documented in Appendix A and B of this report and integrated into the site database. Additional details can be made available on request.

Surface Water Field Data Collection: In 2018 and 2019, Tatham Engineering conducted the following field investigations:

- Wetland Water Level Monitoring
- Surface Water Flow Measurements
- Surface Water Quality Testing
- Geodetic Level and Pond Bathymetry Survey

All of the above-noted field measurements have been compiled into the site database. Key findings and insights informed the development and calibration of the integrated surface water/groundwater model and were used throughout this groundwater assessment report. In addition, the integrated model results were provided to Tatham Engineering for the preparation of the surface water assessment. The details of the surface water data collection and the surface water assessment are documented in a companion report by Tatham Engineering (2020).

1.3.2 Site Characterization and Baseline Conditions Analysis

Sections 3 through 5 of this report present a description of the physical setting, including local geology, hydrogeology, and surface water features in and around the site, as per the MNRF guidelines. Additional interpretation of the surface water resources and quarry water management are included in the Tatham Engineering companion report.

An integrated surface water/ groundwater model was developed as part of a comprehensive evaluation of site conditions. An overview of the development and calibration of the model is described in Section 6. The calibration includes a detailed assessment of the effects of the quarry face advancement over the 2003 to 2012 time period, as observed in the monitoring data. More complete descriptions regarding the model construction and calibration are included in Appendix C, D, and E.

Section 7 of the report presents a numerical simulation of the current or “Baseline” conditions at the site. A continuous transient (time-dependent) assessment is presented, illustrating how the surface water and groundwater systems behave on a daily basis over the last 10 years. Included in this assessment time period is a severe Provincial Low Water Response Level 2 drought (2016), and an above-average wet year (2017). This baseline provides a realistic long-term frame of reference for comparison and assessment of the proposed quarry extension and rehabilitation phases.

The baseline assessment provides:

- Daily groundwater levels and groundwater flows under a range of climate conditions;
- Daily surface water flows and levels under a range of climate conditions;
- Comprehensive quarry and wetland water budgets.

Model results were aggregated over time to assess monthly, annual, average month, and long-term average response. Results were also aggregated spatially to conduct feature-based water budgets around wetlands and other surface water features.

1.3.3 Level 2 Development Impact Assessment and Mitigation Measures

The Level 2 impact assessment is included in Section 8 of this report. Each of the major development phases of quarry extension and rehabilitation is simulated and compared to the baseline flows and levels on a daily basis using the same 10-year climate inputs. In this way, the results of future scenarios can be directly compared to baseline conditions and thereby provide significant insight into the effects of the proposed development on a daily, seasonal, and inter-annual basis and over a range of climatic conditions (e.g., drought and wet years).

The integrated model provides daily results across the entire study area. To simplify the analysis and presentation of results, the transient response was also compared at key surface water and groundwater locations in and around the proposed quarry extension. The beneficial effects of replicating an existing irrigation channel and pond on the West Lands (infiltration pond) were also evaluated across a range of climate conditions. As well, detailed water budgets were prepared for key wetlands, ponds, and streams for each scenario and compared to baseline conditions.

1.3.4 Stream, Wetland, Pond and Lake Model Representations

The graphical presentation and use of the term “ditches”, “wetlands”, “ponds”, “lakes”, “rivers” and “streams” on figures and in the text of this report refers to features that are represented in the numerical model. These terms do not imply that the feature is considered an officially classified hydrologic feature by the regulatory agencies (including MNRF). For example, in some figure presented below, stream segments (blue lines) are shown on the maps to represent streams, roadside ditches and surface drainage swales in the model. These lines represent overland runoff drainage pathways mapped from the digital elevation model (DEM), but they may not correspond to MNRF mapped (and classified) streams. The MNRF does not classify roadside ditches, for example.

Similarly, there are model representations and discussions of dugouts, wetlands, ponds and lakes that represent depressions in the DEM, but they may not correspond to a MNRF mapped wetland or water body. For example, the golf course ditches and ponds are simulated but not considered key hydrologic features or key natural heritage features.

Another example is the numerical model representation of subsurface karst conduits. The Karst Study (Appendix B) identified disappearing streams in the study area. The subsurface portion of the stream conduit is, in some figures, illustrated as a blue line, but that does not imply that the feature exists on surface and is a MNRF classified stream. In these cases, the model is representing the routing of water through a leaky subsurface conduit.

1.3.5 Surface Water Effects Analysis, Water Management, and Water Budgets

The results of the integrated model have been shared and integrated into the surface water effects analysis completed by Tatham Engineering (Tatham Engineering, 2020) and provided under separate cover. Of particular interest was the estimated groundwater seepage, if any, into the quarry and wetland areas as well as groundwater flow across sub-catchment boundaries under current and future conditions.

1.3.6 Adaptive Management Plan (AMP)

The long-term transient simulations were used to aid in identifying groundwater threshold levels for the Adaptive Management Plan (AMP). The AMP is provided in a separate report. The statistical methodology for identifying the AMP threshold levels is based on that used for the Ontario Low Water Response Program.

A numerical simulation of the proposed quarry extension and rehabilitation was conducted under a range of climate conditions, including the 2016 Level 2 drought. Daily model results were post-processed to determine statistical values (percentiles) to assign as groundwater threshold levels for contingency planning. This approach provided significant insight and confidence in the future management of the site because it provided a better understanding of the range of response likely to be observed in the different phases of the quarry extension and rehabilitation and under variable climate conditions.

The numerical model was also used to identify the available drawdown in the aquifer under baseline and future conditions. Results indicated that groundwater resources would remain sustainable under these conditions, as discussed further on in this report.

1.3.7 Level 1/Level 2 Methodology Summary

This report, the companion documents, the integrated model, and the detailed field investigations and analyses represent an exceptionally comprehensive assessment of the proposed development. The same methodology as used for advanced Tier 3 Source Water Protection Water Budgets and Risk Assessment studies was employed for the model development. An extensive long-term, monitoring record was assessed as part of the baseline analyses. Surface water and groundwater flow and groundwater/surface water interaction were evaluated in a fully quantitative and integrated manner under a wide range of climate conditions. Results of the modelling analyses were used to quantitatively assess the likely effects of future quarry extension and rehabilitation.

1.4 Study Area Extents

This investigation centered on the existing Burlington Quarry and the area surrounding the South and West extension lands. To fully assess the effects of quarry extension and rehabilitation, the numerical model developed for this study extended outward to natural hydrologic and hydrogeologic boundaries. Figure 1.3 shows the areal extent of the integrated surface water/groundwater model. Information on geology, hydrology, and hydrogeology were compiled and analyzed for this extended region to develop a conceptual understanding of the study area. Some data sets, such as climate information and geologic data from nearby quarries were also collected, on an as-needed basis, from beyond the study area extents.

1.4.1 Model Extraction Area Extents

The final proposed extraction area in the West Lands Extension is shown with an orange line in Figure 1.2. After completion of the numerical simulations presented in this report, the decision was to remove the western-most corner of the Phase 5 extraction area. This reduced the extraction area by 0.2 ha (from 35.9 ha down to 35.7 ha). The model simulations presented in this report reflect that slightly larger extraction area, and thus over-estimate, by a very small amount, the effects of extraction in that area. The overall effect on the surface and groundwater analysis is insignificant.

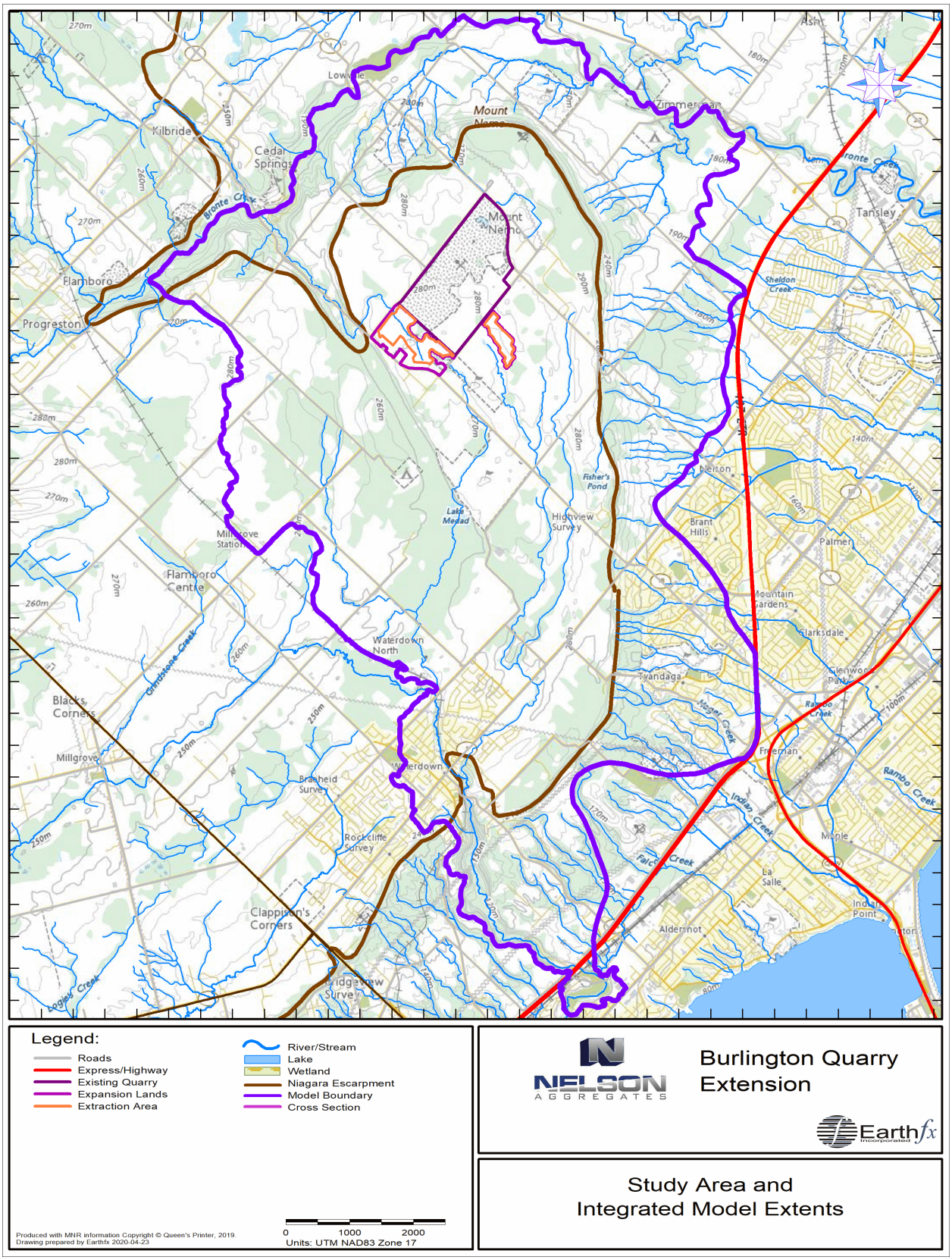

Figure 1.3: Study area and integrated model extents.

2 Background

2.1 Previous Studies

Golder Associates Limited (Golder) conducted extensive hydrologic and hydrogeologic investigations in support of a previously proposed south quarry extension (Golder, 2004). The previously proposed south extension, at 75 ha, was more than four times larger than the South Lands extension proposed at this time (18 ha). The Golder investigation included aquifer testing; installation of monitoring wells; installation of surface water flow and stage measuring points; and the development of a steady-state groundwater model. The investigation was conducted in 2003 and 2004 and is documented in Golder (2004). Additional hydrogeologic field studies of wetland/groundwater interaction were conducted in 2006 (Golder, 2006). Other Golder studies include an assessment of water budgets for individual wetlands in the south extension area (Golder, 2007a); a study of the shallow overburden (Golder, 2007b); and an update of the 2004 groundwater modelling analyses (Golder, 2008).

Additional investigations were conducted regarding the presence of karst features in the quarry vicinity (Worthington Groundwater, 2006). This study examined the walls of the existing quarry, surveyed karst features within and nearby the south extension lands, surveyed springs within the Medad Valley (located southwest of the existing quarry), and conducted tracer tests at wells and sinking streams.

The extensive data collected during and since these investigations have been fully incorporated into this assessment. Data has been collected over time at key locations in the Golder monitoring network since 2006, and new data were collected for this assessment to confirm the results and patterns that were observed in the earlier Golder studies.

2.2 Long Term Monitoring Network

Local monitoring data and site characterization information collected for the Golder studies, as well as ongoing monitoring data, were obtained from Nelson and compiled into a relational database for this study. Other regional data, including climate data, streamflow data, water well information, topographic mapping, and geologic mapping, were obtained from sources including Environment Canada, the Ontario Ministry of Conservation and Parks (MECP), other provincial agencies, Halton Region, and Conservation Halton.

All historical data have been compiled, including the capture of all spreadsheets and databases provided; data were also transcribed from older paper reports. All regional and site information was compiled, including geologic descriptions, well construction logs, transient water levels, streamflow measurements, and quarry discharges (both manual and data logger readings) into a comprehensive site database. A map showing the extent of the groundwater monitoring network is provided in Figure 2.1. A map showing the extent of surface water monitoring network is provided in Figure 2.2.

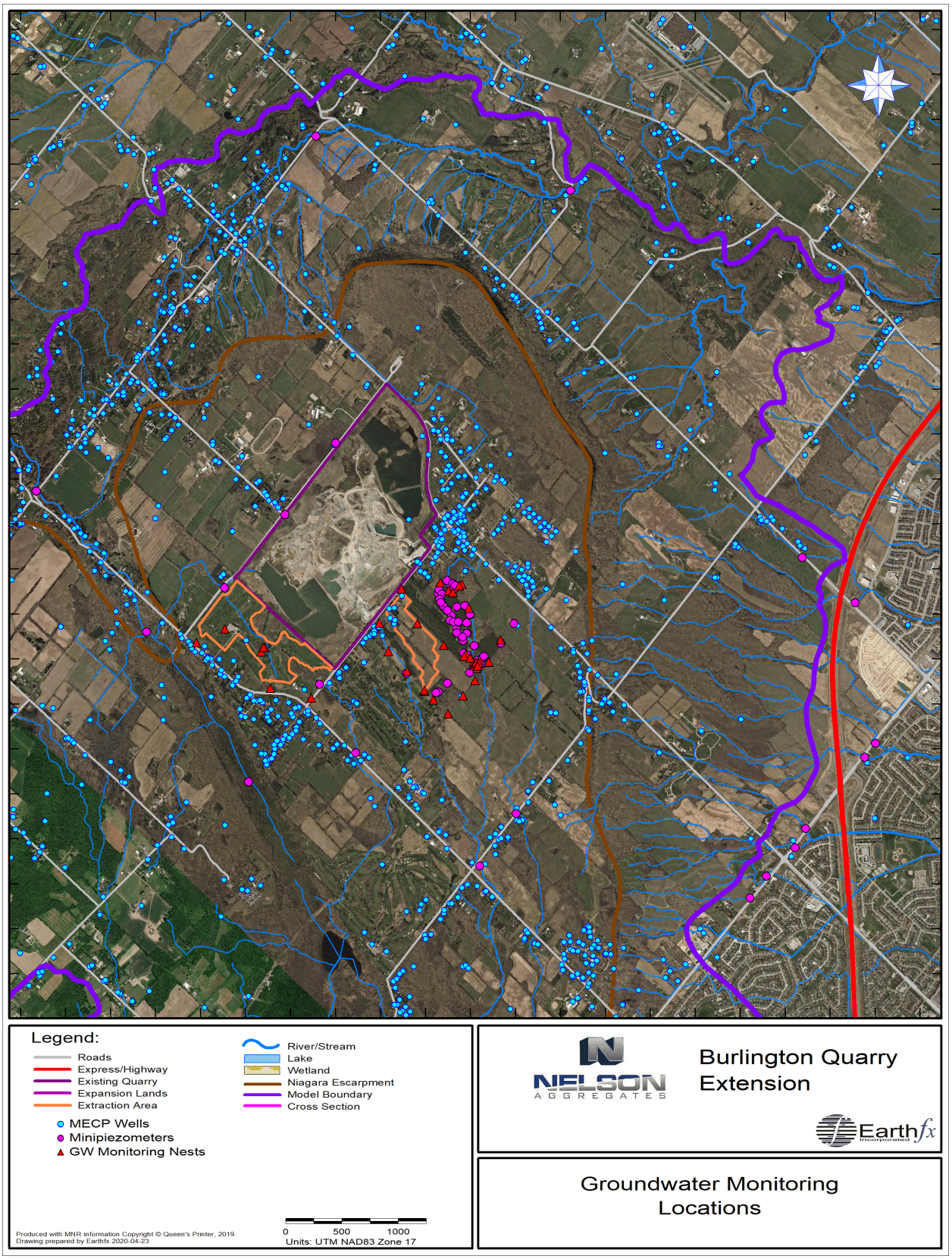

Figure 2.1: Groundwater monitoring locations.

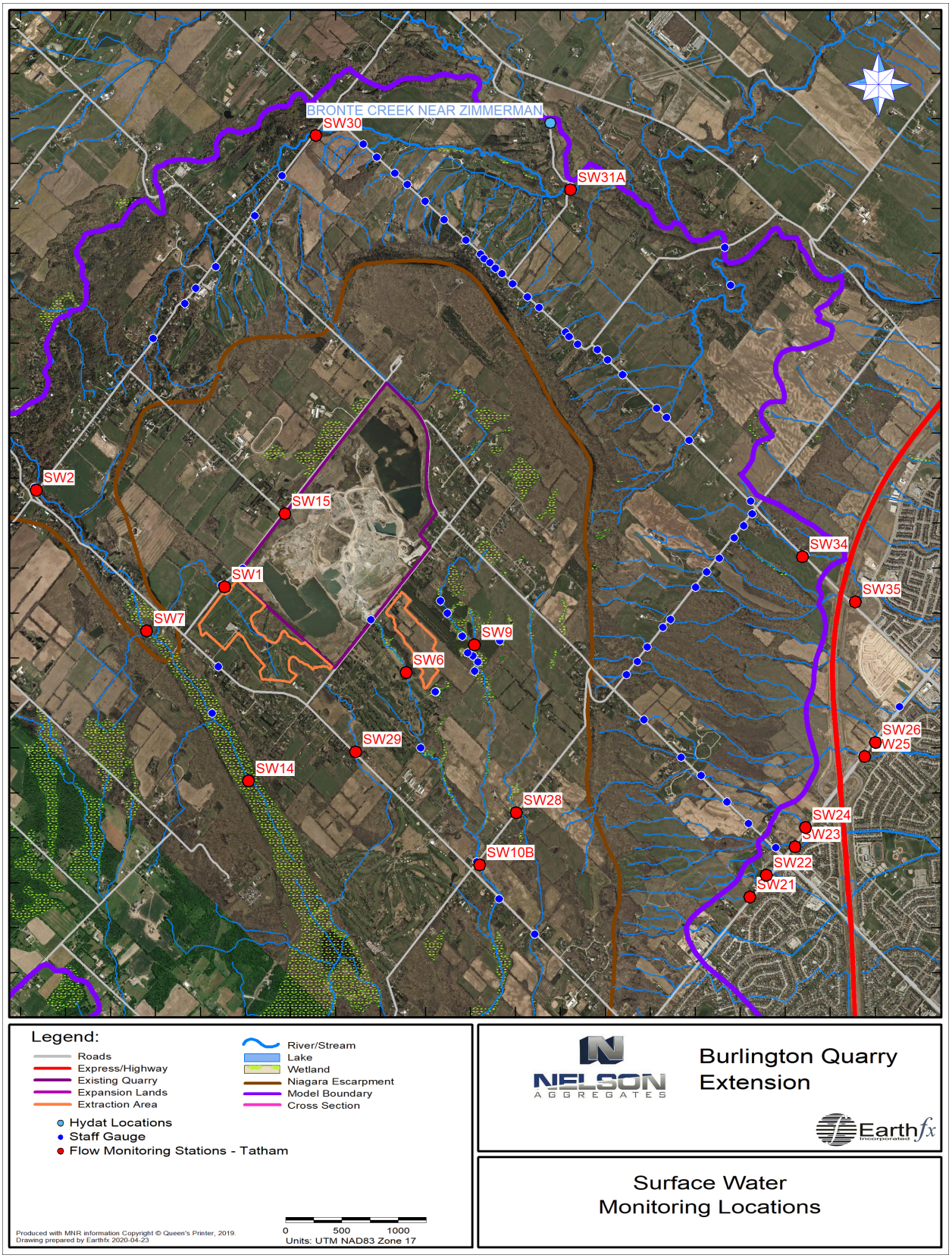

Figure 2.2: Surface water monitoring locations.

2.3 Background Analysis and Updates

The analyses undertaken in this assessment build on the previous work and long-term monitoring data. This study significantly updates and improves on the earlier analyses. Some of these improvements include:

- The study area and model have been enlarged to fully assess the Medad Valley and all tributaries that flow off the Niagara Escarpment;
- New packer test measurements and downhole borehole televiewer logs have been collected to assess the in-situ rock mass and fracture distribution;
- The groundwater-only model has been upgraded to a fully-integrated surface water/groundwater model that simulates the entire hydrologic and hydrogeologic flow system on a daily basis. All geologic layers, streams, wetlands, quarry lakes, and ponds are fully represented in the model.
- The numerical analysis has been upgraded from a steady-state (average conditions) simulations to a fully transient assessment of daily, seasonal, and inter-annual (wet year/dry year) groundwater and surface water conditions.
- Vertical fractures and karst features have been represented in the model.
- The assessment of effects has been expanded from a comparison of average before-and-after conditions to a detailed daily assessment of system behavior under a range of observed climate conditions. The effects of surface and groundwater storage, wet year, and drought year conditions are fully evaluated.
- The integrated model has been used to assess changes in the surface and groundwater water budget of the quarry and surrounding wetlands and ponds.

2.4 Integrated Modelling Studies

The application of integrated models to the analysis of quarry effects is relatively new. Earthfx pioneered the use of integrated models for Source Water Protections studies at the Tier 3 Water Budget and Risk Assessment level. Earthfx conducted Tier 3 studies in the similar geologic settings Region of Halton for the Kelso and Campbellville municipal wellfields (Earthfx, 2012, 2014a,) and for the Greensville Municipal Well in Hamilton (Earthfx, 2014b, 2017). Both studies involved large active quarries adjacent to the Niagara Escarpment, and the effects of future quarry extension and rehabilitation on nearby wellfields, streams, and wetlands were represented in the modelling assessments. A follow-up study (Earthfx, 2016) involved the application of the Greensville Tier 3 model to review a Level 1/Level 2 Hydrogeology and Hydrology Technical Report for a proposed quarry extension. Experience gained in these studies was directly transferrable to the current investigation.

3 Physical Setting

3.1 Topography

Land surface topography for the study area is shown in Figure 3.1. The topographic mapping used for this study was created by merging the 5-m digital elevation model (DEM) produced by the MNRF as part of the Southwest and South-Central Ontario Orthophotography Projects (SWOOP and SCOOP). Within the quarry area, 1-m cell high-resolution elevation data were collected by aerial drone; additional pond bathymetry data were also collected (Figure 3.2). Maximum elevations of about 298 metres above sea level (masl) occur in the Mount Nemo Conservation Area in the northeast part of the study area. Minimum elevations in the study area are about 80 masl occurring along Grindstone Creek in Burlington.

The quarry area is generally flat; gently rising from the southwest towards the crest of the Niagara Escarpment. Local relief is supplied mainly by ridges forming the Waterdown Moraine. Significant changes in elevations occur at the Niagara Escarpment to the northeast and east of the quarry; the steepest changes occur at of Mount Nemo where there are roughly 125 metres (m) of local relief. Elevations decrease less rapidly at the Niagara Escarpment northwest and southeast of the quarry and at the Medad Valley southwest of the quarry. Elevations rise again west of the Medad Valley approaching the topographic divide formed by another ridge of the Waterdown Moraine.

3.2 Physiography

The study area includes parts of four physiographic regions, as described by Chapman and Putnam (1984). The bulk of the study area lies within the Niagara Escarpment or Norfolk sand plain physiographic regions, while the northern and southern extremes of the study area touch on the South slope and the Iroquois plain (Figure 3.3). The Niagara Escarpment is the well-recognized bedrock cuesta that traverses southern Ontario from the Niagara River to Manitoulin Island. Numerous headwaters streams drain the base of the Niagara Escarpment and flow towards Bronte Creek in the north, Grindstone Creek to the south, or eastward to streams that discharge directly to Lake Ontario.

The Norfolk sand plain generally has low relief and is characterized by a layer of fine lacustrine sand overlying or flanking drumlins and till moraines. The latter includes the Waterdown Moraines, a group of seven moraine ridges that parallel the edge of the Niagara Escarpment from north of Dundas to Mount Nemo (Karrow, 1963). The older, western moraines are generally smoother and are mostly covered with sand from glacial lakes ponded ahead of the younger (eastern) ridges. The narrow ridges are mostly composed of silty Halton Till. The Medad Valley is also found in this physiographic region, and is a partly-buried gorge that carried meltwater from the receding ice for a period of time (Karrow, 1987).

The South slope, which lies below the Niagara Escarpment, extends from the southern slope of the Oak Ridges Moraine towards Lake Ontario. Locally, the Trafalgar Moraine separates a fluted till plain to the south from a beveled till plain to the north. The beveled till plain is covered by thin sands and varved clays. The Trafalgar Moraine is a younger moraine, also composed of Halton Till, that rests on a bedrock ridge. The sandy Iroquois plain, below the Niagara Escarpment, is a plain of gravel and lacustrine sand deposits left by Glacial Lake Iroquois.

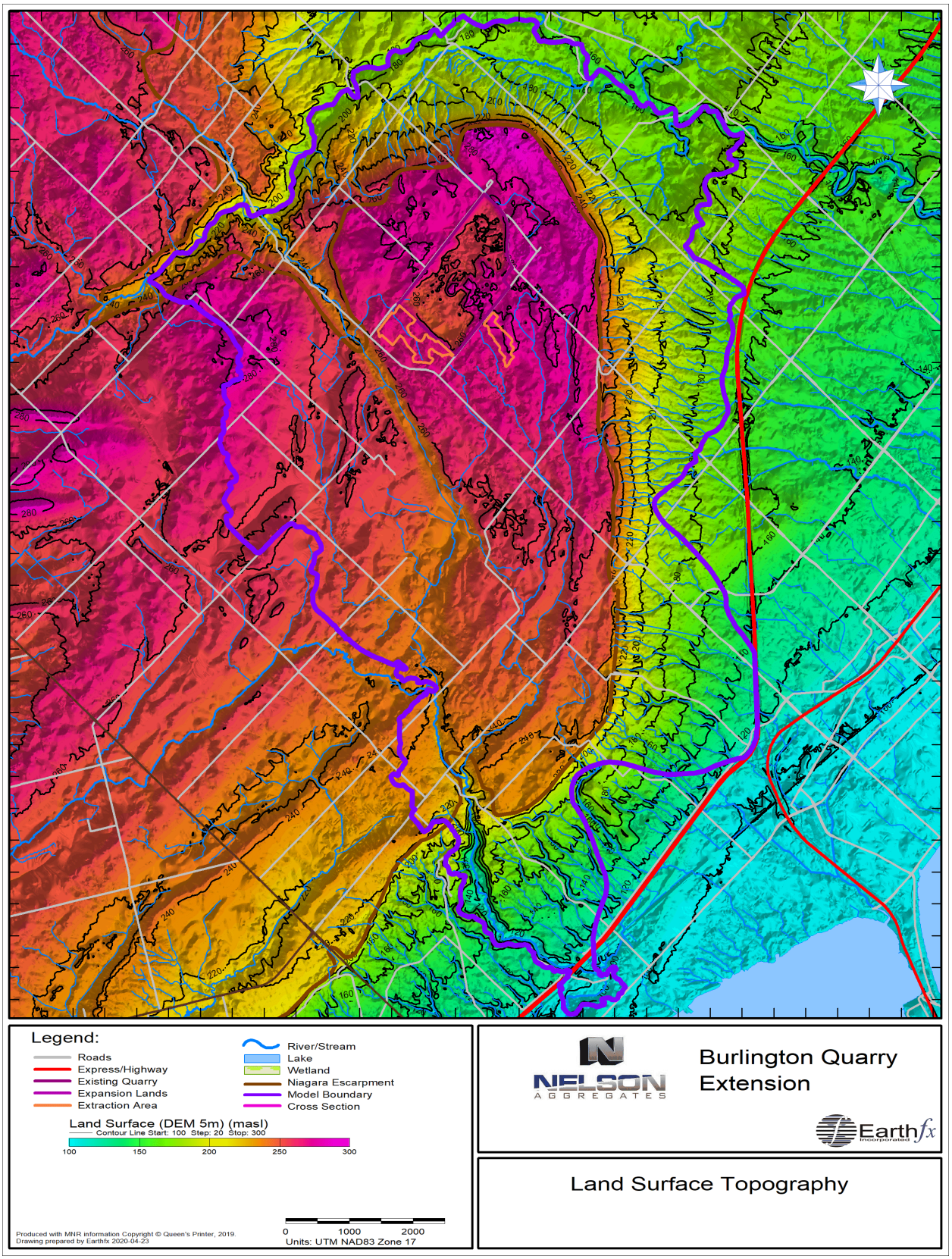

Figure 3.1: Land surface topography from the 5-m digital elevation model.

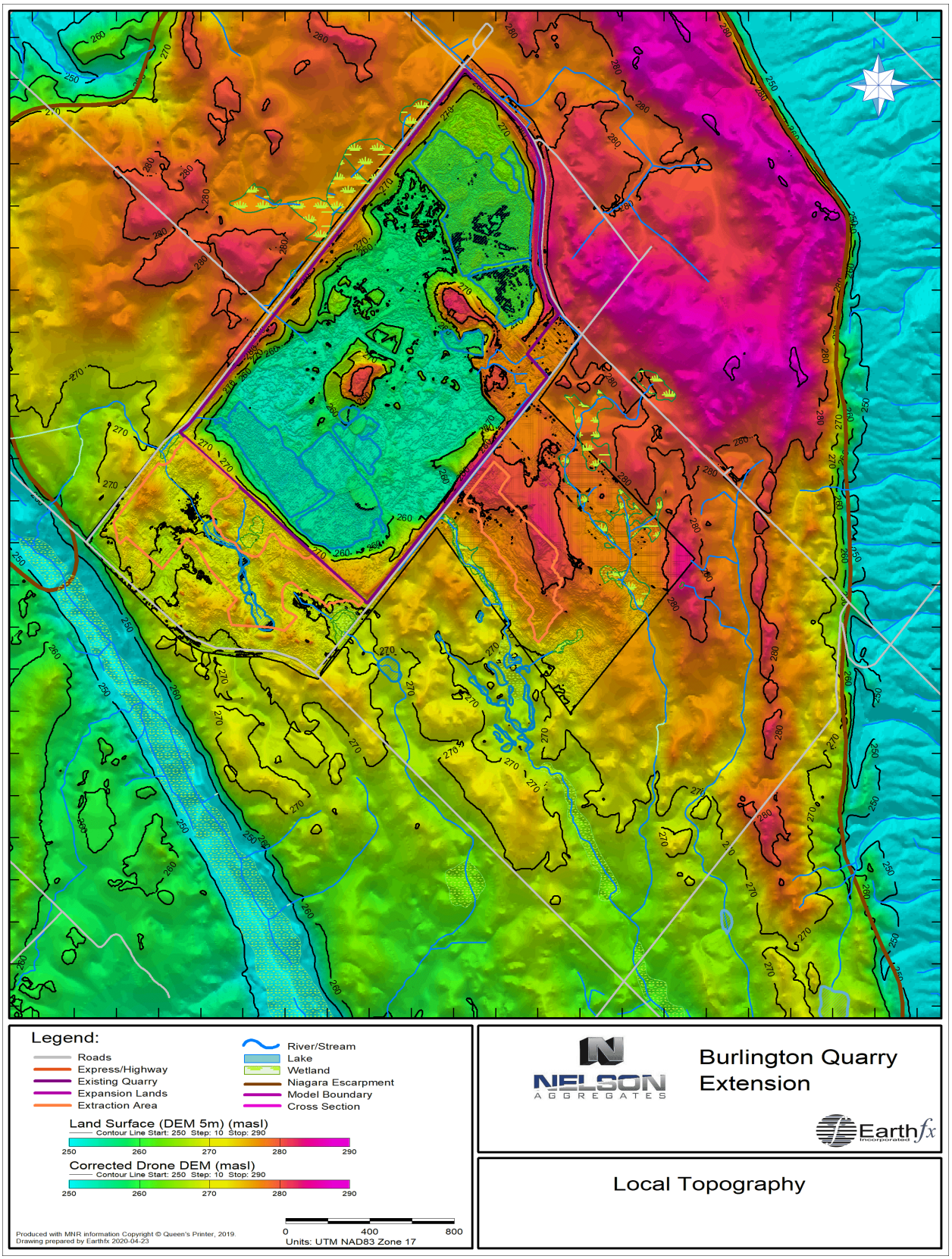

Figure 3.2: Local topography in the vicinity of the Burlington Quarry.

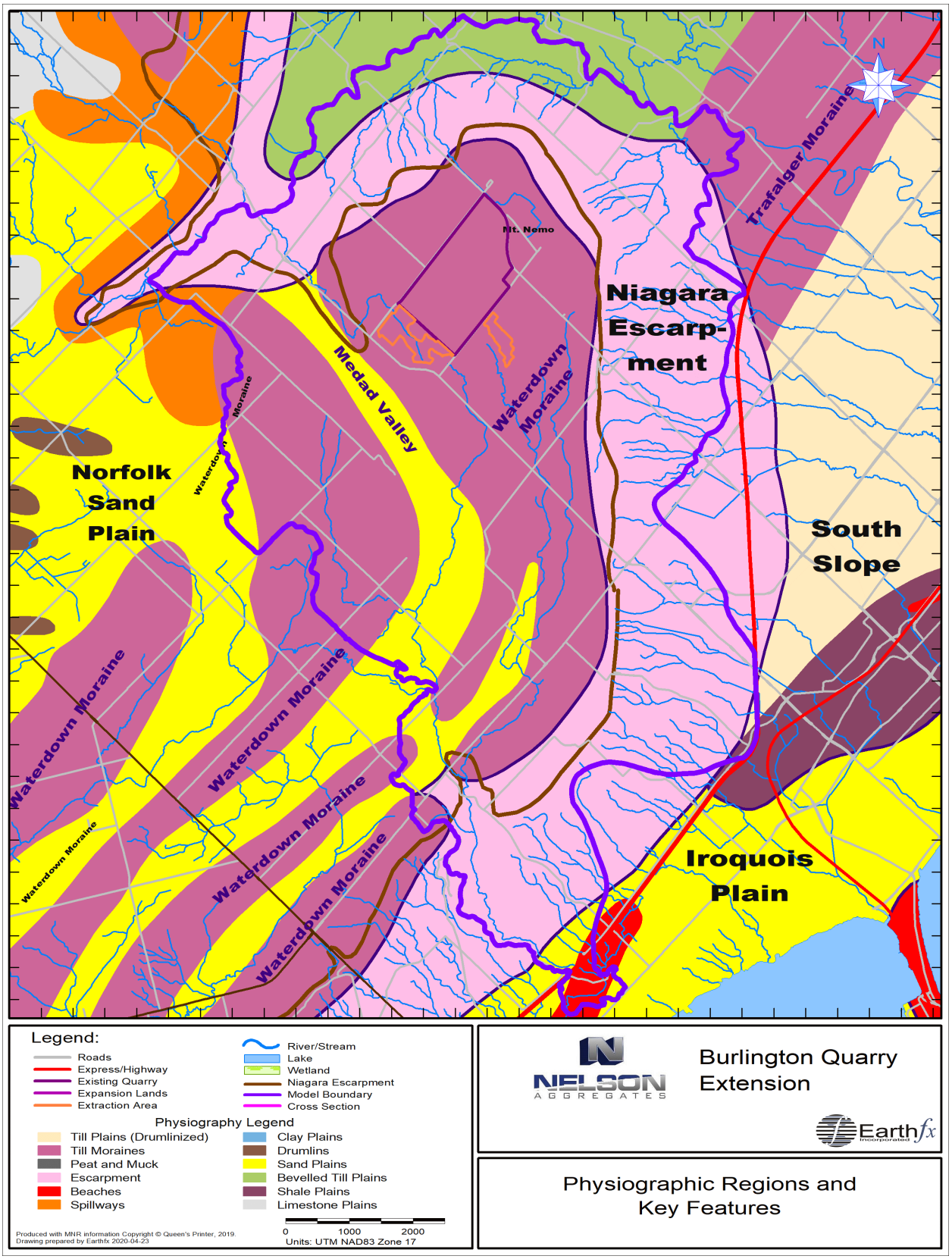

Figure 3.3: Physiographic units and features (from Chapman and Putnam, 2007).

3.3 Drilling and Field Investigation Program Overview

The geologic and hydrogeologic conditions described in the following sections of this report were developed from two extensive drilling and monitoring programs spanning the time period of 2003 to 2019. The Golder (2004) investigations described conditions in the South Extension area. Subsequent monitoring in this area has provided extremely useful insight into the long-term behaviour of the groundwater and surface water systems under a range of quarry development and climatic conditions.

In 2018, new groundwater and surface water field investigations were begun by Azimuth Environmental and Tatham Engineering. These investigations updated and expanded the monitoring in the South Extension area and evaluated conditions in the West Extension area. In addition, an investigation of the karst conditions in the study area was completed by Worthington Groundwater in 2006. An update of that investigation was completed in 2019.

The following is a summary of these extensive field investigation programs. Additional details are included in the Appendices.

3.3.1 Golder 2004 Drilling and Monitoring Program

An extensive borehole drilling and monitoring well installation program was undertaken as part of the Golder (2004) assessment. Golder summarized the program as follows (Golder, 2004, p. 5):

- Eight cored drillholes to provide for a detailed characterization of the limestone bedrock of the Amabel Formation which will be quarried in the proposed extension;
- A total of 70 packer tests were conducted in the open cored drillholes to develop an estimate of the hydraulic conductivity at discrete intervals of the rock;
- A geophysical survey using electrical resistivity imaging (ERI) techniques to assess the possible presence of voids or karst conditions in the bedrock around the perimeter of the proposed extension;
- The installation of 3 additional monitoring wells to validate the results of the geophysical survey;
- Installation of 90 monitoring wells in limestone bedrock and overlying glacial till materials to permit monitoring of groundwater levels on and adjacent to the proposed extension and collection of groundwater quality samples;
- Installation of eight shallow monitoring wells at and adjacent to the wetlands, to observe the relationship of wetland water levels and groundwater levels;
- Laboratory analysis of 32 soil samples to classify grain size distribution;
- Completion of 54 single well response tests;
- Ongoing collection of depth-to-groundwater measurements from the monitoring wells;
- Pumping of a test well to characterize the bulk hydraulic properties of the dolostone and to assess the response of groundwater levels, especially in the vicinity of the wetland, to a lowering of water levels in the bedrock;
- Ongoing measurement of surface water flows at 70 locations on and below the Escarpment;
- Collection of water samples from monitoring wells, streams, and springs to characterize local water quality.

A map showing the borehole locations, completed as part of this program, is shown in Figure 3.4. A sample borehole log from the investigations is shown in Figure 3.5.

3.3.2 Azimuth Environmental 2018 - 2019 Drilling and Monitoring Program

In 2018, Azimuth Environmental began an extensive drilling, testing, and monitoring program that covered the South and West Extension areas. A detailed discussion of the field program is presented in Appendix A (under separate cover). In brief, high-resolution dataloggers were added to some of the existing monitoring wells and a total of seven new boreholes were drilled. A program of borehole televiewer, flow meter, packer testing, and water level/water quality monitoring was initiated. The locations of the new boreholes in the West Extension area are shown in Figure 3.6. A sample borehole log from the West Extension area is shown in Figure 3.7. A detailed discussion of the field program is presented in Azimuth (2019) (Appendix A).

3.3.3 Site Development History

Continued site development has progressed within the existing quarry extraction limits in the intervening time between the 2005 investigations (Figure 3.8) and the 2019 investigations (Figure 3.9). The south quarry face advanced to the northeast by approximately 350 m. The effects of this quarry excavation and expanded dewatering have been observed in the monitoring data collected since 2005; this information is discussed in detail in the following sections. For example, the line of sight distance to the quarry face changed for three of the monitoring nests as follows:

Monitor ID	Distance to Face: 2005	Distance to Face: 2019
OW03-14	175 m	40 m
MW03-30	550 m	300 m
OW03-19	1125 m	1000 m

The results of this progression provided very useful insight into the likely effects of quarry development on the surrounding area. Monitor OW03-19 also serves as a long-term background monitor.

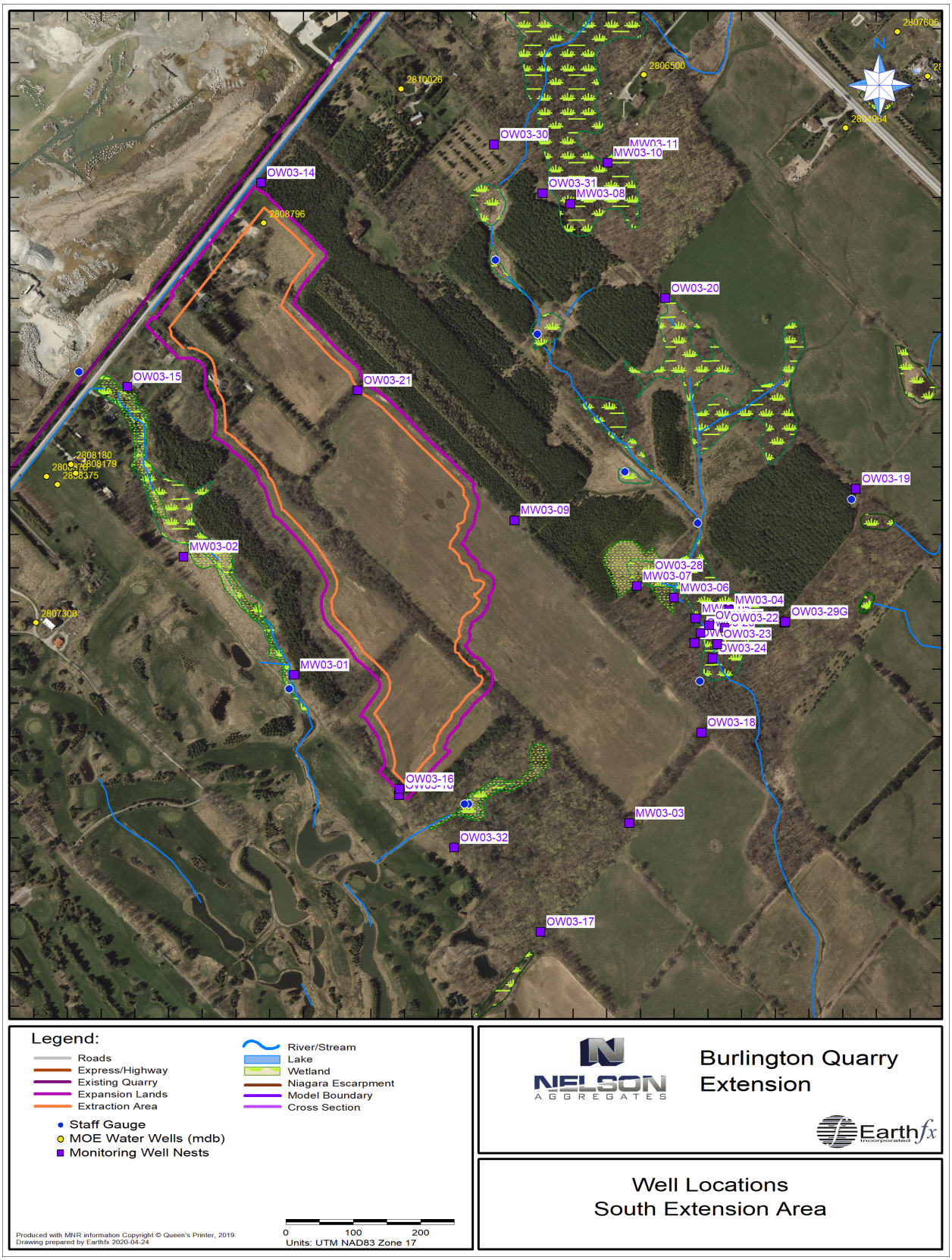

Figure 3.4: Well locations - South Extension area.

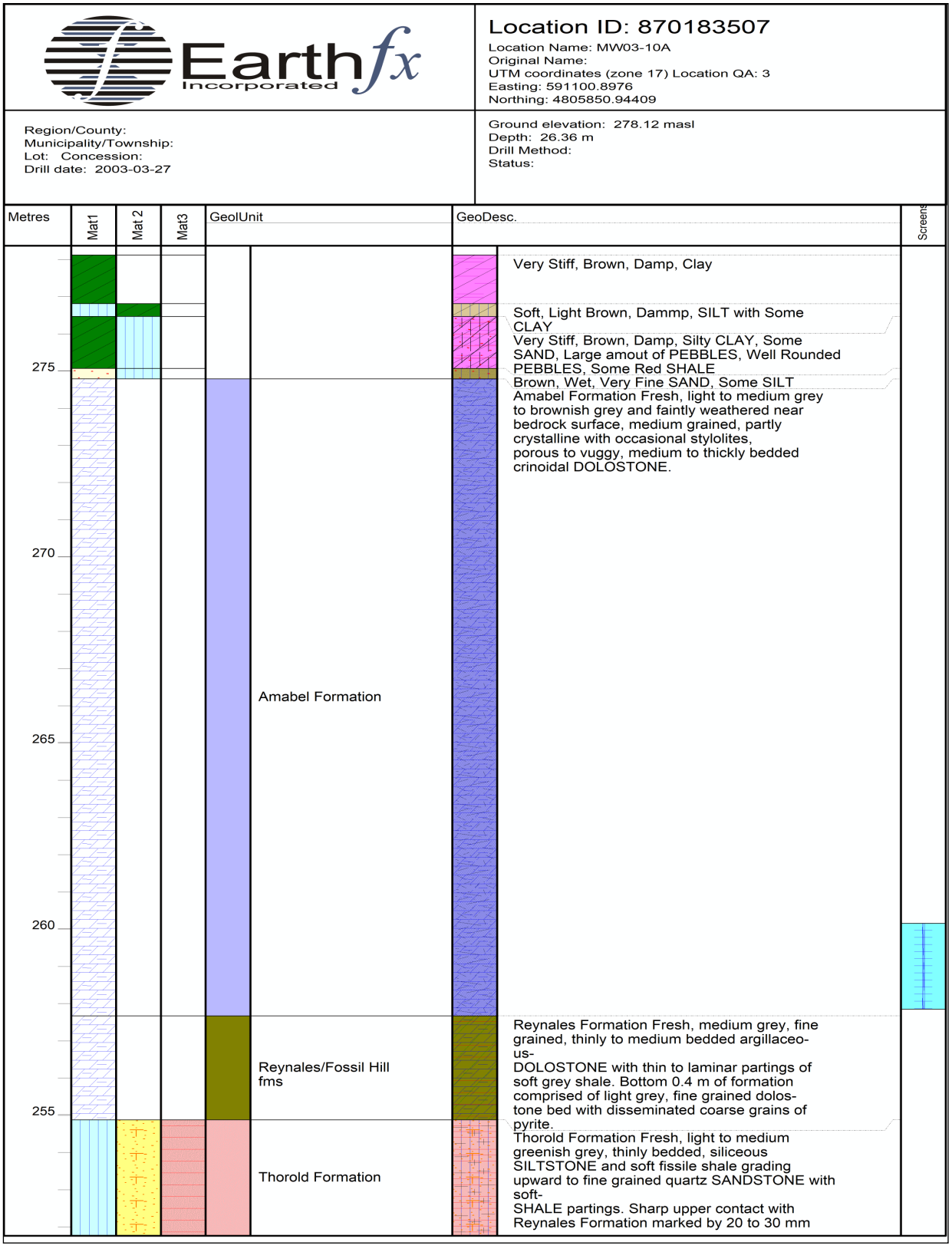

Figure 3.5: Sample borehole log from the South Extension area.

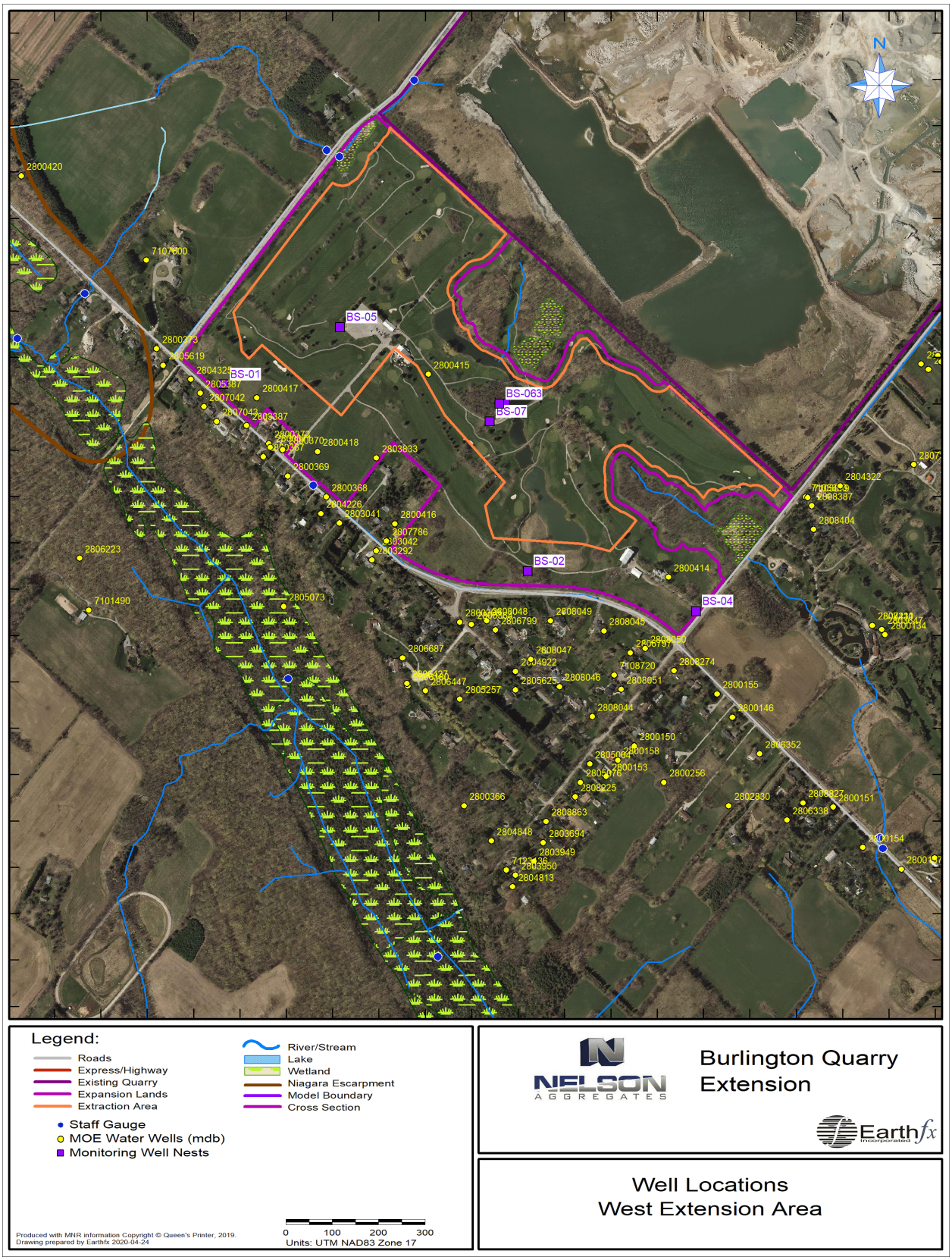

Figure 3.6: Well locations: West Extension area.

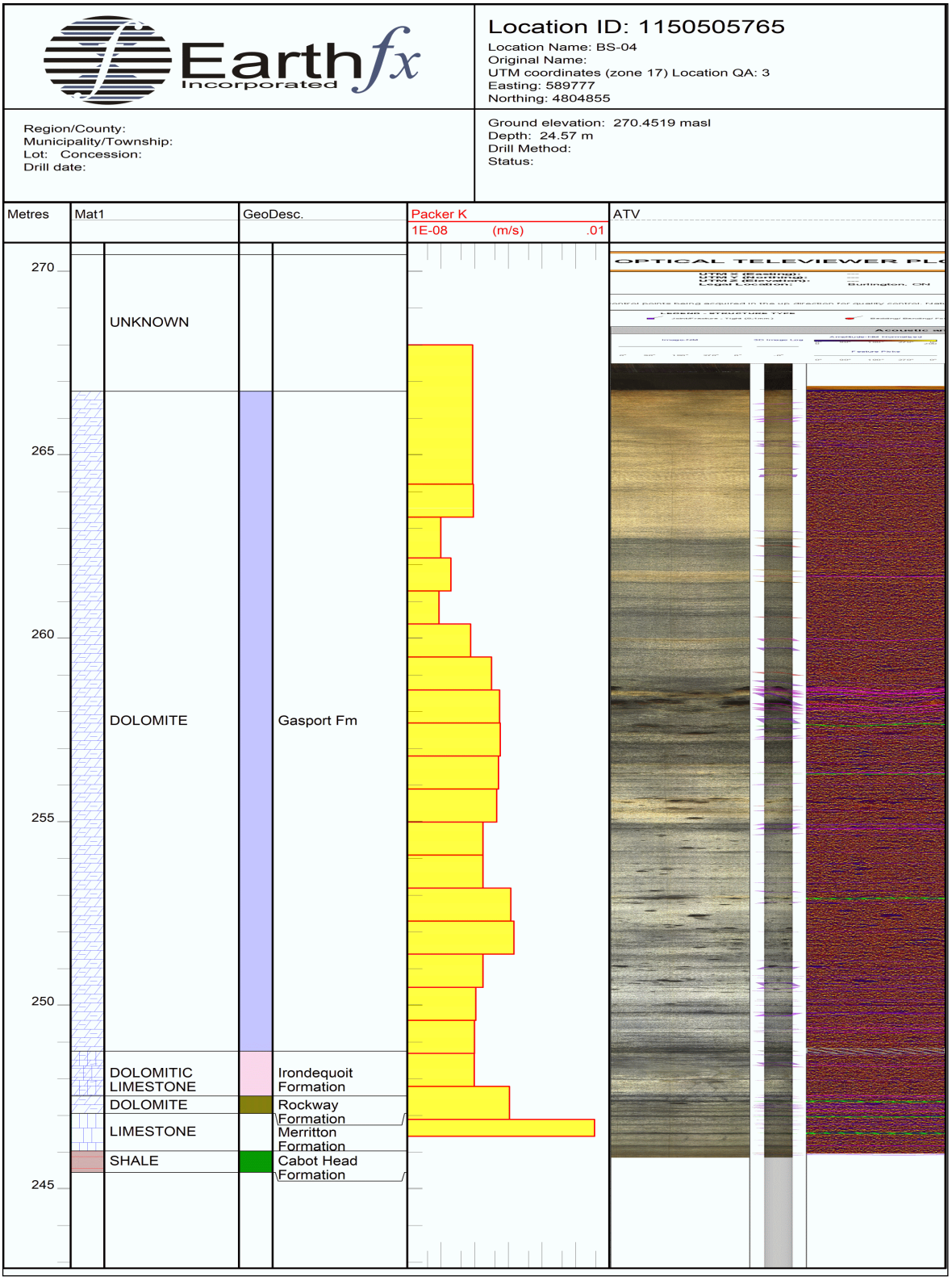

Figure 3.7: Sample borehole log from the West Extension area (BS-04).

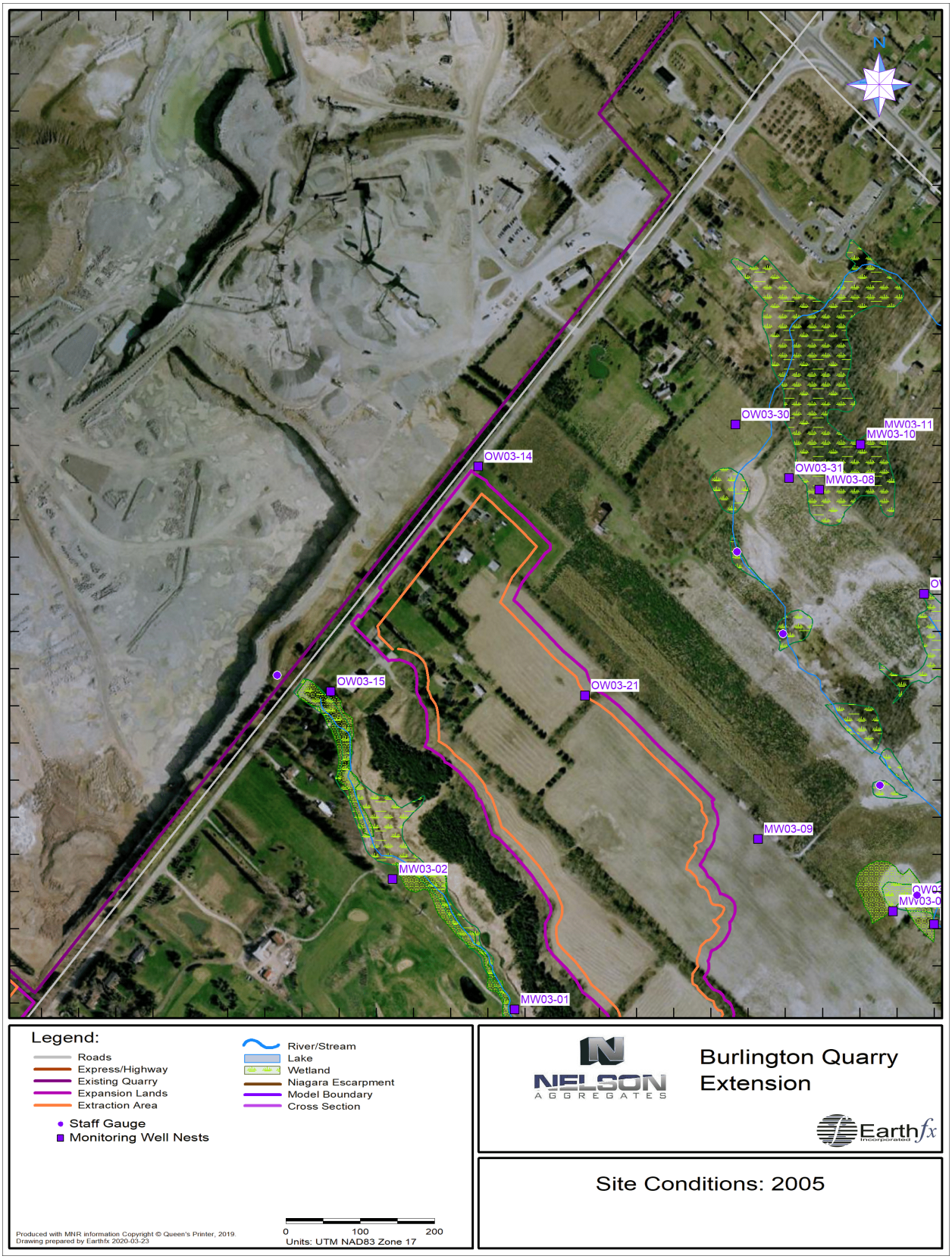

Figure 3.8: Site development conditions in 2005.

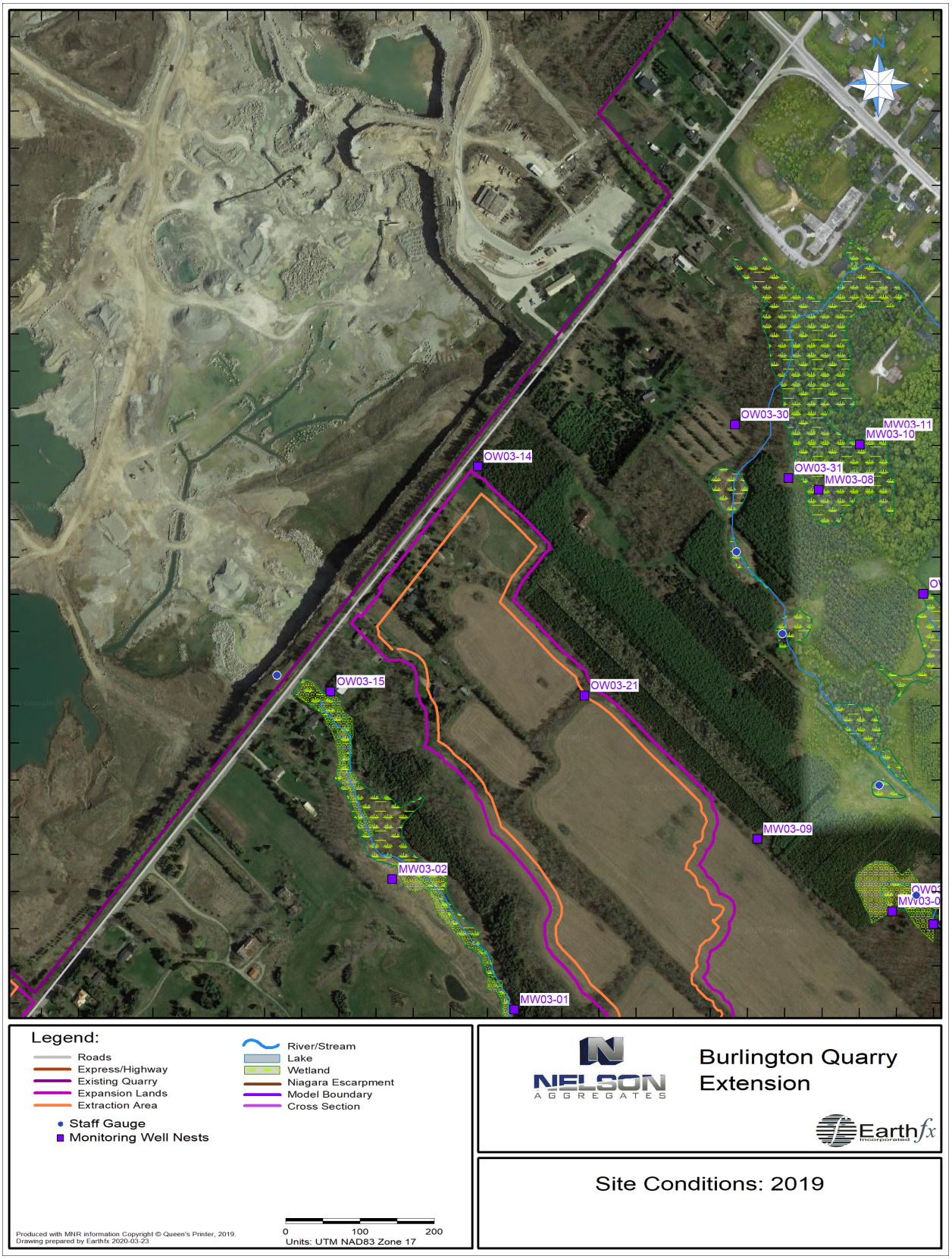

Figure 3.9: Site development conditions in 2019.

3.4 Paleozoic Geology

The study area is underlain by clastic and carbonate sedimentary rocks of Late Ordovician to Middle Silurian age. The site is located at the transition between stratigraphic nomenclature traditionally used in the Niagara Region and that used northwards to the Bruce Peninsula. The complex stratigraphic relationships between these units are shown in Figure 3.11. The stratigraphic unit designations have been updated by the Ontario Geologic Survey (OGS) (Brunton, 2008, 2009) to include the subdivision of the Amabel formation into the upper Goat Island Formation and lower Gasport Formation.

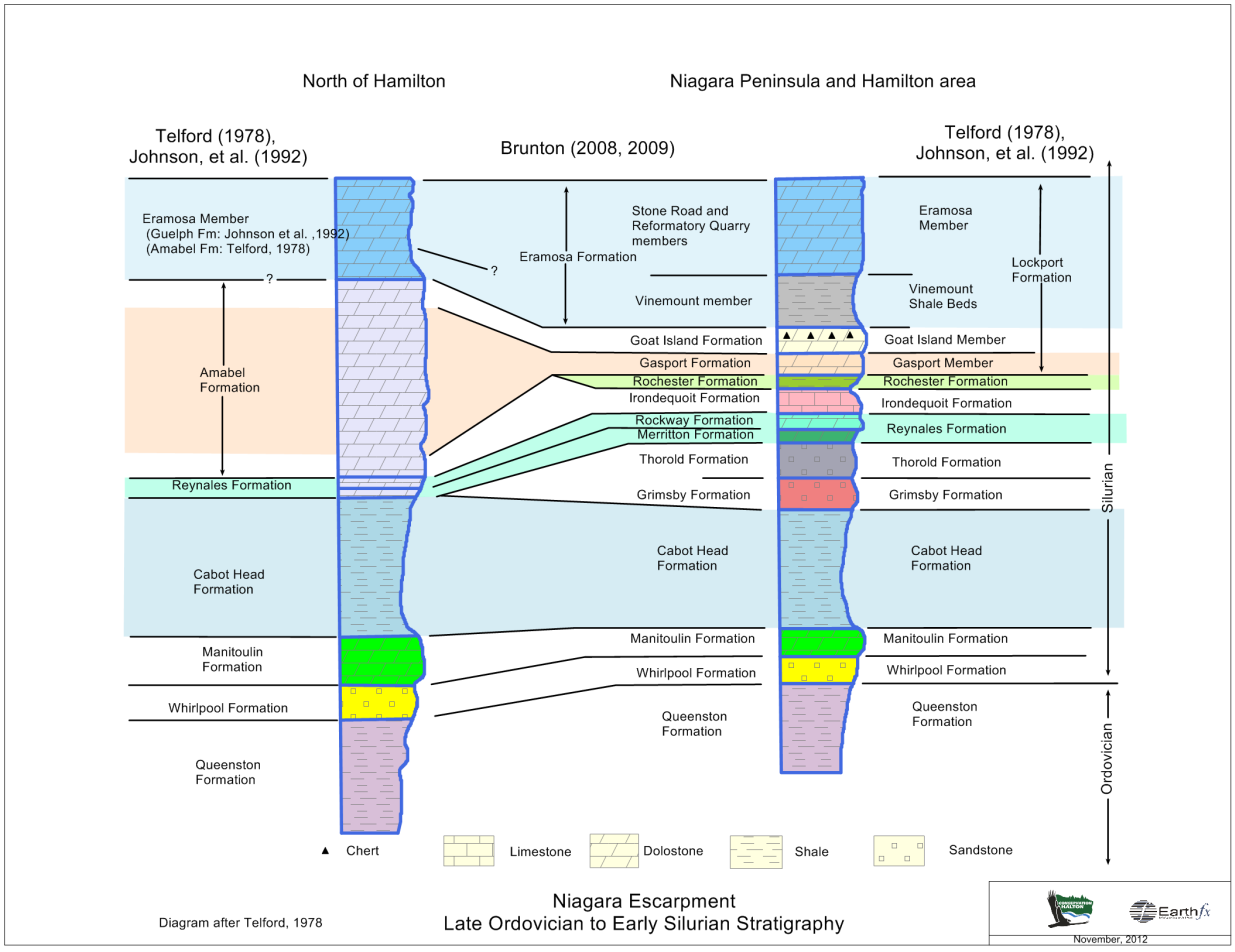

Figure 3.10: Stratigraphic relationships and comparison of stratigraphic nomenclature.

Figure 3.11 shows the uppermost bedrock units in the study area. The units, which dip gently to the southwest, include parts of three major depositional sequences (Johnson *et al.*, 1991), with outcropping rocks generally becoming younger from northeast to southwest.

A conceptual west to east section passing through the quarry site and the Niagara Escarpment is shown in Figure 3.12. The study area is located in the easternmost portion of the conceptual section. Many of the thin units shown on Figure 3.12 are not present or identifiable in the local boreholes.

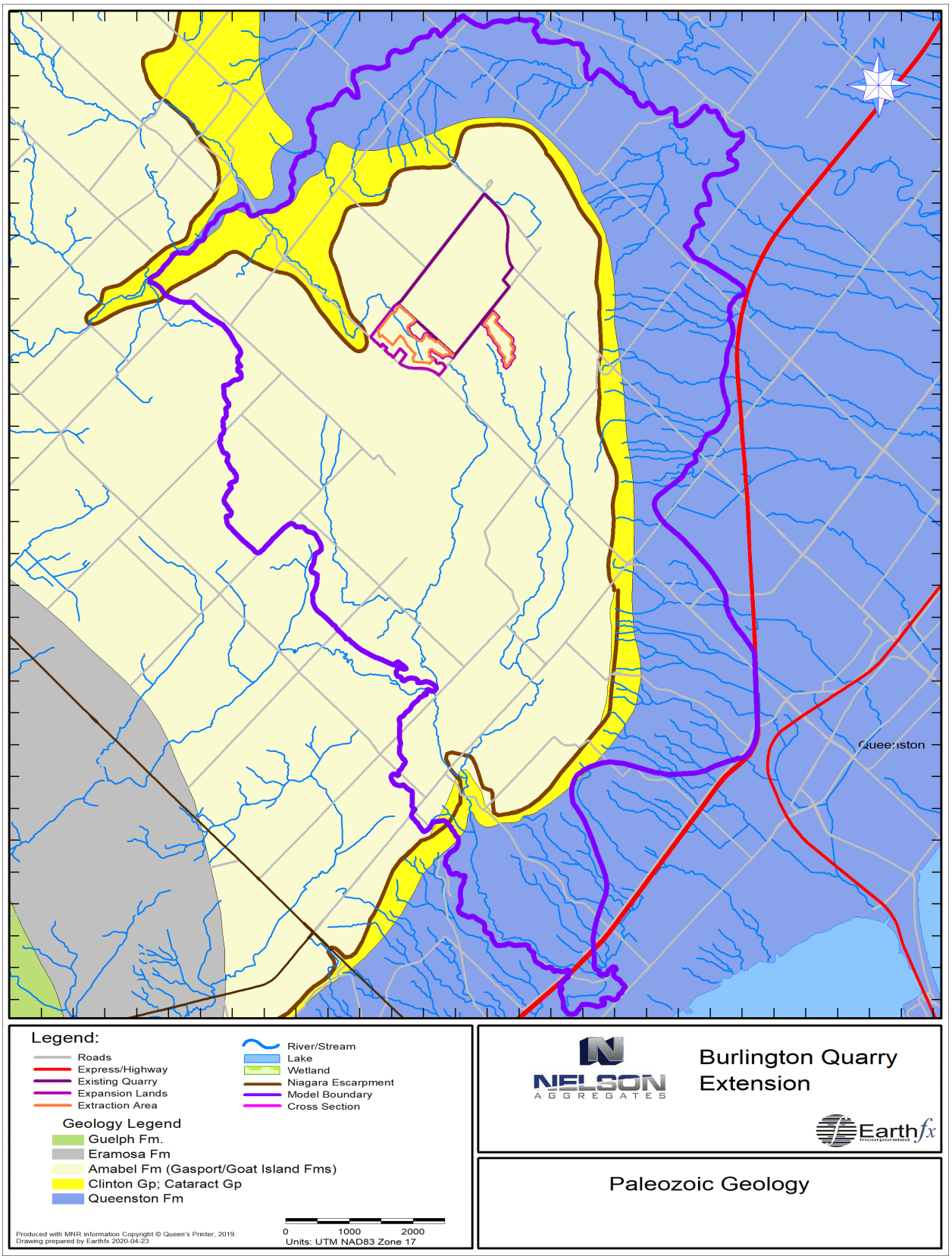

Figure 3.11: Bedrock geology for the study area (from Armstrong and Dodge, 2007).

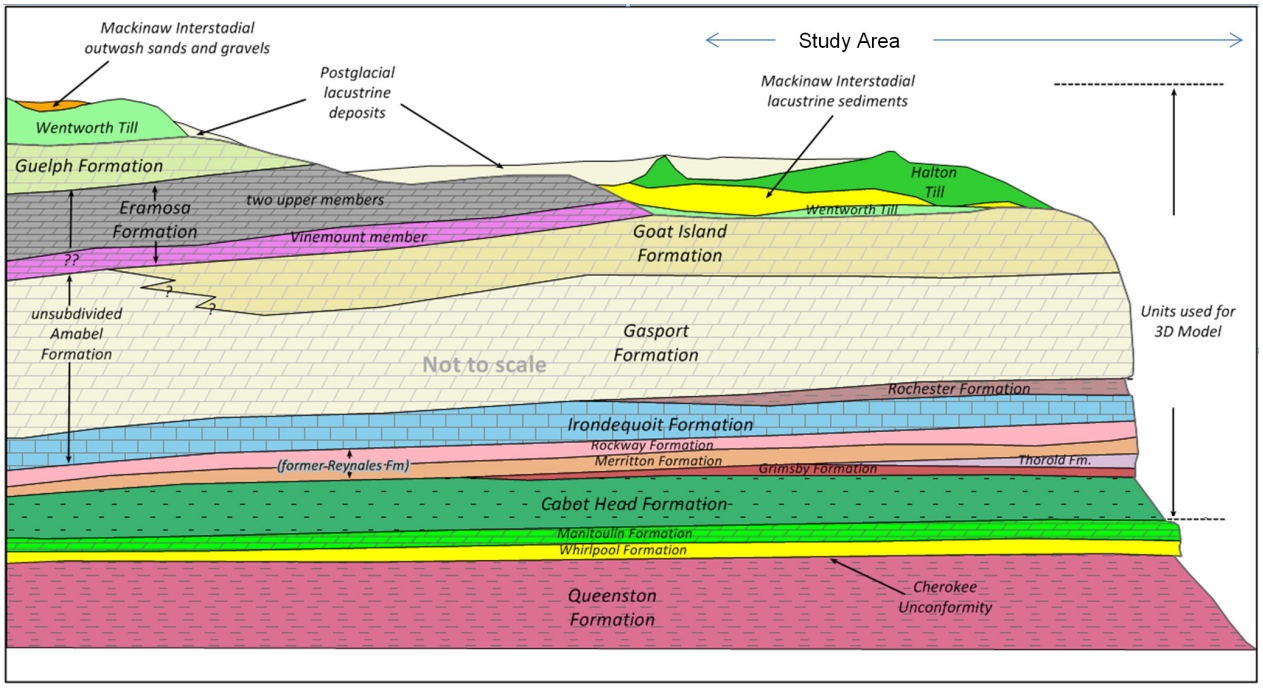

Figure 3.12: Conceptual stratigraphic cross section.

3.4.1 Queenston Formation

The oldest bedrock unit is the Late Ordovician Queenston Formation, which consists of predominantly dark red, fissile, hematitic, calcareous shale with green-coloured reduction zones that are either parallel or discordant to bedding (Liberty, *et al*., 1976). The unit outcrops in incised stream channels below the Niagara Escarpment. The top of the Queenston Formation is marked by an erosional surface known as the Cherokee Unconformity (Brett *et al*., 1990).

3.4.2 Whirlpool Formation

The Whirlpool Formation is composed mainly of fine-grained quartz sandstone, which locally may have thin shale partings (Bond, *et al*., 1976). This unit is approximately 3.3 m thick in a deep borehole south of the site. Whirlpool Formation outcrops are found at the face of the Escarpment and the formation serves as a "caprock" to the underlying Queenston shale. The Whirlpool Formation is succeeded gradationally by the thin- to medium-bedded fossiliferous dolostone of the Manitoulin Formation (Johnson *et al*., 1992), which is approximately 1 m thick in the study area. The contact with the overlying Cabot Head Formation is gradational.

3.4.3 Cabot Head Formation

The rocks of the Cabot Head Formation are predominantly thinly laminated grey and green, noncalcareous shales with minor interbeds of sandstone, limestone, and dolostone (Johnson *et al*., 1992). The Cabot Head dips southwest (Figure 3.13) and is approximately 20-30 m thick (Figure 3.14) in the study area and is locally incised by the Medad Valley. The Cabot Head is a regionally-extensive low-permeability aquitard underlying the study area and functionally directs groundwater discharge to the Escarpment face and the Medad Valley.

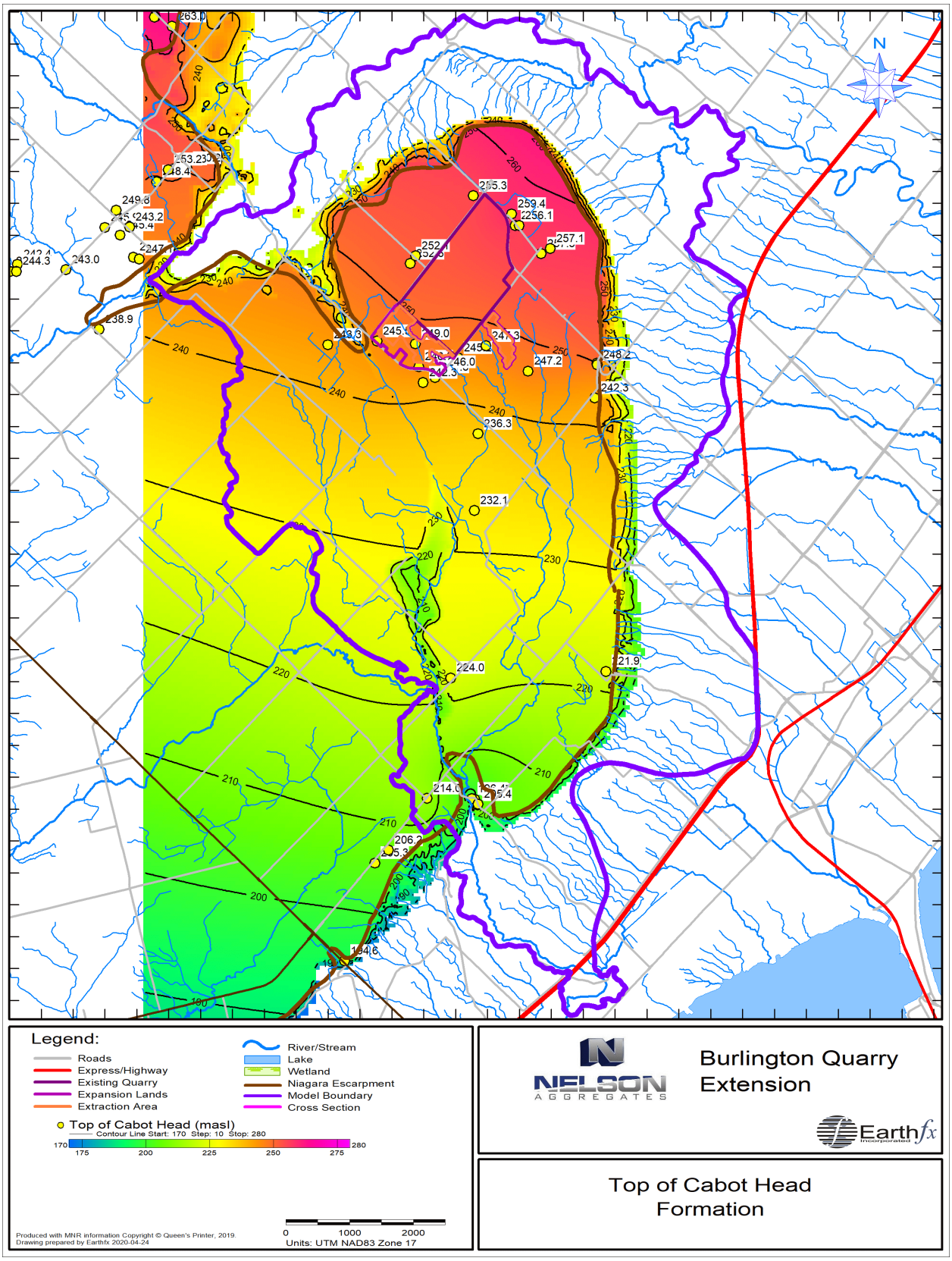

Figure 3.13: Top of the Cabot Head Formation (masl).

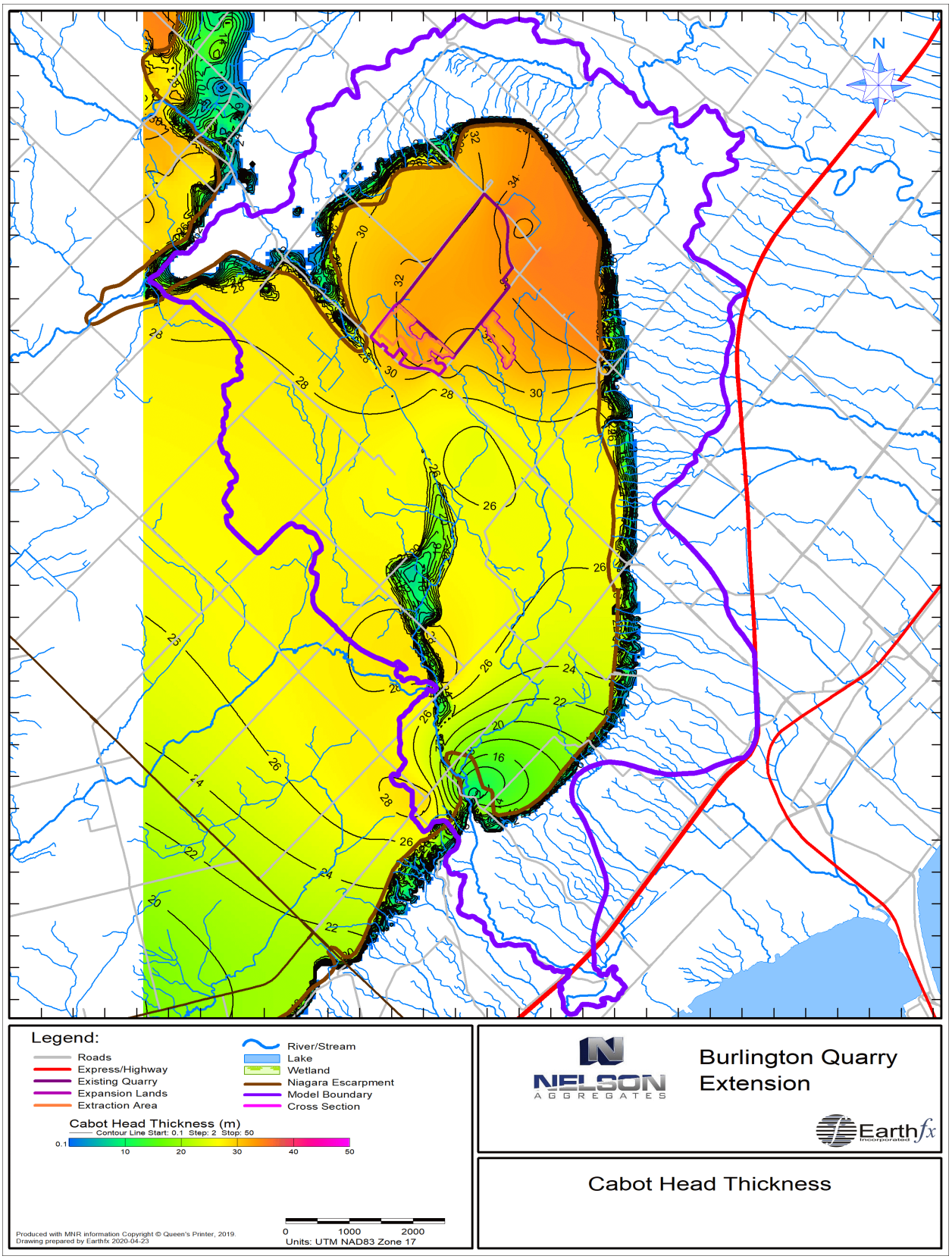

Figure 3.14: Thickness of the Cabot Head Formation (m).

3.4.4 Silurian Units

The Silurian-age units are generally thin and can be difficult to identify in this regional transition area. Furthermore, the recent changes in interpretation and nomenclature can cause some confusion. To address this uncertainty, Dr. Brunton of the Ontario Geologic Survey was asked to review the new drilling and televiewer results collected as part of this study.

OGS staff (Dr. Frank Brunton) reviewed the borehole data and confirmed the following stratigraphy, from top to bottom.

- Gasport Formation (also known as the Amabel Formation)
- Irondequoit Formation (previously included in basal Amabel Formation – where Rochester Formation is cut-down/removed tectonically – due to fore bulge migration and uplift and erosion of unlithified Rochester sediments)
- Rockway Formation (also known as Reynales Formation)
- Merritton Formation (also known as Reynales Formation)
- Cabot Head Formation

The Rochester, Grimsby or Thorold formations were not identified in the boreholes at this site. At the King City Quarry, southwest of the site (a Provincial Geologic ANSI), the Rochester Formation is observed to be 1 m thick, but it thins to the north. In general, some of the upper Clinton Group and Lockport Group rock units thin and/or are eroded completely in a westerly and northerly direction from Niagara Falls to Hamilton and extending along the Niagara Escarpment region, due to the interplay between tectonics (forebulge uplift and downwarping), global sea level fluctuations and glaciations, and resultant changes in regional marine sedimentation.

Brett *et al*. (1995) subdivided the Reynales Formation into the Merritton and Rockway formations. The Merritton Formation disconformably overlies the Cabot Head Formation and consists of finely-crystalline dolostone with dark shale partings (Brett, et al., 1995 and Brunton, 2008). Brunton (2008) noted that the Merritton Formation appears to thin eastward from the Guelph area towards the Niagara Escarpment. The Rockway Formation disconformably overlies the Merritton Formation and is described by Brunton (2008) as an argillaceous dolomicrite to wackestone with a distinctive, greenish-grey finely crystalline matrix with thin shaley partings.

Previous work by Golder on the site identified the following Silurian units below the Amabel Formation:

- Amabel Formation
- Reynales Formation
- Thorold Formation
- Grimsby Formation

Golder did not identify the Irondequoit at the site. It should be noted that Voss (1969) suggested that it can be difficult to identify the Irondequoit due to the similarity with the overlying dolostone. The Cabot Head Formation was also not identified in Golder borehole logs, but was delineated on cross sections in the Golder reports. Golder refers to the top of the Thorold Formation as the “Top of Shale” (Golder, 2004, Figure F2) and assigned both the Thorold and Grimsby the same low hydraulic conductivity value, suggesting that those units have hydraulic properties similar to the Cabot Head Formation.

Golder (2004, page 8) described the Reynales Formation as follows:

> *The Reynales Formation is approximately 2.3 m to 2.8 m in thickness beneath the proposed extension. It is comprised of medium greenish grey, fine-grained, thinly to medium bedded, dolostone with argillaceous dolostone beds and occasional shaley bed partings. The formation*

is currently used by Nelson as a source for some aggregate products and may be extracted in the proposed extension. The basal section of the formation contains pyrite mineralization. The upper contact with the overlying Amabel Formation is sharp.

The identification of these units in records from the MECP water well information system (WWIS) is difficult; however, careful inspection of the records revealed log description patterns that proved useful during the construction of the stratigraphic model layers. Some water well records in the area identify a "Shale, Layered" unit above another unit simply described as "Shale". The terms "Limestone, Shale, Layered" and "Shale, Limestone, Layered" also appears in a number of boreholes. Together, these descriptions are interpreted to represent the Reynales (Rockway and Merritton) unit above the Cabot Head Formation shales.

For the purpose of this study, the various descriptions (Golder, Brunton, MECP well records) were reconciled by defining a single unit above the Cabot Head shale. The following approach was taken:

- based on OGS staff interpretation of the site logs, Golder's Thorold and Grimsby shale units were integrated into the Cabot Head Shale;
- while Brunton (2008) was able to subdivide the Reynales, these units are hydrogeologically similar (dolostone with shale partings) and are un-subdivided in the Golder and MECP logs; for simplicity, the Rockway and Merritton unit is referred to herein as the Reynales Formation.

The top of the Reynales Formation dips gently to the southwest (Figure 3.15). The Reynales Formation is approximately 3 to 5 m thick in the study area and is eroded and missing in the Medad Valley (Figure 3.16).

The stratigraphic units are further illustrated by a series of cross sections drawn through the study area. The cross-section locations are shown in (Figure 3.17). The Guelph Line cross section (Figure 3.18) illustrates the layering near the crest of Mount Nemo and the very thin overburden coverage north of the existing quarry. The Blind Line cross section (Figure 3.19) passes through a pocket of thicker overburden to the northwest of the existing quarry and then traverses the thick Paleozoic section present in the South Quarry Extension area. The Cedar Spring cross section (Figure 3.20) illustrates the bedrock layering immediately west of the proposed West Quarry extension and illustrates the drop off into the Medad Valley to the northwest.

The final two cross sections clearly illustrate the north-east to south-west dip of the units towards the Medad Valley. The 2nd Side Road section (Figure 3.21) passes through the north portion of the South Extension and the south boundary of the West Extension. Finally, a West-East cross section through the quarry illustrates the existing excavation relative to the Medad Valley.

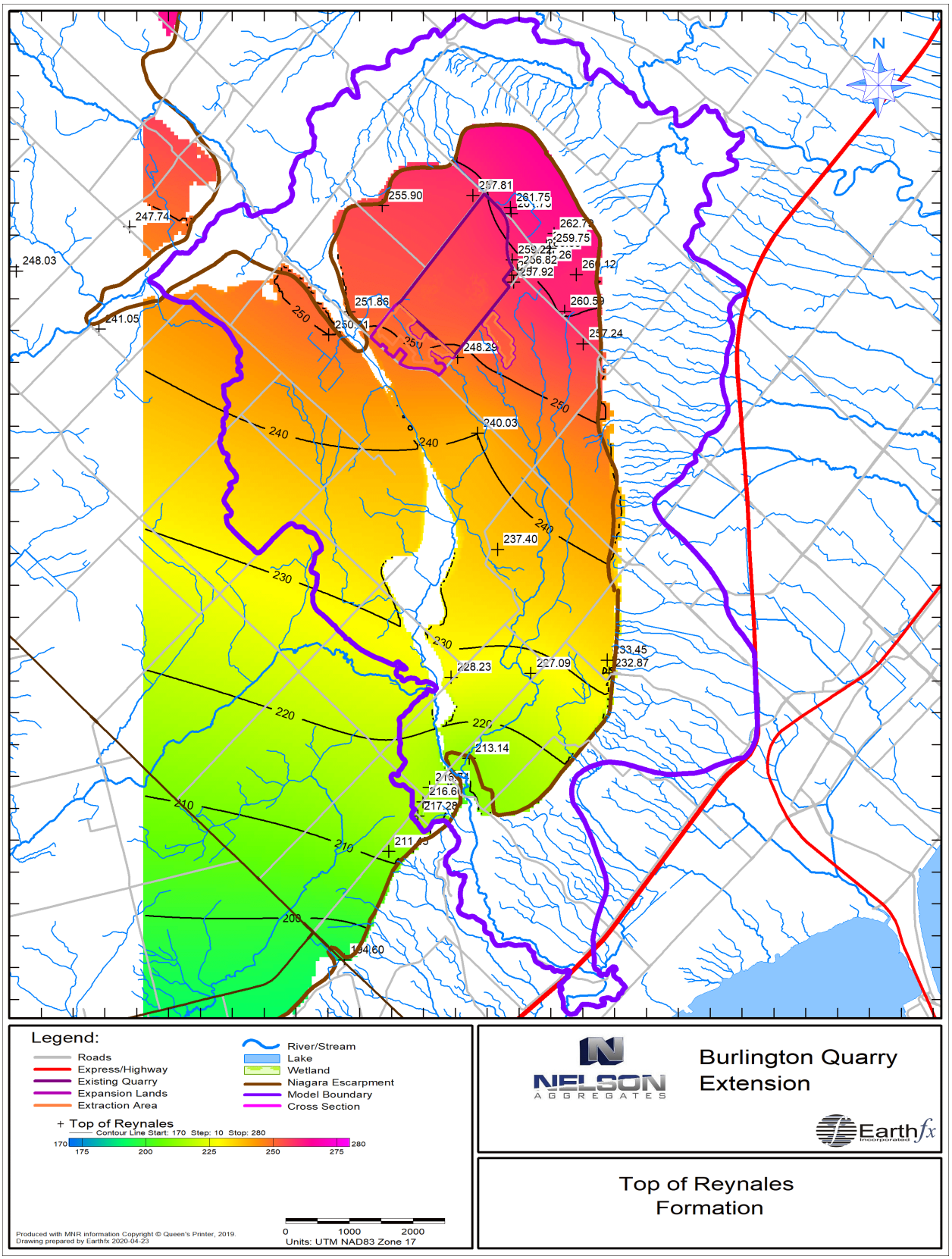

Figure 3.15: Top of the Reynales Formation (masl).

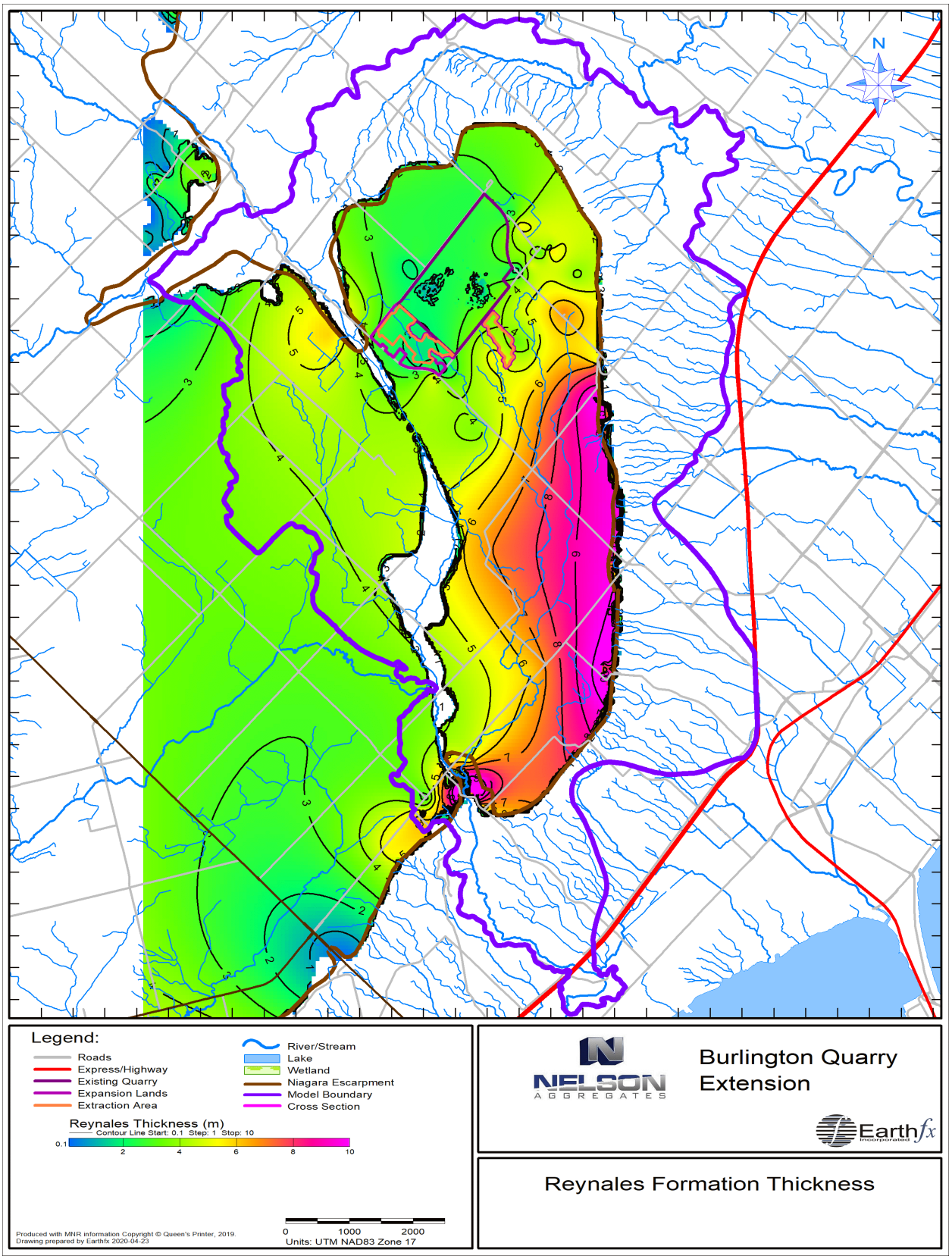

Figure 3.16: Thickness of the Reynales Formation (m).

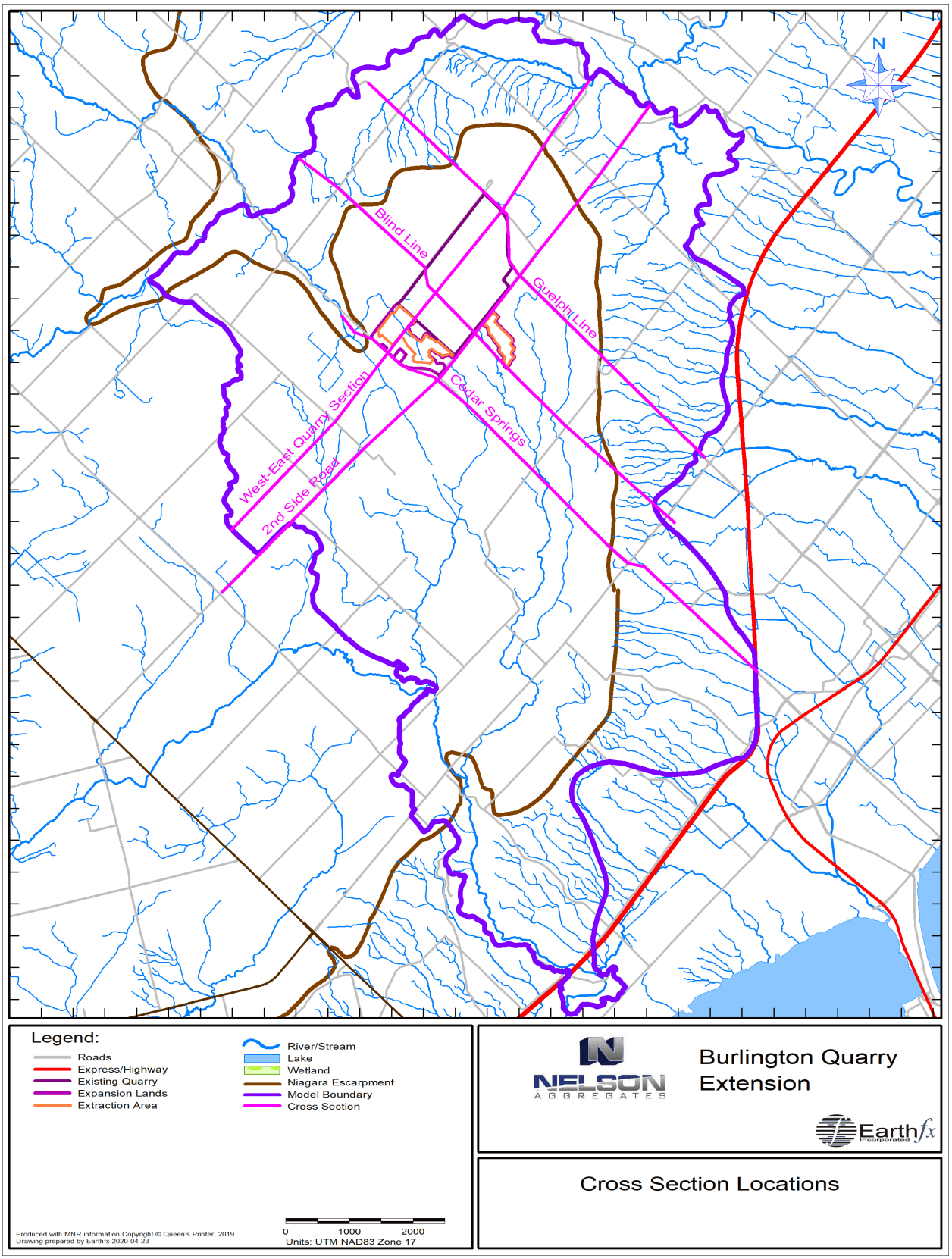

Figure 3.17: Cross section locations.

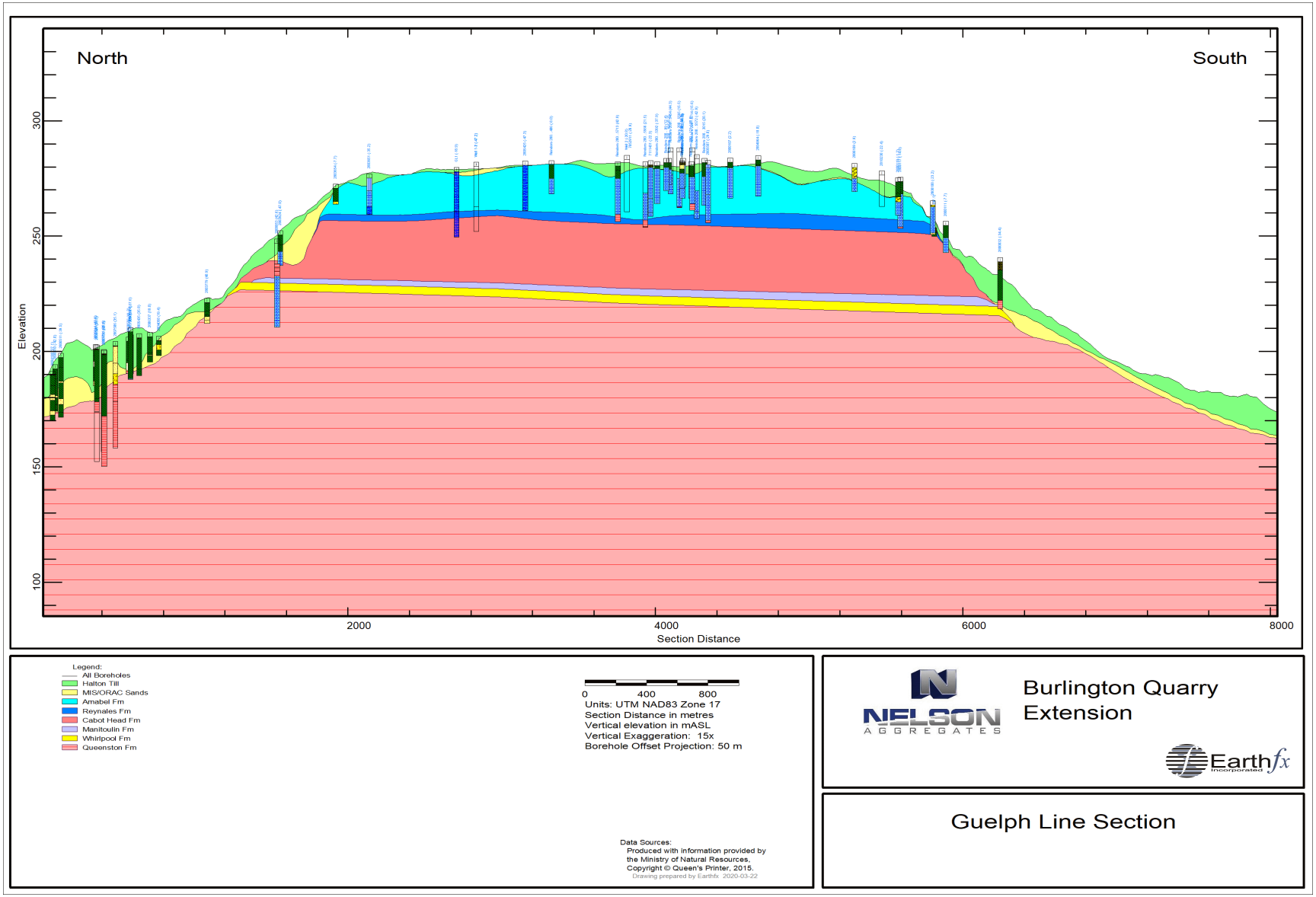

Figure 3.18: Guelph Line cross section.

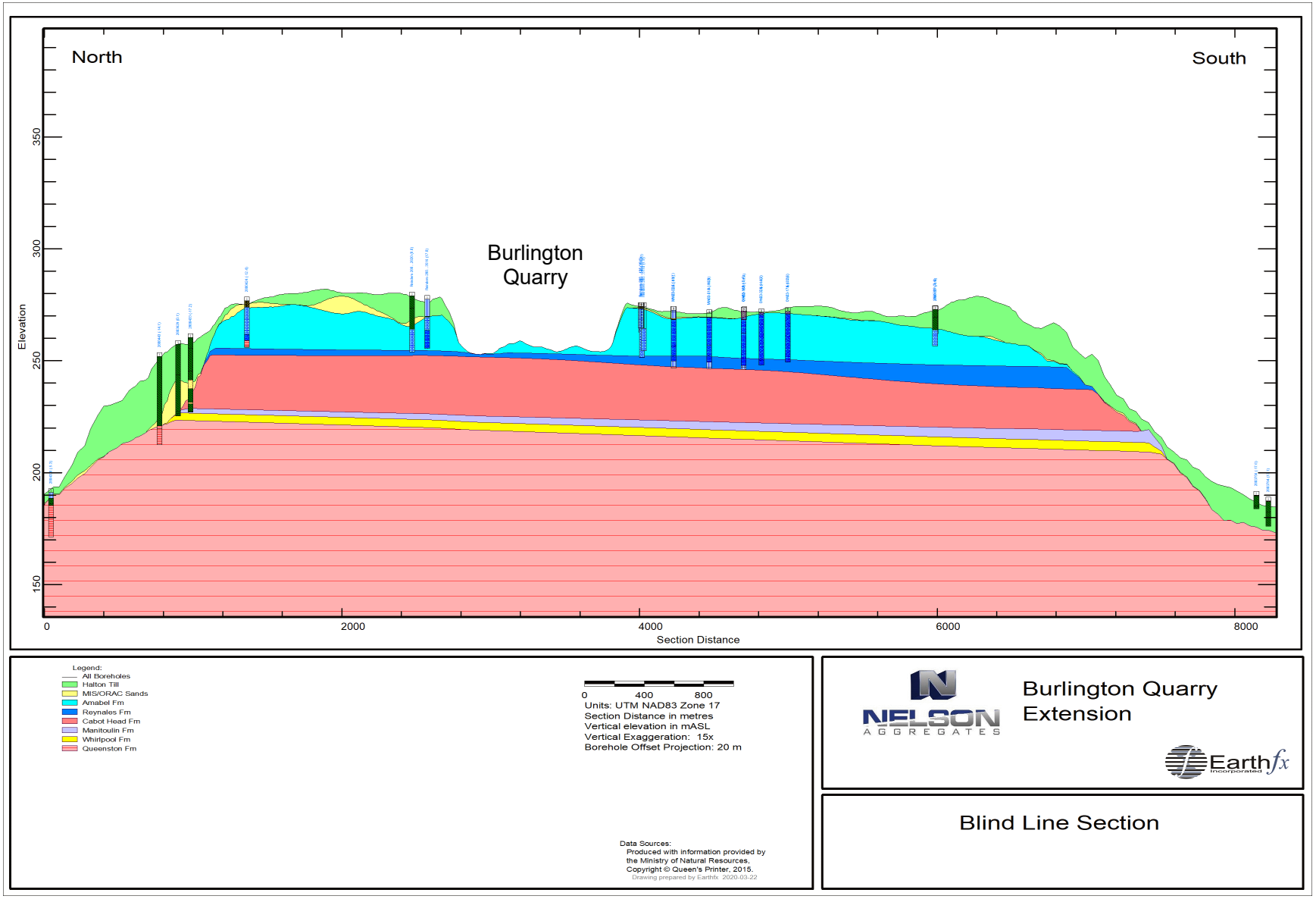

Figure 3.19: Blind Line cross section.

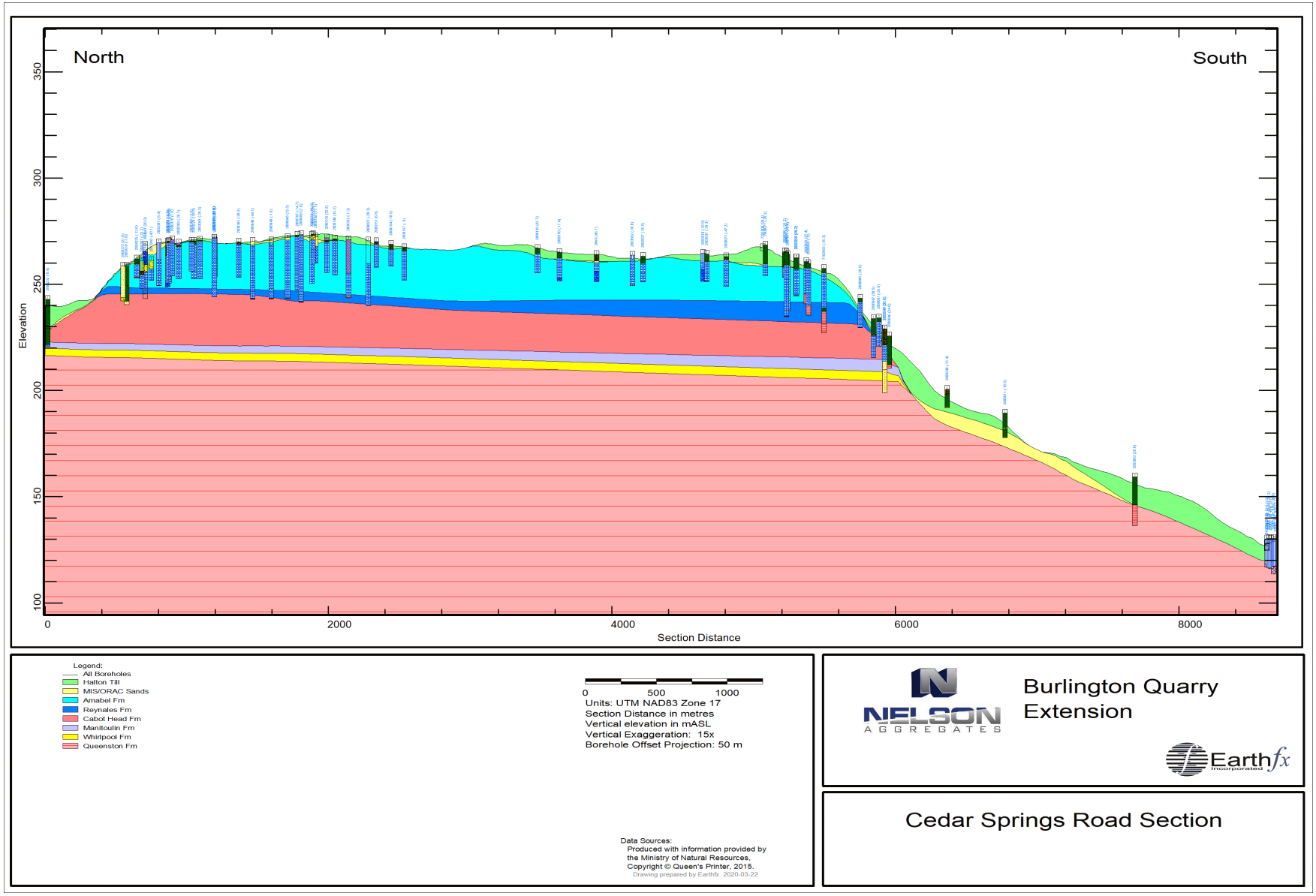

Figure 3.20: Cedar Springs Road cross section.

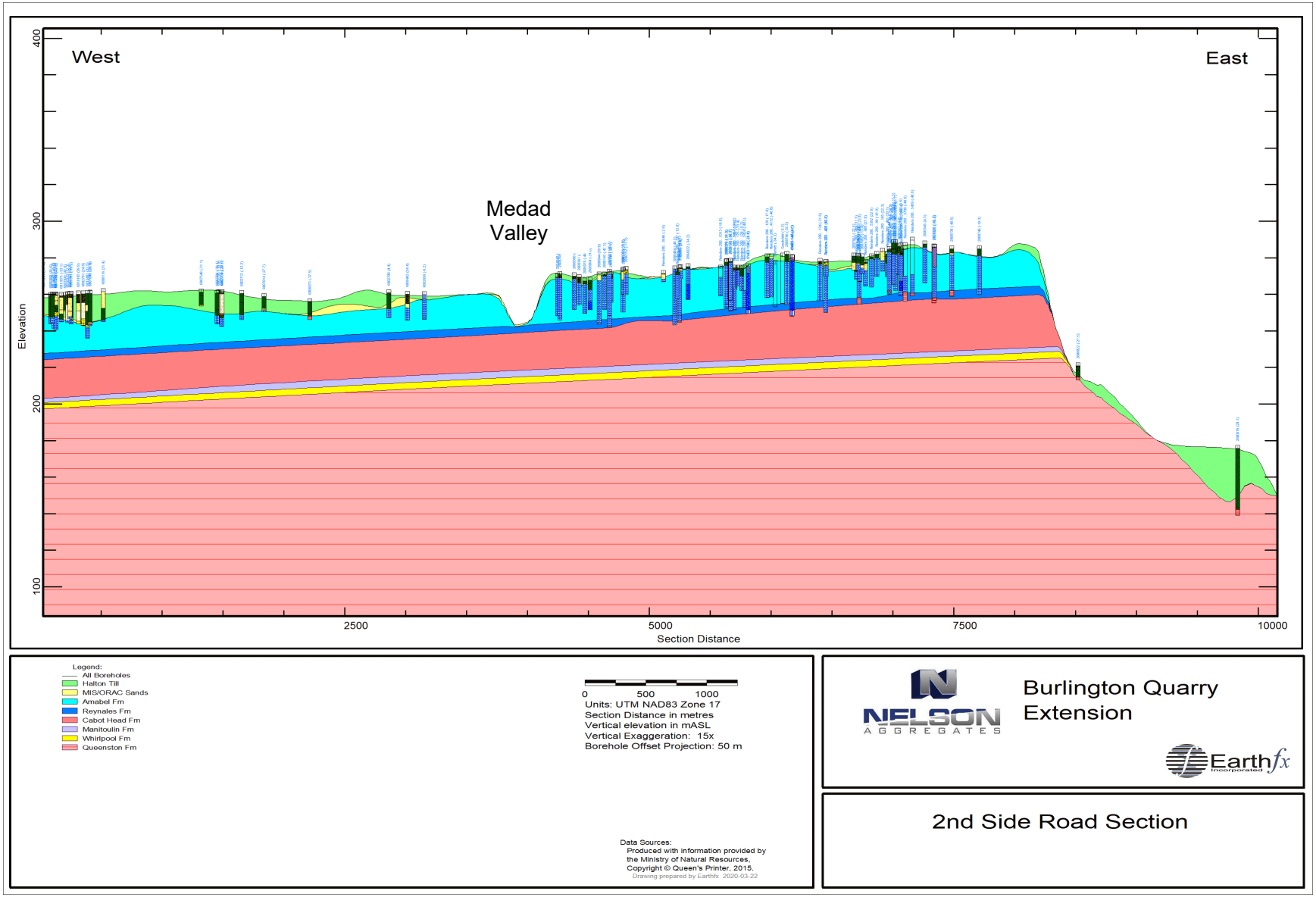

Figure 3.21: 2nd Side Road cross section.

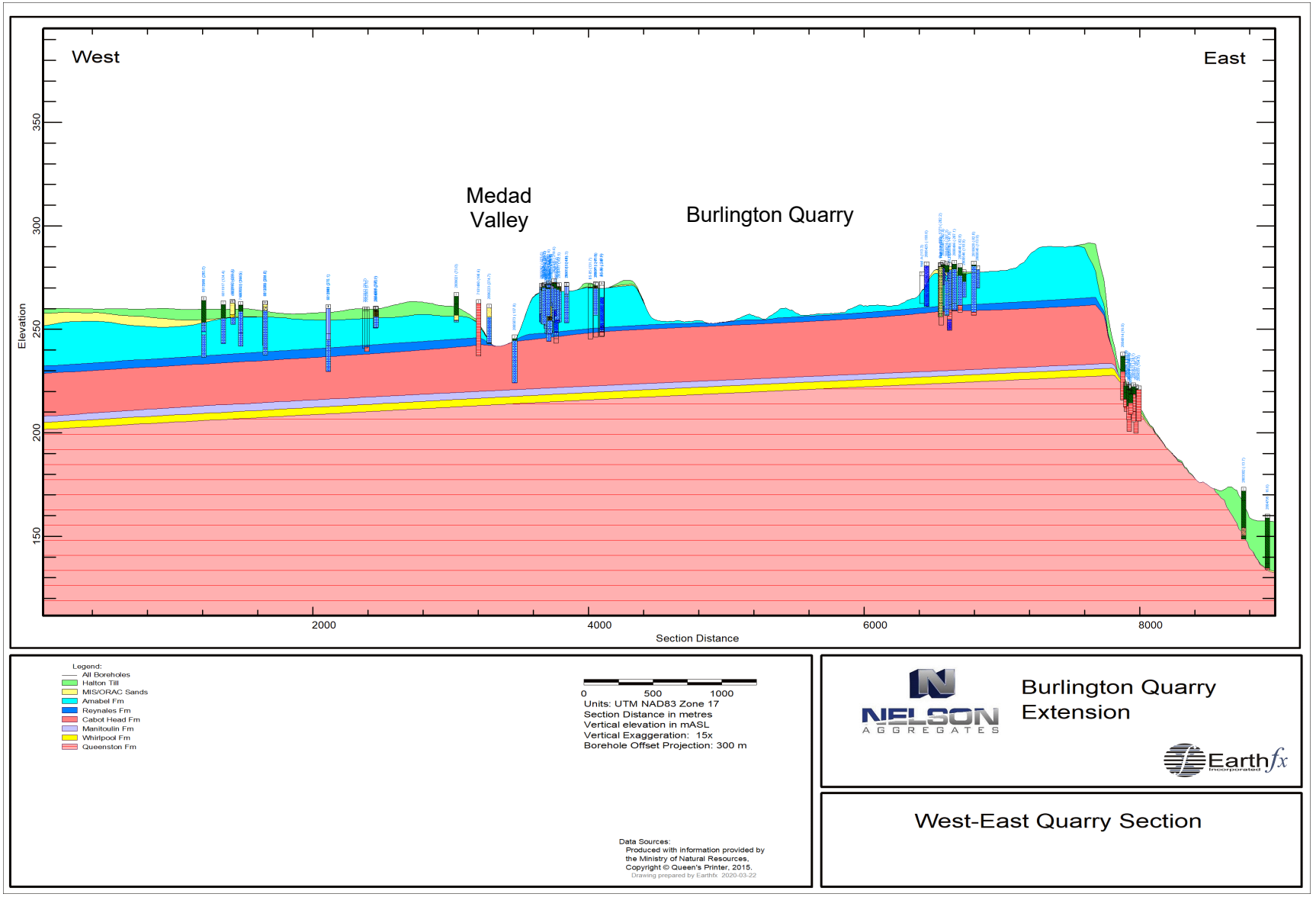

Figure 3.22: West-East quarry cross section.

3.4.5 Amabel Formation

The Reynales (Rockway) Formation is disconformably overlain by thickly-bedded dolomitic grainstones of the Early Silurian Amabel Formation, which form the caprock of the Niagara Escarpment (Figure 3.18 and Figure 3.23).

The Amabel Formation ranges in thickness from less than 10 m to more than 30 m (Figure 3.24). This unit was subdivided by Brunton (2008, 2009), into the Goat Island, Gasport and Irondequoit formations of the Lockport Group (Figure 3.10). The Gasport Formation makes up the bulk of the unsubdivided Amabel in the study area, overlying the two- to three- metre thick Irondequoit Formation. The Gasport Formation is characterized by massive, blue-grey, dolomitic limestones with some bioherms that could be indicative of subaerial exposure (Johnson *et al*., 1992). The Goat Island Formation is a thinner bedded, finer crystalline, grey dolostone that can be cherty and shaley (Bolton, 1957).

As noted in the previous section, OGS staff evaluated the borehole information from the 2019 West Quarry Extension drilling program. The Goat Island Formation was identified in one borehole (BS-01 in Figure 3.25), but was not identified in any other nearby boreholes, such as BS-04 (Figure 3.7). Golder (2004) did not subdivide the Amabel formation (Figure 3.5).

Because the Irondequoit, Gasport and Goat Island formations are hydrogeologically similar, and because the Amabel was not subdivided in the Golder and MECP borehole logs, these units were combined for the purpose of this study and are collectively referred to herein by their former Amabel Formation name.

The upper portion of the Amabel Formation is typically weathered to a depth of up to 5 m. Golder (2004) notes that the weathered section is brown in colour and contains more weathered fractures than the underlying fresh rock mass.

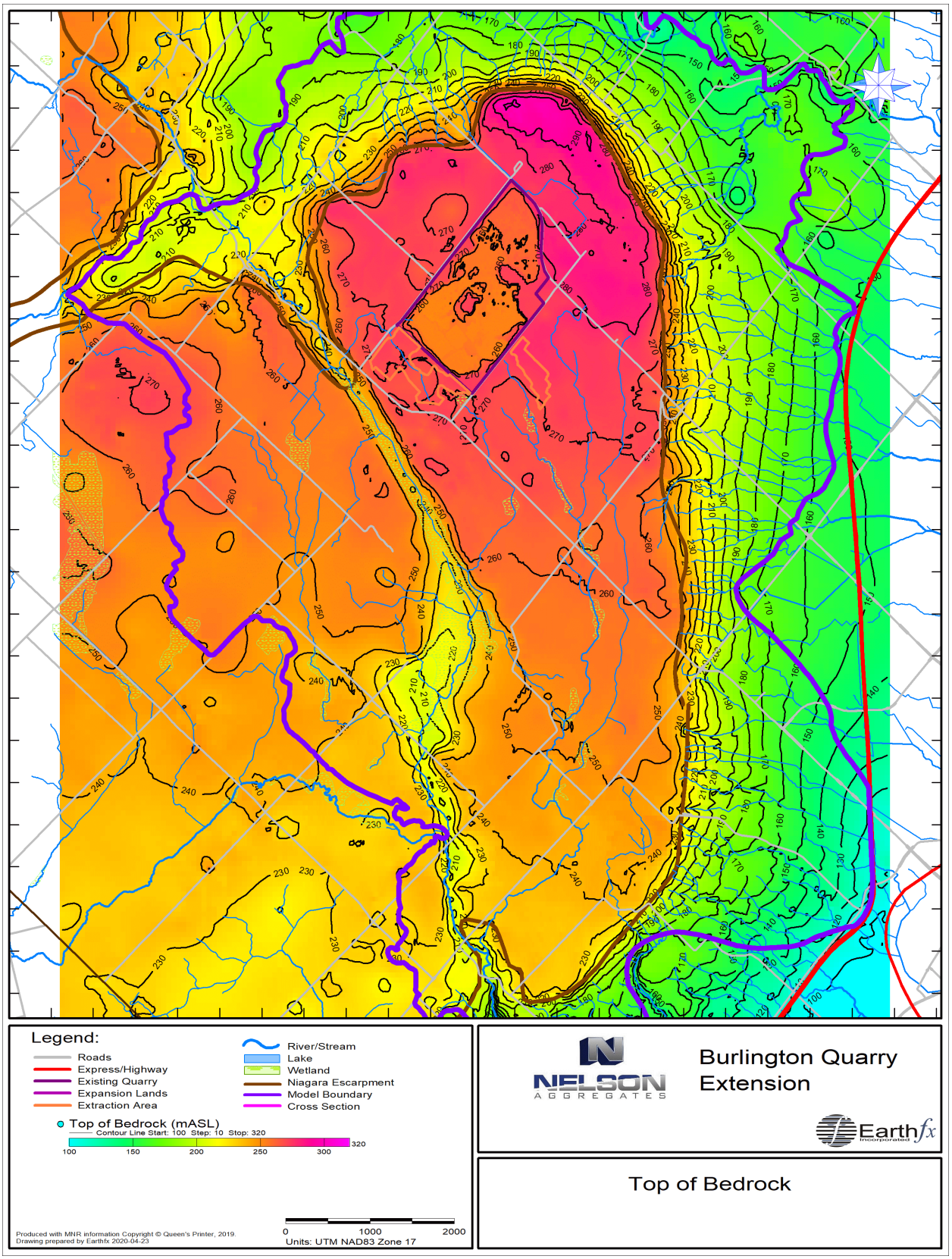

Figure 3.23: Top of bedrock (top of Amabel above the Niagara Escarpment), in masl.

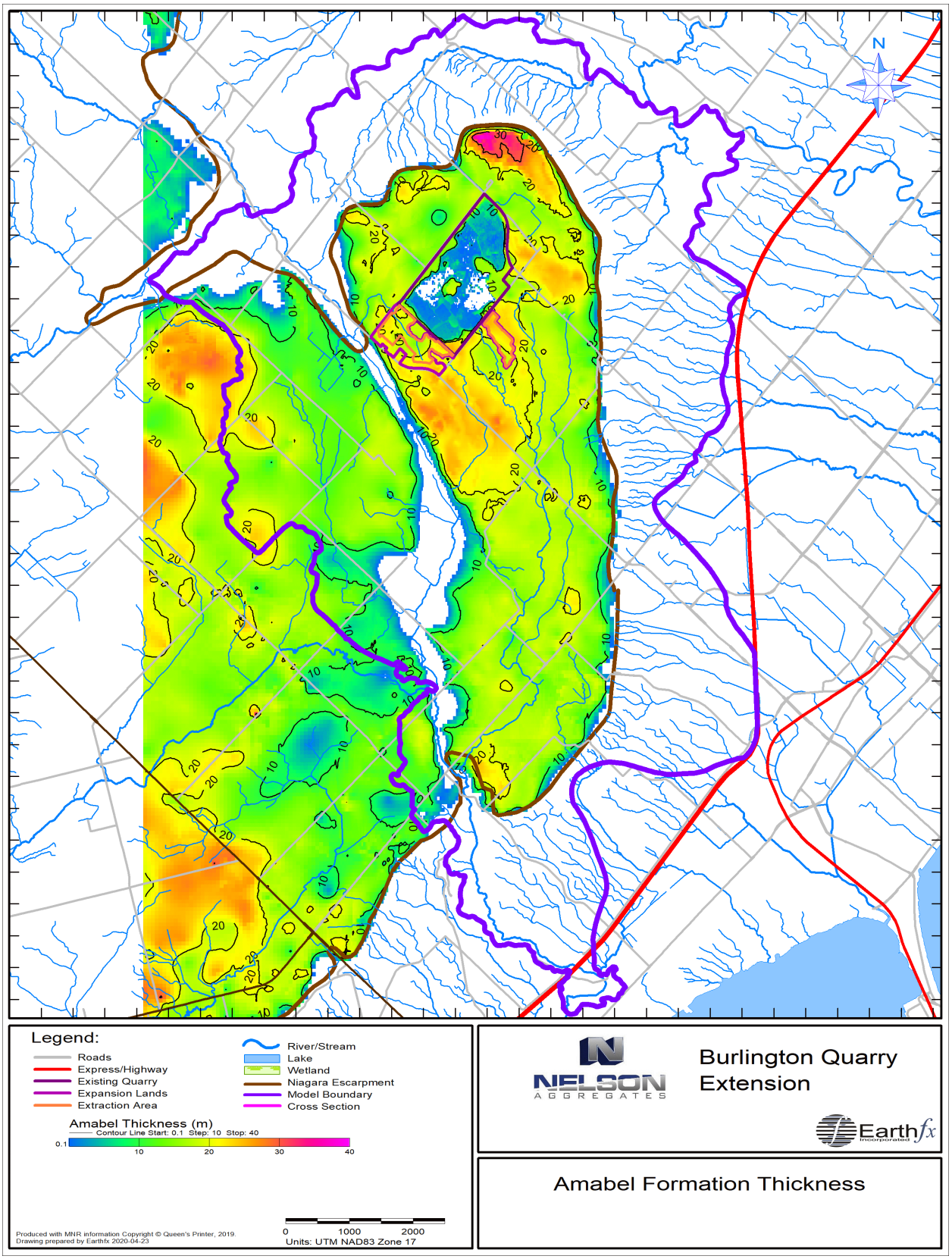

Figure 3.24: Thickness of the Amabel Formation (m).

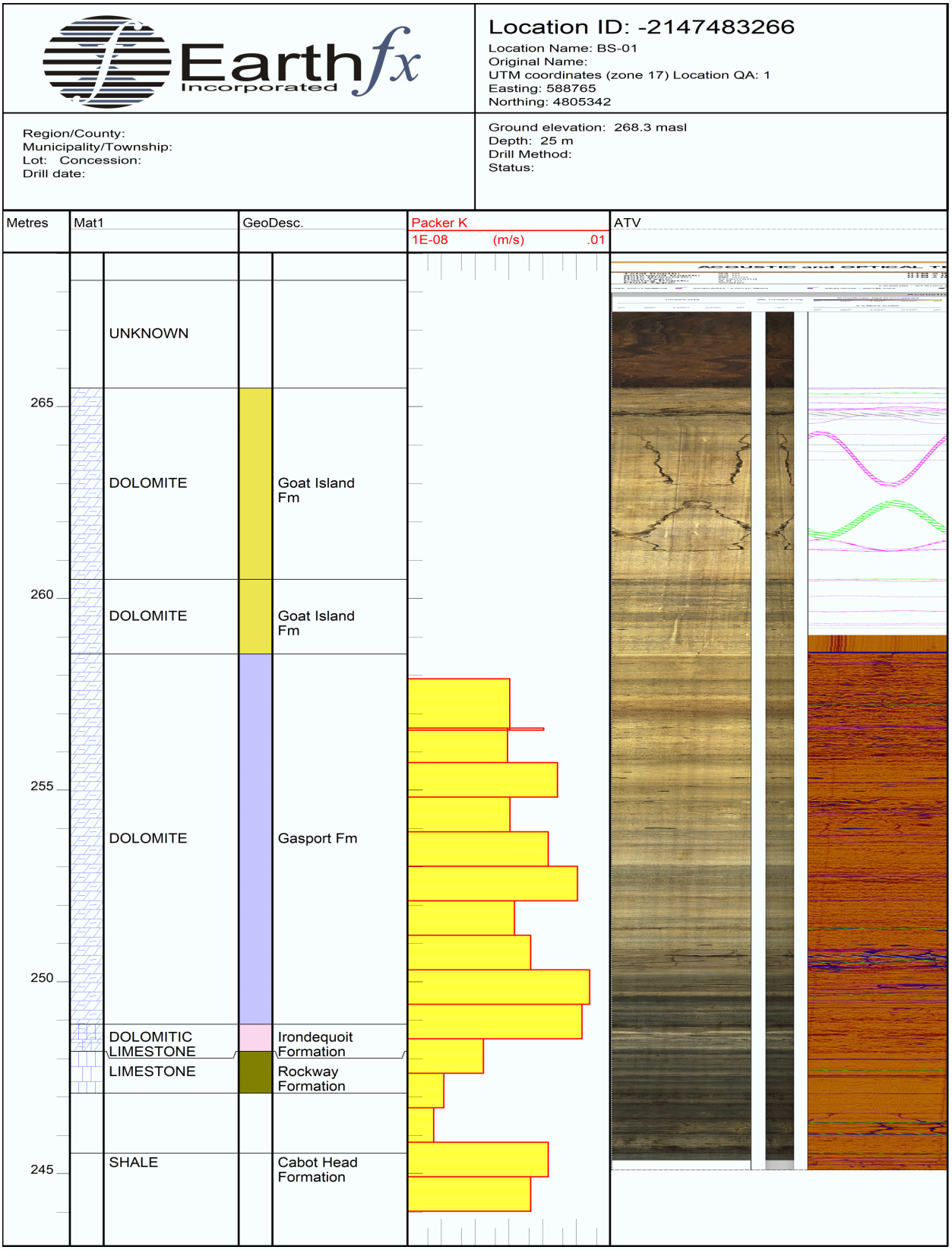

Figure 3.25: BS-01 Borehole log showing the Goat Island Formation.

3.5 Quaternary Geology

Quaternary geology was mapped for the Hamilton NTS map by P.F. Karrow (1987). The map was included in the OGS digital compilation map of southern Ontario Quaternary geology (OGS, 2010). Surficial geology for the study area, based on OGS (2010), is shown in Figure 3.26.

Like all of southern Ontario, the study area was repeatedly glaciated during the Pleistocene Epoch, although locally, there is only clear evidence for glacial activity during the Wisconsinan, the final major glacial episode. Regionally, sediments of Quaternary age form a complex blanket of unlithified deposits on the bedrock surface. Most of these sediments were deposited either directly from glacial ice, in meltwater streams, or in ice-marginal or ice-dammed lakes. The pattern of glaciation in the Great Lakes region is typically lobate, with relatively thin glacial ice flowing from the north and also filling the lake basins (including the Lake Ontario basin) and then spreading out radially.

Sediments in the study area are primarily Late Wisconsinan to Recent in age. The primary till unit is the Halton Till (Port Huron phase). West of the study area, the older Wentworth Till was deposited in the late Port Bruce to early Mackinaw phases and outcrops as large westerly-trending drumlins. Both of these tills were deposited by ice flowing westward out of the Lake Ontario basin.

3.5.1 Halton Till

The Halton Till ranges texturally from a loam to silty clay matrix and is far less stony than the Wentworth Till (White, 1975 and Karrow 1987 and 2005). It outcrops in most of the study area, including above and below the Niagara Escarpment. The till forms a series of north-northeast trending recessional moraines known as the Waterdown Moraines (Karrow, 1987). The first Waterdown Moraine ridge, west of the study area, marks the western limit of the Halton Till advance.

The Halton Till is patchy throughout the study area, generally filling depressions in the bedrock surface (Figure 3.27). The till forms an effective aquitard where present. Golder (2006) studied the properties of the Halton Till in the South Extension Area for the purpose of evaluating the hydraulic connection between the wetlands and the groundwater levels in the bedrock. Golder (2006, p. 6) found that the presence of silty clay in the sediments effectively limited the interaction between the surface and groundwater systems.

3.5.2 Mackinaw Interstadial Sediments

During times of glacial recession, the area was affected by ice-marginal and ice-dammed lakes, such as Glacial Lake Whittlesey and Lake Peel (see Chapman and Putnam, 1984 and Barnett, 1992). Glaciolacustrine sediments of probable Mackinaw Phase age were locally deposited above the Wentworth Till, or directly on bedrock. These deposits range from fine sand to stratified silts and clays. Coarse-grained glaciofluvial deposits, mapped in the center and west of the study area, are thought to be of similar age and locally appear to overlie or flank deposits of Wentworth Till (Karrow, 1987) and infill the Medad Valley. Collectively these deposits are referred to here as the Mackinaw Interstadial Sediments (MIS) sands, but they are time-coincident with the Maple Formation of Georgetown and the Oak Ridges Aquifer Complex (ORAC) to the northeast.

The total thickness of the MIS sands is shown in Figure 3.28. In general, these units are very thin in the vicinity of the extension areas. While there are limited data in the Medad Valley, there is some evidence that the sand deposits are thicker in the valley to the north and south of the site.

3.5.3 Postglacial lacustrine sands

Postglacial lacustrine sands are found at surface in the westernmost portion of the study area, locally overlying both the Wentworth and Halton tills in the central part of the study area, and partly blanketing the Waterdown Moraines. Other postglacial surficial deposits include organic deposits in wetland areas and alluvium along parts of Bronte Creek and lower Grindstone Creek.

3.6 Stratigraphic Interpretation - Conclusions

While the stratigraphic interpretation of the sediments in the study area is complex and continues to evolve, the stratigraphy in the quarry vicinity can be summarized rather simply: there is a thin cover of silty clay (Halton Till), overlying the 25 m thick Amabel Dolostone unit with some intervening, discontinuous MIS sands. The Amabel Formation forms the principal aquifer in the area and is also a key aggregate resource. The Amabel Formation and all lower bedrock units dip southwest toward the Medad Valley. Finally, the Cabot Head Formation shales form a low permeability base to the main groundwater flow system.

The hydrostratigraphy of the study area, including the effects of fracturing and karst, is discussed in Section 5.

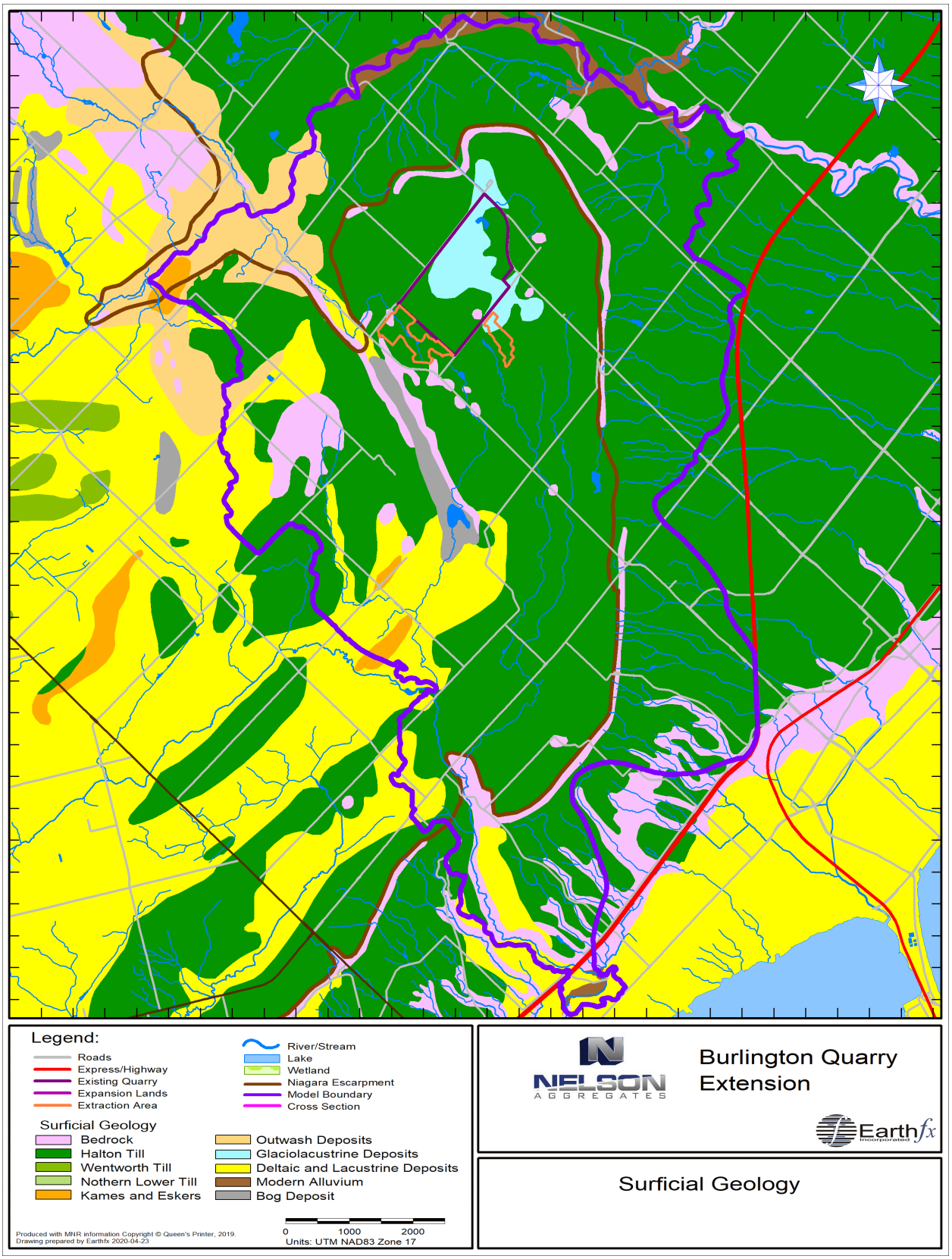

Figure 3.26: Surficial geology (data from OGS, 2010).

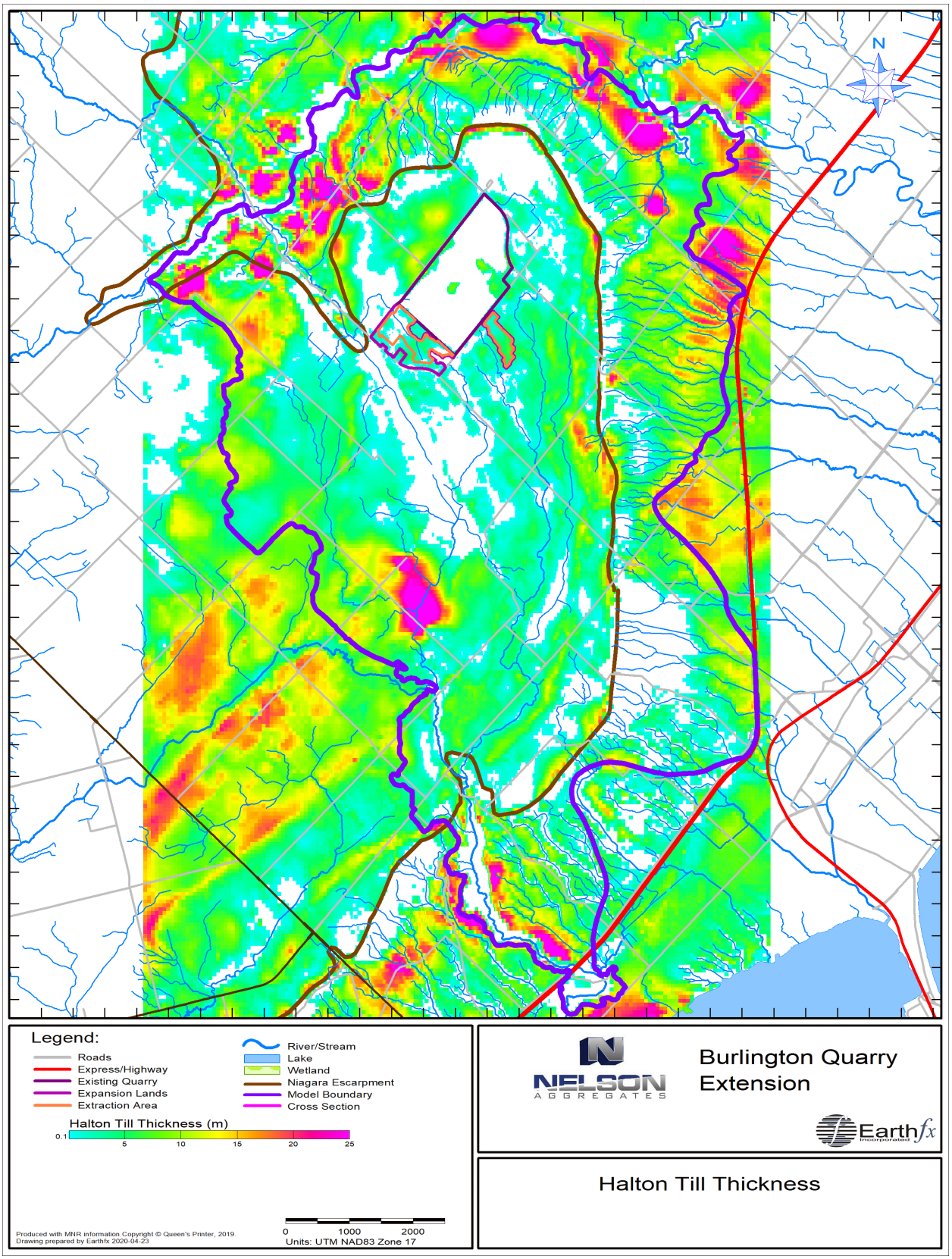

Figure 3.27: Thickness of the Halton Till (m).

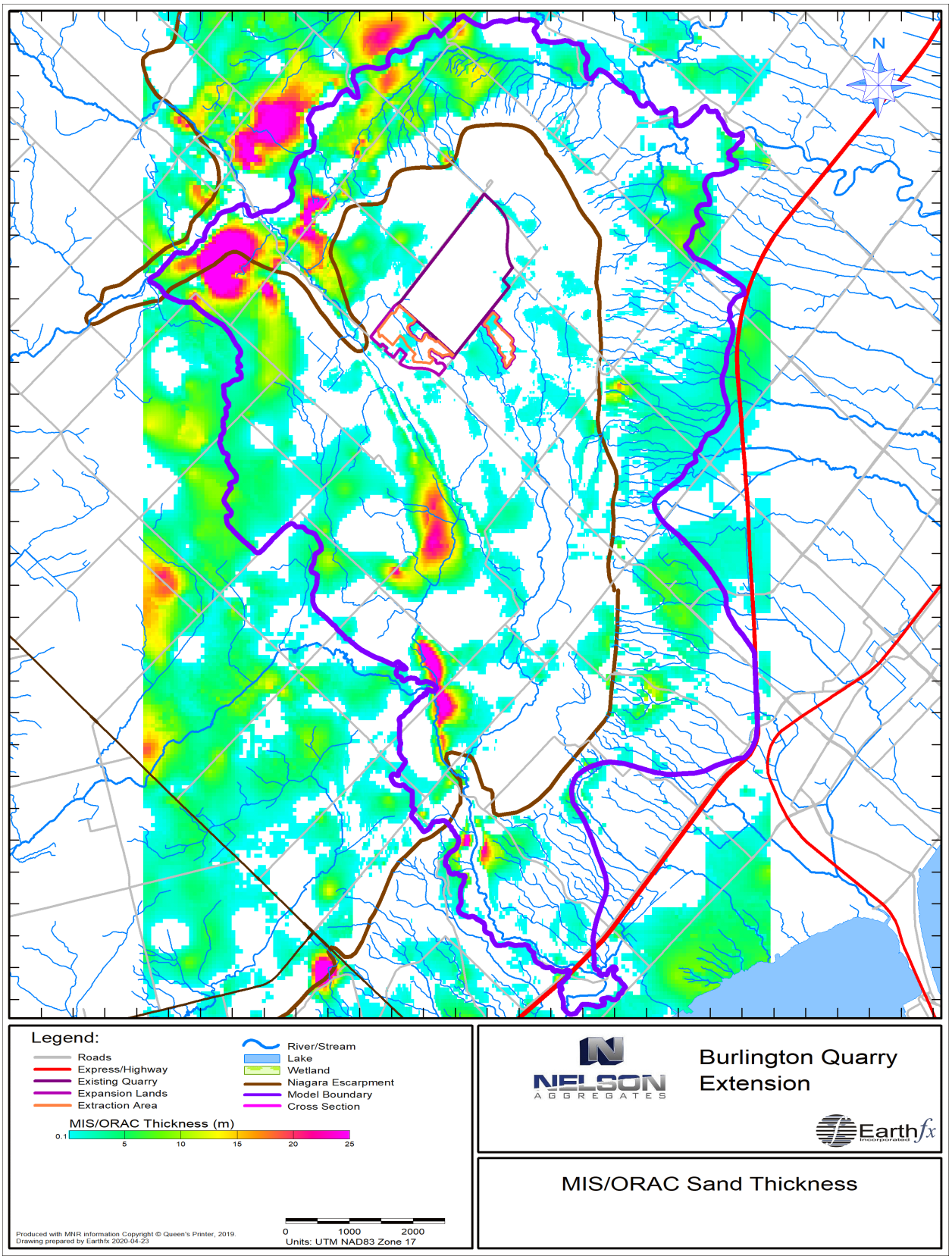

Figure 3.28: Thickness of MIS sands above the Niagara Escarpment and ORAC sands below (m).

4 Hydrologic Setting

A detailed analysis of the surface water hydrology of the Burlington Quarry site and extension lands has been prepared and submitted in a companion document (Tatham Engineering, 2020). The following discussion builds on the field data and analyses presented in the Tatum Engineering report and presents a synthesis of the hydrologic, hydraulic, and climate data needed to construct the integrated surface water/groundwater model for the study area. The integrated GSFLOW model is described further on in Section 6.

4.1 Climate

Three main climate datasets were analysed to characterize the climate of the study area. The datasets include 1) precipitation, 2) maximum and minimum daily air temperature, and 3) net incoming solar irradiation. Climate data used for this study have been compiled primarily from Environment Canada's Atmospheric Environment Service (AES). Data from the University of Waterloo, The University of Toronto, York University, and the Grand River Conservation Authority (GRCA) were used to supplement the solar radiation data when AES data were unavailable.

4.1.1 Precipitation and Temperature

Precipitation and temperature data, collected at Environment Canada AES stations proximal to the study area, were obtained and reviewed. Figure 4.1 shows a subset of the stations within a 25 km radius of the study area. The period of record varies among the available climate data sources; however, it was possible to prepare a continuous climate dataset beginning in water year (WY) 1951 through WY2019 (note: water years begin on October 1 of the preceding calendar year). A total of 121 stations proximal to the study area had records for some or all of this time period. The period of record of each of the 121 stations is shown in Figure 4.2. Figure 4.1 also shows the small number of currently active stations within 25 km of the site.

Figure 4.3 presents the annual average precipitation observed in the study area for a 69-year period showing long-term trends and the number of available stations. As can be seen, the number of available stations has declined steadily since 1970. The annual data shows considerable variation, but, overall, the 7-year average is fairly consistent. The last 50 years have been wetter, on average, than the previous 50 years. Figure 4.4 shows the same estimate broken into precipitation forms (i.e., rain and snow). Measured average annual precipitation between WY1951 and WY2019 was 853 millimetres per year (mm/yr) with a range in values between 655 and 1172 mm/yr. Figure 4.5 presents the average annual temperature over the same time period. The average annual temperature over the 69-year period was 7.7 ºC. The running average shows a rise in the late 1990s, but average temperatures have been steady over the last 25 years.

Measurements recorded at each climate station were processed to generate an estimate of the spatial distribution of both precipitation (broken into rain and snow) and temperature on a daily basis for use as inputs for the integrated GSFLOW model. Station data were interpolated to a 500 m grid using an inverse-distance weighting technique. The average annual precipitation and temperature are shown in Figure 4.6 and Figure 4.7, respectively. The precipitation distribution shows a decreasing trend from west to east. This behaviour may be related to the Niagara Escarpment, where lower elevations tend to receive less precipitation. Unfortunately, the station density near the Escarpment is low, making it difficult to confirm this phenomenon. Temperature tends to decrease in a southeasterly direction and may also be inversely related to topography with lower temperatures corresponding to higher elevations.

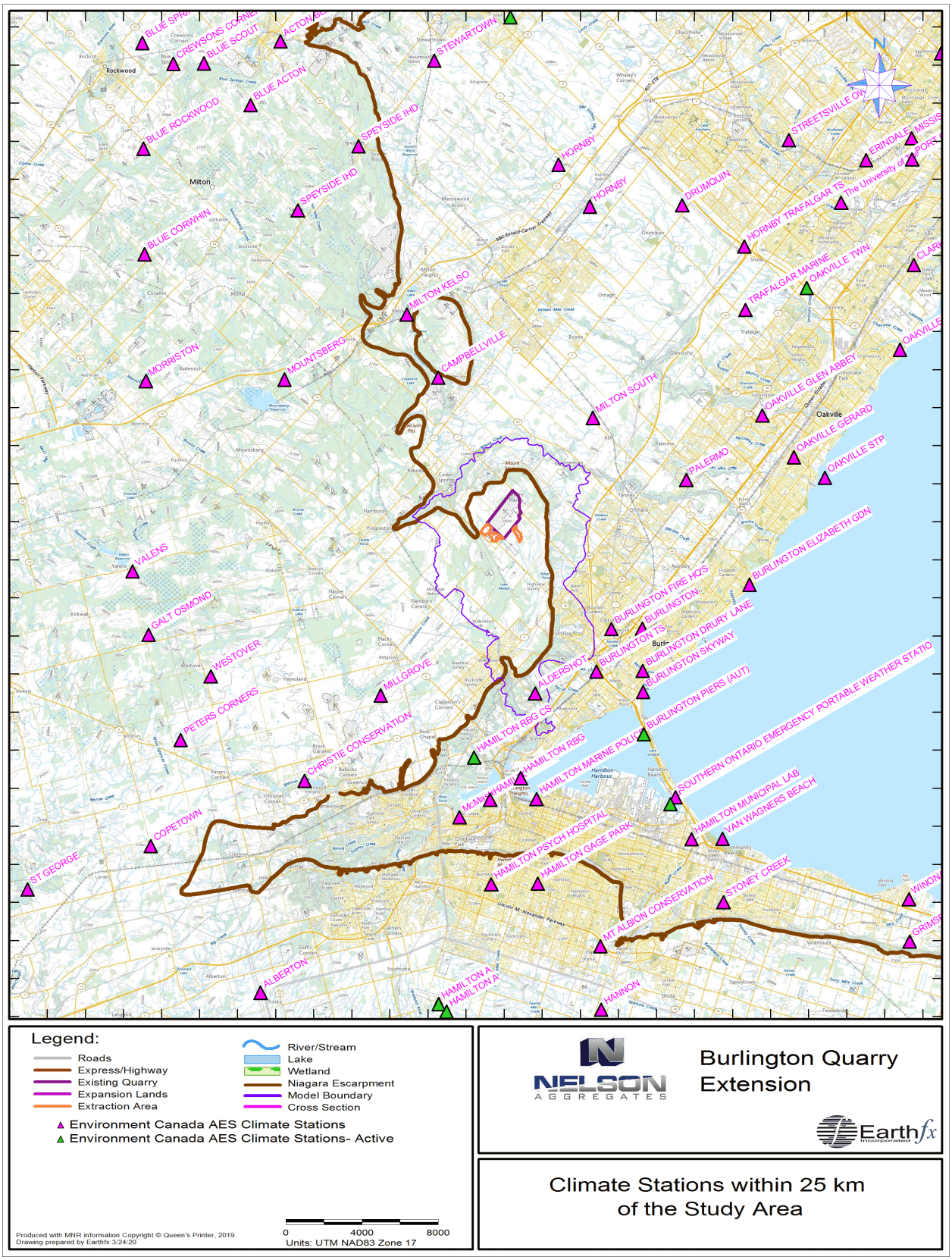

Figure 4.1: Environment Canada climate stations within about 25 km of the Burlington Quarry.

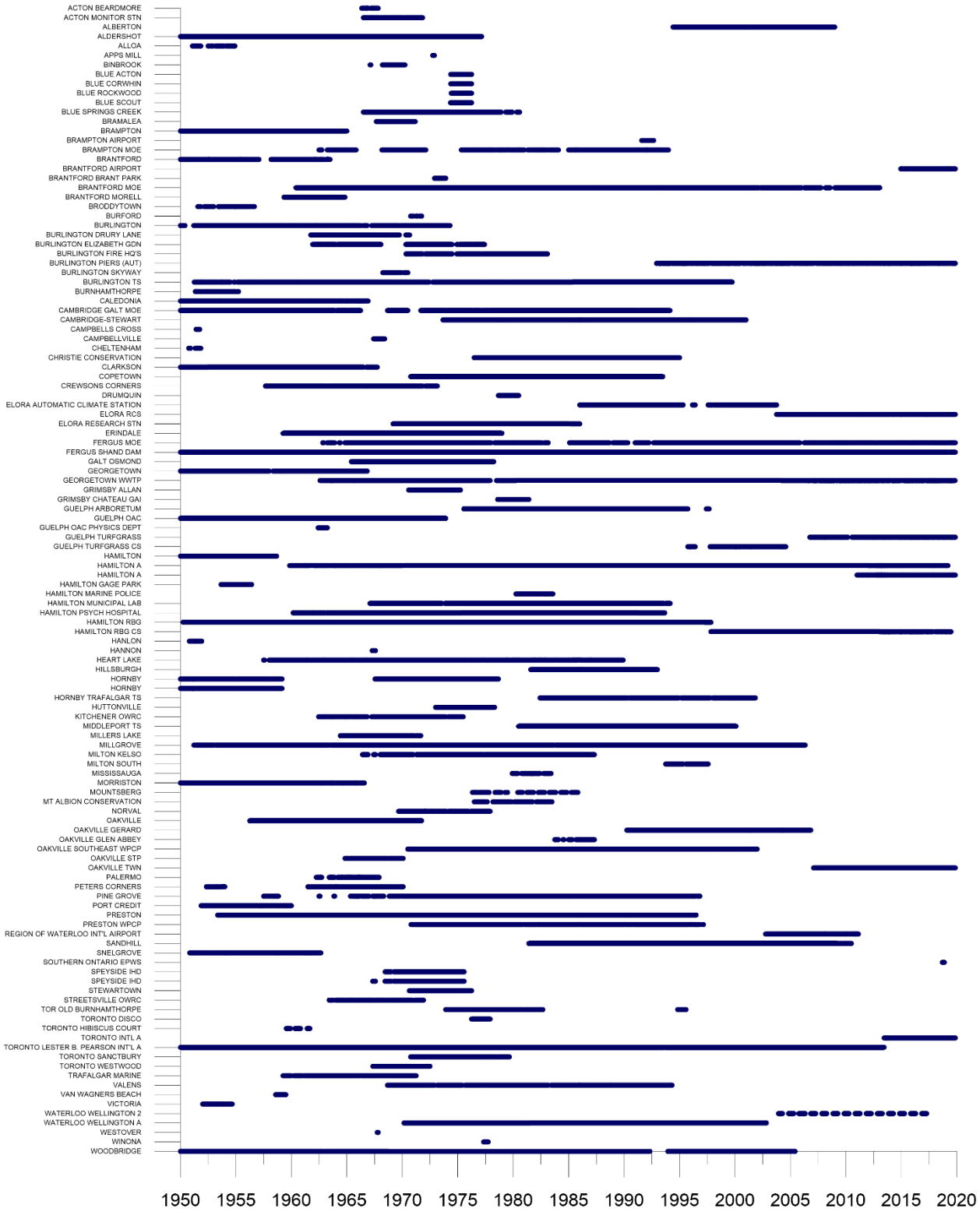

Figure 4.2: Period of record of climate stations proximal to the study area.

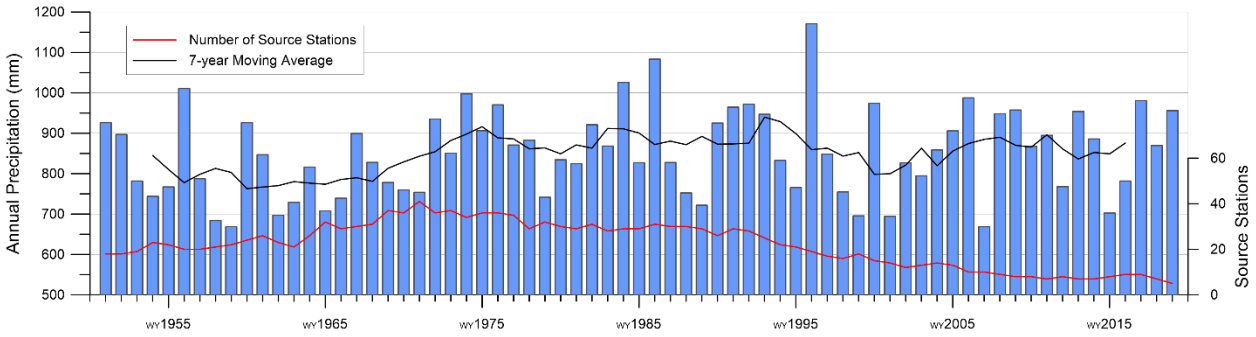

Figure 4.3: Average annual precipitation from WY1951 to WY2019 with the total number of reporting stations.

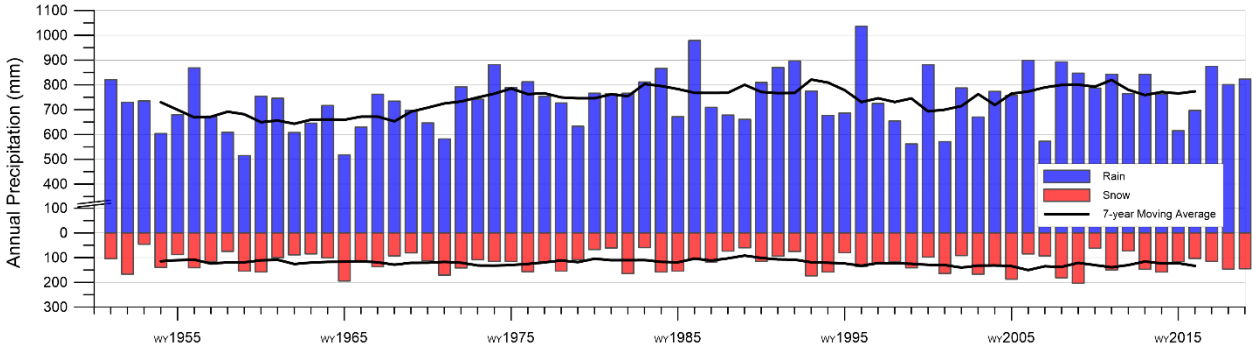

Figure 4.4: Average annual rain and snow from WY1951 to WY2019.

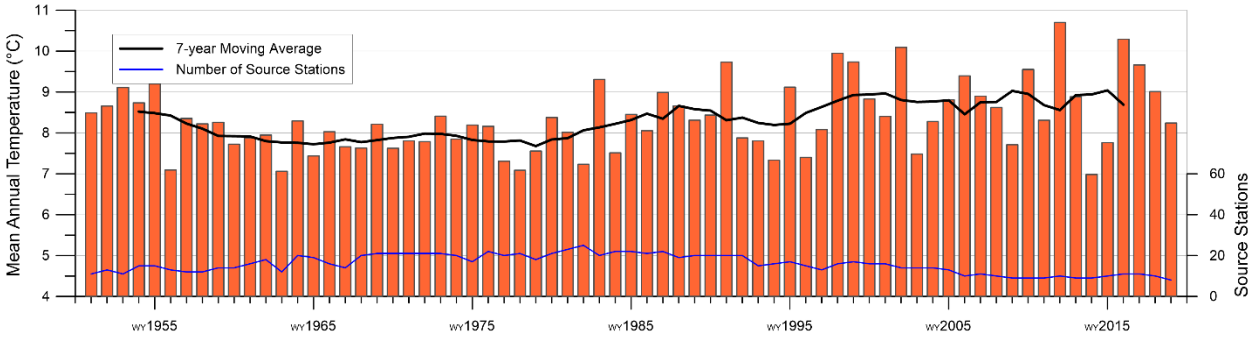

Figure 4.5: Average annual temperature from WY1951 to WY2019 with the total number of reporting stations.

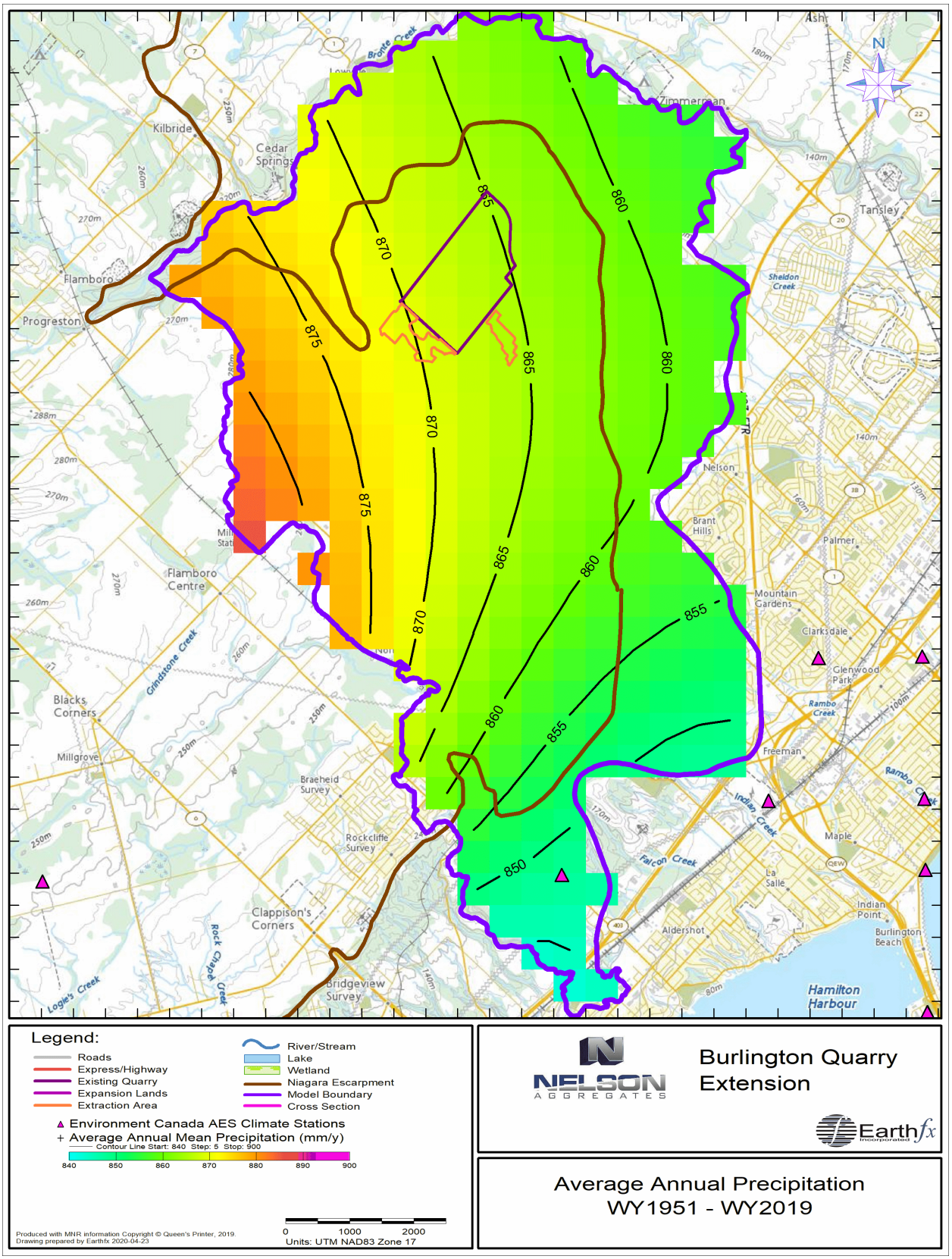

Figure 4.6: Interpolated average annual precipitation WY1951 – WY2019.

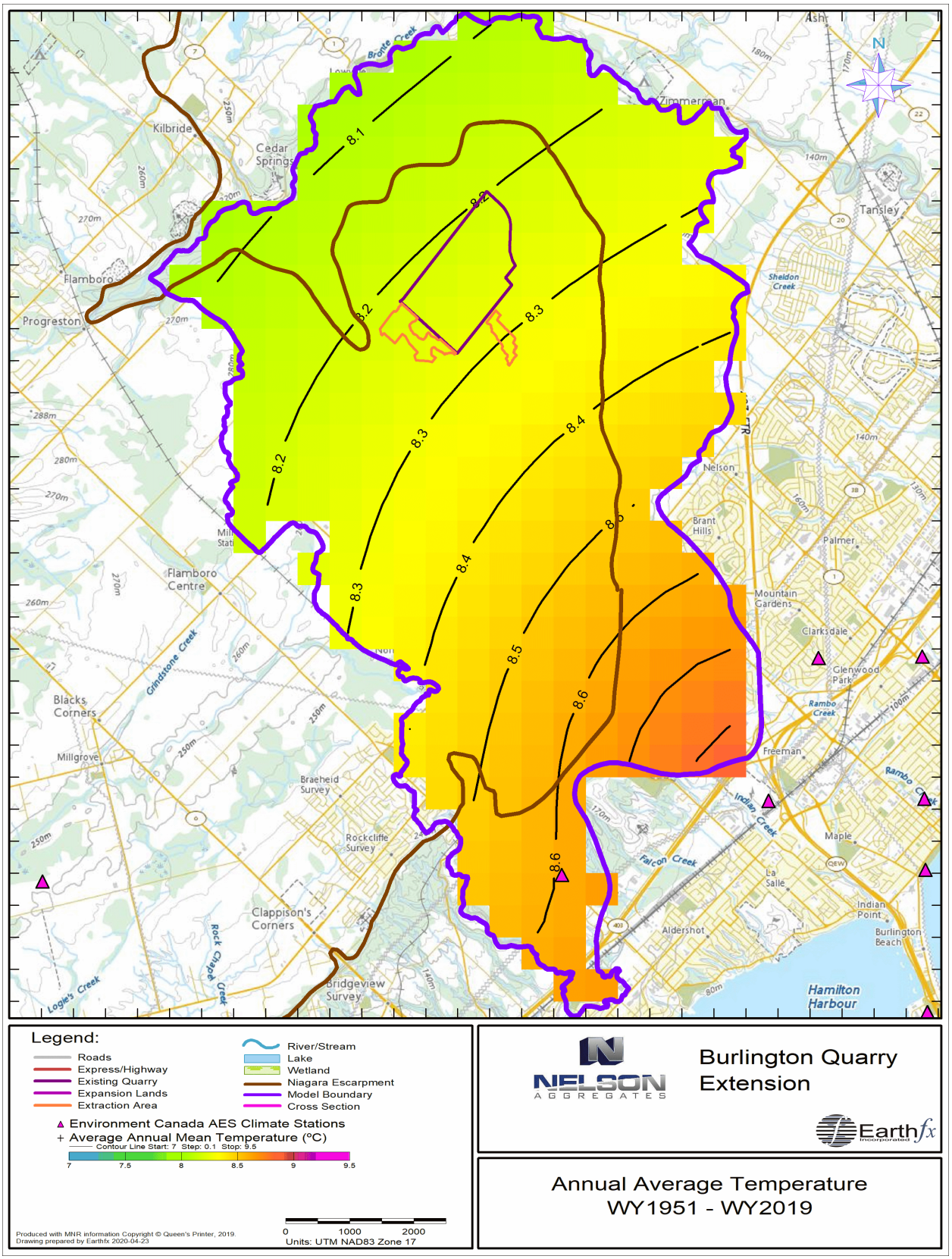

Figure 4.7: Interpolated annual average temperature WY1951 – WY2019.

4.1.2 Solar radiation

Incoming solar radiation is controlled primarily by the number of possible hours of sunshine per day and the percent cloud cover. Solar radiation data are collected at very few stations in Ontario; therefore, the data have to be compiled from a variety of sources. Through linear regression analysis, it was shown (Earthfx, 2010) that the widely-separated Ontario solar radiation stations exhibited good inter-station correlation. Accordingly, a continuous dataset was created by averaging and infilling of daily solar radiation information from 11 southern Ontario stations.

The incoming solar radiation dataset was based primarily on the average of measurements from four climate stations maintained by EC between 1956 and 2003. These stations include: 611KBE0 (Egbert CARE); 6142285 (Elora Research Station); 6158350 (Toronto); and 6158740 (Toronto MET Research Station). The period of record of these four sites only extends to August 31, 2003; therefore the remaining data up to 2019 had to be infilled using a combination of measurements from the University of Waterloo, York University, University of Toronto Mississauga campus, and the Burford Tree Farm (GRCA). Where direct observations were unavailable, solar radiation was estimated by the Hargreaves and Samani (1982) method, which uses the daily minimum and maximum temperatures.

4.2 Land Use and Soil Properties

Land use or land cover, along with surficial soil properties, are important to the hydrologic function of the study area because they influence the rates of overland runoff and evapotranspiration. The primary source for land use/land cover data was the Southern Ontario Land Resource Information System (SOLRIS v3, MNRF, 2019) (Figure 4.8). The source of the surficial soil mapping was the Ministry of Natural Resources Soil Survey Complex (v.4, MNR, 2013) (Figure 4.9). (Please note that the MNR changed its name to MNRF in 2014).

The land use and land cover in the study area ranges from urban development to natural forests and wetlands. Land use in the vicinity of the Burlington Quarry is dominated by agriculture and undifferentiated open fields. There are also several wetland areas adjacent to the quarry and in the Medad valley. As a result, overland runoff is mainly limited by the plant canopy interception, infiltration capacity of the soils, and by local depressions in the topography, rather than imperviousness. Surficial soils are widely classified as loam with varying degrees of sand and silt. As a result of the diverse range in land use and soil type, the hydrologic response of the study area is expected to vary spatially with more runoff being generated on clay soils and in urban areas.

4.3 Surface Water Resources

Surface water data from several sources, including streamflow measurements, previous modelling efforts, and surface feature mapping, were compiled. Stream networks were mapped and classified using streamflow mapping by the Halton and Hamilton Conservation Authorities, while lakes and wetlands were obtained from the MNRF Ontario Hydro Network (OHN) V1.2 coverage. The collected stream, lake, and wetland coverage was processed and is illustrated on Figure 4.10. Also shown are the locations of the Environment Canada - Water Survey of Canada stream gauges and the quaternary watershed boundaries within the study area.

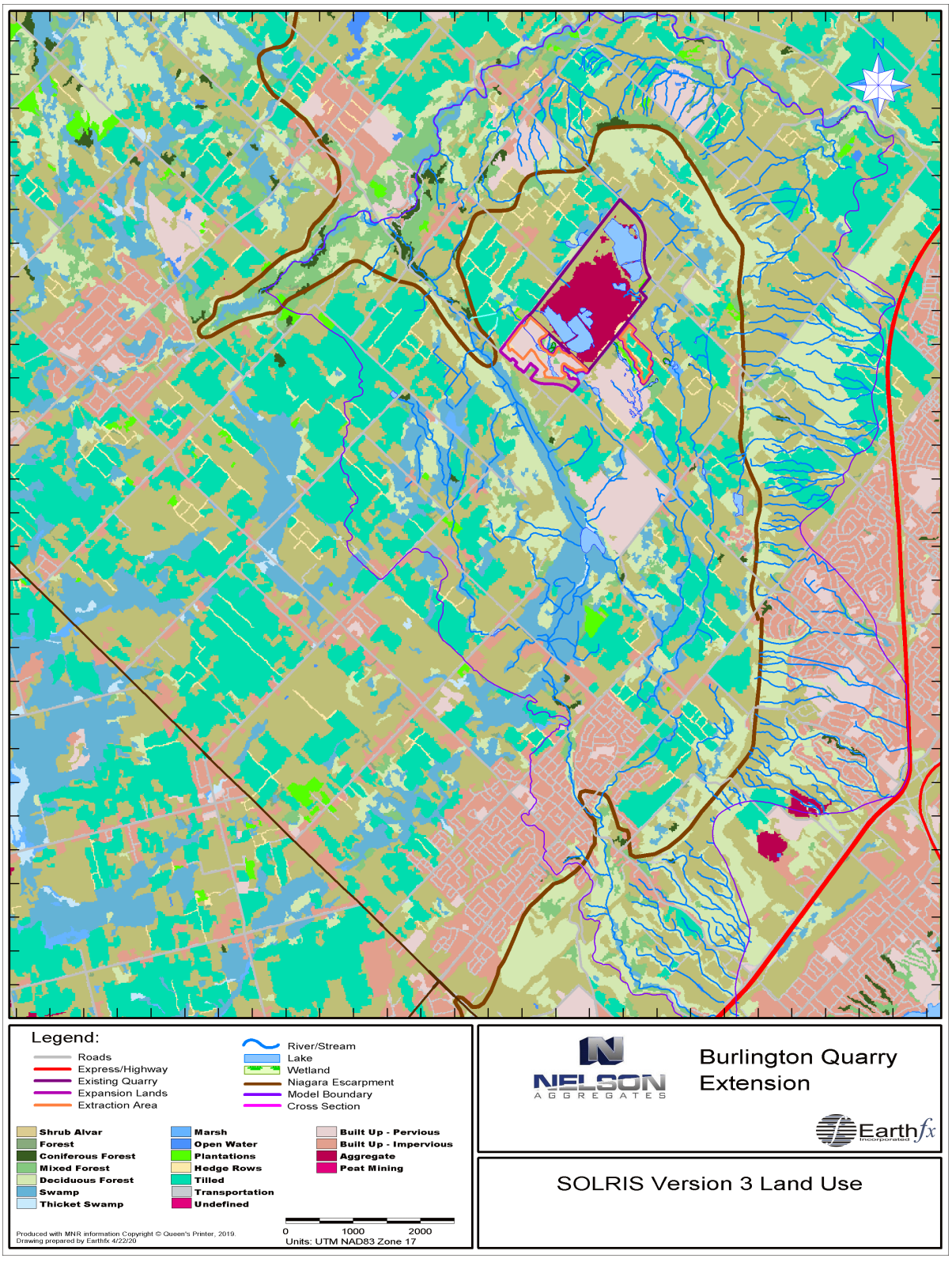

Figure 4.8: SOLRIS v3 (after MNRF, 2019) land use classification.

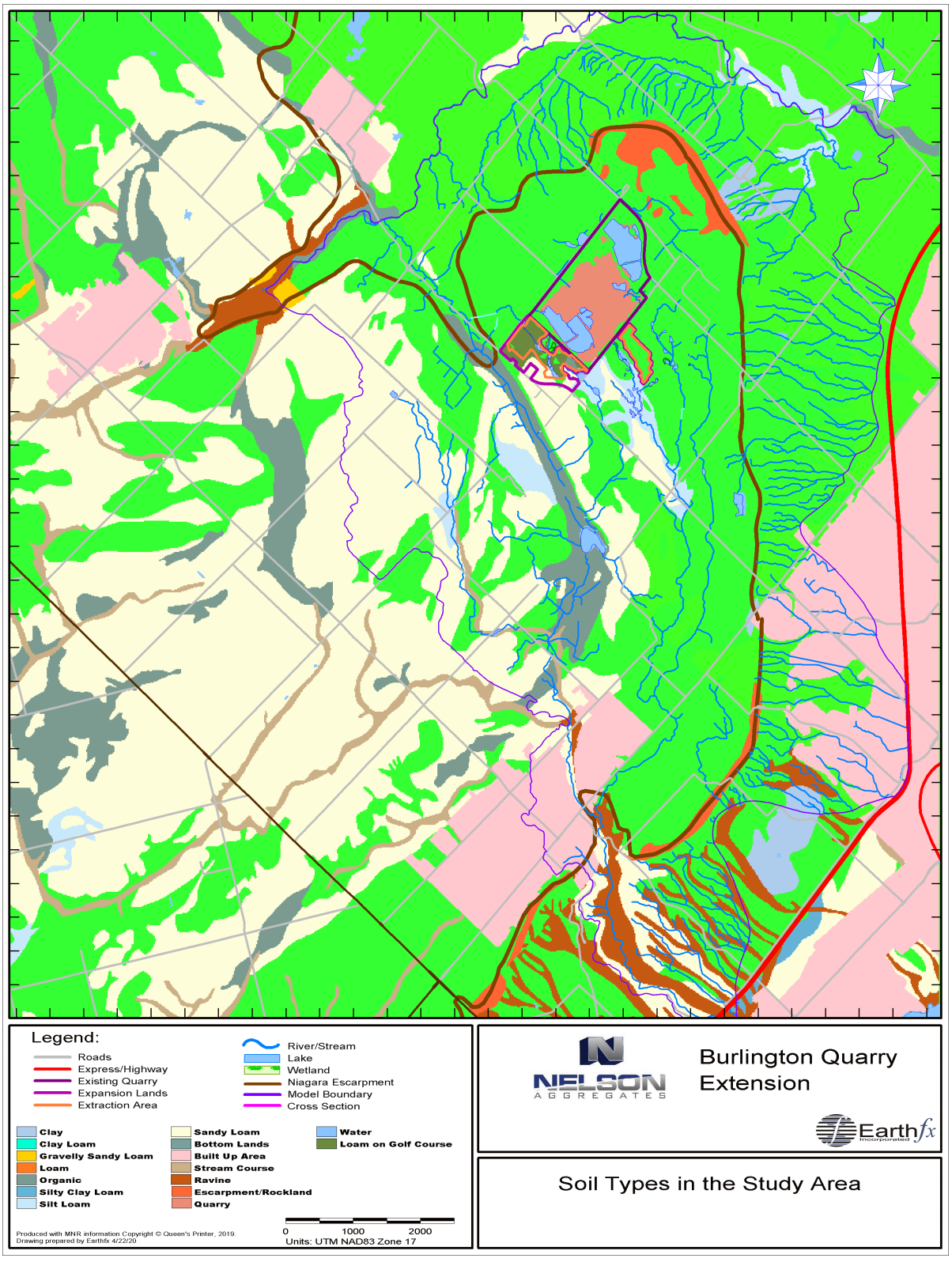

Figure 4.9: Surficial soil complex mapping (after MNR, 2013).

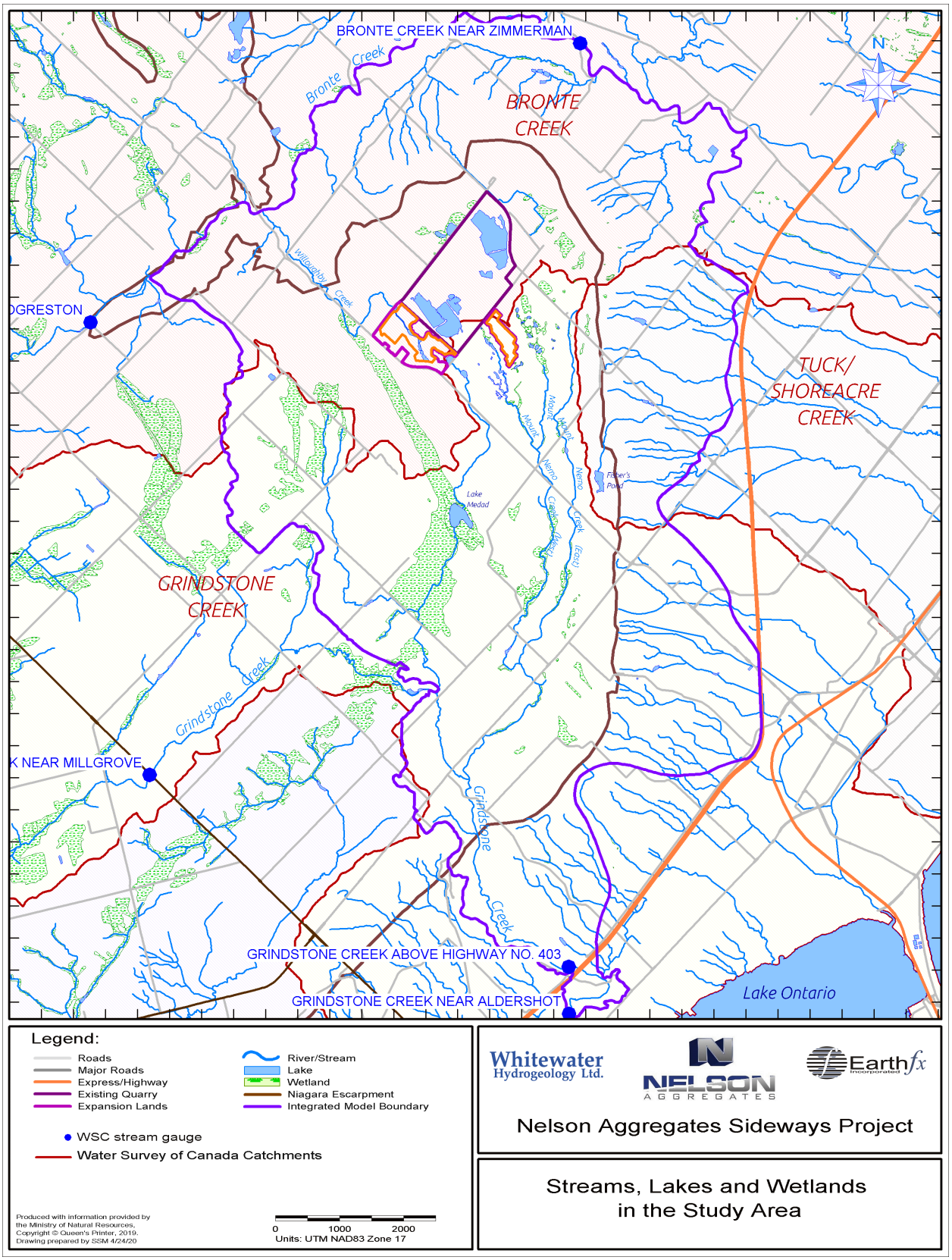

Figure 4.10: Streams, lakes, and wetlands in the study area.

4.3.1 Stream Network and Streamflow

The study area occupies several watersheds with the Burlington Quarry straddling the watershed divide separating Bronte Creek and Grindstone Creek (see Figure 4.10). The Burlington Quarry discharges to the north, to Willoughby Creek (a tributary to Bronte Creek), and to the south, to the west branch of Mt. Nemo Creek, which discharges to Grindstone Creek (see Section 4.3.5). The majority of the streams that contribute to Bronte Creek within the study area are located below the Niagara Escarpment. Several other streams originating below the Escarpment also contribute to the Tuck Creek/ Shoreacre Creek watershed.

Grindstone Creek flows over the Niagara Escarpment in Waterdown at Smokey Hollow Falls, where it continues south to Lake Ontario. A WSC (02HB012) gauge is located in Aldershot and captures the majority of the flow in the watershed, with the exception of some lower-order streams that bypass the gauge and discharge directly to Lake Ontario. While several small headwater tributaries of Grindstone Creek originate southeast of the Burlington Quarry, the large majority of the flow comes from the western portion of the watershed, outside the study area. The main branch of Grindstone Creek enters the study area north of Waterdown at Parkside Drive. Figure 4.11 and Figure 4.12 show the daily observed streamflow and log streamflow, respectively, at the Aldershot gauge. Flow in Grindstone creek at Millgrove (02HB028) is also shown on the graphs to illustrate that much of the flow at the Aldershot gauge originates in the western part of the watershed, outside the study area. Comparison of Figure 4.3 and Figure 4.11 shows that trends in streamflow appear to correlate well with the observed trends in precipitation.

4.3.2 Karst Sinks and Springs

An investigation of local karst features was prepared by Worthington Water (2006, 2020). Karst features have been identified north, south, and west of the Burlington Quarry. Information on the location of sinks, springs, and disappearing streams was incorporated into the construction of the integrated model. Details on how the karst sinks and springs were represented in the model can be found in Section 5.2.4.

The goal of the karst investigation was to (1) document the presence of surficial karst features that are relevant to hydrogeologic processes such as sinking streams, springs, and discharges from quarry walls; (2) to carry out subsurface investigations to characterize the apertures and spacing of solutionally-enlarged fractures; and (3) interpret the results to explain how water flows through the dolostone aquifer (Worthington, 2020). The study results concluded that, except for the sink to west of the West Extension lands and the sink and springs along the east arm of the west branch of Mount Nemo Creek, there is a notable absence of surface karst features in or adjacent to the extension areas. This is in marked contrast to areas close to the Niagara Escarpment, where the overburden in thinner and surface karst features are common.

The karst investigation also concluded that a dense network of solutionally enhanced fractures is likely present in the underlying bedrock. Worthington Groundwater (2020) suggests that treating the aquifer as an equivalent porous medium is reasonable for steady-state groundwater flow modelling; however, transient modelling of flow is more complicated because of the dominance of fracture flow over the short-term such term while the effects of water released from or contributing storage in the bulk matrix over the longer term (e.g., due to seasonal or inter-year changes in recharge) are significant. Section 5.2.5 discusses numerical model refinements implemented to better represent the function vertical and horizontal fractures and solution enhancement.

4.3.3 Lakes and Ponds

Lake Ontario represents the regional topographic low elevation and is the ultimate discharge point of all the major streams in the study area. Most of the lakes or ponds in the area are relatively small, comprising only a few hectares or less. Of these small features, Lake Medad is the most notable because it is located within an Area of Natural and Scientific Interest (ANSI). The 8-hectare (ha) lake is located approximately 2 km south of the Burlington Quarry in the Medad Valley (Figure 4.10). The lake is a discharge point for several groundwater springs and small tributaries. Lake Medad drains to the south and ultimately reaches the main branch of Grindstone Creek. Fisher's pond is another small (3-ha) named feature located approximately 2.7 km southeast of the Burlington Quarry, near the edge of the Niagara Escarpment.

Many other small un-named natural and man-made features also exist in the study area, including a series of golf course ponds located in the western extension lands. These ponds are man-made features designed to store irrigation water for the Burlington Springs Golf Course.

Also shown in Figure 4.10 are unmapped irrigation ponds on the Burlington Springs Golf Course and the quarry ponds in the base of the Burlington Quarry. These ponds do not show on the OHN mapping and were added manually from aerial photography. The discrepancy between the OHN mapping and the observed golf course and quarry ponds is due to the time period in which the OHN study was completed and the fact that the quarry ponds have changed location and shape over time.

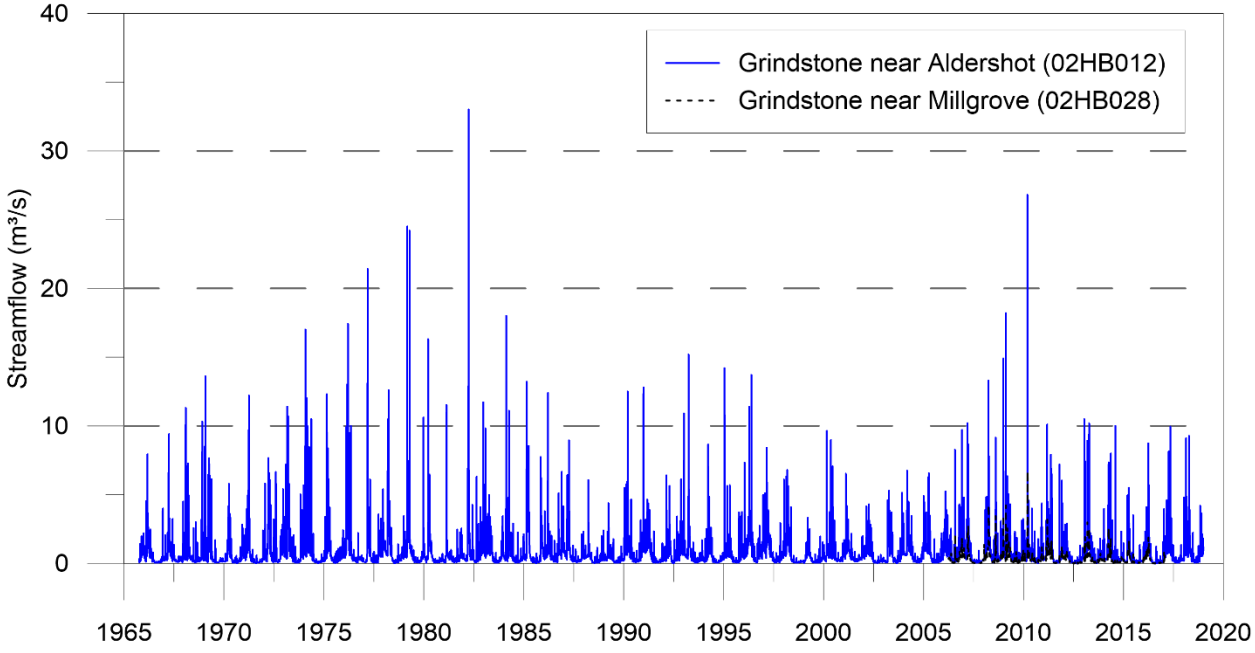

Figure 4.11: Daily measured streamflow at Grindstone Creek near Aldershot (02HB012) and Grindstone Creek near Millgrove (02HB028).

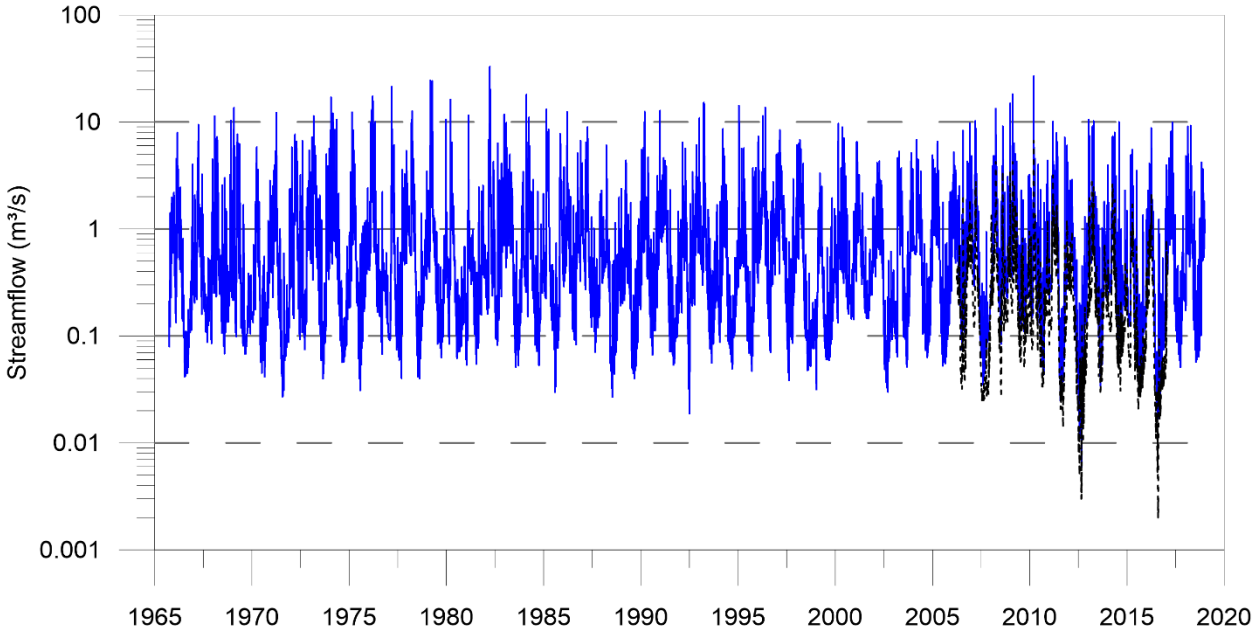

Figure 4.12: Daily measured log-streamflow at Grindstone Creek near Aldershot (02HB012) and Grindstone Creek near Millgrove (02HB028).

4.3.4 Wetlands

There are several wetlands and wetland complexes within the study area, most of them located above the Niagara Escarpment and within the lowlands between the ridges of the Waterdown Moraines or within the Medad Valley. Figure 4.10 displays all of the mapped wetlands in the study area. The largest of the wetlands is found in the Medad Valley and is classified as both a PSW and an ANSI. Several other large PSWs belonging to the Flamborough Centre Complex are located west of the Medad Valley. Clusters of smaller PSWs are also located to the southeast of the existing Burlington Quarry and further south, near Waterdown. A detailed evaluation of the significance and function of key wetlands is presented in a companion report (Tatham Engineering, 2020) and in the natural heritage report (Savanta, 2020).

4.3.5 Surface Water Takings and Diversions

Surface water takings in the province are governed by the Ontario Water Resources Act (OWRA) and the Water Taking Regulation (O. Reg. 387/04); a regulation under the OWRA. Section 34 of the OWRA requires anyone taking more than a total of 50,000 litres of water in a day to obtain a PTTW from the MECP. A detailed review of the permitted surface water takings within 5 km of the Burlington Quarry was completed.

The study area contains six permitted surface water takings, all related to golf course operations. Two of the surface water permits are above the Niagara Escarpment; (1) the adjacent Burlington Springs golf course and (2) the Hidden Lake golf club, which draws water from Lake Medad.

The Burlington Quarry is permitted under PTTW No. 96-P-3009 to discharge water off-site through two locations. Note that while the quarry discharges to surface water, the permit is classified as a groundwater source. This permit is discussed in Section 5.4.

4.4 Surface Water Investigations: Overview

Streamflow Monitoring: A streamflow monitoring program was executed by Tatham Engineering and summarized under separate cover Tatham Engineering (2020). Data from the monitoring sites, shown in Figure 2.2, and in more detail in Figure 4.14, were used in the calibration of the integrated model. The figure also maps the karst features (sinks and springs) identified by Worthington Groundwater (2006, 2019) near the quarry. For a full description of the monitoring program, the reader is referred to Tatham Engineering (2020).

Bathymetry Survey: A bathymetry survey of the irrigation ponds, located on the western extension subject lands (Burlington Springs Golf Course), and key wetland features, located on the southern extension subject lands, was completed by Tatham Engineering. The bathymetry values were used to locally adjust the shallow layer elevations in the integrated model to better represent these features. For a full description of the bathymetry survey methodology and results, the reader is referred to Tatham Engineering (2020).

Wetland and Pond Water Level Monitoring: A wetland monitoring program was executed by Tatham Engineering and summarized under separate cover. Key wetlands were instrumented (Figure 4.14) with staff gauges and shallow groundwater piezometers to assess the hydroperiod and potential groundwater – surface water interactions within the wetlands. The wetland monitors served as important calibration points for the GSFLOW model. For a full description of the monitoring program, the reader is referred to Tatham Engineering (2020).

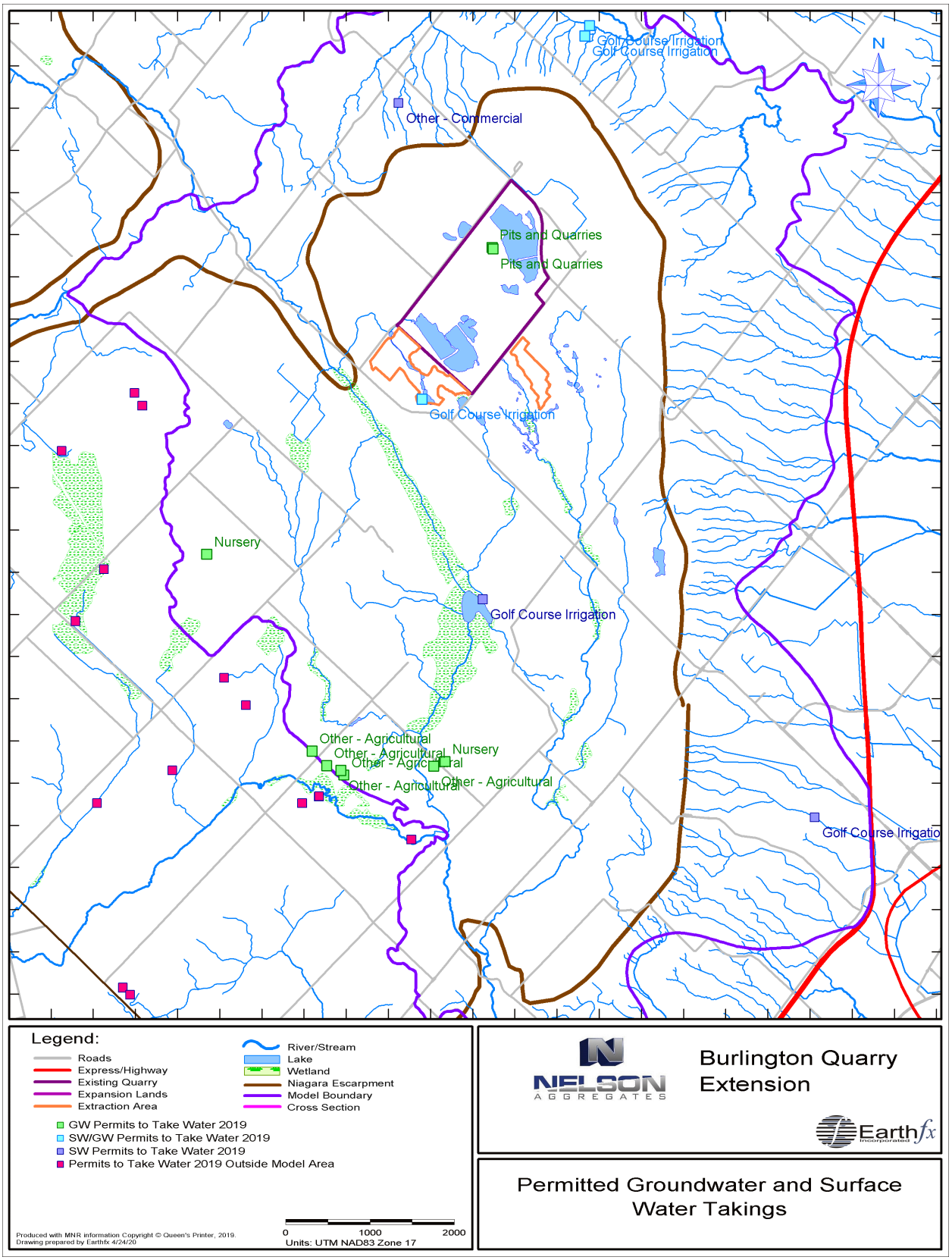

Figure 4.13: Permitted water takings in the study area.

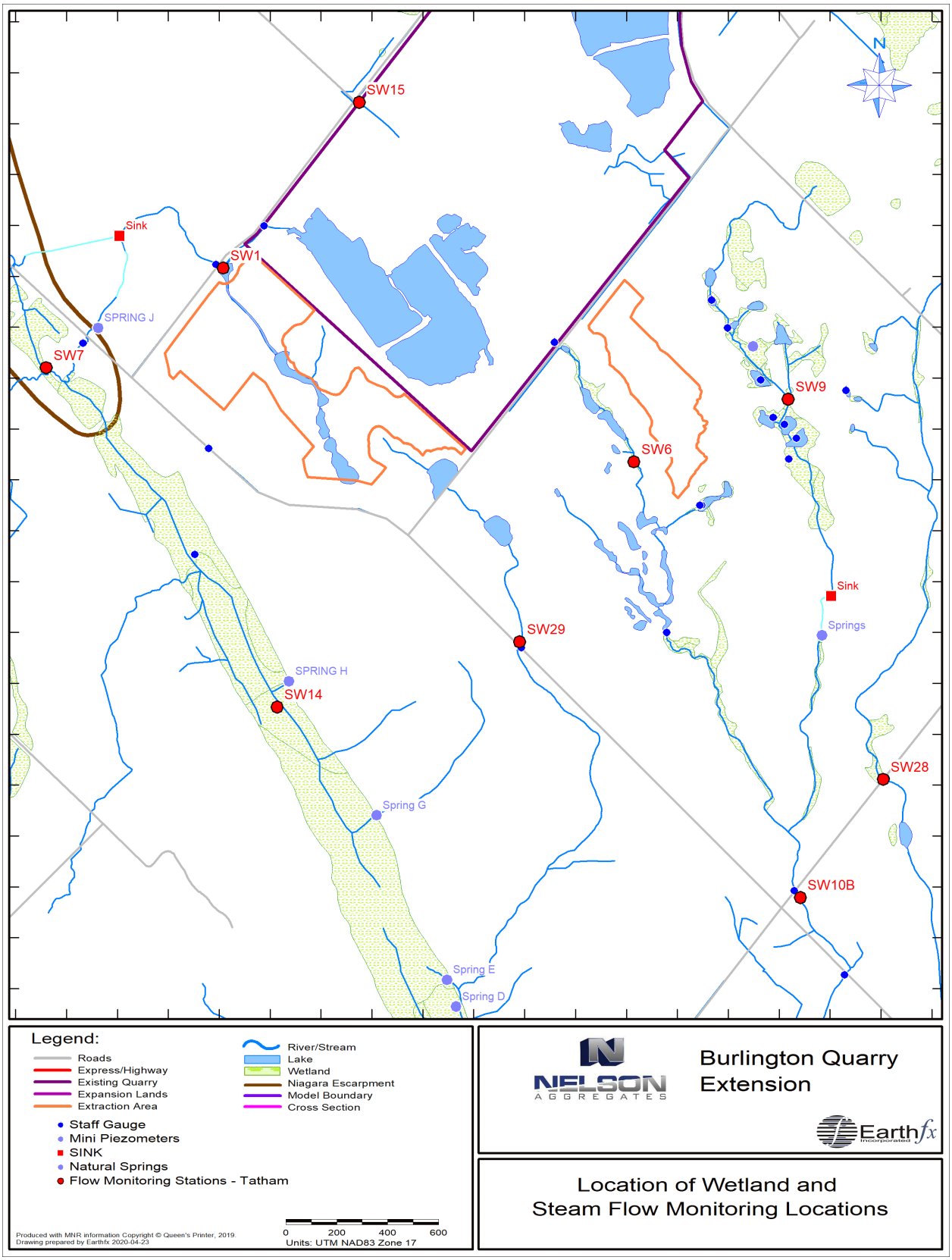

Figure 4.14: Locations of wetland and streamflow monitoring locations and karst features.

5 Hydrogeologic Setting

5.1 Introduction

The development of a numerical flow model involves a multi-stage analysis and model development process. The process begins with a conceptual description of the geologic setting and then proceeds through the development and refinement of stratigraphic, hydrostratigraphic, and finally flow model layers optimized for the numerical simulations.

A significant benefit of an integrated model-driven, quarry assessment approach is that every aspect of the surface and groundwater flow system must be described, quantified, reconciled, and assessed. The integrated numerical model requires accounting for 100% of the water budget. Measured precipitation is added to the top of the model, and all surface water and groundwater flows and levels must be evaluated in a unified manner. The following describe the major model layer development stages followed in this study:

Stratigraphic Model: The stratigraphic model (presented in Sections 3.4 and 3.5) describes and represents the underlying geologic depositional and erosional history of the study area.

Hydrostratigraphic Model: The hydrostratigraphic model (presented in Section 5.2, below) describes the aquifer and aquitard layers and their hydrogeologic characteristics. For the most part, the stratigraphic model layers correspond to the aquifers and aquitards in the study area. The hydrostratigraphic model differs in that it also considers weathering, fracturing, and other processes that affect groundwater flow, so layers may be subdivided or combined as appropriate. For example, the upper bedrock surface is generally weathered, and is frequently represented as a continuous aquifer layer across all bedrock units.

Numerical Flow Model Layers: Finally, the hydrostratigraphic model is converted into a form that is suitable for input into the numerical flow model. Some modifications may be made for model efficiency and because the numerical model does not allow layers to “pinch out”. Layers must be continuous across the model domain and minor adjustments to layer properties are necessary, such as assuming a minimum layer thickness. For example, to represent the removal of materials within the quarry excavations, the tops of the shallow models model layers were shifted downward so that the top of the first layer represented the quarry floor, underlying layers were assigned a minimum thickness, and hydraulic properties were assigned to the shifted layers to match that for the aquitard layer that underlies the quarry.

5.2 Hydrostratigraphic Model Layers

A 9-layer hydrostratigraphic model was created by modifying the stratigraphic layers based on the interpretation of the hydrogeologic data and additional study area conceptualization. The surfaces represent an integrated interpretation of the borehole logs, packer test results, televiewer logs, outcrops, groundwater levels, streamflow, and other supporting information. Three overburden and six bedrock layers are described below, followed by an interpretation of the regional and local transient water level patterns.

The hydrostratigraphic layers are best illustrated on a series of cross sections through the study area (Figure 5.1). Three of the cross sections (Figure 5.2 through Figure 5.4) illustrate the broader hydrostratigraphic setting, while the remaining four sections (Figure 5.5 through Figure 5.8) are focussed on the local conditions in the extension areas.

The 2nd Side Road cross section (see Figure 5.2), which spans the Medad Valley in the west then and follows 2nd Side Road past the quarry towards the crest of the Niagara Escarpment, illustrates the general hydrostratigraphic patterns. Wells screens and open-hole intervals are found throughout the upper bedrock, and the recorded static water levels from the MECP WWIS database show high variability for several reasons. Water levels in wells less than 15 m deep and those greater than 15 m deep are shown as symbols and as potentiometric surface elevation lines on the section. In the west, the water levels drop into the Medad valley, which acts as a regional discharge area. The variable nature of the water levels reflects the fracture patterns, variable well depths, well construction effects, seasonal and inter-annual conditions at the time of drilling, and, through the middle of the section, the influence of the existing quarry.

A similar pattern can be seen in the Colling Road cross section shown in Figure 5.3. Depression of the water levels near the Medad Valley is evident, while the high shallow groundwater levels to the immediate east are likely due to leakage from the stream accepting quarry discharge (discussed in more detail below).

The third regional section follows Cedar Springs Road (Figure 5.4). The northern portion of this cross section begins in the Medad Valley and then rises to the south as the section climbs up the Escarpment. Both well depth and water levels show high variability and reflect the factors outlined above. Variability is noted in wells close to the Medad Valley but also in the middle of the section.

5.2.1 Layer 1: Post-Glacial (Surficial) Deposits

Hydrostratigraphic Layer 1 is defined as a 1 m thick layer of surficial materials that includes both weathered overburden materials and weathered bedrock (where bedrock is mapped at surface). Pond and wetland substrate materials, including organics, are also represented in this layer. Where Halton Till is at surface, Layer 1 and 2 both represent that unit with the upper layer assumed to be more weathered. Hydrogeologic property assignments are consistent with surficial geology mapping (Figure 3.26) and Layer 1 can include some surficial sands deposited on the Halton Till between the Waterdown Moraines in the southwest portion of the model. The resulting hydraulic conductivity of this layer is shown in Figure 18.11.

5.2.2 Layer 2: Halton Till Aquitard

The second hydrostratigraphic layer represents the unweathered Halton Till, which is found across the entire model area, both above and below the Niagara Escarpment. The Halton Till is a discontinuous layer (see Figure 3.27), dominated by silt, with moderate fractions of sand (~20%) and clay (~30%) (Golder, 2007). The till is of low permeability and serves to limit recharge and/or leakage to the underlying aquifers. Where the Halton Till is absent, the properties of the adjacent layers are used in the model (Table 18.4).

5.2.3 Layer 3: Mackinaw Interstadial Sediments (MIS)

Layer 3 represents Mackinaw Interstadial Sediments (MIS) that occur in limited pockets around the quarry area (Figure 3.28). The materials associated with this unit are variable in composition; however, they generally consist of glaciolacustrine and glaciofluvial sand and gravels. This unit infills the Medad Valley and can be quite thick below the Niagara Escarpment. From a functional perspective, this unit likely acts as a single aquifer in conjunction with the weathered bedrock over which it lies. The unit can be intermittently saturated depending on the relative local elevation and season.

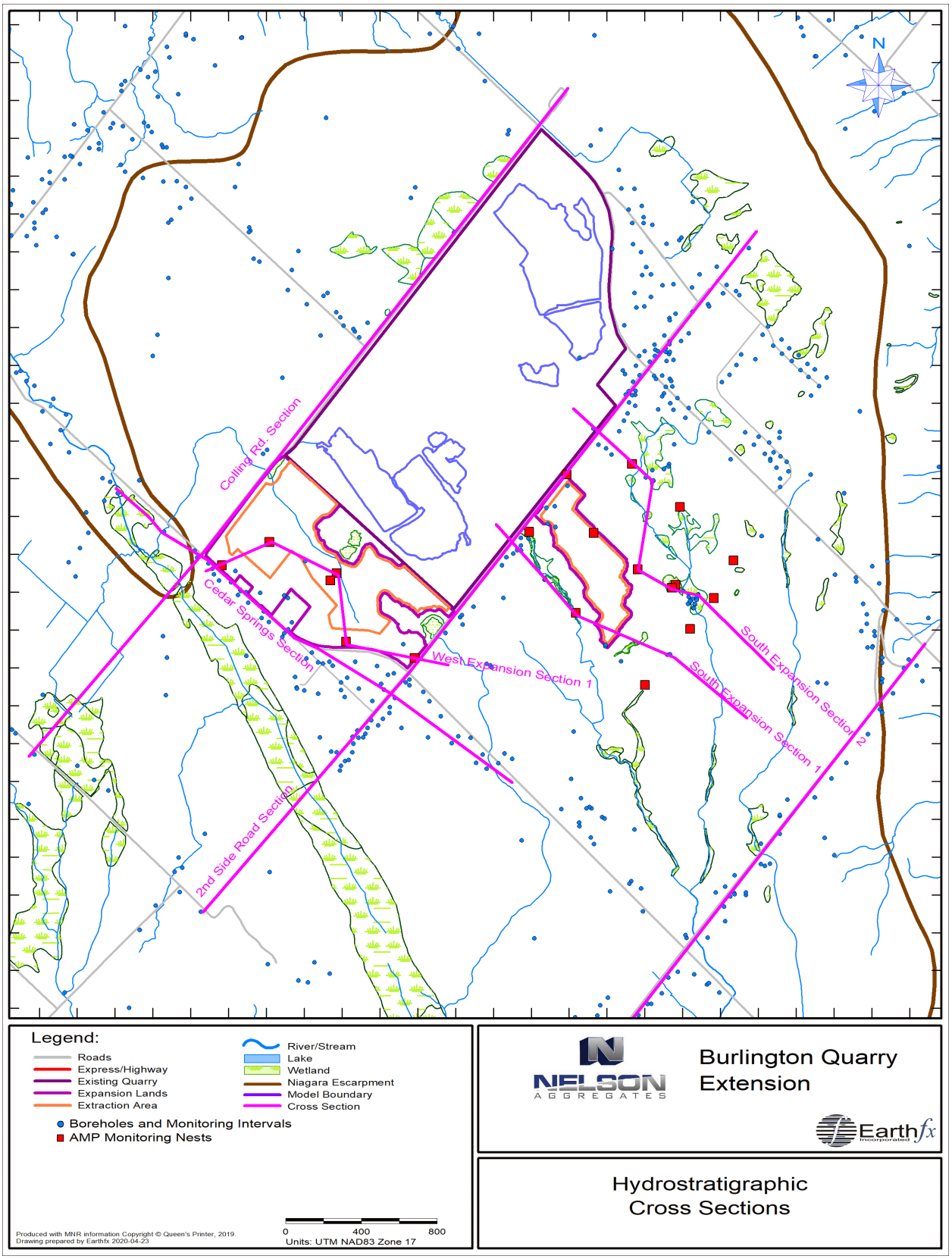

Figure 5.1: Hydrostratigraphic cross section locations.

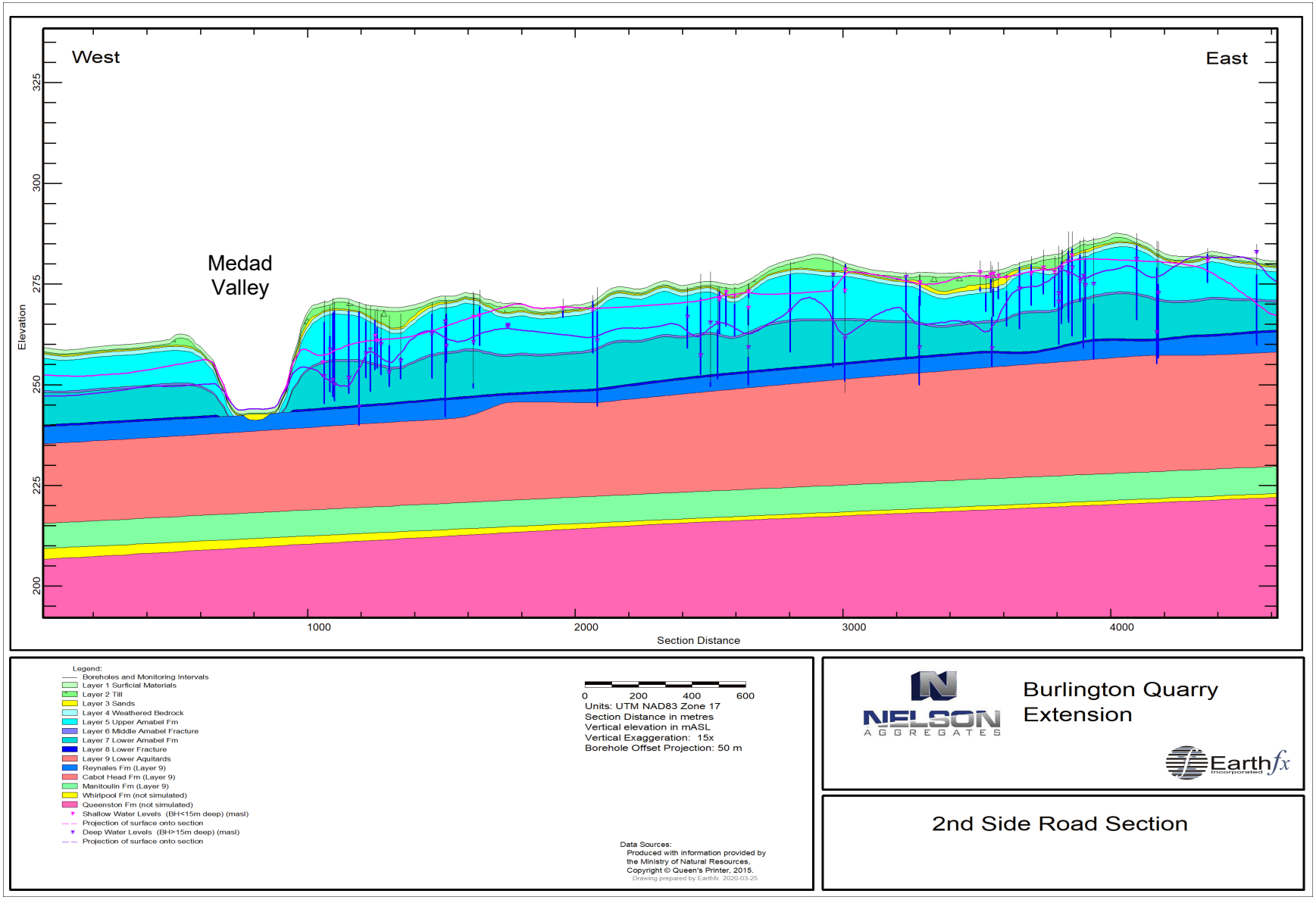

Figure 5.2: 2nd Side Road section.

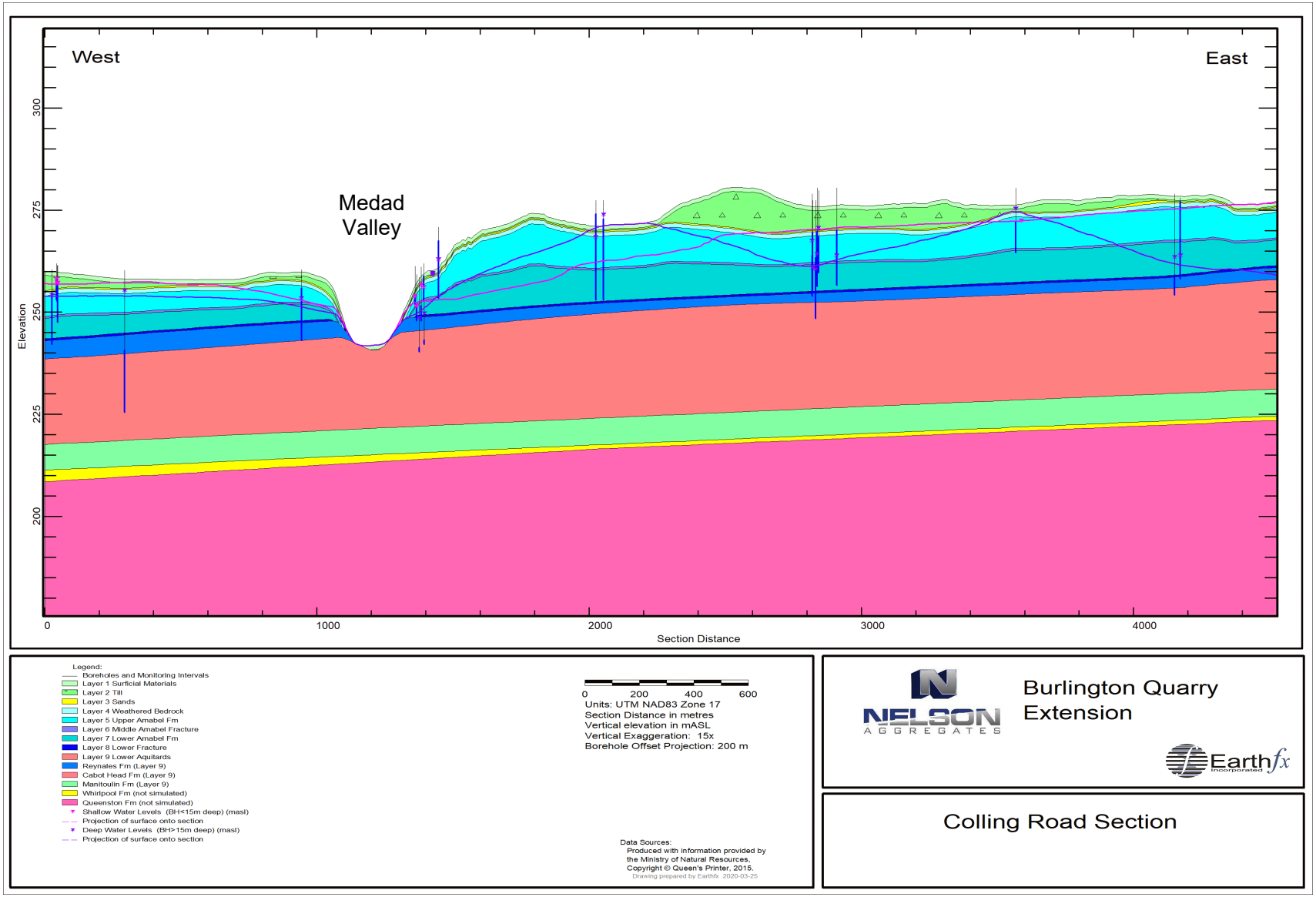

Figure 5.3: Colling Road hydrostratigraphic cross section.

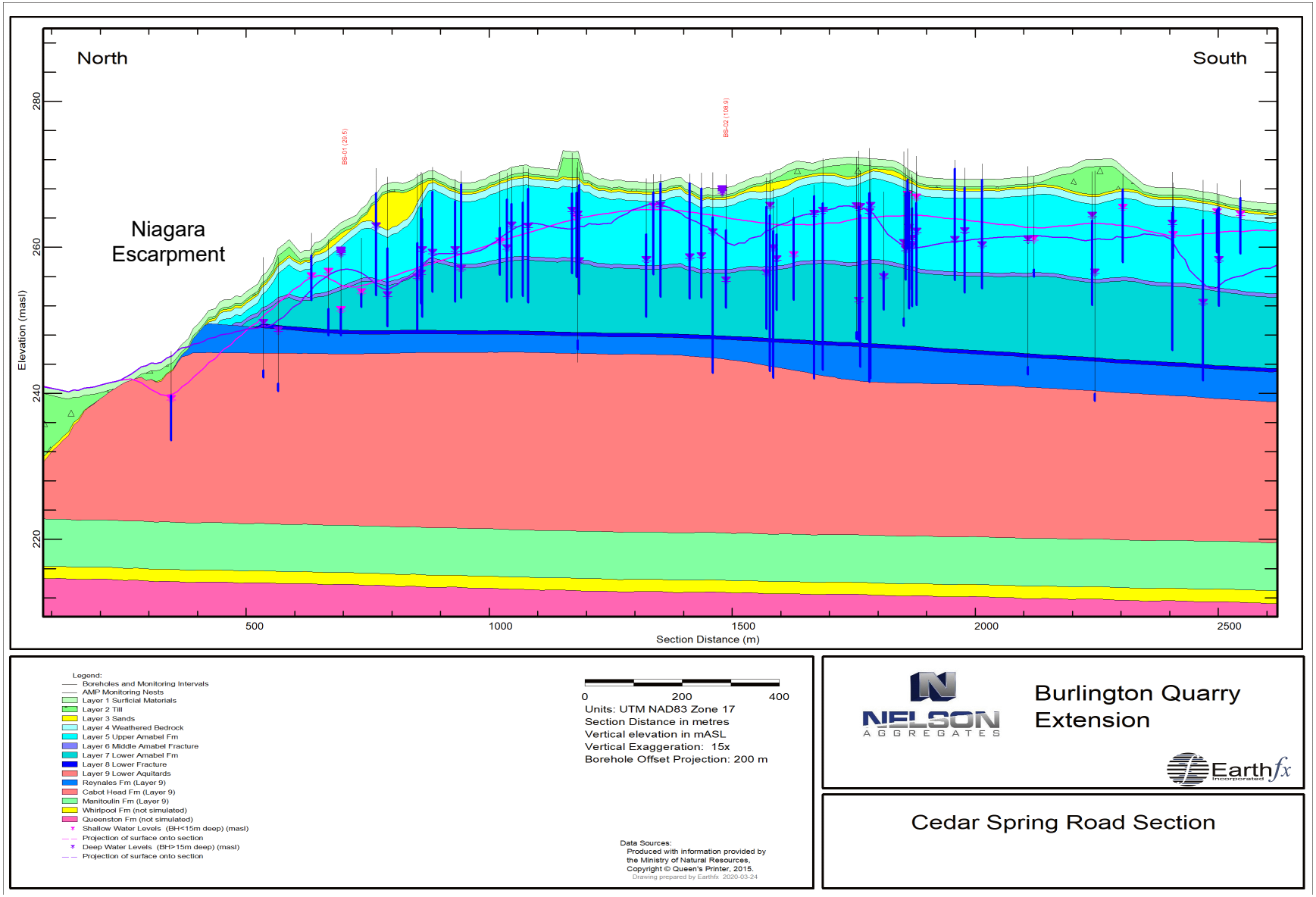

Figure 5.4: Cedar Springs Road section.

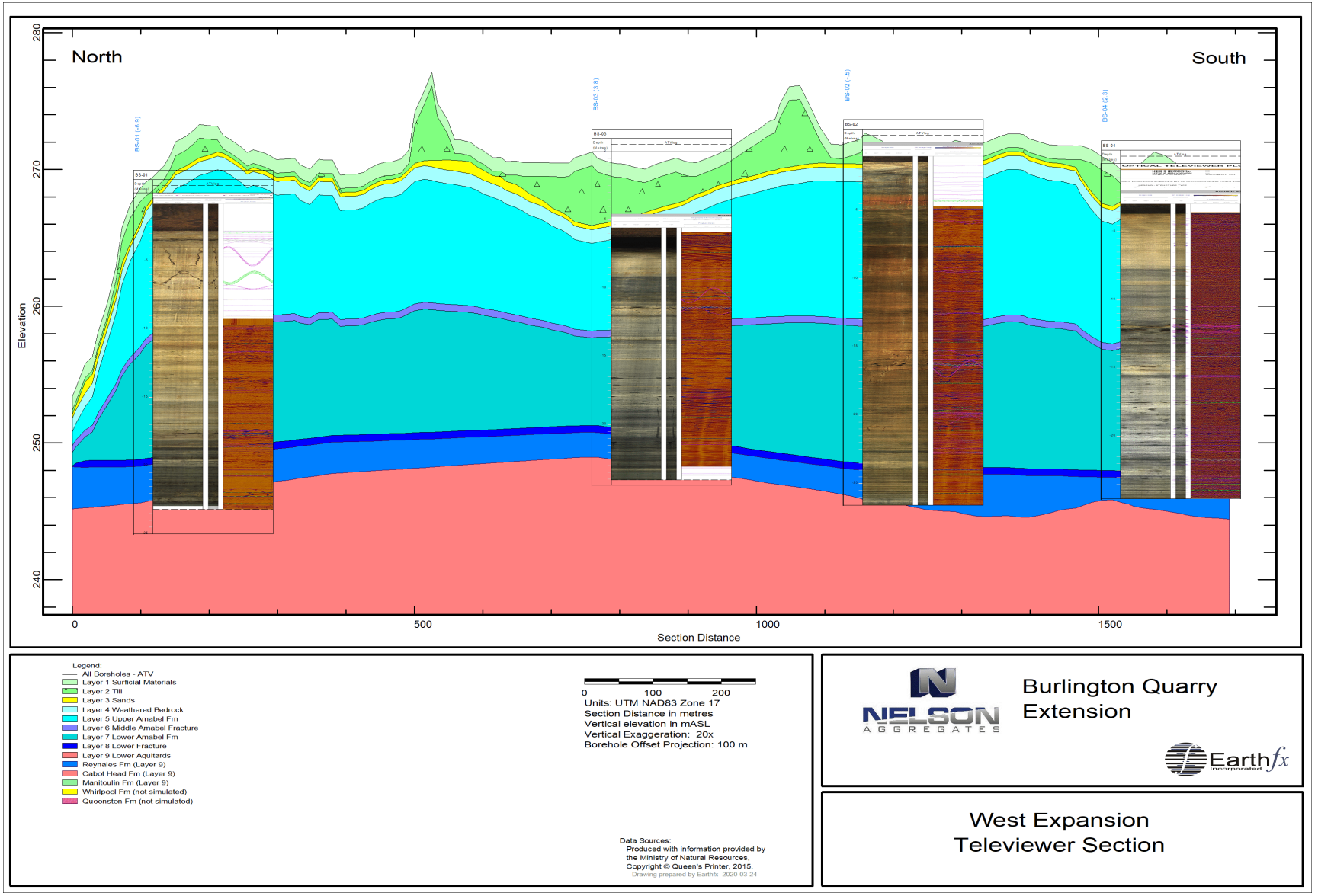

Figure 5.5: Televiewer cross section through the West Extension Area.

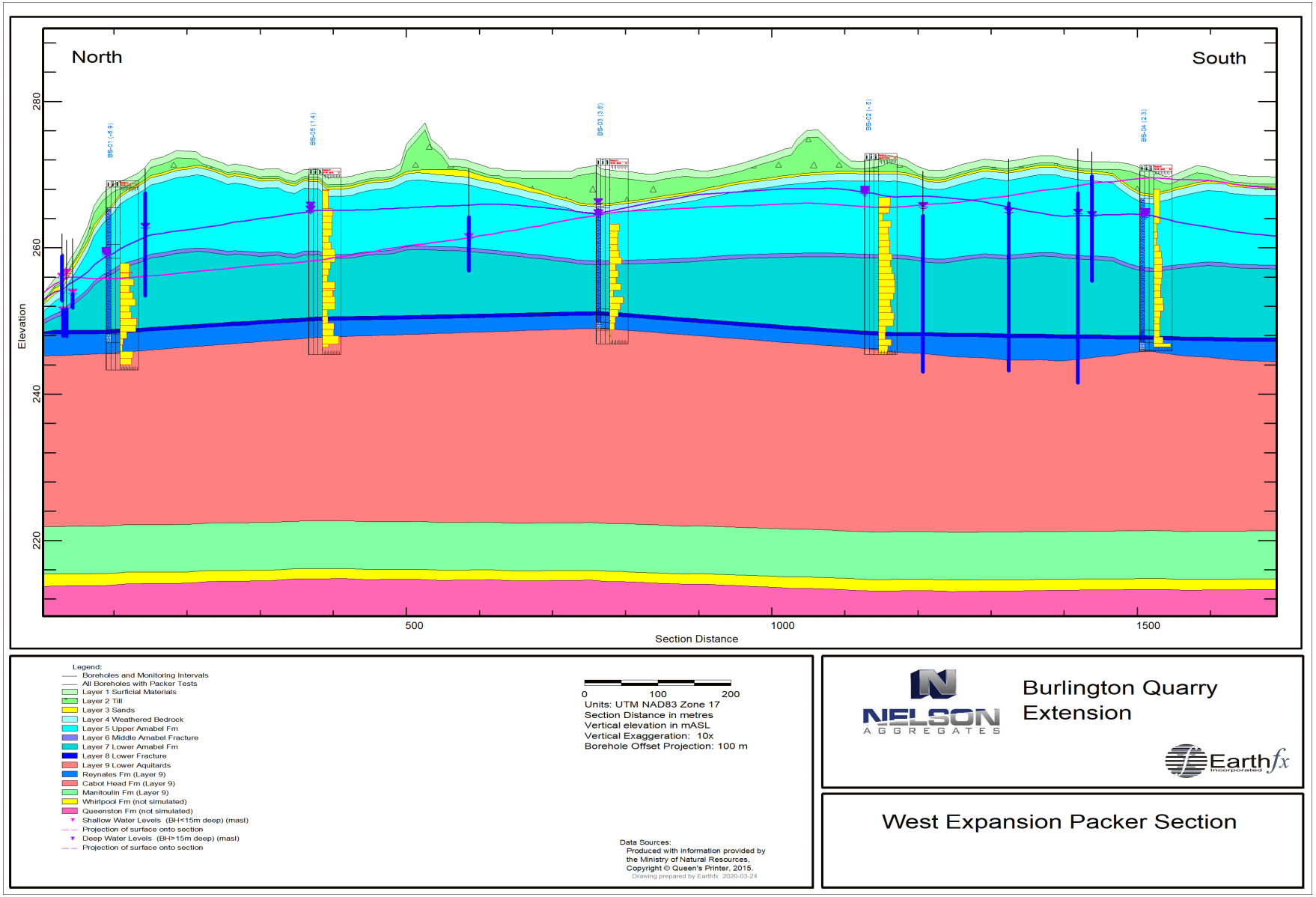

Figure 5.6: West Extension packer test section.

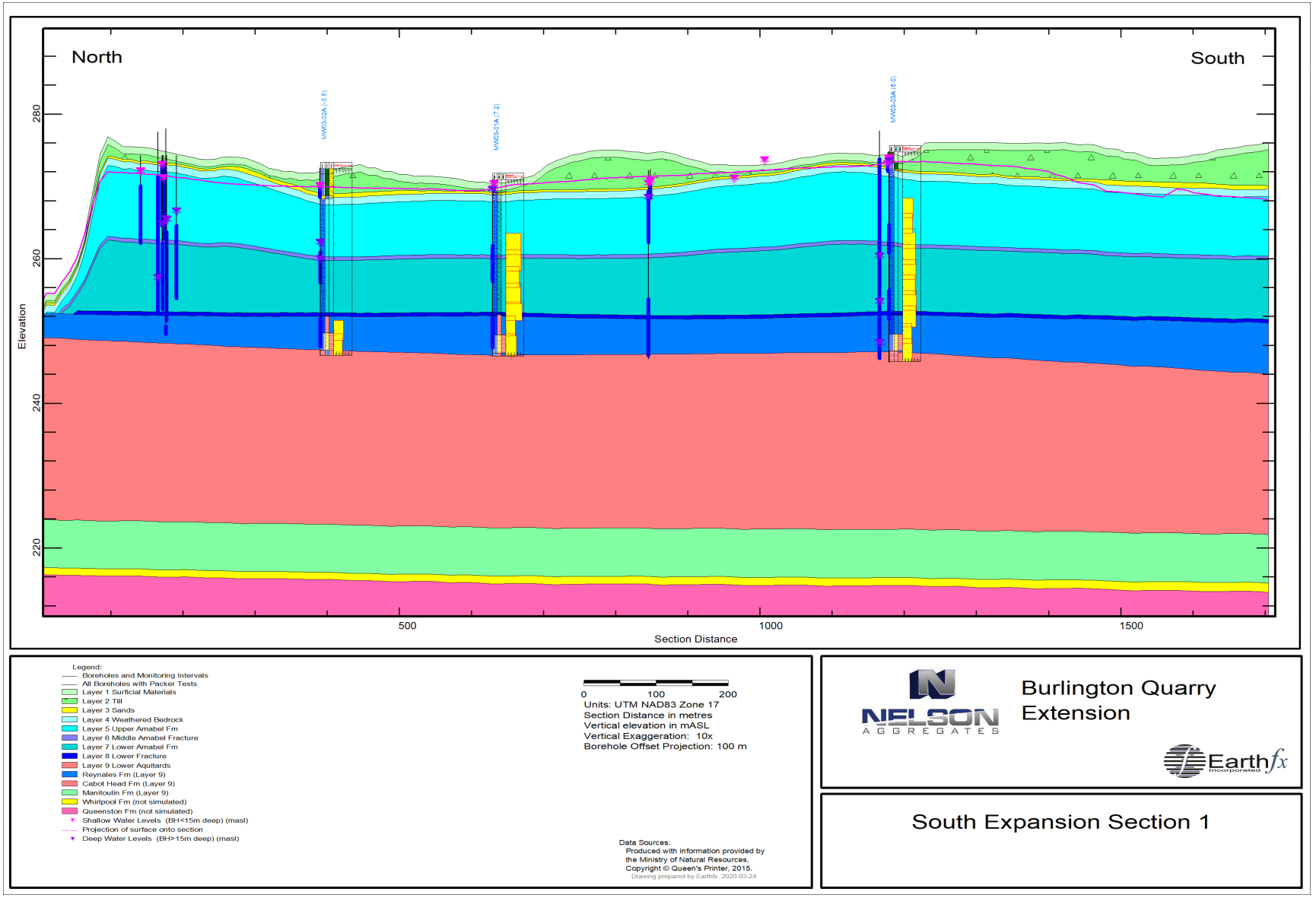

Figure 5.7: South Extension packer test Section 1.

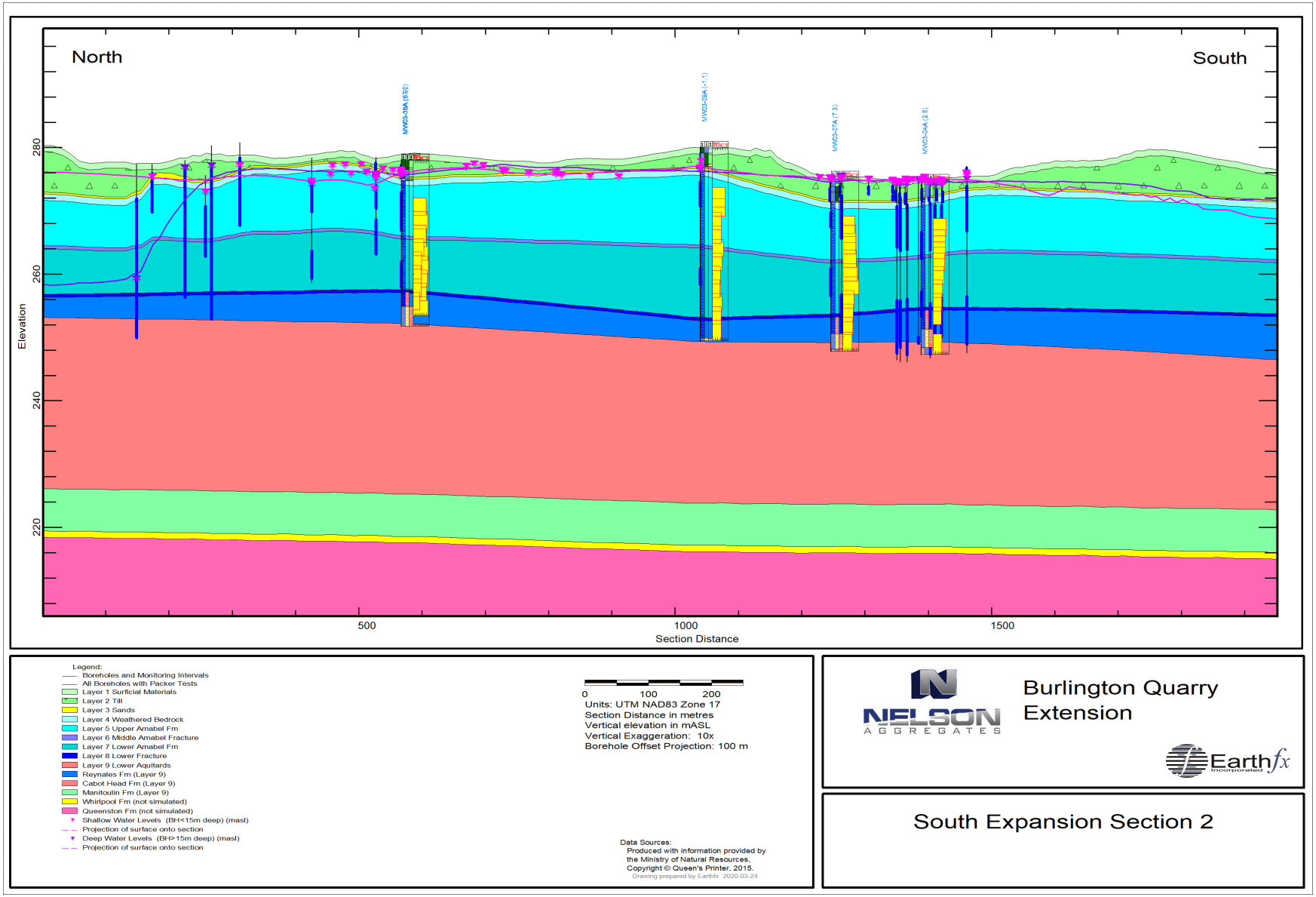

Figure 5.8: South Extension packer test Section 2.

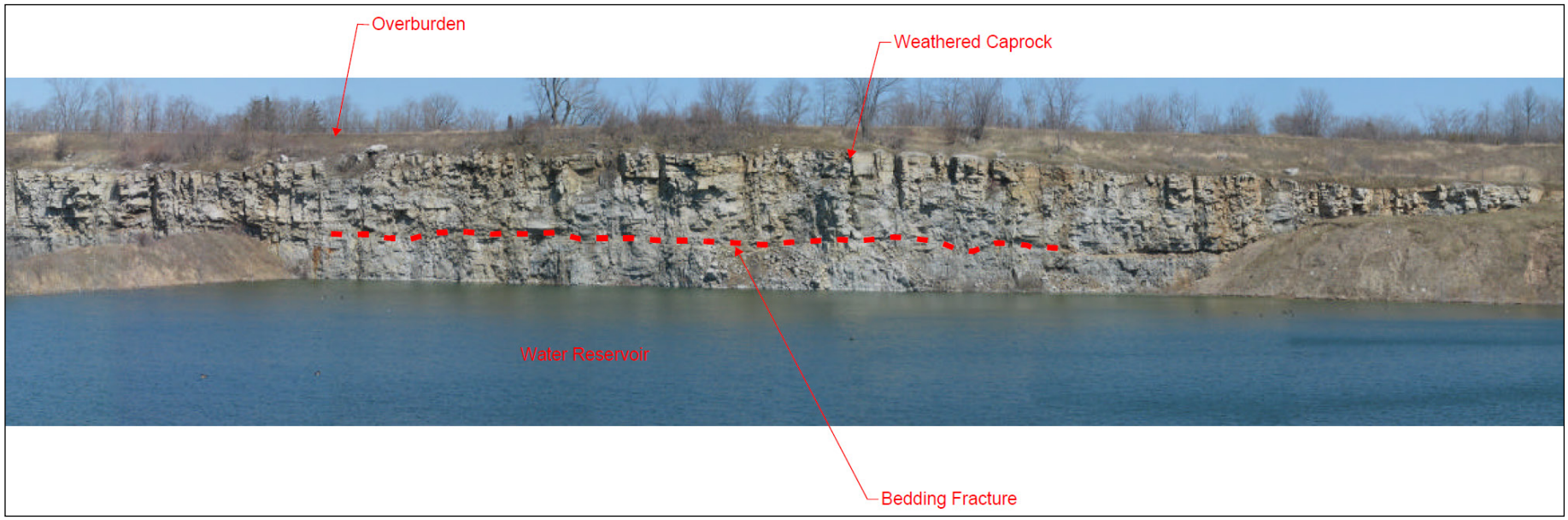

Figure 5.9: Burlington Quarry Amabel outcrop profile (from Golder 2004, Plate 1).

5.2.4 Layer 4: Weathered Bedrock/Overburden Interface Aquifer

A bedrock surface or "contact zone" aquifer is widely observed in the upper portion of the limestone and dolostone units across southern Ontario. Differential weathering and erosion of the bedrock, exposed for over 300 million years in this area of Southern Ontario, has created this aquifer unit. Enhanced permeability is also generally attributed to a combination of weathering, glacial modification, and stress relief fracturing. The weathered bedrock is observed in the quarry outcrops, as illustrated in Figure 5.9, where Golder (2004) notes it can appear to have a brownish tone.

This aquifer is mapped and assumed to be present across the entire study area, although its properties were variable and related to which formation is exposed at the bedrock surface (e.g., the Amabel or Queenston formation). An assumed depth of weathering equal to 0.3 m was applied across the model, extending down from the top of bedrock (Figure 5.6).

Layer 4 (and together with Layer 3) may function as a confined, semi-confined, or unconfined aquifer across the study area, depending largely upon the composition and thickness of overlying Halton Till. Layer 4 is generally not used for water supply wells in the Escarpment upland area of Mt. Nemo, as the water levels in the unit fluctuate seasonally. Water wells are generally cased into or through the weathered bedrock (Figure 5.4); however, leakage from this layer may enter the well around the casing or through vertical or sub-vertical fractures intersecting the borehole.

Shallow Karst Representation: Worthington Groundwater (2006, 2019) completed extensive investigations and mapped karst features, including sinks and springs in the shallow bedrock in the study area. The karst feature locations are shown in Figure 4.14. The Ontario Geological Survey also mapped karst features in the Medad Valley in the study area (OGS, 2008). Karst sinks were represented in the model as disappearing stream segments, where streams flowing across Layer 1 drop down into Layer 4. In Layer 4, the karst flow is represented as a subsurface conduit that leaks or picks up flow. At the mapped karst springs, the stream is again mapped as a Layer 1 stream. The subsurface karst stream segments are generally represented at light blue lines on the figures (for example, see Figure 3.6, with some exceptions for model presentation or stream flow color ramp presentation). An extensive discussion of the karst conditions is included in Appendix B (Section 16).

5.2.5 Layer 5: Upper Bulk Amabel Aquifer

The Amabel Formation was subdivided into multiple hydrostratigraphic layers to reflect a variety of observations related to horizontal and vertical fracturing and anisotropy. Layer 5 represents the uppermost of the subdivided Amabel. The discussion below provided a basis for this representation.

It was previously noted that the upper Amabel may be subdivided into the Goat Island Formation, the Goat Island Formation was only identified in one borehole in the study area. A stratigraphy-based subdivision of the unit was not possible.

An extensive bedding plane fracture observed across the exposed face in the Burlington Quarry provides compelling evidence that supports the delineation of an upper Amabel unit (Figure 5.9) and a middle Amabel fracture zone. A cross section presenting televiewer data through the West Extension area suggests that the upper Amabel has a slightly different tone (Figure 5.5), and a middle Amabel zone is evident upon close inspection (see Figure 3.7). Packer test results in the West Extension area illustrate an increase in hydraulic conductivity in the middle Amabel (Figure 5.6), but the evidence is less clear in the Golder packer test data (Figure 5.7 and Figure 5.8). Well screens are frequently set across the middle Amabel zone (Figure 5.4), further suggesting that a more permeable middle Amabel bedding plane fracture zone extends across the study area.

While the middle Amabel bedding plane fracture is more permeable, the rock mass of the upper Amabel unit is both horizontally and vertically fractured, and this is represented in the bulk hydraulic conductivity of the layer. Two significant numerical model refinements were implemented to better represent the function vertical and horizontal fracturing in this layer (see Section 6. and Appendix D).

5.2.5.1 Amabel Formation Hydraulic Conductivity

The hydraulic conductivity of the Amabel Formation has been studied at sites across the Niagara Escarpment. Two sites near the Burlington Quarry were of interest, including the Freelton Wellfield, approximately 10 km west of the site, and another quarry north of Freelton. The results of several of the tests are summarized in Table 5.1.

Table 5.1: Summary of hydrogeologic properties of the Amabel Formation.

Study	K – low (m/s)	K – high (m/s)
Jagger Himms (2003)*	2.04×10^{-4}	3.56×10^{-4}
Charlesworth & Associates (2006)*	7.18×10^{-5}	3.09×10^{-4}
Dillon (2008)*	3.19×10^{-5}	1.25×10^{-4}
Gartner Lee (2005)/ AECOM (2009)*	4.4×10^{-5}	7.04×10^{-4}
OGS (2010)*	8.44×10^{-4}	2.27×10^{-3}
Wood (2018a)*	3.15×10^{-4}	
Earthfx Interpretation of Wood (2018a) *	2.6×10^{-4}	
Golder (2005) Nelson Model	4.0×10^{-6}	4.0×10^{-5}
Earthfx (2020) Burlington Quarry Model Weathered Bedrock		5.0×10^{-5}
Earthfx (2020) Burlington Quarry Model Amabel Bulk	5.0×10^{-6}	
Earthfx (2020) Burlington Quarry Model Middle Fracture Zone		5.0×10^{-5}
Earthfx (2020) Burlington Quarry Model Lower Fracture Zone		1.0×10^{-4}

Note *: Assumed 25 m thick formation

The hydraulic conductivity of the Amabel has been investigated at the Burlington Quarry using a variety of methods and scales of evaluation. While all methods are useful, each has its own limitations. The packer test results (presented in the previous section) provide detailed insight but can fail to capture the bulk response of the system. The Golder (2005) pump test and the wellfield tests presented in Table 5.1 provide a bulk measurement, but the interpretation of the pump test results requires aquifer layer and property assumptions that may not be well-suited for a layered fractured rock setting. Finally, karst investigations can provide insight into the high permeability conduits that may be present in the system.

While all of this information has been considered in completing this assessment, perhaps the most representative measure of system response is from the observation wells that recorded the progression of the quarry face over the last 10 years (the site development history is presented in Section 3.3.3). While all the field measurements have been integrated into this assessment, the model calibration to the seasonal and long-term groundwater level fluctuations and drawdown as recorded in the monitoring network ultimately provided the best estimate of the hydraulic conductivity of the units. A summary of the calibrated values is presented in Table 5.1 for comparison.

5.2.5.2 Anisotropy and Vertical Flow Patterns

It is widely recognized that the dolostones of the Niagara Escarpment have a high degree of vertical to horizontal anisotropy. Maslia and Johnston (1984) studied the “effectiveness of horizontal (bedding) joints versus vertical joints as water-transmitting openings”. They concluded that vertical hydraulic

conductivity (K_v) to horizontal hydraulic conductivity (K_h) anisotropy of 100:1 to 1000:1 was typical of the Lockport (Amabel) Formation.

Discussions with Dr. Worthington (a partner on this project team) regarding the karst characteristics of the Amabel Formation further suggest that there are low storage/high permeability fractures that interact with a bulk rock mass that has higher storage but lower permeability. These are also discussed in Worthington Groundwater (2019).

These features and characteristics have been incorporated into the conceptual hydrostratigraphic model for the Amabel Formation layers. Based on these insights and model calibration to match the vertical gradient observed in the long-term monitoring wells near the quarry face, the bulk anisotropy of Layer 5 (upper bulk Amabel) was estimated to be 500:1 (K_h/K_v) and Layer 7 (lower bulk Amabel) to be 1000:1 (K_h/K_v).

Simulations with these values alone indicated that, while these anisotropy ratios are within the range of published values, model results failed to represent the observed water level interconnection response observed in the monitoring record. In particular, the lower layers showed a strongly attenuated response to seasonal change. To better represent the presence of vertical fractures which connect the shallow and deeper systems, 5% of the model cells in Layer 5 and Layer 7 were randomly assigned an anisotropy value of 1:1 (K_h/K_v) (Figure 18.20). The 5% figure was based on a set of calibration runs with varying percentages.

The combination of high bulk anisotropy, together with a degree of vertical interconnection, was found to best match the observed well responses. Near the south quarry face, the water table generally remains in the shallow bedrock for much of the year, particularly when spring recharge to the shallow system is higher than the leakage rate downwards through the vertical fractures. In closer proximity to the face, where the deep system is under-drained, highly erratic changes in water levels (greater than 5 m) can be observed in response to recharge events filling the shallow system storage and then leaking downwards over time.

The vertical fracture network and anisotropy patterns also exist, but downward leakage over the broad area tends to minimize the differences in the head between the shallow and deeper bedrock layers. Groundwater flow through the network of vertical and horizontal bedding plane fractures is sufficient for allowing the Amabel aquifer to serve as a source for private water supply.

5.2.6 Layer 6: Middle Amabel Fracture Zone

The preceding discussion of the hydrostratigraphy of Layer 5 (bulk Upper Amabel) introduced many of the concepts and data that support the delineation of Layer 6 as the middle Amabel fracture zone. As noted above, the bedding plane fracture observed in the quarry wall (Figure 5.9), together with the West Extension area packer tests, televiewer logs, and monitoring data, provide compelling evidence of a relatively continuous horizontal fracture zone with preferential flow.

The presence of a production zone in the Gasport (Amabel) Formation has been noted in several studies. In the Freelton wellfield, municipal supply wells FDF01 and FDF03 have been interpreted to intersect the highly permeable fractured zone in the middle of the Gasport Formation. Brunton (2007) also identifies a production zone in the middle of the Gasport Formation in the Guelph area.

5.2.7 Layer 7: Lower Bulk Amabel Aquifer

The Gasport (Amabel) Formation is dominated by thick- to massive-bedded, fine- to coarse-grained dolostone and dolomitic limestone, with minor argillaceous dolostone beds. There is anecdotal evidence that the lower portion of the Amabel, together with the Irondequoit, may be more massive than the upper Amabel within the Burlington Quarry (Figure 5.10).

The hydrogeologic properties of the lower bulk Amabel are represented in a similar manner to that of the upper bulk Amabel. The calibrated vertical anisotropy of Layer 7 is lower, at 1000:1 (Kh/Kv), to reflect the more massive nature of the lower Amabel.

5.2.8 Layer 8: Lower Fracture Zone

A lower flow zone has been identified in a number of boreholes, monitoring data sets, and in observations at the base of the quarry face (Figure 5.10). The most compelling evidence of a lower flow zone is found in the monitoring data. A hydrograph from monitoring location OW03-15, south of the 2nd Side Road (see Figure 3.4) is shown in Figure 5.11. Water levels in the deepest monitor (OW03-15A) at this location are over 13 m below those of the water table (OW03-15C), clearly indicating that the lower system is connected to the quarry by a permeable lower fracture.

Figure 5.10: Lower zone quarry discharge near OW03-15 (Worthington Groundwater, 2006).

A similar pattern is observed in monitor nest OW03-14 (Figure 5.12). When the monitor was installed in 2004, the quarry face was 175 m from the monitor (Figure 3.8). Between 2004 and 2009 the quarry face advanced to within 40 m of the monitor, and during that time the heads in the lower system dropped 14 m. This provides particularly useful information, for it suggests that the quarry influence is less than 200 m from the active face.

Evidence for a lower flow zone is also evident in the packer test data (Figure 5.6 and Figure 5.8, for example); however, technical problems with testing at the bottom of the borehole may have limited the effectiveness of this method.

The exact depth and thickness of the lower fracture zone is difficult to identify precisely, but the presence of the zone and relatively high permeability can be clearly identified in the monitoring data. The lower flow zone may contain a combination of fractures and bulk permeability likely near the sharp contact with the top of the Reynales Formation.

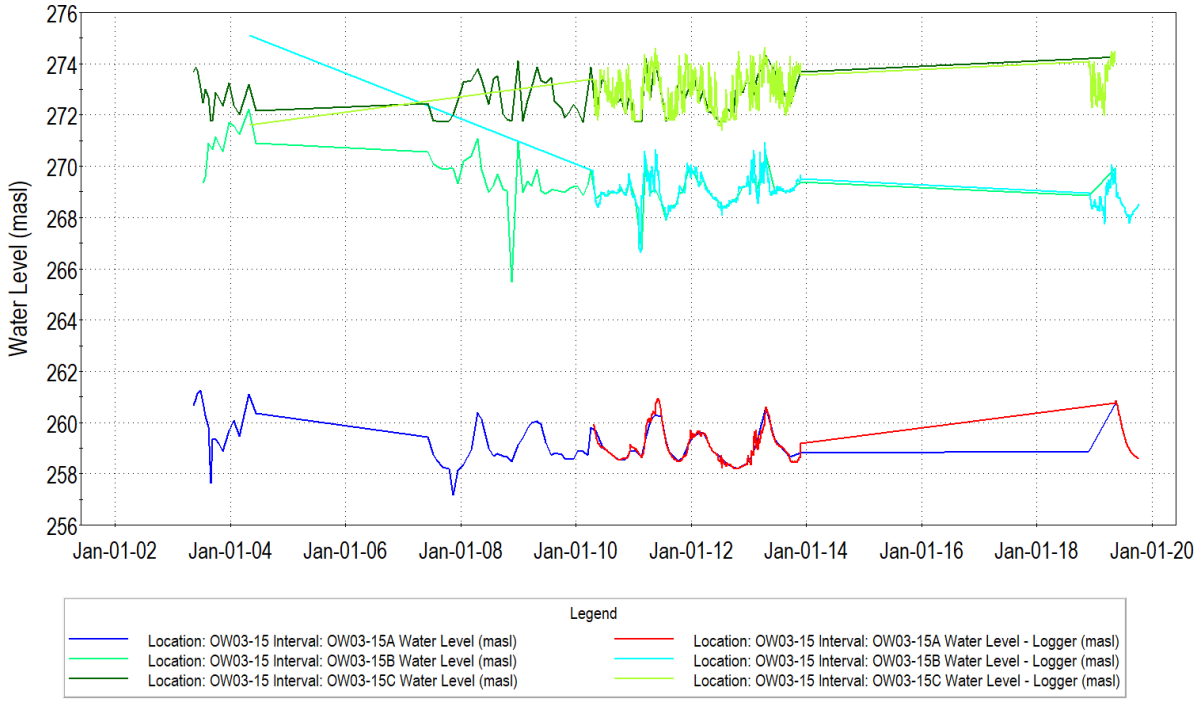

Figure 5.11: Water levels recorded in Monitoring Well OW03-15 (50 m from Quarry face).

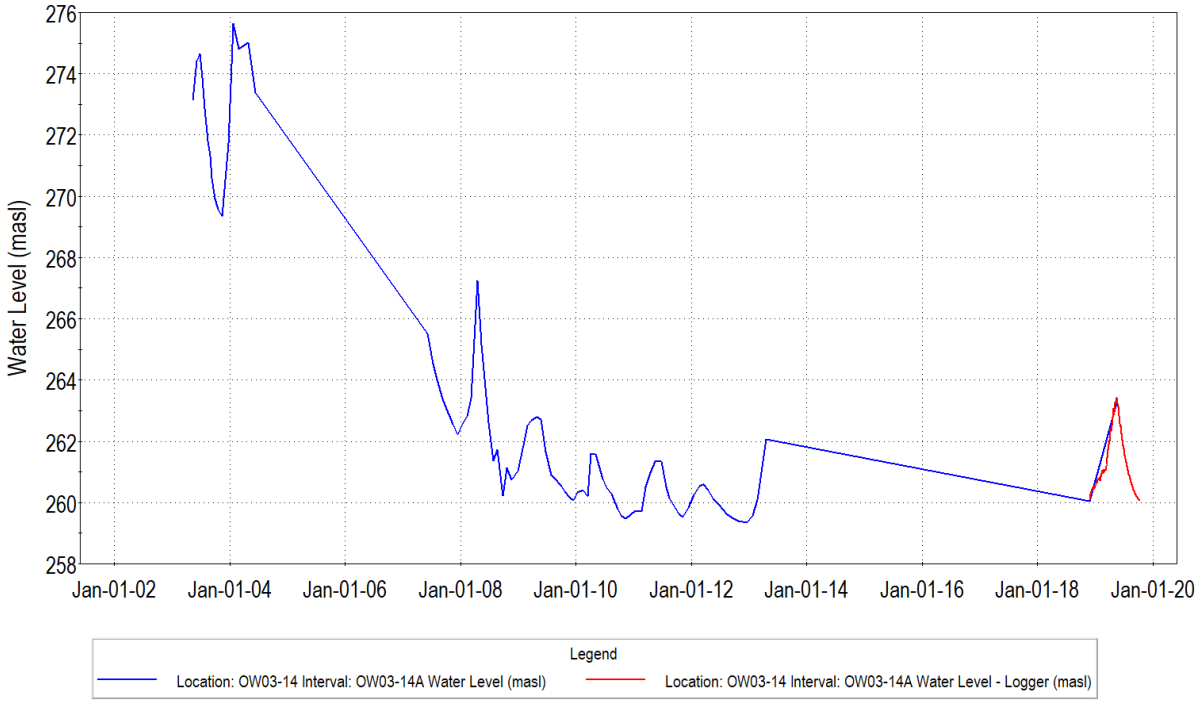

Figure 5.12: Water levels recorded in Monitoring Well OW03-14 (175 m to 40 m from Quarry face).

5.2.9 Layer 9: Lower Aquitard

Because groundwater flow in the lower system is dominated by the lower fracture zone, the multiple aquitard layers below that zone have a limited impact on groundwater flow in the lower system. For this reason, the lower aquitards were grouped into a single Layer 9 Lower Aquitard layer. For the simulations in this study, a collective hydraulic conductivity of $1x10^{-7}$ m/s was selected.

5.2.10 Summary

A 9-layer hydrostratigraphic model was developed from the stratigraphic layers and conceptual and numerical analysis of the field measurements. A number of key hydrogeologic concepts and observations, including weathering, karst, fracturing, anisotropy, and monitoring observations have been incorporated into the hydrostratigraphic model.

As will be discussed in Section 6.10.1 and Appendix D, further refinement was done to transform the hydrostratigraphic model layers into numerical model layers for the GSFLOW model. This includes, for example, ensuring that a minimum thickness was preserved for each of the layers. Unique hydraulic properties were assigned to the units represented by these surfaces.

The hydrostratigraphic model surfaces were also used to assignment well screens and pumped intervals to particular model layers. This information was used in the presentation of groundwater levels and in the selection of calibration targets, as discussed in the next section.

5.3 Groundwater Levels

5.3.1 Water Level Data Sources and Monitoring Record

Water-level data are available from two primary sources: the “static water level” data in the Ontario Ministry of Environment, Conservation, and Parks (MECP) Water Well Information System (WWIS) database and from monitoring wells established for Nelson. There are nearby Provincial Groundwater Monitoring Network (PGMN) wells; however, all are located outside the study area. The water level data provide useful information on groundwater flow rates and directions in the study area as well as provide the primary targets for the calibration of the numerical groundwater model.

5.3.1.1 Static Water Level Data

Static water level data from these wells provide a general insight into the regional groundwater level patterns. The static water levels represent one-time measurements taken at the time of well construction. Numerous issues (bias towards shallow wells, the effect of variation in seasonal and inter-annual groundwater levels on how representative the data are) and errors (survey error, well recovery, etc.) are known to affect the water well record data. Assessment of the intrinsic error and variation in this data set is discussed at length in Kassenaar and Wexler (2006). Despite these limitations, the WWIS data represents the best spatial coverage available.

5.3.1.2 Transient Water Level Data

Nelson maintains a groundwater monitoring network with wells and mini-piezometers around the Burlington Quarry (Figure 3.4). Monthly water level data were collected by Golder starting in 2003, and continuous data were collected in most wells from 2007 to 2013 and starting again in October 2018 by Azimuth Environmental. Mini-piezometer data were collected by Golder from 2007 to 2013, and new mini-piezometers were installed in wetlands by Tatham Engineering in 2018. Although there are gaps, the data provide useful insight into how the wells respond to rainfall events and to seasonal and inter-annual climate variability. The wells also provide insight into how water levels may have been affected over time by quarry excavation and seasonal changes in dewatering activities. Other monitoring sites in the study area were also incorporated into this analysis.

5.3.2 Regional Water Level Patterns

Regional water level patterns were evaluated using static water levels obtained from the MECP WWIS database, static water levels from other geotechnical and consultant wells, and average water levels from long-term water-level monitoring sites. Static water levels were examined visually and using statistical outlier detection techniques to identify obvious errors in water levels. Not all large differences between nearby wells could be classified as erroneous. Possible causes could be slow recovery times in low yielding wells or different degrees of connectivity within the fractured bedrock system (e.g., one site could be well connected to a relatively continuous fracture system while another is poorly connected). Wells with uncertain locations were eliminated. Data for wells with anomalous values were checked against the original borehole logs for transcription errors.

The water-level data were interpolated to a regular grid covering the study area using a geostatistical technique known as “kriging”. Kriging is a weighted-averaging interpolation method that attempts to minimize variance and bias in the results while honouring the local values at the data points. Points along the higher-order stream were added to the interpolation process because these were assumed to correspond closely to the actual water table elevations. Wells above and below the Niagara Escarpment were treated as separate populations for variogram analysis and for interpolation.

Figure 5.13 shows the results of the kriging of the groundwater levels along with the original data posted as colour-coded dots. Only data from wells with completion depths less than 15 m below ground surface were used to approximate the position of the water table. The highest water levels, exceeding 280 masl, are observed in the northwest portion of the study area in the vicinity of Mt. Nemo. The lowest water levels, at approximately 105 masl, are located in the southern portion of the study area along Grindstone Creek. Similar to topography, the water levels are relatively flat above the

Escarpment. Steep gradients are present below the crest of the Niagara Escarpment. In general, groundwater flow is radially outward from Mt. Nemo; however, the flow direction is predominantly to the southwest towards the Medad Valley in the quarry vicinity.

Figure 5.14 shows the results of the kriging of the groundwater levels from wells with completion depths greater 15 m below ground surface. Some low values are observed, particularly in the Medad Valley, confirming the Medad as a local groundwater discharge zone.

5.3.2.1 Vertical Head Differences

The vertical head differences between the shallow and deep system were obtained by subtracting the two interpolated surfaces, and are shown in Figure 5.15. While there are some clear patterns of downward gradients near the Escarpment face (shown in blue), the limitations in the MECP water well record data and spatial distribution result in limited usefulness. The long well screens or open holes used in water well construction often result in water levels that reflect multiple layers, as illustrated in the cross section shown in Figure 5.2 and Figure 5.4.

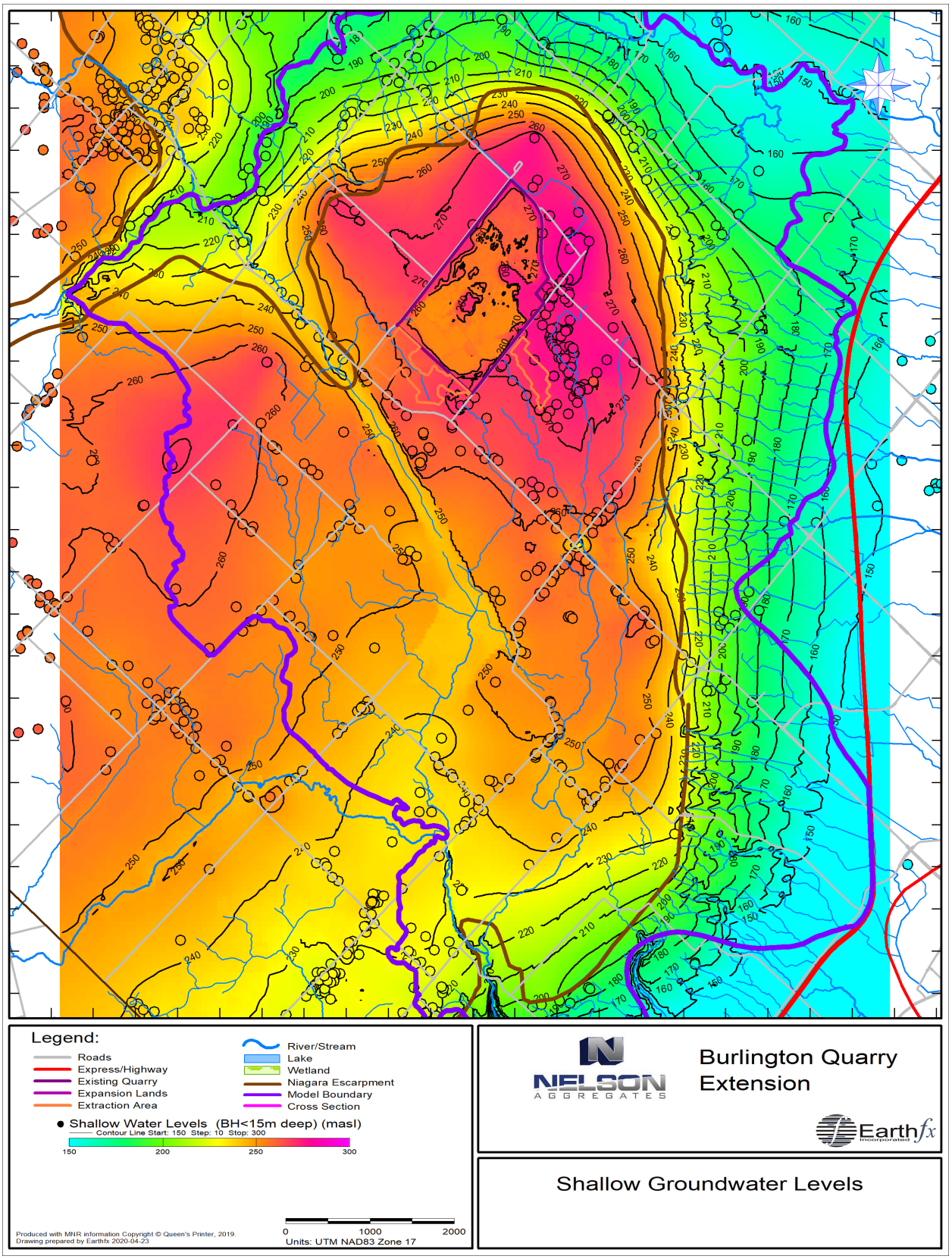

Figure 5.13: Groundwater levels (m) from wells less than 15 m deep.

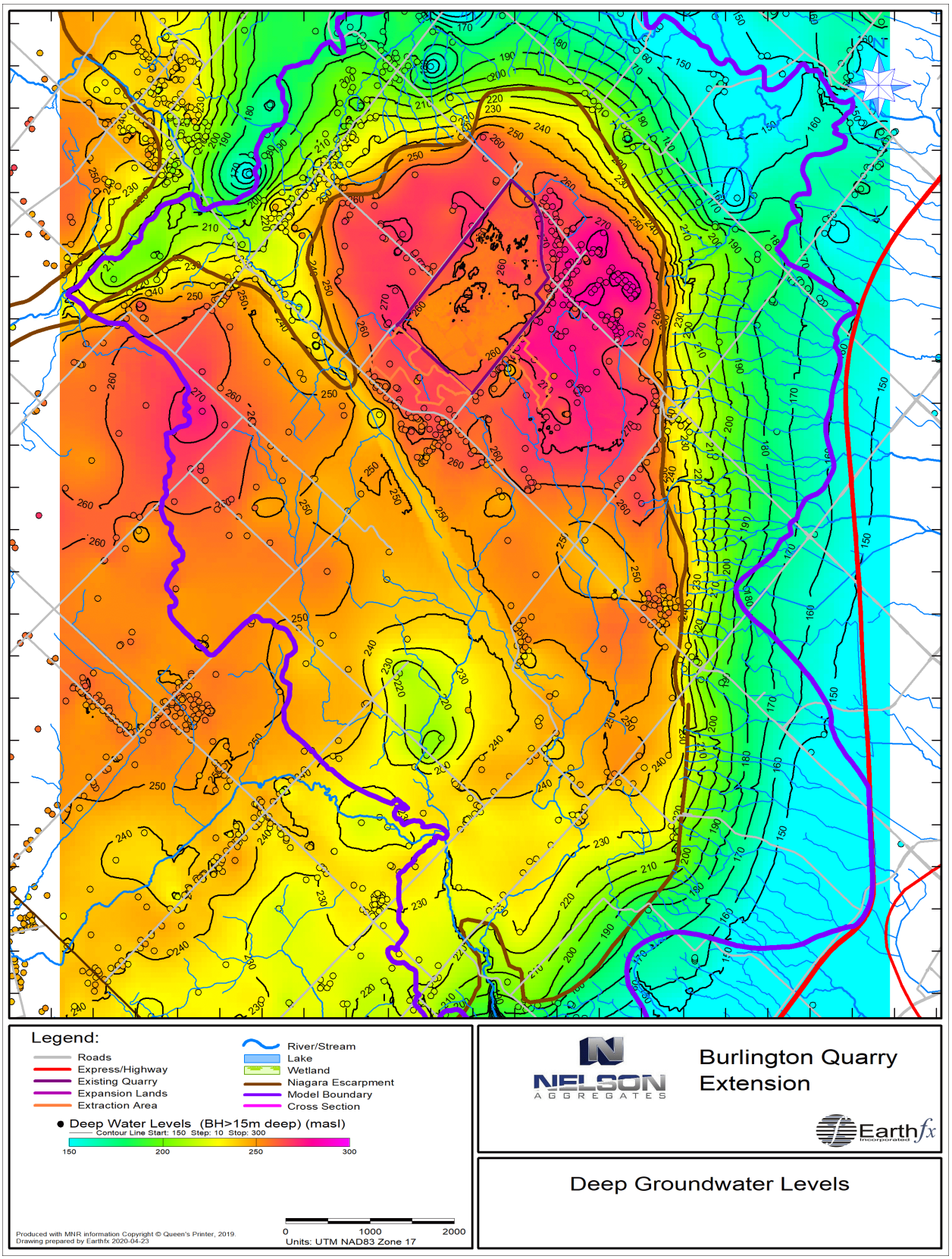

Figure 5.14: Groundwater levels (m) from wells greater than 15 m deep.

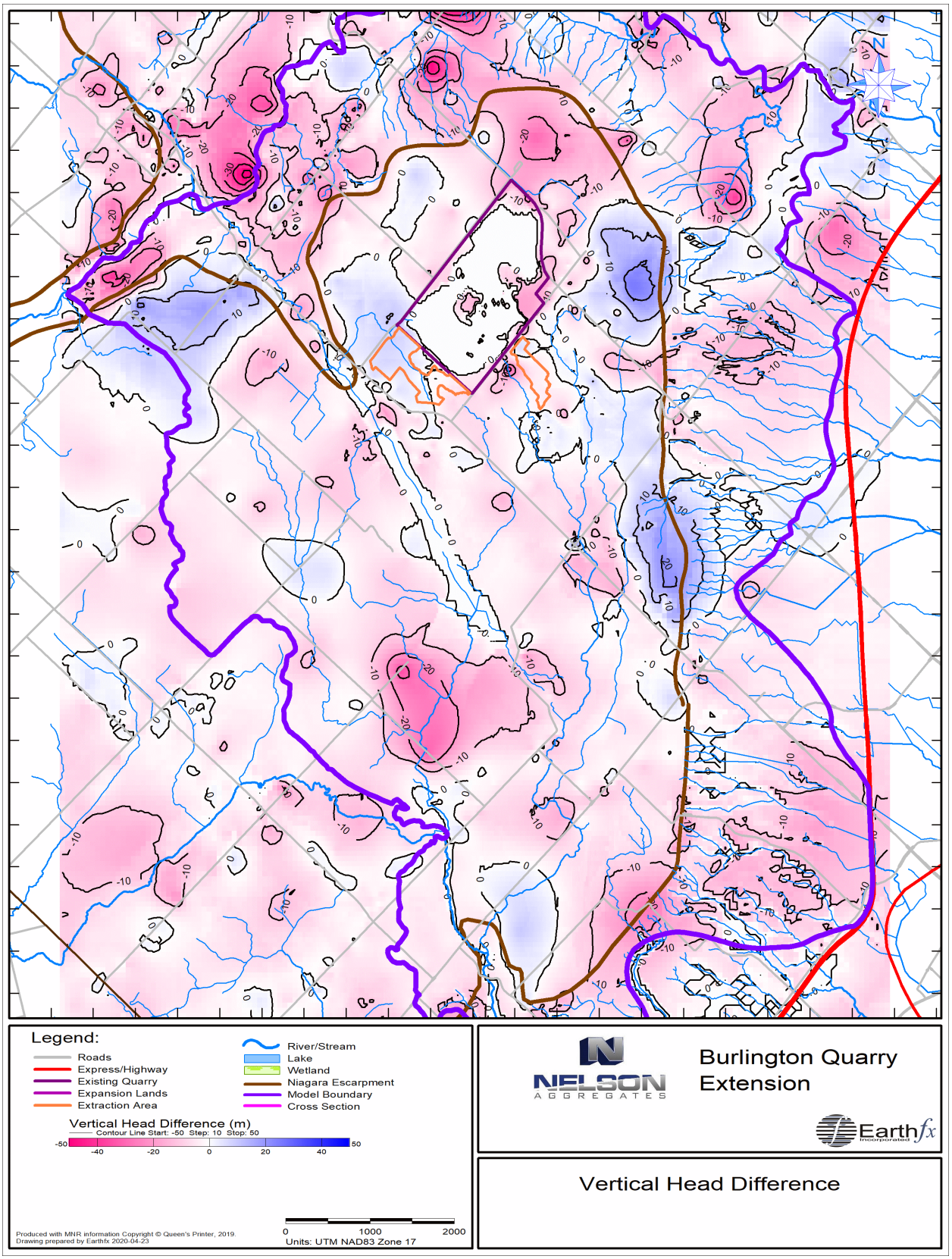

Figure 5.15: Vertical head differences (shallow minus deep groundwater levels, in m).

5.3.3 Water Level Fluctuations

5.3.3.1 Seasonal and Inter-annual Patterns

A review of long-term water level data indicates that natural seasonal variation in water levels can be significant. The storage capacity of the bedrock fractures is limited, and water level response to infiltration events is rapid. Fractures in areas where the water table is in the upper bedrock will also drain rapidly in response to changes in recharge while the bulk matrix drains more slowly.

Figure 5.16 presents a hydrograph for monitoring well MW03-30B, which shows typical seasonal water level patterns (Monitoring locations are shown in Figure 3.4). Groundwater levels show a muted response in the late fall and early winter as the ground freezes, precipitation decreases, and snow accumulates. Peak water levels generally occur in early to mid-April primarily due to recharge from precipitation and snowmelt events after the ground has thawed. Groundwater levels decline through the summer because few infiltration events reach the water table, and most of the water in the soil zone is lost to evapotranspiration. Groundwater levels typically recover in the early fall due to increased precipitation and decreased ET.

The seasonal response pattern varies from year to year due to climatic variations in temperature and precipitation. For example, a warm wet winter will limit the amount of snowmelt available for the spring freshet. There are a number of above-average wet and dry years in the 10-year period used in model simulations (WY2009-WY2019) with a wide range of average monthly precipitation and temperature values. As an example, Figure 5.17 shows inter-annual variations in groundwater levels in PGMN well W000005-1 located west of the study area. Even though rainfall and snowmelt were high in the spring, the dry fall of 2011 and the dry summer of 2012 caused groundwater levels to appear to decline more than normal.

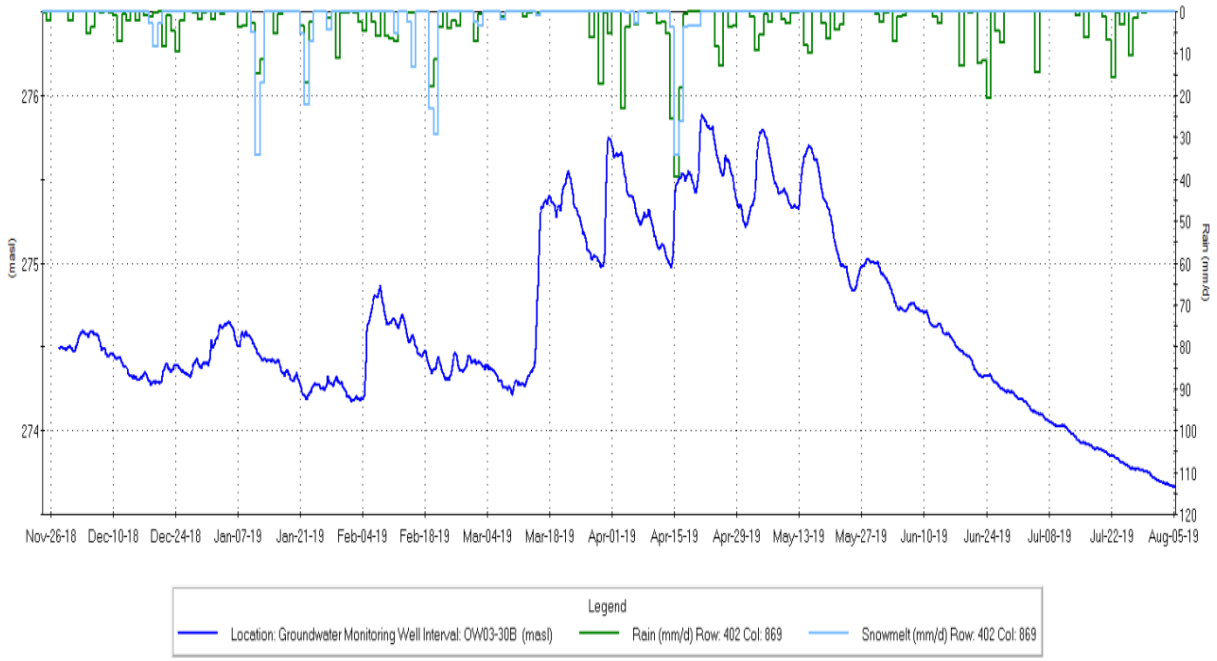

Figure 5.16: Transient groundwater response to precipitation and (simulated) snowmelt events.

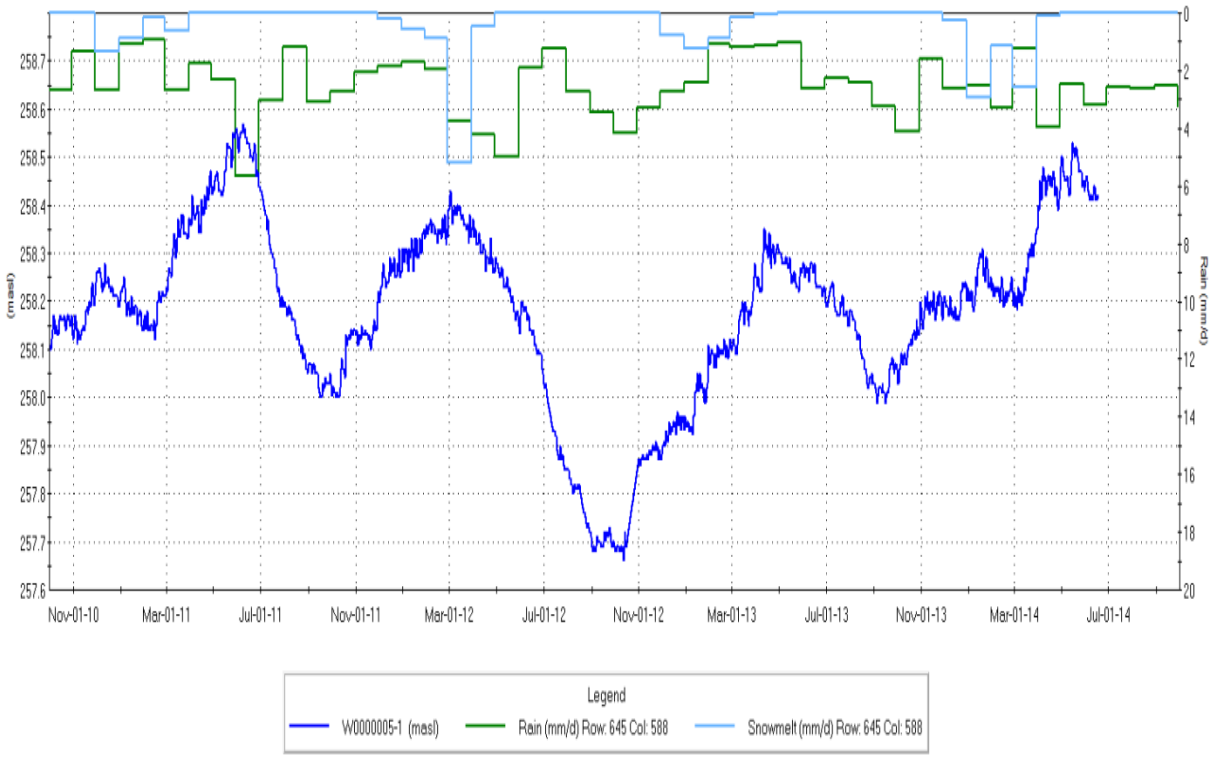

Figure 5.17: Inter-annual variation in groundwater levels at PGMN Well W000005-1 versus monthly average precipitation and snowmelt.

5.3.3.2 Quarry Water Level Patterns

The effects of the quarry have been observed in the South Quarry Extension area monitoring network for many years. A characteristic water level response pattern has been observed that is affected by distance from the active quarry face. Wells in close proximity to the quarry (e.g., OW03-15, which is 50 m from the face) exhibit more than 14 m of vertical head difference between the Layer 4 shallow bedrock and Layer 8 deep fracture zone, as illustrated in Figure 5.11. As noted earlier, this decline in water levels has been observed as the quarry face advanced (Figure 5.12).

With increasing distance from the quarry, the difference in head between the shallow and deep system is reduced. At 300 m from the face, the difference in head has decreased to 10 m (Figure 5.18), and the water levels in the deep system become much more variable (as much as 6 m). This variability is due to the effects of seasonal recharge that serve to replenish the lower system. During the spring freshet, higher rates of recharge and higher water table are able to fill the vertical fractures and drive flow to the lower system faster than it drains laterally to the quarry. Water levels in the deeper system rise significantly in response. Over the summer, the deep system water levels drop as recharge rates and the water table declines.

At 650 m from the quarry face, the difference between the deep potentiometric head and the water table is further reduced. Similar seasonal water level patterns are observed, with up to 4 m in head difference.

Finally, at 1000 m from the quarry, the spring freshet provides an excess of water to the water table and, with minimal deep system drainage to the quarry, the water levels in the shallow and deep system are nearly identical. Normal seasonal fluctuations in the water table are observed.

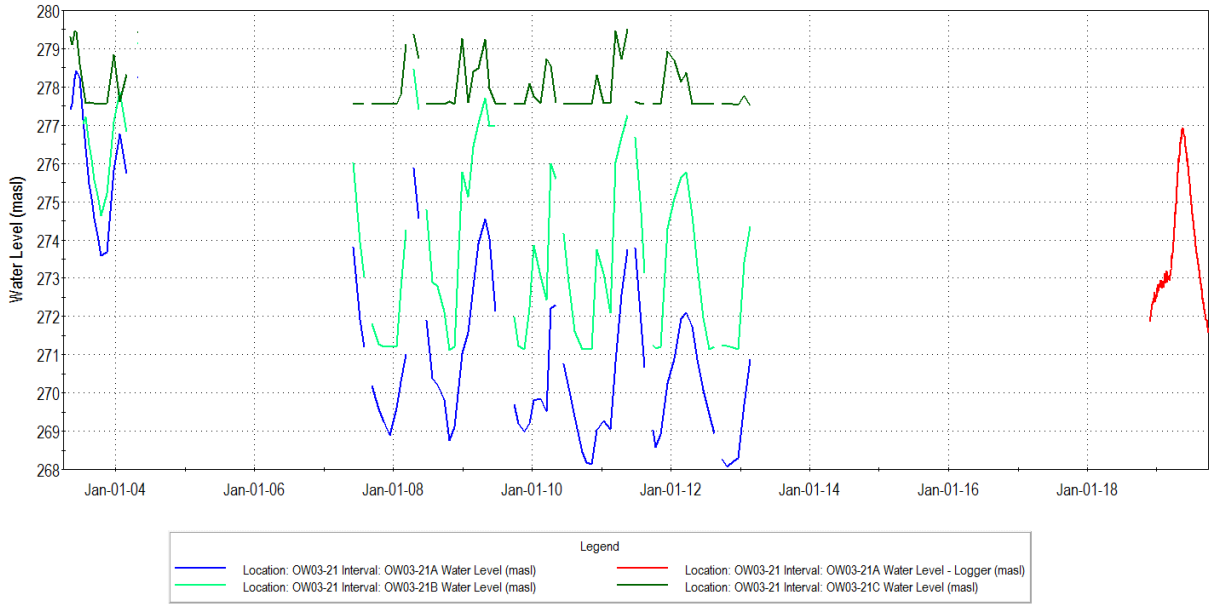

Figure 5.18: Monitor OW03-21, located 300 m from quarry face

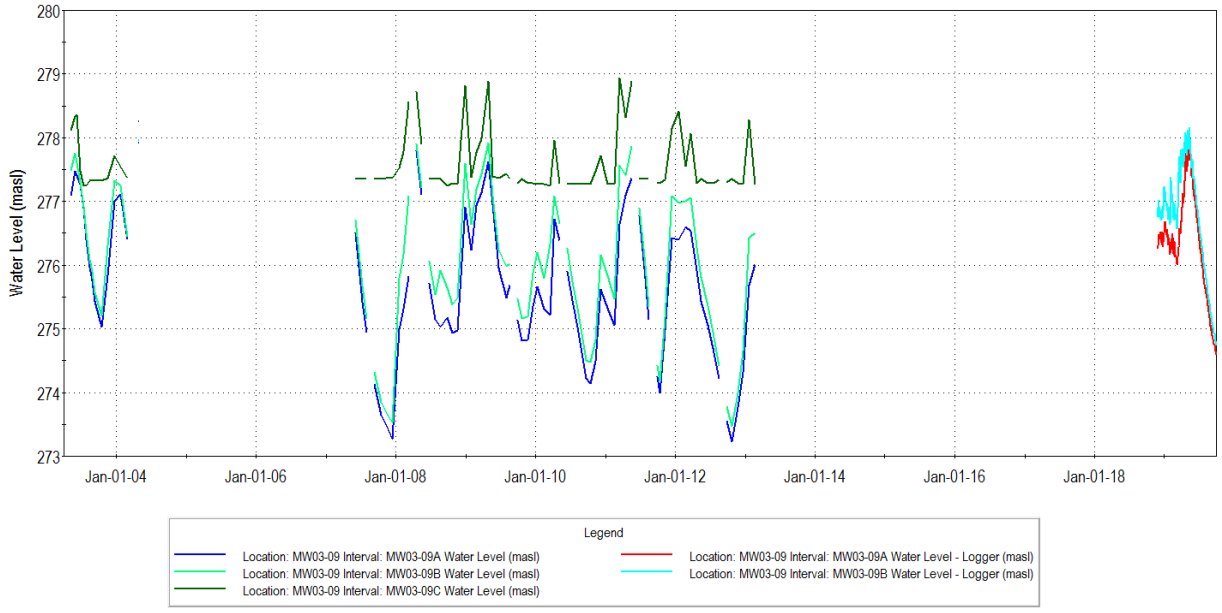

Figure 5.19: Monitor MW03-09, located 650 m from the quarry face.

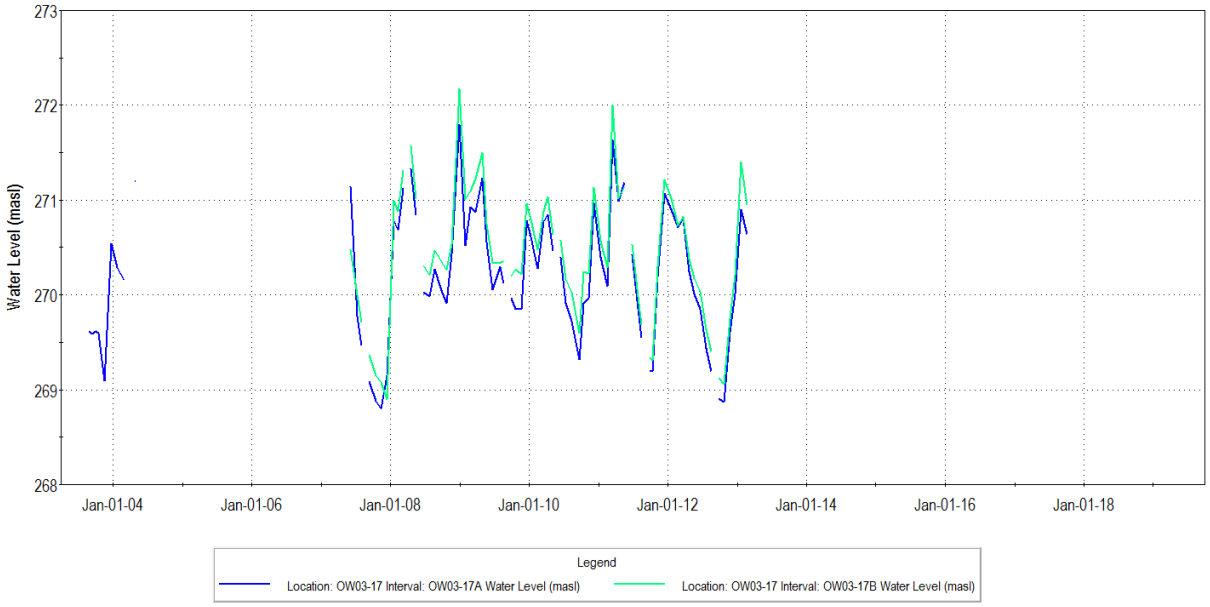

Figure 5.20: Monitor OW03-17, located 1050 m from the quarry face.

5.4 Groundwater Use

Groundwater takings in the province are governed by the Ontario Water Resources Act (OWRA) and the Water Taking Regulation (O. Reg. 387/04); a regulation under the OWRA. Section 34 of the OWRA requires anyone taking more than a total of 50,000 litres of groundwater in a day to obtain a PTTW from the MECP. A detailed review of the permitted groundwater takings within 5 km of the Burlington Quarry was completed.

Agricultural Takings: Results indicated that there are 3 active groundwater PTTWs within 5 km of the Burlington Quarry in the study area (Table 5.2 and Figure 4.13). It was determined that the groundwater takings for agricultural use are relatively distant from the quarry (on the opposite side of the Medad Valley) and are generally small in volume. They were, therefore, not simulated in the model.

Table 5.2: Groundwater PTTW (within 5 km)

Permit No.	Purpose	Source	Max L/Min	Max hrs/d	Days per Year	Distance (km)
4854-9WXRVT	Field Crops	Well	25	8	200	4.38
6781-8SNQ9Q	Nursery	Ponds (spring fed)	4,314	6	60	4.53
8886-8D8T3C	Field Crops	Well	75	10	100	4.39
		Ponds (spring fed)	4,096	16	100	

Industrial/Commercial Water Takings: To extract aggregate from below the water table and operate in dry conditions at the Burlington Quarry, Nelson holds a PTTW (No.: 96-P-3009). The PTTW allows for the site to operate a water management program to control water that enters the quarry footprint as precipitation and groundwater seepage. The PTTW permits the taking of water from two sources:

Quarry Sump 0100 (Northwest Sump) and Quarry Sump 0200 (South-Central sump) at an instantaneous pumping rate of 4,090 L/min (5890 m^3/d) and 945 L/min (1361 m^3/d), respectively. Unlike other water takers, aggregate producers are primarily water handlers and not consumers. The actual amount of water consumed at the Burlington Quarry is relatively small. Well over 90% of the water handled is returned to the local watershed.

Some discharge from Quarry Sump 0100 is diverted, via gravity flow, to the Burlington Springs Golf course for use as irrigation under a separate permit. The remainder is discharged northwest to the roadside ditch along Colling Road, which drains into a tributary of Willoughby Creek north of Colling Road. Water taken from Quarry Sump 0200 is discharged southeast across No. 2 Sideroad to the upstream end of the West Arm of the West Branch of Mount Nemo Creek which is a tributary of Grindstone Creek.

5.4.1 Private Water Wells

A preliminary private door-to-door water well survey was completed by Nelson personnel and a Professional Geoscientist on July 29th and July 30th, 2019. The survey was completed for all residents located within 1 km of the proposed extension lands, including those located on both the north and south sides of Sideroad No. 1. In total, 156 homes were visited. The purpose of the water well survey was to:

- inform the homeowner of the proposed extension planned by Nelson;
- match water well records to properties and confirm well locations;
- obtain baseline information on local water use (quality and quantity) from the homeowner; and
- to offer a voluntary domestic water well monitoring program to those residents located within 1 km of the Burlington Quarry extension lands. This program has been designed to act as an early warning system and would identify any potential adverse interference that may compromise the integrity of the domestic water supply.

Of the 156 homes visited, only eleven homeowners indicated that they were interested in participating in the monitoring program. Seven of the eleven private domestic water wells were accessible and, as a result, have been added to the current groundwater monitoring program (Figure 10.1).

If the ARA licence is issued, Nelson will complete a follow-up door-to-door water well survey to inform residents that they are still able to participate in the program if interested. Particular focus will be on wells located within 500 m of the proposed extraction area and wells that have an available drawdown of less than 10 m. Based on the information obtained from the MECP database, there are 36 water wells that meet this requirement (Table 5.3).

5.5 Conclusions

The hydrogeologic setting in the study area reflects the underlying stratigraphic layering, but with significant additional effects related to weathering, karst, anisotropy, and vertical and horizontal fracturing. The final hydrostratigraphic model layers reflect an integrated interpretation of all the field data, including borehole logs, packer tests, and transient water level patterns. The monitoring of the quarry extraction face advancement since 2003 has provided a direct measure of the effects of quarry development.

Table 5.3: Private wells located within 500 m of extraction boundary and have less than 10 m of available drawdown.

MECP Well ID	Total Depth (m)	Static Water Level (m)	Available Drawdown (m)
2800149	15.2	13.1	2.1
2803646	4.6	2.4	2.2
2807043	9.4	5.8	3.6
2800418	17.4	12.2	5.2
2800487	7.6	2.1	5.5
2800364	17.1	11.6	5.5
2800365	17.1	11.6	5.5
2803292	16.8	11	5.8
7105879	6.1	0	6.1
2803545	15.5	9.1	6.4
2800152	13.7	6.7	7
2806799	18.3	11.3	7
2800415	14	7	7
2805625	15.2	8.2	7
2800362	14	6.7	7.3
2805564	20.4	12.8	7.6
2800368	14	6.4	7.6
2805313	15.2	7.6	7.6
2804226	17.7	9.8	7.9
2807042	11.3	3.4	7.9
2800371	18	10.1	7.9
2800373	16.5	8.5	8
2800126	11.6	3.4	8.2
2804325	9.1	0.9	8.2
2800153	17.7	9.4	8.3
2800369	16.8	8.5	8.3
2800125	9.8	1.5	8.3
2800490	27.4	18.3	9.1
2800358	13.7	4.6	9.1
2800416	16.5	7.3	9.2
2810191	12.2	3	9.2
2805619	18.3	9.1	9.2
2804922	20.7	11.3	9.4
2803042	14.9	5.2	9.7
2800128	12.2	2.4	9.8
2800115	12.8	3	9.8

6 Integrated Model Development and Calibration

6.1 Introduction

Hydrologic (surface water flow) and groundwater flow models are often applied to estimate and help mitigate the effects of quarry development on nearby features (e.g., streams and wetlands) as well as to better predict and manage inflows into the quarry. Typically, the hydrologic and groundwater models are developed separately, with the groundwater flow model run for steady-state (i.e., long-term equilibrium) conditions. A less common approach is the use of integrated groundwater and surface water models, which can assess the changes to the surface water and groundwater systems on a transient (time-dependent) basis. This section presents an overview of the integrated modelling approach and addresses the following:

1. How is the movement of water between the surface and groundwater systems (dynamic feedback) represented in the integrated model?
2. What are the benefits and possible disadvantages of integrated modelling as it applies to the objectives of this study and the unique features of the study area?

The overview describes how each of the sub-model components are developed, pre-calibrated, and then coupled and "final calibrated". It is intended to help the reader better understand the technical details presented in subsequent discussions of model results. More detailed descriptions of model construction and calibration are provided in Appendix C, D, and E of this report.

6.2 Integrated Modelling - Overview

6.2.1 Integrated Modelling

An integrated model represents the entire hydrologic cycle in a comprehensive, complete, and coupled manner. The hydrologic cycle includes:

- Hydrologic processes (e.g., precipitation, interception, snow accumulation and melt, overland runoff, infiltration, interflow, evapotranspiration (ET), and groundwater recharge and discharge)
- Hydraulic processes (i.e., streamflow) and wetland and lake water balances
- Groundwater processes (i.e., saturated and unsaturated subsurface flow)

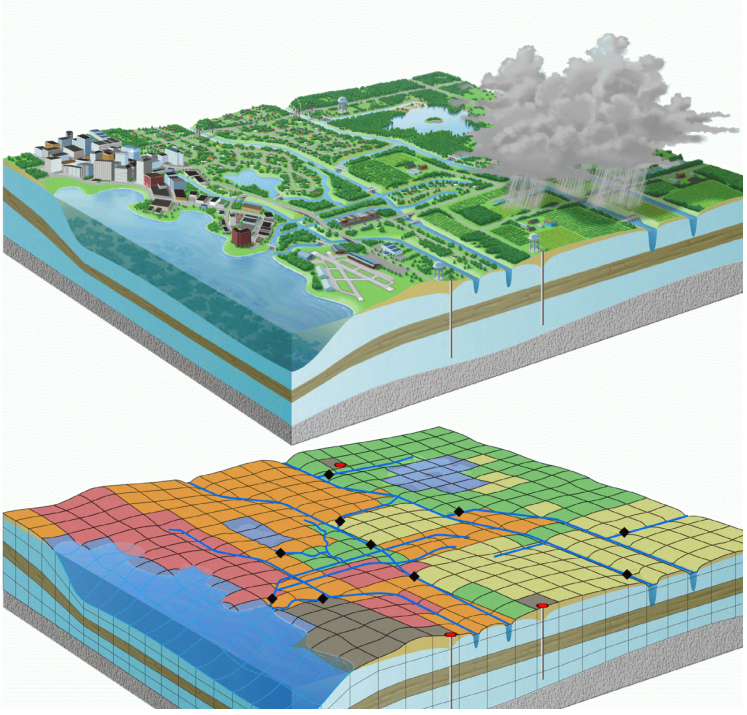

Figure 6.1: Integrated numerical representation of the surface and subsurface using a cell based approach (USGS Image).

A comprehensive and complete representation of the hydrologic cycle is one in which the overall water

budget is tracked through both the surface water and groundwater systems and where water cannot be created or lost. The term "integrated" denotes that the transfer of water between the surface water and groundwater domains is simulated and that key feedback mechanisms are represented. Integrated models determine the flows in the groundwater and surface water systems at the same point in time by solving the governing equations simultaneously or in an iterative manner.

An integrated approach provides additional benefits that are related to the development and calibration of the model. When surface water and groundwater models are developed separately, simplifying assumptions must be made in each model to account for processes that occur in the other model domain. For example, groundwater recharge must be independently estimated and applied to a groundwater model. Similarly, in surface water models, the multi-aquifer systems and complex hydrostratigraphy is often represented as simple linear reservoir accepting excess water and groundwater flow across the catchment boundaries is rarely considered. Finally, there are many processes, such as rejected recharge when groundwater levels are high, have complex dynamic feedback.

These simplified assumptions may not be valid when using the models to evaluate future response under different climate and water use conditions. With an integrated model, the sub-models are often "pre-calibrated" using a traditional model development processes, but final calibration is undertaken with the feedback mechanisms active and without the need to rely on simplifying assumptions and estimates.

6.3 USGS GSFLOW Overview

The USGS GSFLOW code (Markstrom *et al.*, 2008) was used in developing the integrated groundwater/surface water model for the area surrounding the Burlington Quarry. GSFLOW is an open-source, well-documented code and has been used to investigate groundwater/surface water interaction in a number of recent peer-reviewed studies (e.g., Huntington and Niswonger, 2012; Hunt *et al.*, 2013; Ely and Kahle, 2012; Tanvir Hassan *et al.*, 2014; and Niswonger *et al.*, 2014). Earthfx has applied the code to a number of nearby watersheds as part of advanced water-budget studies for the Ontario Source Water Protection program.

GSFLOW was developed from two widely-recognized USGS submodels: The Precipitation Runoff Modelling System, PRMS (Leavesly *et al.*, 1986), and the modular groundwater flow model MODFLOW-NWT (Niswonger *et al.*, 2011). Version 1.1.6 of GSFLOW was used in this study, which integrates PRMS version 3.0.5 and MODFLOW-NWT version 1.0.7. The MODFLOW-NWT code has three key process modules: the UZF unsaturated flow module (Niswonger *et al.*, 2006), the SFR2 streamflow routing module (Niswonger and Prudic, 2005), and the LAK3 lake module (Merritt and Konikow, 2000). The different processes and submodels in GSFLOW are listed in Table 6.1 and are shown schematically in Figure 6.2. The submodels include numerical representations of the physical system and the processes that occur within each submodel domain.

Table 6.1: Processes and GSFLOW submodels.

Zone	Process Component	GSFLOW Submodel
1	Hydrology – Soil Water Processes	PRMS Hydrologic Submodel
2	Streamflow	SFR2 module for MODFLOW
	Lakes, and Wetlands	LAK3 module for MODFLOW
3	Unsaturated Flow	UZF module for MODFLOW
	Groundwater flow	MODFLOW-NWT Groundwater Submodel

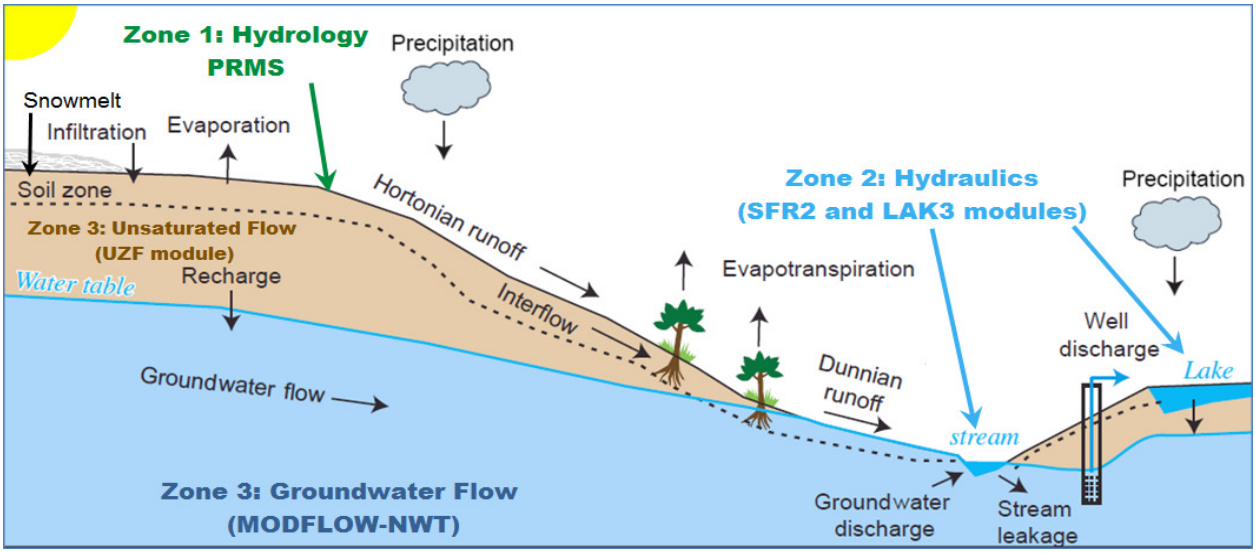

Figure 6.2: Schematic diagram of the GSFLOW process regions.

6.3.1 Spatial Representation

The MODFLOW groundwater flow submodel in GSFLOW is a fully-distributed model, meaning that groundwater processes are simulated using a cell-based representation of the study area. The PRMS hydrology sub-model is also run in a fully-distributed manner, with each cell having unique physical properties. Cells are assigned spatially variable soil and land cover properties as part of model construction. During a simulation, cells receive spatially-variable inputs, such as daily rainfall, snowfall, temperature, and solar radiation. Overland runoff and interflow are routed between cells and to the receiving streams or lakes through a topographically-driven cascade flow network.

The spatial representation in GSFLOW is particularly flexible. Three different grid resolutions can be used for the climate, surface hydrology, and subsurface groundwater processes, respectively (Figure 6.3). This allows for different levels of refinement in each of the three regions to meet the accuracy requirements associated with those processes. The grids in this study share a common origin and, although they have different spacing, the grids are generally aligned so that MODFLOW cells can contain integer multiples of PRMS cells.

Topography, soil properties, and land use vary widely across the study area, so a fine resolution was used to represent local-scale natural features and anthropogenic modifications such as the quarry, agricultural land use, and urban development (Figure 6.3). Sub-cell hydrologic processes are also represented, where each cell in the PRMS submodel is divided into pervious (grass or soil) and impervious (roads, parking lots, buildings) zones (Figure 6.3, right side enlargement), with different processes, storage properties, and interactions simulated in each sub-cell zone.

Rivers and streams in GSFLOW are represented as a network of one-dimensional line elements with open-channel flow routing through the network. The storage associated with small wetlands can be represented in the PRMS soil zone, while larger lakes are represented with the LAK3 module and can be incised into one or more groundwater layers. Wetlands in close proximity to the Burlington Quarry were represented as shallow lakes in this study.

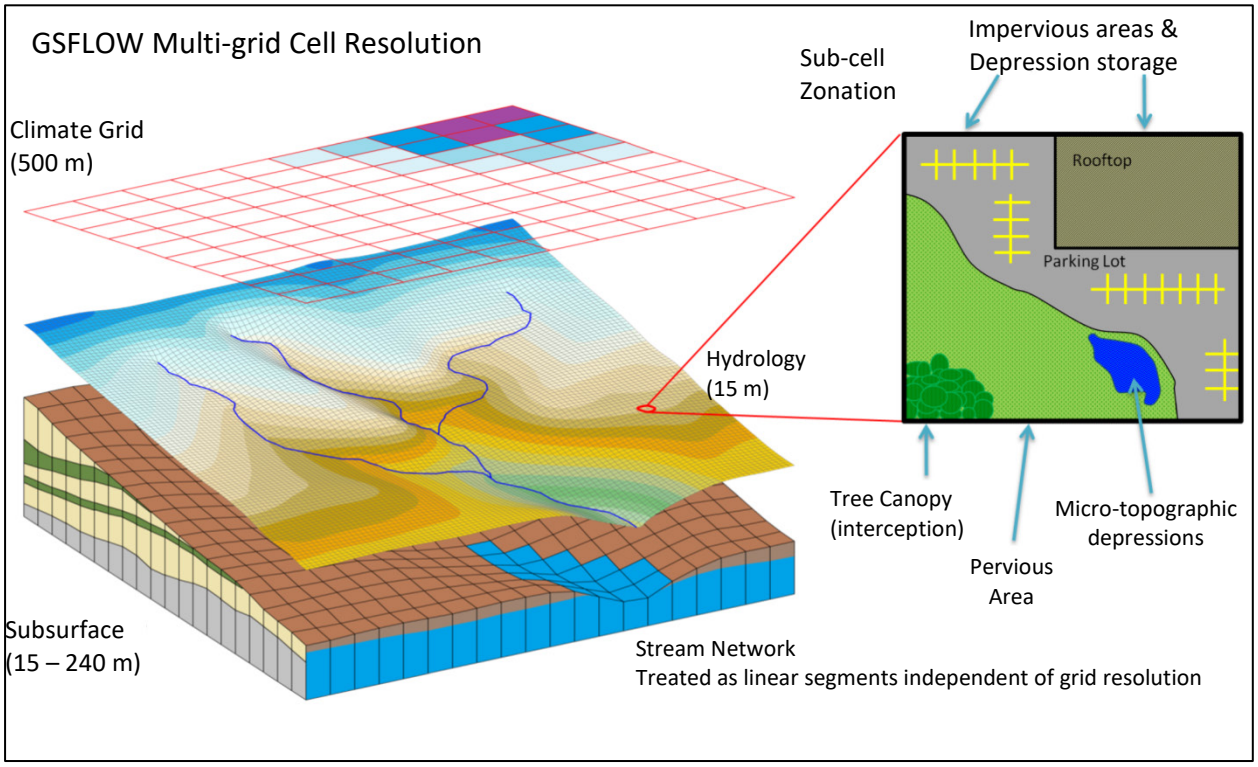

Figure 6.3: Different grid resolutions are available for each process region within GSFLOW.

Groundwater flow processes can generally be represented at a coarser scale. The MODFLOW submodel allows a variable cell size grid. In this study, the grid was locally refined in the vicinity of the quarry to better represent nearby wetlands and streams and drawdowns.

Finally, climate inputs, such as rain, snow, and temperature data are available on a wider geographic distribution. GSFLOW allows a separate coarser grid resolution for the interpolation of climate data between stations to represent spatially-variable temperature and precipitation.

6.3.2 PRMS Submodel Soil Zone Processes

The PRMS submodel represents the vegetative canopy, pervious and impervious surfaces, and the soil zone as a series of reservoirs with finite capacity. The reservoirs are filled and depleted by different hydrologic processes and discharge to one or more reservoirs when the capacity is exceeded. For example, vegetation intercepts rainfall at rates dependent on the plant type and percent of vegetative cover under winter and summer conditions. Intercepted water is subject to evaporation (Figure 6.4). Water in excess of canopy interception capacity is passed to the land surface reservoir or to the snow pack (if present) as "throughfall" or net precipitation. Net precipitation that falls on impervious soils can fill the depression storage reservoir and is subject to evaporation. Water in excess of depression storage is routed as Hortonian overland runoff through the Cascade Flow module in GSFLOW and, if it does not re-infiltrate along the pathway, it passes from PRMS to SFR2 or the LAK3 modules and routed through the stream/lake network.

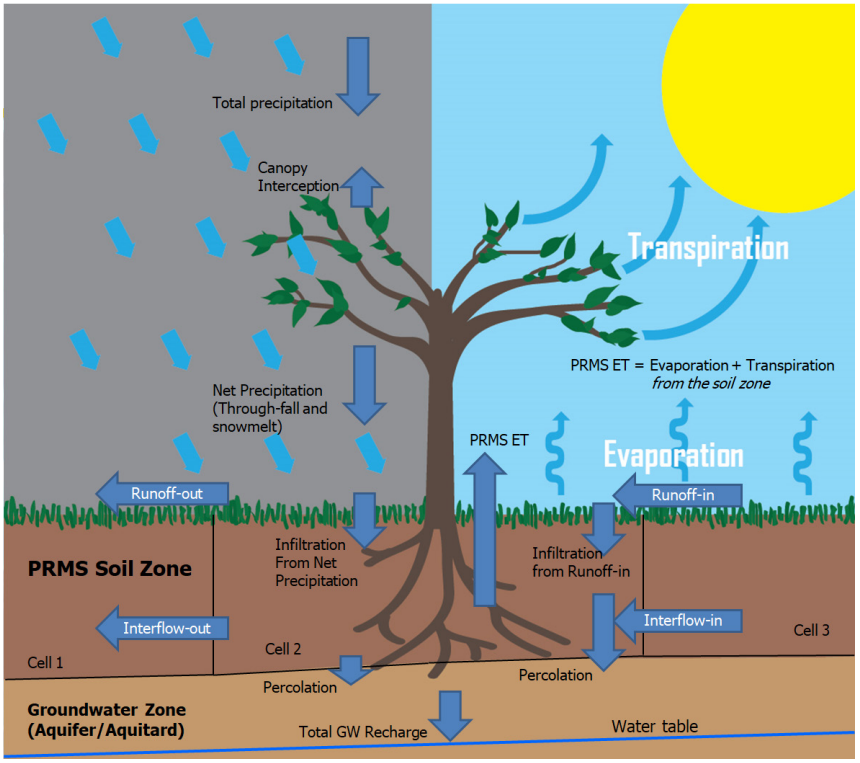

Figure 6.4: PRMS Soil Zone Processes

In a similar manner, net precipitation on pervious soils can infiltrate into the soil zone. If the infiltration capacity is exceeded, the water is discharged as Hortonian runoff (Hortonian runoff) and routed downslope to other cells and ultimately to the stream/lake network. Infiltrating water fills the soil zone reservoir where it is subject to evapotranspiration. Excess water above field capacity is partitioned between interflow and gravity drainage. Interflow is routed to downslope cells along the cascade network. Gravity drainage is directed to the unsaturated zone represented with the UZF module. Water is returned to the soil zone as rejected recharge if the percolation capacity is exceeded, otherwise, the water moves downward to the saturated zone as groundwater recharge. Excess water in the soil zone (above saturation) and any rain falling on the cell is discharged to the cascade network as Dunnian overland runoff.

6.3.3 GSFLOW Process and Region Integration

A key aspect of the integrated model is the representation of processes that move water between the three main model domains, as shown in Figure 6.5. The next sections provide a brief description of the key inter-region processes.

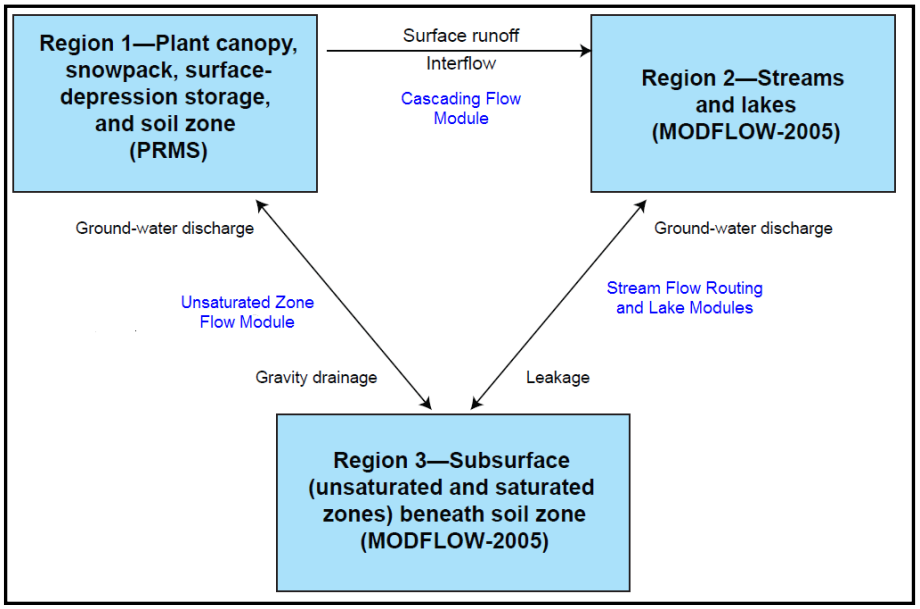

Figure 6.5: Processes moving water between GSFLOW regions.

MODFLOW-NWT simulates the saturated flow system that moves groundwater from recharge areas to points of discharge to streams, lakes, wetlands, and wells. Groundwater can discharge to the soil zone when the water table rises to intersect the base of the soil zone. Discharging groundwater is passed from MODFLOW to PRMS through the UZF module and is added to the soil zone reservoir. Groundwater discharge to the soil zone in low-lying areas often fills the soil zone reservoir and then discharges as Dunnian runoff.

6.3.4 Groundwater/Surface Water Feedback

Rejected Recharge and Contributing Area: The portion of the model area where direct feedback from the groundwater system occurs can change with seasonal fluctuations in the water table or in response to rainfall events. The portion of the watershed where the water table is near-surface and contributes to Dunnian runoff (rejected recharge) has been referred to as the "contributing area" (Dickinson and Whiteley, 1970). Figure 6.6 is a schematic illustrating the change in the contributing area due to the shift in the position of the water table between spring and summer. Rainfall and snowmelt events generate more runoff during the spring because the "contributing area" is larger and saturation excess (Dunnian runoff) is more prevalent.

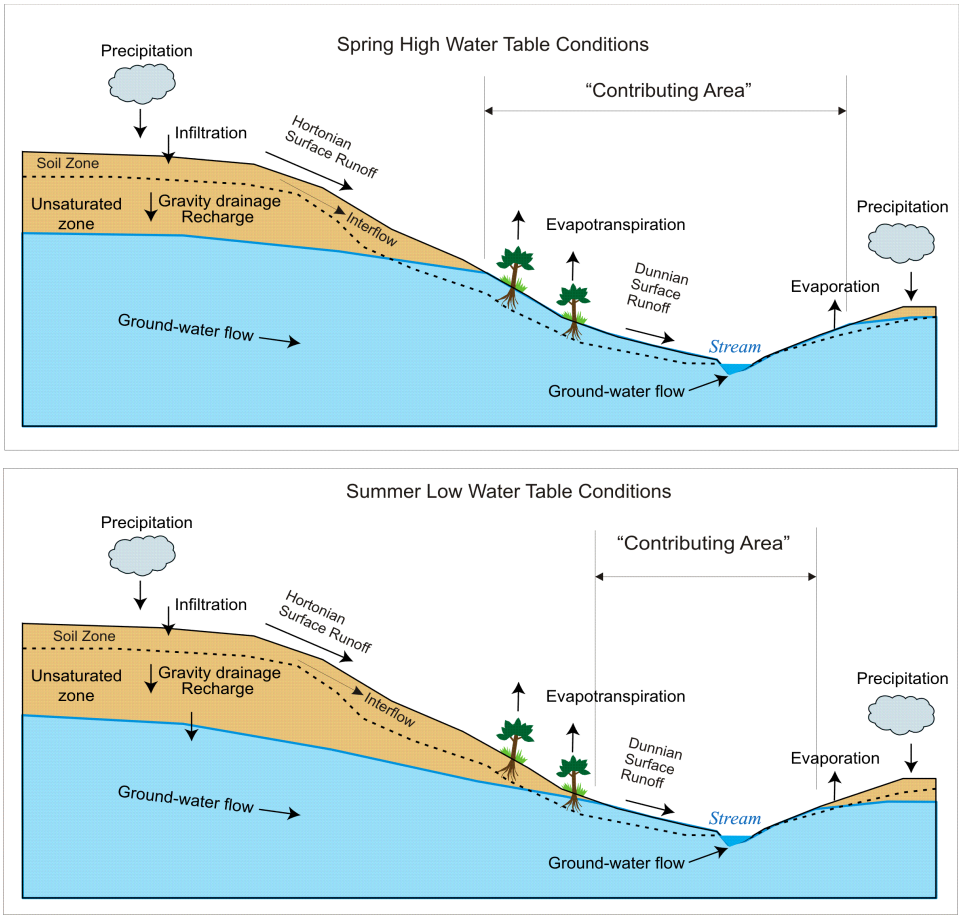

Figure 6.6: Changes in the spring and summer position of the water table increasing Dunnian runoff and the size of the "Contributing Area" (from Markstrom *et al.*, 2008).

Stream/aquifer interaction occurs in the hyporheic zone where water is exchanged between the stream and the groundwater system. This exchange is represented in the GSFLOW model as head-dependent discharge or leakage (Figure 6.7) with the assumption that the rate of water movement between the aquifer system and the stream is proportional to (1) the difference between the head in the aquifer and the stream stage, and (2) the permeability of the intervening streambed. The exchange of water can occur in either direction. Flow across the streambed is presumed to be independent of the water table position when the water table falls below the streambed bottom (Harbaugh, 2005). Similar exchange can occur between a lake and the underlying aquifer across the lakebed materials as lake levels, and groundwater heads change over time.

Often, only the exchange of water across the streambed is represented in separate groundwater models. Studies with the GSFLOW model have shown that considerable amounts of water are exchanged as groundwater discharge to the soil zone in riparian area, which subsequently emerges as Dunnian overland runoff. It should also be noted that groundwater discharge across the streambed is locally suppressed or even reversed as stream stage temporarily rises after precipitation or snowmelt events (Freeze and Cherry, 1979). Groundwater then seeps back out to the stream as the stage subsides (bank storage). While the representation of the groundwater discharge to streams in GSFLOW is more physically correct, it is sometimes more difficult to separate the surface water and groundwater components of discharge to streams in an integrated model.

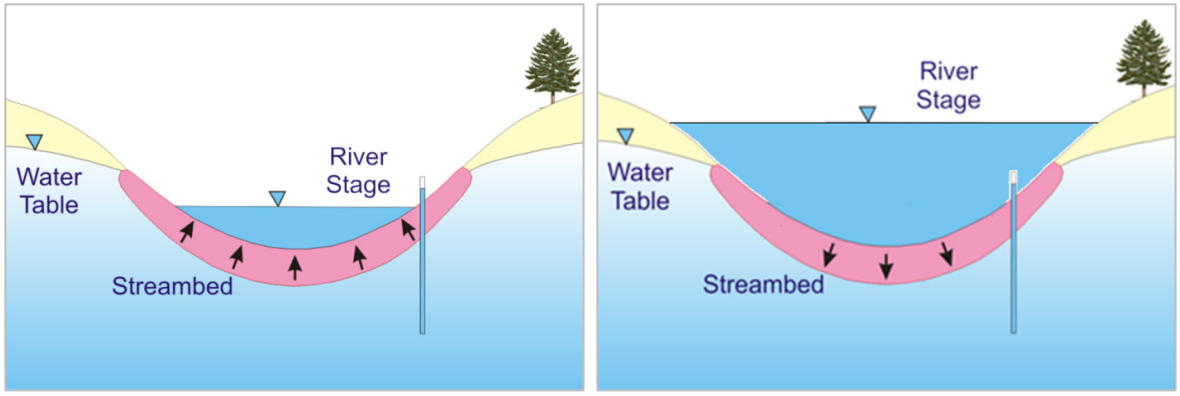

Figure 6.7: Head-dependant groundwater discharge to streams (l) and leakage from streams (r).

6.3.5 Temporal Discretization and Submodel Coupling

During a GSFLOW simulation, each submodel receives a set of daily inputs (e.g., daily climate data for PRMS and daily recharge and pumping rates for MODFLOW). The PRMS submodel calculates a new water balance for each cell in response to the climate inputs and passes updated estimates of groundwater recharge, overland runoff to streams, and residual ET demand to the MODFLOW submodel. In turn, the MODFLOW submodel solves the groundwater flow equations to compute new groundwater levels and the resulting changes in storage, groundwater ET, and groundwater discharge to the soil zone, lakes, and streams. Surface water flows, based on inputs including direct precipitation, evaporation, overland runoff, and groundwater gains or losses, are routed downstream and new stage values in lakes and streams are calculated using the SFR2 and LAK3 modules. The process is repeated in an iterative manner until the exchange of water calculated by the two submodels converges. The final soil water balance, groundwater recharge rates, change in discharge to streams, streamflow, lake stage, groundwater heads (including the updated water table position) are then computed and saved and the model progresses to the next day. A schematic showing the iterative computations executed as the model progresses through time is presented in Figure 6.8.

6.4 GSFLOW Model Development Process

Developing an integrated watershed model is more complicated than building an independent hydrologic model or groundwater model. However, many of the basic model development steps and procedures are similar. Model development begins with the collection of available data. The next steps, as documented in the previous sections of this report, include describing and assessing the features and critical processes active in the study area. Information on the topographic, physiographic, hydrologic, geologic, and hydrogeologic settings is synthesized and used to formulate conceptual models of the soil zone, surface water flow system (lakes, wetlands, and streams), stratigraphy, and hydrostratigraphy.

With data compilation and conceptualization completed, the next step involves converting the conceptual model and data into input data and into parameter values for the PRMS and MODFLOW submodels. This translation is described in Appendix C for the PRMS submodel and Appendix D for MODFLOW. For this study, the submodels were tested, “pre-calibrated” independently, and then combined in the GSFLOW framework for final calibration, as described in Appendix E.

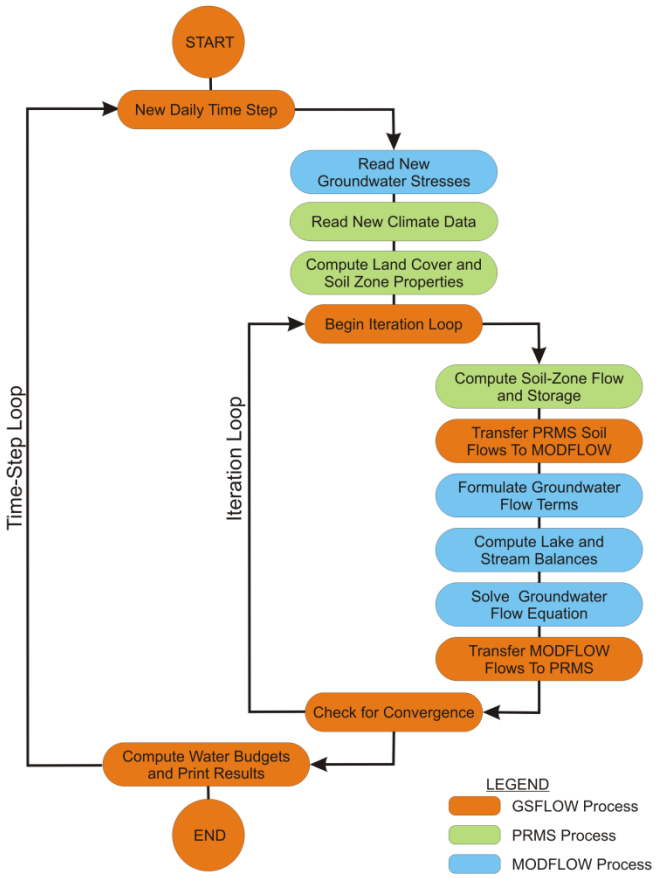

Figure 6.8: Computational sequence for an integrated PRMS/MODFLOW simulation in GSFLOW (modified from Markstrom *et al.* (2008)).

It is important to note that the overall process of data assimilation, conceptual model development, and integrated model calibration is also iterative. Analysis of preliminary model results often pointed to gaps in the previous analyses. The gaps were addressed by obtaining additional data or re-evaluating the data analysis and assumptions made in the conceptualization phases. Model parameters, as well as the underlying conceptual geologic model, were revised several times during the study as our understanding of the study area grew.

6.5 PRMS Submodel Development Overview

Two versions of the PRMS submodel were constructed. The first version of the PRMS submodel was developed for pre-calibration purposes and encompassed the entire gauged portion of the Grindstone Creek. A second version of the PRMS submodel was used in the GSFLOW integrated model simulations covered a smaller area focussed on the Burlington Quarry and Mt. Nemo area. Daily inflows into the GSFLOW model from the western portion of the Grindstone Creek watershed, which was excluded from the GSFLOW model, were estimated from results of the larger, Grindstone Creek PRMS submodel. Similar parameter values were used in both models. Further discussion of the Grindstone Creek PRMS submodel is presented in Appendix C.

Spatial and Temporal Discretization: The GSFLOW model area was represented by 372,368 active model cells covering 83 km². This grid resolution corresponded well with the MODFLOW-NWT groundwater submodel. Cells located outside of the PRMS submodel boundaries were designated as inactive and were not included in the water balance computations. A small portion of the study area, showing the 15 m grid, is presented in Figure 6.9. The version of PRMS included in GSFLOW runs on a daily time step. Streamflows generated by the PRMS model are assumed to represent average daily streamflow.

6.6 Parameter Assignment

Initial estimates of model parameters were assigned based on available data and were updated during the model calibration process. For parsimony, consistent assumptions and parameter values were applied across the study area, where possible. Model parameters fall into five key groups, discussed briefly below. More detail can be found in Appendix C.

Topography-related Properties: Topography for the model area is based on a 5-metre DEM produced by MNRF and infilled with local drone survey data in the vicinity of the Burlington Quarry and proposed extension lands. Slope and slope aspect values were calculated from the DEM after resampling to the PRMS grid. The cascade overland flow routing network was also generated from the DEM.

Soil Properties: MNR Soil Survey Complex (2013) mapping was indexed and resampled to the PRMS grid (Figure 4.9). Soil properties, including porosity (n), field capacity (fc), and wilting point (wp), and hydraulic conductivity were assigned to cells using tabulated look-up values (see Table 17.1 in Appendix C). Soil properties have a significant influence on hydrological processes because they control the amount of water that can infiltrate and be transmitted to the water table as well as the amount of water lost to actual ET. Parameters that controlled the partitioning of flow between interflow and percolation to the water table were also specified as soil-type properties. As an example, Figure 17.11 shows the spatial distribution of groundwater seepage rates.

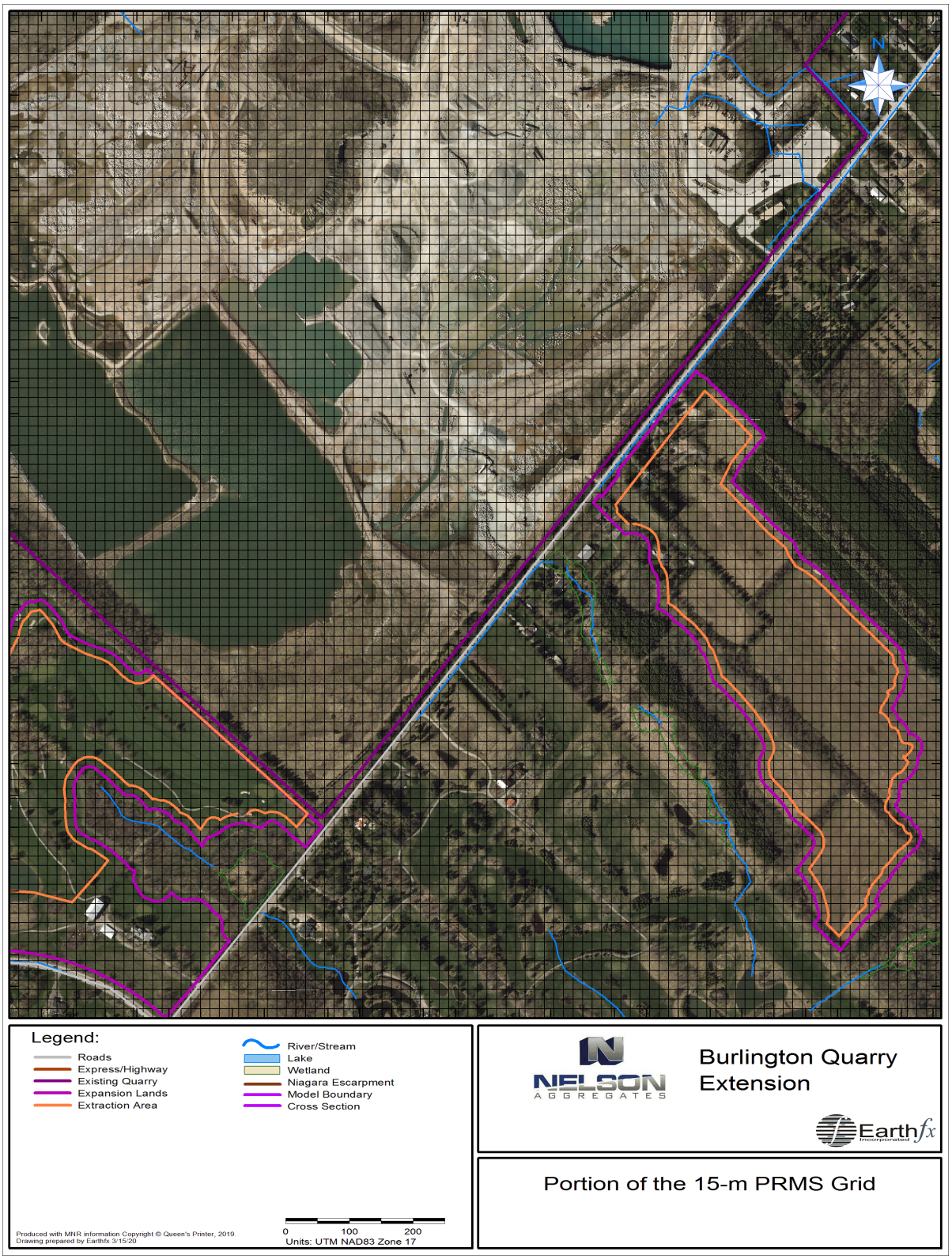

Figure 6.9: Portion of the PRMS model grid in the quarry vicinity.

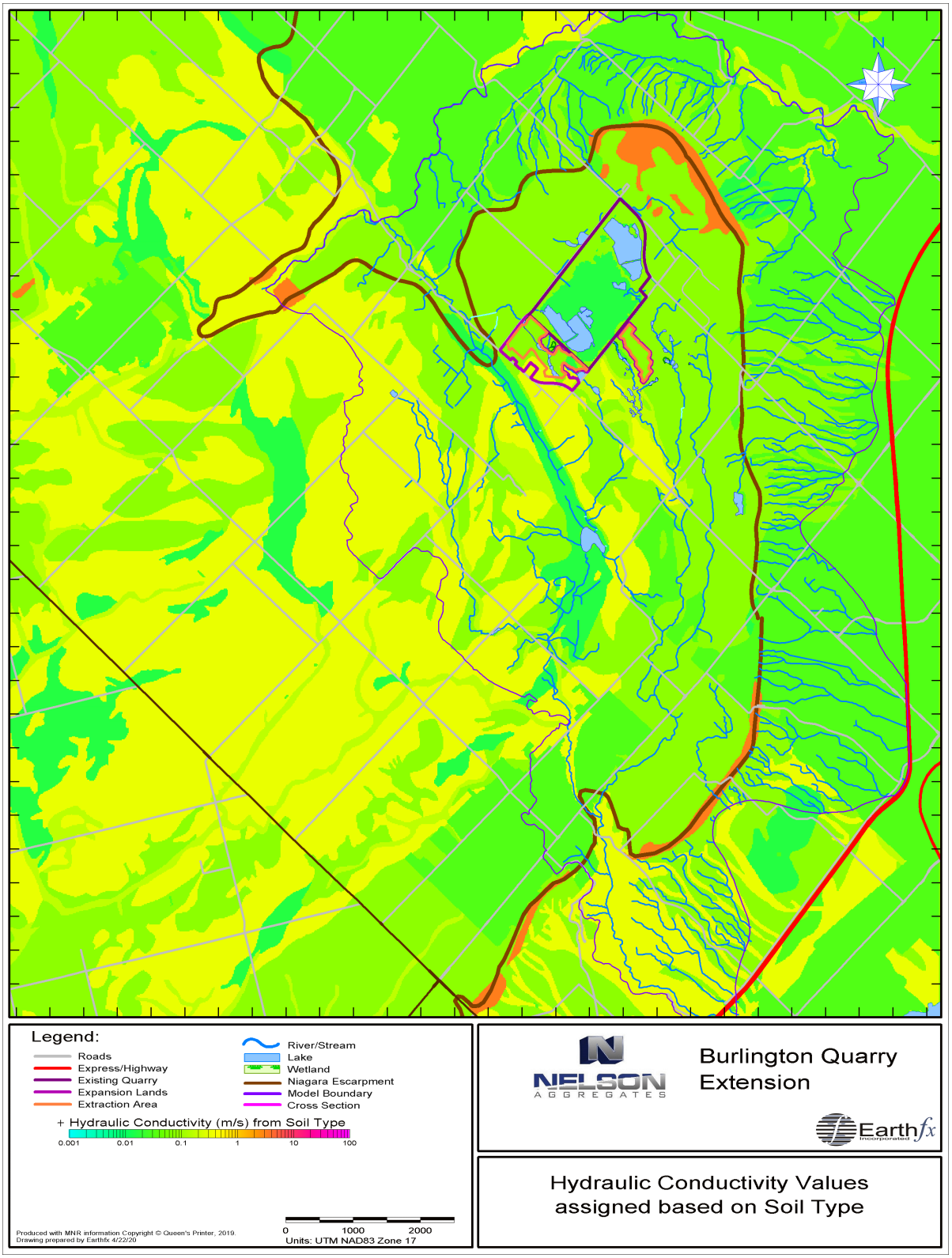

Figure 6.10: Surficial soil hydraulic conductivity.

Land Use-related Properties: Land use/land cover data was obtained from the Southern Ontario Land Resource Information System (SOLRIS v3; MNRF, 2019). The data were indexed and resampled to the PRMS grid (Figure 4.8). Properties including percent imperviousness, depression storage, vegetation index, vegetative cover density, canopy interception storage, and soil zone and extinction depth thickness were assigned to model cells using a look-up table (see Table 17.2 in Appendix C). The urban areas were subdivided into "built-up area pervious" and "built-up area impervious" which may be overly simplified; however, the portion of the study area with these classifications is small. Figure 6.11 shows the percent impervious cover per 15-m as assigned based on the SOLRIS Version 3 land use data.

Hydrological Processes Parameters: Parameters values were estimated for many of the submodel processes, such as snowpack accumulation, snowmelt, and potential ET (PET) calculation. These were generally estimated from "book values" or the results of previous Earthfx investigations in the Halton/Hamilton area.

6.7 Climate Data

The availability of climate data in the study area is discussed in Section 4.1. Three main climate datasets were assembled as inputs to the PRMS submodel. The datasets include 1) precipitation, 2) maximum and minimum daily air temperature, and 3) net incoming solar irradiation. The period of record varies among the available climate data sources; but a continuous climate dataset was compiled. Daily measurements of precipitation and temperature at 121 climate stations were interpolated to a 500 m grid covering the study area.

Incoming solar radiation is controlled primarily by the number of possible hours of sunshine per day and the percent cloud cover. Solar radiation data are collected at very few stations in Ontario, and a continuous dataset was created by averaging and infilling of daily solar radiation information from 11 stations across southern Ontario. Previous studies (Earthfx, 2010) showed that the station data was well correlated despite the large inter-station distances. Solar radiation was estimated by the Hargreaves and Samani (1982) method when direct observations were unavailable.

6.8 PRMS Model Calibration Results

Appendix C describes the calibration of the Grindstone Creek PRMS submodel to match observed streamflow at two Environment Canada/Water Survey of Canada gauges on Grindstone Creek. Figure 6.12 shows simulated and observed streamflow, in m^3/s, at the Grindstone Creek near Millgrove gauge along with precipitation and snowmelt, while Figure 6.13 shows the simulated and observed streamflow at the Grindstone Creek near Aldershot gauge. The observed flows are well correlated to the simulated rainfall and snowmelt events, and the timing of the peak flows in the simulated response generally match the observed events. There are exceptions, possibly due to limitations in the precipitation monitoring network and possibly due to simplifications in the PRMS model and snowmelt computations. The model achieved acceptable Nash-Sutcliffe Efficiencies (Eq. 17.1) of 0.52 and 0.44 for the upstream and downstream gauges, respectively. The model was deemed sufficiently well calibrated for its primary purpose of estimating daily inflows from the upper part of Grindstone Creek, not represented in the GSFLOW model.

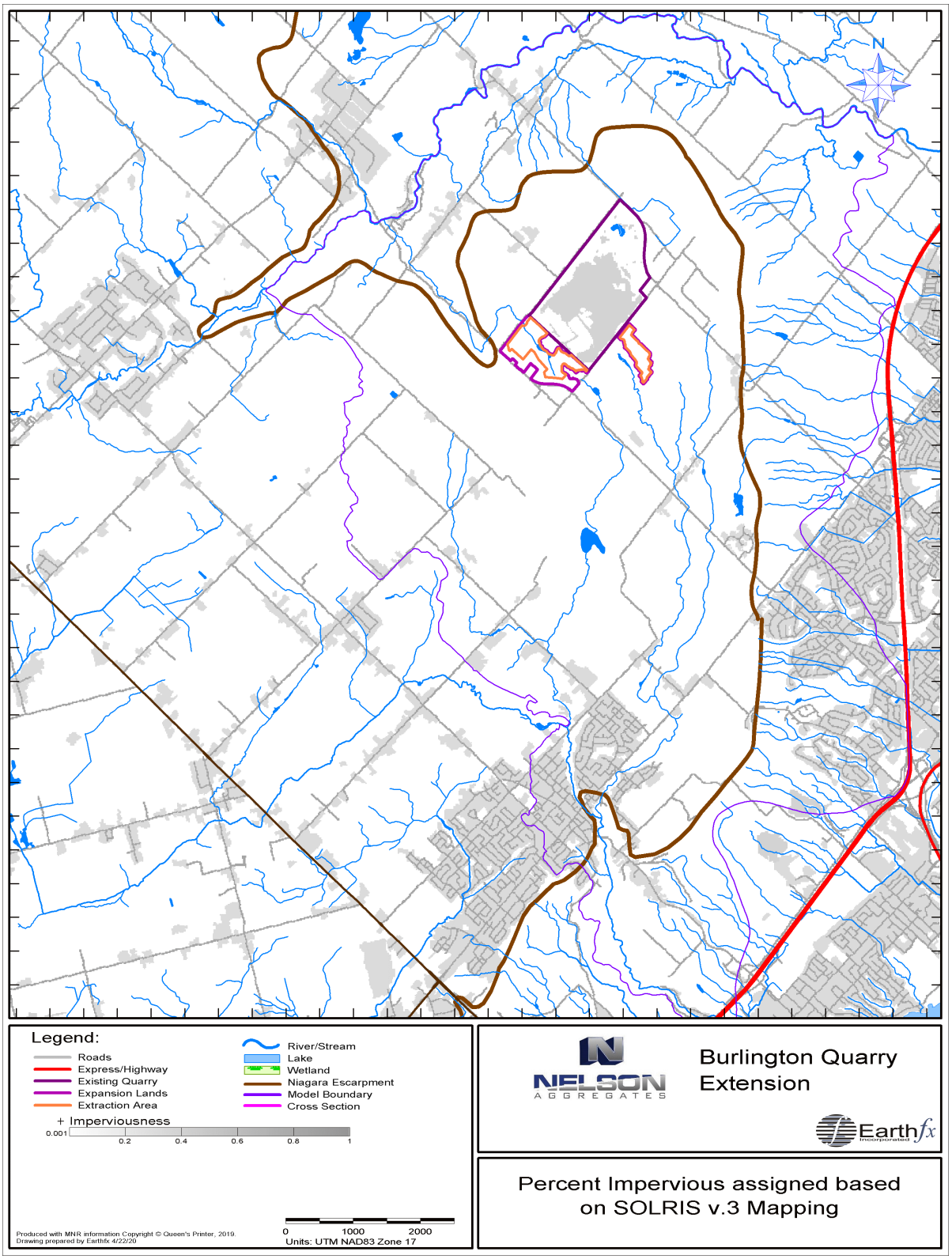

Figure 6.11: Percent impervious cover per cell assigned based on SOLRIS v.3 land cover.

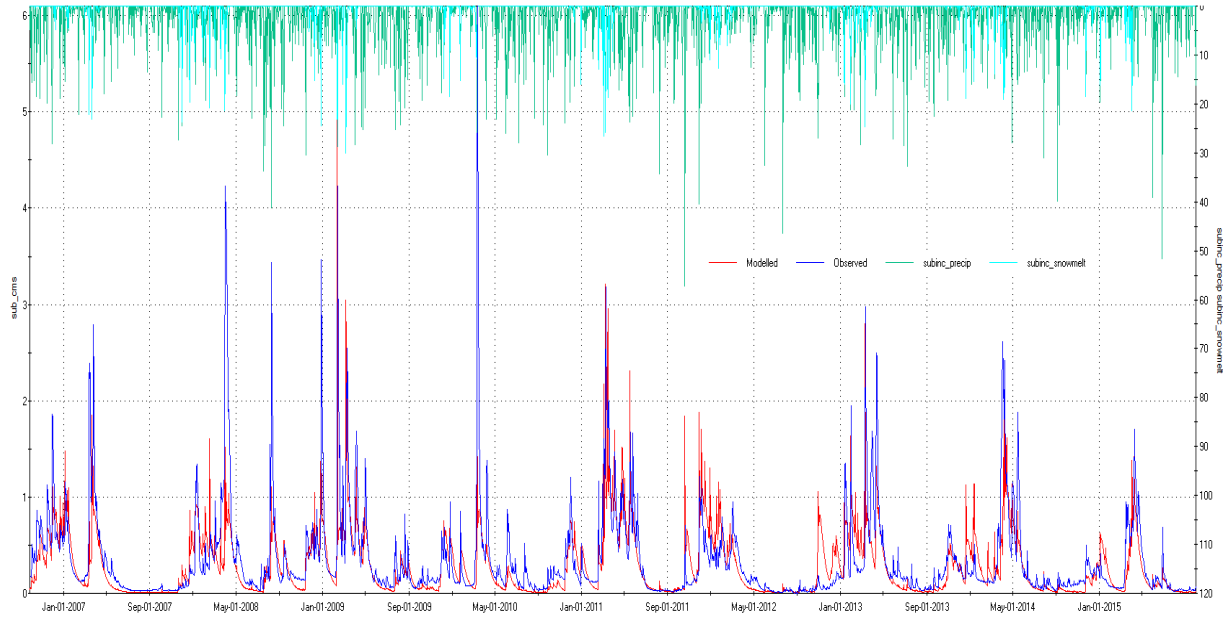

Figure 6.12: Simulated and observed streamflow (in m^3s) at the Grindstone Creek near Millgrove gauge along with precipitation and snowmelt.

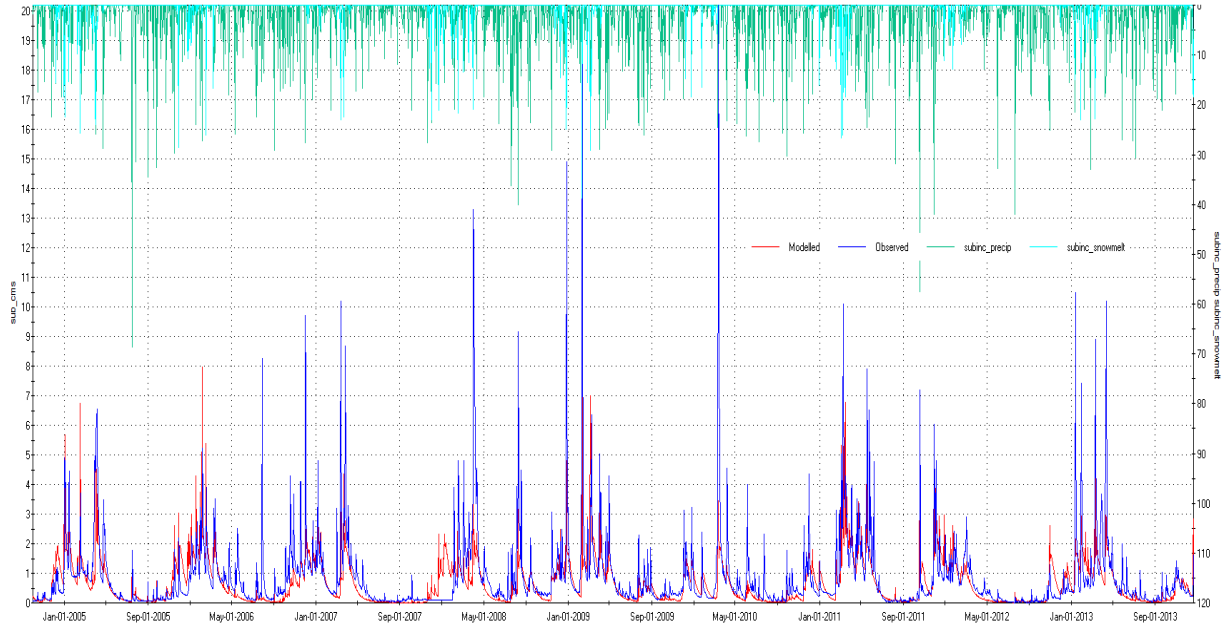

Figure 6.13: Simulated and observed streamflow (in m^3s) at the Grindstone Creek near Aldershot gauge along with precipitation and snowmelt.

6.9 PRMS Submodel Outputs

The PRMS submodel provides daily values for all components of the water budget including precipitation, interception, snowmelt, evapotranspiration, overland runoff, infiltration, and groundwater recharge. The daily values can be presented as hydrographs or maps, and can be aggregated spatially and/or over time so that local water balances can be readily produced.

Figure 6.14 shows the average cell-based average daily precipitation. Values vary over a small range, from 904 mm/yr in the northeast end of the model area to 931 mm/yr in the south. The blockiness of the results is due to the 500 m grid resolution of the input climate data.

Figure 6.15 shows the average annual cascading runoff, shown in volumetric terms (i.e., m^3/d as opposed to mm/yr). A log-scale is used for the color ramp to highlight results. Cascading flow defines the average volume of water moving along the cascade flow path at a given location and includes interflow, Hortonian runoff, and Dunnian runoff.

Excess snowmelt, net precipitation and upslope Hortonian run-on (that does not contribute to runoff from the cell) enters the capillary reservoir as infiltration. Water is removed from the capillary reservoir by ET. Potential ET was computed based on daily temperature and solar radiation and ranged from 542 to 1159 mm/yr. Actual ET can be rate-limited, especially during summer months, if there is insufficient water available in the soil zone. The distribution of total actual evapotranspiration (AET) is presented in Figure 6.16 and includes canopy interception, sublimation, and evaporation from impervious areas but not lake evaporation. AET values ranged between 100 to 1025 mm/yr. High rates occur over the lakes, in the Medad Valley and other areas where soil water is not limited. Rates can exceed infiltration where upslope Dunnian runoff, upslope interflow, and groundwater discharge to the soil zone occur.

PRMS calculates the potential groundwater recharge, which is equal to all water entering the gravity drainage reservoir after interflow is removed. The values often exceed the actual infiltration capacity of the soils underlying the soil zone. Figure 6.17 shows average annual net groundwater recharge for the study area. When coupled with GSFLOW, this value represents the groundwater recharge sent by PRMS to the groundwater model minus groundwater discharge back from MODFLOW. The white areas in Figure 6.17, such as in the Medad Valley, represent areas where groundwater discharge exceeds groundwater recharge.

Groundwater recharge ranges between 100 to 300 mm/yr with the variation due to the different combinations of soil types, land use, and topography. Cells near the end of the long cascade flow paths can have higher rates of focused groundwater recharge. Groundwater discharges to the stream either as baseflow in the stand-alone PRMS model or as a combination of hyporheic discharge (groundwater discharge directly to the stream channel) and groundwater discharge to the soil zone in the riparian areas when PRMS is coupled with MODFLOW.

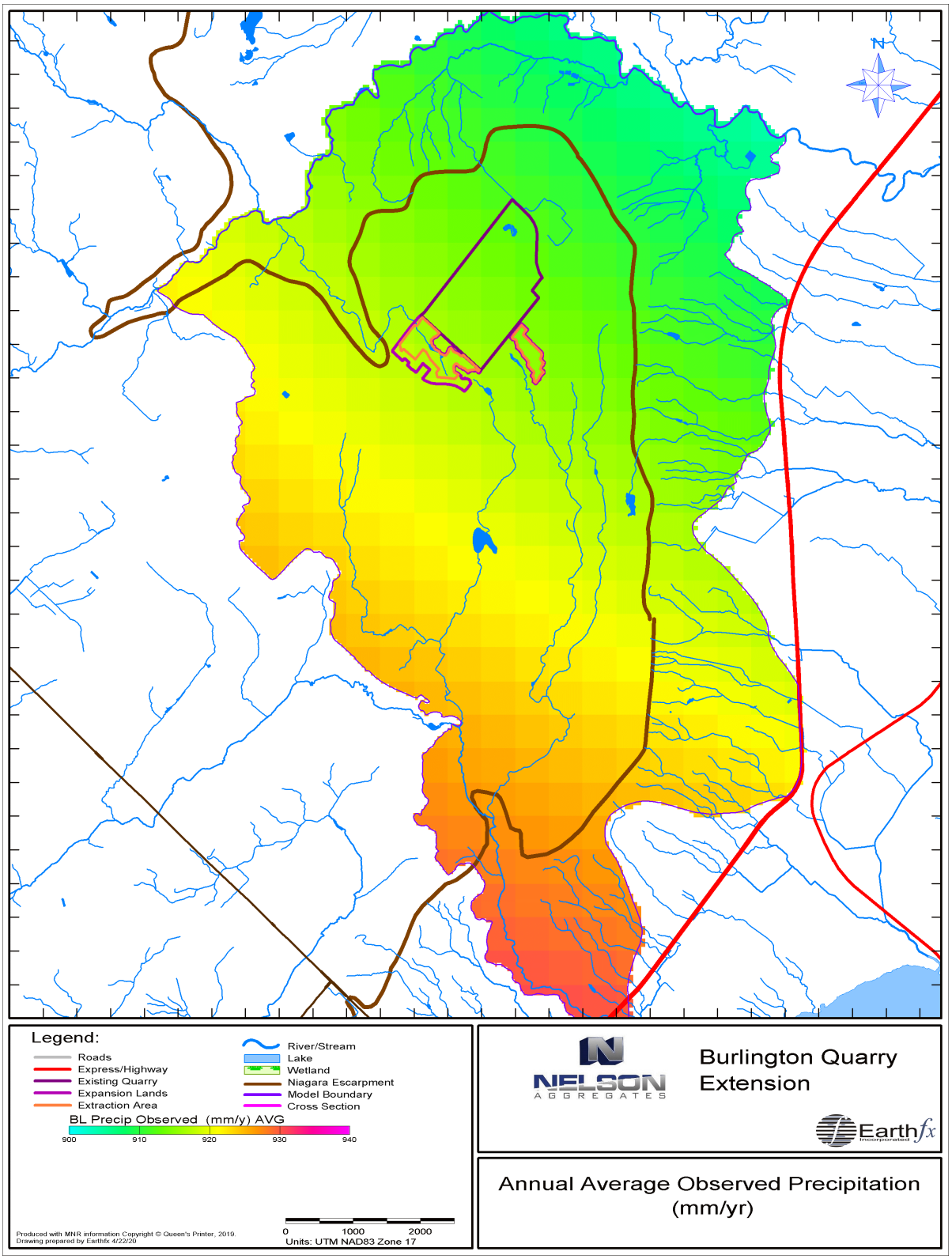

Figure 6.14: Simulated annual average precipitation in the PRMS submodel in mm/yr.

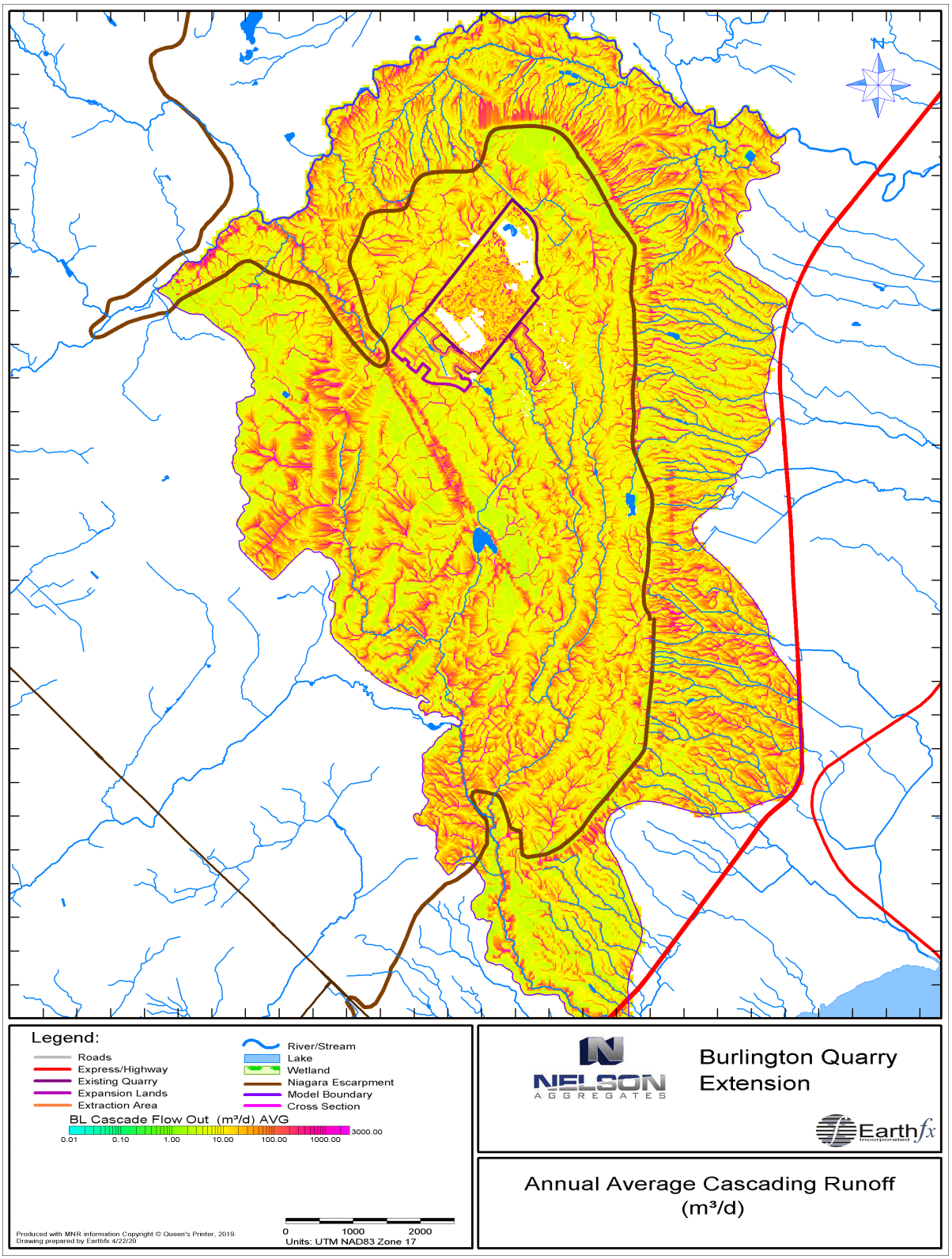

Figure 6.15: Simulated annual average cascading runoff (Hortonian, Dunnian, and interflow) passing through each cell in m^3/d.

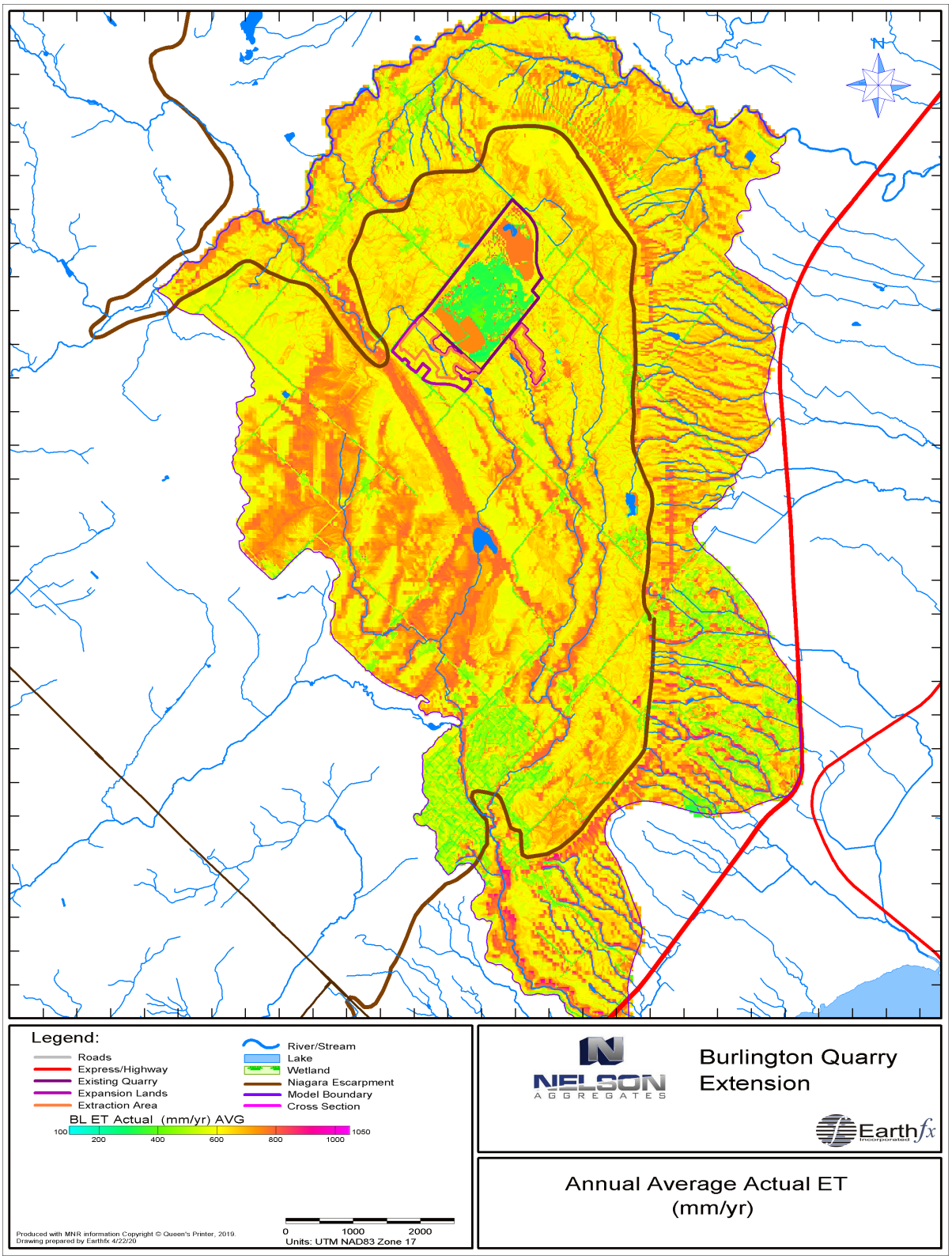

Figure 6.16: Simulated annual average actual evapotranspiration (soil zone ET, canopy losses and sublimation) in mm/yr.

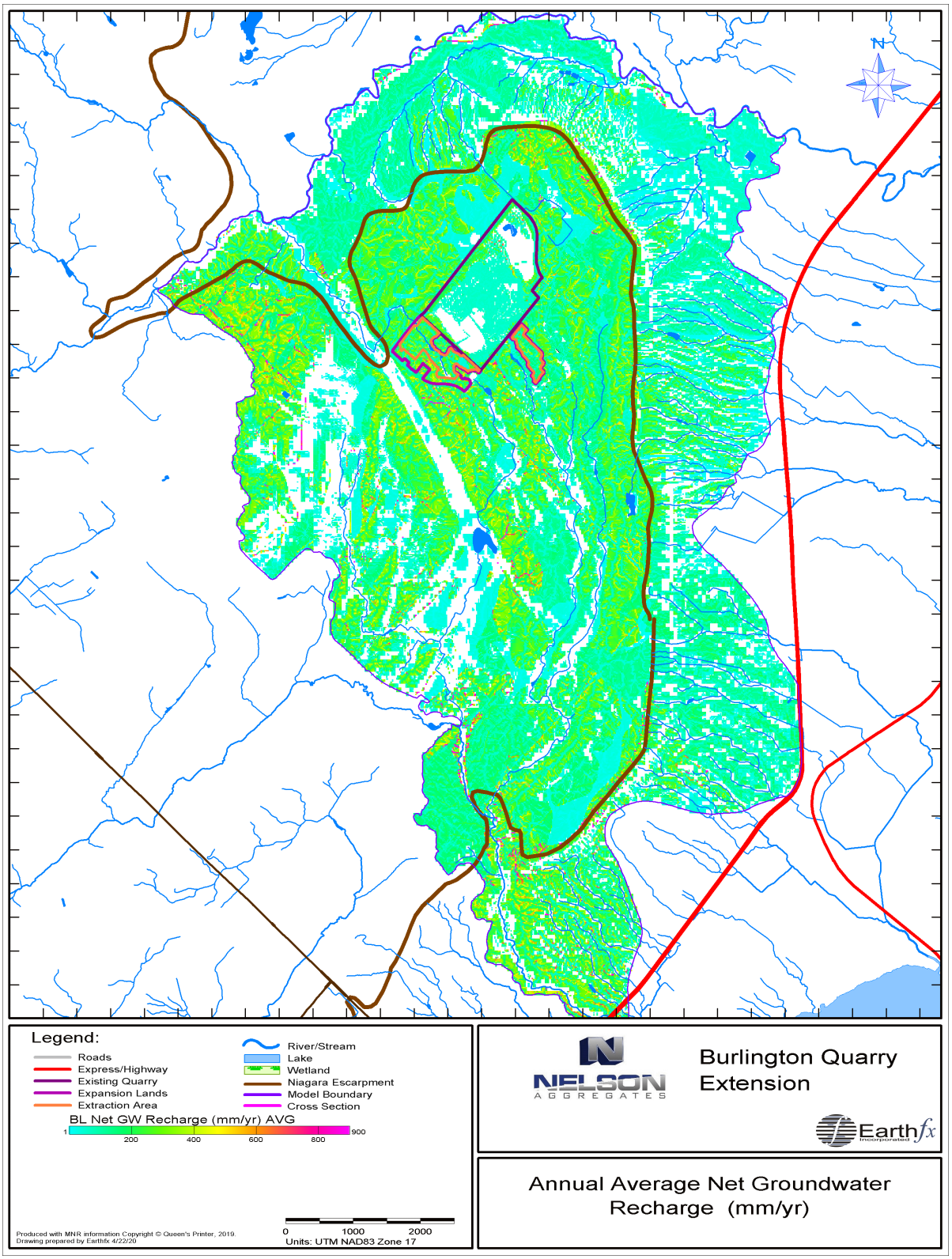

Figure 6.17: Simulated annual net average groundwater recharge in mm/yr.

6.10 MODFLOW Submodel Development Overview

The MODFLOW submodel was developed for the Burlington Quarry study area to represent the complex physical, hydrologic, and hydrogeological processes that affect the rates and direction of groundwater flow. The development proceeded in two stages. First, a steady-state model was constructed to approximate long-term average groundwater levels (also referred to as groundwater potentials or heads) and groundwater discharge to streams and lakes. The steady-state groundwater levels are dependent primarily on the hydraulic conductivity values and the rates of recharge assumed in the model and, therefore, provided an opportunity to separately assess these values. Recharge estimates were obtained from long-term simulations with the PRMS submodel prior to linking with GSFLOW. The steady-state model is described in brief in this section and in more detail in Appendix C.

In the second stage, the PRMS and MODFLOW models were run in an integrated manner with PRMS providing daily values for groundwater recharge and remaining ET demand, and the MODFLOW model returning daily rates of groundwater discharge to the soil zone, streams, and lakes. Final calibration focused primarily on updating aquifer/aquitard storage properties and properties that were most sensitive to transient groundwater/surface water interaction processes. The focus also shifted to improving the calibration in the quarry vicinity to better match data from the groundwater monitoring network around the existing quarry. Final calibration is described in Section 6.11 and in more detail in Appendix E

6.10.1 Model Construction

Model Code: The groundwater flow submodel used in this study was built with the USGS MODFLOW computer code (Harbaugh, 2005). MODFLOW solves the groundwater flow equation using a gridded finite difference approach on a steady-state or transient (time-dependent) basis. The MODFLOW code is well-documented and can simulate groundwater flow in multi-layered aquifer systems with irregular boundaries, complex stratigraphy, and variations in hydrogeologic properties. This study used a newer version of the MODFLOW code, MODFLOW-NWT (Niswonger et al., 2011), which is particularly well-suited for areas with thin aquifers and sharp changes in model layer stratigraphy, and with steep slopes such as those that occur at the edges of the Burlington Quarry and at the Niagara Escarpment.

Model Grid: The finite-difference method requires that the study area be subdivided into a grid of small square or rectangular cells and multiple layers. Separate numerical model layers were used to represent the bedrock and overburden hydrostratigraphic layers discussed in the hydrogeological conceptualization (see Section 5.2). The grid developed for this study has a high level of refinement in the quarry vicinity with 15 m square cells in the extension areas and 60 m cells in the model periphery. Rectangular cells are used in transition zones. The model grid, shown in Figure 18.4, consists of 377 rows and 366 columns for a total of 137,982 active grid cells for each model layer.

Model Layers: The nine numerical model layers used in this study generally correspond to the hydrostratigraphic units with a few exceptions. Layer 1 represented the upper surficial deposits in the study area and was comprised primarily of weathered Halton Till above and below the Niagara Escarpment and surficial sands in the Medad Valley and to the west. Layer 2 represented the unweathered portion of the Halton Till. Layer 3 represented the MIS Formation above the Niagara Escarpment, where present, and the Oak Ridges Aquifer Complex (ORAC) sands below the Niagara Escarpment.

Layers 4 through 8 represent the fracture system and karst and features within the principal Amabel bedrock aquifer (Goat Island, Gasport, and Irondequoit Formations). In brief, Layer 4 represented the upper, weathered portion of the Amabel aquifer and was assumed to have relatively high hydraulic

conductivity, lower storage properties, and a minimum of 1.0 m thick. Layer 5 represented the bulk Amabel aquifer, which is assumed to have higher storage but less horizontal fracturing. Layer 6 represents a thin zone in which fractures are more frequent and/or continuous. A lower bulk aquifer zone (Layer 7) separates the middle fracture zone from Layer 8, which represented a thin lower fracture zone. The location and frequency of vertical fracturing within the Amabel aquifer is not explicitly unknown. As an approximation, a percentage of cells (5% in the final model calibration) in Layers 5 and 7 were selected at random (with different cells in each layer) and assigned a lower storage value but higher vertical hydraulic conductivity to represent this vertical fracturing in the model.

Layer 9 represented the lower hydraulic conductivity units separating the upper bedrock aquifer from the underlying Whirlpool Formation. The amount of water transmitted through these units is expected to be limited. The mapping of hydrostratigraphic units to model layers is summarized in Table 6.2.

Table 6.2: Mapping of model layers to hydrostratigraphic units.

Numerical Model Layer	Hydrostratigraphic Unit		
	Above Escarpment	Below Escarpment	Layer Description
1	Surficial Deposits	Surficial Deposits	Mainly weathered till and surficial sands
2	Halton Till	Halton Till	Unweathered till
3	MIS Sands	ORAC Sands	Discontinuous sand unit
4	Weathered Amabel Aquifer	Weathered Queenston	Weathered Bedrock
5	Upper Bulk Amabel	Weathered Queenston	Goat Island/ Gasport, and Irondequoit Formations (Weathered Queenston below Escarpment)
6	Middle Fracture Zone	Weathered Queenston	
7	Lower Bulk Amabel	Weathered Queenston	
8	Lower Fracture Zone	Weathered Queenston	
9	Lower aquitards	Lower aquitards	Rochester, Cabot Head, Rockway, /Merritton, Manitoulin (Unweathered Queenston below Escarpment

External Model Boundary Conditions: Model boundaries extended to physical boundaries, which included regional watershed divides and major streams. The model was extended below the Niagara Escarpment so that any effect on escarpment headwater streams could be evaluated. Boundary conditions were specified for cells that lie along lines corresponding to the physical boundaries of the groundwater flow system. Three general types of boundary conditions were used in the groundwater flow model: constant head, no-flow, and head-dependent discharge boundaries. Constant head cells were applied along model boundaries corresponding to major water courses, including Bronte Creek along the northern boundary, and at points where the larger stream tributaries (Strahler Class 3) crossed the eastern model boundary. Control elevations for the constant head boundaries were estimated from the DEM for the study area. The remaining external boundaries were defined by watershed divides and were represented as no-flow boundaries and presumed that groundwater flow across the watershed divides was relatively small. A no-flow boundary was imposed along the base of the model, assuming that inflow into the model from below the lower aquitard units would also be negligible.

Head-dependent Flux Boundaries: Head-dependent flux boundaries were used to represent groundwater/surface water interaction between streams and lakes within the model area. Flow

between the groundwater system and streams was assumed to be exchanged as “leakage” across the streambeds and dependent primarily on the difference between stream stage and aquifer head. Stream stage is calculated daily by the SFR2 module, based on stream channel properties and the sum of upstream inflows, precipitation, evaporation, and overland flow to the reach. All mapped streams segments were simulated in the model. Stream channel properties are discussed in Appendix C.

Leakage between the aquifer and other water bodies, such as lakes, ponds, and shallow wetlands, was calculated daily using the LAK3 module. Lake volumes are calculated as the sum of upstream inflows (as computed by the SFR2 module), precipitation, evaporation, overland flow to the lake, and outflow from the lake (also calculated by SFR2 based on lake stage). Lake stage is calculated from stage-volume relationships. Shallow wetland features close to the quarry and extension lands were represented as shallow MODFLOW lakes to better simulate the intermittent occurrence of standing water. Wetland lakes were assigned to Layer 1. Additional details relating to the wetlands are provided in Appendix C.

Dewatering of the existing quarry was simulated passively in the model. Quarry drains were represented with the SFR2 module and conveyed groundwater discharge from the face and floor of the quarry to the quarry lakes. Controls were set on lake stage such that excess volumes were automatically discharged to the stream segments, as per permit rules and regulations, representing the south-central and northwest discharge points.

Model Parameters: Initial estimates for hydraulic conductivity were made based on previous hydrogeologic investigations at the quarry site (e.g., Golder Associates Ltd., 2007), recent field work and aquifer testing (see Appendix A), and on other modelling studies in the vicinity (e.g., Earthfx, 2012). Properties were adjusted in the steady-state model to match observed water levels and general groundwater flow patterns determined primarily from static water level data in the MECP Water Well Information System (WWIS) database and supplemented by average levels from observation wells in the quarry vicinity. The water level data and general flow patterns are described in Section 5.3.

Uniform properties were assigned to each of the hydrostratigraphic units and adjusted through model calibration. Maps showing the spatial distribution of the calibrated hydraulic conductivity values for model layers 1 through 9 are presented in Appendix C (Figure 18.11 through Figure 18.19). Table 18.4 lists the calibrated properties for each of the hydrostratigraphic units. The properties listed represent final calibration values for the integrated model.

Average steady state simulated heads in Layer 6 (middle fracture zone) are shown in Figure 19.2. Static and average water level data are posted on the figure using colour-shaded symbols. Differences between the colour inside the dot and in the surrounding area indicate a deviation from the observations. A visual comparison of the observed and simulated values shows that a good match was achieved although, as was noted in Section 5.3, there is considerable scatter in the static water level data because of the fractured nature of the bedrock; deviations are less prevalent below the Niagara Escarpment. A good match was also achieved across the model with the key study area groundwater flow patterns.

6.11 GSFLOW Model Calibration

Once the PRMS and MODFLOW submodels were reasonably well pre-calibrated, the focus shifted to the integrated GSFLOW final calibration. The final calibration for the GSFLOW model is discussed in detail in in Appendix E.

6.11.1 GSFLOW Surface Water Streamflow Calibration

In brief, parameters in the PRMS submodel in GSFLOW were refined to improve the match to observed streamflow at the Grindstone Creek near Aldershot gauge. Figure 6.18 shows the simulated and observed flow at the Aldershot gauge. A Nash-Sutcliffe Efficiency of 0.67 was achieved with the GSFLOW model (This is a significant improvement over the 0.4 NSE in the PRMS-only model). An NSE of 0.6 is considered a reasonable calibration value (Chiew and McMahon, 1993).

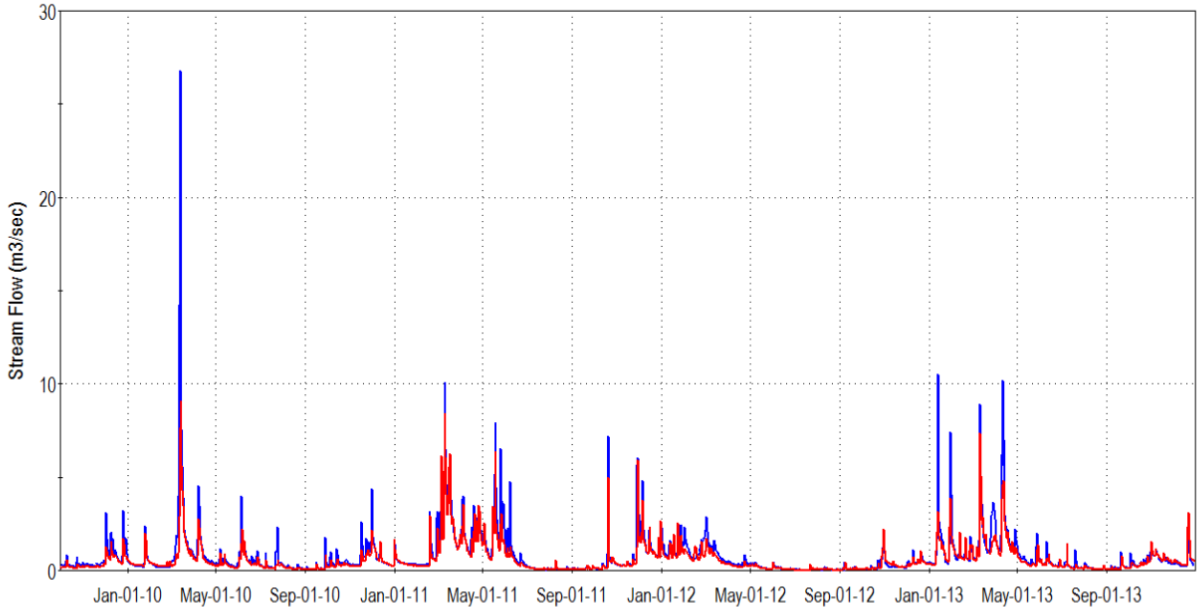

Figure 6.18: Simulated (red) and observed streamflow (blue, in m^3s) at the Grindstone Creek near Aldershot gauge.

Local streamflow measurements collected at streams in the vicinity of the Burlington Quarry were compared visually against simulated streamflow and found to also match well. Numerous hydrographs are provided in Appendix E. As an example, simulated and observed streamflow at SW-10B are presented in Figure 6.19 for WY2019. The gauge location is shown on Figure 2.2. SW10B is an important stream gauge because it represents the confluence of flows from two tributaries on either side of the proposed South Extension area. The observed data includes some data gaps (i.e. winter months, when loggers cannot function), but the calibration to the new 2019 streamflow data is excellent (Figure 6.19).

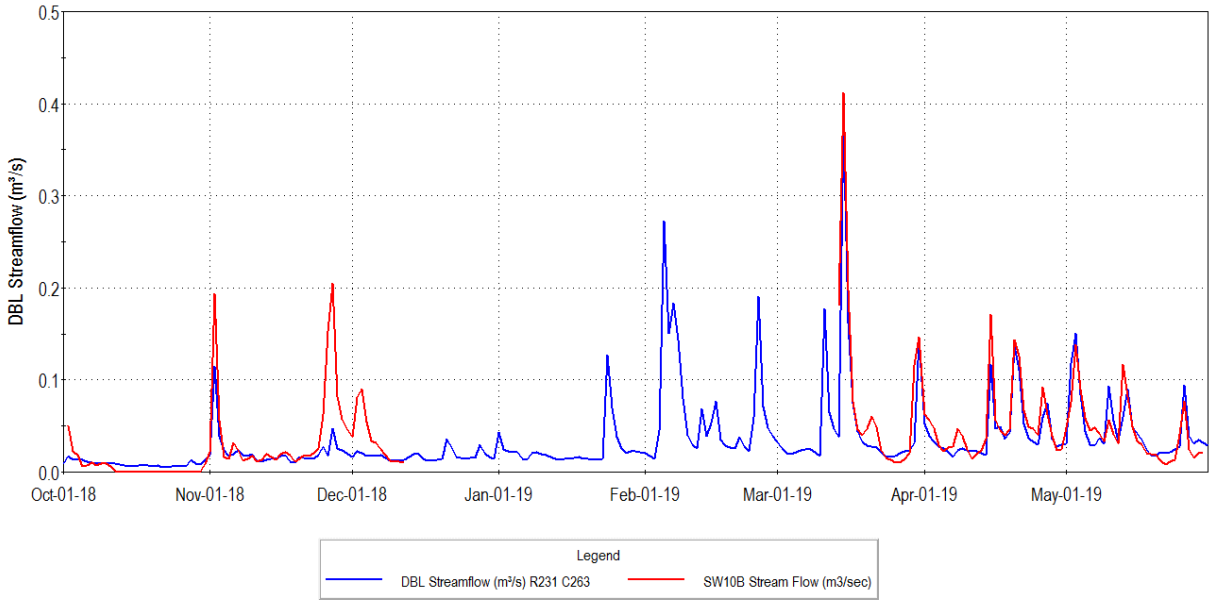

Figure 6.19: Simulated and observed flow at SW10B for WY2019.

Another important local gauge is SW9, located in the chain of wetlands to the east of the proposed P12 extension area. Matching this gauge provides confidence that the model is predicting current local conditions and the resulting effects of new developments. The calibration to SW9 is very good, particularly to the new data collected in 2019 (Figure 6.20). The calibration to the mini-piezometers and wetland ponds in the vicinity of SW9 is discussed in more detail below.

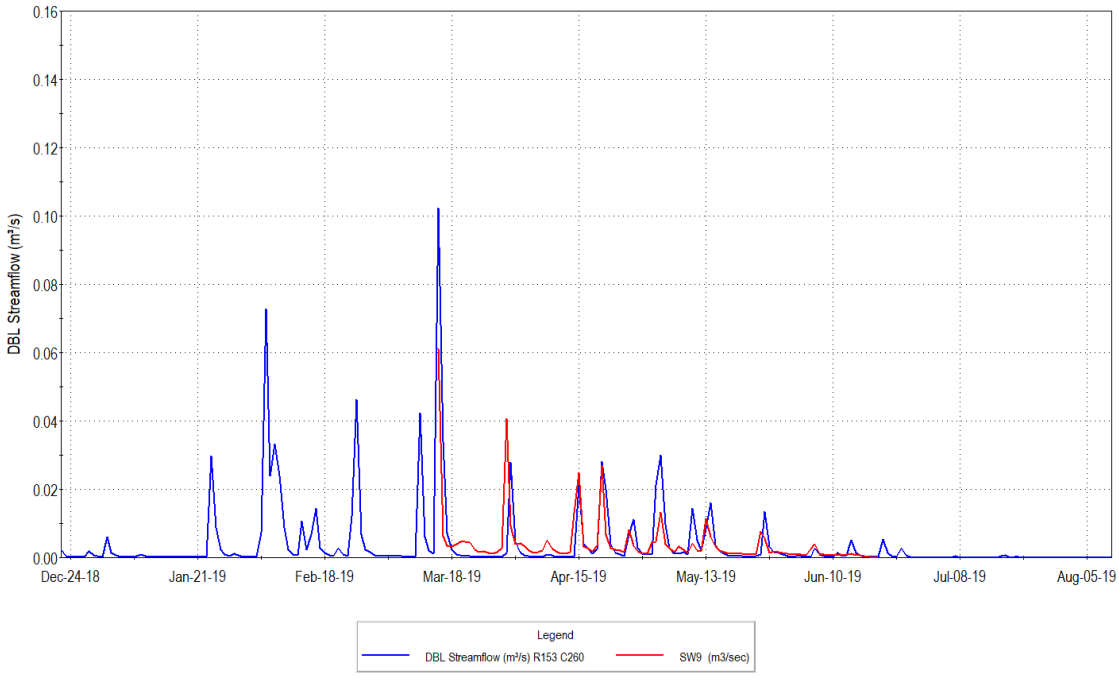

Figure 6.20: Simulated SW9 Streamflow in 2019 (blue) very closely matches the observed values.

6.11.2 Regional GSFLOW Calibration

Further adjustments and refinements were made to the MODFLOW submodel on conversion into GSFLOW. In particular, aquifer and aquitard storage properties were assigned to the layers. The MODFLOW sub-model pre-calibration is based on a "steady state" formulation with no representation of aquifer storage. The regional GSFLOW calibration was based on calculating the average water level from a multi-year transient simulation with a daily time step. The effects of seasonal and inter-annual climate variation, and the buffering effects of aquifer storage on drought and wet year response, are fully represented in the GSFLOW simulation.

Nelson maintains a detailed groundwater monitoring network in the vicinity of the quarry. Water levels from these wells provided transient calibration targets for matching the groundwater system response to rainfall events and to seasonal and inter-annual climate variability. Adjusting the storage parameters provided an improved match to these responses and increased confidence in the model's ability to predict how water levels will be affected by quarry excavation and seasonal changes in climate and dewatering activities.

The final GSFLOW regional calibration is measurably better than the MODFLOW pre-calibration. The overall regional Mean Error calibration statistic for the GSFLOW model is -1.33 m (Figure 19.3), which is a reduction from the Mean Error from -1.86 m determined from the MODFLOW pre-calibration.

6.11.3 Calibration to Local Transient Water Level Data

Additional calibration analysis was focused on matching transient responses at individual local wells, and in particular, the observed patterns in water levels between the upper and lower units and their influence on wetlands and water supply wells.

Appendix E presents numerous hydrographs comparing observed and simulated groundwater levels at well clusters in the vicinity of the proposed South Extension. Results are shown for WY2010 to WY2014, the period of the longest overlap between simulated and continuous observed measurements.

To further support the following discussion of complex transient water level patterns and calibration, two cross sections have been prepared to illustrate the model simulation of current conditions in the south extension area. The monitoring wells and cross section locations are shown on Figure 6.21. The cross sections, showing the average simulated water levels, are presented in Figure 6.22 and Figure 6.23 Additional calibration cross sections are included in Section 19.5.1.

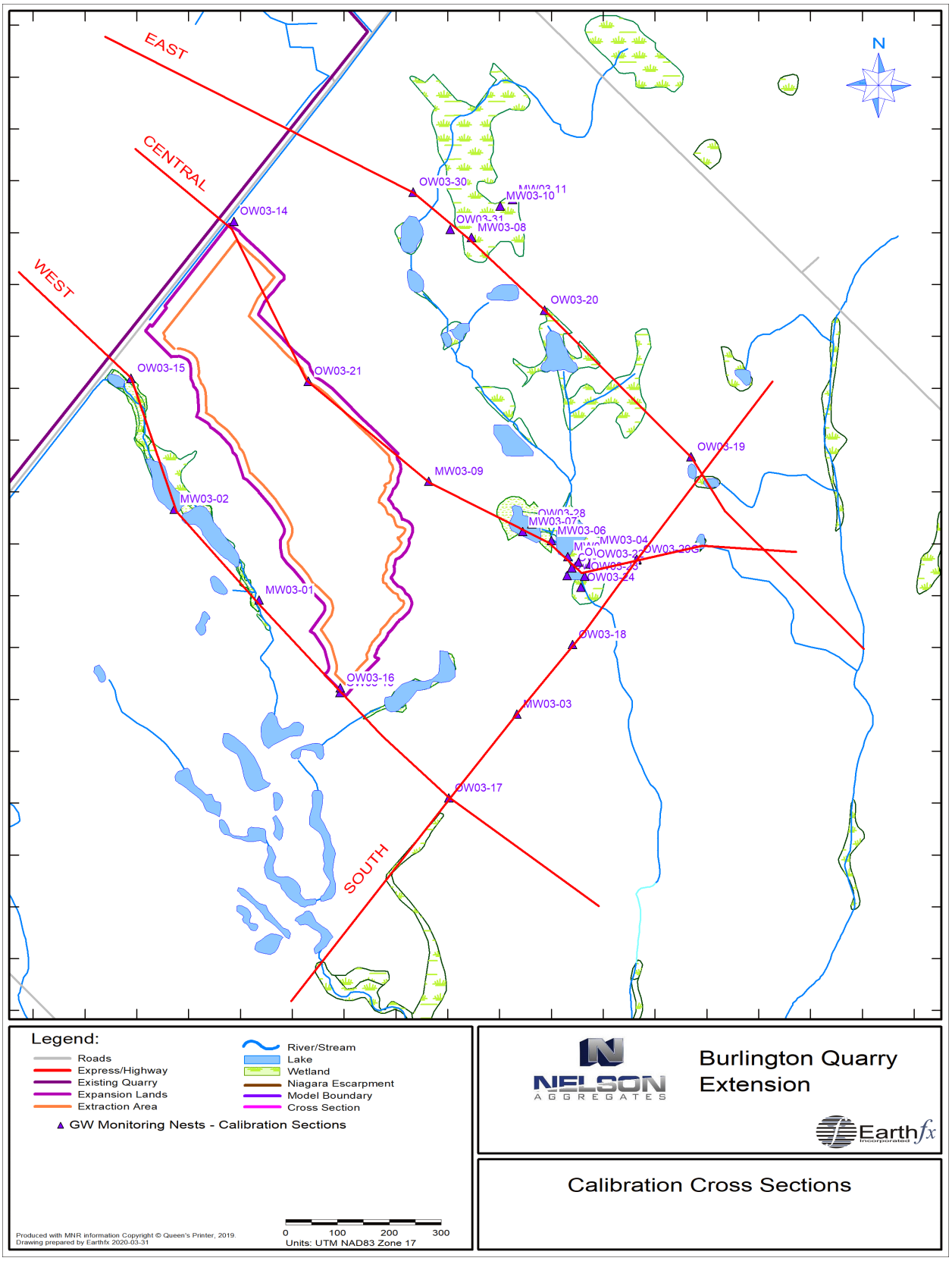

Figure 6.21: Well locations and calibration cross sections.

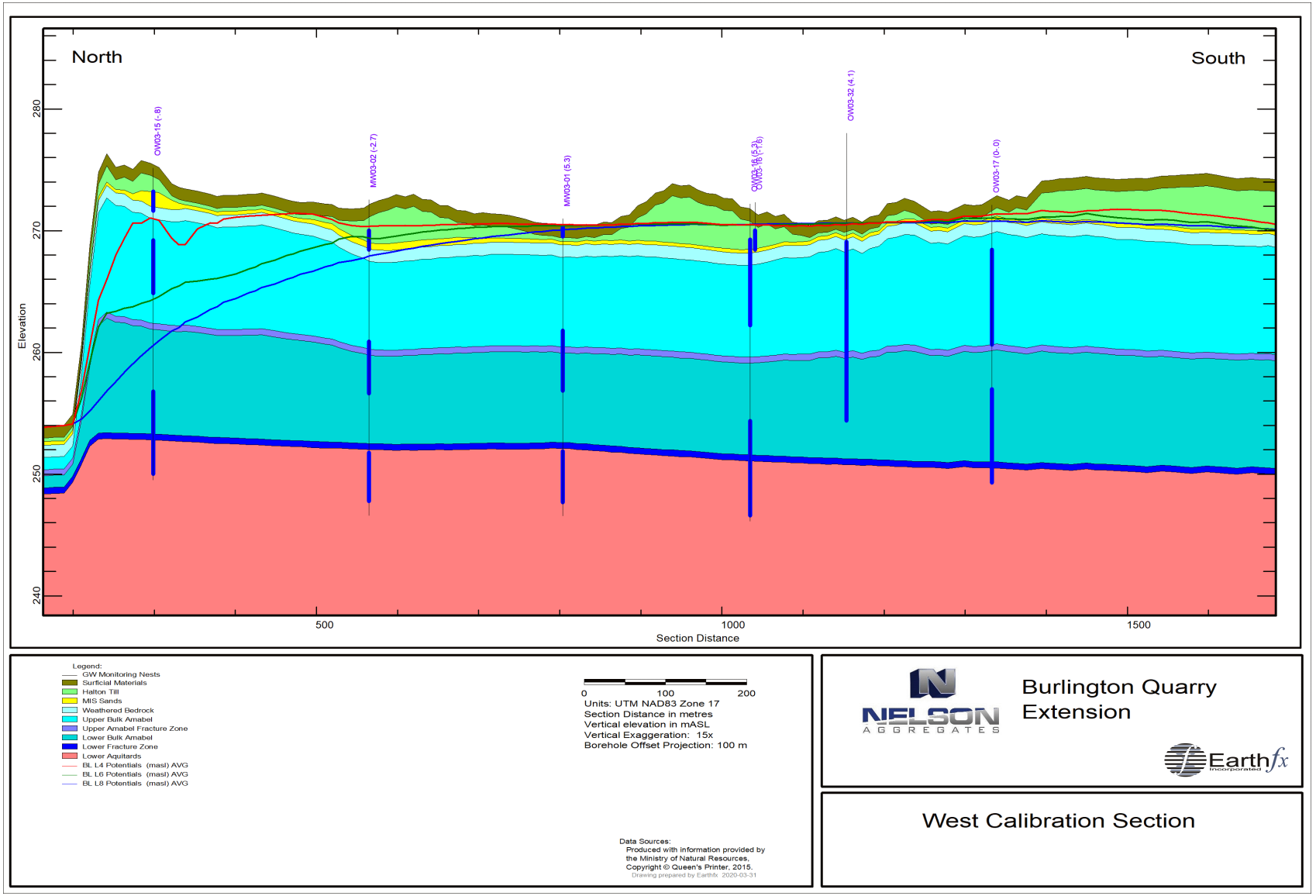

Figure 6.22: West calibration section.

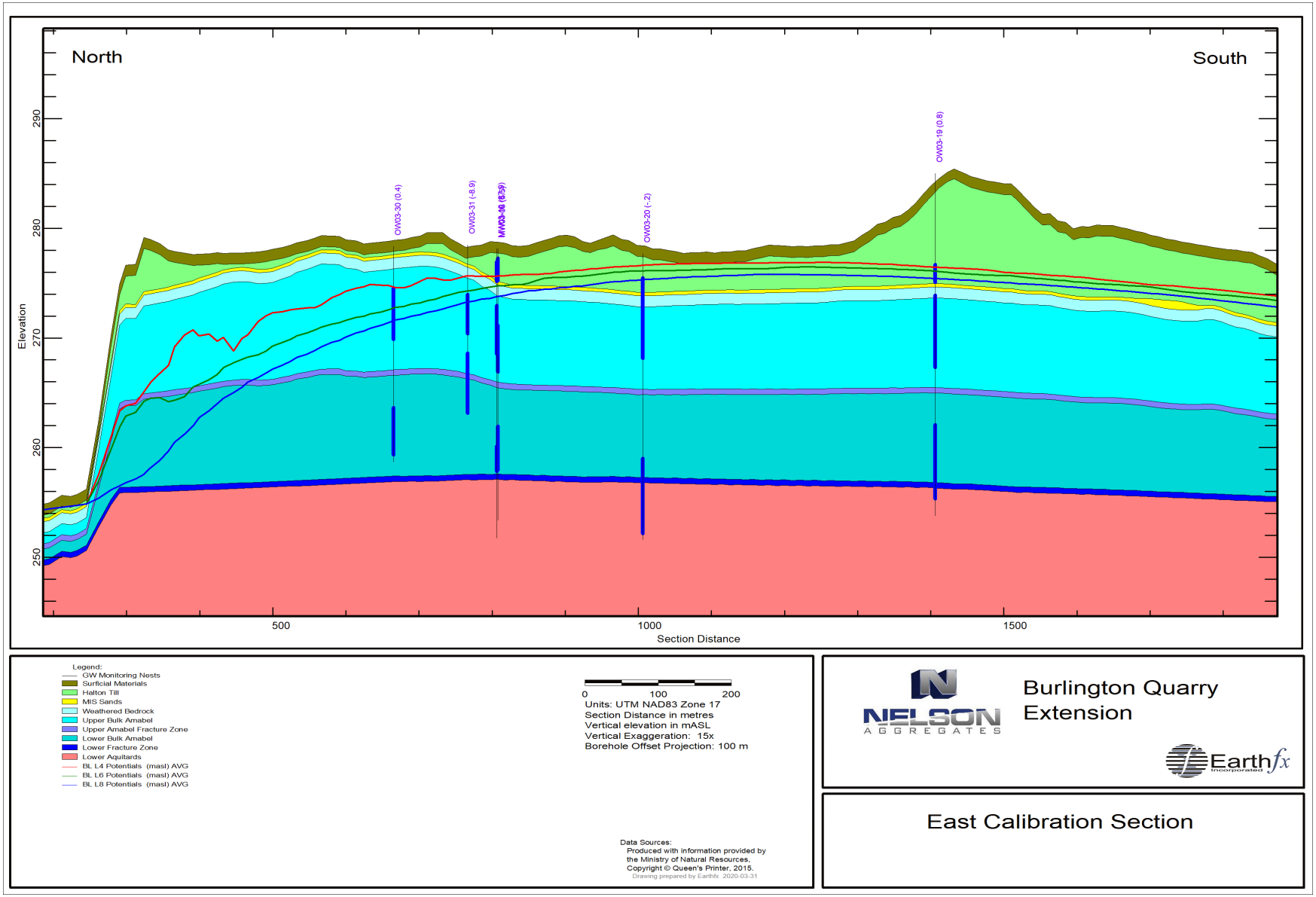

Figure 6.23: East calibration section.

6.11.3.1 Wells within 100 m of the Quarry Face

A distinctive pattern of water levels is observed in the transient monitoring in the study area. Near the quarry (less than 100 m – see Figure 6.22), a head difference of as much as 14 m is observed between the shallow (layer 4, weathered bedrock) and deep monitors (Layer 8, lower fracture zone). With distance from the quarry face, a distinctive wet season/dry season transient water level pattern is observed, and at larger distances, there is no significant difference between shallow and deep levels.

For example, the OW03-15 well cluster is very close to the quarry face (55 m) and a large difference is head is observed. Simulated water levels are shown in Figure 6.24 for Layers 4 and 8 to represent the weathered Amabel and deep fracture zone. The model matches this extreme local response, despite the very close proximity to the face. Water levels at this location are further influenced by stream leakage related to the south quarry discharge.

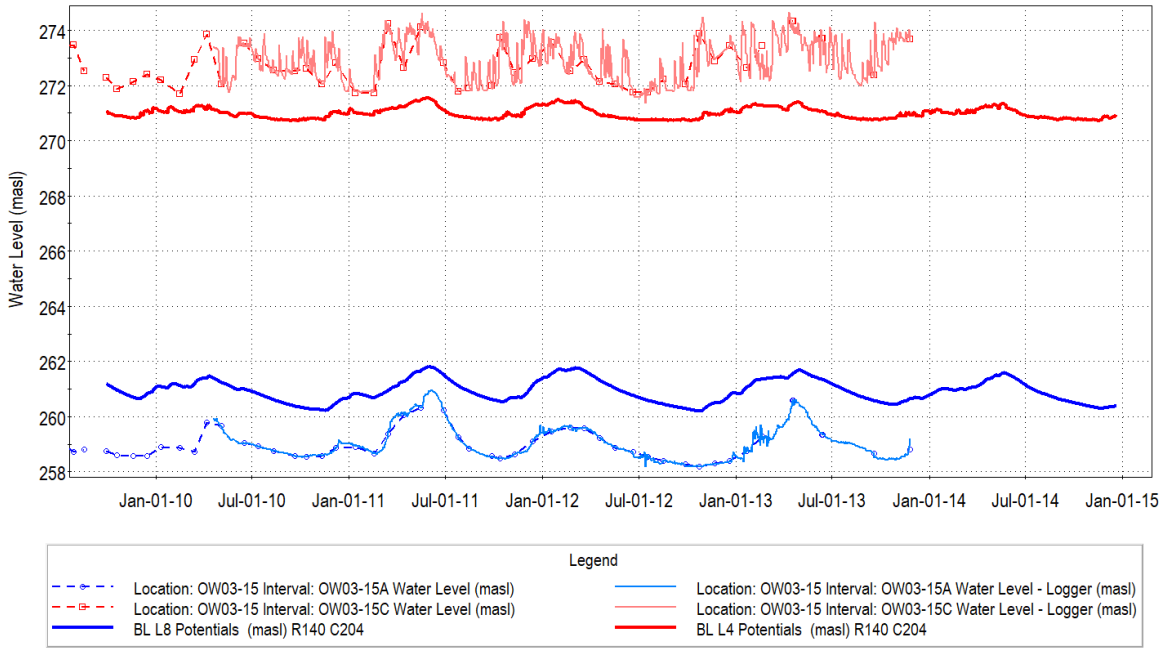

Figure 6.24: Comparison of simulated (thick line) and observed (thin line) potentials in Layers 4 (red) and 8 (blue) at wells OW03-15A and OW03-15C.

6.11.3.2 Wells between 100 m and 800 m of the Quarry Face

With increasing distance, the head in the lower aquifers rise. The shallow aquifers exhibit higher seasonal variability as the system is replenished during the spring, and subsequently drains through the summer and fall to the lower system.

Figure 6.25 shows the simulated and observed monthly water levels at the OW03-21 well cluster, located 350 m from the quarry face (Figure 6.23). This monitor exhibits a water level response that is typical of wells at this distance that are only partially influenced by the quarry. The manual measurements from the intermediate level monitor, OW03-21B (in light green), show a seasonal variation of more than 5 m, and the shallow monitor (in red) is frequently dry, as indicated by the constant water level minimum value. This wide variation in the intermediate zone water level indicates that the shallow and middle aquifer systems are replenished by spring recharge, but then they drain

to the lower system in the late spring and summer. The model simulates this highly complex pattern exceptionally well, as illustrated by comparing the light green manual measurements to the dark green simulated results. The calibration to the water levels in the deep system is also excellent (compare blue lines).

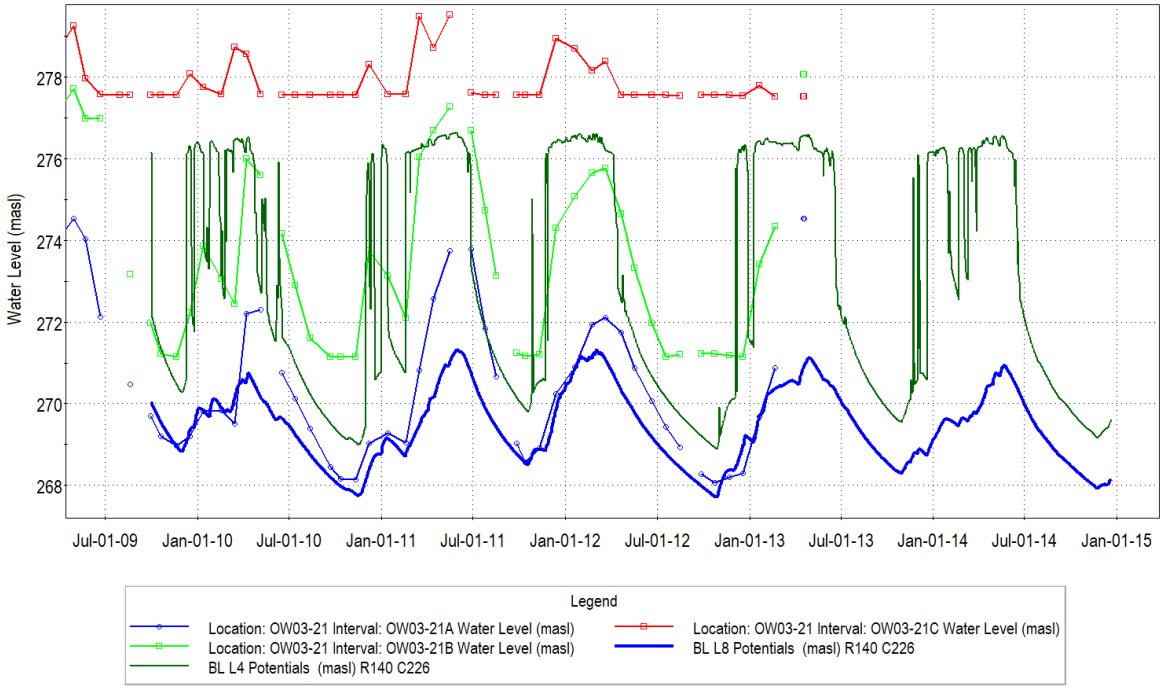

Figure 6.25: Comparison of Observed and Predicted water levels at Monitor OW03-21

This characteristic variability in seasonal water levels disappears with further distance from the quarry. Monitor OW03-31, located 420 m from the quarry face (Figure 6.21), exhibits a more muted water level response (Figure 6.26). The nearly 7 m range in inter-annual water levels is larger than for background wells, but the summer drainage to the lower fracture zone is not observed.

6.11.3.3 Wells greater than 800 m from the Quarry Face

At a distance of more than 800 m from the quarry face, the water levels in all layers are typically very similar. For example, monitoring nest OW-03-29, located over 1000 m from the quarry face (Figure 6.21) exhibits a head difference of less than 0.5 m and a seasonal variation of less than 2 m (Note the reduced scale range in Figure 6.27). The model replicates this pattern across all distal monitoring wells.

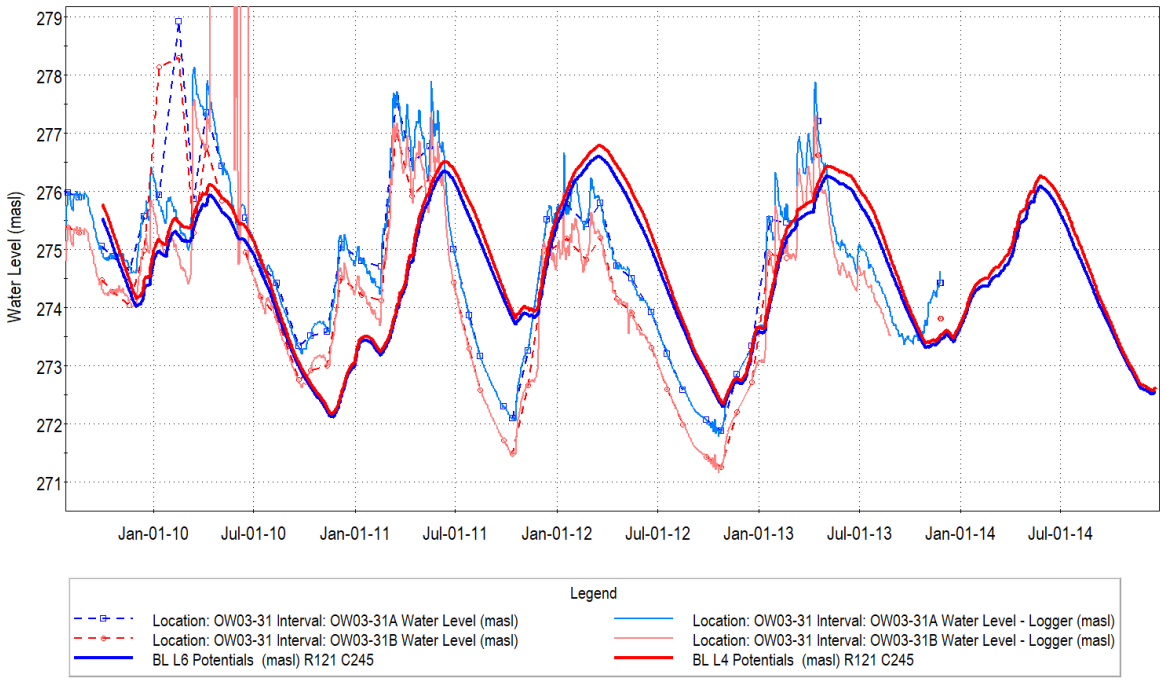

Figure 6.26: Comparison of observed and simulated water levels at monitor OW03-31 (Note: deep monitor in layer 6, shallow monitor in Layer 4-5).

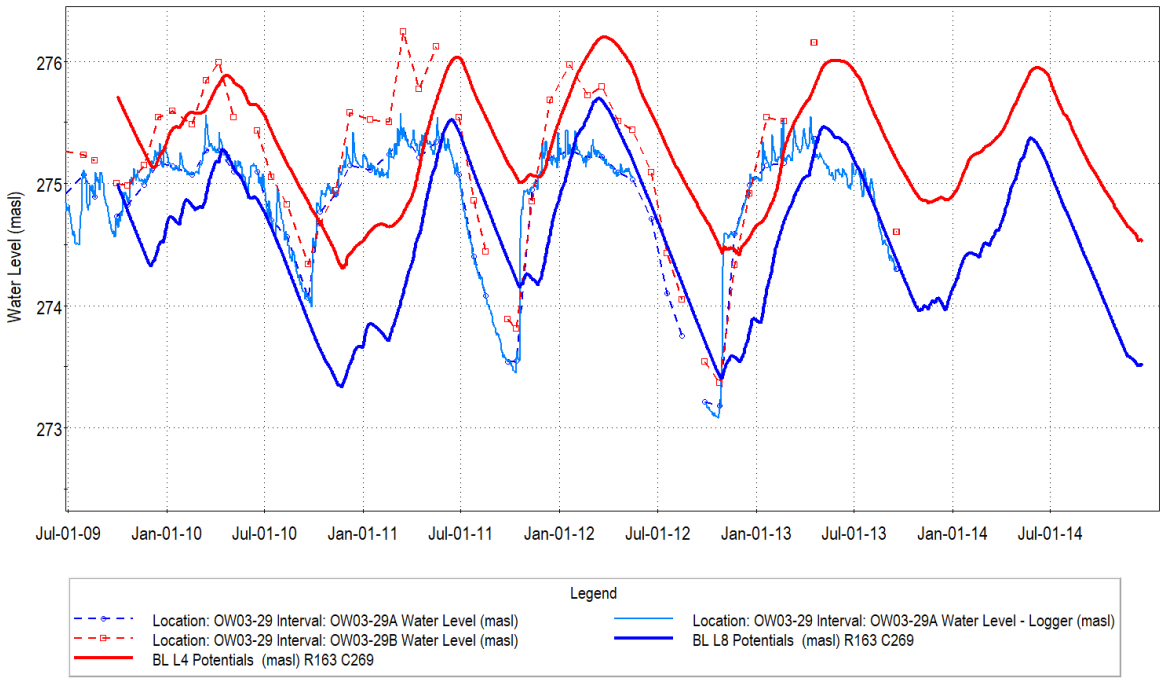

Figure 6.27: Comparison of observed and simulated water levels at monitor OW03-29.

6.11.3.4 Quarry Effects Calibration: Conclusions

Numerous additional examples of each of these water level patterns are included in Section 19. The numerical model universally replicates the patterns, indicating an excellent calibration to the observed effect of the existing quarry. The close calibration to these commonly observed patterns confirms that the model can accurately predict the future effects of the quarry extension.

6.11.4 Shallow Groundwater Calibration

The calibration of the model to shallow water levels observed in the mini-piezometers and wetland pond staff gauges provides further insight into both the behaviour of the model and groundwater and surface water interactions.

The mini-piezometer and pond staff gauge locations that were used for calibration span the wetland complex to the east of the proposed P12 extenson area (Figure 6.28). It is important to note that a single hydraulic conductivity value was used for the Halton Till across the entire study area, so no local modifications were implemented to match specific calibration issues. This consistency demonstrates that the model can be applied broadly across the study area.

Figure 6.29 shows the observed and simulated water levels at mini-piezometer location MP16, which is located in a wetland immediately south of the proposed P12 extension area (Wetland 20, as shown in Figure 19.49). The water levels in MP16 follow a characteristic pattern: rising through the wet seasons and dropping below the base of the monitor at other times (flat line readings). The simulated water levels match the magnitude and patterns very well, and illustrate where water levels recede to during the dry periods. Note the small scale of the graph, and that the calibration peaks match within 10 cm.

Figure 6.30 presents the results for MP6, located just on the edge of another large wetland/pond complex. The calibration and response are similar to that observed at MP16, and many other mini-piezometers across the study area. MP6, which is close to the Wetland 13032, illustrates that the model is representing the shallow system well in that area.

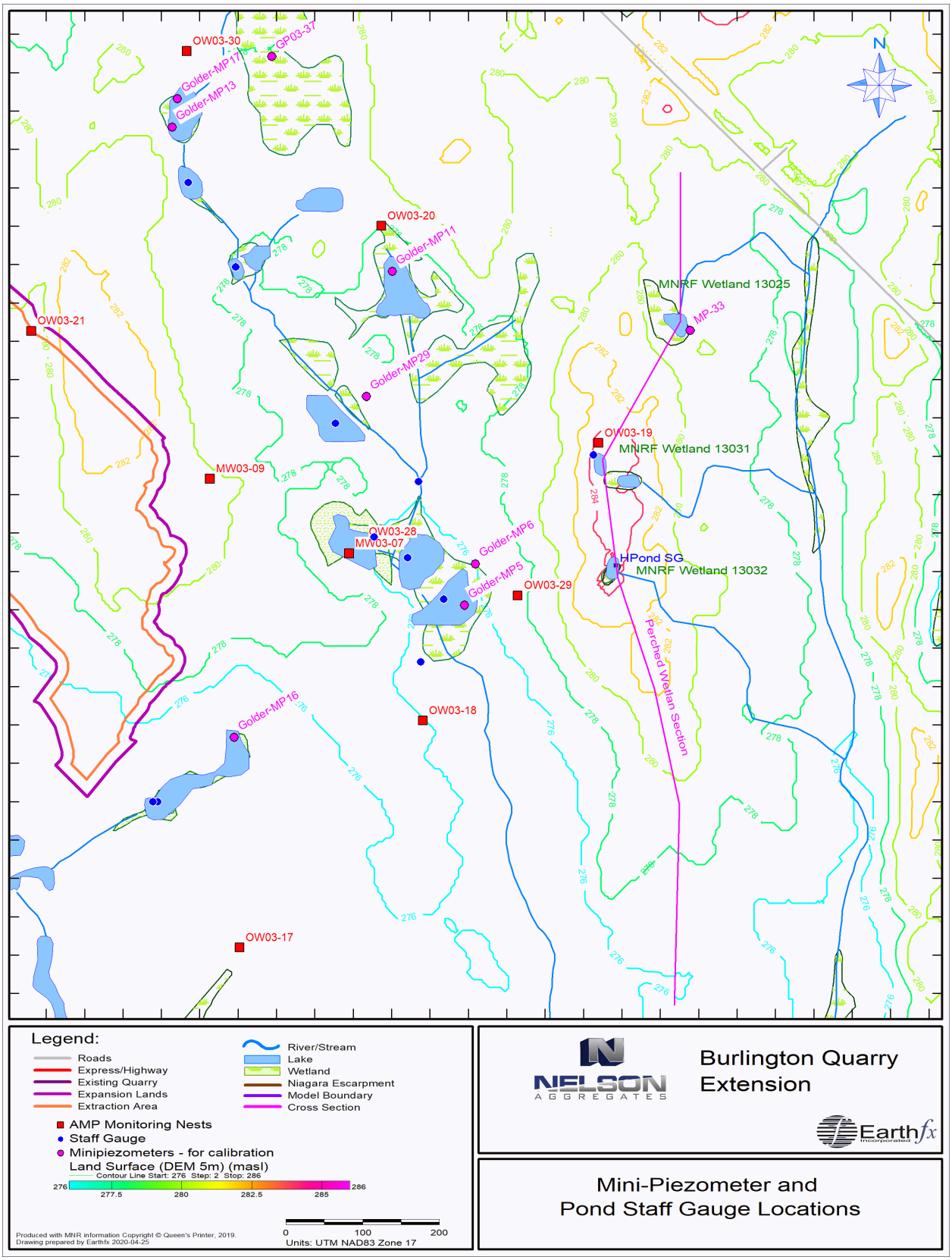

Figure 6.28: Mini-piezometer and pond staff gauge locations.

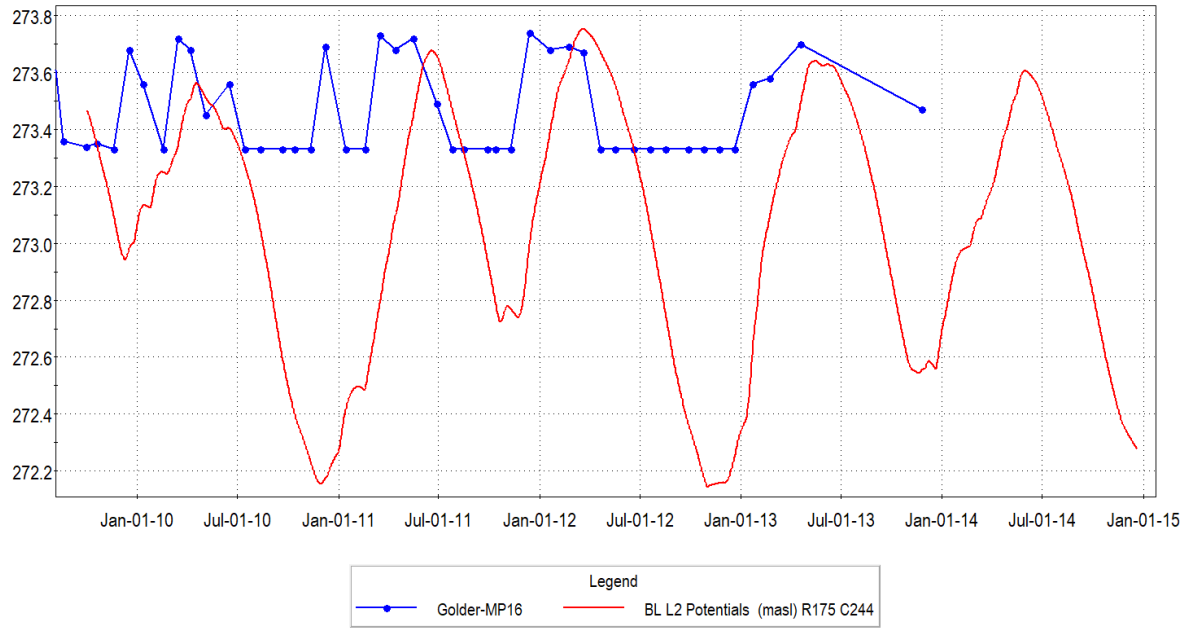

Figure 6.29: Observed and simulated pond elevation at MP16.

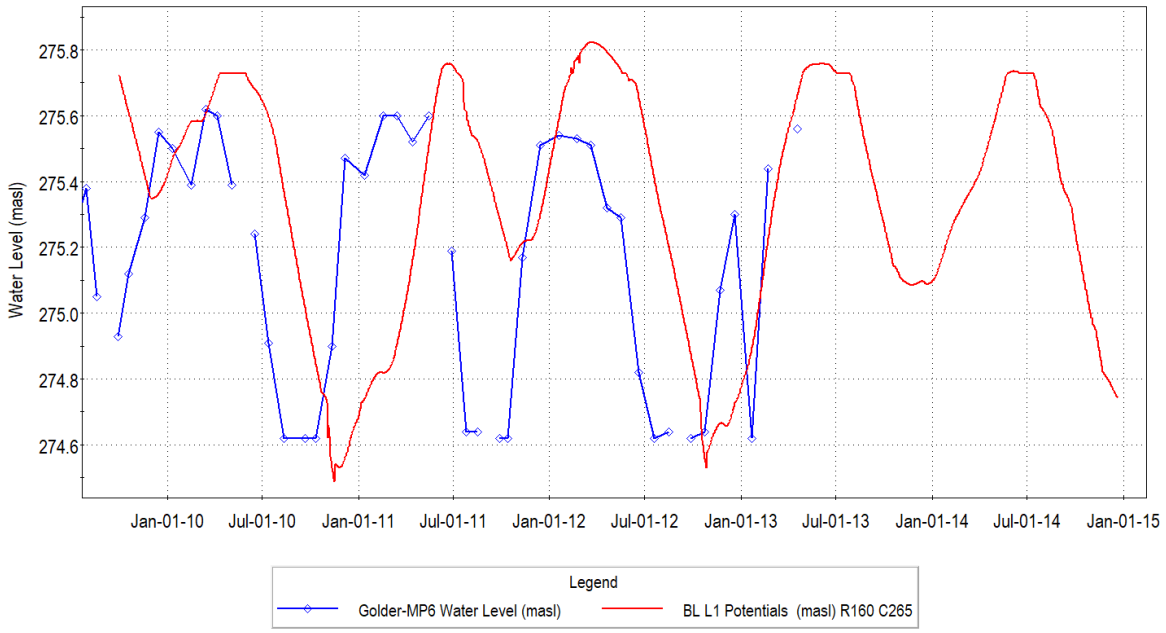

Figure 6.30: Observed and simulated shallow water levels at MP6.

6.11.5 Wetland and Pond Calibration

The calibration to Staff Gauge SG2 and Mini-piezometer MP5 is particularly interesting, for it shows both pond and the underlying groundwater level fluctuations (Figure 6.31). The measurements are from the southern portion of Wetland 17 (Figure 19.49), and the pond is immediately south of Stream Gauge SW9 (Figure 6.28). Groundwater levels, shown in blue, indicate that the water levels in the shallow groundwater system are at times above pond levels, and, in the summer recession, below the pond levels. This suggests that the pond both receives and loses to groundwater, depending on the time of year. The simulated water levels under the pond match the observed values generally very well, capturing this changing vertical gradient, and the calibration to pond levels is also very good (compare red lines). The model matches the trends and range in the pond levels, particularly given the size and complexity of the wetland bathymetry in this area. The results from a number of additional ponds are included in Section 19.

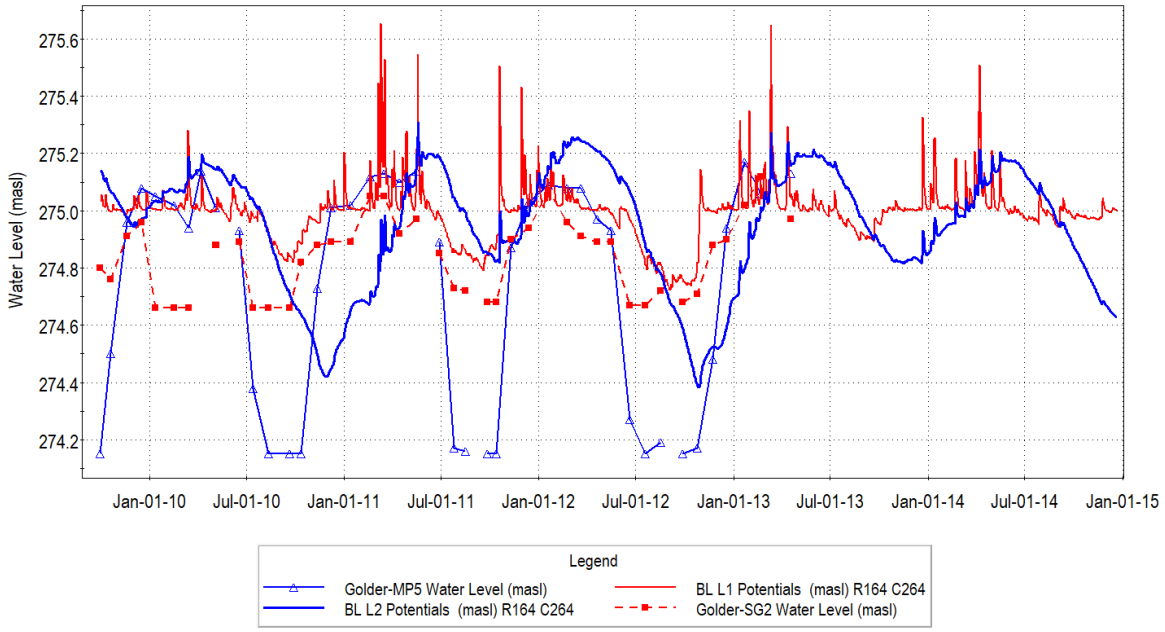

Figure 6.31: Observed and simulated pond and mini-piezometer elevation at Golder SG2 and MP5.

6.11.6 Perched Wetland Ponds

A north-south trending ridge of Halton Till is located approximately 575 m west of the P12 extraction area (Figure 6.28). The ridge rises approximately 8 m above the local lowlands, and may have been deposited in a similar manner to the Waterdown Moraines that are found west of the study area. While the majority of the wetlands in the study area are located in the lowlands, three perched wetland ponds are located along this ridge.

There are no recognizable geologic or hydrologic processes that can create shallow ponds at the top of a ridge or till moraine. It is very likely that the wetland ponds might have been manually excavated as watering holes for livestock, agricultural purposes, or historically as a location to create winter ice blocks for subsequent summer cold storage. OMFRA discusses the construction of dugouts for livestock purposes at the following web page:
http://www.omafra.gov.on.ca/english/livestock/beef/news/vbn0211a5.htm

A north-south cross section (location shown in Figure 6.28) illustrates the wetland pond elevation relative to the water table (Figure 6.32). (The wetland position is shown with both their MNRF Wetland ID Number and corresponding staff gauge or mini-piezometer name). The cross section shows that ponds are located many metres above the water table.

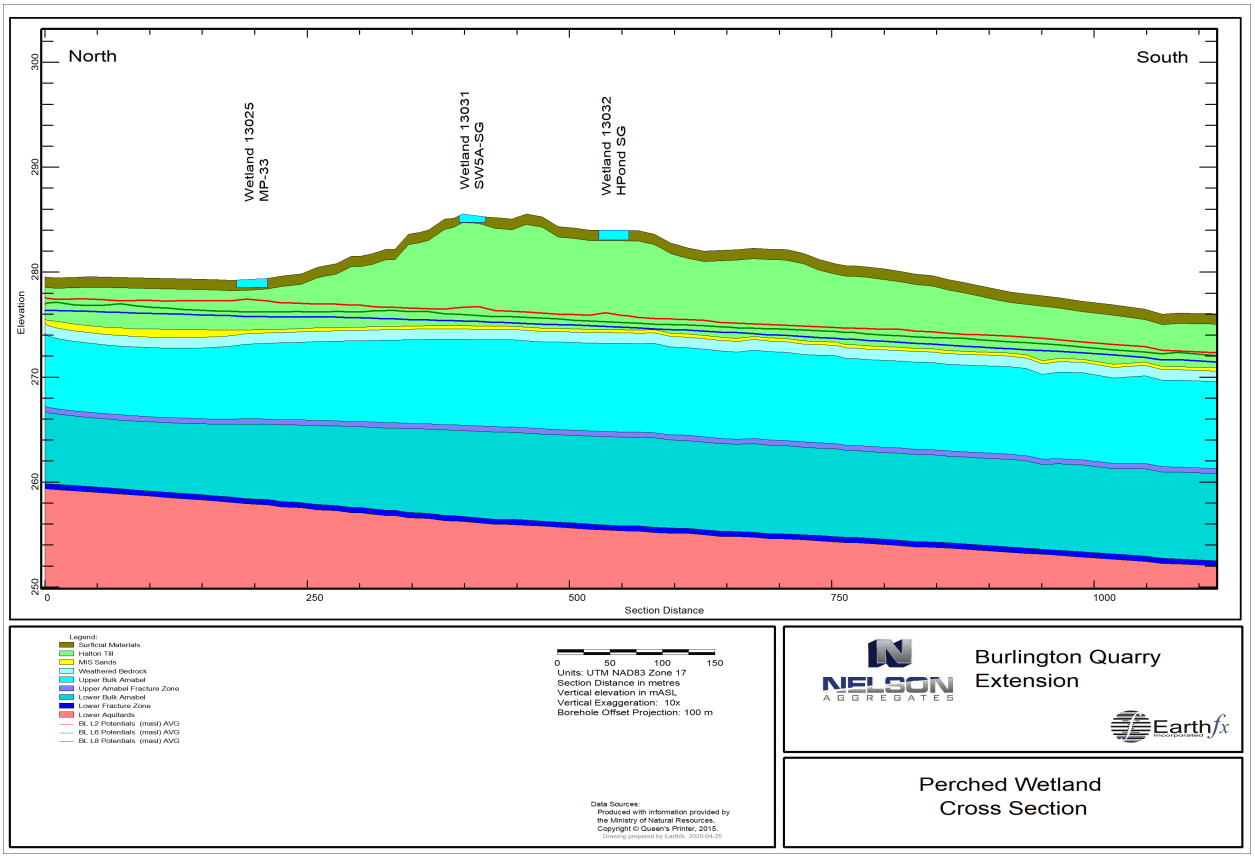

Figure 6.32: Perched Wetland Cross Section

6.11.6.1 MNRF Wetland 13025

The northern-most wetland, MNRF 13025, has been monitored for some years by mini-piezometer MP-33. This wetland is the lowest of the three, and is located 4 m below the top of the ridge (on the eastern flank). MP-33 is located at the eastern edge of the wetland pond, and extensive manual and data logger measurements are available (Figure 6.33). The measured water levels illustrate that the pond fills in the winter and spring, and then water levels recede over the summer. The simulated water levels in the pond (in dark red) closely matches the observed values. The model also matches the rate of spring recession in the pond levels very closely, indicating that the model is correctly matching the hydrologic processes and function of the wetland. Water levels in this wetland are always higher than the water table (shown as the Layer 2 potentials in Figure 6.33).

In summary, this perched wetland fills in the spring with snowmelt, rainfall and runoff, and then water levels gradually decline over the summer through evapotranspiration and vertical leakage of water down to the water table. The pond never receives groundwater inflow.

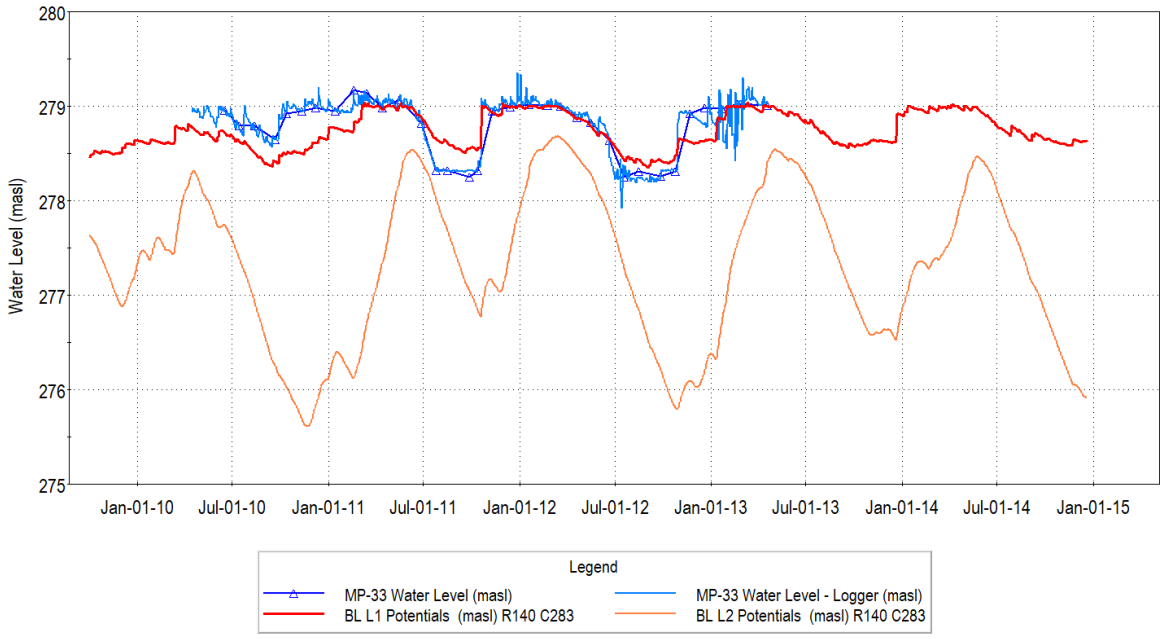

Figure 6.33: Wetland 13025 simulated pond water levels compared to MP-33 measurements

6.11.6.2 MNRF Wetland 13031

MNRF Wetland 1301, located at the top of the ridge, has been monitored by Staff Gauge SW5A-SG and nearby groundwater monitoring nest OW03-19. The observed water levels in the wetland pond are nearly 10 m above the measured water table in monitor OW03-19C (Figure 6.34), confirming that this a highly perched wetland. The model matches the water level variation and recession pattern, but slightly over-predicts water level elevations in the pond. No bathymetry data was available for this pond, so the offset between the observed and predicted pond elevation is likely due to a simple geometric offset in the base of the pond.

The groundwater levels measured in OW03-19C span a 10-year period and are consistently 9 m below the water levels observed in the pond. The model simulation of the water table very closely matches the observed level, including the seasonal and inter-annual fluctuations (Figure 6.34).

The field observations, together with the model simulations, confirm that this is a fully perched wetland pond with no interaction with the water table or groundwater system. The wetland fills in the spring with snowmelt, rainfall and runoff. Water levels gradually decline over the summer through evapotranspiration and vertical leakage of water down to the water table.

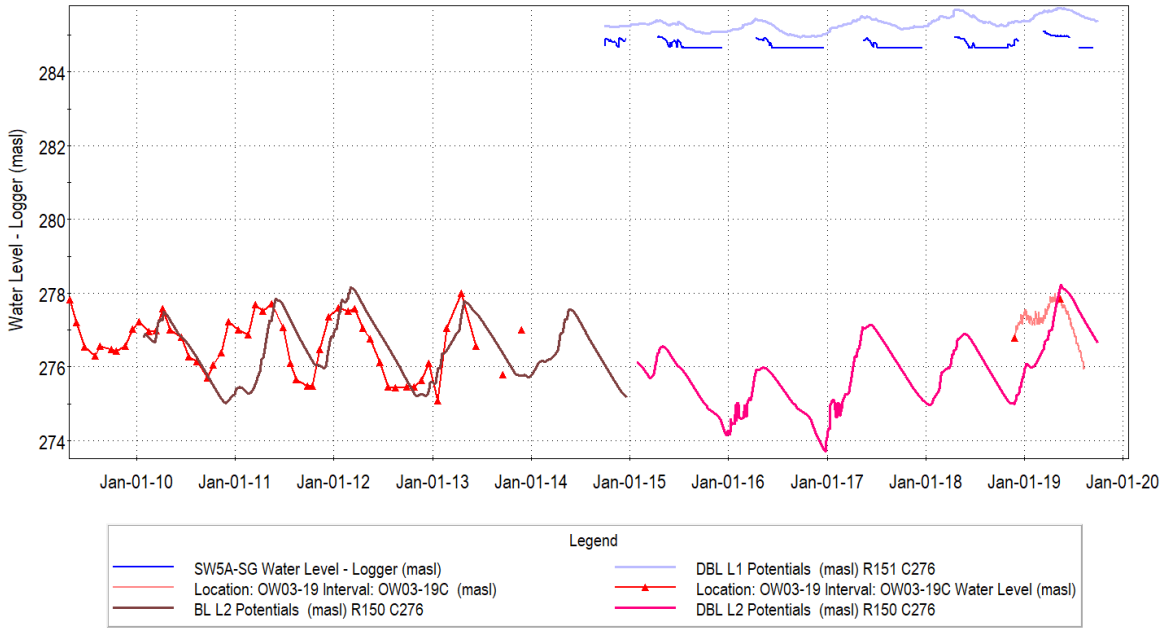

Figure 6.34: Wetland 13031 water levels compared to water table monitor OW03-19C

6.11.6.3 MNRF Wetland 13032 (Earthfx Wetland Number 19)

MNRF Wetland 13032, also located at the top of the ridge, was monitored in 2007 by the H Pond Staff Gauge (HPond SG) (Table 6.3). (This wetland is also referred to as Earthfx Wetland 19 in subsequent water budget analysis – alternate numbers were needed to better delineate water bodies). In addition to the staff gauge in the pond, two drive points (mini-piezometers) were installed near this pond in 2007. These drive points were always dry, indicating that the pond is perched above the water table.

Table 6.3: Wetland 13032 pond and drive point water levels. (Source: Ray Blackport, provided by David Donnelly via email July 8, 2010)

Water Level Measurement Summary			
	Pond	DP1	DP2
Ref:	283.09	284.09	283.31
GS:	-	283.29	282.63
Date	Water Level Elevations		
17-May-07	283.40	#N/A	#N/A
11-Jul-07	283.21	282.25dry	281.83dry
notes:	Ref. = reference point elevation GS = ground surface elevation		

Note: DP1 is adjacent to the pond (north)
DP2 is about 20 m north (downslope) of the pond

The field measurements indicate that the pond level dropped 19 cm between May 17, 2007 and July 11, 2007 (a dry year). While 2007 was not simulated, the model simulation of pond water level recession in 2016 (also a dry year) declines from 283.91 down to 283.68 masl, or 23 cm, over the May 17, 2016 to July 11, 2016 time period (Figure 6.35). The simulated water level recession of 23 cm is very similar to the measured value of 19 cm over a similar spring time period. The simulations further indicate that this water level recession is similar in other years (Figure 6.36).

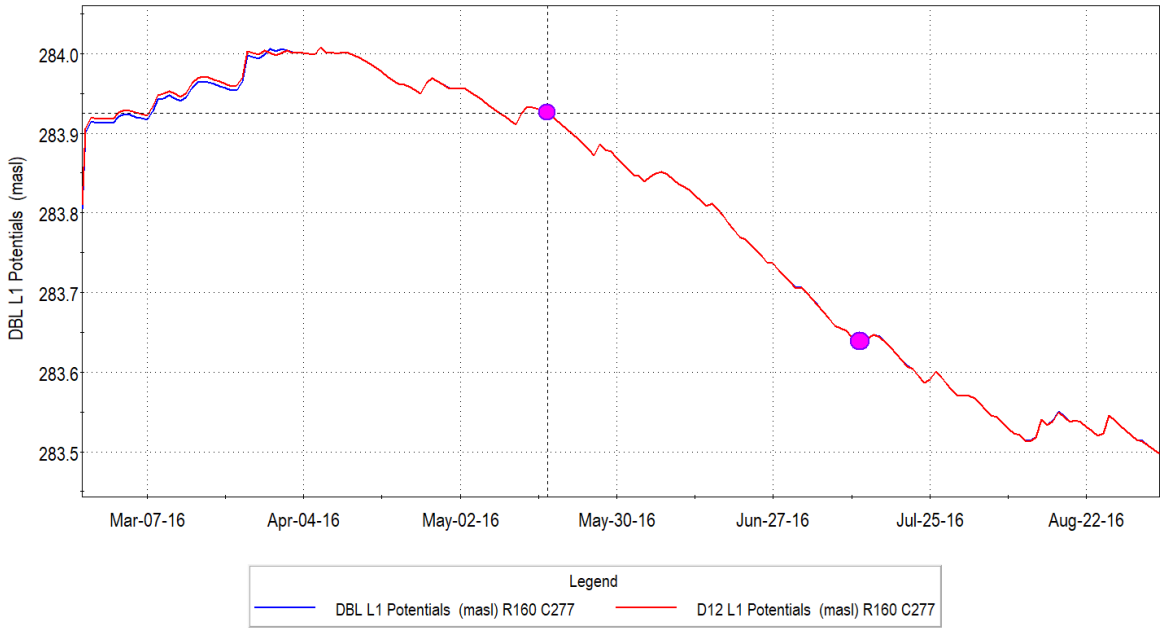

Figure 6.35: Wetland 13032 water level recession. Purple symbols mark the water level recession between the May 17 and July 11 time period.

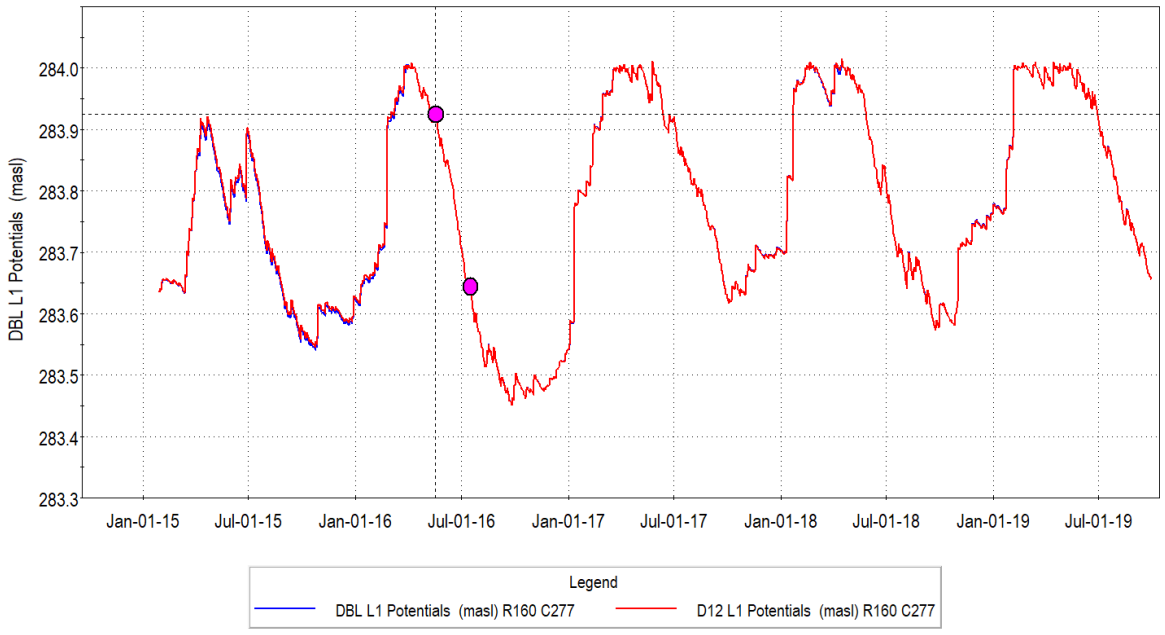

Figure 6.36: Wetland 13032 simulated water level showing similar spring recession patterns.

The field measurement of pond level recession confirms that the model is correctly simulating the hydrologic processes and pond water budget. The spring recession is a relatively good time to evaluate the pond function, for the dominant loss processes in a perched wetland are evapotranspiration and leakage to groundwater. The observed and simulated results at this highly perched wetland confirm that it is functionally identical to Wetland 13031, which has been extensively monitored for a number of years by both surface and groundwater instrumentation. Both the long-term monitoring record and the long-term simulations confirm that both wetlands are fully disconnected from the groundwater system.

6.11.6.4 Perched Wetland Conclusions

Both the field observations and model simulations of the three wetlands on the till ridge clearly demonstrate that these ponds are perched high above the water table. The close match between the model simulations and the field measurements confirm that the model is accurately simulating the hydrologic processes (snowmelt, rainfall, runoff, ET) that drive the wetland function and water budget. No groundwater inflows are observed or simulated into these wetlands.

The field observations and model simulations confirm that seasonal and inter-annual changes in the water table have no impact on the ponds. The ponds respond only to local climate-driven processes.

6.11.7 GSFLOW Outputs

Primary GSFLOW model outputs include daily streamflow, groundwater heads, and lake stage. The PRMS submodel also provides daily values for all components of the water budget including precipitation, interception, snowmelt, evapotranspiration, overland runoff, infiltration, and groundwater recharge. The GSFLOW code contains routines to sum many of the daily values over the basin. Earthfx added additional components to the output and aggregated other flow components so that local (cell-based) and subcatchment-based water balances can be readily produced. Average results from the PRMS submodel for key water budget components for the study area were presented in Appendix C and in Figure 6.14 and Figure 6.17.

Additional groundwater submodel outputs include the flows across constant head boundaries; groundwater recharge and groundwater ET; lateral and vertical flows between each cell; well discharge; groundwater discharge to streams and lakes; and groundwater discharge to the soil zone (also referred to as surface leakage). The daily values can be aggregated over time to provide monthly, seasonal, and annual water budgets. Values can also be aggregated spatially to provide water budgets at the subwatershed scale and for particular areas of interest, including individual wetlands.

As an example, Figure 6.37 shows the average March simulated heads in the Layer 4 (weathered bedrock) and simulated streamflow (in m^3/d). Groundwater levels and streamflow are at or near their highs for the year. Figure 6.38 shows the average September simulated heads and streamflow, which are at or near their lows for the year. Heads drop between 0 and 1 m in the quarry vicinity and up to 3 m at Mt. Nemo. Many of the lower-order streams have negligible flow.

As another example, the daily flows were averaged to create an average monthly water budget (Figure 6.37) that illustrates seasonal trends in the water balance. Water goes into storage during the fall through early spring and comes out of storage during the drier summer months. The rate of recharge also decreases significantly in the late spring and summer as do groundwater discharge to the soil zone and to streams.

6.11.8 GSFLOW Calibration Conclusions

The calibration analysis shows that the GSFLOW model represents surface water and groundwater flow patterns at both the regional and local scale. The use of uniform layer properties across all scales demonstrates that the model is broadly applicable across the study area.

The comparisons to transient data show excellent calibration matches, particularly considering the uncertain nature of the fractured rock and the inherent simplifications of the numerical model. The model is able to represent the complex effects of the existing quarry across multiple layers and distances, despite the use of uniform layer properties.

The calibration to the shallow mini-piezometers illustrates that the model is representing the shallow flow system well. There is a slight lag in the simulated response, suggesting there might be less storage in the Halton Till, but overall, the calibration is excellent, particularly given the fact that the model uses a single uniform Halton till hydraulic conductivity across the entire study area.

The calibration to pond water levels is also very good, indicating that the model is representing the wetlands and their interactions with the groundwater system very well. While water levels are easy to measure in the field, there is some uncertainty in the wetland pond bathymetry due to the difficulties measuring through thick wetland vegetation.

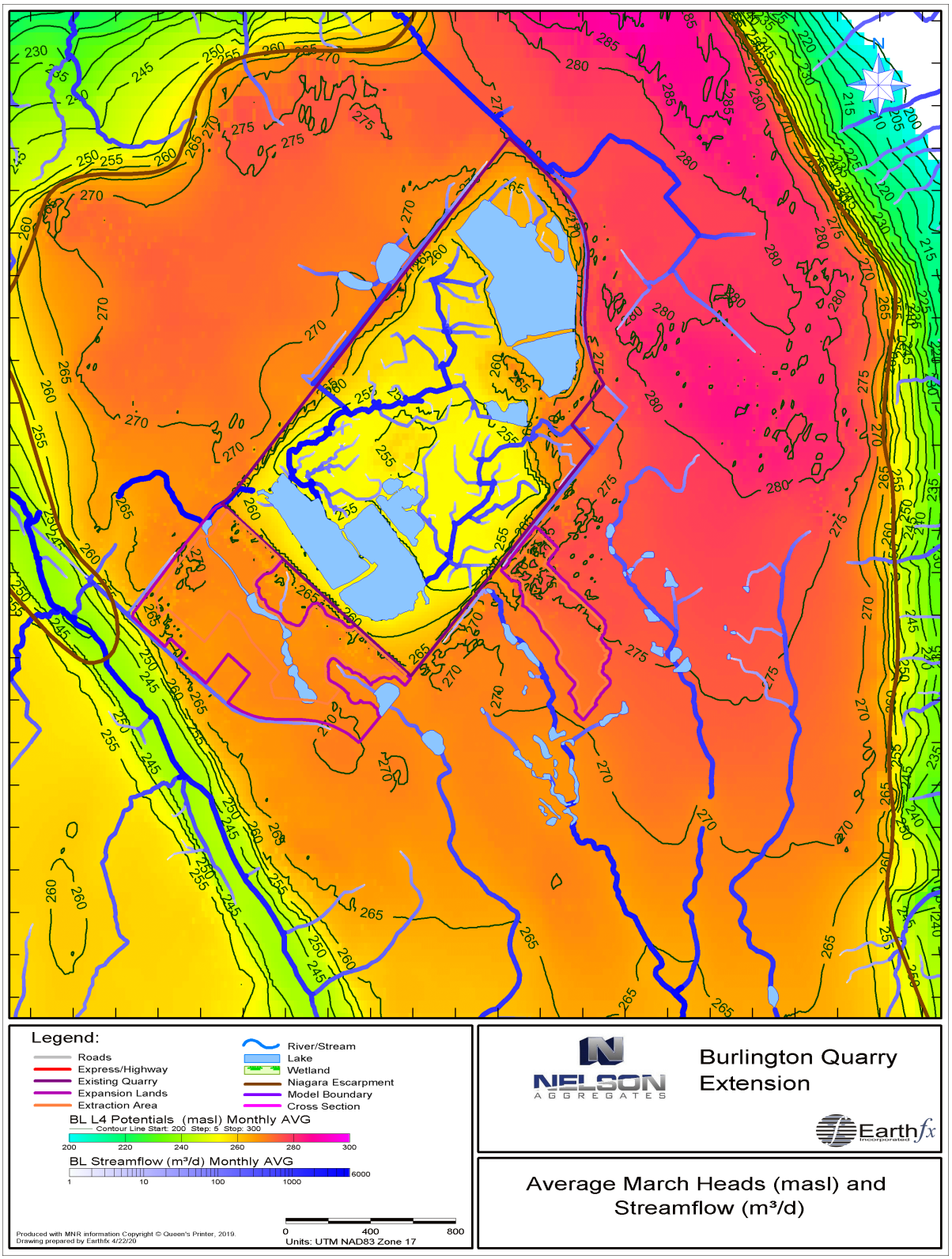

Figure 6.37: Average monthly simulated heads (in masl) and streamflow (in m^3/d) for March.

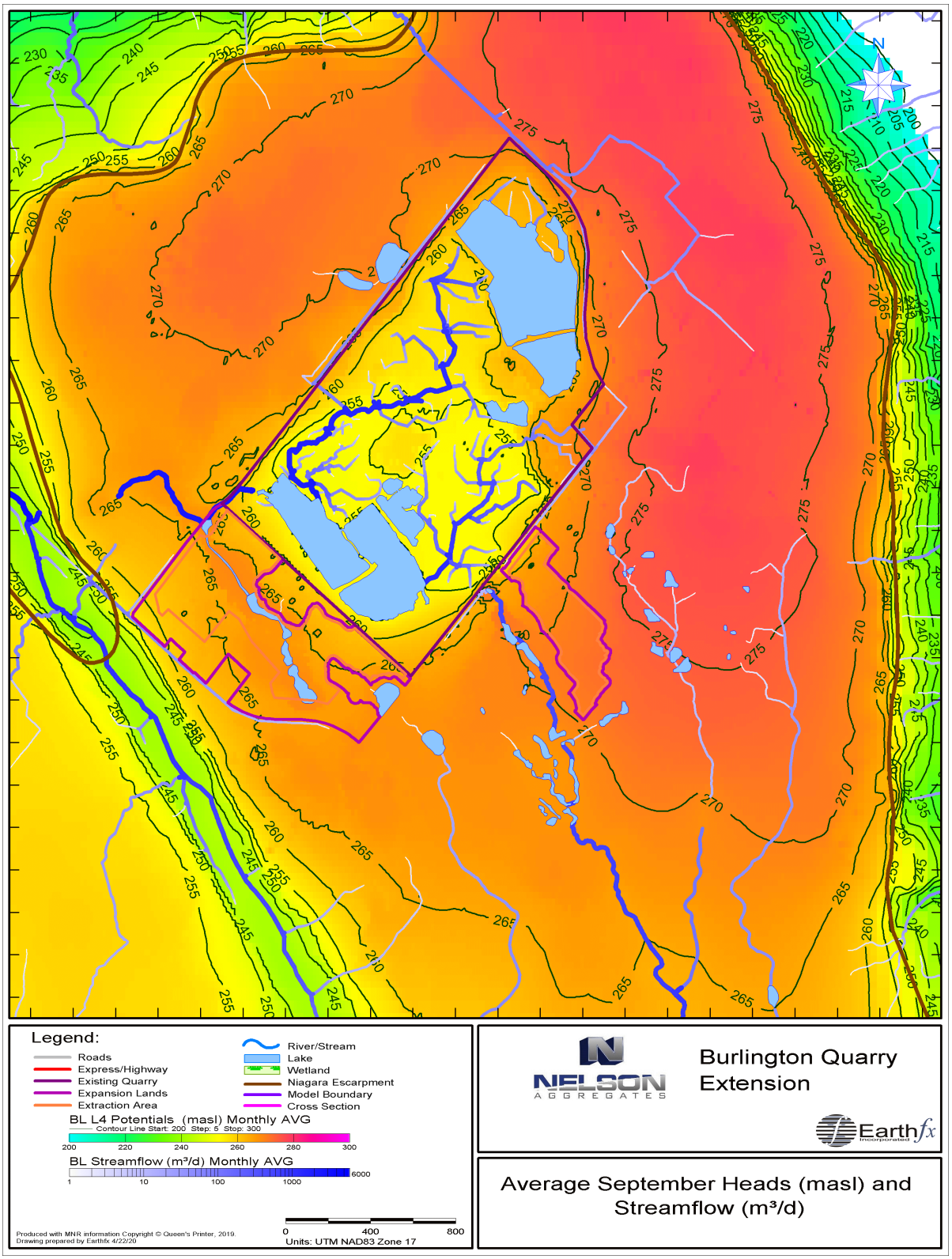

Figure 6.38: Average monthly simulated heads (in masl) and streamflow (in m^3/d) for September.

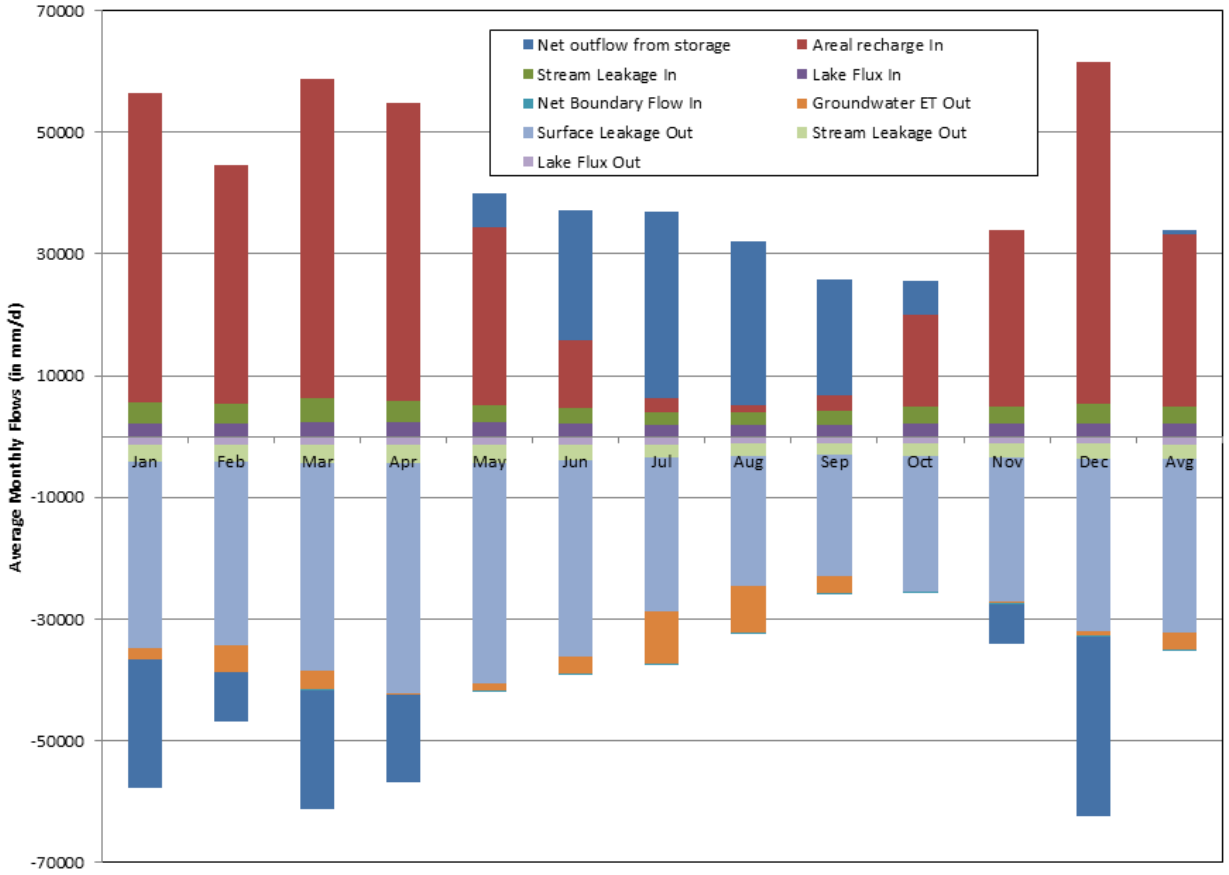

Figure 6.39: Average monthly groundwater budget for the study area (all flows in m^3/d).

7 Baseline Conditions Analysis

7.1 Introduction

The integrated surface water/groundwater model was used to compute the daily groundwater levels, surface water flows, and lake/wetland stage under baseline conditions for the study area. In addition, the model was used to compute all components of the water budget for significant groundwater and surface water features. The significant features were chosen through collaboration with other members of the project team and include streams, wetlands, and the current and future quarry excavations (see Tatham, 2020; Savanta 2020).

The model was run for a ten-year period (WY2010 to 2019) and calibrated to regional and local observation data collected during this time. As such, the calibrated model represents current groundwater and surface water conditions in and around the Burlington Quarry across a range of climatic conditions, including seasonal and interannual wet and dry years. The model results for this period represent a highly realistic baseline for comparison with other scenarios.

Transient Assessment Approach: The GSFLOW model was run in transient mode at a daily time step. The transient approach offers several benefits over a steady-state, or long-term average, approach because it can represent the seasonal variability in key hydrologic parameters such as streamflow and groundwater levels.

A key factor in the analysis was that the same daily climate inputs were used for both the Baseline and for all the future extraction and rehabilitation scenarios. This was done because (1) the future climate is unknown; (2) the WY2010 through WY2019 period is representative of wet, dry and average climate years; and (3) a consistent transient climate input allows direct comparison of the effects of quarry extension and rehabilitation on the surface water and groundwater systems. With this approach, maps and hydrographs of different scenarios could be directly compared to baseline conditions to determine the incremental effects of the proposed changes.

For example, drawdowns (i.e., the change in groundwater levels) in each aquifer during the Phase 1 and 2 extraction were computed by subtracting the simulated groundwater heads in each cell from the simulated groundwater heads for that day in each corresponding cell under Baseline Conditions. This operation was repeated for each day in the simulation. In this way, daily, mean, maximum, minimum, and percentile changes in water levels were determined across the entire simulation period. The same procedures were followed for assessing changes in simulated streamflow, wetland/lake stage, and water budget components.

7.2 Baseline Assessment

7.2.1 Time Period

As noted above, the time period chosen for the Baseline and quarry extension/rehabilitation scenarios was October 1, 2009 to September 31, 2019 (WY2010 – WY2019). The time period was chosen because, as a whole, it represented an average climate period, while still containing years of above average and below average precipitation. The time period was also consistent with the up-to-date land use mapping (SOLRIS v3) used to assign many key model parameters.

The model required long run times, with the 10-year simulations taking 14 days to complete. The time requirement is mainly due to the MODFLOW submodel; PRMS simulations are relatively fast. The long model run times can be attributed to the extremely fine resolution of the MODFLOW grid in the

quarry vicinity combined with numerical stability challenges at the sharp Niagara Escarpment rock face.

7.2.2 Scenario Summary and Nomenclature

The exceptionally long model run times and model stability challenges required practical model management solutions. In some cases, the long model runs were completed as two simulations spanning the 10-year assessment time period. For example, the first 5 years of the baseline scenario was completed as one continuous simulation, with an emphasis on the assessment of the Golder monitoring data. The second part of the baseline assessment started in October 2014 and covered:

- the WY2015-WY2016 drought period (including a Level 2 Low Water Advisory),
- the WY2017 wet period, and finally,
- the WY2018-WY2019 new data collection period.

A complete list of the baseline and development scenarios is included in Table 7.1. Details about the other scenarios are discussed in the following chapter.

Throughout this report, the model simulation results include a “Prefix” describing the scenario. For example, the Baseline Layer 4 simulated potentiometric head results are referred to as “BL L4 Potentials (masl)”. The second part of the Baseline simulation, covering the 2015-2016 drought period, is referred to as the “DBL” or Drought Baseline simulation. The scenario name and prefixes are listed in Table 7.1.

Table 7.1: Scenario summary.

Scenario	Prefix	Period	Start Date	End Date	Years	Comment
Baseline	BL	Start	WY2010	WY2014	5	Golder calibration period
	DBL	Drought	WY2015	WY2019	5	Validation and drought
Phase 1/2	P12	Start	WY2010	WY2011	2	
	D12	Drought	WY2015	WY2019	5	Drought assessment
Phase 3/4	P34	Start/Drought	WY2010	WY2016	7	P34 and P12 Recovery
Phase 3456	P3456	Start/Drought	WY2009	Mid-WY2019	9.6	Full P3456 Build and P12 recovery
Rehabilitation Plan 1	RHB1	Start	WY2010	WY2011	3	Conversion to Park
Rehabilitation Plan 2	RHB2	Start	Mid-WY2010	Mid-WY2015	5	One Quarry Lake

7.2.3 Surface Water Flows

The GSFLOW model provides daily streamflow for every stream reach (length of stream within a MODFLOW model cell). A set of common assessment points, including several of the existing streamflow gauges, was selected for the Baseline and Scenario comparative analyses. These locations, shown on Figure 7.1, are located at a range of distances from the quarry and extension areas.

Figure 7.2 shows the average simulated streamflow for the baseline period. The blue stream color intensity and line thickness are proportional to the flow in the stream (Note: See Section 1.3.4 for important information about the stream network representation). The flows range from 0.0001 m^3/s

(8.64 L/s) to 0.1 m^3/s. The highest flow occurs downstream of SW07, past the confluence with the karst spring that carries quarry discharge.

Figure 7.4 through Figure 7.15 show hydrographs of simulated streamflow, in m^3/s, for the six streamflow analysis points. The hydrographs are split to show five years on each for better visualization. The first five sites are to the south or east of the existing quarry while the last site, SW07, is in the Medad valley. Note that flows at SW36 are affected by the south quarry discharge.

The hydrographs for WY2015 to WY2019 include an extreme dry year (WY2015), a dry year (2016), and an extreme wet year (2017). Daily precipitation and snowmelt were added to the hydrograph for SW10B (Figure 7.13). It is interesting to note that the lowest flows occurred in the summer of 2016, not 2015, because storage in the groundwater system supported baseflow through the early part of the drought.

7.2.4 Seasonal and Inter-annual Groundwater Levels

The GSFLOW model provides daily groundwater levels in each model layer. A set of groundwater assessment points (some close to existing wells, some located near residential areas, and some near the centre of a wetland complex) were selected for the Baseline and Scenario comparative analyses. Assessment point locations are shown on Figure 7.1, and represent a range of distances from the existing quarry and extension areas.

The color contours presented in Figure 7.2 show the average simulated heads in Model Layer 6, representing the middle fracture zone in the Amabel aquifer, for the period WY2010-WY2014. Figure 7.16 shows the transient water levels in Layer 6 for the 8 groundwater assessment points over the same time period. Natural water level fluctuations become more muted at points close to the Medad Valley because it is a natural discharge area.

Figure 7.17 shows a similar plot for the simulated heads for WY2015 to WY2019 (including the drought period). The heads at most assessment points reach a minimum in the fall of 2015 in response to the lower than average precipitation in WY2015, but reach a similar low in fall of 2016, even though it is a wetter year, because of natural climate-driven depletion of groundwater storage in the previous year.

Figure 7.3 presents a summary of the groundwater supply conditions in the study area. This figure shows the available groundwater drawdown in the Amabel Formation. At any location in the vicinity of the quarry a private water well could be drilled to the Layer 8 fracture zone and would have up to 22 m of available drawdown. Near the existing quarry that drawdown is reduced by the effects of the quarry dewatering, but many wells are both shallow, and in close proximity to the quarry, and yet have had suitable water supply for many years.

In summary, the model provides a wealth of information about the water levels and stream flows across the study area and assessment time period. Results are presented both spatially and temporally (on hydrographs) to illustrate the flow patterns and natural response to changing climate.

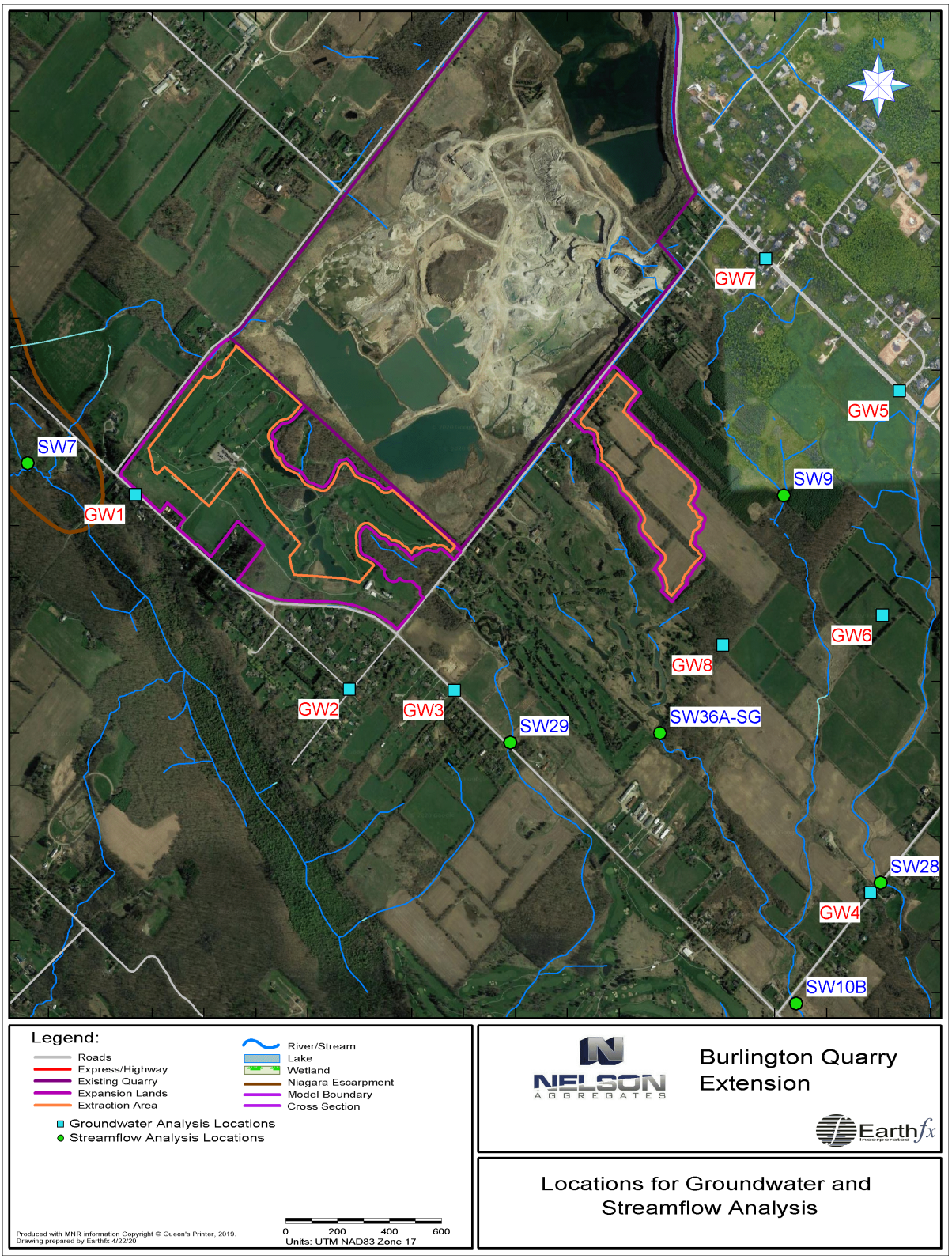

Figure 7.1: Locations selected for comparative analyses of streamflow and groundwater levels.

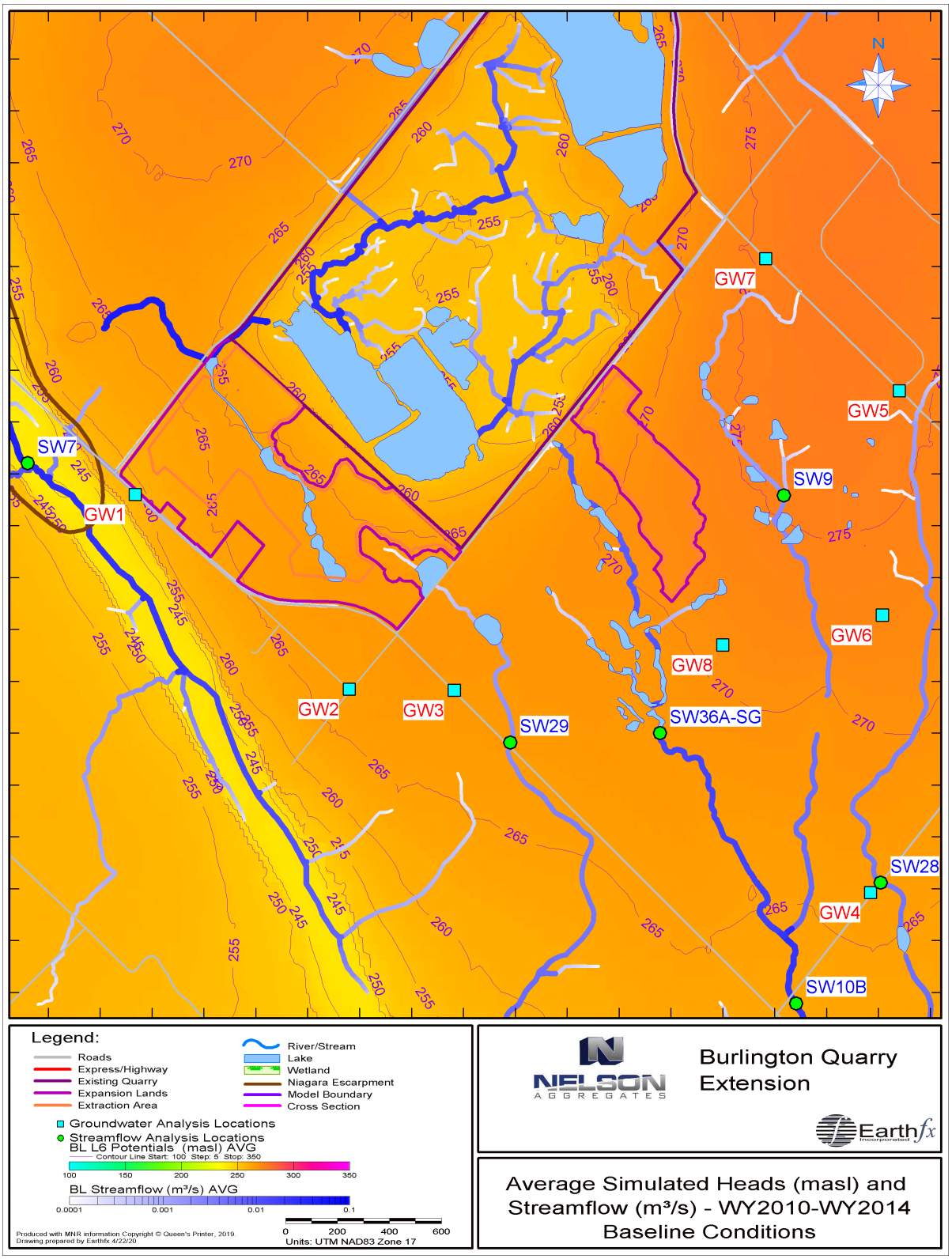

Figure 7.2: Average simulated heads in Model Layer 6 (masl) and streamflow (m^3/s) for WY2010 to WY2014.

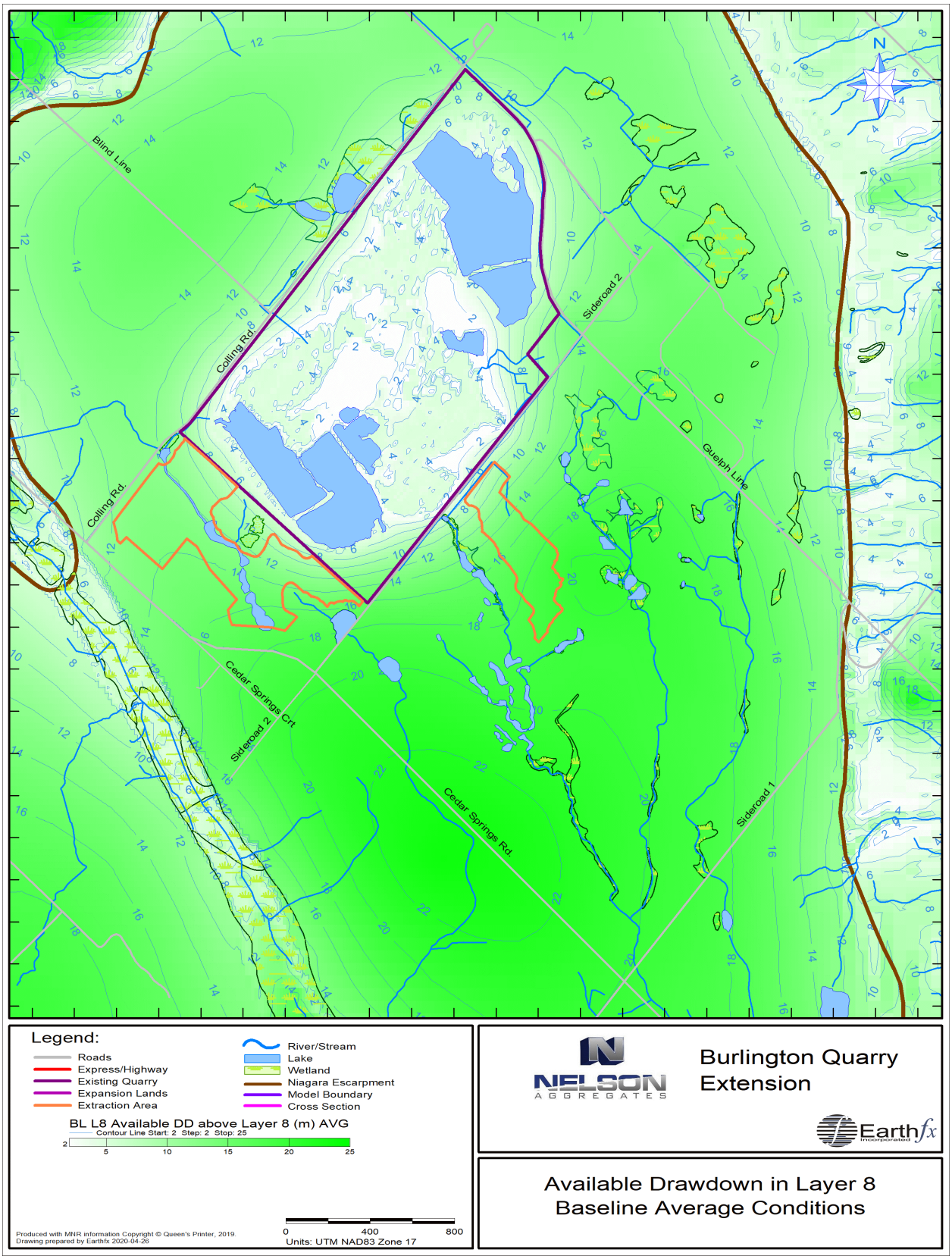

Figure 7.3: Available Drawdown in Layer 8 - Baseline Conditions

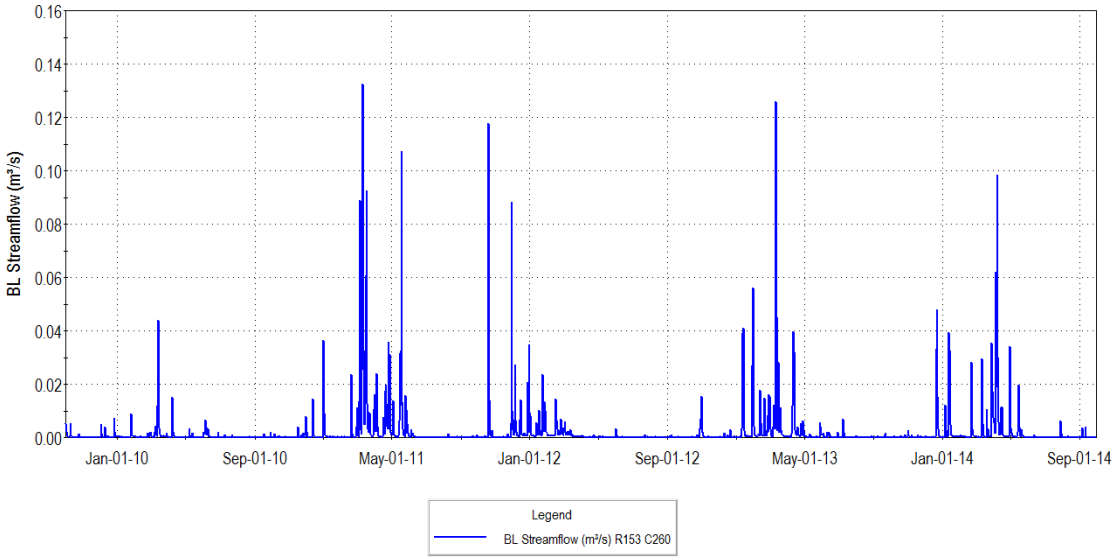

Figure 7.4: Simulated streamflow at SW09 for WY2010 to WY2014 - Baseline Conditions.

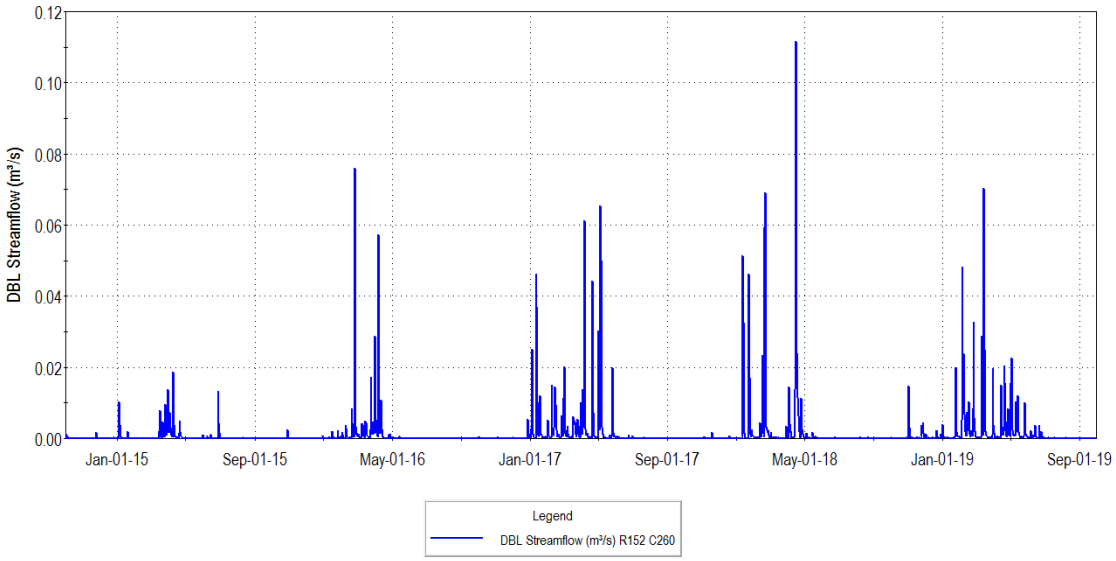

Figure 7.5: Simulated streamflow at SW09 for WY2015 toWY2019 - Baseline Conditions.

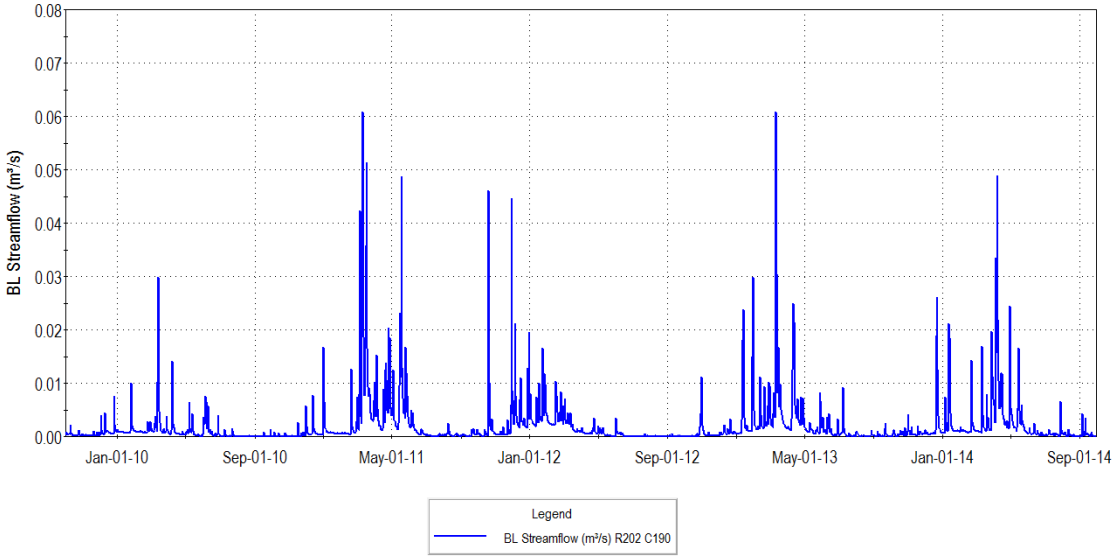

Figure 7.6: Simulated streamflow at SW29 for WY2010 to WY2014 - Baseline Conditions.

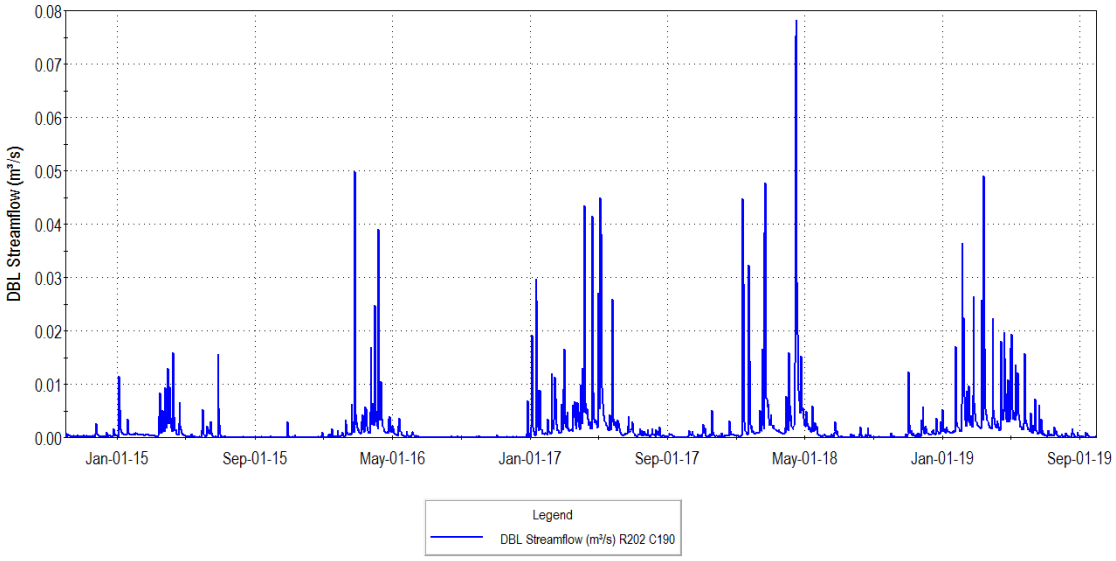

Figure 7.7: Simulated streamflow at SW29 for WY2015 to WY2019 - Baseline Conditions.

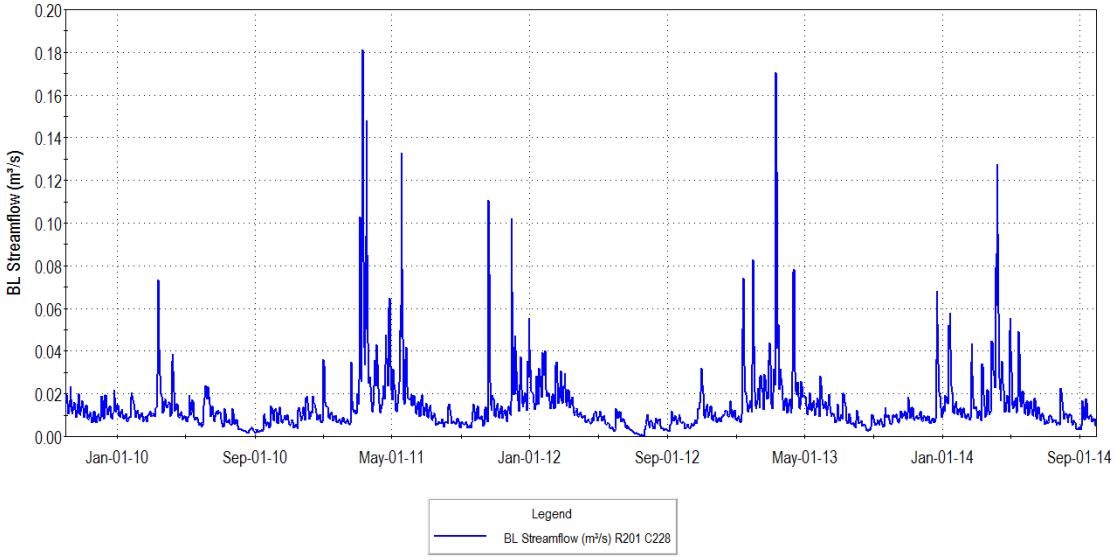

Figure 7.8: Simulated streamflow at SW36A for WY2010 to WY2014 - Baseline Conditions.

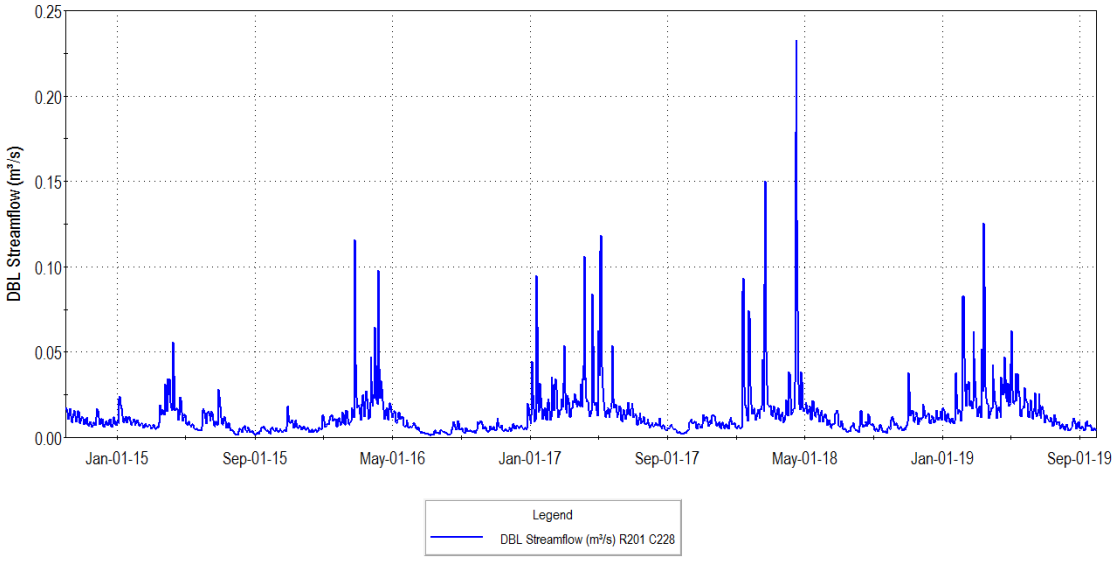

Figure 7.9: Simulated streamflow at SW36A for WY2015 to WY2019 - Baseline Conditions.

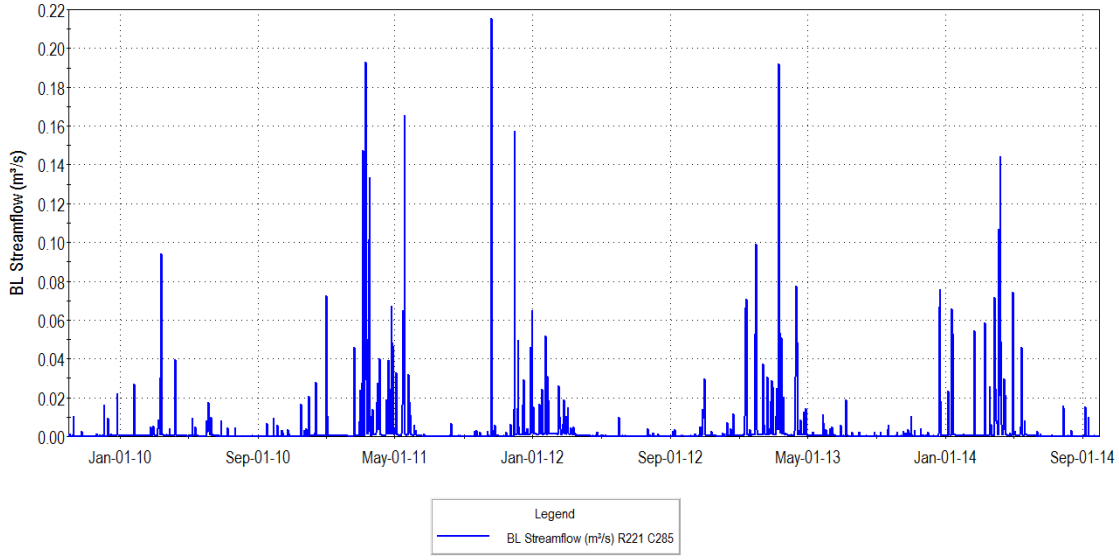

Figure 7.10: Simulated streamflow at SW28 for WY2010 to WY2014 - Baseline Conditions.

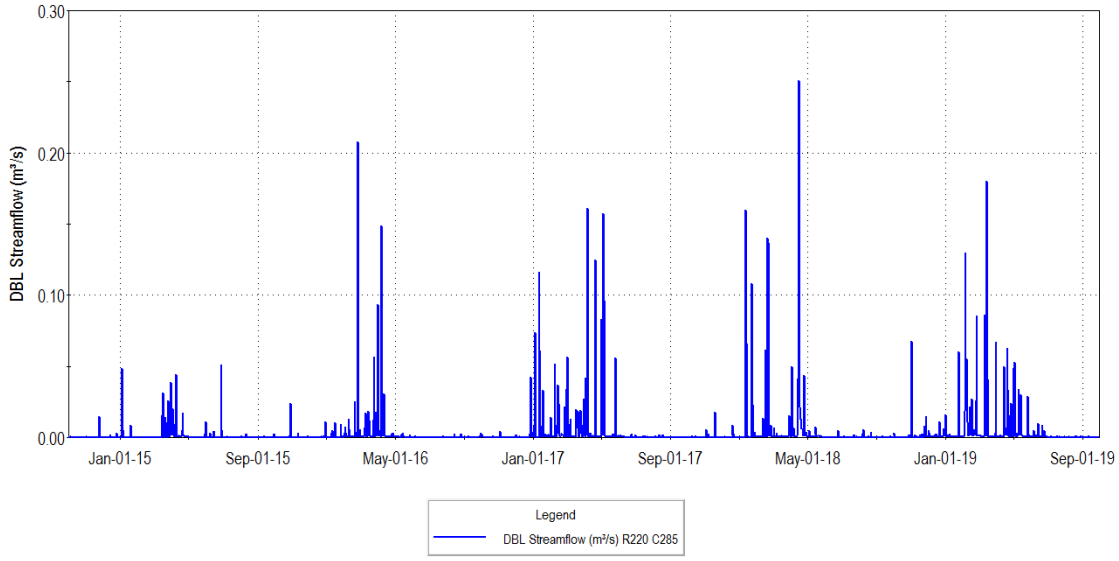

Figure 7.11: Simulated streamflow at SW28 for WY2015 to WY2019 - Baseline Conditions.

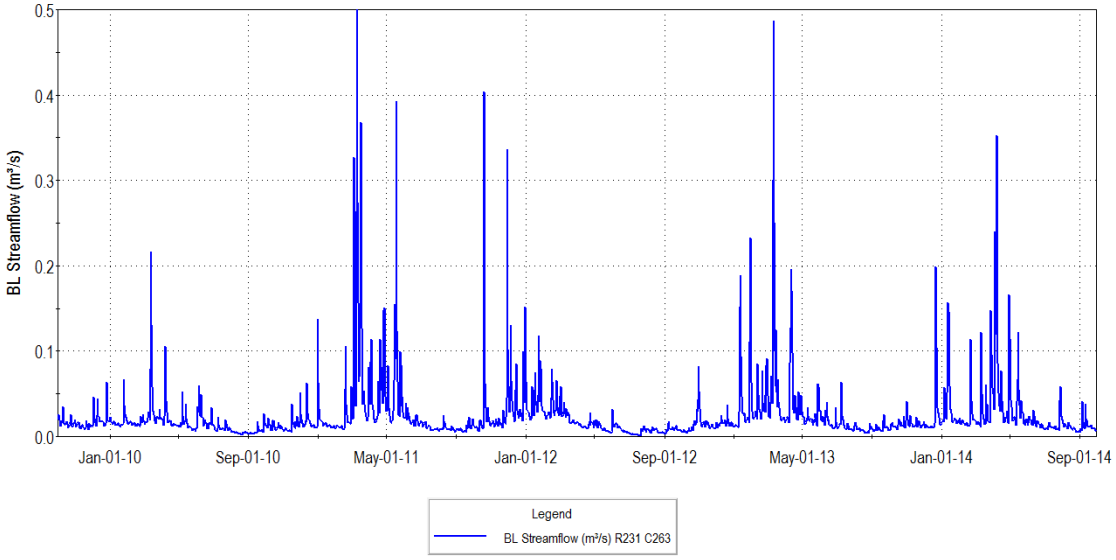

Figure 7.12: Simulated streamflow at SW10B for WY2010 to WY2014 - Baseline Conditions.

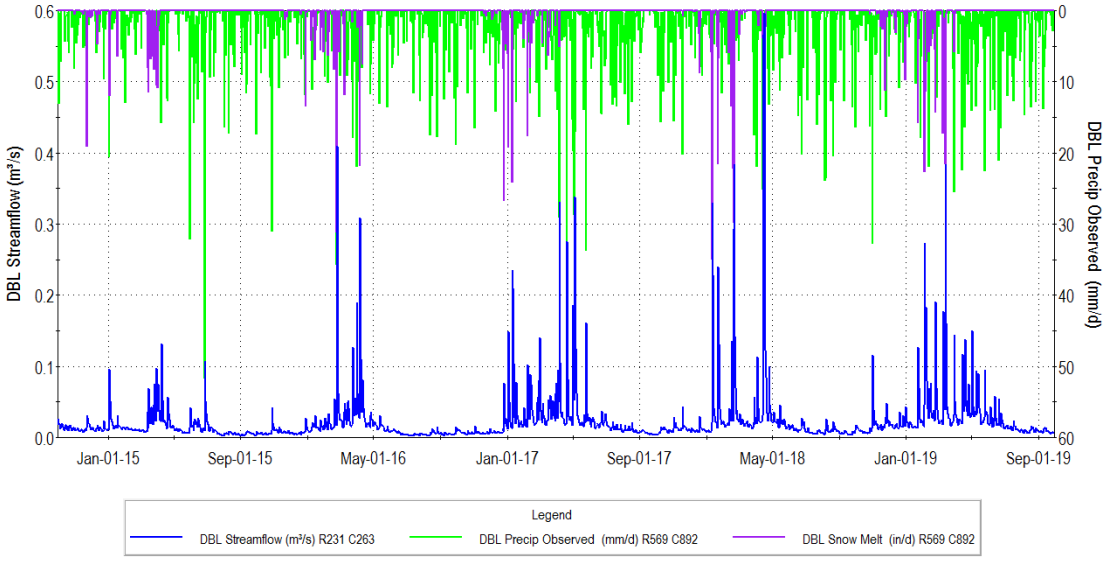

Figure 7.13: Simulated precipitation and streamflow at SW10B for WY2015 to WY2019 - Baseline Conditions.

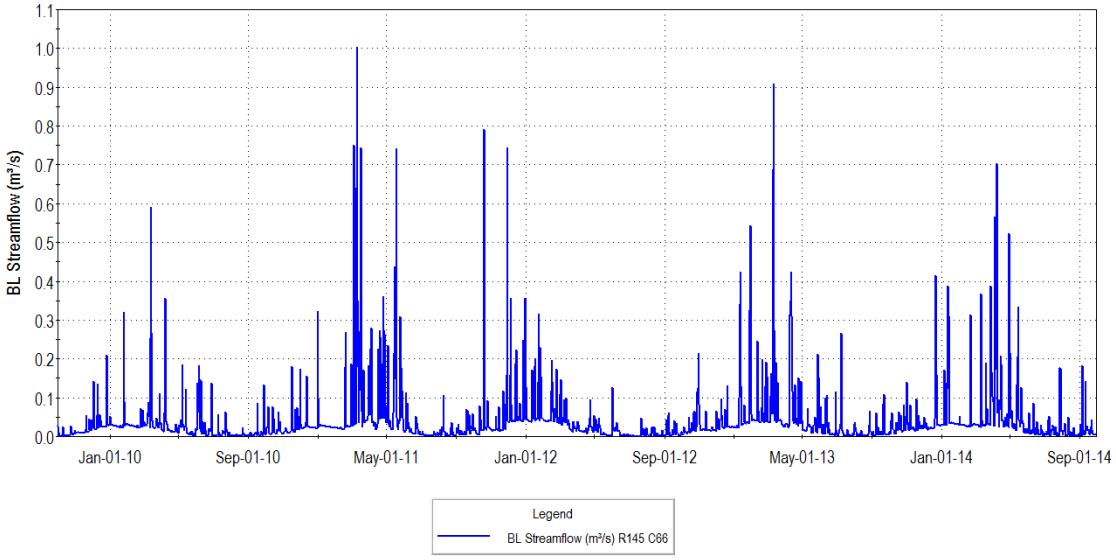

Figure 7.14: Simulated streamflow at SW07 for WY2010 to WY2014 - Baseline Conditions.

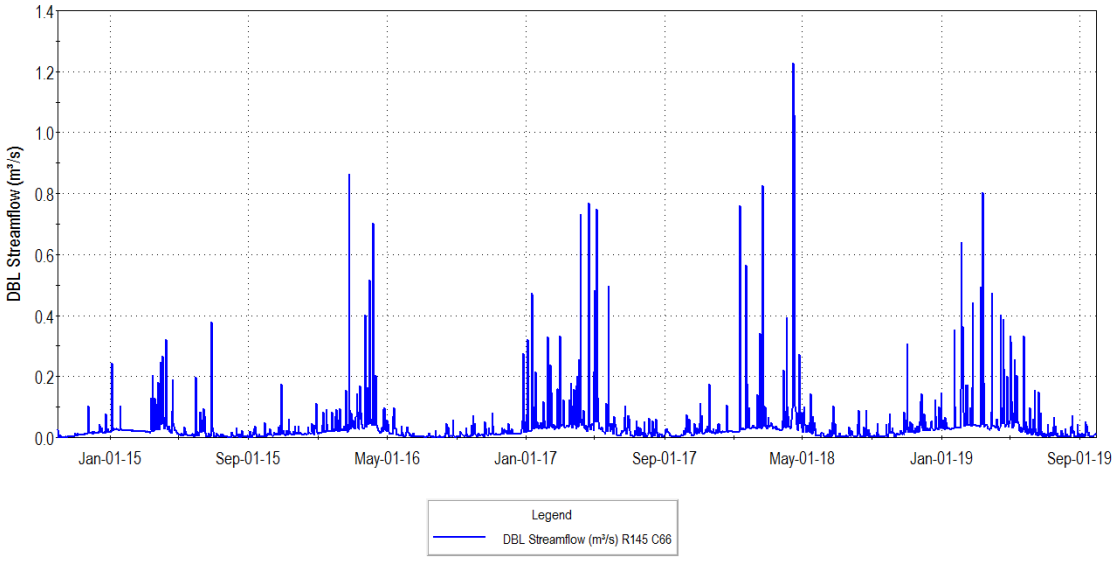

Figure 7.15: Simulated streamflow at SW07 for WY2015 to WY2019 - Baseline Conditions.

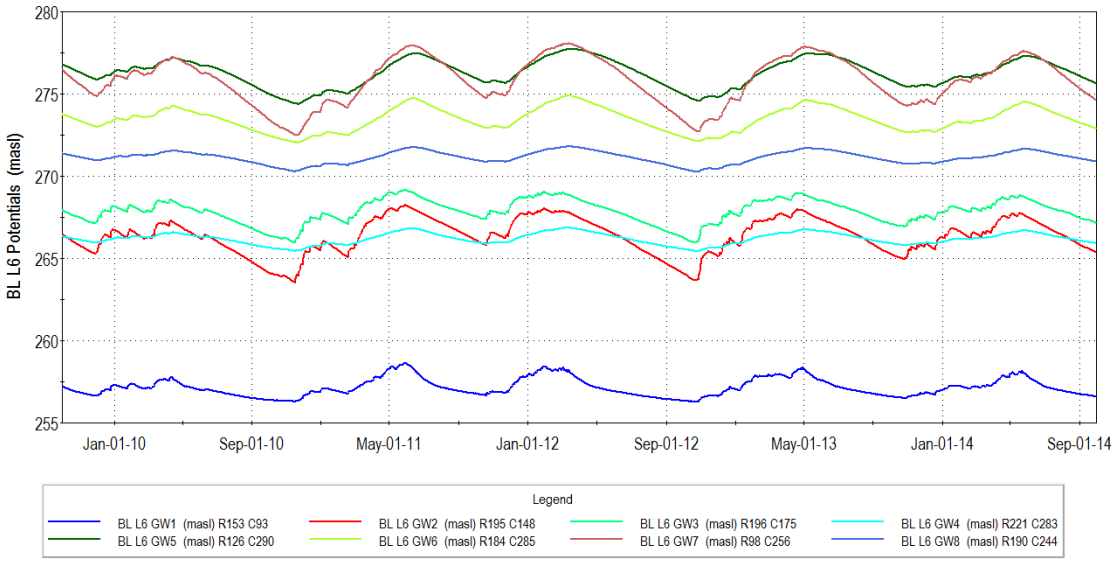

Figure 7.16: Simulated heads in Model Layers 6 at groundwater assessment locations GW1 to GW-8 for WY2010 to WY 2014 - Baseline Conditions.

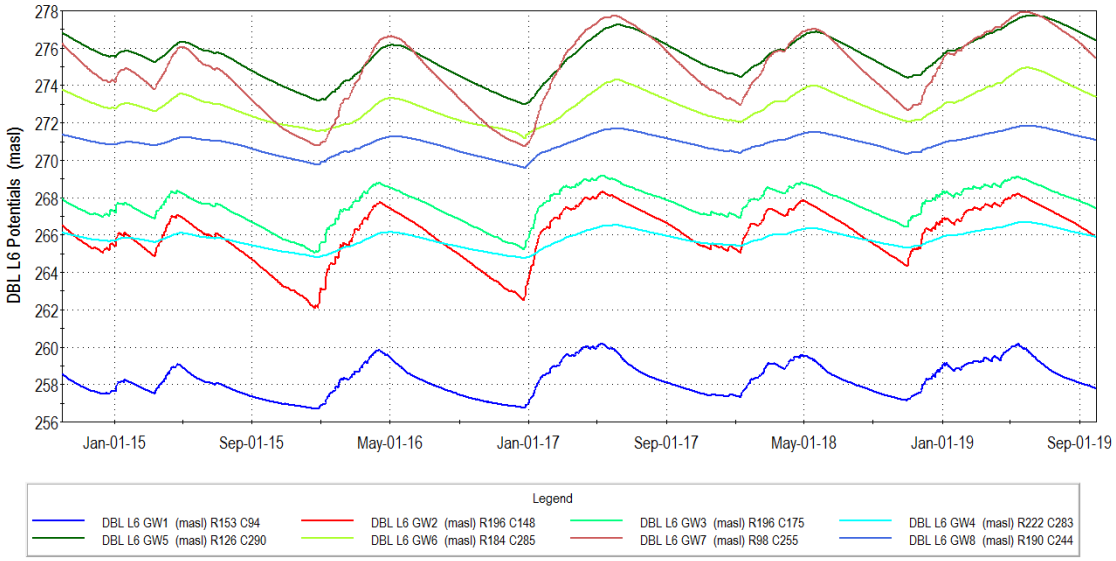

Figure 7.17: Simulated heads in Model Layers 6 at groundwater assessment locations GW1 to GW-8 for WY2015 to WY2019 - Baseline Conditions.

7.2.5 Surface Water/Groundwater Interaction

A key strength of the GSFLOW model is its ability to represent and quantify the interaction between groundwater and surface water. As noted in Section 6.3, traditional groundwater-only models assume that direct groundwater discharge to streams (hyporheic exchange) is the principal mechanism of groundwater/surface water interaction. This is incorrect, for there are multiple additional feedback and interaction mechanisms, including rejected recharge, groundwater ET and groundwater discharge to the soil zone (See Section 6.3.4).

The following discussion presents an overview of the Baseline conditions groundwater and surface water interactions. Subsequent comparative scenario analysis focuses on the change in these interactions.

7.2.5.1 Recharge

As noted in Section 6.3, the PRMS code estimates daily seepage from the soil zone, but the feedback between the PRMS and MODFLOW submodels determines how much of this seepage becomes groundwater, and how much is rejected back to the soil zone as Dunnian runoff.

Figure 7.18 shows the average simulated net groundwater recharge in the quarry vicinity for Baseline Conditions. Recharge is relatively uniform across the Halton Till, although focussed recharge occurs in areas where topographically-driven overland runoff concentrates. The white areas, such as in the Medad valley and around the Mt. Nemo Creek tributaries are indicative of groundwater discharge.

7.2.5.2 Groundwater ET

Lake, soil zone and groundwater ET are all simulated in the model. The PRMS model passes any unsatisfied soil zone ET demand down to the groundwater system where it can be met by evaporative uptake from the shallow water table. Figure 7.19 shows the average simulated groundwater ET for Baseline Conditions, and groundwater ET occurs in the riparian areas where the water table is near the surface. It is interesting to note that that high groundwater ET rates occur on the quarry floor because there is no vegetative cover and most of the potential soil zone ET demand is passed to the groundwater model. The proposed changes in quarry footprint and land cover processes are modest, so ET changes are not significant.

7.2.5.3 Surface Discharge

Figure 7.20 presents the average simulated groundwater discharge to the soil zone under Baseline Conditions. This is a key mechanism in the riparian and wetland areas, for groundwater seepage to the soil and wetlands can become Dunnian overland flow into the streams. Lowering the water table can change the surface discharge, but major areas of surface discharge, including the Medad Valley, are already at a lower elevation than the quarry, and are therefore less sensitive to water table changes associated with the proposed extraction.

7.2.5.4 Stream Leakage (Hyporheic Exchange)

Figure 7.21 presents the average simulated streamflow loss to groundwater (blue lines) and groundwater discharge to streams (red lines) under Baseline Conditions. As most streams are perched above the water table, they generally lose rather than gain flow from the groundwater system. The streams are primarily located in Halton Till, so the low permeability of the till limits GW/SW interactions.

The Medad Valley is an interesting setting, for Figure 7.20 shows that there is groundwater discharge to the soil zone along the flanks of the valley, yet the main stream in the centerline of the valley is leaking water to the groundwater system (Figure 7.21). This demonstrates that the incised Medad wetlands and streams are somewhat isolated from, and functionally different than, the streams and wetlands of the upland plateau (where the quarry is located). Despite this loosing condition, there is still a net pickup of water in the stream between gauges SW14 and SW07 (Figure 2.2).

7.2.6 Wetland Water Budgets

There are 24 wetlands within the study area (locations are shown in Figure 7.22). Detailed feature-based water budgets were calculated to analyze the inflows and outflows to 22 of these local wetlands. Two of these features, known as the Weir Pond (MNRF ID 13202) and the elongated Medad Valley Wetland Complex, receive the primary quarry discharge water from Sump 0100 and are discussed in detail in Section 8.7.5 and 8.7.6. (Further discussion of the form and function of these two features can be found in Tatham (2020) and Savanta (2020)).

The integrated water budgets presented here supplement and complement the surface water assessment of Tatham (2020). (The groundwater components of the Tatham analysis were taken from the integrated model.) The main difference is that the Tatham water budgets are based on subcatchment analysis, while these water budgets are “feature-based”, meaning that they are calculated based on the local mapped boundaries of the wetland or pond.

The water budget assessment areas are generally based on the MNRF wetland mapping, however additional zones were needed, so a new Earthfx Water Budget ID number was created. The Earthfx and corresponding MNRF wetland ID numbers are shown in Figure 7.22,and a table correlating the ID numbers is shown in Table 7.2. Wetland descriptions can be found in Tatum Engineering (2020). (Also please note the feature representation issues discussed in Section 1.3.4).

Table 7.2: MNRF Wetland ID Numbers vs Earthfx ID Numbers.

Earthfx ID	MNRF Wetland ID Numbers
9	13014
10	13015
11	13016
12	13017, 13018
13	13030
14	13019
15	13021
16	13022
17	13033
18	None
19	13032
20	13036, 13037, 13038, 13039

21	13201
22	13200
23	13202 (Weir Pond)
24	Medad Valley Wetland Complex

The Earthfx GSFLOW processor was used to compute all flows within each area as well as lateral groundwater flow, streamflow, overland runoff, and interflow crossing the wetland boundaries. Figure 7.23 through Figure 7.30 present schematic summaries showing detailed water budgets for key wetland areas 9, 16, 17, 18, 19, 20, 21, and 22, respectively. The wetlands are located at various distances from the existing quarry and the extension areas. All areas are net contributors to groundwater, which is typical of wetlands that are perched for most or all of the year. Wetlands 16, 17, and 20 have ponded areas within the wetland that were treated as shallow lakes with separate water budgets.

A summary of the groundwater interactions with the wetlands is presented in Table 7.3. The groundwater component is presented as a percentage of the total inflow or outflow. The table shows that the wetlands have generally limited interaction with the groundwater system. None of the wetlands receive more than 3% of their total inflows from the groundwater system: Groundwater inflows are not a significant component of the wetland water budget.

The groundwater outflow results indicate that the wetlands generally leak water down to the groundwater system. This is expected for runoff dominated wetlands that are generally perched in the Halton Till above the water table.

Table 7.3: Summary of groundwater-wetland interactions.

Earthfx Wetland ID	MNRF ID	Baseline	
		GW Outflow %	GW Inflow %
9	13014	10.19%	0.00%
16	13022	1.25%	0.34%
17	13033	2.51%	1.31%
18	None	5.98%	2.42%
19	13032	19.82%	0.00%
20	13036-13039	12.84%	1.76%
21	13201	12.78%	2.98%
22	13200	26.31%	0.00%
GW Outflow = Groundwater outflows as a percentage of total outflows from the feature			
GW Inflow = Groundwater inflows as a percentage of total inflows to the feature			

The components of the water budget are expected to vary to some degree as the quarry is expanded and then rehabilitated. The changes for wetlands with little interaction with groundwater are expected to be minor. The comparative wetland analysis is presented in Section 8.

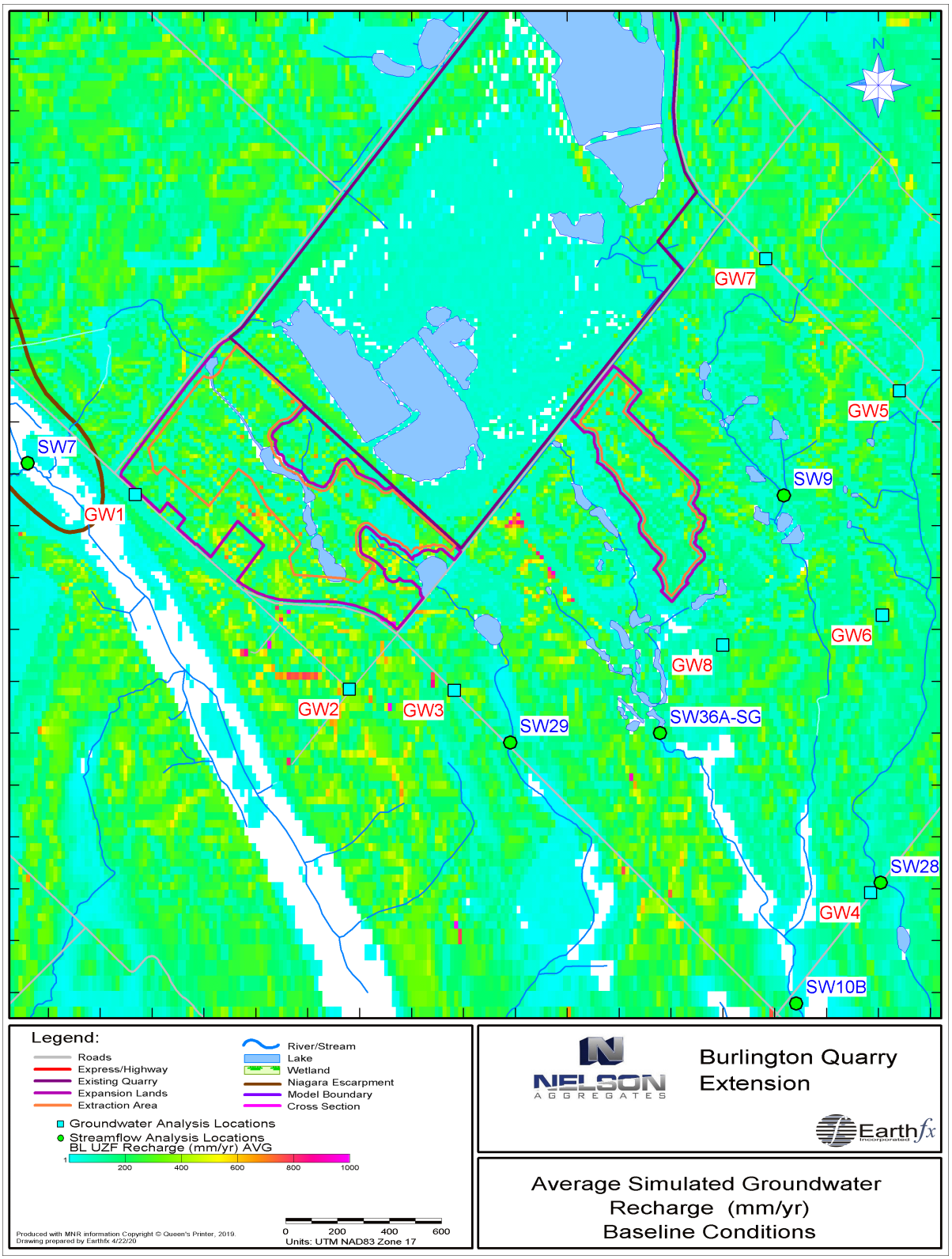

Figure 7.18: Average simulated groundwater recharge (mm/yr) under Baseline Conditions.

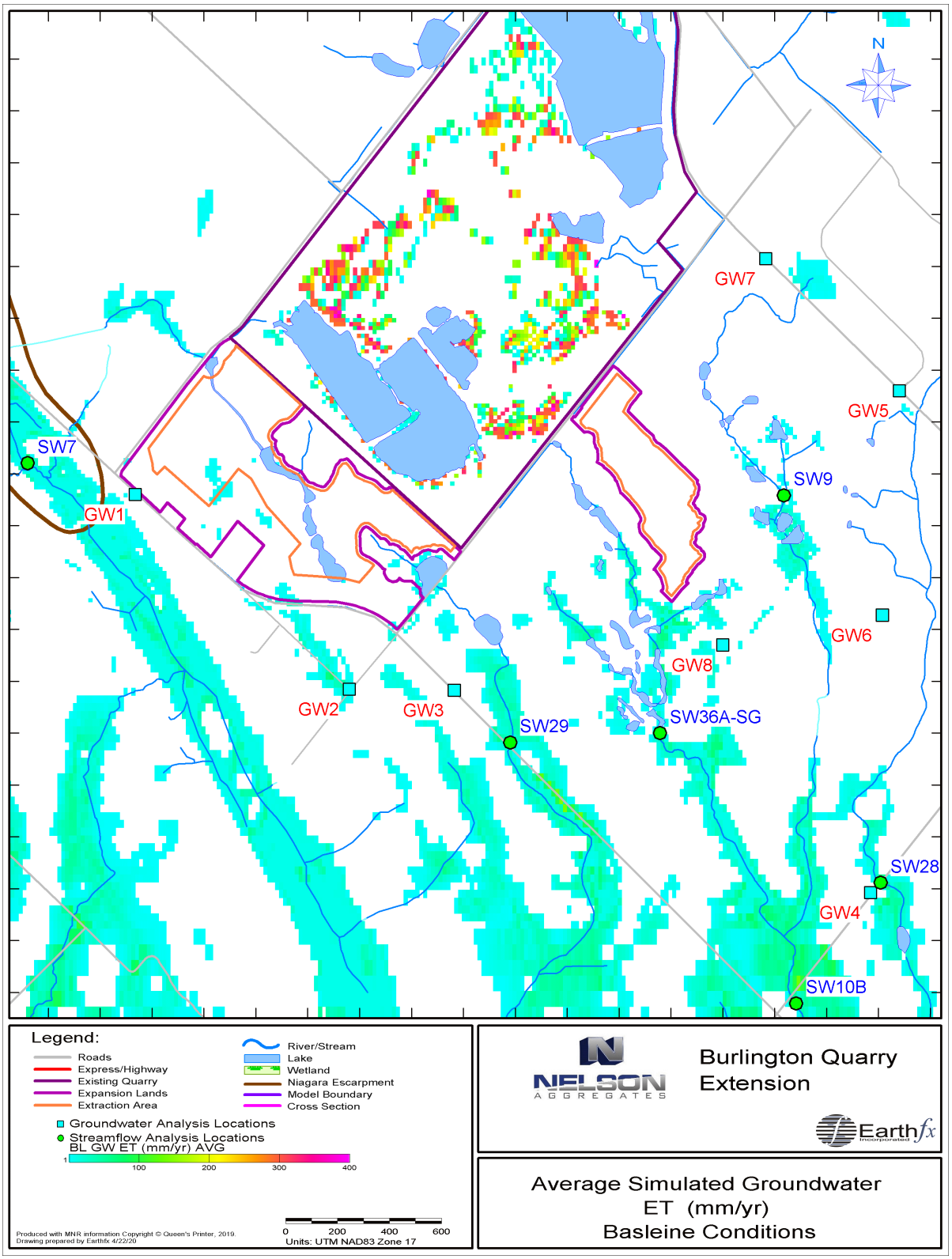

Figure 7.19: Average simulated groundwater ET (mm/yr) under Baseline Conditions.

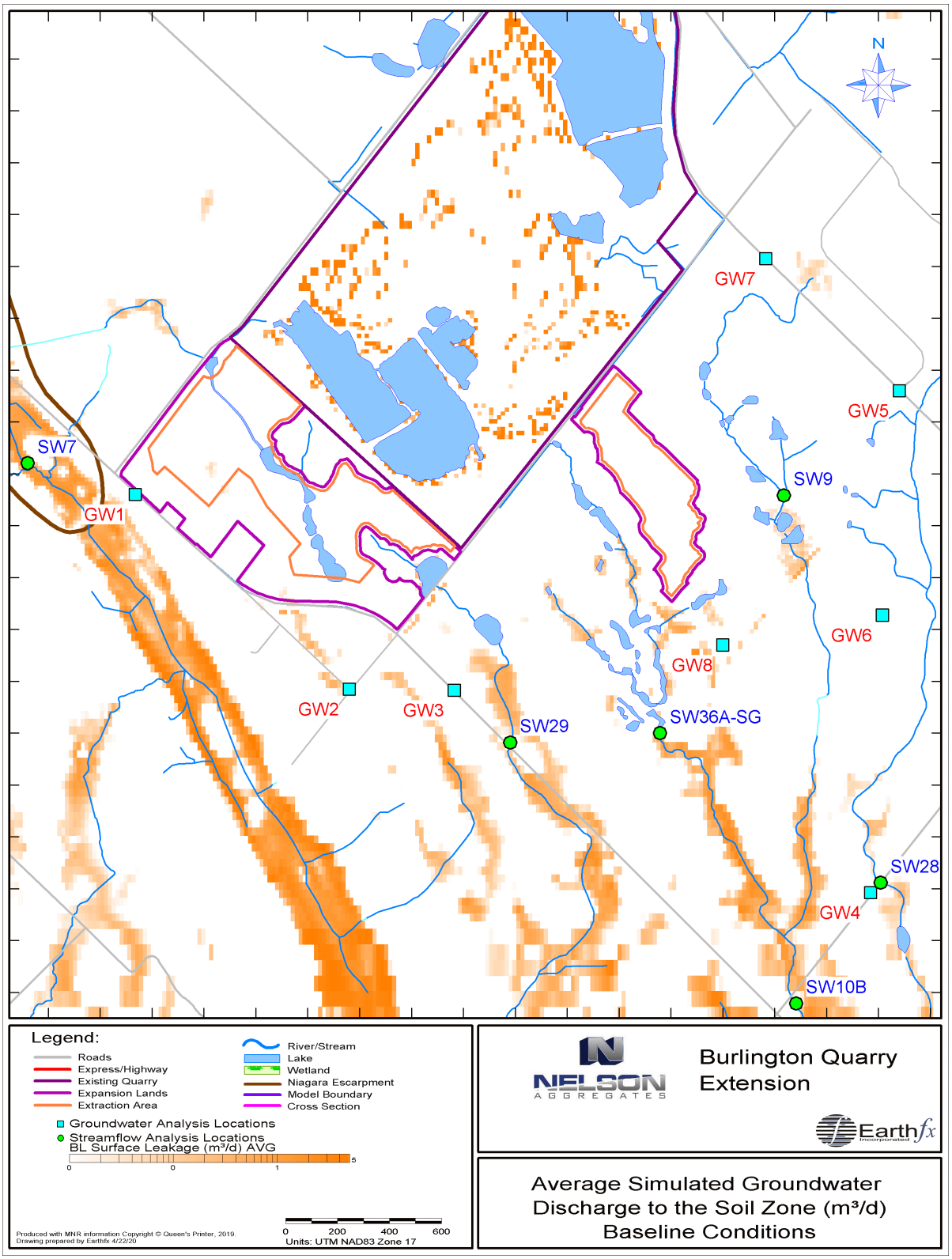

Figure 7.20: Average simulated groundwater discharge to the soil zone (m^3/d) under Baseline Conditions.

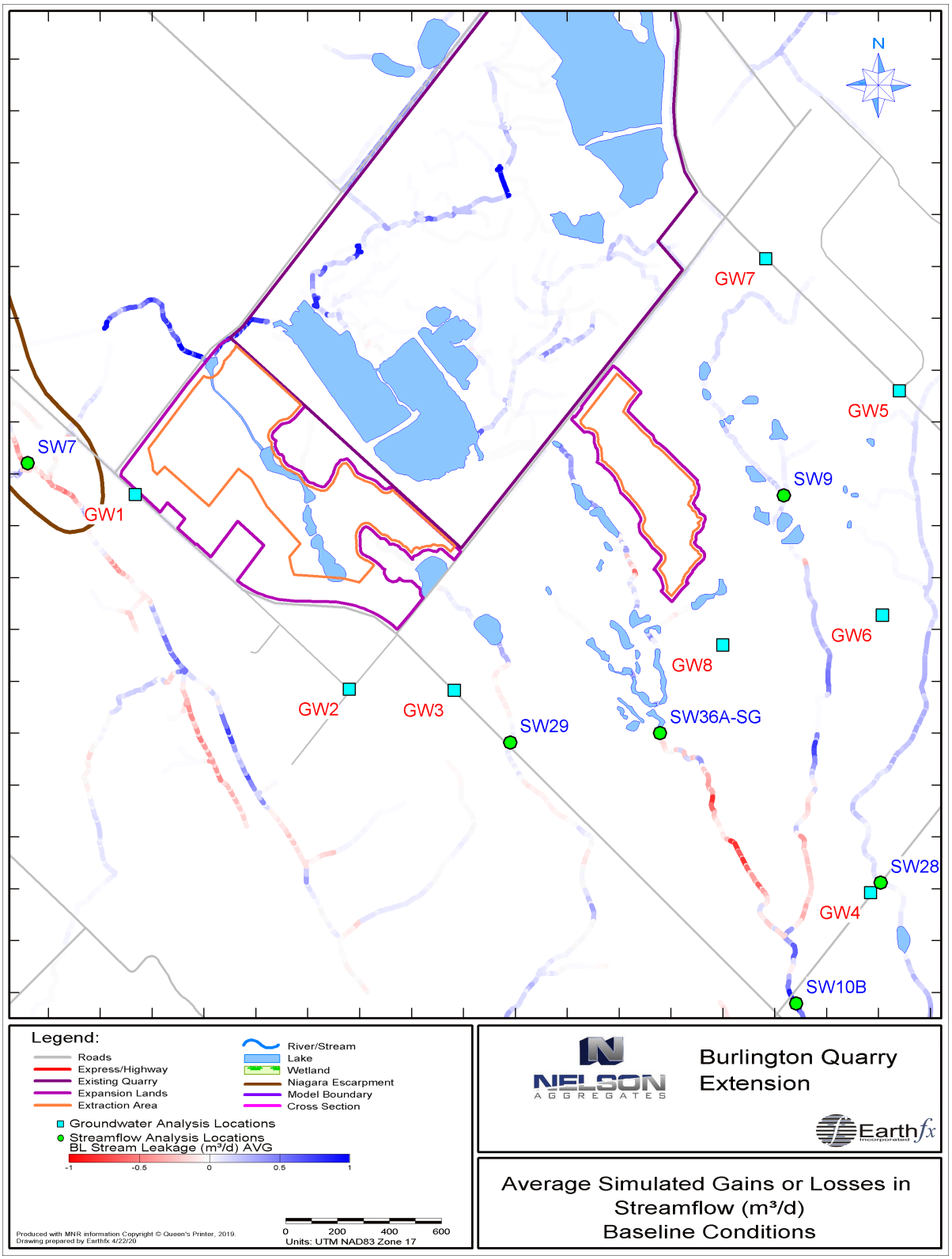

Figure 7.21: Average simulated streamflow loss to groundwater (blue) or groundwater discharge to streams (red) (m^3/d) under Baseline Conditions.

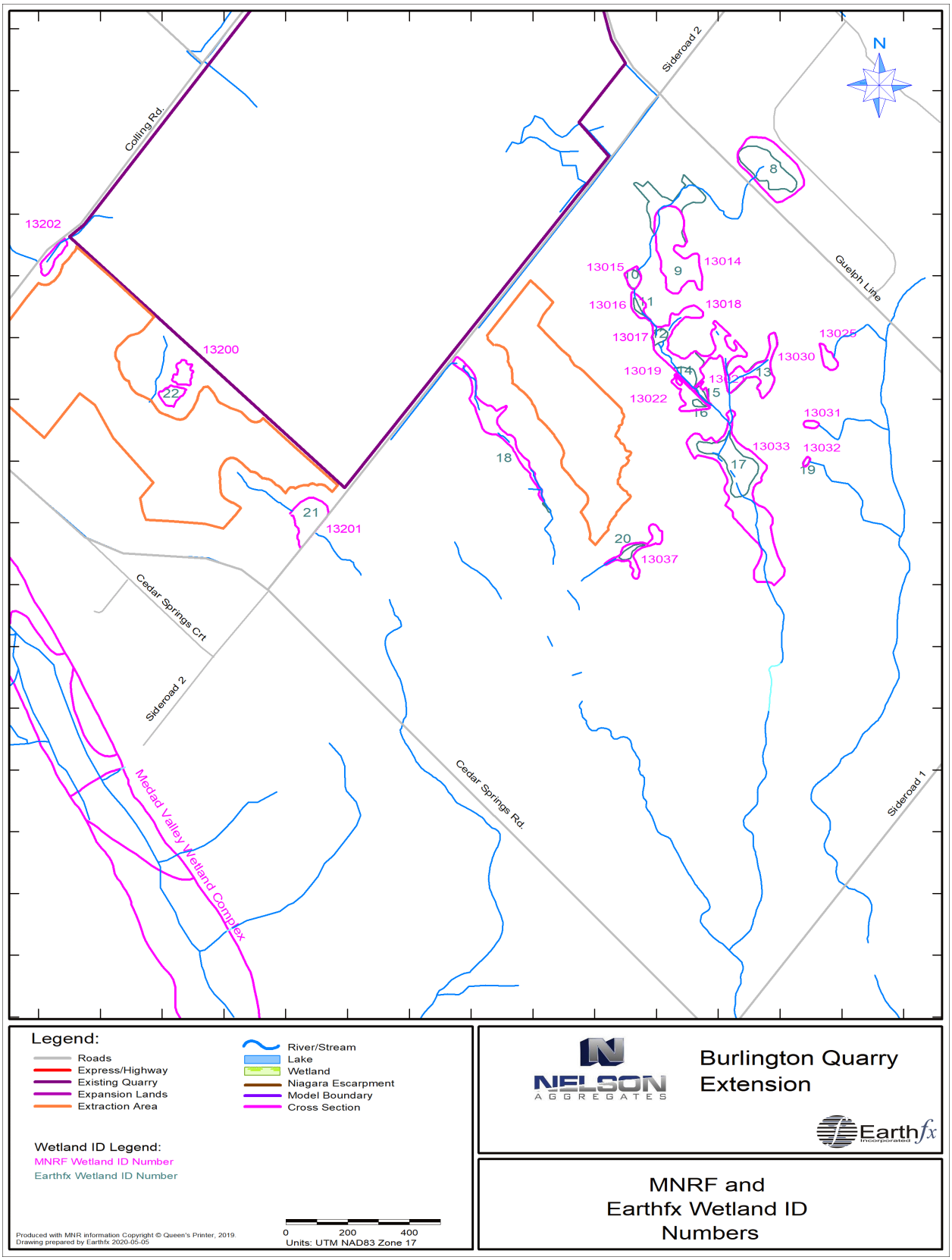

Figure 7.22: Significant wetland features selected for water budget analysis

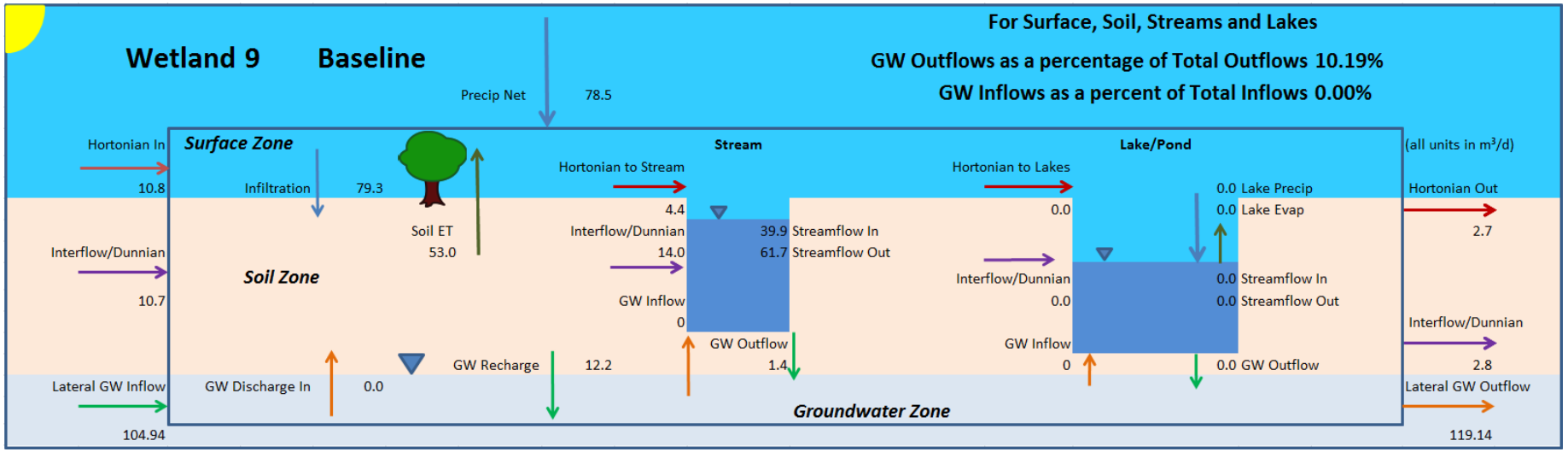

Figure 7.23: Detailed water budget for Wetland 9 averaged over WY2010 to WY2014 under Baseline Conditions.

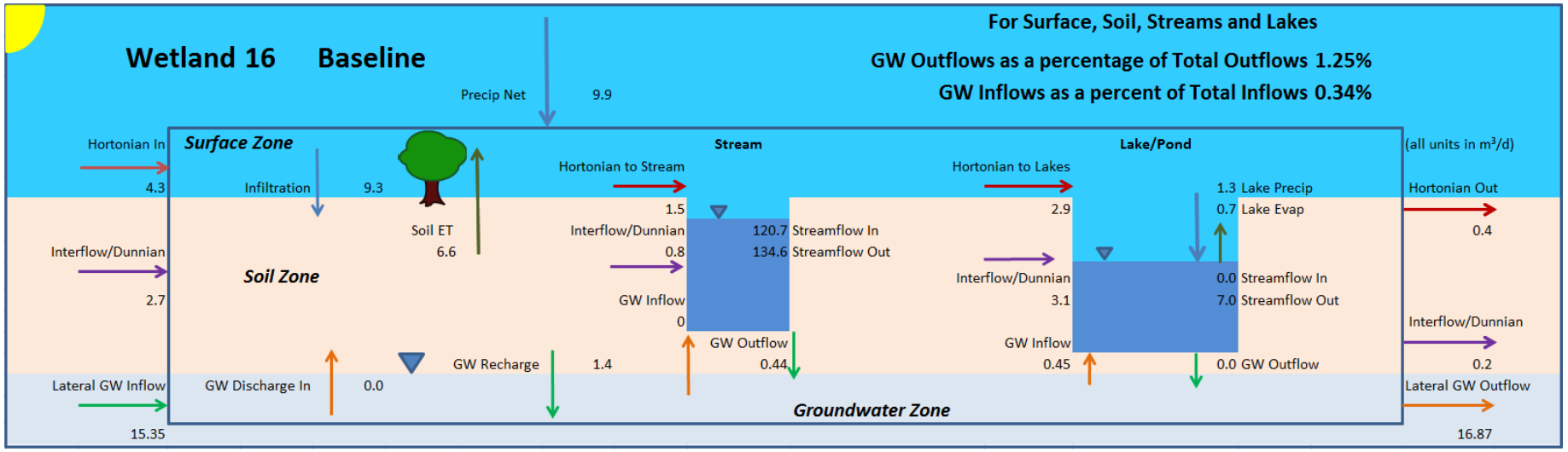

Figure 7.24: Detailed water budget for Wetland 16 averaged over WY2010 to WY2014 under Baseline Conditions.

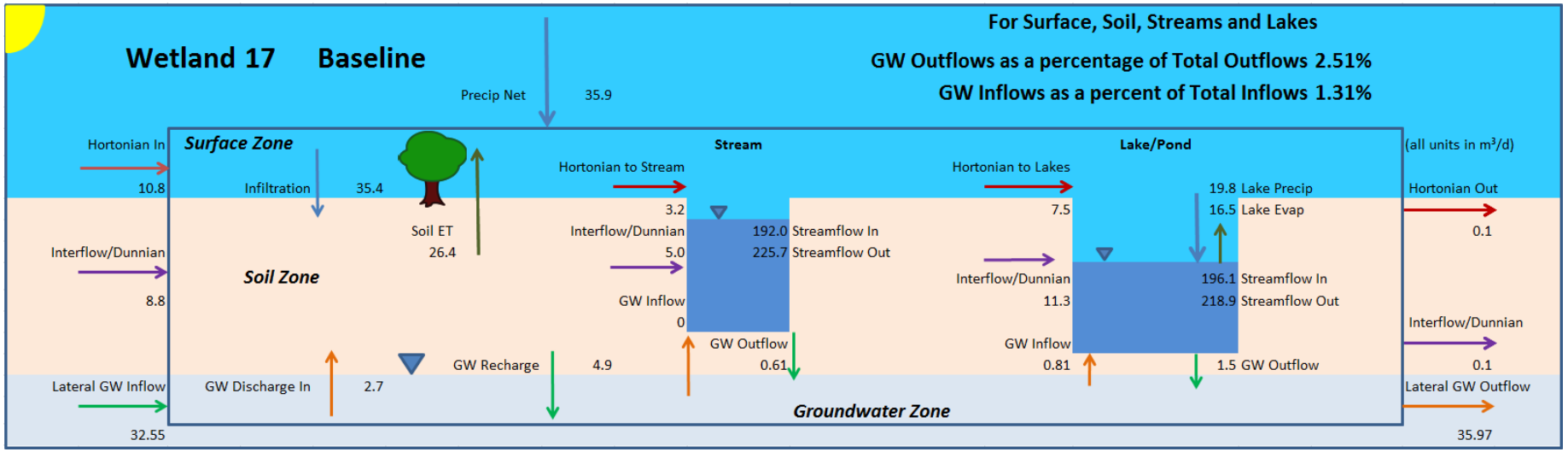

Figure 7.25: Detailed water budget for Wetland 17 averaged over WY2010 to WY2014 under Baseline Conditions.

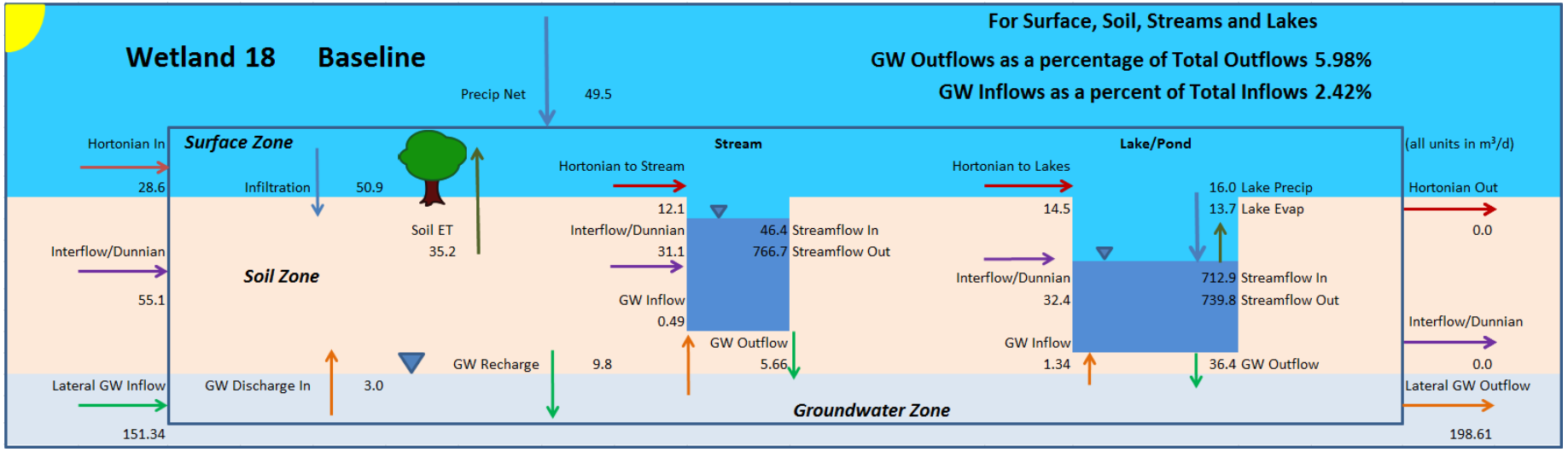

Figure 7.26: Detailed water budget for Wetland 18 averaged over WY2010 to WY2014 under Baseline Conditions.

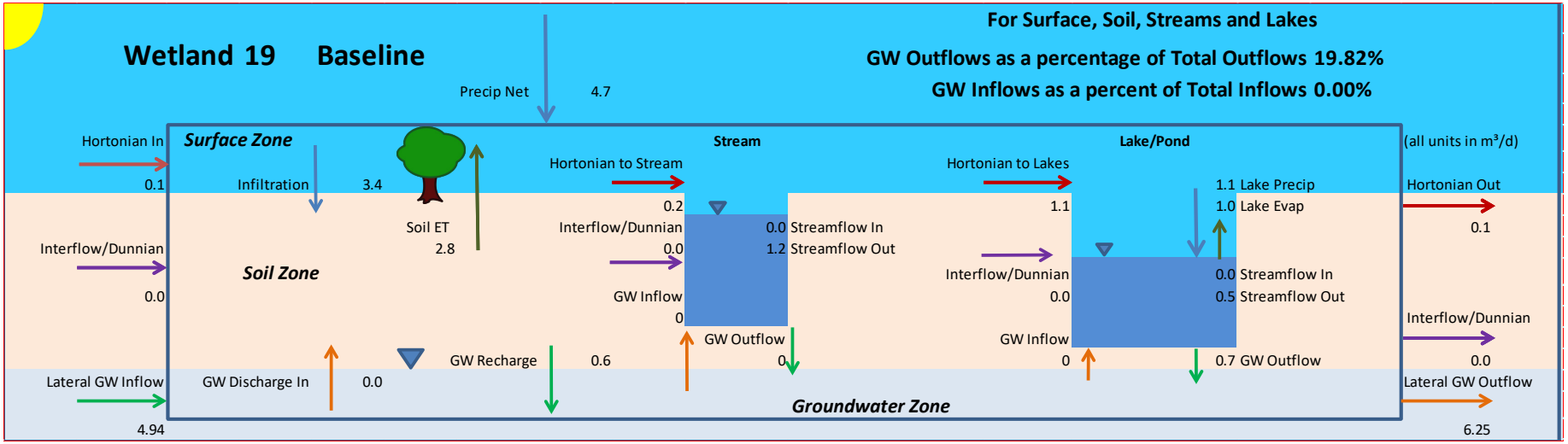

Figure 7.27: Detailed water budget for Wetland 19 averaged over WY2010 to WY2014 under Baseline Conditions.

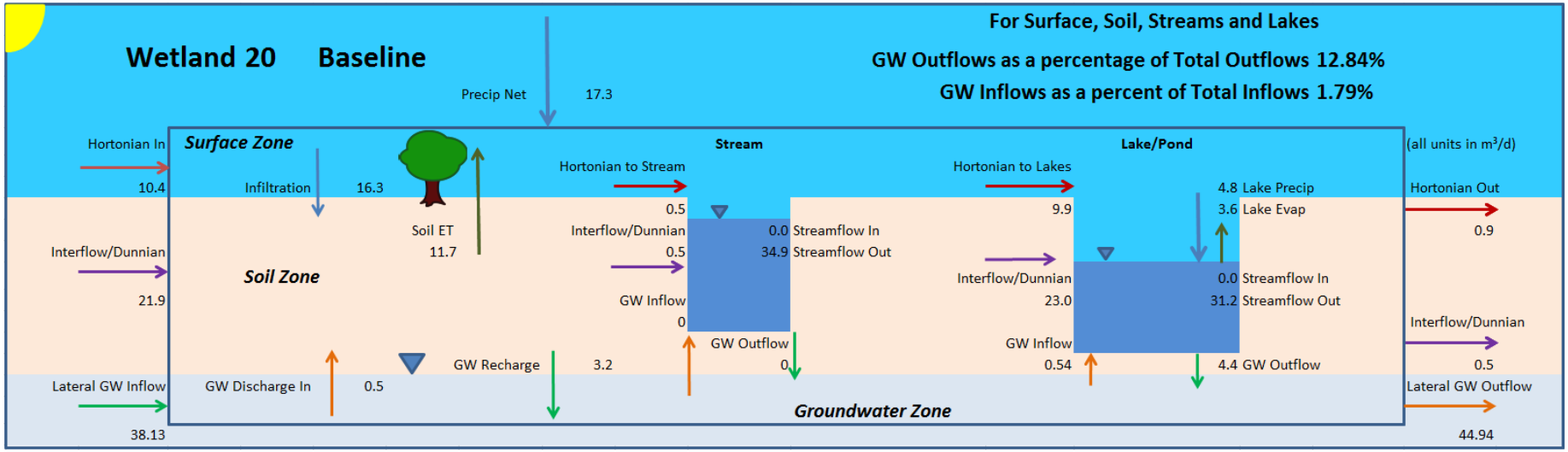

Figure 7.28: Detailed water budget for Wetland 20 averaged over WY2010 to WY2014 under Baseline Conditions.

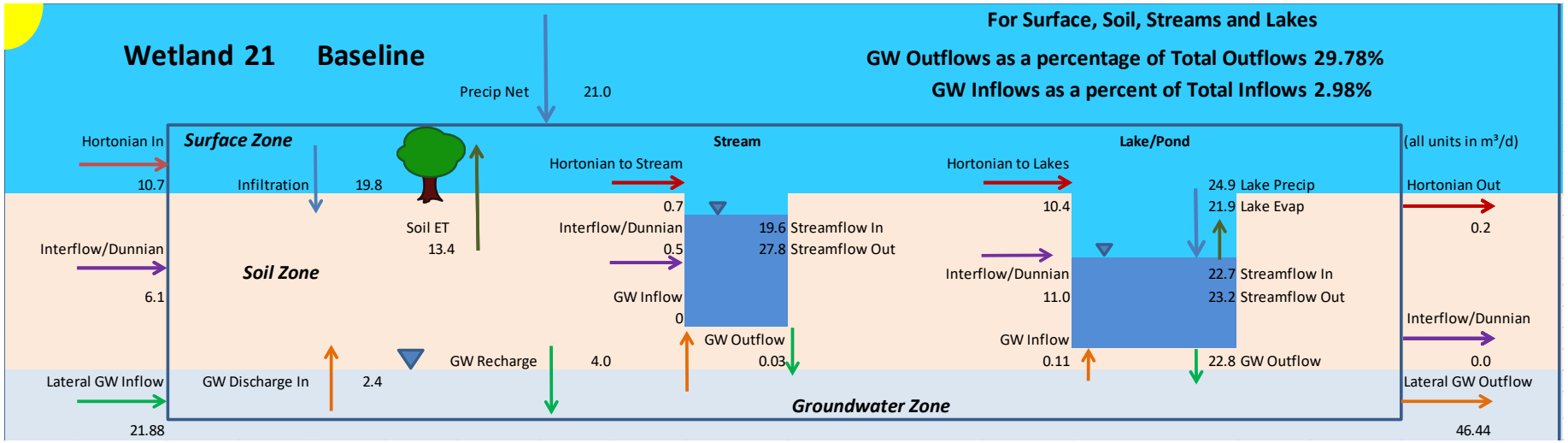

Figure 7.29: Detailed water budget for Wetland 21 averaged over WY2010 to WY2014 under Baseline Conditions.

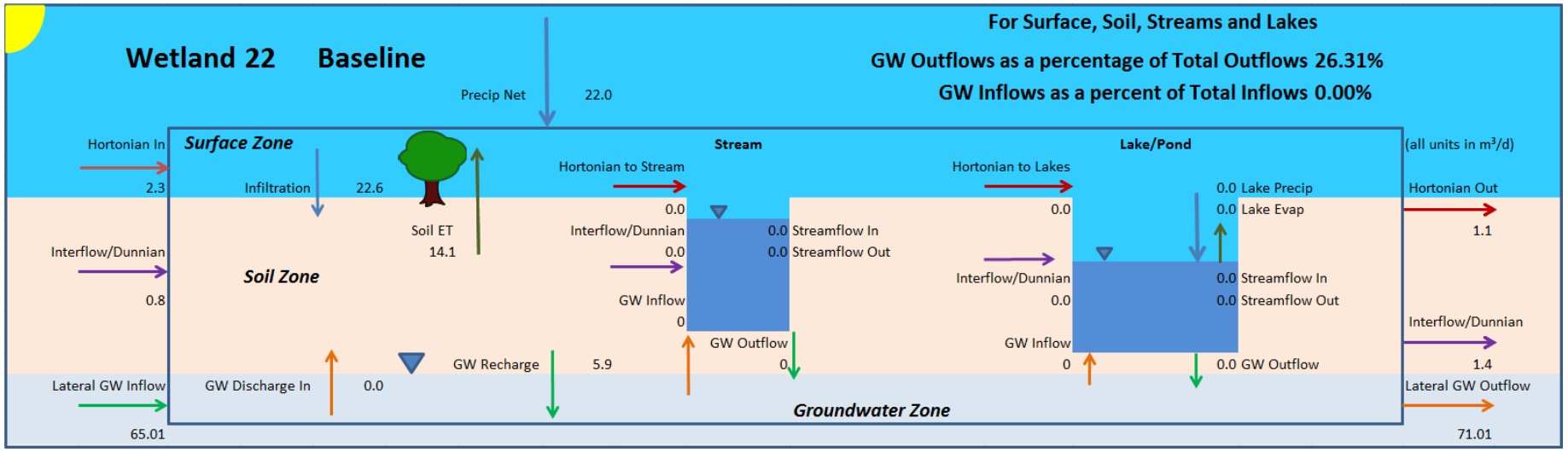

Figure 7.30: Detailed water budget for Wetland 22 averaged over WY2010 to WY2014 under Baseline Conditions.

7.3 Baseline Conclusions

The Baseline Conditions scenario provides a detailed and fully integrated transient numerical simulation of the study area. The average condition maps present only an overview of more than 3600 daily outputs that are available for each model layer and each model parameter. The hydrographs from the assessment locations present a key view of the dynamic and complex surface and groundwater processes. (The reader may also refer to the Model Calibration chapter and Appendices for additional discussions about specific surface water and groundwater features.)

The Baseline surface water analysis demonstrates that, while there are some interactions between the surface and groundwater systems, they are frequently limited by the regionally extensive, and low permeability, Halton Till. None of the wetlands in the immediate vicinity of the quarry receive significant groundwater inflows.

Figure 7.3 presents a useful summary of the existing groundwater supply conditions in the study area. This figure shows that, at any location in the vicinity of the quarry, a private water well could be drilled to the Layer 8 fracture zone and it would have up to 22 m of available drawdown. Near the existing quarry that available drawdown is reduced, but many existing wells are in close proximity to the quarry, and yet have been providing suitable water supply for many years.

8 Level 2 Future Conditions Evaluation

8.1 Proposed Extraction

The site plans prepared by MHBC Planning outline the 6 phases of the proposed extraction. Mining will be conducted with groundwater dewatering as per the current site license. A surface water management strategy has been developed for the proposed quarry extension during and post extraction (Tatham, 2020). The existing drainage patterns within Burlington Quarry will remain as is through extraction in the south and west extensions. The quarry will drain internally to a series of settling ponds constructed in the quarry floor and water will be discharged off-site from Quarry Sump 0100 and 0200 to the two existing discharge locations. The configuration of the existing settling ponds will be altered during different phases of extraction in the west extension as operations require. The configuration will be altered to facilitate extraction in the west expansion lands and to maintain dry operating conditions. However, the off-site discharge will continue as per the conditions of Nelson's PTTW and ECA.

During the south extraction, water will accumulate on the quarry floor in a sump and be discharged to a settling pond constructed at surface within the extraction area. The settling pond will discharge to the West Arm after treating the quarry water at rates set to mimic existing conditions. For the western extraction area, the existing sump (0100) will continue to operate and discharge water to the Collins Road roadside ditch and into the Weir Pond. The existing golf course irrigation ditch and pond will be relocated to an area outside of the extraction area but inside of the license boundary to replicate the artificial groundwater mound they currently create.

As per the Ministry of Natural Resources and Forestry (MNRF) standards, a Level 1 and/or a Level 2 evaluation are needed for an aggregate license application. An overview of the ARA requirements is presented in Section 1, including a summary of the various companion reports and studies that make up this application.

8.2 Level 2 Evaluation Requirements

Table 8.1 summarizes the requirements for a Level 1 and Level 2 assessment, with an overview of the issues particular to this application. Given the local presence of water wells, springs and wetlands, a Level 2 evaluation, as described by MNRF, is needed.

8.3 Level 2 Assessment Overview

The Level 2 Assessment surface and groundwater issues are fully addressed by the integrated model. To facilitate the impact assessment, a number of groundwater and surface water assessment or evaluation points have been selected around the development area. These points, introduced in the preceding baseline analysis chapter, are shown in Figure 7.1.

The Baseline Conditions assessment indicates that, from a hydrogeological perspective, the proposed West and South development are located in areas favorable to extraction, but for different reasons. The South Extension is located in an area with thick aquifer layers, extensive available drawdown, and the presence of a deep fracture zone that provides a regionally significant aquifer resource. The distance of the excavation from Cedar Springs Road and Guelph Line further minimizes the effects on private groundwater wells located along those roads.

The West Extension area is also in a hydrologically favorable location. The Medad Valley is a locally significant groundwater discharge area, and as such it is less susceptible to seasonal and inter-annual water level fluctuations. For example, a comparison of Baseline Layer 8 water level fluctuations at Location GW1 (near the Medad Valley, as shown in Figure 7.1) versus those at location GW7 (east of the existing quarry) illustrates that there is nearly 2 m more water level decline in the 2015-2016 drought at GW7 than at GW1 (Figure 8.1). This demonstrates that the Medad is less drought sensitive. (Note that while Location GW7 is more drought sensitive, it does fortunately have over 12 m of available drawdown.)

These, and many more, aspects of the groundwater and surface water impact assessment are discussed below.

Table 8.1: Evaluation of need for Level 2 Hydrogeological Assessment

Category	Level 1 Assessment	Level 2 Assessment Needed?
Water Wells	Water wells located within 120 metres of the Site obtain water from sand and gravel aquifer.	Level 2 Assessment for water wells required.
Springs	Springs located downgradient of Site in in the Medad Valley, and headwater streams located in and around the Mt. Nemo escarpment area.	Level 2 assessment needed to assess potential impact on springs.
Groundwater Aquifers	Extraction will occur in the local Amabel Bedrock aquifer.	Level 2 assessment required to assess the potential reduction in water levels in the wells. Limited potential for water quality effects as groundwater dewatering will maintain flow directions into the quarry.
Discharge to Surface Water	The Site will be operating in geological materials that are contiguous with off-site surface water features.	Level 2 assessment required to evaluate the impact of changes to ponds.
Water Diversion, Storage and Drainage Facilities On-Site	Water diverted into excavations	A Level 2 assessment is required to address alterations to water diversion, storage and drainage facilities. Assessment of site water management completed under separate cover by Tatham Engineering (Tatham, 2020), with input from the integrated model results documented in this report.
Water Balance	There will be an increase in evaporation from the Site.	Level 2 assessment is needed to evaluate changes in the water balance. Assessment of site water balance completed under separate cover by Tatham Engineering, with inputs from the integrated model results document in this report.

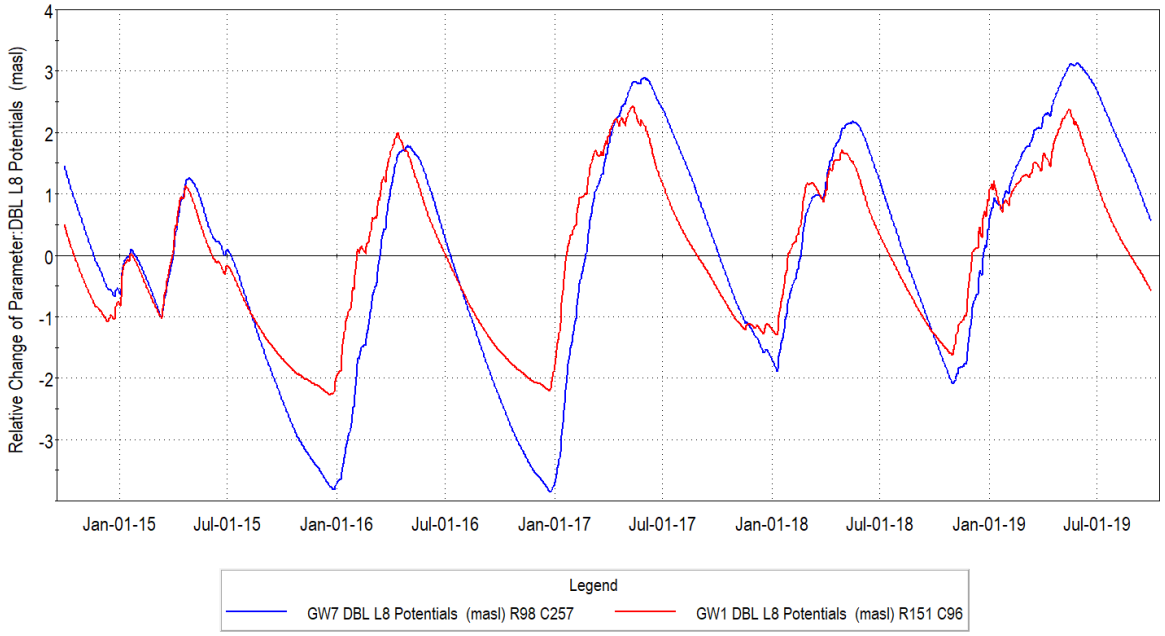

Figure 8.1: Comparison of water level fluctuations at Location GW1 (near the Medad) versus GW7 indicates that the Medad location is no drought sensitive.

8.4 Model Evaluation of Extraction Phases

The baseline GSFLOW scenario was modified to create five additional scenarios representing the proposed extraction and rehab conditions. The future scenarios were simulated through the same ten-year time period (WY2010 – WY2019) as the baseline scenario, with identical precipitation, temperature and solar radiation inputs, to facilitate direct comparative analysis of streamflow, groundwater levels, and other water budget components on a daily basis.

The proposed extension of the Burlington Quarry is to occur in six phases of extraction, as shown in Figure 8.2. The details and timing of the extraction, along with the proposed quarry rehabilitation plans have been submitted under separate cover. The model was revised, as outlined in Table 8.2, to incorporate the specifics of the extraction and rehabilitation plans for scenario.

8.4.1 Scenario Summary

As noted in the last chapter, the long model run times required, in some cases, that the scenario be completed as two simulations spanning the 10-year assessment time period. Some scenarios were complete as long simulations, or, in other cases, as shorter scenarios if the assessment results could be fully determined from a shorter model run. A complete list of the baseline and development scenarios is included in Table 8.3 (reproduced from Table 7.1).

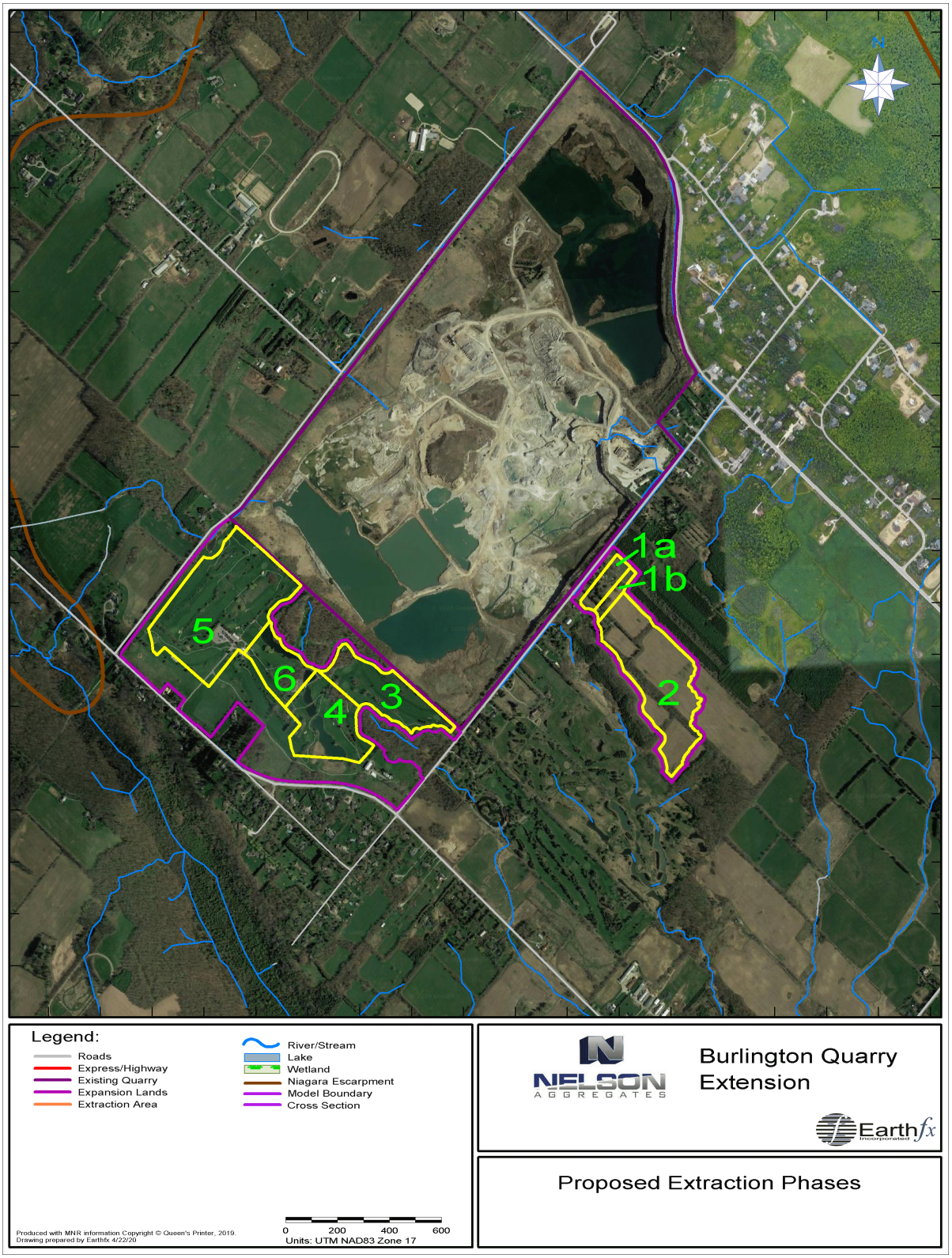

Figure 8.2: Proposed extraction phases.

Table 8.2: Summary of changes relative to Baseline Conditions for each future scenario

Scenario Name	Changes to MODFLOW submodel	Changes to PRMS submodel
P12	• Layer 1 top lowered to 270.5 masl in Phase 1a, 269.5 masl in Phase 1b, and 252.5 masl in Phase 2.	• Land use and surficial soil classes adjusted in P12
	• Layer elevations adjusted in P12 as required.	• Lookup parameters reset based on new land use and soil classes
	• Layer properties adjusted in P12 as required.	• Topography, slope and aspect adjusted in P12
	• Quarry floor drains and conduit stream types added to SFR2 module	• Cascade network regenerated for new topography and quarry floor drains.
P34	• Layer 1 top adjusted to 272.5 masl in P12	• Land use and surficial soil classes adjusted in in P12 and P34
	• P12 area defined as lake and added to LAK3 module	• Lookup parameters reset based on new land use and soil classes
	• Layer 1 top lowered to 252.5 masl in P34.	• Topography, slope and aspect adjusted in P12 and P34
	• Layer elevations adjusted in P12 and P34 as required	• Cascade network regenerated for new topography, lake, and quarry drainage stream segments.
	• Layer properties adjusted in P12 and P34 as required	
	• Partial removal of Burlington Springs GC ponds from LAK3 module	
	• Quarry floor drains and conduit stream types added to SFR2 module for P34.	
	• Infiltration pond added to LAK3 module between P3456 and Cedar Springs Road. Diversion added to SFR2	
P3456	• Layer 1 top adjusted to 272.5 masl in P12	• Land use and surficial soil classes adjusted in P12 and P3456
	• Phase 12 area defined as lake and added to LAK3 module	• Lookup parameters reset based on new land use and soil classes
	• Layer 1 top lowered to 252.5 masl in P3456	• Topography, slope and aspect adjusted in P12 and P3456
	• Layer elevations adjusted in P12 and P3456 as required	• Cascade network regenerated for new topography, lake, and quarry drainage stream segments
	• Layer properties adjusted in P12 and P3456 as required	
	• Full removal of Burlington Springs GC ponds from LAK3 module	
	• Quarry floor drains and conduit stream types added to SFR2 module for P3456.	
	• Infiltration pond added to LAK3 module between P3456 and Cedar Springs Road. Diversion added to SFR2	
RHB1	• Layer 1 top adjusted to 272.5 masl in P12	• Land use and surficial soil classes adjusted in P12 and P3456
	• P12 lake added to LAK module	• Lookup parameters reset based on new land use and soil classes
	• Layer 1 top assigned as per the backfill specifications in the closure plan in P3456	• Topography, slope and aspect adjusted in P12 and P3456
	• Lakes modified in P3456 and existing quarry as per closure plan	• Cascade network regenerated for new topography, lake, and quarry drainage stream segments
	• Stream segment added to SFR2 between P5 lake and P4 pond.	
	• Infiltration pond added to LAK3 module between P3456 and Cedar Springs Road. Diversion added to SFR2	
RHB2	• Layer 1 top adjusted to 272.5 masl in P12	• Land use and surficial soil classes adjusted in P12 and P3456
	• P12 lake added to LAK3 module	• Lookup parameters reset based on new land use and soil classes
	• A lake was defined within the existing and proposed western extension for every model cell below 272 masl.	• Topography, slope and aspect adjusted in P12 and P3456
	• New lake bathymetry was set equivalent to the topography of Scenario R1.	• Cascade network regenerated for new topography, lake, and quarry drainage stream segments
	• Infiltration pond left in place but no diversion in SFR2	

As previously noted, model simulation results include a “Prefix” abbreviation describing the scenario. For example, the Phase 1 and 2 simulated potentiometric head results for Layer 4 are referred to as “P12 L4 Potentials (masl)”. The scenario name and abbreviations are listed in Table 8.3, and, for ease of review, the mapping of hydrostratigraphic units to model layers is again summarized in Table 8.4.

Table 8.3: Scenario Summary

Scenario	Prefix	Period	Start Date	End Date	Years	Comment
Baseline	BL	Start	WY2010	WY2014	5	Golder calibration period
	DBL	Drought	WY2015	WY2019	5	Validation and drought
Phase 1/2	P12	Start	WY2010	WY2011	2	
	D12	Drought	WY2015	WY2019	5	Drought assessment
Phase 3/4	P34	Start/Drought	WY2010	WY2016	7	P34 and P12 Recovery
Phase 3456	P3456	Start/Drought	WY2009	Mid-WY2019	9.6	Full P3456 Build and P12 recovery
Rehabilitation Plan 1	RHB1	Start	WY2010	WY2011	3	Conversion to Park
Rehabilitation Plan 2	RHB2	Start	Mid-WY2010	Mid-WY2015	5	One Quarry Lake

Table 8.4: Numerical model layers and corresponding hydrostratigraphic layers

Model Layer	Hydrostratigraphic Unit	
	Above Escarpment	Below Escarpment
1	Surficial Deposits and Wetlands	Surficial Deposits and Wetlands
2	Halton Till	Halton Till
3	MIS Sands	ORAC Sands
4	Weathered Bedrock	Weathered Queenston
5	Upper Bulk Amabel	Weathered Queenston
6	Middle Amabel Fracture Zone	Weathered Queenston
7	Lower Bulk Amabel	Weathered Queenston
8	Lower Fracture Zone	Weathered Queenston
9	Lower Aquitards	Lower Aquitards

8.5 Scenario P12

Scenario P12 represents the extraction of aggregate from the Phases 1a, 1b, and 2 areas. For the purposes of this comparative analysis, it is assumed that the Phase 1a, 1b, and 2 extraction is at its maximum depth and dewatering is ongoing. The final elevation of the quarry floor is 252.5 masl in the Phase 2 footprint. Figure 8.3 shows the modified topography in the quarry vicinity in the P12 scenario.

Land use and soil class were modified in the extraction footprint (changing from a variety of classes to “Quarry”) and all the soil and land use based PRMS model parameter values were updated. Topography, slope, and aspect were also adjusted. Quarry floor drains and conduit stream types were added to the SFR2 module to convey quarry discharge from Phase 1 and 2 into the West Branch of Mount Nemo Creek. A new cascade network was created to account for the new stream network and topography.

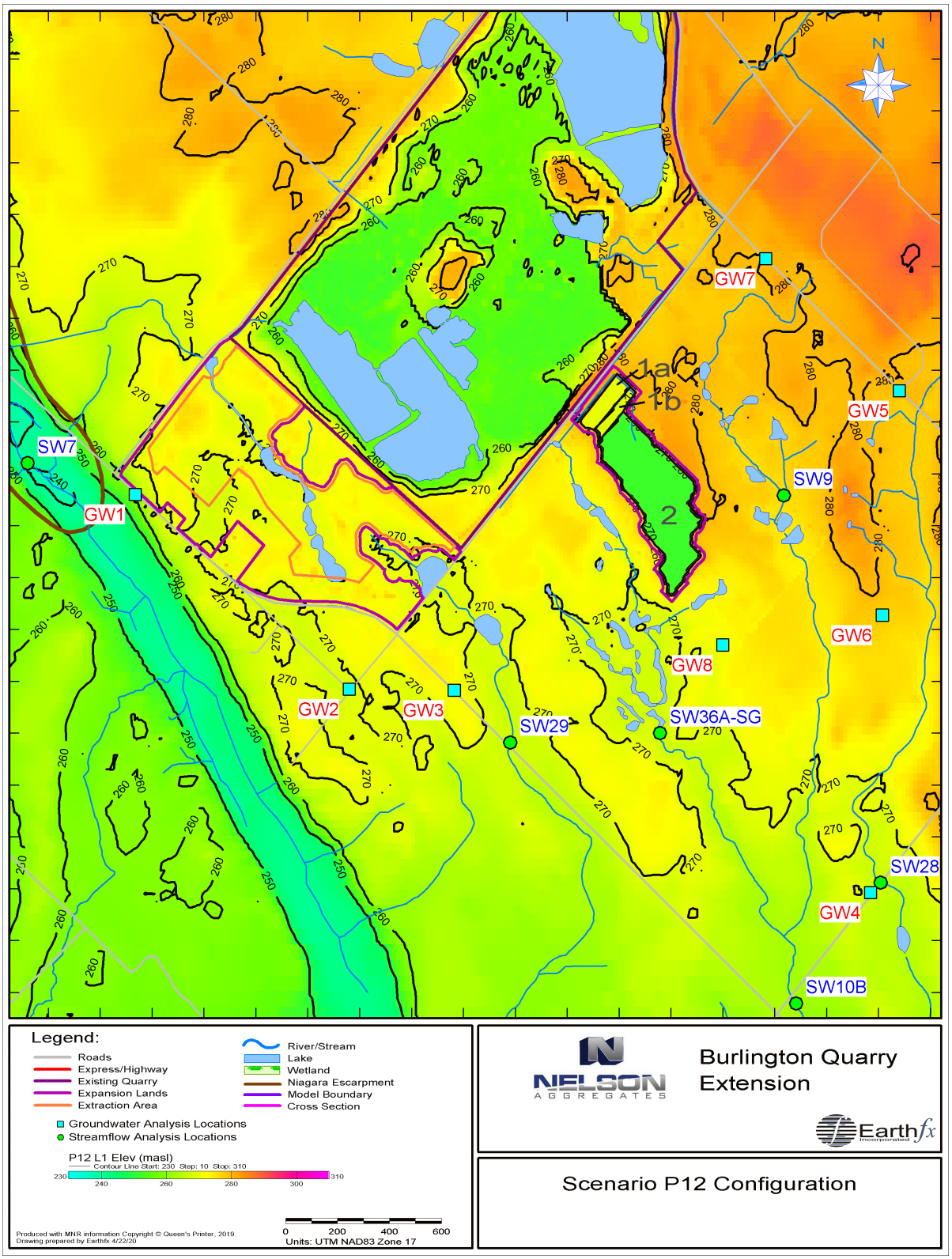

Figure 8.3: Scenario P12 configuration.

The GSFLOW model was run with the modified inputs for Scenario P12 and model results were post-processed and compared to Baseline Conditions. The discussions below focus on the WY2014-2019 period because the two dry years in that period showed the most significant change in heads, streamflow, and water budget components.

The effect of the changes can be relatively small when comparing streamflow and heads away from the extraction footprint. To highlight changes, additional maps showing average drawdowns (i.e., changes in simulated heads) and average changes in stream flow and leakage are presented along with hydrographs showing changes in daily flows and groundwater levels.

8.5.1 P12 Drawdowns and Surface Water Flows

Figure 8.4 shows the average simulated heads in Model Layer 6, the middle Amabel fracture zone, along with average simulated streamflow for the same period. Figure 8.5 shows the average simulated drawdown in Model Layer 6 between baseline and P12 extraction. The simulated drawdowns decrease sharply with distance from the excavation, and fall to below 2.0 m at a distance of approximately 850 m from the excavation. The location of P12, centrally located between Guelph Line and Cedar Springs Road, is optimally located to minimize the effects on the private wells along those roads. The maximum drawdown near those two roads is less than 2 m, which is within the range of natural variability.

Figure 8.5 also shows the average simulated change in streamflow. There is a modest change in quarry discharge flow patterns because the south extension directly intercepts some of the inflow that previously leaked more broadly in from the south face. Drawdowns on the southwest side of the South Extension are attenuated by leakage from the nearby discharge stream. Other streams show small decreases in average flow compared to Baseline Conditions.

Figure 8.6 through Figure 8.11 shows hydrographs comparing simulated daily streamflow under Scenario P12 to Baseline Conditions, in m^3/s, for the six streamflow analysis points (locations shown in Figure 8.3). Change in streamflow is shown inverted on the secondary (right) y-axis. Flows at SW36A and SW10B show net increases, due to quarry discharge. The other stations show very small decreases in baseflow and small losses during storm or snowmelt events. SW07 (Figure 8.11) in the Medad valley (Figure 8.3) shows that there will be a virtually unmeasurable change in flow during the spring, related to small changes in relative discharge between the north and south sump.

In summary, P12 has a very minor impact on the local streams. The discharge through the stream to the west of the P12 maintains surface water conditions in a manner consistent with current discharge patterns. The small stream to the east of P12 is mostly perched through the wetland chain, so lowering the water table has no impact on the streamflow passes by the excavation.

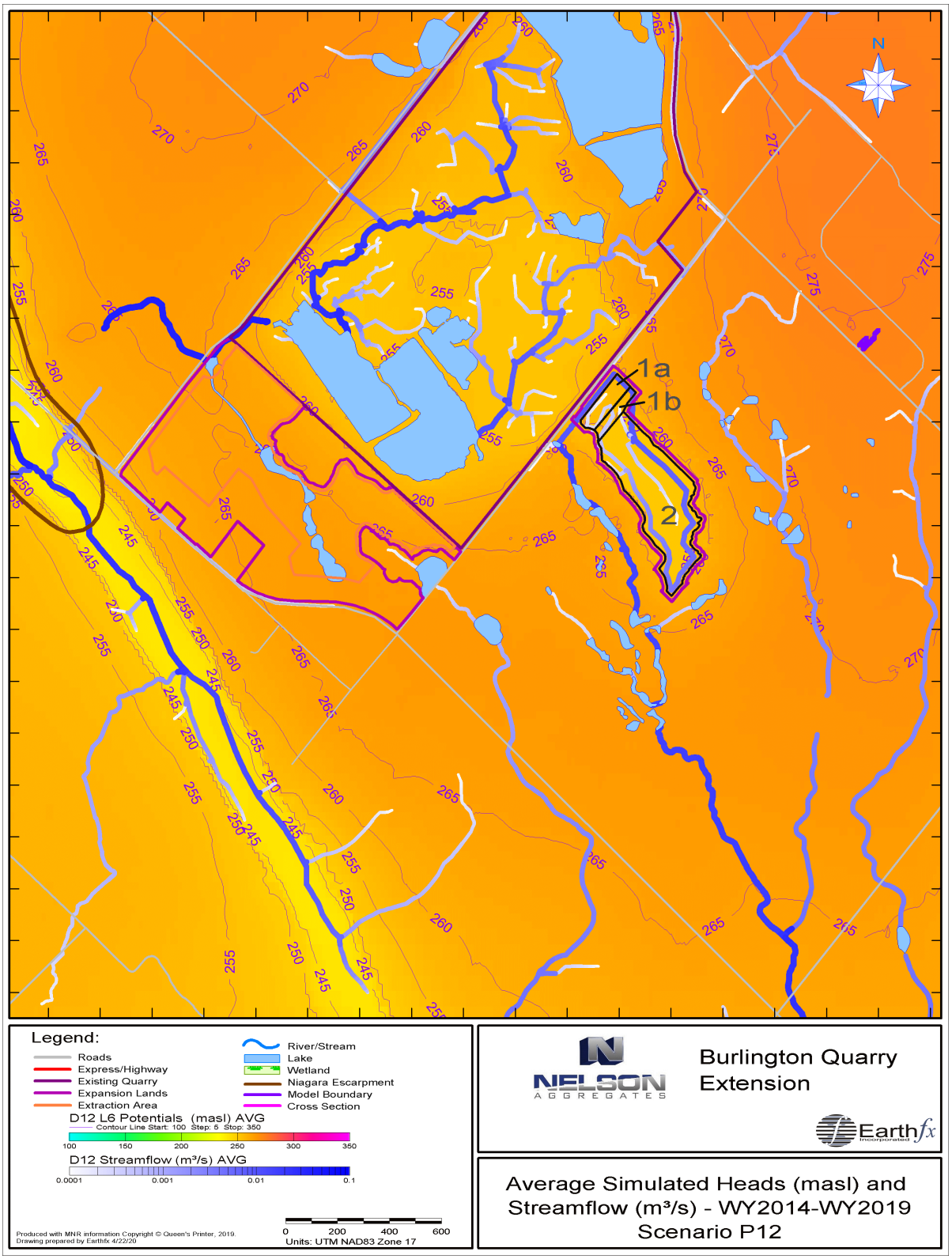

Figure 8.4: Average simulated heads in Model Layer 6 (masl) and streamflow (m^3/s) for WY2014 to WY2019 under Scenario P12.

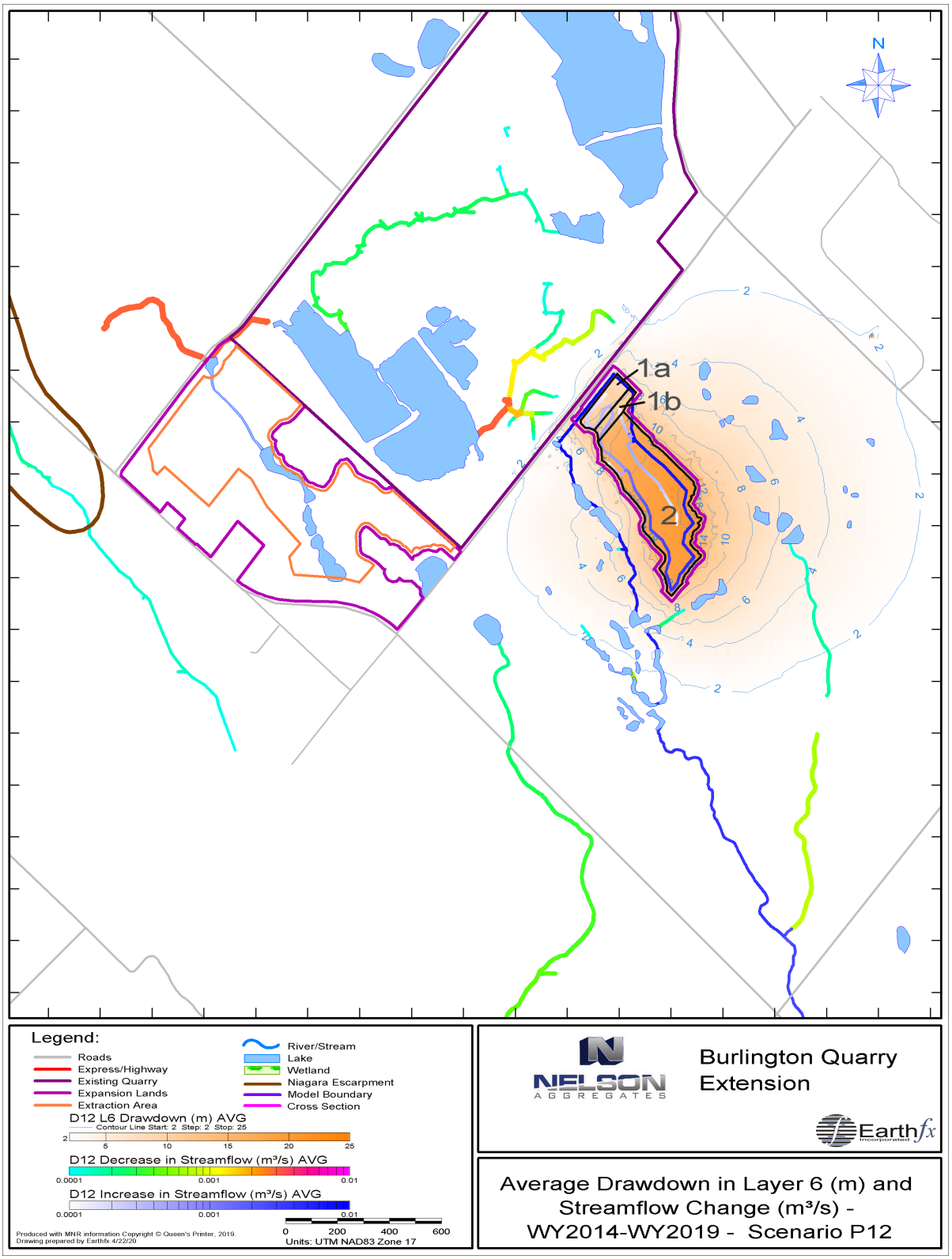

Figure 8.5: Average simulated drawdown in Model Layer 6 (m) and increase/decrease in streamflow (m^3/s) for WY2014 to WY2019 under Scenario P12.

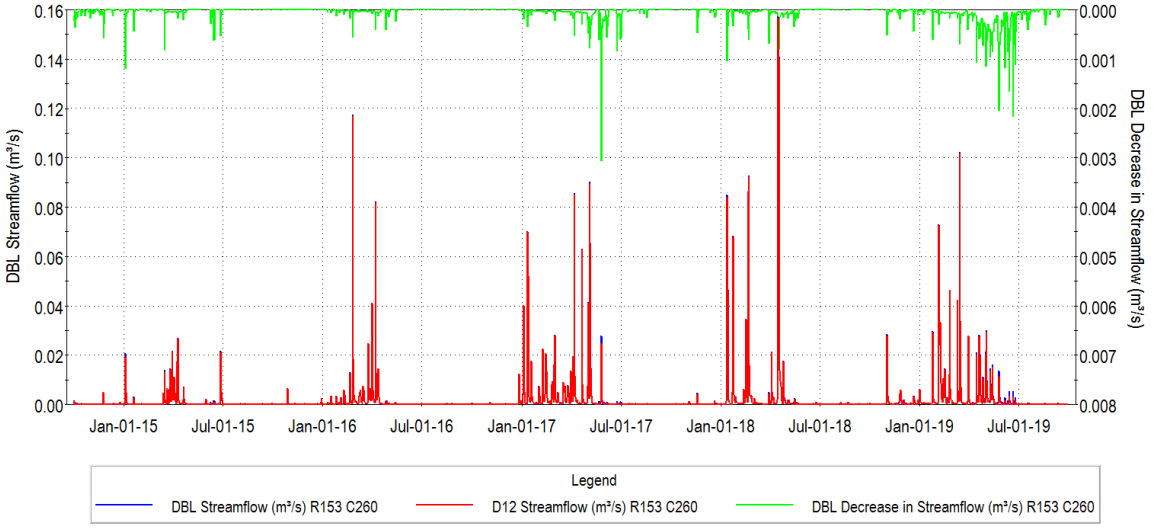

Figure 8.6: Simulated streamflow at SW09 for WY2014 to WY2019 – P12 and Baseline Conditions.

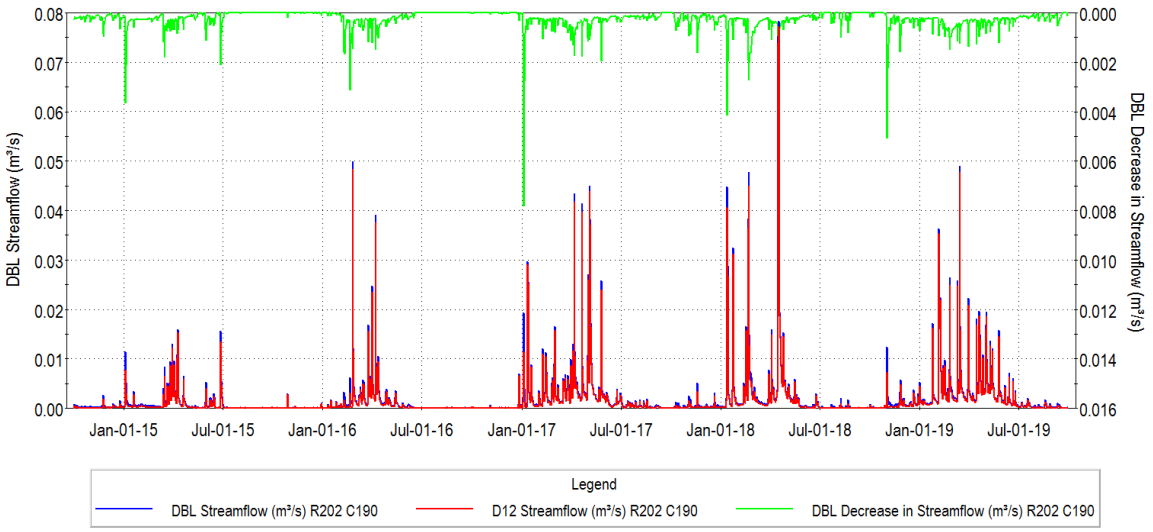

Figure 8.7: Simulated streamflow at SW29 for WY2014 to WY2019 – P12 and Baseline Conditions.

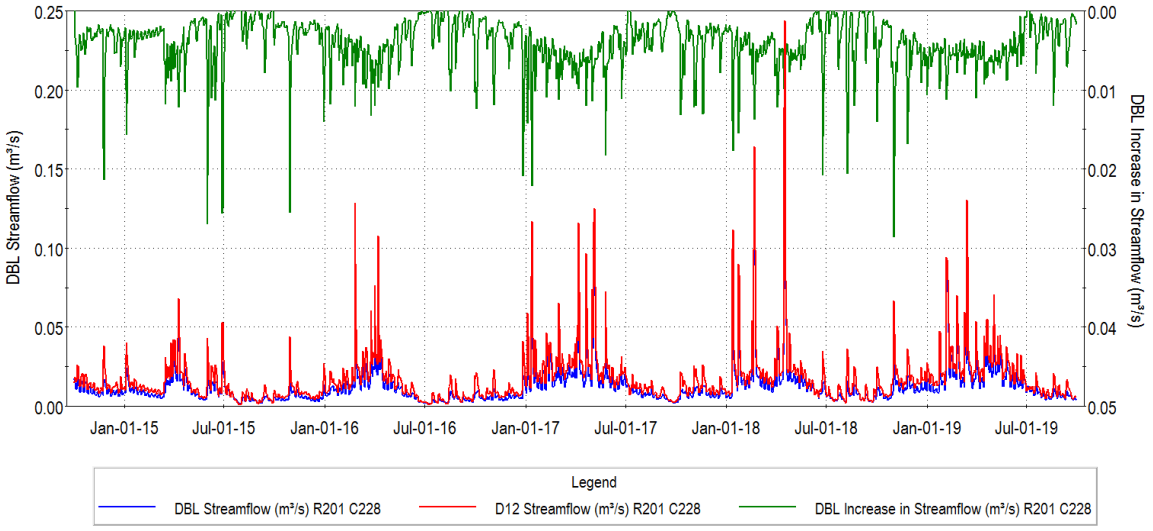

Figure 8.8: Simulated streamflow at SW36A for WY2014 to WY2019 – P12 and Baseline Conditions.

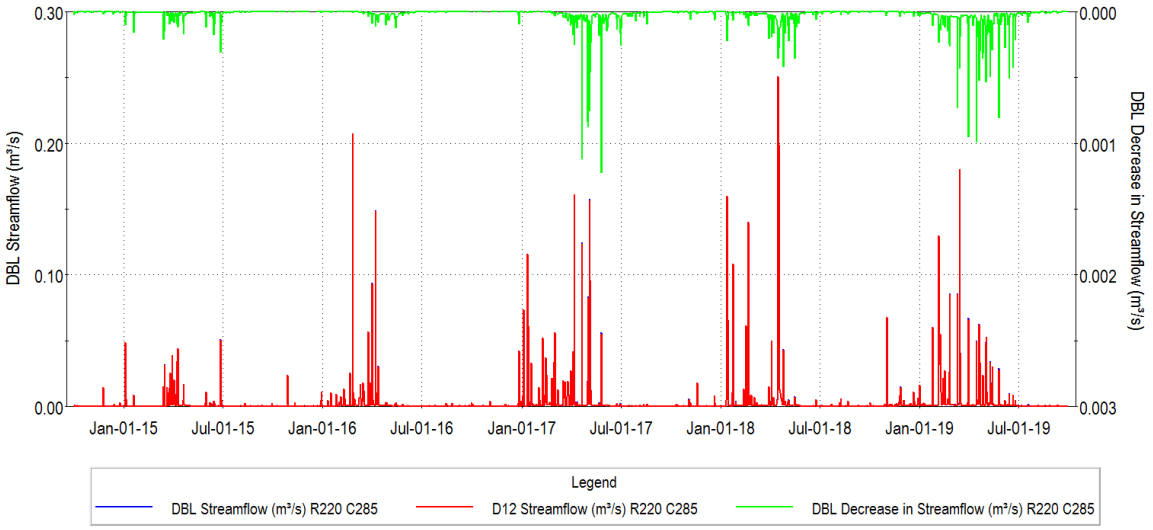

Figure 8.9: Simulated streamflow at SW28 for WY2014 to WY2019 – P12 and Baseline Conditions.

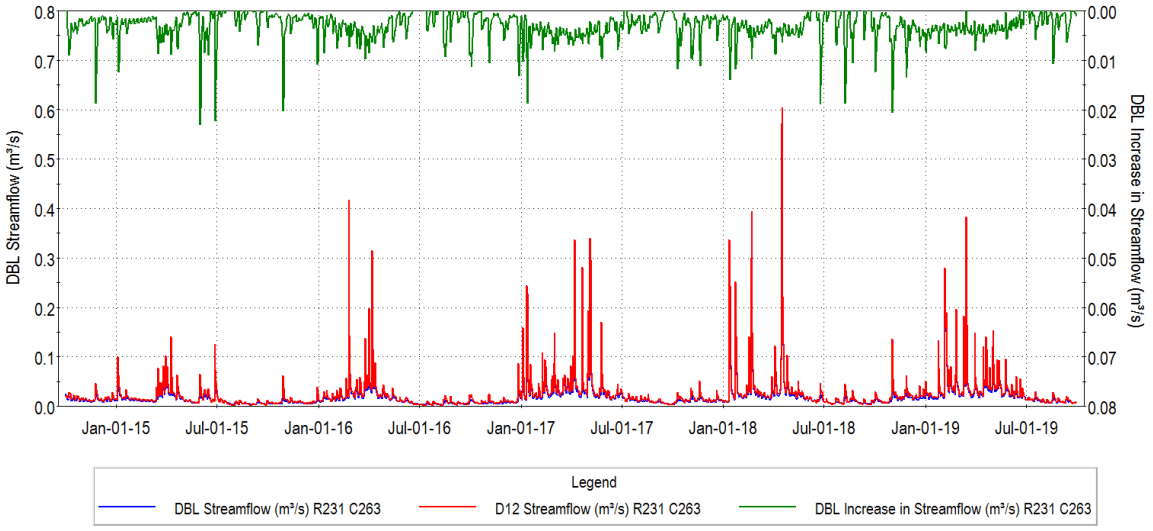

Figure 8.10: Simulated streamflow at SW10B for WY2014 to WY2019 – P12 and Baseline Conditions.

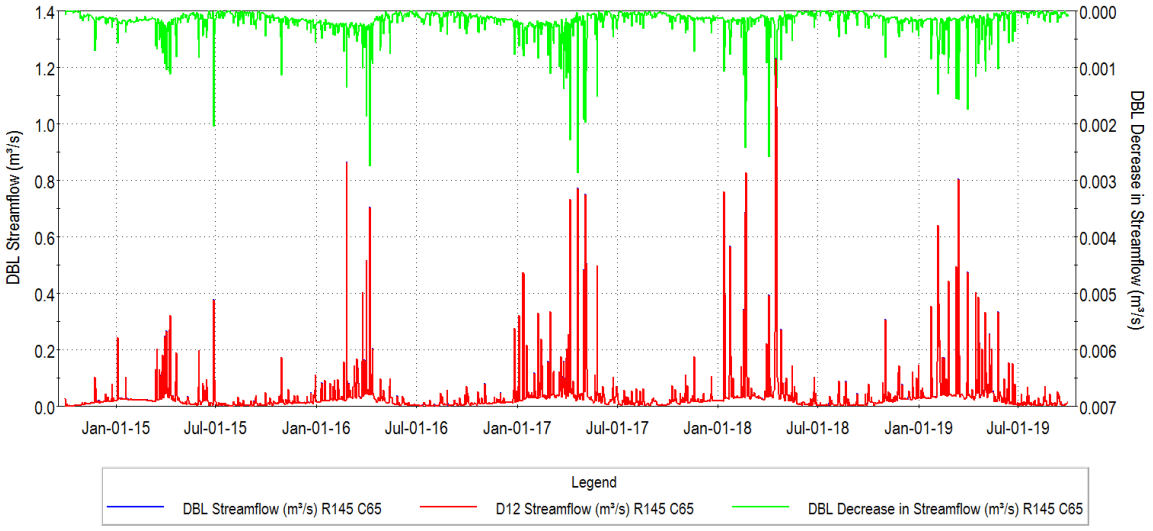

Figure 8.11: Simulated streamflow at SW07 for WY2014 to WY2019 – P12 and Baseline Conditions.

8.5.2 P12 Seasonal and Inter-Annual Groundwater Levels

The transient simulations through 2015-2016 provide insight into the effects of P12 during seasonal and interannual variation, including a Level 2 drought. Figure 8.12 through Figure 8.19 show the simulated heads in Model Layer 6, representing the middle fracture zone in the Amabel aquifer, for WY2014 to WY2019 for the eight assessment points (locations shown in Figure 8.3). Drawdowns are also shown on the hydrographs (on the inverted secondary y-axis).

The maximum daily incremental drawdown over baseline occurs at GW8 (the closest assessment point to the Phase 2 extraction area) and range between 2.3 to 5.2 m (Figure 8.19). The drawdowns at other assessment points decrease quickly with distance from the P12 footprint. Daily drawdowns are near zero for GW1, the farthest point from the extraction area (Figure 8.12).

On a seasonal basis, the maximum incremental drawdown typically occurs in late December (Figure 8.19), and the minimum drawdown occurs on the late spring, after the aquifer storage has been naturally replenished by snowmelt. (The drawdowns are not constant over time, because non-linear system response and storage, which can significantly buffer the response to climate variability.)

The development of P12 will create a local drawdown in the Amabel aquifer surrounding the P12 excavation. Wells in the vicinity of the excavation will experience a loss of available drawdown, however there will, on average, remain up to 22 m of available drawdown in the aquifer (Figure 8.20) as measured from the basal Layer 8 lower fracture zone.

Under drought conditions, the heads at most assessment points still reach a local minimum in the late fall of 2015, but reach a similar low in late fall of 2016, even though it was a wetter year, because of depletion of groundwater storage in the previous year.

Under worst case drought conditions, such during the Level 2 Provincial Low Water Advisory that was issued in 2016, water levels in the vicinity of P12 will be an additional 1.5 m lower than average extraction levels. Under drought conditions there will, however, continue to be up to 20 m of available drawdown in the Amabel Aquifer (Figure 8.21).

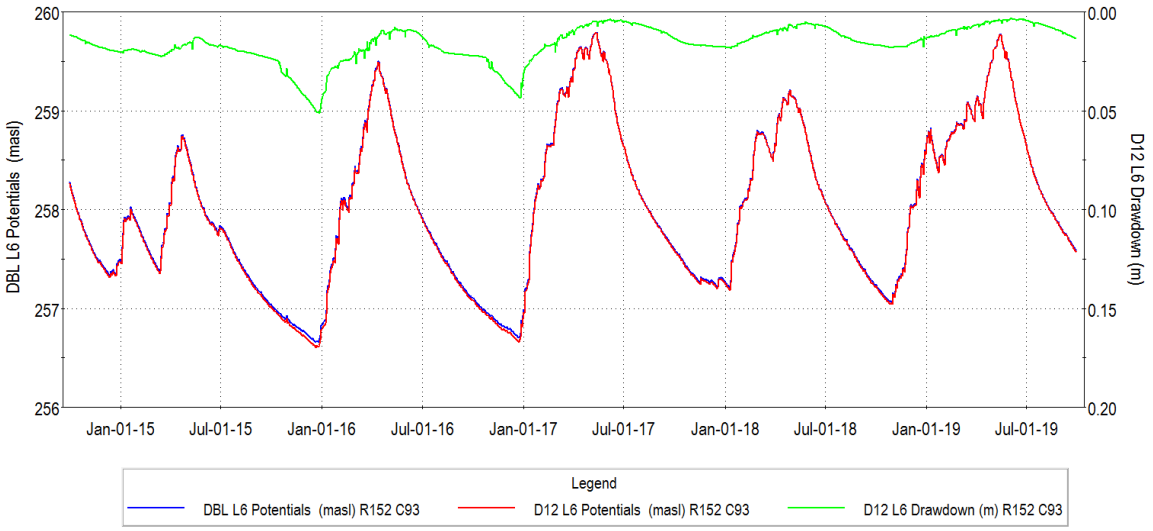

Figure 8.12: Simulated heads and drawdowns in Model Layers 6 at GW1 for WY2014 to WY2019 - P12 and Baseline Conditions.

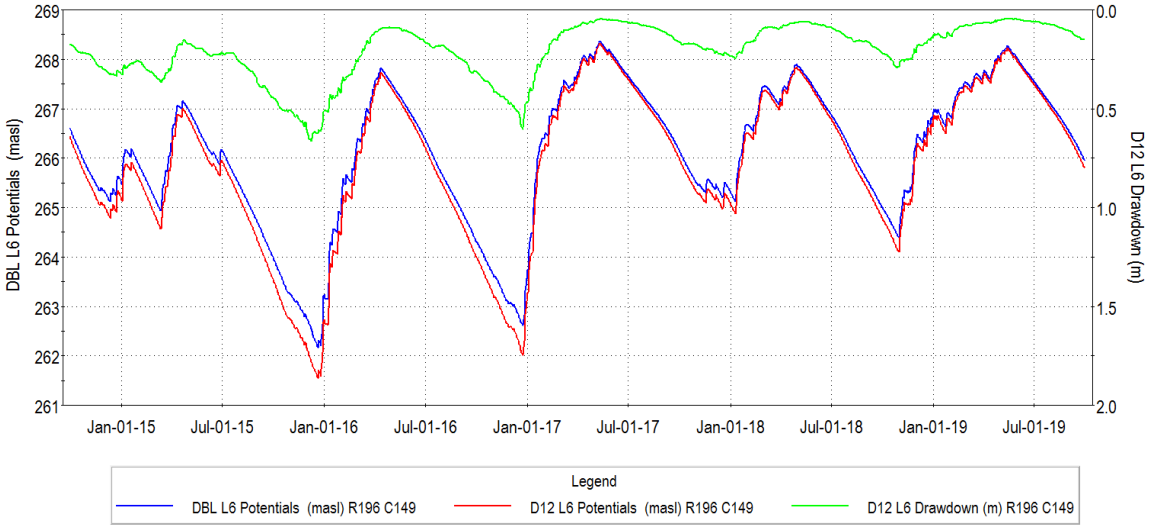

Figure 8.13: Simulated heads and drawdowns in Model Layers 6 at GW2 for WY2014 to WY2019 - P12 and Baseline Conditions.

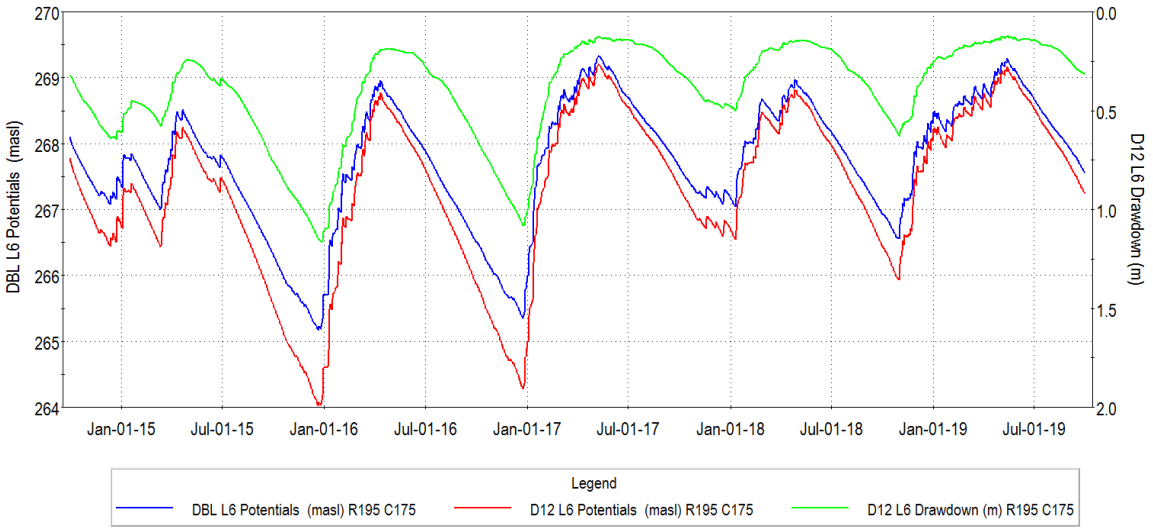

Figure 8.14: Simulated heads and drawdowns in Model Layers 6 at GW3 for WY2014 to WY2019 - P12 and Baseline Conditions.

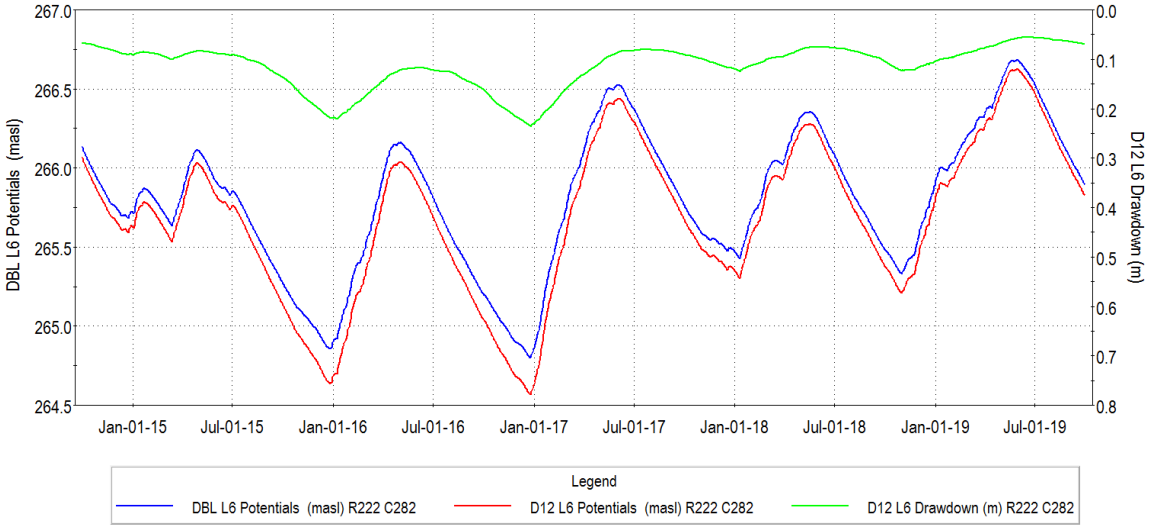

Figure 8.15: Simulated heads and drawdowns in Model Layers 6 at GW4 for WY2014 to WY2019 - P12 and Baseline Conditions.

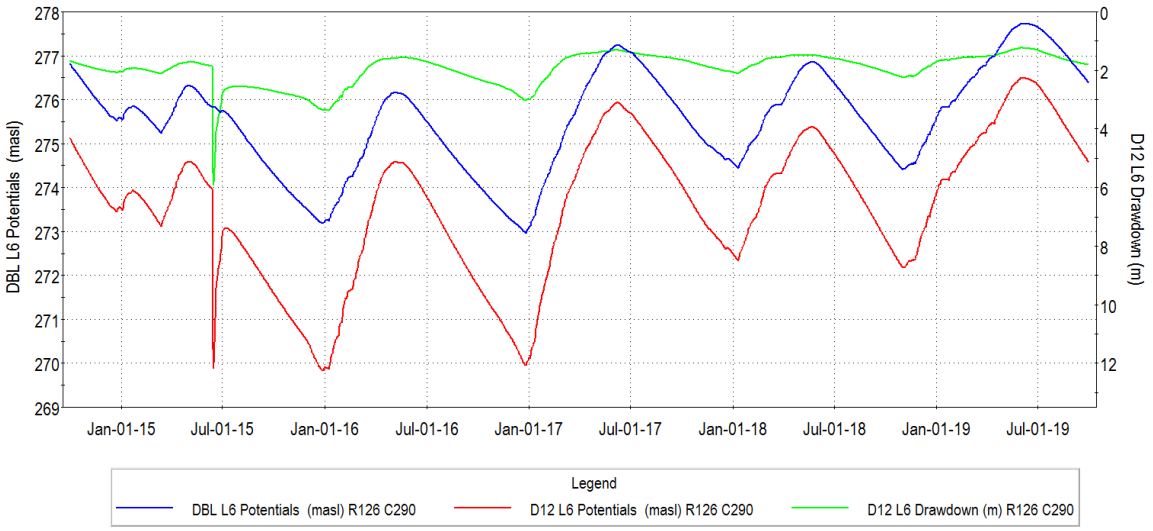

Figure 8.16: Simulated heads and drawdowns in Model Layers 6 at GW5 for WY2014 to WY2019 - P12 and Baseline Conditions.

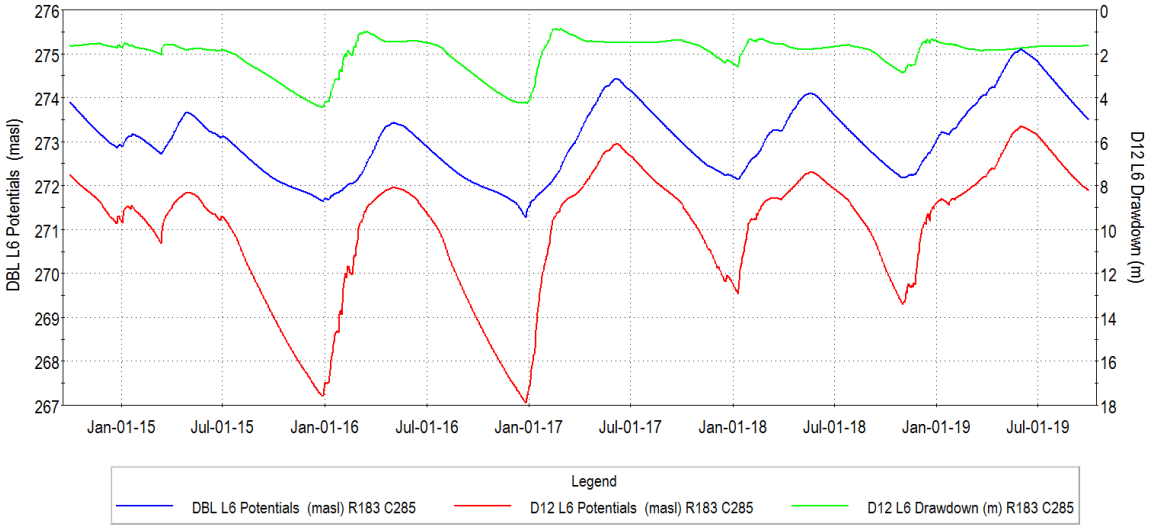

Figure 8.17: Simulated heads and drawdowns in Model Layers 6 at GW6 for WY2014 to WY2019 - P12 and Baseline Conditions.

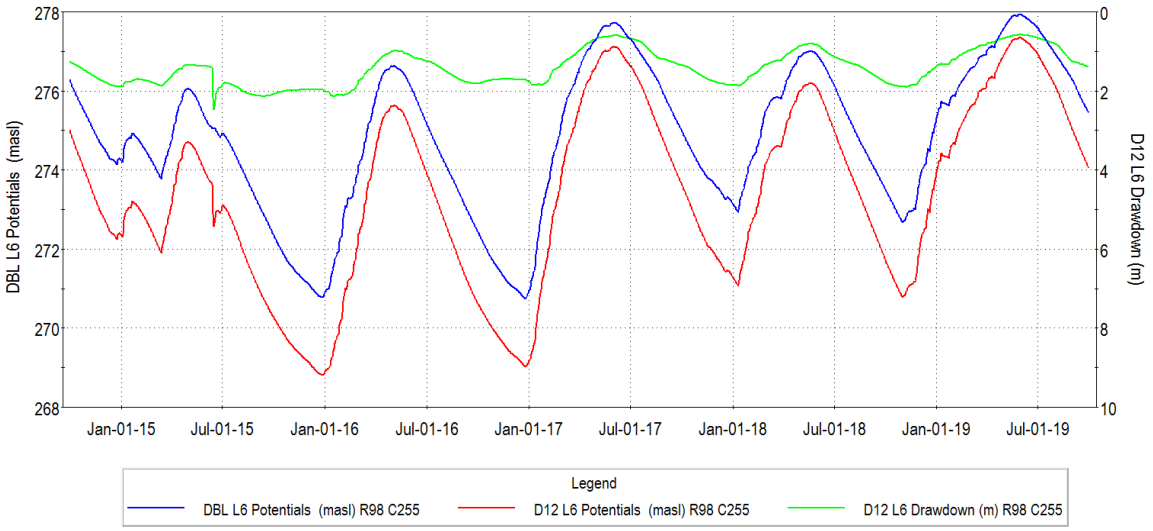

Figure 8.18: Simulated heads and drawdowns in Model Layers 6 at GW7 for WY2014 to WY2019 - P12 and Baseline Conditions.

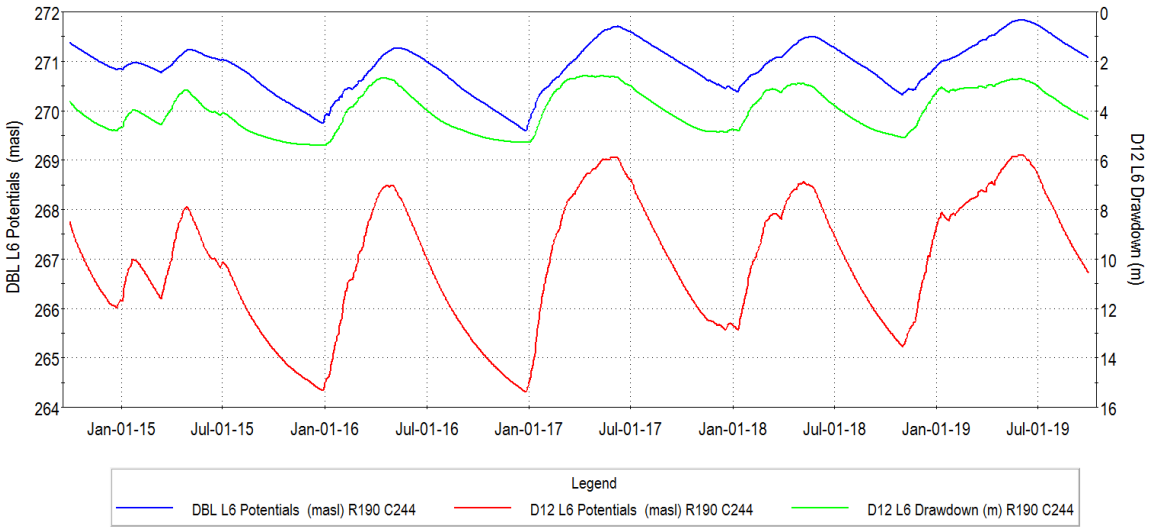

Figure 8.19: Simulated heads and drawdowns in Model Layers 6 at GW8 for WY2014 to WY2019 - P12 and Baseline Conditions.

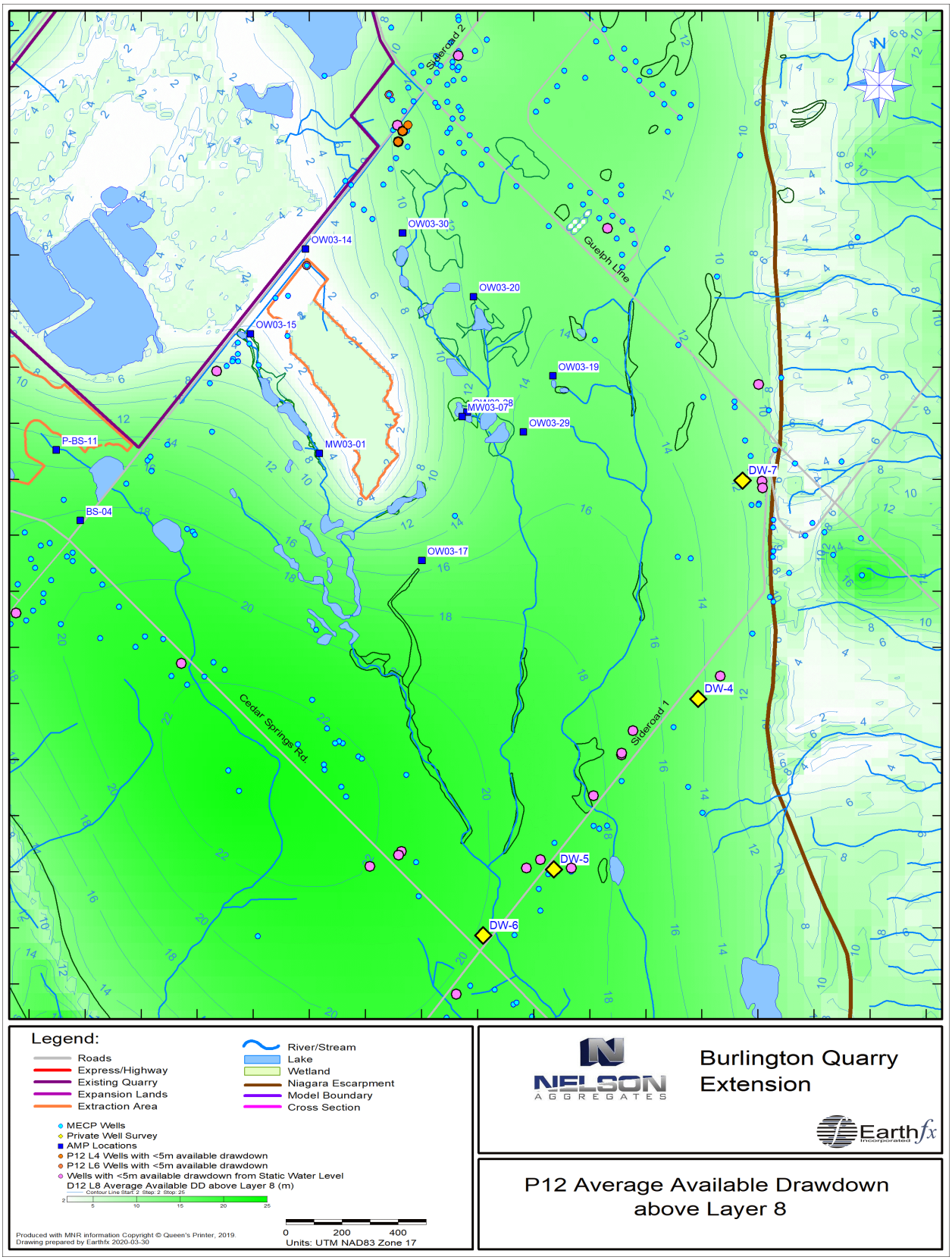

Figure 8.20: Average available drawdown under P12 conditions.

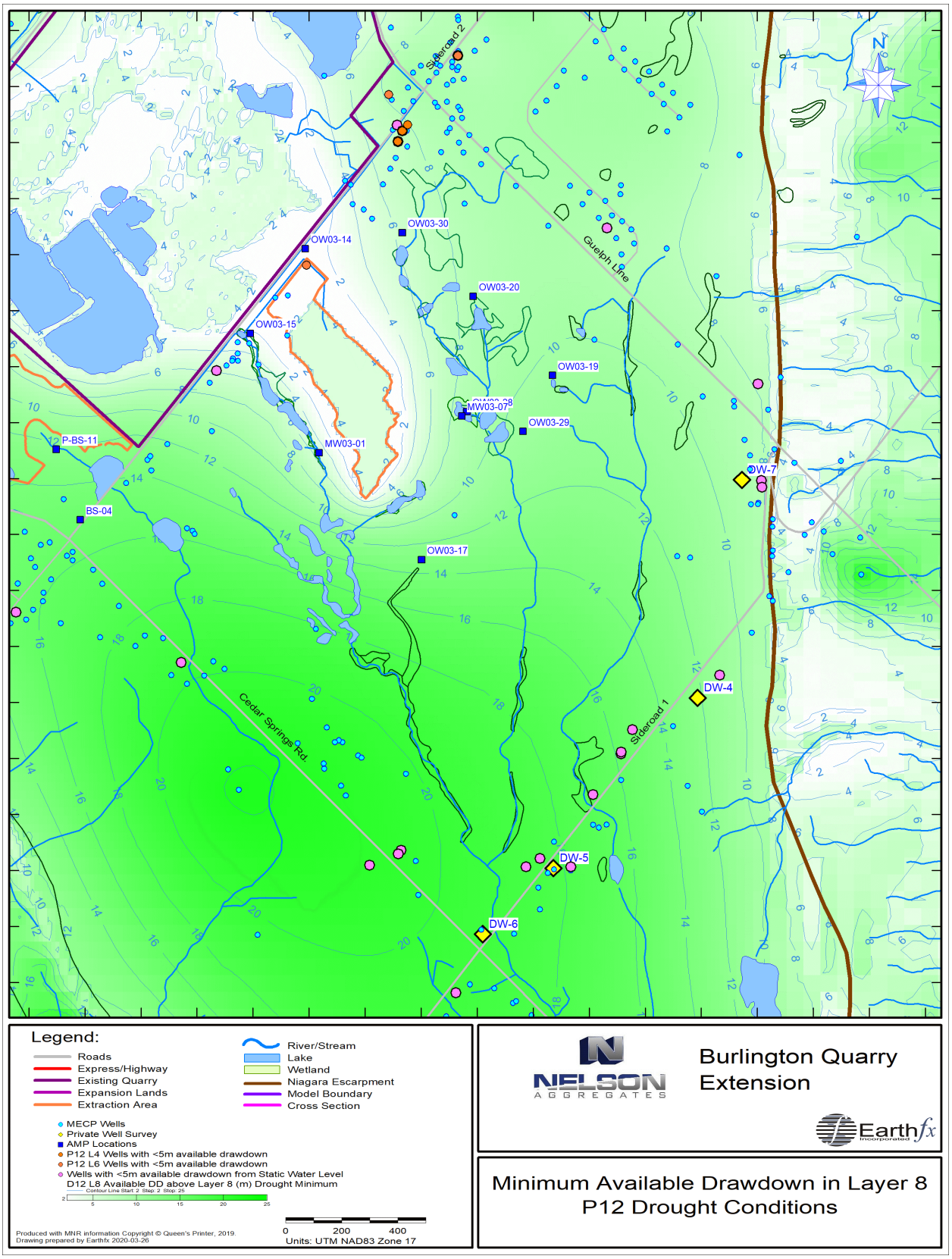

Figure 8.21: Minimum available drawdown under P12 Drought conditions.

8.5.3 P12 Surface Water/Groundwater Interaction

Figure 8.22 shows the average simulated net groundwater recharge in the quarry vicinity for Scenario P12. The decrease in recharge, compared to the Baseline Conditions (Figure 7.18) is focused on the P12 extraction area where soils and land use parameters were changed. Similarly, Figure 8.23 shows that average simulated groundwater ET has increased significantly in the P12 footprint, compared to the Baseline Conditions (Figure 7.19), because of the extra PET demand passed to the groundwater model.

Figure 8.24 presents the average simulated streamflow loss to groundwater (blue areas) and the areas of groundwater discharge to streams (red areas). Little change is seen compared to the Baseline Conditions (Figure 7.21), except in the small streams in the wetland complex to the west of P12. Figure 8.25 presents the average simulated groundwater discharge to the soil zone under Scenario P12. The most significant change compared to the Baseline Conditions (Figure 7.20) is groundwater discharge within the P12 quarry footprint. This flow is picked up as Dunnian runoff by the quarry floor drains and included in quarry discharge.

A cross section through the wetlands provides insight into the interactions between the surface and groundwater system. The section location is shown in Figure 8.26, and the cross section is shown in Figure 8.27. The cross section shows water levels in the Halton Till (layer 2) under both baseline and P12 extraction conditions. Under P12 conditions, water levels have declined by up to 5 m under Wetland 17 (the effects of this on the wetland water budget is discussed in the next section).

A detailed discussion of the field measurements and model simulation of perched wetlands was presented in Section 6.11.6. A perched wetland, such as Wetland 19 (MNRF 13032), is located 9 m above the water table under baseline conditions, but that increases to 11 m under P12 extraction conditions. Wetland 19 never receives groundwater inflows because it is always perched above the water table.

A comparison of water levels in the pond under baseline and P12 conditions is shown in Figure 8.28. There is no change in the water level fluctuations in the pond between the two scenarios, because the wetland is located high above the water table and the P12 development has no impact on the local hydrologic function.

The effect of lowering the water table on leakage from a highly perched wetland is illustrated in Figure 8.29. The figure presents a time series graph of the leakage from the Wetland 19 pond to the groundwater system. The leakage rate varies on a seasonal basis, as the pond levels fill during the spring with rainfall and snowmelt, and drop through the summer and fall due to leakage downwards and evapotranspiration. The graph shows that the leakage from the pond is identical under both Baseline and P12 conditions, and that lowering the water table under the pond has no impact on the hydrologic function of the pond.

The wetland water budgets, including Wetland 19, are discussed below.

8.5.4 P12 Wetland Water Budgets

Water budgets were completed to analyze inflows and outflows to 22 local wetlands (locations shown in Figure 7.22). All flows within each area are computed as well as lateral groundwater flow, streamflow, overland runoff, and interflow crossings the wetland area boundaries. Figure 8.30 through Figure 8.37 present schematics showing detailed average water budgets for wetland areas 9, 16, 17,

18, 19, 20, 21, and 22, respectively. These can be compared with Figure 7.23 through Figure 7.30 for Baseline Conditions. For example, the water budget for Wetland 19 (MNRF 13032) remains unchanged because it is perched above the water table and therefore unaffected by any changes in groundwater levels.

The wetlands are located at various distances from the existing quarry and the extension areas. All except Wetlands 21 and 22 are in the vicinity of the P12 extraction area. The wetland areas are net contributors to groundwater, which is typical of wetlands that are perched for most (or all) of the year and are fed by runoff or stream inflows.

The effects of P12 on the wetlands is illustrated by comparing the baseline and P12 water budget summaries. Under baseline conditions, none of the wetlands receive more than 3.0% of their total inflows from the groundwater system (Table 8.5), and many receive no groundwater inflow at all because they are perched. The wetlands that do receive minor groundwater inflow become perched under P12 conditions, and will loose up to 3.0% of their outflow water budget. The wetlands will leak more to the groundwater system, but the effect of this change is generally so small that it cannot be measured in the field and will not change the overall water budget of the wetland.

Table 8.5: Water budget comparison between Baseline and P12 conditions.

Earthfx Wetland ID	MNRF ID	Baseline		P12		Change in Water Budget P12 -BL	
		GW Outflow %	GW Inflow %	GW Outflow %	GW Inflow %	Change in Outflow %	Change in GW Inflow %
9	13014	10.19%	0.00%	9.67%	0.00%	-0.52%	0.00%
16	13022	1.25%	0.34%	1.31%	0.00%	0.06%	-0.34%
17	13033	2.51%	1.31%	5.71%	0.00%	3.20%	-1.31%
18	na	5.98%	2.42%	9.95%	0.00%	3.97%	-2.42%
19	13032	19.82%	0.00%	19.35%	0.00%	-0.47%	0.00%
20	13037	12.84%	1.76%	15.90%	0.00%	3.06%	-1.76%
21	13201	12.78%	2.98%	30.38%	1.76%	17.60%	-1.22%
22	13200	26.31%	0.00%	25.24%	0.00%	-1.07%	0.00%
Note:	GW Outflow = Groundwater outflows as a percentage of total outflows from the feature						
	GW Inflow = Groundwater inflows as a percentage of total inflows to the feature						

Wetland 21 is located at the south edge of the West Extension area, and its function is impaired by the road and a limited culvert, so its function and water budget are compromised. This wetland will receive a review and supplemental inflows, as described in the Tatham, 2020 report. The planned supplementation has not been represented in the model, so the Wetland 21 water budget is not fully representative of future conditions.

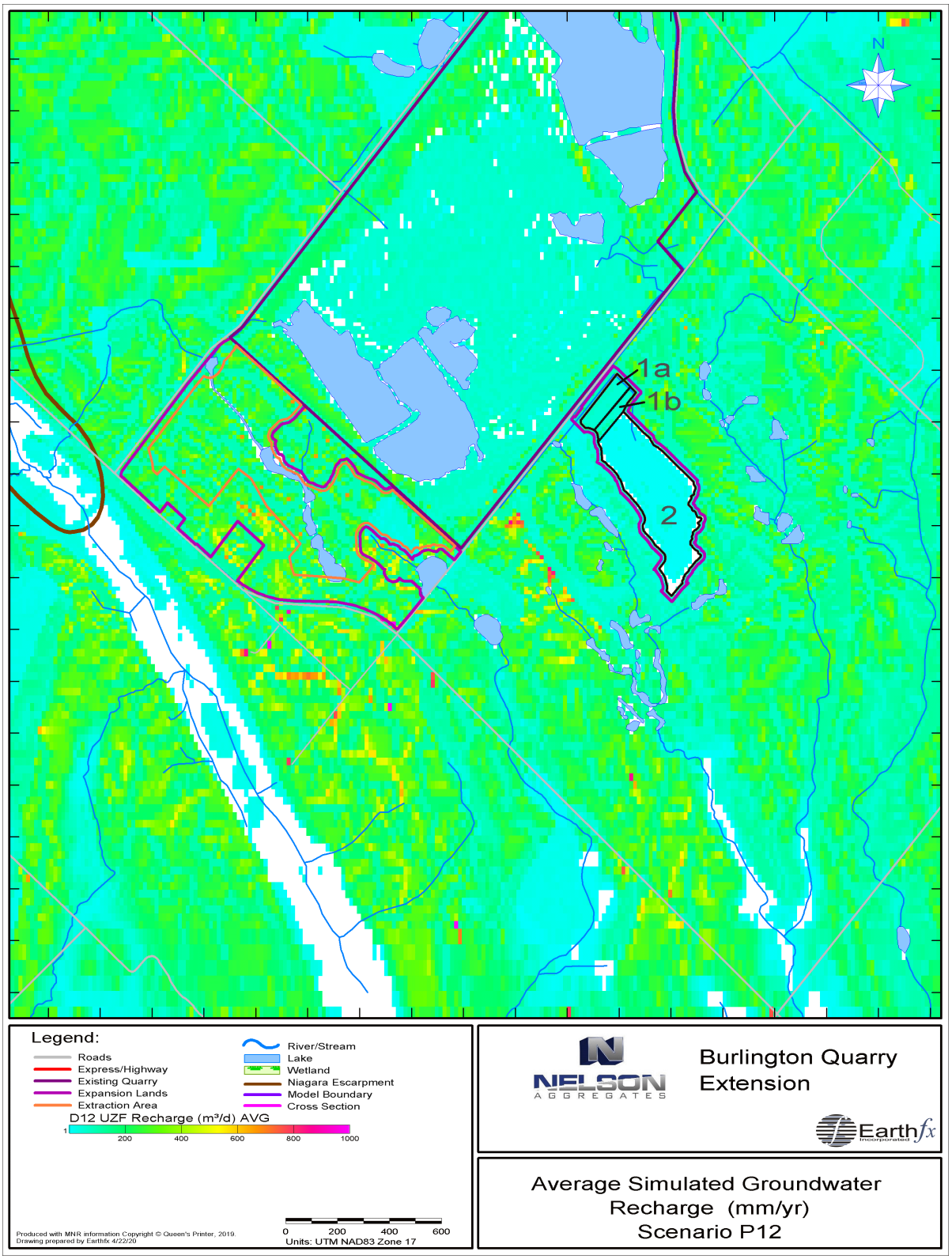

Figure 8.22: Average simulated groundwater recharge (mm/yr) for WY2014 to WY2019 – Scenario P12.

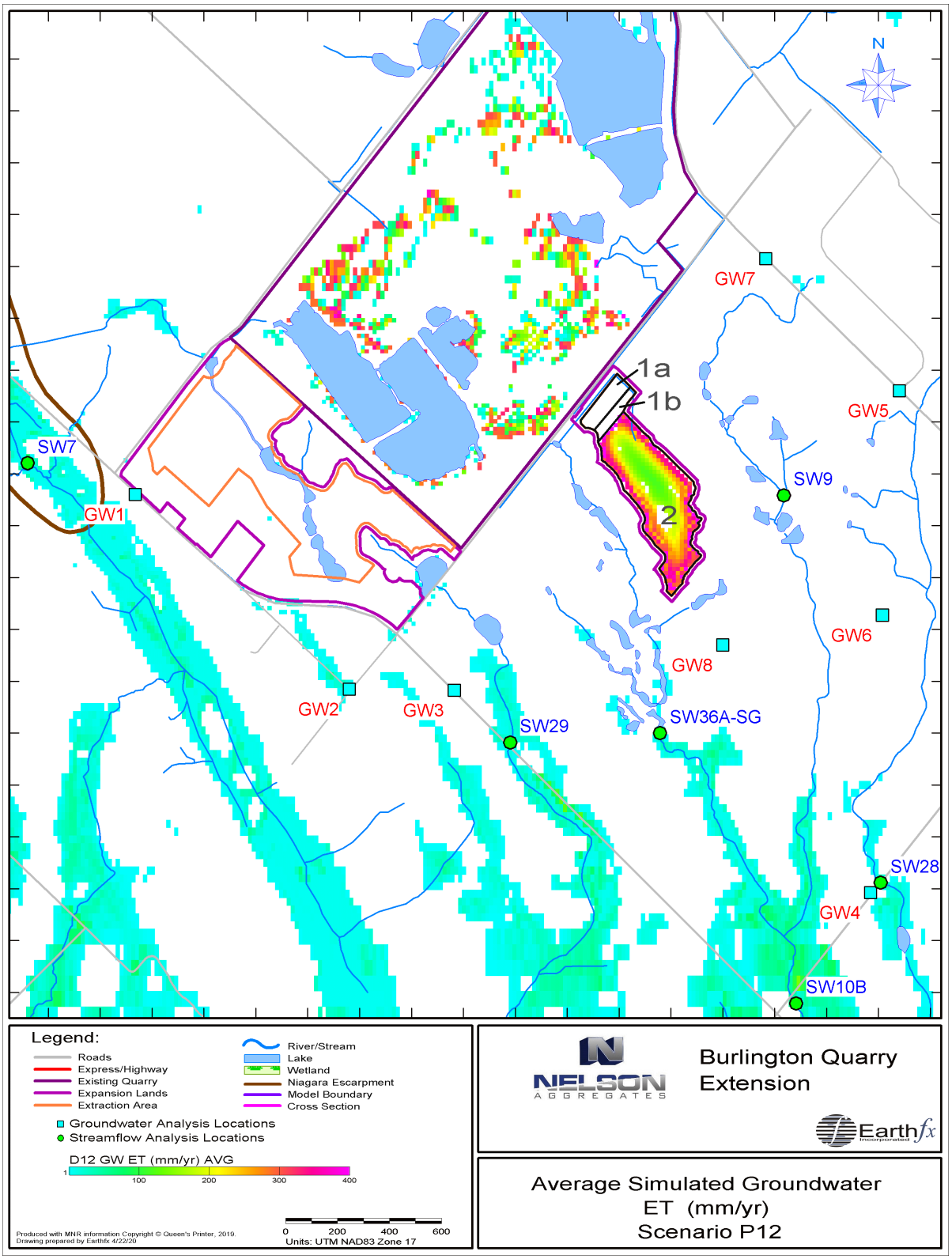

Figure 8.23: Average simulated groundwater ET (mm/yr) for WY2014 to WY2019 – Scenario P12.

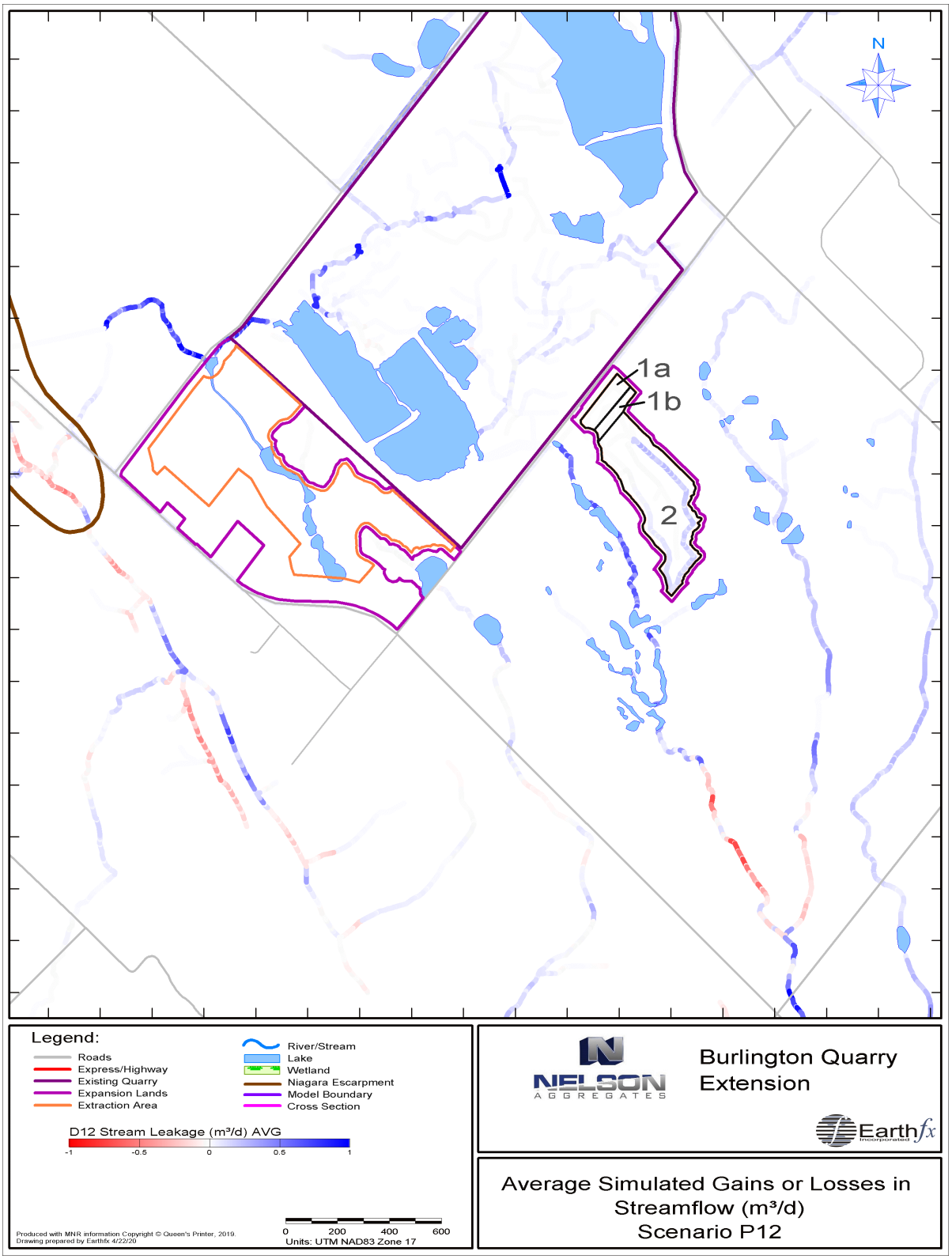

Figure 8.24: Average simulated streamflow loss (blue) to groundwater or groundwater discharge to streams (red) (m^3/d) for WY2014 to WY2019 – Scenario P12.

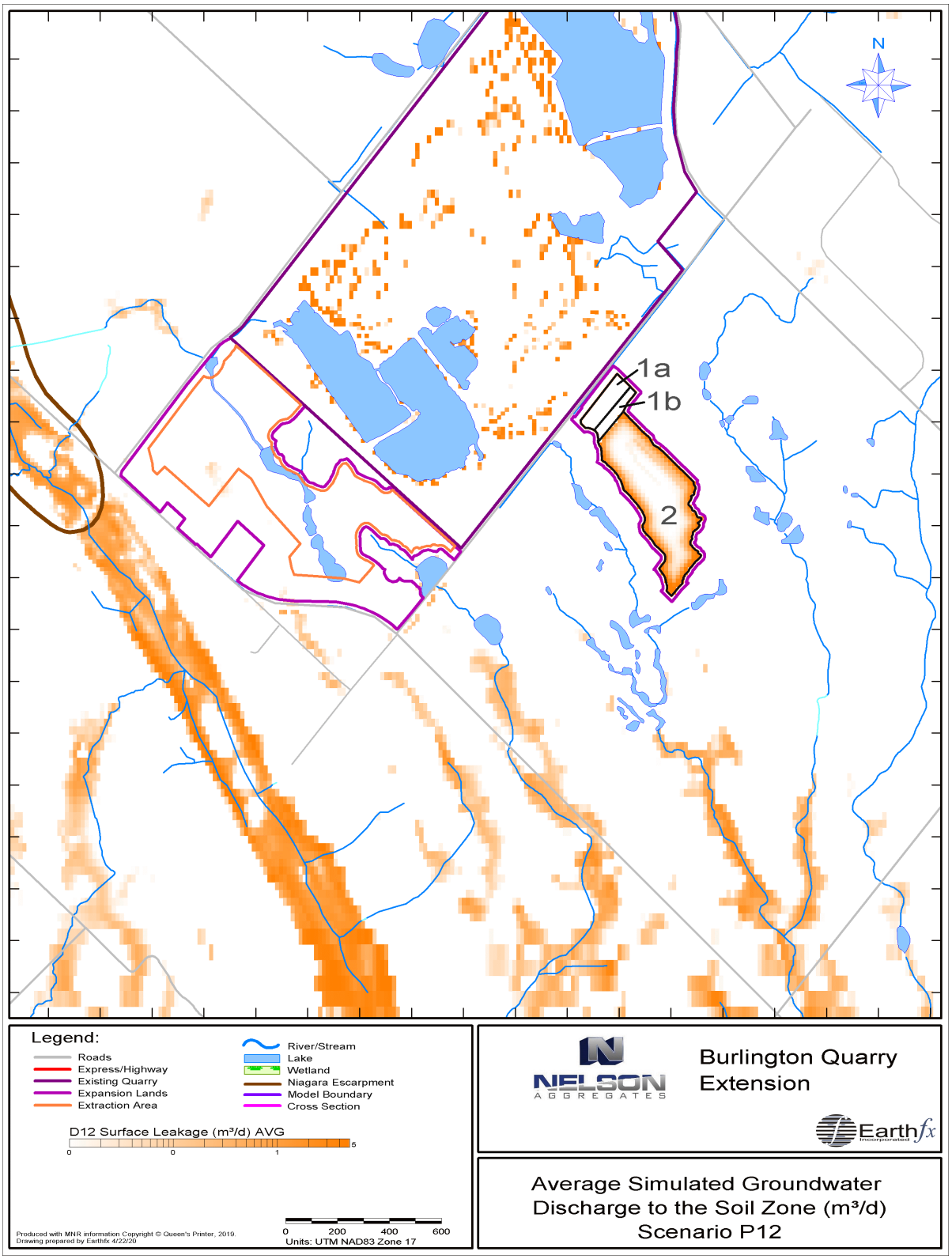

Figure 8.25: Average simulated groundwater discharge to the soil zone (m^3/d) for WY2014 to WY2019 – Scenario P12.

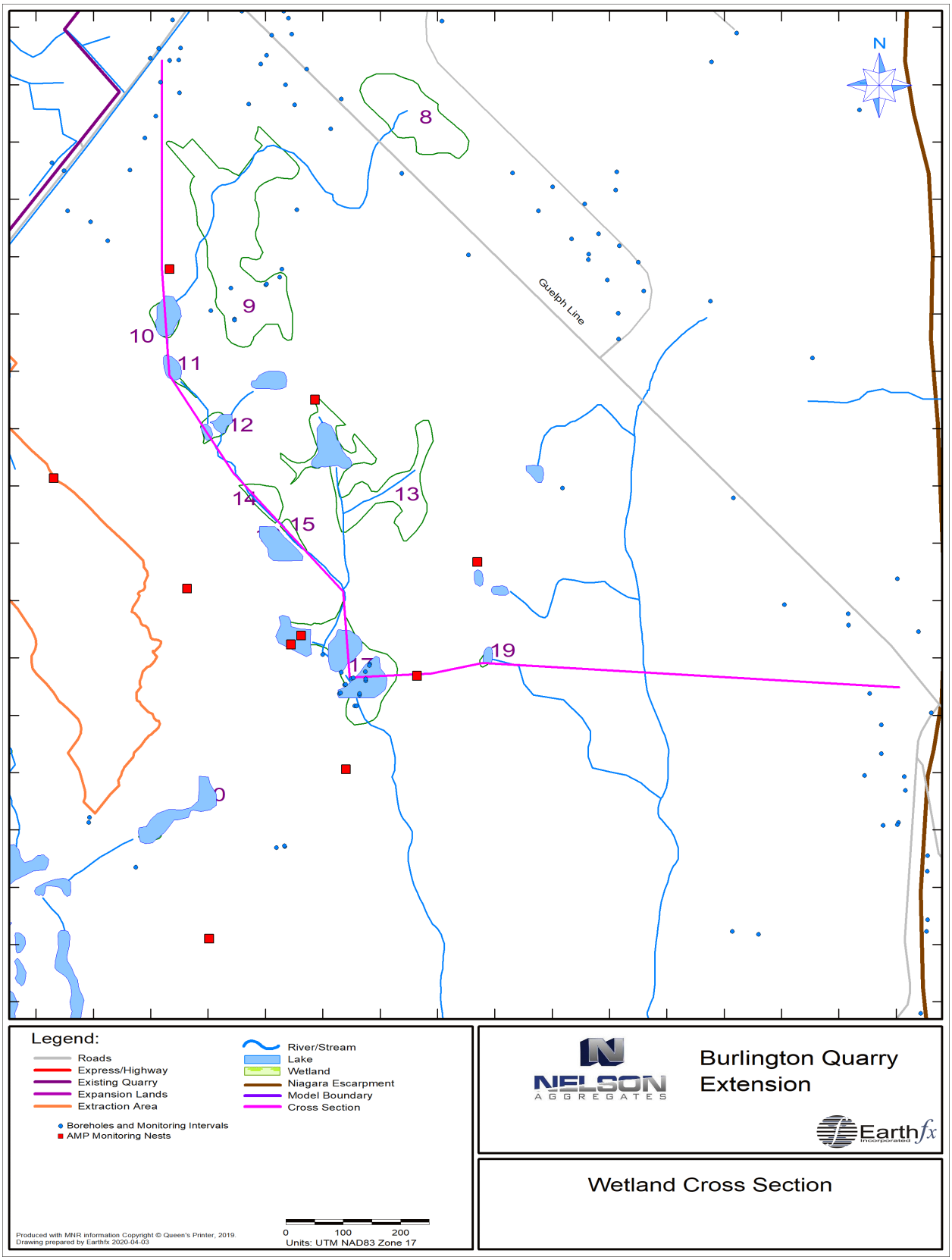

Figure 8.26: Wetland cross section location.

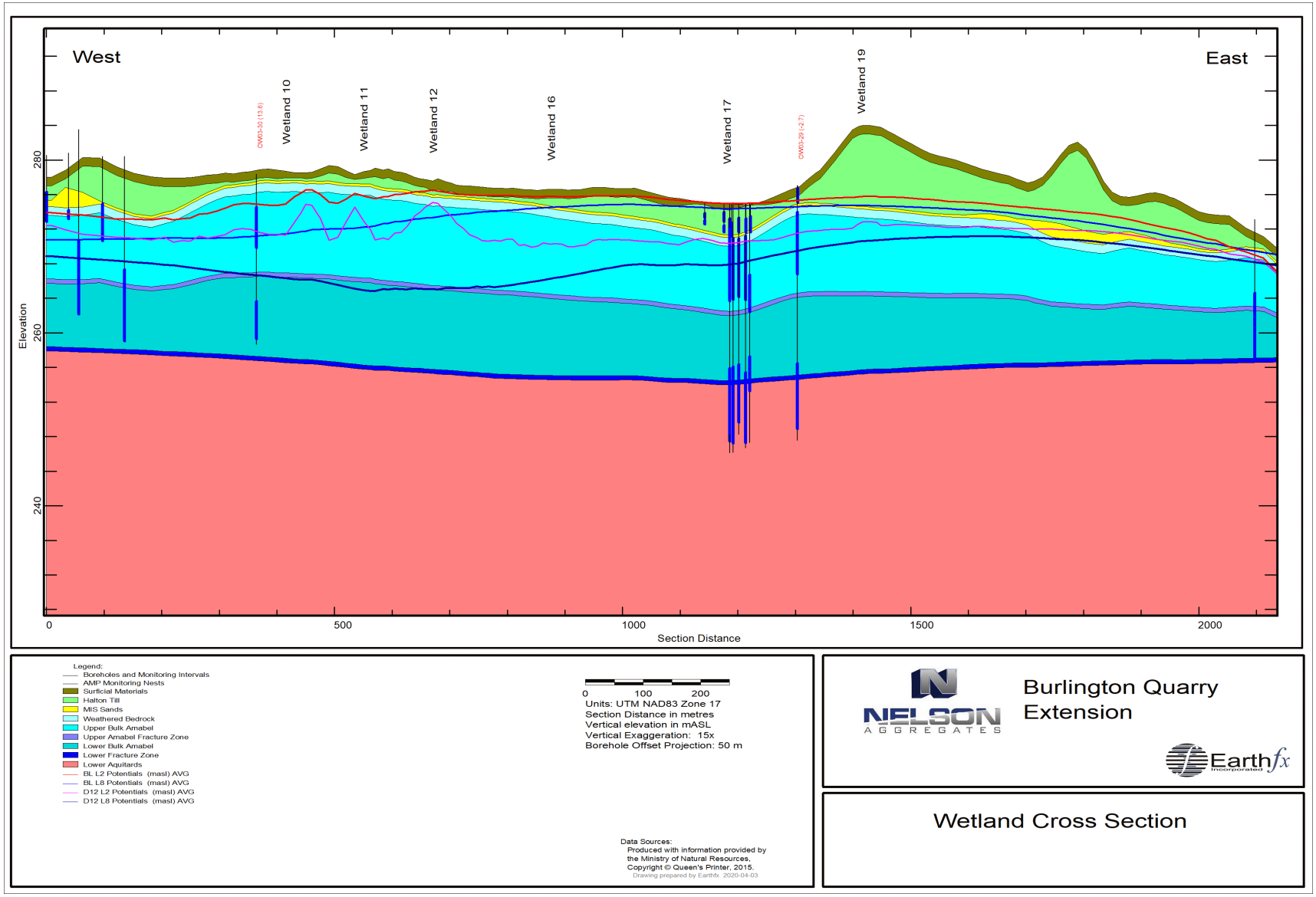

Figure 8.27: Wetland cross section.

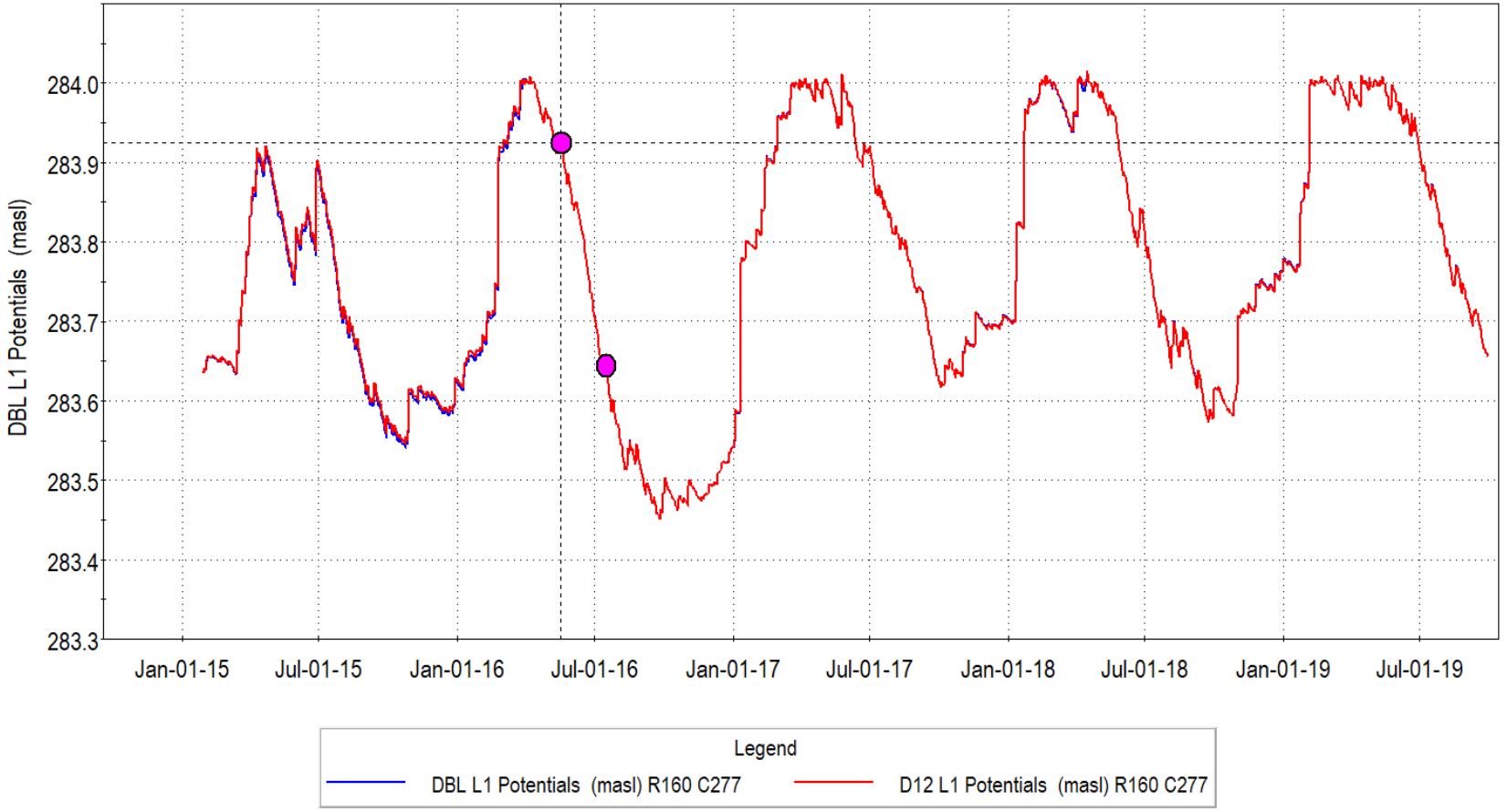

Figure 8.28: Comparison of pond water levels in Wetland 19 (MNRF 13032) under baseline (blue) and P12 conditions (red). Purple symbols show spring recession period.

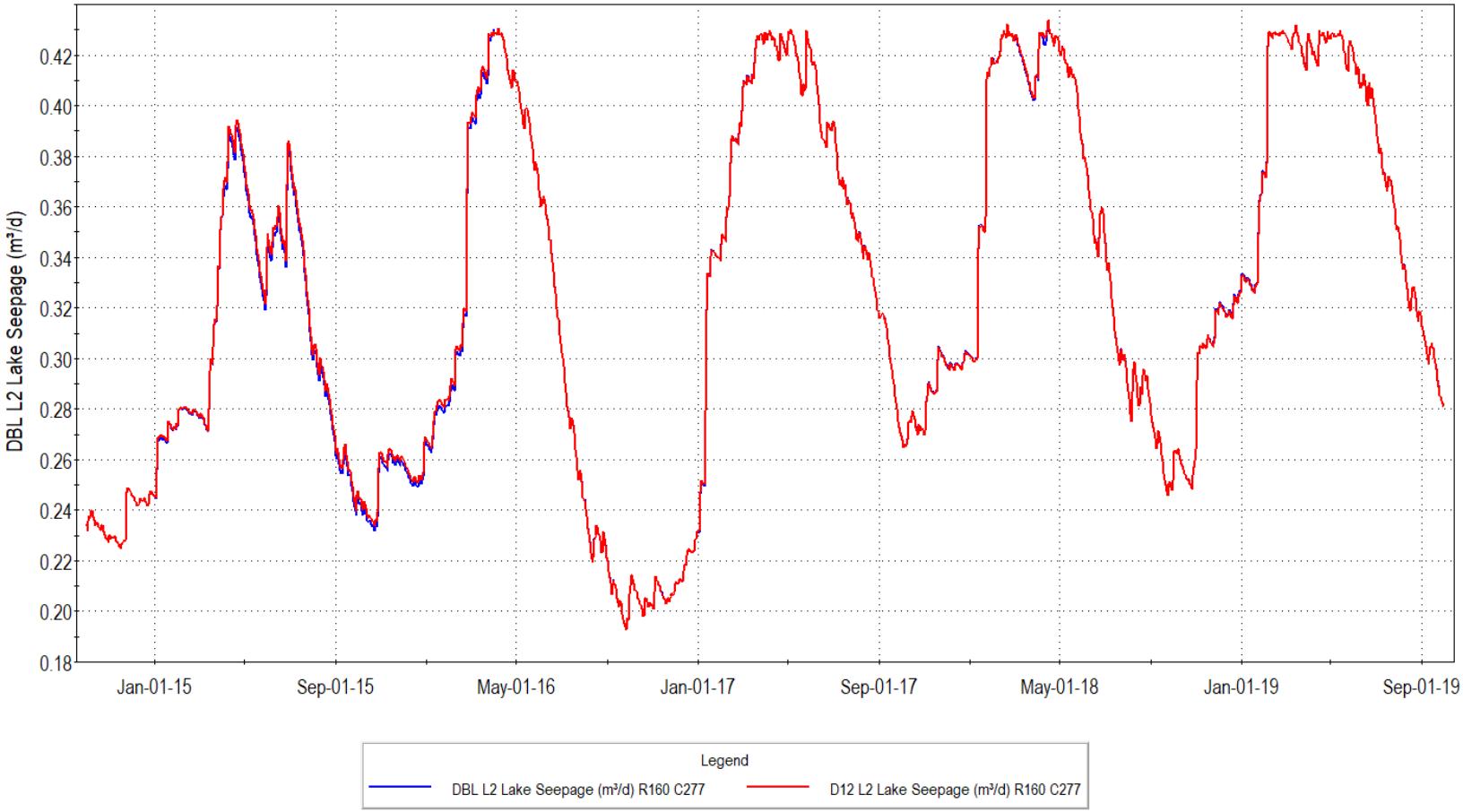

Figure 8.29: Comparison of leakage from Wetland 19 to groundwater under Baseline and P12 conditions.

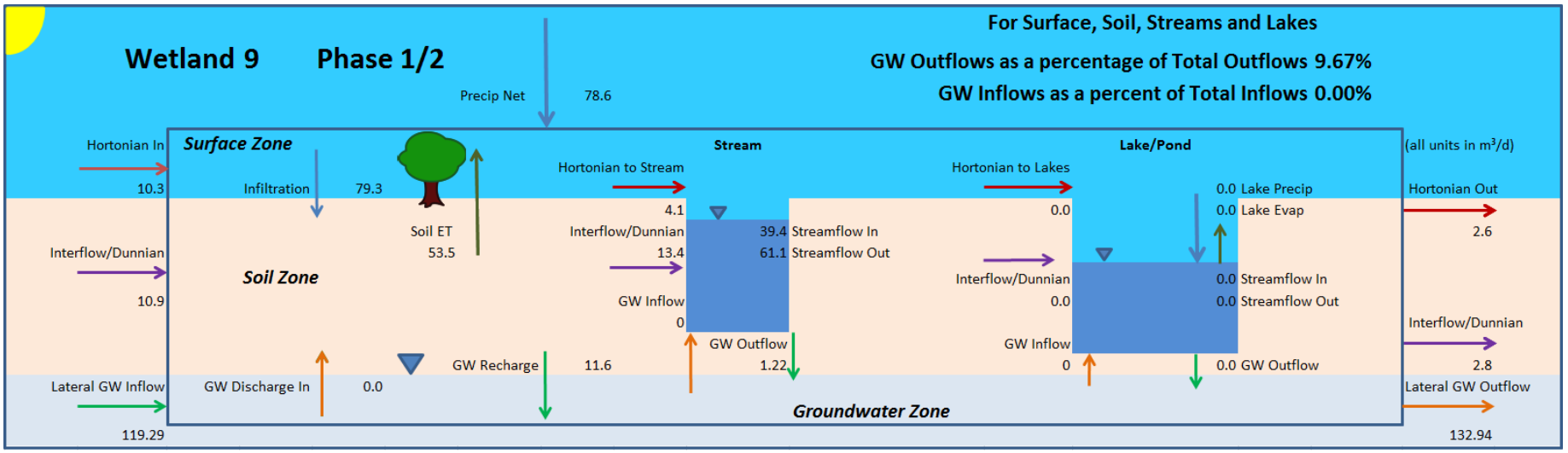

Figure 8.30: Detailed water budget for Wetland 9 averaged over WY2010 and WY2011 under Scenario P12.

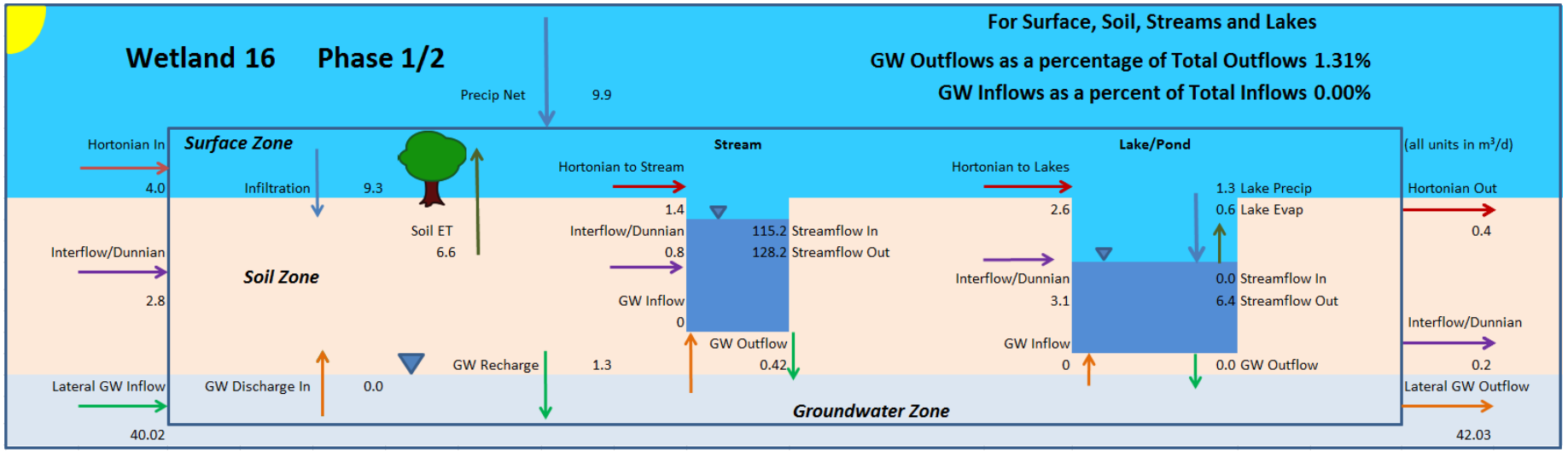

Figure 8.31: Detailed water budget for Wetland 16 averaged over WY2010 and WY2011 under Scenario P12.

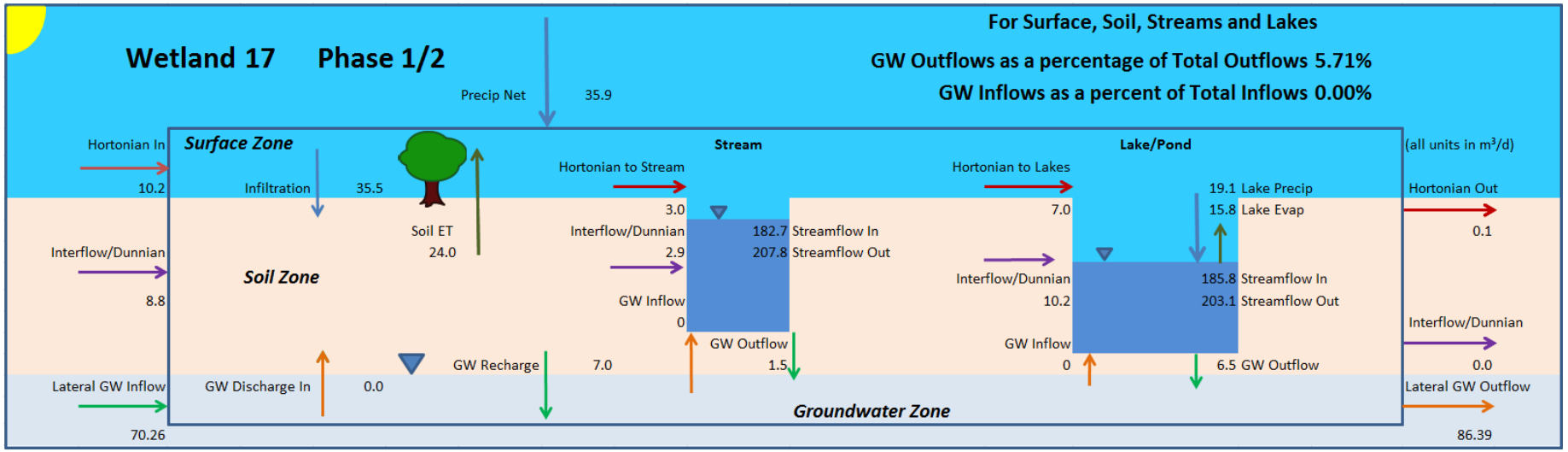

Figure 8.32: Detailed water budget for Wetland 17 averaged over WY2010 and WY2011 under Scenario P12.

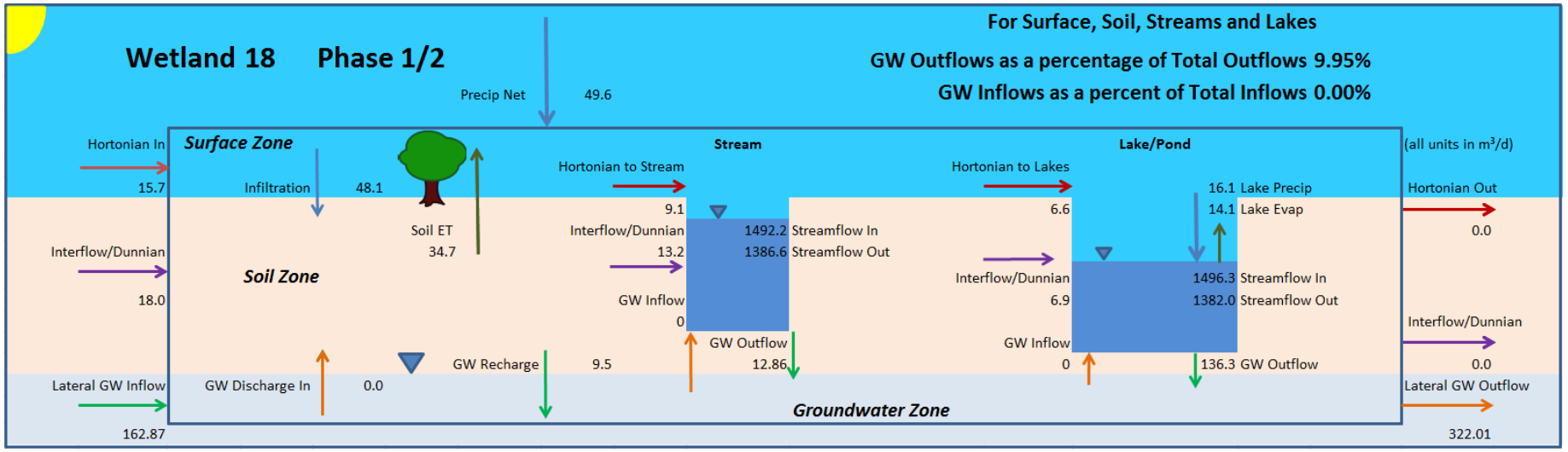

Figure 8.33: Detailed water budget for Wetland 18 averaged over WY2010 and WY2011 under Scenario P12.

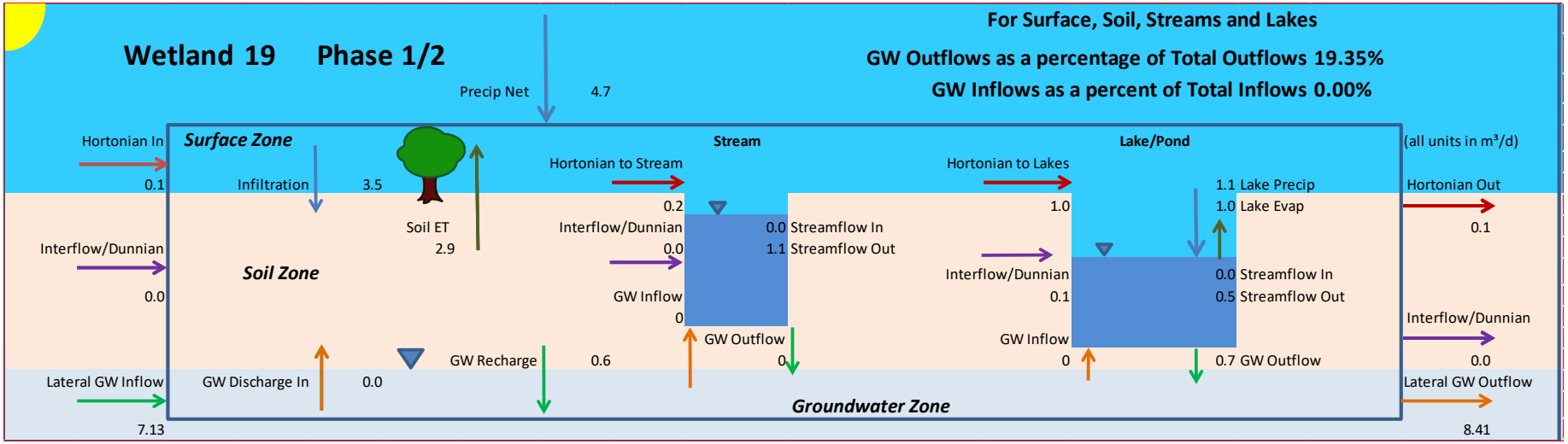

Figure 8.34: Detailed water budget for Wetland 19 averaged over WY2010 and WY2011 under Scenario P12.

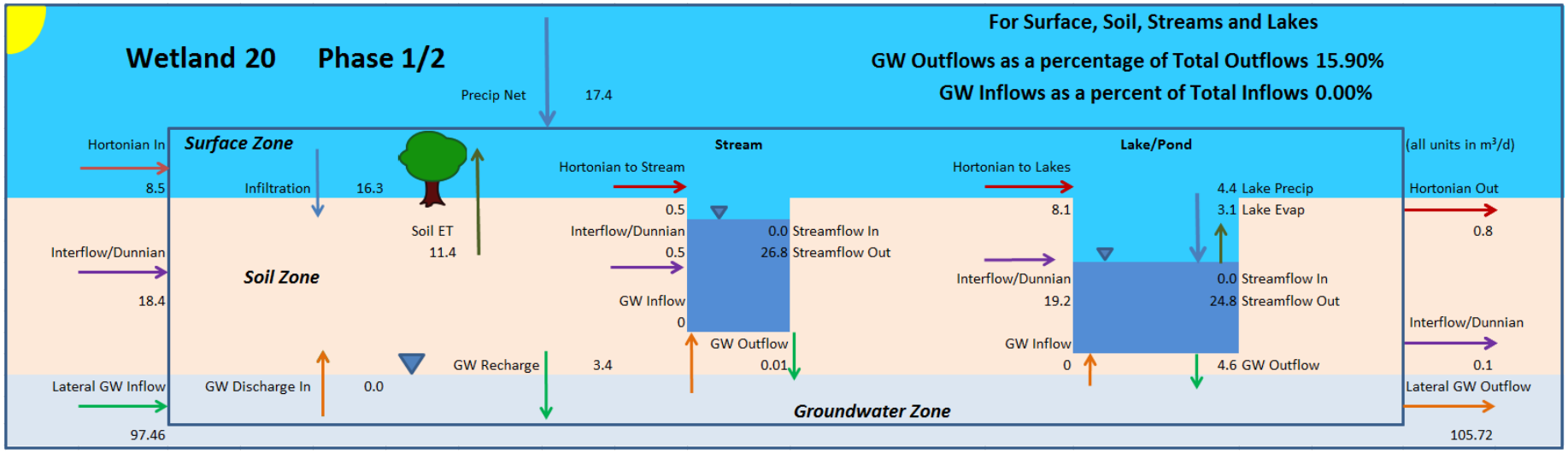

Figure 8.35: Detailed water budget for Wetland 20 averaged over WY2010 and WY2011 under Scenario P12.

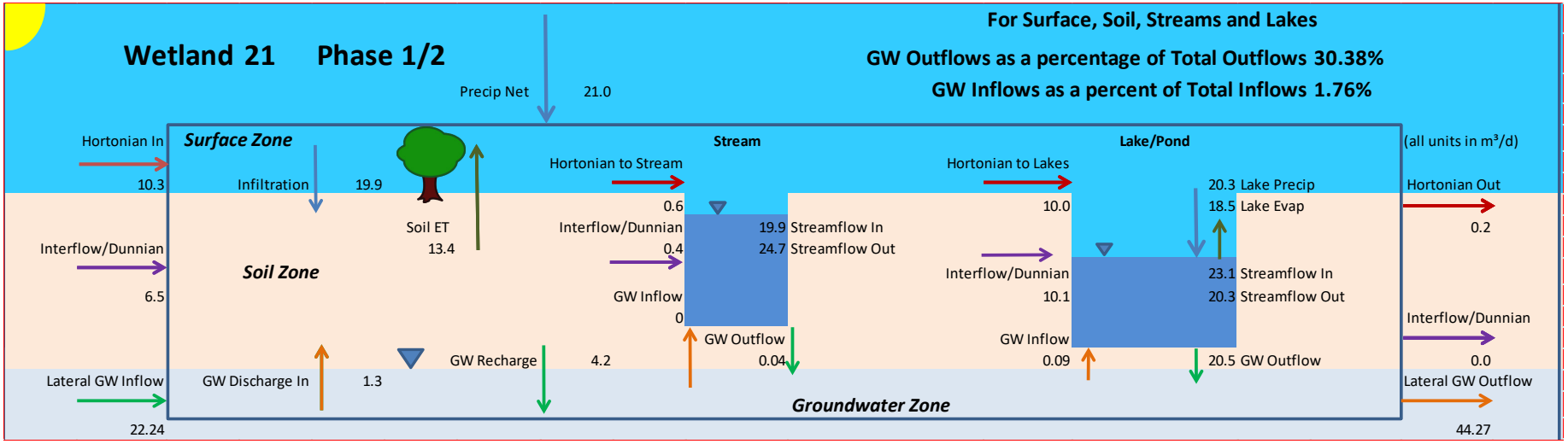

Figure 8.36: Detailed water budget for Wetland 21 averaged over WY2010 and WY2011 under Scenario P12.

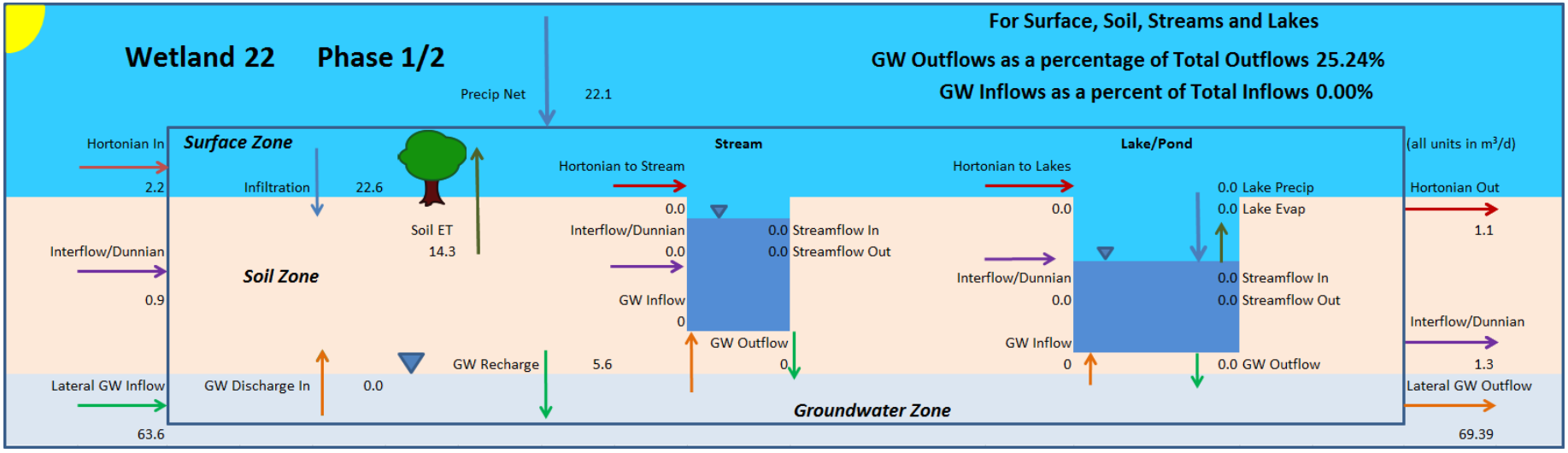

Figure 8.37: Detailed water budget for Wetland 22 averaged over WY2010 and WY2011 under Scenario P12.

8.5.5 P12 Level 2 Conclusions

The development of P12 will create a local drawdown in the Amabel aquifer surrounding the P12 excavation. Wells in the vicinity of the excavation will experience a loss of available drawdown, however there will, on average, remain up to 22 m of available drawdown in the aquifer (Figure 8.20) as measured from the basal Layer 8 lower fracture zone.

Under worst case drought conditions, such during the Level 2 Provincial Low Water Advisory that was issued in 2016, water levels in the vicinity of P12 will be an additional 1.5 m lower than average extraction levels. There will, however, continue to be up to 20 m of available drawdown in the Amabel Aquifer (Figure 8.21).

Figure 8.24 presents the average simulated streamflow loss to groundwater (blue areas) and the areas of groundwater discharge (upwelling) to streams (red areas). Little change is seen compared to the Baseline Conditions (Figure 7.21), except in the small streams in the wetland complex immediately to the west of P12.

The wetland water budgets confirm that the wetlands will leak a small amount more to the groundwater system under P12 conditions, but the effect of this change is so small that it cannot be measured in the field and will not change the overall water budget of the wetland

8.6 Scenario P34

Scenario P34 represents the extraction of aggregate from the Phases 3 and Phase 4 areas. For the purposes of this analysis, it is assumed that extraction is at its maximum depth and dewatering is ongoing. The final elevation of the quarry floor is 252.5 masl in the P34 footprint. Quarry discharge is directed to the existing quarry lakes and eventually discharged from the Northwest sump. Figure 8.38 shows the modified topography and drainage in the quarry vicinity in the P34 scenario.

One key aspect of this phase is that operations in Phase 1 and 2 are assumed to be complete. The Phase 2 excavation is allowed to fill completely with water to its natural elevation (see Figure 8.38) and water is no longer discharged to the tributary to Mt. Nemo Creek.

Land use and soil class were modified in the P34 extraction footprint (changing from a variety of classes to “Quarry”) and in the P12 footprint (from Quarry to “Open Water”). All the soil and land use-based PRMS model parameter values were updated. Topography, slope, and aspect were also adjusted in both areas. Quarry floor drains and conduit stream types were added to the SFR2 module to convey quarry discharge from P34 to the quarry lakes and drains that were removed from P12. MODFLOW layer geometry was modified in the P34 and P12 areas and the P12 Lake and infiltration ponds were added to the LAK3 module and the golf course ponds were adjusted. A new cascade network was generated to account for the new stream network, lakes, and topography.

The GSFLOW model was run with the modified inputs for Scenario P34 and model results were post-processed and compared to Baseline Conditions. Maps similar to those from Scenario P12 were generated and are discussed below. Because this is an interim development step and greater impacts exist in the full Phase 3 to Phase 6 extension, hydrographs showing changes in heads, streamflow, and the water budget for wetlands in the P34 area are not provided.

8.6.1 Infiltration Pond

Another aspect of this phase is addition of an infiltration pond that in the West Lands between Cedar Springs Road and the extraction area (see Figure 8.38). Water is currently routinely diverted from the north quarry discharge pond, through golf course ditches, to the golf course ponds. This water is used for irrigation and a portion also likely infiltrates directly to the groundwater system. The proposed infiltration pond is intended to function in a similar manner to the irrigation ditches and golf course ponds, so as to help maintain the current surface and groundwater system patterns. In addition, based on the findings of this report, Tatham (2020), and Savanta (2020), pumping to the north and south (Quarry discharge locations Sump 0100 and 0200), must be maintained.

8.6.2 P34 Drawdowns and Surface Water Flows

Figure 8.39 shows the average simulated heads in Model Layer 6, representing the middle fracture zone in the Amabel aquifer and average simulated streamflow for the same period. Stage in the P12 lake averaged 270.0 masl. Figure 8.40 shows the average simulated drawdown in Model Layer 6, which is focused on the extraction. The simulated drawdowns decrease sharply with distance and fall below 2.0 m at a maximum distance of 470 m from the active face.

Figure 8.40 also shows the average simulated change in streamflow. Increases in simulated flow occur at the Northwest sump (and in new quarry floor drains and the conduits carrying flow to the infiltration pond). Decreases in simulated flow occur in the Medad Valley, reaching a maximum of approximately $1x10^{-3}$ m^3/s (1 L/s) in the Medad creek immediately west of the P34 excavation.

8.6.3 P12 Recovery

With the filling and recovery of P12, water levels rise and stream flows are reduced in that area (also due to changes in south quarry discharge). Decreases range from $1x10^{-4}$ m^3/s (0.1 L/s) to $7.8x10^{-4}$ m^3/s at the downstream end of the eastern tributary to Mt. Nemo Creek that carries quarry discharge (compared to $8x10^{-4}$ m^3/s under P12). Flow decreased by $9x10^{-4}$ m^3/s at the downstream end of a tributary to Lake Medad (compared to $4x10^{-4}$ m^3/s under P12) due to excavation in the P34 area.

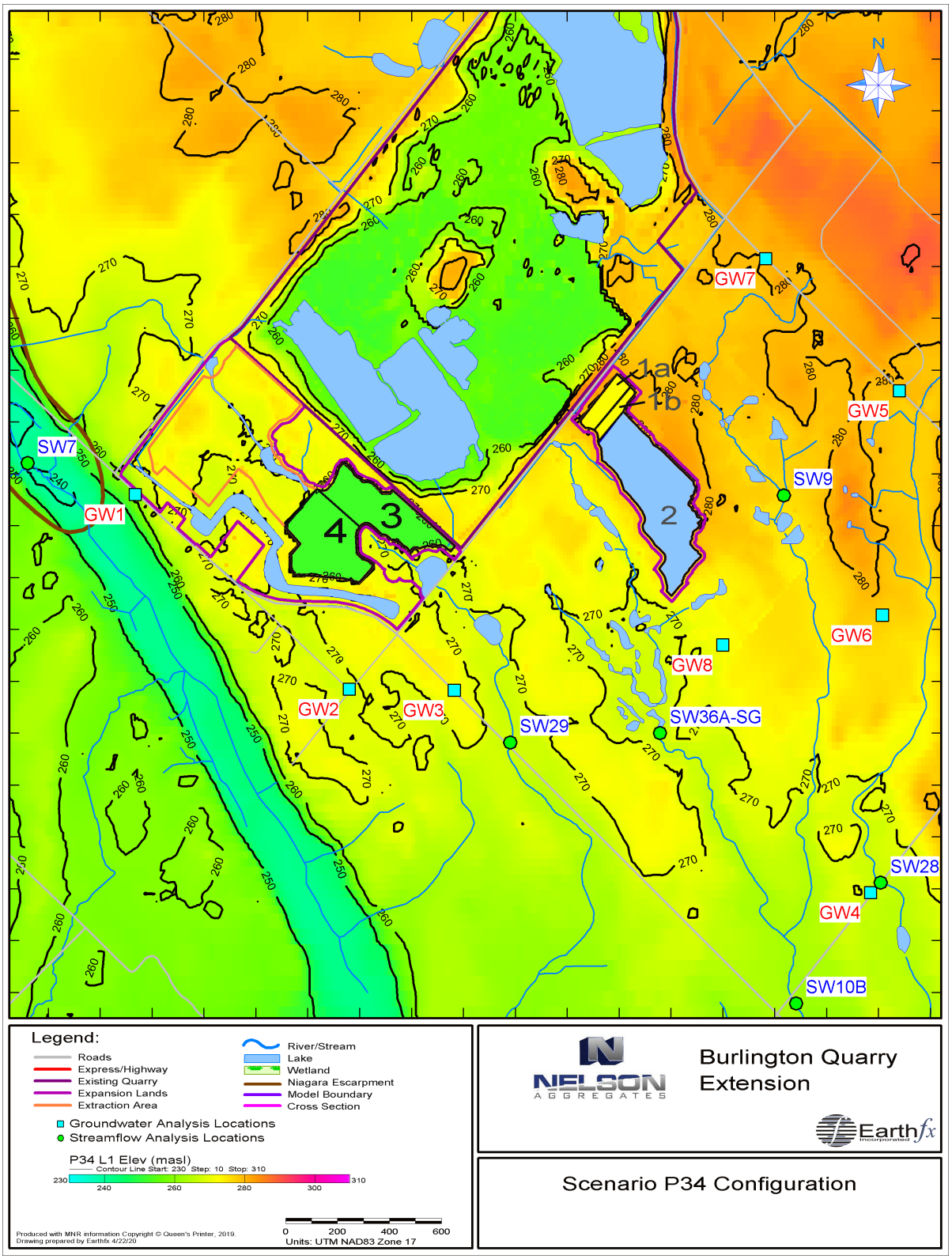

Figure 8.38: Scenario P34 configuration.

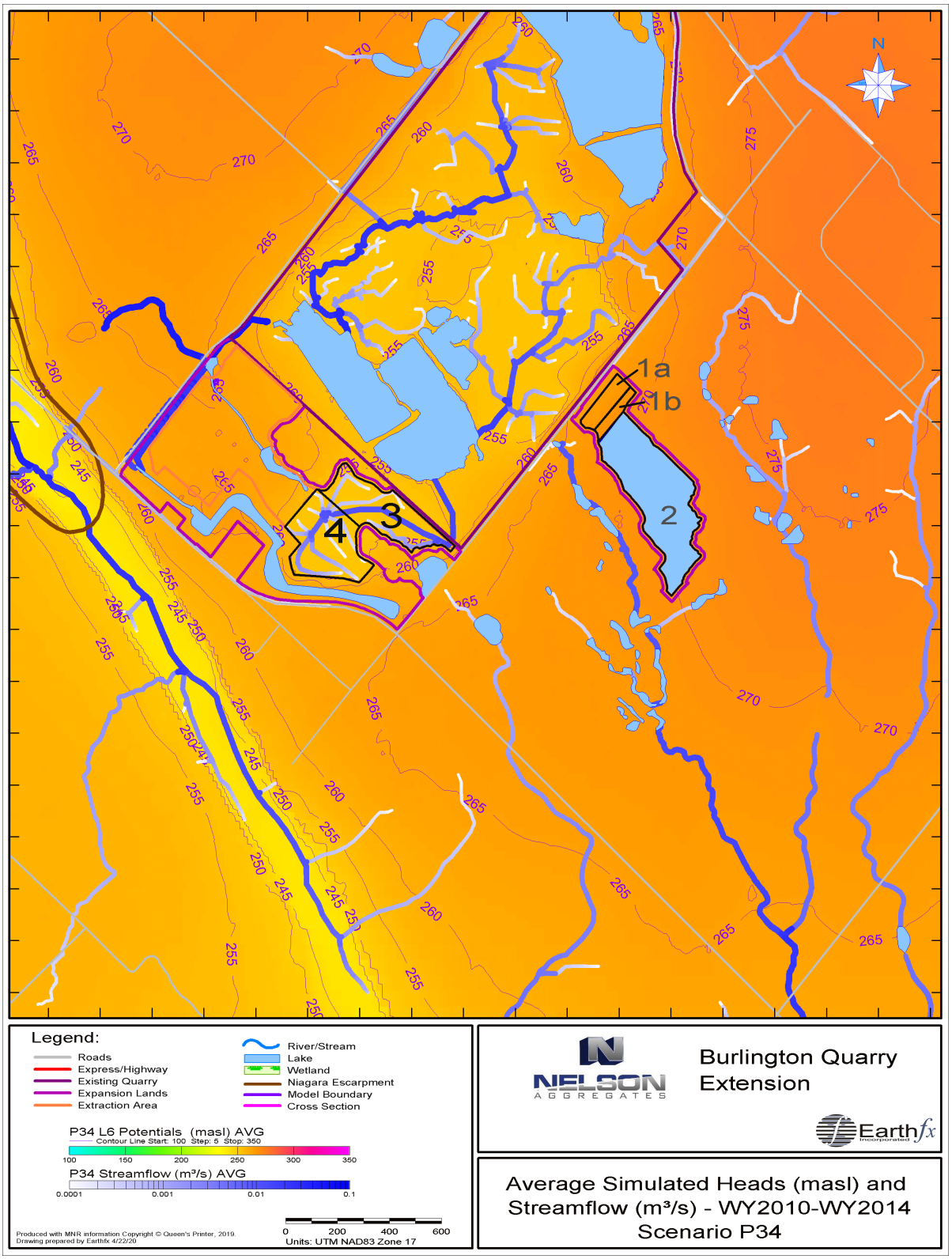

Figure 8.39: Average simulated heads in Model Layer 6 (masl) and streamflow (m^3/s) for WY2010 to WY2014 under Scenario P34.

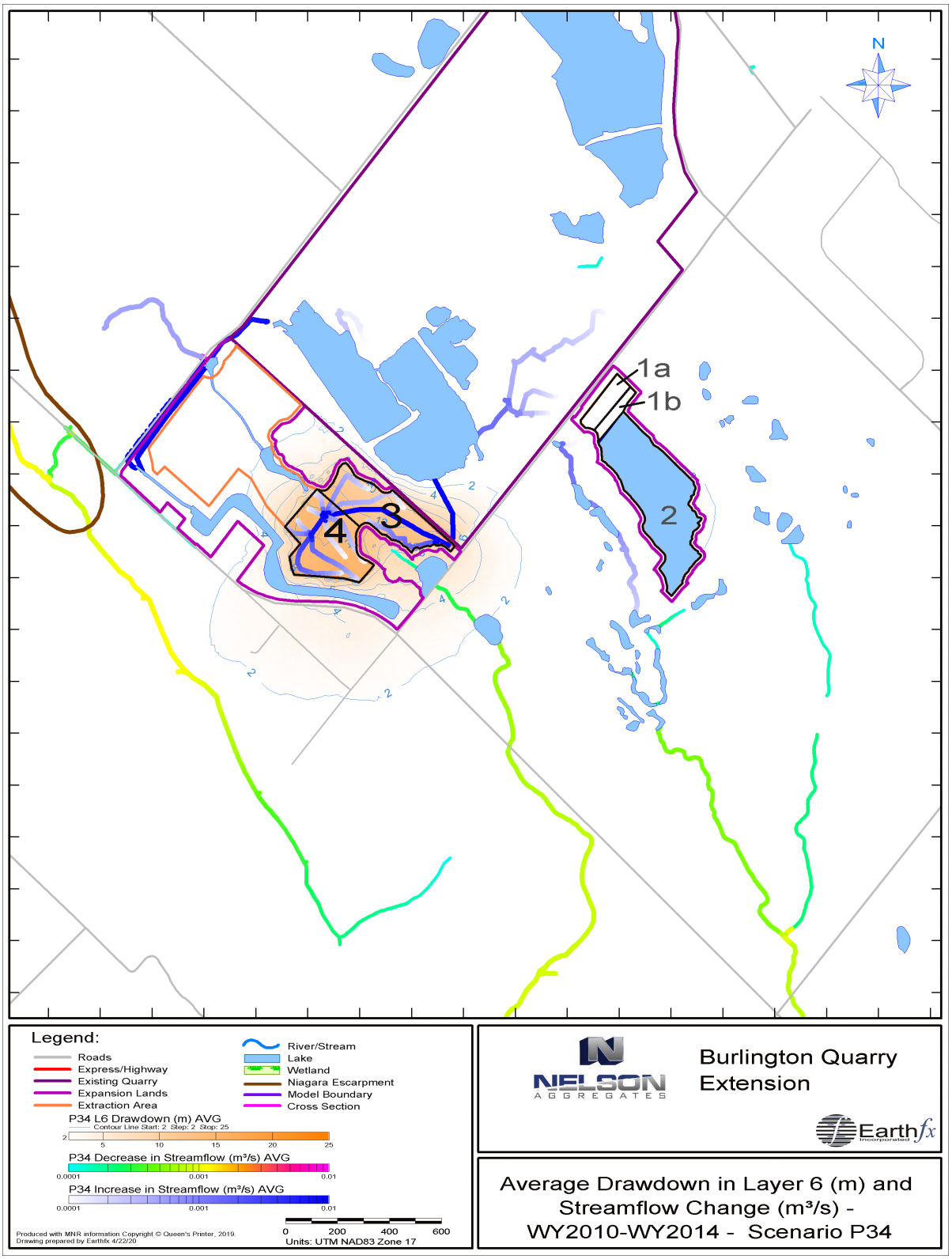

Figure 8.40: Average simulated drawdown in Model Layer 6 (m) and increase/decrease in streamflow (m^3/s) for WY2010 to WY2015 under Scenario P34.

8.7 Scenario P3456

Scenario P3456 represents the extraction of aggregate from the Phases 3 through Phase 6. For the purposes of this analysis, it is assumed that extraction is at its maximum depth and dewatering is ongoing in all four extraction areas. The final elevation of the quarry floor is 252.5 masl in the P3456 footprint. Quarry discharge is directed to the existing quarry lakes and eventually discharged from the Northwest sump. Figure 8.41 shows the modified topography and drainage in the quarry vicinity in the P3456 scenario.

As in P34, operations in Phase 1 and 2 are complete and the P12 excavation has filled to its natural elevation (see Figure 8.41). Water from quarry discharge at the northwest sump is still diverted to the infiltration pond between Cedar Springs Road and the extraction area (see Figure 8.41) to preserve the effect of the existing golf course ponds.

Land use and soil class were modified in the P3456 extraction footprint (changing from a variety of classes to “Quarry”) and in the P12 footprint (from Quarry to “Open Water”). All the soil and land use-based PRMS model parameter values were updated. Topography, slope, and aspect were also adjusted in both areas. Quarry floor drains and conduit stream types were added to the SFR2 module to convey quarry discharge from P3456 to the quarry lakes and drains were removed from P12. MODFLOW layer geometry was modified in the P3456 and P12 areas and the P12 Lake and infiltration ponds were added to the LAK3 module and the golf course ponds were removed. Stage in the P12 lake averaged 270.0 masl. A new cascade network was generated to account for the new stream network, lakes, and topography.

The GSFLOW model was run with the modified inputs for Scenario P3456 and model results were post-processed and compared to Baseline Conditions. The discussions below focus on the WY2014-2019 period which had the two dry years and showed the most significant change in heads, streamflow, and water budget components. Additional maps showing average drawdowns (i.e., changes in simulated heads) and average changes in stream flow and leakage are presented along with hydrographs showing changes in daily flows and groundwater levels.

8.7.1 P3456 Drawdowns and Surface Water Flows

Figure 8.42 shows the average simulated heads in Model Layer 6, representing the middle fracture zone in the Amabel aquifer and average simulated streamflow for the same period under Scenario P3456. Figure 8.43 shows the average simulated drawdown in Model Layer 6. The water levels rise rapidly with distance from the excavation, and exhibit less than 2.0 m of drawdown at a distance of 500 m from the active face.

Under this scenario, discharge continues to the north from Sump 0100 and to the south from Sump 0200 as per the recommendations presented in the Tatham (2020) and Savanta (2020) reports.

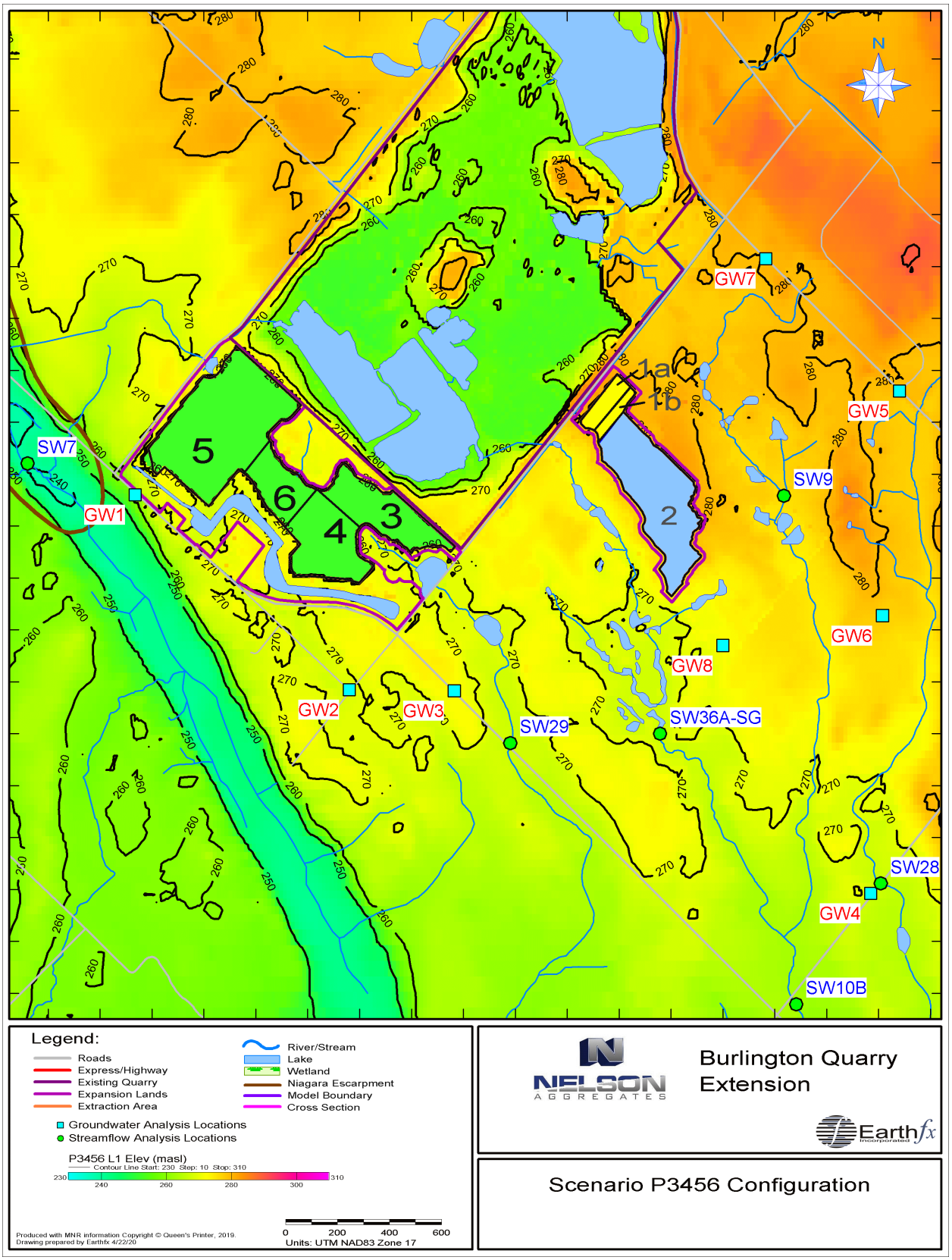

Figure 8.41: Scenario P3456 configuration.

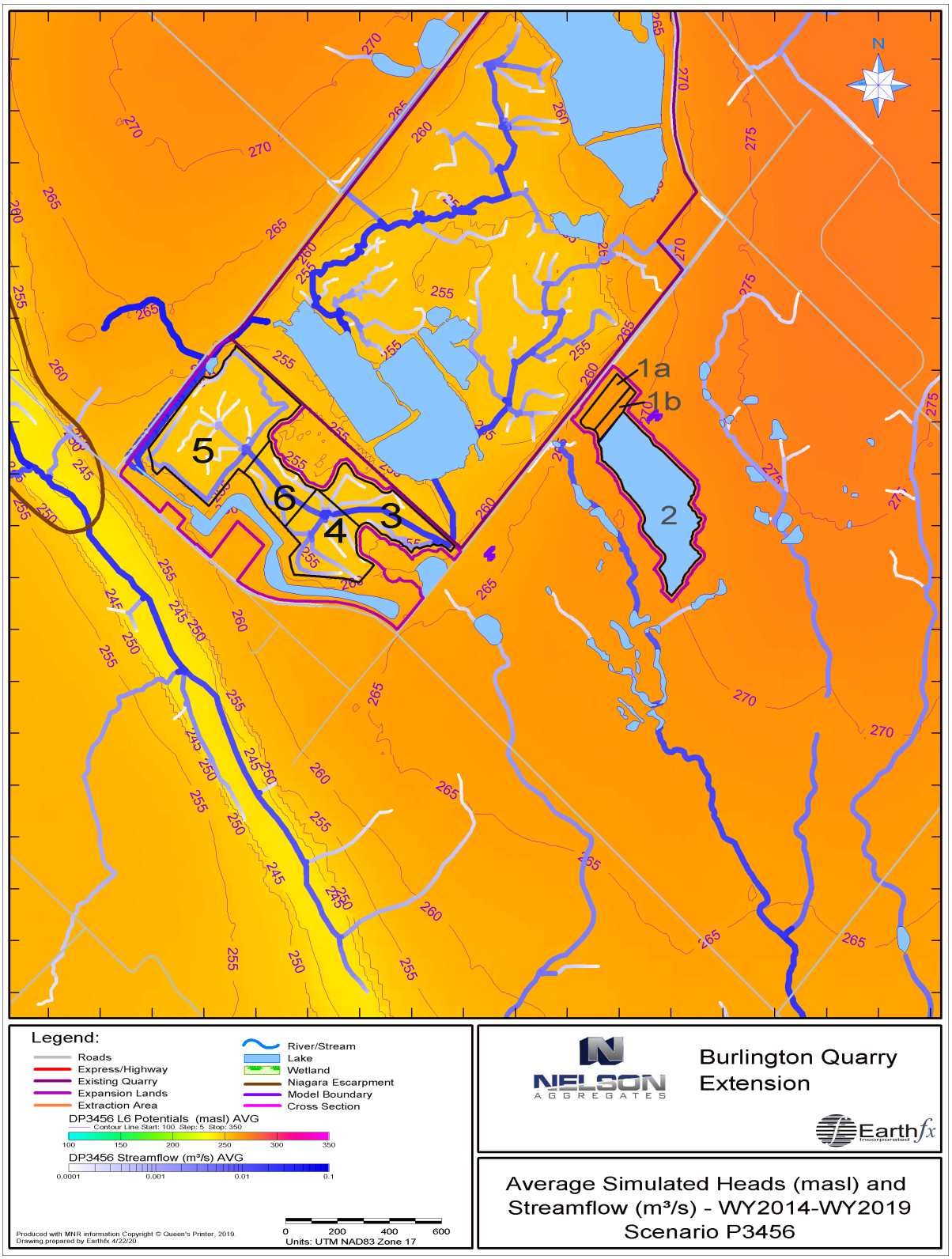

Figure 8.42: Average simulated heads in Model Layer 6 (masl) and streamflow (m^3/s) for WY2010 to WY2014 under Scenario P3456.

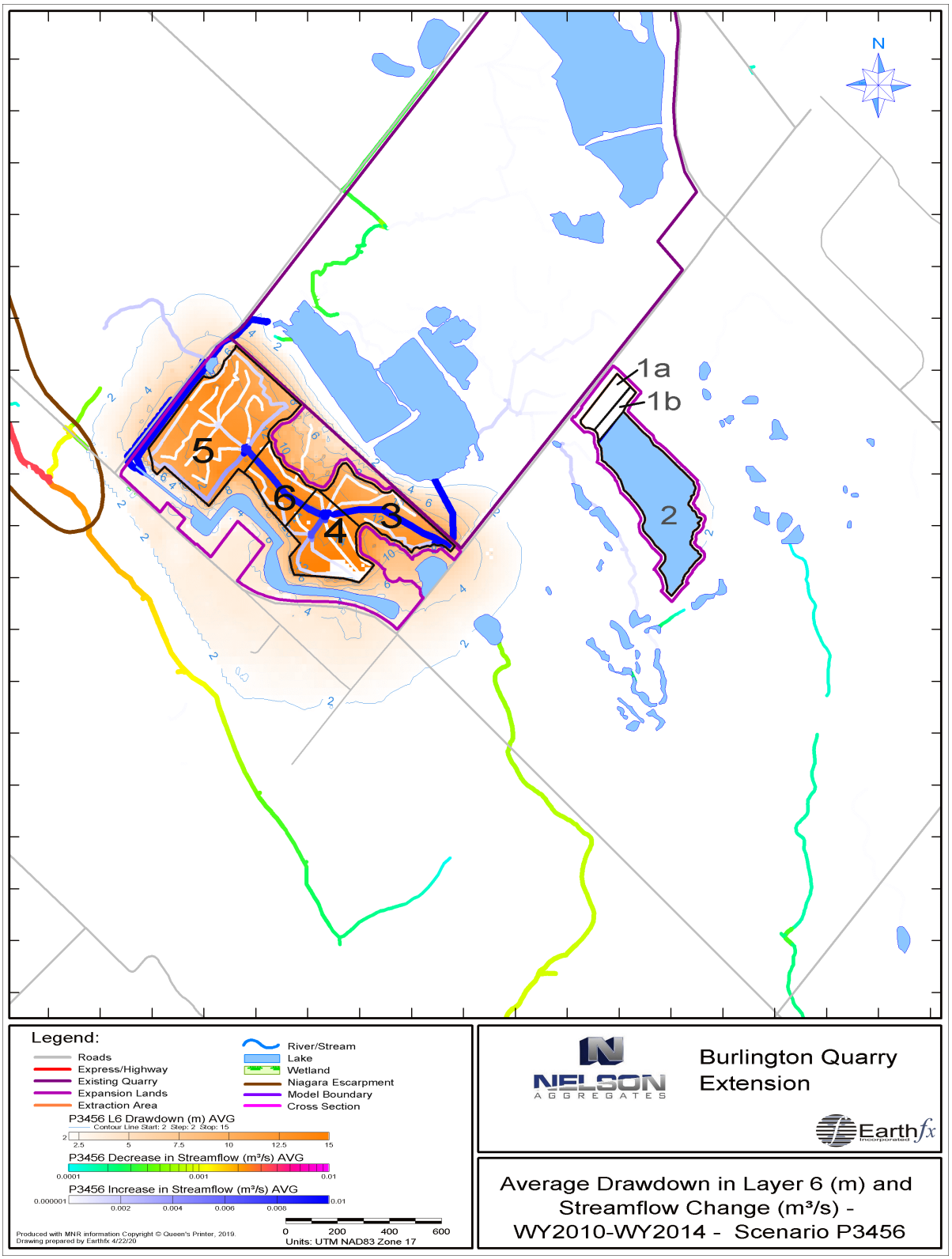

Figure 8.43: Average simulated drawdown in Model Layer 6 (m) and increase/decrease in streamflow (m^3/s) for WY2010 to WY2014 under Scenario P3456.

Figure 8.43 also shows the average simulated change in streamflow. Increases in simulated flow occur within the P3456 area, at the Northwest sump, and in the conduits carrying flow to the infiltration pond. Decreases in simulated flow occur in the Medad Valley, and other streams in the P12 east area show small decreases in average flow compared to Baseline Conditions.

Figure 8.44 through Figure 8.49 show hydrographs comparing simulated daily streamflow under Scenario P3456 to Baseline Conditions, in m^3/s, for the six streamflow analysis points (locations shown in Figure 8.41). (Note that the first year of data in these hydrographs may be affected by model spin-up.) Changes in streamflow on shown inverted on the secondary y-axis. Flows at SW36A and SW10B show small increases in baseflow, due to leakage from the lake in P12 to the main quarry drains, as well as small decreases in peak flows. The other stations show very small decreases in baseflow and small losses during storm or snowmelt events.

8.7.2 P3456 Seasonal and Inter-annual Groundwater Levels

Figure 8.50 through Figure 8.57 show the simulated transient heads in Model Layer 6, representing the middle fracture zone in the Amabel aquifer, for WY2014 to WY2019 for the eight assessment points, respectively (locations shown in Figure 8.41). Drawdowns are also shown on the hydrographs (on the inverted secondary y-axis). (The first year of data in these hydrographs may be affected by model spin-up.) Maximum daily drawdowns occur at GW2 (3.8 m), close to the Phase 4 extraction area. Maximum daily drawdowns at GW1 and GW3, also close to the Phase 3456 extraction area, are about 2.2 and 2.4 m, respectively. As noted, the drawdowns decrease sharply with distance from the P3456 footprint. Maximum daily drawdowns range from 0.7 to 1.2 m for the other assessment points.

The heads at most assessment points reach a minimum in the fall of 2015 in response to the lower than average precipitation in WY2015, and reach a similar low in fall of 2016, even though it was a wetter year, because of depletion of groundwater storage in the previous year.

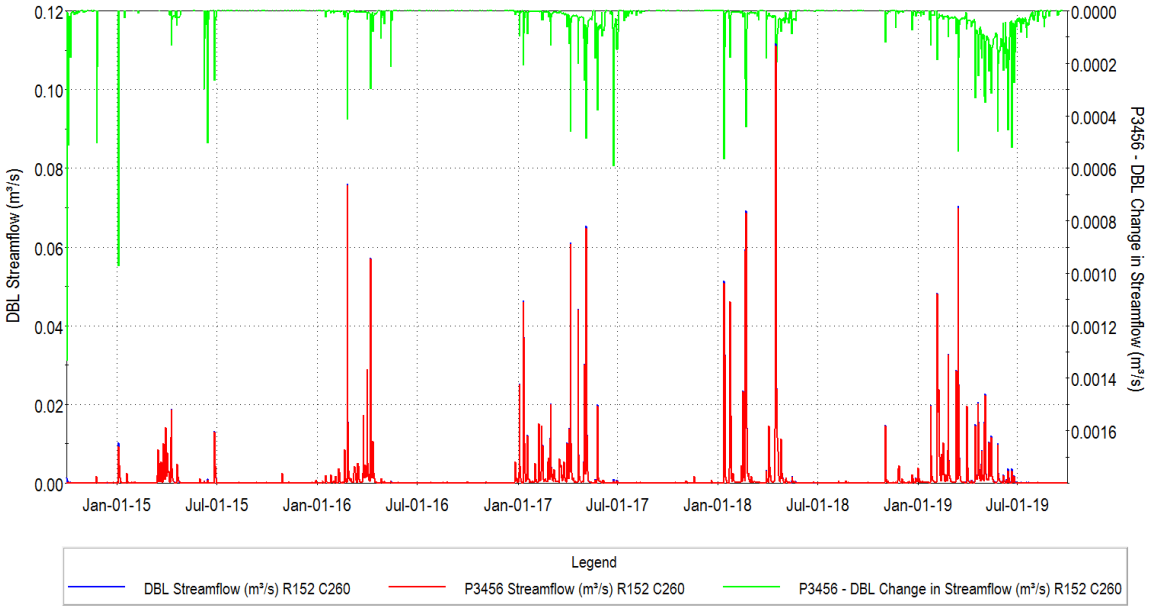

Figure 8.44: Simulated streamflow at SW09 for WY 2014-2019 – P3456 and Baseline Conditions.

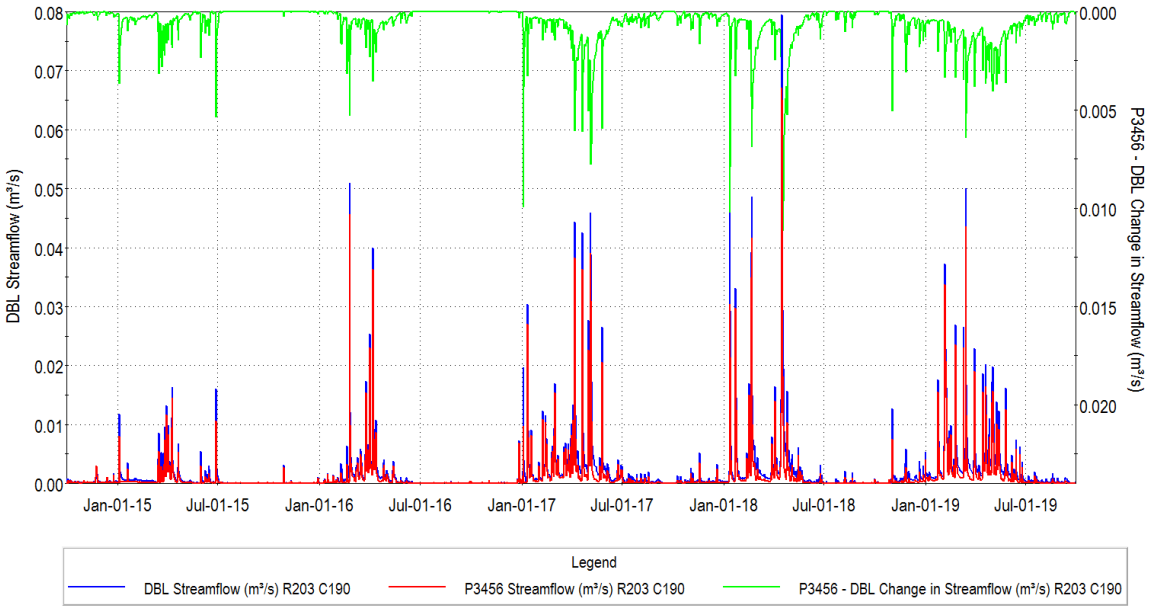

Figure 8.45: Simulated streamflow at SW29 for WY 2014-2019 – P3456 and Baseline Conditions.

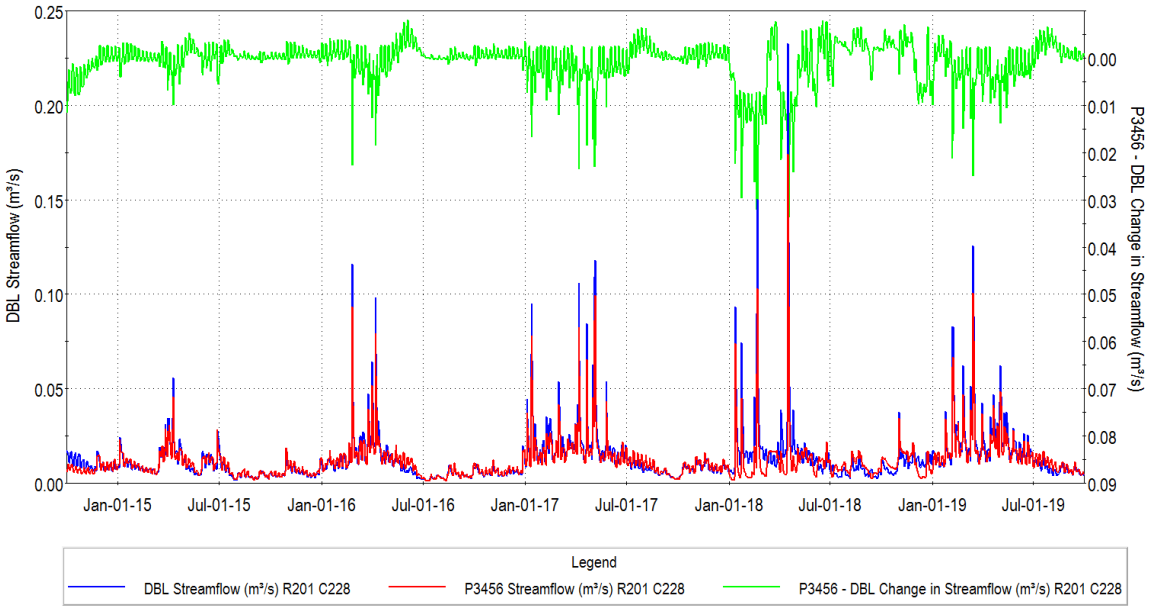

Figure 8.46: Simulated streamflow at SW36A for WY 2014-2019 – P3456 and Baseline Conditions.

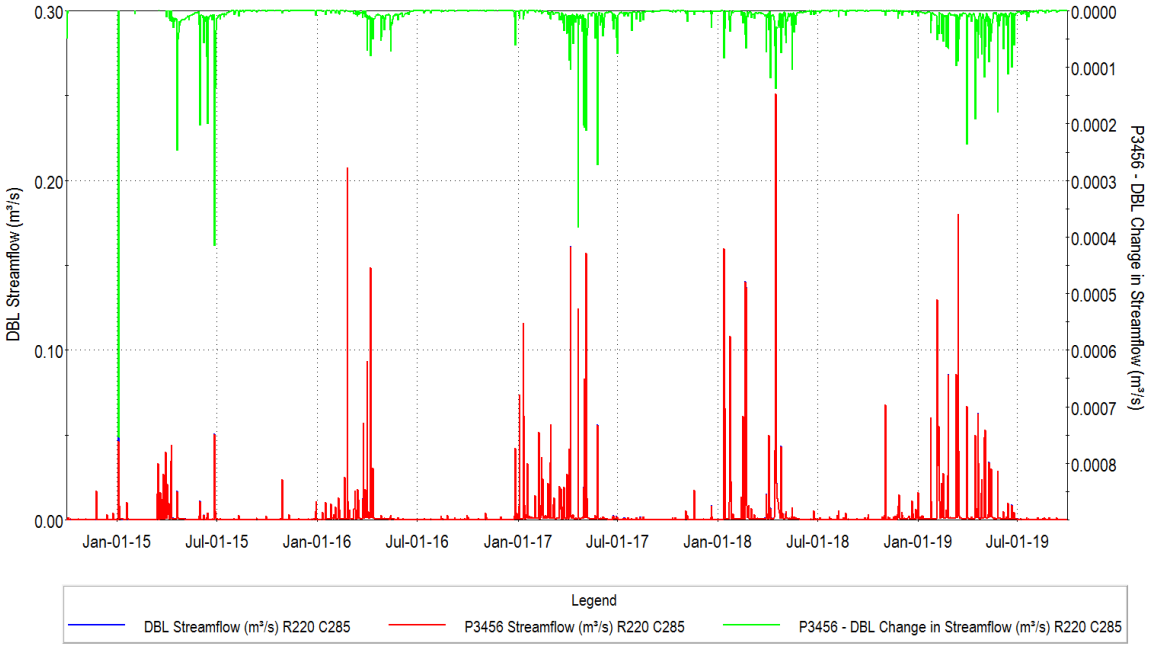

Figure 8.47: Simulated streamflow at SW28 for WY 2014-2019 – P3456 and Baseline Conditions.

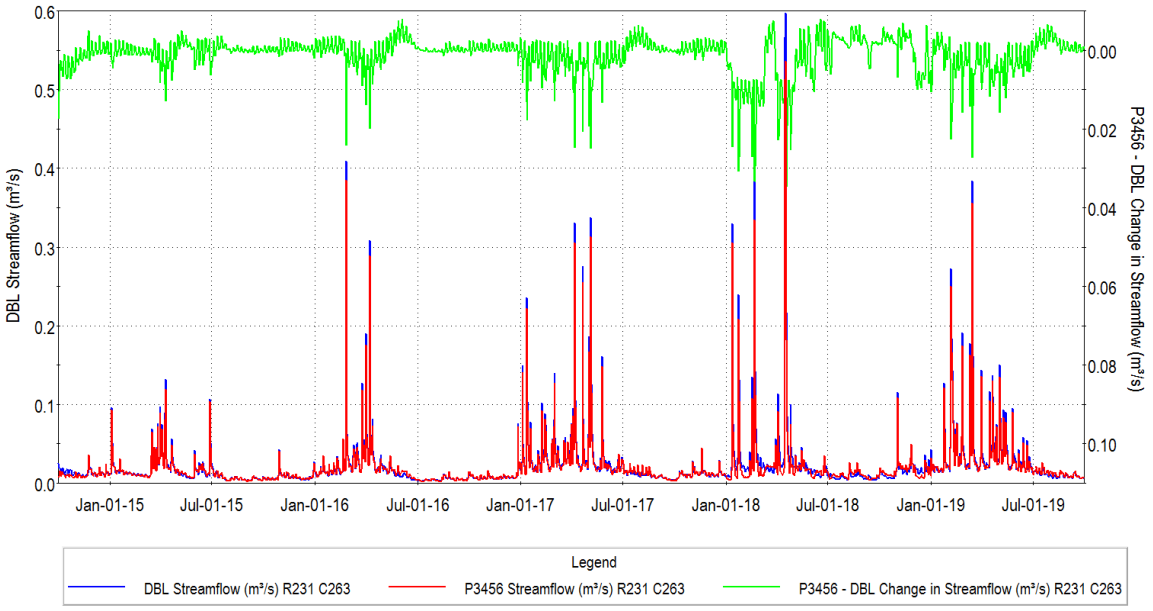

Figure 8.48: Simulated streamflow at SW10B for WY 2014-2019 – P3456 and Baseline Conditions.

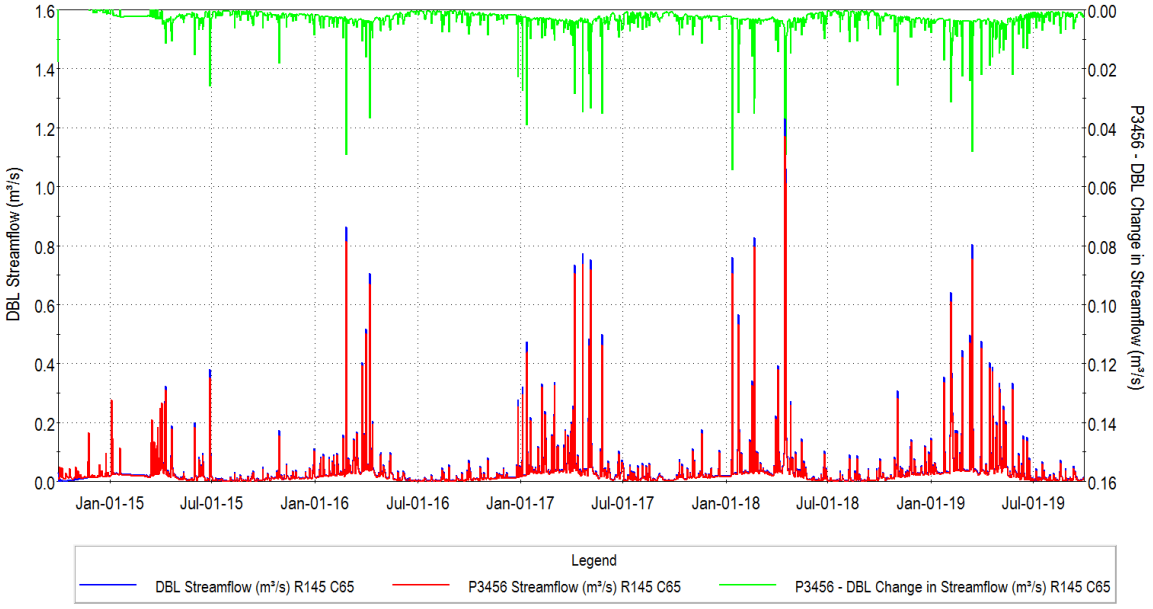

Figure 8.49: Simulated streamflow at SW07 for WY 2014-2019 – P3456 and Baseline Conditions.

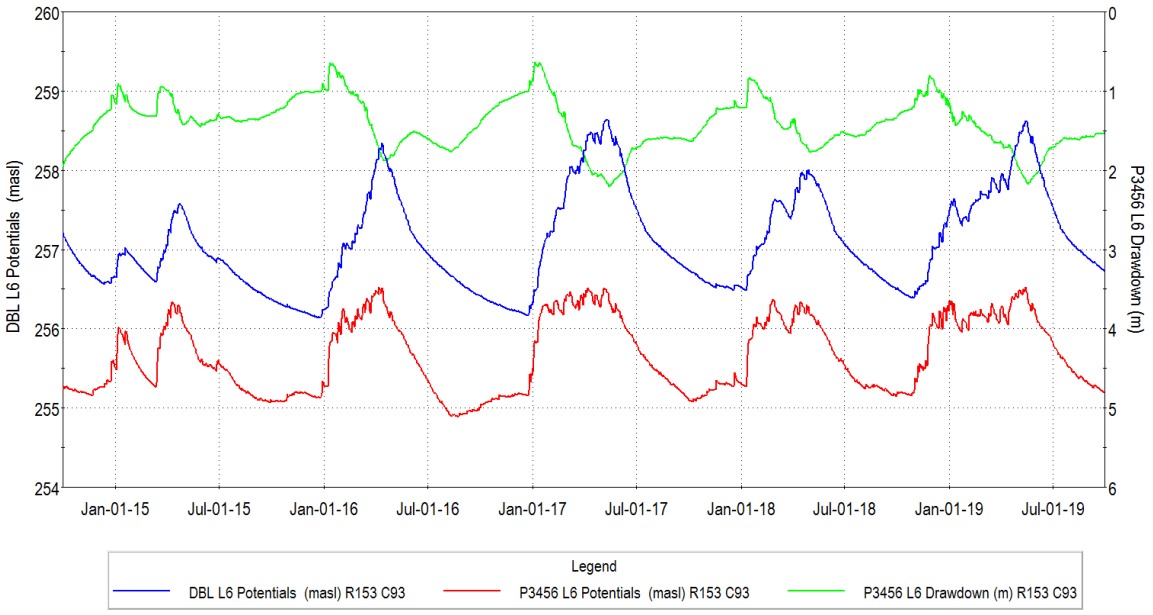

Figure 8.50: Simulated heads and drawdowns in Model Layers 6 at GW1 for WY 2014-2019 - P3456 and Baseline Conditions.

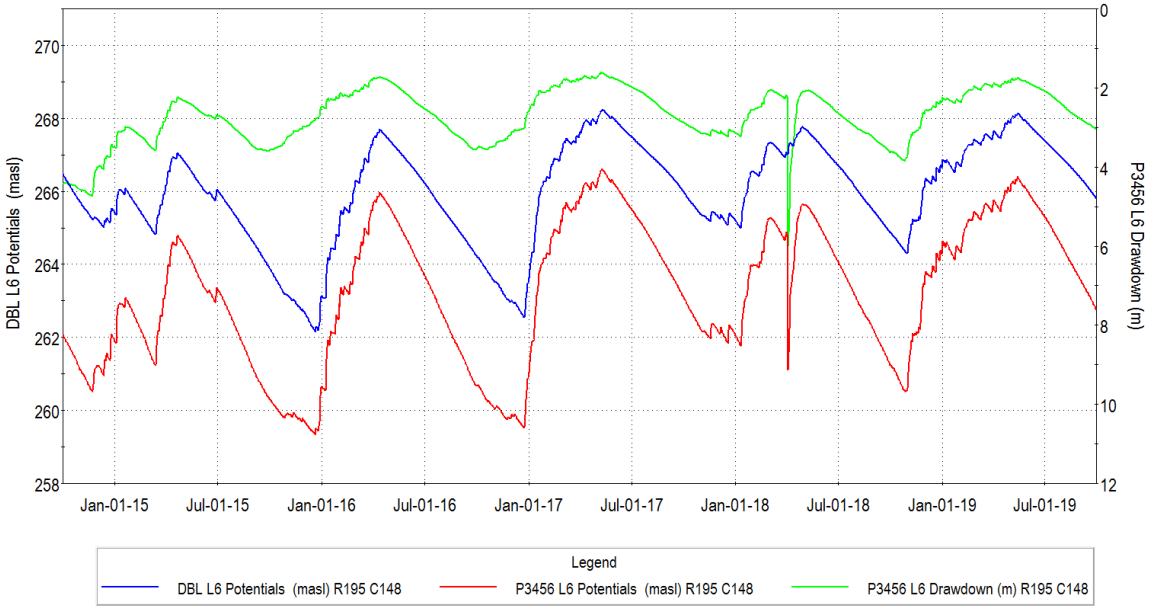

Figure 8.51: Simulated heads and drawdowns in Model Layers 6 at GW2 for WY 2014-2019 - P3456 and Baseline Conditions.

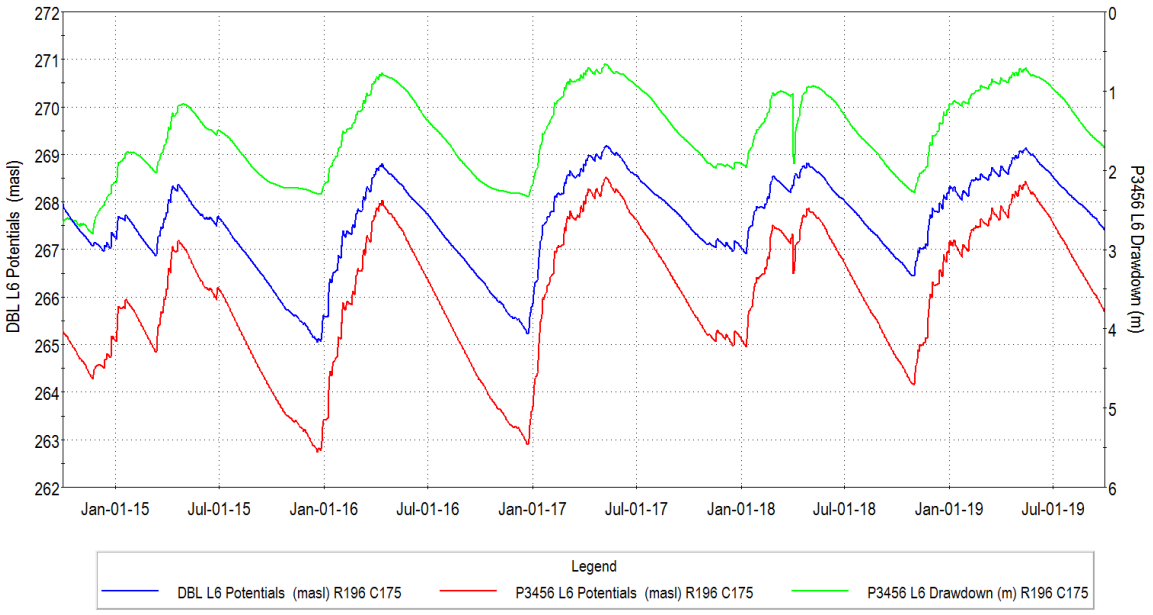

Figure 8.52: Simulated heads and drawdowns in Model Layers 6 at GW3 for WY 2014-2019 - P3456 and Baseline Conditions.

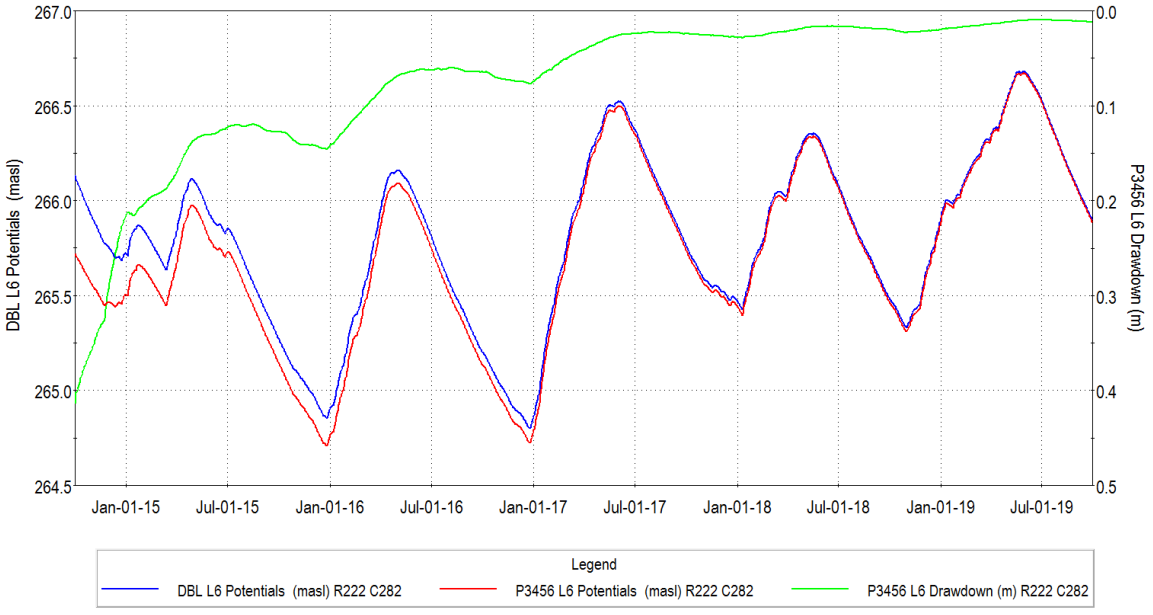

Figure 8.53: Simulated heads and drawdowns in Model Layers 6 at GW4 for WY 2014-2019 - P3456 and Baseline Conditions.

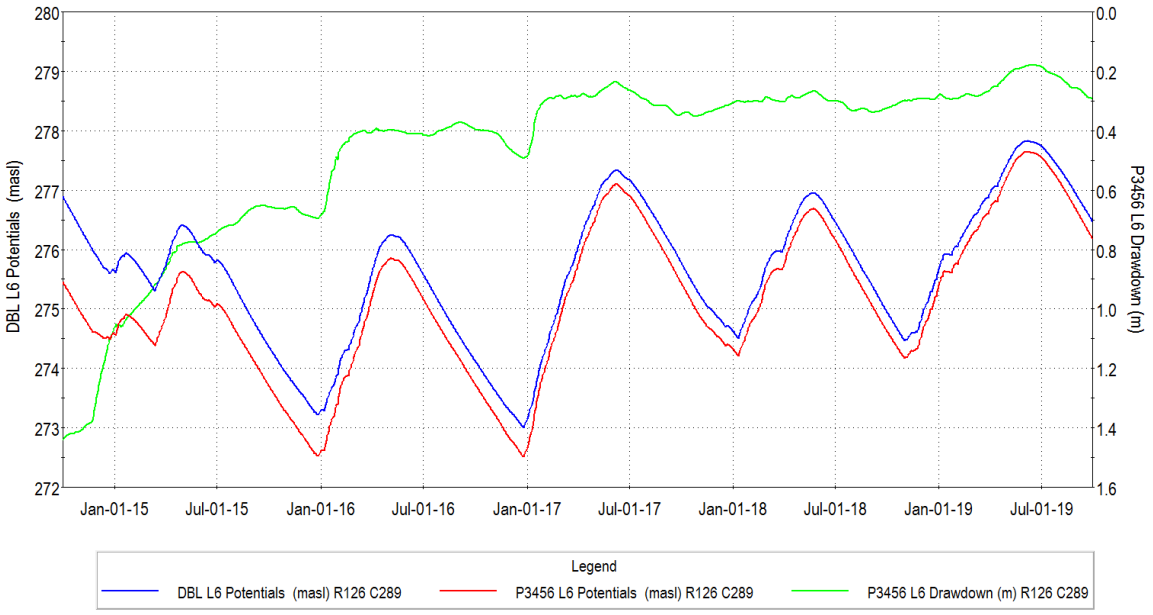

Figure 8.54: Simulated heads and drawdowns in Model Layers 6 at GW5 for WY 2014-2019 - P3456 and Baseline Conditions.

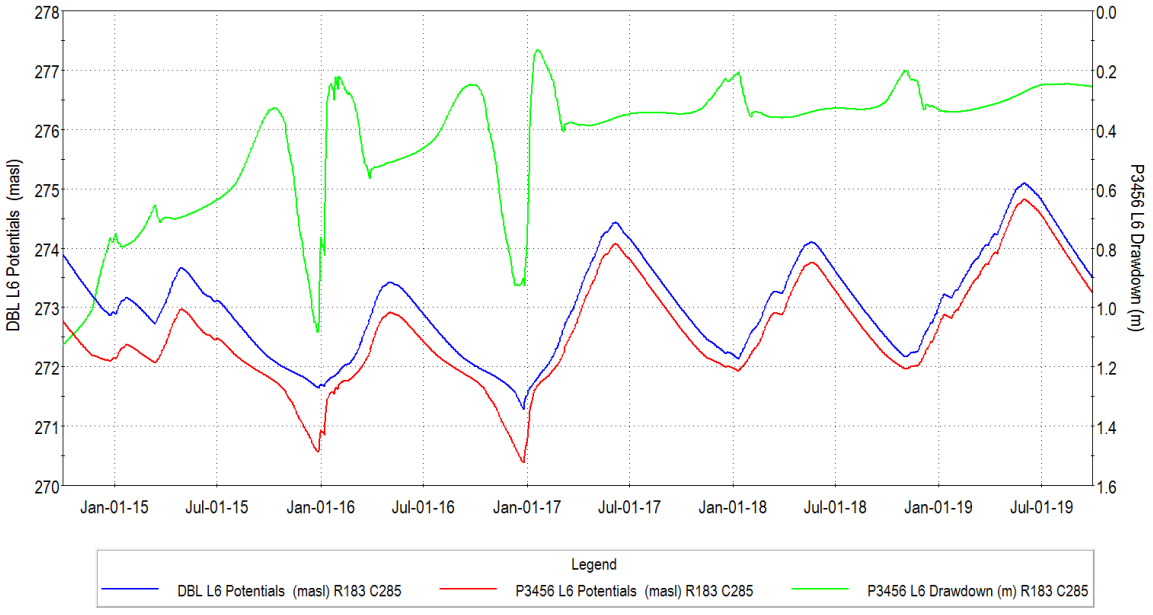

Figure 8.55: Simulated heads and drawdowns in Model Layers 6 at GW6 for WY 2014-2019 - P3456 and Baseline Conditions.

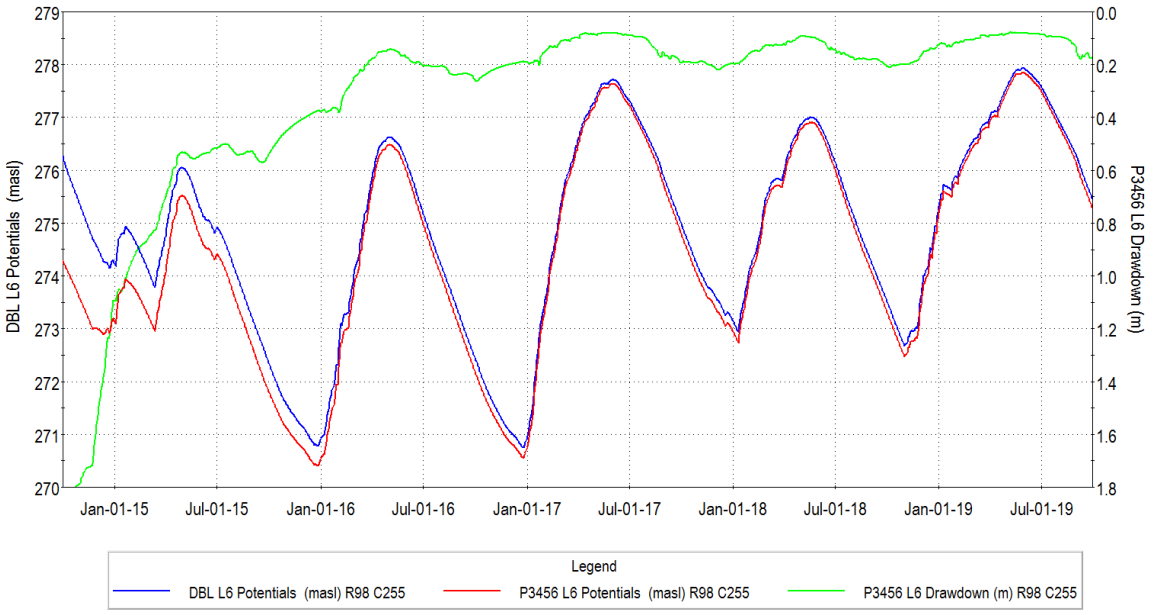

Figure 8.56: Simulated heads and drawdowns in Model Layers 6 at GW7 for WY 2014-2019 - P3456 and Baseline Conditions.

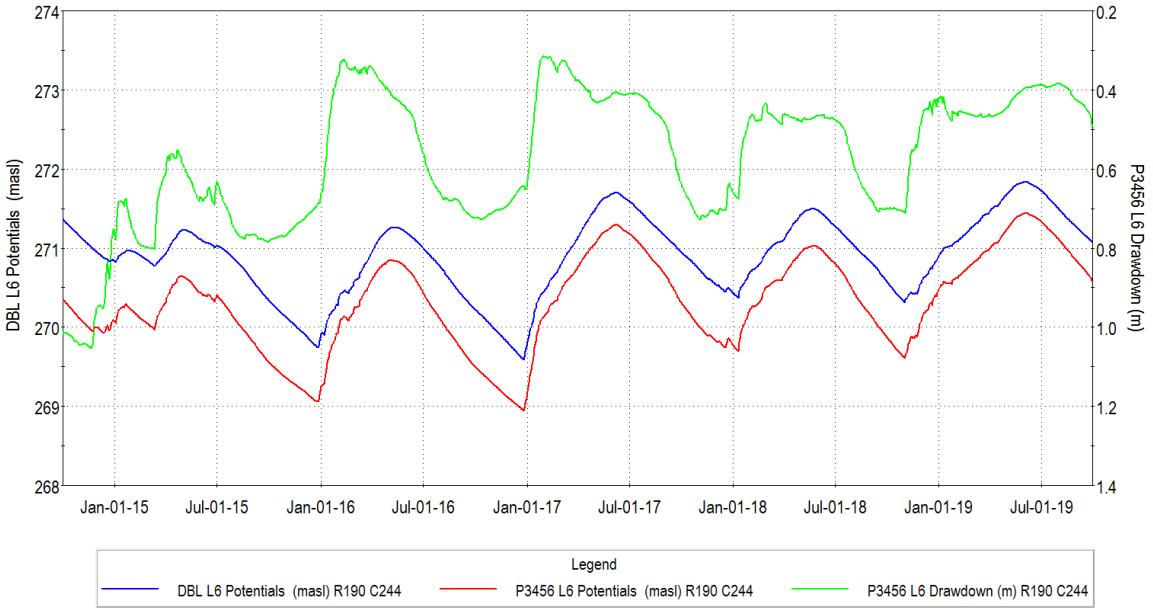

Figure 8.57: Simulated heads and drawdowns in Model Layers 6 at GW8 for WY 2014-2019 - P3456 and Baseline Conditions.

8.7.3 P3456 Surface Water/Groundwater Interaction

Figure 8.58 shows the average simulated net groundwater recharge in the quarry vicinity for Scenario P3456. The decrease in recharge, compared to the Baseline Conditions (Figure 7.18) is focused on the P3456 extraction area where soils and land use parameters were changed. Similarly, Figure 8.59 shows that average simulated groundwater ET has increased in the P3456 footprint, compared to the Baseline Conditions (Figure 7.19), because of the removal of the golf course sediments.

Figure 8.60 presents the average simulated streamflow loss to groundwater (blue areas) and the areas of groundwater discharge to streams (red areas). Little change is seen compared to the Baseline Conditions (Figure 7.21), except in the vicinity of tributaries on the west side of Medad Creek. Figure 8.61 presents the average simulated groundwater discharge to the soil zone under Scenario P3456. The most significant change compared to the Baseline Conditions (Figure 7.20) is groundwater discharge within the P3456 footprint.

8.7.4 P3456 Wetland Water Budgets

Average water budgets were completed to analyze inflows and outflows to 22 local wetlands (locations shown in Figure 7.22). All flows within each area are computed as well as lateral groundwater flow, streamflow, overland runoff, and interflow crossings the wetland area boundaries. Figure 8.62 through Figure 8.69 present schematics showing detailed water budgets for wetland areas 9, 16, 17, 18, 19, 20, 21, and 22, respectively. The water budgets were compiled for WY2010 to 2014. These can be compared with Figure 7.23 through Figure 7.30 for Baseline Conditions averaged over the same period.

The wetlands are located at various distances from the existing quarry and the extension areas. Wetland 22 is located between the P3456 extraction area and the existing quarry. This wetland had no change in the water budget compared to baseline conditions because it is perched year-round and there was no change in the contributing area.

Wetland 21 is located at the south edge of the West Extension area, and its function is impaired by the road and a limited culvert, so its baseline function and water budget are compromised. This wetland will receive a review and supplemental inflows, as described in the Tatham, 2020 report. The planned supplementation has not been represented in the model, so the Wetland 21 water budget is not representative of future conditions.

The effects of P3456 on the wetlands in the vicinity of the excavation has been fully quantified by the water budget analysis. Under baseline conditions, none of the wetlands receive more than 3.0% of their total inflows from the groundwater system (Table 8.6). Under P3456 conditions, the P12 excavation has been filled with water and the water table has recovered to a new level consistent with the P12 lake. This recovery has restored a degree of groundwater discharge to the wetlands in the vicinity of P12. For example, Wetland 17 will receive 0.34% of its inflows from the groundwater system after infilling of P12. Both the predicted percent impacts, and predicted percent recovery levels, are so small as to be unmeasurable in the field.

Table 8.6: P3456 wetland water budget comparison.

Earthfx Wetland ID	MNRF ID	Baseline		P3456		Change in Water Budget P3456 -BL	
		GW Outflow %	GW Inflow %	GW Outflow %	GW Inflow %	Change in Outflow %	Change in GW Inflow %
9	13014	10.19%	0.00%	10.17%	0.00%	-0.02%	0.00%
16	13022	1.25%	0.34%	1.34%	0.00%	0.09%	-0.34%
17	13033	2.51%	1.31%	4.18%	0.34%	1.67%	-0.97%
18	na	5.98%	2.42%	7.11%	0.04%	1.13%	-2.38%
19	13032	19.82%	0.00%	19.79%	0.00%	-0.03%	0.00%
20	13037	12.84%	1.76%	16.29%	0.00%	3.45%	-1.76%
21	13201	29.78%	2.98%	51.69%	0.01%	21.91%	-2.97%
22	13200	26.31%	0.00%	26.31%	0.00%	0.00%	0.00%
Note:	GW Outflow = Groundwater outflows as a percentage of total outflows from the feature						
	GW Inflow = Groundwater inflows as a percentage of total inflows to the feature						

8.7.5 P3456 North Quarry Discharge and Infiltration Pond

The north quarry discharge passes through the Weir Pond (MNRF ID 13202); a non-provincially significant wetland pond immediately north of Phase 5. Discharge from this pond flows northward, through a karst conduit, and into the Medad valley stream network. Under current conditions this pond is also used to support golf course operations and, when necessary, a portion of the quarry discharge is diverted south through a ditch into the golf course pond system.

Under P3456 conditions, current levels of quarry discharge will continue to pass through this pond. Diversions for golf course operations will no longer be necessary, however a portion of flow will be diverted to the newly constructed infiltration pond, which will locally support groundwater levels in a similar manner to the current golf course ditch and pond system.

Under P3456 conditions, the pond and the stream reach flowing north of P5 will be within the drawdown cone of the P5 excavation (Figure 8.43). This will locally increase in leakage to groundwater from the pond and stream. Figure 8.60 presents the average simulated streamflow loss to groundwater (blue segments) and the areas of groundwater discharge to streams (red areas). A small increase in leakage is seen compared to the Baseline Conditions (Figure 7.21). The extra leakage to groundwater will ultimately discharge into the Medad Valley, however a portion will also recirculate back through the P5 excavation. The net effect is very small, and virtually all the water will end up in the Medad Valley in any case.

Stream Gauge SW07 (Figure 8.49) reflects most of the cumulative effects associated with the P3456 extension. Some of the changes in flow in P3456 will, however, appear in the Medad Valley just downgradient of SW07. Figure 8.49 shows that the predicted change in flow at SW07 is a slight reduction in peak flows in the winter and spring.

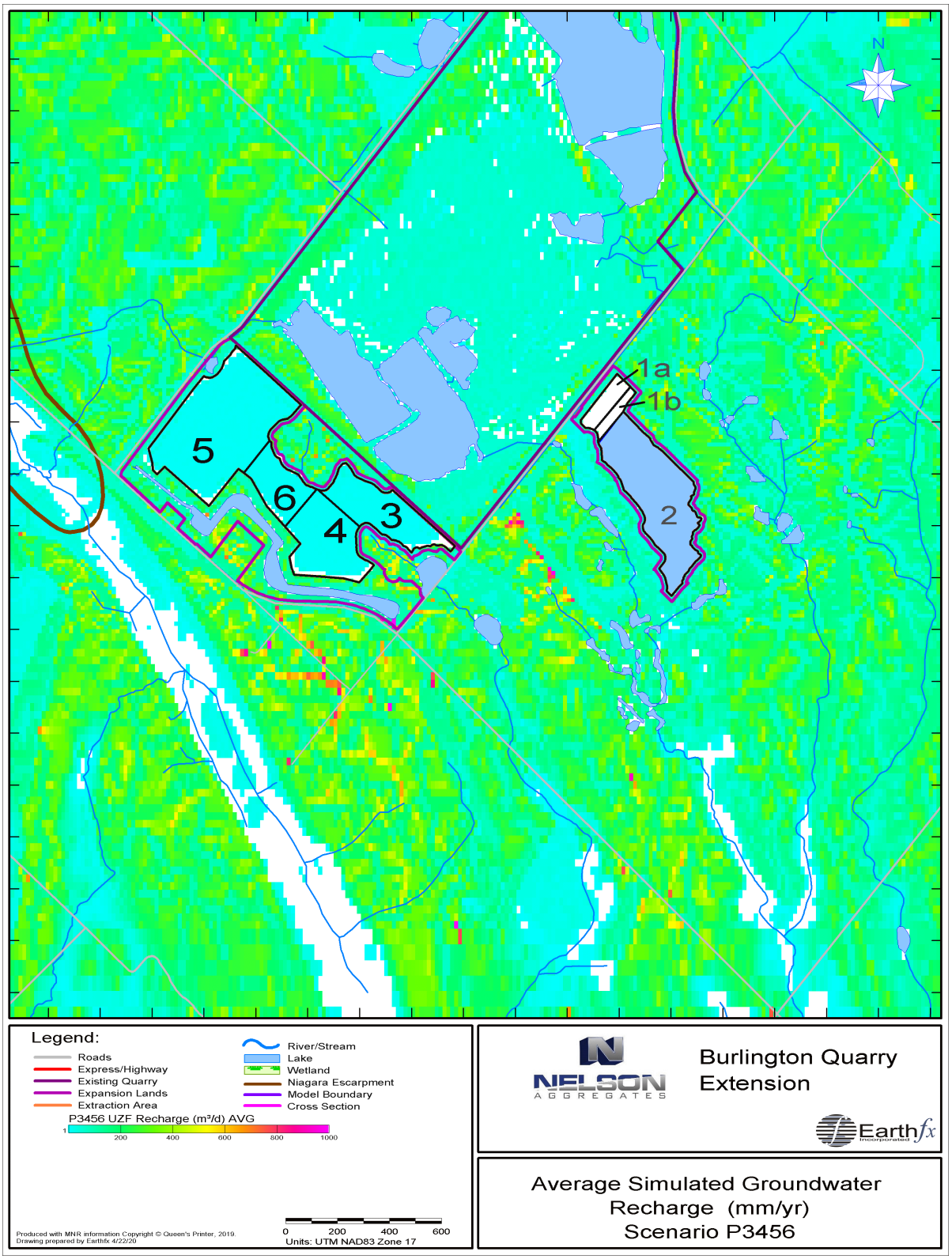

Figure 8.58: Average simulated groundwater recharge (mm/yr) for WY 2010-2014 – Scenario P3456.

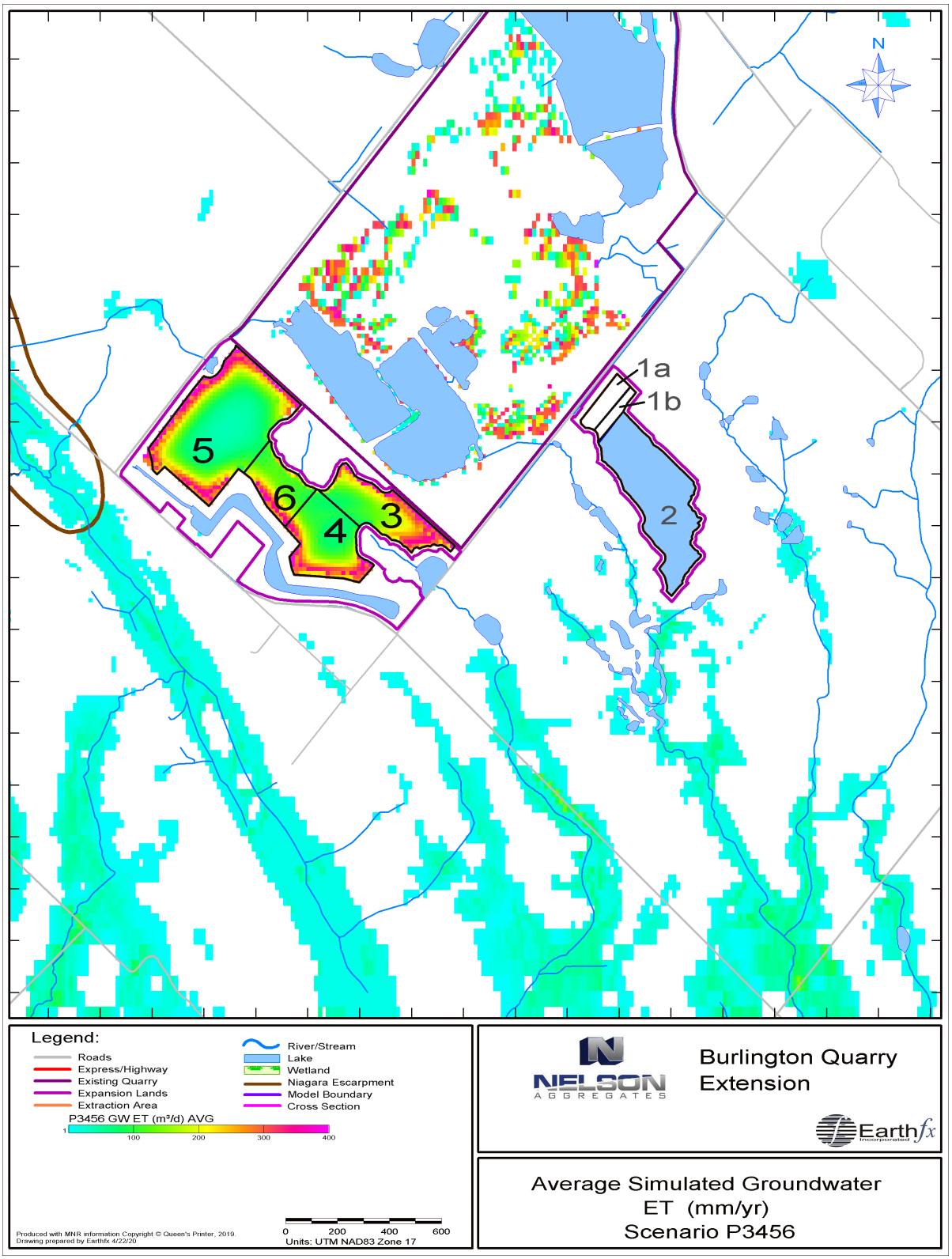

Figure 8.59: Average simulated groundwater ET (mm/yr) for WY 2010-2014 – Scenario P3456.

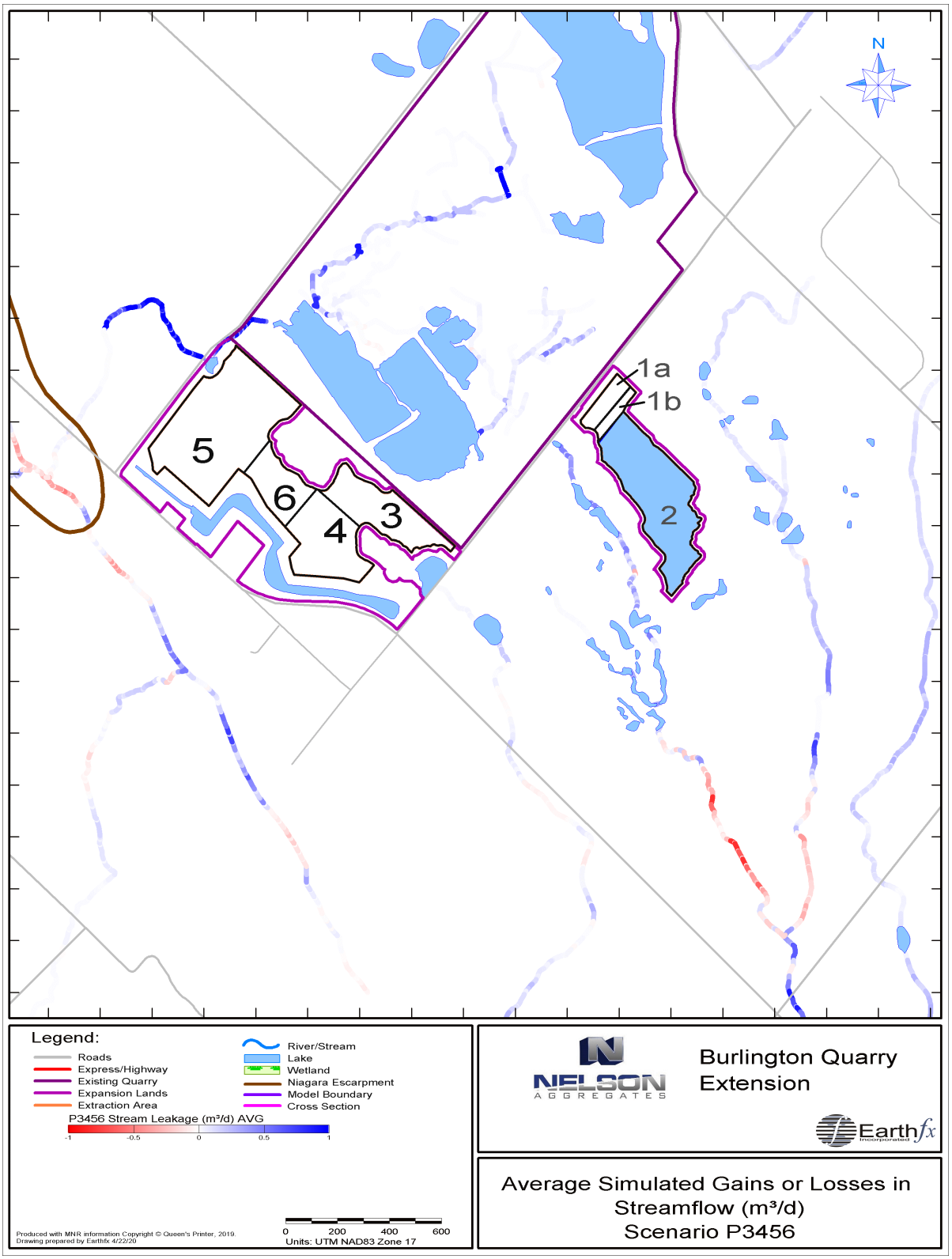

Figure 8.60: Average simulated streamflow loss to groundwater or groundwater discharge to streams (m^3/d) for WY 2010-2014 – Scenario P3456.

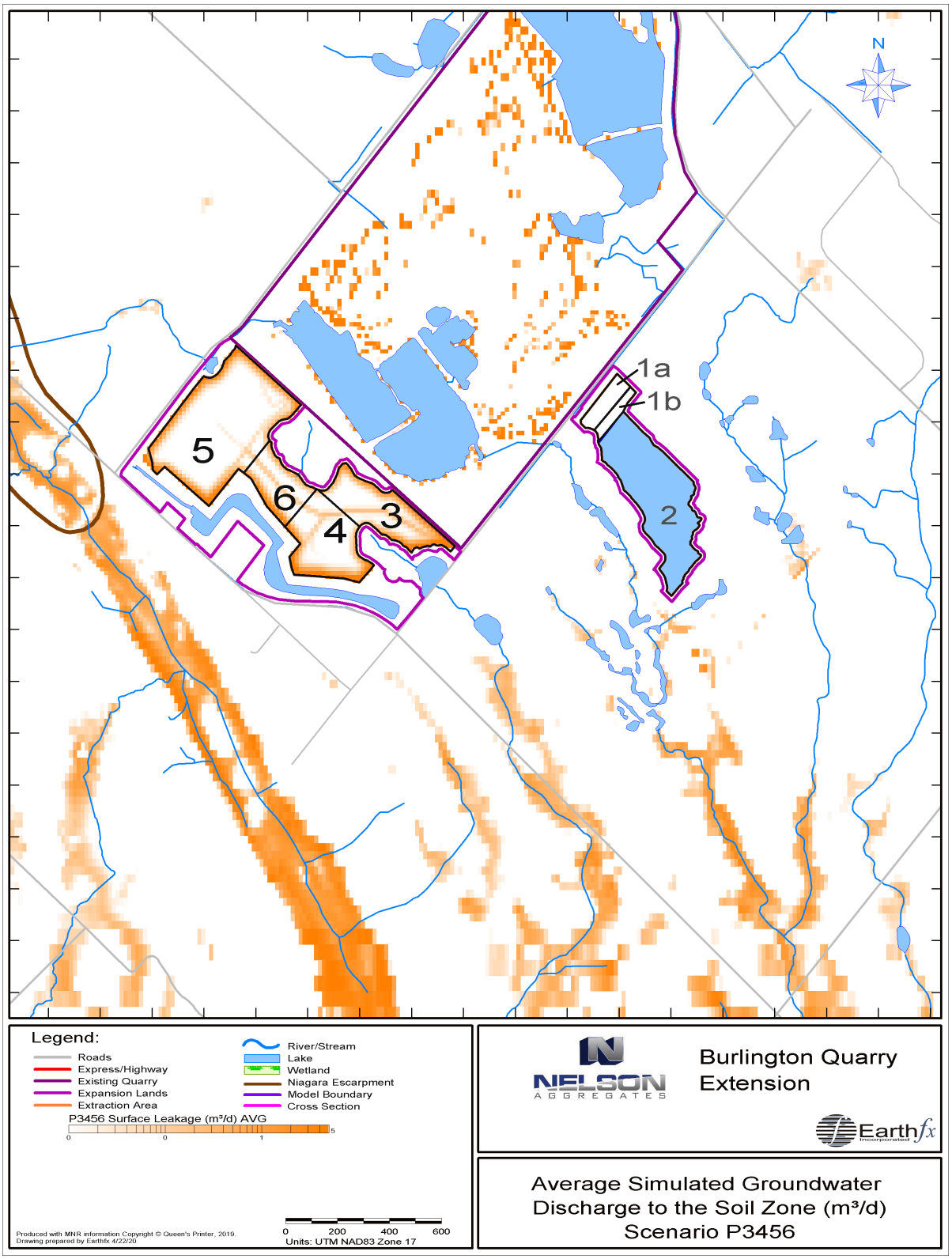

Figure 8.61: Average simulated groundwater discharge to the soil zone (m^3/d) for WY 2010-2014 – Scenario P3456.

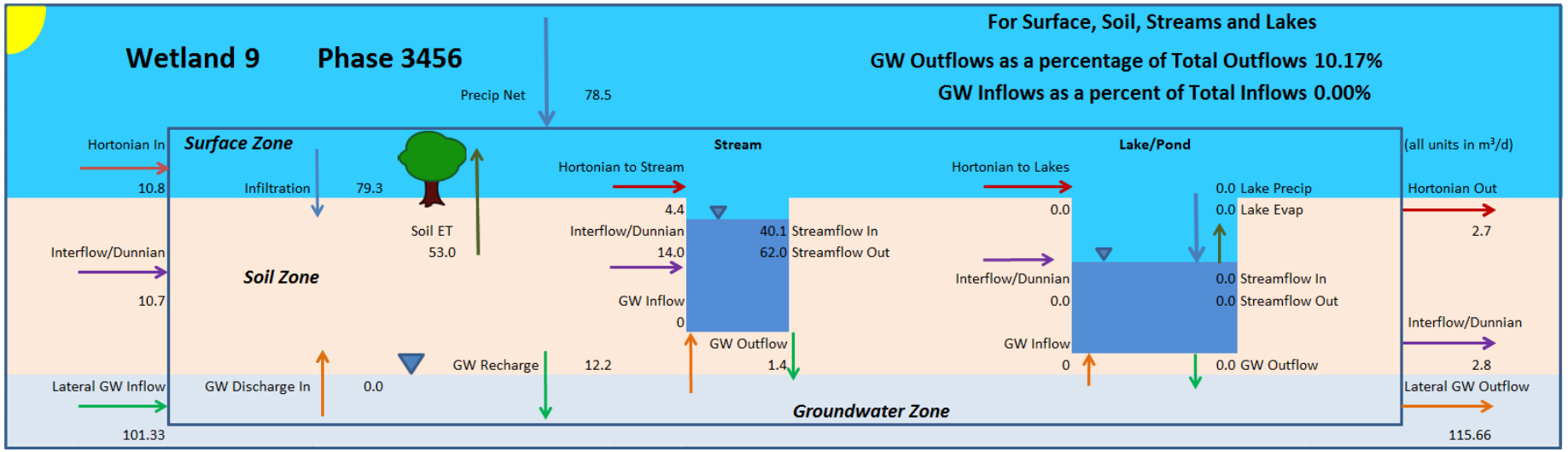

Figure 8.62: Detailed water budget for Wetland 9 averaged over WY2010 and WY2011 under Scenario P3456.

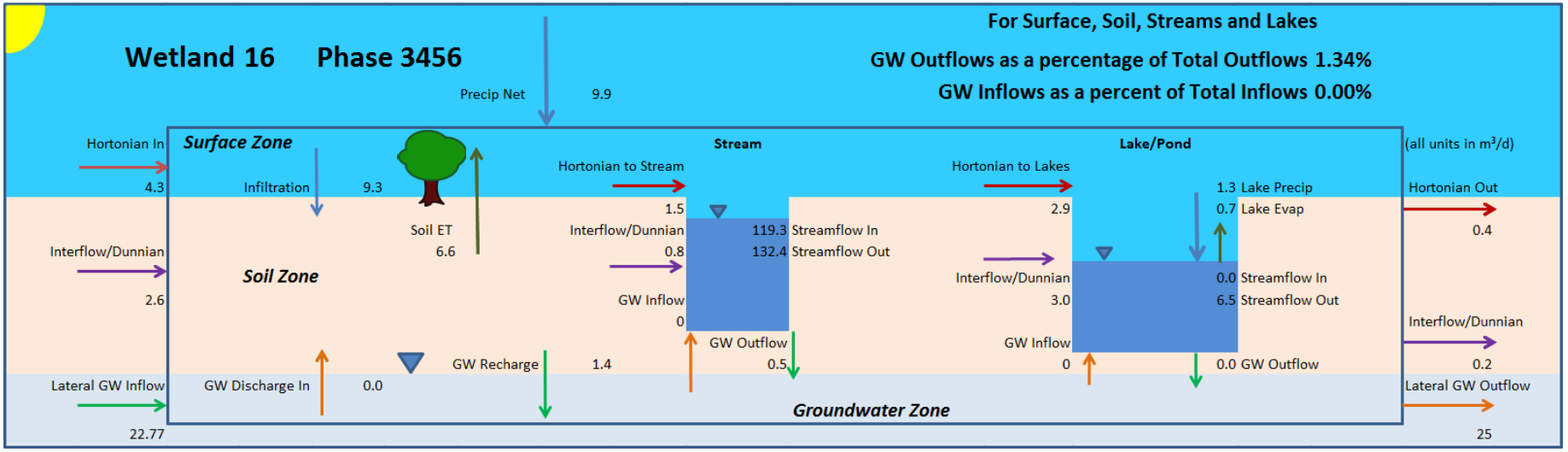

Figure 8.63: Detailed water budget for Wetland 16 averaged over WY2010 and WY2011 under Scenario P3456.

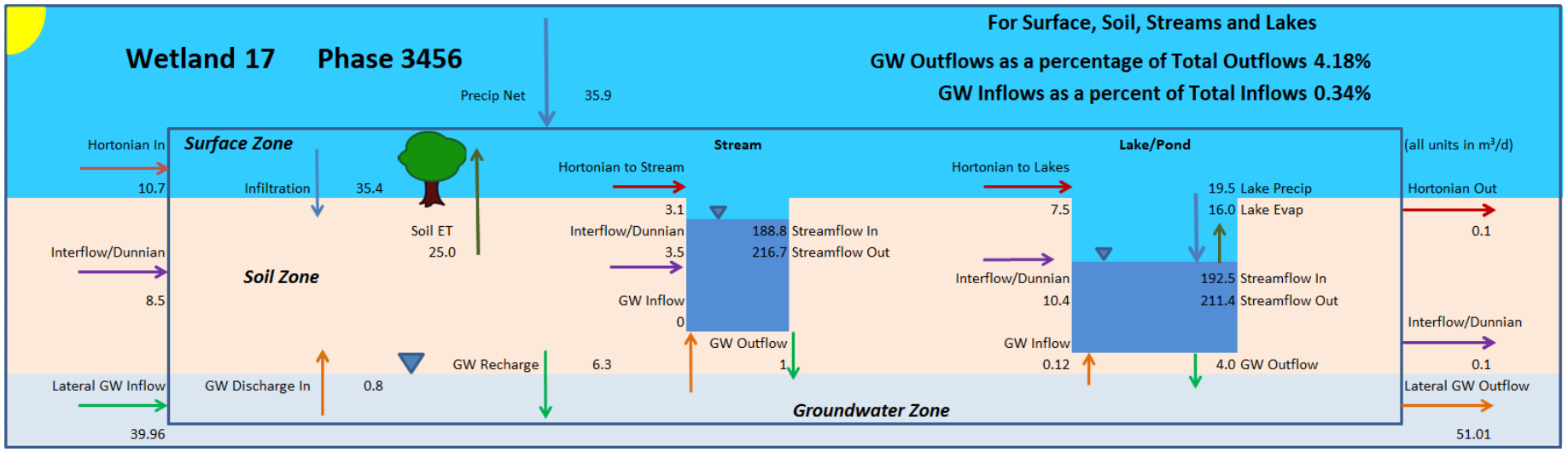

Figure 8.64: Detailed water budget for Wetland 17 averaged over WY2010 and WY2011 under Scenario P3456.

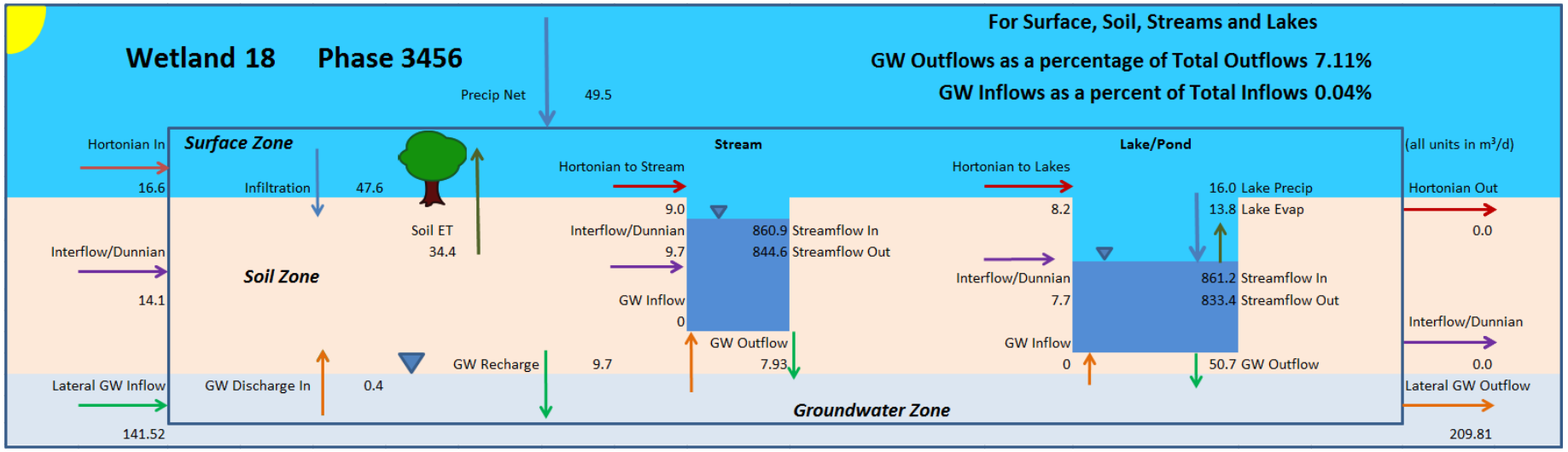

Figure 8.65: Detailed water budget for Wetland 18 averaged over WY2010 and WY2011 under Scenario P3456.

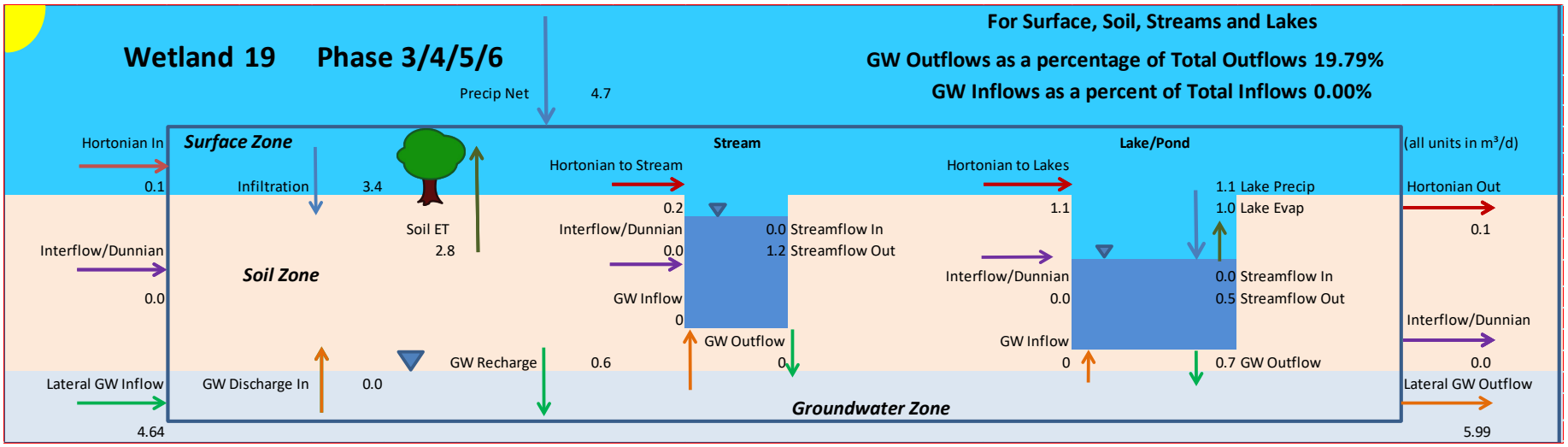

Figure 8.66: Detailed water budget for Wetland 19 averaged over WY2010 and WY2011 under Scenario P3456.

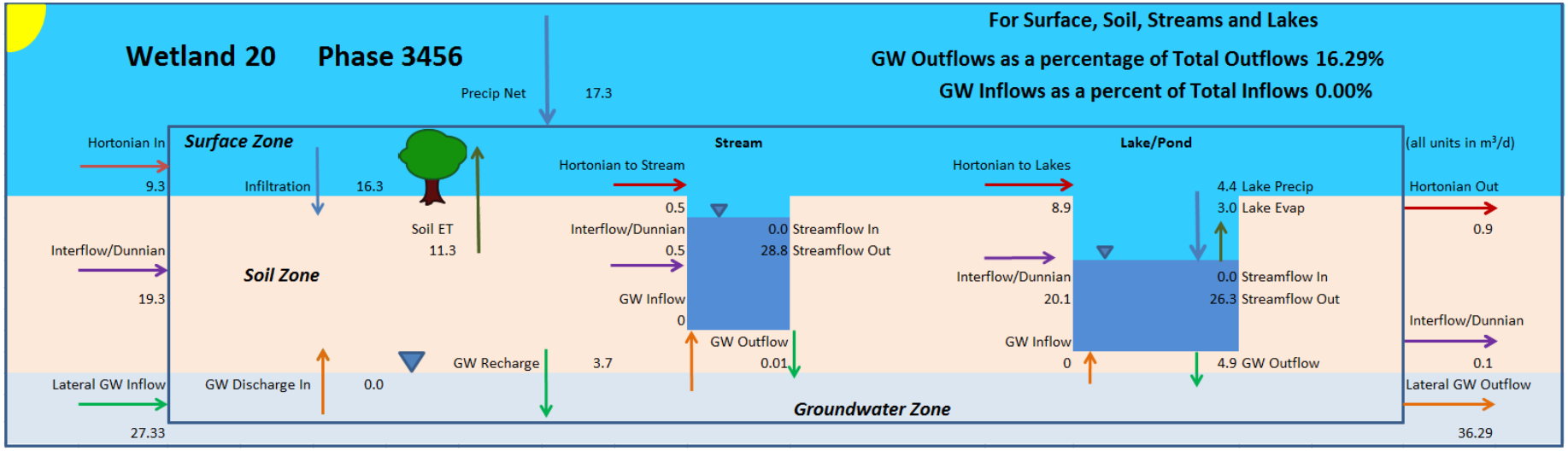

Figure 8.67: Detailed water budget for Wetland 20 averaged over WY2010 and WY2011 under Scenario P3456.

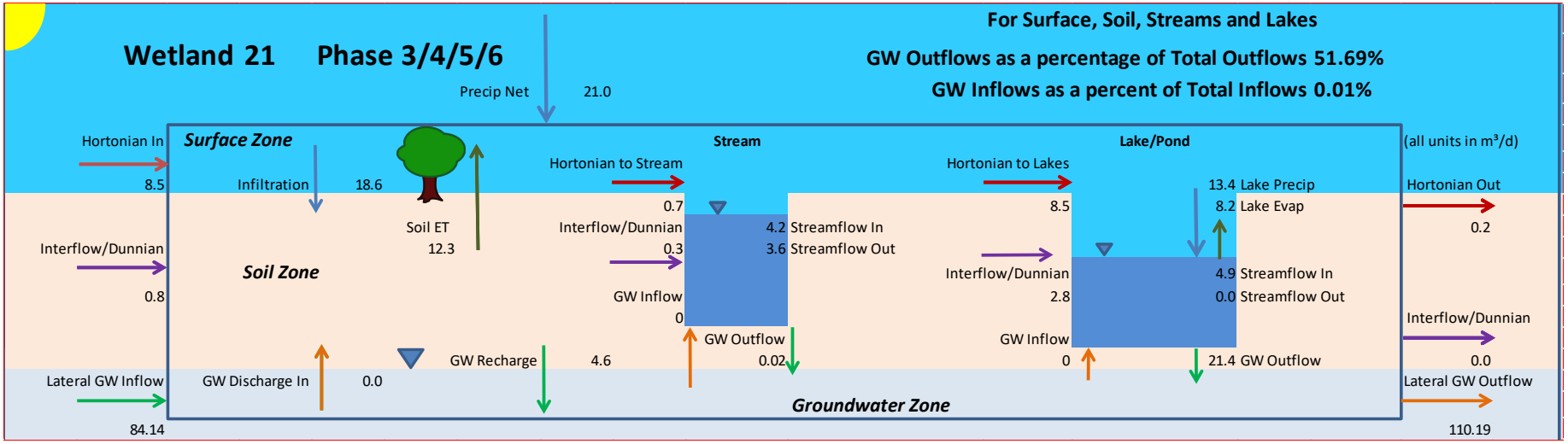

Figure 8.68: Detailed water budget for Wetland 21 averaged over WY2010 and WY2011 under Scenario P3456.

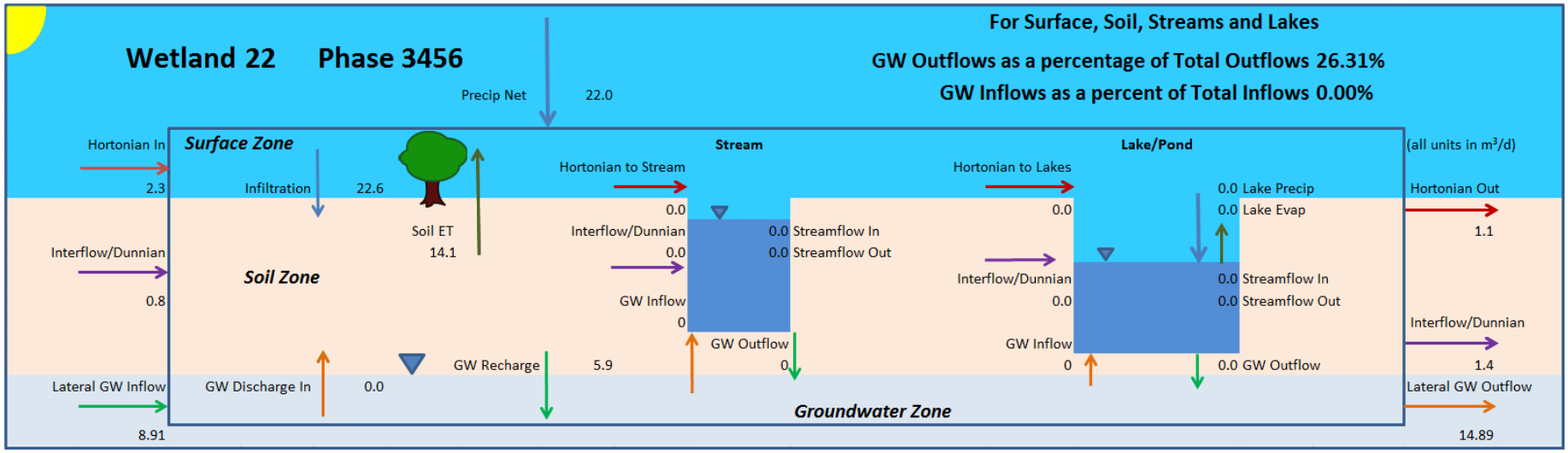

Figure 8.69: Detailed water budget for Wetland 22 averaged over WY2010 and WY2011 under Scenario P3456.

8.7.6 P3456 Effects on Medad Valley

The effects of P3456 development on the Medad Valley is distributed across this elongated feature. Figure 8.70 shows the areas where changes in groundwater discharge to the soil zone (seepage) will occur between the baseline and P3456 scenarios. (Values are presented on a cell-by-cell basis in m^3/d). Summing those values from the start-of-flow- of Medad Creek to SW07 yields a net average decrease in seepage of 2.1 L/s at SW07. The hydrograph for SW07 (Figure 8.49) shows that the change is primarily a minor reduction in winter and spring peak flows.

Figure 8.71 shows the spatial distribution of the average increase (in blue) or decrease in streamflow. The figure shows that there will be an increase in flow through the north quarry discharge stream, and that the flow will continue through the karst conduit as under current conditions. As noted above, the increase in flow will enter the Medad Valley just downstream of SW07, so there will be no significant change downstream at SW1.

To better illustrate the effects on the valley, a point 250 m upstream of SW07 was selected for further analysis. This location is upstream of the SW02 tributary entry point, and near where Colling Road would cross the valley. Figure 8.72 shows a flow hydrograph for WY2010 to WY2014. The inverted Y2 right axis shows the difference in flow (green), with an average decrease of approximately 2 L/s. Figure 8.73 shows the change in flow for WY2012, and the enlargement better illustrates that the largest change occurs in the winter months and peak flow events.

Figure 8.74 shows the change in flow at SW14, with an average of about 0.41 L/s over the simulation period.

Overall, the construction of the west extension has a minor impact on the Medad Valley. No water is diverted away from this natural discharge zone, but some water is discharged slightly to the north via north quarry discharge stream.

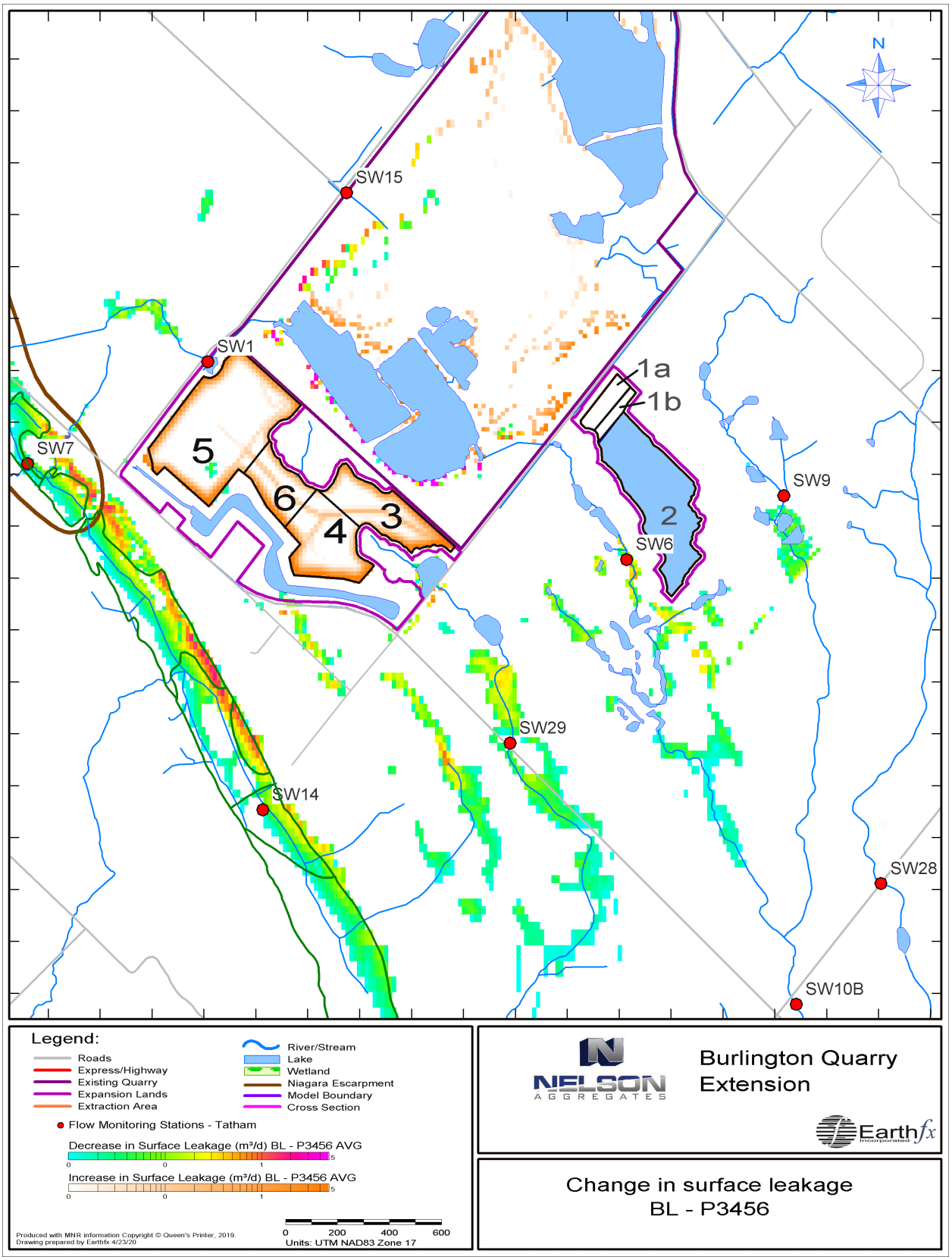

Figure 8.70: Change in groundwater discharge to the soil zone between Baseline and P3456.

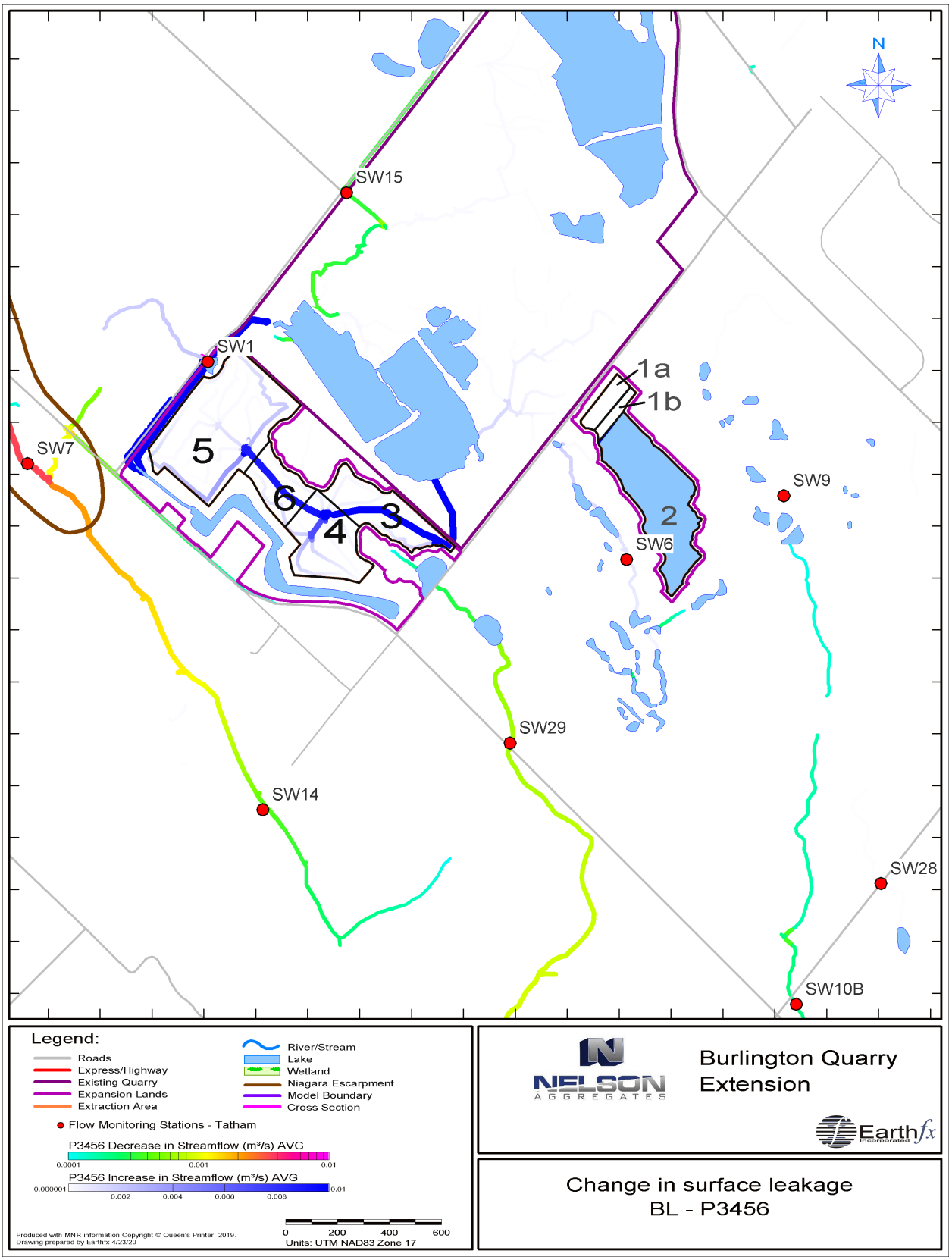

Figure 8.71: Change in streamflow between Baseline and P3456

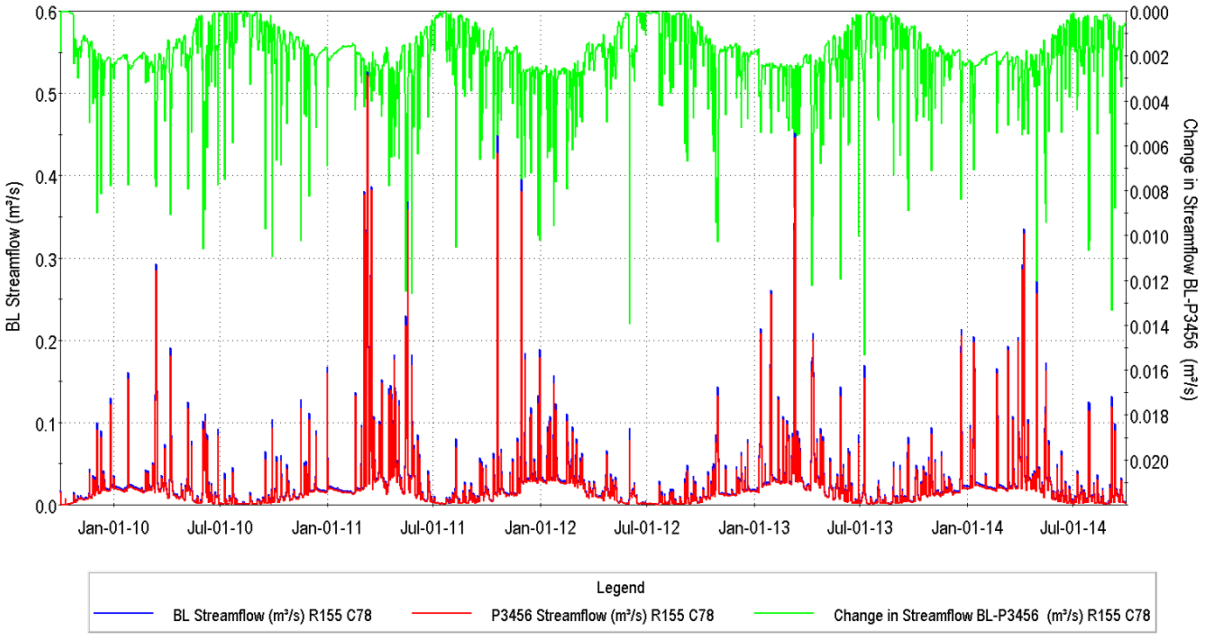

Figure 8.72: Hydrograph showing stream flow 250 m upstream of SW07 for WY2010 to WY2014

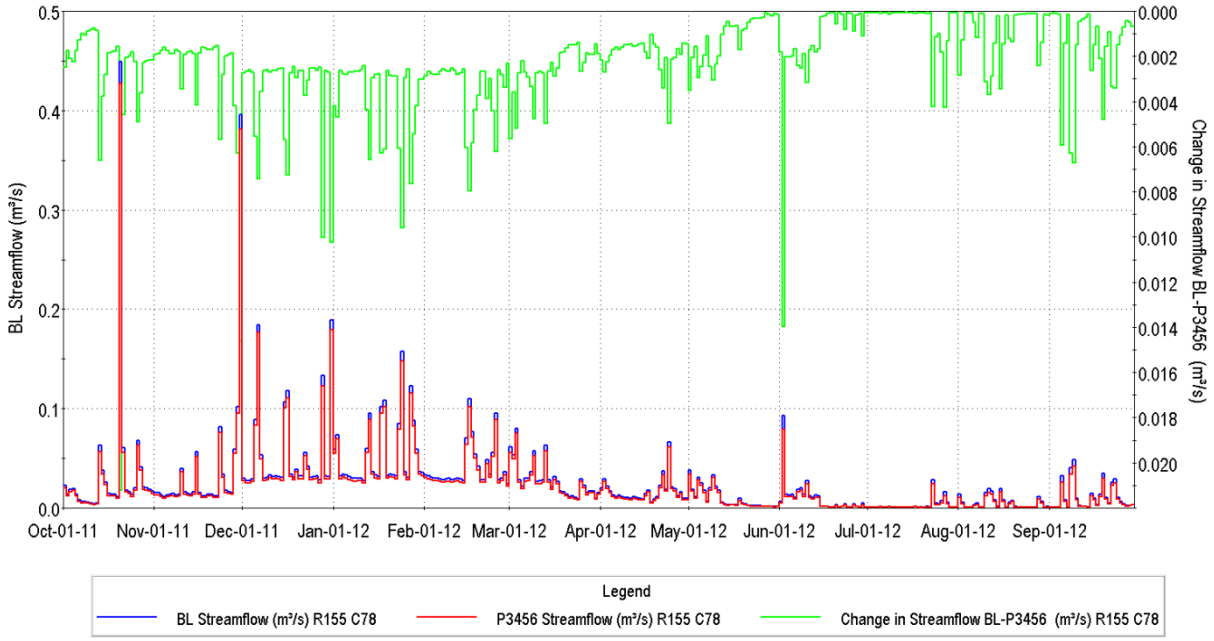

Figure 8.73: Hydrograph showing stream flow 250 m upstream of SW07 for WY2012 (enlargement to show detail)

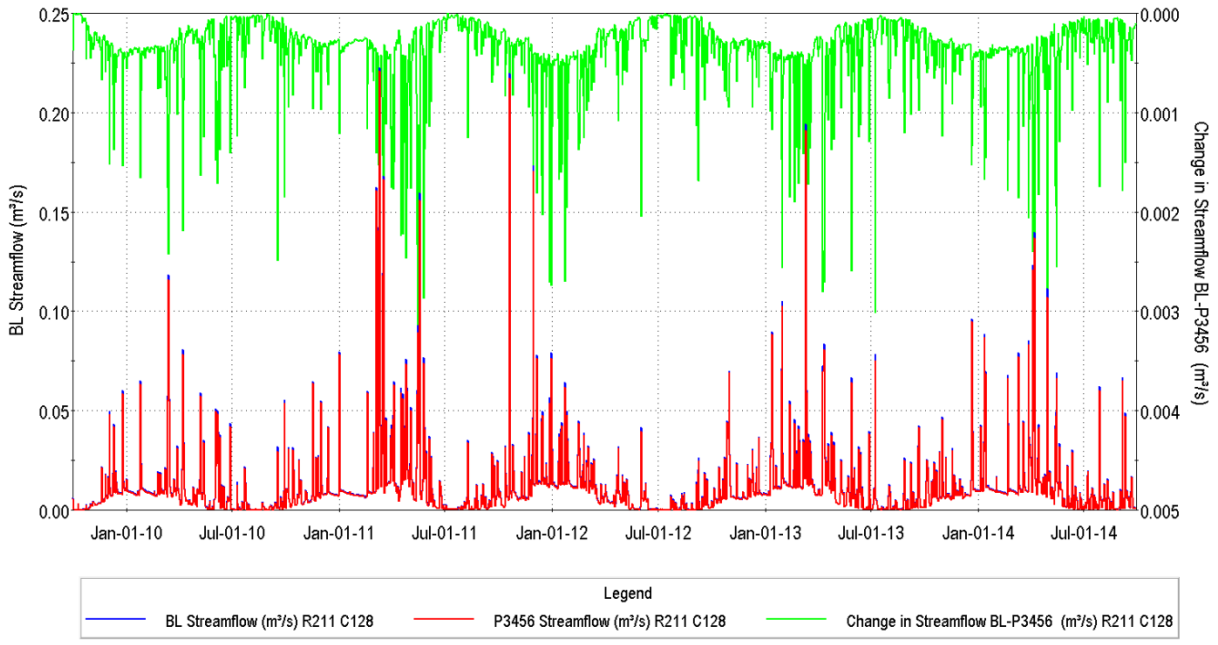

Figure 8.74: Baseline vs P3456 Change in flow at SW14

8.7.7 P3456 Level 2 Conclusions

The development of P3456 will create a drawdown in the Amabel aquifer that will propagate north and south of the excavation. The water levels rise rapidly with distance from the excavation, and exhibit less than 2.0 m of drawdown at a distance of 500 m from the active face.

The basal Layer 8 lower fracture will maintain, on average, between 6 and 20 m of available drawdown in the aquifer (Figure 8.75). As a result, private domestic water wells, some of which are partially penetrate the Amabel Formation, could be deepened if necessary. The proposed groundwater monitoring program has been designed to ensure that there are no changes to the quantity or quality of private water supplies (Section 9.3).

Under worst case drought conditions, such during the Level 2 Provincial Low Water Advisory that was issued in 2016, water levels in the vicinity of P3456 will be an additional 1 m lower than average extraction conditions. There will, however, continue to be between 5 and 20 m of available drawdown in the Amabel Aquifer (Figure 8.76).

Figure 8.60 presents the average simulated streamflow loss to groundwater (blue areas) and the areas of groundwater discharge to streams (red areas). Little change is seen compared to the Baseline Conditions (Figure 7.21). The increase in leakage from the North Quarry discharge stream is due to the local drawdown created by the excavation, and the extra leakage either flows as groundwater directly into the Medad or returns to the P5 excavation.

The effects of P3456 on the wetlands in the vicinity of the excavation has been demonstrated by the water budget analysis. Under baseline conditions, none of the wetlands receive more than 3% of their total inflows from the groundwater system (Table 8.6). Under P3456 conditions, the P12 excavation has been filled with water and the water table has recovered to a new level consistent with the P12 lake. This recovery has restored a degree of groundwater discharge to the wetlands near P12.

The effects of the quarry extension are small and distributed across the long Medad Valley wetland. SW07, in the northern section of the Medad, shows some gains and losses in baseflow (Figure 8.43), but the largest change in flows at SW07 are a loss in peak flows, due to the increased buffering effect of the west extension (Figure 8.49). The changes in SW07 flows are so small that they will not be measurable in the field.

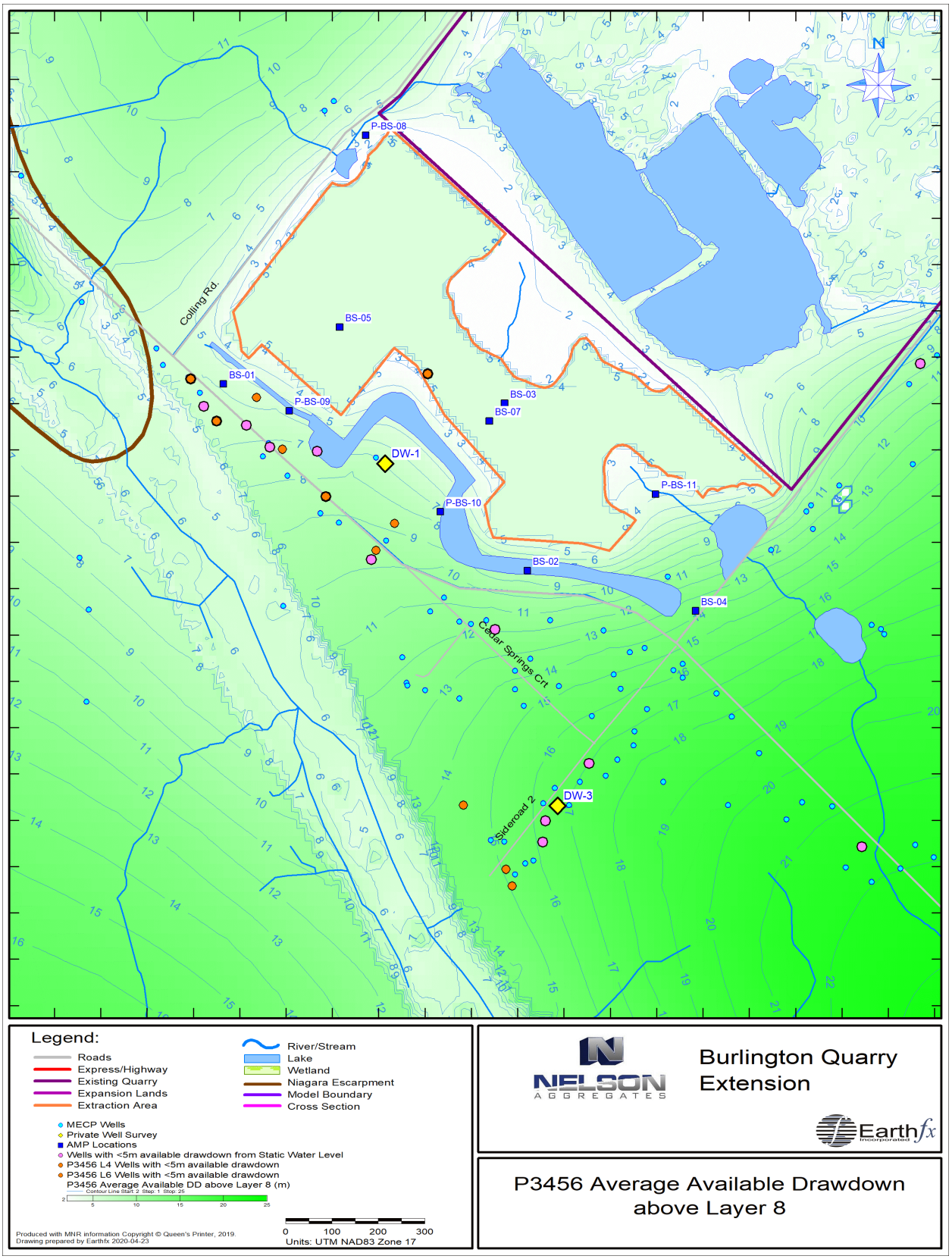

Figure 8.75: Average available drawdown under P3456 conditions.

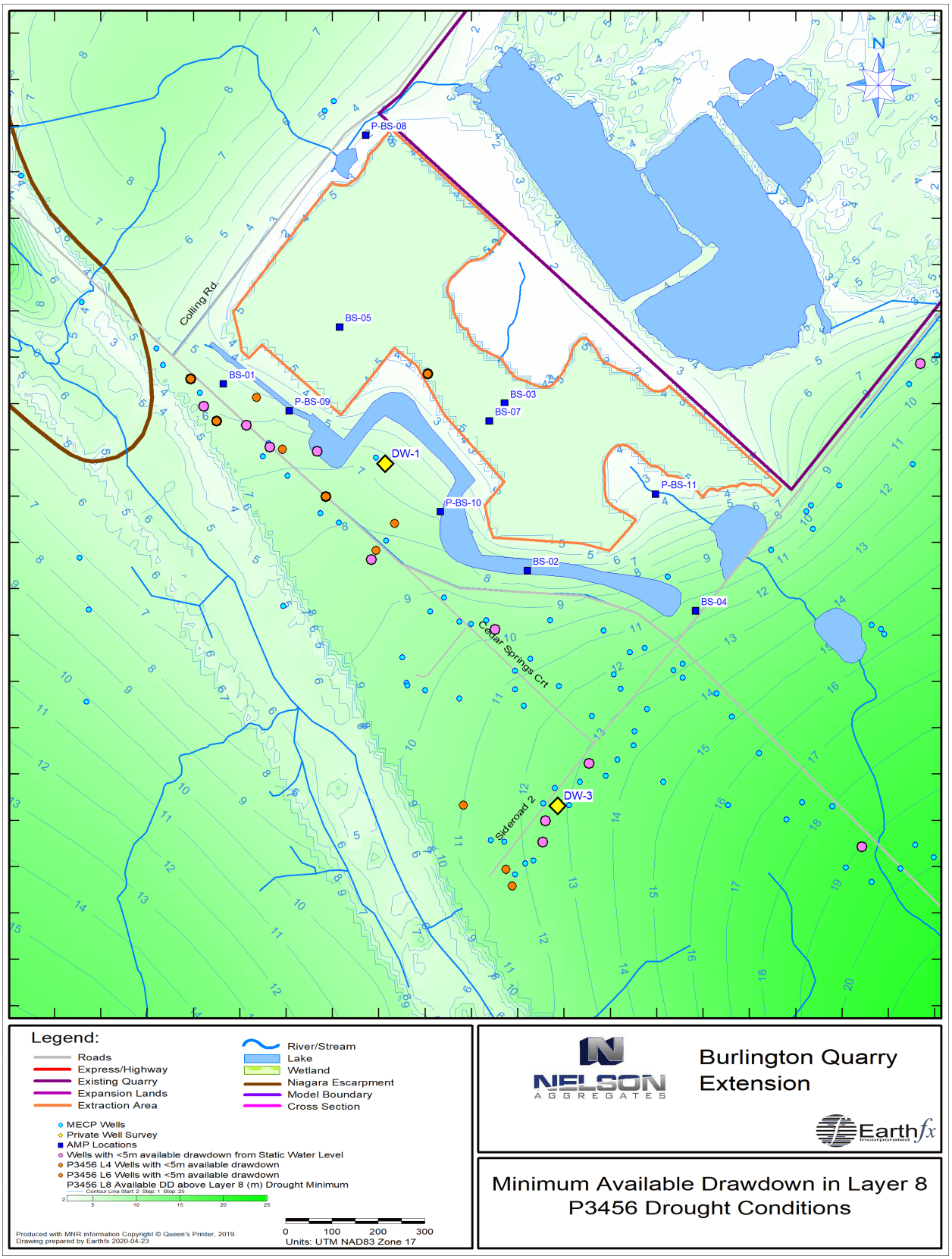

Figure 8.76: Minimum available drawdown under P3456 drought conditions.

8.8 Scenario RHB1

Scenario RHB1 represents the first of two simulations of conditions after the excavation of all material in Phase 3 to Phase 6 and the implementation of quarry rehabilitation. The quarry rehabilitation plan is laid out in reports by MHBC (2020). The GSFLOW model was modified to incorporate key components of the plan into the model. In Scenario RHB1, much of the Phase 5 area is converted into a new consolidated lake that extends into the existing quarry pond (Figure 8.77). A small portion of Phase 4 is also to be converted to a pond while the remaining excavated area, including Phase 3 and 6 are to be backfilled and graded to specified elevations. The small pond in Phase 4 discharges to the Phase 5 lake through a small stream channel.

Scenario RHB1 represents a managed rehabilitation and it is assumed that discharge from the Sump 0100 will be ongoing to maintain dry conditions in the rest of the quarry area and to keep the P5 lake at the specified elevation of 255.5 masl. The control elevation for the P4 pond is 256 masl. Figure 8.77 shows the modified topography and drainage in the quarry vicinity in the RHB1 scenario. Water from quarry discharge at the northwest sump is assumed to still be diverted to the infiltration pond between Cedar Springs Road and the extraction area (in a manner similar to the current golf course ditches and ponds). As in previous scenarios the P12 excavation is filled to its natural elevation.

Land use and soil class were modified from the P3456 scenario and changed from “Quarry” to “Open Water” in the new P5 lake and P4 pond footprints. Similar modifications were made to the soil and land use types within the existing quarry to reflect the new lake configuration. All the soil and land use-based PRMS model parameter values were updated. Topography, slope, and aspect were also adjusted in all quarry areas. Quarry floor drains and conduit stream types were added or modified as needed module to drain the existing quarry and P3456 area to convey quarry discharge to the new P5 lake. MODFLOW layer geometry was modified and the input to the LAK3 module was adjusted to represent all the changes to the lake configurations. A new cascade network was generated to account for the new stream network, lakes, and topography.

In summary, the RHB1 scenario is very similar to the P3456 scenario. The infiltration pond continues to function in a manner similar to the golf course ditches and ponds. The main difference with P3456 is that the quarry ponds have been reconfigured and the P5 lake is maintained at a slightly higher elevation, which will reduce drawdowns.

8.8.1 RHB1 Drawdowns and Surface Water Flows

Figure 8.78 shows the average simulated heads in Model Layer 6, representing the middle fracture zone in the Amabel aquifer and average simulated streamflow for the same period under Scenario RHB1. Stage in the P5 lake averaged 255.5 masl, as designed, but varied between 255.0 and 256.5 over the simulation period.

Figure 8.79 shows that the average simulated drawdown in Model Layer 6 is mostly contained within the P3456 footprint. The simulated water levels recover quickly with distance and fall below 2.0 m at a distance of approximately 330 m from the active face.

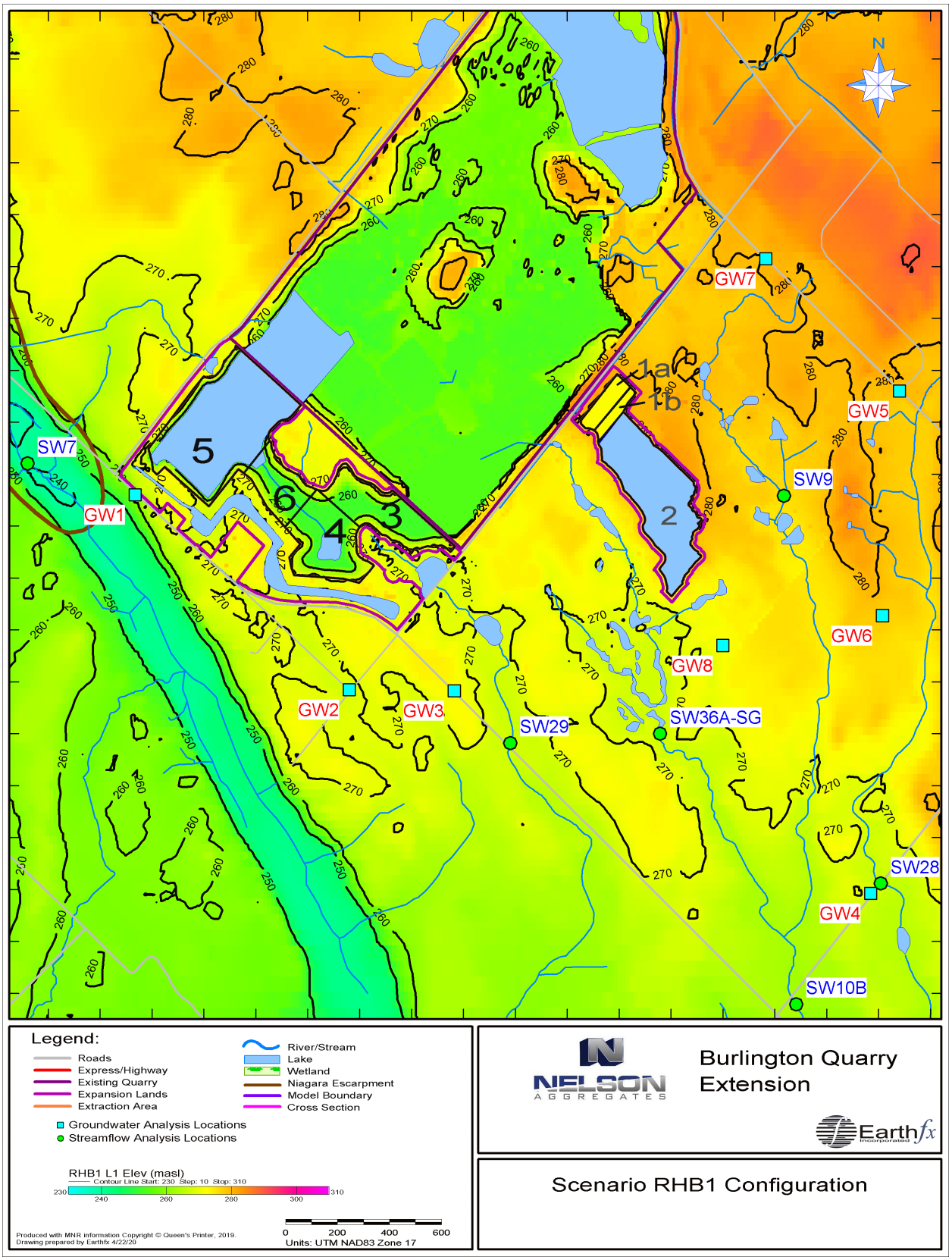

Figure 8.77: Scenario RHB1 configuration.

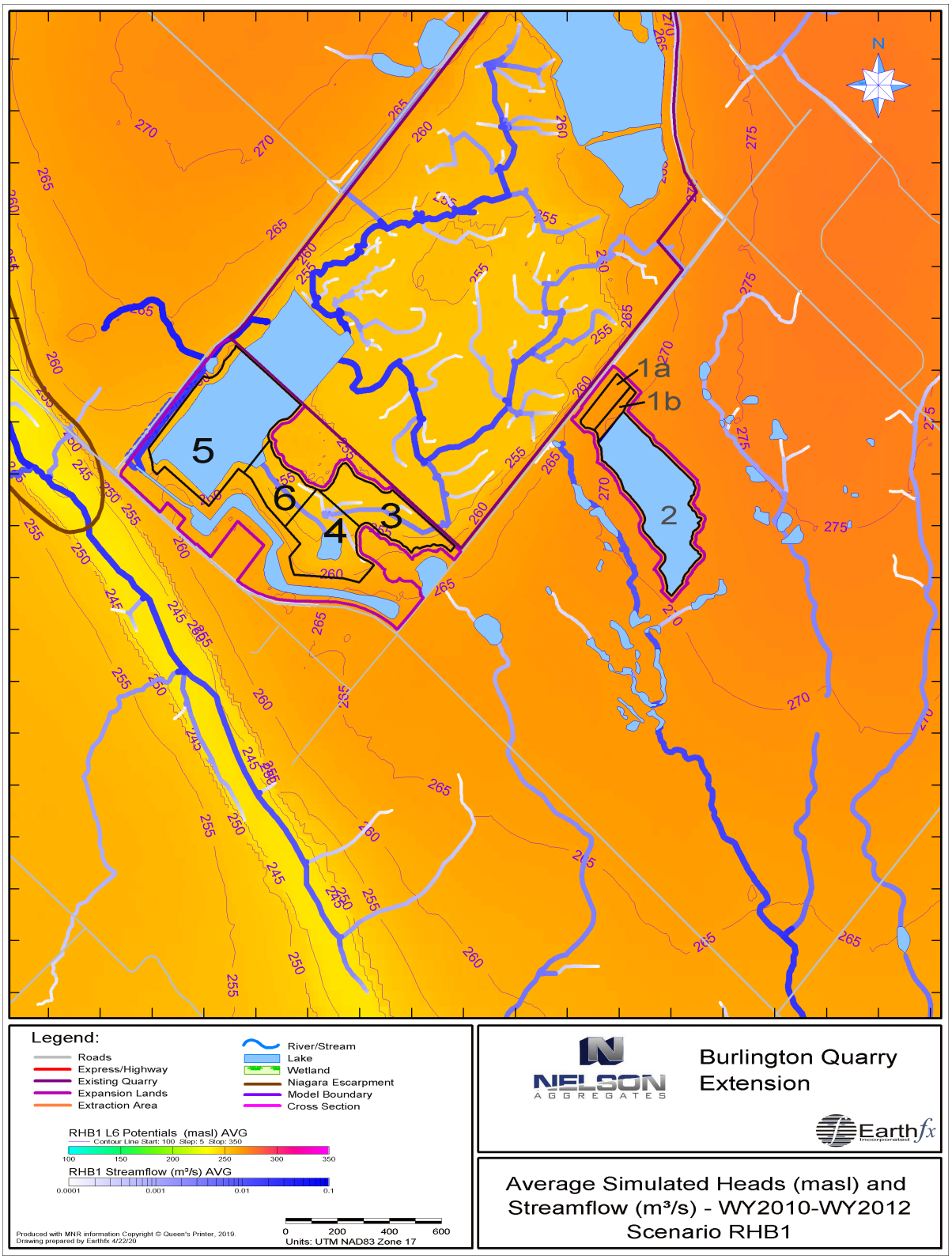

Figure 8.78: Average simulated heads in Model Layer 6 (masl) and streamflow (m^3/s) for WY2010 to WY2012 under Scenario RHB1.

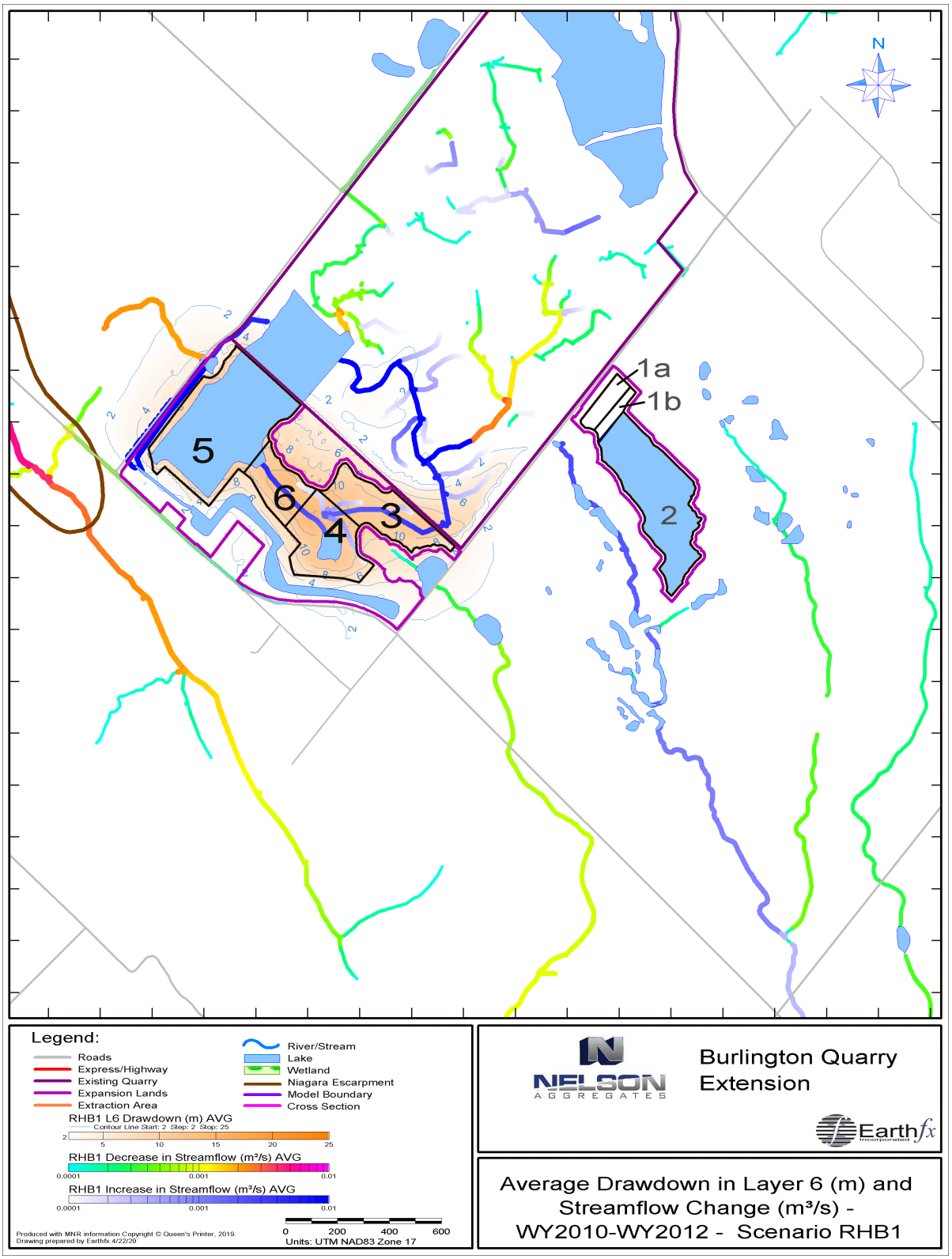

Figure 8.79: Average simulated drawdown in Model Layer 6 (m) and increase/decrease in streamflow (m^3/s) for WY2010 to WY2012 under Scenario RHB1.

Figure 8.79 also shows the average simulated change in streamflow. There are general decreases in flows within the existing quarry footprint and an overall decrease in the discharge from the Northwest sump. Decreases in simulated flow occur in the Medad Valley as a result, reaching a maximum of $5.2x10^{-3}$ m^3/s (5.2 L/s) compared to $3.6x10^{-3}$ m^3/s under Scenario P3456. Other streams in the east show small decreases in average flow compared to Baseline Conditions. Decreases in streamflow have been moderated compared to Scenario P12 due to the cessation of quarry dewatering at P12. The decreases range from $1x10^{-4}$ m^3/s (0.1 L/s) as a cut-off value to $4x10^{-4}$ m^3/s at the downstream end of an eastern tributary that joins the Mt. Nemo Creek tributary carrying the quarry discharge (compared to $8x10^{-4}$ m^3/s under P12). Flow decreased by $1x10^{-3}$ m^3/s at the downstream end of a tributary to Lake Medad (compared to $4x10^{-4}$ m^3/s under P12) due to continued dewatering in the P3456 area.

Figure 8.80 through Figure 8.85 show hydrographs comparing simulated daily streamflow under Scenario RHB1 to Baseline Conditions, in m^3/s, for the six streamflow analysis points (locations shown in Figure 8.77). Flows at SW36A and SW10B show small increases in baseflow, due to leakage from the lake in P12 to the main quarry drains as well as small decreases in peak flows. Flows at SW09 and SW28 have essentially returned to Baseline Conditions with very small decreases in event flows, about an order of magnitude less than under Scenario P3456. Decreases at SW29 are about double that of Scenario P12 because of the proximity to the P3456 excavation area and about the same as for Scenario P3456 (with a different averaging period). SW07 in the Medad valley shows some gains and losses in baseflow, most likely due to changes in discharge from the Northwest sump that recharges the groundwater system as it flows through the karst feature. Decreases in event flows reach a maximum value of 0.05 m^3/s, about 10 times the losses under Scenario P12 but the hydrograph does not appear that different compared to (Figure 8.49) for Scenario P3456 despite the higher average decrease in flow.

8.8.2 RHB1 Seasonal and Inter-annual Groundwater Levels

Figure 8.86 through Figure 8.93 show the simulated heads in Model Layer 6, representing the middle fracture zone in the Amabel aquifer, for WY2010 to WY2012 for the eight measurement points, respectively (locations shown in Figure 8.77). Drawdowns are also shown on the hydrographs (on the inverted secondary y-axis). Maximum daily drawdowns occur at GW2 (1.8 m), close to the Phase 4 extraction area and further from the quarry pond. Maximum daily drawdowns at GW1 and GW3, also close to the Phase 3456 extraction area, are about 1.7 and 1.15 m, respectively. In general, average drawdowns at the points are less than half of those for Scenario P3456. Heads at GW4 and GW7 are back to Baseline Conditions.

Under this scenario, discharge continues to the north from Sump 0100 and to the south from Sump 0200 as per the recommendations presented in the Tatham (2020) and Savanta (2020) reports.

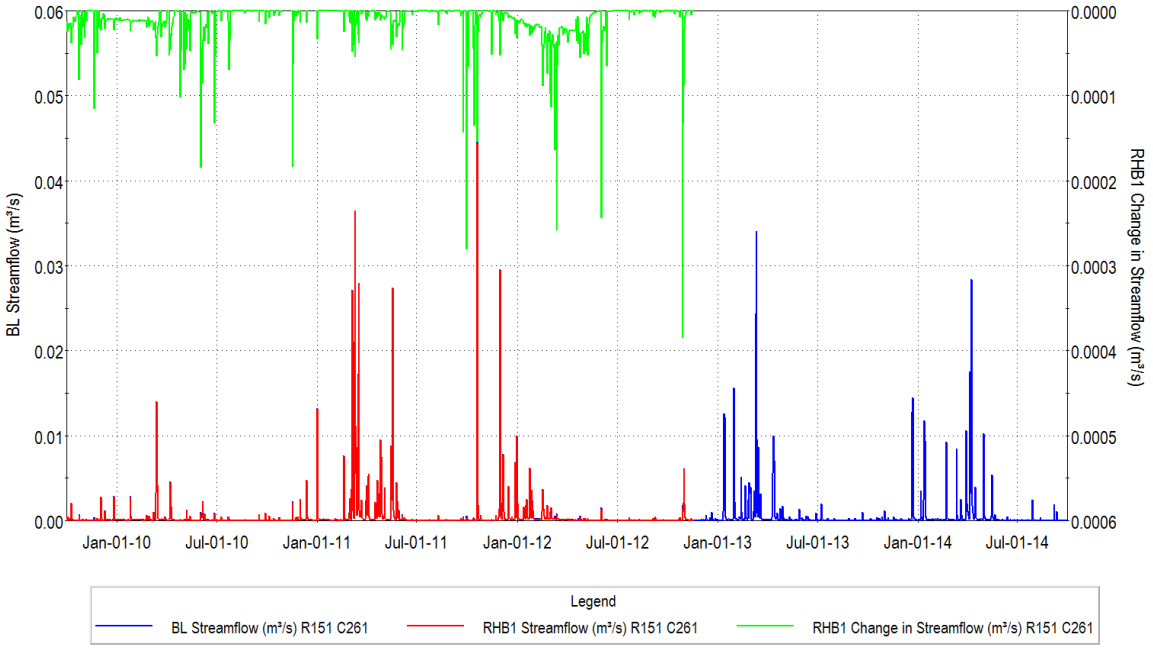

Figure 8.80: Simulated streamflow at SW09 for WY 2010-2012 – RHB1 and Baseline Conditions.

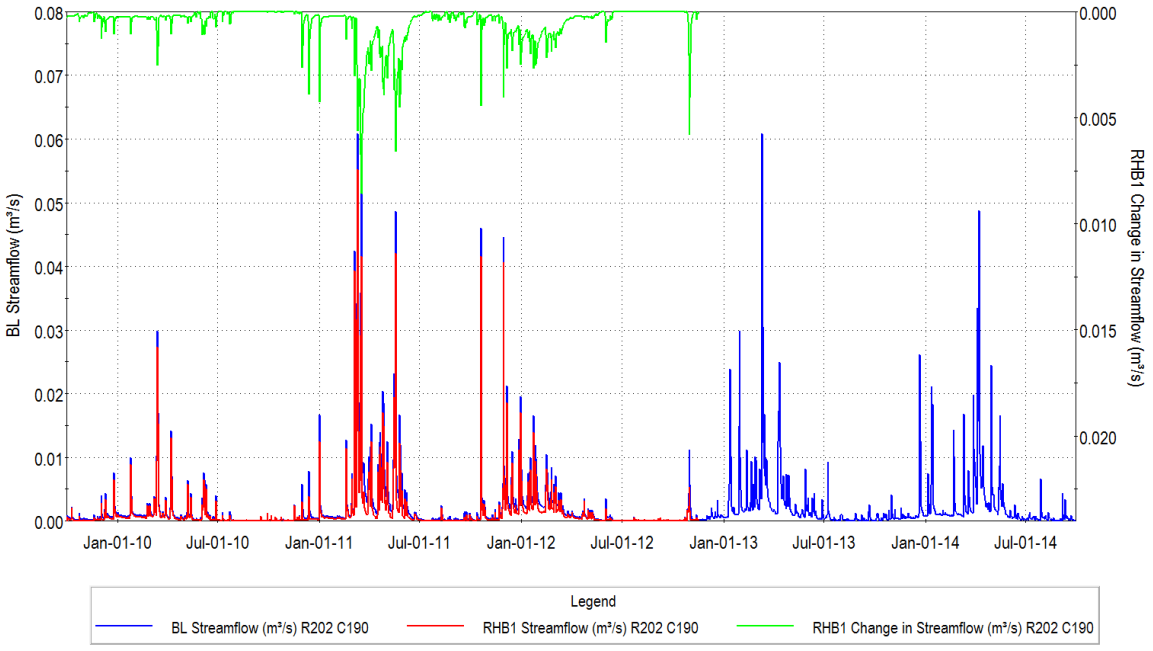

Figure 8.81: Simulated streamflow at SW29 for WY2010-WY2012 – RHB1 and Baseline Conditions.

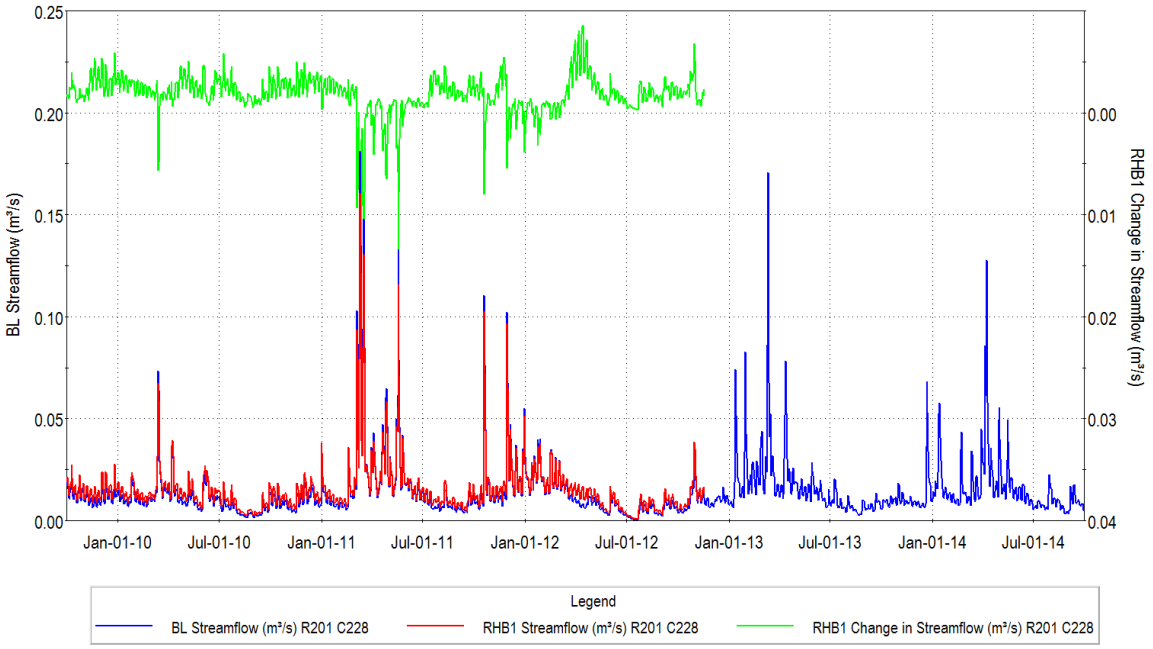

Figure 8.82: Simulated streamflow at SW36A for WY2010-WY2012 – RHB1 and Baseline Conditions.

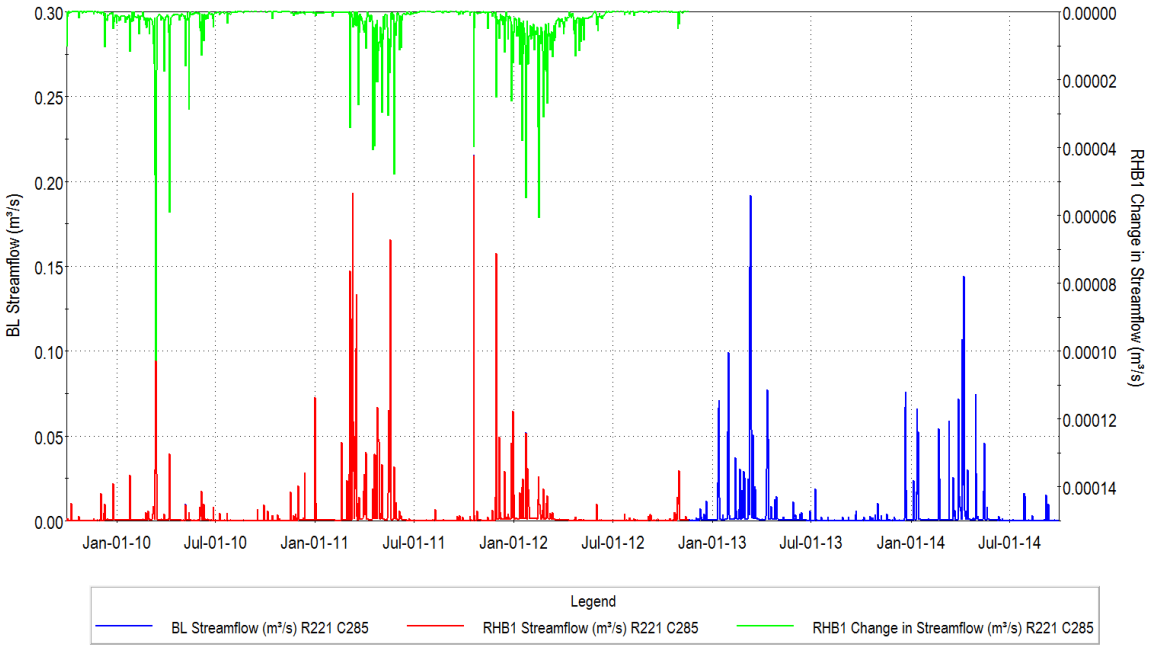

Figure 8.83: Simulated streamflow at SW28 for WY2010-WY2012 – RHB1 and Baseline Conditions.

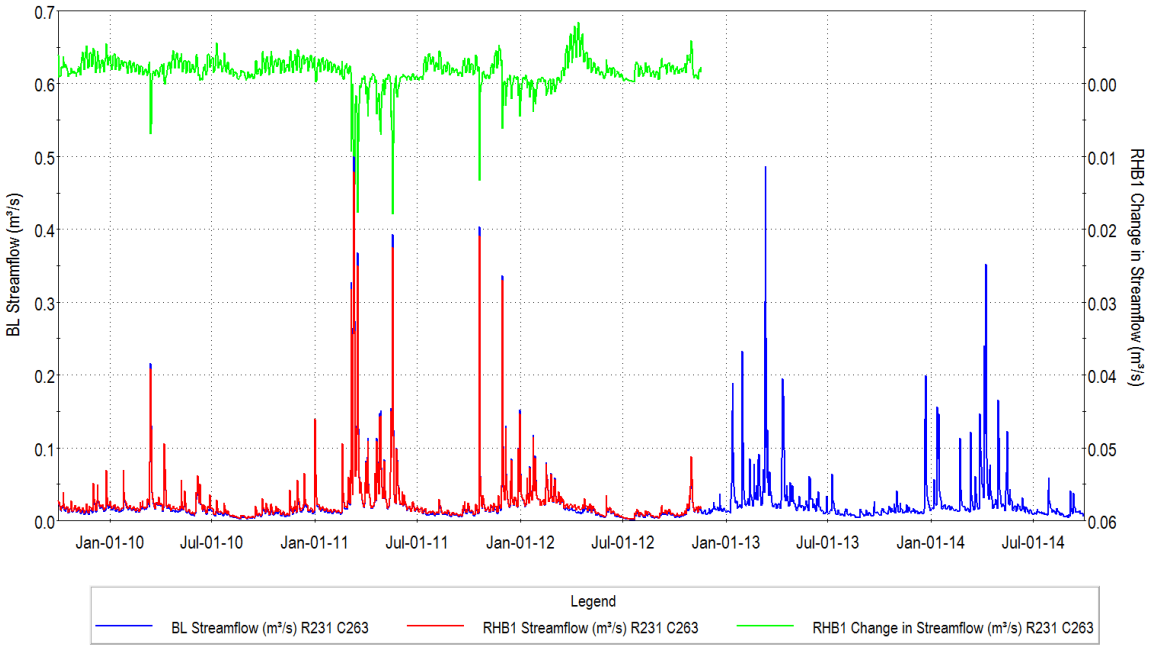

Figure 8.84: Simulated streamflow at SW10B for WY2010-WY2012 – RHB1 and Baseline Conditions.

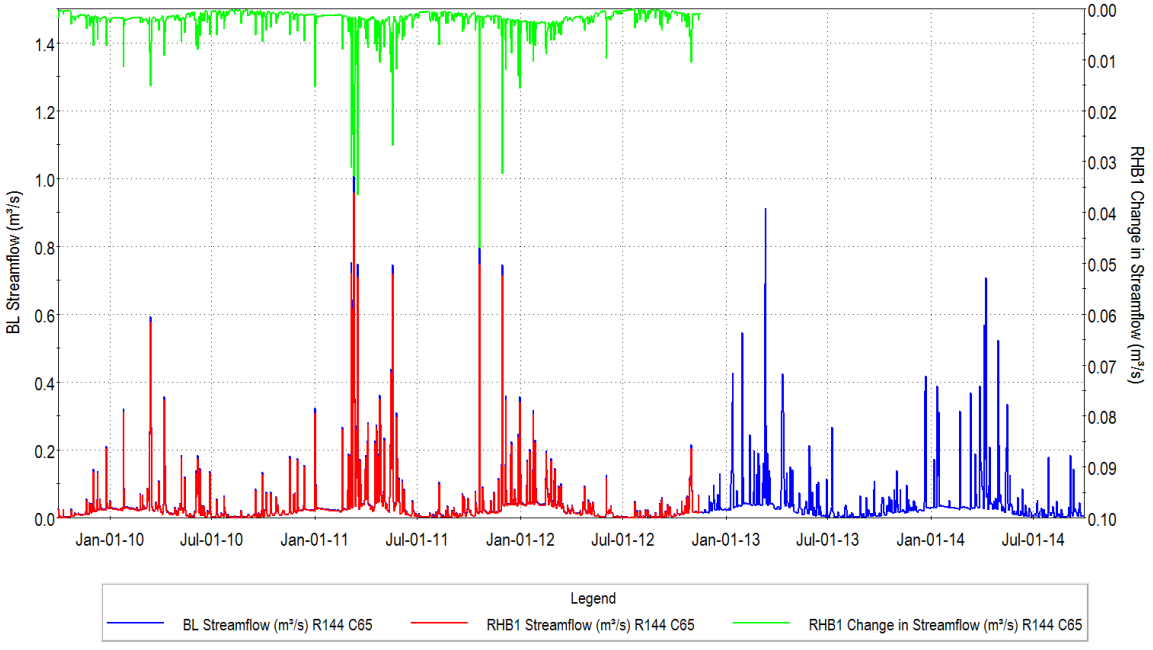

Figure 8.85: Simulated streamflow at SW07 for WY2010-WY2012 – RHB1 and Baseline Conditions.

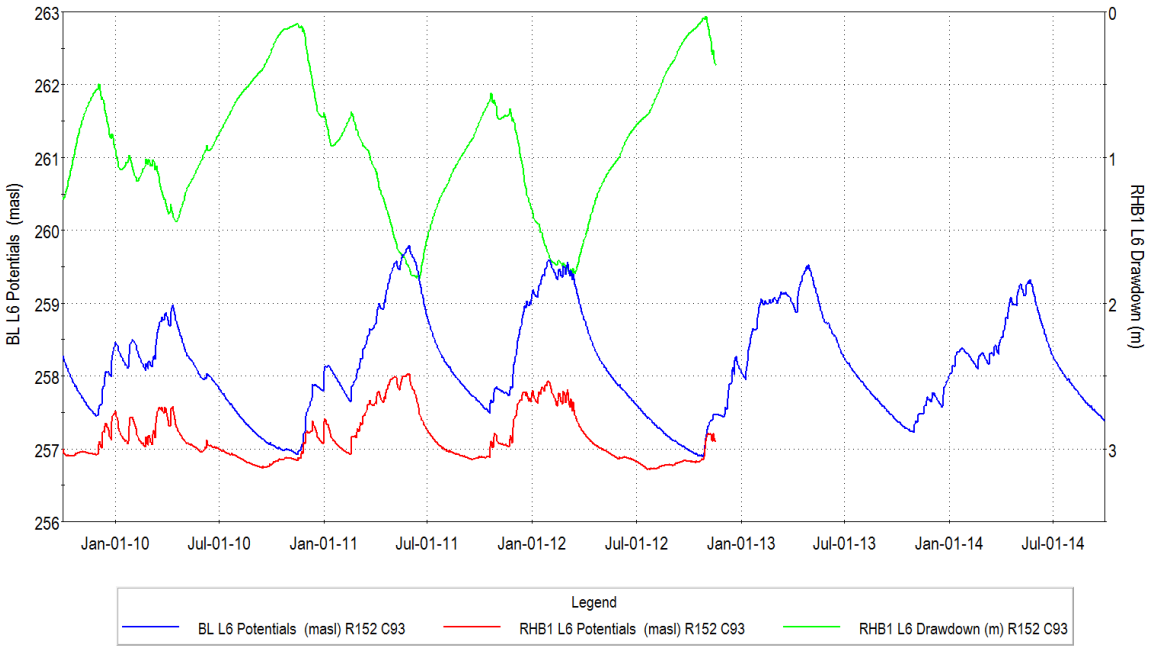

Figure 8.86: Simulated heads and drawdowns in Model Layers 6 at GW1 for WY2010-WY2012 – RHB1 and Baseline Conditions.

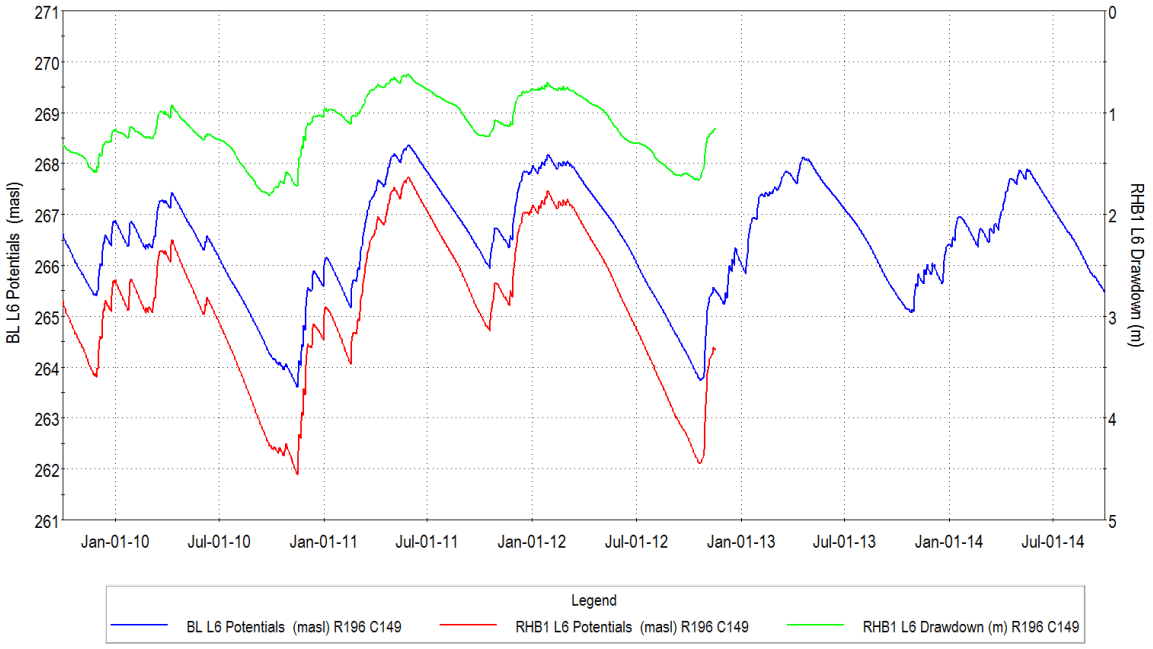

Figure 8.87: Simulated heads and drawdowns in Model Layers 6 at GW2 for WY2010-WY2012 – RHB1 and Baseline Conditions.

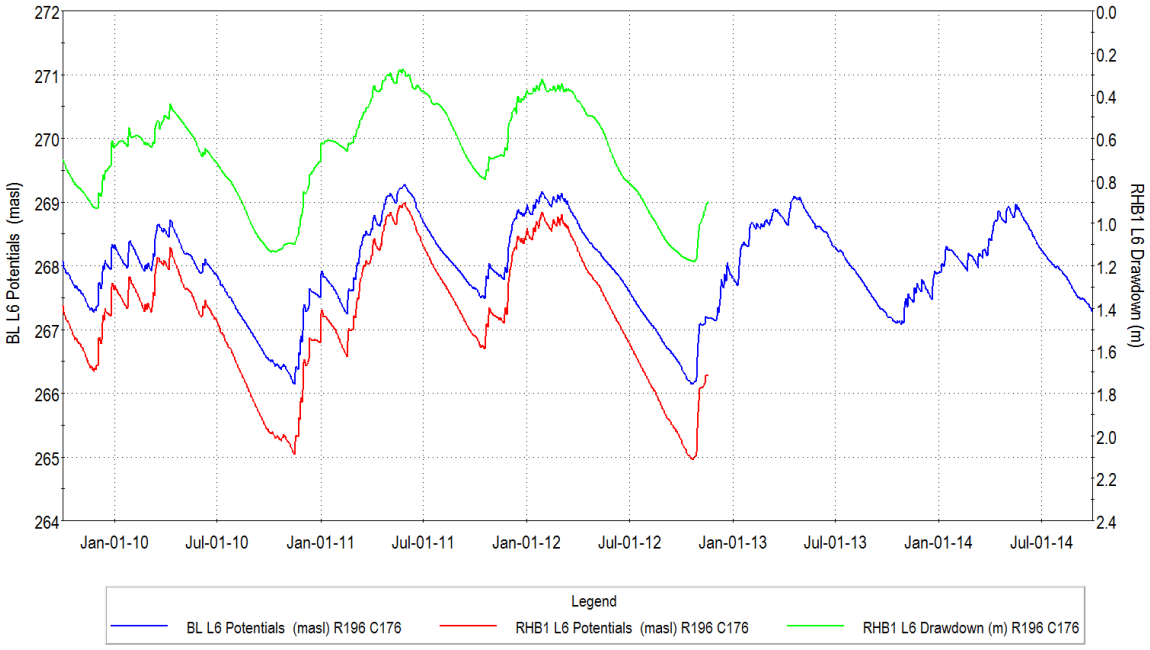

Figure 8.88: Simulated heads and drawdowns in Model Layers 6 at GW3 for WY2010-WY2012 – RHB1 and Baseline Conditions.

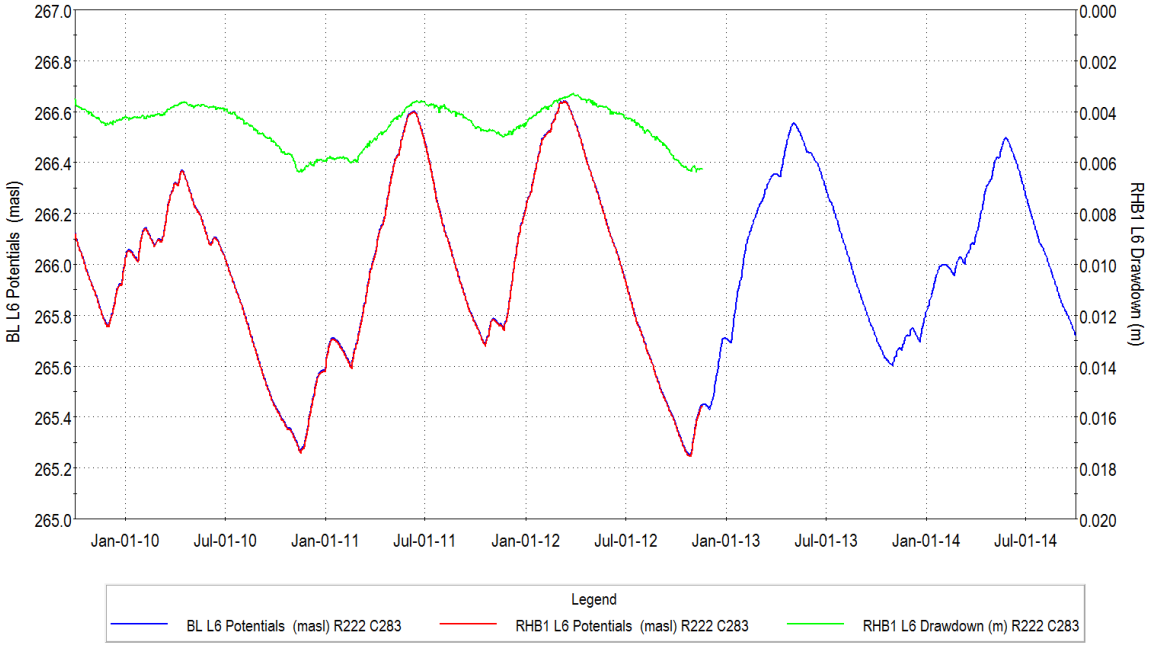

Figure 8.89: Simulated heads and drawdowns in Model Layers 6 at GW4 for WY2010-WY2012 – RHB1 and Baseline Conditions.

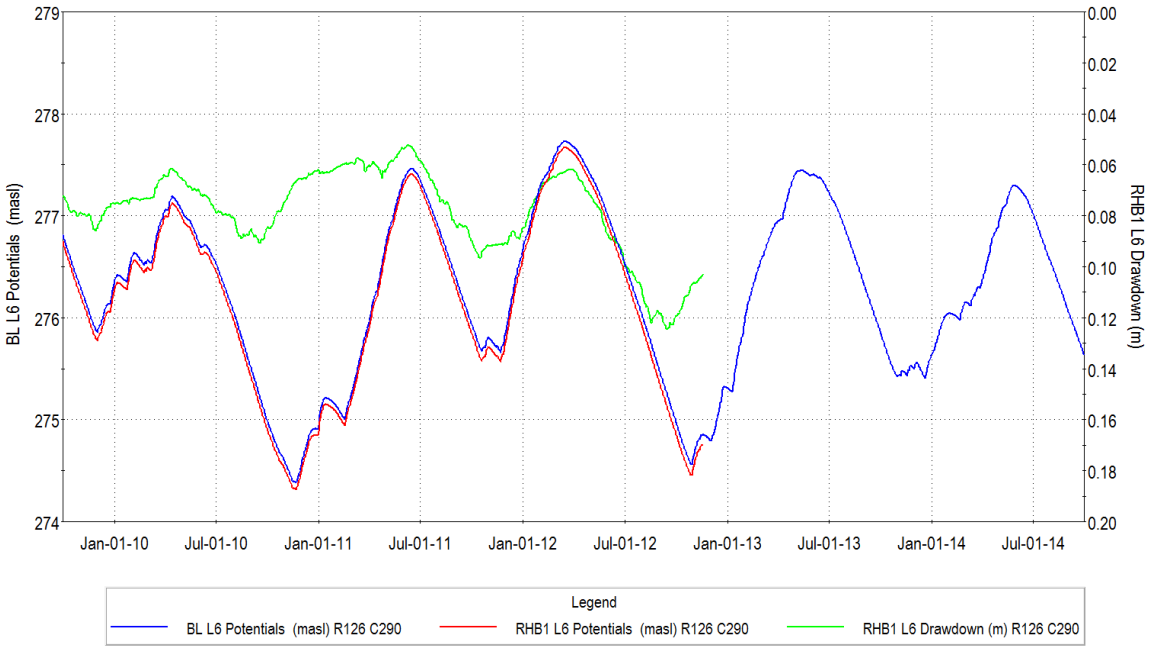

Figure 8.90: Simulated heads and drawdowns in Model Layers 6 at GW5 for WY2010-WY2012 – RHB1 and Baseline Conditions.

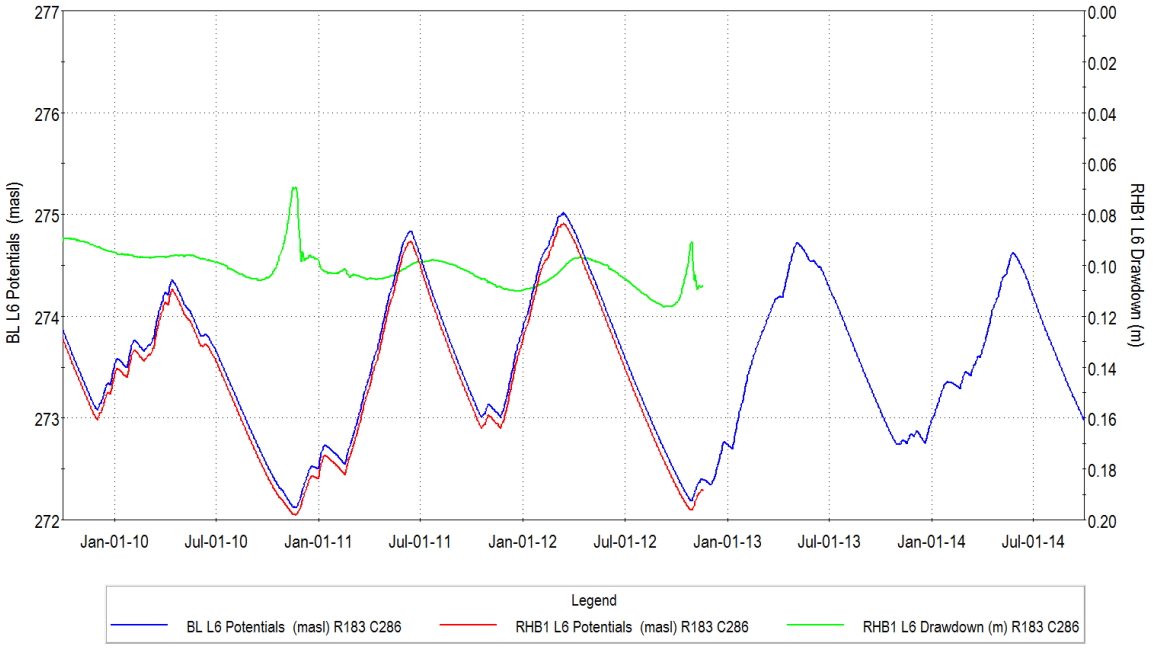

Figure 8.91: Simulated heads and drawdowns in Model Layers 6 at GW6 for WY2010-WY2012 – RHB1 and Baseline Conditions.

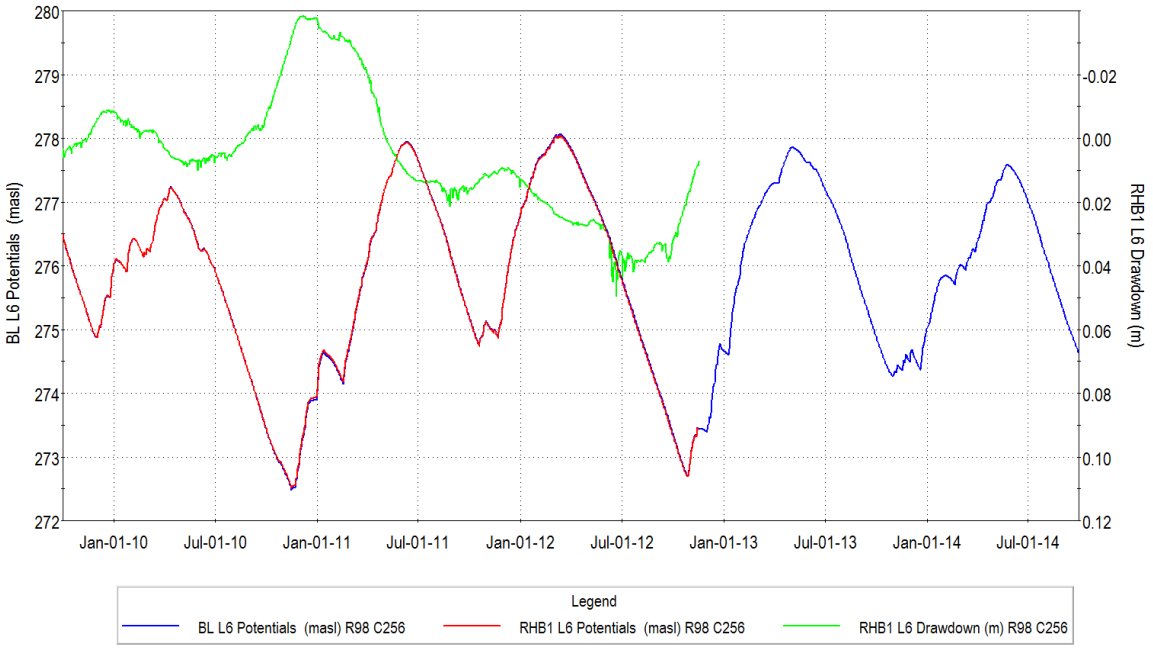

Figure 8.92: Simulated heads and drawdowns in Model Layers 6 at GW7 for WY2010-WY2012 – RHB1 and Baseline Conditions.

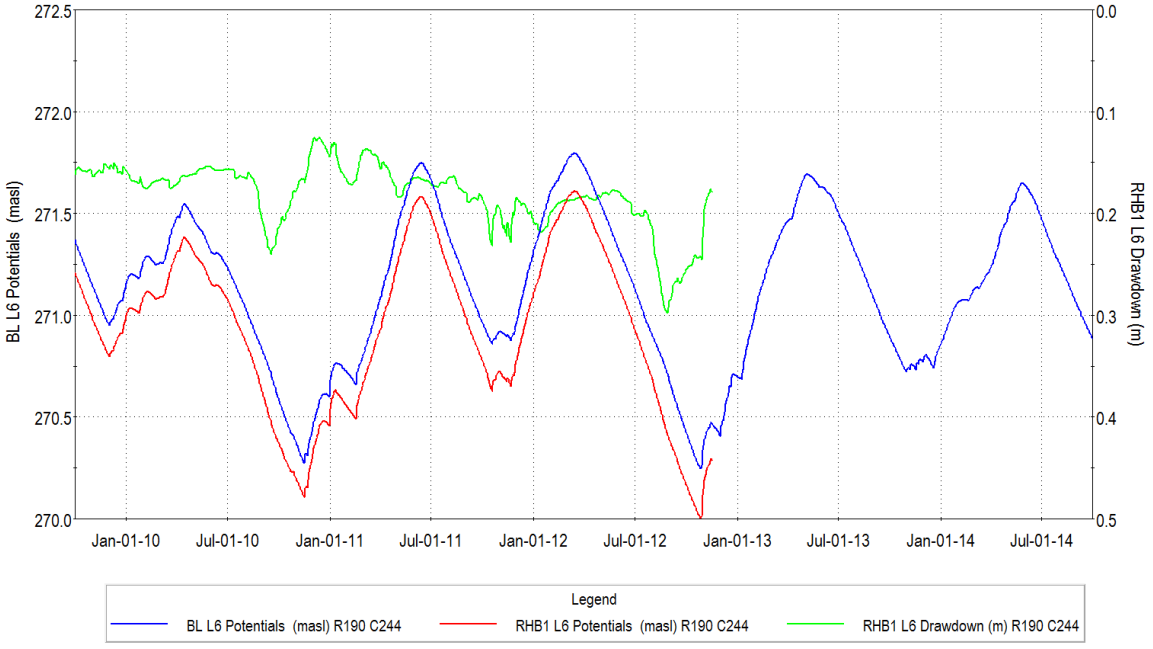

Figure 8.93: Simulated heads and drawdowns in Model Layers 6 at GW8 for WY2010-WY2012 – RHB1 and Baseline Conditions.

8.8.3 RHB1 Surface Water/Groundwater Interaction

Figure 8.94 shows the average simulated net groundwater recharge in the quarry vicinity for Scenario RHB1. The decrease in recharge, compared to the Baseline Conditions (Figure 7.18) remains focused on the Phase 3, 4, 5 and 6 extraction areas where soils and land use parameters were changed in the excavation. Similarly, Figure 8.95 shows that average simulated groundwater ET has increased significantly in the extraction area footprint compared to the Baseline Conditions (Figure 7.19), because of the extra PET demand passed to the groundwater model. Values are noticeably higher than for Scenario P3456 (Figure 8.59) because the water table is 1 to 2 m higher due to leakage from the P5 lake.

Figure 8.96 presents the average simulated streamflow loss to groundwater (blue areas) and the areas of groundwater discharge to streams (red areas). Some small changes are noted in comparison to Scenario P3456 including increases in flow within the existing quarry footprint due to changes in the quarry lake and drain configurations. Figure 8.97 presents the average simulated groundwater discharge to the soil zone under Scenario RHB1. The most significant change compared to Scenario P3456 (Figure 8.61) occurs within the P3456 footprint due to internal drainage and lake reconfiguration.

8.8.4 RHB1 Wetland Water Budgets

Average water budgets were completed to analyze inflows and outflows to 22 local wetlands (locations shown in Figure 7.22). All flows within each area are computed as well as lateral groundwater flow, streamflow, overland runoff, and interflow crossings the wetland area boundaries. Figure 8.98 through Figure 8.103 present schematics showing detailed water budgets for wetland areas 9, 16, 17, 18, 20, and 22, respectively. The water budgets were compiled for WY2010 to 2012. These can be compared with Figure 7.23 through Figure 7.30 for Baseline Conditions averaged over the same period and with those for Scenario P3456 (Figure 8.62 to Figure 8.69).

The wetlands are located at various distances from the existing quarry and the extension areas. Wetland 22 is located between the P3456 extraction area and the existing quarry. This wetland had no change in the water budget compared to baseline conditions because it is perched year-round and there was no change in the contributing area. Most of the other wetland areas are slightly more similar to baseline conditions than P3456 because of internal quarry configuration changes.

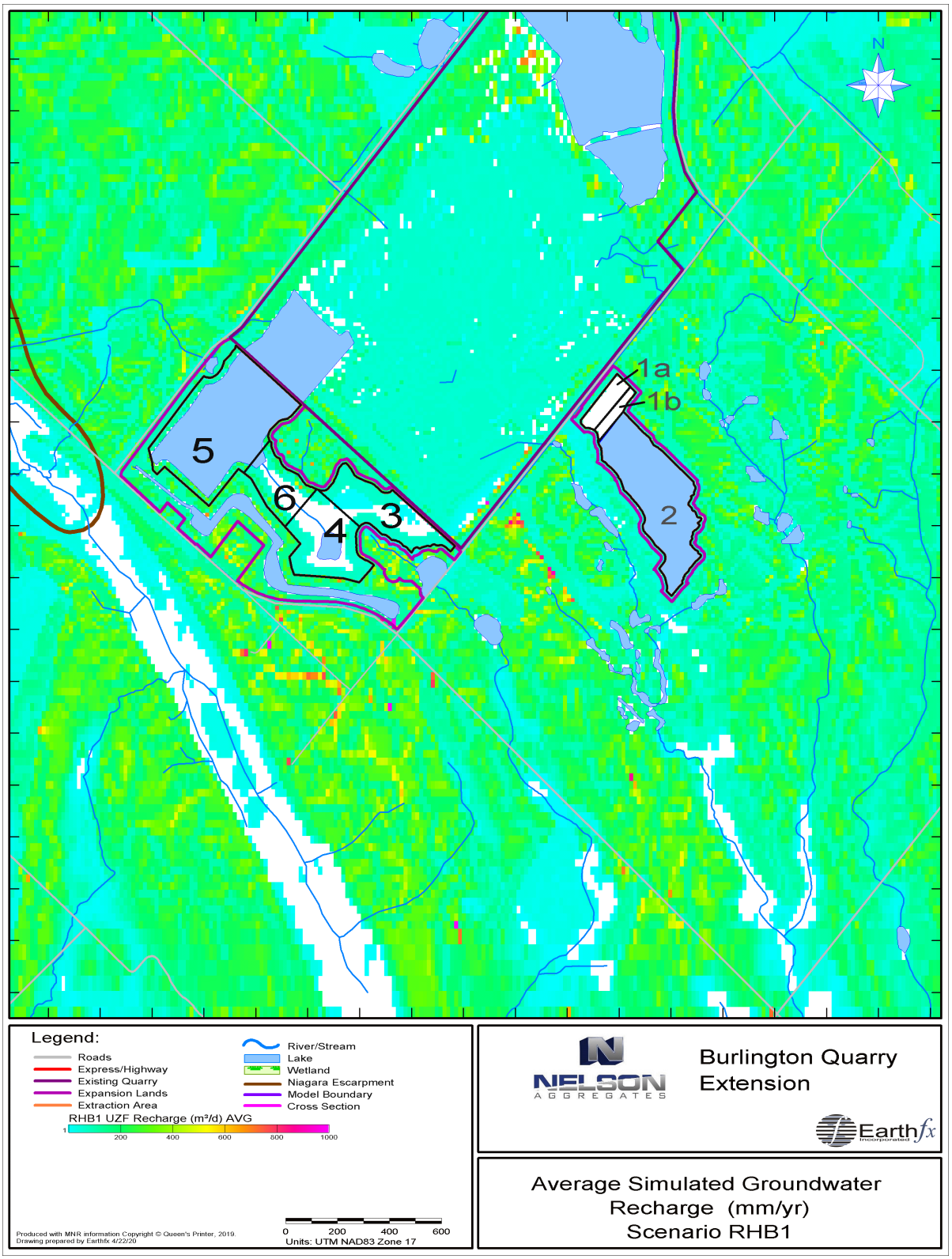

Figure 8.94: Average simulated groundwater recharge (mm/yr) for WY2010-WY2012 – Scenario RHB1.

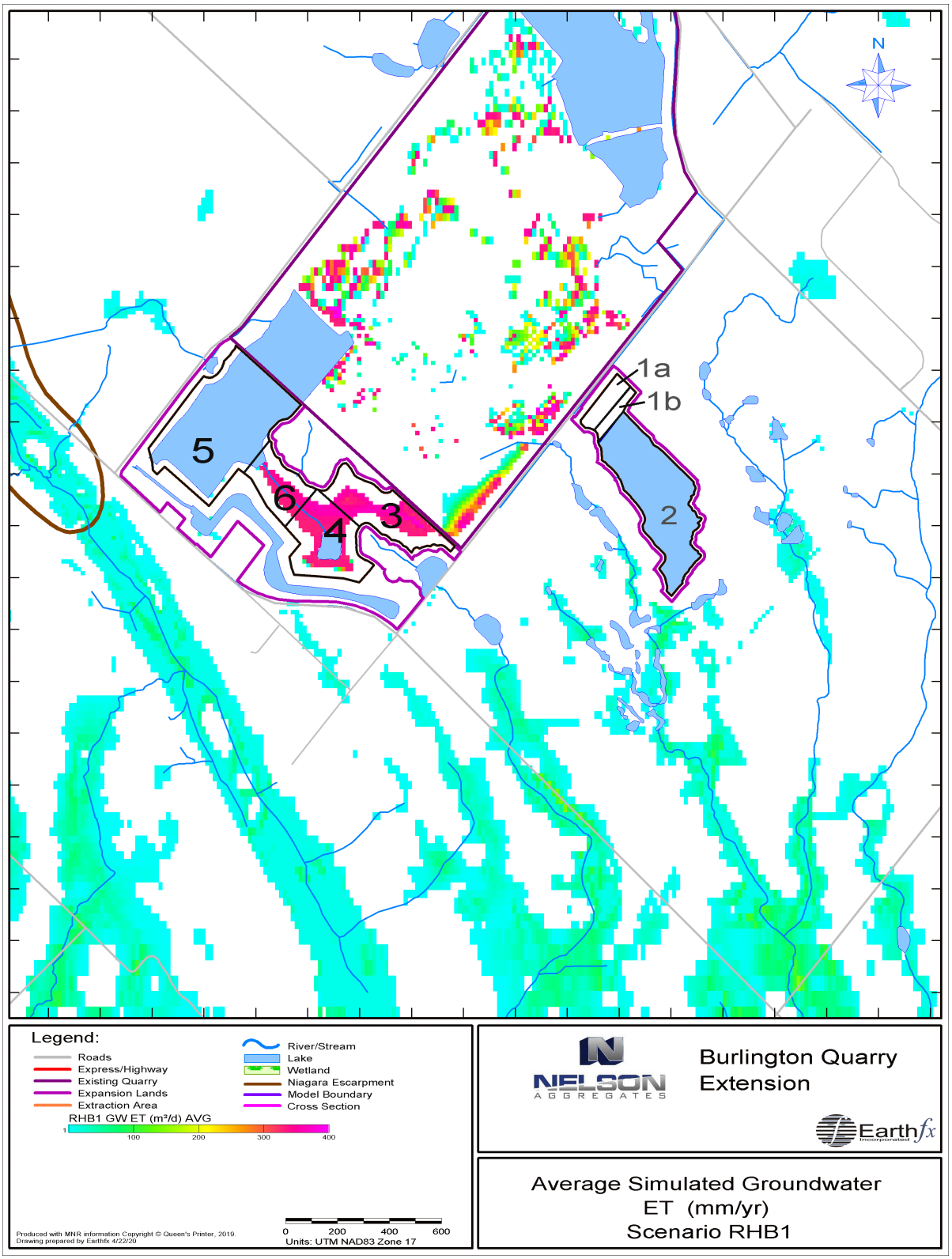

Figure 8.95: Average simulated groundwater ET (mm/yr) for WY2010-WY2012 – Scenario RHB1.

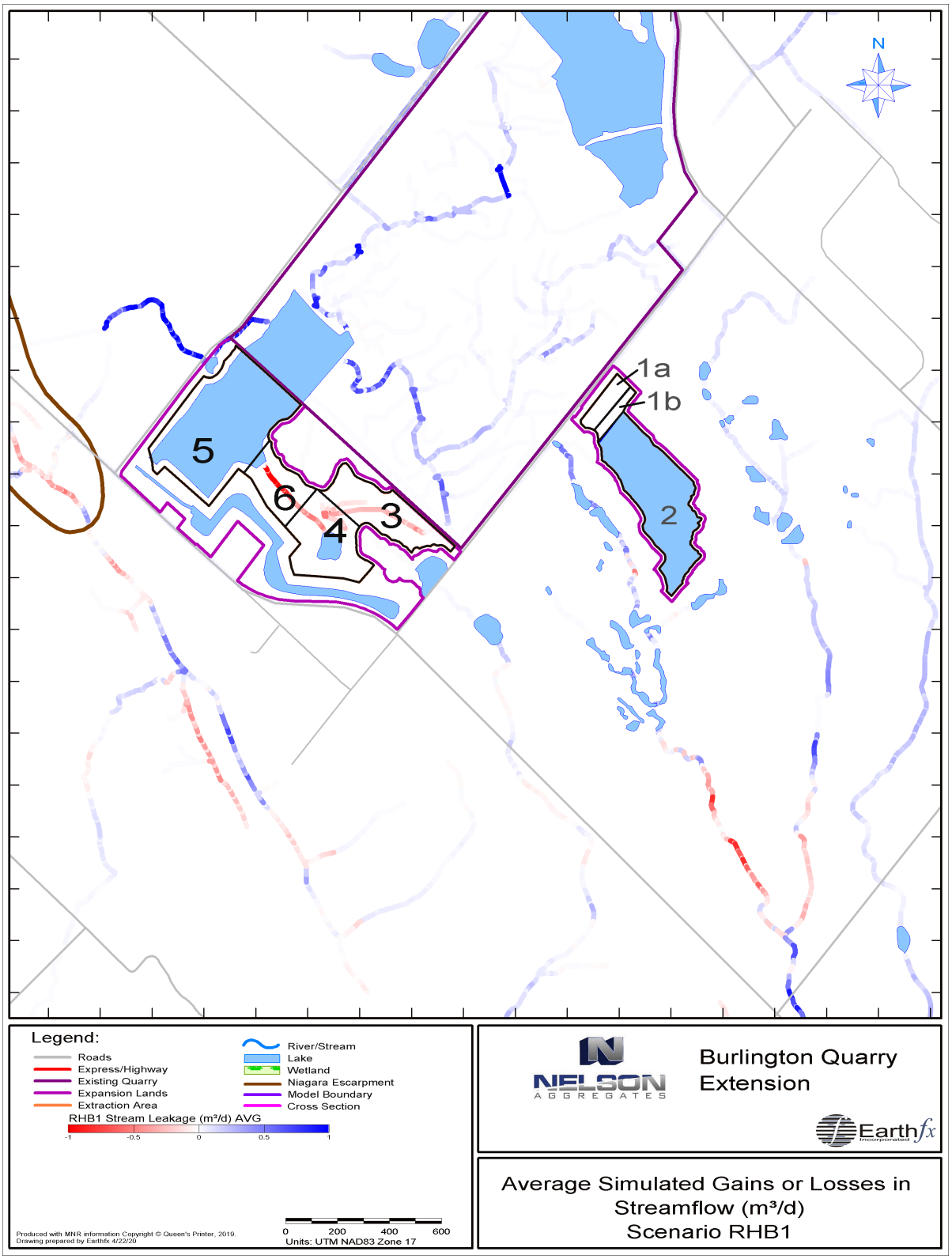

Figure 8.96: Average simulated streamflow loss to groundwater or groundwater discharge to streams (m^3/d) for WY2010-WY2012 – Scenario RHB1.

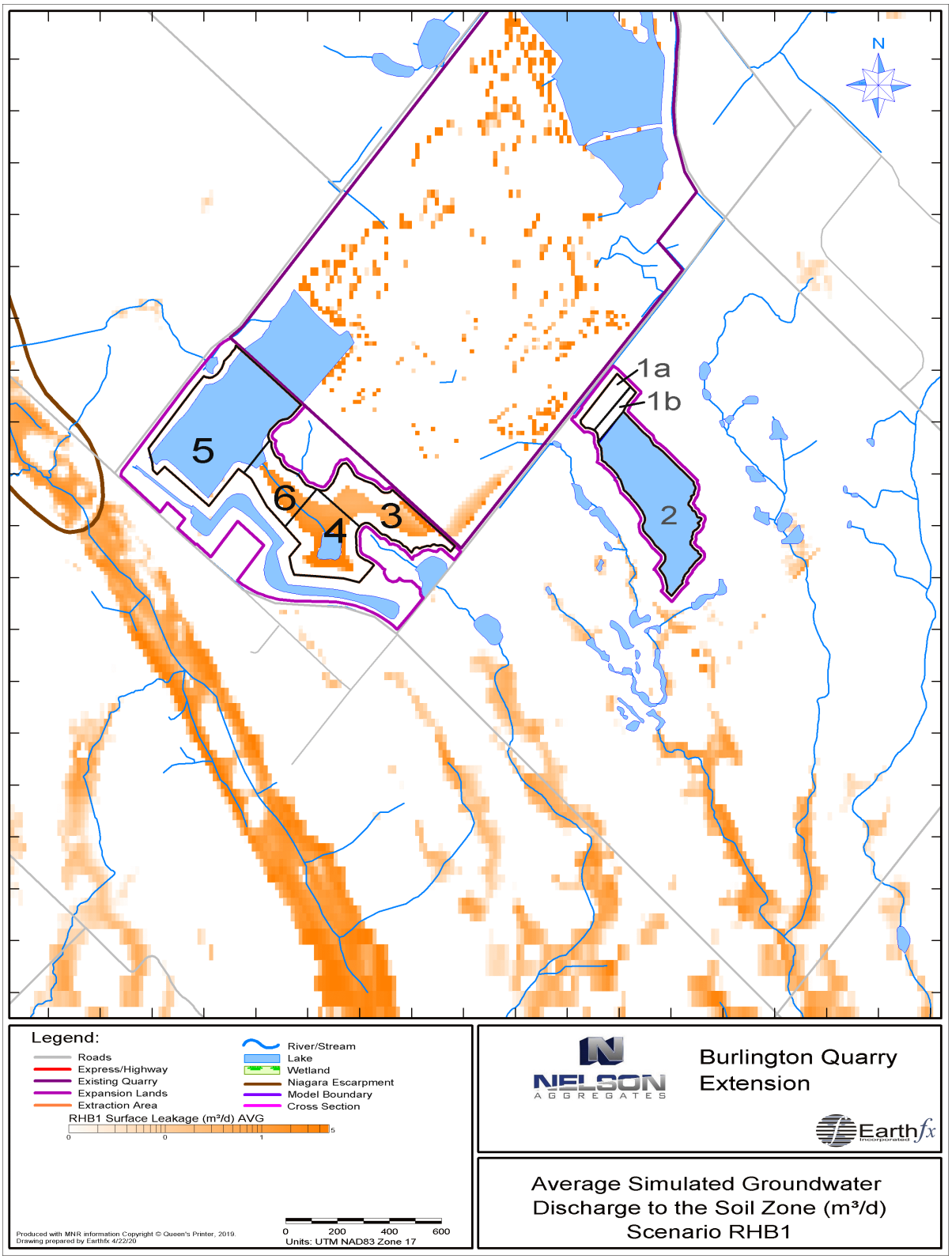

Figure 8.97: Average simulated groundwater discharge to the soil zone (m^3/d) for WY2010-WY2012 – Scenario RHB1.

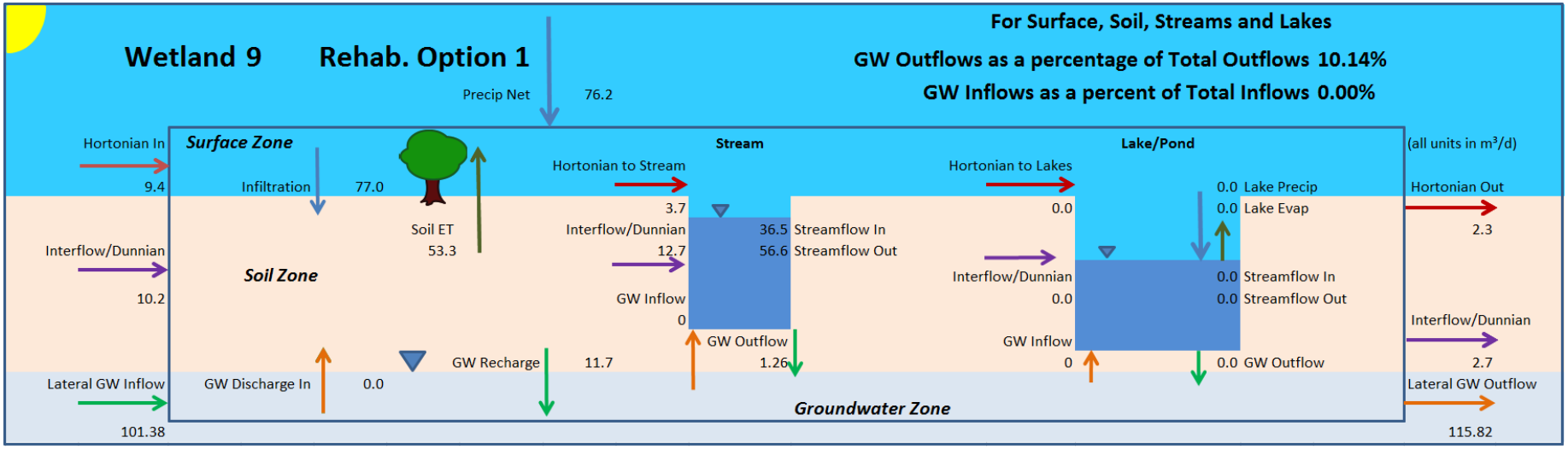

Figure 8.98: Detailed water budget for Wetland 9 averaged over WY2010 to WY2012 under Scenario RHB1.

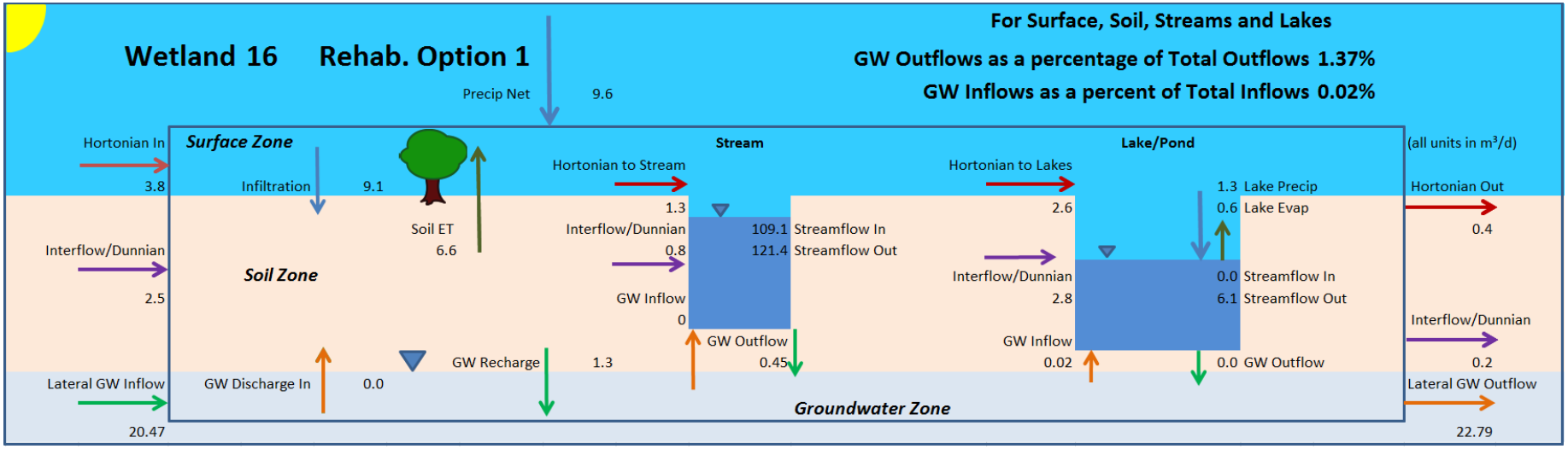

Figure 8.99: Detailed water budget for Wetland 16 averaged over WY2010 to WY2012 under Scenario RHB1.

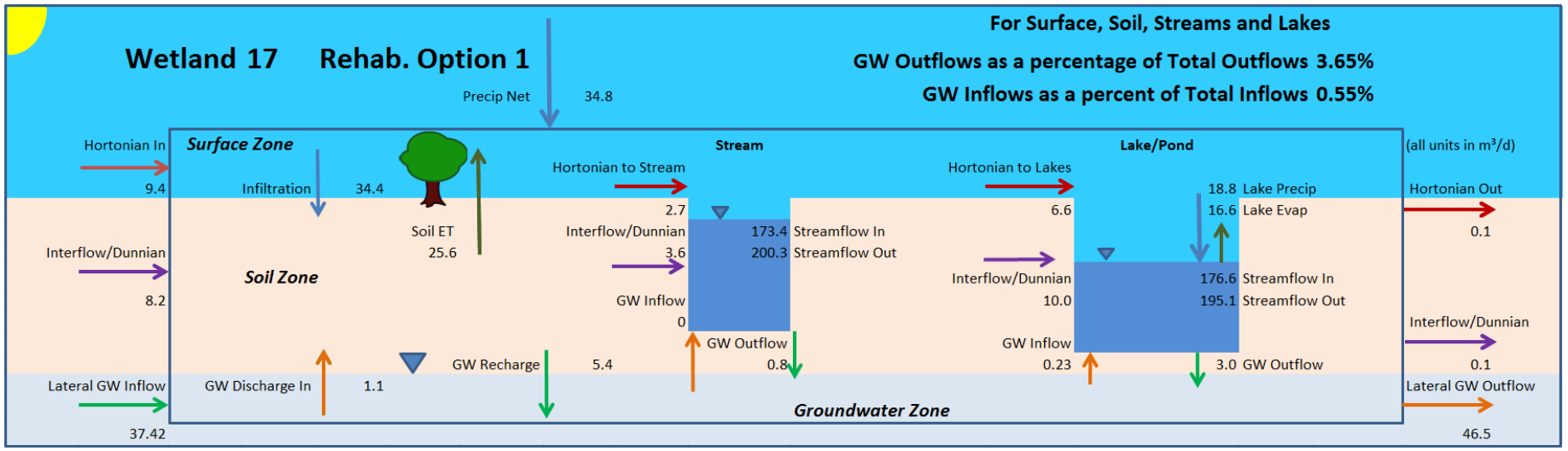

Figure 8.100: Detailed water budget for Wetland 17 averaged over WY2010 to WY2012 under Scenario RHB1.

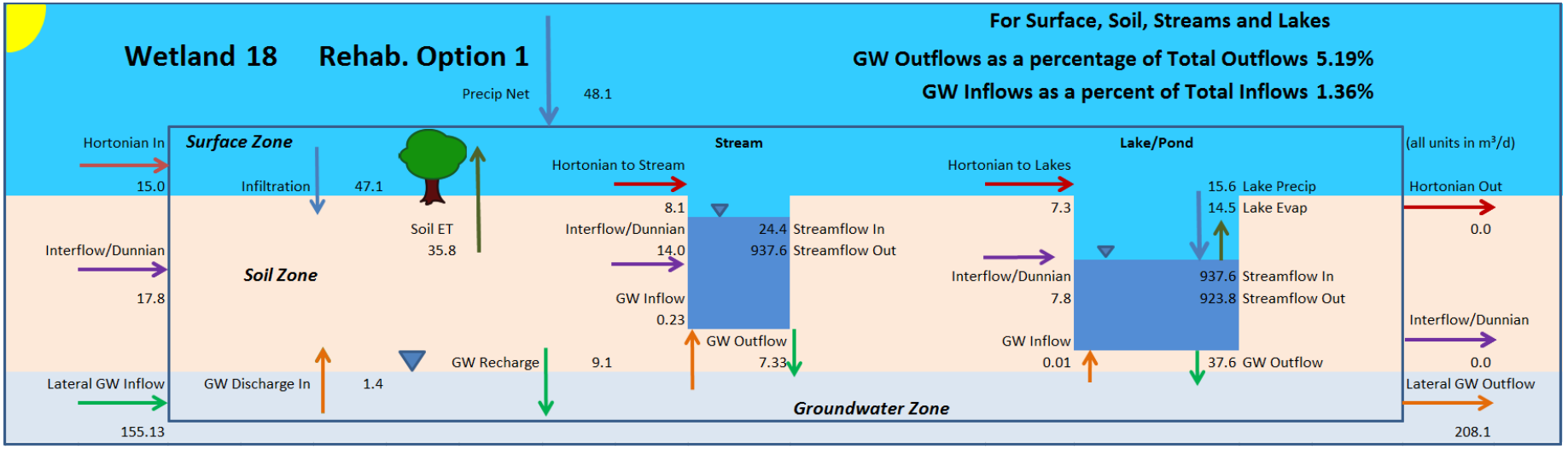

Figure 8.101: Detailed water budget for Wetland 18 averaged over WY2010 to WY2012 under Scenario RHB1.

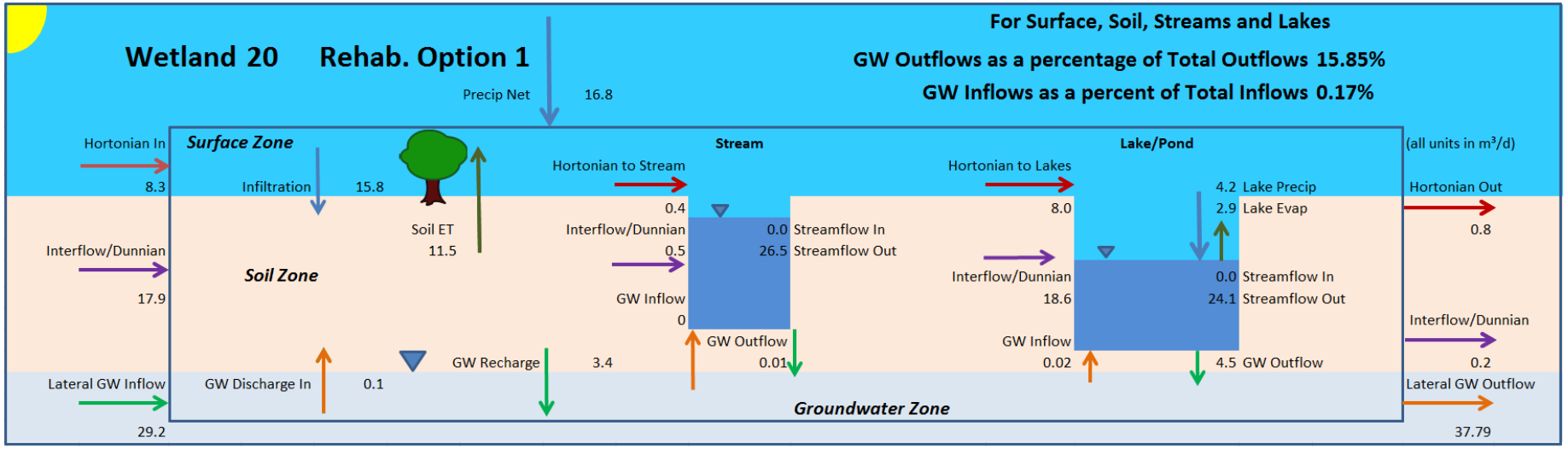

Figure 8.102: Detailed water budget for Wetland 20 averaged over WY2010 to WY2012 under Scenario RHB1.

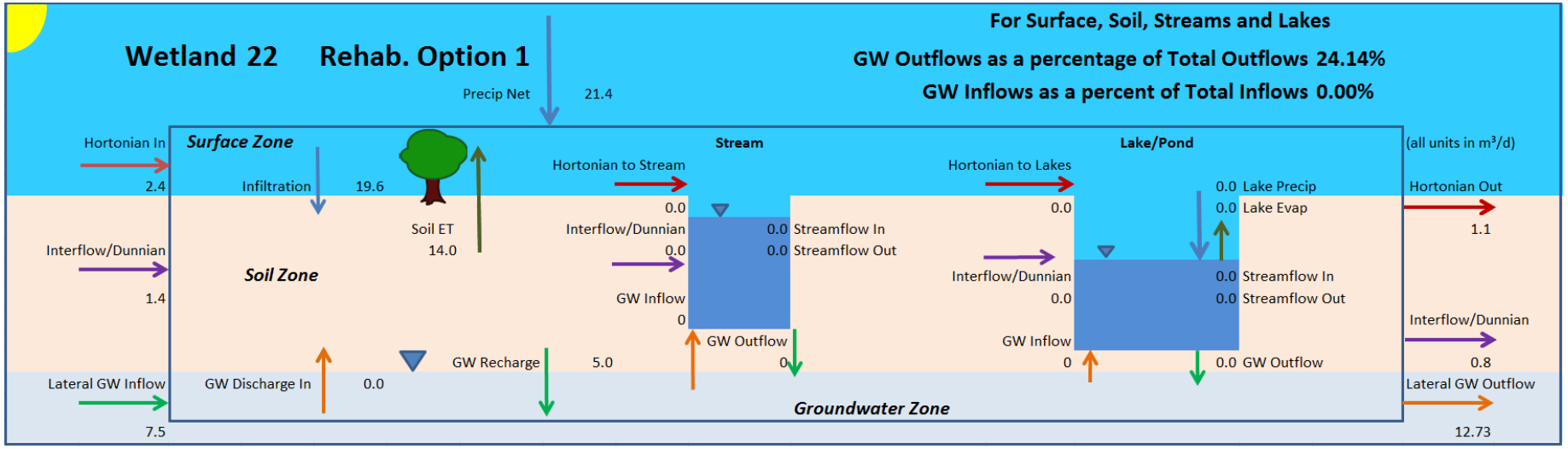

Figure 8.103: Detailed water budget for Wetland 22 averaged over WY2010 to WY2012 under Scenario RHB1.

8.8.5 RHB1 Level 2 Conclusions

From a groundwater perspective, the differences between P3456 and the RHB1 scenario are minor. Under RHB1, a small rise in the water levels in the modified quarry ponds has a minor but positive effect on the water levels in the vicinity of the private wells near the Medad Valley. Quarry discharge and operations are similar. In summary, the Level 2 analysis of available drawdown and wetland function conclusions, presented for P3456 (Section 8.7.7) is essentially the same for RHB1.

Note that the effects of rehabilitation of the P12 excavation (lake filling) are discussed in Section 8.7.7.

8.9 Scenario RHB2

Scenario RHB2 represents the second of two simulations of conditions after excavation of all material in Phase 3 to Phase 6 and implementation of quarry rehabilitation. Scenario RHB2 represent a "walk-away" condition where all dewatering has stopped and the quarry would be allowed to fill to its new equilibrium condition. In this scenario much of the extracted area footprint is converted into a single quarry lake (Figure 8.104). Scenario RHB2 assumes that Scenario RHB1 grading was built first, and, therefore, the topography and backfill on-site is reflective of Scenario RHB1 with the addition of a lake on top of the final graded surface.

The GSFLOW model was modified to incorporate key components of the plan into the model. All quarry lakes were removed, except P12, and replaced with the single large lake extending from the existing quarry to P3456. All quarry drains were removed and the discharge from the Northwest and South-Central sumps was curtailed. The infiltration pond was left in place but there was no active diversion of flow. As in previous scenarios the P12 excavation fills to its natural elevation. Figure 8.77 shows the modified topography and drainage in the quarry vicinity in the P3456 scenario.

Land use and soil class were modified from the RHB1 scenario and changed from "Quarry" to "Open Water" in the new lake footprint. Topography, slope, and aspect were also adjusted in all quarry areas. MODFLOW layer geometry was modified and the input to the LAK3 module was adjusted to represent all the changes to the lake configurations. A new cascade network was generated to account for the new stream network, lakes, and topography.

The GSFLOW model was run with the modified inputs for Scenario RHB2. There were some start-up issues with the model and the longest continuous run was for March 2010 to February 2015 (second half of WY2010 to first half of WY2015). Model results for this period were post-processed and compared to Baseline Conditions. Maps showing average groundwater levels and streamflow, drawdowns and average changes in streamflow and leakage (averaged over WY2010 to WY2014), are presented along with hydrographs showing changes in daily flows and groundwater levels for that period.

8.9.1 RHB2 Drawdowns and Surface Water Flows

Figure 8.105 shows the average simulated heads in Model Layer 6, representing the middle fracture zone in the Amabel aquifer and average simulated streamflow for the same period under Scenario RHB1. Stage in the main rehabilitation lake P12 lake averaged 269.0 masl and varied between 268.75 and 269.3 over the simulation period.

Figure 8.106 shows the simulated change in average head in Model Layer 6. Only a very small area west of Phase 5 had a drawdown greater than 2 m, which was due to the elimination of quarry

discharge and leakage to groundwater. Some residual drawdowns, less than 1.3 m, are noted in the P12 area, due to the flattening of the water table in the vicinity of the P12 lake. Most of the quarry vicinity showed a significant increase in heads ranging from 0 to 12 m, with the 2 m rise extending out up to 630 m from the west side of the existing quarry.

Surface water flow in the upper reaches of a tributary of Willoughby Creek and the West Arm of the West Branch of Mount Nemo Creek will cease when the quarry discharge is discontinued, resulting in an adverse impact to downstream fish habitat compared to baseline conditions (See Savanta, 2020 and Tatham, 2020 for details).

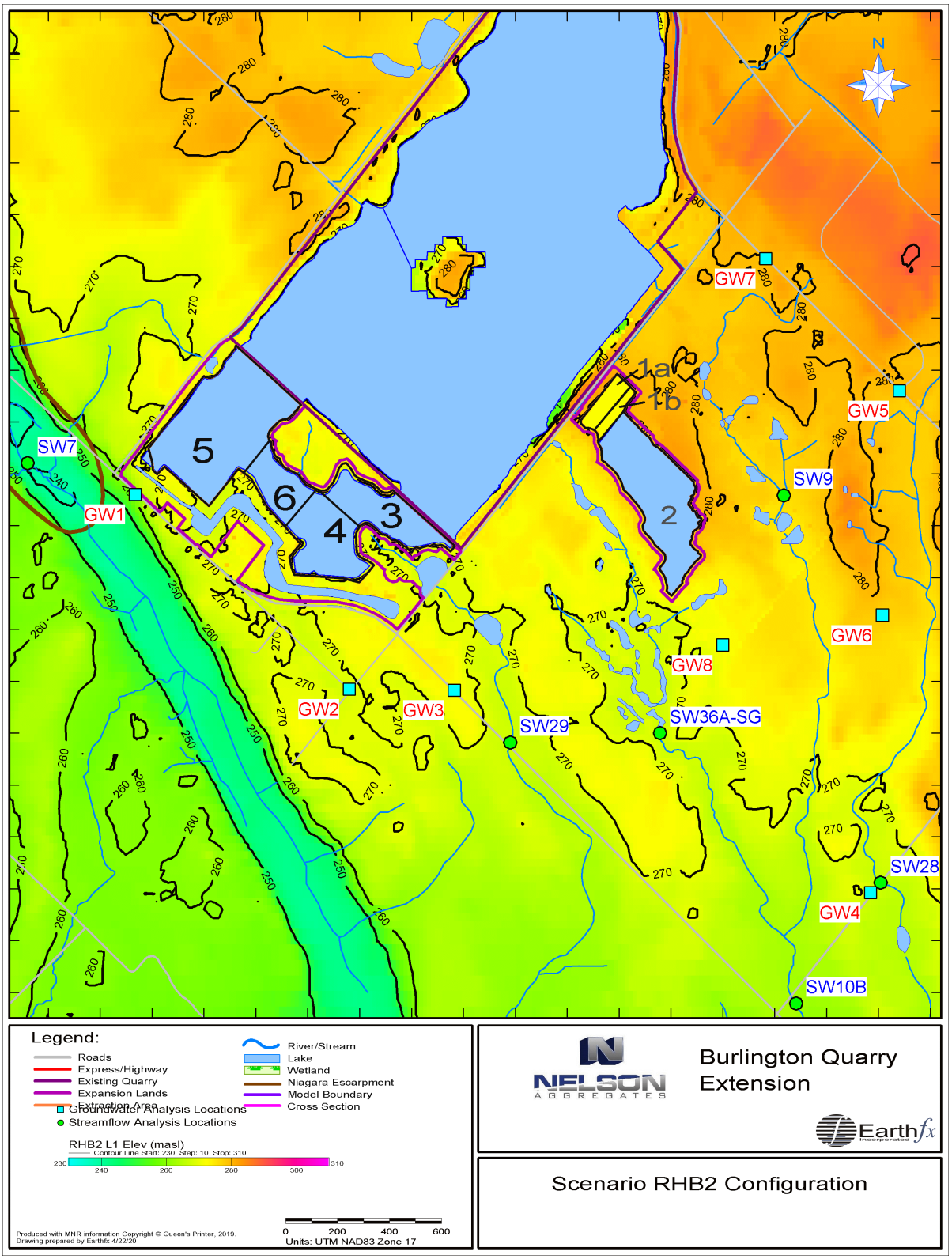

Figure 8.104: Scenario RHB2 configuration.

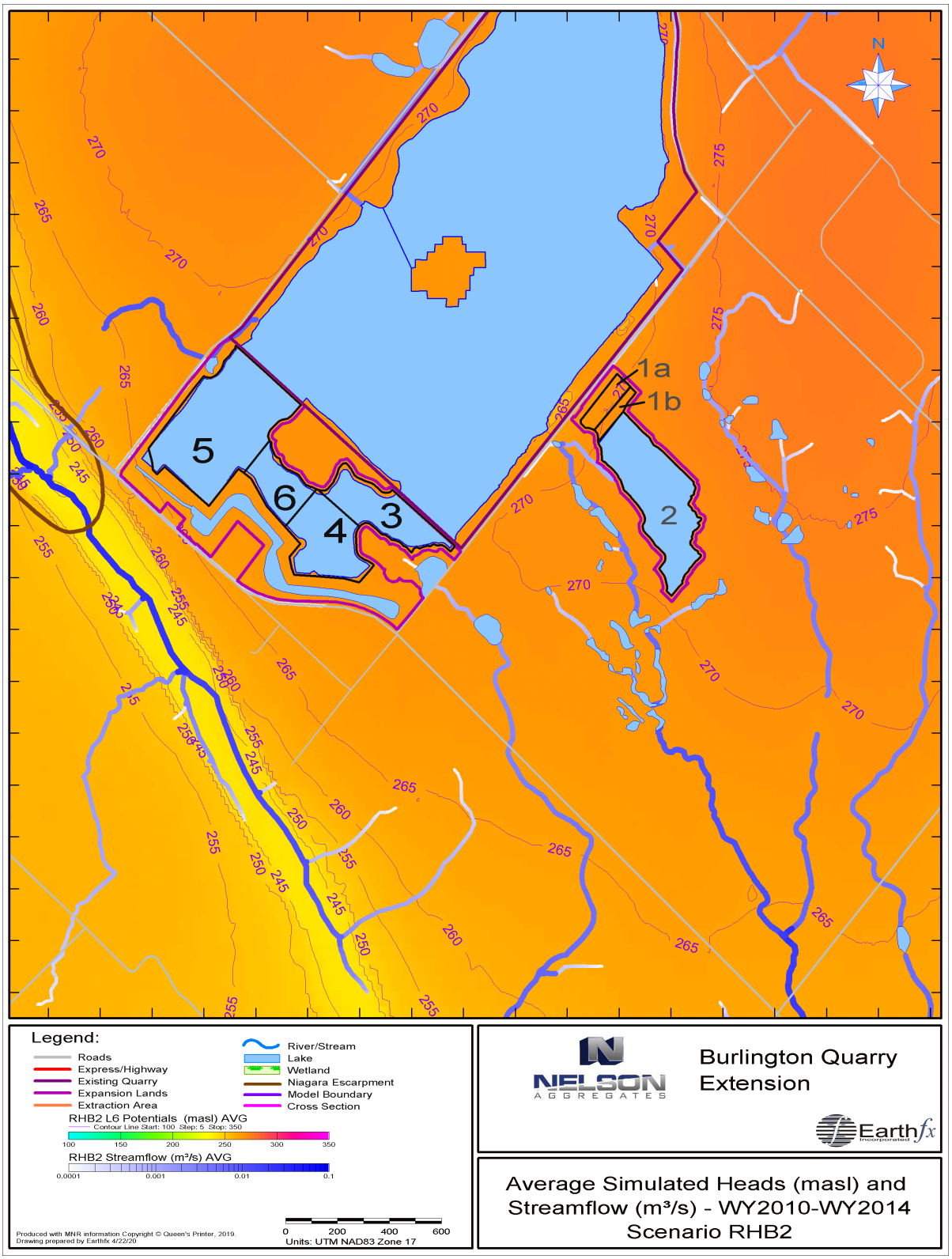

Figure 8.105: Average simulated heads in Model Layer 6 (masl) and streamflow (m^3/s) for WY2010 to WY2014 under Scenario RHB2.

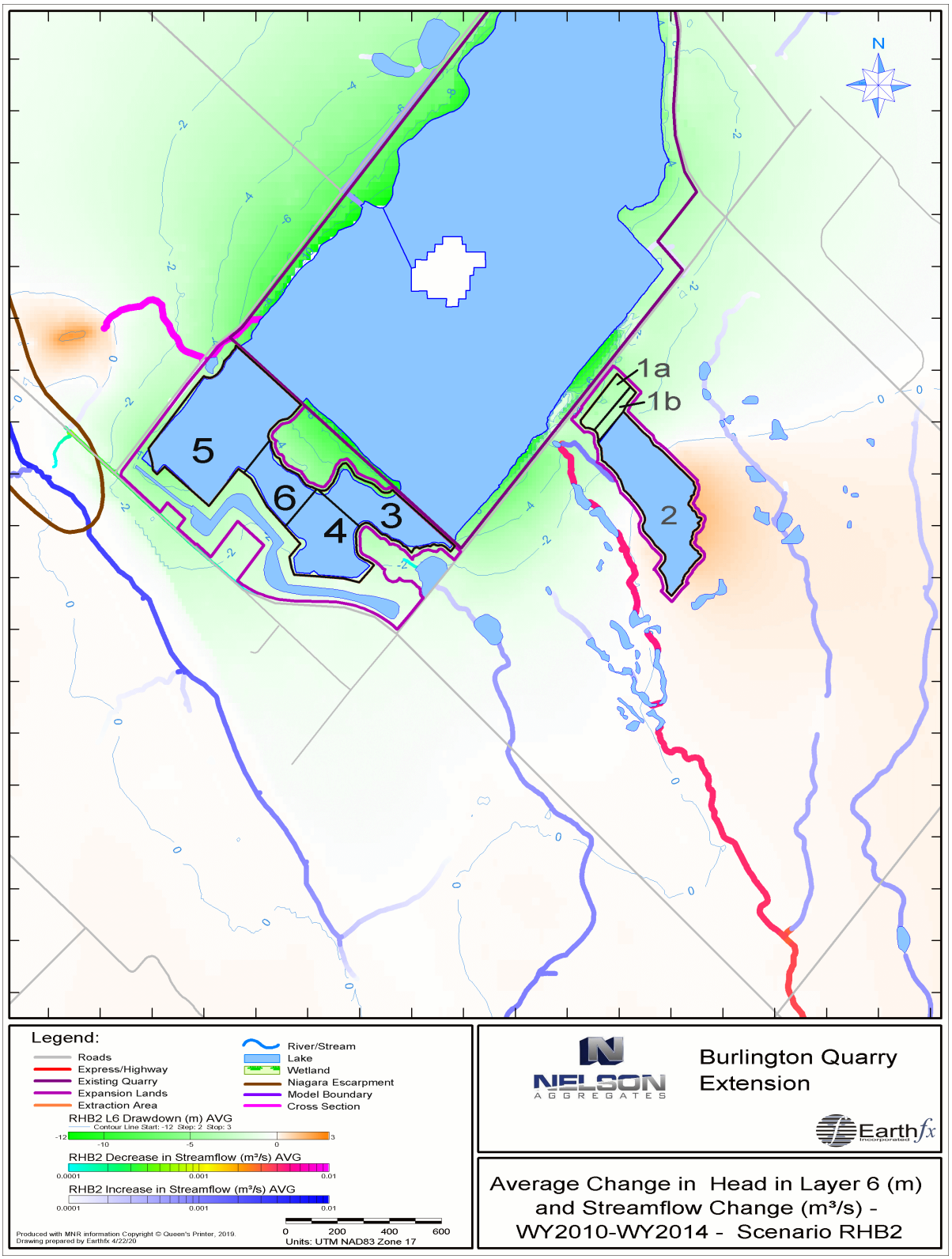

Figure 8.106: Average simulated change in head in Model Layer 6 (m) and increase/decrease in streamflow (m^3/s) for WY2010 to WY2014 under Scenario RHB2.

Figure 8.106 also shows the average simulated change in streamflow. As might be expected, there are significant decreases in flow in the streams that previously accepted quarry discharge. All other streams show net increases in flow ranging from $7x10^{-4}$ m^3/s for the eastern Mt. Nemo Creek tributary, $1x10^{-3}$ m^3/s for the tributary to Lake Medad, and $4.7x10^{-3}$ m^3/s for Medad Creek (despite the cessation of quarry discharge)

Figure 8.107 through Figure 8.112 show hydrographs comparing simulated daily streamflow under Scenario RHB2 to Baseline Conditions, in m^3/s, for the six streamflow analysis points (locations shown in Figure 8.104). The first year of data in these hydrographs appears affected by model spin-up. Flows at SW09 and SW28 have essentially returned to Baseline Conditions with very small increases or decreases in event flows. Small increase in baseflow (0 to 0.002 m^3/s) can be seen at SW29 but there are also small decreases in event-based flows compared to Baseline Conditions (about 0.004 m^3/s). Flows at SW36A and SW10B show small decreases in both baseflow and in event flows (up to 0.03 m^3/s) compared to Baseline Conditions due to the cessation of quarry discharge from the South-Central Sump. SW07 in the Medad valley shows very small gains in baseflow, most likely due to cessation of discharge from the Northwest Sump that served to recharge the groundwater system as it flowed through the karst feature. Decreases in event flows reach a maximum value of 0.05 m^3/s.

8.9.2 RHB2 Seasonal and Inter-annual Groundwater Levels

Figure 8.113 through Figure 8.120 show the simulated heads in Model Layer 6, representing the middle fracture zone in the Amabel aquifer, for WY2010 to WY2012 for the eight measurement points, respectively (locations shown in Figure 8.104). Drawdowns are also shown on the hydrographs (on the inverted secondary y-axis). Heads are consistently higher than Baseline conditions at GW1 (about 2.1 m on average), GW2 ((about 0.5 m on average), GW3 (about 0.3 m on average), GW5 (about 0.25 m on average) and GW7 (about 1.4 m on average) after the start-up period. GW6 (about 0.05 m on average) and GW8 (about 0.1 m on average) show slight decreases in water levels and are affected by the changes induced by the lake level in P12. GW4, which is further east from GW6 and GW8 shows a very slight decrease but is close to Baseline Conditions at the end of the WY2014.

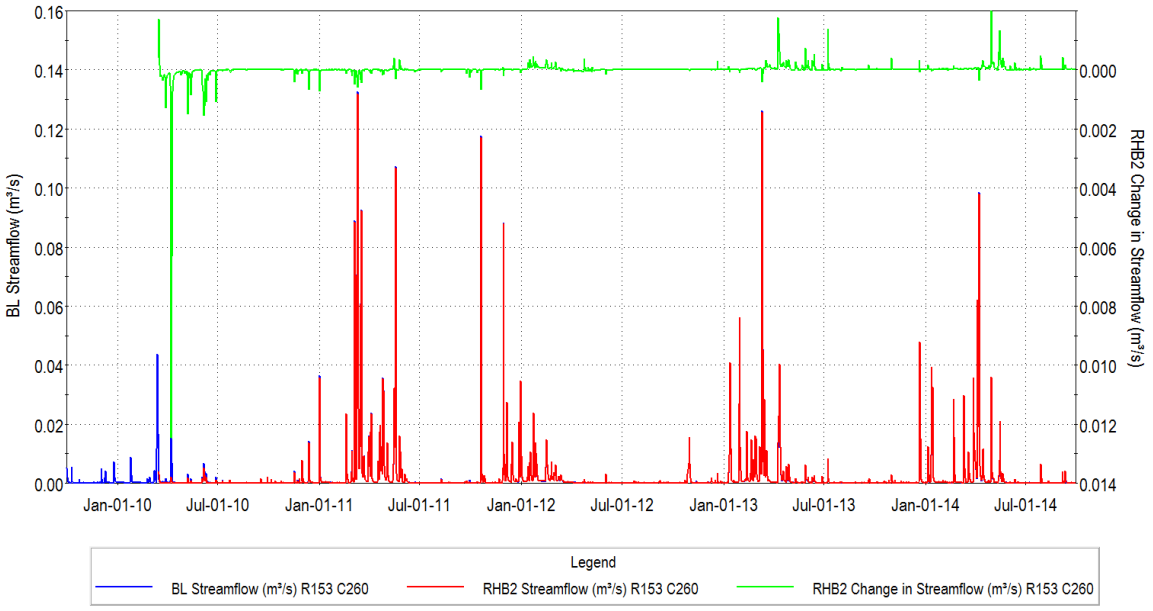

Figure 8.107: Simulated streamflow at SW09 for WY 2010-2014 – RHB2 and Baseline Conditions.

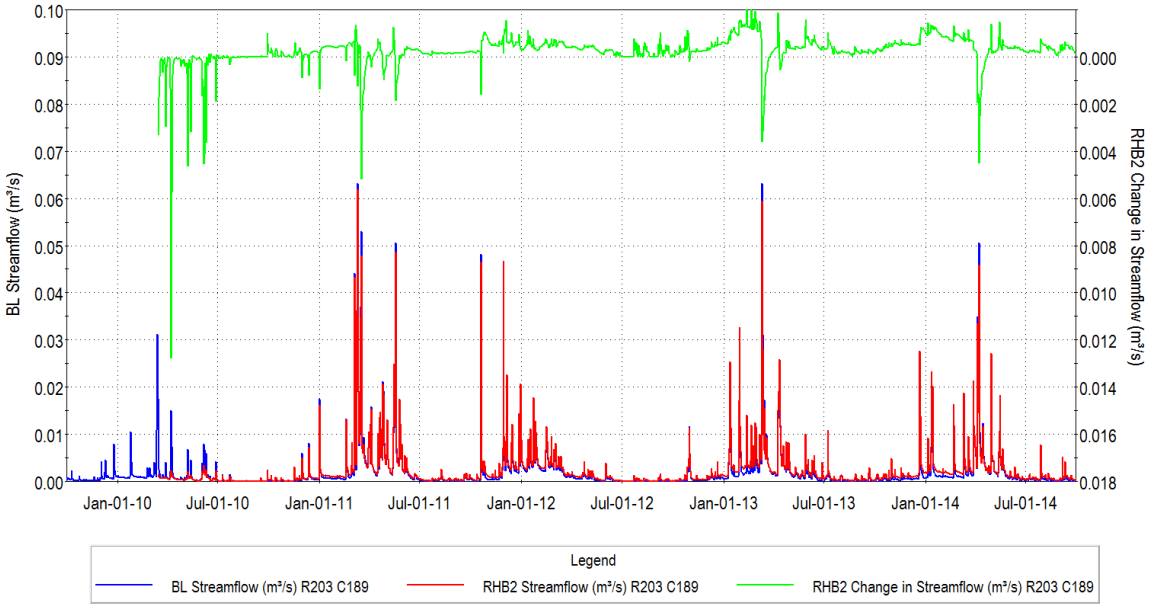

Figure 8.108: Simulated streamflow at SW29 for WY2010-WY2014 – RHB2 and Baseline Conditions.

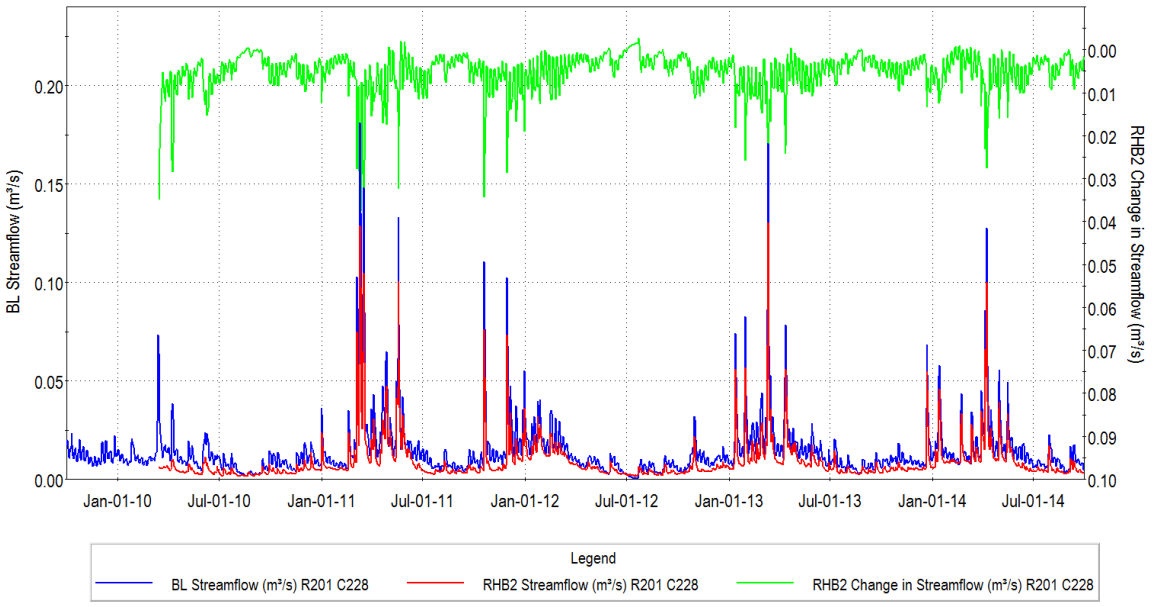

Figure 8.109: Simulated streamflow at SW36A for WY2010-WY2014 – RHB2 and Baseline Conditions.

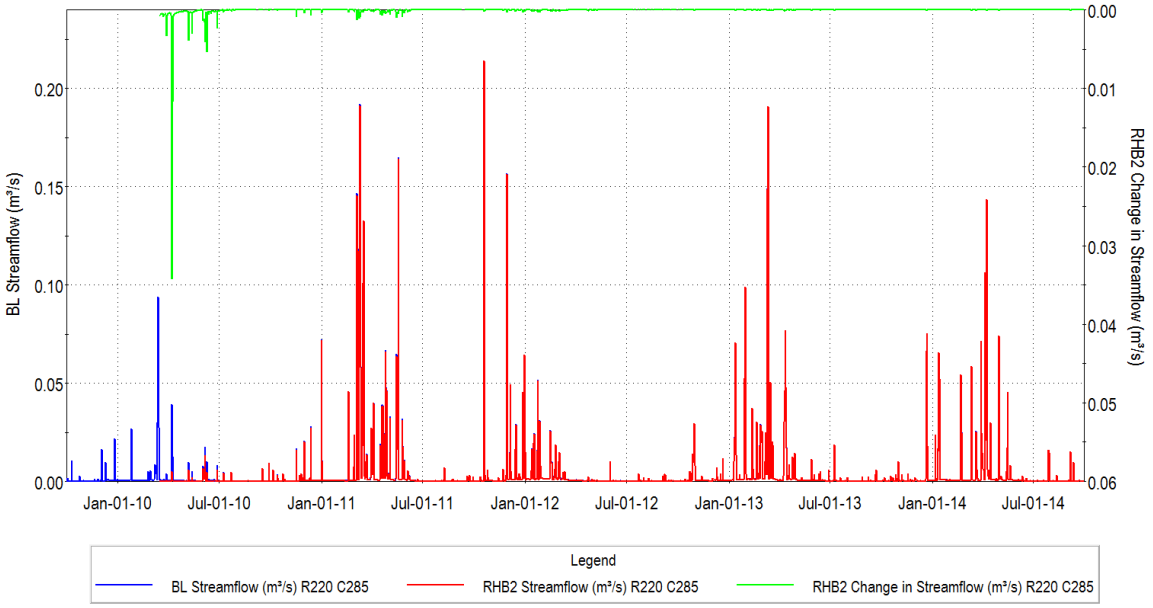

Figure 8.110: Simulated streamflow at SW28 for WY2010-WY2014 – RHB2 and Baseline Conditions.

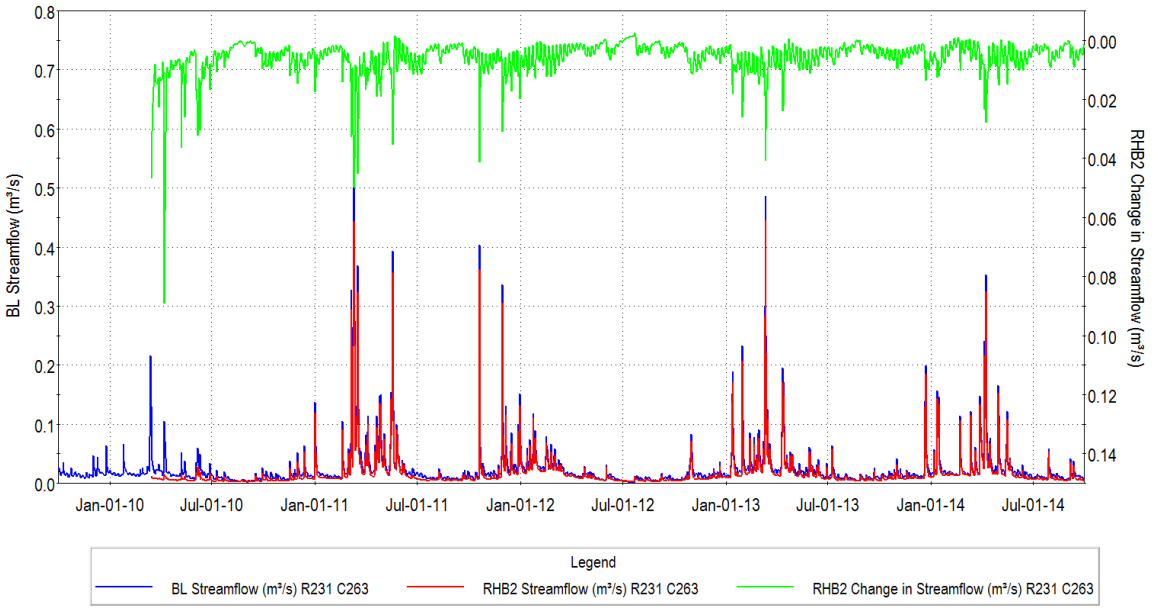

Figure 8.111: Simulated streamflow at SW10B for WY2010-WY20142 – RHB2 and Baseline Conditions.

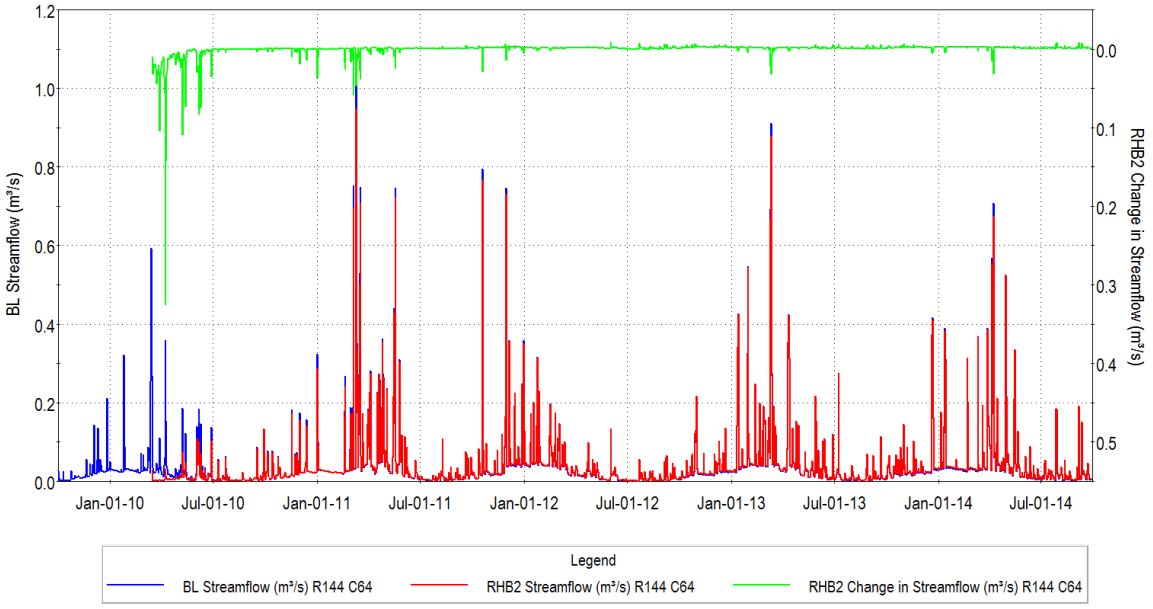

Figure 8.112: Simulated streamflow at SW07 for WY2010-WY2014 – RHB2 and Baseline Conditions.

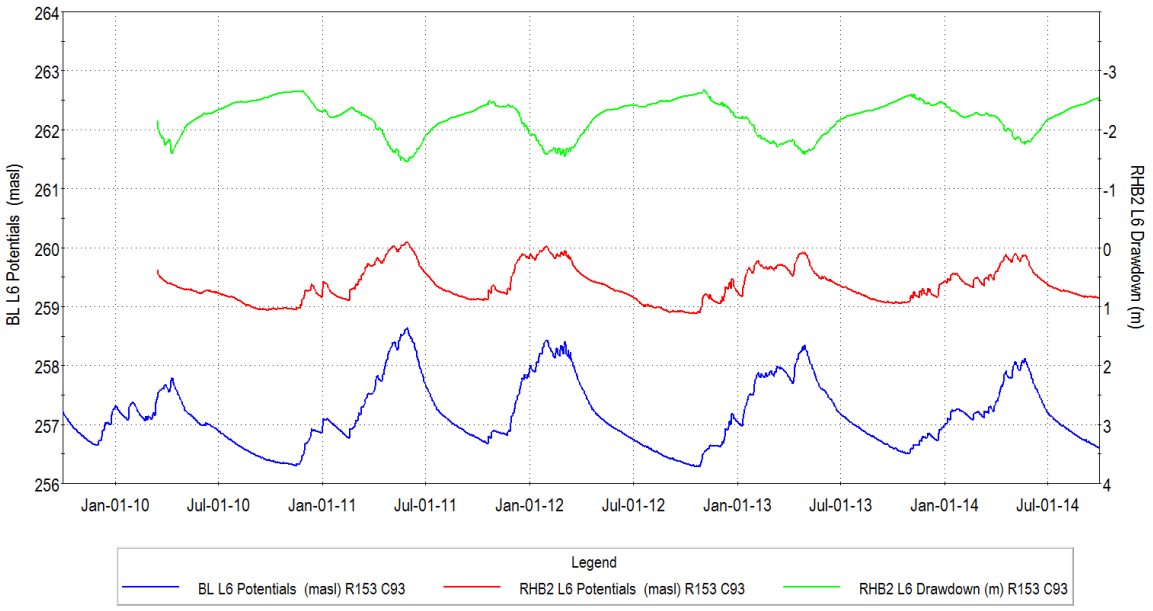

Figure 8.113: Simulated heads and drawdowns in Model Layers 6 at GW1 for WY2010-WY2014 – RHB2 and Baseline Conditions.

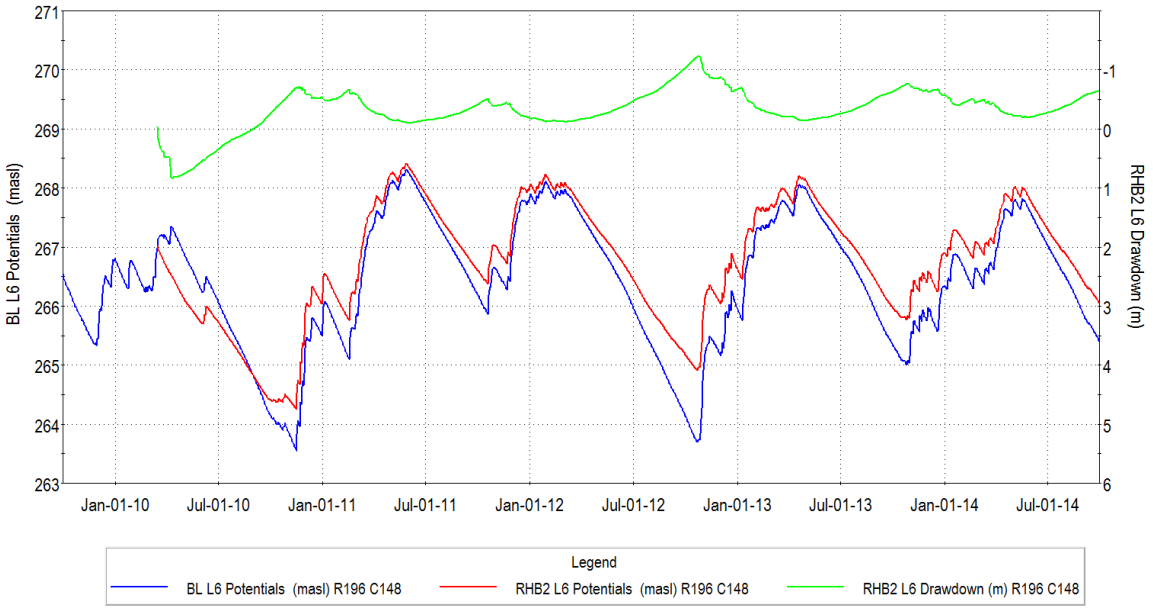

Figure 8.114: Simulated heads and drawdowns in Model Layers 6 at GW2 for WY2010-WY2014 – RHB2 and Baseline Conditions.

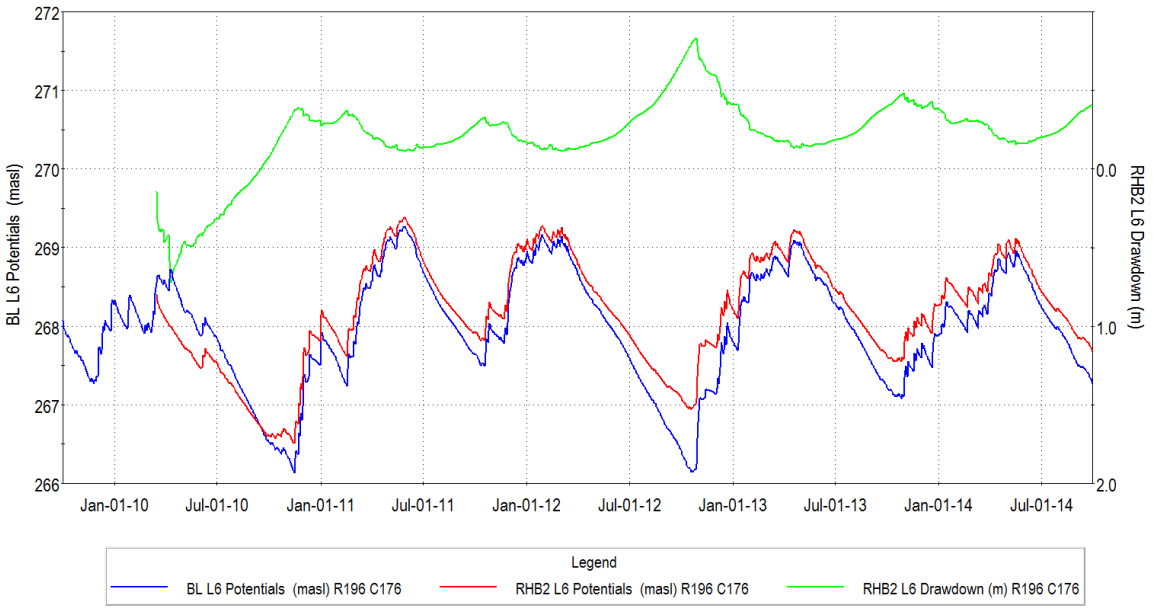

Figure 8.115: Simulated heads and drawdowns in Model Layers 6 at GW3 for WY2010-WY2014 – RHB2 and Baseline Conditions.

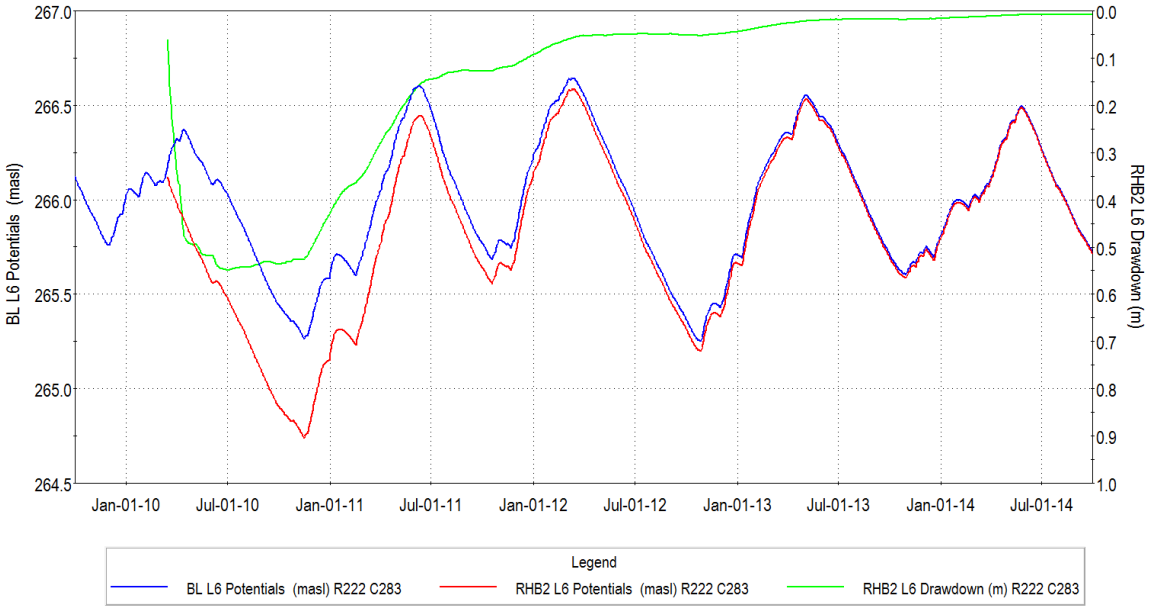

Figure 8.116: Simulated heads and drawdowns in Model Layers 6 at GW4 for WY2010-WY2014 – RHB2 and Baseline Conditions.

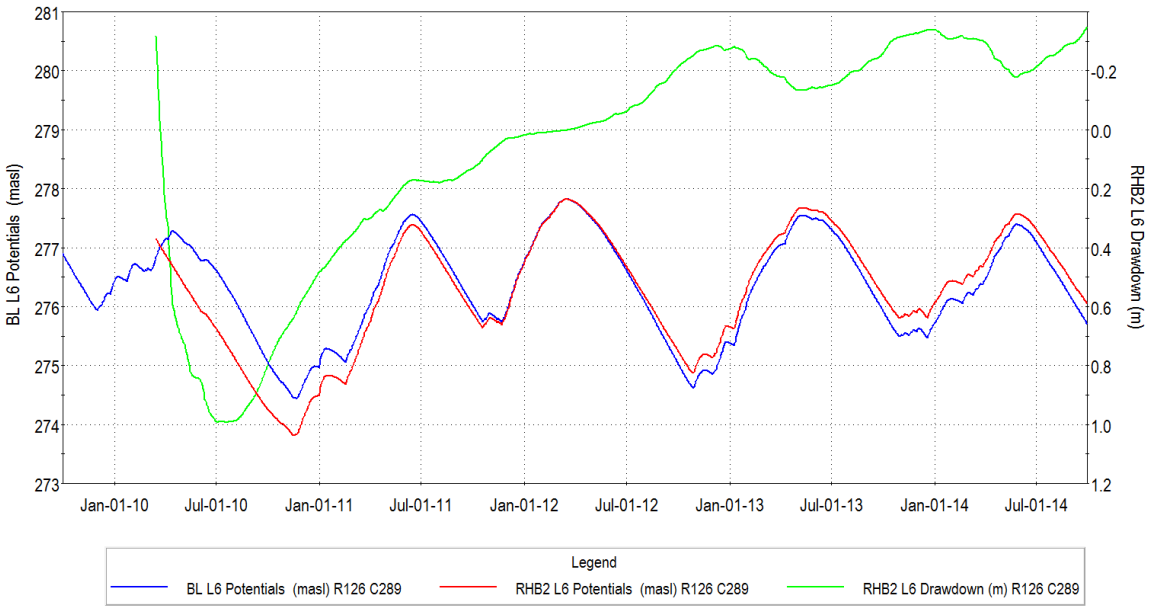

Figure 8.117: Simulated heads and drawdowns in Model Layers 6 at GW5 for WY2010-WY2014 – RHB2 and Baseline Conditions.

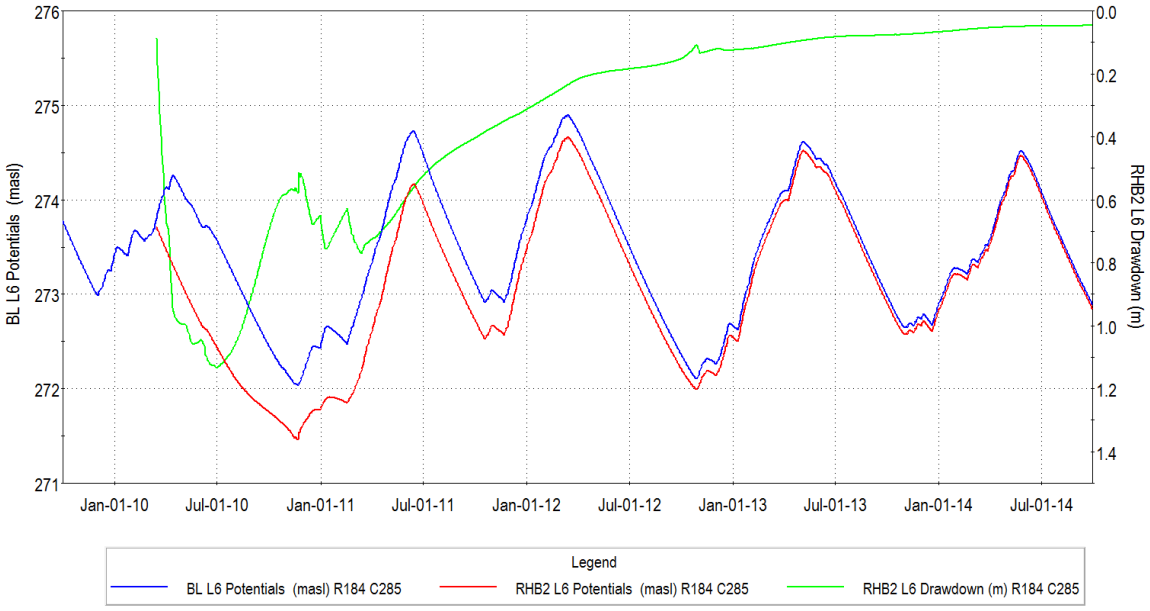

Figure 8.118: Simulated heads and drawdowns in Model Layers 6 at GW6 for WY2010-WY2014 – RHB2 and Baseline Conditions.

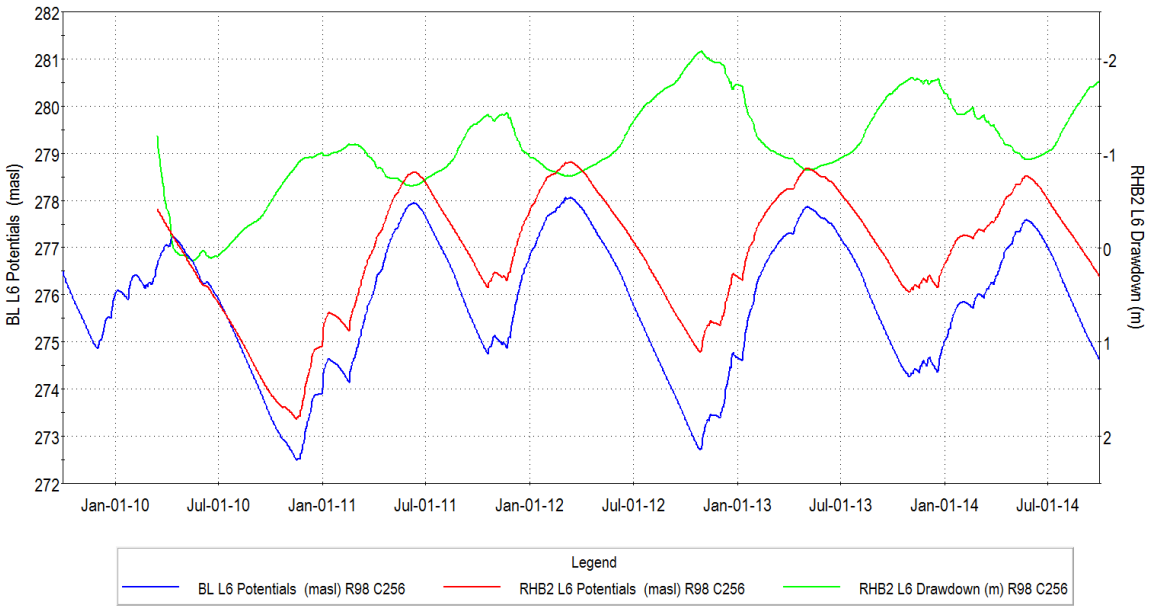

Figure 8.119: Simulated heads and drawdowns in Model Layers 6 at GW7 for WY2010-WY2014 – RHB2 and Baseline Conditions.

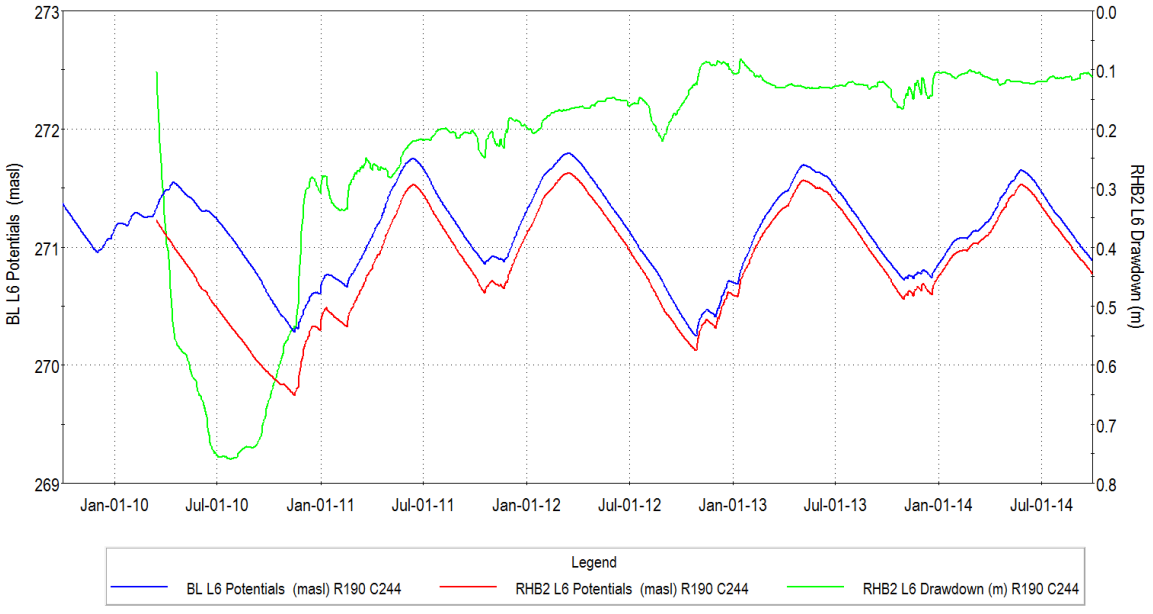

Figure 8.120: Simulated heads and drawdowns in Model Layers 6 at GW8 for WY2010-WY2014 – RHB2 and Baseline Conditions.

8.9.3 RHB2 Surface Water/Groundwater Interaction

Figure 8.121 shows the average simulated net groundwater recharge in the quarry vicinity for Scenario RHB2. The recharge rates outside the quarry lake are nearly the same as for baseline conditions. Similarly, Figure 8.122, which shows that average simulated groundwater ET, is also nearly identical to Baseline Conditions. Leakage below the final quarry lake contributes to the groundwater flow system and contributes to the higher heads outside of the quarry.

Figure 8.123 presents the average simulated streamflow loss to groundwater (blue areas) and the areas of groundwater discharge to streams (red areas). The only significant change compared to Baseline Conditions is the decrease in the seepage out of the stream that carried quarry discharge from the Northwest Sump. Figure 8.124 presents the average simulated groundwater discharge to the soil zone under Scenario RHB2. The appears to be little change from Baseline Conditions except in the area north of P5 where increases in heads have created shallow water table conditions.

8.9.4 RHB2 Wetland Water Budgets

Average water budgets were completed to analyze inflows and outflows to 22 local wetlands (locations shown in Figure 7.22). All flows within each area are computed as well as lateral groundwater flow, streamflow, overland runoff, and interflow crossings the wetland area boundaries. Figure 8.125 through Figure 8.130 present schematics showing detailed water budgets for wetland areas 9, 16, 17, 18, 20, and 22, respectively. The water budgets were compiled for WY2010 to 2014. These can be compared with Figure 7.23 through Figure 7.30 for Baseline Conditions averaged over the same period.

The wetlands are located at various distances from the existing quarry and the extension areas. Wetland 9 shows a small increase in overland runoff and interflow into the wetland and a corresponding increase in groundwater outflow compared to Baseline Conditions. Similar conditions are noted in Wetlands 16 17, and 20 with a slight increase in groundwater (compared to previous scenarios) in to the ponded area. Wetland 18 shows a net decrease in overland runoff and interflow into the wetland area but a notable increase in groundwater inflow into the ponded area (9.54 versus 1.34 m^3/d). Wetland 22 is located between the P3456 extraction area and the existing quarry. This wetland had no change in the water budget compared to baseline conditions because it is perched year-round and there was no change in the contributing area.

8.9.5 RHB2 Level 2 Conclusions

The conversion of the quarry excavation area into lakes will raise groundwater levels throughout the area, with the exception of a small area south of P12, where the lake effect will flatten the water table. In addition, a small decline in water levels will also be observed near the north quarry discharge tributary, as with quarry discharge halted, leakage from the stream will be reduced and groundwater levels will decline modestly in that local area.

The RHB2 scenario is not significantly better for most surface water features than RHB1 because under both scenarios the P12 area is flooded and has returned near baseline conditions. In the west expansion area, the Medad Valley receives essentially the same amount of water under both scenarios because, with its lower relative elevation, it continues to function as a locally significant discharge area in any case.

Surface water flow in the upper reaches of a tributary of Willoughby Creek and the West Arm of the West Branch of Mount Nemo Creek will cease when the quarry discharge is discontinued, resulting in an adverse impact to downstream fish habitat compared to baseline conditions (See Savanta, 2020 and Tatham, 2020 for details).

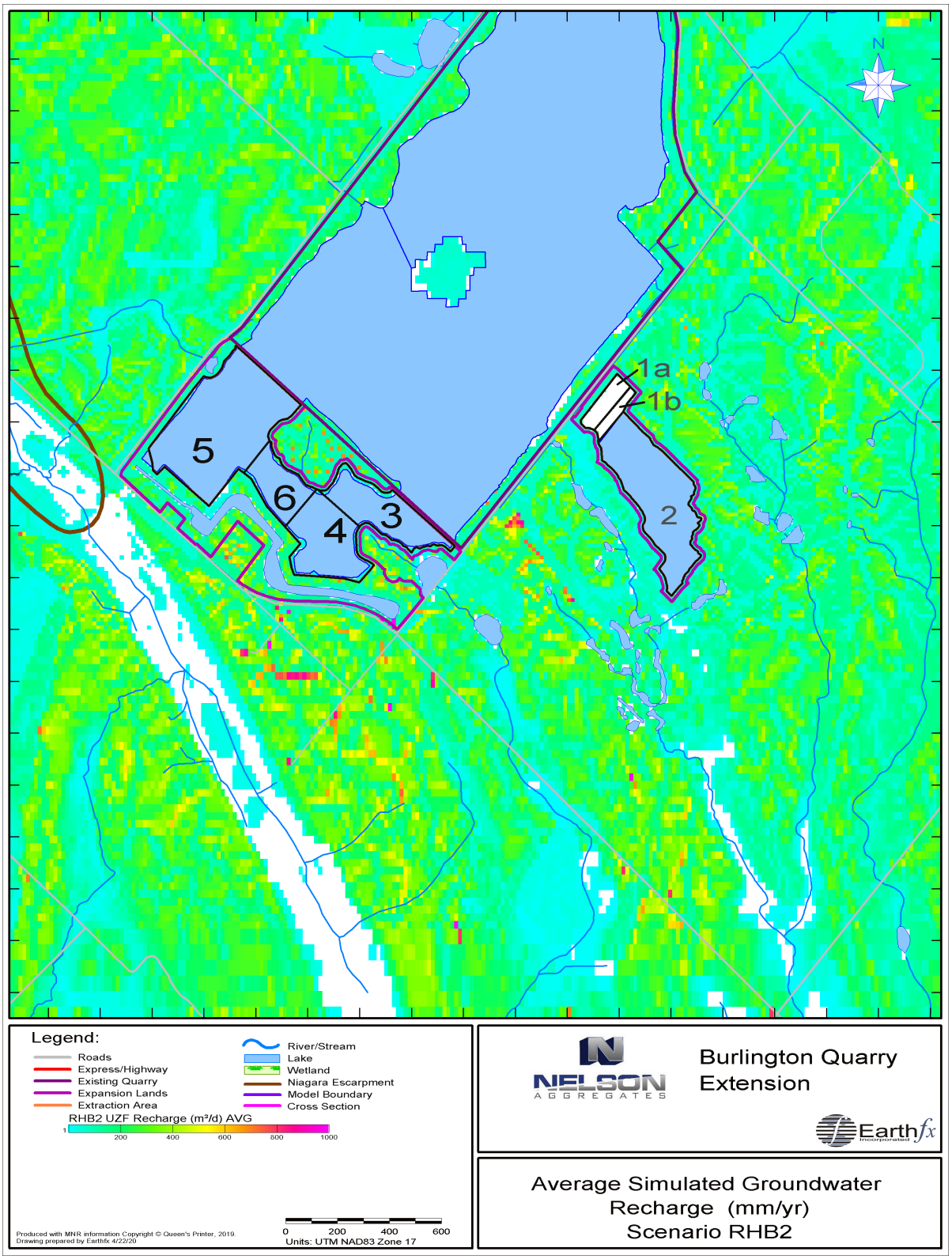

Figure 8.121: Average simulated groundwater recharge (mm/yr) for WY2010-WY2014 – Scenario RHB2.

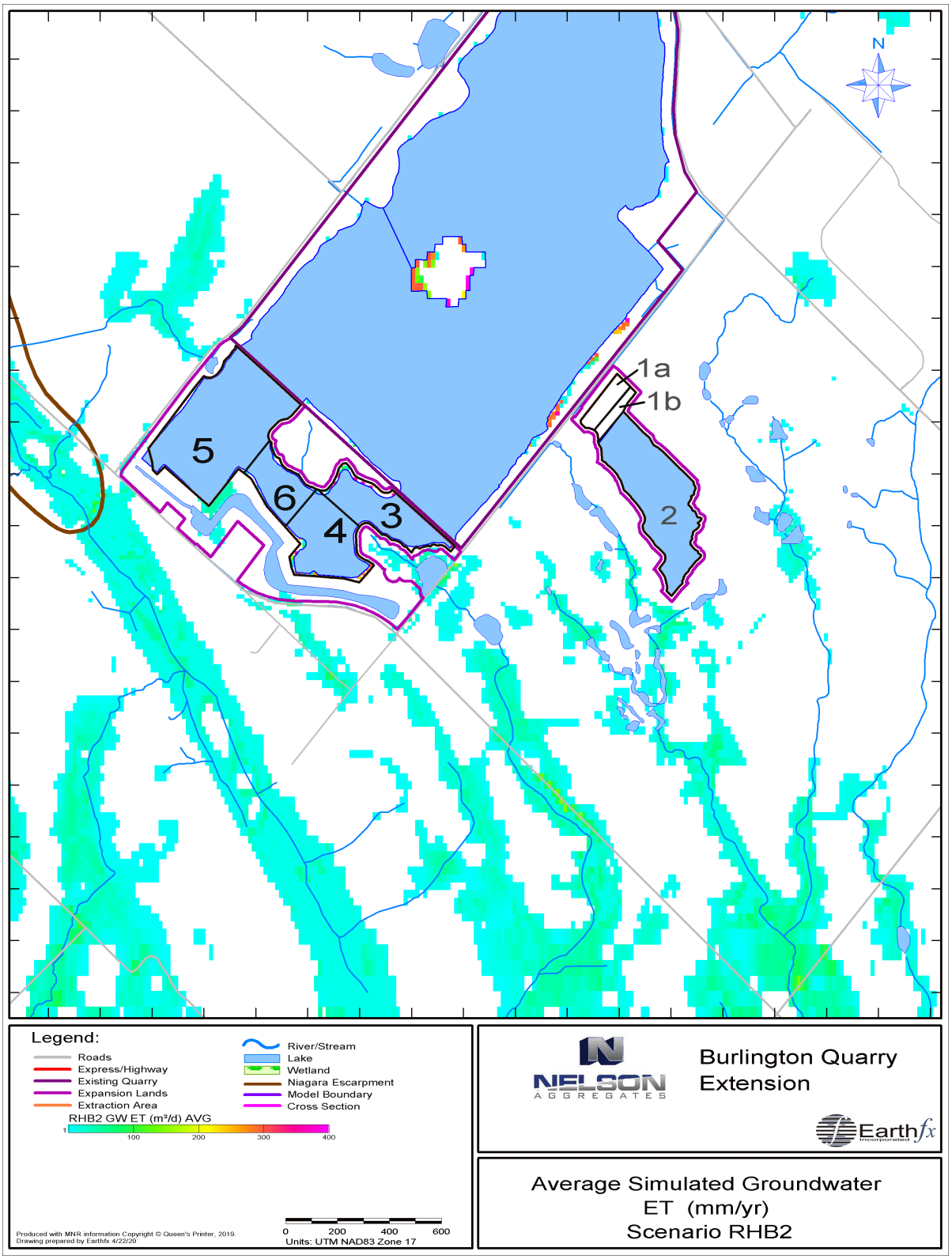

Figure 8.122: Average simulated groundwater ET (mm/yr) for WY2010-WY2014 – Scenario RHB2.

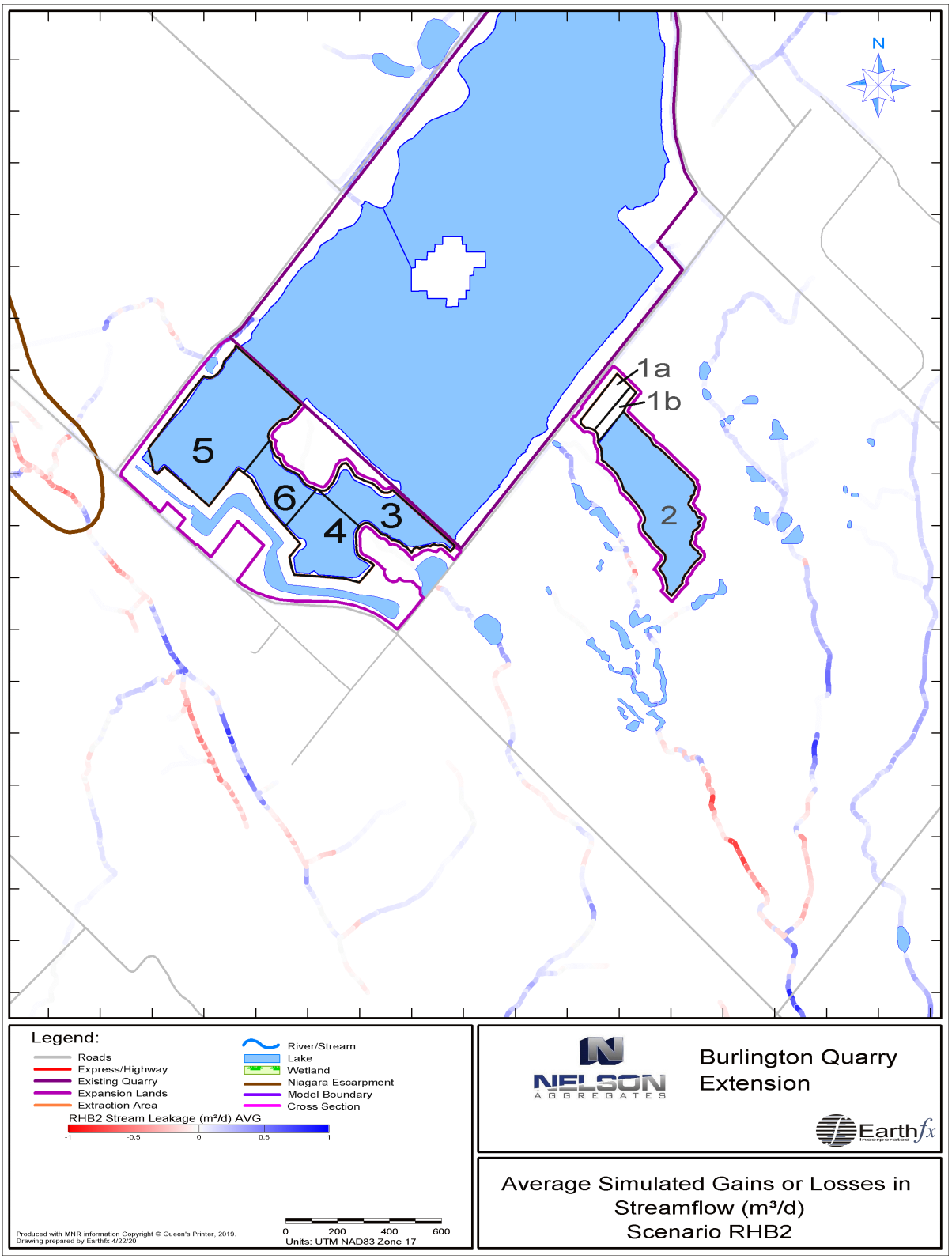

Figure 8.123: Average simulated streamflow loss to groundwater or groundwater discharge to streams (m^3/d) for WY2010-WY2014 – Scenario RHB2.

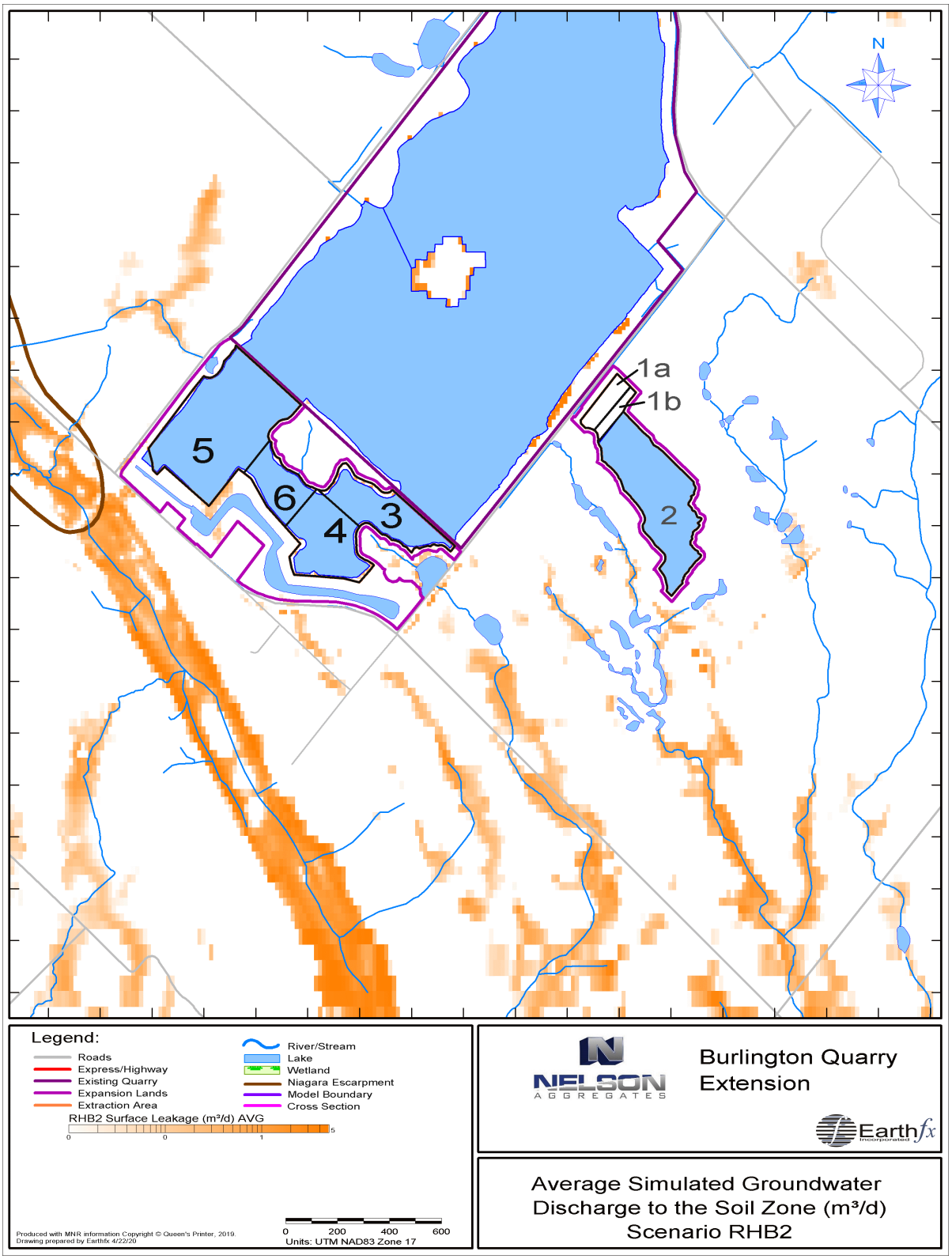

Figure 8.124: Average simulated groundwater discharge to the soil zone (m^3/d) for WY2010-WY2014 – Scenario RHB2.

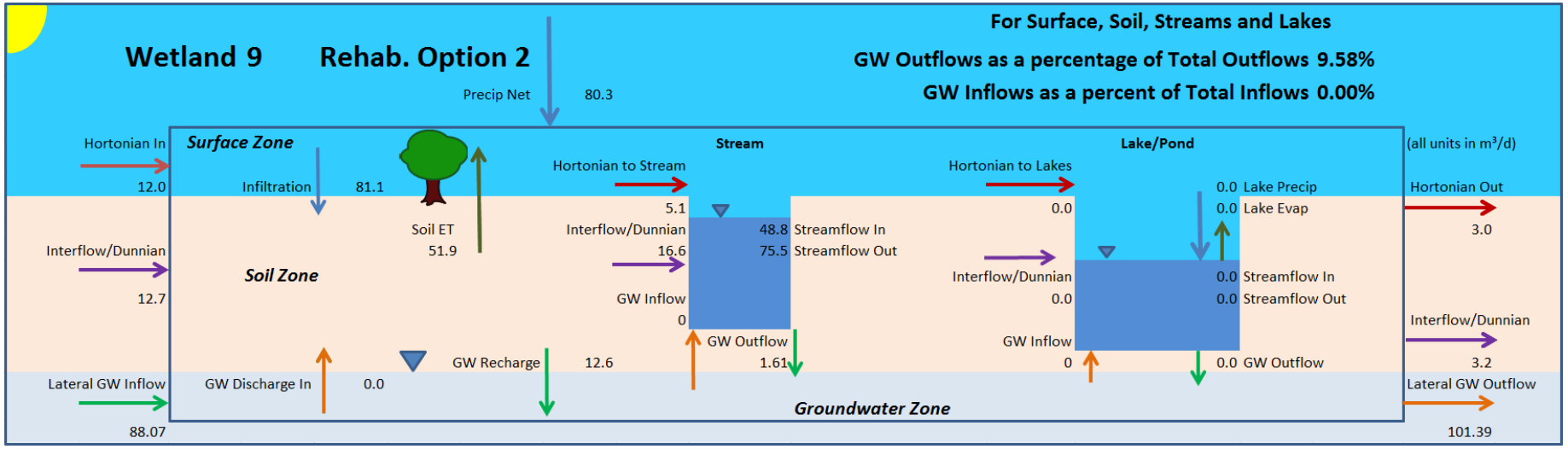

Figure 8.125: Detailed water budget for Wetland 9 averaged over WY2010 to WY2014 under Scenario RHB2.

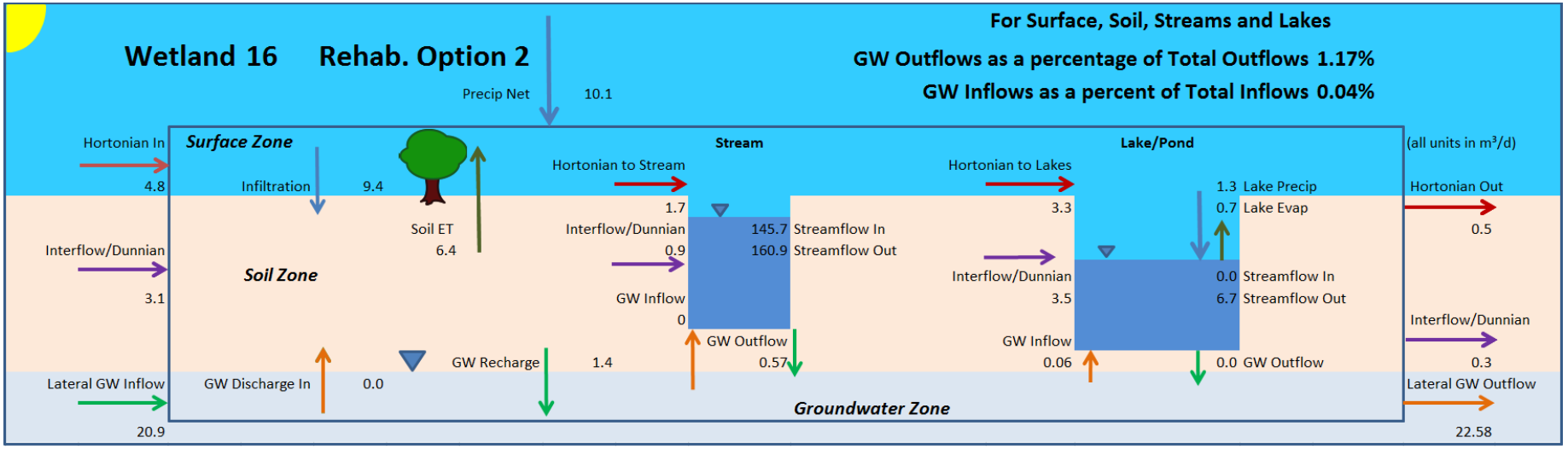

Figure 8.126: Detailed water budget for Wetland 16 averaged over WY2010 to WY2014 under Scenario RHB2.

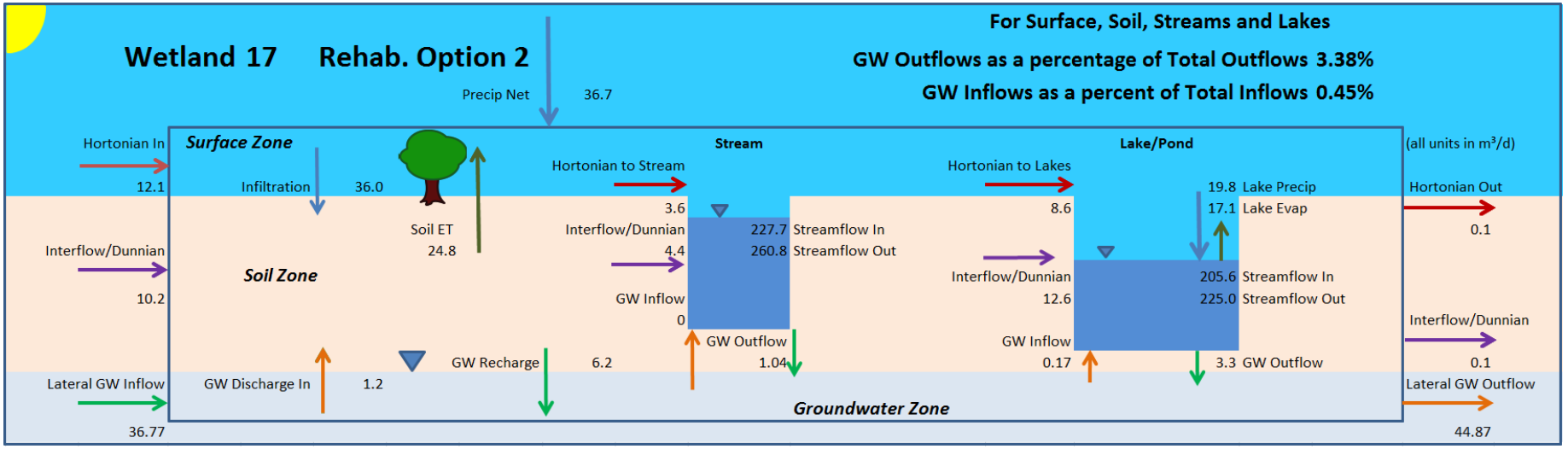

Figure 8.127: Detailed water budget for Wetland 17 averaged over WY2010 to WY2014 under Scenario RHB2.

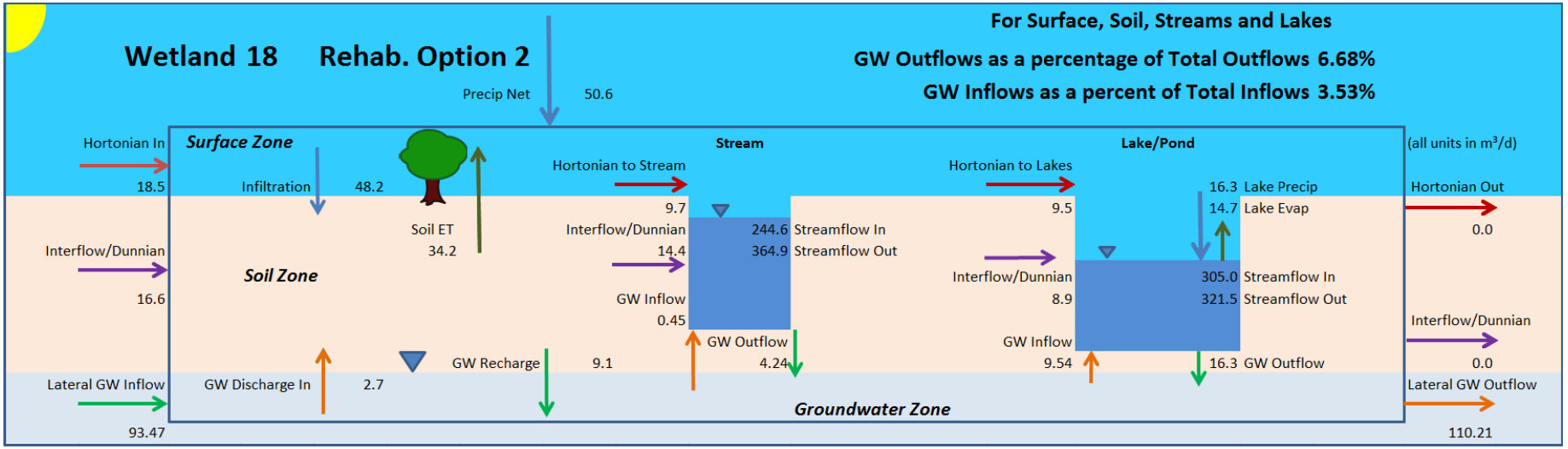

Figure 8.128: Detailed water budget for Wetland 18 averaged over WY2010 to WY2014 under Scenario RHB2.

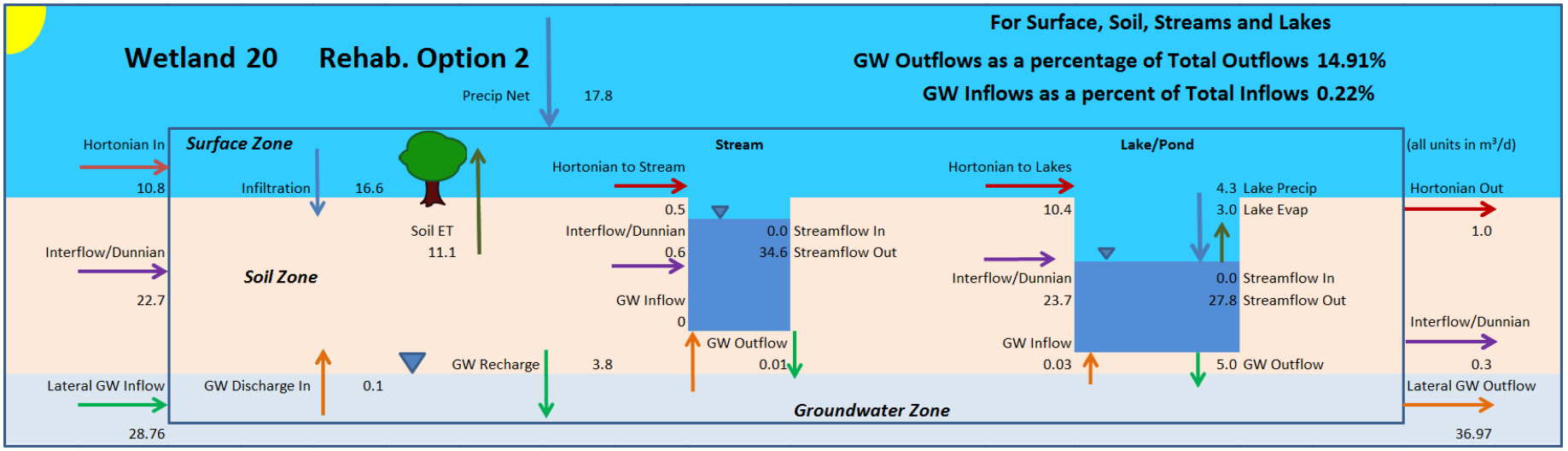

Figure 8.129: Detailed water budget for Wetland 20 averaged over WY2010 to WY2014 under Scenario RHB2.

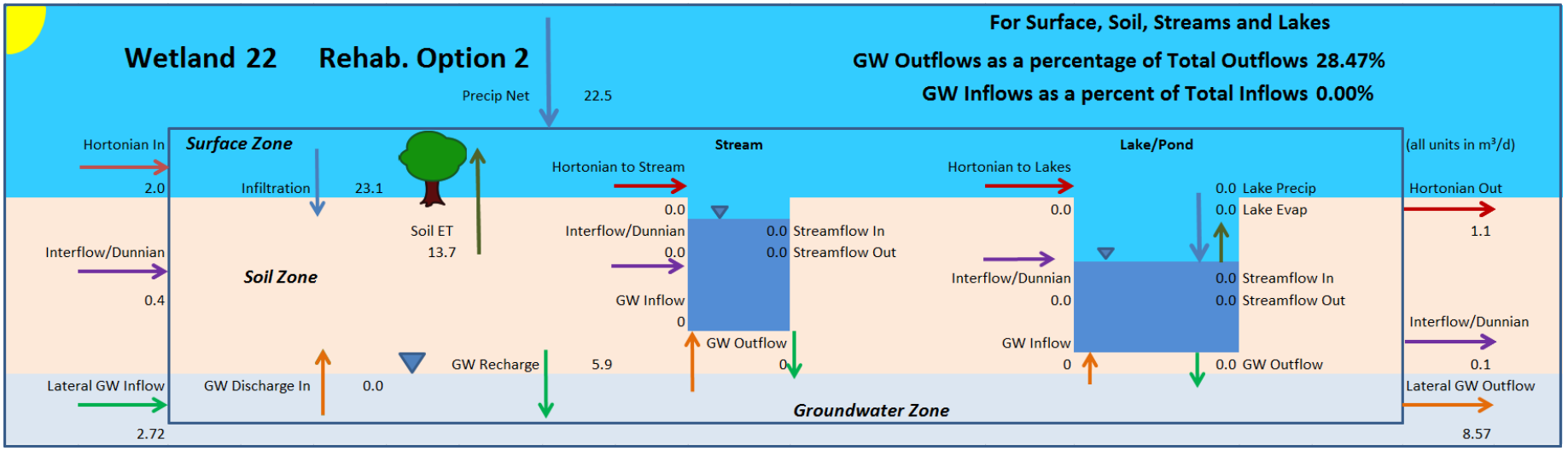

Figure 8.130: Detailed water budget for Wetland 22 averaged over WY2010 to WY2014 under Scenario RHB2.

8.10 Level 2 Impact Assessment Conclusions

The Level 2 impact assessment scenarios present a detailed and exhaustive comparison of the proposed developments to the baseline conditions. All pertinent aspects of the surface water and ground water system have been compared across a wide range of climate conditions. The integrated approach ensures that surface and groundwater functions and water budgets are fully reconciled.

After this detailed analysis, a few key findings become very clear, including:

8.10.1 System Understanding

The system behaviour in and around the existing quarry is extremely well understood. The long-term monitoring (including the monitoring of the 2005-2019 advancement of the south extraction face) provides a clear groundwater response that has been accurately simulated by the transient integrated model. The detailed field investigations, together with the simulation of this large-scale response, provides significant confidence in the assessment.

Similarly, the extensive record of stream flow and wetland monitoring produces an unprecedented level of understanding of the shallow surface water and ground water system. The model closely matches both flows and levels in streams, wetlands and ponds. This includes wetlands that are part of the stream network and received significant stream flows and surface runoff, and also those that are isolated and perched high above the water table.

8.10.2 Drawdowns

As noted above, the model closely matches the existing drawdowns in and around the quarry, including recent developments.

The local conditions associated with each of the extension phases does result in somewhat different drawdown patterns, but the overall conclusions and general patterns are the same.

The 2.0 m drawdown cone associated with P12 extends up to 1000 m from the excavation. P12 is, however, optimally located, as it is located in an area with up to 22 m of available drawdown in the Amabel Aquifer. P12 is also relatively isolated from private wells along Cedar Springs Road, Sideroad 1 and Guelph Line, so the effects will not impact those private wells.

The 2.0 m drawdown cone associated with P3456 extends 330 m to 450 m from the excavation. P3456 is next to a locally significant groundwater discharge area, so water levels are relatively stable and less subject to drought, seasonal fluctuations and the effects of excavation.

8.10.3 Water Supply

While the simulations identify drawdown effects, they also clearly demonstrate that the Amabel aquifer will continue to be a productive and sustainable local water supply resource. The analysis confirms that there is between 5 and 23 m of available drawdown across the study area, confirming that there is ample groundwater available for current and future private water supply use.

8.10.4 Stream and Wetland Function

The wide distribution of low permeability Halton Till in and round the quarry is the dominant feature controlling surface and groundwater interaction. The wetlands and streams are generally perched above the water table and isolated from the groundwater system by the low permeability till. None of the wetlands receive significant groundwater inflow, and are thus isolated from any changes in the water table due to quarry development.

As a locally significant groundwater discharge area, the Medad Valley wetlands will continue to receive groundwater and surface water discharge both during P3456 extraction, and after closure, whether under RHB1 or RHB2 conditions. There will be some changes in where the discharge will enter the valley, but ultimately, the same amount of water will reach the outlet of the valley.

Under the preferred rehabilitation scenario (RHB1), discharge continues to the north from Sump 0100 and to the south from Sump 0200 as per the recommendations presented in the Tatham (2020) and Savanta (2020) reports.

9 Development of the Groundwater Monitoring Program

9.1 Objectives

The intent of the groundwater monitoring program is to serve four (4) primary purposes: These are listed as:

1. to determine the background quality and seasonal groundwater level fluctuations in the vicinity of the extraction activities;
2. to assess and characterize the quality and seasonal groundwater level fluctuations throughout the quarry operations and upon closure of the Burlington Quarry;
3. to evaluate whether unforeseen changes within the groundwater regime is occurring from the extraction of aggregate and quarry dewatering; and if they are
4. to determine the presence of, and risk to, private well receptors of the unforeseen changes and if the implementation of mitigation measures is required to off-set the unexpected changes in the groundwater regime.

Groundwater monitoring will not be used to assess potential impacts to surface water features form and function. Recent studies[1] have highlighted the difficulties of using groundwater drawdown thresholds for monitoring and protection of groundwater-dependent ecosystems (springs and groundwater-fed springs). In response, Nelson has proposed an alternative surface water monitoring and threshold strategy (presented in the AMP under separate cover).

9.2 On-Site Monitoring Wells

Based on the findings of the impact assessment, key sentry groundwater monitoring wells have been selected and incorporated into the long-term groundwater monitoring program. The groundwater monitoring program consists of water level and water quality monitoring. Water levels will be collected manually on a monthly basis as well as continuously with automatic water level transducers. The manual measurements are used to calibrate the continuous data, which allows for a comprehensive assessment of the water level responses and trends.

The groundwater monitoring network consists of well nests, which monitor discrete intervals in the bedrock aquifer, as well as, open holes, which are constructed to straddle water-bearing flow zones. Well nests have monitoring wells with either A or B following the well label (for example: W03-1A and M03-1B). The A monitor is constructed in the regionally extensive lower bedrock aquifer system found below the quarry floor elevation. The B monitor is constructed within the upper/middle dolostone unit that intersects the quarry extraction face.

Water quality sampling will be completed on a semi-annual basis. Parameters will include general water quality parameters, metals, major and minor ions and cations, and hydrocarbons (F1-F4 and VOCs).

9.3 Off-Site Domestic Water Wells

[1]Drawdown ''Triggers'': A Misguided Strategy for Protecting Groundwater-Fed Streams and Springs, Currell, Vol. 54, No. 5–Groundwater–September-October 2016

The MECP requires that all PTTW holders take the necessary actions to ensure residents and their water supplies are protected from potential impacts associated with the water takings at aggregate operations. To be proactive and to alleviate the complaint driven process, Nelson shall implement a voluntary domestic water well monitoring program to those residents located within 1 km of the Burlington Quarry extension lands. This program will be designed to act as an early warning system and would identify any potential adverse interference that may compromise the integrity of the domestic water supply.

A follow-up door-to-door water well survey will be completed to attempt to expand the Private Well Monitoring Program. This program will be offered to residents within 1 km of the extension lands by a qualified well technician (as is required by law [Ontario Regulation 903, as amended]). This program will be designed to establish baseline conditions of existing domestic water wells. Domestic water wells need to be determined case-by-case as the physical characteristics of each well will need to be evaluated and documented to provide an understanding of the current conditions, including water quality, well yield and the available drawdown.

This monitoring program will be completed only at locations where permission has been granted by the property owner. Furthermore, the domestic water wells, which will be incorporated into the AMP shall be constructed to comply with Ontario Regulation 903 (as amended).

9.4 Groundwater Impact Assessment Methodology

The Level 1 and 2 Hydrogeological Assessment must identify potential receptors, outline the compliance monitoring program, as well as identify threshold values to assess and mitigate the potential impact to those receptors that may be impacted by the quarry development.

The impact assessment methodology has been developed for the initial five (5) years of quarry operation. During these five (5) years, Nelson will have only operated in the south extension and will have completed extraction from Phase 1 and will have partially extracted Phase 2. The area surrounding the south extension area has been monitored extensively for over seven (7) years. As a result, the awareness of how the groundwater regime behaves is enough to develop the assessment tools, such as threshold values and threshold trend analysis for the south extension.

The impact assessment methodology proposed for the Burlington Quarry extension involves both an evidence-based and a predicted-based approach to ensure that the complexity of fractured rock hydrogeology is addressed. The evidence-based approach requires a comprehensive understanding of the natural variability of groundwater elevations at key monitoring locations. This understanding requires several years of monitoring data that shows the groundwater systems natural response to varying climatic conditions, including how the aquifer responds during and following dry/drought conditions. The baseline conditions allow for an improved ability to identify unforeseen trends in water level data, which could be a result of the quarry operations.

The predictive-based approach relied upon the simulated water level drawdowns in the bedrock aquifers resulting from both climatic conditions and quarry dewatering. The predicted water levels during drought conditions represent a worst-case scenario that may be encountered during the initial phases of quarry operation (Phase 1 and 2).

A key component of the evidence-based groundwater monitoring program is the availability of background water level data that reports the natural conditions during quarry extraction.

9.4.1 Monitoring of Background Groundwater Conditions

To assist in the evaluation of the water levels measured as part of the groundwater monitoring program, a background monitoring well has been incorporated to the program. The background monitoring well is a domestic water well located north of the existing quarry at 2377 Collins Road (referred to as DW2; Figure 9.1). The purpose of this background monitoring well is to document the natural variability of the groundwater elevation fluctuations and trends under various future climatic conditions. This background monitoring well has shown to have no drawdown from the proposed quarry extension.

As discussed in the following sections, the impact assessment will be assessing short and long-term trends identified in the data. Being able to identify trends that are resulting from either prolonged climatic changes or those which are largely associated with aquifer dewatering are a fundamental component of the AMP. On-going monitoring data from DW2 will be used to represent the natural background conditions.

9.4.2 Comprehensive Groundwater Elevation Trend Analysis

Traditionally, AMPs have set seasonal site-specific trigger water level elevations at select sentry monitoring wells. These trigger values are determined based on the evaluation of baseline water level data and the predicted maximum extent of the cone of influence under full extraction limits. By defining the maximum extent of the cone of influence, trigger values are set that would activate mitigation measures if the observed values collected through the groundwater monitoring program are lower than predicted during set periods (seasonal triggers).

Trigger values set based on the traditional approach have caused numerous false positive trigger exceedances. The reasons for these exceedances include the oversimplification of the methodology to setting trigger values in a fractured rock environment (fundamental principles of how aquifers respond to abstraction), and more importantly the neglect to account for the full impact of climate change. Seasonal variability in groundwater level as well as season creep, which refers to observed changes in the timing of the seasons, have been widely observed in Ontario.

A key objective of the impact assessment methodology is to utilize the important concept of long-term trends from either prolonged climatic changes or those which are largely associated with aquifer dewatering. Prolonged climatic changes mean sustained periods of departure from "normal" precipitation amounts, for example droughts. These precipitation trends, when severe and lengthy, leave noticeable effects on groundwater levels. Short-term trends (seasonal) should also be evaluated. However, they should not cause a concern if an exceptionally dry year results in water levels that drop below a minimum reported or predicted water level.

Nelson will rely on the Seasonal Mann-Kendall Test to statistically interpret trend analysis of groundwater elevations at select sentry wells. The Nottawasaga Valley Conservation Authority has relied on the Seasonal Mann-Kendall Test to interpret Provincial Groundwater Monitoring Network (PGMN) groundwater levels after it was recognized that statistically definable results can be utilized to manage groundwater resources, assess drought conditions, evaluate the impact of human activities on groundwater and evaluate long-term groundwater trends.

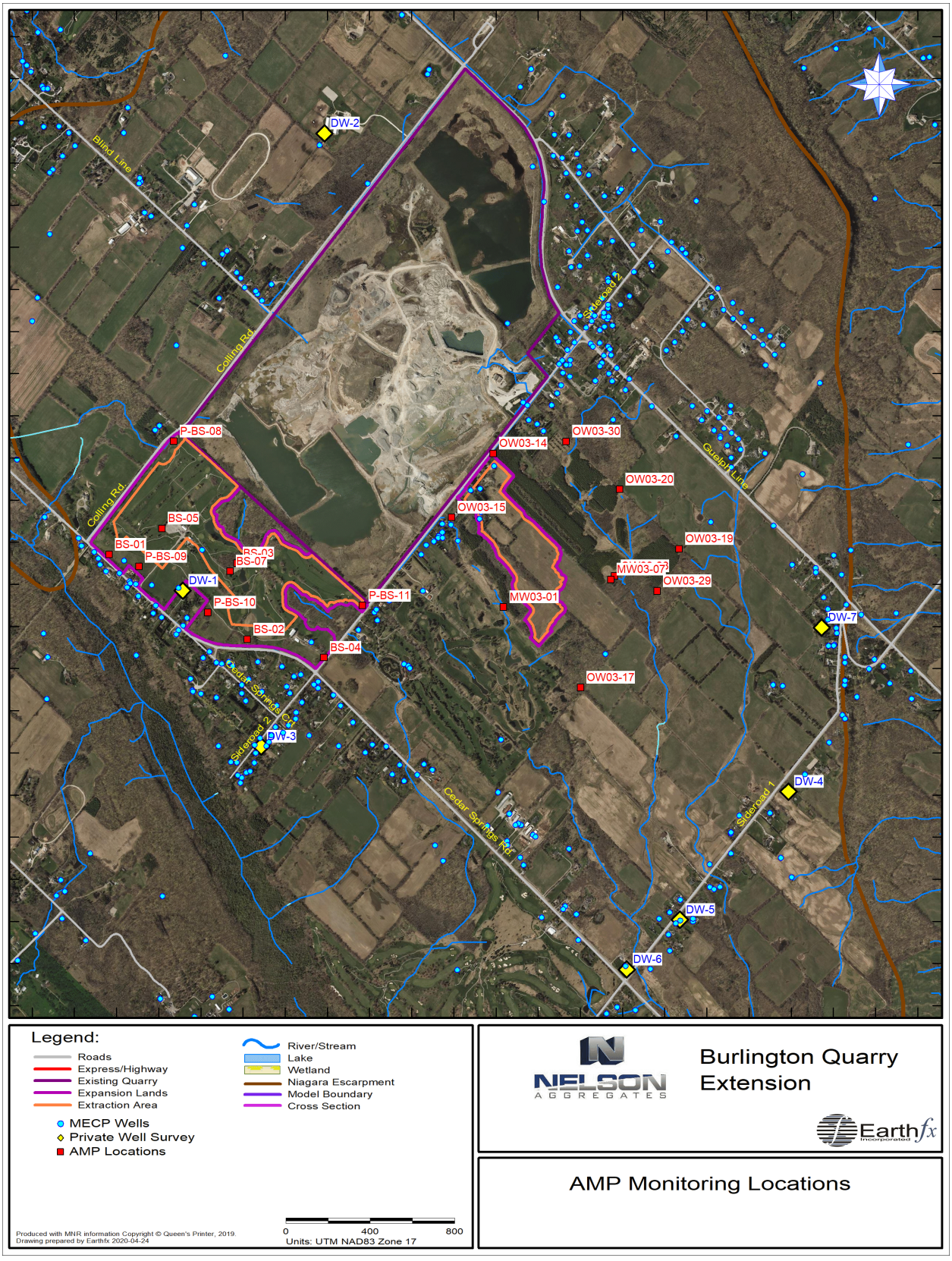

Figure 9.1: Location of Well DW2

The Seasonal Mann-Kendall Test considers the seasonality of the data series. This means that for monthly data with seasonality of 12 months, one will not try to find a trend in the overall series, but a trend from one of January to another, and from one February and another, and so on. The Seasonal Mann-Kendall test is established on the basis that the trend is cyclically varying in relation to the seasons of the year. It is used to analyse time series data for the possible existence of an upward or downward trend, at a significance level, while accounting for the effect of seasonality.

If a decreasing trend is determined by the results of the Seasonal Mann-Kendall Test, the trend will be analyzed using a Theil-Sen slope. The Theil-Sen test is also nonparametric and provides a more robust slope estimate than the least-squares method because outliers or extreme values in the time series affect it less. Therefore, this test provides an estimate of the true slope of an existing trend (as change per year). If the trend is decreasing, the date at which the water level is predicted to drop below a threshold of 5 m of available drawdown is calculated. If the trend is not decreasing, the test will conclude that the slope is not statistically decreasing. The slope of the trend line is used to make a conclusion on future groundwater conditions.

9.4.3 Proposed Groundwater Threshold Levels

A decreasing trend in local groundwater elevations that has been confirmed to be the result of quarry operations must be identified before a threshold value can be exceeded. Nelson proposes to rely upon the percentile method for establishing groundwater thresholds. For the standard statistical method, a percentile is a statistic that gives the relative standing of a numerical data point when compared to all other data points in a distribution. A percentile value ranges from 0 to 100. The value indicates the percentage of the data is equal to or below it.

The proposed thresholds have been calculated from the simulated water level elevations from the difference between the simulated average baseline water levels and the simulated drought water levels with Phase 1 and 2 extracted during a drought period. If the 0th percentile equals the minimum water level simulated, the 10th and 5th percentile values will be relied upon for the threshold values. Level 1 Threshold conditions occur when the measured water level falls below the Threshold 1 value (10th percentile) for a 15-day period. Level 2 conditions occur when the water level falls below the Threshold 2 value (5th percentile) for a 15-day period. This statistical approach to reviewing and assessing the impacts associated with the quarry development meets the objectives of the AMP, which is to implement a system that allows for a comprehensive evaluation of how the groundwater regime behaves with quarry development and to identify unforeseen changes in this system that provides time to implement appropriate mitigation strategies to protect local water use.

9.4.4 Proposed Groundwater Mitigation Measures

As stipulated in the General Conditions of all Ontario Water Resource Act (OWRA) Section 34 Permit to Take Water (PTTW), if the taking of water is observed to cause any negative impact to groundwater supplies, the Permit Holder shall take such action necessary to make available to those affected, a supply equivalent in quantity and quality to their normal takings. If the permitted water taking at the Burlington Quarry causes permanent interference, Nelson shall restore the water supplies of those permanently affected. Nelson acknowledges and endorses this responsibility under Section 34 of the OWRA for the replacement of the water supply, which must be of equivalent quality and quantity. To ensure a cooperative and fair treatment with all concerned, Nelson will work diligently with their neighbours on these issues.

A key finding of the Level 1 and 2 Hydrogeological Assessment and Numerical Modelling (Earthfx et. al., 2020), is that the drawdown associated with the extension of the Burlington Quarry does not adversely impact the available drawdown in the regional bedrock aquifer found at an elevation beneath

252 masl (elevation of the quarry floor). The available drawdown is the distance between the static water level (either pre or post quarry development) and the top of the aquifer. Interference with available drawdown can reduce the maximum yield of a well. It is generally accepted that 5 m of available drawdown is a safe available drawdown for domestic water wells constructed in bedrock aquifers.

The available drawdown at the private water wells is based on the well construction. If the well does not straddle the regional bedrock aquifer, available drawdown may be limited. Private wells are not always designed to obtain the maximum possible yield, but only an acceptable yield for domestic use. Nelson has determined the level of risk based on the total available drawdown for each well identified within the predicted area of influence. This information has been superimposed onto the model results showing available drawdown within the stratigraphic units, and the results show that wells can be deepened, if needed, to increase the available drawdown at each location. Data collected from existing domestic water wells along No. 2 Sideroad, which are within 80 m of the quarry, show that wells constructed in the hydrostratigraphy layer beneath the quarry floor (Layer 8) can meet peak domestic water demands with between 2 and 5 m of available drawdown.

The Seasonal Mann-Kendall Test will act as an early warning tool to identify any deviation from predicted water level trends and impacts. This test will be applied to private water wells where permission to monitor has been granted. However, the sentry wells are key locations to monitor trends and identify any unforeseen impacts before the influence is reported off-site. This approach limits the time required to complete traditional investigations that are triggered only if a specific water level threshold has been exceeded. Nelson will commence with planning the required compensation if unforeseen trends suggest off-site impacts will be greater than predicted and threaten the available drawdown in private wells. Compensation must be acceptable to the homeowner and the quarry operator and could include all or part of the costs associated with drilling of a new well, deepening a well, and abandonment of the old well.

In addition to providing a new private water supply well in a deeper aquifer system, Nelson will ensure that the quality of this source is equivalent or better than that of the well being replaced. Upon completion of the well construction, a comprehensive water quality analysis will be completed to characterize the water supply. If it is shown that the water quality has deteriorated from intercepting poor water quality at depth (for example increased chlorides and sulphates), the appropriate water treatment system will be purchased and installed.

The integrated surface water/groundwater model results predict groundwater mounding beneath the existing irrigation ponds in the West Extension. This groundwater mounding is generally maintained year-round by the diversion of quarry discharge into the irrigation ponds and raises groundwater levels in the area artificially. Through extraction, the irrigation ponds will be eliminated, and groundwater water levels will be lowered in the area. To replicate the existing artificial groundwater mounding produced by the irrigation ponds, a pond will be constructed outside the extraction area within the licence boundary between the extraction limit and Cedar Springs Road. The pond will be constructed at depths and elevations consistent with the existing irrigation ponds.

9.5 Groundwater Monitoring Network and Thresholds (Phase 1 and 2: Southern Extraction Area)

9.5.1 Groundwater Monitoring Program

The effect the extension will have on the groundwater regime will be controlled by the depth, timing, and direction of extraction. Interference will be in part masked or, coupled by local climatic conditions. Key groundwater monitoring locations that have over 7 years of water level data have been selected to act as the long-term sentry wells to ensure the influence on the groundwater regime is consistent with the predicted influence from quarry operations (Figure 9.2). The monitoring locations, well construction details, and predicted drawdown conditions during a drought period (expressed as water level elevation, simulated drawdown, and simulated available drawdown), are provided on Table 9.1.

As discussed, it is generally accepted that 5 m of available drawdown is a safe available drawdown for domestic water wells constructed in bedrock aquifers. To identify potential groundwater receptors, domestic water wells that have less than 5 m of available drawdown have been plotted on Figure 9.3. The purple well symbols indicate wells that have less than 5 m of available drawdown based on the static water level recorded when the well was drilled, which indicates that these wells had limited available drawdown prior to the proposed aggregate extraction in Phases 1 and 2. The orange well symbols identify wells that have less than 5 m of available drawdown from the average simulated water level during the extraction of Phase 1 and Phase 2. The yellow symbols identify domestic water wells that are currently part of the on-going groundwater monitoring program.

A noteworthy finding of the model results is the simulated available drawdown in Layer 8 (lower aquifer) during drought conditions which will continue to have enough available drawdown to support private water supplies (i.e., > 5 m). Figure 9.3 shows contour intervals (shaded in green) that represent the available drawdown above the base of Layer 8 under drought conditions.

The groundwater monitoring wells are constructed within the Upper Bedrock Aquifer (Layer 6) and the Lower Bedrock Aquifer (Layer 8) of the numerical model. The wells constructed within Layer 6 are relied upon to assess the influence on the water-bearing fracture network that is intercepted by the quarry face.

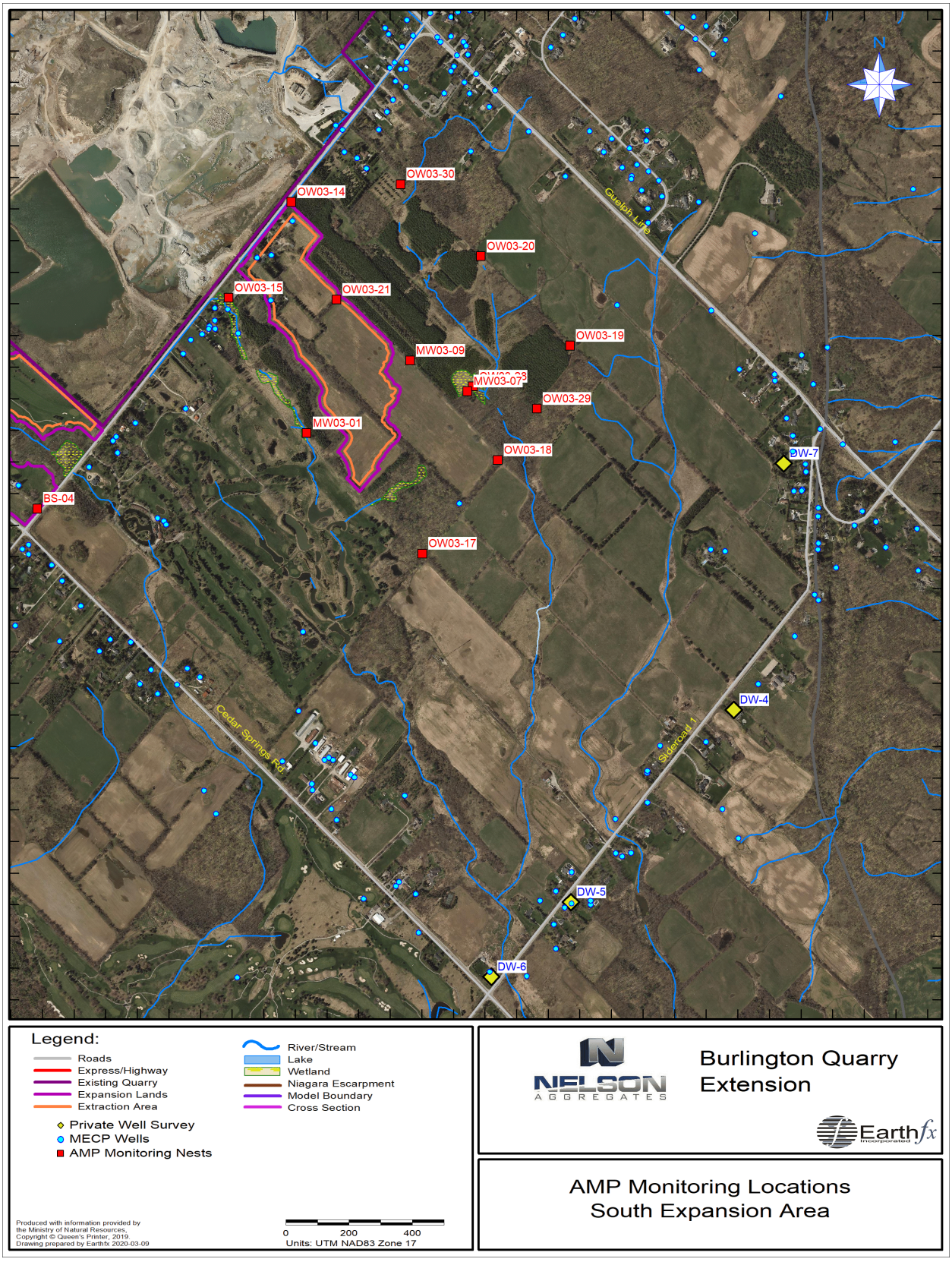

Figure 9.2: Groundwater Monitoring Network (Southern Extension)

Table 9.1: Monitoring Well Details (Southern Extension)

Borehole	Well ID	Survey Coordinates (NAD83)		Well Depth (m)	Simulated Water Levels (masl)	Simulated Drawdown (m)	Simulated Available Drawdown in Aquifer (m)
		Easting	Northing		Post-Extraction (Phase 1 and 2) During Extreme Drought Conditions		
MW03-01	M03-01A	590,635	4,805,092	24.4	256.34	12.20	5.7
	M03-01B			14.1	259.54	9.63	
MW03-07	M03-07A	591,145	4,805,222	27.6	259.89	11.75	9.2
	M03-07B			7.9	260.96	11.40	
MW03-09	M03-09A	590,963	4,805,320	30.7	253.95	16.41	4.1
	M03-09B			9.4	254.50	16.15	
OW03-14	M03-14A	590,587	4,805,821	32.1	254.70	5.20	1.5
	M03-14B			7.4	251.88	8.59	
OW03-15	M03-15A	590,389	4,805,517	25.6	254.57	5.35	2.8
	M03-15B			10.2	258.40	4.59	
OW03-17	M03-17A	591,001	4,804,710	22.3	262.71	6.63	13.7
	M03-17B			11.4	263.14	6.36	
OW03-18	M03-18A	591,469	4,805,367	31.1	262.25	9.13	11.2
	M03-18B			17.6	262.88	9.06	
OW03-19	M03-19A	591,469	4,805,367	31.1	264.44	8.30	10.8
	M03-19B			17.6	264.92	8.45	
OW03-20	M03-20A	591,168	4,805,650	26.1	262.08	9.57	9.0
	M03-21B			8.9	262.75	9.70	
OW03-28	M03-28A	591,163	4,805,239	27.3	260.21	11.53	9.3
OW03-29	M03-29A	591,363	4,805,168	29.5	263.28	8.91	11.1
	M03-29B			10.2	263.71	8.95	
OW03-30	M03-30A	590,933	4,805,878	24.3	260.08	7.85	6.8
	M03-30B			8.5	260.08	8.55	

The wells constructed in Layer 8 monitor the aquifer unit beneath the quarry floor to ensure that there will be an available drawdown of at least 5 m, which would be utilized as a potable water supply if private water wells need to be deepened.

The simulated available drawdown in the regional bedrock aquifer (Layer 8) at the on-site groundwater monitoring wells show that, except for M03-9, M03-14, and MW03-15, the available drawdown remains above 5 m. M03-14, and MW03-15 are located between the existing quarry and the proposed extension to the south along No. 2 Sideroad. The closest receptor (private water well) is located approximately 120 m to the west of MW03-15, and currently has 4.6 m of available drawdown. Model results show that the aquifer will have approximately 5 m of available drawdown. Therefore, mitigation options are available, if required. MW03-9 is located immediately adjacent to the quarry face and therefore a greater drawdown in anticipated.

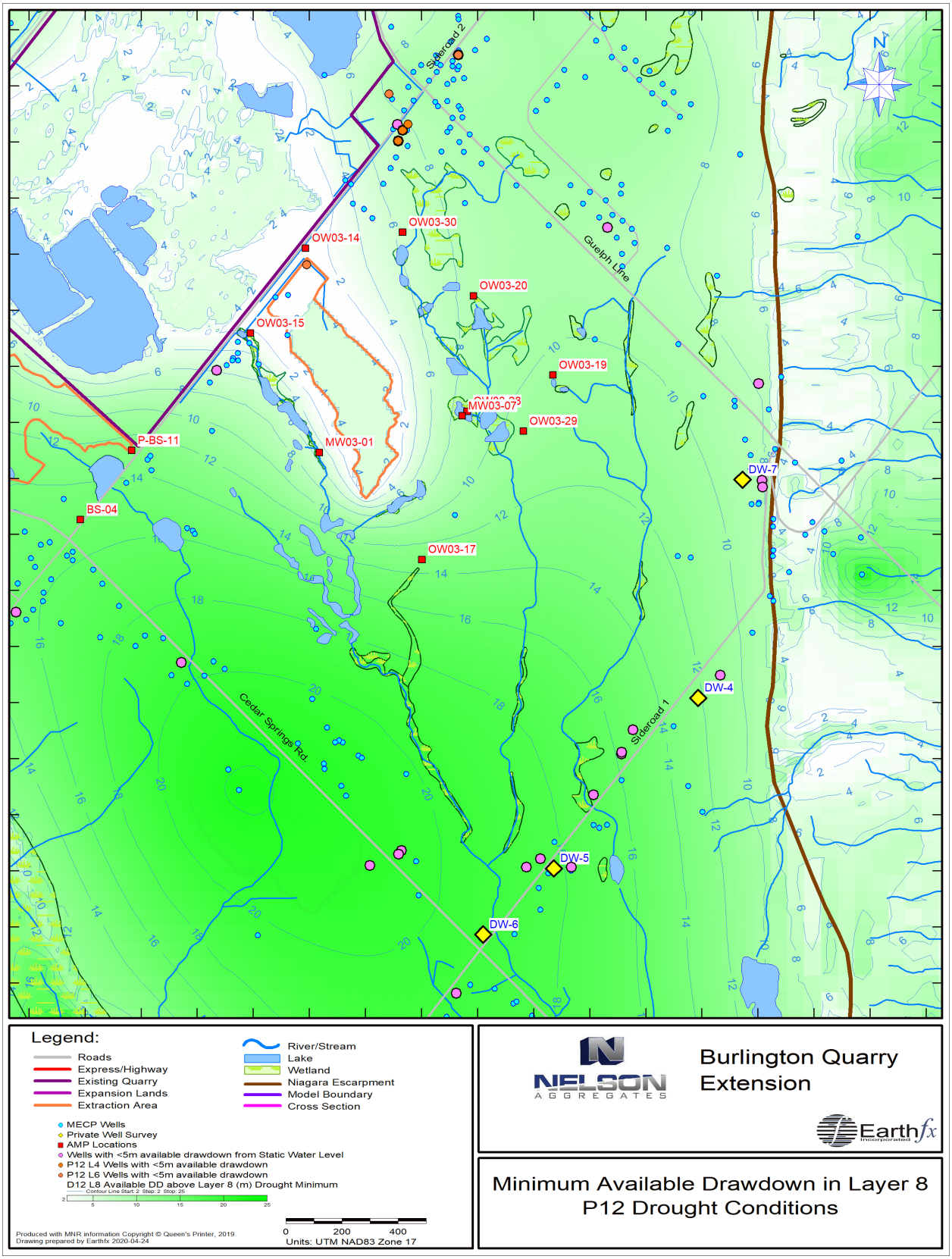

Figure 9.3: Available Drawdown (Southern Extension)

9.5.2 Groundwater Thresholds

Preliminary groundwater threshold values have been assigned to key Sentry Wells that are located outside of the extraction area. As discussed, these threshold values represent the 10th and 5th percentile of the water levels simulated under the 2016 drought conditions with the southern extension fully extracted (Phase 1 and 2 complete) and no rehabilitation.

Level 1 Threshold conditions occur when the measured water level falls below the Threshold 1 value (10th percentile) for a 15-day period. Level 2 conditions occur when the water level falls below the Threshold 2 value (5th percentile) for a 15-day period. These threshold levels are set as early warning water level elevations were the cumulative influence of drought conditions and quarry dewatering have lowered the water levels to an early warning threshold, where local private wells (adjacent to or in close proximity to the quarry) may start to notice a decrease in well yield.

Table 9.2: Groundwater Threshold Values

Well ID	Water Level Elevation (masl)		
	Simulated Min	Level 1 Threshold Value (10%)	Level 2 Threshold Value (5%)
MW03-01A	257.88	258.08	257.97
MW03-07A	262.40	263.26	262.75
OW03-14A	256.73	257.19	256.92
OW03-15A	256.46	256.69	256.56
OW03-17A	255.60	255.69	255.64
OW03-18A	264.13	264.81	264.42
OW03-19A	264.35	265.40	264.80
OW03-20A	267.10	268.36	267.64
OW03-28A	265.72	266.68	266.08
OW03-29A	253.83	253.84	253.84
OW03-30A	262.74	263.63	263.11

The response to a Level 1 Threshold condition, would prompt Nelson to:

- mail out a letter to all residents located within 1 km of the southern extension lands informing them of the low water levels;
- notify the SLC, MECP and MNR in writing; and
- post a notice on the Nelson website.

The letter mailed to the residents shall include the estimated drawdown anticipated in their private water supply well based on simulated results along with Nelson's contact information. It will be requested that Nelson be notified immediately if the residents have noticed any change in the water quality or quantity. A licenced water well technician will preform an investigation on any wells located within 1 km, where a change has been reported. The results will be compared to background conditions, if available. If an impact to the resident's water supply has occurred as a result of the quarry operations, Nelson will immediately replace the private water supply with a deeper bedrock well.

The process will be repeated if a Level 2 Threshold condition is met. In addition to a second mail out letter, Nelson will attempt to notify the residents in person; and post a notification of the local groundwater conditions in the local news outlets. Instructions to contact Nelson if anyone has experienced any issues with their water supply within 1 km of the quarry will be outlined.

9.6 Groundwater Monitoring Network and Thresholds (Western Extension)

9.6.1 Drilling of Groundwater Sentry Wells

In response to the lack of current interest from the residents who reside along Cedar Springs Road to have their private water well monitored, Nelson will be supplementing the existing groundwater monitoring program on the western extension lands. The sentry well drilling program will be completed within the first year of extraction (Phase 1). Drilling and well construction will occur at 4 locations along Cedar Springs Road (Figure 9.4). At each location, two wells will be drilled:

- one (1) to the depth of the quarry floor (252 masl); and
- one (1) drilled to the lower aquifer unit (~244 masl).

These wells will be constructed as water wells (cased into the upper bedrock) and left as an open hole through the dolostone units. The intent of this construction is to mimic / understand the behavior in the adjacent water supply wells which are constructed above and below the base of the quarry floor.

These wells will be added to the on-going groundwater monitoring program. At least 8-years of baseline data will be collected during Phases 1 and 2 of extraction which will be used to assess seasonal fluctuations prior any influence from the quarry operations. The setting of the trend analysis techniques and trigger mechanisms will be defined between year 8 and 9 in consultation with the review agencies.

9.6.2 Groundwater Monitoring Program

The monitoring locations, well construction details, and predicted drawdown conditions during a drought period (expressed as water level elevation, simulated drawdown, and simulated available drawdown), are provided in Table 9.3. Groundwater monitoring at several monitoring wells on the West Extension commenced in 2018 and 2019. The monitoring of water levels and water quality shall continue for the duration of this AMP. Data collected will represent background conditions for as long as Phases 3-6 remain undisturbed.

The simulated available drawdown in the regional bedrock aquifer (Layer 8) at the on-site groundwater monitoring wells show that, except for BS-03, BH-05, and BS-07, the available drawdown remains above 5 m. BS-03, BH-05, and BS-07 are located within the proposed extraction footprint and therefore will see the most impact. Model results show that the aquifer will have approximately 5 m of available drawdown. Therefore, mitigation options are available, if required.

Table 9.3: Monitoring Well Details (Western Extension)

Borehole	Well ID	Survey Coordinates (NAD83)		Well Depth (m)	Simulated Water Levels (masl)	Simulated Drawdown (m)	Available Drawdown in Aquifer (m)
		Easting	Northing		Post-Extraction (Phase 3-6) During Drought Conditions		
BS-01	BS-01A	588,765	4,805,342	18.50	258.43	6.71	5.9
	BS-01B			15.20	257.90	3.41	
BS-02	BS-02A	589,421	4,805,342	23.1	262.72	10.08	7.7
	BS-02B			18.9	263.63	6.25	
BS-03	BS-03A	589,368	4,805,298	18.8	262.34	12.27	1.7
	BS-03B			12.8	263.64	13.44	
BS-04	BS-04A	589,777	4,804,855	24.5	264.07	7.61	11.9
	BS-04B			19.9	264.90	5.91	
BS-05	BS-05A	589,015	4,805,462	24.3	261.05	11.43	2.5
	BS-05B			18.2	261.65	12.45	
BH-07	BS-07	589,363	4,805,271	25.0	262.31	12.47	2.1
P-BS-08	BS-08A	589,072	4,805,879	Well to be drilled and constructed during the extraction of Phase 1			
	BS-08B						
P-BS-09	BS-09A	588,907	4,805,284				
	BS-09B						
P-BS-10	BS-10A	589,233	4,805,066				
	BS-10B						
P-BS-11	BS-11A	589,968	4,805,104				
	BS-11B						

9.6.3 Groundwater Thresholds

The extraction of the proposed West Extension (Phase 3 through to 6) is scheduled to commence approximately 10-years following the issuance of the ARA licence. No groundwater thresholds are proposed until enough groundwater monitoring data is collected to establish baseline conditions. The groundwater monitoring program outlined in Section 9.6.2, shall commence before the extraction begins in Phase 1. Once there is enough seasonal water level data and the behavior of the groundwater response in the vicinity of the West Extension is understood enough to develop the assessment tools, threshold values will be assigned, and threshold trend analysis will be then completed. These values must be defined and approved by the MNRF before extraction commences in the West Extension.

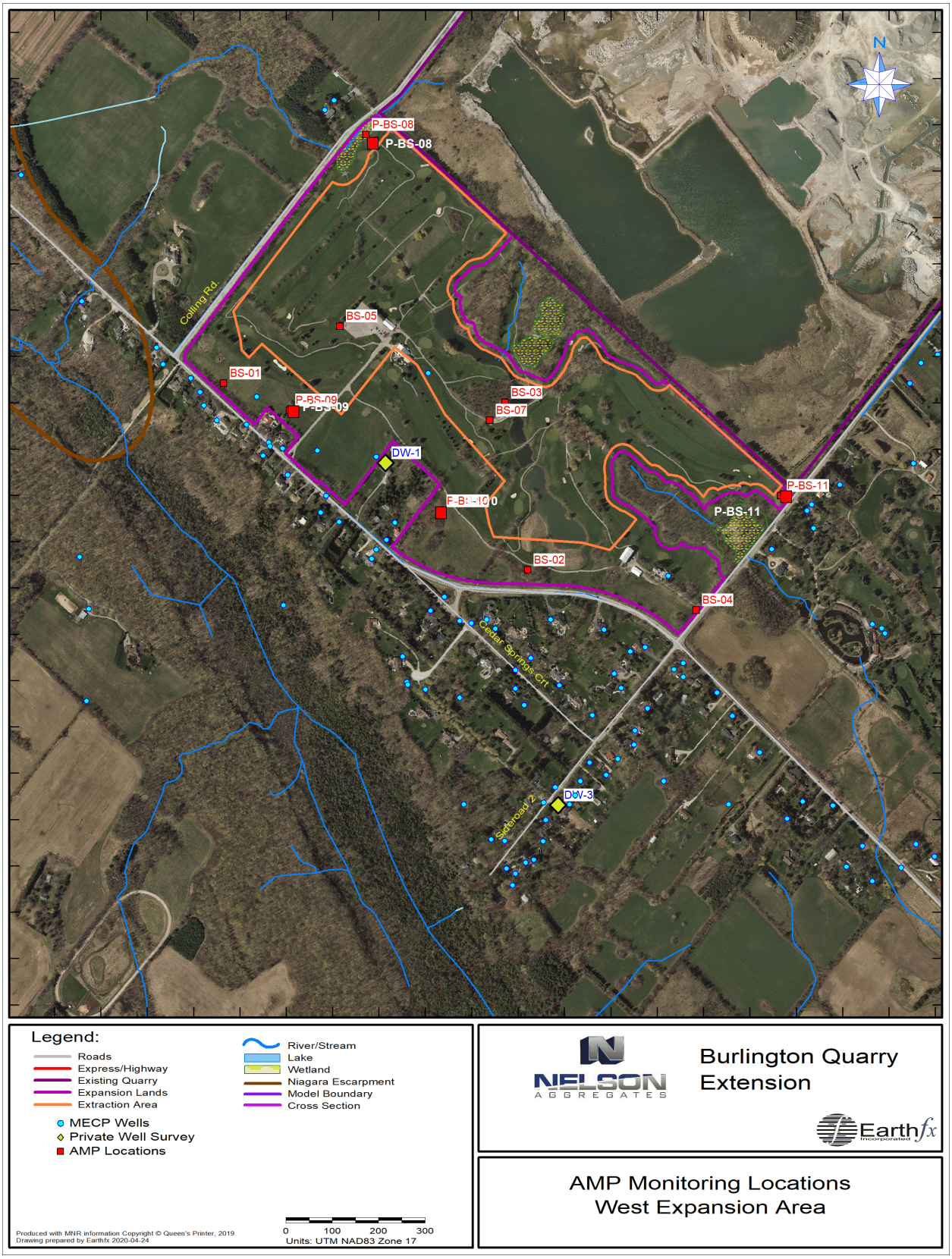

Figure 9.4: Groundwater Monitoring Locations (West Extension)

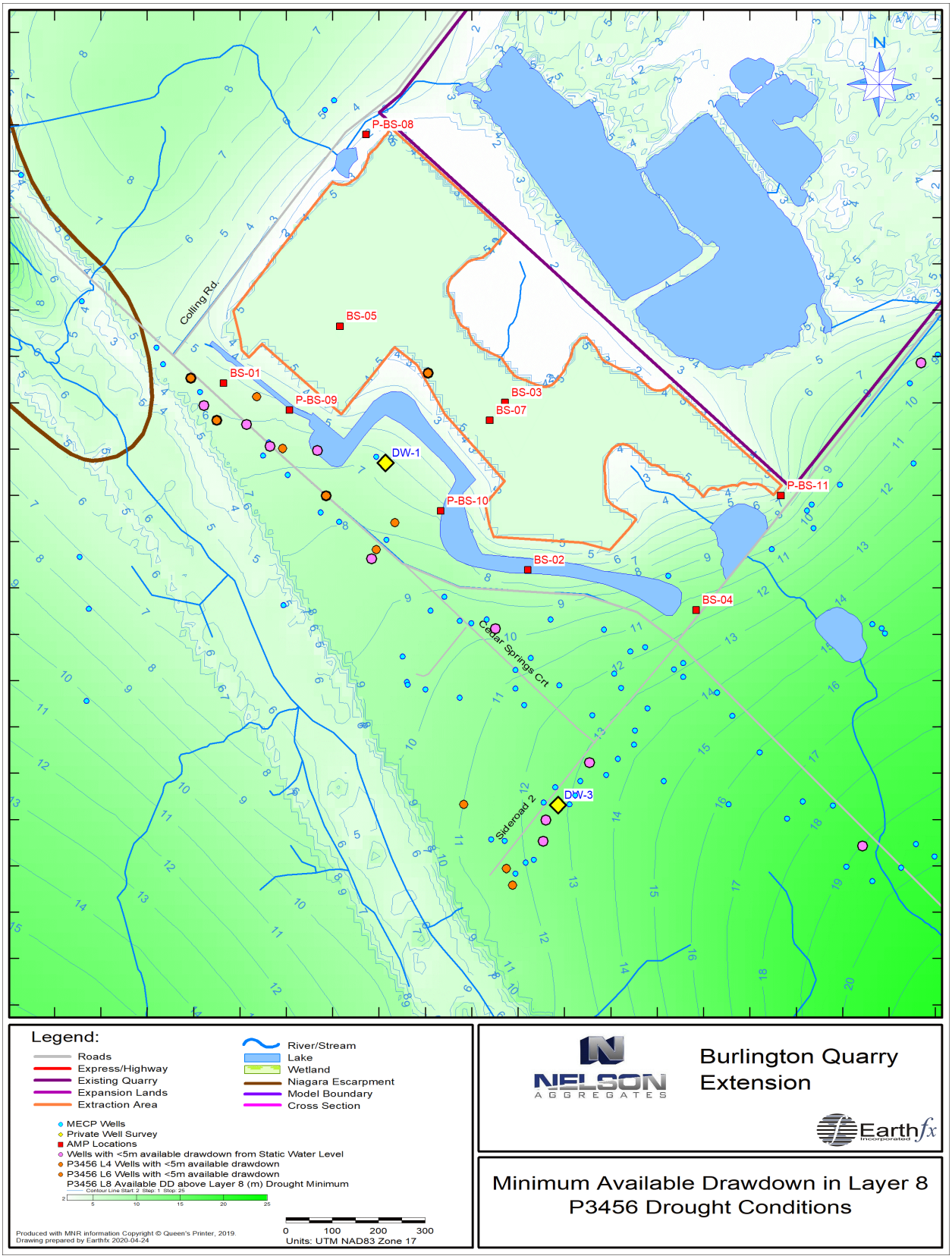

Figure 9.5: Available Drawdown (West Extension)

9.7 Water Well Interference Complaint Protocol

The Nelson Well Interference Complaint process is provided on Nelson's website.

https://www.nelsonaggregate.com/copy-of-licensing-1

If a water well complaint is received by the licencee, the following actions will be taken:

- The licencee will notify MNRF and MECP of the complaint.
- The licencee will contact a well contractor in the event of a well malfunction and residents will be provided a temporary water supply within 24 hours, if the issue cannot be easily determined and rectified.
- The well contractor will contact the resident with the supply issue and rectify the problem as expediently as possible, provided landowner authorization of the work. If the issue raised by the landowner is related to loss of water supply, the licencee will have a consultant/contractor determine the likely causes of the loss of water supply, which can result from a number of factors, including pump failure (owner's expense), extended overuse of the well (owner's expense) or lowering of the water level in the well from potential quarry interference (licencee expense). This assessment process will be carried out at the expense of the licencee and the results provided to the homeowner.
- If it has been determined that the quarry caused the water supply interference, the quarry shall continue to supply water at the licencee's expense until the problem is rectified. The following mitigation measures shall be considered, and the appropriate measure(s) implemented at the expense of the licencee:
    - adjust pump pressure;
    - lowering of the pump to take advantage of existing water storage within the well;
    - deepening of the well to increase the available water column;
    - widening of the well to increase the available storage of water;
    - relocation of the well to another area on the property;
    - drilling multiple wells; and
    - only at the request of a landowner would a cistern be installed.

If the issue raised by the land owner is related to water quality, the licencee will have a consultant/contractor determine the likely causes of the change in water quality, and review monitoring results at the quarry and background monitoring results from the baseline well survey to determine if there is any potential correlation with the quarry. If it has been determined that the quarry caused a water quality issue, the quarry shall continue to supply water at the licencee's expense until the problem is rectified. The licencee shall be responsible for restoring the water supply by replacing the well or providing a water treatment system. Only at the request of a landowner would a cistern be supplied. The licencee is responsible for the expense to restore the water quality.

10 Compliance Monitoring and Assessment

10.1 Groundwater Monitoring Program

10.1.1 On-Site Groundwater Monitoring Program

The groundwater monitoring program is outlined in Table 10.1 and Table 10.2, and shown on Figure 10.1.

Table 10.1: On-Site Groundwater Monitoring and Evaluation Program

Extraction Area	Borehole	Well ID	Water Level Monitoring		Water Quality Sampling		Analysis		
			Monthly Manual	Continuous (4-hour frequency)	Semi-Annual	Annual	Trend Analysis	%10 Threshold (masl)	%5 Threshold (masl)
Southern Extraction Area	M03-01	M03-01A	X	X	X		X	258.08	257.97
		M03-01B	X	X	X	X	X	NVR	NVR
	M03-07	M03-07A	X	X	X		X	263.26	262.75
		M03-07B	X	X	X	X	X	NVR	NVR
	M03-09	M03-09A	X	X	X		X	257.19	256.92
		M03-09B	X	X	X	X	X	NVR	NVR
	M03-14	M03-14A	X	X	X		X	256.69	256.56
		M03-14B	X	X	X	X	X	NVR	NVR
	M03-15	M03-15A	X	X	X		X	255.69	255.64
		M03-15B	X	X	X	X	X	NVR	NVR
	M03-17	M03-17A	X	X	X		X	264.81	264.42
		M03-17B	X	X	X	X	X	NVR	NVR
	MW03-18	M03-18A	X	X	X		X	265.40	264.80
		M03-18B	X	X	X	X	X	NVR	NVR
	M03-19	M03-19A	X	X	X		X	268.36	267.64
		M03-19B	X	X	X	X	X	NVR	NVR
	M03-20	M03-20A	X	X	X		X	266.68	266.08
		M03-20B	X	X	X	X	X	NVR	NVR
	M03-21	M03-21A	X	X	X		X	253.84	253.84
		M03-21B	X	X	X	X	X	NVR	NVR

	M03-28	M03-28A	X	X	X		X	263.63	263.11
		M03-28B	X	X	X	X	X	NVR	NVR
	M03-29	M03-29A	X	X	X		X	266.85	266.18
		M03-29B	X	X	X	X	X	NVR	NVR
	M03-30	M03-30A	X	X	X		X	264.42	263.92
		M03-30B	X	X	X	X	X	NVR	NVR
Western Extraction Area	BS-01	BS-01A	X		X		X	TBD	TBD
		BS-01B	X	X	X	X	X	TBD	TBD
	BS-02	BS-02A	X		X		X	TBD	TBD
		BS-02B	X	X	X	X	X	TBD	TBD
	BS-03	BS-03A	X		X		X	TBD	TBD
		BS-03B	X	X	X	X	X	TBD	TBD
	BS-04	BS-04A	X		X		X	TBD	TBD
		BS-04B	X	X	X	X	X	TBD	TBD
	BS-05	BS-05A	X		X		X	TBD	TBD
		BS-05B	X	X	X	X	X	TBD	TBD
	BH-07	BS-07	X		X		X	TBD	TBD
Proposed West Extension	P-MW-08	MW-08	X	X	X	X	X	TBD	TBD
	P-MW-09	MW-09	X	X	X	X	X	TBD	TBD
	P-MW-10	MW-10	X	X	X	X	X	TBD	TBD
	P-MW-11	MW-11	X	X	X	X	X	TBD	TBD
	NVR = No value required (shallow well) TBD = value to be determined before extraction commences from Western Extension								

Table 10.2: Groundwater Quality Parameters

Water Quality Sampling Frequency	Parameters
Semi-Annual	pH, Conductivity, Alkalinity, Hardness, Bicarbonate, Total Phosphorus, Metals (Antimony, Arsenic, Barium, Beryllium, Boron, Cadmium, Calcium, Cobalt, Copper, Lead, Iron, Magnesium, Manganese, Mercury, Molybdenum, Nickel, Potassium, Selenium, Sodium, Silver, Strontium, Sulfur, Thallium, Thorium, Tin, Titanium, Tungsten, Uranium, Vanadium, Zinc),
Annual	Petroleum Hydrocarbons (BTEX, F1-F4)

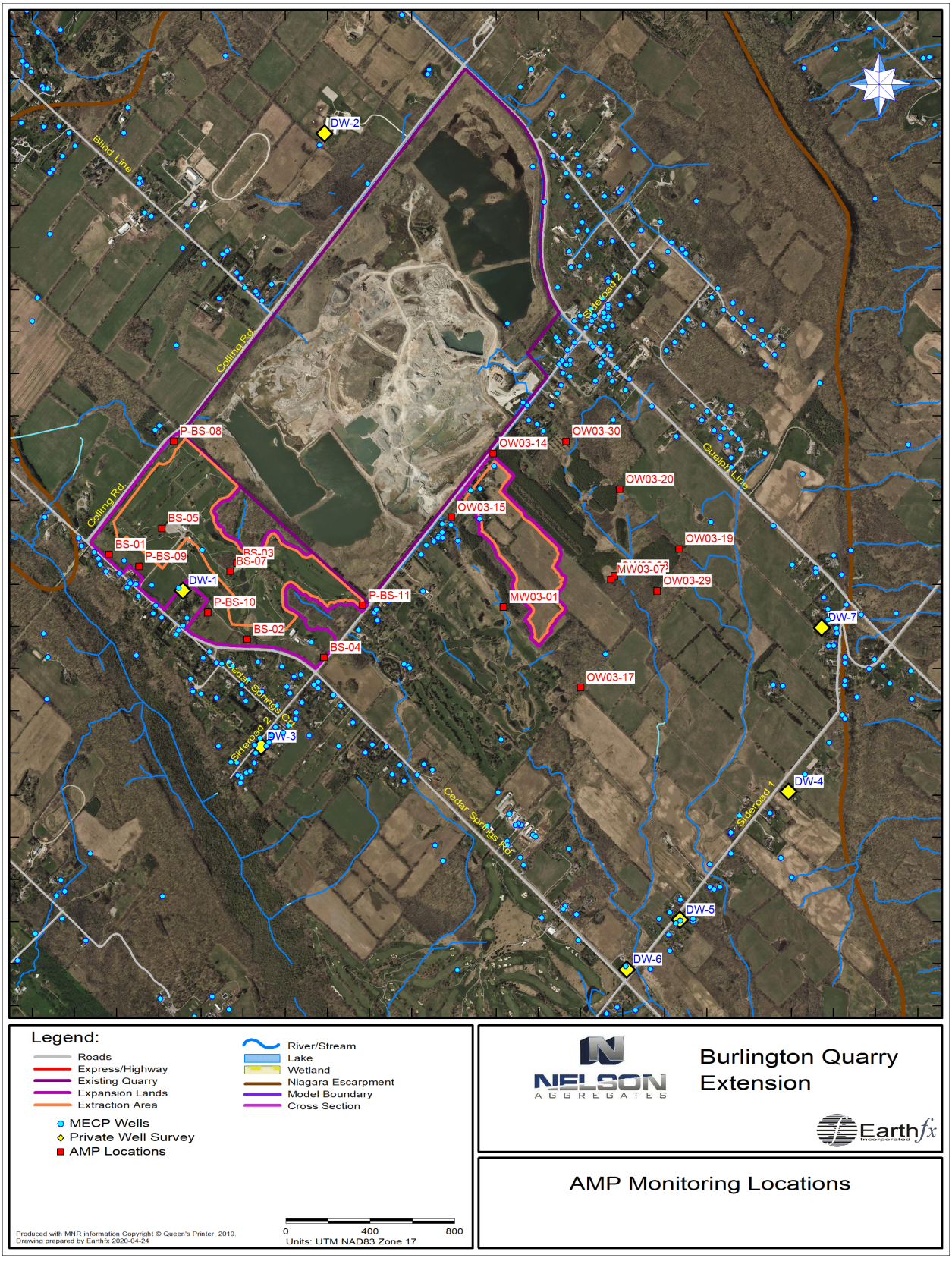

Figure 10.1: AMP Groundwater Monitoring Locations

10.1.2 Private Water Well Monitoring

The Private Well Monitoring Program includes the collection of water quality samples and water levels, like the on-site monitoring program outlined in Section 10.1.1. Similarly, the impact assessment on each well will include a trend analysis and threshold value. The current domestic water well monitoring locations are provided in Table 10.3.

Each domestic well that becomes a part of the groundwater monitoring program will be assigned independent threshold values, which will be based on the well construction details and the proximity to the proposed extraction face.

Nelson will continue efforts to expand the domestic water well monitoring network. It is anticipated that the residents will become increasingly more interested in having their potable water supply monitored if the aggregate licence is issued.

Table 10.3: Private Monitoring Well Locations

Borehole	MECP Well ID	Survey Coordinates (NAD83)	
		Easting	Northing
DW-1	28-03833	589114	4805170
DW-2	na	589786	4807340
DW-3	7276141	589486	4804431
DW-4	na	591987	4804216
DW-5	2800063	591472	4803608
DW-6	na	591220	4803372
DW-7	na	590916	4806143

11 Summary and Conclusions

11.1 Introduction

The objective of this Level 2 ARA investigation was to characterize the existing conditions at the quarry site, describe the development of an integrated groundwater/surface water assessment model, and predict any likely changes to the hydrologic and hydrogeologic conditions at different phases of extraction and final rehabilitation.

The assessment methodology used in this study is the same as that used by Earthfx for multiple Source Water Protection Tier 3 Water Budget and Wellhead Protection studies conducted for the Province of Ontario. The same model and methodology were used, and the key aspects of the approach include:

5. Fully integrated analysis and simulation of all surface water and groundwater processes
6. Fully transient assessment of system behaviour on a daily basis for a period of years; including significant drought and wet year conditions.
7. Detailed daily comparative assessment including evaluation of the minimum, average and maximum impact of development
8. Full water budget accounting on a daily basis.

Earthfx has used the same methodology for Source Water Protection studies for the Region of Halton, Conservation Halton, City of Hamilton, Region of York, Region of Peel, Toronto and Region Conservation Authority, Lake Simcoe Conservation Authority, Grand River Conservation Authority, City of Toronto and other water management agencies across Canada and the USA.

11.2 Hydrogeologic and Hydrologic System Summary

The study area is predominantly covered by the low permeability Halton Till, a fine grained silty to clayey till that was deposited approximately 13,000 years ago by a glacial lobe that advanced out of the Lake Ontario basin. Beneath the Halton Till are occasional deposits of sands on the bedrock surface. These sands and the upper weathered bedrock form an upper water table aquifer.

The upper most bedrock unit is commonly referred to as the Amabel Formation, but in recent literature it has been subdivided into the Goat Island and Gasport Formations. The Amabel is a massive, fine grained dolostone with an average thickness of 25 m. The Amabel includes occasional vertical fractures and there is good evidence of an intermediate and lower fracture zone. Beneath the Amabel are thin interbedded shale and limestone units and the thick, low permeability Cabot Head Shale.

The highest measured ground water elevations are located near the crest of Mt. Nemo, northwest of the existing quarry. There is radial flow in all directions from this regional high, but, in general, the predominant groundwater flow direction follows the dipping topography and bedrock layers to the south and west. The Medad Valley is incised into the Cabot Head shale aquitard and receives groundwater discharge from the overlying dolostones.

Water supply wells in the area are typically constructed as open boreholes drilled 10 to 15 m into the Amabel formation. Wells are drilled sufficiently deep to encounter one or more bedrock fractures with adequate flow for domestic use. Static water levels in these wells are highly variable, depending on local fracture conditions and seasonal recharge.

In general, there is limited interaction between the local streams and groundwater system because of the low permeability of the surficial Halton Till aquitard. The water table is generally found in the shallow bedrock but in low lying areas in the spring it can rise into the overburden and discharge to the streams and wetlands. There are two karstic streams to the south and north of the quarry where streamflow disappears into the shallow bedrock and reappears a few hundred metres downslope as small groundwater springs. There are other groundwater springs (and karst discharge features) in the Medad Valley, but these are masked by the wetlands that fill the valley.

Groundwater monitoring since 2003 has delineated the effects of quarry development on water levels in and around the active quarry. A distinctive pattern of water level changes in the Amabel layers are observed as the quarry advances, with enhanced water level variability observed up to 650 m from the quarry face during the late summer. Baseline (current condition) numerical model simulations closely replicate this pattern and illustrate how groundwater recharge in the spring replenishes the system through downward in the vertical fractures.

The numerical simulations confirm that the majority of the wetlands and streams are isolated from the water table by the low permeability Halton Till. A total of 5 of the 22 mapped wetlands in and around the quarry receive groundwater upwelling in the spring, however groundwater is in every case a very small percentage (less than 3%) of the overall inflows into the wetland.

11.3 Level 2 Impact Assessment

11.3.1 Baseline Conditions

The system behaviour in and around the existing quarry is extremely well understood. The long-term monitoring (including the monitoring of the 2005-2019 advancement of the south extraction face) provides a clear groundwater response that has been accurately simulated by the transient integrated model. The detailed field investigations, together with the simulation of this large-scale response, provides significant confidence in the numerical model and the resulting impact assessment.

The local conditions around each extension phase result in somewhat different drawdown patterns for each expansion scenario, however the overall conclusions and general patterns are consistent with the existing quarry. The configuration of the excavation, local recharge, hydrogeologic setting and proximity to the existing quarry affect the area of influence.

The Level 2 impact assessment scenarios present a detailed and exhaustive comparison of the proposed developments to the baseline conditions. All pertinent aspects of the surface water and ground water system have been compared across a wide range of climate conditions. The integrated approach ensures that surface and groundwater functions and water budgets are fully reconciled. Many wells in the upland area exhibit more than 2 m of seasonal and inter-annual variation, so distinguishing quarry influence below this level would be difficult.

11.3.2 Summary of South Extension Area Effects

11.3.2.1 Area of Influence

The drawdowns associated with the South Extension diminish rapidly with distance from the excavation. The 2.0 m drawdown cone extends up to 1000 m from the excavation in the middle Amabel aquifer, but the 2.0 m drawdown is much more limited in the springtime, extending less than 700 m, because of the higher recharge and water levels associated with the spring snowmelt.

11.3.2.2 Wetlands and Surface Water Features

The majority of the wetlands in the vicinity of the South Extension are perched above the water table in the low permeability Halton Till. As noted, a total of 5 of the 22 wetlands evaluated do receive groundwater inflow in the spring, but the percentage of groundwater inflows relative to the total inflows is less than 3%. During South Quarry extraction, the drawdown in the water table will limit groundwater upwelling into those five wetlands that do normally receive groundwater inflow. The effects of this change, a loss of 3% of the inflow, will be so small that it cannot be measured in the field. This reduction in upwelling occurs in the springtime when the wetlands are already relatively wet, further minimizing the hydrologic effects.

11.3.2.3 Domestic Water Wells

From a water supply perspective, the South Extension is optimally located, as it is in an area with up to 22 m of available drawdown in the Amabel Aquifer. The excavation is also relatively distant and isolated from private wells along Cedar Springs Road, Sideroad 1 and Guelph Line, so it is unlikely to impact those wells.

Existing private water supply wells generally draw from the middle to lower portions of the Amabel, with a few tapping into the deep fracture zone at base of Amabel. There is extensive additional available drawdown for all wells, should they require increased supply, as they could be extended the full depth and into the lower Amabel fracture zone.

11.3.3 Summary of West Extension Area Effects

11.3.3.1 Area of Influence

The 2.0 m drawdown cone associated with the West Extension extends up to 500 m from the excavation in the middle Amabel aquifer. The West Extension is next to a locally significant groundwater discharge area, so water levels are less subject to drought and seasonal fluctuations. The proximity to the discharge area helps to mitigate the local effects of the excavation.

11.3.3.2 Wetlands and Surface Water Features

There are two perched wetlands in the immediate vicinity of the West Extension. Neither of these receive groundwater inflows, so lowering the water table will not affect their hydrogeologic interactions and function.

The Medad Valley is a locally significant groundwater discharge area that receives the majority of the groundwater that flows in and around the existing and proposed quarry. The development of the West Extension will shift some of the groundwater discharge to the north, through the North Discharge pond, but ultimately all of this discharge simply enters the Medad Valley in a similar manner to the current discharge.

The central ditch and pond system in the existing golf course extraction area will be removed during excavation. This system is currently supplied by the diversion of discharge from the existing quarry. To help preserve the current groundwater and surface water flow conditions created by this ditch and pond system, a new infiltration pond will be constructed between the West Extension and Cedar Springs Road.

11.3.3.3 Domestic Water Wells

The private wells in the vicinity of the West Extension will see a decline of approximately 2 m in available drawdown, however the majority of the wells have between 10 and 16 m of Amabel Aquifer drawdown after excavation, so deepening a well is a viable mitigation measure. Near the intersection of Colling Road and Cedar Springs Road there are a few wells that will have between 5 and 10 m of available drawdown, however these are in a significant discharge area so it is likely that there will be sufficient flow to meet their private supply needs.

11.3.4 Rehabilitation and Closure

Two rehabilitation options were evaluated. Under both scenarios the South Extension will be allowed to re-fill and become a natural lake. This lake will return groundwater water levels to current conditions, with some minor flattening of the water table around the lake. Surface water interactions and private well levels will return to current conditions.

Under Rehabilitation Scenario 1, the main quarry and West Extension will be rehabilitated, including regrading and consolidation of the quarry lakes. The overall hydrogeologic and hydrologic conditions will be similar to the final excavation phase, with some recovery in water levels due to the consolidation of the quarry lakes.

Under Rehabilitation Scenario 2, the quarry floor will be regraded, pumping will cease, and the entire quarry will be allowed to fill to become a single large lake. Groundwater levels will rise, except near the stream segments that currently carry the discharge, where they will fall due to the reduction in stream leakage.

Furthermore, surface water flow in the upper reaches of a tributary of Willoughby Creek and the West Arm of the West Branch of Mount Nemo Creek will cease when the quarry discharge is discontinued, resulting in an adverse impact to downstream fish habitat compared to baseline conditions (See Savanta, 2020 and Tatham, 2020 for details).

11.4 Conclusions

This Level 2 ARA Impact Assessment presents a detailed comparative evaluation of the effects of the proposed extension of the Nelson Burlington Quarry. The existing (baseline) site conditions are fully characterized and the numerical model closely replicates the observed surface water and groundwater processes and water budget. The predicted effects of the South and West Extension have been systematically evaluated on a daily basis across a range of seasonal and inter-annual (wet and dry year) climate conditions. The predicted effects on groundwater levels are consistent with the existing quarry, and significant available groundwater resources remain through the development and closure phases. The streams and wetlands in the study area are relatively isolated from the predicted changes in the groundwater system by the low permeability Halton Till, and no measurable change will occur in the nearby wetland water budgets.

The final rehabilitation plan will preserve the form and function of the upper reaches of a tributary of Willoughby Creek and the West Arm of the West Branch of Mount Nemo Creek as quarry discharge will continue.

At the subwatershed scale, the proposed extension will not change the overall surface water and groundwater flow system. There will be no cross-watershed impacts, groundwater recharge rates will be preserved, and groundwater and surface water in and around the quarry will continue to flow toward

the Medad Valley. The quality and quantity of groundwater needed for the natural environment and wells will be protected, and no municipal wellhead protection areas will be impacted. Both of the evaluated rehabilitation options preserve and restore the surface water and groundwater system. A comprehensive monitoring and response plan has been developed based on the statistical percentile methodology as defined in the Ontario Low Water Response Program. The additional available groundwater resources have been quantified, and a well mitigation program has been proposed.

12 Recommendations

Based on the findings of the hydrogeological assessment, it is recommended that the following steps be taken:

1. Current approvals for the existing quarry will stop the water discharge pumping at both locations once extraction is complete, which would have a negative impact on and associated fish habitat in both watercourses (Savanta, 2020 and Tatham, 2020). The proposed revised rehabilitation plan recommends that the dewatering and pumping should continue at the same locations and in the same manner to ensure there are no negative impacts to any of the hydrological features that rely on this water input. This will result in long-term enhancements to downstream fish habitat compared to the existing approved post-extraction water management plan (See Savanta, 2020 and Tatham, 2020 for details).

2. Incorporate the mitigation and monitoring requirements as outlined in this report into the Adaptive Management Plan (Earthfx and Tatham, April 2020) for the site; as outlined in Sections 9 and 10 of this report.

3. The licensee is required to operate in accordance with the Adaptive Management Plan, prepared by Earthfx Inc. and Tatham Engineering, dated April 23, 2020, as may be amended from the time to time with approval from MNRF, in consultation with NEC, Region of Halton, City of Burlington and Conservation Halton.

4. Prior to extraction commencing, the licensee shall complete another residential well survey for properties within 1 km of the extraction area.

5. The licensee is required to implement the Water Well Interference Complaint Protocol as outlined in Section 9.7 of this report.

6. Post rehabilitation, maintain the west extension in a dewatered state and main discharge to north and south from Quarry Sump 0100 and 0200 in accordance with the conditions of the PTTW and ECA to provide public water management benefits.

13 Limitations

As with all models, it must be recognized that there are inherent simplifications in the model conceptualization of distributed hydrologic and hydrogeologic processes and in the simplified assignment of parameters. There are also limitations and uncertainty in the input and calibration target data and potential for erroneous data or inputs to affect results.

With regards to the intrinsic uncertainty in the input data, the data used to describe the geologic, hydrogeologic, and hydrologic setting of the study area is presented in Sections 3 through 5. Data from a wide variety of sources, including climate records, streamflow measurements, static and transient groundwater levels, and geologic logs were collected, reviewed, and synthesized. In general, the data coverage for the study area is quite high, however some limitations were noted in the soils mapping, topographic mapping, and the number of transient groundwater monitors and significant gaps in the record. This study built on a large base of previous investigations conducted in the quarry vicinity.

Stream flow data were available for the area from gauges on Grindstone Creek as well as flow data collected for local streams in the quarry vicinity. Climate data coverage is sufficient but has deteriorated in recent times due the large number of discontinued stations.

With regards to the intrinsic uncertainty in the modelling approach, the integrated modelling approach applies a physically-based approach to quantifying groundwater recharge and groundwater/surface water interaction rather than using simplifying assumptions and relying on automated calibration to estimate these components of the groundwater flow system. By integrating the PRMS and MODFLOW submodels in GSFLOW, feedback mechanisms between the groundwater and surface water systems are better represented. The reasonableness of submodel outputs (e.g., groundwater recharge values from the hydrologic submodel and groundwater discharge to the soil zone from the groundwater submodel) and the overall water budget were tested much more rigorously than possible with separate, non-integrated models. Although no model can perfectly match the observed behaviour due to inherent simplifications and incomplete information, it is felt that the model results are reasonable, physically-based, and scientifically sound.

With regards to the uncertainty related to the model calibration, the results obtained with the PRMS-submodel appear reasonable and the observed streamflow was matched well in most gauges. The GSFLOW model was calibrated to a wide range of conditions, including wet and dry-year conditions, and validated over extended simulation periods to increase the degree of confidence in model results. Improvements can always be made, however, through additional data collection and refinement of model parameters.

The results of the groundwater model calibration yielded a good match to the static groundwater levels and groundwater flow patterns despite using uniform parameter values for the hydrogeologic units. The calibration to transient data highlighted that, although reasonable parameter values were obtained that could be applied consistently across the study area, the local calibration is very good. This model is intended to serve as a framework for continued monitoring.

14 References Cited

Azimuth Environmental Consulting Inc., 2019, Appendix A – Hydrogeologic Field Investigations: in Level 1 and Level 2 Hydrogeological Assessment Proposed Burlington Quarry Extension – Appendix A and B, report prepared by Earthfx Inc. for the Nelson Aggregates Co., November 2019, 70 p.

Bear, J., 1979, Hydraulics of Groundwater: McGraw Hill International Book Co., New York, 567 p.

Bolton, T.E., 1957, Silurian Stratigraphy and Palaeontology of the Niagara Escarpment in Ontario: Geological Survey of Canada, Memoir 289, 145p.

Brunton, F.R. and Dodge, J.E.P. 2008. Karst of southern Ontario and Manitoulin Island; Ontario Geological Survey, Groundwater Resources Study 5. ISBN 978-1-4249-8376-6 (ZIP FILE); ISBN 978-1-4249-8375-9 (DVD)

Chiew, F.H.S. and McMahon, T.A., 1993, Assessing the adequacy of catchment streamflow yield estimates: Australian Journal of Soil Research, 31: 665-680.

DeWalle, D.R., and Rango, A., 2008, Principles of snow hydrology: Cambridge University Press, Cambridge, U.K., 410 p.

Di Biase, Stephen M., 2005, Constraints on Maintaining Groundwater Recharge via Stormwater Infiltration: M.Sc. Thesis, Department of Geology, University of Toronto.

Dickinson, W.T. and Whiteley, H.Q., 1970, Watershed areas contributing to runoff: International Association of Hydrologic Sciences Publication 96, p. 1.12-1.28.

Doherty, J., 2015, Calibration and Uncertainty Analysis for Complex Environmental Models: Watermark Numerical Computing, Brisbane, Australia. ISBN: 978-0-9943786-0-6.

Earthfx Incorporated, 2012, Tier 3 Water Budget and Local Area Risk Assessment for the Kelso and Campbellville Groundwater Municipal Systems - Model Development and Calibration Report: prepared for the Halton Region Conservation Authority, December 2012.

Earthfx Incorporated, 2014a, Tier 3 Water Budget and Local Area Risk Assessment for the Kelso and Campbellville Groundwater Municipal Systems - Phase 2 Risk Assessment Report: prepared for the Halton Region Conservation Authority, February 2014

Earthfx Incorporated, 2014b, Tier 3 water budget and local area risk assessment for the Greensville groundwater municipal system, Phase 1 model development and calibration report: prepared for the Conservation Halton, May 2014.

Earthfx Incorporated, 2015, Tier 3 water budget and local area risk assessment for the Greensville groundwater municipal system, Phase 2 risk assessment report: prepared for the Conservation Halton, March 2015.

Earthfx Incorporated, 2016, Model Assessment and Review of the Proposed Dundas South Quarry Extension, Level 1/2 Hydrogeology and Hydrology Technical Report (Phase 1)

Earthfx Incorporated, 2017, Update to the Tier 3 Water Budget and Local Area Risk Assessment for the Greensville Groundwater Municipal System - Updated Risk Assessment Report: draft report prepared for Conservation Halton, March 2017, 180 p.

Earthfx and Tatham Engineering, 2020. Preliminary Adaptive Management Plan, Proposed Burlington Quarry Extension, Nelson Aggregates Co. Version 1, April 2020

Golder Associates Limited, 2004, Report on Hydrogeological and Water Resources Assessment of the Proposed Nelson Quarry Co. Extension: report submitted to Nelson Aggregate Co., Project No. 021-1238, October 2004.

Golder Associates Ltd., 2006, Additional Hydrogeologic Field Studies at the Proposed Nelson Quarry Co. Extension: report submitted to Nelson Aggregate Co., April 2006, 58 p.

Golder Associates Ltd., 2007a, Monthly Water Budgets for Individual Wetland Areas: report submitted to Nelson Aggregate Co., September 2007, 90 p.

Golder Associates Ltd., 2007b, Report on Characterization of Shallow Overburden Hydrogeology at the Proposed Nelson Quarry Co. Extension, Burlington, Ontario: report submitted to Nelson Aggregate Co., September 2007, 85 p.

Golder Associates Ltd., 2008, Addendum report on Water Resources Impact Assessment and Contingency Design Updates - Proposed Nelson Quarry Co. Extension, Burlington, Ontario: report prepared for Nelson Aggregate Co., January 2008, 203 p.

Harbaugh, A.W., 2005, MODFLOW-2005, the U.S. Geological Survey modular ground-water model—the Ground-Water Flow Process: U.S. Geological Survey Techniques and Methods 6-A16, variously paged.

Hargreaves, G. H. and Samani, Z. A., 1982, Estimating potential evapotranspiration: Journal of the Irrigation and Drainage Division, 108(3), 225-230.

Jensen, M.E., and Haise, H.R., 1963, Estimating evapotranspiration from solar radiation: Proc. of the American Soc. of Civil Engineers, Journal of Irrigation and Drainage, v. 89, no. IR4, p. 15-41.

Kassenaar, J.D.C., 2013, VIEWLOG (version 4). Microsoft Windows, v.3.1 through 8.1. Toronto, ON: VIEWLOG Systems Inc.

Leavesley, G.H., Lichty, R.W., Troutman, B.M., Saindon, L.G., 1983, Precipitation-Runoff Modeling System–User's Manual: USGS Water Resources Investigations Report 83–4238

Markstrom, S.L., Niswonger, R.G., Regan, R.S., Prudic, D.E., and Barlow, P.M., 2008, GSFLOW-coupled ground-water and surface-water FLOW model based on the integration of the Precipitation-Runoff Modeling System (PRMS) and the Modular Ground-Water Flow Model (MODFLOW-2005): USGS Techniques and Methods book 6, chap. D1, 240 p.

Maslia, M.L. and Johnston, R.H., 1984. Use of a digital model to evaluate hydrogeoligic controls on groundwater flow in a fractured rock aquifer at Niagara Falls, NY, J. Hydro!., 75: 167-194.

Markstrom, S. L., Regan, R. S., Hay, L. E., Viger, R. J., Webb, R. M., Payn, R. A., and LaFontaine, J. H., 2015, PRMS-IV, the precipitation-runoff modeling system, version 4: U.S. Geological Survey Techniques and Methods, book 6, chap. B7, 158 p., http://dx.doi.org/10.3133/tm6B7.

Merritt, M.L., and Konikow, L.F., 2000, Documentation of a computer program to simulate lake-aquifer interaction using the MODFLOW groundwater flow model and the MOC3D solute-transport model: USGS Water-Resources Investigations Report 00-4167, 146 p.

MHBC Regional and Urban Planning & Resource Development, 2004-2008, Operational and Rehabilitation Plans - 2004, 2005, 2006, and 2008.

Nash, J.E. and Sutcliffe, J.V., 1970, River flow forecasting through conceptual models, Part I - A discussion of principles. Journal of Hydrology 10, p. 282-290.

Niswonger, R.G., and Prudic, D.E., 2005, Documentation of the Streamflow-Routing (SFR2) Package to include unsaturated flow beneath streams — A modification to SFR1: U.S. Geological Survey Techniques and Methods 6-A13.

Niswonger, R.G., Prudic, D.E., and Regan, R.S., 2006, Documentation of the Unsaturated-Zone Flow (UZF1) Package for modeling unsaturated flow between the land surface and the water table with MODFLOW-2005: USGS Techniques and Methods Book 6, Chapter A19, 62 p.

Niswonger, R.G., Panday, Sorab, and Ibaraki, Motomu, 2011, MODFLOW-NWT, A Newton formulation for MODFLOW-2005: USGS Techniques and Methods 6–A37, 44 p.

Ontario Ministry of Natural Resources and Forestry (MNRF), 2014, Southern Ontario Land Resource Information System (SOLRIS) Version 2.0 [Computer File]. Peterborough, ON (Accessed August 2015).

Ontario Ministry of Natural Resources (MNR), 2005, Provincial Digital Elevation Model, Version 2.0.0 [Computer File]. Peterborough, ON (Accessed August 2006).

Ontario Ministry of Agriculture and Food, Ontario Ministry of Rural Affairs (OMAFRA), 2003, Soil Survey Complex [Computer File]. Guelph, ON (Accessed October 2014).

Savanta Inc., 2020, Natural Environment Technical Report – Nelson Aggregate Burlington Quarry Extension

Tatham Engineering, 2020, Burlington Quarry Extension Surface Water Assessment: prepared for Nelson Aggregates Co., April 8, 2020, 555 p.

Worthington Groundwater, 2006, Karst Investigations at the Proposed Nelson Quarry Co. Extension: report prepared for Nelson Aggregate Co. by S.R.H. Worthington, April 13, 2006.

Worthington Groundwater, 2019, Appendix B – Karst Investigation: in Level 1 and Level 2 Hydrogeological Assessment Proposed Burlington Quarry Extension – Appendix A and B, report prepared by Earthfx Inc. for the Nelson Aggregates Co., November 2019, 41 p.

15 Appendix A: Hydrogeologic Field Investigations

Appendix A summarizes the hydrogeological field investigation methodology. The results of each task have been interpreted and relied upon for the development of the site conceptual geological and hydrogeological model. Where the interpretation of the results has not been discussed in detail in the body of the report, they have been included in the following sections. Due to the immense volume of data and interpretative results, the data presented may not be inclusive. The field data and interpretations are available and can be presented in any format upon request.

Appendix A includes:

- Drilling Program
- Hydraulic Testing Program, including packer testing and a long-term pumping test
- Monitoring Well Construction Program
- Geophysical Logging
- Borehole Televiewer Results
- Groundwater Monitoring Program
- Hydrogeochemical Testing
- Private Well Survey Resutls

15.1 Drilling Program

The current monitoring well network has been implemented in stages over the past 17 years (Figure 2.1). Most of the monitoring wells were constructed as part of the previous ARA application in 2006 with all wells located on the Southern Lands. In total, this original monitoring well network included a total of 84 wells at 32 nested locations with wells targeting both varying bedrock depths and overburden. Several additional overburden monitoring wells were also installed by Golder across the Southern Lands and some of these wells were included in the 2018 / 2019 monitoring program completed by Azimuth. The methodology of the original drilling program has been previously summarized in the Golder Associates Hydrogeological & Water Resources Assessment of the Proposed Nelson Quarry Co. Extension (Golder, 2006), while borehole logs have been included in for reference. To supplement the previous work conducted by Golder, Orbit Garant (formerly Lantech) Drilling Services Inc. drilled an additional three boreholes in July 2016, while Keith Lang Water Well Drilling completed four additional boreholes in May 2019, all on the Western Lands (Figure 3.6). The boreholes completed by Orbit Garant were drilled to depths of approximately 24 to 27 m relating to a bottom of hole elevation of 244 to 246 masl, while the Keith Lang boreholes were all drilled to a target depth of 25 m relating to a bottom elevations of 245 to 247 masl.

The Orbit Garant boreholes were advanced using HQ coring equipment to obtain a 4-inch hole which would allow for, packer testing and downhole geophysics to be completed along with the installation of two monitoring wells. Core recovery was typically greater than 95% in all boreholes which allowed for a completed stratigraphic log. Immediately after extracted from the core barrel, the core was photographed digitally, producing electronic logs of the core of the deep boreholes to aid in the identification of lithologic units. The core was then logged in detail for lithology and fracture frequency. All breaks in the rock were identified as either mechanical or open (natural) fractures. The natural fractures were identified for the presences of infilling (generally calcite), and by evidence of weathering. The characteristics of the fractures can lead to the identification of potential flow zones. The Keith Lang boreholes were drilled to supplement the original HQ boreholes and expand the geological and hydrogeological coverage of the Western Lands. These boreholes are 6-inch in diameter and were constructed using a conventional rotary water well rig. As such, no core was recovered in these boreholes.

Finally, two additional overburden monitoring wells were constructed in November 2019 at the southeast corner of the Southern Lands (MW18-1 and MW18-2). These two-inch monitoring wells were installed to gain a better understanding of both the ground water elevations and hydraulic conductivity in the overburden where the overburden thickness was noted to be greater than the remainder of the Site.

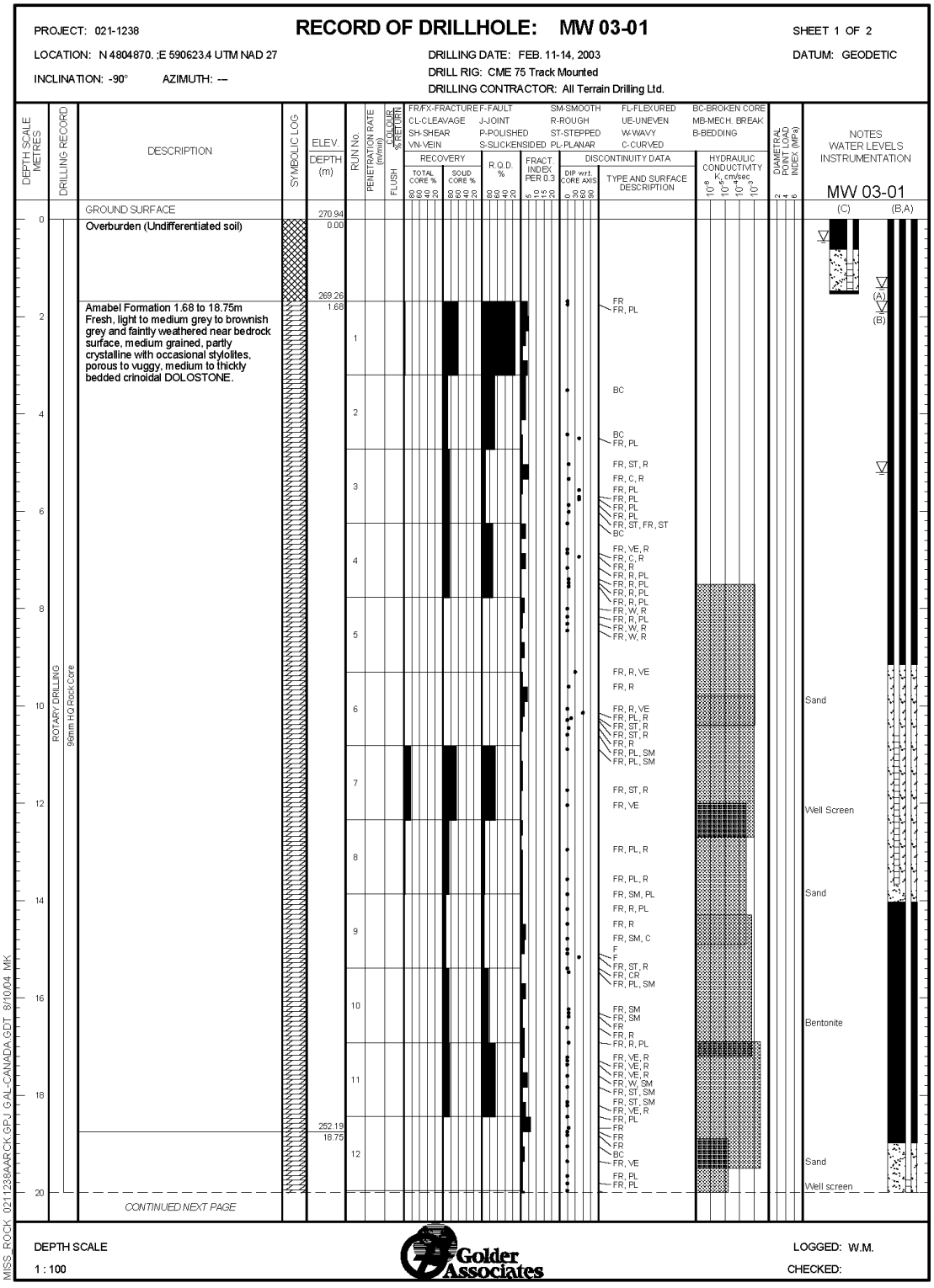
PROJECT: 021-1238
RECORD OF DRILLHOLE: MW 03-01
SHEET 1 OF 2
LOCATION: N 4804870. ;E 590623.4 UTM NAD 27
DRILLING DATE: FEB. 11-14, 2003
DATUM: GEODETIC
INCLINATION: -90° AZIMUTH: ---
DRILL RIG: CME 75 Track Mounted
DRILLING CONTRACTOR: All Terrain Drilling Ltd.
DEPTH SCALE METRES
DRILLING RECORD
ROTARY DRILLING
96mm HQ Rock Core
DESCRIPTION
SYMBOLIC LOG
ELEV. DEPTH (m)
RUN No.
PENETRATION RATE (mm/min)
FLUSH
COLOUR % RETURN
FR/FX-FRACTURE
CL-CLEAVAGE
SH-SHEAR
VN-VEIN
F-FAULT
J-JOINT
P-POLISHED
S-SLICKENSIDED
SM-SMOOTH
R-ROUGH
ST-STEPPED
PL-PLANAR
FL-FLEXURED
UE-UNEVEN
W-WAVY
C-CURVED
BC-BROKEN CORE
MB-MECH. BREAK
B-BEDDING
RECOVERY
TOTAL CORE %
SOLID CORE %
R.Q.D. %
FRACT. INDEX PER 0.3
DISCONTINUITY DATA
DIP wrt. CORE AXIS
TYPE AND SURFACE DESCRIPTION
HYDRAULIC CONDUCTIVITY K, cm/sec
DIAMETRAL POINT LOAD INDEX (MPa)
NOTES WATER LEVELS INSTRUMENTATION
MW 03-01
(C)
(B,A)
(A)
(B)
GROUND SURFACE
270.94
0.00
Overburden (Undifferentiated soil)
269.26
1.68
Amabel Formation 1.68 to 18.75m
Fresh, light to medium grey to brownish grey and faintly weathered near bedrock surface, medium grained, partly crystalline with occasional stylolites, porous to vuggy, medium to thickly bedded crinoidal DOLOSTONE.
252.19
18.75
CONTINUED NEXT PAGE
Sand
Well Screen
Sand
Bentonite
Sand
Well screen
DEPTH SCALE
1 : 100
Golder Associates
LOGGED: W.M.
CHECKED:
MISS_ROCK 021 1238AARCK.GPJ GAL-CANADA.GDT 8/10/04 MK

PROJECT: 021-1238

RECORD OF DRILLHOLE: MW 03-01

SHEET 2 OF 2

LOCATION: N 4804870. ;E 590623.4 UTM NAD 27

DRILLING DATE: FEB. 11-14, 2003

DATUM: GEODETIC

INCLINATION: -90° AZIMUTH: ---

DRILL RIG: CME 75 Track Mounted

DRILLING CONTRACTOR: All Terrain Drilling Ltd.

FR/FX-FRACTURE, CL-CLEAVAGE, SH-SHEAR, VN-VEIN; F-FAULT, J-JOINT, P-POLISHED, S-SLICKENSIDED; SM-SMOOTH, R-ROUGH, ST-STEPPED, PL-PLANAR; FL-FLEXURED, UE-UNEVEN, W-WAVY, C-CURVED; BC-BROKEN CORE, MB-MECH. BREAK, B-BEDDING

DEPTH SCALE METRES	DRILLING RECORD	DESCRIPTION	SYMBOLIC LOG	ELEV. DEPTH (m)	RUN No.	PENETRATION RATE (mm/min)	FLUSH % RETURN	RECOVERY TOTAL CORE %	RECOVERY SOLID CORE %	R.Q.D. %	FRACT. INDEX PER 0.3	DISCONTINUITY DATA: DIP wrt. CORE AXIS	DISCONTINUITY DATA: TYPE AND SURFACE DESCRIPTION	HYDRAULIC CONDUCTIVITY K, cm/sec	DIAMETRAL POINT LOAD INDEX (MPa)	NOTES WATER LEVELS INSTRUMENTATION
		--- CONTINUED FROM PREVIOUS PAGE ---														MW 03-01 (C) (B,A)
20	ROTARY DRILLING 96mm HQ Rock Core	Reynales Formation 18.75 to 21.53m Fresh, medium grey, fine grained, thinly to medium bedded argillaceous DOLOSTONE with thin to laminar partings of soft grey shale. Bottom 0.4 m of formation comprised of light grey, fine grained dolostone bed with disseminated coarse grains of pyrite. Sharp contact with overlying Amabel Formation			13								FR, C FR, PL FR, PL FR, C FR, PLR, FR, PLR FR, PLR, FR, PLR FR, PL, SM				
22				249.41 21.53									FR, PL, FR, PL			Well screen
		Thorold Formation 21.53 to 24.01m Fresh, light to medium greenish grey, thinly bedded, siliceous SILTSTONE and soft fissile shale grading upward to fine grained quartz SANDSTONE with soft SHALE partings. Sharp upper contact with Reynales Formation marked by 20 to 30 mm thick layer of dark green, medium grained, detrital phosphate grains..			14								FR, PL FR, PL, FR, PL FR, C FR, R, FR, R FR, C SM FR, R, FR, R FR, R FR, R FR, PL FR, PL FR, PL, FRPL, R, FR, PL, R FR, PL, SM, FR, PLR, FR FR, FR FR, FR B FR			Sand
24				246.93 24.01	15											Bentonite
		Grimsby Formation 24.01 to 24.45m Fresh, medium reddish brown, fissile, slake susceptible SHALE with interbedded SILTSTONE. Gradational contact with overlying formation		246.49 24.45												Wells constructed with 1" dia. Schedule 40 PVC flush threaded pipe and No. 10 slot screen Note: Water levels taken on May 28, 2003.
		END OF BOREHOLE														
26																
28																
30																
32																
34																
36																
38																
40																

DEPTH SCALE
1 : 100

Golder Associates

LOGGED: W.M.
CHECKED:

MISS_ROCK 0211238AARCK.GPJ GAL-CANADA.GDT 8/10/04 MK

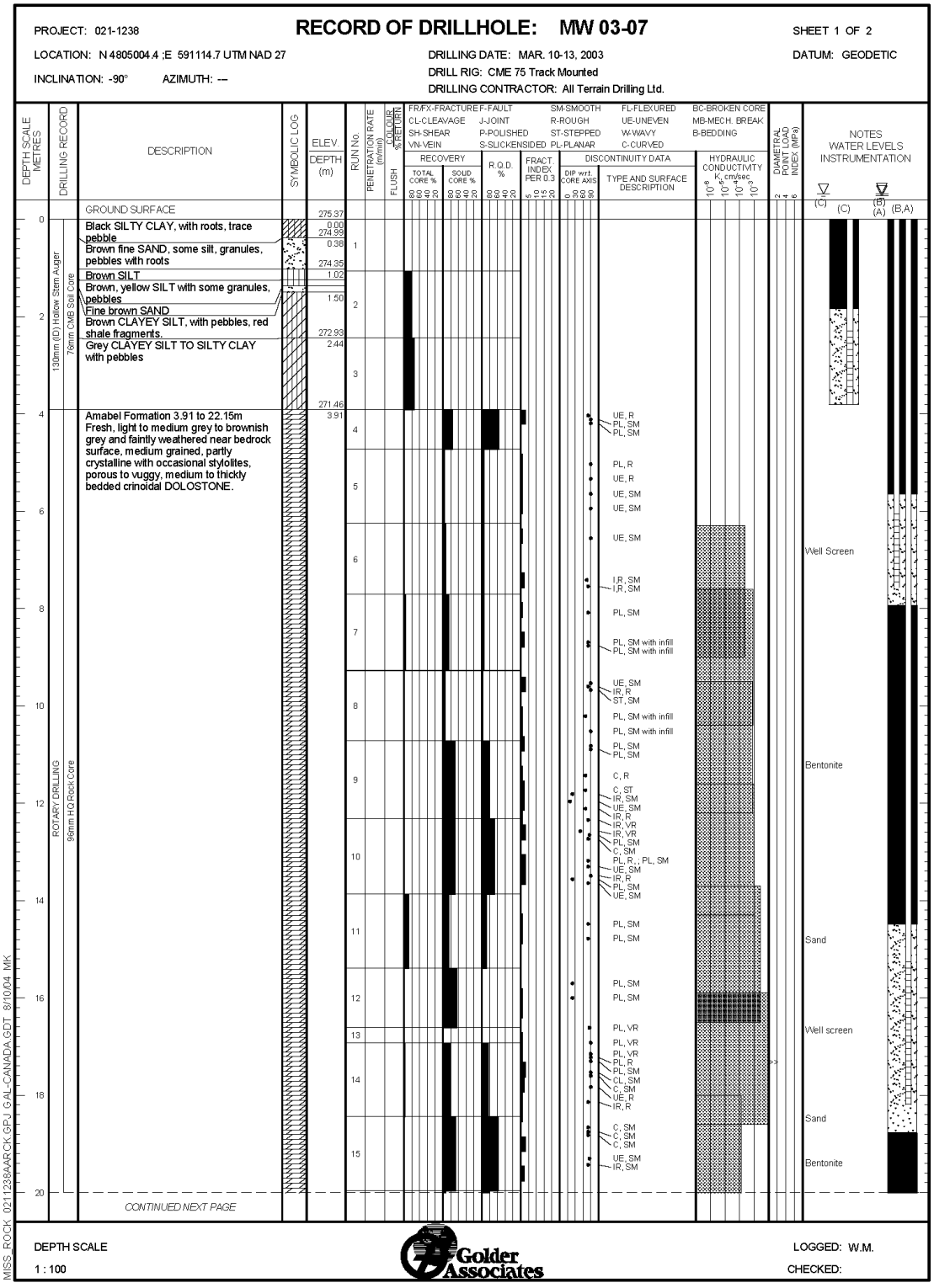
RECORD OF DRILLHOLE: MW 03-07
PROJECT: 021-1238
LOCATION: N 4805004.4 ;E 591114.7 UTM NAD 27
INCLINATION: -90° AZIMUTH: ---
DRILLING DATE: MAR. 10-13, 2003
DRILL RIG: CME 75 Track Mounted
DRILLING CONTRACTOR: All Terrain Drilling Ltd.
SHEET 1 OF 2
DATUM: GEODETIC
DEPTH SCALE METRES
DRILLING RECORD
DESCRIPTION
SYMBOLIC LOG
ELEV. DEPTH (m)
RUN No.
PENETRATION RATE (min/m)
FLUSH
COLOUR
% RETURN
RECOVERY
TOTAL CORE %
SOLID CORE %
R.Q.D. %
FRACT. INDEX PER 0.3
DISCONTINUITY DATA
DIP wrt. CORE AXIS
TYPE AND SURFACE DESCRIPTION
HYDRAULIC CONDUCTIVITY K, cm/sec
DIAMETRAL POINT LOAD INDEX (MPa)
NOTES WATER LEVELS INSTRUMENTATION
FR/FX-FRACTURE
CL-CLEAVAGE
SH-SHEAR
VN-VEIN
F-FAULT
J-JOINT
P-POLISHED
S-SLICKENSIDED
SM-SMOOTH
R-ROUGH
ST-STEPPED
PL-PLANAR
FL-FLEXURED
UE-UNEVEN
W-WAVY
C-CURVED
BC-BROKEN CORE
MB-MECH. BREAK
B-BEDDING
GROUND SURFACE
275.37
Black SILTY CLAY, with roots, trace pebble
0.00
274.99
Brown fine SAND, some silt, granules, pebbles with roots
0.38
274.35
Brown SILT
1.02
Brown, yellow SILT with some granules, pebbles
1.50
Fine brown SAND
Brown CLAYEY SILT, with pebbles, red shale fragments.
272.93
Grey CLAYEY SILT TO SILTY CLAY with pebbles
2.44
271.46
Amabel Formation 3.91 to 22.15m
Fresh, light to medium grey to brownish grey and faintly weathered near bedrock surface, medium grained, partly crystalline with occasional stylolites, porous to vuggy, medium to thickly bedded crinoidal DOLOSTONE.
3.91
130mm (ID) Hollow Stem Auger
76mm CMB Soil Core
ROTARY DRILLING
96mm HQ Rock Core
UE, R
PL, SM
PL, SM
PL, R
UE, R
UE, SM
UE, SM
UE, SM
IR, SM
IR, SM
PL, SM
PL, SM with infill
PL, SM with infill
UE, SM
IR, R
ST, SM
PL, SM with infill
PL, SM with infill
PL, SM
PL, SM
C, R
C, ST
IR, SM
UE, SM
IR, R
IR, VR
IR, VR
PL, SM
C, SM
PL, R, , PL, SM
UE, SM
IR, R
PL, SM
UE, SM
PL, SM
PL, SM
PL, SM
PL, SM
PL, VR
PL, VR
PL, VR
PL, R
PL, SM
CL, SM
C, SM
UE, R
IR, R
C, SM
C, SM
C, SM
UE, SM
IR, SM
Well Screen
Bentonite
Sand
Well screen
Sand
Bentonite
(C)
(B)
(A)
(B,A)
CONTINUED NEXT PAGE
DEPTH SCALE
1 : 100
Golder Associates
LOGGED: W.M.
CHECKED:
MISS_ROCK 021123BAARCK.GPJ GAL-CANADA.GDT 8/10/04 MK

PROJECT: 021-1238

RECORD OF DRILLHOLE: MW 03-07

SHEET 2 OF 2

LOCATION: N 4805004.4 ;E 591114.7 UTM NAD 27

DRILLING DATE: MAR. 10-13, 2003

DATUM: GEODETIC

INCLINATION: -90° AZIMUTH: ---

DRILL RIG: CME 75 Track Mounted

DRILLING CONTRACTOR: All Terrain Drilling Ltd.

FR/FX-FRACTURE F-FAULT SM-SMOOTH FL-FLEXURED BC-BROKEN CORE
CL-CLEAVAGE J-JOINT R-ROUGH UE-UNEVEN MB-MECH. BREAK
SH-SHEAR P-POLISHED ST-STEPPED W-WAVY B-BEDDING
VN-VEIN S-SLICKENSIDED PL-PLANAR C-CURVED

DEPTH SCALE METRES	DRILLING RECORD	DESCRIPTION	SYMBOLIC LOG	ELEV. DEPTH (m)	RUN No.	PENETRATION RATE (mm/min)	FLUSH % RETURN	COLOUR	RECOVERY TOTAL CORE %	RECOVERY SOLID CORE %	R.Q.D. %	FRACT. INDEX PER 0.3	DISCONTINUITY DATA DIP wrt. CORE AXIS	DISCONTINUITY DATA TYPE AND SURFACE DESCRIPTION	HYDRAULIC CONDUCTIVITY K, cm/sec	DIAMETRAL POINT LOAD INDEX (MPa)	NOTES WATER LEVELS INSTRUMENTATION
		--- CONTINUED FROM PREVIOUS PAGE ---															(C) (B,A)
20	ROTARY DRILLING 96mm HQ Rock Core	Amabel Formation 3.91 to 22.15m Fresh, light to medium grey to brownish grey and faintly weathered near bedrock surface, medium grained, partly crystalline with occasional stylolites, porous to vuggy, medium to thickly bedded crinoidal DOLOSTONE.			16									PL, R UE, R PL, R UE, R UE, R IR, R C, R IR, R PL, SM			
22				253.22										IR, SM			
		Reynales Formation 22.15 to 24.79m Fresh, medium grey, fine grained, thinly to medium bedded argillaceous DOLOSTONE with thin to laminar partings of soft grey shale. Bottom 0.4 m of formation comprised of light grey, fine grained dolostone bed with disseminated coarse grains of pyrite. Sharp contact with overlying Amabel Formation		22.15	17									UE, SM PL, SM PL, SM PL, SM, infilling PL, SM, infilling PL, SM, infilling PL, SM			Bentonite
24					18									PL, SM PL, SM PL, SM PL, SM PL, SM PL, R			
				250.58													
		Thorold Formation 24.79 to 27.25m Fresh, light to medium greenish grey, thinly bedded, siliceous SILTSTONE and soft fissile shale grading upward to fine grained quartz SANDSTONE with soft SHALE partings. Sharp upper contact with Reynales Formation marked by 20 to 30 mm thick layer of dark green, medium grained, detrital phosphate grains.		24.79	19									PL, R PL, SM PL, SM PL, SM PL, SM PL, SM			
26					20									PL, SM PL, SM PL			
				248.12													
		Grimsby Formation 27.25 to 27.58m Fresh, medium reddish brown, fissile, slake susceptible SHALE with interbedded SILTSTONE. Gradational contact with overlying formation		27.25													
		END OF BOREHOLE		27.58													Wells constructed with 1" dia. Schedule 40 PVC flush threaded pipe and No. 10 slot screen Note: Water levels taken on May 28, 2003.
28																	
30																	
32																	
34																	
36																	
38																	
40																	

DEPTH SCALE
1 : 100

Golder Associates

LOGGED: W.M.
CHECKED:

MISS_ROCK 0211236AARCK.GPJ GAL-CANADA.GDT 8/10/04 MK

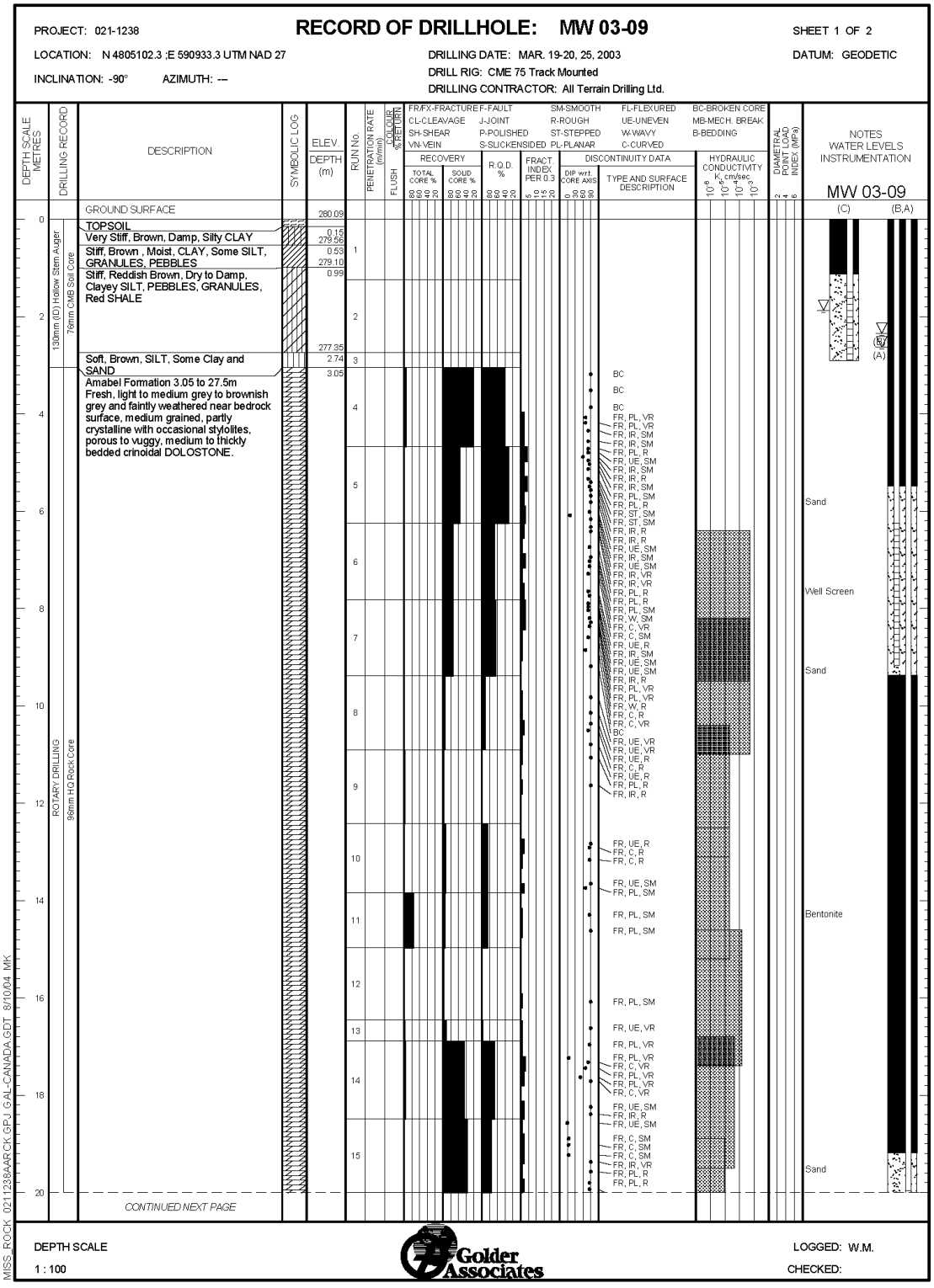
RECORD OF DRILLHOLE: MW 03-09
PROJECT: 021-1238
LOCATION: N 4805102.3 ;E 590933.3 UTM NAD 27
INCLINATION: -90° AZIMUTH: ---
DRILLING DATE: MAR. 19-20, 25, 2003
DRILL RIG: CME 75 Track Mounted
DRILLING CONTRACTOR: All Terrain Drilling Ltd.
SHEET 1 OF 2
DATUM: GEODETIC
DESCRIPTION
GROUND SURFACE
TOPSOIL
Very Stiff, Brown, Damp, Silty CLAY
Stiff, Brown , Moist, CLAY, Some SILT, GRANULES, PEBBLES
Stiff, Reddish Brown, Dry to Damp, Clayey SILT, PEBBLES, GRANULES, Red SHALE
Soft, Brown, SILT, Some Clay and SAND
Amabel Formation 3.05 to 27.5m
Fresh, light to medium grey to brownish grey and faintly weathered near bedrock surface, medium grained, partly crystalline with occasional stylolites, porous to vuggy, medium to thickly bedded crinoidal DOLOSTONE.
CONTINUED NEXT PAGE
130mm (ID) Hollow Stem Auger
76mm CMB Soil Core
ROTARY DRILLING
96mm HQ Rock Core
NOTES WATER LEVELS INSTRUMENTATION
MW 03-09
Sand
Well Screen
Sand
Bentonite
Sand
DEPTH SCALE 1 : 100
LOGGED: W.M.
CHECKED:
Golder Associates
MISS_ROCK 0211238AARCK.GPJ GAL-CANADA.GDT 8/10/04 MK

PROJECT: 021-1238

RECORD OF DRILLHOLE: MW 03-09

SHEET 2 OF 2

LOCATION: N 4805102.3 ;E 590933.3 UTM NAD 27

DRILLING DATE: MAR. 19-20, 25, 2003

DATUM: GEODETIC

INCLINATION: -90° AZIMUTH: ---

DRILL RIG: CME 75 Track Mounted

DRILLING CONTRACTOR: All Terrain Drilling Ltd.

FR/FX-FRACTURE F-FAULT SM-SMOOTH FL-FLEXURED BC-BROKEN CORE
CL-CLEAVAGE J-JOINT R-ROUGH UE-UNEVEN MB-MECH. BREAK
SH-SHEAR P-POLISHED ST-STEPPED W-WAVY B-BEDDING
VN-VEIN S-SLICKENSIDED PL-PLANAR C-CURVED

DEPTH SCALE METRES	DRILLING RECORD	DESCRIPTION	SYMBOLIC LOG	ELEV. DEPTH (m)	RUN No.	PENETRATION RATE (mm/min)	FLUSH	COLOUR % RETURN	RECOVERY TOTAL CORE %	RECOVERY SOLID CORE %	R.Q.D. %	FRACT. INDEX PER 0.3	DISCONTINUITY DATA DIP w.r.t. CORE AXIS	DISCONTINUITY DATA TYPE AND SURFACE DESCRIPTION	HYDRAULIC CONDUCTIVITY K, cm/sec	DIAMETRAL POINT LOAD INDEX (MPa)	NOTES WATER LEVELS INSTRUMENTATION
		--- CONTINUED FROM PREVIOUS PAGE ---															MW 03-09 (C) (B,A)
20	ROTARY DRILLING 96mm HQ Rock Core	Amabel Formation 3.05 to 27.5m Fresh, light to medium grey to brownish grey and faintly weathered near bedrock surface, medium grained, partly crystalline with occasional stylolites, porous to vuggy, medium to thickly bedded crinoidal DOLOSTONE.												FR, IR, SM FR, IR, SM FR, IR, SM FR, PL, SM			Well screen
					16												
22														FR, UE, SM FR, IR, R FR, PL, R FR, PL, SM FR, PL, R FR, PL, R			Sand
					17												
24					18									FR, PL, SM FR, PL, SM FR, PL, R FR, PL, R FR, C, SM FR, PL, R FR, PL, R			
					19									FR, PL, SM FR, PL, R FR, PL, SM FR, PL, R			
26					20									BC FR, PL, SM FR, W, SM FR, PL, R FR, PL, R			Bentonite
				252.59													
28		Reynales Formation 27.5 to 30.27m Fresh, medium grey, fine grained, thinly to medium bedded argillaceous DOLOSTONE with thin to laminar partings of soft grey shale. Bottom 0.4 m of formation comprised of light grey, fine grained dolostone bed with disseminated coarse grains of pyrite. Sharp contact with overlying Amabel Formation		27.50										FR, PL, SM			
					21									FR, PL, SM FR, PL, SM FR, PL, SM FR, PL, SM FR, PL, SM			
30					22									FR, PL, SM FR, UE, R FR, UE, SM FR, PL, SM			
				249.82										FR, PL, SM			
		Thorold Formation 30.27 to 30.67m Fresh, light to medium greenish grey, thinly bedded, siliceous SILTSTONE and soft fissile shale grading upward to fine grained quartz SANDSTONE with soft SHALE partings. Sharp upper contact with Reynales Formation marked by 20 to 30 mm thick layer of dark green, medium grained, detrital phosphate grains.		30.27 249.42										FR, PL, SM			
32		END OF BOREHOLE		30.67													Wells constructed with 1" dia. Schedule 40 PVC flush threaded pipe and No. 10 slot screen Note: Water levels taken on May 28, 2003.
34																	
36																	
38																	
40																	

DEPTH SCALE
1 : 100

Golder Associates

LOGGED: W.M.
CHECKED:

MISS_ROCK 0211238AARCK.GPJ GAL-CANADA.GDT 8/10/04 MK

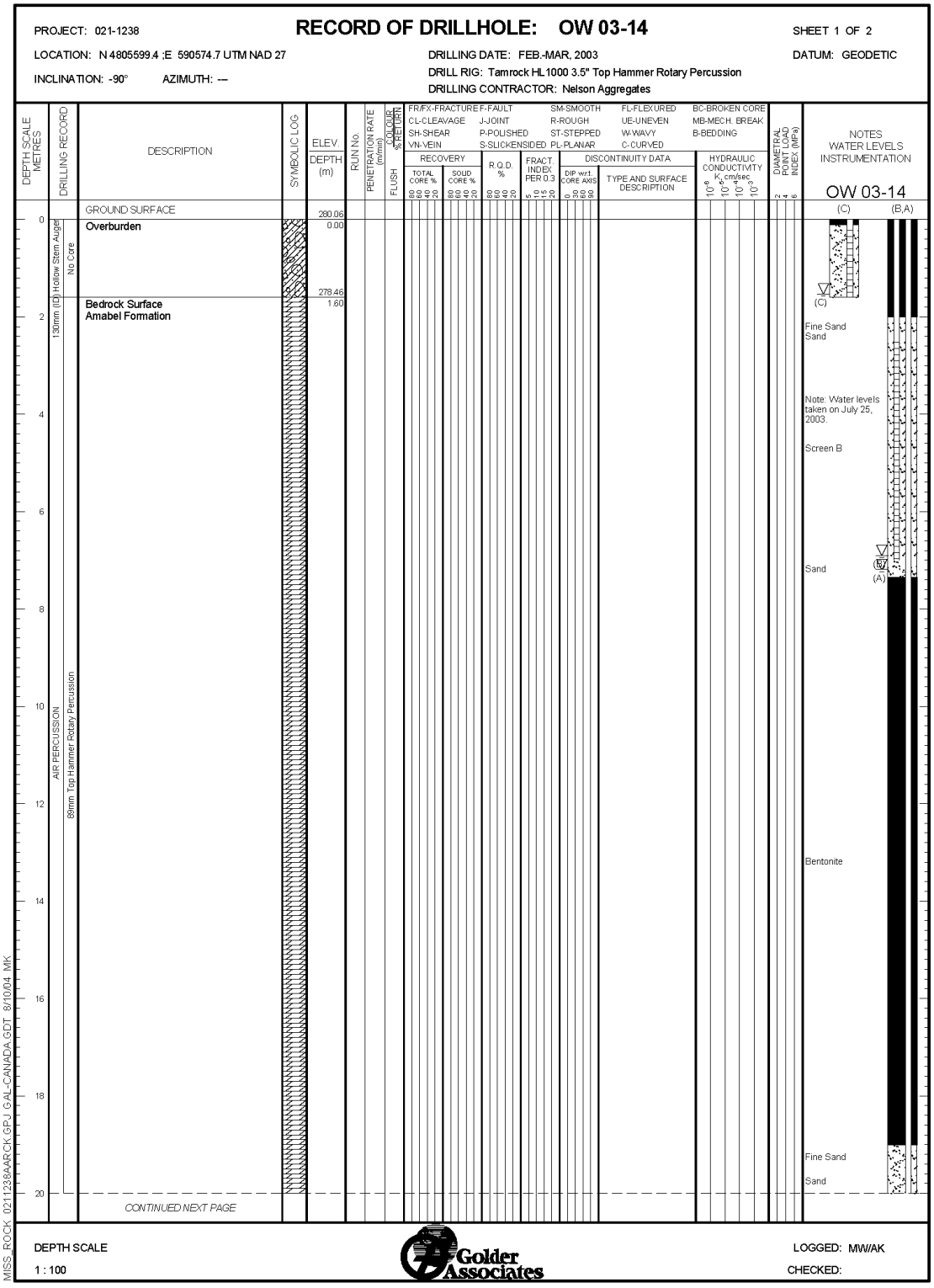
RECORD OF DRILLHOLE: OW 03-14
PROJECT: 021-1238
LOCATION: N 4805599.4 ;E 590574.7 UTM NAD 27
INCLINATION: -90° AZIMUTH: ---
DRILLING DATE: FEB.-MAR, 2003
DRILL RIG: Tamrock HL1000 3.5" Top Hammer Rotary Percussion
DRILLING CONTRACTOR: Nelson Aggregates
SHEET 1 OF 2
DATUM: GEODETIC
DEPTH SCALE METRES
DRILLING RECORD
DESCRIPTION
SYMBOLIC LOG
ELEV. DEPTH (m)
RUN No.
PENETRATION RATE (mm/min)
FLUSH
COLOUR % RETURN
RECOVERY
TOTAL CORE %
SOLID CORE %
R.Q.D. %
FRACT. INDEX PER 0.3
DISCONTINUITY DATA
DIP wrt. CORE AXIS
TYPE AND SURFACE DESCRIPTION
HYDRAULIC CONDUCTIVITY K, cm/sec
DIAMETRAL POINT LOAD INDEX (MPa)
NOTES WATER LEVELS INSTRUMENTATION
OW 03-14
GROUND SURFACE
280.06
Overburden
0.00
278.46
Bedrock Surface
Amabel Formation
1.60
130mm (ID) Hollow Stem Auger
No Core
AIR PERCUSSION
89mm Top Hammer Rotary Percussion
CONTINUED NEXT PAGE
Fine Sand
Sand
Note: Water levels taken on July 25, 2003.
Screen B
Sand
Bentonite
Fine Sand
Sand
DEPTH SCALE
1 : 100
Golder Associates
LOGGED: MW/AK
CHECKED:
MISS_ROCK 0211238AARCK.GPJ GAL-CANADA.GDT 8/10/04 MK

PROJECT: 021-1238

RECORD OF DRILLHOLE: OW 03-14

SHEET 2 OF 2

LOCATION: N 4805599.4 ;E 590574.7 UTM NAD 27

DRILLING DATE: FEB.-MAR, 2003

DATUM: GEODETIC

INCLINATION: -90° AZIMUTH: ---

DRILL RIG: Tamrock HL1000 3.5" Top Hammer Rotary Percussion

DRILLING CONTRACTOR: Nelson Aggregates

FR/FX-FRACTURE F-FAULT SM-SMOOTH FL-FLEXURED BC-BROKEN CORE
CL-CLEAVAGE J-JOINT R-ROUGH UE-UNEVEN MB-MECH. BREAK
SH-SHEAR P-POLISHED ST-STEPPED W-WAVY B-BEDDING
VN-VEIN S-SLICKENSIDED PL-PLANAR C-CURVED

DEPTH SCALE METRES	DRILLING RECORD	DESCRIPTION	SYMBOLIC LOG	ELEV. DEPTH (m)	RUN No.	PENETRATION RATE (mm/min)	FLUSH	COLOUR % RETURN	RECOVERY TOTAL CORE %	RECOVERY SOLID CORE %	R.Q.D. %	FRACT. INDEX PER 0.3	DISCONTINUITY DATA DIP wrt. CORE AXIS	DISCONTINUITY DATA TYPE AND SURFACE DESCRIPTION	HYDRAULIC CONDUCTIVITY K, cm/sec	DIAMETRAL POINT LOAD INDEX (MPa)	NOTES WATER LEVELS INSTRUMENTATION
		--- CONTINUED FROM PREVIOUS PAGE ---							80 60 40 20	80 60 40 20	80 60 40 20	5 10 15 20	0 30 60 90		10^{-6} 10^{-5} 10^{-4} 10^{-3}	2 4 6	OW 03-14 (C) (B,A)
20	AIR PERCUSSION 89mm Top Hammer Rotary Percussion	Bedrock Surface Amabel Formation															
22																	
24																	Screen A
26																	
28				251.10													
		Inferred Thorold Formation Contact		28.96													
30																	Caved Material
32				247.96													
		END OF BOREHOLE		32.10													A and B wells constructed with 1" dia. Schedule 40 PVC flush threaded pipe and No. 10 slot screen, C well constructed with 2" dia. Schedule 40 PVC flush threaded pipe and No. 10 slot screen
		Notes: 1. Rotary Percussion Borehole drilled and logged by Nelson 2. Monitoring well installation constructed by Golder															Note: Water levels taken on May 28, 2003.
34																	
36																	
38																	
40																	

MISS_ROCK 0211238AARCK.GPJ GAL-CANADA.GDT 8/10/04 MK

DEPTH SCALE
1 : 100

Golder Associates

LOGGED: MW/AK
CHECKED:

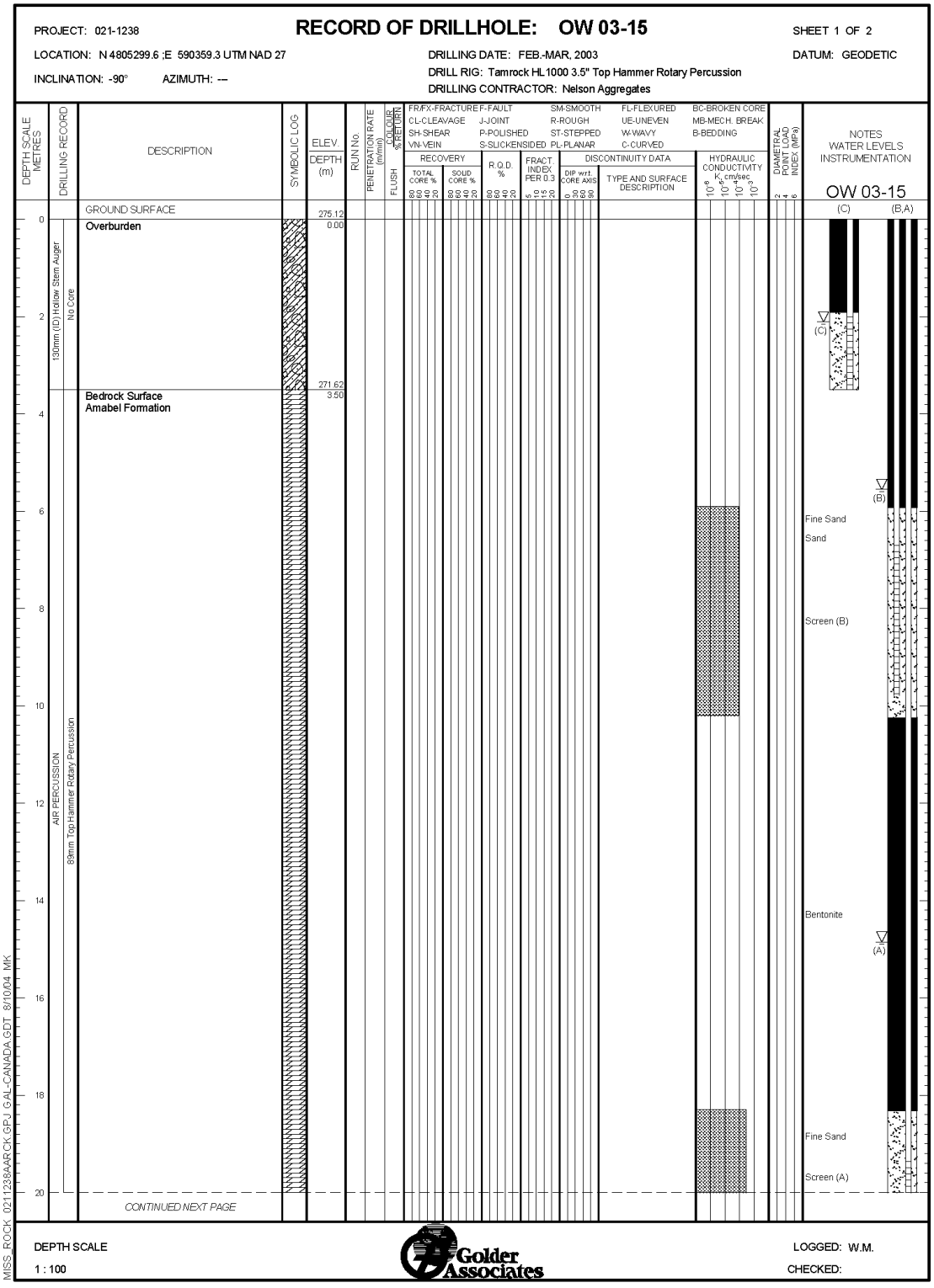
RECORD OF DRILLHOLE: OW 03-15
PROJECT: 021-1238
LOCATION: N 4805299.6 ;E 590359.3 UTM NAD 27
INCLINATION: -90° AZIMUTH: ---
DRILLING DATE: FEB.-MAR, 2003
DRILL RIG: Tamrock HL1000 3.5" Top Hammer Rotary Percussion
DRILLING CONTRACTOR: Nelson Aggregates
SHEET 1 OF 2
DATUM: GEODETIC
DEPTH SCALE METRES
DRILLING RECORD
DESCRIPTION
SYMBOLIC LOG
ELEV. DEPTH (m)
RUN No.
PENETRATION RATE (mm/min)
FLUSH
COLOUR % RETURN
RECOVERY
TOTAL CORE %
SOLID CORE %
R.Q.D. %
FRACT. INDEX PER 0.3
DISCONTINUITY DATA
DIP wrt. CORE AXIS
TYPE AND SURFACE DESCRIPTION
HYDRAULIC CONDUCTIVITY K, cm/sec
DIAMETRAL POINT LOAD INDEX (MPa)
NOTES WATER LEVELS INSTRUMENTATION
OW 03-15
GROUND SURFACE
275.12
Overburden
0.00
271.62
Bedrock Surface
Amabel Formation
3.50
130mm (ID) Hollow Stem Auger
No Core
AIR PERCUSSION
89mm Top Hammer Rotary Percussion
CONTINUED NEXT PAGE
Fine Sand
Sand
Screen (B)
Bentonite
Fine Sand
Screen (A)
DEPTH SCALE
1 : 100
Golder Associates
LOGGED: W.M.
CHECKED:

PROJECT: 021-1238

RECORD OF DRILLHOLE: OW 03-15

SHEET 2 OF 2

LOCATION: N 4805299.6 ;E 590359.3 UTM NAD 27

DRILLING DATE: FEB.-MAR, 2003

DATUM: GEODETIC

INCLINATION: -90° AZIMUTH: ---

DRILL RIG: Tamrock HL1000 3.5" Top Hammer Rotary Percussion

DRILLING CONTRACTOR: Nelson Aggregates

FR/FX-FRACTURE CL-CLEAVAGE SH-SHEAR VN-VEIN

F-FAULT J-JOINT P-POLISHED S-SLICKENSIDED

SM-SMOOTH R-ROUGH ST-STEPPED PL-PLANAR

FL-FLEXURED UE-UNEVEN W-WAVY C-CURVED

BC-BROKEN CORE MB-MECH. BREAK B-BEDDING

DEPTH SCALE METRES	DRILLING RECORD	DESCRIPTION	SYMBOLIC LOG	ELEV. DEPTH (m)	RUN No.	PENETRATION RATE (mm/min)	FLUSH % RETURN COLOUR	RECOVERY TOTAL CORE %	RECOVERY SOLID CORE %	R.Q.D. %	FRACT. INDEX PER 0.3	DISCONTINUITY DATA DIP wrt. CORE AXIS	DISCONTINUITY DATA TYPE AND SURFACE DESCRIPTION	HYDRAULIC CONDUCTIVITY K, cm/sec	DIAMETRAL POINT LOAD INDEX (MPa)	NOTES WATER LEVELS INSTRUMENTATION
		--- CONTINUED FROM PREVIOUS PAGE ---														OW 03-15 (C) (B,A)
20	AIR PERCUSSION 89mm Top Hammer Rotary Percussion	Bedrock Surface Amabel Formation														
22																Screen (A)
				251.65												
24		Inferred Thorold Formation Contact		23.47												Sand
				249.52												Bentonite
26		END OF BOREHOLE		25.60												
		Notes: 1. Rotary Percussion Borehole drilled and logged by Nelson 2. Monitoring well installation constructed by Golder														A and B wells constructed with 1" dia. Schedule 40 PVC flush threaded pipe and No. 10 slot screen, C well constructed with 2" dia. Schedule 40 PVC flush threaded pipe and No. 10 slot screen Note: Water levels taken on July 25, 2003.
28																
30																
32																
34																
36																
38																
40																

MISS_ROCK 0211238AARCK.GPJ GAL-CANADA.GDT 8/10/04 MK

DEPTH SCALE

1 : 100

Golder Associates

LOGGED: W.M.

CHECKED:

PROJECT: 021-1238

RECORD OF DRILLHOLE: OW 03-17

SHEET 1 OF 2

LOCATION: N 4804488.6 ;E 590989.7 UTM NAD 27

DRILLING DATE: AUGUST 19, 2003

DATUM: GEODETIC

INCLINATION: -90° AZIMUTH: ---

DRILL RIG: Tamrock HL1000 3.5" Top Hammer Rotary Percussion

DRILLING CONTRACTOR: Nelson Aggregates

DEPTH SCALE METRES	DRILLING RECORD	DESCRIPTION	SYMBOLIC LOG	ELEV. DEPTH (m)	RUN No.	PENETRATION RATE (mm/min)	FLUSH % RETURN	COLOUR	RECOVERY TOTAL CORE %	RECOVERY SOLID CORE %	R.Q.D. %	FRACT. INDEX PER 0.3	DISCONTINUITY DATA DIP wrt. CORE AXIS	DISCONTINUITY DATA TYPE AND SURFACE DESCRIPTION	HYDRAULIC CONDUCTIVITY K, cm/sec	DIAMETRAL POINT LOAD INDEX (MPa)	NOTES WATER LEVELS INSTRUMENTATION
		GROUND SURFACE		272.54													OW 03-17 (B,A)
0	130mm (ID) Hollow Stem Auger / No Core	Overburden		0.00													
		Bedrock Surface Amabel Formation		271.47 1.07													
2	AIR PERCUSSION / 89mm Top Hammer Rotary Percussion																Bentonite
4																	Sand
6																	
8																	Screen (B)
10																	
12																	Sand
14																	Bentonite
16																	Sand
18																	Screen (A)
20		CONTINUED NEXT PAGE															

FR/FX-FRACTURE CL-CLEAVAGE SH-SHEAR VN-VEIN

F-FAULT J-JOINT P-POLISHED S-SLICKENSIDED

SM-SMOOTH R-ROUGH ST-STEPPED PL-PLANAR

FL-FLEXURED UE-UNEVEN W-WAVY C-CURVED

BC-BROKEN CORE MB-MECH. BREAK B-BEDDING

DEPTH SCALE 1 : 100

LOGGED:

CHECKED:

Golder Associates

MISS_ROCK 0211238AARCK.GPJ GAL-CANADA.GDT 8/10/04 MK

PROJECT: 021-1238

RECORD OF DRILLHOLE: OW 03-17

SHEET 2 OF 2

LOCATION: N 4804488.6 ;E 590989.7 UTM NAD 27

DRILLING DATE: AUGUST 19, 2003

DATUM: GEODETIC

INCLINATION: -90° AZIMUTH: ---

DRILL RIG: Tamrock HL1000 3.5" Top Hammer Rotary Percussion

DRILLING CONTRACTOR: Nelson Aggregates

FR/FX-FRACTURE CL-CLEAVAGE SH-SHEAR VN-VEIN

F-FAULT J-JOINT P-POLISHED S-SLICKENSIDED

SM-SMOOTH R-ROUGH ST-STEPPED PL-PLANAR

FL-FLEXURED UE-UNEVEN W-WAVY C-CURVED

BC-BROKEN CORE MB-MECH. BREAK B-BEDDING

DEPTH SCALE METRES	DRILLING RECORD	DESCRIPTION	SYMBOLIC LOG	ELEV. DEPTH (m)	RUN No.	PENETRATION RATE (mm/min)	FLUSH % RETURN COLOUR	RECOVERY TOTAL CORE %	RECOVERY SOLID CORE %	R.Q.D. %	FRACT. INDEX PER 0.3	DISCONTINUITY DATA DIP wrt. CORE AXIS	DISCONTINUITY DATA TYPE AND SURFACE DESCRIPTION	HYDRAULIC CONDUCTIVITY K, cm/sec	DIAMETRAL POINT LOAD INDEX (MPa)	NOTES WATER LEVELS INSTRUMENTATION
		--- CONTINUED FROM PREVIOUS PAGE ---														(B,A)
20	AIR PERCUSSION	Bedrock Surface Amabel Formation														Screen (A)
22				249.77												Sand
		END OF BOREHOLE		22.77												Wells constructed with 1" dia. Schedule 40 PVC flush threaded pipe and No. 10 slot screen
24		Note 1) Rotary Percussion Borehole drilled and logged by Nelson Note 2) Monitoring well installation constructed by Golder														Note: Water levels taken on April 27, 2004.
26																OW 03-17
28																
30																
32																
34																
36																
38																
40																

DEPTH SCALE
1 : 100

Golder Associates

LOGGED:

CHECKED:

MISS_ROCK 0211238AARCK.GPJ GAL-CANADA.GDT 8/10/04 MK

PROJECT: 021-1238

RECORD OF DRILLHOLE: OW 03-18

SHEET 1 OF 2

LOCATION: N 4804786.5 ;E 591209.4 UTM NAD 27

DRILLING DATE: FEB.-MAR, 2003

DATUM: GEODETIC

INCLINATION: -90° AZIMUTH: ---

DRILL RIG: Tamrock HL1000 3.5" Top Hammer Rotary Percussion

DRILLING CONTRACTOR: Nelson Aggregates

FR-FRACTURE, CL-CLEAVAGE, SH-SHEAR, VN-VEIN, F-FAULT, J-JOINT, P-POLISHED, S-SLICKENSIDED, SM-SMOOTH, R-ROUGH, ST-STEPPED, PL-PLANAR, FL-FLEXURED, UE-UNEVEN, W-WAVY, C-CURVED, BC-BROKEN CORE, MB-MECH. BREAK, B-BEDDING

DEPTH SCALE METRES	DRILLING RECORD	DESCRIPTION	ELEV. DEPTH (m)
		GROUND SURFACE	275.64
0	130mm (ID) Hollow Stem Auger, No Core	**Overburden**	0.00
4		**Bedrock Surface** **Amabel Formation**	271.04 4.60
20	AIR PERCUSSION, 89mm Top Hammer Rotary Percussion	*CONTINUED NEXT PAGE*	

RUN No. | PENETRATION RATE (mm/min) | FLUSH | COLOUR % RETURN | RECOVERY: TOTAL CORE % | SOLID CORE % | R.Q.D. % | FRACT. INDEX PER 0.3 | DISCONTINUITY DATA: DIP wrt. CORE AXIS | TYPE AND SURFACE DESCRIPTION | HYDRAULIC CONDUCTIVITY K, cm/sec | DIAMETRAL POINT LOAD INDEX (MPa)

NOTES WATER LEVELS INSTRUMENTATION

OW 03-18

(C) (B,A)

(C) (A) (B)

Fine Sand

Sand

Screen (B)

Sand

Bentonite

Fine Sand

Screen (A)

DEPTH SCALE 1 : 100

Golder Associates

LOGGED: W.M.

CHECKED:

MISS_ROCK 0211236AARCK.GPJ GAL-CANADA.GDT 8/10/04 MK

PROJECT: 021-1238

RECORD OF DRILLHOLE: OW 03-18

SHEET 2 OF 2

LOCATION: N 4804786.5 ;E 591209.4 UTM NAD 27

DRILLING DATE: FEB.-MAR, 2003

DATUM: GEODETIC

INCLINATION: -90° AZIMUTH: ---

DRILL RIG: Tamrock HL1000 3.5" Top Hammer Rotary Percussion

DRILLING CONTRACTOR: Nelson Aggregates

FR/FX-FRACTURE CL-CLEAVAGE SH-SHEAR VN-VEIN

F-FAULT J-JOINT P-POLISHED S-SLICKENSIDED

SM-SMOOTH R-ROUGH ST-STEPPED PL-PLANAR

FL-FLEXURED UE-UNEVEN W-WAVY C-CURVED

BC-BROKEN CORE MB-MECH. BREAK B-BEDDING

DEPTH SCALE METRES	DRILLING RECORD	DESCRIPTION	SYMBOLIC LOG	ELEV. DEPTH (m)	RUN No.	PENETRATION RATE (mm/min)	FLUSH % RETURN COLOUR	RECOVERY TOTAL CORE %	RECOVERY SOLID CORE %	R.Q.D. %	FRACT. INDEX PER 0.3	DISCONTINUITY DATA DIP wrt. CORE AXIS	DISCONTINUITY DATA TYPE AND SURFACE DESCRIPTION	HYDRAULIC CONDUCTIVITY K, cm/sec	DIAMETRAL POINT LOAD INDEX (MPa)	NOTES WATER LEVELS INSTRUMENTATION
		--- CONTINUED FROM PREVIOUS PAGE ---														OW 03-18 (C) (B,A)
20	AIR PERCUSSION 89mm Top-Hammer Rotary Percussion	Bedrock Surface Amabel Formation														
22																
24																Screen (A)
26		Inferred Thorold Formation Contact		250.34 25.30												Sand
28																Caved Material
30		END OF BOREHOLE Notes: 1. Rotary Percussion Borehole drilled and logged by Nelson 2. Monitoring well installation constructed by Golder		246.74 28.90												A and B wells constructed with 1" dia. Schedule 40 PVC flush threaded pipe and No. 10 slot screen, C well constructed with 2" dia. Schedule 40 PVC flush threaded pipe and No. 10 slot screen Note: Water levels taken on July 25, 2003.
32																
34																
36																
38																
40																

MISS_ROCK 0211238AARCK.GPJ GAL-CANADA.GDT 8/10/04 MK

DEPTH SCALE

1 : 100

Golder Associates

LOGGED: W.M.

CHECKED:

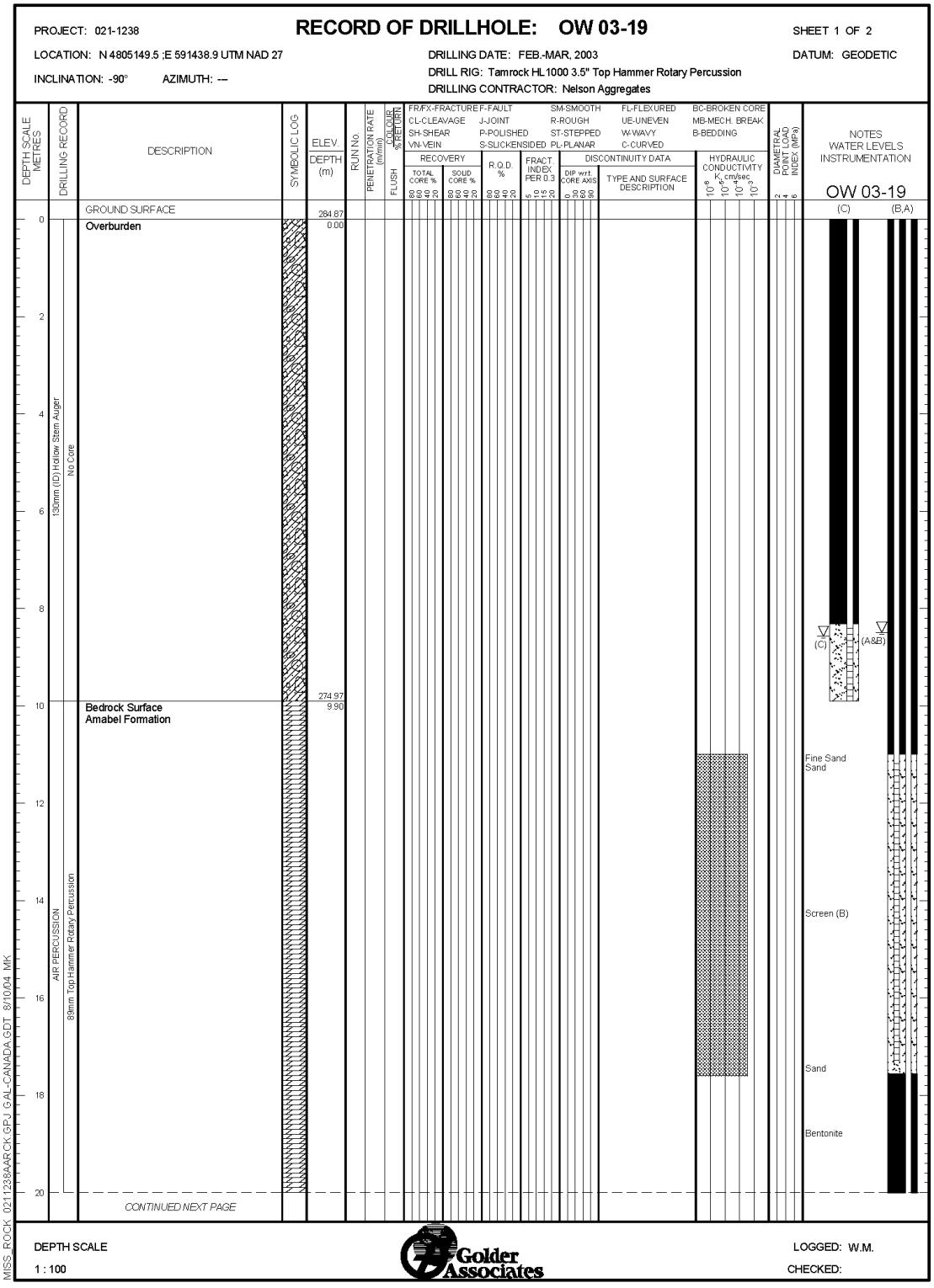
RECORD OF DRILLHOLE: OW 03-19
PROJECT: 021-1238
LOCATION: N 4805149.5 ;E 591438.9 UTM NAD 27
INCLINATION: -90° AZIMUTH: ---
DRILLING DATE: FEB.-MAR, 2003
DRILL RIG: Tamrock HL1000 3.5" Top Hammer Rotary Percussion
DRILLING CONTRACTOR: Nelson Aggregates
SHEET 1 OF 2
DATUM: GEODETIC
DEPTH SCALE METRES
DRILLING RECORD
DESCRIPTION
SYMBOLIC LOG
ELEV. DEPTH (m)
RUN No.
PENETRATION RATE (mm/min)
FLUSH
COLOUR % RETURN
RECOVERY
TOTAL CORE %
SOLID CORE %
R.Q.D. %
FRACT. INDEX PER 0.3
DISCONTINUITY DATA
DIP wrt. CORE AXIS
TYPE AND SURFACE DESCRIPTION
HYDRAULIC CONDUCTIVITY K, cm/sec
DIAMETRAL POINT LOAD INDEX (MPa)
NOTES WATER LEVELS INSTRUMENTATION
OW 03-19
GROUND SURFACE
284.87
0.00
Overburden
130mm (ID) Hollow Stem Auger
No Core
274.97
9.90
Bedrock Surface
Amabel Formation
AIR PERCUSSION
89mm Top Hammer Rotary Percussion
CONTINUED NEXT PAGE
Fine Sand
Sand
Screen (B)
Sand
Bentonite
(C)
(A&B)
DEPTH SCALE
1 : 100
Golder Associates
LOGGED: W.M.
CHECKED:

PROJECT: 021-1238

RECORD OF DRILLHOLE: OW 03-19

SHEET 2 OF 2

LOCATION: N 4805149.5 ;E 591438.9 UTM NAD 27

DRILLING DATE: FEB.-MAR, 2003

DATUM: GEODETIC

INCLINATION: -90° AZIMUTH: ---

DRILL RIG: Tamrock HL1000 3.5" Top Hammer Rotary Percussion

DRILLING CONTRACTOR: Nelson Aggregates

FR/FX-FRACTURE F-FAULT SM-SMOOTH FL-FLEXURED BC-BROKEN CORE
CL-CLEAVAGE J-JOINT R-ROUGH UE-UNEVEN MB-MECH. BREAK
SH-SHEAR P-POLISHED ST-STEPPED W-WAVY B-BEDDING
VN-VEIN S-SLICKENSIDED PL-PLANAR C-CURVED

DEPTH SCALE METRES	DRILLING RECORD	DESCRIPTION	SYMBOLIC LOG	ELEV. DEPTH (m)	RUN No.	PENETRATION RATE (mm/min)	FLUSH	COLOUR % RETURN	RECOVERY TOTAL CORE %	RECOVERY SOLID CORE %	R.Q.D. %	FRACT. INDEX PER 0.3	DISCONTINUITY DATA DIP wrt. CORE AXIS	DISCONTINUITY DATA TYPE AND SURFACE DESCRIPTION	HYDRAULIC CONDUCTIVITY K, cm/sec	DIAMETRAL POINT LOAD INDEX (MPa)	NOTES WATER LEVELS INSTRUMENTATION
		--- CONTINUED FROM PREVIOUS PAGE ---															OW 03-19
20	AIR PERCUSSION 89mm Top Hammer Rotary Percussion	Bedrock Surface Amabel Formation															(C) (B,A)
22																	Bentonite
24																	Fine Sand Sand
26																	Screen (A)
28																	
30																	Sand
				253.77													Caved Material
		END OF BOREHOLE		31.10													
32		Notes: 1. Rotary Percussion Borehole drilled and logged by Nelson 2. Monitoring well installation constructed by Golder															A and B wells constructed with 1" dia. Schedule 40 PVC flush threaded pipe and No. 10 slot screen, C well constructed with 2" dia. Schedule 40 PVC flush threaded pipe and No. 10 slot screen Note: Water levels taken on July 25, 2003.
34																	
36																	
38																	
40																	

MISS_ROCK 0211238AARCK.GPJ GAL-CANADA.GDT 8/10/04 MK

DEPTH SCALE
1 : 100

Golder Associates

LOGGED: W.M.
CHECKED:

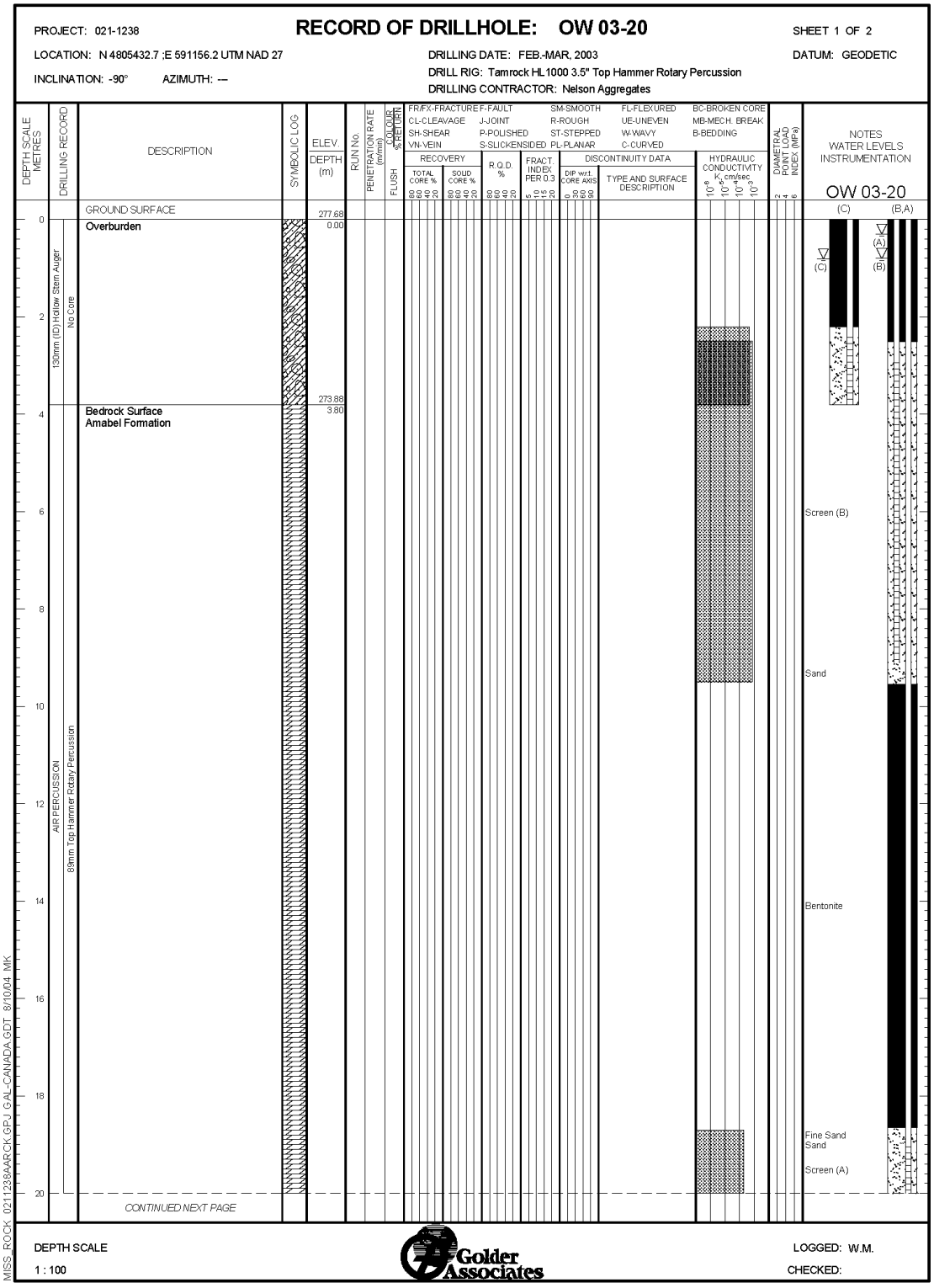
RECORD OF DRILLHOLE: OW 03-20
PROJECT: 021-1238
LOCATION: N 4805432.7 ;E 591156.2 UTM NAD 27
INCLINATION: -90° AZIMUTH: ---
DRILLING DATE: FEB.-MAR, 2003
DRILL RIG: Tamrock HL1000 3.5" Top Hammer Rotary Percussion
DRILLING CONTRACTOR: Nelson Aggregates
SHEET 1 OF 2
DATUM: GEODETIC
DEPTH SCALE METRES
DRILLING RECORD
DESCRIPTION
SYMBOLIC LOG
ELEV. DEPTH (m)
RUN No.
PENETRATION RATE (mm/min)
FLUSH
COLOUR % RETURN
FR/FX-FRACTURE CL-CLEAVAGE SH-SHEAR VN-VEIN
F-FAULT J-JOINT P-POLISHED S-SLICKENSIDED
SM-SMOOTH R-ROUGH ST-STEPPED PL-PLANAR
FL-FLEXURED UE-UNEVEN W-WAVY C-CURVED
BC-BROKEN CORE MB-MECH. BREAK B-BEDDING
RECOVERY
TOTAL CORE %
SOLID CORE %
R.Q.D. %
FRACT. INDEX PER 0.3
DISCONTINUITY DATA
DIP wrt. CORE AXIS
TYPE AND SURFACE DESCRIPTION
HYDRAULIC CONDUCTIVITY K, cm/sec
DIAMETRAL POINT LOAD INDEX (MPa)
NOTES WATER LEVELS INSTRUMENTATION
OW 03-20
GROUND SURFACE
277.68
Overburden
0.00
273.88
Bedrock Surface
Amabel Formation
3.80
130mm (ID) Hollow Stem Auger
No Core
AIR PERCUSSION
89mm Top Hammer Rotary Percussion
CONTINUED NEXT PAGE
Screen (B)
Sand
Bentonite
Fine Sand
Sand
Screen (A)
(C)
(B,A)
(A)
(B)
DEPTH SCALE
1 : 100
Golder Associates
LOGGED: W.M.
CHECKED:
MISS_ROCK 0211238AARCK.GPJ GAL-CANADA.GDT 8/10/04 MK

PROJECT: 021-1238

RECORD OF DRILLHOLE: OW 03-20

SHEET 2 OF 2

LOCATION: N 4805432.7 ;E 591156.2 UTM NAD 27

DRILLING DATE: FEB.-MAR, 2003

DATUM: GEODETIC

INCLINATION: -90° AZIMUTH: ---

DRILL RIG: Tamrock HL1000 3.5" Top Hammer Rotary Percussion

DRILLING CONTRACTOR: Nelson Aggregates

FR/FX-FRACTURE CL-CLEAVAGE SH-SHEAR VN-VEIN

F-FAULT J-JOINT P-POLISHED S-SLICKENSIDED

SM-SMOOTH R-ROUGH ST-STEPPED PL-PLANAR

FL-FLEXURED UE-UNEVEN W-WAVY C-CURVED

BC-BROKEN CORE MB-MECH. BREAK B-BEDDING

DEPTH SCALE METRES	DRILLING RECORD	DESCRIPTION	SYMBOLIC LOG	ELEV. DEPTH (m)	RUN No.	PENETRATION RATE (mm/min)	FLUSH % RETURN COLOUR	RECOVERY TOTAL CORE %	RECOVERY SOLID CORE %	R.Q.D. %	FRACT. INDEX PER 0.3	DISCONTINUITY DATA DIP wrt. CORE AXIS	DISCONTINUITY DATA TYPE AND SURFACE DESCRIPTION	HYDRAULIC CONDUCTIVITY K, cm/sec	DIAMETRAL POINT LOAD INDEX (MPa)	NOTES WATER LEVELS INSTRUMENTATION
		--- CONTINUED FROM PREVIOUS PAGE ---														OW 03-20 (C) (B,A)
20	AIR PERCUSSION 89mm Top Hammer Rotary Percussion	Bedrock Surface Amabel Formation		253.30												Screen (A)
24		Inferred Thorold Formation Contact		24.38 251.58												Sand Caved Material
26		END OF BOREHOLE Notes: 1. Rotary Percussion Borehole drilled and logged by Nelson 2. Monitoring well installation constructed by Golder		26.10												A and B wells constructed with 1" dia. Schedule 40 PVC flush threaded pipe and No. 10 slot screen, C well constructed with 2" dia. Schedule 40 PVC flush threaded pipe and No. 10 slot screen Note: Water levels taken on July 25, 2003.
28																
30																
32																
34																
36																
38																
40																

DEPTH SCALE
1 : 100

Golder Associates

LOGGED: W.M.
CHECKED:

MISS_ROCK 0211238AARCK.GPJ GAL-CANADA.GDT 8/10/04 MK

PROJECT: 021-1238

RECORD OF DRILLHOLE: OW 03-28

SHEET 1 OF 2

LOCATION: N 4805021.2 ;E 591133.0 UTM NAD 27

DRILLING DATE: FEB.-MAR, 2003

DATUM: GEODETIC

INCLINATION: -90° AZIMUTH: ---

DRILL RIG: Tamrock HL1000 3.5" Top Hammer Rotary Percussion

DRILLING CONTRACTOR: Nelson Aggregates

FR/FX-FRACTURE CL-CLEAVAGE SH-SHEAR VN-VEIN

F-FAULT J-JOINT P-POLISHED S-SLICKENSIDED

SM-SMOOTH R-ROUGH ST-STEPPED PL-PLANAR

FL-FLEXURED UE-UNEVEN W-WAVY C-CURVED

BC-BROKEN CORE MB-MECH. BREAK B-BEDDING

DEPTH SCALE METRES	DRILLING RECORD	DESCRIPTION	SYMBOLIC LOG	ELEV. DEPTH (m)	RUN No.	PENETRATION RATE (mm/min)	FLUSH % RETURN	COLOUR	RECOVERY TOTAL CORE %	RECOVERY SOLID CORE %	R.Q.D. %	FRACT. INDEX PER 0.3	DISCONTINUITY DATA DIP wrt. CORE AXIS	DISCONTINUITY DATA TYPE AND SURFACE DESCRIPTION	HYDRAULIC CONDUCTIVITY K, cm/sec	DIAMETRAL POINT LOAD INDEX (MPa)	NOTES WATER LEVELS INSTRUMENTATION
		GROUND SURFACE		275.46													OW 03-28
0	130mm (ID) Hollow Stem Auger No Core	Overburden		0.00													(C) (B,A)
2																	(C) (B) (A)
				272.36													
4	AIR PERCUSSION 89mm Top Hammer Rotary Percussion	Bedrock Surface Amabel Formation		3.10													Fine Sand Sand
6																	Screen (B)
8																	
10																	Sand
12																	
14																	Bentonite
16																	
18																	
20		CONTINUED NEXT PAGE															Fine Sand Sand Screen (A)

DEPTH SCALE 1 : 100

Golder Associates

LOGGED: W.M.

CHECKED:

MISS_ROCK 0211238AARCK.GPJ GAL-CANADA.GDT 8/10/04 MK

PROJECT: 021-1238

RECORD OF DRILLHOLE: OW 03-28

SHEET 2 OF 2

LOCATION: N 4805021.2 ;E 591133.0 UTM NAD 27

DRILLING DATE: FEB.-MAR, 2003

DATUM: GEODETIC

INCLINATION: -90° AZIMUTH: ---

DRILL RIG: Tamrock HL1000 3.5" Top Hammer Rotary Percussion

DRILLING CONTRACTOR: Nelson Aggregates

FR/FX-FRACTURE F-FAULT SM-SMOOTH FL-FLEXURED BC-BROKEN CORE
CL-CLEAVAGE J-JOINT R-ROUGH UE-UNEVEN MB-MECH. BREAK
SH-SHEAR P-POLISHED ST-STEPPED W-WAVY B-BEDDING
VN-VEIN S-SLICKENSIDED PL-PLANAR C-CURVED

DEPTH SCALE METRES	DRILLING RECORD	DESCRIPTION	SYMBOLIC LOG	ELEV. DEPTH (m)	RUN No.	PENETRATION RATE (mm/min)	FLUSH	COLOUR % RETURN	RECOVERY TOTAL CORE %	RECOVERY SOLID CORE %	R.Q.D. %	FRACT. INDEX PER 0.3	DISCONTINUITY DATA DIP wrt. CORE AXIS	DISCONTINUITY DATA TYPE AND SURFACE DESCRIPTION	HYDRAULIC CONDUCTIVITY K, cm/sec	DIAMETRAL POINT LOAD INDEX (MPa)	NOTES WATER LEVELS INSTRUMENTATION
		--- CONTINUED FROM PREVIOUS PAGE ---															OW 03-28 (C) (B,A)
20	AIR PERCUSSION 89mm Top Hammer Rotary Percussion	Bedrock Surface Amabel Formation															
22																	Screen (A)
24				251.08													
		Inferred Thorold Formation Contact		24.38													
26				248.94													Sand
		Inferred Grimsby Formation Conatact		26.52													
				248.16													Caved Material
28		END OF BOREHOLE Notes: 1. Rotary Percussion Borehole drilled and logged by Nelson 2. Monitoring well installation constructed by Golder		27.30													A and B wells constructed with 1" dia. Schedule 40 PVC flush threaded pipe and No. 10 slot screen, C well constructed with 2" dia. Schedule 40 PVC flush threaded pipe and No. 10 slot screen Note: Water levels taken on July 25, 2003.
30																	
32																	
34																	
36																	
38																	
40																	

DEPTH SCALE
1 : 100

Golder Associates

LOGGED: W.M.
CHECKED:

MISS_ROCK 0211238AARCK.GPJ GAL-CANADA.GDT 8/10/04 MK

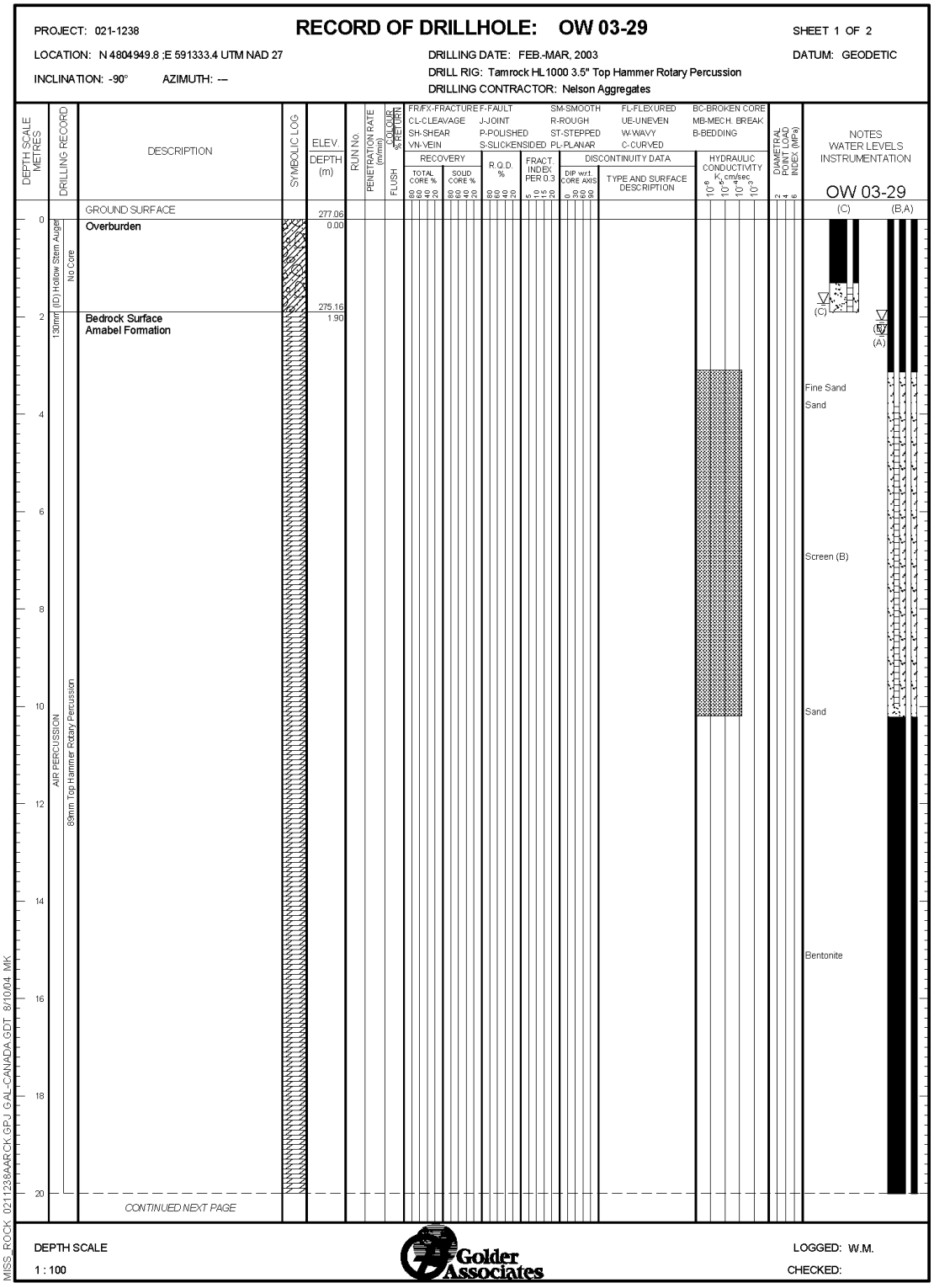
RECORD OF DRILLHOLE: OW 03-29
PROJECT: 021-1238
LOCATION: N 4804949.8 ;E 591333.4 UTM NAD 27
INCLINATION: -90° AZIMUTH: ---
DRILLING DATE: FEB.-MAR, 2003
DRILL RIG: Tamrock HL1000 3.5" Top Hammer Rotary Percussion
DRILLING CONTRACTOR: Nelson Aggregates
SHEET 1 OF 2
DATUM: GEODETIC
DEPTH SCALE METRES
DRILLING RECORD
DESCRIPTION
SYMBOLIC LOG
ELEV. DEPTH (m)
RUN No.
PENETRATION RATE (mm/min)
FLUSH
COLOUR % RETURN
RECOVERY
TOTAL CORE %
SOLID CORE %
R.Q.D. %
FRACT. INDEX PER 0.3
DISCONTINUITY DATA
DIP wrt. CORE AXIS
TYPE AND SURFACE DESCRIPTION
HYDRAULIC CONDUCTIVITY K, cm/sec
DIAMETRAL POINT LOAD INDEX (MPa)
NOTES WATER LEVELS INSTRUMENTATION
OW 03-29
GROUND SURFACE
277.06
Overburden
0.00
275.16
Bedrock Surface
Amabel Formation
1.90
130mm (ID) Hollow Stem Auger
No Core
AIR PERCUSSION
89mm Top Hammer Rotary Percussion
Fine Sand
Sand
Screen (B)
Sand
Bentonite
CONTINUED NEXT PAGE
DEPTH SCALE
1 : 100
Golder Associates
LOGGED: W.M.
CHECKED:

PROJECT: 021-1238

RECORD OF DRILLHOLE: OW 03-29

SHEET 2 OF 2

LOCATION: N 4804949.8 ;E 591333.4 UTM NAD 27

DRILLING DATE: FEB.-MAR, 2003

DATUM: GEODETIC

INCLINATION: -90° AZIMUTH: ---

DRILL RIG: Tamrock HL1000 3.5" Top Hammer Rotary Percussion

DRILLING CONTRACTOR: Nelson Aggregates

FR/FX-FRACTURE F-FAULT SM-SMOOTH FL-FLEXURED BC-BROKEN CORE
CL-CLEAVAGE J-JOINT R-ROUGH UE-UNEVEN MB-MECH. BREAK
SH-SHEAR P-POLISHED ST-STEPPED W-WAVY B-BEDDING
VN-VEIN S-SLICKENSIDED PL-PLANAR C-CURVED

DEPTH SCALE METRES	DRILLING RECORD	DESCRIPTION	SYMBOLIC LOG	ELEV. DEPTH (m)	RUN No.	PENETRATION RATE (mm/min)	FLUSH % RETURN	RECOVERY TOTAL CORE %	RECOVERY SOLID CORE %	R.Q.D. %	FRACT. INDEX PER 0.3	DISCONTINUITY DATA DIP wrt. CORE AXIS	DISCONTINUITY DATA TYPE AND SURFACE DESCRIPTION	HYDRAULIC CONDUCTIVITY K, cm/sec	DIAMETRAL POINT LOAD INDEX (MPa)	NOTES WATER LEVELS INSTRUMENTATION
		--- CONTINUED FROM PREVIOUS PAGE ---														OW 03-29 (C) (B,A)
20	AIR PERCUSSION 89mm Top Hammer Rotary Percussion	Bedrock Surface Amabel Formation														Bentonite
22																Fine Sand
24																Sand
26				250.85												Screen (A)
		Inferred Thorold Formation Contact		26.21												
28				248.41												Sand
		END OF BOREHOLE		28.65												Caved Material A and B wells constructed with 1" dia. Schedule 40 PVC flush threaded pipe and No. 10 slot screen, C well constructed with 2" dia. Schedule 40 PVC flush threaded pipe and No. 10 slot screen
30		Notes: 1. Rotary Percussion Borehole drilled and logged by Nelson 2. Monitoring well installation constructed by Golder														Note: Water levels taken on July 25, 2003.
32																
34																
36																
38																
40																

MISS_ROCK 0211238AARCK.GPJ GAL-CANADA.GDT 8/10/04 MK

DEPTH SCALE
1 : 100

Golder Associates

LOGGED: W.M.
CHECKED:

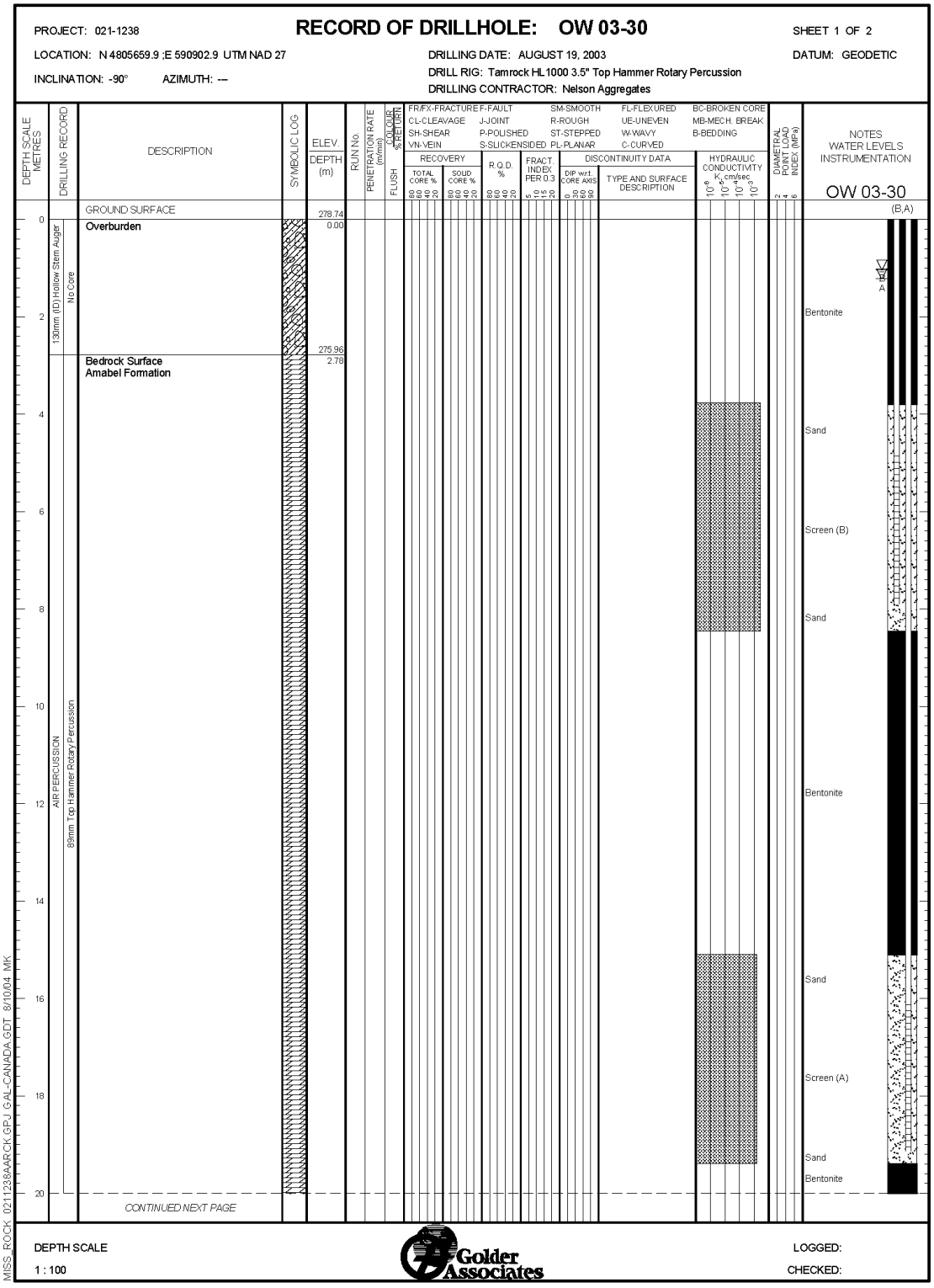
PROJECT: 021-1238
RECORD OF DRILLHOLE: OW 03-30
SHEET 1 OF 2
LOCATION: N 4805659.9 ;E 590902.9 UTM NAD 27
DRILLING DATE: AUGUST 19, 2003
DATUM: GEODETIC
INCLINATION: -90° AZIMUTH: ---
DRILL RIG: Tamrock HL1000 3.5" Top Hammer Rotary Percussion
DRILLING CONTRACTOR: Nelson Aggregates
DEPTH SCALE METRES
DRILLING RECORD
DESCRIPTION
SYMBOLIC LOG
ELEV. DEPTH (m)
RUN No.
PENETRATION RATE (mm/min)
FLUSH
COLOUR % RETURN
RECOVERY
TOTAL CORE %
SOLID CORE %
R.Q.D. %
FRACT. INDEX PER 0.3
DISCONTINUITY DATA
DIP wrt. CORE AXIS
TYPE AND SURFACE DESCRIPTION
HYDRAULIC CONDUCTIVITY K, cm/sec
DIAMETRAL POINT LOAD INDEX (MPa)
NOTES WATER LEVELS INSTRUMENTATION
OW 03-30
GROUND SURFACE
278.74
Overburden
0.00
275.96
Bedrock Surface
Amabel Formation
2.78
130mm (ID) Hollow Stem Auger
No Core
AIR PERCUSSION
89mm Top Hammer Rotary Percussion
Bentonite
Sand
Screen (B)
Sand
Bentonite
Sand
Screen (A)
Sand
Bentonite
CONTINUED NEXT PAGE
DEPTH SCALE
1 : 100
LOGGED:
CHECKED:
Golder Associates

PROJECT: 021-1238

RECORD OF DRILLHOLE: OW 03-30

SHEET 2 OF 2

LOCATION: N 4805659.9 ;E 590902.9 UTM NAD 27

DRILLING DATE: AUGUST 19, 2003

DATUM: GEODETIC

INCLINATION: -90° AZIMUTH: ---

DRILL RIG: Tamrock HL1000 3.5" Top Hammer Rotary Percussion

DRILLING CONTRACTOR: Nelson Aggregates

DEPTH SCALE METRES	DRILLING RECORD	DESCRIPTION	SYMBOLIC LOG	ELEV. DEPTH (m)	RUN No.	PENETRATION RATE (mm/min)	FLUSH / % RETURN	RECOVERY: TOTAL CORE %	RECOVERY: SOLID CORE %	R.Q.D. %	FRACT. INDEX PER 0.3	DISCONTINUITY DATA: DIP wrt. CORE AXIS	DISCONTINUITY DATA: TYPE AND SURFACE DESCRIPTION	HYDRAULIC CONDUCTIVITY K, cm/sec	DIAMETRAL POINT LOAD INDEX (MPa)	NOTES WATER LEVELS INSTRUMENTATION
		--- CONTINUED FROM PREVIOUS PAGE ---														OW 03-30
20	AIR PERCUSSION 89mm Top Hammer Rotary Percussion	Bedrock Surface Amabel Formation														(B,A)
22																Bentonite
24				254.41												
		END OF BOREHOLE		24.33												Wells constructed with 1" dia. Schedule 40 PVC flush threaded pipe and No. 10 slot screen
26		Note 1) Rotary Percussion Borehole drilled and logged by Nelson Note 2) Monitoring well installation constructed by Golder														Note: Water levels taken on April 27, 2004.
28																
30																
32																
34																
36																
38																
40																

FR/FX-FRACTURE CL-CLEAVAGE SH-SHEAR VN-VEIN

F-FAULT J-JOINT P-POLISHED S-SLICKENSIDED

SM-SMOOTH R-ROUGH ST-STEPPED PL-PLANAR

FL-FLEXURED UE-UNEVEN W-WAVY C-CURVED

BC-BROKEN CORE MB-MECH. BREAK B-BEDDING

DEPTH SCALE 1 : 100

LOGGED:

CHECKED:

Golder Associates

MISS_ROCK 0211238AARCK.GPJ GAL-CANADA.GDT 8/10/04 MK

AZIMUTH ENVIRONMENTAL CONSULTING, INC.
Environmental Assessments & Approvals

Project: Sideways Quarry	**Project Number:** 18-223	**Client:** Nelson Aggregates	**Borehole ID:** BS01
Project Location: Burlington Springs Golf Club, Burlington, ON		**Drilling Contractor:** Lantech Drilling Services	**Drilling Method:** HQ Coring
Logged By: Colin Ross *(geophysical imagery)*	**Date:** Drilled June 2016 Instrumented Jan. 23/19	**Stickup (m):** 0.95	**Borehole Depth (mbgs):** 24.37
UTM: (NAD 83, Zone 17T)	**Ground Elevation (masl):** 268.3	**Water Level (mbgs):** 9.37 (Nov. 12/18) (open hole)	**Borehole Diameter (mm)** 96
Easting: 588765	**Well Screen Type:**	**Riser Pipe Type:**	**Monitoring Well Diameter (mm)**
Northing: 4805342	10-Slot PVC, schedule 40	schedule 40 PVC	25

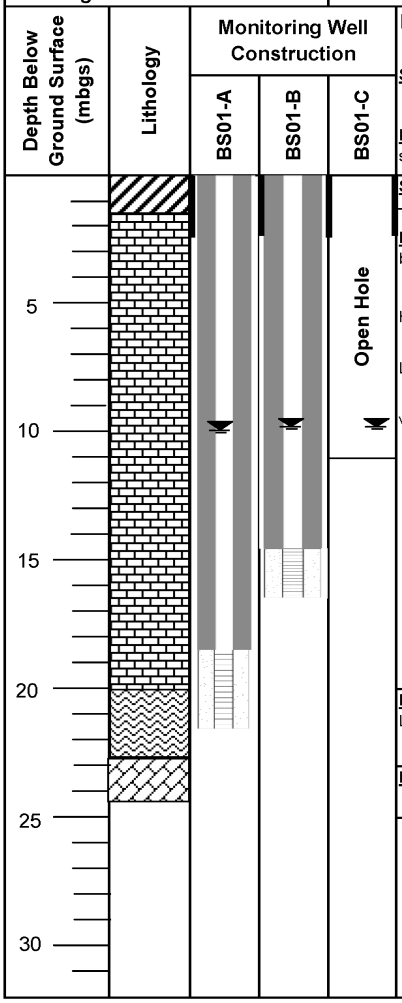

Lithology Description

Soil Group Name: grain size,color, density/consistency, moisture, stratification, other descriptors

Rock Description: modifier, color, hardness/degree of concentration, bedding and joint characteristics, solutions, void conditions.

Silty Clay Till: Brown silty clay with stones, compact, dry to moist, poorly sorted

Bedrock (Amabel Formation): Light brown to grey with depth dolostone, medium to thickly bedded with vuggy with stylolites and fractures throughout.

Heavily fractured at 3.5m and 17.5m

Larger fractures at7.8m, 8.7m and 11.7m

vertical / angular fractures of approximately 1.2m length noted at 4.0m and 5.8m

Bedrock (Reynales): Grey fine grained dolostone with thin laminar bedding planes throughout. Larger fractures noted at 20.3m, 20.6m, 20.75m, 21.2m, 22m, 22.3m and lower contact

Bedrock (Thorold Formation): Greenish grey siltstone, thinly bedded.

Ground Water Level Upon Well Completion (mbgs)
Seal (grout / hole plug)
Silica Sand Pack
Well Screen
Well Casing

AZIMUTH ENVIRONMENTAL CONSULTING, INC.
Environmental Assessments & Approvals

Project: Sideways Quarry	**Project Number:** 18-223	**Client:** Nelson Aggregates	**Borehole ID:** BS02
Project Location: Burlington Springs Golf Club, Burlington, ON		**Drilling Contractor:** Lantech Drilling Services	**Drilling Method:** HQ Coring
Logged By: Colin Ross *(geophysical imagery)*	**Date:** Drilled June 2016 Instrumented Jan. 23/19	**Stickup (m):** 0.72	**Borehole Depth (mbgs):** 27.3
UTM: (NAD 83, Zone 17T)	**Ground Elevation (masl):** 272	**Water Level (mbgs):** 4.58 (Nov. 12/18) (open hole)	**Borehole Diameter (mm)** 96
Easting: 589421	**Well Screen Type:** 10-Slot PVC, schedule 40	**Riser Pipe Type:** schedule 40 PVC	**Monitoring Well Diameter (mm)** 25
Northing: 4804939			

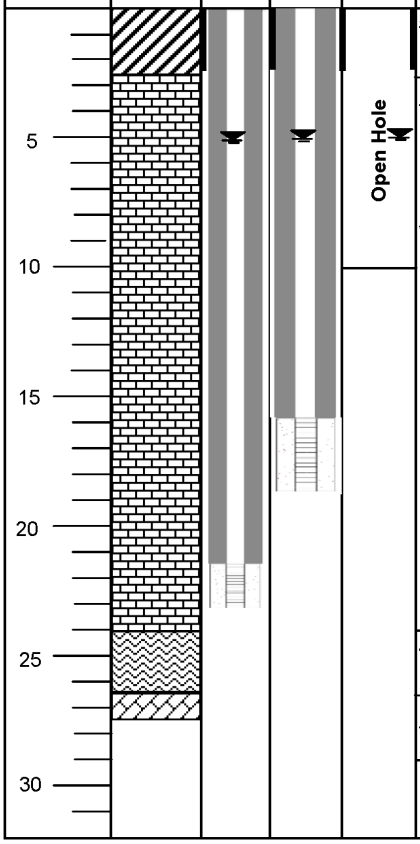

Lithology Description

Soil Group Name: grain size,color, density/consistency, moisture, stratification, other descriptors

Rock Description: modifier, color, hardness/degree of concentration, bedding and joint characteristics, solutions, void conditions.

Silty Clay Till: Brown silty clay with stones, compact, dry to moist, poorly sorted

Bedrock (Amabel Formation): Light brown to grey with depth dolostone, medium to thickly bedded with vuggy with stylolites and fractures throughout.

Larger fractures at 4.1m, 4.9m, 7.6m, 13.9m and 14.7m

vertical / angular fractures of approximately 1.2m length noted between 15.3 and 17.8m

Bedrock (Reynales): Grey fine grained dolostone with thin laminar bedding planes throughout. Larger fractures noted at upper contact, 24.9m, 25.7m, 26.5m and lower contact

Bedrock (Thorold Formation): Greenish grey siltstone, thinly bedded.

Ground Water Level Upon Well Completion (mbgs)
Seal (grout / hole plug)
Silica Sand Pack
Well Screen
Well Casing

Page 1 of 1

AZIMUTH ENVIRONMENTAL CONSULTING, INC.
Environmental Assessments & Approvals

Project: Sideways Quarry	**Project Number:** 18-223	**Client:** Nelson Aggregates	**Borehole ID:** BS03
Project Location: Burlington Springs Golf Club, Burlington, ON		**Drilling Contractor:** Lantech Drilling Services	**Drilling Method:** HQ Coring
Logged By: Colin Ross *(geophysical imagery)*	**Date:** Drilled June 2016 Instrumented Aug. 14/19	**Stickup (m):** 0.68	**Borehole Depth (mbgs):** 24.4
UTM: (NAD 83, Zone 17T)	**Ground Elevation (masl):** 271.3	**Water Level (mbgs):** 6.11 (Nov. 12/18) (open hole)	**Borehole Diameter (mm)** 96
Easting: 589366	**Well Screen Type:** 10-Slot PVC, schedule 40	**Riser Pipe Type:** schedule 40 PVC	**Monitoring Well Diameter (mm)** 25
Northing: 4805299			

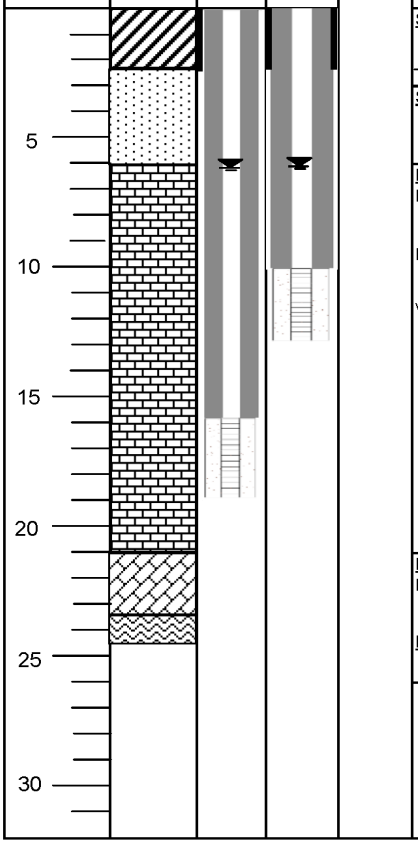

Lithology Description

Soil Group Name: grain size,color, density/consistency, moisture, stratification, other descriptors

Rock Description: modifier, color, hardness/degree of concentration, bedding and joint characteristics, solutions, void conditions.

Silty Clay Till: Brown silty clay with stones, compact, dry to moist, poorly sorted

Sand & Gravel: Brown sand and gravel

Bedrock (Amabel Formation): Light brown to grey with depth dolostone, medium to thickly bedded with vuggy with stylolites and fractures throughout.

Larger fractures at 7.4m, 8.9m, 9.4m, 10.3m 10.7m, 12m, 13.8m, 15.2m, 17.2m and 19.4m

vertical / angular fractures of approximately 0.5m length noted between 10.7m and 12.0m

Bedrock (Reynales): Grey fine grained dolostone with thin laminar bedding planes throughout. Larger fractures noted at upper contact, 21.3m, 21.5m and lower contact

Bedrock (Thorold Formation): Greenish grey siltstone, thinly bedded.

Ground Water Level Upon Well Completion (mbgs)
Seal (grout / hole plug)
Silica Sand Pack
Well Screen
Well Casing

Page 1 of 1

AZIMUTH ENVIRONMENTAL CONSULTING, INC.
Environmental Assessments & Approvals

Project: Sideways Quarry	**Project Number:** 18-223	**Client:** Nelson Aggregates	**Borehole ID:** BS04
Project Location: Burlington Springs Golf Club, Burlington, ON		**Drilling Contractor:** Keith Lang Well Drilling	**Drilling Method:** Rotary Prescussion
Logged By: Colin Ross *(geophysical imagery)*	**Date:** Drilled May 27/19 Instrumented Aug. 14/19	**Stickup (m):** 0.56	**Borehole Depth (mbgs):** 24.6
UTM: (NAD 83, Zone 17T)	**Ground Elevation (masl):**	**Water Level (mbgs):** 3.35 (May 28/19) (open hole)	**Borehole Diameter (mm)** 152
Easting: 589775	**Well Screen Type:** 10-Slot PVC, schedule 40	**Riser Pipe Type:** schedule 40 PVC	**Monitoring Well Diameter (mm)** 32
Northing: 4804851			

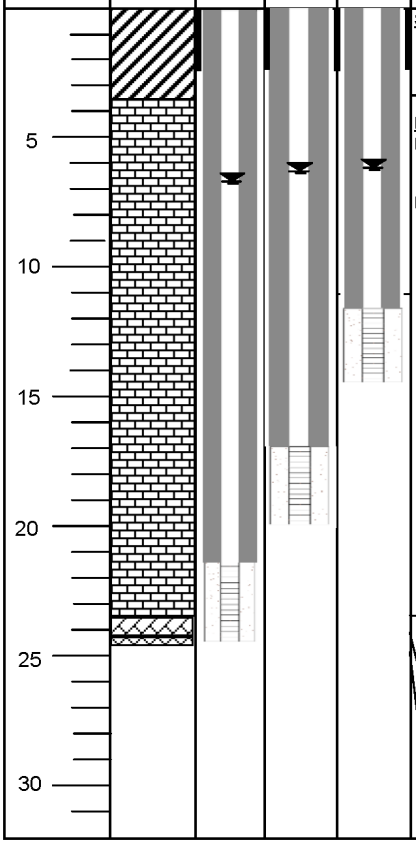

Lithology Description

Soil Group Name: grain size,color, density/consistency, moisture, stratification, other descriptors

Rock Description: modifier, color, hardness/degree of concentration, bedding and joint characteristics, solutions, void conditions.

Silty Clay Till: Brown silty clay with stones, compact, dry to moist, poorly sorted

Bedrock (Amabel Formation): Light brown to grey with depth dolostone, medium to thickly bedded with vuggy with stylolites and fractures throughout.

Larger fractures at 8.7m, 15.6m, 20.6m, 21.2m 23m and 23.4

Bedrock (Reynales): Grey fine grained dolostone with thin laminar bedding planes throughout.

Larger fractures noted at upper contact, 23.9m and lower contact

Bedrock (Thorold Formation): Greenish grey siltstone, thinly bedded.

Ground Water Level Upon Well Completion (mbgs)
Seal (grout / hole plug)
Silica Sand Pack
Well Screen
Well Casing

Page 1 of 1

AZIMUTH ENVIRONMENTAL CONSULTING, INC.
Environmental Assessments & Approvals

Project: Sideways Quarry	**Project Number:** 18-223	**Client:** Nelson Aggregates	**Borehole ID:** BS05
Project Location: Burlington Springs Golf Club, Burlington, ON		**Drilling Contractor:** Keith Lang Well Drilling	**Drilling Method:** Rotary Prescussion
Logged By: Colin Ross *(geophysical imagery)*	**Date:** Drilled May 28/19 Instrumented Aug. 14/19	**Stickup (m):** 0.52	**Borehole Depth (mbgs):** 24.6
UTM: (NAD 83, Zone 17T)	**Ground Elevation (masl):**	**Water Level (mbgs):** 3.96 (May 28/19) (open hole)	**Borehole Diameter (mm)** 152
Easting: 589019	**Well Screen Type:**	**Riser Pipe Type:**	**Monitoring Well Diameter (mm)**
Northing: 4805464	10-Slot PVC, schedule 40	schedule 40 PVC	32

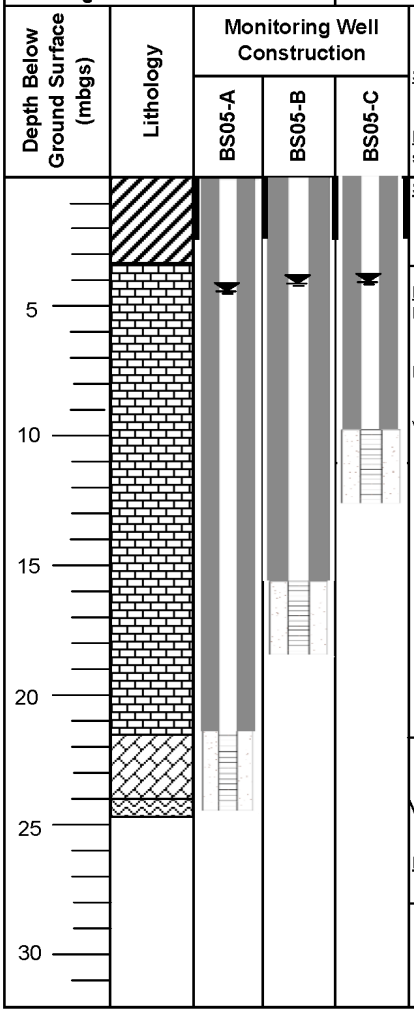

Lithology Description

Soil Group Name: grain size,color, density/consistency, moisture, stratification, other descriptors

Rock Description: modifier, color, hardness/degree of concentration, bedding and joint characteristics, solutions, void conditions.

Silty Clay Till: Brown silty clay with stones, compact, dry to moist, poorly sorted

Bedrock (Amabel Formation): Light brown to grey with depth dolostone, medium to thickly bedded with vuggy with stylolites and fractures throughout.

Larger fractures at 6.2m, 16.3m, 18.3m and 20.1m

vertical / angular fractures of approximately 0.5m length noted between 11.5m and 12.1m

Bedrock (Reynales): Grey fine grained dolostone with thin laminar bedding planes throughout.
Larger fractures noted at upper contact, 21.7m, 23.6m and lower contact
vertical / angular fractures of approximately 0.8m length noted between 22.0m and 22.8m

Bedrock (Thorold Formation): Greenish grey siltstone, thinly bedded.

Ground Water Level Upon Well Completion (mbgs)
Seal (grout / hole plug)
Silica Sand Pack
Well Screen
Well Casing

Page 1 of 1

AZIMUTH ENVIRONMENTAL CONSULTING, INC.
Environmental Assessments & Approvals

Project: Sideways Quarry	**Project Number:** 18-223	**Client:** Nelson Aggregates	**Borehole ID:** BH-18-2 / MW-18-2
Project Location: Burlington, ON		**Drilling Contractor:** Orbit Garant	**Drilling Method:** HS Auger / SS
Logged By: B. Pettersone	**Drilling Start Date:** 26-Nov-2018	**Stickup (m):** 0.75	**Well Depth (m bgs):** 3.45
UTM: (NAD 83, Zone 17T)	**Ground Elevation (masl):** 281.1	**Water Level (m bgs):** 2.51	**Well Diameter (mm)** 51
Easting: 591429	**Well Screen Type:** 10-Slot PVC, schedule 40	**Riser Pipe Type:** schedule 40 PVC	**Well Screen Length (m):** 1.5
Northing: 4805258			

Depth Below Ground Surface (mbgs)	Sample Type	Sample Number	RKI (ppm)	Lithology	Monitoring Well Construction	Lithology Description
						Soil Group Name: grain size,color, density/consistency, moisture, stratification, other descriptors **Rock Description:** modifier, color, hardness/degree of concentration, bedding and joint characteristics, solutions, void conditions.
						Topsoil: Brown, silty topsoil with some organics, wet and compact (0.0-0.15 m)
1	GS	1				**Silt / Sandy Silt:** Reddish brown, dry, silt with some sand and gravel (ML Type), mottled, dense. Greater sand and gravel content within the finer textured soil matrix with depth. Borehole not saturated at time of drilling.
2	GS	2				Sand seam @ 1.8m bgs;
3						END BH @ 5.0 m
4						
5	GS	3				
6						

Ground Water Level Upon Well Completion (mbgs)

Seal (grout / hole plug) | Silica Sand Pack | Well Screen | Well Riser

Page 1 of 1

AZIMUTH ENVIRONMENTAL CONSULTING, INC.
Environmental Assessments & Approvals

Project: Sideways Quarry	**Project Number:** 18-223	**Client:** Nelson Aggregates	**Borehole ID:** BH-18-1 / MW-18-1
Project Location: Burlington, ON		**Drilling Contractor:** Orbit Garant	**Drilling Method:** HS Auger / SS
Logged By: B. Pettersone	**Drilling Start Date:** 26-Nov-2018	**Stickup (m):** 0.8	**Well Depth (m bgs):** 6.04
UTM: (NAD 83, Zone 17T)	**Ground Elevation (masl):** 284.6	**Water Level (m bgs):** Dry	**Well Diameter (mm)** 51
Easting: 591472	**Well Screen Type:** 10-Slot PVC, schedule 40	**Riser Pipe Type:** schedule 40 PVC	**Well Screen Length (m):** 3
Northing: 4805360			

Depth Below Ground Surface (mbgs)	Sample Type	Sample Number	RKI (ppm)	Lithology	Monitoring Well Construction	Lithology Description
						Soil Group Name: grain size,color, density/consistency, moisture, stratification, other descriptors **Rock Description:** modifier, color, hardness/degree of concentration, bedding and joint characteristics, solutions, void conditions.
						Sand Fill: Saturated with preciptation, compact, brown sand and gravel fill (SP type) (0.0-0.05 m)
						Topsoil: Brown, silty buried topsoil with some organics, wet and compact (0.05-0.15 m)
1	GS	1				**Till - Silt / Sandy Silt:** Reddish brown, dry, silt with some sand and gravel (ML Type), mottled, dense. Greater sand and gravel content within the finer textured soil matrix with depth. Borehole not saturated at time of drilling.
2	GS	2				Silt lens and moist @ 2.8 m bgs;
3						END BH @ 6.0 m
4						
5	GS	3				
6						

Ground Water Level Upon Well Completion (mbgs)

Seal (grout / hole plug) | Silica Sand Pack | Well Screen | Well Riser

Page 1 of 1

15.2 Hydraulic Testing Program

15.2.1 Downhole Packer Testing

Unlike equivalent porous media (sand and gravel aquifers), determining the hydraulic characteristics of a fractured bedrock aquifer requires a hydraulic testing program designed to isolate and test discrete zones over the entire depth of the borehole as open fractures may intersect a borehole at any depth. For the purpose of this investigation, the hydraulic testing program was developed from the preliminary conceptual model of the fracture network and ground water flow system. The hydraulic testing program involved slug injection testing techniques (water) using both a single and double-packer system (i.e. packer testing). Packer tests are preferred over the conventional "pumping tests" as the vertical distribution of transmissivity can be determined by systematically testing the length of the borehole in sections. Whereas pumping tests require pumping from an open hole which draws water from all water bearing zones.

Shapiro and Hsieh (1998) determined that interpreting slug tests in fractured rock by using a homogeneous model of formation properties may be adequate in providing order of magnitude estimates of transmissivity in the vicinity of the borehole in most fractured rock terrains. However, caution should be used in applying the estimates of transmissivity from slug tests, because the slug tests stress only a small volume of the formation and thus cannot be used to interpret formation heterogeneity or large-scale formation properties.

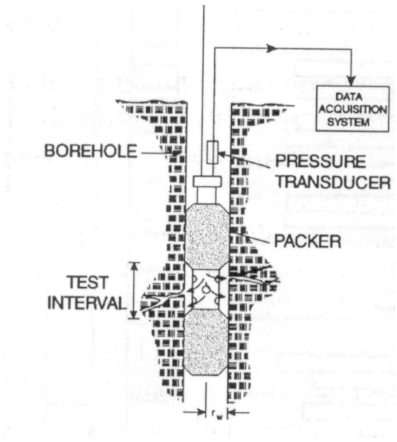

Packer testing consists of lowering inflatable rubber glands separated a fixed distance down a borehole to test a selected zone. The rubber glands are inflated with compressed nitrogen, which seals the glands against the borehole wall thus isolating the zone between the packer glands from the remainder of the borehole. The packed off interval and the wellbore annulus was instrumented so that the fluid pressure in each zone could be monitored at land surface by directly measuring a water level open to the atmosphere using a pressure transducer datalogger. Monitoring the packed off zone and the annulus also allowed for the detection of communication around the top packer. In addition, a datalogger was also attached to the base of the lower packer for the purposes of establishing pressure response and potential detection of communication around the bottom packer. Although this logger did not provide real-time data as there was no connection to the surface during testing, it was downloaded at the end of the testing sequence to assess the data collected. These dataloggers were programmed to take fluid pressure readings every second.

Once the packers were inflated, the isolated zone was then slug tested to determine the permeability of the test interval and if possible, the static hydraulic head for the zone. The test involved pouring a known volume of water into the isolated zone. By measuring the interval response of back to an equilibrium condition, the transmissivity of the zone was calculated using Hvorslev (1951). As noted by Lapcevic *et al.* (1999) slug tests conducted in fracture rock frequently exhibits results, which deviate from the ideal Cooper *et al.*, (1967) response. The deviation was a result of the limitations of the numerical software that could not account for a storativity value less than 1×10^{-20}. In general, the Hvorslev (1951) method was consistently used to obtain an estimate of hydraulic conductivity. It is noted that the Hvorslev (1951) method compared favourably with other analytical techniques evaluated.

The separation between the two rubber packers was set to be 1.1 m. This choice of test zone length was selected based on the expected fracture spacing with depth derived through review of the previously completed packer testing on the Southern Lands. Too short of an interval would have led to an unnecessarily large number of tests, while an overly long interval would not have captured the variability in transmissivity of the discrete fractures. To ensure full coverage of the borehole the packer system was only raised 0.9 m before another test event was conducted, thus there was a 0.2 m overlap. The packer testing completely covered the entire length of the borehole due to the use of the overlap strategy in the testing program. Given the bottom 1.0 to1.5 m of the borehole would have been isolated from the internal packed interval, the use of the datalogger instrumented below the bottom packer provided data that was utilized to calculate the hydraulic properties of the basal borehole fractures. This was completed by analyzing the inflation pressure response below the packer system. As this basal zone was isolated from the atmosphere upon inflation of the packer system, the pressure response during inflation either over-pressured this zone (in the event there was no permeable fracture to facilitate the displacement of water resulting from “squeeze” of the inflating packer bladder), or a measured displacement response was observed. In instances where the latter was observed, the displacement response was analyzed like that of the transient slug tests completed within the packed intervals.

In addition to the packer testing, similar slug testing was completed at monitoring wells in these boreholes following monitoring well instrumentation, as well as at select monitoring well locations on the Southern Lands. The Southern Lands locations were to confirm previously completed slug testing in some of the Golder Wells, and two new overburden monitoring wells located at the southeastern corner of the property (MW18-1 & MW18-2), as well as five drive point monitoring wells installed within the Southern Lands wetlands as part of the current surface water monitoring program completed by Tatham Engineering. These tests were all completed by creating displacement by either removal or addition of a water “slug”. Addition of a slug was completed by adding a known volume of water, while removal was completed by purging a known volume. Water level recovery was monitored through pressure transducers set to a one second interval.

The packer testing results are provided on the borehole records (Section 11.1). A summary discussion of the results is provided below.

15.2.1.1 BS-01 Packer Test Interpretation

Based on the detailed review of the packer testing results at BS-01, it is generally concluded that the most conductive zone in the rock profile likely exists at depth (243.6 to 243.8 masl). A single packer test was not conducted for the bottom hole condition, but the monitoring below the bottom packer indicates that no squeeze was seen during the deepest double packer test. There was only 0.2 m of space below this bottom packer, indicating a very transmissive zone that responded faster than the packer inflation (i.e., at least $>10^{-3}$ m^2/s based on response from other testing). The static water level below the bottom packer did not changed as the equipment moved up the hole suggesting that the deep fracture controlled the open hole water level. This depth is below the proposed floor of the quarry at ~252 masl.

It was also noted that two other transmissive zones were measured at 249.2 to 251.0 masl having an estimated transmissivity of $2x10^{-3}$ m^2/s and $3x10^{-3}$ m^2, respectively. This interval represents 69% of the total profile response. The other zone occurred at 252.8 to 253.7 masl having an estimated transmissivity of $1x10^{-3}$ m^2/s which represents 19% of the total profile response. Four other zones had an interval transmissivity about an order of magnitude lower than the two zones noted above and essentially represent the remaining 12% of the total profile response.

15.2.1.2 BS-02 Packer Test Interpretation

Based on the detailed review of the packer testing results at BS-02, it is generally concluded that this borehole illustrates a more conductive profile. The borehole transmissivity is roughly twice that seen elsewhere. However, most tested intervals are more conductive than 10^{-5} m^2/s. it is speculated that the borehole proximity to the Medad Valley might account for this situation being the stress relief propagating laterally into this area.

This borehole was drilled deeper into the subsurface and as a result the bottom of the borehole is impervious. A conductive zone was located at the same general depth as other boreholes; but it is not as conductive as that seen elsewhere. The most conductive zone in the rock profile is higher in the profile (i.e., 249.6 to 253.2 masl). This conductive zone is a series of four intervals with the middle two intervals being about a half order more permeable than that tested on either flank, (i.e., $8x10^{-4}$ m^2/s, $21x10^{-4}$ m^2/s, $18x10^{-4}$ m^2/s, and $9x10^{-4}$ m^2/s, respectively). Overall, the testing suggests that 60% of total profile transmissivity is evident at this sequence. This conductive zone correlates with the proposed floor of the quarry at 252 masl;

It was also noted that a second transmissive zone was measured at 246.0 to 247.8 masl having an estimated transmissivity of $6x10^{-4}$ m^2/s and $9x10^{-4}$ m^2, respectively. This interval represents 24% of the total profile response.

15.2.1.3 BS-04 Packer Test Interpretation

Based on the detailed review of the packer testing results at BS-04, it is generally concluded that the most conductive zone in the rock profile likely exists at depth (i.e., 247 to 246 masl). The interval testing provided an estimated transmissivity of $2x10^{-5}$ m^2/s located at the bottom of the well. Theoretically, this interval represents 33% of the total borehole response. Two additional flow zones are found at 252 to 253 masl and 253 to 254 masl, which reported a transmissivity of $1x10^{-5}$ m^2/s and $7x10^{-6}$ m^2/s, respectively.

15.2.1.4 BS-05 Packer Test Interpretation

Based on the detailed review of the packer testing results at BS-05, it is generally concluded that the most conductive zone in the rock profile exists at between 24.2 m below ground level (mbgl) and 23.2 mbgl, or between 247.8 m above mean seal level (masl) and 248.8 masl. This zone represents ~84% of the total borehole transmissivity measured over the saturated bedrock profile and is found below the proposed floor of the quarry of 252 masl.

It was also noted that a relatively low permeability zone exists from 250.7 masl to 252.5 masl. This horizon appears to isolate the deeper conductive zone from the next permeable feature detected between 252.5 masl and 254.3 masl. This conductive zone between 252.5 masl and 254.3 masl only represents 4% of the total borehole transmissivity. There were two other zones higher in the borehole profile also each represent 4% of the total borehole transmissivity being 255.2 masl to 256.3 masl; and 259.0 masl to 260.8 masl.

Above 260.8 masl, the borehole transmissivity declines by a half order of magnitude over the next 6 m of saturated rock. There is no conductive fracture plane at or near the water table elevation of 268.5 masl or 3.5 mbgl. Furthermore, the annular testing at top of the saturated borehole profile showed that no conductive zones were evident up to 269 masl or 3 mbgl.

15.2.2 Pumping Test

In order to supplement the hydraulic data collected has part of the packer testing program, a pumping test was completed at a 6-inch well located on the Western Lands (BS-06). This well was constructed along with another proximal 6-inch well (BS-07) in the area of BS-03 such that interference from the pump test could be evaluated both in close proximity, as well as more distantly with the other monitoring wells located on the Western Lands. When BS-06 was constructed in May 2019, the well records indicated a potential well yield of 30 IGPM (135 L/min). As a result, a temporary Permit to Take Water (PTTW) was required and obtained, which would authorize the withdrawal of ground water in excess of 50,000 L/day. In the Temporary PTTW application documentation, a maximum rate of 65 IGPM (300 L/min) was requested. This rate was based on a potentially more elevated yield than what was assessed when the well was drilled.

The temporary PTTW was issued by the MOE to Bestway Springs Golf & Country Club as they are currently the owners of the Western Lands on October 3, 2019 (No. 4818-BGJHZ3). As monitoring is a requirement under Ontario Regulation 387/04, specific monitoring conditions were stipulated. All the monitoring requirements outlined in the PTTW were incorporated into the groundwater and surface water monitoring program discussed in the following sections.

15.2.2.1 Monitoring Program

A. Notification to Well Owners

On October 11, 2019, representatives from Azimuth delivered a letter notifying all properties within 500 m of the pump test location. The notification included the expected date, time, duration of the pumping test, and the contact telephone numbers that may be used to report any interference with water supplies. Letters were distributed by Azimuth staff on October 11, 2019 to 28 properties located along Cedar Springs Road and Cedar Springs Court, west of the pumping test well.

B. Test Well Monitoring

The Test Well (BS-06) was continuously monitored (30 second interval) for water level, temperature, and specific conductance prior to, during and post pumping. In addition, manual water level readings were taken to calibrate the datalogger data. The pumping rates were measured and recorded to ensure that the rate remained relatively constant throughout the duration of the test with the flow rate of 26 IGPM (120 L/min). Some minor adjustments to the flow rate were made throughout the pumping period which resulted in small fluctuations in water levels in the pumping well.

During the pumping test, two water quality samples of the discharge water were collected at 1.5-hour and 72-hour intervals over the course of the 72-hour pump test. These samples were submitted to Caduceon and Testmark Laboratories respectively, with both analyzed for general water quality package, although with slightly differing parameter lists. The purpose of the water quality sampling program was to determine if the quality of the water changed as a result of pumping.

C. Observation Well Monitoring

The existing ground water monitoring network for the Western Lands was utilized for monitoring purposes throughout the pumping test as locations were present northwest, west, southwest and south of the pumping well between the pumping well and neighbouring private wells. As such, the monitoring network was sufficient to delineate potential interference issues beyond the Site boundaries, as well as to determine the influence and radial extent of the pumping. Dataloggers within these monitoring wells were set to a similar 30 second interval and were installed at BS-01A, BS-02A, BS-03A, BS-03B,

BS-04A, BS-04B, BS-04C, BS-05A, BS-05B, BS-07, as well as within a stilling well installed in the adjacent golf course irrigation pond. It is noted that no dataloggers were instrumented in BS-01B, BS-02B or BS-02C as the long term data trends for these locations have been shown to plot similarly to the deep intervals such that these monitoring points were determined to be redundant, while BS-01C was noted to be dry during prior to initiation of the pump test.

In addition to the monitoring well network, the private well located at 5161 Cedar Springs Road as it is included in the long-term monitoring program. The datalogger within this well was set to a similar 30 second interval as the remaining monitoring locations.

15.2.2.2 Pumping Test Interpretation

The pumping test was conducted in BS-06 for a period of 72-hours, which commenced on October 16, 2019 and ran until October 21, 2019. BS-06 was an open wellbore about 25 m in depth. The submersible pump was installed close to the wellbore bottom to facilitate the full drawdown of the well.

The initial water level was measured as 7.88 m below the top of the well casing. This correlated to the transducer pressure of 25.47 m of water head. The pumping rate varied slightly over the testing duration; but the rate was maintained at about 120 L/min (32 USGPM). The rate was varied by the field crew on occasion and accounts for the noticeable shifts in the water level over time. These small changes did not alter the pumping rate significantly enough that a multi-rate evaluated was needed to assess the drawdown curves generated over the testing sequence. The transducer compares favourably to the manual measurements taken during the pumping test.

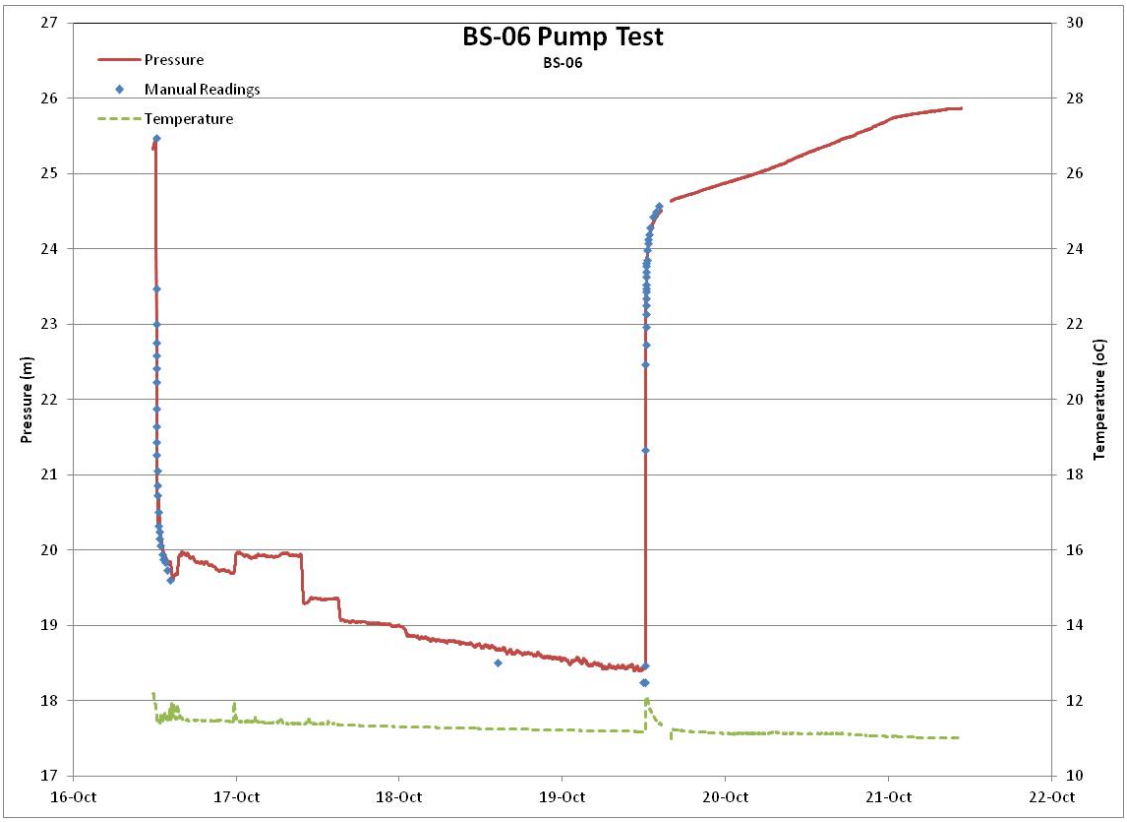

Pressure transducers were placed in BS-01A, BS-02A, BS-04 (three zones), BS-05 (three zones), BS-07, BS-03A, and BS-03B. In addition, the pond adjacent to the pumping well was monitored and the

closest residence being 5161 Cedar Springs Road. These transducers were installed on October 13, 2019 in order to obtain some baseline water level measurements prior to the start of the pumping test.

The data from these monitoring wells is presented for thoroughness. However, no meaningful response was detected at these monitoring well locations except for BS-03 and BS-07. All the monitoring well plots employ a vertical line to denote the start and end of the 72-hour pumping test. The data is plotted using an exaggerated pressure scale of order to detect any evidence of response in the recorded data. The pressure data represents a gauge reading relative to the depth that the transducer was positioned into the water column. The slight variations in the pressure data are attributed to barometric variations. The deep zone was used since the packer testing data indicated it was the most transmissive zone tested.

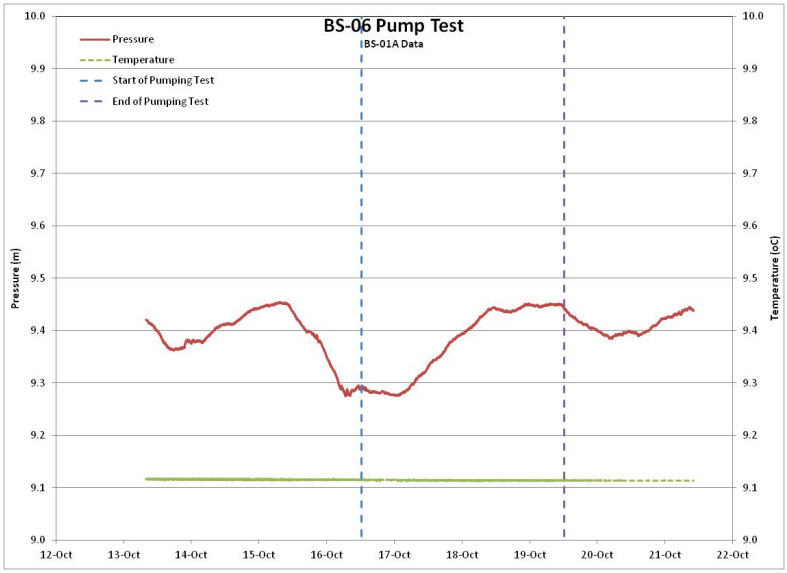

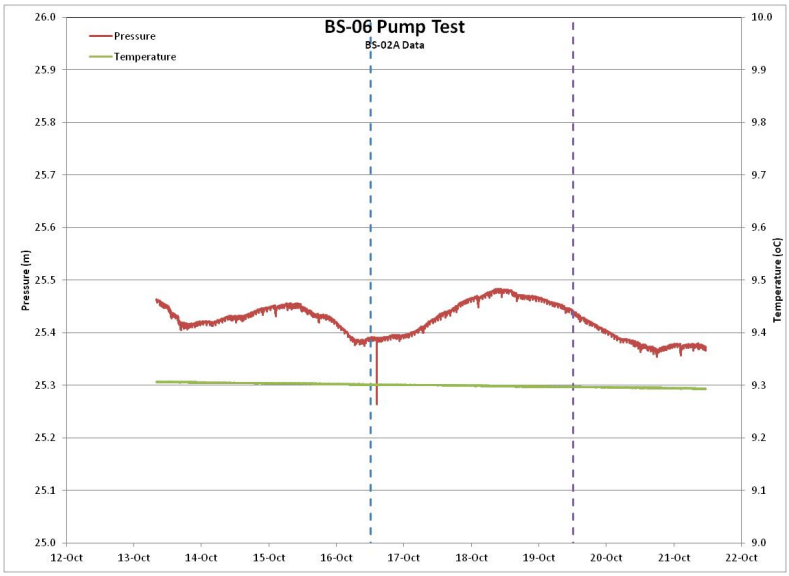

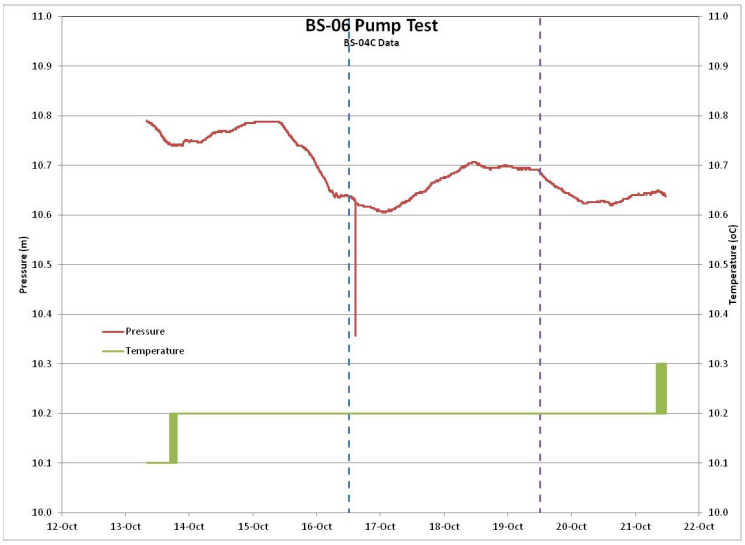
BS-06 Pump Test
BS-04C Data
Pressure (m)
Temperature (oC)
Pressure
Temperature
12-Oct
13-Oct
14-Oct
15-Oct
16-Oct
17-Oct
18-Oct
19-Oct
20-Oct
21-Oct
22-Oct

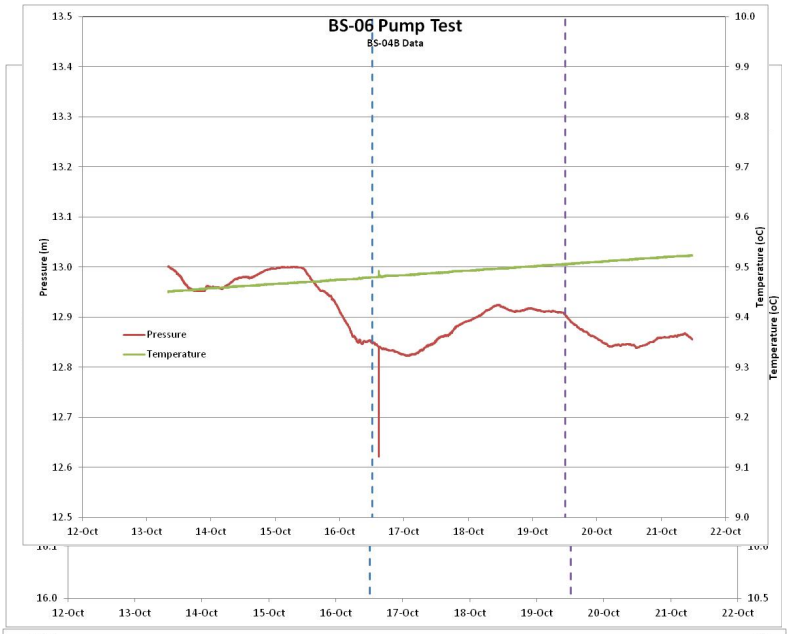
BS-06 Pump Test
BS-04B Data
Pressure (m)
Temperature (oC)
Pressure
Temperature
12-Oct
13-Oct
14-Oct
15-Oct
16-Oct
17-Oct
18-Oct
19-Oct
20-Oct
21-Oct
22-Oct

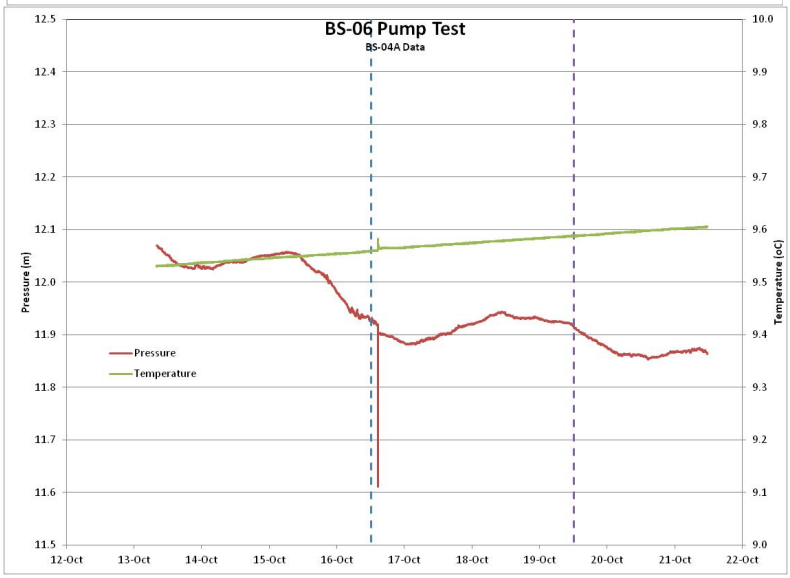
BS-06 Pump Test
BS-04A Data
Pressure (m)
Temperature (oC)
Pressure
Temperature
12-Oct
13-Oct
14-Oct
15-Oct
16-Oct
17-Oct
18-Oct
19-Oct
20-Oct
21-Oct
22-Oct

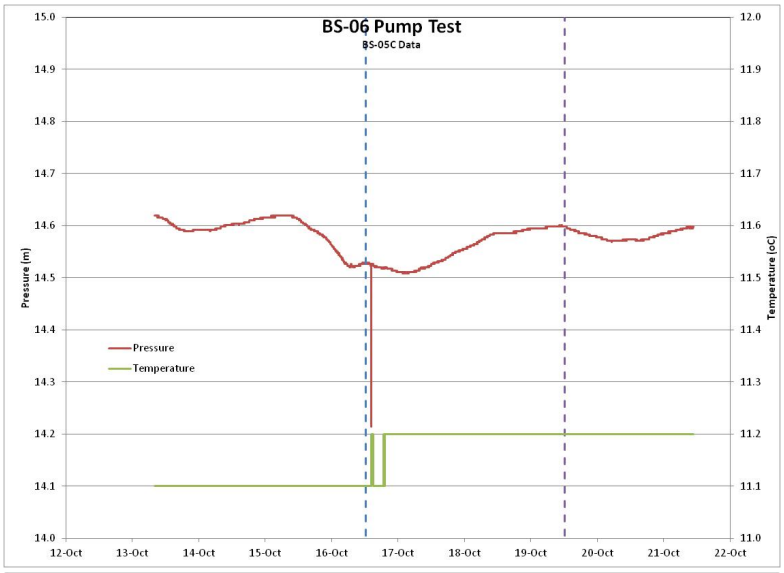
BS-06 Pump Test
BS-05C Data
Pressure (m)
Temperature (oC)
Pressure
Temperature
12-Oct
13-Oct
14-Oct
15-Oct
16-Oct
17-Oct
18-Oct
19-Oct
20-Oct
21-Oct
22-Oct

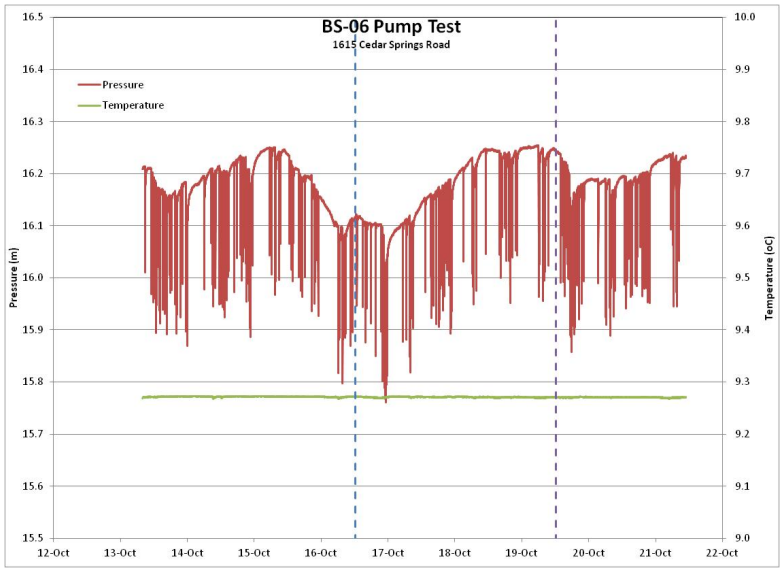
BS-06 Pump Test
1615 Cedar Springs Road
Pressure (m)
Temperature (oC)
Pressure
Temperature
12-Oct
13-Oct
14-Oct
15-Oct
16-Oct
17-Oct
18-Oct
19-Oct
20-Oct
21-Oct
22-Oct

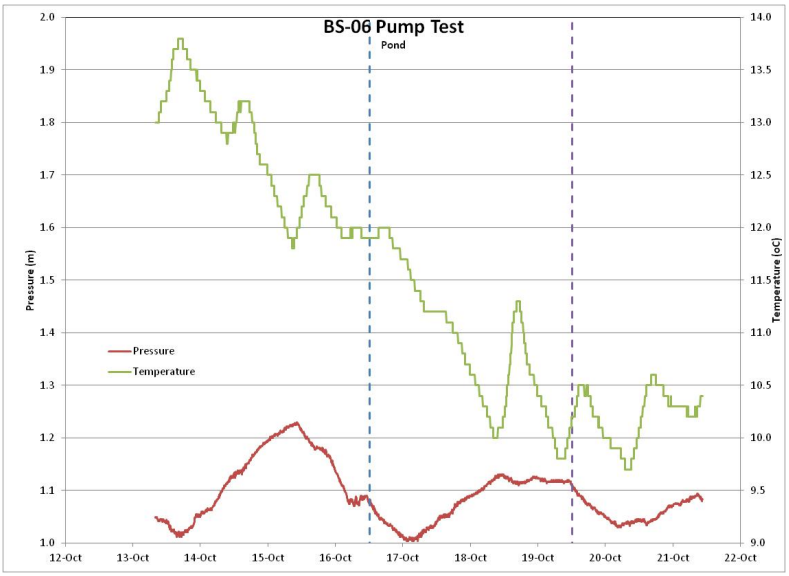
BS-06 Pump Test
Pond
Pressure (m)
Temperature (oC)
Pressure
Temperature
12-Oct
13-Oct
14-Oct
15-Oct
16-Oct
17-Oct
18-Oct
19-Oct
20-Oct
21-Oct
22-Oct

The BS-04A well response shows the same barometric response, although the water level in the monitor is declining over the monitoring period. This accounts for the data trend recorded at this location. The data appears to "jog" at about 2:30 pm on October 16, 2019; but this is attributable to manual water levels being collected at the various monitoring wells. The pressure transducers needed to be removed in order to collect the manual reading. When re-installed subtle shifts in the water level were noted in some locations.

An analogous response was measured at the BS-04B well and will not be discussed further. The same can be stated for the BS-04C well. It is noted that transducers with different resolution scales were used and thus the temperature data for BS-04C reflects this lower resolution threshold. The same can be stated for the BS-05 wells as are presented below and the closest home (i.e., 1615 Cedar Springs Road) as well as the adjacent pond.

The remaining monitoring wells were sufficiently close to the pumping well (i.e., BS-06) such that they were able to detect a response to the pumping sequence. One of the monitoring wells in proximity to BS-06 was instrumented (i.e., BS-03) and the other BS-07 remained as an open borehole. The two monitored intervals for BS-03 as well as that for BS-07are shown below. The pumping response in the BS-03 intervals is essentially analogous to the response recorded in the pumping well (i.e., BS-06), albeit not to the same magnitude given the estimated 7 m separation between these wells.

The data acquisition in the BS-07 open hole began essentially when the pumping test was about to commence and therefore did not record the pre-test sequence as occurred at other monitoring locations. In fact, BS-07 was to originally be used as the pumped well. However, the water level in this well drew down too quickly and therefore the test was abandoned and the pump moved to the BS-06 well which proved to be more conductive than BS-07. The estimated distance between these two wells is 14 m or twice that of the BS-03 well. The original drawdown is detected in BS-07; but is quite muted representing a decline of less than a meter or about an order of magnitude less than that measured at BS-03. The downward trend in the data fails this initial response. In fact, the barometric response would appear to define this well's response following the initial decline which is likely due to the limited influence measured at the well (i.e., competing responses). The BS-07 response to the pumping test recovery is also quite limited.

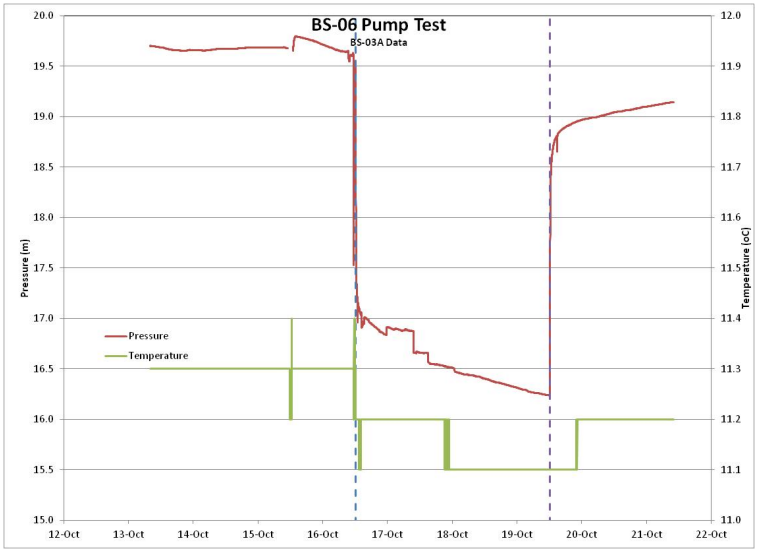

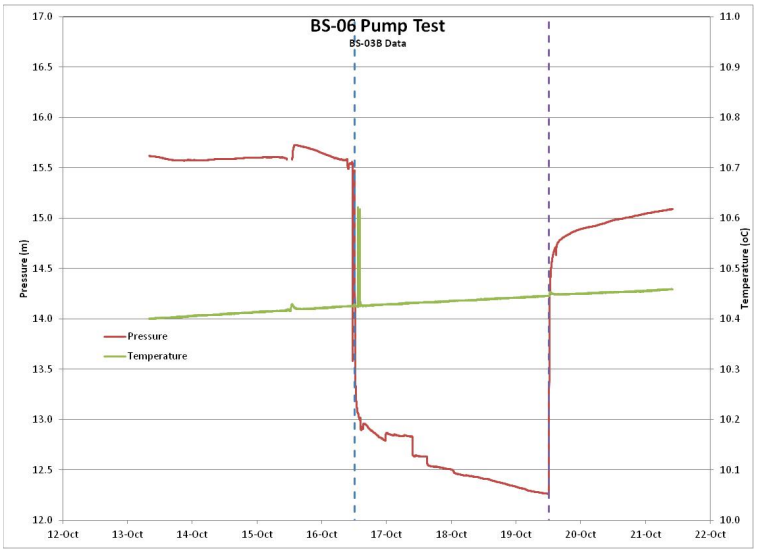

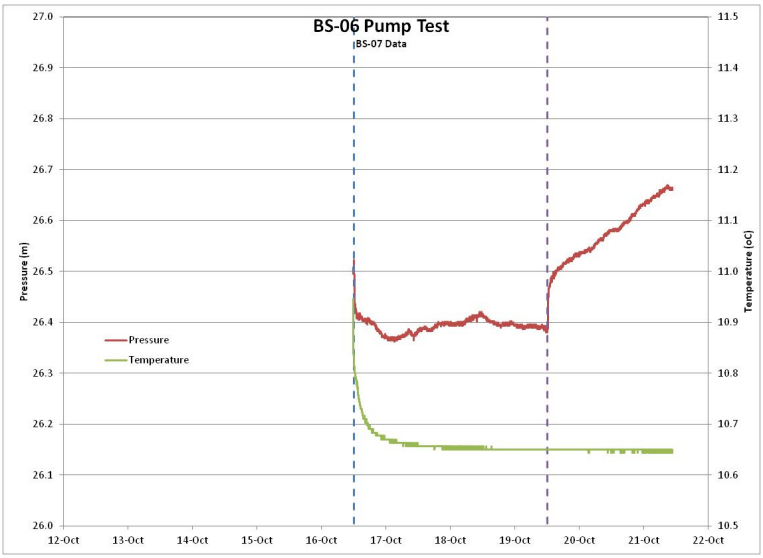

Evaluation of the response in the pumping well, the two intervals in BS-03 and the open hole at BS-07 were conducted and in general yielded similar results. The small fluctuations in the pumping rate did impact on the data and made the "late time" assessment of the drawdown data much more subjective. As a result, the pumping test recovery curves provided a superior database for analysis.

The most comprehensive fit to the recovery data was obtained using an unconfined solution (i.e., Neuman, 1974) since both the "early time" and "late time" data were matched to the sequence. However, several other solutions were also attempted on specific portions of the response data and in general yielded comparable results.

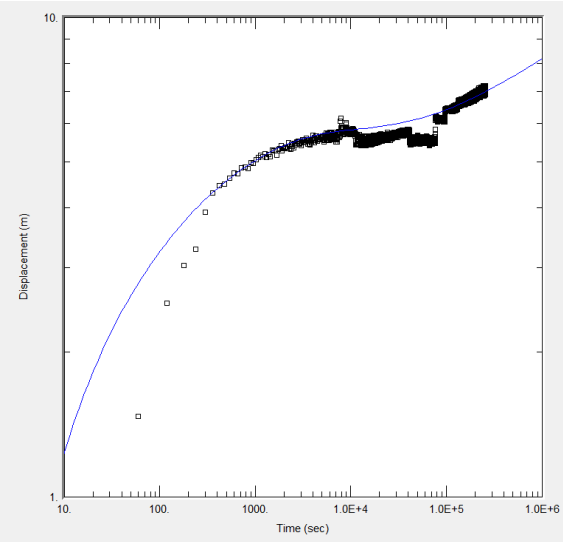

The evaluation of the BS-06 pumping response using the Neuman (1974) solution is presented in the adjacent graphic. The solution provides an estimated formation transmissivity of $2x10^{-4}$ m^2/s which is in keeping with the packer testing results for the saturated profile. The estimated storativity was 0.2 and the specific yield (Sy) was 20. The unconfined well function (ß) was estimated to be 0.001 which would infer that the vertical permeability is 50 times larger than the horizontal permeability. This could be anticipated in proximity to the wellbore where the water table drawdown is most acute. The limits of the solution are also being taxed since the drawdown magnitude is comparable to the saturated water thickness (i.e., underlying assumptions to the analytical equation).

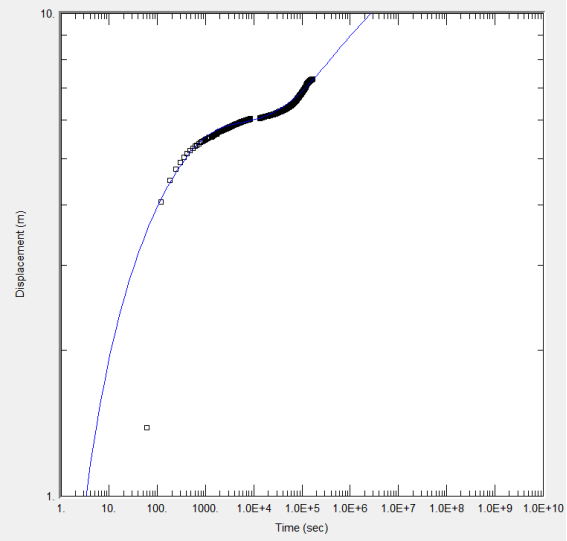

The same general parameters were obtained for the pumping test recovery curve using the Neuman (1974) solution. An estimated formation transmissivity of $2x10^{-4}$ m^2/s was used with a S of 0.1 and a Sy of 11. The ß remained at 0.001. The curve match isn't perfect; but it is reasonably close to the measured recovery data. In general, parameter estimates within an order of magnitude are typically considered to be representative of the accuracy obtained through this evaluation technique and thus, the pumping test and recovery data considered equivalent for the purposes of this evaluation.

The Neuman (1974) solution for the BS-03A and BS-03B pumping test data yielded similar results to the pumping well.

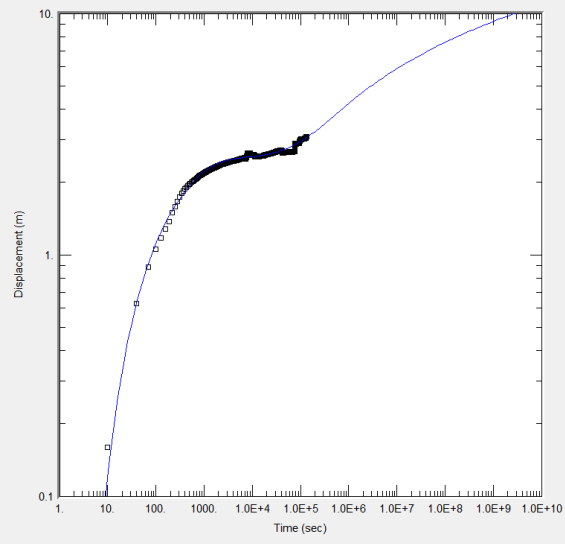

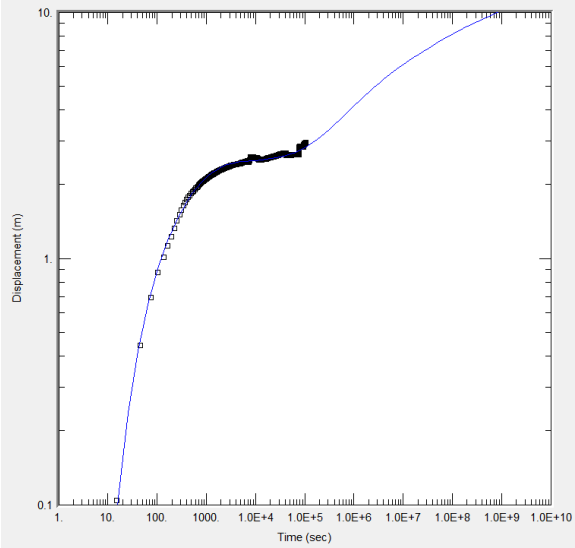

Pumping Data	T (m2/s)	S	Sy	ß
BS-06	2x10-4	0.2	20	0.001
BS-03A	2x10-4	0.0002	0.03	0.01
BS-03B	2x10-4	0.0003	0.07	0.02
BS-07	2x10-3	0.007	NA	NA

Storativity values estimated from pumping well data are not typically relied upon because of well efficiency issues and thus the observation well data is often relied upon to estimate these values. In the case of BS-07 there was no usable "late time" data in order to match the Neuman (1974) solution and therefore a Theis (1935) curve match to the "early time" data was performed. If the curve match is to be trusted; then the ß value would suggest that the horizontal permeability is about 10 times greater than the vertical permeability.

As can be seen above, the "late time" data curves are not well established and thus the late time match is suspect. In general, the same can be indicated for the pump test recovery data as presented below.

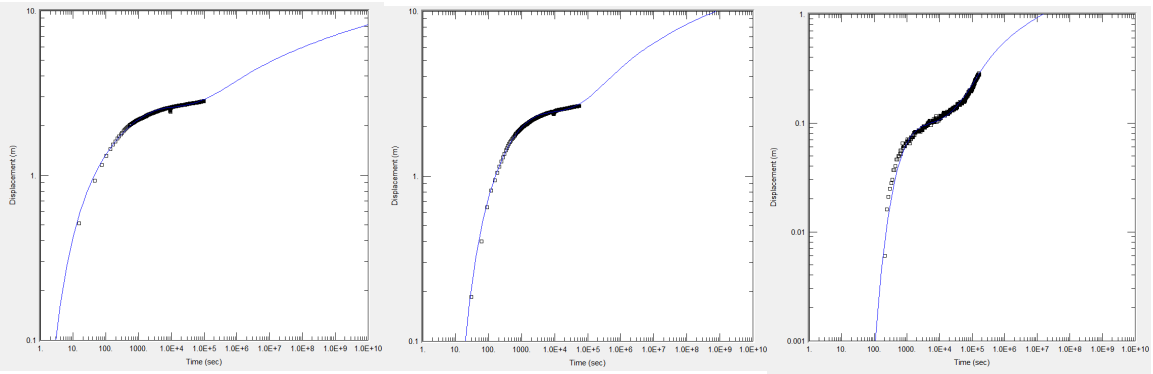

Recovery Data	T (m2/s)	S	Sy	ß
BS-06	2x10-4	0.1	11	0.001
BS-03A	3x10-4	0.00008	0.006	0.001
BS-03B	1x10-4	0.0004	0.07	0.02
BS-07	1x10-3	0.007	0.4	0.5

The "late time" data does not yield much of the Theis (1935) curve and therefore the data matching is suspect except for the BS-07 data which has a well defined "late time" curve. The ß value for the BS-07 match would suggest that the K_V to K_H ratio was about 1.

The pumping test for the Western Lands yielded a formation transmissivity estimate comparable to that determined through the packer testing program. This is not unexpected given that this testing sequence would draw most of the bedrock response from the most conductive fracture planes.

The analytical solution used for the testing sequence is base on an unconfined aquifer response. The pumping test data give inference to this solution; but the full response was not obtained for all

observation wells. Thus, the late time data matching is more speculative in nature; but as noted below, not overly important to the formation evaluation.

The test response for the Westerns Lands is unique in terms of the unconfined response and is attributed to the local setting at the pumping well. This is stated since the bedrock profile at the pumping well is overridden by a thickness of sand which has not been seen elsewhere on the Western Lands and the Southern Lands. This delayed response (i.e., late-time unconfined response) is attributed to the overlying sand sequence as opposed to the larger interconnected fractured rock network. This also accounts for the fact that the same response was not observed during the former Golder pumping test sequences (Golder, 2006). The clay till overburden evident over the regional setting has no capacity to yield any significant response.

The delayed response is effective in illustrating the vertical interconnectivity of the bedrock regime. The ability to detect this response given the uniqueness of the geologic setting at the production well location was considered to be an opportune situation and reinforces the conceptual model for the host rock sequence as had been inferred by the long term ground water monitoring data.

15.3 Monitoring Well Construction

Based on the packer testing results, geophysics, and detailed core logging, discrete fracture (or flow) zones were identified. These conductive fracture zones were targeted for the well screens in the monitoring wells. The screened zone isolates the discrete fractures through a permanently constructed monitoring system. Isolating these discrete zones allows for the monitoring of the hydraulic head and water quality. The construction details of the monitoring wells are provided in the borehole logs and were determined by generally selecting the most conductive zones as presented in the packer testing data.

For the three HQ (4-inch diameter) boreholes (BS-01, BS-02, & BS-03), the borehole diameter limited the installation of two formal monitoring well instrumentations, both of which were standard one-inch (25 mm) diameter PVC construction, while BS-01 and BS-02 had the upper part of the boreholes left open such that they targeted the upper saturated fractures and could be monitored and sampled similar to the deeper well constructions. The larger diameter 6-inch water wells (BS-04 & BS-05) were able to have three formal monitoring well installations with 1.25-inch (32 mm) diameter PVC construction. All these wells were constructed with either a 1.5 m or 3 m machine slotted well screen with standard monitoring well sand pack. The intervening borehole spacing was sealed with bentonite holeplug to ensure proper vertical sealing between monitoring wells within each borehole.

It is noted that all well construction was completed by licensed well technicians from Orbit Garant Drilling Services in 2019

15.4 Geophysical Logging

Logistics and Final Report

2018 Azimuth Environmental Consulting Inc – Barrie, ON.
Acoustic Televiewer, Optical Televiewer, and Flow Meter Surveys – Burlington, ON.

Prepared By:

DGI Geoscience Inc.
119 Spadina Avenue, Suite 405
Toronto, Ontario, M5V 2L1
Tel: +1 416 361 3191
www.dgigeoscience.com

Prepared For:

Azimuth Environmental Consulting Inc.

Main Contact:

Dave Ketcheson, P. Eng., M.A.Sc. – Senior Environmental Engineer

1. INTRODUCTION

1.1. Project Overview

DGI Geoscience Inc. (DGI) was contracted by Azimuth Environmental Consulting Inc. (Azimuth) to survey three (3) boreholes located near the Burlington Springs Golf Club. The goals of this project were to acquire; geotechnical, structural and hydrogeological data to support an environmental study in the area. This information can be used for advanced interpretation and understanding of the subsurface in the area of study.

Data acquisition commenced on October 9th, 2018 and ended on October 11th, 2018. During this time the following parameters were surveyed: Optical Televiewer, Acoustic Televiewer and Heatpulse Flow Meter. Data processing was completed simultaneously with data acquisition. Prior to the delivery of this report, all final plots were provided to Azimuth via FTP and will remain downloadable for one year from the delivery of this report.1.2. DGI Geoscience Profile

DGI Geoscience Inc. is a dynamic and innovative company that maximizes the investment in drilling by providing in-situ borehole geophysical measurements for mining, exploration, geotechnical and environmental applications. DGI applies strict standard operating procedures, utilizes calibration facilities, and well-defined calibration methodologies, to obtain quantifiable geophysical data.

To extract the most value from client's datasets, DGI developed a proprietary data analysis technique referred to as the 2-4C Process. The 2-4C Process is a robust data-driven technique that uses a combination of data validation, machine learning, cluster analysis and conventional statistics to extract value from complex datasets. Key applications of the 2-4C Process include: defining unbiased classification schemes via the establishment of petrophysical domains and establishing proxy relationships between traditionally isolated geoscience datasets. In general, physical rock properties are used to quantitatively link geology with geophysics and estimate geochemistry, geometallurgy, and grade in a rapid and cost- effective manner.

DGI is focused on applying cutting edge, proven technologies to its clients' projects. Indeed, DGI is proud to be the first company in North America to have commercial experience deploying Borehole Magnetic Resonance technology for continuous Porosity, Permeability, and Dry Weight Density data acquisition.

In addition, DGI has developed techniques and has experience in surveying flat dipping and up-direction boreholes, introducing rapid, high accuracy, and in-situ data acquisition with unique applications in rock mechanics and risk analysis, thus allowing risk mitigation and safer underground operations, in tunneling and underground mining works.

2. SURVEY DETAILS

2.1. Location

The boreholes surveyed on this project were located at the Burlington Springs Golf Club., near Burlington, Ontario. The Burlington Springs Golf Club is approximately 135 km south-west of DGI's Operation Centre in Barrie, ON.

2.2. Personnel

Project Manager

Alejandro Rojas

Field Personnel

Kevin Smylie (Field Technician) Olga Fomenko (Field Technician)

Data Analysts

Pamela Patraskovic (Senior Data Analyst) Steve Reese (Data Analyst)

2.3. Logistics

The surveys were completed in a single mobilization. DGI personnel prepared all necessary gear for the surveys prior to mobilizing to the project site. A local mobilization was completed on October 9th. Data acquisition commenced the same day and finished on October 11th of 2018. Boreholes were accessed and surveyed via a purposed built 4x4 surveying vehicle and a portable geophysical survey equipment suite. A total of three (3) boreholes were surveyed over two (2) days at the project site, with zero Lost Time incidents and zero incidents requiring First Aid.

3. PARAMETERS

Table 2 shows which probes were run during the project. In the appendix, a more detailed description is given, indicating which parameters were run on each borehole, survey depth, and survey date.

PROBE	MANUFACTURER	SERIAL NUMBER	LOGS
Acoustic Televiewer	ALT	112301	Borehole Azimuth, Inclination, Acoustic Amplitude and Travel Time
Optical Televiewer	ALT	170709	Borehole Azimuth, Inclination, High resolution borehole-wall image
Heatpulse Flow Meter	MSI	6160	Magnitude and direction of vertical fluid flow

Table 2: Parameters collected.

4. DATA PROCESSING

4.1. Client Deliverables

The following files were provided for each borehole surveyed by DGI:

1. [HoleID]_ATVOTV_Draft1.WCL
2. [HoleID]_ATVOTV_Draft1.pdf (preliminary results – processed images with no feature picks)
3. [HoleID]_ATVOTVFlowmeter_111318.pdf
4. [HoleID]_ATVOTVFlowmeter_111318.WCL (final processed data, televiewers and flowmeter, with feature pick orientations)
5. [HoleID]_HistogramPlot_All Features.pdf
6. [HoleID]_SchmidtPlot_All Features.pdf (area equal projection in the southern hemisphere)
7. [HoleID]_StructureAnalysis.xlsx (export of feature dip and dip direction, fracture frequency and RQD values)
8. [HoleID]_Flowmeter.xlsx *(export of flowmeter values)*

All data can be downloaded via DGI's ftp site, using the credentials provided below. We recommend accessing this through a FTP program such as FileZilla (open source software, downloadable free of charge). The results will remain downloadable for a period of one year after the delivery of this report.

4.2.1. Televiewers

Optical Televiewer

Optical Televiewer (OTV) produces a true colour (RGB), oriented, high-resolution, 360-degree image of the borehole wall. This allows bedding/foliation, contacts, joints/fractures, and veins to be visible in detail, and provides important information regarding the lithological characterization and structure of rock formations. In areas of low core recovery, OTV provides valuable and continuous oriented information. The OTV operates in wet and dry conditions, however if fluid is present the transparency of the fluid is observed in the image. DGI has developed unique techniques to treat the borehole fluid, maximizing the quality of the OTV images collected.

Acoustic Televiewer

Acoustic Televiewer (ATV) produces an oriented acoustic 360-degree image of the borehole wall. This allows bedding, joints/fractures, faults and breakouts to be visible in detail, and provides important information regarding the structure and geotechnical competency of rock formations. Joints can be seen open or closed and any width/aperture of a feature can be measured accurately. This ability has made the Acoustic Televiewer (ATV) probe important for precision engineering studies. In areas of low RQD, disking etc. Acoustic Televiewer provides a complete record and true orientation of structural and geotechnical features. The ATV requires fluid to be present to transmit the signal and the probe should be centralized in the borehole to provide the best image.

Another relevant application for Acoustic Televiewer data is the identification of zones of potential underground fluid flow. The information derived from ATV surveys can be used to target areas for hydrogeological studies, flow measurement and monitoring instrumentation set up.

DGI's data analyst completed the QA/QC, processing and plotting of the ATV data acquired, including noise filtering, depth shifting and centralization.

4.2.2. Hydrogeological Data

Heatpulse Flow Meter:

The Heat Pulse Flow Meter probe measures low flow rates within the borehole fluid column. Zones of interest are identified through data acquired by the full suite of parameters. The probe is lowered to these zones of interests and remains stationary while field personnel acquire measurements above and below a possible fracture zone. The Heat Pulse Flow Meter uses a heat grid to heat a sheet of water within the borehole fluid column. Sensors located above and below the heat grid record the time required for this heated sheet of water to reach the sensors. This data indicates direction and magnitude of fluid flow within the borehole fluid column.

Data collected with the Acoustic Televiewer probe was used to identify potential zones of flow. DGI data analysts used this data to select the areas for flow measurement. The potential zones of flow were then provided to the operators to conduct the flow measurements. The results from the flow meter surveys where analyzed and plotted along with the Televiewer data acquired on each borehole. In addition, the flow meter data was presented in a csv format showing depth of measurement, magnitude and direction (a positive value indicates an up-flow, and negative value indicates down-flow) of the flow.

4.2.3. Data Processing – Acoustic and Optical Televiewer and Flowmeter Composite Plot

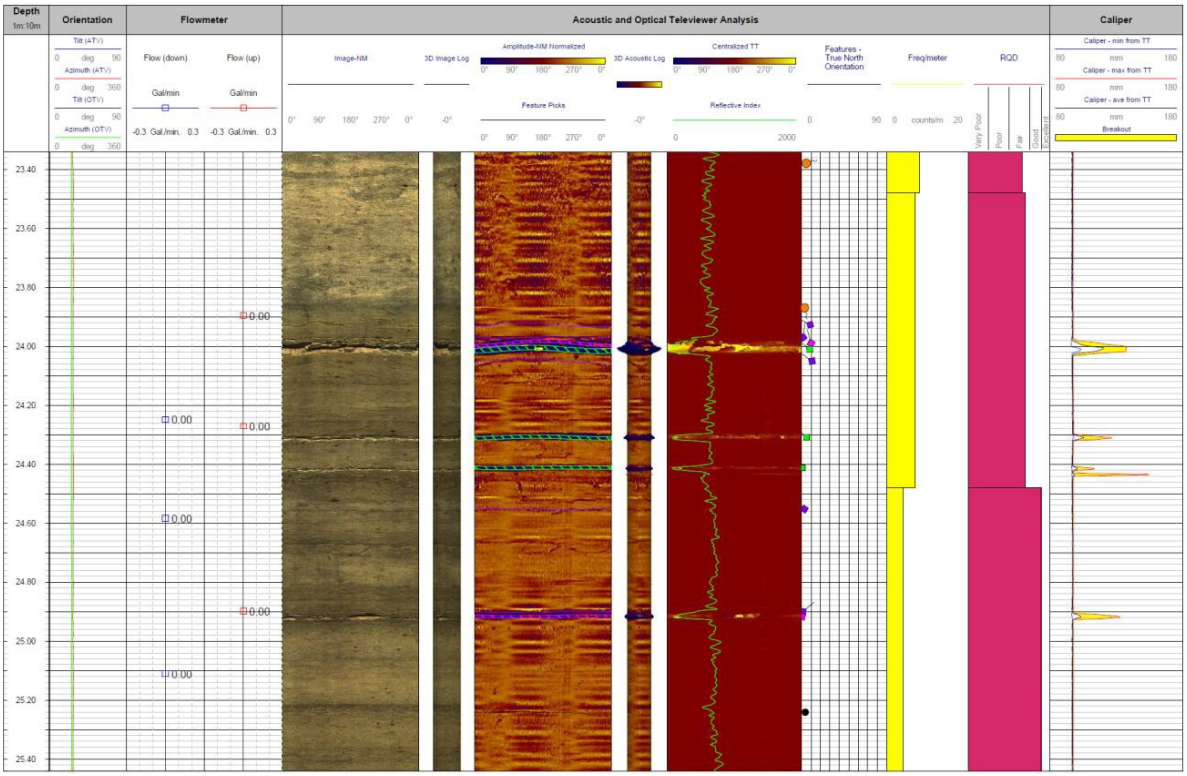

The above figure shows a sample of the acoustic and optical televiewer, and flowmeter composite plots provided by DGI. This includes picked borehole features, fracture frequency, RQD, synthetic caliper calculated from the acoustic televiewer, and flowmeter data. The following describes the logs present in the plot:

A. Tilt and Azimuth

Both the acoustic and optical televiewer contain a built-in, high precision deviation sensor which measures the borehole tilt and azimuth during data acquisition.

Tilt: inclination of the borehole measured from the vertical axis. Tilt = 0 degrees corresponds to a vertical borehole; Tilt = 90 degrees indicates a horizontal borehole.

Azimuth: the raw probe azimuth is represented with respect to ***magnetic north,*** plotted from 0 to 360 degrees. Note that the azimuth is influenced by magnetics. When the probe azimuth is used for feature orientation, these regions of magnetic interference are interpolated through.

B. 3D Acoustic and Image Logs

For visual reference, the unwrapped acoustic and optical images are also plotted in WellCAD as 3D logs. These logs are a three-dimensional outside view of the borehole wall. The synthetic caliper calculated from the acoustic travel time was applied to the 3-D Acoustic log to better visually represent regions of borehole blowouts.

C. Acoustic Televiewer Logs

Amplitude Normalized

Amplitude of the returned pulse with a high pass normalization filter applied. **Highs** (orange) represent regions where the formation is smooth, or more acoustically reflective, while **lows** (blue) represent regions where the acoustic signal is being preferentially absorbed by the formation. These regions of absorption typically are the result of fractures present in the formation.

Reflective Index

The median of the acoustic amplitude log per vertical sample interval. This value is indicative of **relative** rock hardness. As with the amplitude log, low values indicated high absorption/low reflectivity while highs indicate a low absorption/high reflectivity.

Centralized TT

The travel time log filtered and corrected for centralization. Highs indicate that there are open fractures/joints present.

Synthetic Caliper Logs

Using the centralized travel time log, the two-way travel time, the probe radius, and an assumed fluid velocity of 1450m/s, DGI produces a synthetic caliper log by computing a radius value for each recorded travel time data point along the borehole path. Opposite radius values are then added to get the actual borehole caliper. This value is outputted and displayed as the minimum, maximum and average value for each vertical interval resulting in three caliper logs (min, max and average). The "Breakout" log is the shaded area between "Caliper – Ave from TT" and "Caliper – Max from TT" and is a visual indicator of hole enlargement caused by fracturing and/or borehole breakouts.

D. Televiewer Rock Quality Designation and Fracture Frequency

DGI generates a Televiewer Rock Quality Designation (RQD) and a Fracture Frequency log for each borehole. This data is displayed in the WellCAD plot as well as exported to excel for the client. Both measurements are calculated using the following feature pick classes:

Broken Zone/Undifferentiated Joint/Fracture - Fault/Wide Open (30mm+) Joint/Fracture - Moderately Open (10-30mm) Joint/Fracture - Open (1-10mm) Joint/Fracture - Tight (0-1mm)

Freq/meter: Fracture frequency per 1m; the number of occurrences per meter.

Televiewer Rock Quality Designation (RQD): a measure of the drill core quality or intensity of fracturing. This is measured as a percentage of drill core in length of 0.1 meters and is derived from the televiewer feature picks.

RQD	W Description
0-25%	Very Poor
25-50%	Poor
50-75%	Fair
75-90%	Good
90-100%	Excellent

4.2.4. Data Processing – Televiewer Feature Classification and Orientation

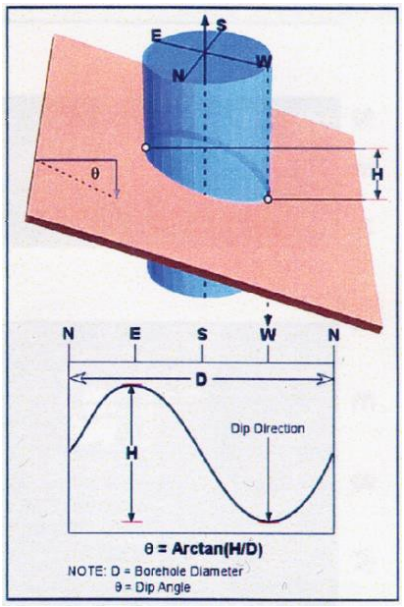

All planar geological features appear in the unwrapped acoustic and optical televiewer images as sinusoidal waves. From this, the dip and dip direction were determined as follows:

Dip: amplitude of the sinusoid
Dip Direction: radial position of the sine wave minimum

These features were provided to the client oriented to true north orientation. To correct the feature picks to true north orientation, DGI used the tilt and azimuth information collected by the televiewer probes, along with the magnetic declination at site (-10.714 degrees). The magnetic declination was determined using the Natural Resources Canada website using the following location: **Latitude**: 43.3255° North, **Longitude**: 79.7990° West.

All feature picks were plotted in WellCAD both in projection view ("Feature Picks" Log) and as tadpoles ("Features – True North Orientation" Log). All feature pick orientations were provided exported in .xlsx format which can be imported by the client into their preferred software. Furthermore, DGI also provided the feature picks in a histogram plot, and plotted in a Schmidt plot, for client convenience.

4.2.5. Data Processing – Televiewer Classification Scheme

The following feature classes were interpreted from the acoustic and optical televiewer data set:

CODE	SYMBOL	DESCRIPTION
BZ		Broken Zone/Undifferentiated
F1		Joint/Fracture - Fault/Wide Open (30mm+)
F2		Joint/Fracture - Moderately Open (10-30mm)
F3		Joint/Fracture - Open (1-10mm)
F4		Joint/Fracture - Tight (0-1mm)
BF		Bedding/ Banding/ Foliation
CT		Contact
0		Bottom of Casing
1		Water Level

Joints/Fractures were defined as classes F1 through F4 based on their aperture. A class F4 fracture was defined as having an aperture of less than 1mm, a class F3 fracture had an aperture between 1 and 10mm, a class F2 fracture had an aperture between 10-30mm and a class F1 fracture had an aperture greater than 30mm. The BZ designation was used to identify zones in the borehole where a large amount of fracturing is present, but where no accurate orientation could be assigned to these features. Fractures were identified primarily from the acoustic televiewer image when available, and from the optical televiewer image when above water level.

Bedding/Banding/Foliation appeared in the optical televiewer image as parallel, repetitive sinusoids. These were picked and oriented approximately every 5m, when visible.

Contacts were also picked primarily from the optical televiewer image and identified as distinct changes throughout the log. Some texturally distinct contacts were also visible in the acoustic televiewer data.

4.2.5. Data Processing General Comments

Good quality acoustic and optical televiewer and flowmeter data was collected on each borehole by DGI field technicians. This allowed for the successful identification and orientation of planar borehole features which were provided to the client. Each planar feature identified and classified by the data analysts had an associated true dip and dip direction, depth reference point, and aperture value.

The televiewer also allowed for the selection of flowmeter collection points/stations throughout each borehole. All three boreholes showed a significant amount of fracturing throughout, as well as some voids in the formation. Flowmeter stations were collected above and below selected major fracture zones to test for water flow. Borehole BS-01 contained some flow throughout the entire borehole. BS-02 exhibited flow associated with fracturing near the top of the borehole, with no flow deeper in the borehole. BS-03 recorded no flow other than one flowmeter station.

5. QUALITY CONTROL

DGI employs a rigorous QA/QC process to ensure all deployed equipment are always functioning appropriately. Standard Operating Procedures (SOP) are developed over three key stages: pre-mobilization, on-site, and post-project. Adherence to SOPs at each stage enables early detection and solution when issues are encountered. Prevention is our goal, but identification and contingency plans are equally important when unforeseen challenges occasionally arise. Our QA/QC process and attention to detail assures client confidence and top-quality results.

DGI has established a baseline for all probes and parameters at the Geologic Survey of Canada's (GSC) Bells Corners Calibration Facility near Ottawa, Canada. The GSC calibration borehole is well understood with detailed core analysis and published papers in support of results. Repeated acquisition of data at this facility has enabled the development of a baseline for each probe's individual functionality based on expected geophysical signatures. DGI has developed a calibration data set, using the GSC facility, to create field calibration procedures that supplement manufacturer recommendations.

To expand the quality and breadth of calibration procedures, DGI has established an additional calibration borehole. DGI has leveraged proven baselines from the GSC Calibration Facility for each probe and parameter, by transferring calibration to our own calibration borehole in Levack, Ontario. The exceptional geology of the Levack borehole provides geophysical signatures with extensive variance; well supported by documented drilling data, core analysis and lab assay. The Levack calibration borehole enables our

equipment to be checked for nominal function, calibration and performance in an environment approximating a project site. Our full calibration infrastructure enables DGI to conduct an auditable logging process for each project from pre-mobilization through to project completion.

Once equipment has been mobilized to site, QA/QC measures are in place to ensure field personnel have confidence in equipment functionality. SOPs are defined based on the specific suite of geophysical probes, site conditions and overall goals of the client's project. Each geophysical probe has unique measures in place that may include:

- On-site calibrations to correct for regional variance and/or borehole size;
- Bench tests conducted in the field to ensure probes meet baseline values;
- Calibration checks recorded before and after each survey, if applicable;
- Transferred calibration enabling establishment of an on-site calibration borehole with representative geology for long-term projects.

6. CONCLUSIONS AND RECOMMENDATIONS

DGI Geoscience Inc. successfully surveyed three (3) boreholes over the course of two (2) days at the Azimuth's area of study near Burlington, ON. DGI obtained three important types of information the boreholes. 1) Geotechnical information through Acoustic Televiewer data, which will help understand fracture and fault networks present in the area. 2) Important structural and lithological information through Optical Televiewer surveys, including true dip and dip direction of bedding, joints, fractures and faults. 3) Hydrogeological information through Heatpulse Flow Meter borehole measurements, that will allow evaluate the magnitude and direction of underground fluids within the subsurface fractures and faults network.

The combination of geotechnical, structural and hydrogeological information can greatly assist with the understanding in the area of study's subsurface. All deliverables have been provided to the client as of the delivery of this report. All data has been quality assured by our strict quality control procedure.

15.5 Groundwater Monitoring Program

Ground water elevations were monitoring by Azimuth field staff during 2018 and 2019 at both the existing monitoring well network located on the Southern Lands, as well as with the newly constructed monitoring wells on the Western Lands. This monitoring program targeted the bedrock and overburden wells associated with these bedrock wells, but did not include a number of shallow overburden monitoring wells located across the Southern Lands ("MP"'s and "GP"'s - Golder, 2006) as many have either been destroyed or could not be located in 2018.

In total, 100 monitoring wells were monitored at 39 locations (nested locations) with dataloggers targeting 34 monitoring wells for at least part of the monitoring period of November 2018 to October 2019. It is also noted that a single domestic well located at 5161 Cedar Springs Road was also included in this monitoring program and had a datalogger installed for continuous monitoring. Manual measurements were completed along with downloading of all loggers during November 2018, May 2019, August 2019 and November 2019 such that all continuous datalogger data could be properly calibrated to reference ground water elevations. An on-site barometric datalogger was also utilized to barometrically correct all datalogger data. This monitoring supplemented the previous monitoring data completed by Golder on the Southern Lands, which includes a dataset of 2004 to 2013 at several locations.

Hydrographs for the monitoring wells that are recommended for the long-term groundwater monitoring program are provided below.

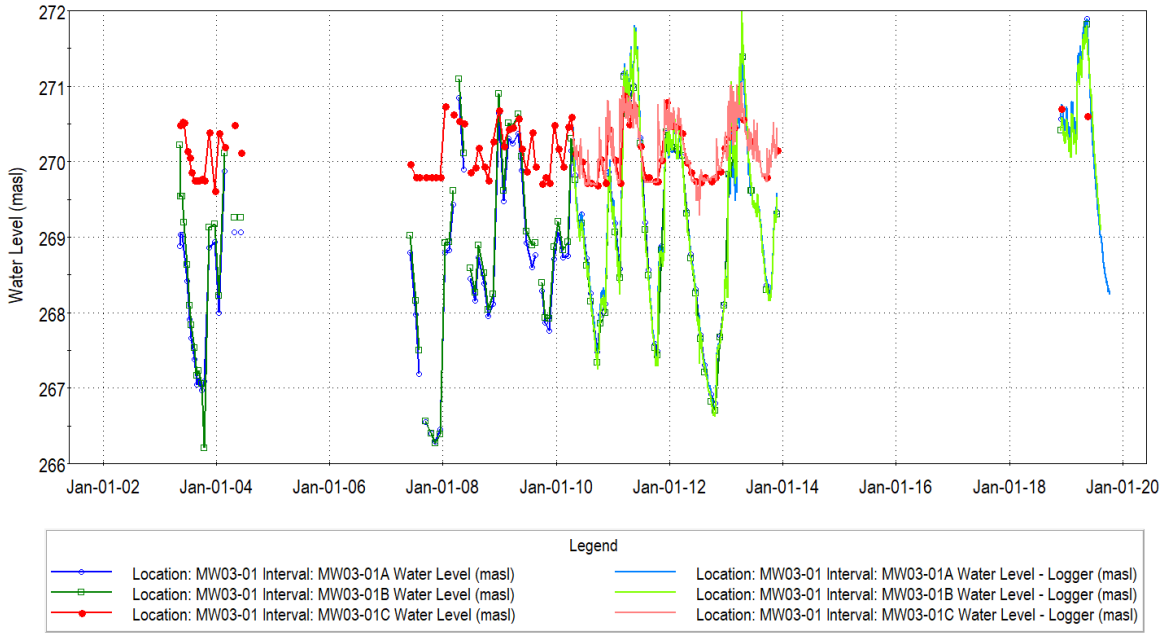

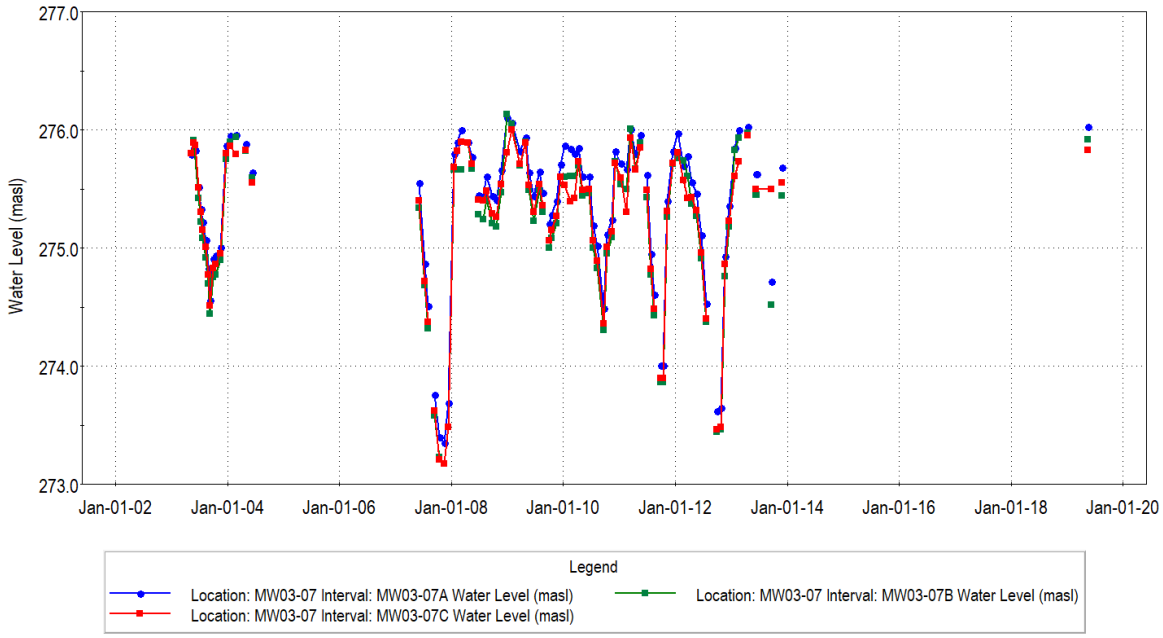
277.0
276.0
275.0
274.0
273.0
Water Level (masl)
Jan-01-02
Jan-01-04
Jan-01-06
Jan-01-08
Jan-01-10
Jan-01-12
Jan-01-14
Jan-01-16
Jan-01-18
Jan-01-20
Legend
Location: MW03-07 Interval: MW03-07A Water Level (masl)
Location: MW03-07 Interval: MW03-07B Water Level (masl)
Location: MW03-07 Interval: MW03-07C Water Level (masl)

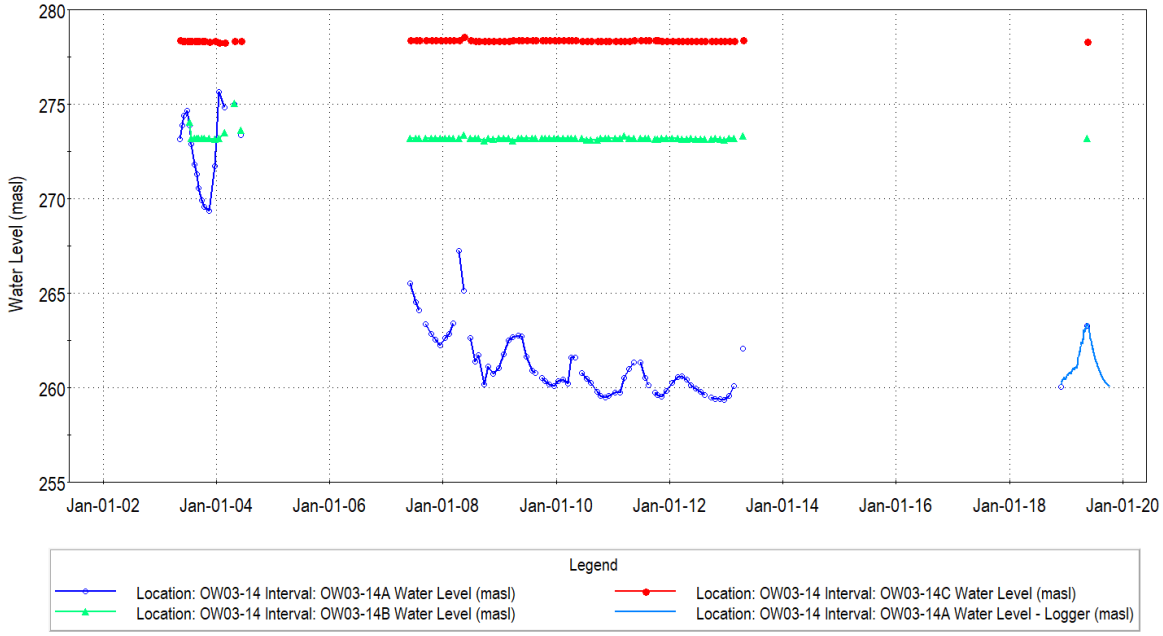
280
275
270
265
260
255
Water Level (masl)
Jan-01-02
Jan-01-04
Jan-01-06
Jan-01-08
Jan-01-10
Jan-01-12
Jan-01-14
Jan-01-16
Jan-01-18
Jan-01-20
Legend
Location: OW03-14 Interval: OW03-14A Water Level (masl)
Location: OW03-14 Interval: OW03-14B Water Level (masl)
Location: OW03-14 Interval: OW03-14C Water Level (masl)
Location: OW03-14 Interval: OW03-14A Water Level - Logger (masl)

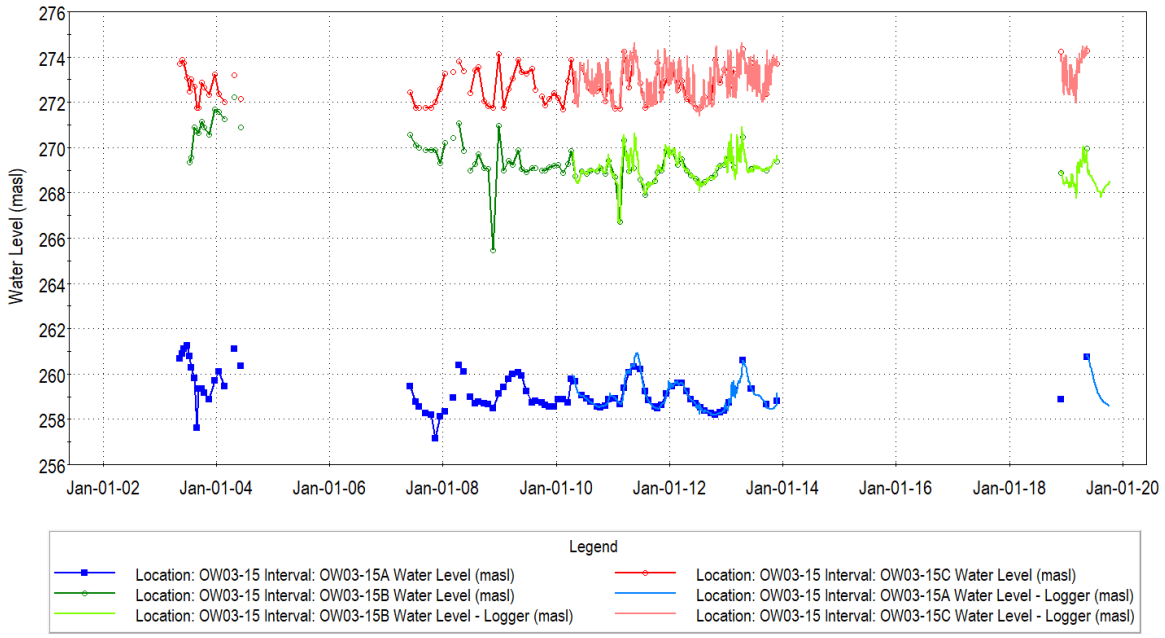
Water Level (masl)
276
274
272
270
268
266
264
262
260
258
256
Jan-01-02
Jan-01-04
Jan-01-06
Jan-01-08
Jan-01-10
Jan-01-12
Jan-01-14
Jan-01-16
Jan-01-18
Jan-01-20
Legend
Location: OW03-15 Interval: OW03-15A Water Level (masl)
Location: OW03-15 Interval: OW03-15B Water Level (masl)
Location: OW03-15 Interval: OW03-15B Water Level - Logger (masl)
Location: OW03-15 Interval: OW03-15C Water Level (masl)
Location: OW03-15 Interval: OW03-15A Water Level - Logger (masl)
Location: OW03-15 Interval: OW03-15C Water Level - Logger (masl)

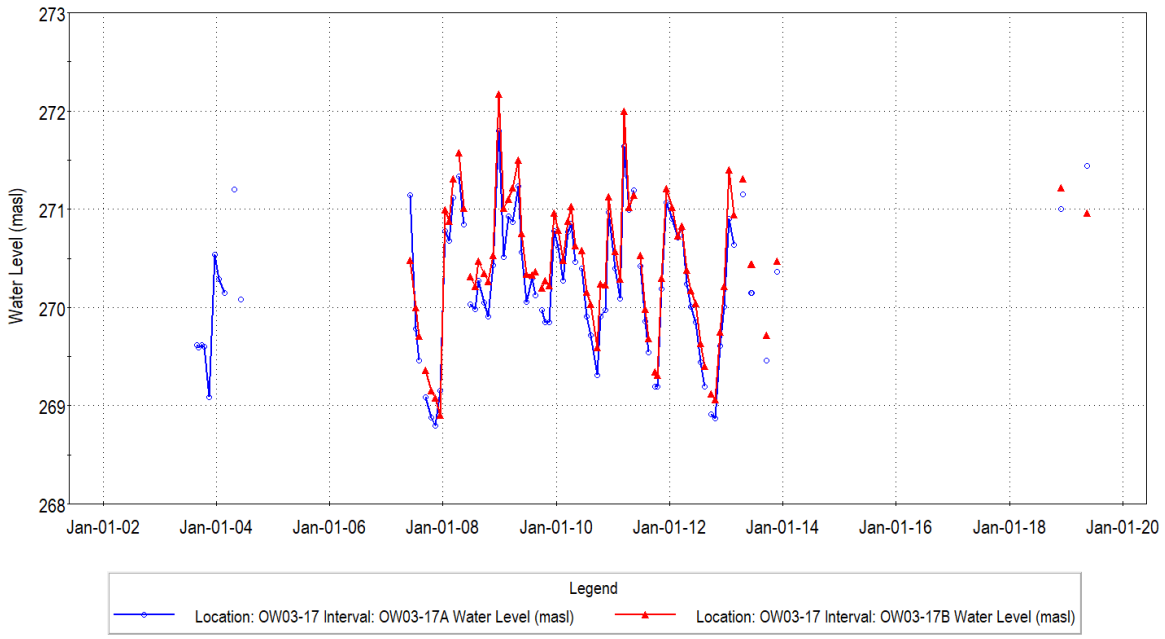
Water Level (masl)
273
272
271
270
269
268
Jan-01-02
Jan-01-04
Jan-01-06
Jan-01-08
Jan-01-10
Jan-01-12
Jan-01-14
Jan-01-16
Jan-01-18
Jan-01-20
Legend
Location: OW03-17 Interval: OW03-17A Water Level (masl)
Location: OW03-17 Interval: OW03-17B Water Level (masl)

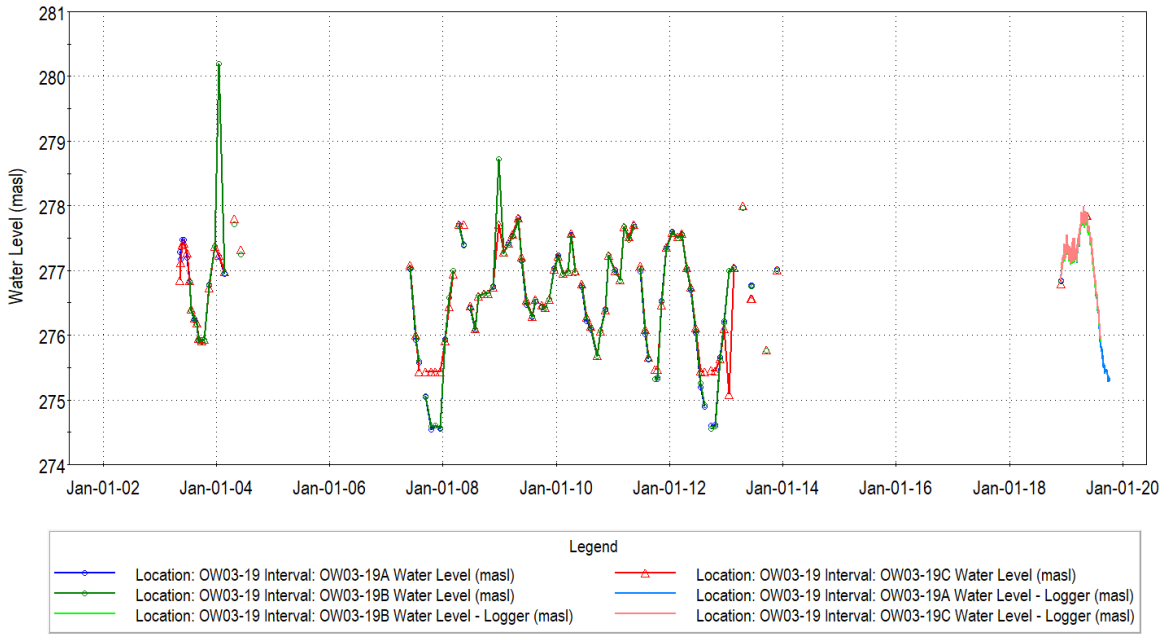
Water Level (masl)
281
280
279
278
277
276
275
274
Jan-01-02
Jan-01-04
Jan-01-06
Jan-01-08
Jan-01-10
Jan-01-12
Jan-01-14
Jan-01-16
Jan-01-18
Jan-01-20
Legend
Location: OW03-19 Interval: OW03-19A Water Level (masl)
Location: OW03-19 Interval: OW03-19B Water Level (masl)
Location: OW03-19 Interval: OW03-19B Water Level - Logger (masl)
Location: OW03-19 Interval: OW03-19C Water Level (masl)
Location: OW03-19 Interval: OW03-19A Water Level - Logger (masl)
Location: OW03-19 Interval: OW03-19C Water Level - Logger (masl)

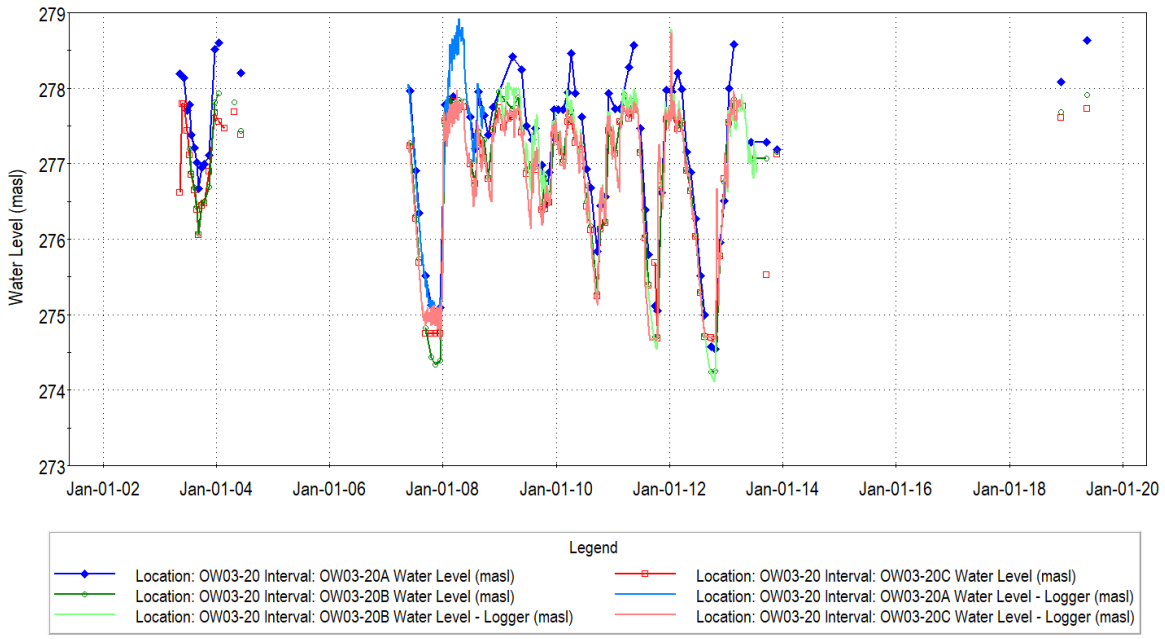
Water Level (masl)
279
278
277
276
275
274
273
Jan-01-02
Jan-01-04
Jan-01-06
Jan-01-08
Jan-01-10
Jan-01-12
Jan-01-14
Jan-01-16
Jan-01-18
Jan-01-20
Legend
Location: OW03-20 Interval: OW03-20A Water Level (masl)
Location: OW03-20 Interval: OW03-20B Water Level (masl)
Location: OW03-20 Interval: OW03-20B Water Level - Logger (masl)
Location: OW03-20 Interval: OW03-20C Water Level (masl)
Location: OW03-20 Interval: OW03-20A Water Level - Logger (masl)
Location: OW03-20 Interval: OW03-20C Water Level - Logger (masl)

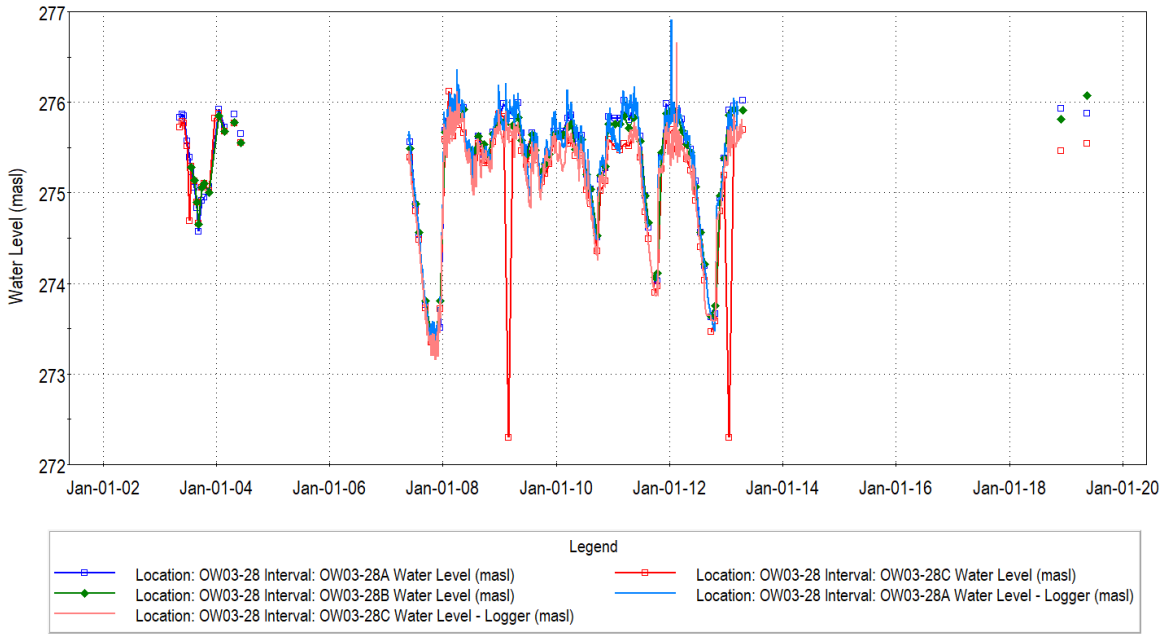
277
276
275
274
273
272
Water Level (masl)
Jan-01-02
Jan-01-04
Jan-01-06
Jan-01-08
Jan-01-10
Jan-01-12
Jan-01-14
Jan-01-16
Jan-01-18
Jan-01-20
Legend
Location: OW03-28 Interval: OW03-28A Water Level (masl)
Location: OW03-28 Interval: OW03-28B Water Level (masl)
Location: OW03-28 Interval: OW03-28C Water Level - Logger (masl)
Location: OW03-28 Interval: OW03-28C Water Level (masl)
Location: OW03-28 Interval: OW03-28A Water Level - Logger (masl)

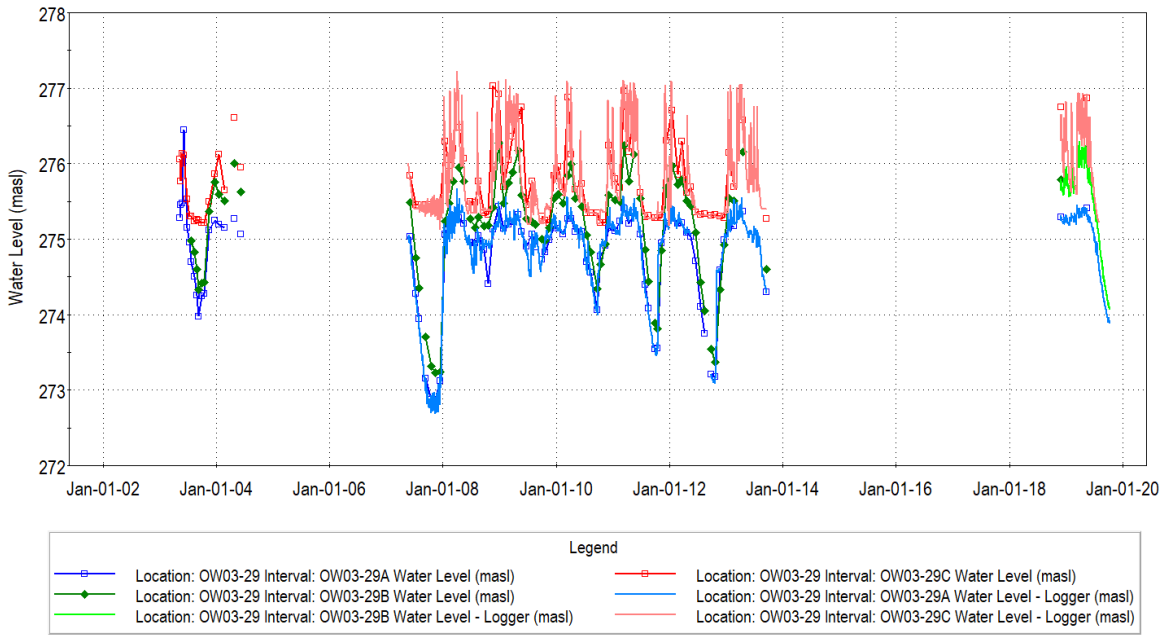
278
277
276
275
274
273
272
Water Level (masl)
Jan-01-02
Jan-01-04
Jan-01-06
Jan-01-08
Jan-01-10
Jan-01-12
Jan-01-14
Jan-01-16
Jan-01-18
Jan-01-20
Legend
Location: OW03-29 Interval: OW03-29A Water Level (masl)
Location: OW03-29 Interval: OW03-29B Water Level (masl)
Location: OW03-29 Interval: OW03-29B Water Level - Logger (masl)
Location: OW03-29 Interval: OW03-29C Water Level (masl)
Location: OW03-29 Interval: OW03-29A Water Level - Logger (masl)
Location: OW03-29 Interval: OW03-29C Water Level - Logger (masl)

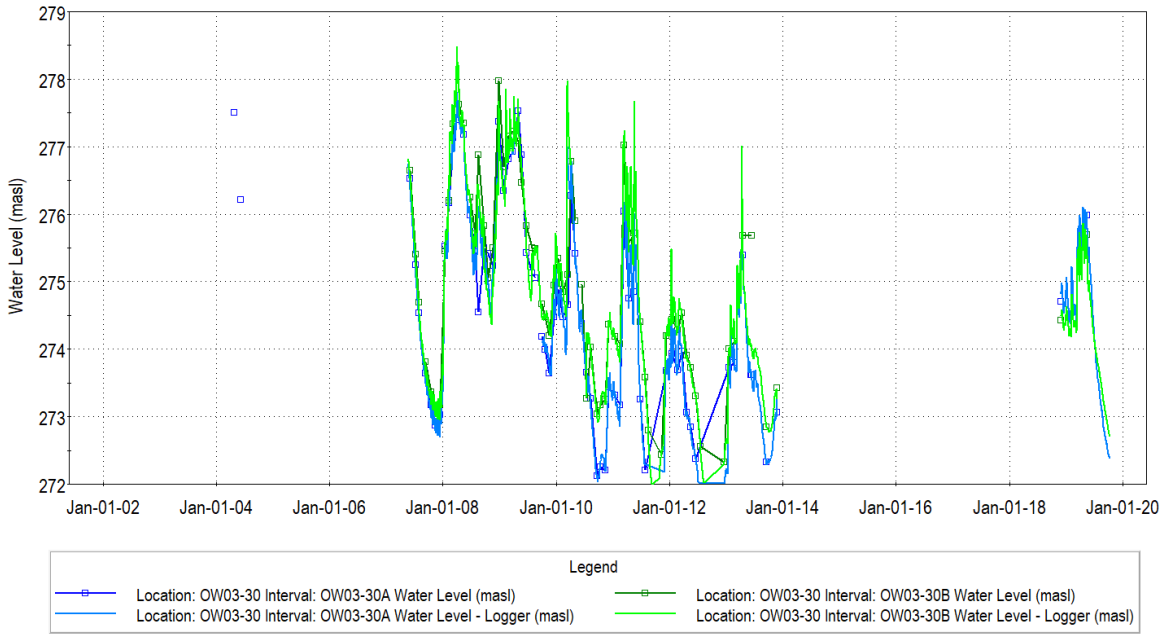
279
278
277
276
275
274
273
272
Water Level (masl)
Jan-01-02
Jan-01-04
Jan-01-06
Jan-01-08
Jan-01-10
Jan-01-12
Jan-01-14
Jan-01-16
Jan-01-18
Jan-01-20
Legend
Location: OW03-30 Interval: OW03-30A Water Level (masl)
Location: OW03-30 Interval: OW03-30A Water Level - Logger (masl)
Location: OW03-30 Interval: OW03-30B Water Level (masl)
Location: OW03-30 Interval: OW03-30B Water Level - Logger (masl)

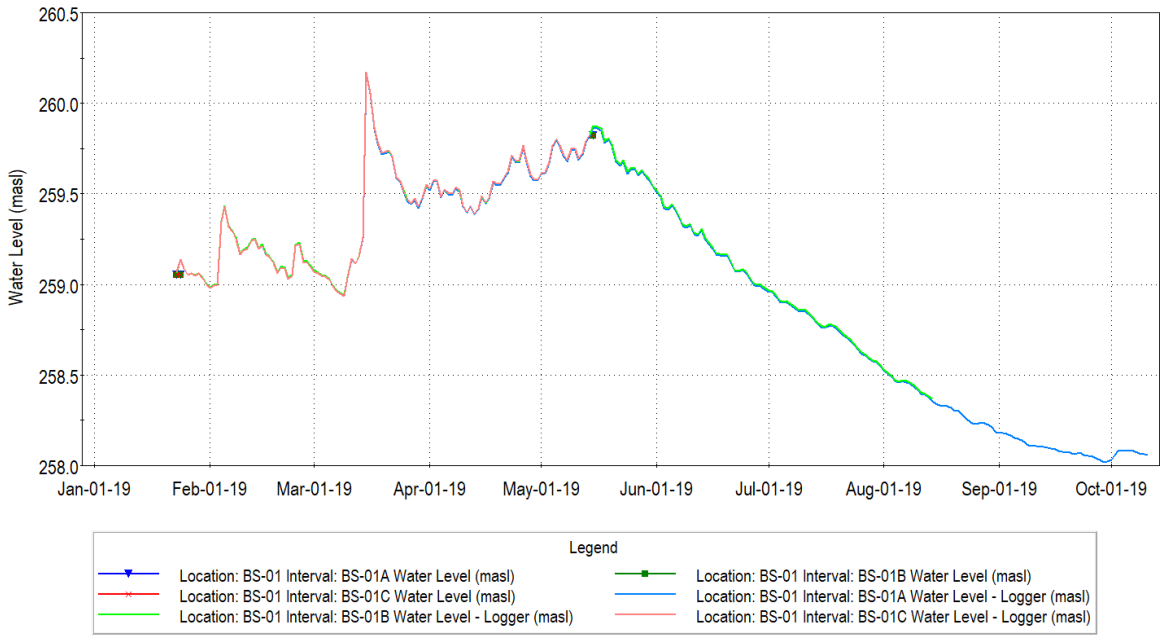
260.5
260.0
259.5
259.0
258.5
258.0
Water Level (masl)
Jan-01-19
Feb-01-19
Mar-01-19
Apr-01-19
May-01-19
Jun-01-19
Jul-01-19
Aug-01-19
Sep-01-19
Oct-01-19
Legend
Location: BS-01 Interval: BS-01A Water Level (masl)
Location: BS-01 Interval: BS-01C Water Level (masl)
Location: BS-01 Interval: BS-01B Water Level - Logger (masl)
Location: BS-01 Interval: BS-01B Water Level (masl)
Location: BS-01 Interval: BS-01A Water Level - Logger (masl)
Location: BS-01 Interval: BS-01C Water Level - Logger (masl)

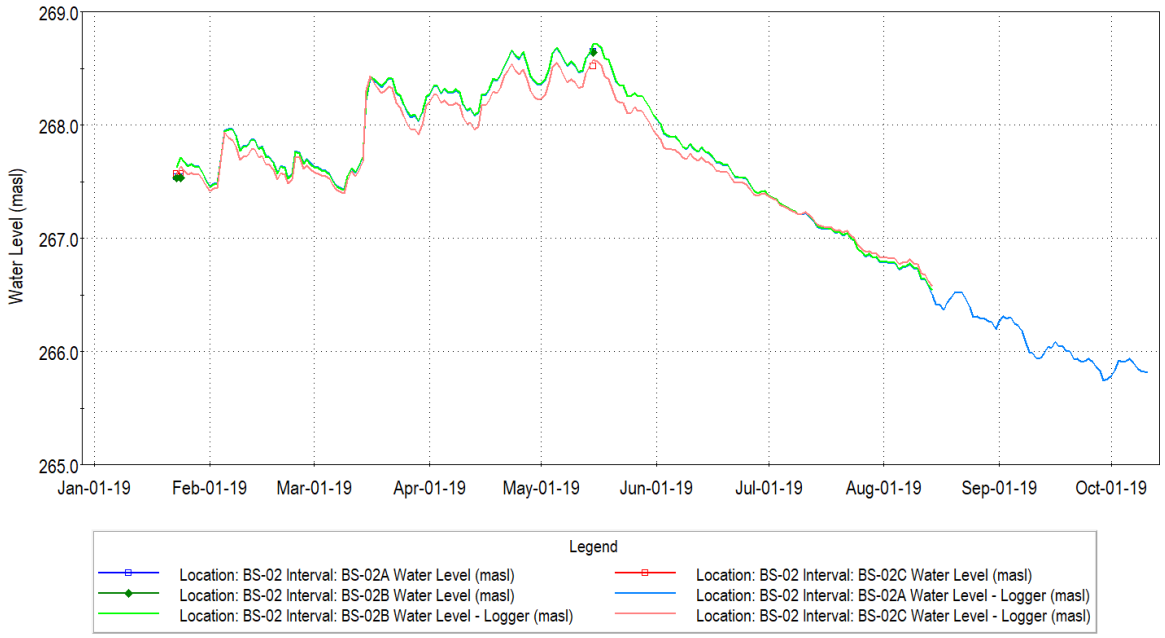
269.0
268.0
267.0
266.0
265.0
Water Level (masl)
Jan-01-19
Feb-01-19
Mar-01-19
Apr-01-19
May-01-19
Jun-01-19
Jul-01-19
Aug-01-19
Sep-01-19
Oct-01-19
Legend
Location: BS-02 Interval: BS-02A Water Level (masl)
Location: BS-02 Interval: BS-02B Water Level (masl)
Location: BS-02 Interval: BS-02B Water Level - Logger (masl)
Location: BS-02 Interval: BS-02C Water Level (masl)
Location: BS-02 Interval: BS-02A Water Level - Logger (masl)
Location: BS-02 Interval: BS-02C Water Level - Logger (masl)

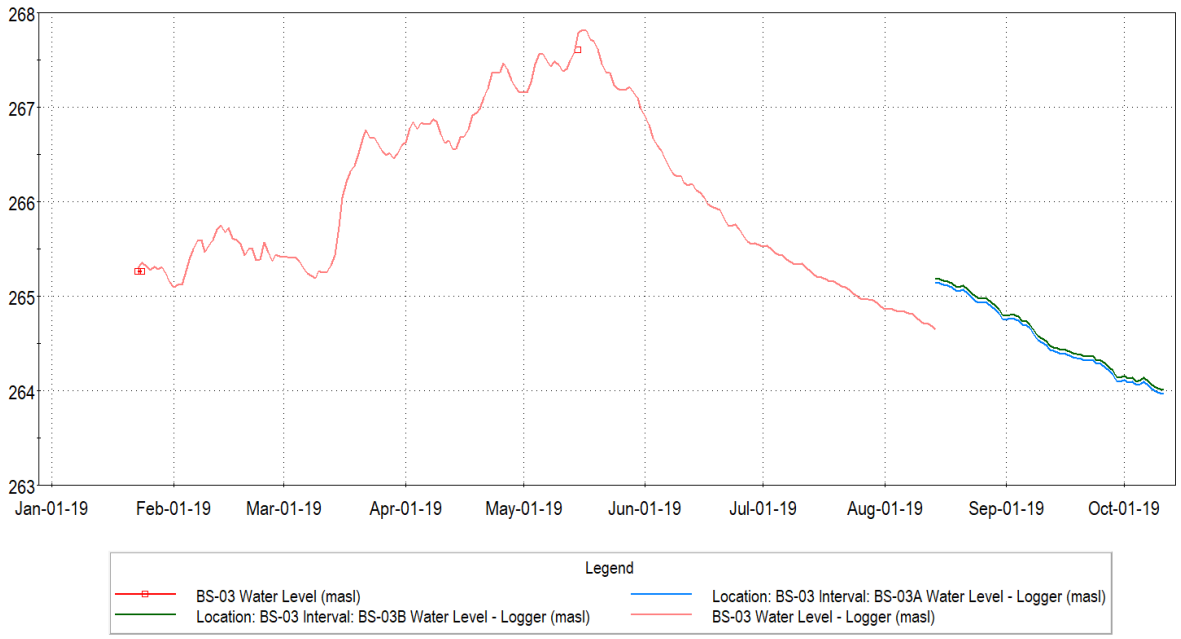
268
267
266
265
264
263
Jan-01-19
Feb-01-19
Mar-01-19
Apr-01-19
May-01-19
Jun-01-19
Jul-01-19
Aug-01-19
Sep-01-19
Oct-01-19
Legend
BS-03 Water Level (masl)
Location: BS-03 Interval: BS-03B Water Level - Logger (masl)
Location: BS-03 Interval: BS-03A Water Level - Logger (masl)
BS-03 Water Level - Logger (masl)

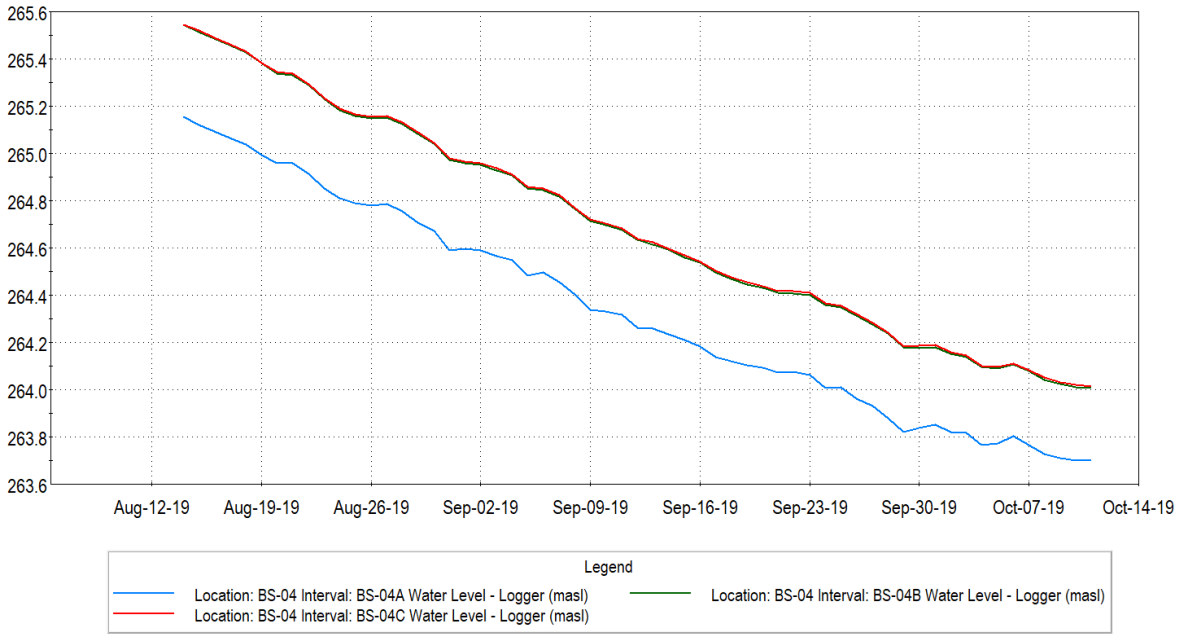
265.6
265.4
265.2
265.0
264.8
264.6
264.4
264.2
264.0
263.8
263.6
Aug-12-19
Aug-19-19
Aug-26-19
Sep-02-19
Sep-09-19
Sep-16-19
Sep-23-19
Sep-30-19
Oct-07-19
Oct-14-19
Legend
Location: BS-04 Interval: BS-04A Water Level - Logger (masl)
Location: BS-04 Interval: BS-04B Water Level - Logger (masl)
Location: BS-04 Interval: BS-04C Water Level - Logger (masl)

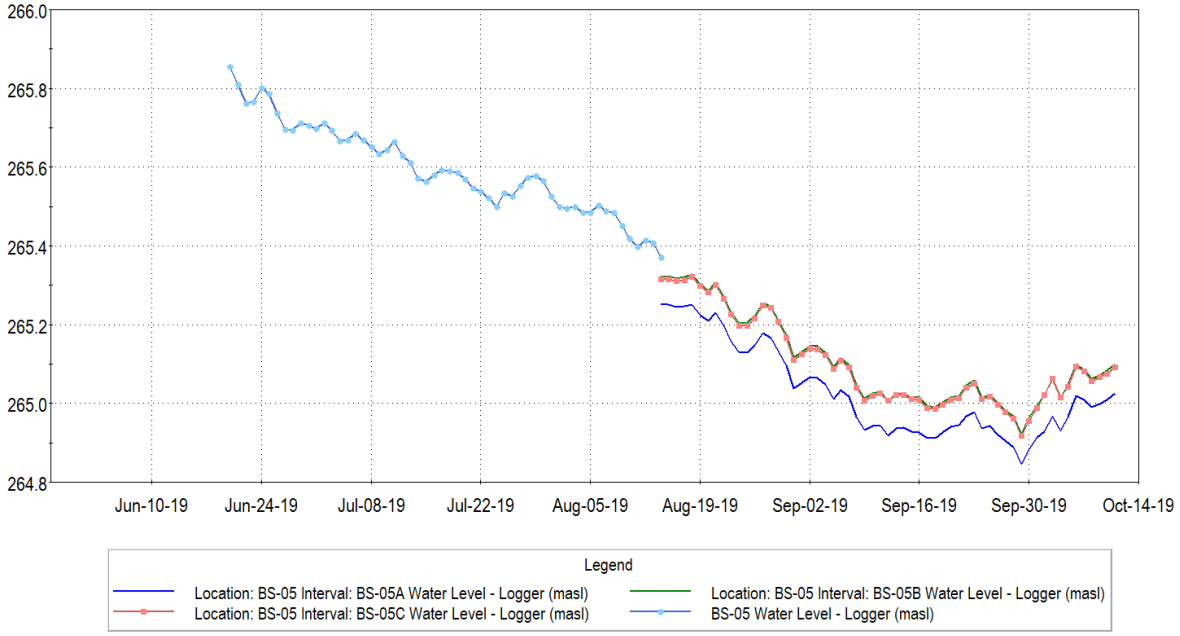
266.0
265.8
265.6
265.4
265.2
265.0
264.8
Jun-10-19
Jun-24-19
Jul-08-19
Jul-22-19
Aug-05-19
Aug-19-19
Sep-02-19
Sep-16-19
Sep-30-19
Oct-14-19
Legend
Location: BS-05 Interval: BS-05A Water Level - Logger (masl)
Location: BS-05 Interval: BS-05B Water Level - Logger (masl)
Location: BS-05 Interval: BS-05C Water Level - Logger (masl)
BS-05 Water Level - Logger (masl)

15.6 Hydrogeochemical Testing

During the field program completed by Azimuth in 2019, 24 ground water samples were collected from 13 locations, while eight additional samples were collected from the Southern Lands to complement the previous geochemical sampling completed by Golder in 2003. This previous sampling of the Southern Lands included 22 water quality samples collected from 21 locations. Waterra tubing and inertial foot valve pumps were equipped in the wells to acquire the water samples, which were collected during the May and August monitoring events to assess potential seasonal water quality variance at the Site. The parameters collected for each water quality sample included a total of 49 parameters including general inorganics, nutrients and trace metals. The water quality package is a standard package routinely utilized to characterize the water type and can be used to identify aquifer recharge areas, aquifer flow processes, and the degree of hydraulic connection between differing aquifers.

All samples collected by Azimuth field staff were completed using contemporary sampling protocols with the purging of at least three borehole volumes prior to sample collection. In all instances where the wells were found to dry out, samples were collected following sufficient recovery such that a representative water sample could be collected. Caduceon Laboratories, which is CALA certified was utilized for all analytical work on this project with all samples submitted to the laboratory within 24 hours such that all applicable hold times were achieved.

The reliability of the major ion water quality data was assessed based on the ionic charge balance error (Mandel and Shiftan, 1981; Lloyd and Heathcote, 1985). The ionic charge balance error (C.B.E.) is defined as:

$$CBE = \frac{\sum cations - \sum anions}{(\sum cations + \sum anions)/2} \times 100$$

Where concentrations of cations and anions are expressed as meq/L. A CBE of less than 15% is commonly used as the criterion for acceptance of a water quality analysis. All the CBE for the dataset collected in 2019 are below 15%.

Major ion chemistry was useful to identify some of the more important sources of water to the ground water flow regimes. Piper diagrams (Piper, 1944) were used for the chemical analyses of the ground water. The ratio of the major ion chemistry from a water source tends to remain unchanged, unless influenced by an external factor. This ratio, or “hydrogeochemical signature”, allows an evaluation of different water sources. These diagrams can be used to show the effects of various factors, including major and minor ion composition, of possible source waters, as well as, the effects of aquifer mixing. The effects of hydrogeochemical interactions between water and soil or aquifer minerals may also be indicated. The Amabel Formation consists of dolomite. Dolomite is a mineral (formula $Ca{\cdot}Mg{\cdot}(CO_3)^2$) consisting of a calcium magnesium carbonate.

Geochemical sampling results from both the Southern Lands and Western Lands yield a generally similar geochemical signature. As expected, there is a strong carbonate signature owing to the host limestone. The overlying till soils also have a similar calcium magnesium carbonate geochemical signature since these soils were derived from the host rock setting in Southern Ontario.

Some variations owing to external influences (ex., road salt) have been detected in certain wells at the Western Lands (ex., BS-04 and BS-02). This external influence is far less obvious for the wells geochemically sampled on the Southern Lands.

Similarly, some vertical differences exist at certain monitoring locations. For example, elevated sulphate concentrations were measured in a several monitoring well intervals which possibly represent specific mineralogy (ex., anhydrite presence) for certain conductive fractures. Specific minor ion chemistry also was noted to show some typical limestone mineralogy variations such as the presence of an elevated strontium geochemical signature relative to the water quality of the remaining well intervals.

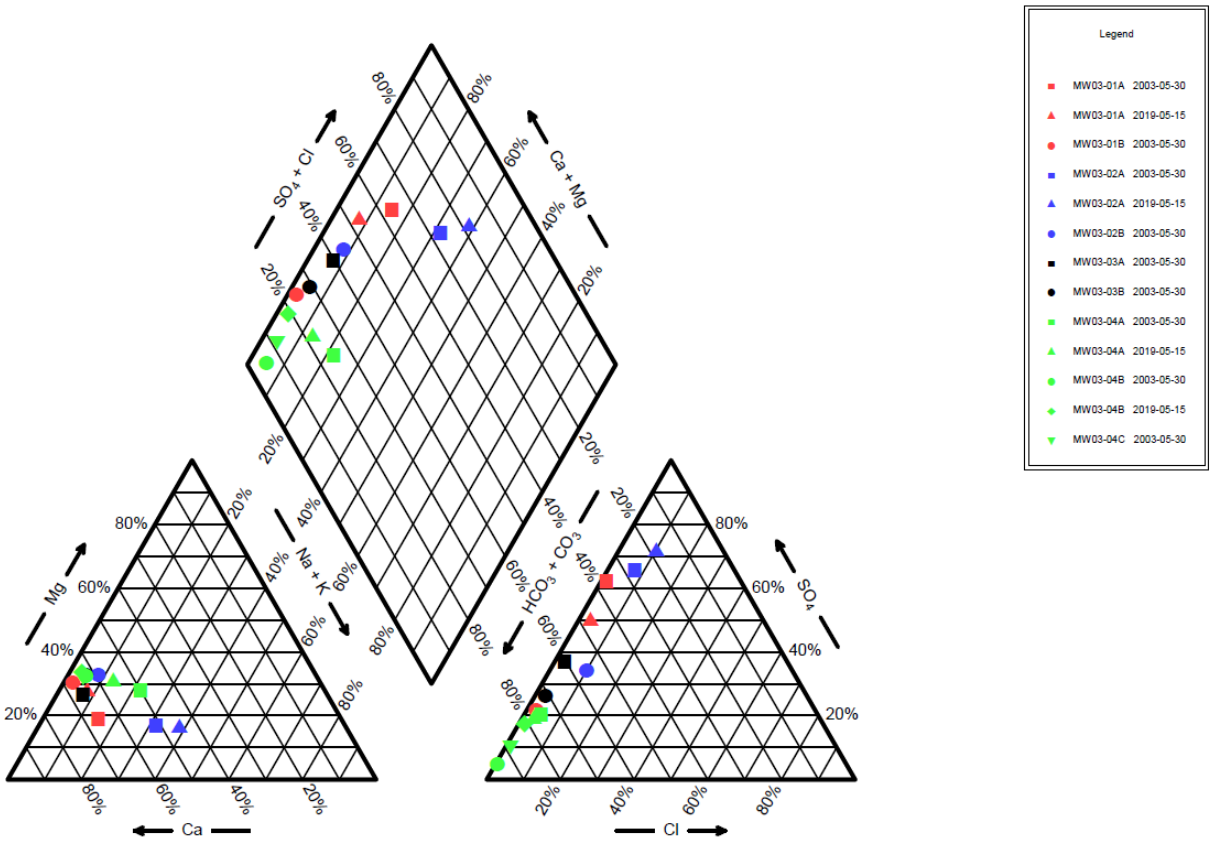

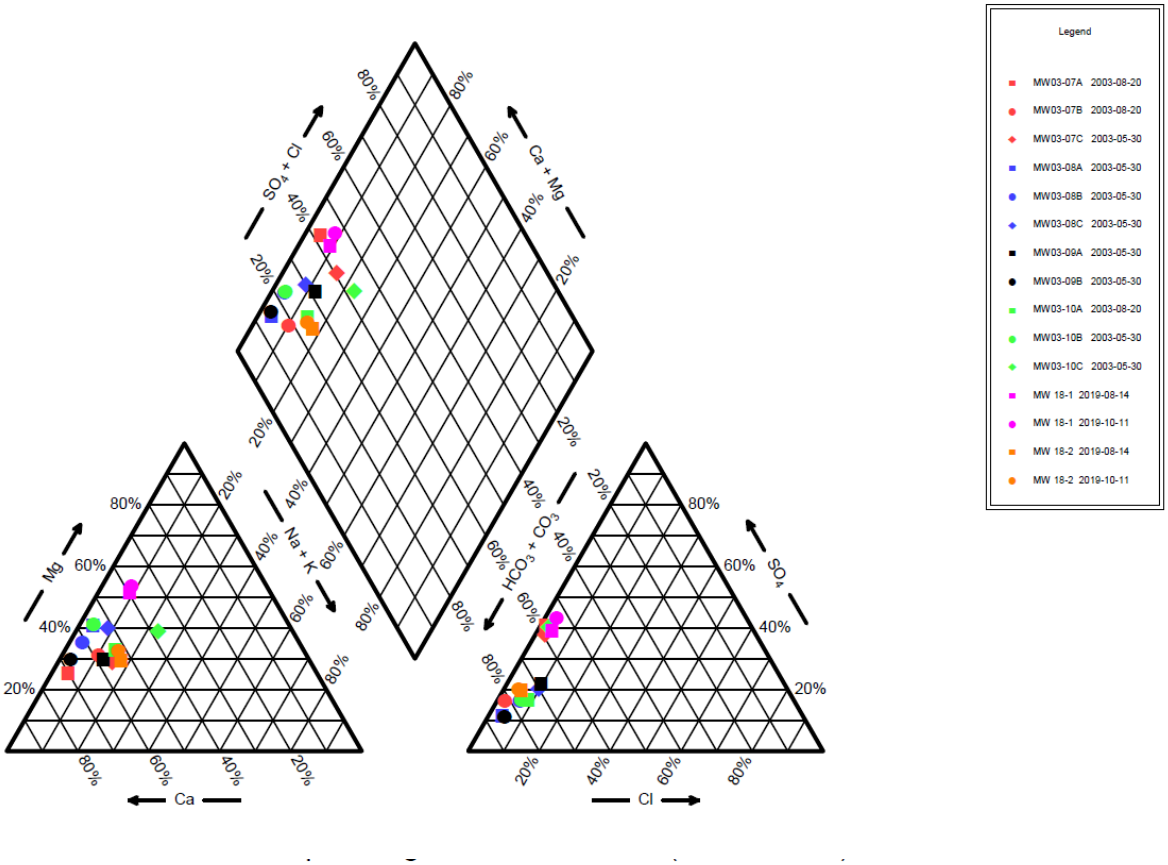
Legend
MW03-07A 2003-08-20
MW03-07B 2003-08-20
MW03-07C 2003-05-30
MW03-08A 2003-05-30
MW03-08B 2003-05-30
MW03-08C 2003-05-30
MW03-09A 2003-05-30
MW03-09B 2003-05-30
MW03-10A 2003-08-20
MW03-10B 2003-05-30
MW03-10C 2003-05-30
MW 18-1 2019-08-14
MW 18-1 2019-10-11
MW 18-2 2019-08-14
MW 18-2 2019-10-11
SO4 + Cl
Ca + Mg
Na + K
HCO3 + CO3
Mg
SO4
Ca
Cl

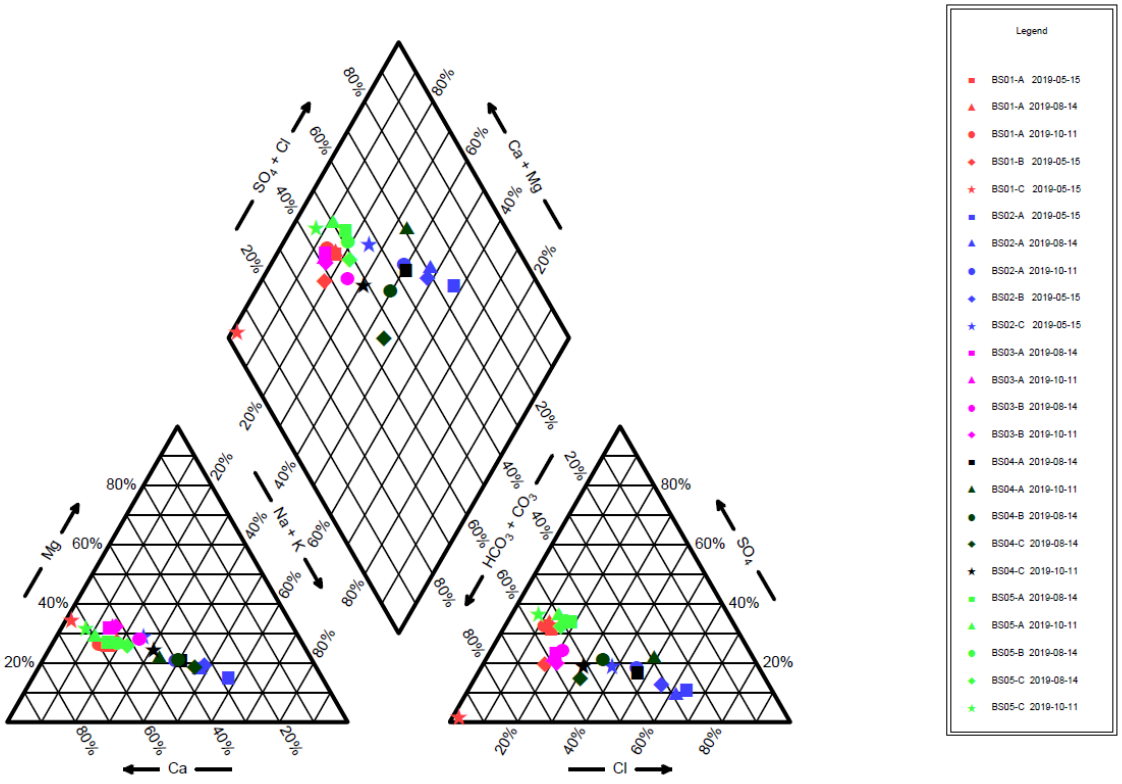
Legend
BS01-A 2019-05-15
BS01-A 2019-08-14
BS01-A 2019-10-11
BS01-B 2019-05-15
BS01-C 2019-05-15
BS02-A 2019-05-15
BS02-A 2019-08-14
BS02-A 2019-10-11
BS02-B 2019-05-15
BS02-C 2019-05-15
BS03-A 2019-08-14
BS03-A 2019-10-11
BS03-B 2019-08-14
BS03-B 2019-10-11
BS04-A 2019-08-14
BS04-A 2019-10-11
BS04-B 2019-08-14
BS04-C 2019-08-14
BS04-C 2019-10-11
BS05-A 2019-08-14
BS05-A 2019-10-11
BS05-B 2019-08-14
BS05-C 2019-08-14
BS05-C 2019-10-11
SO4 + Cl
Ca + Mg
Na + K
HCO3 + CO3
Mg
SO4
Ca
Cl

15.7 Residential Well Survey

A preliminary private door-to-door water well survey was completed by Nelson personnel and a Professional Geoscientist on July 29th and July 30th, 2019. The survey was completed to all residents located within 1 km of the proposed expansion lands, including those located on both the north and south sides of Sideroad No.: 1. In total, 156 homes were visited. The purpose of the water well survey was to collect baseline information on the local water use (quality and quantity) to ensure the sustained quality and quantity of the water supply and to discuss the proposed expansion. If residents were not home, an information package was left at their front door. The package included an informative flier on the proposed application, details about the well monitoring program, and Nelson's contact information.

Of the 156 homes visited, only eleven (11) homeowners indicated that they were interested in participating in the monitoring program. Seven (7) of the eleven (11) private domestic water wells were accessible and, as a result, have been added to the current groundwater monitoring program

16 Appendix B: Karst Investigation

Karst investigations and conceptual model of the bedrock aquifer at the proposed Nelson Quarry extensions

Stephen R.H. Worthington

Worthington Groundwater

April 25, 2020

16.1 Introduction

The existing Nelson Quarry and proposed extensions are located in dolostone rocks of the Goat Island and Gasport Formations. Flow in dolostone rocks is somewhat different from flow in sediments such as sand, and a common question is whether these rocks are karstified, and if so, what are the practical implications. This report described the investigations that were carried to answer these questions, and describes how water flows through the dolostone aquifer.

The Gasport Formation is named after Gasport, New York, which is 110 km east of Burlington. Goat Island is located between the Horseshoe Falls and American Falls, at Niagara Falls. The usage of these names such a long distance from the type localities is an indication of the lateral persistence of these rocks. Consequently, only minor variations in lithology are expected in the area of the site, and studies from elsewhere can inform the expected aquifer characteristics at the site. For instance, extensive measurements of the matrix of the rock have been made in the Smithville and Cambridge areas, showing that the mean porosity of the rock is about 7% and mean matrix hydraulic conductivity is about 10-7 m/s (Novakowski et al., 1999; Perrin et al., 2011). Pumping tests and numerical models of the site have shown that the total hydraulic conductivity of the aquifer is about 10-5 m/s to 10-4 m/s (see Azimuth and Earthfx reports). This shows that more than 99% of the flow in the aquifer is through the fracture network rather than through the matrix of the rock. This is a common situation in bedrock aquifers, which are referred to as dual-porosity aquifers.

The fractures in the rock were formed by physical processes such as tectonic stresses and unloading of the rock after the melting of the glacier that covered Ontario in the last ice age. Similar fracturing also occurs in shale, such as the Queenston Shale, which outcrops to the east of the Niagara Escarpment. However, the permeability of dolostone is on average four to five orders of magnitude greater than that of shale. The large difference is explained by the greater solubility and higher dissolution rate of dolomite, the main mineral in dolostone, compared to the minerals in shale such as quartz, illite and kaolinite (Worthington et al., 2016). Dissolution of the bedrock is focussed where the most flow is, which is along fractures. This results in a positive feedback loop, creating a network of solutionally-enlarged fractures through which most of the groundwater flows (Worthington and Ford, 2009). Bedrock aquifers where the permeability has been enhanced by dissolution are sometimes called karst aquifers, though there are a number of definitions for the term karst aquifer (Worthington et al., 2017). Where streams flow over dolostone bedrock, then there is the potential for substantial enlargement of underlying fractures, and on occasion these can be enlarged to become caves. However, percolation of rainfall into the bedrock favours the enlargement of the many interconnected fractures through which the water flows, producing a network of enlarged fractures (called channels, solutionally-enlarged fractures, or open fractures) that typically have apertures in the 0.1 mm - 10 mm range (Worthington and Ford, 2009).

The goal of the karst investigation in the study area is (a) to document the presence of surficial karst features that are relevant to aquifer hydrogeology such as sinking streams, springs, and discharges from quarry walls, (b) to carry out subsurface investigations to characterize the apertures and spacing of solutionally-enlarged fractures, and (c) to interpret the results to explain how water flows through the dolostone aquifer. These three tasks are described below in sections 2, 3, and 4, respectively.

16.2 Surficial karst features

2.1 Discharge from the walls of the existing quarry

An examination of quarry faces in winter can give a good indication of the nature of flow in a carbonate aquifer. Small discharges from such faces readily freeze and are visible as deposits of ice on the face. Major discharges may have enough flow of relatively warm groundwater that they only partially freeze, but the large flow of water is readily visible flowing down a quarry face. The quarry faces were visited on two occasions in cold winter conditions. Figure 1a shows the locations of photos taken and of sinks and springs, and Figure 1b shows the location of the wells referred to in this report. Figures 2 and 3 show typical accumulations of ice on quarry faces. In Figure 2, most of the discharge appears to be from several closely-spaced bedding planes close to the base of the face. Such flow is not unexpected because drawdown of the water table around the quarry by pumping from the quarry sumps should result in greater flow near the base of the quarry faces.

The higher parts of the face in Figure 2 as well as the section of face shown in Figure 3 have only sparse deposits of ice. These photos were taken on the eighth consecutive day of sub-zero temperatures, and the mean temperature in this period was -6.3 ^{o}C. Consequently, the ice that accumulated over this period only represents small discharges of groundwater, and represents flow from channels of a few millimetres or less in aperture. A feature of note is the much larger void shown in Figure 3 close to the base of the face. There was no flow of water from this feature, which consequently was an isolated void rather than part of the interconnected channel network.

The overall distribution of ice deposits on the face gives one indication that there is preferential flow in the aquifer along channels and that there are many such channels. The aperture of these channels is likely to be predominantly in the millimetre range.

2.2 Karst features on the extension lands and adjacent properties

The surface features of the South Extension lands were examined during the pumping test on February 10-13, 2006 and on several subsequent occasions. The first was a field trip to examine karst features on March 14, 2006 when Daryl Cowell, the peer review karst expert, was present. On that occasion the perimeter of the extension lands was visited and the East Arm of the West Branch of Mount Nemo Tributary was followed downstream to a sinkpoint (Figure 4) and a series of springs located in a dug pond that was 162 m to the south of the sinkpoints (Figure 5). The second was on March 22, 2006, when a tracer test was carried out at the sinking stream (Figure 6). The third occasion was March 23, 2006, when the extension lands were extensively searched for karst features. The Medad valley was traversed, from south of Lake Medad to the monitoring location SW02B (Figure 1). Several springs were located, and their electrical conductivity, temperature, and discharge were recorded (Table 1). In addition, the adjacent farm property between the extension lands and Guelph Line was also searched for karst features. Additional measurements were made on April 6, 2006 (Table 2).

A series of depressions in a wooded area along the south-east boundary of the property were visited on March 14, 2006. The deepest depression was about 10 m long, 6 m wide and 2 m deep. The consensus at that time was that the depressions represented small glacial kettle holes rather than karstic sinkholes. The visit on March 22, 2006 strengthened this opinion as two of the three largest depressions had standing water in them, covered by a layer of ice (Figure 7). This indicated that the permeability at the base of these depressions was extremely low. The largest depression had no standing water, however, indicating that the permeability at the base of this depression is somewhat higher than the other depressions. There were no channels entering this depression, no evidence of collapse, and the side slopes are gentle, so it is probably glacial rather karstic in origin. However, it is

possible that the focussing of recharge at one point has resulted in dissolution of the underlying bedrock.

In a low-lying wooded area in the south-west part of the extension lands there are a series of small springs. A number of small springs and seeps were noted in an area of 30 m by 30 m. The largest single spring had a discharge of less than 0.5 L/s. All the flows combine to form a creek that had a flow of 4 L/s at the property line, close to monitor OW3-32. The creek flows west from here to join the West Arm of the West Branch of Mount Nemo Tributary. The location of the springs in a shallow valley and the low discharge of these springs indicate they are likely to be depression discharges from the overburden, which has a depth of 1.02 m at OW3-32.

The surface features of the West Extension lands were examined on April 22, 2019. Only one potential karst feature was found, a closed depression about 25 m west of the southernmost of the artificial ponds on the golf course property. The landscape in this area has been heavily modified, so it is not possible to tell whether the depression is natural. Water was ponded in the base of the depression at the time of the visit, so it does not perform a karstic function at the moment, even if it is a natural depression.

With the exception of the sink to spring flow shown in Figures 4 and 5, there is a notable absence of surface karst features in or adjacent to the extension areas. This is in marked contrast to areas close to the Niagara Escarpment, where the overburden in thinner and karst features are common.

2.3 Characterizing the sink to spring connections

Two streams were found to sink into the ground in the study area, and it was assumed that these flow to nearby springs (Figure 1). This assumption was tested by tracer testing from the sink on the East Arm of the West Branch of Mount Nemo Tributary and by water level measurements on Willoughby Creek Tributary, as described below.

2.3.1 East Arm of the West Branch of Mount Nemo Tributary

To the south-east of the South Extension, the East Arm of the West Branch of Mount Nemo Tributary sinks into the ground at several sinkpoints (Figure 4). Several springs are located 162 m to the south (Figures 1 and 5). A fluorescent dye was injected into the sinking stream at the principal sinkpoint (Figure 6). Details of the test are given in Appendix A. The tracer travelled to the springs at a velocity of 1600 m/d, which is typical for conduit velocities in karst. There are several sinkpoints and springs, and flow between them is likely to be through several conduits in the shallow weathered bedrock. The sum of the calculated cross-sections of these conduits is 0.3 m^2.

2.3.2 Willoughby Creek Tributary

Willoughby Creek Tributary flows into a sinkhole downstream from the monitoring point on Colling Road at SW1 (Figure 1). A large spring 400 m to the west in the Cedar Spring valley (Spring K in Figure 1) was presumed to be the resurgence for this sinking stream. To confirm this, water levels were recorded at this spring at 15 minute intervals over a period of two weeks (Figure 8). Figure 9 shows greater detail of the water levels over the last three days of this period. Pumping from the quarry sump took place between 2 am and 5 am on these days. The spring water levels started to increase one hour after the start of pumping, and started to decrease one hour after the cessation of pumping. Part of this lag time is accounted for by flow along the surface creek so the lag time through the sink to spring connection is less than one hour (Figure 1). The short lag time indicates an efficient sink to spring conduit connection. Spring J has a similar electrical conductivity to the sinking stream, which suggests that the stream not only connects with Spring K but also with Spring J.

16.3 Tests using wells

Two types of well tests were used to characterize the aquifer. Pumping tests and tracer tests were both used to characterize the aquifer between wells, and are described in Section 3.1. Single-well tests included packer tests and flowmeter, video, televiewer, electrical conductivity and temperature logging. These are described in Section 3.2.

3.1 Tests between wells

3.1.1 Celerity values from pumping tests

Celerity refers to the speed of a pressure pulse. In aquifers, these are associated with decreases in pressure, such as during a pumping test, and increases in pressure, such as when the water table rises following rain or snowmelt. Celerities in unconfined aquifers can exceed 10 km per day, resulting in rapid response of springs and streams to rain and snowmelt events (Worthington, 2019).

There is a rapid decrease in water level in the pumping well when a pumping test starts, and the arrival time of the drop in pressure is routinely recorded in monitoring wells. Results from pumping tests at PW-1 in 2006 and BS-06 in 2019 give celerities of 3.9 km/d to 49 km/d (Table 3).

3.1.2 Tracer testing during the pumping test at PW-1

Tracer testing was carried out during the February 2006 pumping test to gain more knowledge on fracture apertures and on the connectivity of large-aperture fractures. A summary of tracer results are given in Table 4, and full details of the methodology and results are given in Appendix A.

Fluorescent dyes were introduced over three days into six bedrock monitors located from 14 m to 24 m from the pumping well. Traces from five of the six monitors used gave groundwater velocities of 72 - 160 metres per day, indicating efficient connection with the pumping well through channels. It is likely that many of these channels have diameters in the range 0.1-1 mm, a smaller number are in the range 1-10 mm, and relatively few have diameters > 1cm. The tracer from the sixth monitor was not recovered when the pumping test was terminated 24.3 hours after injection, and this showed that there was no efficient channel connection between this monitor and the pumping well.

3.2 Single well tests

3.2.1 Packer tests

Packer tests made a series of measurements of transmissivity in a well. Packer testing was carried out by Golder Associates in 2003 and by Azimuth in 2019, and results are found in the respective reports. Results presented here are for calculations of fracture characteristics from the packer test results. The calculated mean hydraulic conductivity from the packer testing is 6.15×10^{-5} m/s, with a standard deviation of log hydraulic conductivity of 0.79 (Table 5). This table also shows calculated fracture apertures for the most transmissive interval, assuming that the transmissivity in each well is associated with a single fracture.

The hydraulic conductivity in each well was measured by packer testing, and this enables the aperture of the flowing fractures to be estimated from the cubic law

$K = \rho g N b^3 / 12\mu$

where K is the hydraulic conductivity, ρ is the density of water, g is gravitational acceleration, N is fractures per unit distance, b is fracture aperture, and μ is dynamic viscosity. The calculated maximum fracture apertures for each well are given in Table 5.

The testing in 2019 used a much smaller test interval (~1 m) than the 2003 testing (~3m). The smaller interval allows more accurate determination of fracture porosity values, so only the 2019 data were used to determine fracture porosity. The individual fracture apertures for each tested interval in each well were summed to give the total fracture apertures for each well. These were then divided by the sum of the tested intervals to give the fracture porosity, which ranged from 0.00013 to 0.00059 (Table 6).

3.2.2 Video, televiewer, and flowmeter logging

Video and televiewer logs do not directly produce quantitative data, but they are nevertheless invaluable for developing conceptual models of bedrock aquifers. These visual logs are ideally coupled with measurements of flow from flowmeter logs or of transmissivity from packer tests. The combination shows whether flow in a bedrock aquifer is mostly seeping slowly through the pores of the rock, or whether there is more rapid flow through fractures. If the latter is true, then the shape of the fractures can show whether their apertures are due solely to physical stresses, or whether weathering has dissolve the rock to produce elliptical channels. Select video, televiewer, and flowmeter logs are shown in Appendix B. The full logs are found in the respective Golder and Azimuth reports.

Flow in the dolostone aquifer is principally through fractures, and the fractions of total flow through the most productive fractures can be calculated from flowmeter or packer test data. Results are shown in Table 7, and these results are compared to data from the literature in Figure 10.

3.2.3 Electrical conductivity and temperature logging

Profiling of electrical conductivity and of temperature at monitoring wells during pumping tests can help show the nature of preferential flow in bedrock aquifers, and how water quality can change over time (Worthington and Smart, 2017). Profiling was carried out at Well BS-07 before, during, and after the pumping test at BS-06 in October 2019. Profiling was also carried out in the pumping well before and after the pumping test. Further details and the results are found in Appendix C.

16.4 Conceptual model of the dolostone aquifer

4.1 Large conduits

Large conduits were identified at two locations in the Mount Nemo plateau (Section 2.3). Tracer testing of the 162 m long sink to spring connection on the East Arm of the West Branch of Mount Nemo Tributary gave an estimated conduit cross-section of 0.3 m^2. This is probably divided between several conduits. The conduit along Willoughby Creek Tributary drains a larger area and thus may be larger in size if it is a single conduit. The depth of these conduits is unknown. However, Worthington (2001) showed that depth of conduit flow below the water table is a function of both stratal dip and flow path length. The shallow stratal dip (0.4° at the extension lands) and the short flow paths between sink and spring give predicted conduit depths of less than 1 m below the water table. While such a calculation is not exact, it does indicate that these major conduits are in the upper part of the bedrock.

Further large conduits (with diameters greater than 10 cm) are also likely to occur upgradient of and close to the larger springs that are found at the perimeter of the Mount Nemo plateau. It is possible that large conduits were formed between sinking streams and springs before the last glaciation. It is

most likely that such ancient conduits linking sinks to springs would also have formed in the uppermost bedrock and consequently would have been eroded away during the subsequent glaciation.

4.2 Open fractures

The observations of discharge at the quarry faces (Figures 2 and 3) show that there are many open fractures in the aquifer. The occurrence of many small springs along the Medad Valley (Table 1 and Figure 1) gives an indication of how dissolution and self-organization of flow in the aquifer results in flow to many smaller springs rather than one or two large springs.

The testing between wells (Section 3.1) demonstrates the connectivity of open fractures between wells. Pressure pulses from pumping tests or recharge events propagate through the network of open fractures, and result in the high celerity values of 3.9 km/d to 49 km/d (Table 3). Calculations from tracer testing between wells gives calculated apertures of less than 1 mm (Table 4).

The testing within wells (Section 3.2) gave complementary data of fracture characteristics. Packer testing allows the calculation of maximum fracture apertures (0.17 mm to 1.59 mm - Table 5) and fracture porosity (0.00019 - 0.00059 - Table 6). This porosity largely represents the porosity of bedding-plane fractures. These are much more likely to be intersected by wells than joints, which are almost all close to vertical. The addition of joint porosity would increase fracture porosity somewhat, perhaps to about 0.001. The fracture aperture and fracture porosity calculations in Tables 4, 5, and 6 are all based upon the assumption that fracture flow is through smooth, straight, constant aperture fractures. However, televiewer logs show that fracture enlargement along bedding planes is irregular. This is because dissolution enlarges fractures, with the most dissolution occurring where there is the most flow. This results in a positive feedback loop where parts of the bedding plane are enlarged to form elliptical channels that may have apertures >1 cm, while much of the bedding plane remains minimally enlarged. This is illustrated well in the televiewer images at depths of 1.85 m, 8.09 - 8.13 m and 18.79 - 18.84 m in BH06-1 (Appendix B, pages 31-33) . Occasionally, a well may intercept a joint, and flow from a joint in BS-05 is shown by the flowmeter log, with the televiewer logs showing that the joint is intercepted from a depth of 11.55 m to 12.10 m (Appendix B, page 36). The preferential enlargement of fractures by dissolution results in maximum apertures that are always somewhat larger than are indicated by calculations such as those in Tables 4, 5, and 6.

Packer testing, televiewer, flowmeter and electrical conductivity logs all help show the spacing of the major flowing fractures in a well. Typically half the flow in a bedrock well comes from the most productive fracture, and 20% and 10% come from the second and third most productive fractures, respectively. Measurements show this to be the case in the dolostone aquifer in the study area (Table 7), and it is also true globally, not just in carbonate aquifers but also in other bedrock lithologies (Figure 10).

The data presented above shows that fracture porosity is very low (~0.001) and is much less than the porosity of the matrix (~0.07). Consequently, almost all the storage is in the matrix. Conversely, the hydraulic conductivity of the matrix (~10^{-7} m/s) is very low, and is only a very small fraction of the bulk hydraulic conductivity of the aquifer (~10^{-5} to 10^{-4} m/s). Consequently, almost all the flow is through the fracture network. This combination of properties makes the aquifer a dual-porosity aquifer, like many bedrock aquifers.

4.3 Does the dolostone behave as a karst aquifer?

A common question is whether carbonate aquifers are karst aquifers. This question is considered to be an important one by some hydrogeologists, who divide carbonate aquifers into karstic aquifers and non-karstic aquifers, and who consider that numerical of flow and transport in the former is less predictable than in the latter. The problem in answering this question is that there are several

conflicting definitions of what constitutes a karst aquifer. Worthington et al. (2017) discuss the five major definitions. The aquifer is karstic according to two definitions, having solutionally-enlarged fractures and a hydraulic conductivity >10^{-6} m/s. The aquifer is not karstic according to one definition because it has no caves, and is sparsely karstic according to two definitions, having little turbulent flow and few karst landforms. However, classifying the aquifer as karstic or non-karstic is not important; instead, the important issue in the context of developing a quarry is to understand aquifer behaviour.

A useful way to consider aquifer predictability is to assess the variability between wells by calculating the standard deviation of the logarithm of either transmissivity (SD log T) or hydraulic conductivity (SD log K). A karst aquifer in England which has many caves has SD log T of 1.31, while three other English limestones which are generally considered as not karstic and have very few caves have SD log T values of 0.74, 0.76, and 1.02, respectively (Worthington and Ford, 2009). The SD log K value in the study area for the packer test data is 0.79 (Table 5), suggesting that the aquifer is towards the more predictable end of the spectrum of carbonate aquifers.

4.4 Practical consequences of the aquifer structure

The low value of SD log K reflects the common occurrence of solutionally-enlarged fractures in wells, which shows that the network has a dense network of these fractures. This means that treating the aquifer as an equivalent porous medium can give reliable results for steady-state modelling of flow. However, transient modelling of flow and modelling of transport are somewhat more complicated because of the dominance of fracture flow over the short-term such term, and the addition of drainage from and recharge to the matrix over the long term such as seasonally (Worthington et al., 2019). If this transience is properly accounted for, then there is no reason why numerical models should not give good results for transport.

16.5 References

Golder Associates, 2004, Hydrogeological and water resources assessment of the proposed Nelson Quarry Co. Extension.

Novakowski, N., P. Lapcevic, G. Bickerton, J. Voralek, L. Zanini and C. Talbot, 1999, The development of a conceptual model for contaminant transport in the dolostone underlying Smithville, Ontario. National Water Research Institute, Burlingon, Ontario, 98 p.

Perrin, J., Parker, B.L, Cherry, J.A., 2011. Assessing the flow regime in a contaminated fractured and karstic dolostone aquifer supplying municipal water. Journal of Hydrology, 400, 396-410.

Worthington, S.R.H., 2001. Depth of conduit flow in unconfined carbonate aquifers, Geology, 29, 335-338.

Worthington, S.R.H., 2019. How preferential flow delivers pre-event groundwater rapidly to streams. Hydrological Processes, 33, 2373-2380.

Worthington, S.R.H., Ford, D.C., and Beddows, P.A., 2000b. Porosity and permeability enhancement in unconfined carbonate aquifers as a result of solution, in Speleogenesis: Evolution of karst aquifers, Eds. A. Klimchouk, D.C. Ford, A.N. Palmer and W. Dreybrodt, National Speleological Society, Huntsville, p. 463-472.

Worthington, S.R.H., and D.C. Ford, 2009, Self-organized permeability in carbonate aquifers. Ground Water, 47, no. 3, 326-336.

Worthington, S.R.H. and Smart, C.C., 2017. Transient bacterial contamination of the dual-porosity aquifer at Walkerton, Ontario, Canada. Hydrogeology Journal, 25(4), pp.1003-1016.

Worthington, S.R.H., Davies, G.J., and Alexander, Jr., E.C., 2016. Enhancement of bedrock permeability by weathering. Earth-Science Reviews, 160, 188-202.

Worthington, S.R.H, P-Y. Jeannin, E.C. Alexander, Jr., G. J. Davies, and G.M. Schindel, 2017. Contrasting definitions for the term ‘karst aquifer’. Hydrogeology Journal, 25, 1237-1240.

Worthington, S.R.H. Foley, A.E. and Soley, R.W.N., 2019. Transient characteristics of effective porosity and specific yield in bedrock aquifers. Journal of Hydrology, 578, 124129.

16.6 Tables and Figures

Table 1 Location and details of springs and creek flows measured on March 23, 2006

Grid easting (m)	Grid northing (m)	Electrical conductivity (µS/cm)	Temp. °C	Discharge (L/s)	Notes
590413	4802022	1095	7.7	2	by tank, <50 m from road
590416	4802034	793	7.9	1	
590343	4802077	758	8.3	-	
		853	8.7	5	5 m to north, Spring A
590343	4802081	836	8.4	1	at foot of slope
		799	8.6	1	2 m to north
590236	4802270	842	6.9	5.5	Circular spring in flood plain, flows into L. Medad, Spring B
590230	4802317	803	7.3	0.5	5 m from base of slope, flows into L. Medad
590218	4802352	769	7.3	0.3	below old track, flows into L. Medad
590140	4802486	616	7.3	0.3	at foot of slope, flows into L. Medad
590143	4802506	794	7.1	1.5	behind pump house, flows into L. Medad
590091	4802514	845	7.8	27	north of pump house, flows into L. Medad, Spring C
589963	4802693	881	7.1	1.5	
589993	4802740	809	6.8	0.5	
589915	4802708	779	7.4	3	Spring D
		776	6.7	2	10 m further north, headwaters of L. Medad
589890	4802789	843	6.8	1	in oil pipeline right of way, headwaters of creek flowing north
589880	4802813	722	7.3	3	Spring E
		833	7.5	3	15 m further north, Spring F
589725	4803103	747	5.5	1.5	
589696	4803176	773	5.9	2	
					Dense cedar - end measurement of springs < 3 L/s
589603	4803460	619	7.5	5	Spring G
589259	4803986	989	7.8	3	Spring H
588889	4804485	762	1.2	35	Creek in middle of valley at Second Sideroad right of way
				206	Willoughby Creek at Britannia Road (SW2)

Note: grid locations are with respect to the NAD27 grid

Table 2 Location and details of springs and creek flows measured on April 10, 2006

Electrical conductivity (µS/cm)	Temp. °C	Discharge (L/s)	Notes
1231	8.9	5	discharge from quarry at Colling Road (from small pipe)
1196	12.6	19	Willoughby Creek Tributary at Colling Road (SW1)
1219	6.4	5	Spring J (east of road)
1127	8.9	32	Spring K, at outlet from lake below waterwheel
882	10.1	140	Willoughby Creek at Britannia Road (SW2)

Table 3. Celerity values from pumping tests

Pumping well	Monitoring well	Distance from pumping well (m)	Celerity (m/d)
PW-1	MW03-04	13	3900
	OW03-22	17	8160
	OW03-23	38	16,600
	OW03-24	63	19,300
	OW03-25	57	17,500
BS-06	BS-03	17	49,000
	BS-07	37	15,200

Table 4. Groundwater velcities and fractures apertures from tracer tests to PW-1

Well	Tracer velocity (m/day)	Distance to PW-1 (m)	Channel diameter (mm)
MW03-04A	160	13.7	0.095
MW03-04B	<14	13.7	<0.046
MW03-04B	<14	13.7	<0.028
OW03-22A	72	16.1	0.066
OW03-22B	110	16.1	0.27
OW03-22B	110	16.1	0.15
OW03-27A	120	23.7	0.091
OW03-27A	120	23.7	0.093
OW03-27B	130	23.7	0.19
OW03-27B	130	23.7	0.095
OW03-27B	130	23.7	0.19
OW03-27B	130	23.7	0.096

Table 5. Fracture transmissivities and apertures from packer tests

Well	Hydraulic conductivity (mean- m/s)	Hydraulic conductivity (highest value - m/s)	Fracture aperture (assuming single fracture - mm)
BS-01	3.70E-4	2.50E-3	1.59
BS-02	2.03E-4	1.94E-3	1.46
BS-03	9.19E-6	7.13E-5	0.49
BS-04	1.97E-6	7.17E-6	0.23
BS-05	1.30E-4	2.3E-3	1.54
MW03-01	7.58E-6	1.1E-5	0.26
MW03-02	8.20E-6	1.6E-5	0.29
MW03-03	1.59E-6	3.3E-6	0.17
MW03-04	4.12E-6	1.0E-5	0.25
MW03-07	2.94E-5	1.5E-4	0.62
MW03-08	2.48E-5	5.4E-5	0.44
MW03-09	1.47E-6	5.3E-6	0.20
MW03-10	7.62E-6	2.9E-5	0.36
Mean	**6.15E-5**		
Standard deviation of log K	**0.79**		

Table 6. Fracture porosity from packer tests

Well	Sum of apertures (mm)	Sum of tested intervals (m)	Fracture porosity
BS-01	8.79	14.99	0.00059
BS-02	12.27	21.21	0.00058
BS-03	3.18	16.59	0.00019
BS-04	2.62	20.60	0.00013
BS-05	8.14	21.50	0.00038
Mean			**0.00037**

Table 7. Percentage of the total flows in each well that come from the most productive fractures

Well	Test method	Interval with highest flow or transmissivity (%)	Interval with second highest flow or transmissivity (%)	Interval with third highest flow or transmissivity (%)
OW3-30	Flowmeter	43.2	35.1	13.5
OW3-31	Flowmeter	51.5	24.2	13.3
BS-05	Flowmeter	67.9	20.5	11.4
BS-01	Packer	42.3	25.4	18.6
BS-02	Packer	36.7	17.8	9.6
BS-03	Packer	40.5	22.6	13.5
BS-04	Packer	17.9	13.9	10.1
BS-05	Packer	83.9	2.2	2.2
Mean		**48.0**	**20.2**	**11.5**

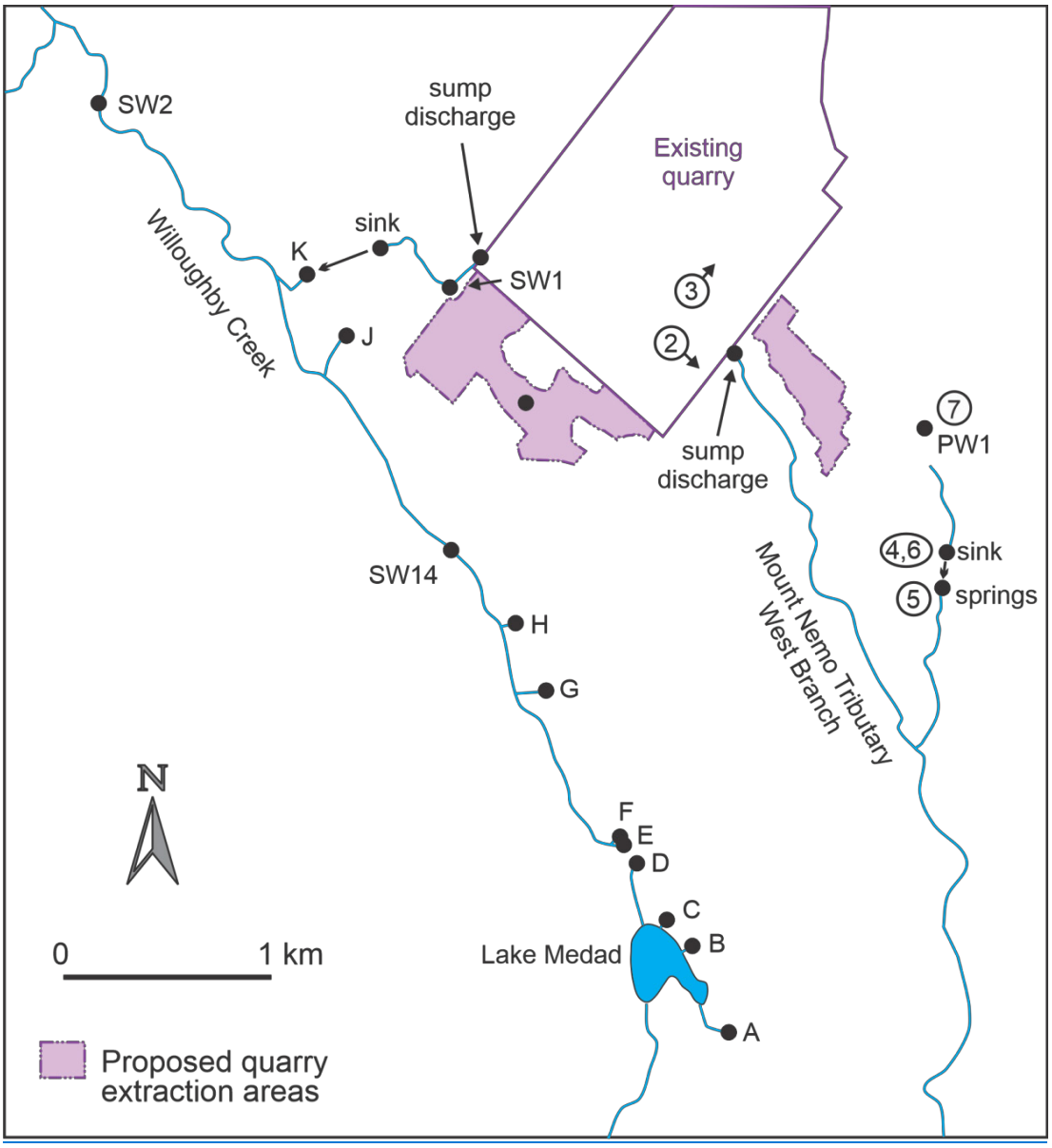

Figure 1a. Location of springs A to K, sinking streams near the quarry, and locations of the photos (circled numbers) shown in Figures 2 to 7.

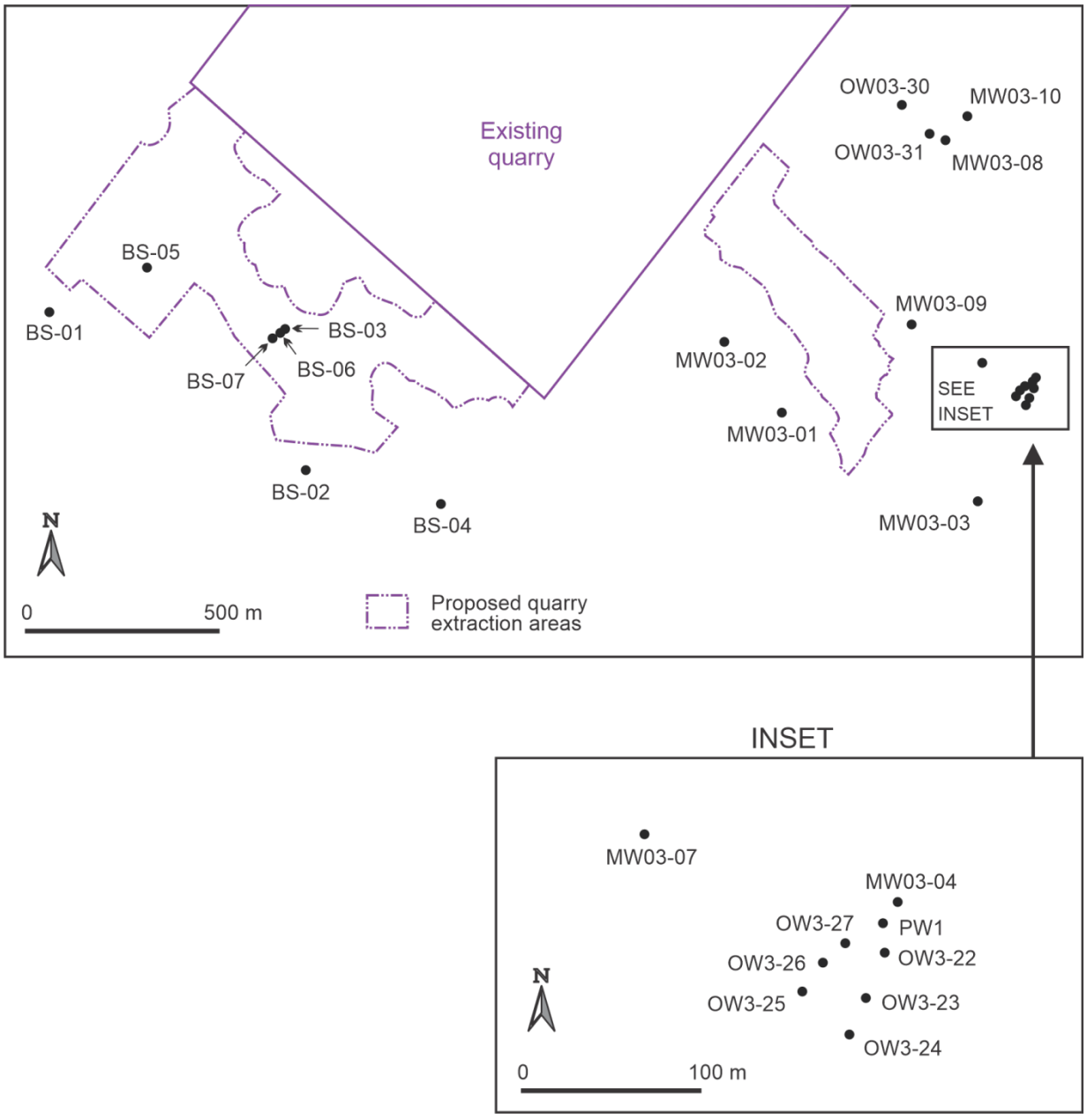

Figure 1b. Location of the wells referred to in this report.

Figure 2. Multiple ice deposits near the base of the quarry wall and spare ice higher in the wall below the processing plant. The location is shown in Figure 1.

Figure 3. A hydrologically-inactive large void near the base of the south-east face of the quarry, together with ice build-ups indicating much smaller channels that are active and discharge water.

Figure 4. Looking north towards the sinkpoint of the East Arm of the West Branch of Mount Nemo Tributary on March 14, 2005

Figure 5. Looking north towards the springs of the East Arm of the West Branch of Mount Nemo Tributary on March 14, 2005

Figure 6. Injection of uranine dye at the sinkpoint of the East Arm of the West Branch of Mount Nemo Tributary on March 22, 2005

Figure 7. Shallow closed depression close to the boundary of the extension lands on March 23, 2006.

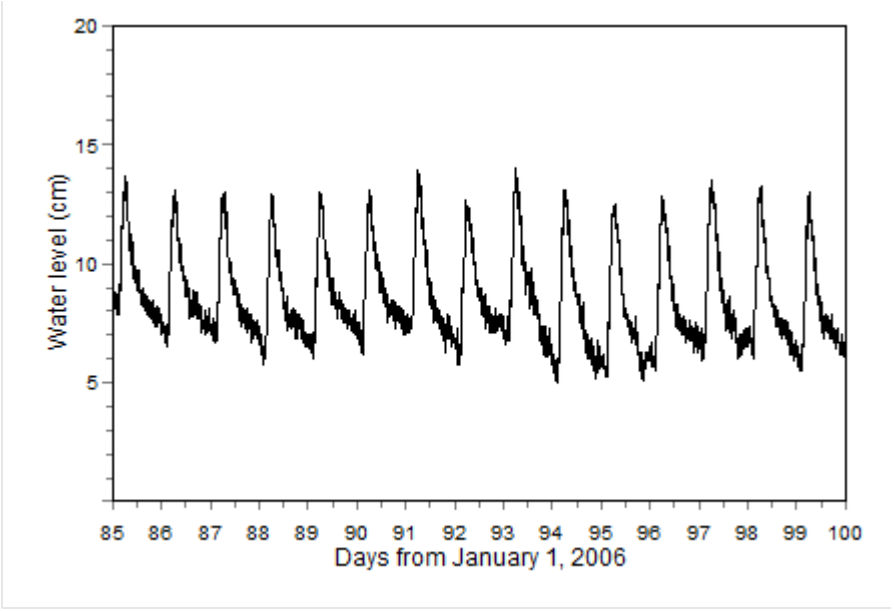

Figure 8. Water levels at Spring K from March 26, 2006 to April 9, 2006, showing a diurnal fluctuation due to pumping from the quarry sump to Willoughby Creek Tributary

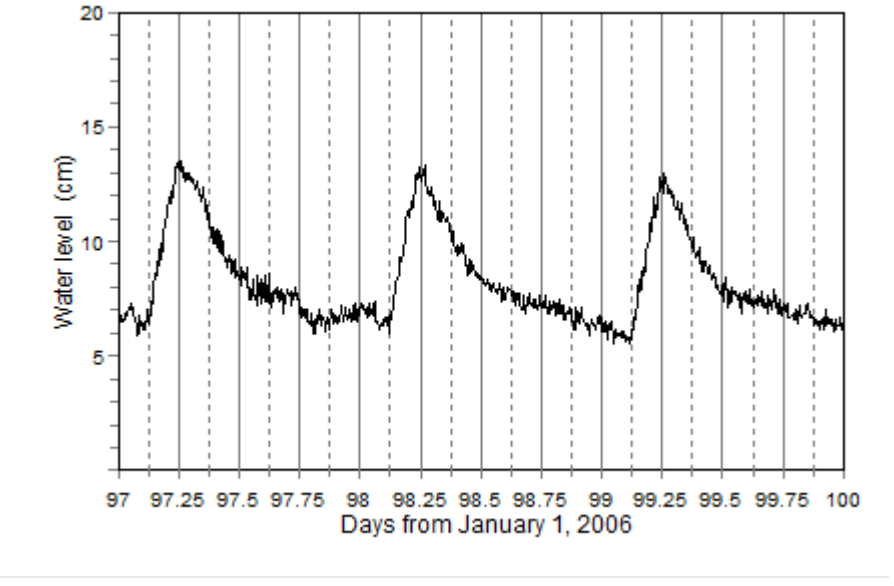

Figure 9. Water levels at Spring K for April 7, 8, and 9, showing a rise in water level at about 3 am and a peak at 6 am each day in response to pumping from the quarry sump.

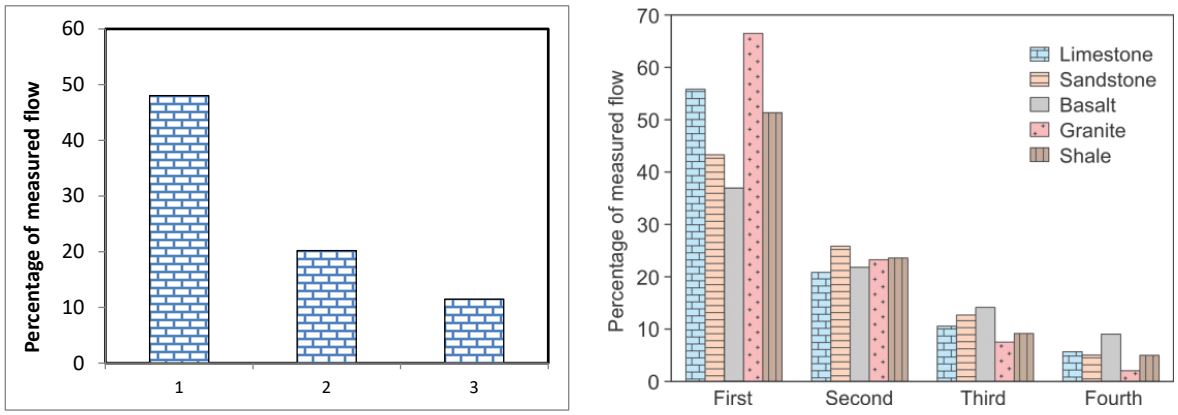

Figure 10. Average percentage of flow from the most produce fractures in the dolostone aquifer at Burlington (left) and in 77 wells in different bedrock lithologies (right). Data is from Table 7 (left) and from Worthington et al., 2016 (right).

16.7 Appendix A: Tracer testing

Tracer methodology for well to well tests

The tracers used were the fluorescent dyes uranine (also known as sodium fluorescein; Colour Index (CI) 45350), eosin (CI 45380) and phloxine B (CI 45410). Sodium fluorescein is the preferred dye since it is the most fluorescent and is the more detectable dye with both field and lab instruments; it was used in four of nine injections. All three dyes have very low toxicity and are approved for use in drugs in Canada (Food and Drugs Act, section C.01.040.2).

Grab samples were collected from the pumped discharge water and saved in 20 mL glass vials. Samples were collected at the end of the discharge line, which was located in a trailer 233 m from the pumping well. Samples were analyzed onsite in near real time on a Turner Designs Picofluor filter fluorometer. This instrument has two channels and can measure concentrations of two different dyes injected at the same time. The analysis on site gave approximate results that were ideal for planning subsequent tracer injections. After the completion of the tracer testing all samples were stored at 4o C and later reanalyzed on the filter fluorometer after being allowed to come to room temperature for 24 hours. Where three dyes were injected simultaneously, the filter fluorometer was only able to give approximate results, and selected samples were reanalyzed on a Photon Technology International scanning fluorometer in the laboratory of Dr. Chris Smart at the University of Western Ontario.

For each injection, the dye (previously diluted into four litres of water) was injected either by siphoning it down tubing to below the water table in each well or by pouring it directly into the monitor. In both cases a further 20 litres of the discharge water pumped from PW-1 was flushed down the tubing to ensure that all the dye was flushed from the container and tubing through the sand pack and into the bedrock. The amount of dye injected was calculated from two equations which give good predictions of tracer concentrations (Worthington and Smart, 2016). Small quantities of dye were used to ensure that there would be no offsite coloration of either surface water or groundwater.

The pumping test commenced at 15:50 on February 9th, 2006. The pumping rate was increased from 25 litres per minute to 32 litres per minute at 09:00 on February 10th to maintain a constant head in the well at a depth of 27.8 m below top of casing. Dye injections were made on February 10th, 11th and 12th. Sample collection followed a logarithmic schedule after dye injection, with the sampling interval increasing gradually from five minutes immediately after injection to one hour at 12 or more hours after injection. Sampling was terminated at the cessation of pumping at 12:40 on February 13th.

Tracer methodology for sink to spring tracer test

A tracer test was carried out on the West Arm of the East Tributary of Mount Nemo Tributary at the point where the stream sinks into the ground. Four springs were noted close to the edge of the pond where surface flow starts again. Conductivity and temperature measurements gave essentially identical readings from all four orifices. Samples were collected by hand from one of the eastern pair of springs and one of the western pair of springs. The springs were about 2 m apart and are 162 m from the injection point in an approximately southerly direction.

Tracing results at PW-1

On overview of the tracing results is shown in Figure A1 and Table A1 and A2. Three dyes were injected on February 10th into the deep bedrock monitors of the three wells closest to the pumping well, MW03-04A, OW03-22A and OW03-22A. Analysis of samples on the two-channel field fluorometer showed that at least two of the three dyes arrived quickly at the pumping well and peaked after a few hours. Slow recessions resulted in substantial concentrations after 24 hours in the pumped water, so larger amounts of dye were used in the injections on February 11th into the shallow bedrock

monitors of OW3-27B and OW3-22B. These arrived travelled quickly to the pumping well but had slow decreases in concentration, so the amount of tracer used was again increased for the final three traces on February 12th.

Only two dyes were injected on February 11th so the results from the filter fluorometer were used for the dye concentrations in Figure A4. Because of the triple dye injections on February 10th and February 12th, the scanning fluorometer was used to define the dye concentrations from these injections (Figures A2, A3, and A5). This analysis gave good results for all traces with the exception of Trace 3 and Trace 7. The peak concentration of Trace 3 was at 18:00 on February 10th, but the maximum concentration at that time is only shown by a higher minimum between the much larger urnaine and phloxine peaks at that time (Figure A3). There was no recovery for Trace 7 in the 24.3 hours until pumping stopped, so the travel time is longer than 24.3 hours.

Tracing results for sink to spring tracer test

Samples were analyzed in the field on a Turner Picofluor fluorometer, and sampling was stopped at 4.7 hours, by which time concentrations had returned to close to background. (Figure A6).

Interpretation of tracer test results for sink to spring tracer test

The sink to spring tracer test gives a groundwater velocity of 65 m/hour (Table A1 and Figure A6). This is close to the 73 m/hour geometric mean from a compilation of 3015 tracer tests (Worthington and Ford, 2009). The elapsed time to tracer arrival at the springs (Ta) was 1.9 hours and the elapsed time to peak concentration (Tp) was 2.5 hours. The Tp/Ta ratio is thus 1.3, which is typical for simple tracer tests in karst along a single conduit. The size of this conduit can be calculated from

$$A = Q / v$$

where A is the cross-section of the conduit, Q is conduit discharge, and v is conduit velocity. A discharge of 6 L/s was measured upstream of the sink, and the calculated conduit cross-section is 0.33 m^2. A discharge of 5.3 L/s was calculated from the dye recovery data, assuming 100% recovery. This latter discharge gives a conduit cross-section of 0.29 m^2.

There are several sinkpoints spread over a distance of several metres. Similarly, at the pond there are several springs spread over several metres. Consequently, the cross-section area of 0.3 m^2 is divided between several conduits at the upstream and downstream end of the flow path. In between there could be a single conduit or multiple conduits that add up to 0.3 m^2. The water table is less than one metre below the surface along most of the flow path and so conduit development in the shallow weathered or epikarst zone is likely. This would favour there being multiple conduits.

The creek discharge downstream of the pond was gauged at 8 L/s, the temperature of the water was 4.2 ^oC and the conductivity was 463 µS/cm. This compares with 1.9 ^oC and 369 µS/cm in the creek upstream of the sink and 2.3 ^oC and 497 µS/cm at the springs that were sampled for dye. These data show that the 2 L/s increase in discharge from the sinkpoint to the pond outlet is accounted for by groundwater with a conductivity of 745 µS/cm. This value is similar to the conductivity measured in bedrock and overburden wells in the proposed extension area (Golder Associates, 2004).

The tracer test does not provide direct information on the depth of the conduit linking the sink to the spring. However, caves in similar environments, such as Nexus Cave in Hamilton follow a generally sub-horizontal pathway in the top few metres of the bedrock (Buck et al., 2002). The conduit here is similarly likely to be found in the top few metres of the bedrock.

Interpretation of tracer test results from well to well tests

The groundwater velocities measured for the well to well tests were all at least an order of magnitude slower than the sink to spring test (Table A2). Furthermore, the dispersion of dye is much greater, with the ratio Tp/Ta ranging from 2.2 to 6.9, which is much higher than the ratio of 1.3 for the sink to spring test. The higher dispersion shows that the flow paths between the injection wells and pumping well cannot be thought of as single fractures or channels. Instead, the traces suggest that there are multiple pathways that the dye followed and that the apertures of these pathways vary substantially. Such multiple pathways are especially clear in traces #1 and #8, which both have two tracer peaks.

The tracing results can be used to calculate a range of fracture or channel apertures, and two methods are used here. Both methods use the simplifying assumption that the pathways are circular channels or pipes. Maximum groundwater gradients can be calculated from the horizontal distance and the difference in head between the tracer injections wells and PW-1. However, the actual groundwater gradients may be less because some of the inflow to the well cascades down the well from further up the well. Following the end of the pumping test on February 13th, 2006, water could be heard cascading into the well until the water level rose to a depth of 6.01 m. The sound of the cascading water gradually diminished over time, indicating that there was inflow from several bedding planes. The gradient from the injection well to -6.01 m in the pumping well represents the minimum hydraulic gradient. Channel diameter can be calculated using the Hagen-Poiseuille equation for laminar flow in a pipe. Results for an assumed groundwater temperature of 10 ^{o}C range from <0.03 mm to 0.27 mm (Table A3). The Hagen-Poiseuille equation assumes flow in a smooth pipe. Channels in the bedrock are not smooth and so actual apertures will be somewhat larger than these calculations indicate.

The second method of calculating utilizes the known pumped discharge from PW-1 (32 L/min). It is assumed that the well intersects a number of circular channels and that water flows from both channel openings into the well in each case. The Darcy-Weisbach equation is used, which assumes turbulent flow, with a friction factor of, which is an average value for karst conduits. The range of hydraulic gradients of 0.18 to 0.86 is the same as in Table A3, and calculations are given for 2, 5, and 10 channels. The results are given in Table A4. The calculated Reynolds Numbers of at least 2100 confirm that flow is turbulent, and the channel diameter ranges from 9 mm to 24 mm.

The results from Tables A3 and A4 bracket the likely range of channel apertures in the aquifer. There are likely to be many channels with diameters in the range 0.1-1 mm, a smaller number in the range 1-10 mm, and relatively few with diameters > 1cm.

References

Buck, M.J., Worthington, S.R.H., and Ford, D.C., 2003. Earth science inventory and evaluation of the Eramosa Karst Area of Natural and Scientific Interest. Ontario Ministry of Natural Resources, Guelph, 51 p.

Golder Associates, 2004, Hydrogeological and water resources assessment of the proposed Nelson Quarry Co. Extension.

Worthington, S.R.H., and D.C. Ford, 2009, Self-organized permeability in carbonate aquifers. Ground Water, 47, no. 3, 326-336.

Worthington, S.R.H., and Smart, C.C., 2016. Determination of tracer mass for effective groundwater tracer tests. Carbonates and Evaporites, 31, 349-356.

Table A1 Tracer Injection details

Test number	Tracer Injection Date	Time	Dye	Mass of dye (g)	Injection location
1	Feb. 10	11:14	Uranine	1.96	MW03-04A
2	Feb. 10	12:26	Phloxine	1.42	OW03-22A
3	Feb. 10	13:04	Eosine	1.58	OW03-27A
4	Feb. 11	11:29	Phloxine	17.83	OW03-27B
5	Feb. 11	11:34	Uranine	6.10	OW03-22B
6	Feb. 12	09:56	Eosine	98.57	OW03-27B
7	Feb. 12	11:09	Uranine	6.25	MW03-04B
8	Feb. 12	11:20	Phloxine	61.24	OW03-27A
9	March 22	11:18	uranine	0.48	Sinking stream

Table A2 Tracer recovery details

Test #	Recovery location	Distance from injection location (m)	Travel time to tracer arrival (Ta – hours)	Travel time to tracer peak (Tp – hours)	Dye recovery (%)	Tp/Ta	Velocity (m/d)
1	PW-1	13.7	0.77	2.1	7.5	2.7	160
2	PW-1	16.1	1.2	5.4	32	4.5	72
3	PW-1	23.7	(2.2)	(4.8)	N.C.*	(2.2)	120
4	PW-1	23.7	1.4	4.5	35	3.8	130
5	PW-1	16.1	0.52	3.6	33	6.9	110
6	PW-1	23.7	1.3	4.4	19	3.4	130
7	PW-1	13.7	>24.3	>24.3	0	-	<13
8	PW-1	23.7	<3	4.7	9.2	-	120
9	Pond spring (west)	162	1.9	2.5	~100	1.3	1600
9	Pond spring (east)	162	1.9	2.5	~100	1.3	1600

* Notes:
N.C. = not calculated

Table A3 Calculated channel apertures from tracer tests

Well	Trace #	Tracer velocity (m/d)	Distance to PW-1	Difference in head (m)	Channel diameter (mm)
MW03-04A	1	160	13.7	23	0.095
MW03-04B	7	<13	13.7	4.3	<0.046
MW03-04B	7	<13	13.7	23	<0.028
OW03-22A	2	72	16.1	23	0.066
OW03-22B	5	110	16.1	4.3	0.27
OW03-22B	5	110	16.1	23	0.15
OW03-27A	3	120	23.7	23	0.091
OW03-27A	8	120	23.7	23	0.093
OW03-27B	4	130	23.7	4.3	0.19
OW03-27B	4	130	23.7	23	0.095
OW03-27B	6	130	23.7	4.3	0.19
OW03-27B	6	130	23.7	23	0.096

Table A4 Calculated channel apertures from inflow to PW-1

Number of channels	Discharge per channel (mL/s)	Hydraulic gradient	Channel velocity (m/s)	Channel diameter (mm)	Reynolds Number
10	53	0.18	0.24	13	2100
10	53	0.86	0.45	9	2800
5	107	0.18	0.28	17	3100
5	107	0.86	0.52	12	4200
2	267	0.18	0.34	24	5400
2	267	0.86	0.63	18	7400

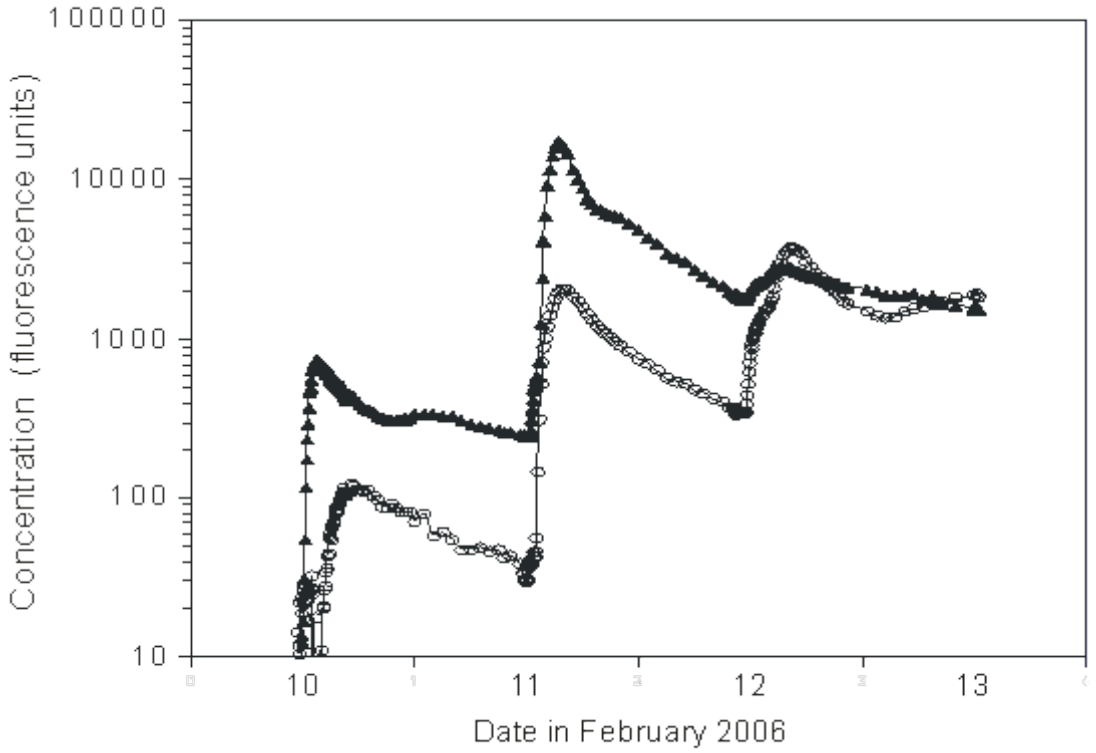

Figure A1 Dye concentrations at PW-1 on February 10-13, 2006 on the green channel (triangles) and red channel (circles) of a Turner Picofluor field fluorometer

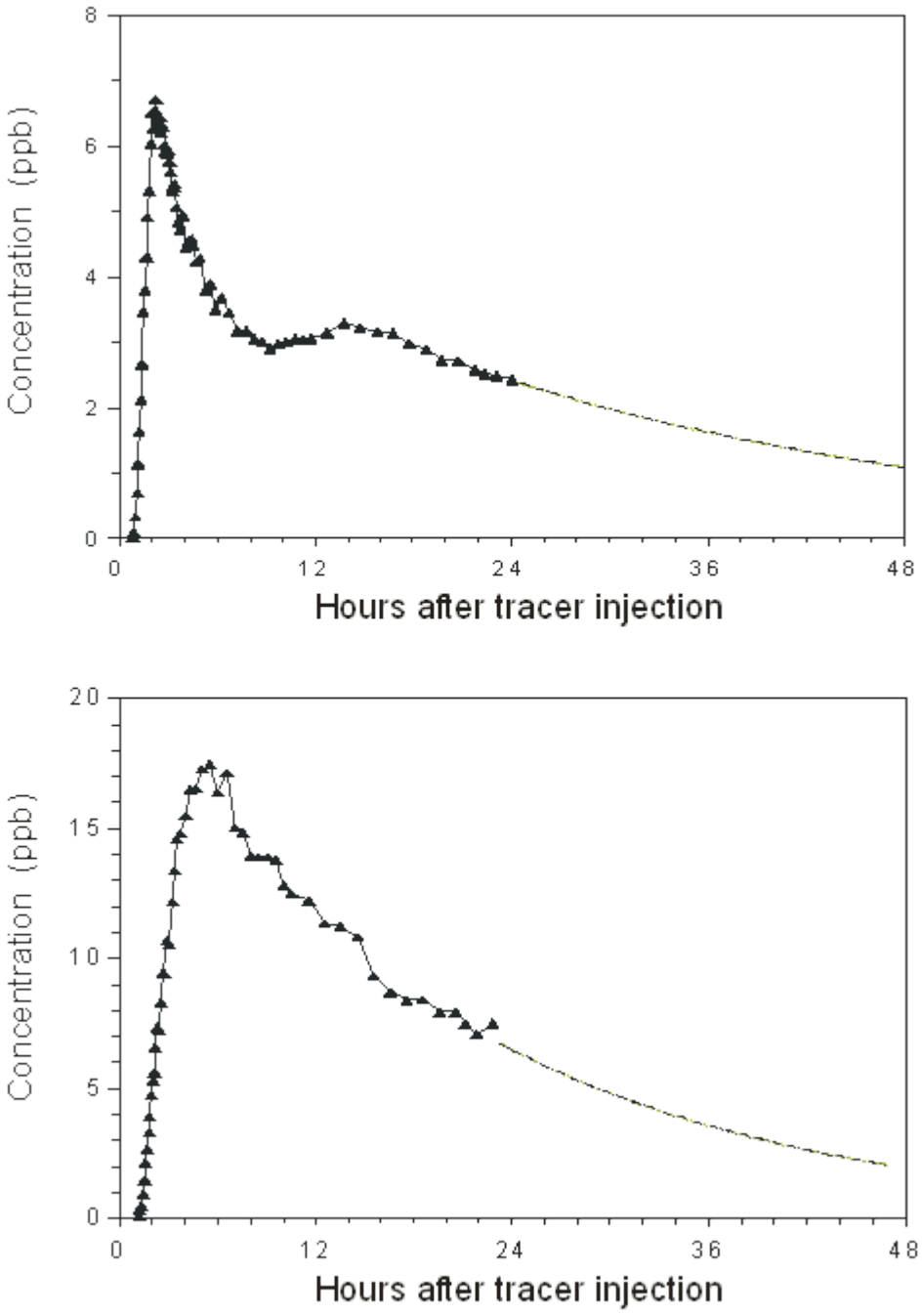

Figure A2 Dye concentrations at PW-1 for Trace 1 (uranine, top) and Trace 2 (phloxine, bottom), showing calculated exponential recessions

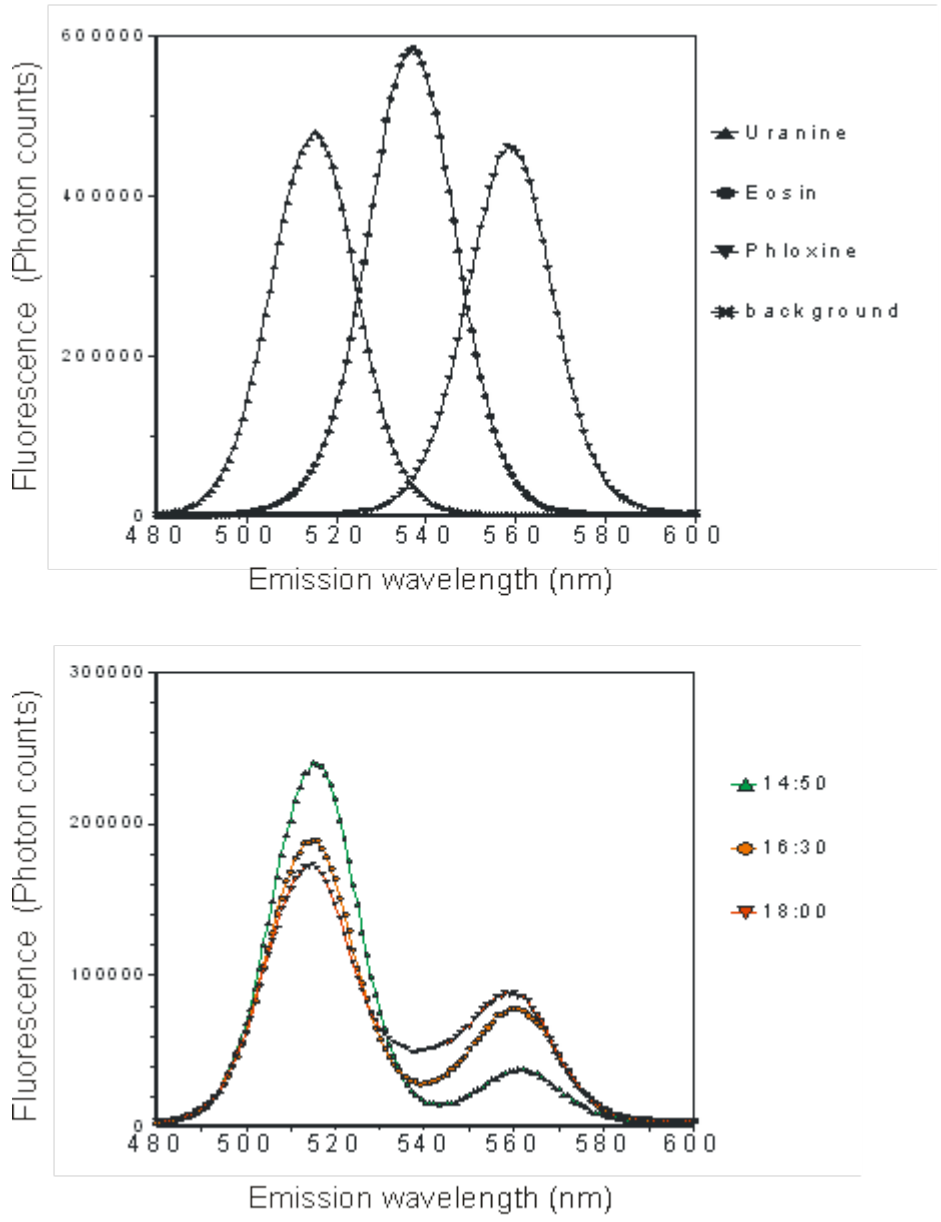

Figure A3 Fluoroscence spectra for standards of 10 µg/L uranine, 100 µg/L eosin and 100 µg/L phloxine (top) and for three samples from PW-1, showing decreasing concentrations of uranine and increasing concentrations of eosin and phloxine between 14:50 and 18:00 on February 10, 2006.

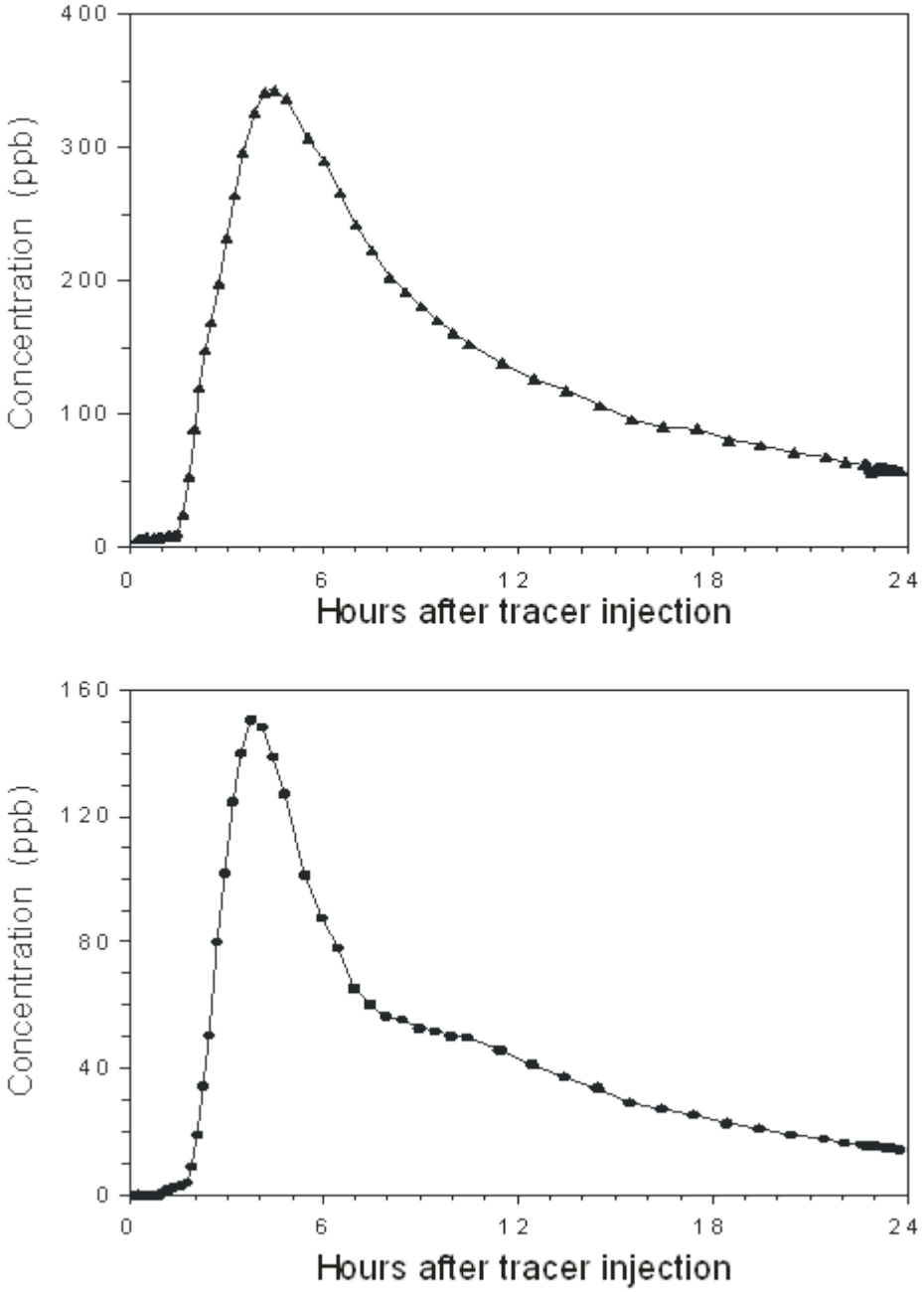

Figure A4 Dye concentrations at PW-1 for Trace 4 (phloxine, top) and Trace 5 (uranine, bottom).

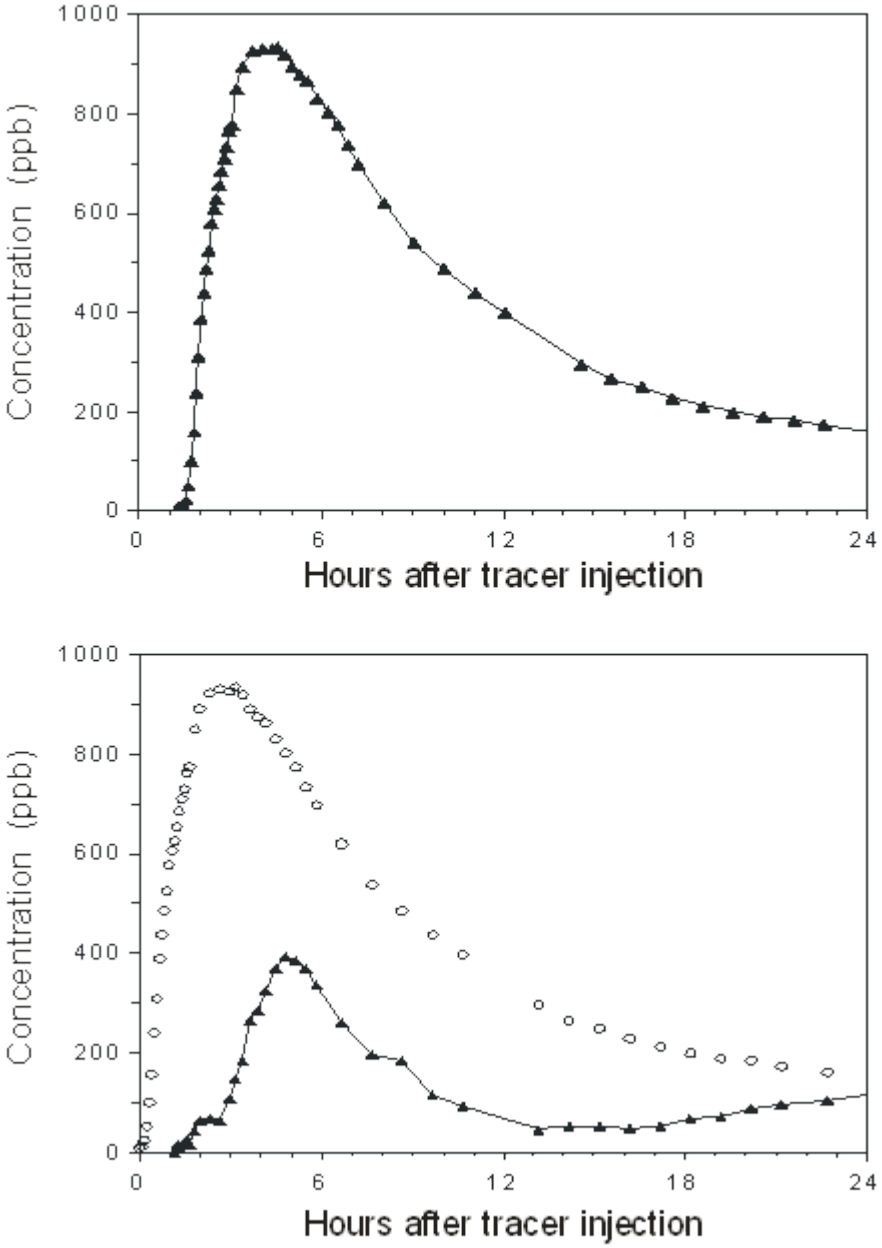

Figure A5 Dye concentrations at PW-1 for Trace 6 (eosin, top) and Trace 8 (phloxine, bottom). In the lower figure, the concentrations of eosin are shown for comparison.

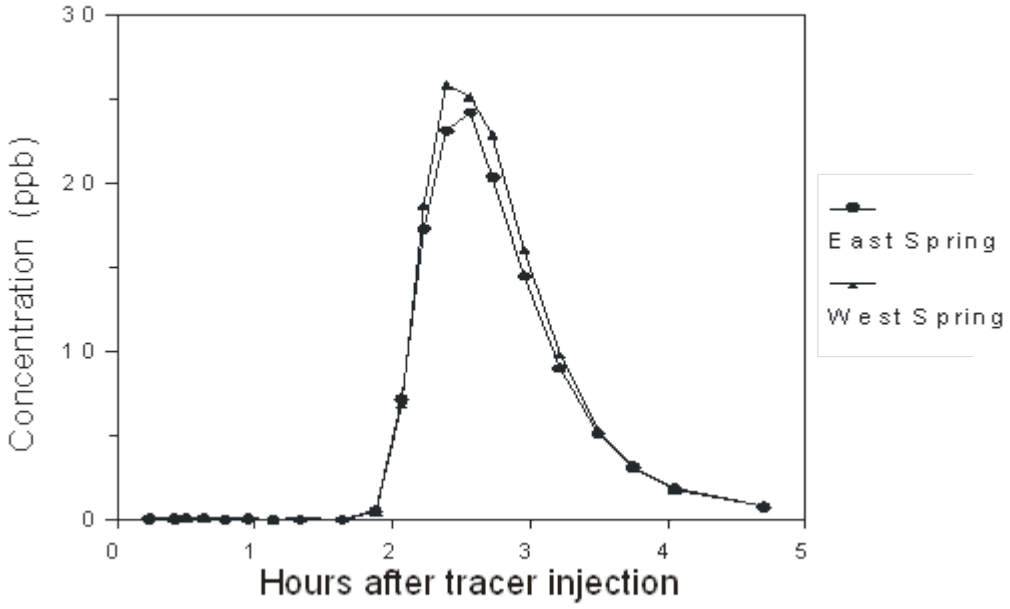

Figure A6 Concentrations of uranine for Trace 9 on March 22, 2006 at two springs in the pond on the East Arm of the West Branch of Mount Nemo Tributary.

Appendix B. Select video, televiewer, and flowmeter logging

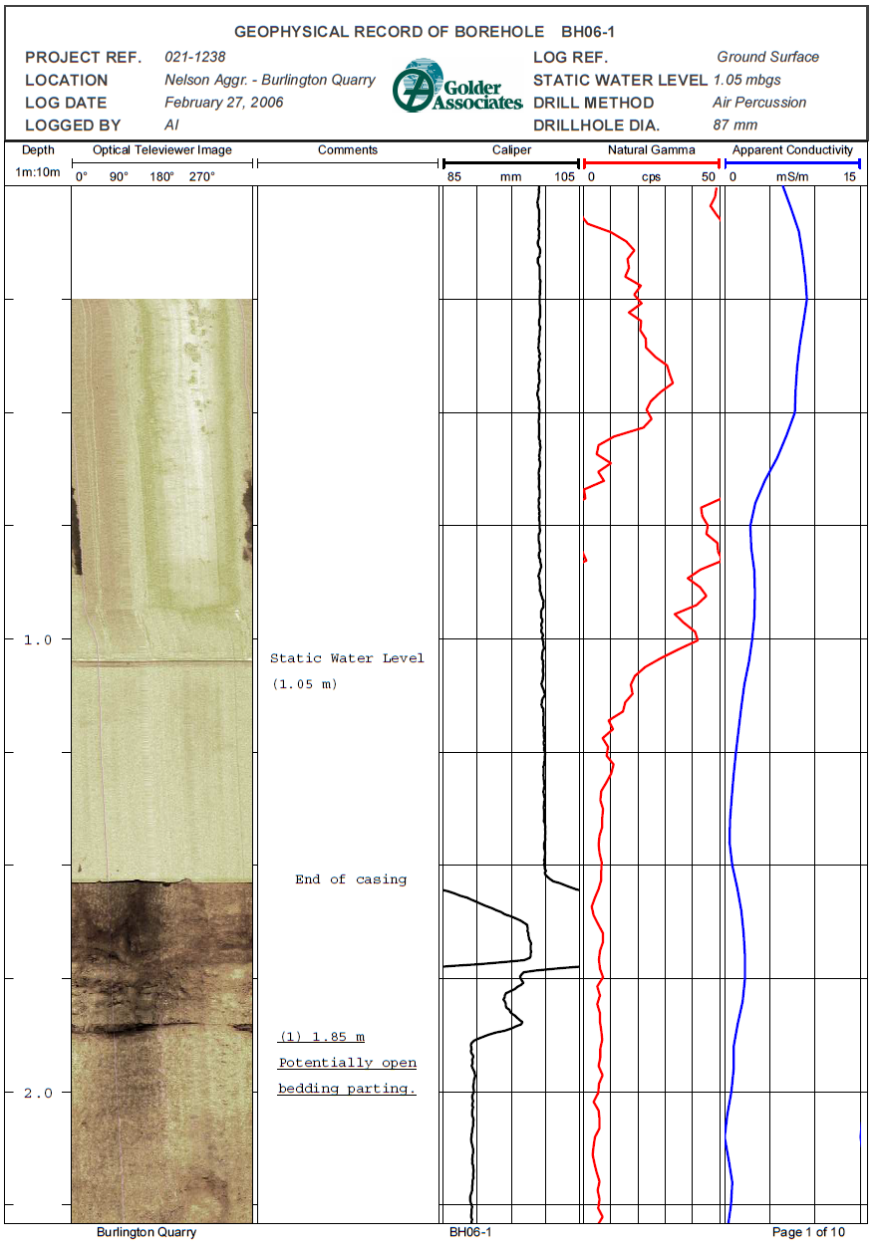

Figure A7. Optical televiewer and other geophysics logs from Well BH06-1

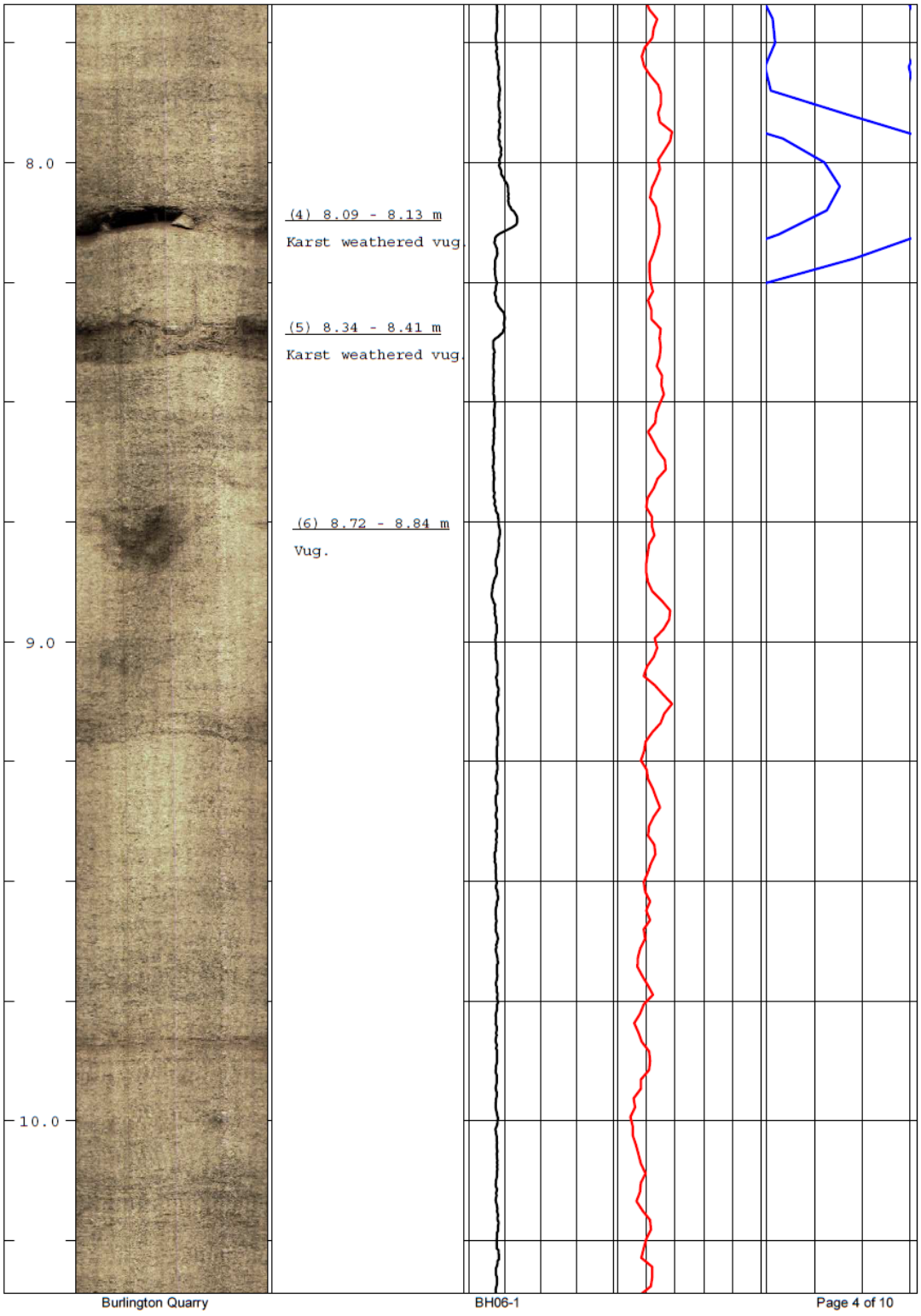

Figure A7. (continued) Optical televiewer and other geophysics logs from Well BH06-1

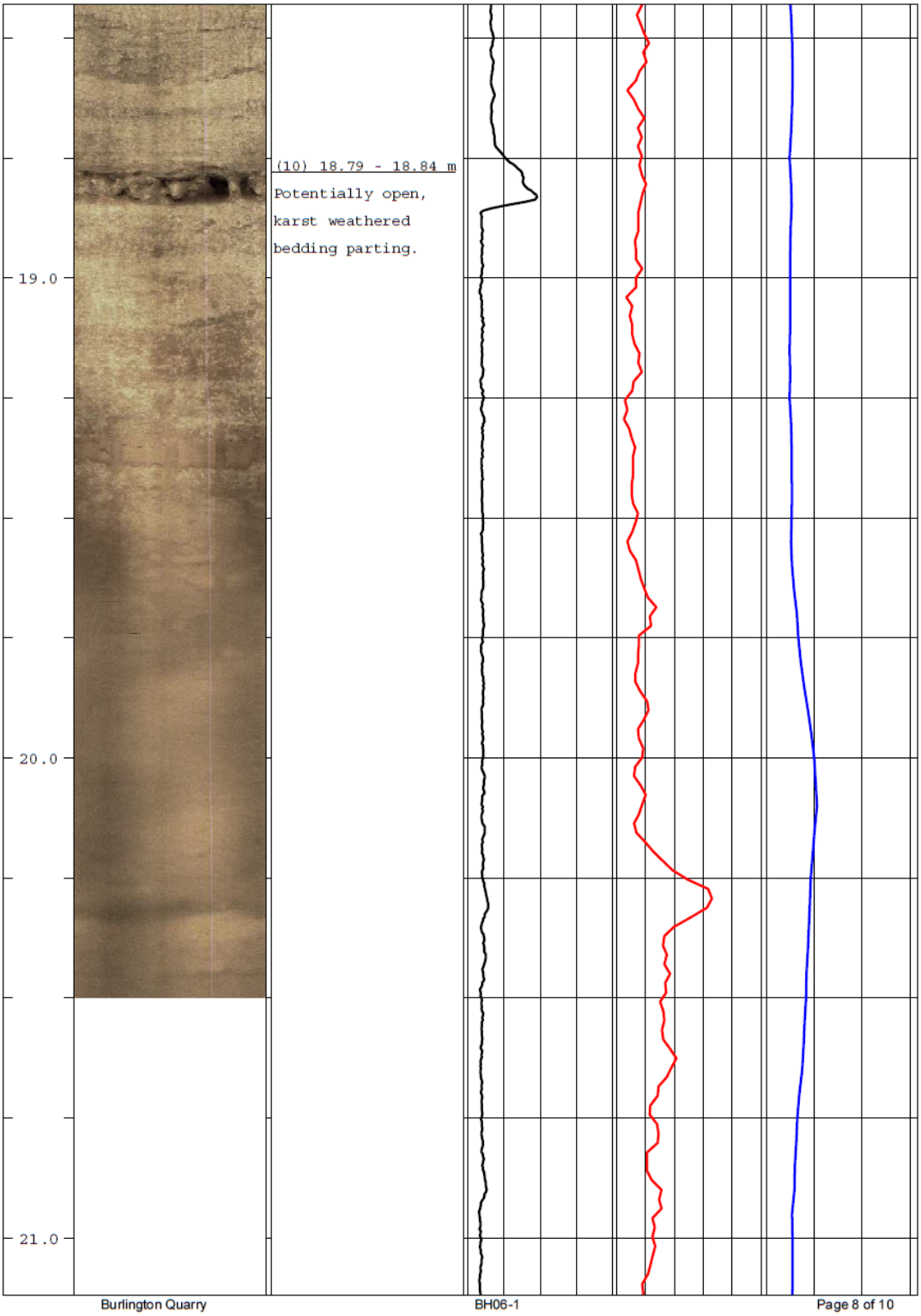

Figure A7. (continued) Optical televiewer and other geophysics logs from Well BH06-1

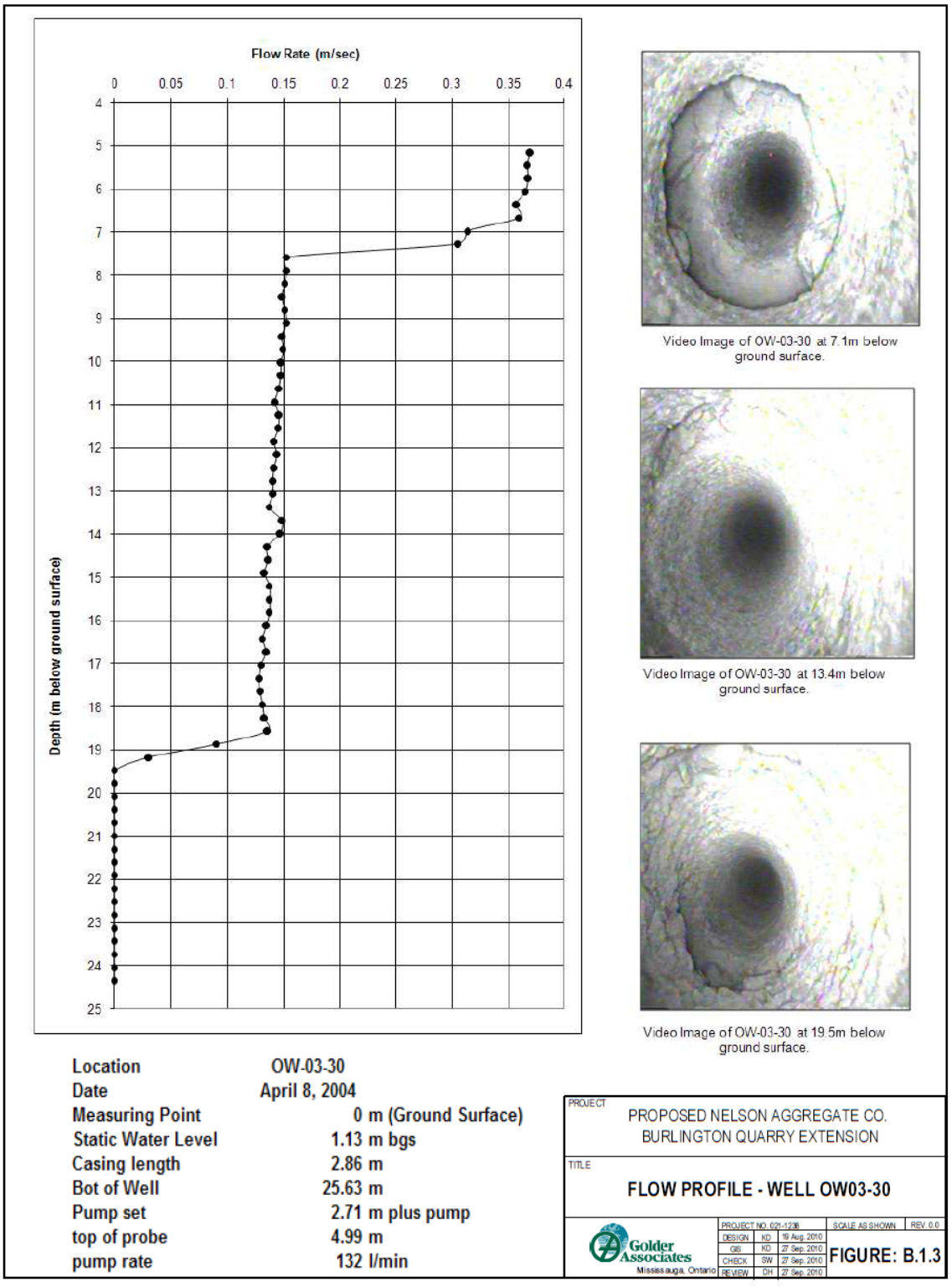

Figure A8. Flowmeter and video images in Well OW3-30

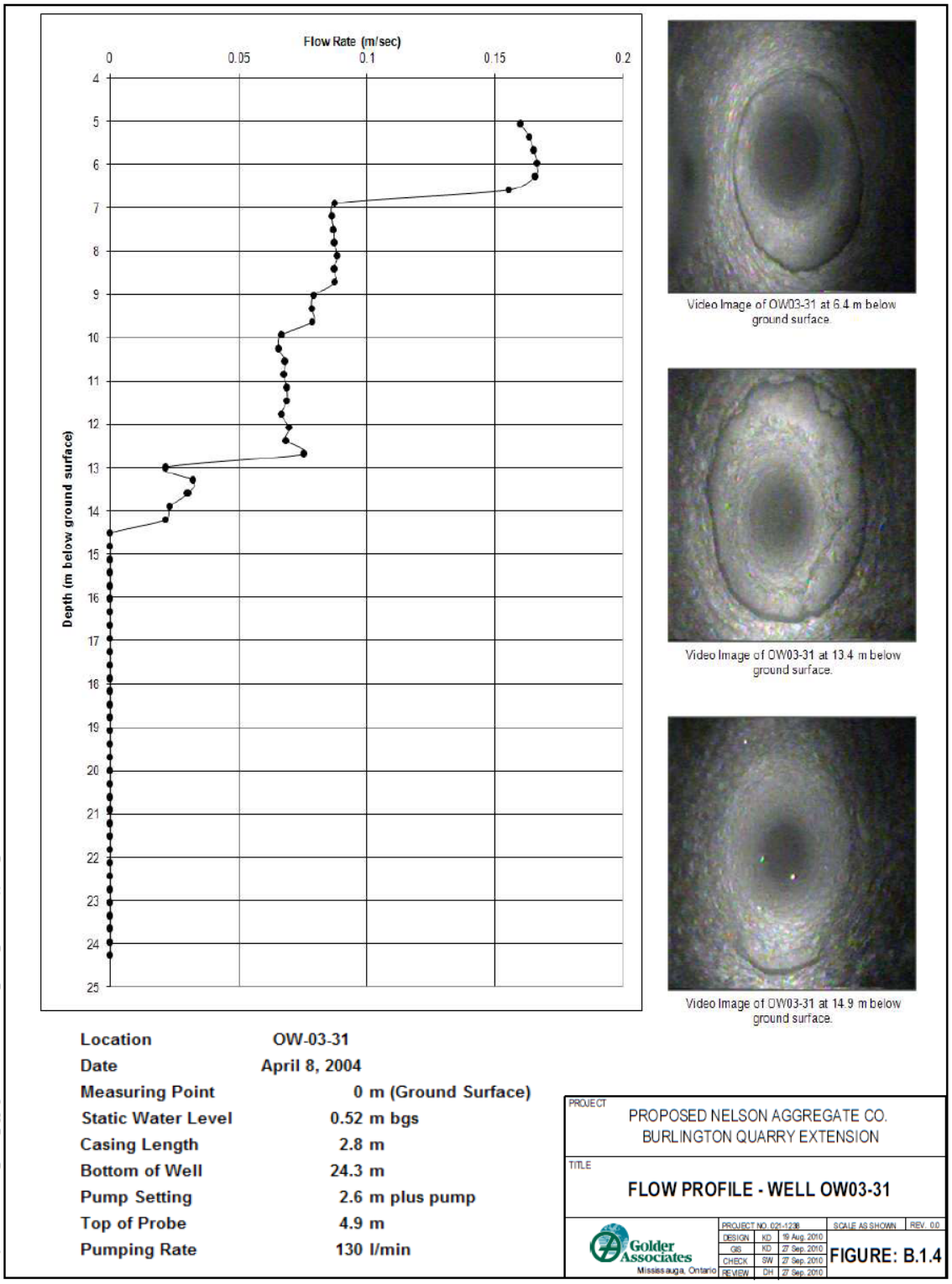

Figure A9. Flowmeter and video images in Well OW3-31

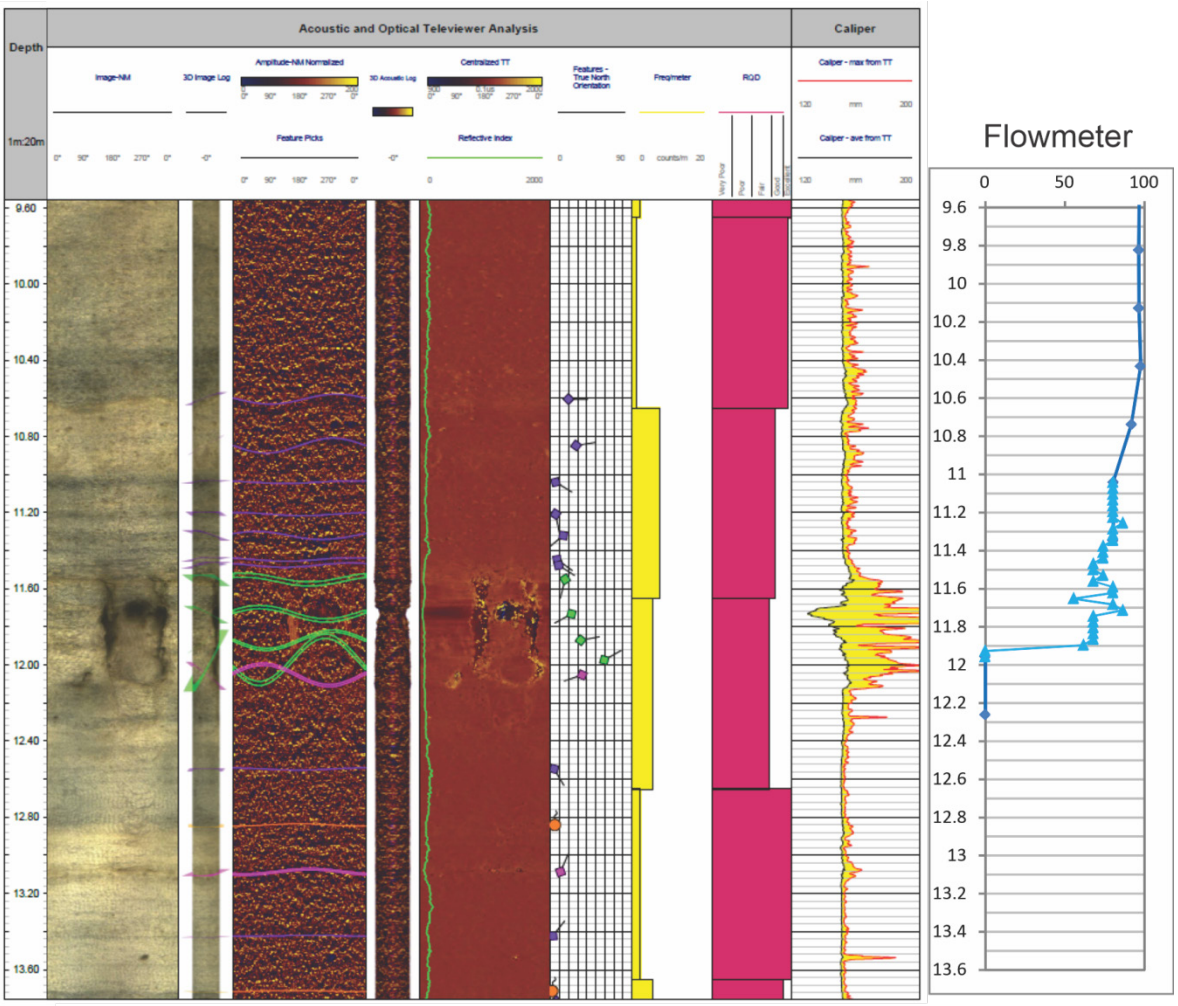

Figure A10. Geophysics logs of Well BS-05

Appendix C. Electrical conductivity and temperature profiles from wells

Electrical conductivity (EC) and temperature profiling was carried out in wells BS-06 and BS-07 using a Heron Instruments Inc. conductivity and temperature meter. The probe was lowered into the well and measurement recorded at 0.5 m intervals. More frequent measurements were made where there were substantial changes in conductivity.

BS-06 was profiled before, during, and after the 72 hour pumping test at BS-06, which is 37 m from BS-07 (Figures A11 and A12). Results show that EC is substantially higher at the bottom of the well, with the greatest change in EC occurring at a depth of 21.0 m to 21.2 m. There is no change in temperature at this depth, but there substantial changes between 8 m and 8.5 m and between 16 m and 19 m. Flow either up or down the well is indicated where there is little change in values with depth, such as between 9 m and 16 m for both EC and temperature. The substantial change in temperature below 16 m suggests that most flow down the well is exiting via a fracture at 16 m. The lowest EC two hours after cessation of pumping, during the recovery phase, suggests that there was ingress of low EC water from a fracture at 9 m depth and that flow was down the well, with most flow exiting the well via at fracture at 21.1 m. Changes in EC at the very bottom of the well suggest that there are one or more active fractures at this depth.

BS-07, the pumping well, was profiled before and after pumping. The EC profile before pumping shows that there was a substantial increase in EC at a depth of 24 - 25 m. A temperature profile was not taken before pumping. The first profile after the end of the pumping test was taken two hours after the cessation of pumping, and immediately after the removal of the submersible pump. There was a rapid increase thereafter in the bottom metre of the well, from 600 µS/cm at 2 hours, to 690 µS/cm at 2.2 hours, to 810 µS/cm at 2.5 hours. This rapid change suggests that the submersible pump, which was close to the bottom of the well and occupied much of its cross-section, was restricting upward flow. There are also changes in EC and temperature at 10.5 to 11 m, and 19 to 21.5 m.

Overall, the changes in EC and temperature with depth and over time suggest that there are one or more open fractures in well BS-07 between 8 m and 9 m, between 16 m and 18 m, and at 21.1 m. In well BS-06, there are major open fractures at 10.8 m and 25.1 m, with probably three less important fractures between 18.5 m and 21.5 m. Furthermore, the changes in EC and temperature suggest that the open fractures must persist laterally and be well-connected, resulting in contrasting values at different depths and rapid changes in values over time.

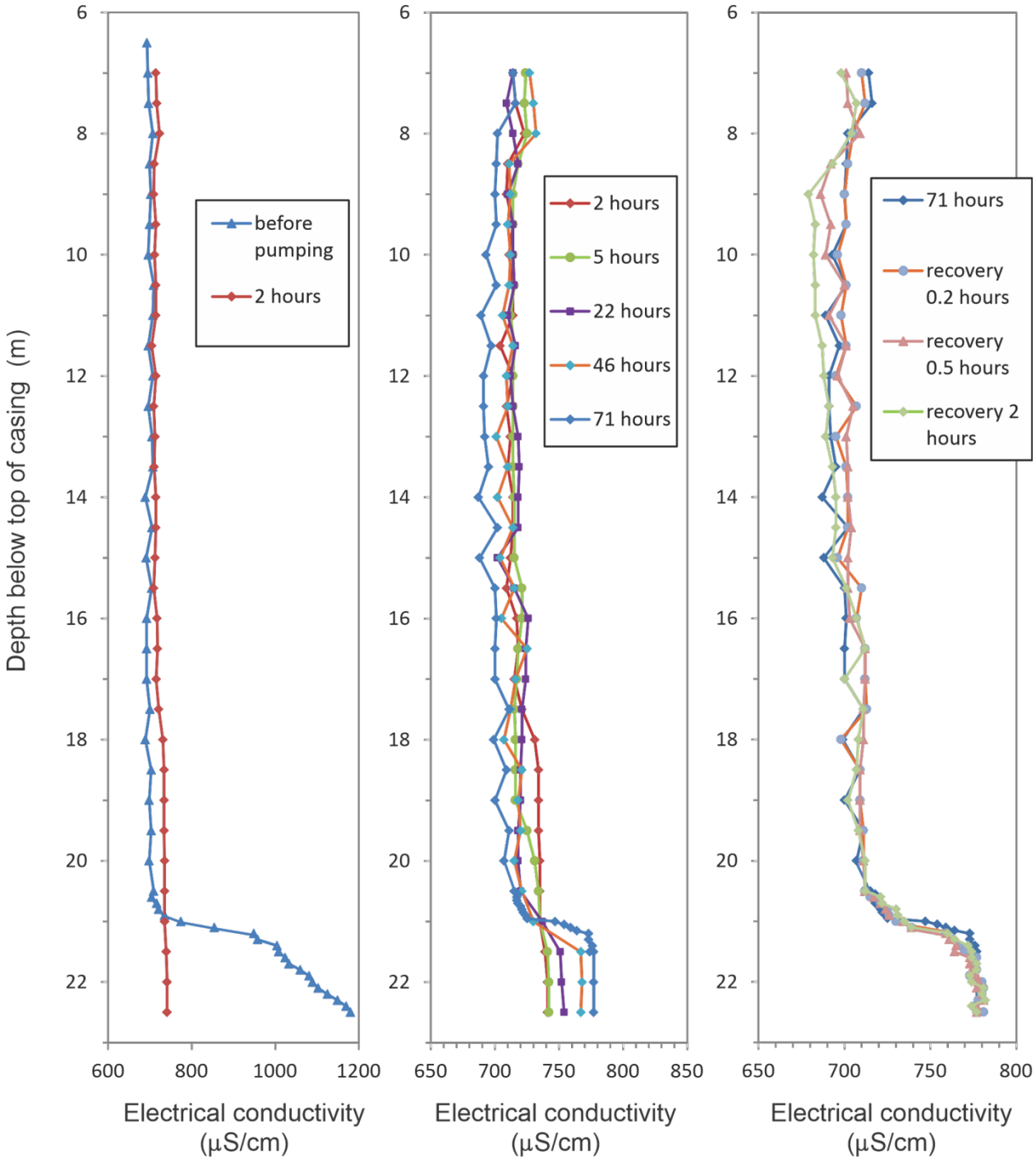

Figure A11. Electrical conductivity profiles at Well BS-07 before, during and after the pumping test at BS-06.

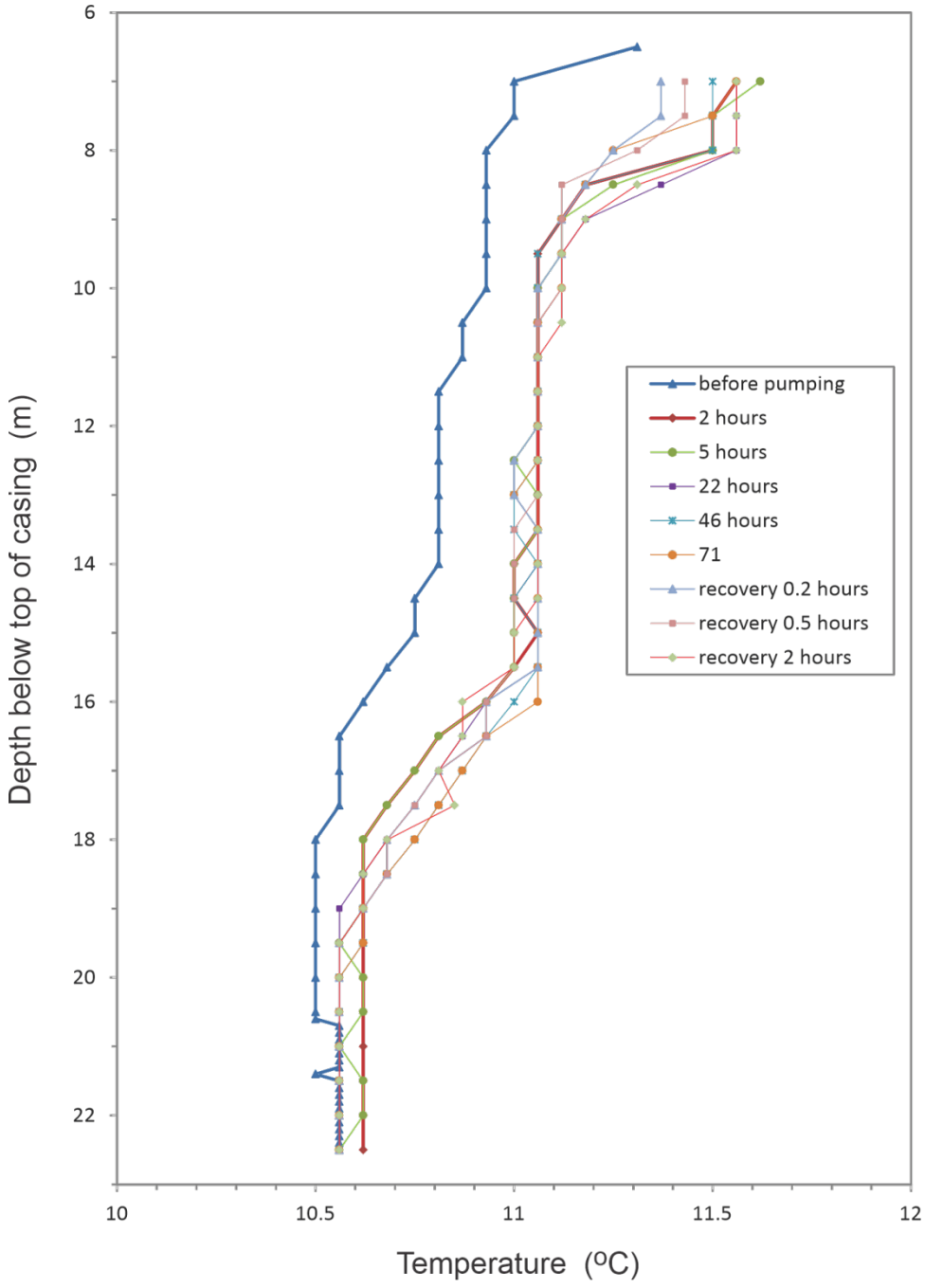

Figure A12. Temperature profiles at Well BS-07 before, during and after the pumping test at BS-06.

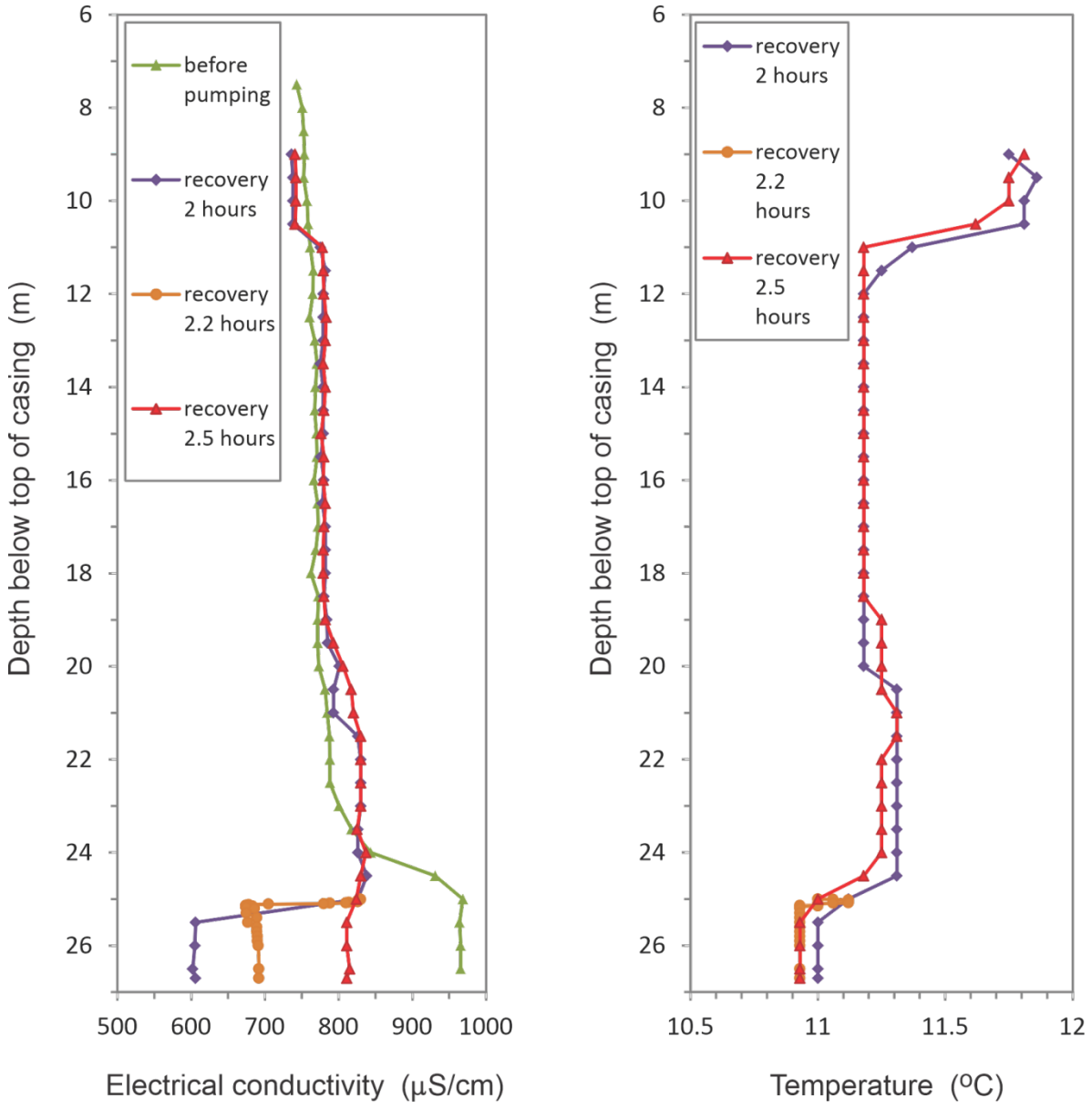

Figure A13. Electrical conductivity and temperature profiles at Well BS-06 before and after the pumping test at BS-06.

17 Appendix C: Hydrologic Sub-model Development

17.1 Introduction

Hydrological processes were simulated using the USGS Precipitation-Runoff Modeling System (PRMS) code. The PRMS code is well documented in Leavesly *et al.* (1983) and Markstrom *et al.* (2008). PRMS is provided as a submodel in GSFLOW and can run in a stand-alone mode or in a fully-integrated manner which links the PRMS submodel to the MODFLOW-NWT groundwater submodel. The stand-alone PRMS submodel was used to pre-calibrate the GSFLOW model and to provide estimates of long-term average groundwater recharge for pre-calibration of the groundwater submodel (Appendix C). Results of the stand-alone PRMS submodel were also used to estimate daily inflows into the GSFLOW model from the western portion of the Grindstone Creek watershed.

The following section presents a brief description of the PRMS submodel, a summary of the climate inputs required to drive the model, an outline of the parameterization process employed in this study, and a brief discussion of the preliminary hydrologic submodel calibration.

17.2 Model Description

PRMS is an open-source code for calculating all components of the hydrologic cycle at a watershed, subwatershed, or cell-based scale. PRMS is a modular, deterministic, physically-based, fully-distributed model developed to evaluate the impacts of various combinations of precipitation, climate, topography, soil type, and land use on streamflow and groundwater recharge.

A flow chart describing the operation of the PRMS code is shown in Figure 17.1. A more complete description of the program code and underlying theory can be found in Leavesly *et al.* (1983), Markstrom *et al.* (2008), and Markstrom *et al.* (2015). In brief, the PRMS model tracks volumes of water for each cell in multiple storage reservoirs. These include interception storage, depression storage, snowpack storage, capillary soil moisture zone storage, gravity soil moisture zone storage (water in excess of field capacity), preferential flow storage, and groundwater storage (when GSFLOW is run in the PRMS-only mode). The main processes were summarized earlier in Section 6. Additional detail is provided here.

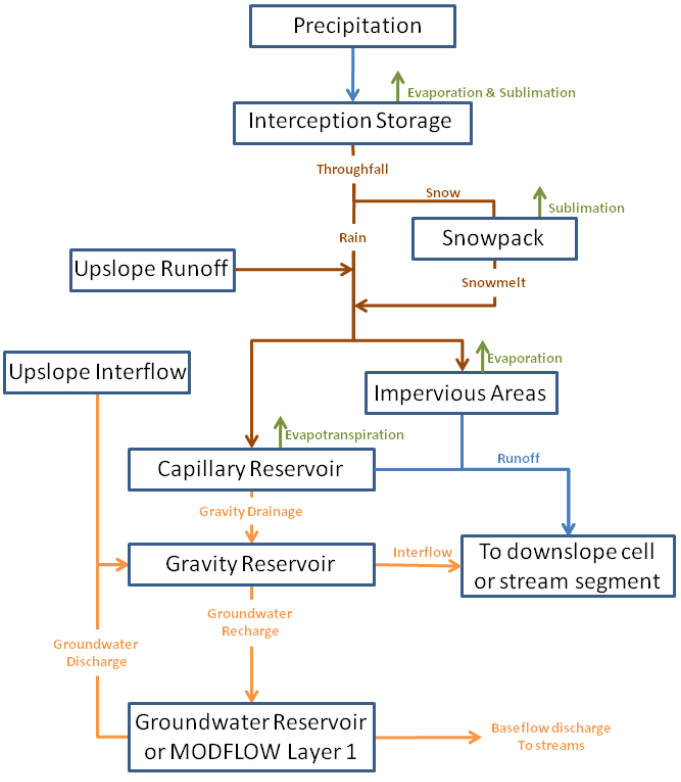

Figure 17.1: PRMS hydrologic processes

To use PRMS as a fully-distributed model, the study area must first be subdivided into a grid of small cells, each representing a small part of the overall water budget. Each cell is then assigned representative values to characterize

slope, slope aspect, elevation, vegetation type, soil type, land use, and surficial geology; such that every cell within the model domain can have a unique set of properties.

Precipitation and Interception: As can be seen in Figure 17.1, the process begins by with daily precipitation. Daily climate data (i.e., precipitation and minimum/maximum temperature) are assigned to each cell based on data from nearby climate stations. Precipitation can be provided in the form of rain or snow or the model can determine the mix of rain and snow from total precipitation, based on air temperature. Daily solar radiation values are also assigned to each cell; these values are adjusted by PRMS for cell slope and aspect.

The model then computes interception by vegetation. The amount intercepted depends on vegetation type, precipitation type (rain, snow, or mixed), and winter/summer vegetation cover density. If interception storage capacity is exceeded, the surplus is allowed to fall though onto the snowpack, if present, or directly onto the ground surface (a process termed throughfall). Water is removed from interception storage by evaporation.

Snowpack: A sub-process model is used in PRMS to represent the snowpack. Snow accumulation and subsequent melting is a key source of spring runoff and groundwater in the spring. Rain-on-snow events and sudden warming can also trigger large runoff events mid-winter. PRMS contains a two-layer, energy-balance model, shown schematically in Figure 17.2, to compute snowpack depth, pack density, change in albedo, temperature, sublimation, and snowmelt on a daily basis using maximum and minimum air temperature, solar radiation, and precipitation data. The linear, energy-balance snowpack model is combined with an areal snow depletion curve to simulate the sub-cell spatial distribution of snowmelt at shallow snowpack depths (DeWalle and Rango, 2008).

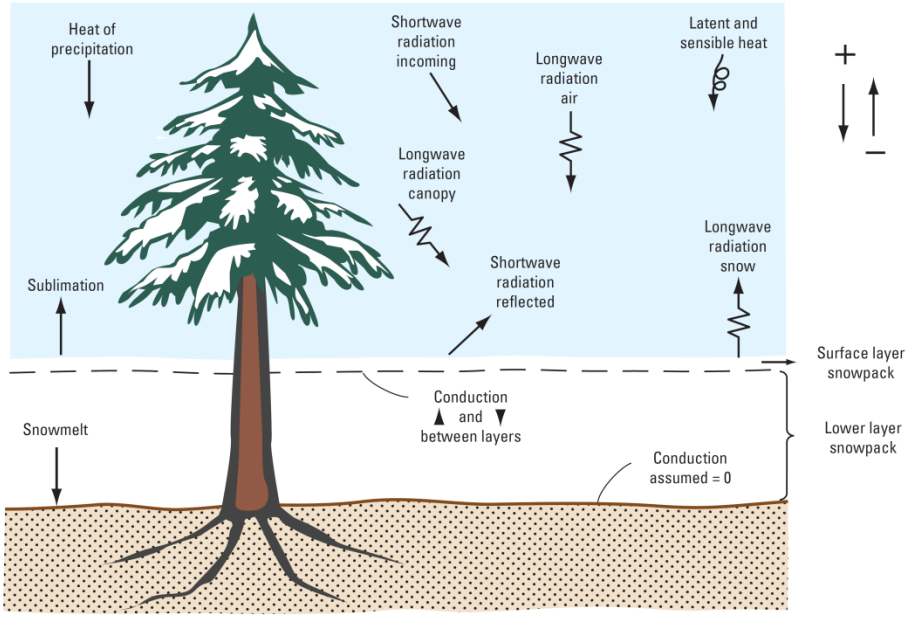

Figure 17.2: PRMS two-layer snowpack conceptualization and components of the snowpack energy balance, accumulation, snowmelt, and sublimation algorithms (from Markstrom *et al.*, 2015).

On days with precipitation, the PRMS code first determines whether a snowpack exists. If the temperature is below a user-defined base temperature (T_b), all throughfall is added to the snowpack as new snow. If the temperature is higher than T_b, the throughfall is added as rain to the snowpack and is used to raise the temperature of the snowpack through sensible and latent heat exchange. If the energy input is high enough and the snowpack has become isothermal, all or part of the snowpack

can melt. The snowpack can also melt or refreeze based on air temperature change and is subject to sublimation. Snowmelt is allowed to infiltrate the soil (in permeable areas) up to a maximum daily amount and any excess is added to the overland (Hortonian) runoff for the cell.

Hortonian Runoff: Each cell can contain both pervious and impervious surfaces; a daily water balance is computed independently for each area type. For impervious areas, the model computes the capture of precipitation and snowmelt by depression storage. When depression storage capacity is exceeded, the surplus is allowed to run off. Water is removed from the depression storage reservoir in each cell by evaporation.

Throughfall (in the absence of a snowpack) and snowmelt on pervious surfaces are partitioned between infiltration and Hortonian runoff. The original PRMS code included a “contributing area” method to partition flows (Dickinson and Whiteley, 1970). Because the contributing area method was originally intended to account for Dunnian (saturation excess) runoff, Earthfx added the Natural Resources Conservation Service (NRCS) Curve Number (CN) method. In the CN method, infiltration is computed based on the retention characteristics of different combinations of soils, vegetation cover type, land use, and antecedent moisture conditions. Water not infiltrating the soil surface is added to Hortonian overland runoff.

Soil Zone Processes: The soil zone in PRMS is split into two main conceptual reservoirs: the capillary reservoir and the gravity drainage reservoir (Figure 17.1.). Water infiltrating into the soil zone in pervious areas enters the capillary reservoir where it is retained against gravity drainage as long as the moisture content is less than field capacity. Evapotranspiration can remove water from the capillary zone (shown schematically in Figure 17.3).

The PRMS model has several methods for calculating potential evapotranspiration (PET). The modified Jensen-Haise method (Jensen and Haise, 1963) was used in this study to estimate daily PET and only requires values for daily temperature, incoming global solar radiation, and two other user-specified parameters. Actual evapotranspiration (AET) depends on available water and is assumed to follow a hierarchy whereby ET is first extracted from interception storage and then depression storage on impervious. Any unmet PET demand is extracted from the capillary reservoir.

A two-layer root zone is used in PRMS. Water is first extracted from the upper zone which is subject to soil evaporation and transpiration. The amount extracted depends on the type of soil, vegetation type, vegetation cover density, and the ratio of available water currently in the soil zone to its maximum available water-holding capacity (field capacity). Remaining ET demand is extracted as transpiration from the lower zone at a rate also dependent on soil, vegetation, and available water. Any remaining PET demand is passed from PRMS to MODFLOW where it can be extracted as groundwater ET from the saturated zone (GWET) at a rate dependent on depth to the water table.

Interflow, Gravity Drainage, and Dunnian Flow: Excess soil moisture (i.e., water above field capacity) is transferred to the gravity reservoir. Water leaves the gravity reservoir as either interflow or gravity drainage. Interflow is given priority and occurs at a rate proportional to the volume in storage (first-order rate). Gravity drainage occurs at a specified maximum daily seepage rate. Water in excess of the amount that can be passed as interflow or gravity drainage is retained in the soil zone and the moisture content may build up to reach saturation. If saturation is exceeded, additional rain or upslope runoff entering the cell will run off as saturation-excess Dunnian flow.

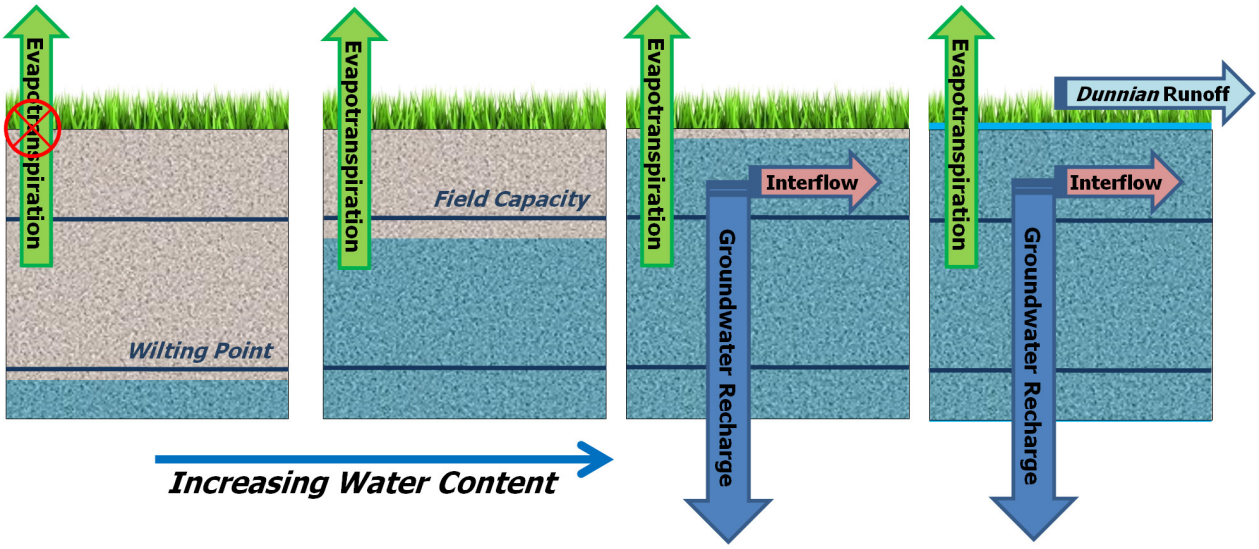

Figure 17.3: Influence of soil zone moisture on recharge, interflow, and runoff processes.

Groundwater Recharge: The maximum daily seepage rate controls the volume of water that is allowed to percolate from the soil zone to recharge the groundwater system. Percolation rates were assigned based on a factor multiplying the estimated saturated vertical hydraulic conductivity of the surficial soils. In PRMS-only simulations, percolating water enters a linear groundwater reservoir associated with each cell. Discharge to streams from the groundwater reservoirs (baseflow) occurs at a rate dependent on the volume of water entering the groundwater reservoir. The groundwater discharge coefficient was selected to best match recession rates observed in streamflow records.

When combined with MODFLOW, groundwater recharge is directed to the underlying MODFLOW cell and MODFLOW simulates the groundwater flow processes. In addition, MODFLOW calculates the volume of water transferred back to the soil reservoirs when the infiltration capacity is exceeded (rejected recharge) or when the water table intersects the soil zone. Discharge from the groundwater system in low-lying areas is treated as Dunnian overland runoff and can be a significant contributor to streamflow.

Cascade Flow: Overland runoff and interflow are routed between cells along a cascade flow network based on basin topography. The cascade directs outflows from each upslope cell as run-on to downslope cells. Hortonian overland runoff is added to snowmelt and net precipitation in the downslope cell where it can re-infiltrate or contribute to the runoff to the next cell. Interflow and Dunnian runoff from upstream cells are added directly to the capillary zone of the downstream cell where it can contribute to interflow, groundwater recharge, or additional Dunnian runoff. Overland runoff and interflow that does not re-infiltrate eventually reaches a stream or lake. Accumulation of runoff from upstream cells creates a generally dendritic flow network with enhanced runoff to streams, infiltration, and groundwater recharge in the downslope areas. ET is also enhanced in these areas because more water is available in the soil zone.

17.3 PRMS Sub-Model Construction

Two versions of the PRMS submodel were constructed. The first version of the PRMS submodel was developed for pre-calibration purposes and encompassed the entire gauged portion of the Grindstone Creek (Figure 17.4). The second version of the PRMS submodel was used in the GSFLOW integrated

model simulations that covered a smaller area focussed on the Burlington Quarry and Mt. Nemo area (also shown in Figure 17.4). Daily inflows into the GSFLOW model from the western portion of the Grindstone Creek watershed, which was excluded from the GSFLOW model, were estimated from results of the larger, Grindstone Creek PRMS submodel. Similar parameter values were used in both models.

Spatial Discretization: The study area was subdivided using a uniform grid with square cells 15 m on a side. The larger model consists of 638,163 active model cells covering 144 km². The GSFLOW model area was represented by 372,368 active model cells covering 83 km². This grid resolution corresponded well with the MODFLOW-NWT groundwater submodel. Cells located outside of the PRMS submodel boundaries were designated as inactive and were not included in the water balance computations. A small portion of the study area, showing the 15 m grid, is presented in Figure 17.5.

The hydrologic processes computed by PRMS were aggregated over four subbasins that represent surface water catchment divides (Figure 17.6). Subbasins 1, and 3 are gauged and observed flows served as primary calibration targets. Other short-term flow records collected in the quarry vicinity were used as secondary checks on the calibration. PRMS results for Subbasin 2 and 3 were used to predict inflows into the integrated model through a methodology described in Section 17.6.4.

Temporal Discretization: The version of PRMS included in GSFLOW runs on a daily time step. Streamflows generated by the PRMS model are assumed to represent average daily streamflow.

17.4 Parameter Assignment

Initial estimates of model parameters were assigned based on available data and were updated during the model calibration process. For parsimony, consistent assumptions and parameter values were applied across the study area, where possible. Model parameters fall into five key groups, including:

- topography-related parameters;
- land-cover related parameters;
- soil parameters derived from soils mapping;
- recharge parameters derived from surficial geology mapping; and,
- other parameters related to hydrological processes, such as snowmelt.

VIEWLOG 5.0 (Kassenaar, 2013) was used to help create, view, re-sample, and/or interpolate most gridded data sets (such as land surface elevations) and to assign parameters using lookups for tabulated values and cell-based indices. Additional data sets were created using VL-GSFLOW, a pre-processor written by Earthfx to generate input data for use in GSFLOW runs. VL-GSFLOW was used to post-process time-series data and perform subbasin water budget analyses. VIEWLOG aided in visualizing and graphing model results and in preparing report figures.

17.4.1 Topography-related Properties

Topography for the model area is based on a 5-metre DEM produced by the Ontario Ministry of Natural Resources (MNRF) and infilled with local drone survey data in the vicinity of the Burlington Quarry and proposed extension lands. The DEM was re-sampled to the 15 m PRMS cells by averaging the 5-m DEM values within each 15 m cell. Topography used in the PRMS submodel is shown for the GSFLOW model area in Figure 17.7. Slope and slope aspect values were calculated from the re-sampled DEM; slope for the PRMS submodel is shown in Figure 17.8, and highlights the extreme slopes in the Niagara Escarpment vicinity and gentler slopes elsewhere.

Terrain analysis techniques were applied to the re-sampled DEM to create the cascade overland flow routing network. An 8-direction steepest-descent method was selected because it generates an efficient many-to-one cascade network. An example of the cascade flow network around the Burlington Quarry, along with the resampled land surface topography, is presented in Figure 17.9. A cascade pathline goes from cell to cell until a stream reach, lake, or a closed depression (referred to in PRMS documentation as a "swale") is encountered.

17.4.2 Soil Properties

Soil properties have a significant influence on hydrological processes because they control the amount of water that can infiltrate and be transmitted to the water table as well as the amount of water lost to actual ET. Soil water-holding capacity in the capillary and gravity reservoirs were calculated in VL-GSFLOW as functions of soil zone thickness (from land cover), porosity (*n)*, field capacity (*fc*), and wilting point (*wp*). Parameters that controlled the partitioning of flow between interflow and percolation to the water table were also specified as soil-type properties.

MNR Soil Survey Complex (2013) mapping was indexed and resampled to the PRMS grid (Figure 17.10). Soil properties were assigned to cells using tabulated look-up values. The surficial soil classes and final parameter values are listed in Table 17.1. Some modification of the soil mapping was done to be more consistent with observed conditions. For instance, the soil code was updated in the vicinity of the quarry to better reflect the location of open water (type 22) and the location of exposed quarry (type 27). A lookup/assignment algorithm was used to distribute soil-type related parameters to the PRMS model cells. The distribution of groundwater seepage rates, as assigned using the lookup procedure, is shown in Figure 17.11 as an example of a spatially-distributed soil-based parameter.

17.4.3 Land Use-related Properties

Land use and land cover are important inputs to the PRMS models because they also strongly influence hydrologic response. The source for land use/land cover data was the Southern Ontario Land Resource Information System (SOLRIS v3; MNRF, 2019). The dataset was indexed and sampled to the PRMS grid (Figure 17.12). Some modification to the mapping was made in the vicinity of the quarry to better reflect the location of open water in the quarry ponds (type 170).

A large number of land-use categories are found in the study area and several hydrologic properties used in PRMS could be correlated with the different categories. These were assigned to model cells using a look-up table with parameter values for each land-use category. An underlying assumption was that properties for a particular land-use class (e.g., "built-up area - pervious") were the same in one part of the model area as another. Hydrologic properties included:

- percent imperviousness - the fraction of the cell area assumed to be impervious;
- depression storage - the amount of water retained over impervious areas;
- vegetation index – dominant vegetation type (bare, grass, shrub, or trees) in the cell;
- vegetative cover density - the fraction of pervious area covered by vegetation and/or tree canopy. Two values are provided: one for the growing season and one for winter;
- interception storage - the amount of precipitation retained on vegetative surfaces and/or tree canopy. Three values are provided: interception storage for summer rain, winter rain, and winter snow. Effective interception capacity is the product of vegetative cover density and interception storage.

- Soil zone and extinction depth thickness – Soil zone thickness is used to calculate the size of the capillary and gravity reservoirs when combined with soil properties (porosity, field capacity and wilting point), as described below. Extinction depth fixes the size of the upper root zone for ET.

The land use lookup table for the study area is provided in Table 17.2. The assumption of consistent property values across the study area was felt to be reasonable for most land use classes. While the breakdown of urban areas into "built-up area pervious" and "built-up area impervious" may be overly simplified, the portion of the study area with these classifications is small. Figure 17.13 shows the percent impervious cover per 15-m as assigned based on the SOLRIS Version 3 land use data.

17.4.4 Hydrological Processes Parameters

As noted earlier, the modified Jensen-Haise method (Jensen and Haise, 1963) was used to estimate daily PET. In addition to daily temperature and incoming global solar radiation values, the method requires two additional user-specified parameters. These can be estimated using regional air temperature, altitude, vapor pressure, and plant cover as discussed in Markstrom *et al.* (2008). The first term serves as a monthly factor to better match measured PET. The second term essentially acts as an elevation correction factor with less ET at higher elevations.

The snowpack submodel has a large number of additional parameters. While many of these can be assigned on a cell-by-cell basis, for simplicity and consistency, uniform (basin-wide) values were used where appropriate. Independent testing of the process submodels was done to determine optimal values for the parameter. For this study, the calculated snow pack depths were compared against measurements of snow depth at Environment Canada climate stations in the study area.

17.5 Climate Data Sets

Three main climate datasets were analysed to characterize the climate of the study area. The same datasets were used as inputs to the integrated GSFLOW model described in Section 6. The datasets include 1) precipitation, 2) maximum and minimum daily air temperature, and 3) net incoming solar irradiation.

17.5.1 Precipitation and Temperature

Precipitation and temperature data collected at Environment Canada AES stations proximal to the study area were obtained and reviewed. The period of record varies among the available climate data sources; however, a continuous climate dataset was compiled beginning in water year (WY) 1951 through WY2019 (note: water years begin on October 1 of the preceding calendar year). Data from 121 stations were available within this time period. Figure 17.14 shows the portion of the 121 stations located within 25 km of the study area.

Daily measurements recorded at each climate station were interpolated to a 500 m grid using an inverse distance weighted technique to approximate their spatial distribution. As an example, the average annual precipitation and temperature are shown in Figure 17.15 and Figure 17.16, respectively. The precipitation distribution shows a decreasing trend from west to east. This behaviour may be related to the Niagara Escarpment where lower elevations tend to receive less precipitation. Unfortunately, the number of stations near the Escarpment is low making it difficult to confirm this phenomenon. Temperature tends to decrease in a southeasterly direction and may also be related to elevation, with lower temperatures corresponding to higher elevations.

17.5.2 Solar radiation

Incoming solar radiation is controlled primarily by the number of possible hours of sunshine per day and the percent cloud cover. Solar radiation data are collected at very few stations in Ontario; therefore, the data had to be compiled from a variety of sources. Through linear regression analysis, it was shown that the widely-separated Ontario solar radiation stations exhibited good inter-station correlation (Earthfx, 2010). Accordingly, a continuous dataset was created by averaging and infilling of daily solar radiation information from 11 southern Ontario stations. Data provided in sub-daily increments were summed to daily energy gains and converted to langleys per day (ly/d = cal/cm²/day or 41.84 kilojoules/m²), the input units required by PRMS.

The incoming solar radiation dataset was based primarily on the average of measurements from four climate stations maintained by EC between 1956 and 2005. These stations include: 611KBE0 (Egbert CARE); 6142285 (Elora Research Station); 6158350 (Toronto); and 6158740 (Toronto MET Research Station). The period of record of these four sites only extends to August 31, 2003; therefore, the remaining data up to 2019 had to be infilled using a combination of measurements from the University of Waterloo, York University, University of Toronto Mississauga campus, and the Burford Tree Farm (GRCA). Where direct observations were unavailable, solar radiation was estimated by the Hargreaves and Samani (1982) method which uses daily minimum and maximum temperatures.

17.6 PRMS Submodel Results

17.6.1 PRMS Calibration Results and Discussion

The PRMS submodel provides daily values for all components of the water budget including precipitation, interception, snowmelt, evapotranspiration, overland runoff, infiltration, and groundwater recharge. The daily outputs are best visualized with hydrographs or animated maps, the latter cannot be provided in printed reports, unfortunately. The code contains routines to sum several of the daily values over the subbasins and the entire model area. Earthfx added additional components to the output and aggregated other flow components so that local (cell-based) and subcatchment-based water balances can be readily produced.

17.6.2 Baseline Conditions Simulation Results

Figure 17.17 shows the cell-based average daily precipitation for the Baseline Conditions scenario for a 5-year simulation period. The results are generally consistent with the long-term average input precipitation (Figure 17.15) but differ because of the different averaging periods. Values vary over a small range, from 904 mm/yr in the northeast end of the model area to 931 mm/yr in the south. The blockiness of the results is due to the 500 m grid resolution of the input climate data.

Average annual net precipitation is shown in Figure 17.18. This value includes loses from canopy interception and sublimation from the snow pack. Values range from 695 mm/yr to 930 mm/yr. Average annual evaporation from interception storage in the canopy and sublimation (the complement of the net precipitation) is shown in Figure 17.19. Both results are strongly influenced by land cover type (Figure 17.12), vegetative cover density, interception storage, as well as the distribution of precipitation. Values for interception/sublimation range from zero for open water (such as the quarry lakes) to 217 mm/yr over forested land. The losses within the quarry are primarily due to sublimation.

Figure 17.20 shows the average annual Hortonian runoff and includes runoff from impervious areas and infiltration-excess runoff from pervious area as computed using the curve number (CN) method.

Values range from 0.0 to 570 mm/yr. Maximum values occur along roads and within the urbanized areas and these results are strongly linked to the distribution of impervious land cover (Figure 17.13). High runoff values within the quarry are due to the high CN value assigned (85) which is comparable to values assigned to soils in urban areas. It should be noted that the values shown are for runoff generated within the cell and do not include Hortonian run-on from upslope cells.

Figure 17.21 shows the average annual cascading runoff, shown in volumetric terms (i.e., m^3/d as opposed to mm/yr). A log-scale is used for the color ramp to highlight results. Cascading flow defines the average volume of water moving along the cascade flow path at a given location and includes interflow, Hortonian runoff, and Dunnian runoff. As was noted earlier, Hortonian runoff from upslope cells is partitioned the same way as snowmelt and net precipitation. Upslope Dunnian runoff and interflow are added directly to the capillary reservoir. Dunnian flow is mainly generated in areas where upslope interflow and Dunnian flow exceed the storage capacity of the gravity reservoir. In GSFLOW simulations, Dunnian flow is also generated where significant groundwater discharge to the soil zone occurs, such as in areas of shallow water table. Figure 17.21 shows the dendritic nature of the runoff and interflow as a result of the cascade network.

From a surface water balance perspective, the important numbers are the components of interflow and runoff that reach the stream network. Figure 17.22 shows the combined average net runoff to streams (Hortonian and Dunnian) and interflow to streams. Runoff to lakes and shallow wetlands are smaller terms and are reported separately.

Snowmelt, net precipitation and upslope Hortonian run-on that does not runoff is assumed to enter the capillary reservoir as infiltration. Figure 17.23 shows the simulated average annual infiltration for the study area. Rates higher than the observed precipitation can occur in downslope areas because of the re-infiltration of Hortonian runoff. Water is removed from the capillary reservoir by ET. As noted earlier, ET demand is based on PET (computed based on daily temperature and solar radiation) and ranged from 542 to 1159 mm/yr. Lowest values occurred below Mt. Nemo in the shadow of the Niagara Escarpment. The ET demand from the soil zone is equal to the PET minus any evaporation from the canopy and sublimation from the snowpack. The distribution of total actual evapotranspiration (AET) is presented on Figure 17.24. This includes canopy interception, sublimation and evaporation from impervious areas, but not lake evaporation. AET values ranged between 100 to 1025 mm/yr. High rates occur over the lakes, in the Medad Valley and other areas where soil water is not limited. Rates can exceed infiltration where upslope Dunnian runoff, upslope interflow, and groundwater discharge to the soil zone occur.

PRMS calculates the potential groundwater recharge, which is equal to all water entering the gravity drainage reservoir after interflow is removed. The values often exceed the actual infiltration capacity of the soils underlying the soil zone. As well, this water would not be able to recharge the aquifer in groundwater discharge areas where the water table at or near land surface. Figure 17.25 shows average annual net groundwater recharge for the study area. When coupled with GSFLOW, this value represents the groundwater recharge sent by PRMS to the groundwater model minus groundwater discharge back from MODFLOW. The white areas in Figure 17.25, such as in the Medad Valley, represent areas where groundwater discharge exceeds groundwater recharge.

Generally, groundwater recharge ranges between 100 to 300 mm/yr with the variation due to the different combinations of soil types, land use, and topography. Cells near the end of the long cascade flow paths can have higher rates of focused groundwater recharge. Groundwater discharges to the stream as baseflow in the stand-alone PRMS model and as a combination of hyporheic discharge (groundwater discharge directly to the stream channel) and groundwater discharge to the soil zone in the riparian area when combined with MODFLOW.

17.6.3 Surface Water Calibration Results

Simulated runoff, interflow, and groundwater discharge to streams was calculated for the four basins shown in Figure 17.6. Results for Subbasins 1 and 3 were compared to the available gauge data on Grindstone Creek. Figure 17.26 shows simulated and observed streamflow, in m^3s, at the Grindstone Creek near Millgrove gauge along with precipitation and snowmelt, while Figure 17.27 shows the simulated and observed streamflow at the Grindstone Creek near Aldershot gauge. The observed flows are well correlated to the simulated rainfall and snowmelt events and the timing of the peak flows in the simulated response generally match the observed events. There are exceptions, possibly due to limitations in the precipitation monitoring network as well as simplifications and limitations in the PRMS and process submodels (e.g., the snowpack/snowmelt process).

The model achieved acceptable Nash-Sutcliffe Efficiencies of 0.52 and 0.44 for the upstream and downstream gauges, respectively. The NSE is given by:

$$\text{Nash Sutcliffe Efficiency} = 1 - \frac{\sum_{n=1}^{nobs}(Q_o - Q_s)^2}{\sum_{n=1}^{nobs}(Q_o - \overline{Q_o})^2} \qquad \text{(Eq. 17.1)}$$

where Qo is the observed flow and Qs is the simulated flow (Nash and Sutcliffe, 1970). The NSE can range from 1 to minus infinity, with 1 being a perfect fit. A Nash-Sutcliffe efficiency of 0.6 is considered a reasonable value (Chiew and McMahon, 1993). It must be recognized that the model simulates flow on a daily basis and would not be expected to achieve a perfect match to observed mean daily flows. The PRMS-only simulations are considered a “pre-calibration” of the GSFLOW model, because they do not include groundwater processes.

Note: A significantly improved NSE was achieved with the GSFLOW model after further integrated model calibration, suggesting that groundwater flow processes likely influenced by the escarpment are occurring in the Grindstone Creek watershed. An NSE of 0.67 was achieved with the GSFLOW model (see Figure 6.18 for the hydrograph). Additional GSFLOW calibration to local quarry streamflow measurements is further discussed Appendix E.

17.6.4 Daily Grindstone Creek Inflows

As noted in Section 17.3, the PRMS submodel used in the integrated GSFLOW model does not encompass the entire headwater region of Grindstone Creek. Consequently, inflows into the PRMS model area were required as input to be used in GSFLOW to simulate streamflow in the lower reaches of Grindstone Creek.

Grindstone Creek enters the GSFLOW model boundary north of Waterdown at Parkside Drive. The contributing area for these flows corresponds to PRMS Subbasin 2, and 3 in the larger-scale PRMS submodel (See Figure 17.6). Subbasin 3 corresponds to the contributing area for the Grindstone Creek near Millgrove gauge (02HB028). Data for the Millgrove gauge are available between 4/1/2006 and 2/1/2017 (Figure 17.28).

A synthesized observed/simulated time-series of daily flows was generated for periods where data were available for the Millgrove gauge by adding the observed flows to the incremental flow contributed by Subbasin 2 estimated by the PRMS submodel. For periods with no observed flow, the PRMS submodel was used to predict inflows for both Subbasin 2 and 3. The PRMS submodel was run for

an extended period (WY2000 – WY2019) to generate the time-series of daily flows in Subbasins 2 and 3 shown in Figure 17.29). A hydrograph showing the resultant time-series of daily inflows is shown in Figure 17.30. Different colours are used to illustrate when different methods of inflow generation were used.

17.7 Tables

Table 17.1: Surficial soil property lookup table.

Soil Index	Soil Texture Code	Soil Description	Porosity	Field Capacity	Wilting Point	Plant Available Water	Soil Type[3]	Hydraulic Conductivity (m/s)
1	C	Clay	0.4	0.37	0.2	0.17	3	$5.0x10^{-9}$
2	CL	Clay Loam	0.4	0.36	0.2	0.16	2	$1.0x10^{-8}$
5	FSL	Fine Sandy Loam[4]	0.3	0.25	0.1	0.15	2	$5.0x10^{-7}$
6	GL	Gravelly Loam	0.27	0.18	0.05	0.13	2	$1.0x10^{-6}$
8	GS	Gravelly Sand[4]	0.22	0.14	0.04	0.1	1	$5.0x10^{-7}$
9	GSL	Gravelly Sandy Loam[4]	0.22	0.2	0.08	0.12	2	$1.0x10^{-7}$
10	L	Loam	0.35	0.25	0.1	0.15	2	[1]$2.5 x10^{-9}$ - $2.5 x10^{-8}$
12	LS	Loamy Sand[4]	0.28	0.17	0.08	0.09	1	$5.0x10^{-8}$
14	ORG	Organic	0.5	0.49	0.2	0.29	2	$5.0x10^{-9}$
15	S	Sand[4]	0.25	0.15	0.05	0.1	1	1.0E-05
17	SICL	Silty Clay Loam	0.35	0.3	0.15	0.15	2	$1.0x10^{-8}$
18	SIL	Silt Loam	0.35	0.27	0.12	0.15	2	$5.0x10^{-8}$
19	SL	Sandy Loam	0.3	0.22	0.1	0.12	2	[1]$1.0x10^{-8}$ - $1.0x10^{-7}$
20	R	Rock[4]	0.25	0.1	0.05	0.05	3	$5.0x10^{-8}$
21		Bottom lands	0.5	0.49	0.1	0.39	2	$5.0x10^{-8}$
22		Water	1	0.99	0	0.99	2	$1.0x10^{-8}$
23		Built Up Area	0.35	0.25	0.1	0.15	2	$1.0x10^{-8}$
24		Stream Course	0.3	0.22	0.1	0.12	2	$5.0x10^{-8}$
25		Ravine	0.35	0.25	0.1	0.15	2	$1.0x10^{-7}$
26		Escarpment and Rockland	0.22	0.14	0.04	0.1	1	$1.0x10^{-6}$
27		Quarry	0.22	0.14	0.04	0.1	1	$5.0x10^{-9}$
28		Clay Pits	0.4	0.35	0.2	0.15	3	$5.0x10^{-9}$
29		Loam on Golf Course[2]	0.35	0.25	0.1	0.15	2	$2.5x10^{-8}$

[1]: Loam and sandy loam hydraulic conductivity educed by a factor of 10 or 2 if classified as imperfectly or poorly drained, respectively.
[2]: “Loam on golf course” was a custom soil type. [3]: 1=sand; 2=loam; 3=clay [4]: Not found in study area in significant quantity

Table 17.2: SOLRIS land use lookup table.

Look-up Index	Description	% Imper-vious	Return from Imper-vious	Depres-sion Storage	Vege-tation Index	Winter Cover Density	Summer Cover Density	Winter Radiation Trans-mission	Snow Inter-ception Storage (mm)	Summer Rain Inter-ception Storage (mm)	Winter Rain Inter-ception (mm)	Soil Zone Depth (mm)	Extinc-tion Depth (mm)
11	Open Beach Bar	0	0	0	1	0.1	0.2	0.95	2.032	1.778	0.762	610	305
21	Open Sand Dune	0	0	0	1	0.1	0.2	0.95	2.032	1.778	0.762	610	305
41	Open Cliff and Talus	0	0	0	1	0.1	0.2	0.95	2.032	1.778	0.762	610	305
52	Shrub Alvar	0	0	0	1	0.1	0.2	0.95	2.032	1.778	0.762	610	305
81	Open Tallgrass Prairie	0	0	0	2	0.4	0.8	0.65	2.032	2.032	1.016	914	305
82	Tallgrass Savannah	0	0	0	3	0.3	0.8	0.5	2.032	2.286	1.27	914	305
83	Tallgrass Woodland	0	0	0	3	0.4	0.8	0.3	2.032	2.54	1.27	914	305
90	Forest	0	0	0	3	0.45	0.8	0.2	3.302	3.302	1.524	1219	305
91	Coniferous Forest	0	0	0	3	0.5	0.8	0.15	3.81	3.048	1.27	1219	305
92	Mixed Forest	0	0	0	3	0.45	0.8	0.2	3.302	3.302	1.524	1219	305
93	Deciduous Forest	0	0	0	3	0.4	0.9	0.25	3.048	3.556	1.27	1219	305
131	Swamp	0	0	0	2	0.3	0.9	0.55	5.08	2.032	0.762	1219	610
135	Thicket Swamp	0	0	0	2	0.3	0.9	0.55	5.08	2.032	0.762	1219	610
140	Fen	0	0	0	2	0.4	0.8	0.65	2.032	2.032	0.762	1219	610
150	Bog	0	0	0	2	0.4	0.8	0.65	2.032	2.032	0.762	1219	610
160	Marsh	0	0	0	2	0.4	0.8	0.65	2.032	2.286	1.016	1219	914
170	Open Water	0	0	0	0	0	0	1	0	0	0	1829	1829
191	Plantations/Tree Farm	0	0	0	3	0.5	0.8	0.25	2.54	2.54	1.27	1219	305
192	Hedge Rows	0	0	0	3	0.5	0.8	0.25	2.54	2.54	1.27	1219	305
193	Tilled	0	0	0	2	0.1	0.8	0.95	0.254	2.032	0.254	914	305
201	Transportation	0.85	0.35	1.27	2	0.25	0.55	0.95	2.032	2.032	1.016	914	305
202	Built-Up Area Pervious	0	0	0	2	0.3	0.55	0.95	2.032	2.032	1.016	914	305
203	Built-Up Area Impervious	0.33	0.35	1.27	2	0.3	0.55	0.95	2.032	2.032	1.016	305	152
204	Extraction - Aggregate	0.4	0	12.7	1	0.1	0.2	1	1.27	2.032	1.016	25	25
205	Extraction – Peat/Topsoil	0.4	0	12.7	1	0.1	0.2	1	1.27	2.032	1.016	25	25
250	Undefined	0	0	0	2	0.3	0.4	0.8	2.032	2.032	1.016	914	305

17.8 Figures

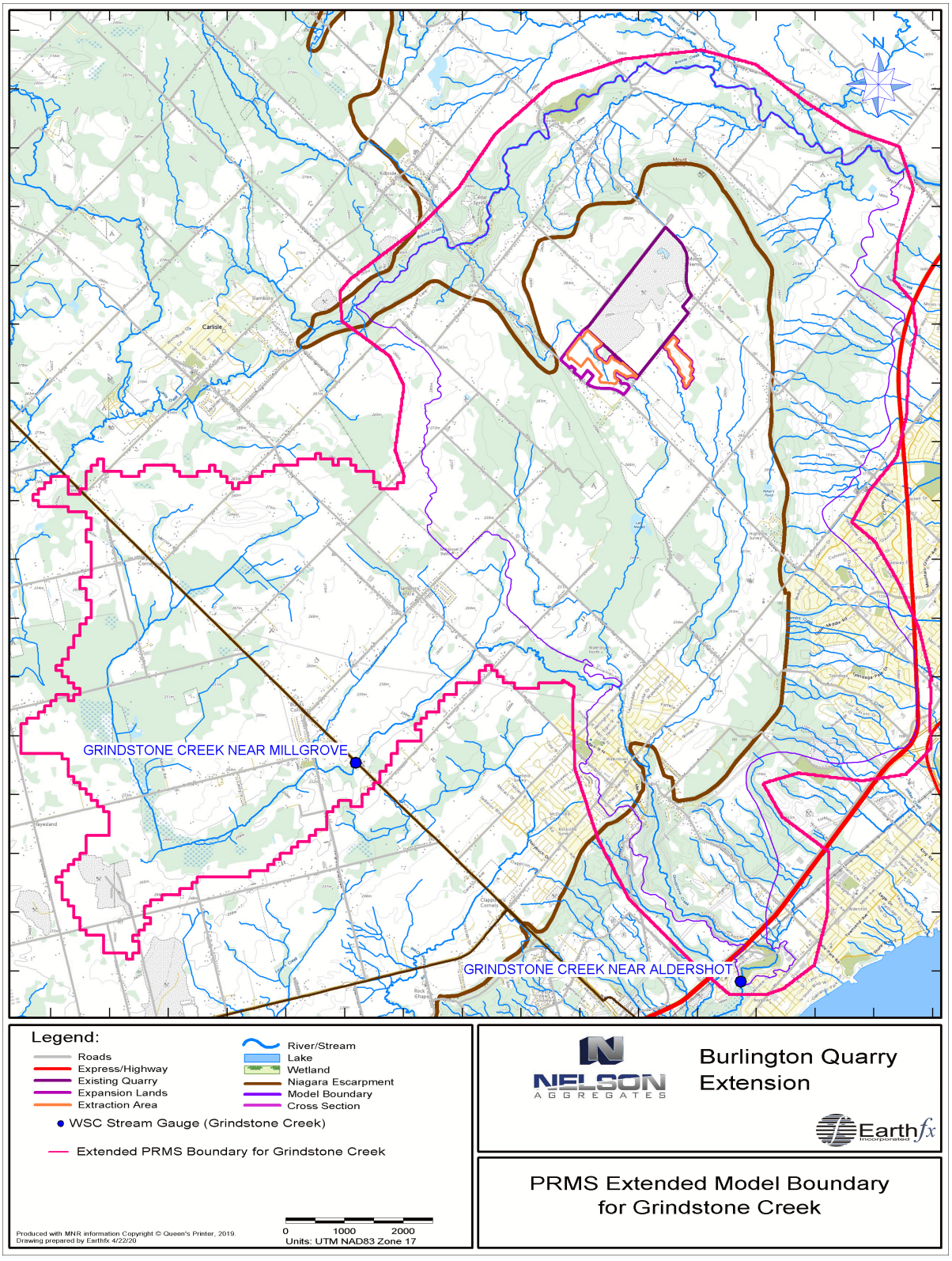

Figure 17.4: PRMS extended model boundary for Grindstone Creek.

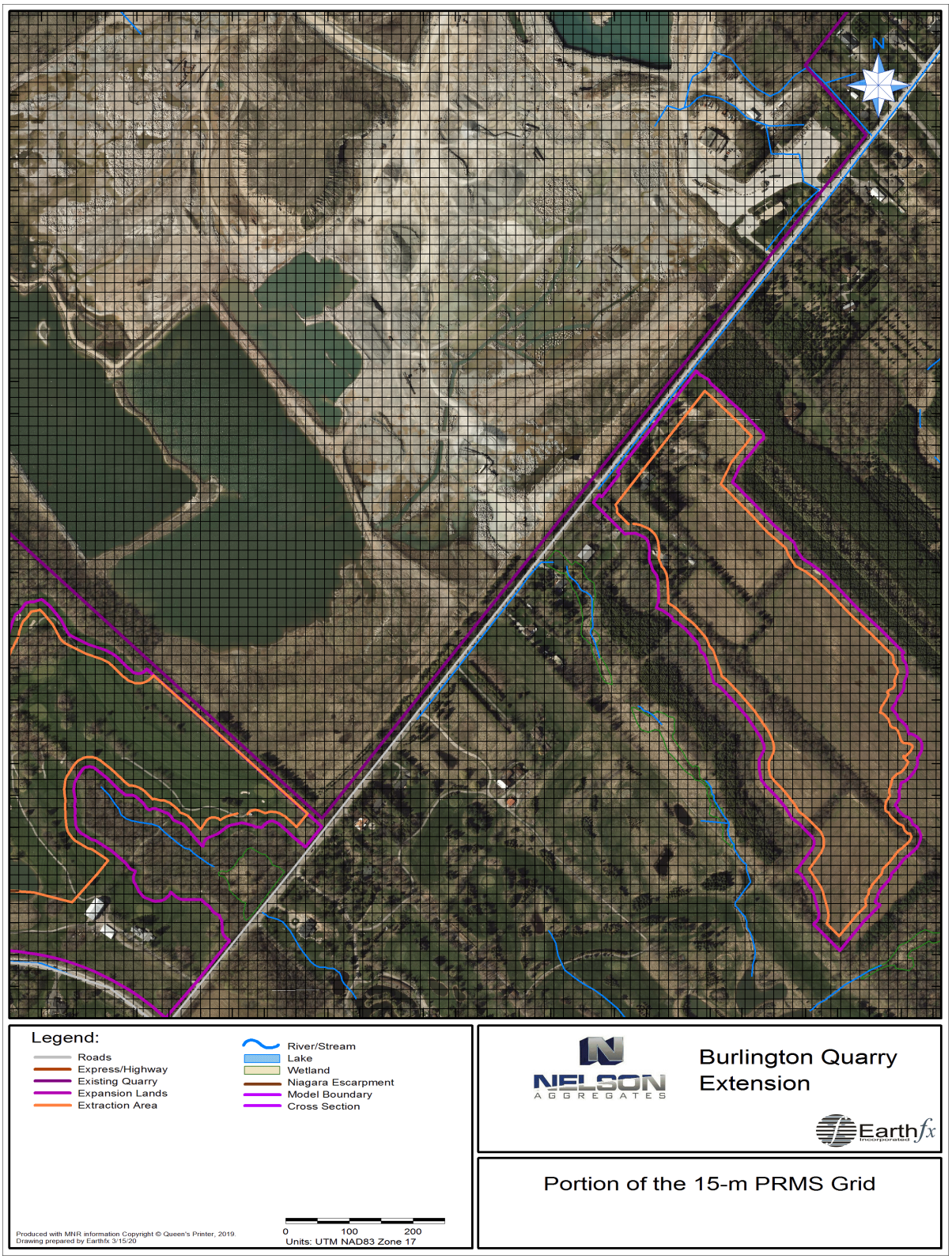

Figure 17.5: Portion of the PRMS model grid in the quarry vicinity.

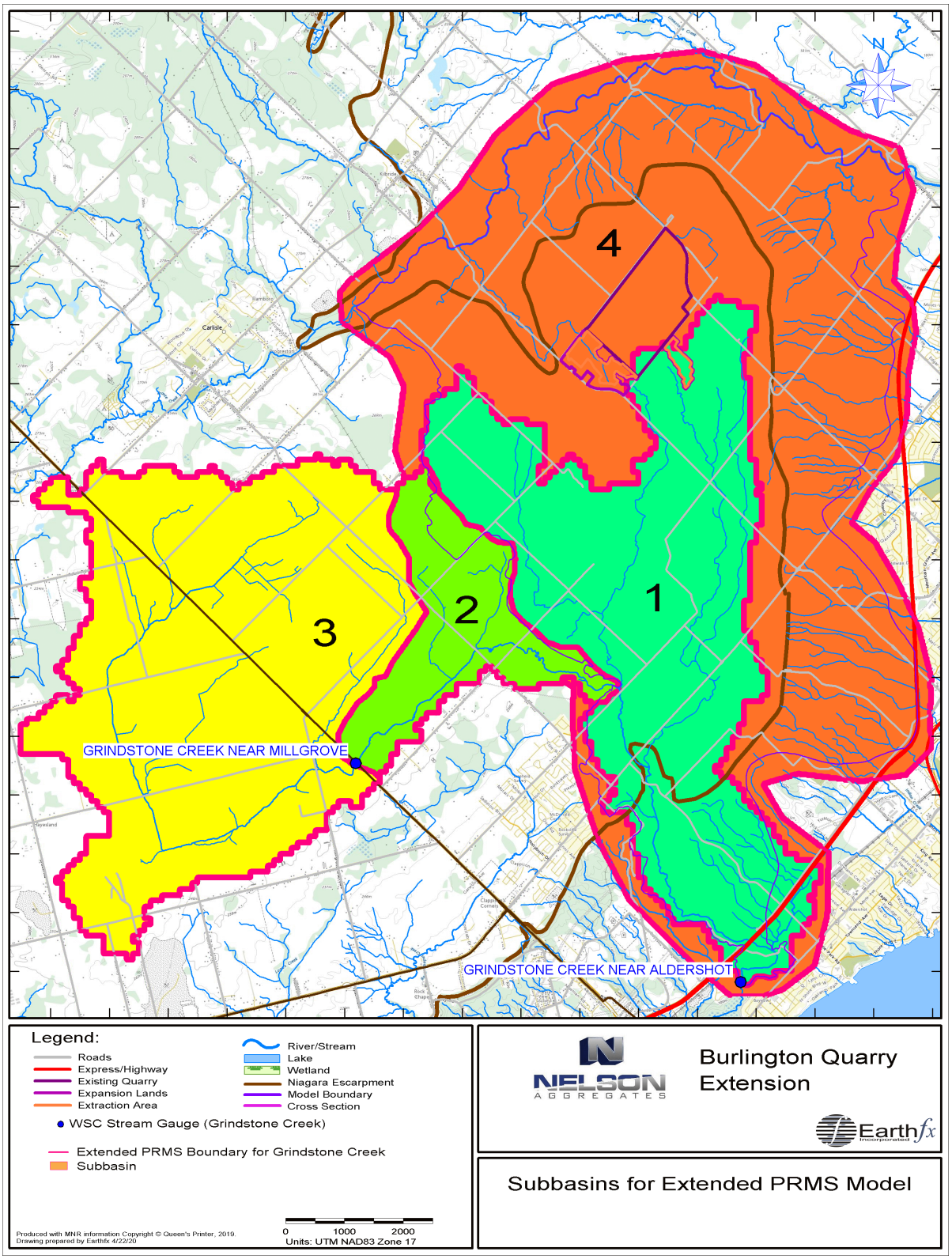

Figure 17.6: PRMS subbasins for the extended PRMS model.

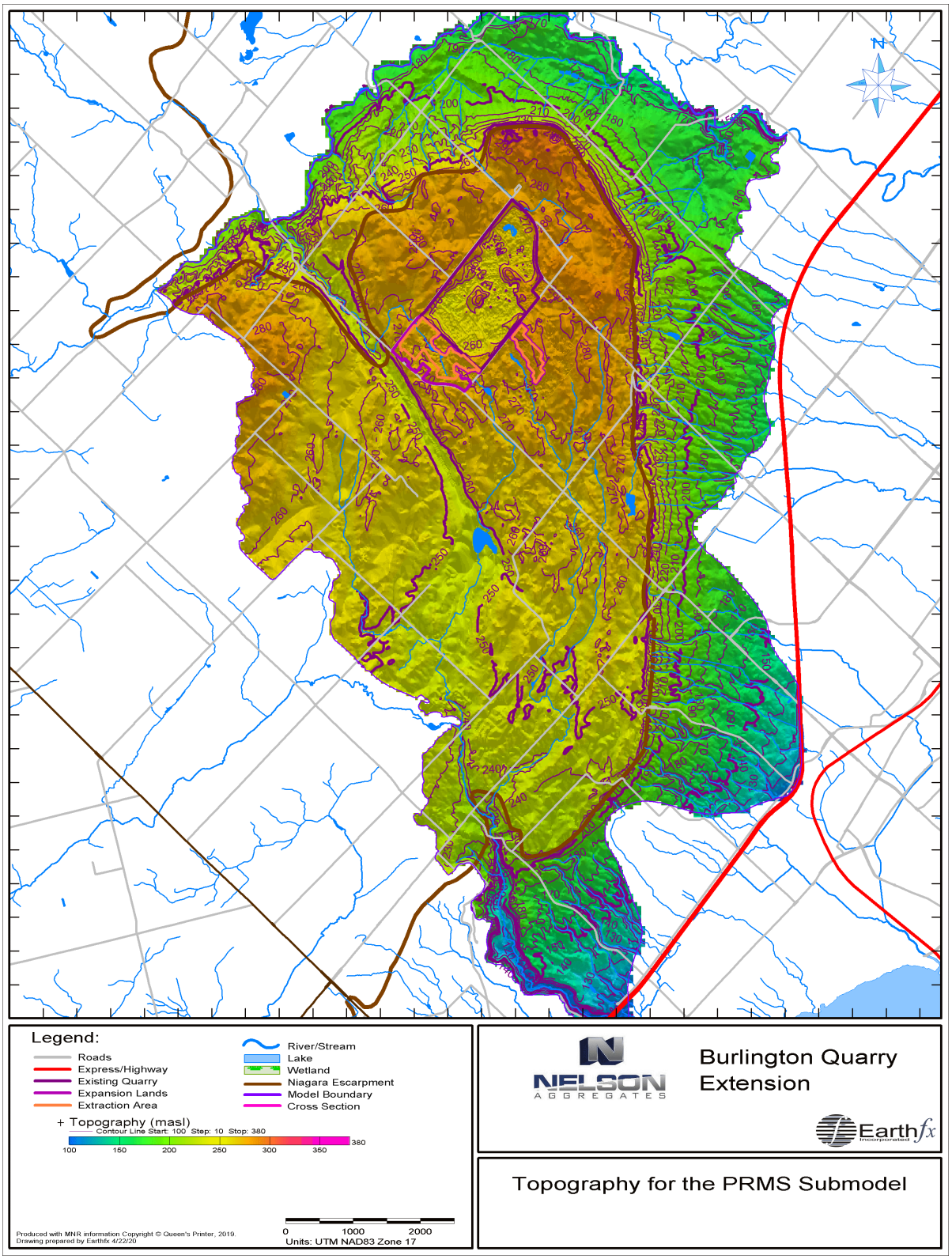

Figure 17.7: PRMS model topography.

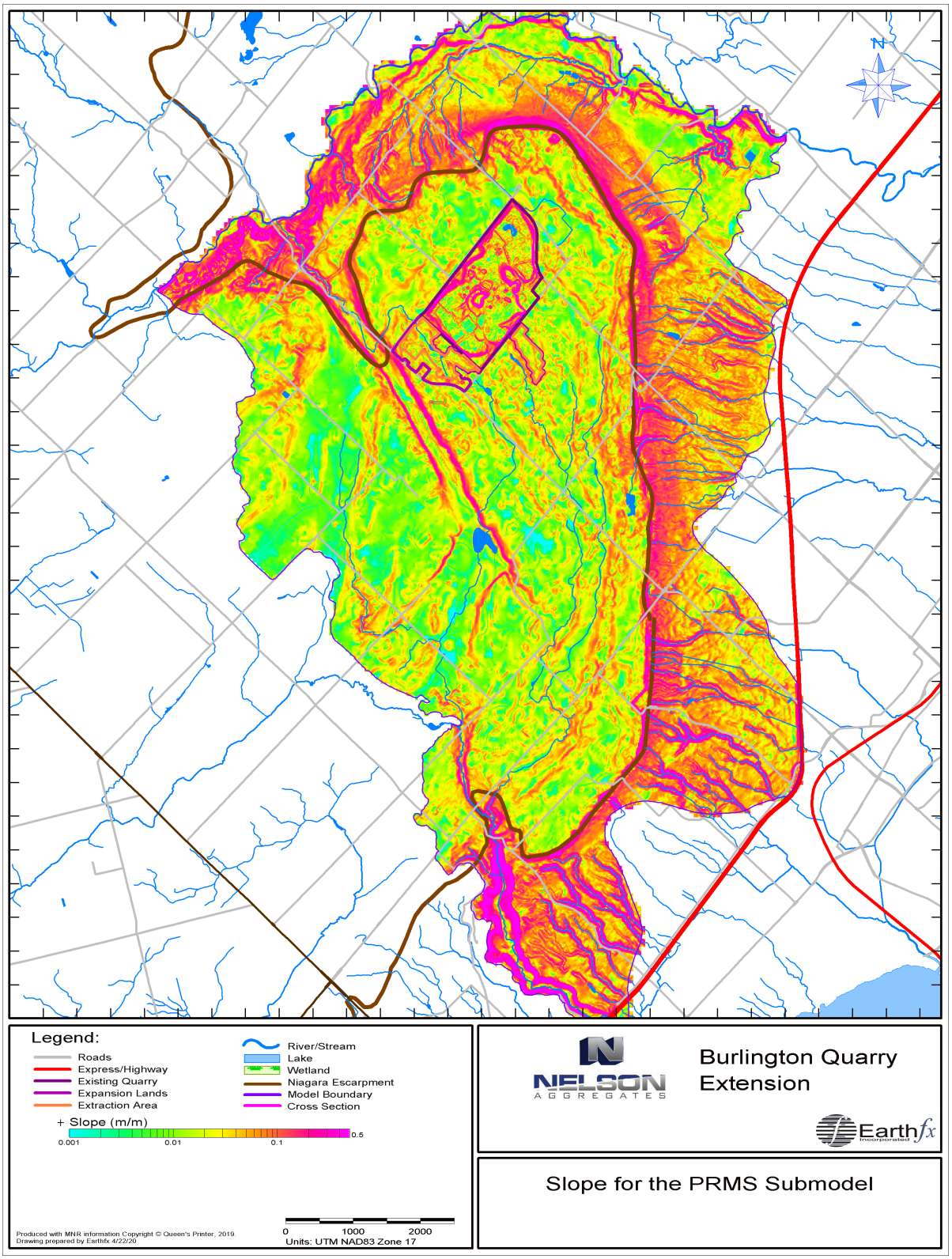

Figure 17.8: PRMS model cell slope.

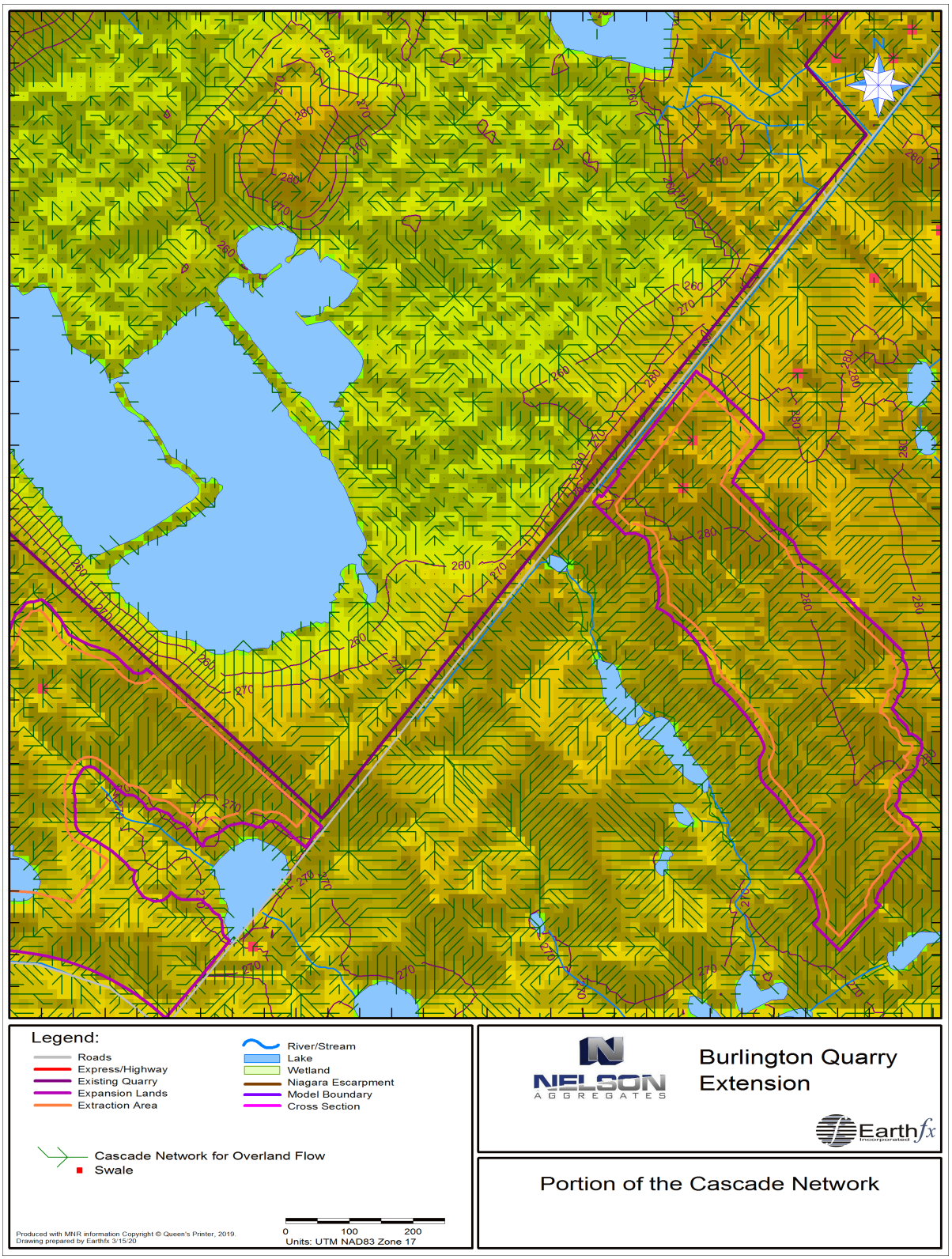

Figure 17.9: Cascade network near the Nelson Burlington Quarry.

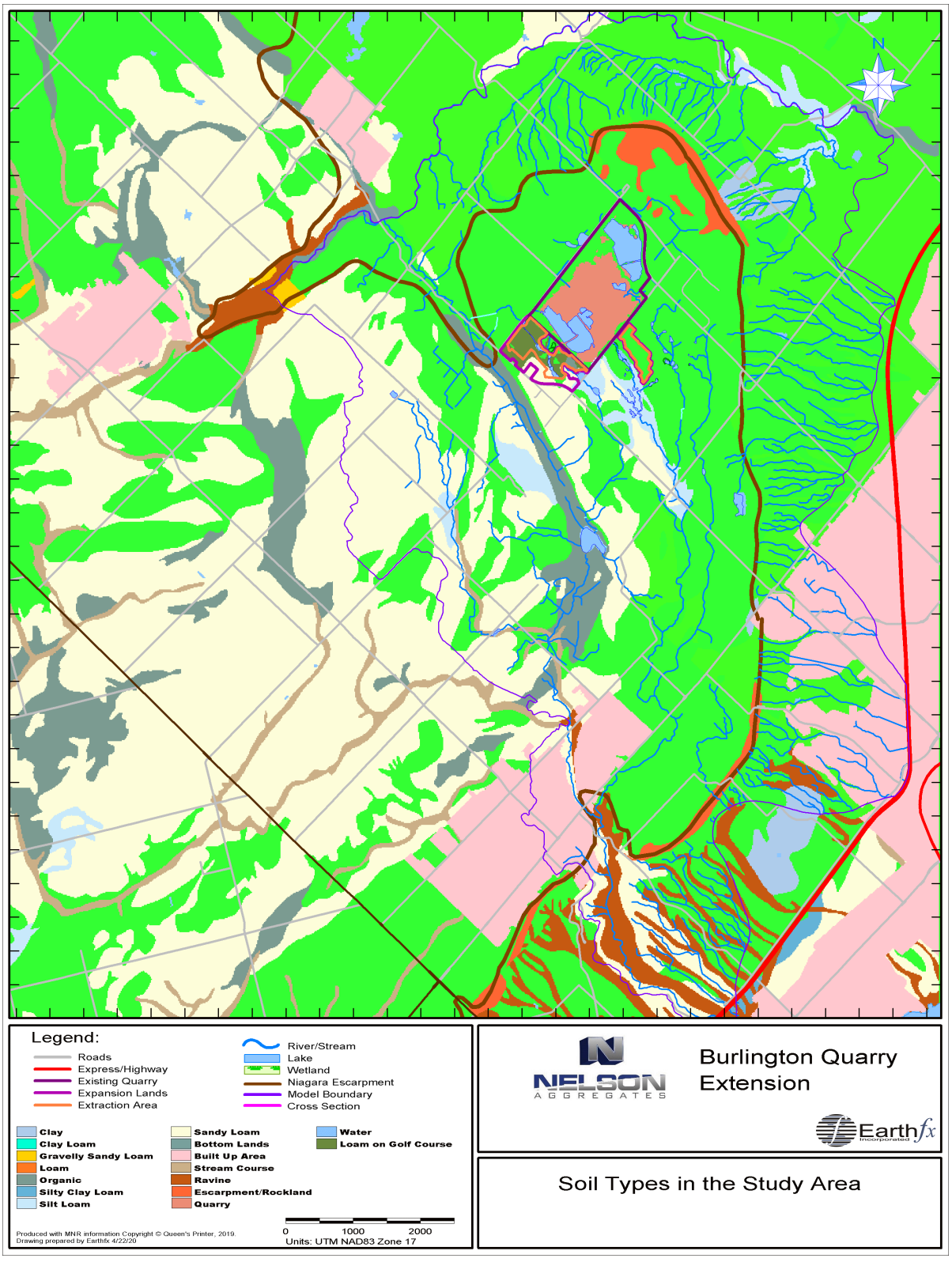

Figure 17.10: Surficial soil index (MNR, 2013).

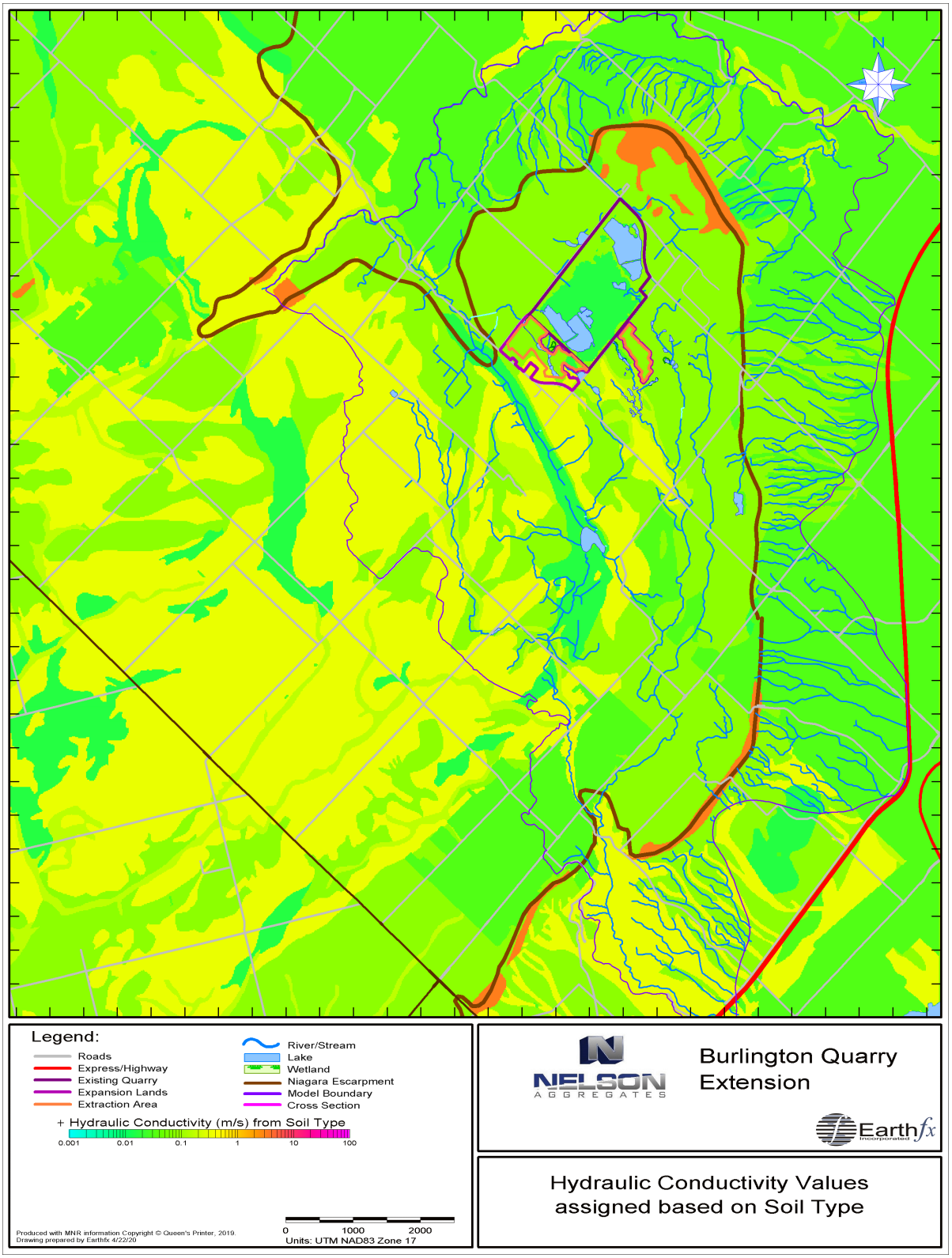

Figure 17.11: Surficial soil hydraulic conductivity.

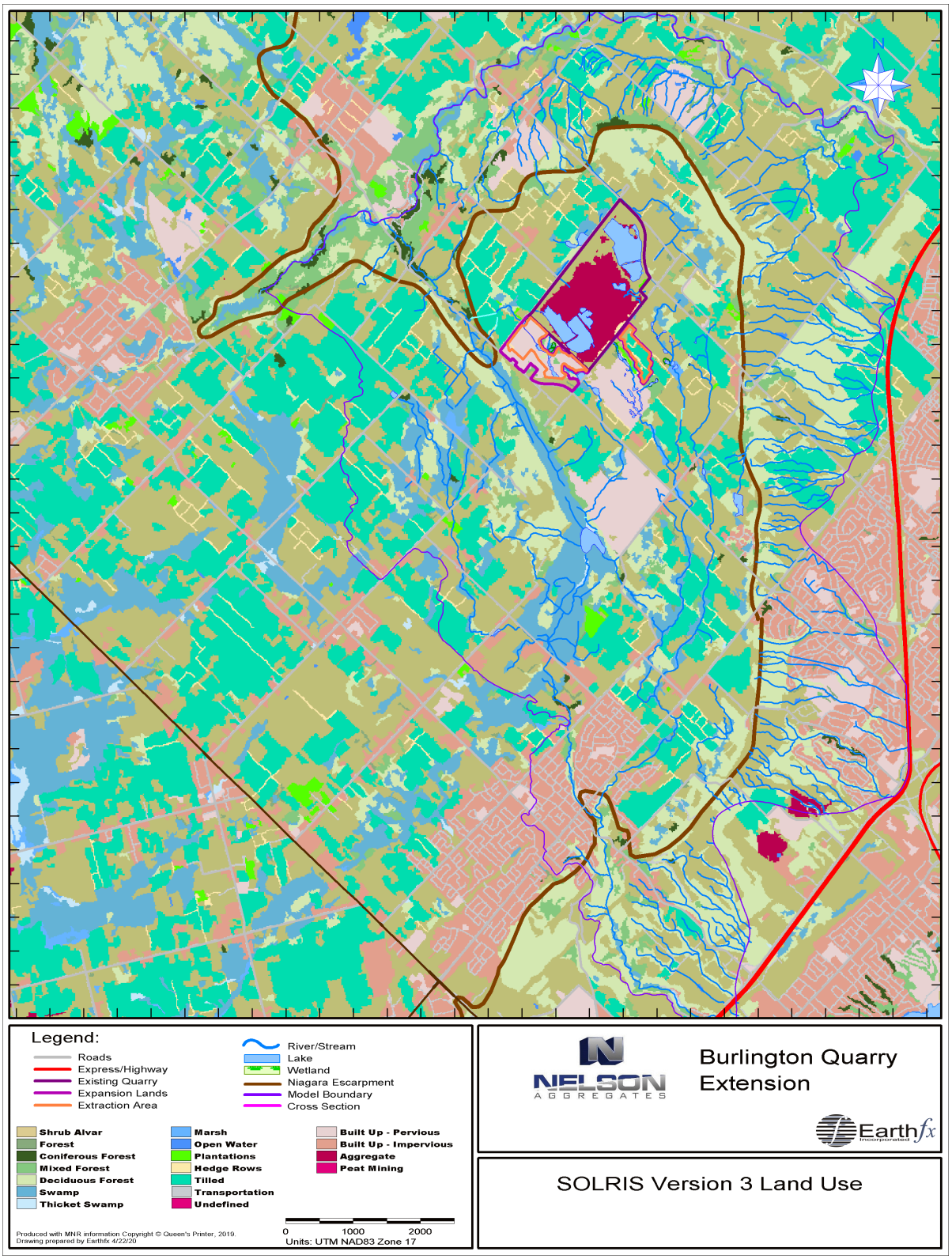

Figure 17.12: SOLRIS v3 (MNRF, 2019) land use index.

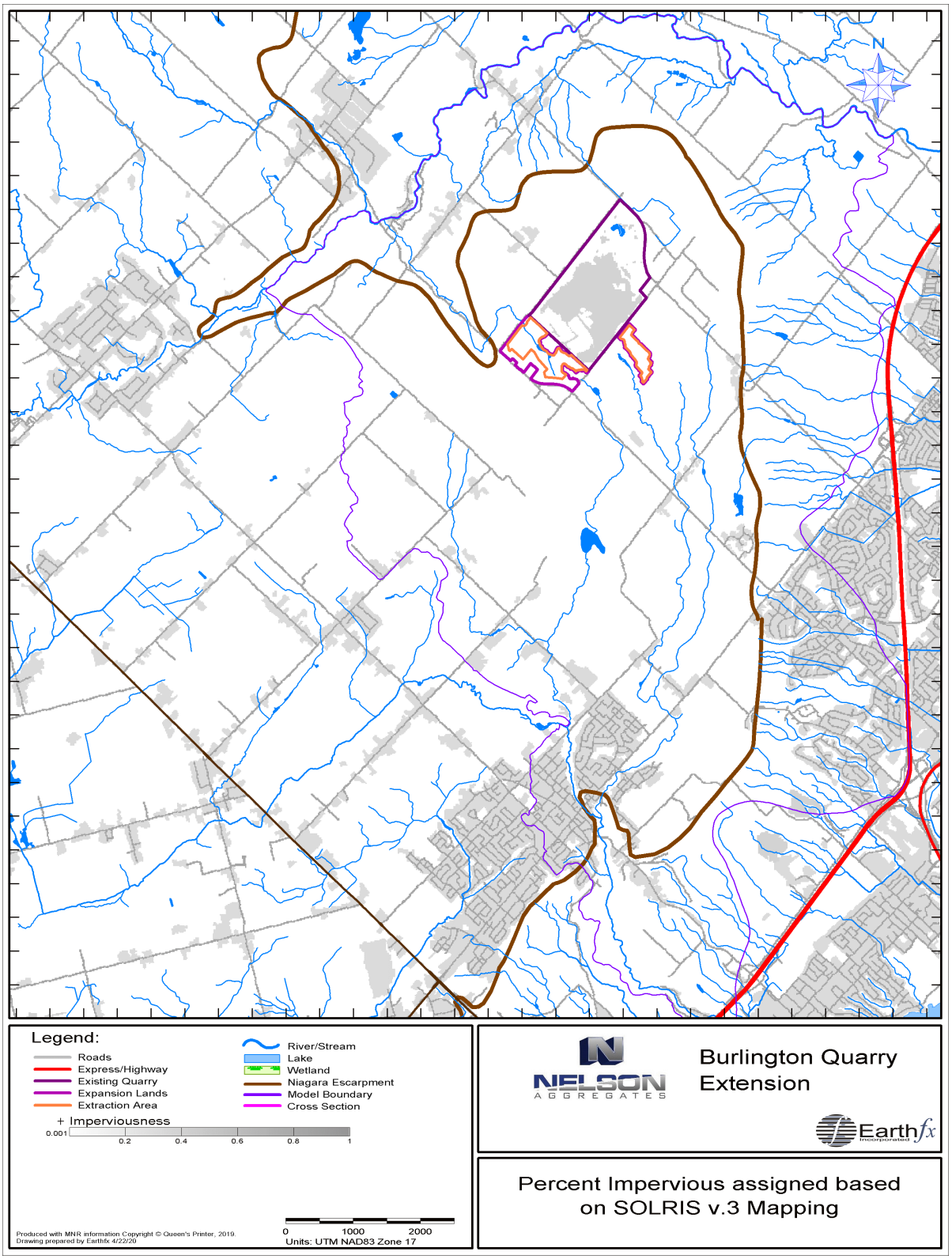

Figure 17.13: Percent impervious cover per cell assigned based on SOLRIS v.3 land cover.

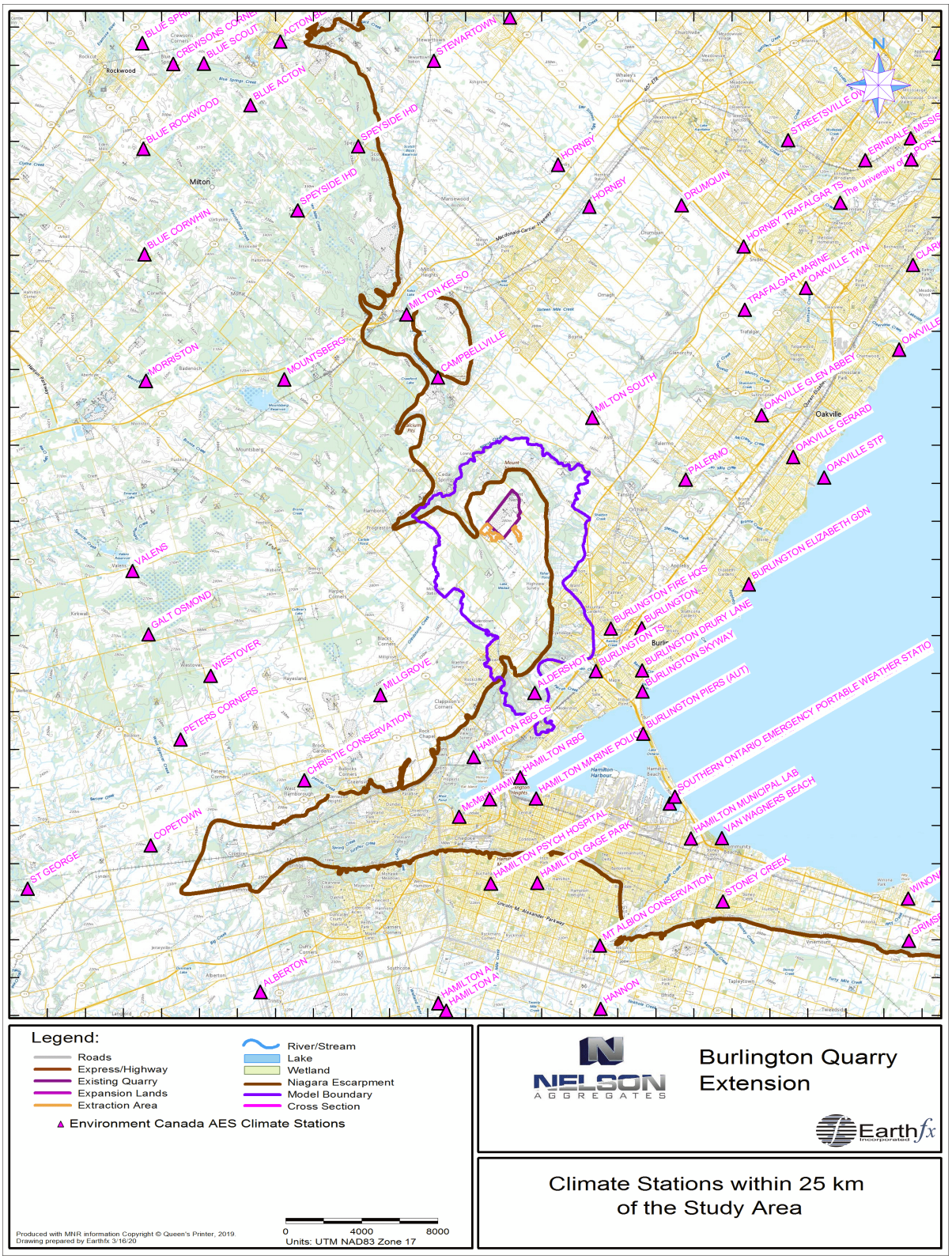

Figure 17.14: Environment Canada AES climate stations within 25 km of the study area.

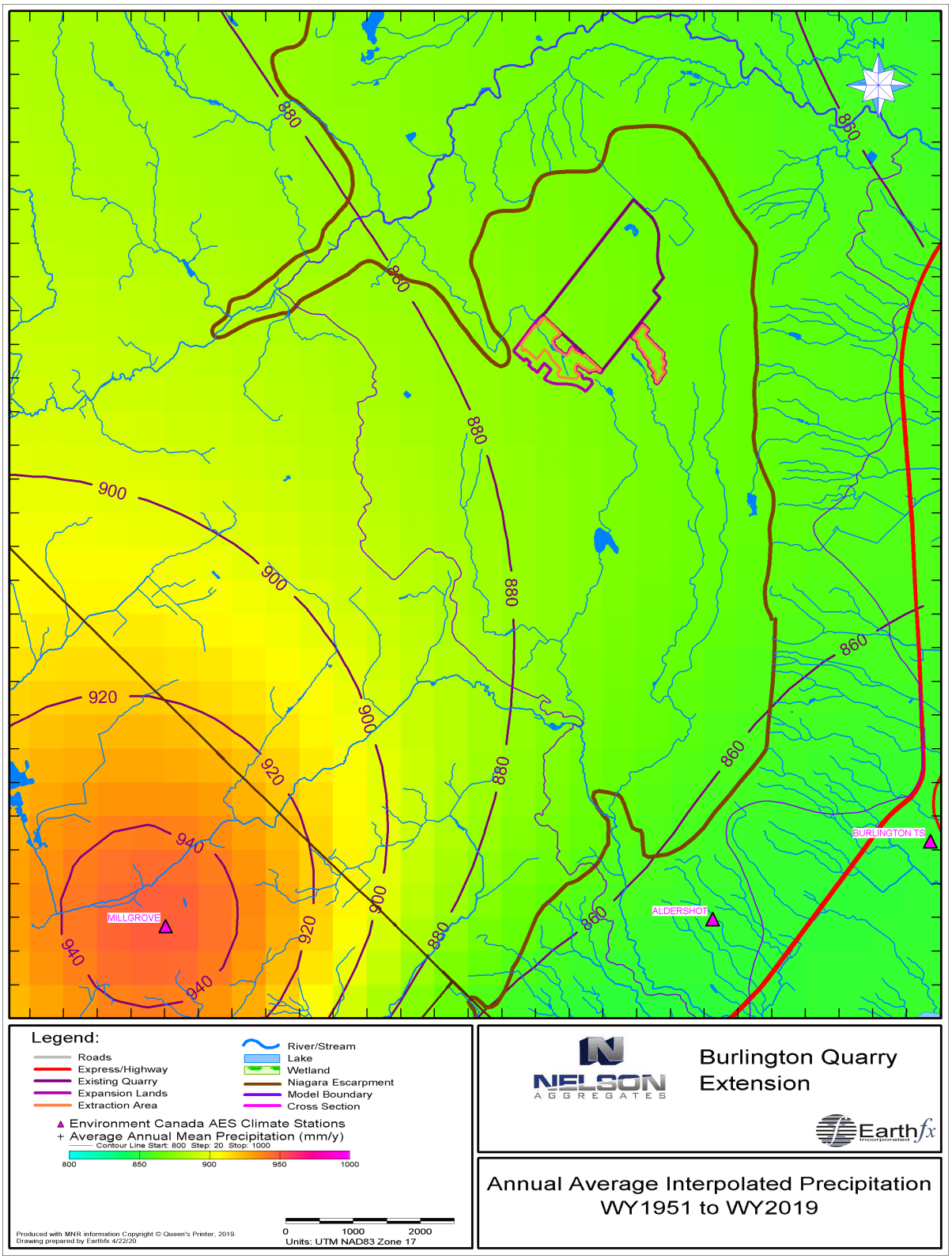

Figure 17.15: Interpolated average annual precipitation (data from WY1951 to WY2019).

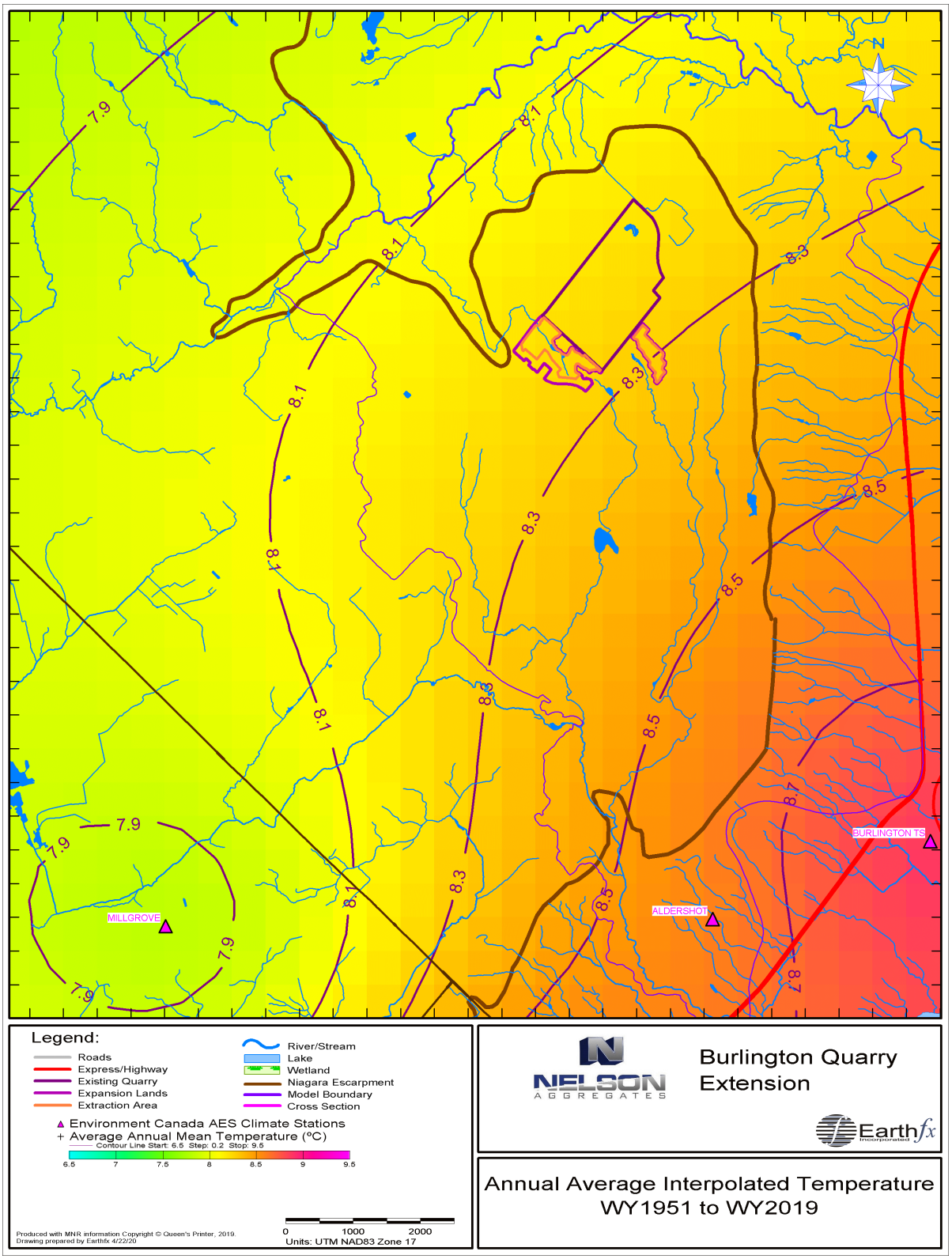

Figure 17.16: Interpolated annual average temperature (data from WY1951 to WY2019).

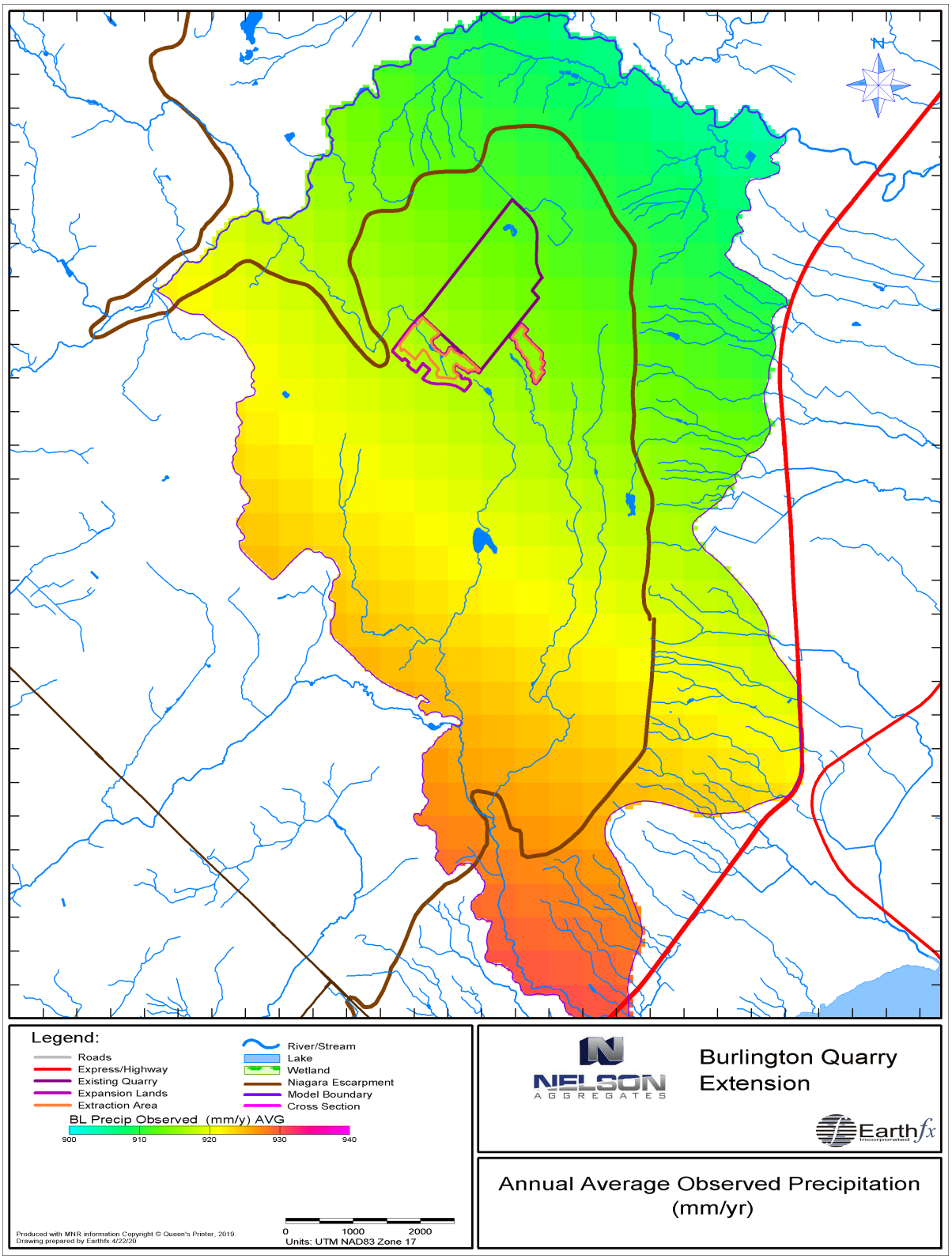

Figure 17.17: Simulated annual average precipitation in the PRMS submodel in mm/yr.

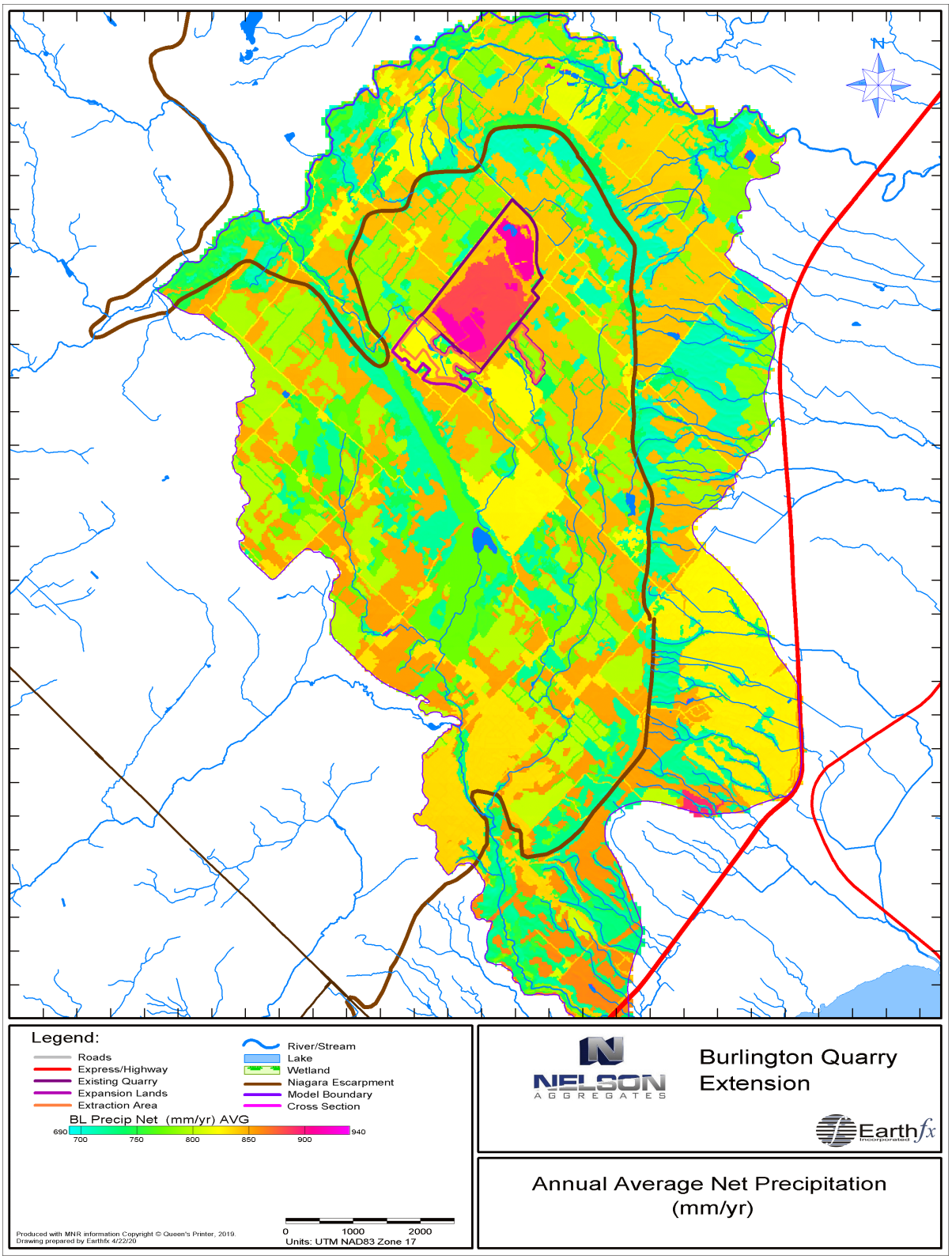

Figure 17.18: Simulated annual average net precipitation (after canopy interception and sublimation) in mm/yr.

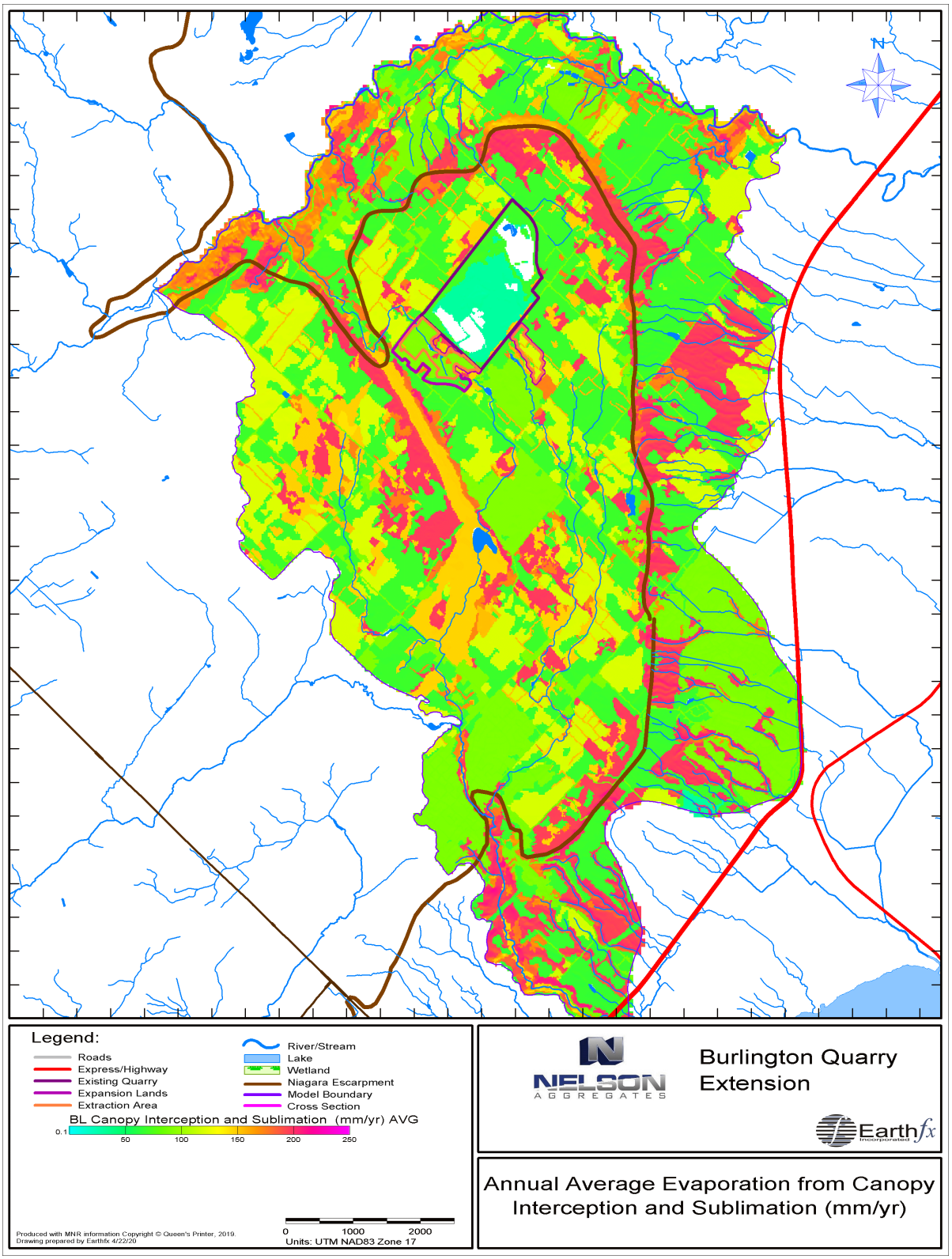

Figure 17.19: Simulated annual average evaporation from canopy interception and sublimation in mm/yr.

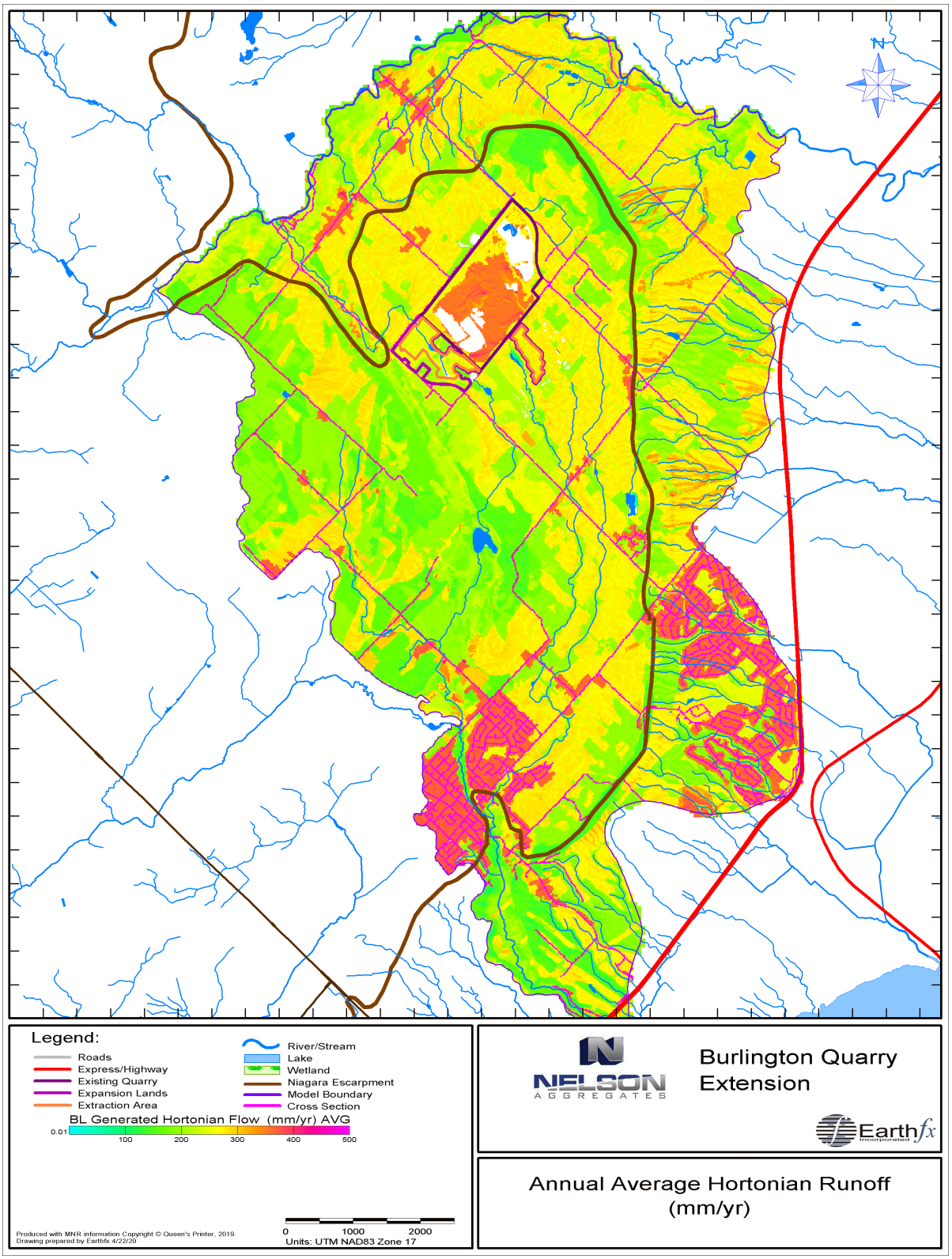

Figure 17.20: Simulated annual average Hortonian overland runoff in mm/yr.

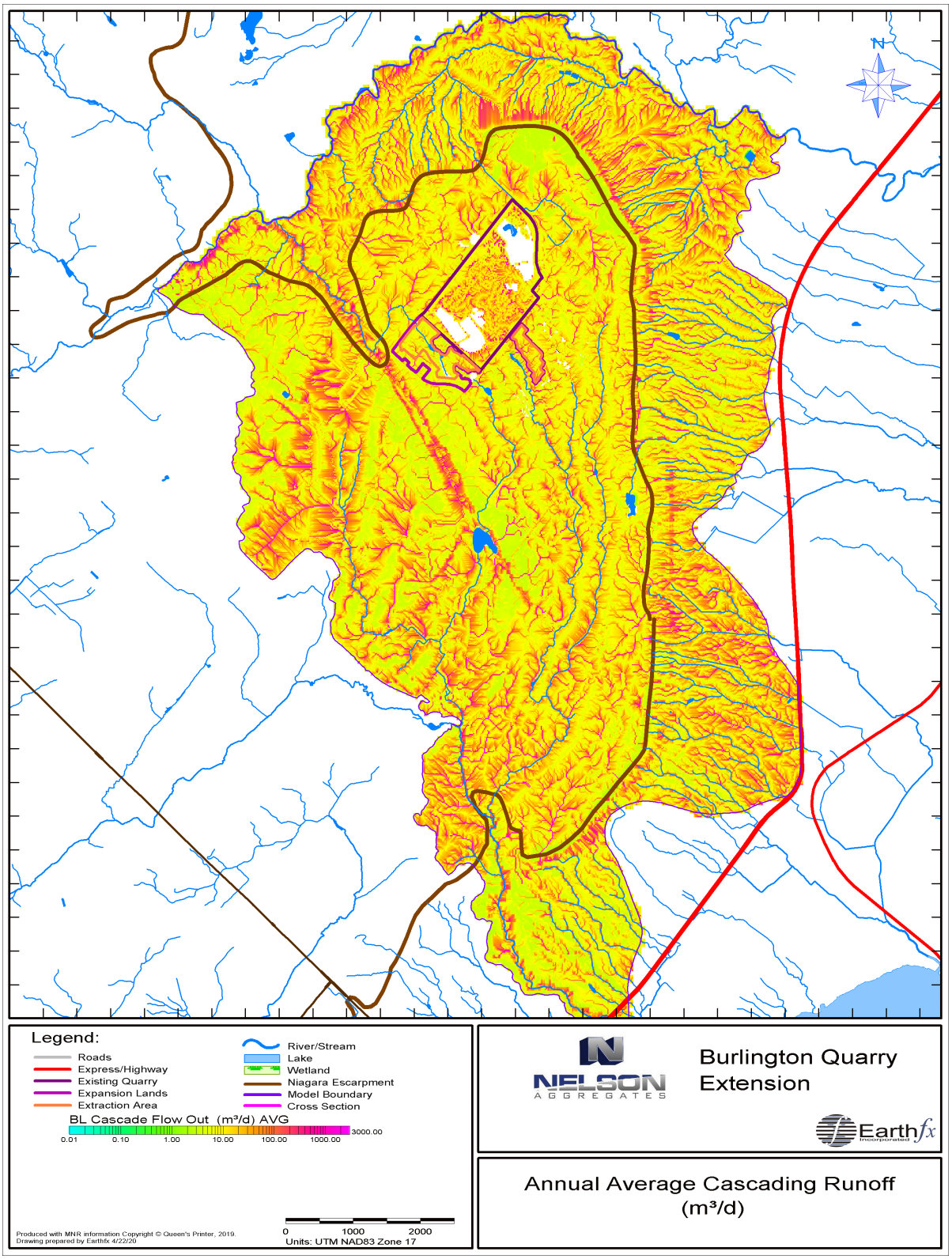

Figure 17.21: Simulated annual average cascading runoff (Hortonian, Dunnian, and interflow) passing through each cell in m^3/d.

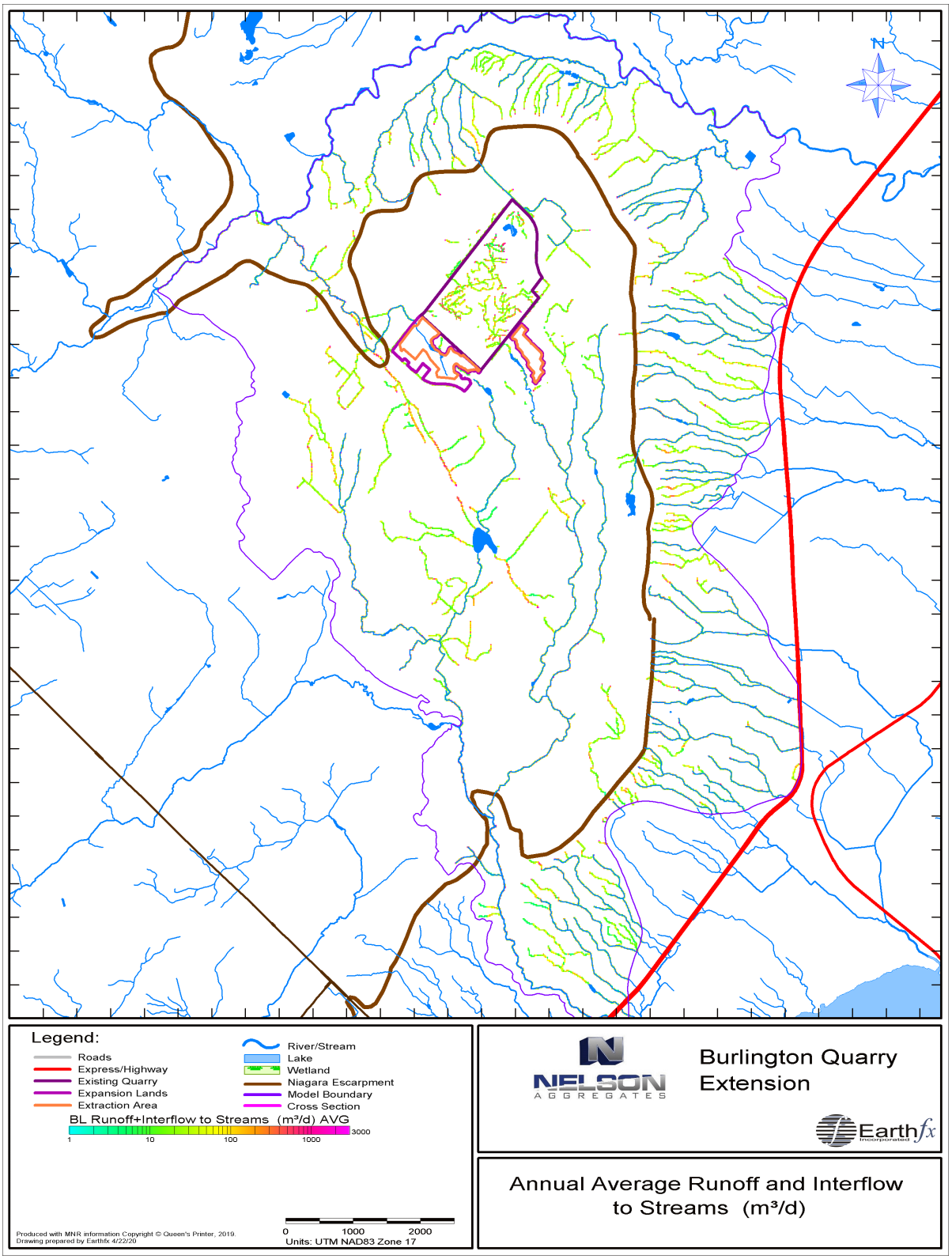

Figure 17.22: Simulated annual average runoff (Hortonian and Dunnian) and Interflow to streams in m^3/d.

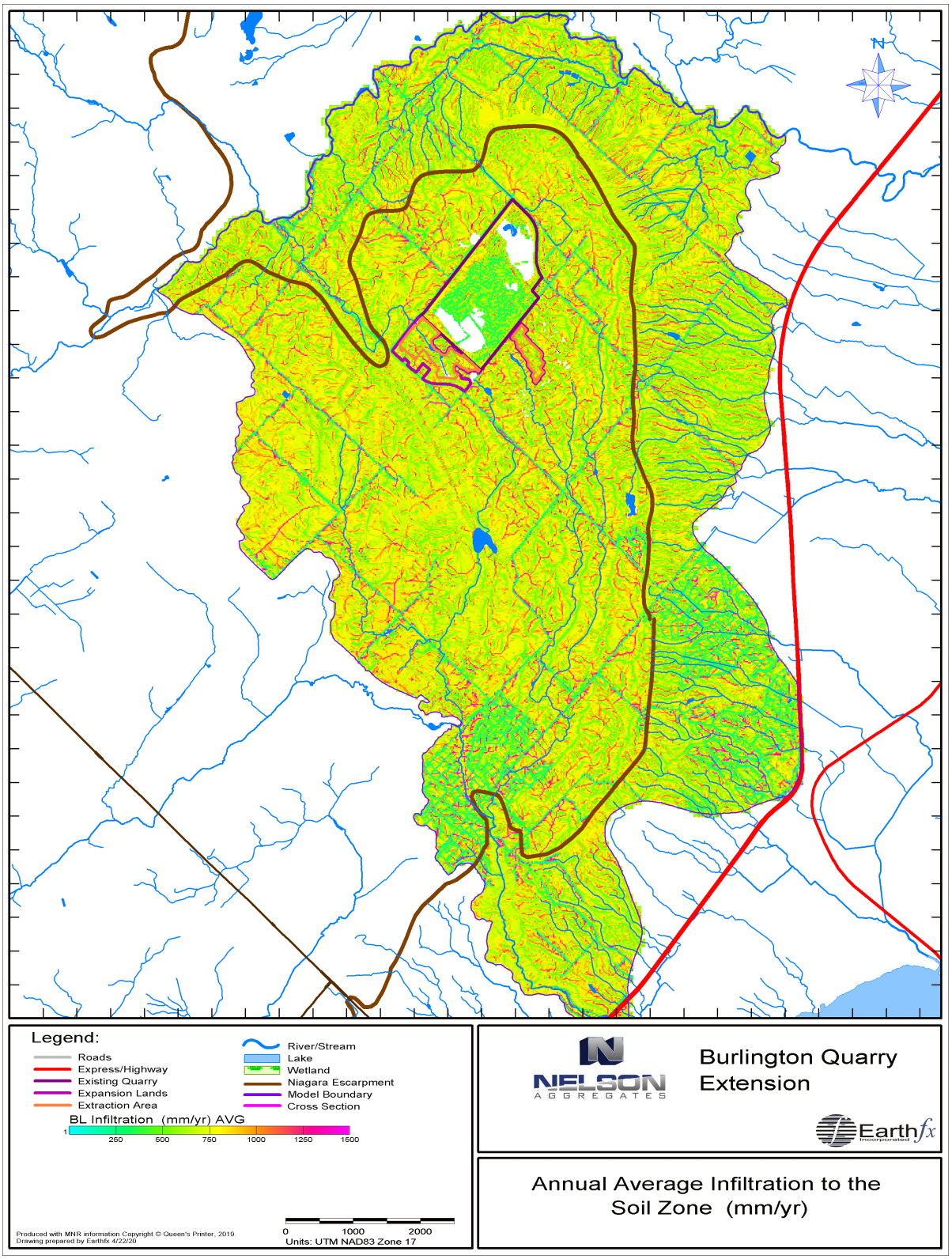

Figure 17.23: Simulated annual average infiltration to the soil zone in mm/yr.

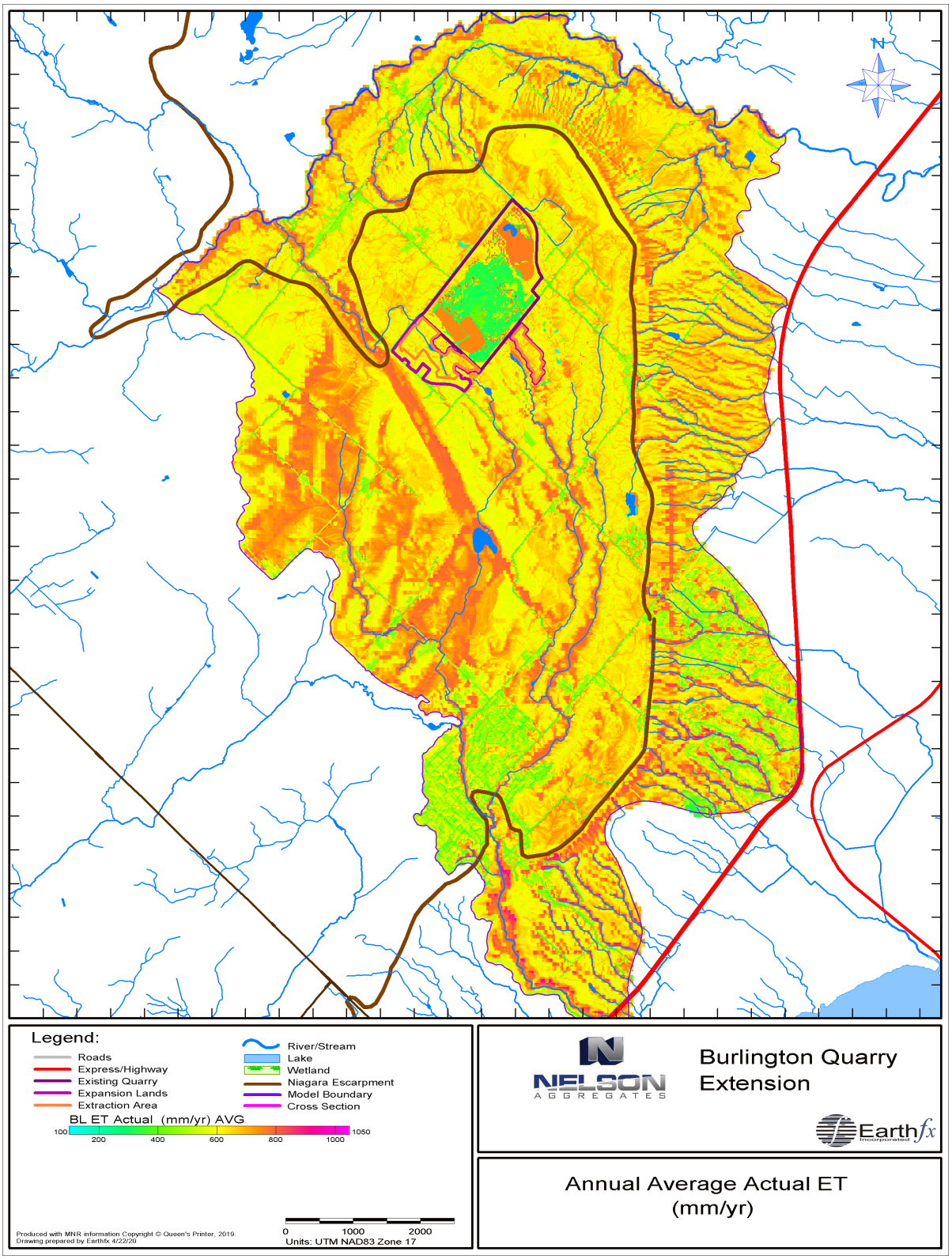

Figure 17.24: Simulated annual average actual evapotranspiration (soil zone ET, canopy losses and sublimation) in mm/yr.

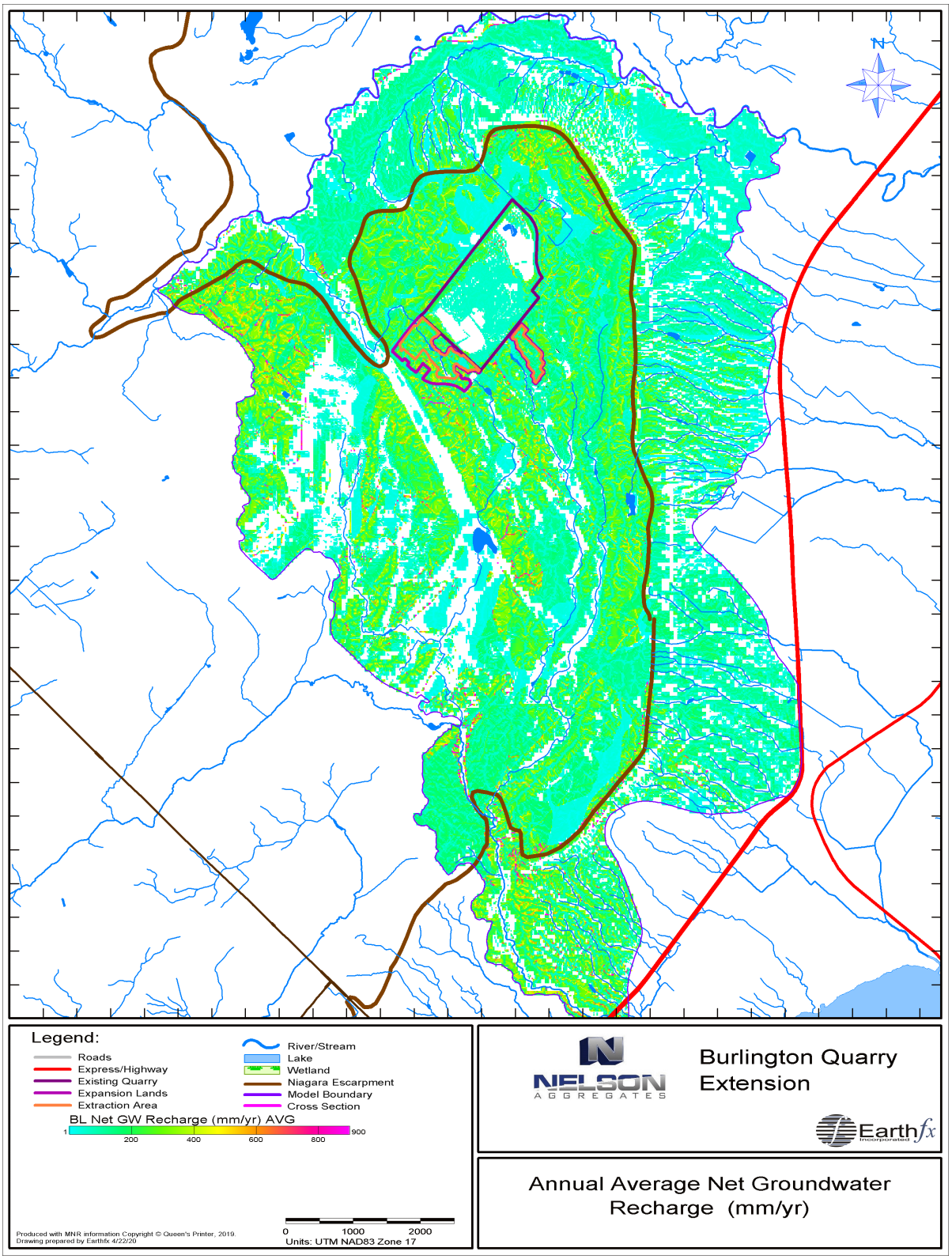

Figure 17.25: Simulated annual net average groundwater recharge in mm/yr.

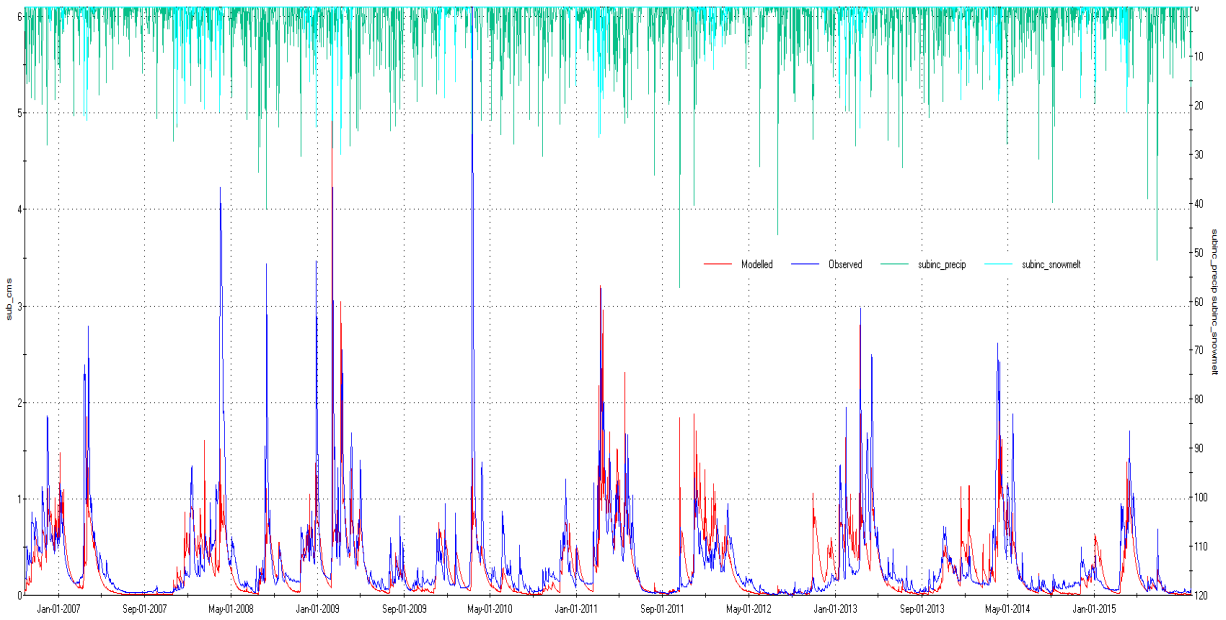

Figure 17.26: Simulated and observed streamflow (in m^3s) at the Grindstone Creek near Millgrove gauge along with precipitation and snowmelt.

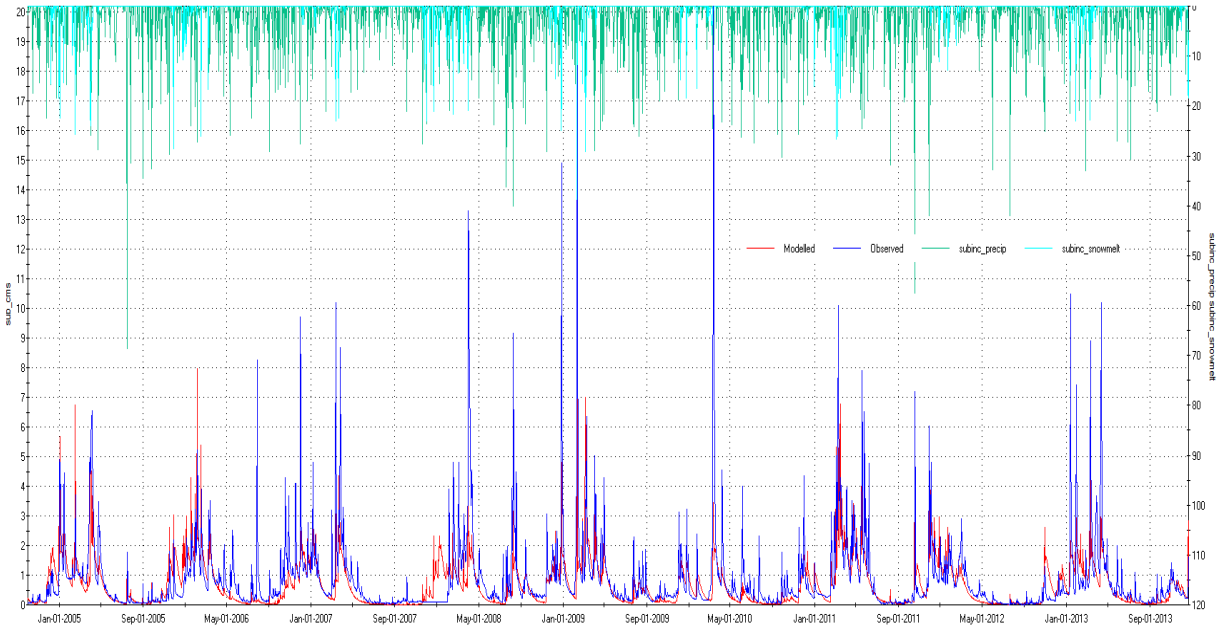

Figure 17.27: Simulated and observed streamflow (in m^3s) at the Grindstone Creek near Aldershot gauge along with precipitation and snowmelt.

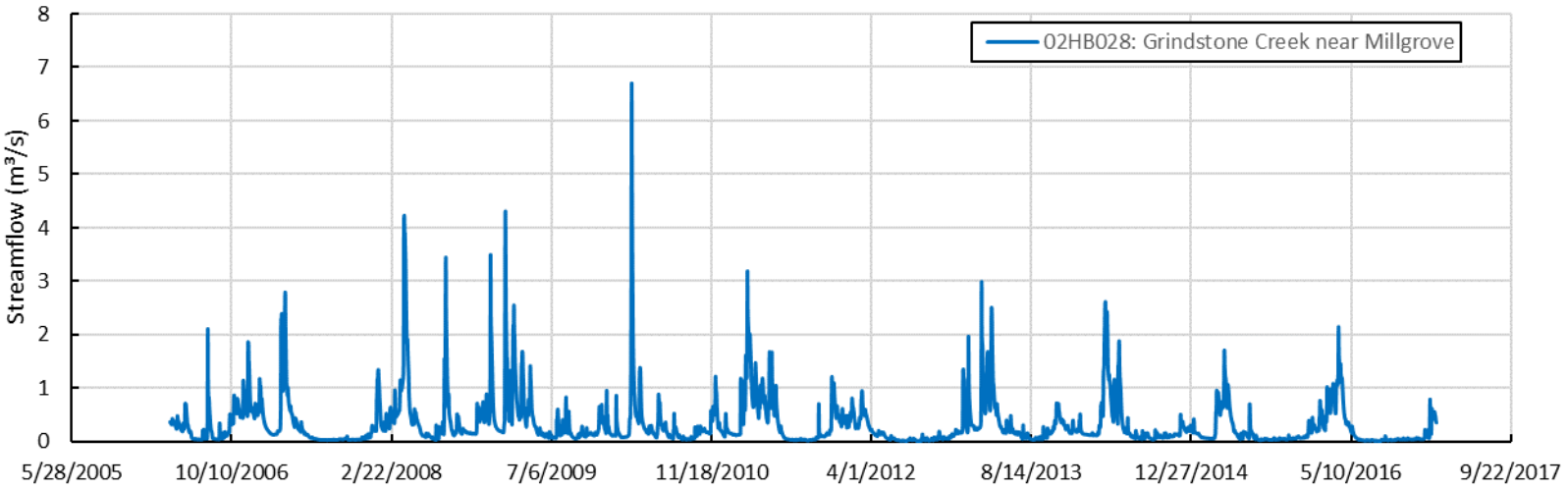

Figure 17.28: Observed streamflow at Grindstone Creek near Millgrove (WSC Station No. 02HB028)

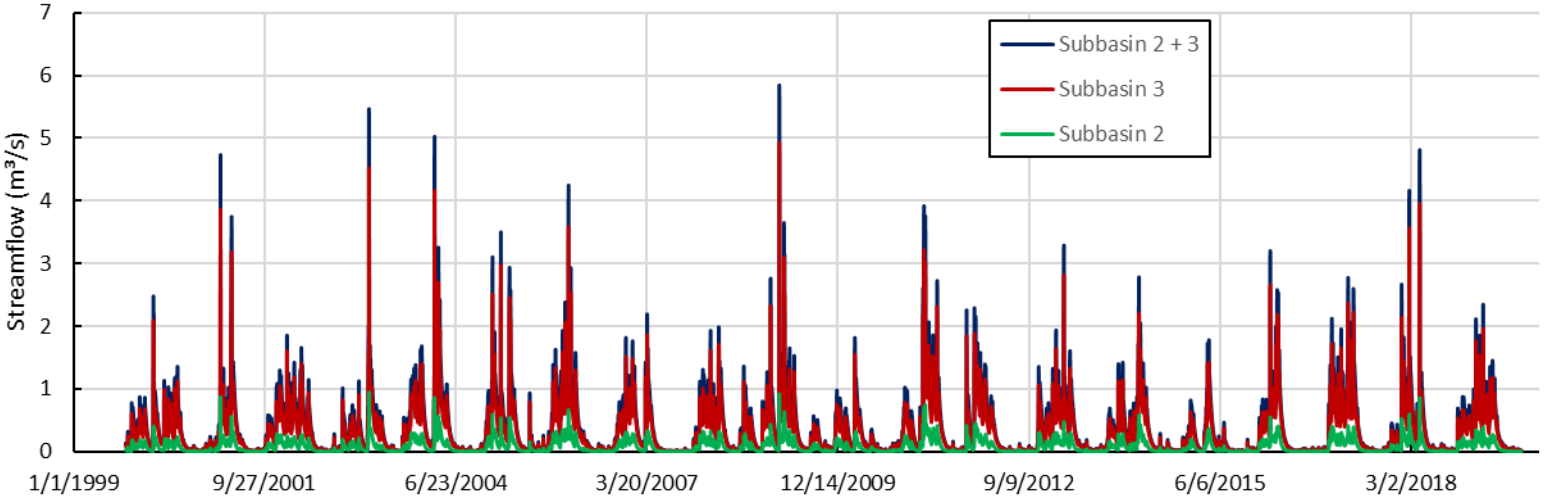

Figure 17.29: Incremental and cumulative simulated streamflow in PRMS subbasin 2 and 3.

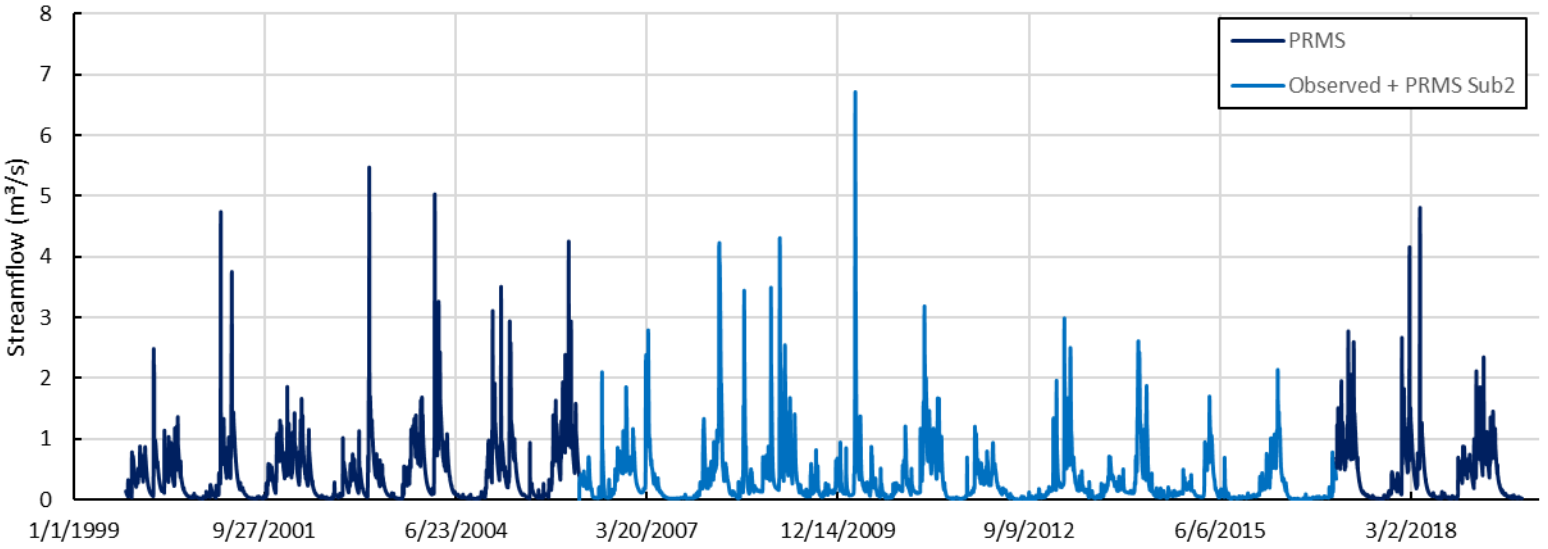

Figure 17.30: Partial synthetic hydrograph of Grindstone Creek inflows to be applied to the integrated GSFLOW model.

18 Appendix D: Groundwater Sub-model Development

18.1 Introduction

A groundwater flow model is a simplified representation of the complex physical, hydrologic and hydrogeological processes that affect the rates and direction of groundwater flow. These processes relate to physical characteristics of the study area and include:

- stratigraphy (the bedrock and overburden stratigraphic layers, their top and bottom surface elevations, lateral extent of the formations, and unit thickness);
- hydrostratigraphy (descriptions of the aquifers and aquitards in the study area, their top and bottom surface elevations, and their lateral extent, thickness, and degree of continuity);
- aquifer and aquitard properties (estimated hydraulic conductivity, anisotropy, saturated thickness, transmissivity, porosity, and storage properties);
- inputs to the hydrologic system (rates of groundwater recharge and discharge and the underlying processes that affect these rates, such as precipitation, ET, overland runoff, infiltration, and baseflow);
- properties of the surface-water system and factors controlling groundwater/surface water interaction;
- anthropogenic inputs and outputs from the groundwater system (e.g., pumping rates for quarry dewatering); and
- other significant features, including surficial geology and topographic features that may affect recharge and discharge rates.

18.1.1 Groundwater Flow Equation

Groundwater flow is governed by Darcy's Law, which states that flow is proportional to the hydraulic gradient and hydraulic conductivity of the aquifer material. Darcy's Law can be written as:

$$q = -K \frac{dh}{dx} \qquad \text{Eq. 18.1}$$

where q is the specific discharge or rate of flow per unit area, K is the hydraulic conductivity, and dh/dx is the hydraulic gradient (change in hydraulic head per unit length). Groundwater flow is also governed by the Law of Conservation of Mass which states that all inflows to an area must be balanced by outflows and/or by a change in aquifer storage. When the mass balance equation is combined with Darcy's Law, it yields the governing equation for three-dimensional groundwater flow.

$$\frac{\partial}{\partial x}\left(K_{xx}\frac{\partial h}{\partial x}\right) + \frac{\partial}{\partial y}\left(K_{yy}\frac{\partial h}{\partial y}\right) + \frac{\partial}{\partial z}\left(K_{zz}\frac{\partial h}{\partial z}\right) = S_0 \frac{\partial h}{\partial t} + R - Q \qquad \text{Eq. 18.2}$$

where:
- K_{xx} = hydraulic conductivity in the x direction;
- K_{yy} = hydraulic conductivity in the y direction;
- K_{zz} = hydraulic conductivity in the z direction;
- h = hydraulic head (also referred to as groundwater levels or potentials);
- S_0 = specific storage; and
- R = rate of groundwater recharge
- Q = other withdrawals from groundwater

In early phases of the study, steady-state conditions, where the time–dependent term is set to zero, were assumed in order to approximate long-term average conditions in the groundwater flow system. The steady-state groundwater levels are dependent primarily on the hydraulic conductivity values and the rates of recharge and, therefore, provide an opportunity to separately assess these values.

In the hydraulic approach to aquifer flow (see Bear, 1979), Eq. 18.2 can be simplified by integrating over the thickness of the aquifer. The resulting steady-state equation for two-dimensional flow in a confined aquifer is written mathematically as:

$$\frac{\partial}{\partial x}\left(T_{xx}\frac{\partial h}{\partial x}\right)+\frac{\partial}{\partial y}\left(T_{yy}\frac{\partial h}{\partial y}\right)+\left[\frac{K'_U}{B'_U}(H_U-h)\right]+\left[\frac{K'_L}{B'_L}(H_L-h)\right]+R-\mathrm{Q}'=0 \qquad \text{Eq. 18.3}$$

where:
- T_{xx} = transmissivity in the x direction (where $T_{XX} = K_{XX}B$);
- T_{yy} = transmissivity in the y direction;
- H = hydraulic head;
- K' = vertical hydraulic conductivity of an overlying (or underlying) confining unit
- B' = thickness of the upper (or lower) confining unit;
- H_L/H_U = head in the aquifer layer overlying/underlying the confining unit;
- Q' = Withdrawal rates (per unit area) from groundwater

Eq. 18.3 can be written for each aquifer in a layered sequence of aquifers and confining units. Eq. 18.3 is the partial differential equation that forms the basis of the mathematical model developed for the study area. Numerical methods are used to solve Eq. 18.3 for each cell in a grid used to represent the model area subject to the boundary conditions and variable aquifer/aquitard properties, geometry, and rates of recharge and discharge across the study area.

18.1.2 Model Description

The groundwater flow submodel used in this study was built with the USGS MODFLOW computer code (Harbaugh, 2005). MODFLOW solves the groundwater flow equation (Eq. 13.3) using a gridded finite difference approach on a steady-state or transient (time-dependent) basis. The basic MODFLOW-2005 code is documented in Harbaugh (2005). The MODFLOW code is well suited for modelling transient groundwater flow in multi-layered aquifer systems and can easily account for irregular boundaries, complex stratigraphy, and variations in hydrogeologic properties. A newer version of the MODFLOW code, MODFLOW-NWT (Niswonger *et al.*, 2011), is especially well suited for representing thin aquifers and sharp changes in model layer stratigraphy, such as those occurring in models with patchy, discontinuous units or with steep slopes such as those that occur at the edges of the Burlington Quarry and at the Niagara Escarpment.

18.1 Model Discretization

The finite-difference method requires that the study area be subdivided into a grid of small square or rectangular cells and multiple layers. Optimal grid design is a balance between achieving the highest resolution possible (i.e., a large number of small cells) and minimizing model run times, which increases proportionally to the number of cells. Separate numerical model layers were used to represent the bedrock and overburden hydrostratigraphic layers discussed in the hydrogeological conceptualization (see Section 5.2).

18.1.1 Model Grid

The grid developed for this study has a high level of refinement in the quarry vicinity with 15 m square cells in the extension areas and 60 m cells in the model periphery. The model grid is shown in Figure 18.4 and consists of 377 rows and 366 columns for a total of 137,982 grid cells for each of the model layers. Cells outside the model area were considered inactive and do not contribute to groundwater flow.

MODFLOW works in a local, grid coordinate system based on row and column numbers. The VIEWLOG-GIS preprocessor (Kassenaar, 2013) was used to translate geo-referenced map data into MODFLOW coordinates. The local origin for the model grid is at 585,105 E and 4,794,585,500 N in the UTM Zone 17 UTM (NAD83) coordinate system. All digital data for the study area were georeferenced to the same UTM coordinate system.

18.1.2 Model Layers

The numerical model consists of nine layers as introduced in Section 5.2. These layers generally correspond to the hydrostratigraphic units with a number of exceptions. The mapping of hydrostratigraphic units to model layers is summarized in Table 18.1 and discussed in detail below.

Layer 1 represented the upper surficial deposits in the study area and was comprised primarily of weathered Halton Till above and below the Niagara Escarpment and surficial sands in the Medad Valley and to the west. Layer 2 represented the unweathered portion of the Halton Till. Layer 3 represented the Mackinaw Interstadial Sediments (MIS) sands and Maple Formation above the Niagara Escarpment, where present, and the Oak Ridges Aquifer Complex sands below the Niagara Escarpment. Both units are thin and can be discontinuous. Older tills may also be present in parts of the study area but were assumed to be patchy and were not represented explicitly in the model.

Principal Aquifer: Considerable thought was given to how best represent the fracture system and karst and features within the principal bedrock aquifer (Goat Island, Gasport, and Irondequoit Formations, collectively referred to as the Amabel formation, as discussed in Section 3.4.5) with the MODFLOW model. Analysis of borehole logs and other hydrogeologic data (see Section 5.2) indicated that multiple horizontal fracture zones were present within the Amabel aquifer and possibly at or below the contact with the Irondequoit Formation. Vertical fracturing occurs less frequently but is still an important mechanism for propagating rapid response to changes to recharge or dewatering to the lower system. The aquifer also exhibits the dual-porosity nature of the fractured rock system which has, on one hand, high primary porosity in the bulk rock and therefore has high storage but slow response due to limited hydraulic conductivity and, on the other hand, has fracture zones with low secondary porosity but rapid response times.

Accordingly, the Amabel was subdivided into five numerical model layers. Layer 4 represented the upper, weathered portion. This layer was assumed to be of relatively high hydraulic conductivity, lower storage properties, and a minimum of 1.0 m thick. Layer 5 represents the bulk Amabel aquifer which is assumed to have higher storage but less horizontal fracturing (or, equivalently, that the fractures are less continuous). Layer 6 represents a thinner (bedding plane) zone in which the fractures are more frequent and/or continuous. A lower bulk aquifer zone (Layer 7) separates the middle fracture zone from Layer 8 representing a thin lower fracture zone.

Vertical fractures occur throughout bulk Amabel layers. As an approximation, a percentage of cells (5% in the final model calibration) in Layers 5 and 7 were selected at random (with different cells in each layer) and assigned a lower storage value but higher vertical hydraulic conductivity.

It is important to note that this conceptual model has been implemented represent a clearly observed hydraulic behaviour in the principal aquifer in the vicinity of the quarry, but it is expected to be consistent across the entire model area. Similar behaviour can be seen in the MECP static water level data. This model representation addresses three key observations (discussed in detail in Section 5.3):

- Relatively rapid response to dewatering occurred away from the quarry, indicating good horizontal connection
- Strong vertical gradients between the upper and lower parts of the aquifer, even in close proximity to the quarry, indicating that vertical connection is limited
- Very rapid response occurs to recharge events in the deeper system, indicating good vertical connection. The seeming contradiction with the previous observation indicates that the vertical connections are present but are distributed spatially.

Finally, Layer 9 represents the underlying suite of lower hydraulic conductivity units separating the upper bedrock aquifer from the underlying Whirlpool Formation. The amount of water transmitted through these units is assumed to be limited. The Whirlpool Formation was not explicitly represented in the model.

Layer Continuity: An important consideration when translating the hydrostratigraphic model layers to numerical model layers is that MODFLOW requires continuity for the simulated numerical layers; whereas the hydrostratigraphic model has layers that pinch out to zero thickness. The hydrostratigraphy of the study area presented a unique challenge because of the discontinuous nature of some of the overburden units and the truncation of the key bedrock units at the quarry face and at the Niagara Escarpment.

To meet the layer continuity requirements for the numerical model, all model units were assigned a minimum thickness which was set to 0.3 m for Layers 1 through 8 and to 4 m for the Layer 9. The top surfaces of underlying units were adjusted downward, as needed, to ensure that the minimum thicknesses were maintained. This resulted in a subdivision of the weathered Queenston Formation into several sublayers below the Escarpment as well as subdivision of layers within the quarry. These layers were assigned similar properties and the use of multiple layers in these zones did not affect model performance or accuracy.

A cross section through the MODFLOW model layers is shown in Figure 18.5 (the Cedar Spring Road cross section location is shown in Figure 5.1). Notice that the model layers are continuous across the section. Figure 18.6 shows the hydraulic conductivity of the continuous layers, and how the thin continuous layers are assigned the same values where layer pinch outs occur. Finally, Figure 18.7 shows the Kh/Kv layer anisotropy, and illustrates how select random cells in the bulk Amabel layers have 1:1 anisotropy to represent random vertical fractures.

18.2 Model Boundary Conditions

While the focus of this study was on the Burlington Quarry and the proposed extension lands, model boundaries still had to extend to physical boundaries including regional watershed divides and major streams. The active model area extended between 2 and 10 km from the Burlington Quarry, as shown in Figure 18.4.

Boundary conditions were specified for cells that lie along lines corresponding to the physical boundaries of the groundwater flow system. Three general types of boundary conditions were used in the groundwater flow model: constant head, no-flow, and head-dependent discharge boundaries.

18.2.1 Constant-Head and No-Flow Boundary Conditions

Figure 18.8 shows the location of constant head and no-flow boundaries for the model. Constant head cells were applied along model boundaries corresponding to major water courses, including Bronte Creek along the northern boundary, and at points where the larger stream tributaries (Strahler Class 3) crossed the eastern model boundary.

Control elevations for the constant head boundaries were estimated from the 5-m DEM for the study area. The remaining boundaries were defined by watershed divides and were represented as no-flow boundaries. The no-flow boundaries have an implicit assumption that groundwater flow across the watershed divide is relatively small and would not affect flow in the area of interest. A no-flow boundary was imposed along the base of the model assuming that inflow into the model from below the lower aquitard units would be negligible.

18.2.2 Head-Dependent Discharge

Head-dependent flux boundaries were used extensively to represent groundwater/surface water interaction between streams and lakes within the model area. Flow between the groundwater system and streams was assumed to be exchanged as "leakage" across the streambeds. All mapped streams segments were simulated in the model. The locations of cells containing streams are shown in Figure 18.8.

Streams segments were assigned channel properties and streambed conductance (hydraulic conductivity divided by bed thickness). The rate of leakage is determined based on Darcy's Law where:

$$Q_{leak} = \frac{K'}{B'} A_L (H_L - h) = -K \frac{dh}{dx} \qquad \text{Eq. 18.4}$$

Where
- Q_{leak} = volumetric flow rate between aquifer and stream;
- K' = vertical hydraulic conductivity of the streambed;
- B' = thickness of the streambed
- A_L = wetted area of the streambed
- H_L = stream stage (in masl); and
- H = head in the aquifer (in masl)

Leakage between the stream and the aquifer is calculated on a cell-by-cell basis using the SFR2 module in MODFLOW (Niswonger and Prudic, 2005). In SFR2, a stream "reach" is defined as the portion of a stream within a model cell (see Figure 18.1). H_L, the stage in the centre of the reach, is calculated based on stream channel properties and the sum of upstream inflows, precipitation, evaporation, and overland flow to the reach. Multiple reaches can occur within a single cell and cell size is set small enough so that the h, the head in the model cell, reasonably represents the head in the aquifer beneath the streambed.

Leakage between the aquifer and water bodies, such as lakes, ponds, and shallow wetlands, is also governed by Eq. 18.4 and is calculated on a cell-by-cell basis using the LAK3 module in MODFLOW (Merritt and Konikow, 2000). In LAK3, a cell can represent all or a portion of a lake (Figure 18.1). The area A_L in Eq. 18.4 is equal to the cell area. H_L is equal to the lake stage and h is equal to the head in the cell underlying the lake. Lake volumes are calculated in a separate water budget analysis based on the sum of upstream inflows (as computed by the SFR2 module), precipitation, evaporation, overland flow to the lake, and outflow from the lake (also calculated by SFR2 based on lake stage). Lake stage is calculated from stage-volume relationships. Lakes can penetrate multiple model layers

and leakage can occur to cells adjacent as well as underlying the lake. The locations of cells representing lakes or shallow wetlands are shown in Figure 18.8.

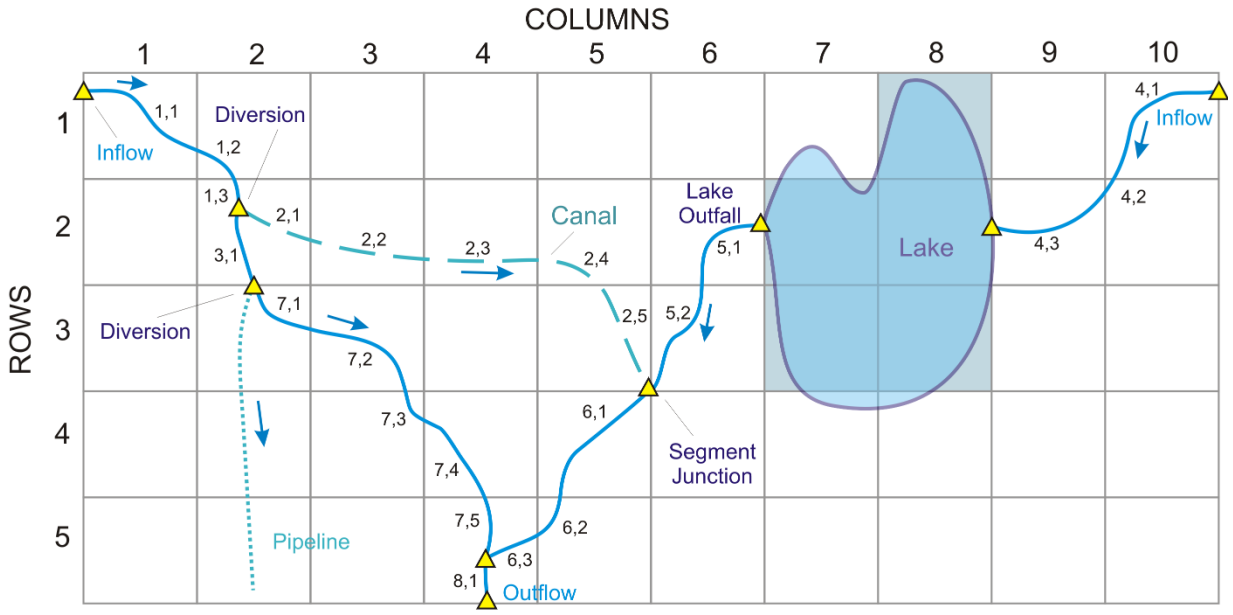

Figure 18.1: Stream network and lake representation in the SFR2 and LAK3 modules (modified from Markstrom, *et al.*, 2008).

18.2.3 Top of Model Flux Boundary

Recharge is specified as a calculated flux across the model top surface. Annual average recharge for the preliminary steady-state model calibration was calculated using long-term average results from the stand-alone PRMS submodel. (In transient GSFLOW simulations, the PRMS submodel calculates recharge on a daily basis and supplies this value, along with any unsatisfied ET demand, to the MODFLOW submodel.)

Head-dependent discharge boundaries are also assigned across the top surface of the model so that groundwater can discharge from the aquifer when the water table rises above ground. When MODFLOW is run in stand-alone mode, this water discharges to land surface and is routed directly to nearby streams as overland flow. Assignment of stream reaches to model cells was based on an analysis of land surface topography. When run in integrated model mode, groundwater is discharged from the aquifer to the soil zone. Excess water in the soil zone contributes to cascading runoff and interflow. All “surface leakage” flows were simulated using the Unsaturated-Zone Flow (UZF1) package for MODFLOW (Niswonger *et al.*, 2006).

18.3 Surface Water Features

18.3.1 Stream Network

The SFR2 module computes both stream leakage as well as flow into and out of each stream reach in the model. Accumulated streamflow is routed down the stream network to an outfall, which may be either a lake or the model boundary.

A locally-corrected version of the MNRF stream network was used in this study. The corrections were done to add local drainage features (such as roadside ditches) and update missing or modified streams in the quarry vicinity. Additional line-work was added to represent drainage on the existing quarry floor. The stream network for baseline conditions and model calibration is shown in Figure 18.8. As noted earlier, the stream network is broken into "segments" and "reaches" as shown in Figure 18.1. The stream network shown in Figure 18.8 contains 685 stream segments and 12,362 reaches. The stream and lake network were adjusted in the other quarry extension scenarios to account for the creation and removal of quarry lakes and diversions of streams.

Stream Channel Properties: To simplify the assignment of stream properties, the stream segments were assigned to different classes. Natural streams were assigned Strahler Class numbers (where headwater streams are assigned a Strahler class of 1 and the class number increases downstream when two tributaries with the same class meet). Additional classes were used to represent outlet structures, karst streams, quarry floor drains, and conduits. Missing channel segments and added ditching were assumed to be of Strahler 1 order. Karst streams were assumed to interact directly with the weathered the bedrock in Layer 4. The location of karst features (as indicated by points where streams dropped into the subsurface or emerged as springs) was informed by Worthington Groundwater (2006). Quarry floor drains were assigned based on topography and aerial imagery.

Structures were assigned to all lakes in-line with the stream network. While most of the lakes did not contain an actual control structure, representing the lake outlet as a wide slotted weir provided continuous flow and helped improve numerical stability. Conduits were added to convey quarry water to a discharge location and represent closed pipes that did not experience leakage or receive surface runoff. (Note: conduits were only for quarry extension scenarios and were not present in the calibration/baseline conditions). Figure 18.9 shows the stream network broken down by type in the vicinity of the Burlington Quarry.

Channel geometry is represented in SFR2 using an 8-point section. Consistent stream cross-section geometry was assumed for each Strahler class and consisted of a primary narrow central channel and a wide outer channel (Figure 18.2). Typically, flow occurs within the narrow central channel. Other channel properties are summarized in Table 18.2, and Table 18.3.

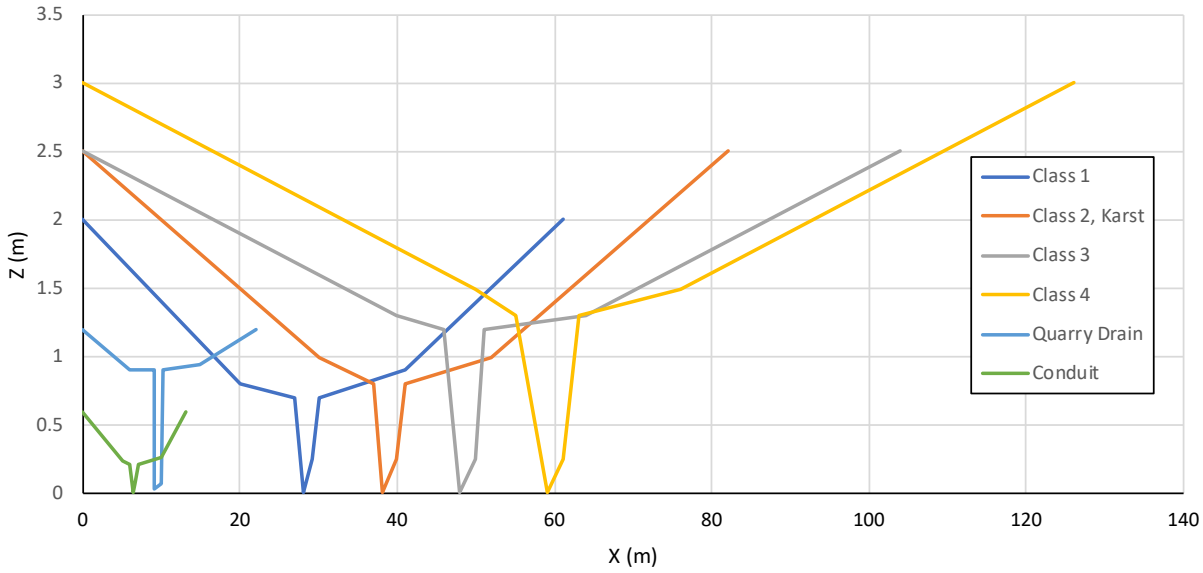

Figure 18.2: Simulated stream channel geometry.

18.3.2 Lake and Wetland Representation

The location and delineation of lakes was done using the Ontario Hydro Network (OHN) water body geospatial dataset. Some updates were made in the quarry vicinity base on aerial imagery and field observations made by the project team. A total of 40 MODFLOW "lakes" were simulated in the model, as shown in Figure 18.9. Some of the smaller ponds were not explicitly represented in the model, particularly if they were located below the Niagara Escarpment.

Lake bathymetry was assigned as the depth below the top of model Layer 1. In most cases, lake bathymetry was assumed to be 1.5 m, with a few exceptions. Lake Medad was assumed to be 3.33 m deep and the quarry ponds were assumed to be between 1.5 and 3 m with the sump of the south pond extending to 6 m. Detailed bathymetry data was provided by Tatham Engineering for the Burlington Springs Golf Course ponds. The bathymetry points were interpolated to the MODFLOW grid and incorporated into the model geometry. Cells in the underlying layers were assigned as lake cells based on bathymetry and the layer top elevations.

Several important shallow wetland features were identified by the project team in close proximity to the existing quarry and proposed future extension lands. These features were represented as shallow MODFLOW lakes to better simulate the intermittent occurrence of standing water. The bathymetry survey completed by Tatham Engineering was also completed through most of the key wetlands and was interpolated to the MODFLOW grid and incorporated into the model. Wetland lakes were assigned to Layer 1 by adjusting the base of Layer 1 to correspond with the interpolated bottom elevation. Care was taken to ensure that the lowest elevation observed in the wetland was honored in the assigned elevations.

18.4 Groundwater Recharge

Groundwater recharge, groundwater ET (i.e., the loss of water from a shallow water table below the soil zone), and unsaturated flow is also simulated using the UZF module (Niswonger *et al*., 2006). When run in stand-alone mode, recharge rates are typically estimated and then adjusted as part of the model calibration procedure. Using this approach, however, would have led to large changes when the submodels were integrated. Instead, the spatially-variable average recharge rates were estimated based on results from long-term simulations from the stand-alone PRMS submodel. In this way, reasonable values for the groundwater model parameters (primarily hydraulic conductivity) were obtained. The final calibration focused on storage properties and parameters controlling groundwater feedback mechanisms.

The average annual groundwater recharge rates from the final GSFLOW model are presented in Figure 18.10. Recharge quantities below the Niagara Escarpment are low, where Halton Till is prevalent. Very low recharge quantities are present in the Medad Valley and other incised river valleys where groundwater discharge is occurring in the model. Recharge is moderate around the Burlington Quarry and higher quantities are found to the west of the Valley in in some swales. Overall, the recharge distribution is highly variable owing to the distributed nature of the hydrologic model used to generate it. Recharge tends to be lowest along topographic highs and increases as runoff and interflow accumulate downslope. The long-term average annual recharge applied to the model is 124 mm/y, which is indicative of the till soils widely distributed throughout the model area.

18.5 Groundwater Takings

Groundwater and surface water are extracted from the aquifers and streams in the study area for quarry dewatering, golf course irrigation, agriculture, commercial and industrial use, and private (domestic) water supply. Private domestic takings are typically small and were not simulated as water is returned locally through the septic systems. Permitted groundwater sources were reviewed and it was determined that most of the groundwater takings are relatively distant from the quarry and are generally small in volume. They were, therefore, not simulated in the model.

Dewatering of the Burlington Quarry was simulated passively in the model so as to reflect actual water control measures. Quarry drains were added to accept groundwater discharge from the face and floor of the quarry. This water was conveyed by SFR2 to the quarry lakes. Controls were set to specify the maximum stage on two of the lakes, such that excess volumes were automatically discharged to the stream segments representing the south-central and northwest discharge points. The control elevations were adjusted until a reasonable match between simulated and observed average was achieved in the initial steady-state MODFLOW-only simulations. For transient simulations, reported discharge values were simulated as specified outflows from the quarry lakes. The control structures served as overflow points when inflow volumes exceeded the reported discharge.

18.6 Groundwater Model Parameters

The properties of the model layers, such as the top and bottom elevations, hydraulic conductivity, and storage properties, were assigned to each model cell. Layer tops and bottoms were assigned primarily based on the geometry of the hydrostratigraphic model developed for this study but modified to assure layer continuity.

Initial estimates for hydraulic conductivity were made based on previous hydrogeologic investigations at the quarry site (e.g., Golder Associates Ltd., 2007), recent field work and aquifer testing (see Appendix A), and on other modelling studies in the vicinity (e.g., Earthfx, 2012).

Uniform properties were assigned to each of the hydrostratigraphic units and adjusted through model calibration. For the bedrock units, an equivalent porous medium (EPM) was assumed. As was noted above, the principal aquifer was subdivided into fracture and non-fracture dominated layers. Uniform properties were assumed for the units although properties likely vary locally depending on the density of fracture occurrences, aperture, orientation, and connectivity.

Maps showing the spatial distribution of the calibrated hydraulic conductivity values for model layers 1 through 9 are presented in Figure 18.11 through Figure 18.19. Maps showing the spatial distribution of the calibrated vertical hydraulic conductivity values for model layers 5 and 7 are presented in Figure 18.20 and Figure 18.21, respectively, and show the assignment of higher values to selected cells. Table 18.4 lists the calibrated properties for each of the hydrostratigraphic units. The properties listed represent final calibration values for the integrated model.

Storage parameters (specific storage and specific yield) for the hydrostratigraphic units represented in the model are also presented in Table 18.4. Storage values were calibrated through comparison of transient model outputs with continuous groundwater level data. Specific yield values for the bedrock units were due to the assumption that groundwater flow in these units is dominated by secondary permeability associated with small–aperture fractures. Specific storage values are also low (on the order of 10^{-6} m^{-1}), due to the incompressibility of the rock matrix.

18.7 Groundwater Model Pre-Calibration

The MODFLOW submodel was pre-calibrated to steady state (average) conditions. Regional calibration was done to match observed water levels and general groundwater flow patterns

determined primarily from static water level data in the MECP Water Well Information System (WWIS). Subsequent to this average condition regional pre-calibration, the GSFLOW model calibration was refined by matching the transient response in long term monitoring wells in the GSFLOW model. The water level data and general flow patterns are described in Section 5.3 of the main report.

The interpolated water levels, showed a number of significant features in the study area that needed to be matched by the numerical model, including:

- the high water levels in the Amabel formation in the Mt. Nemo area above the Niagara Escarpment;
- natural flow in the quarry vicinity is generally from the north to the southwest (towards the Medad valley) or to the southeast towards the Niagara Escarpment;
- Gradients are fairly flat relative to the steep gradients below the Escarpment;
- Water levels are depressed in the immediate vicinity of the quarry due to dewatering;
- Steep declines in heads occur at the Niagara Escarpment
- Flow in the north below the Niagara Escarpment is toward Bronte Creek while flow in the east is toward the numerous streams that flow to Lake Ontario; and
- the influence of the streams of the groundwater system area as seen in the bending of the contours around the streams.

Parameter values, primarily hydraulic conductivity values for the aquifers and aquitards as well as for parameters in the SFR2 and LAK3 modules used to represent streamflow and lake/wetland water balances, were revised from initial estimates in a trial-and-error approach, to improve the match to observed water levels. The parameter estimation code, PEST (Doherty, 2015), was also used to help refine the initial estimates of the groundwater submodel parameter values by minimizing the sum of the squares of the residuals between simulated and observed groundwater levels. The automated calibration procedure had limited success because of high scatter in the static water level data. (PEST requires multiple runs to determine optimal parameter values, so it is impractical to use to calibrate the transient GSFLOW model because of long model run times).

Simulated steady-state heads in Layer 6 (middle fracture zone) are shown in Figure 18.22. Static and average water level data are posted on the figure using colour-shaded symbols. Differences between the colour inside the dot and in the surrounding area indicate a deviation from the observations. A visual comparison of the observed and simulated values shows that reasonably good matches were achieved although, as was noted in Section 5.3, there is considerable scatter in the static water level data because of the fractured nature of the bedrock. Deviations are less prevalent below the Niagara Escarpment. A good match was also achieved across the model with the key study area groundwater flow patterns noted above.

The static groundwater level data and average water levels (at wells with transient data) were used as a primary target to match the overall range in water levels and groundwater flow patterns. The data were filtered to remove wells with obvious errors, such as water levels below the bottom of the monitoring interval, or wells with obviously incorrect spatial coordinates. Wells with a depth of less than 15 m were used for the calibration assessment, and compared to steady state simulated water levels simulated in Layer 6, which represents the middle Amabel fracture zone. MECP wells typically have long well screens or open holes and represent a vertically averaged head measurement. This combination of well depth and middle Amabel model layer simulated head provides the most representative comparison between simulated and observed regional water levels.

A total of 504 observed static water levels made up the final calibration dataset. Three statistics were used to assess the quality of the model calibration: the mean error (ME), mean absolute error (MAE), and root mean squared error (RMSE). These are given by Anderson and Woessner (1992) as:

$$\text{Mean Error} = \frac{1}{n}\sum_{1}^{n}(h_O - h_S)_i \qquad \text{Eq. 18.5}$$

$$\text{Mean Absolute Error} = \frac{1}{n}\sum_{1}^{n}\left|(h_O - h_S)_i\right| \qquad \text{Eq. 18.6}$$

$$\text{Root Mean Squared Error} = \sqrt{\frac{1}{n}\sum_{1}^{n}(h_O - h_S)_i^2} \qquad \text{Eq. 18.7}$$

where:

h_o = observed head;
h_s = simulated head; and
n = number of observations.

The Mean Error in the final calibration was -1.86 m; the negative ME indicates that simulated values are slightly higher than the observed values. The Mean Absolute Error (MAE) and the Root Mean Squared Error (RMSE) provide a good estimate of the average magnitude of the difference and variance between observed and simulated values. An observed-predicted calibration plot is shown in Figure 18.3. The groundwater submodel had a MAE of 3.24 m and a RMSE of 4.23 m. Intrinsic error in the MECP WWIS data makes it difficult to achieve smaller RMSE values; this is further compounded by the natural local variability in groundwater levels in fractured bedrock.

Calibration of the integrated GSFLOW model is discussed further in Appendix E. The GSFLOW model has better average calibration statistics, with a Mean Error of -1.32 m (compared to the MODFLOW-Mean Error of -1.86 m noted above). While the GSFLOW model did improve on the regional calibration, the focus of the GSFLOW calibration was on the transient local water level data across all model layers as well as local streamflow and wetland gauges.

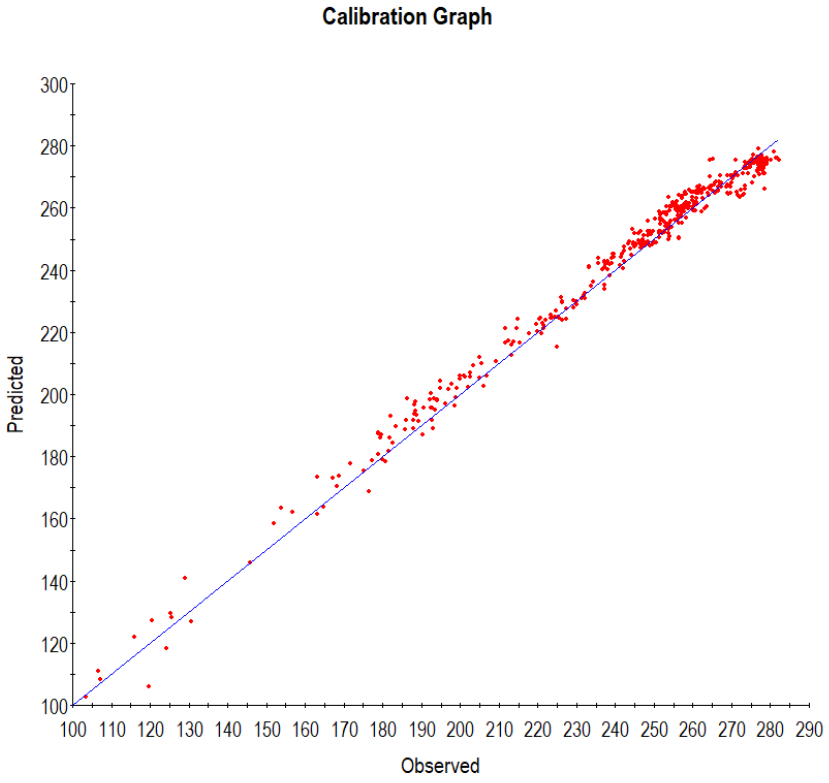

Figure 18.3: Steady State Model Calibration

Calibration Statistics Report

Observation Point Parameter: 2441. Shallow Water Levels (Boreholes < 15 m deep) (masl)
Model Result Parameter: 2803. BL L6 Potentials (masl)
Statistics:(Observed - Predicted)

- Number of points: 504
- Mean Error: -1.86196
- Mean Abs. Error: 3.24992
- RMS Error: 4.23139
- R Squared:0.98861
- Min Abs. Difference: 0.00168
- Max Abs. Difference: 13.02795
- Min Model value: 98.24532
- Max Model value: 281.89999
- Min Obs. value: 92.97000
- Max Obs. value: 281.89999

18.8 Tables

Table 18.1 Numerical model layers and corresponding hydrostratigraphic layers.

Numerical Model Layer	Hydrostratigraphic Unit		
	Above Escarpment	Below Escarpment	Layer Description
1	Surficial Deposits	Surficial Deposits	Mainly weathered till and surficial sands
2	Halton Till	Halton Till	Unweathered till
3	MIS Sands	ORAC Sands	Discontinuous sand unit
4	Weathered Amabel Aquifer	Weathered Queenston	Weathered Bedrock
5	Upper Bulk Amabel	Weathered Queenston	Goat Island/ Gasport, and Irondequoit Formations (Weathered Queenston below Escarpment)
6	Middle Fracture Zone	Weathered Queenston	
7	Lower Bulk Amabel	Weathered Queenston	
8	Lower Fracture Zone	Weathered Queenston	
9	Lower aquitards	Lower aquitards	Rochester, Cabot Head, Rockway, /Merritton, Manitoulin (Unweathered Queenston below Escarpment

Table 18.2: Summary of stream properties organized by type.

Stream Type	Streambed Hydraulic Conductivity (m/s)	Streambed Roughness (Mannings n)	Stream Bank Roughness (Mannings n)	Streambed Thickness (m)
Strahler Class 1-4	$5x10^{-7}$	0.035	0.045	0.5
Karst	$5x10^{-7}$	0.035	0.045	0.1
Quarry Floor Drain	$1x10^{-4}$	0.02	0.02	0.5
Conduit	$1x10^{-12}$	0.035	0.045	0.5

Table 18.3: Summary of outlet structure properties

Structure Type	Width 1	Height 1	Width 2	Height 2	Weir Coefficient	Orifice Coefficient
Slotted Weir - Wide	0.08	1.1	2.5	1.2	2.95	3.2
Slotted Weir - Narrow	0.01	1.1	2.5	1.2	2.95	3.2

Table 18.4: Final calibrated model parameter values.

Hydrostratigraphic Unit	Hydraulic Conductivity [m/s]	Anisotropy Kh:Kz	Specific Yield	Specific Storage [1/m]
Recent Deposits/Late Stage Lacustrine	Variable	1:1	0.15	$1x10^{-4}$
Halton Till	$5x10^{-7}$	3:1	0.035	$1x10^{-5}$
MIS Sands	$5x10^{-6}$	2:1	0.15	$1x10^{-4}$
Weathered Amabel	$5x10^{-5}$	1:1	0.001	$1x10^{-6}$
Upper Bulk Amabel	$5x10^{-6}$	500:1	0.01	$1x10^{-6}$
Upper Bulk Amabel Vertical Fractures	$5x10^{-6}$	1:1	0.01	$1x10^{-6}$
Middle Amabel Bedding Plane Fracture Zone	$5x10^{-5}$	1:1	0.001	$1x10^{-6}$
Lower Bulk Amabel	$5x10^{-6}$	1000:1	0.01	$1x10^{-6}$
Lower Bulk Amabel Vertical Fractures	$5x10^{-6}$	10:1	0.01	$1x10^{-6}$
Lower Fracture Zone	$1x10^{-4}$	1:1	0.001	$1x10^{-6}$
Lower Aquitards	$1x10^{-7}$	10:1	0.05	$1x10^{-6}$
Queenston – Weathered	$5x10^{-7}$	1:1000	0.01	$1x10^{-5}$
Karst Zones	$1x10^{-3}$	1:1	0.1	$1x10^{-5}$
Quarry Backfill	$8x10^{-6}$	3:1	0.15	$1x10^{-4}$

18.9 Figures

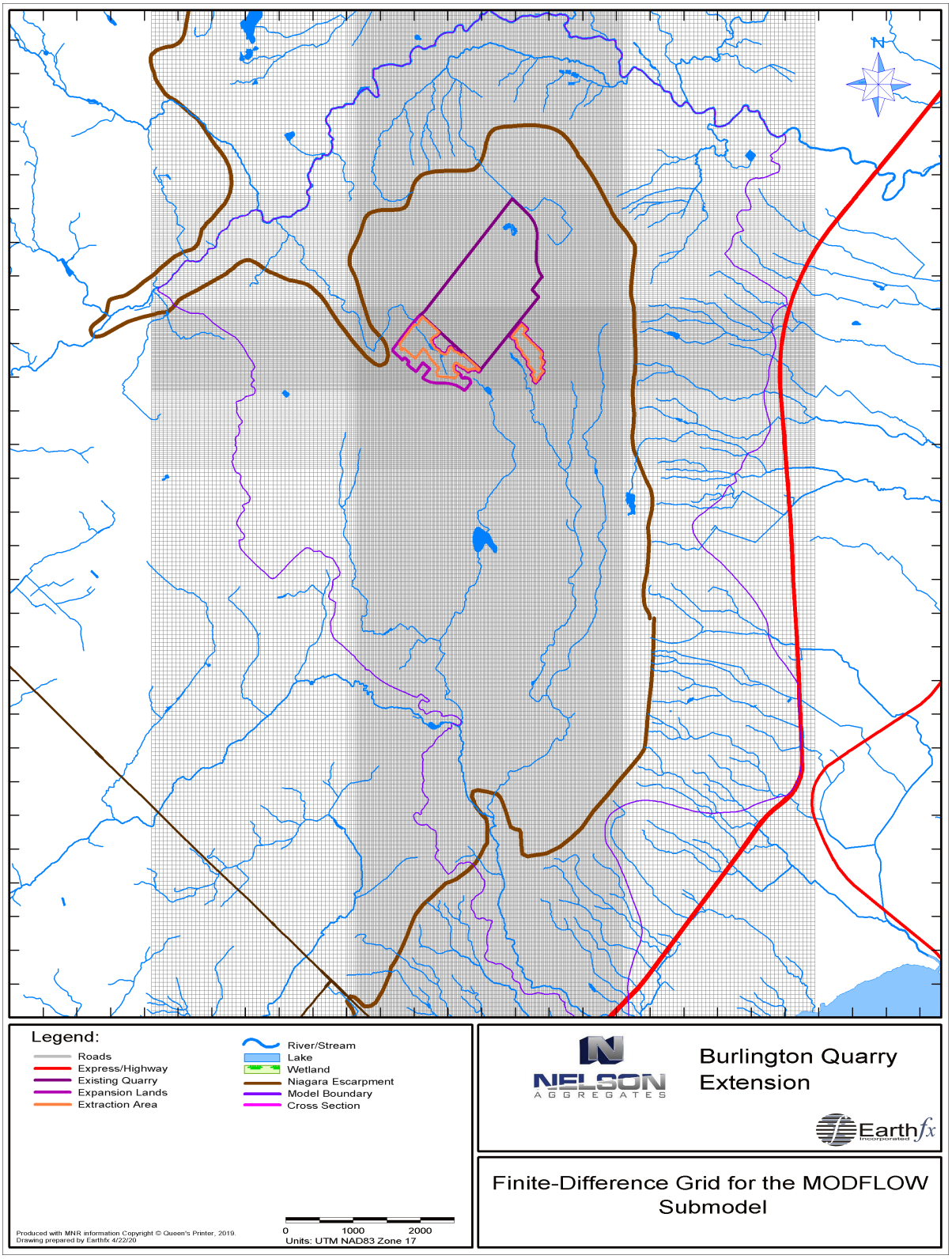

Figure 18.4: Finite-difference grid for the MODFLOW submodel in GSFLOW.

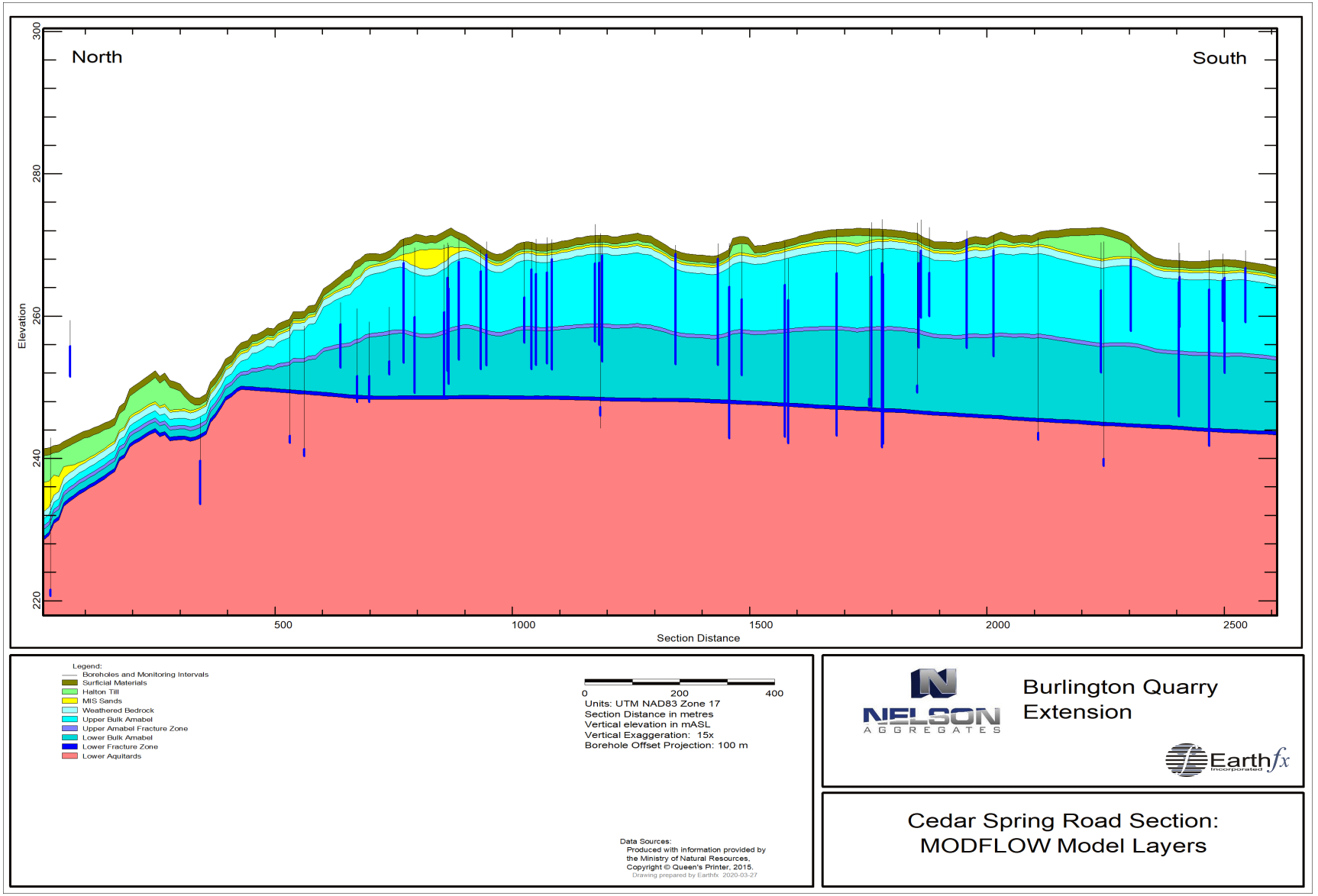

Figure 18.5: MODFLOW Model Layers showing layer continuity.

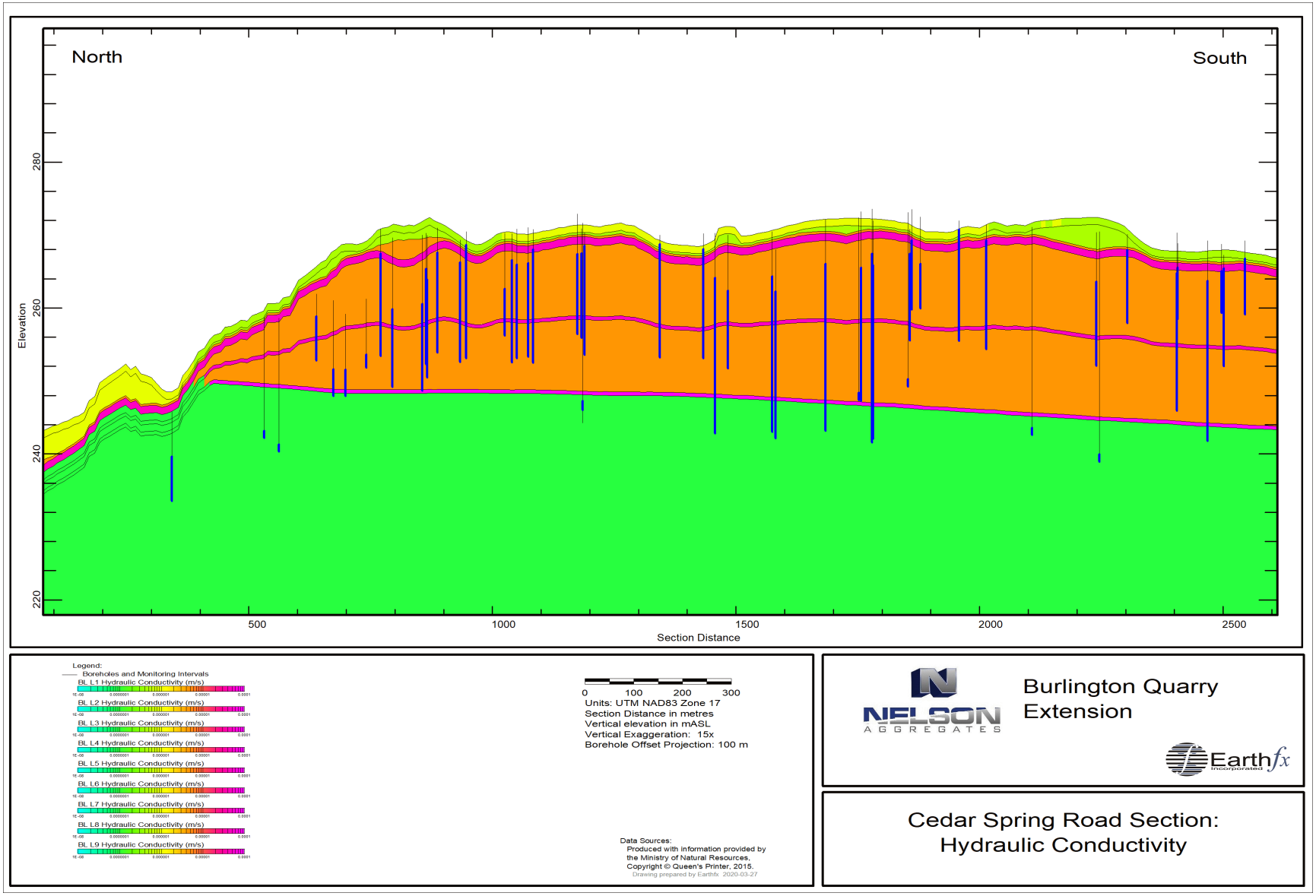

Figure 18.6: MODFLOW layer hydraulic conductivity.

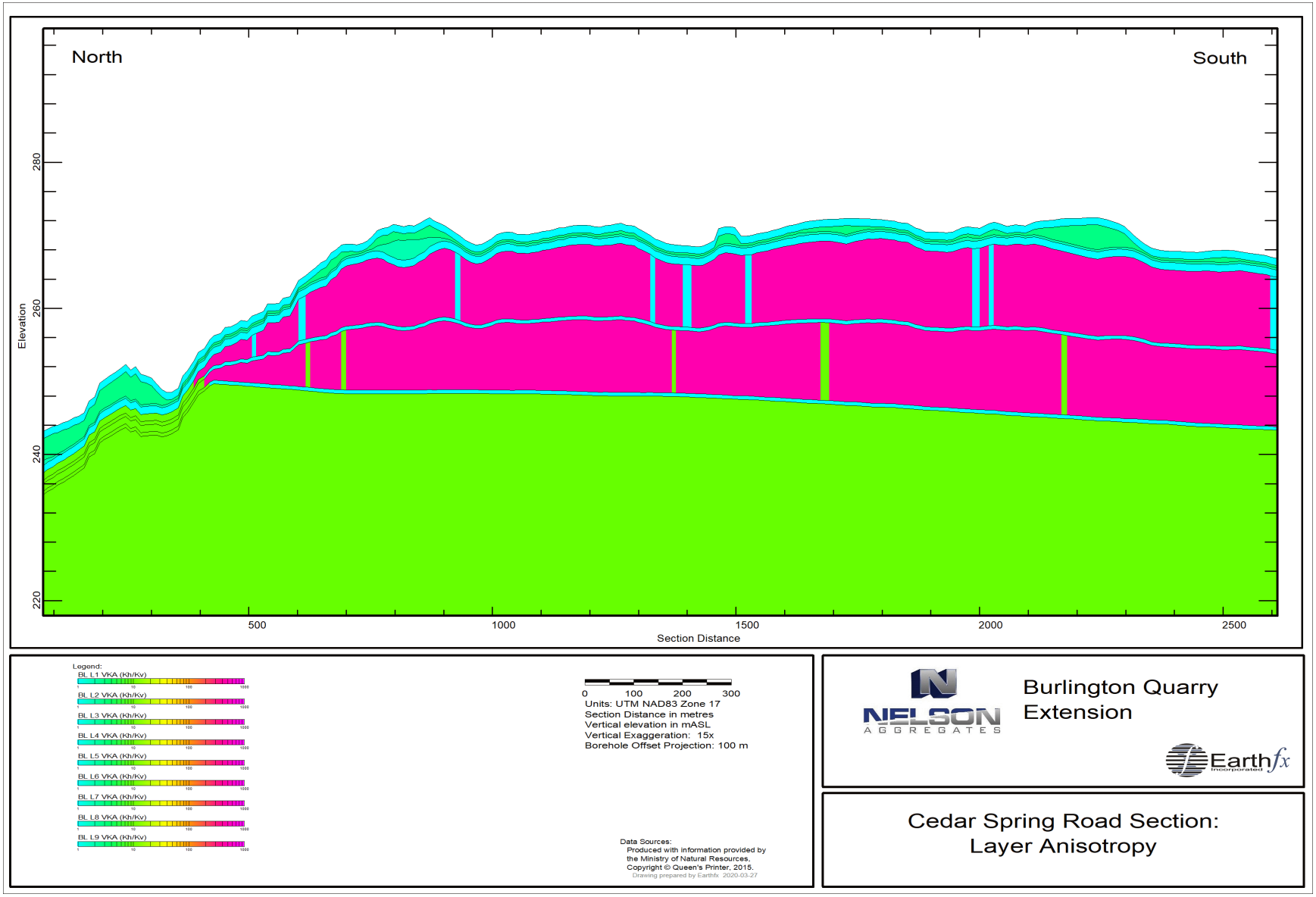

Figure 18.7: MODFLOW layer anisotropy, showing vertical connectivity in the bulk Amabel.

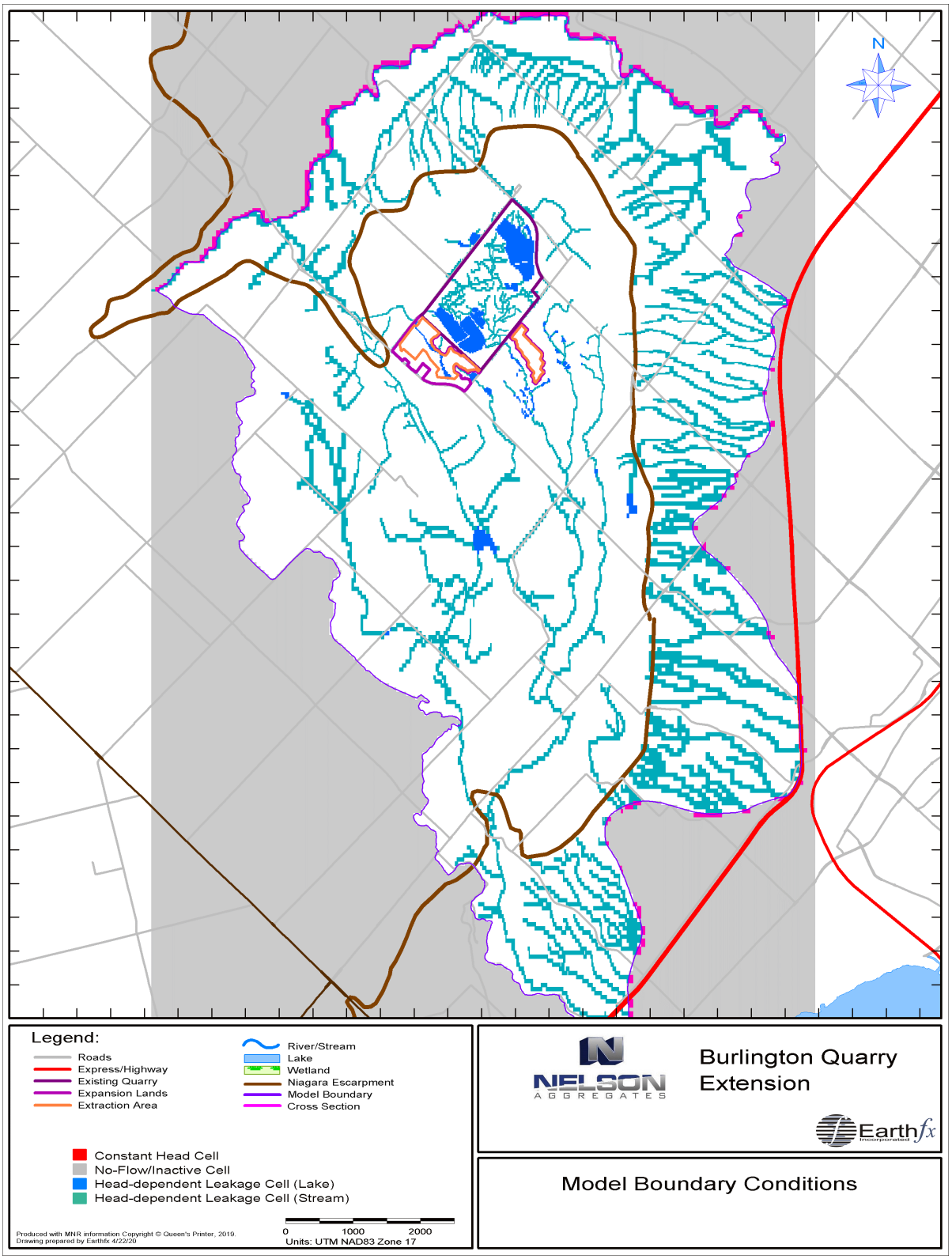

Figure 18.8: Model boundary conditions for the calibration/baseline scenario.

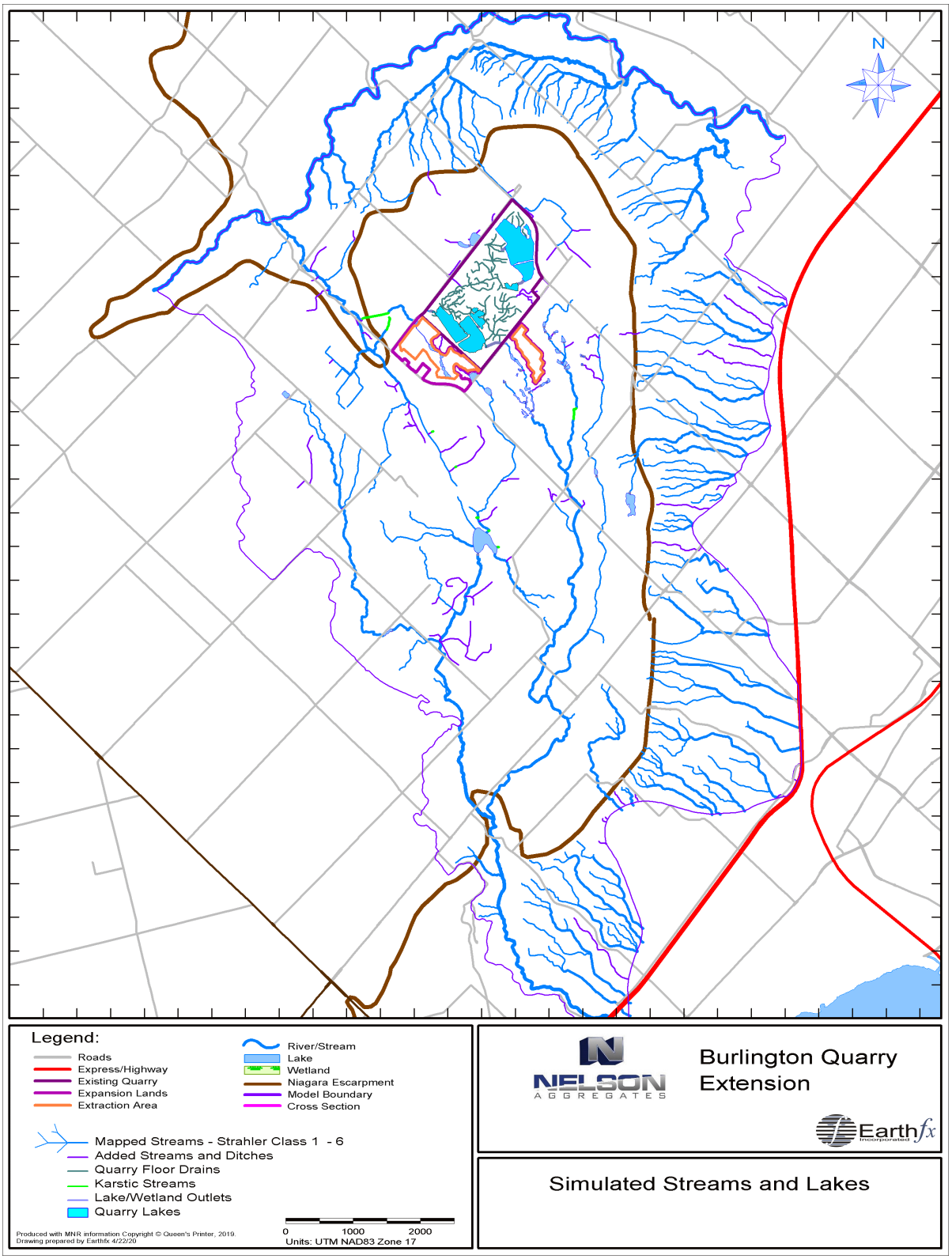

Figure 18.9: Simulated stream and lakes by type.

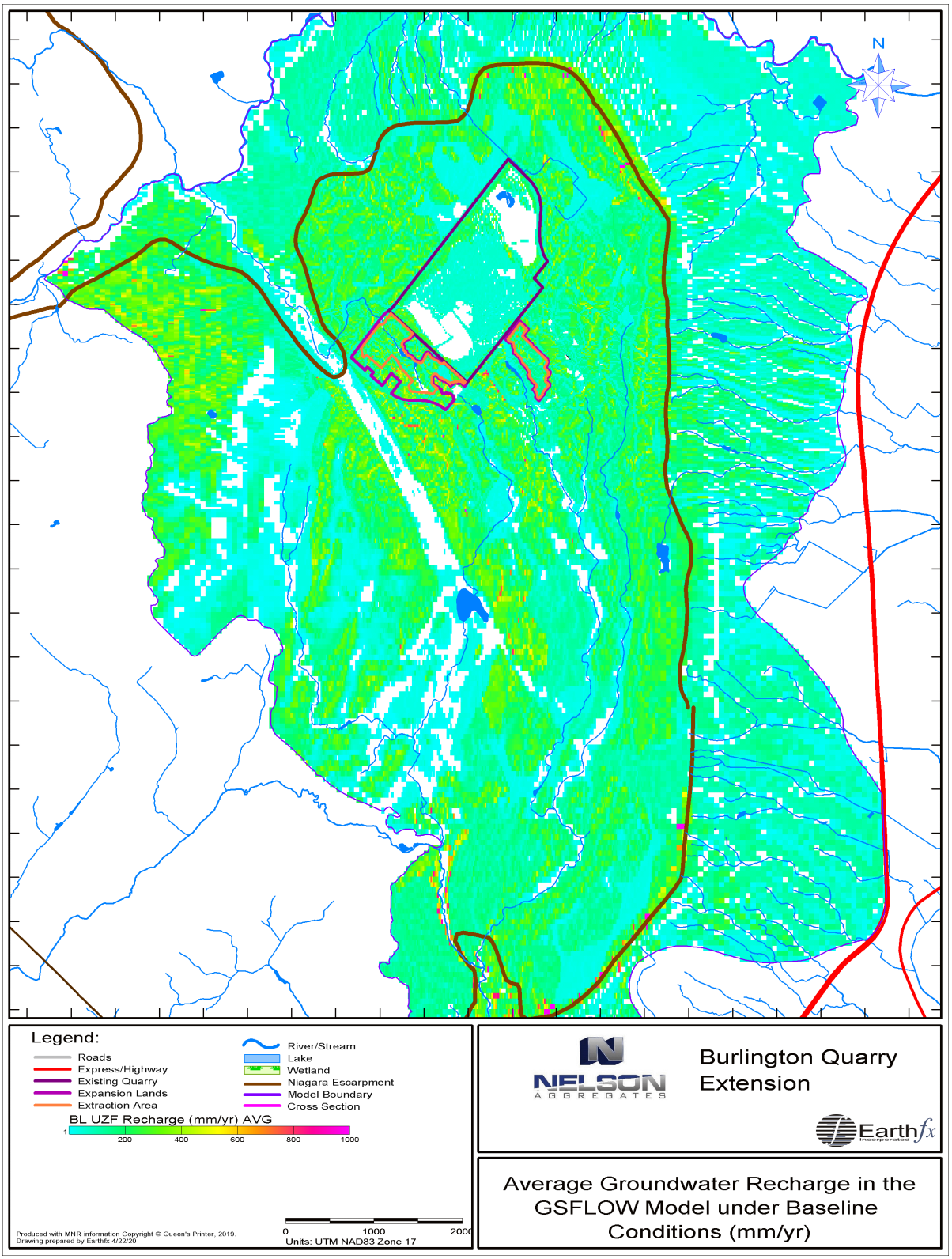

Figure 18.10: Simulated average groundwater recharge in the GSFLOW model under baseline conditions.

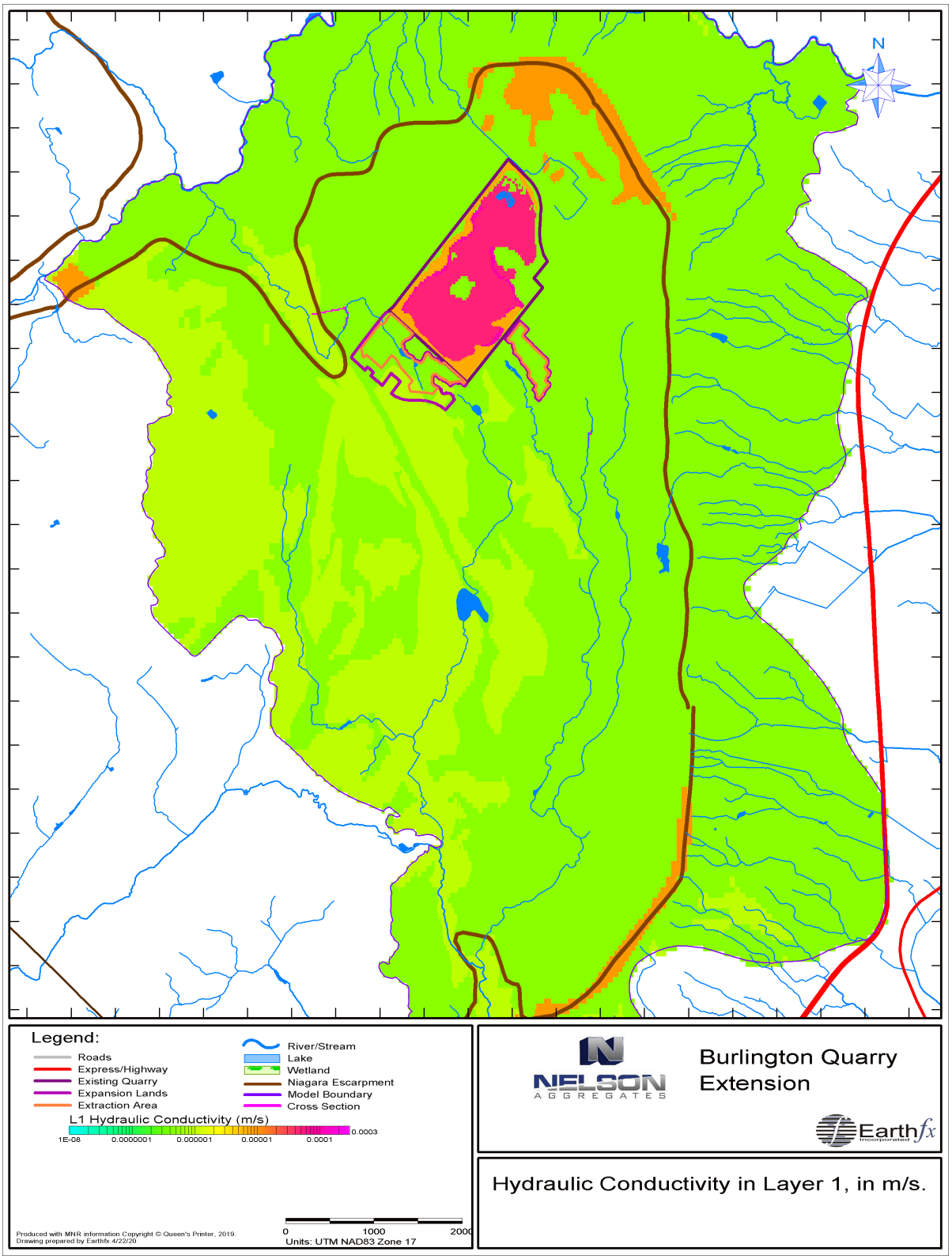

Figure 18.11: Final calibrated hydraulic conductivity values for Layer 1, in m/s, based on surficial geology.

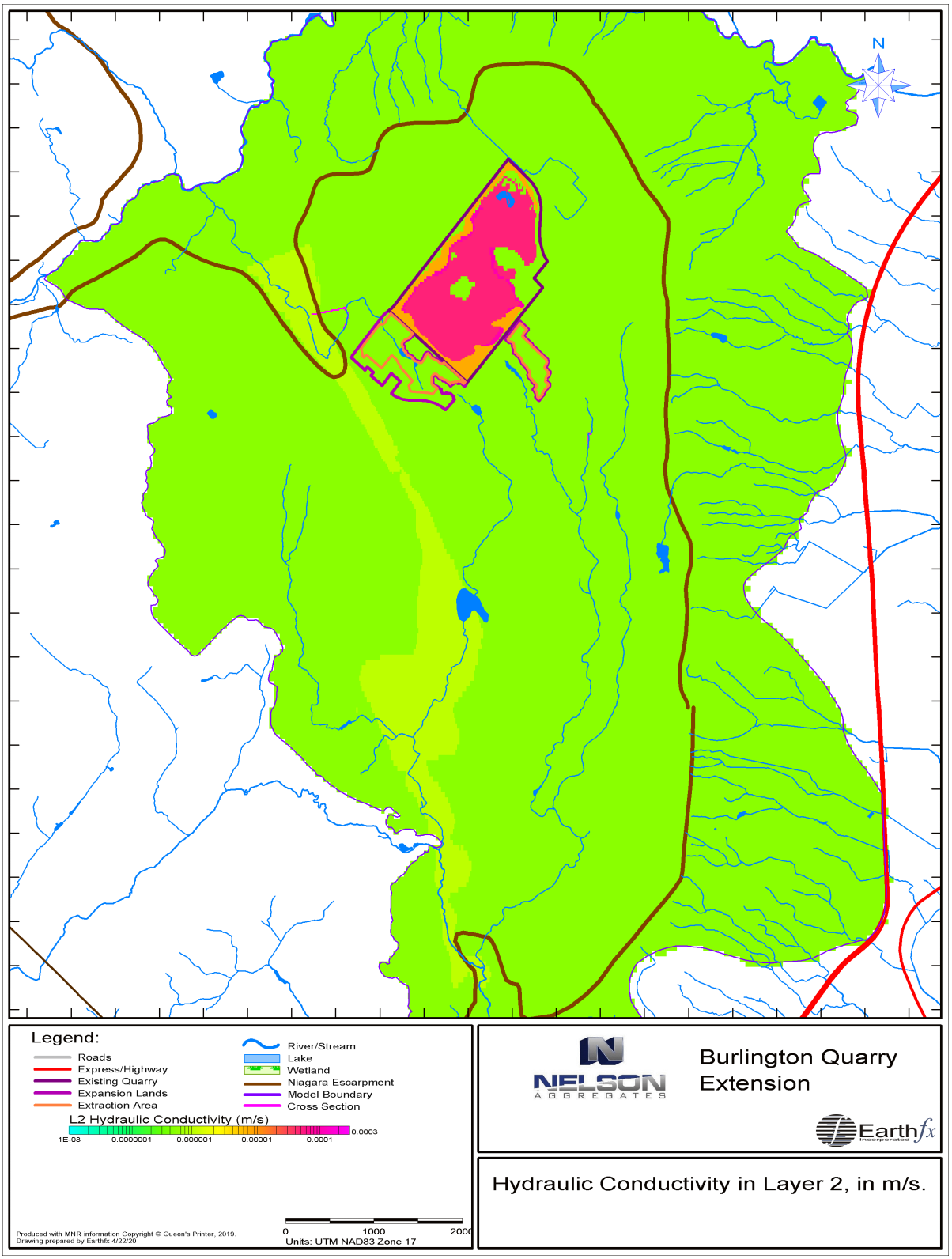

Figure 18.12: Final calibrated hydraulic conductivity values for Layer 2 (mainly Halton Till), in m/s.

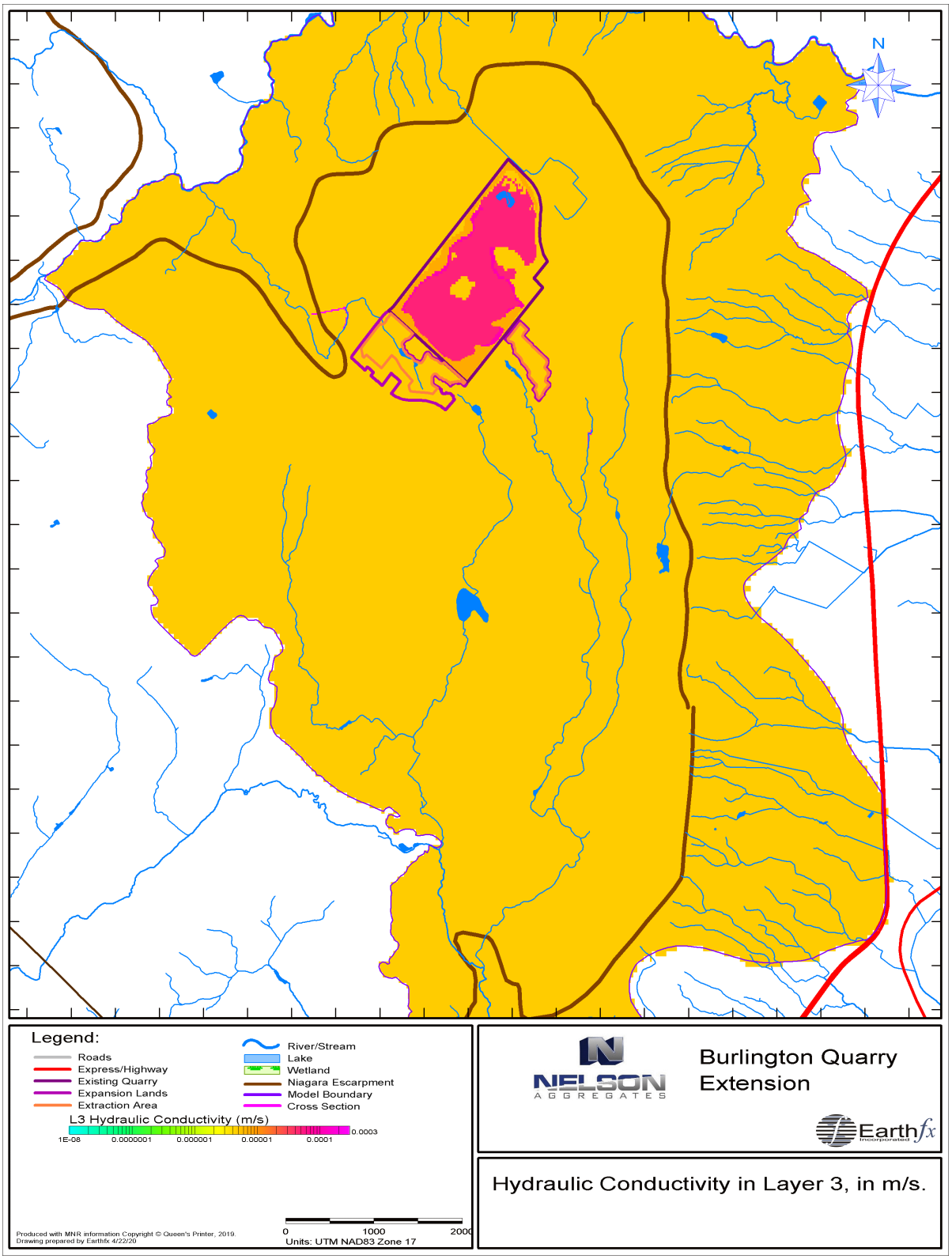

Figure 18.13: Final calibrated hydraulic conductivity values for Layer 3, mainly MIS Fm. and ORAC, in m/s.

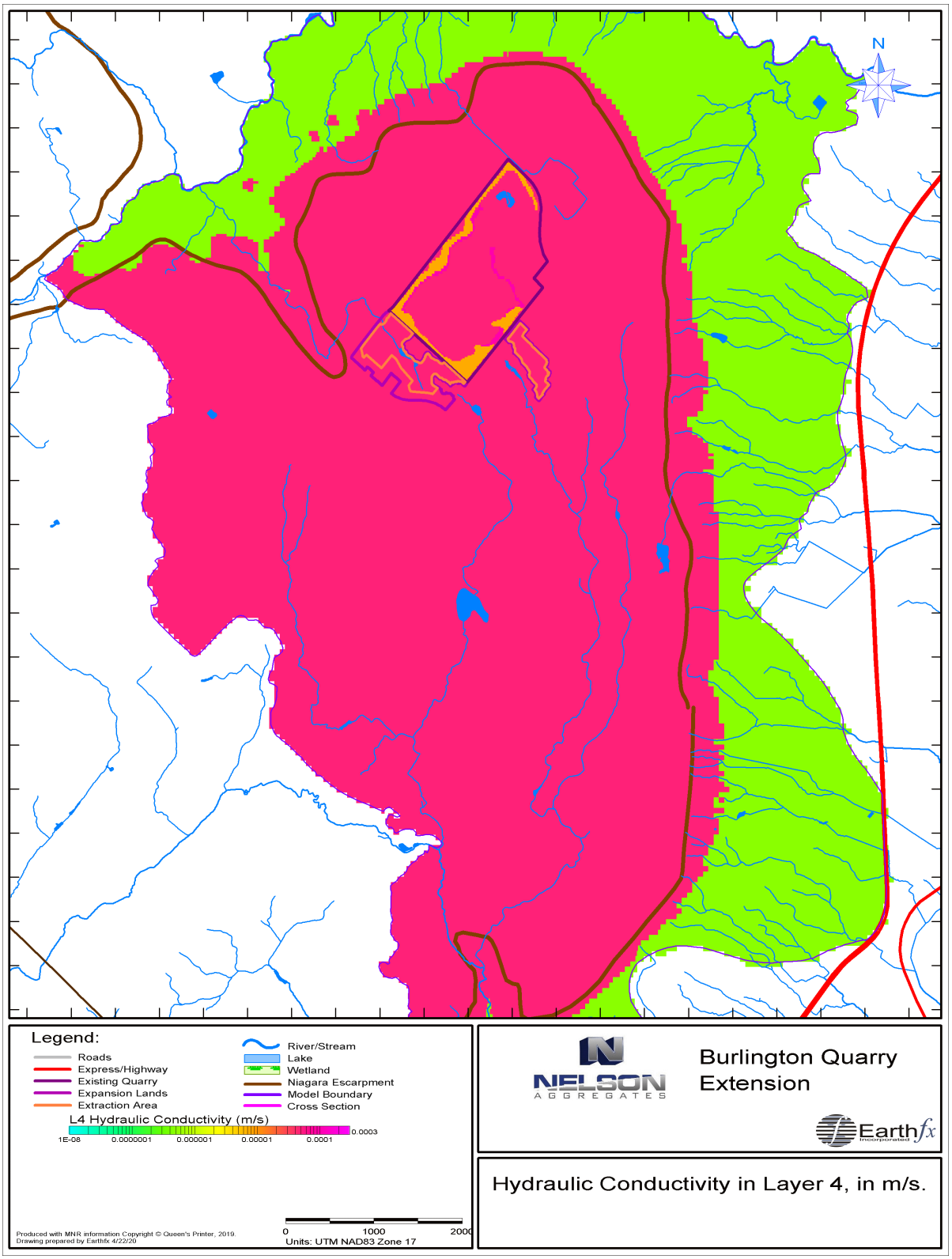

Figure 18.14: Final calibrated hydraulic conductivity values for Layer 4, mainly weathered Goat Island/Gasport Fm. above the Niagara Escarpment, in m/s.

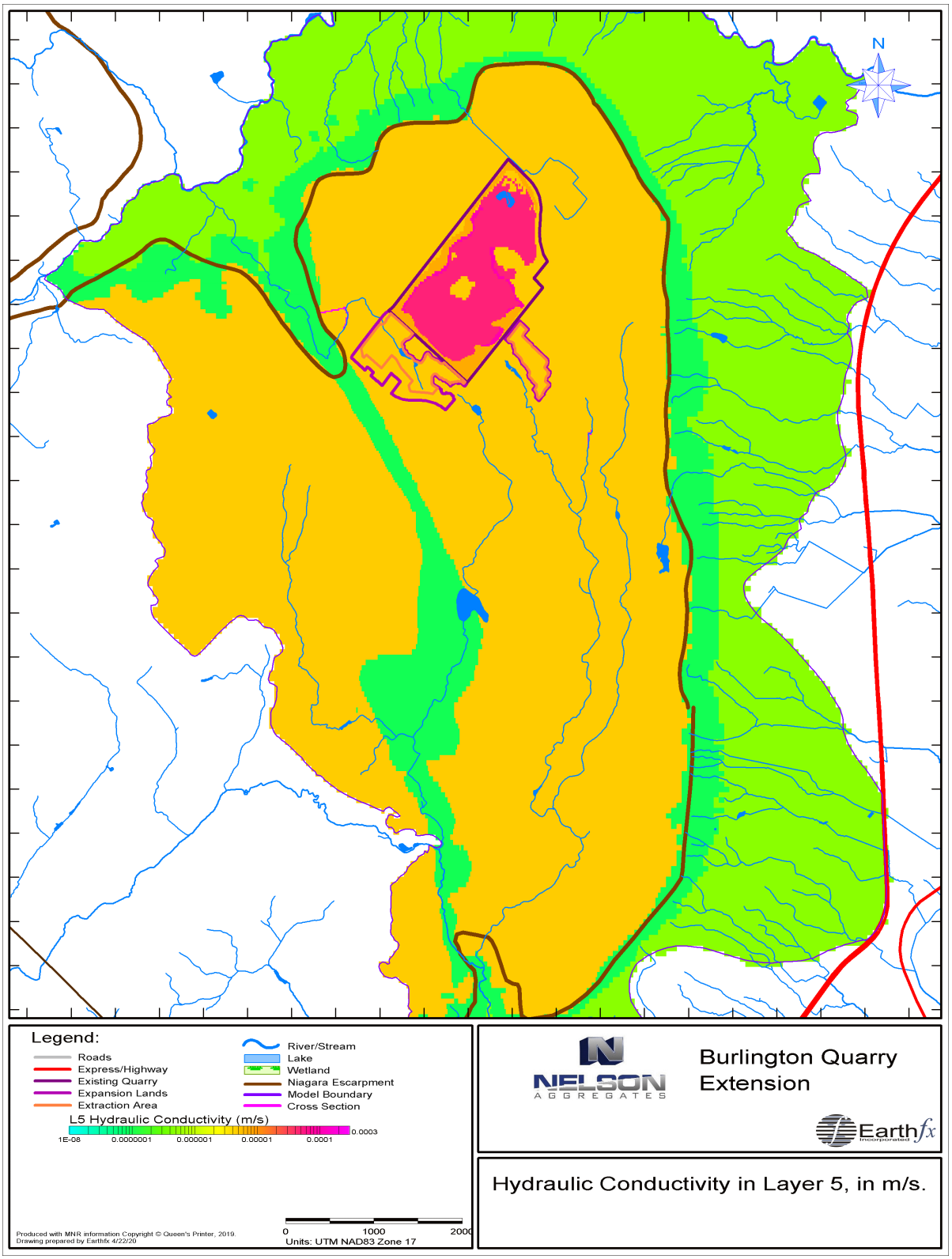

Figure 18.15: Final calibrated hydraulic conductivity values for Layer 5, mainly upper bulk Goat Island/Gasport Fm. above the Niagara Escarpment, in m/s.

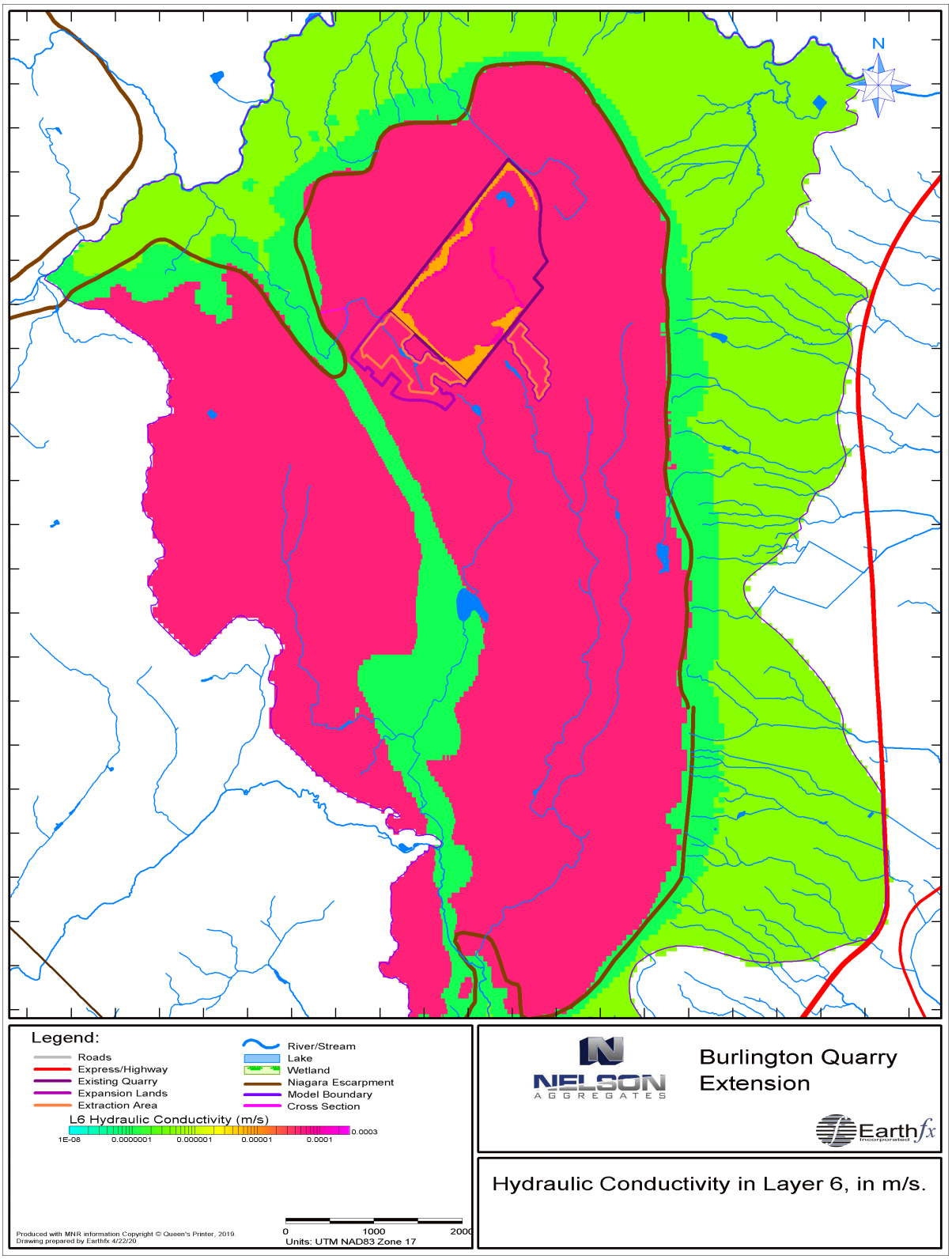

Figure 18.16: Final calibrated hydraulic conductivity values for Layer 6, mainly middle fracture zone in the Goat Island/Gasport Fm. above the Niagara Escarpment, in m/s.

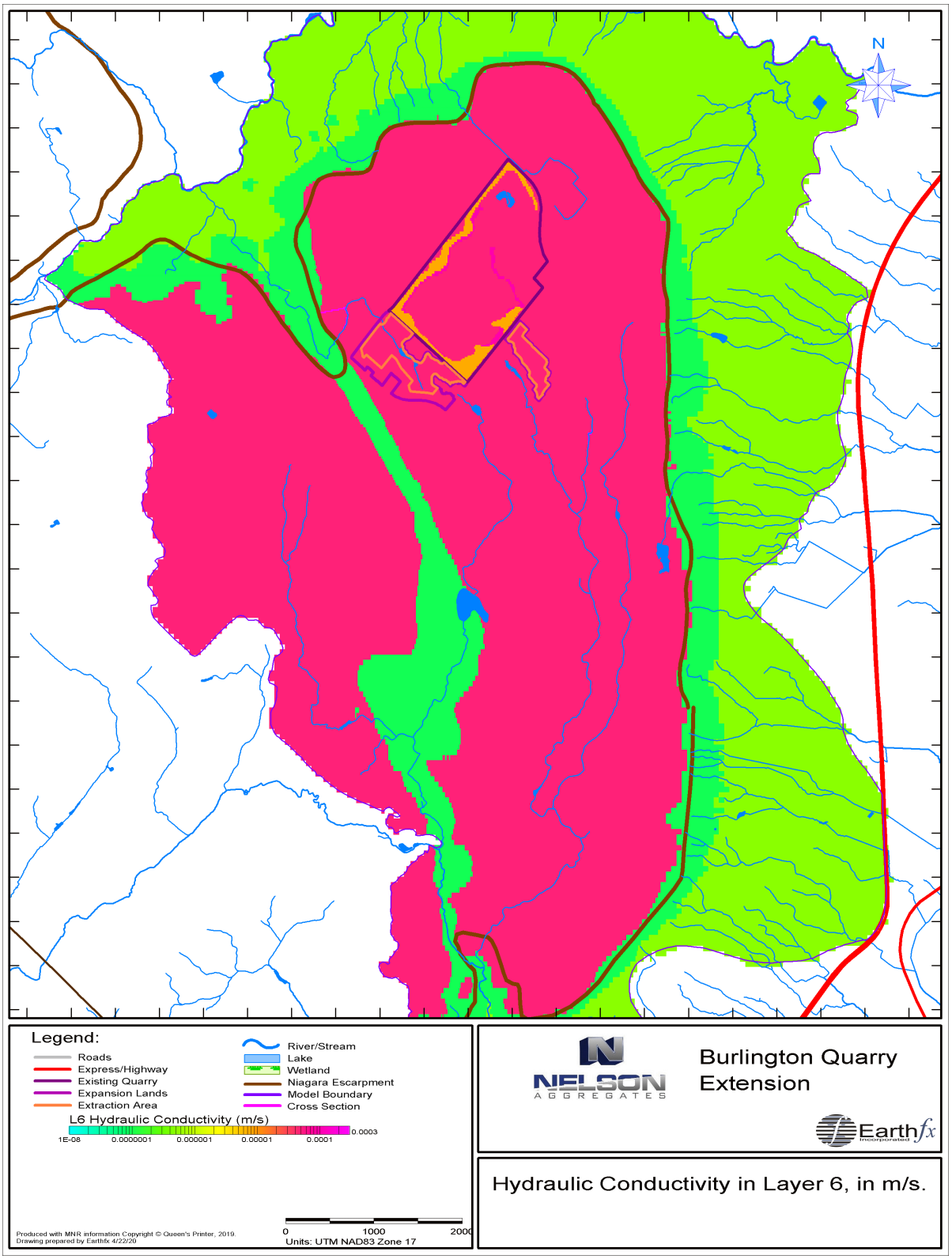

Figure 18.17: Final calibrated hydraulic conductivity values for Layer 7, mainly lower bulk Goat Island/Gasport Fm. above the Niagara Escarpment, in m/s.

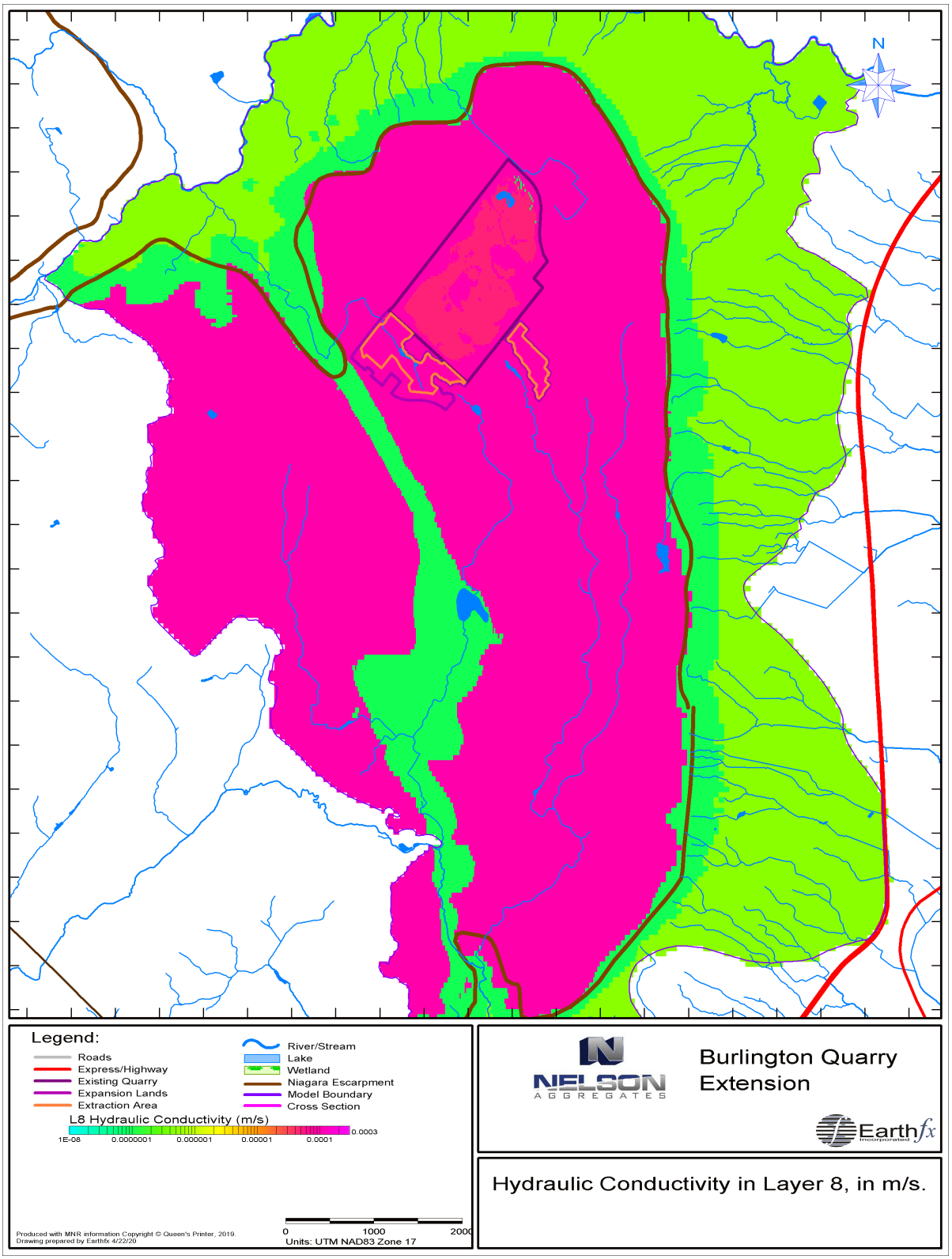

Figure 18.18: Final calibrated hydraulic conductivity values for Layer 8, mainly lower fracture zone in the Goat Island/Gasport Fm. above the Niagara Escarpment, in m/s.

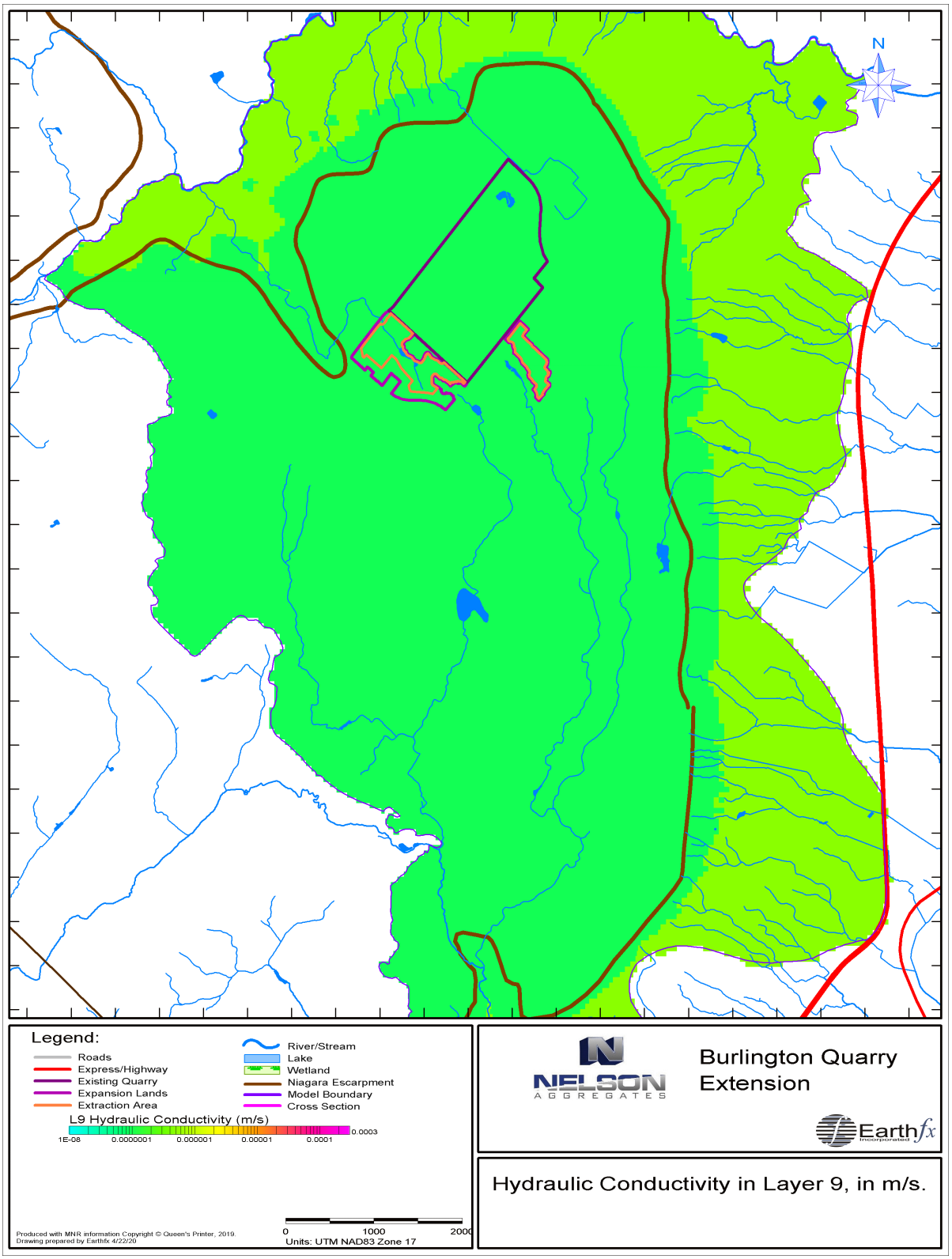

Figure 18.19: Final calibrated hydraulic conductivity values for Layer 9, mainly lower aquitards above the Niagara Escarpment, in m/s.

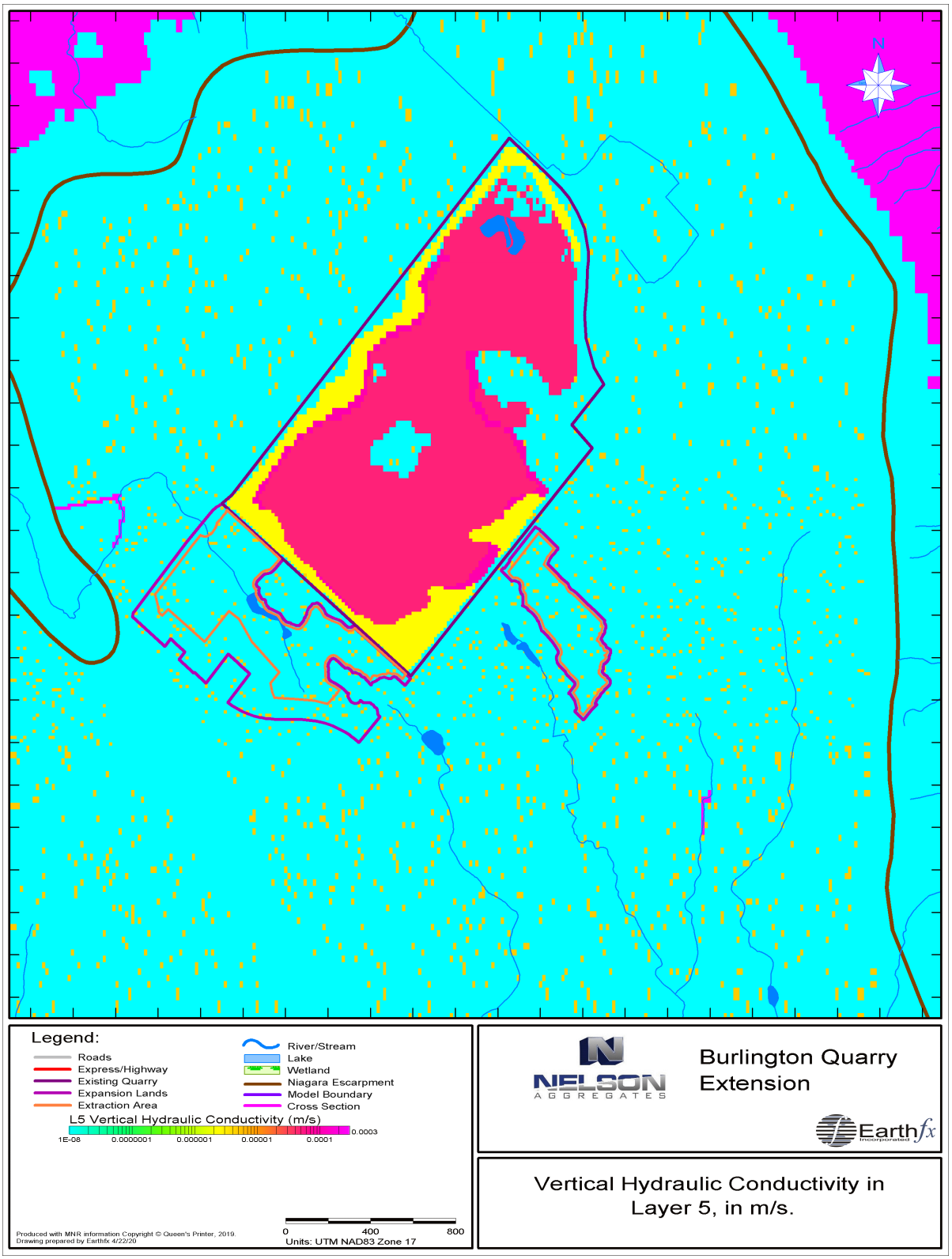

Figure 18.20: Final calibrated vertical hydraulic conductivity values for Layer 5, mainly upper bulk Goat Island/Gasport Fm. above the Niagara Escarpment, in m/s.

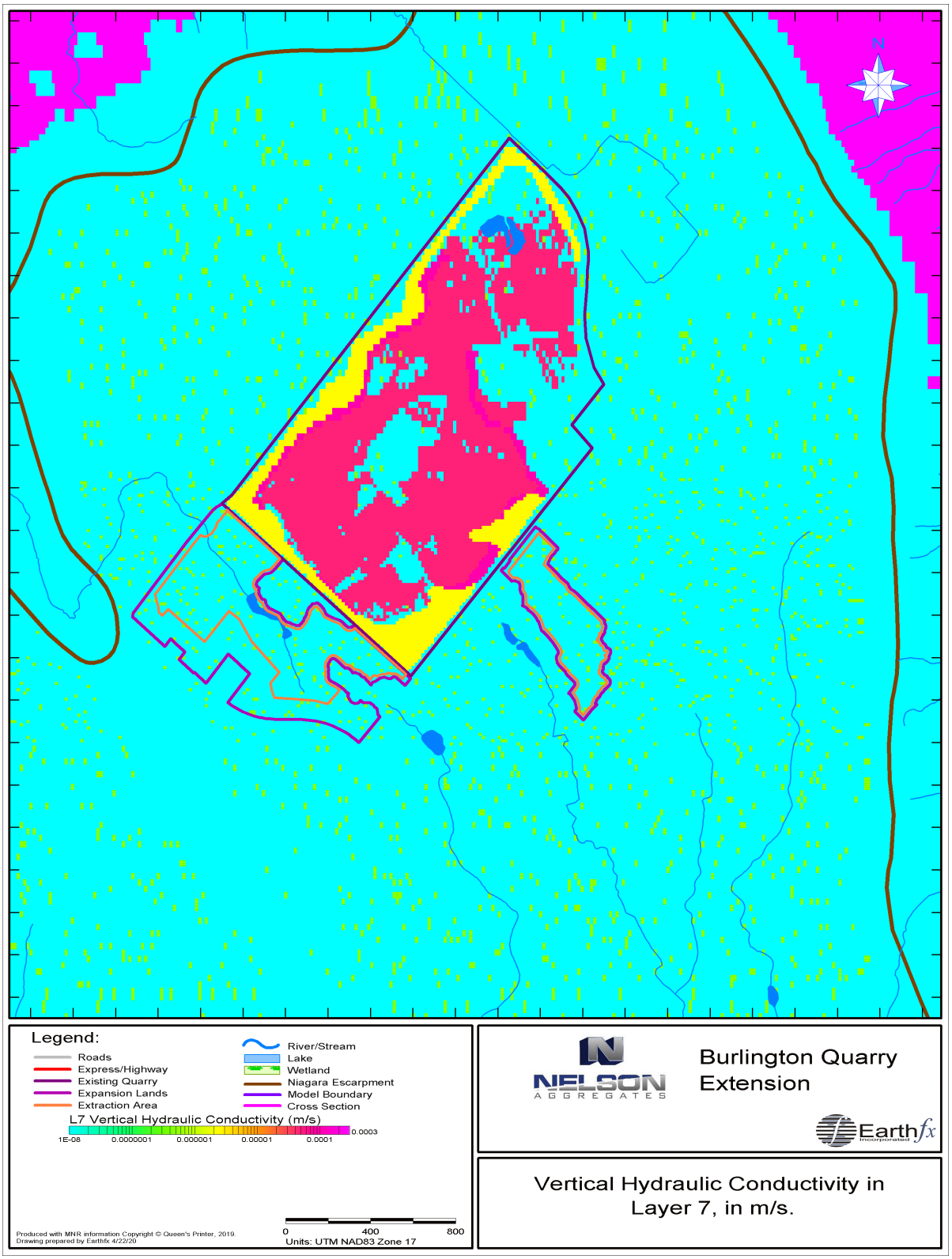

Figure 18.21: Final calibrated hydraulic conductivity values for Layer 7, mainly lower bulk Goat Island/Gasport Fm. above the Niagara Escarpment, in m/s.

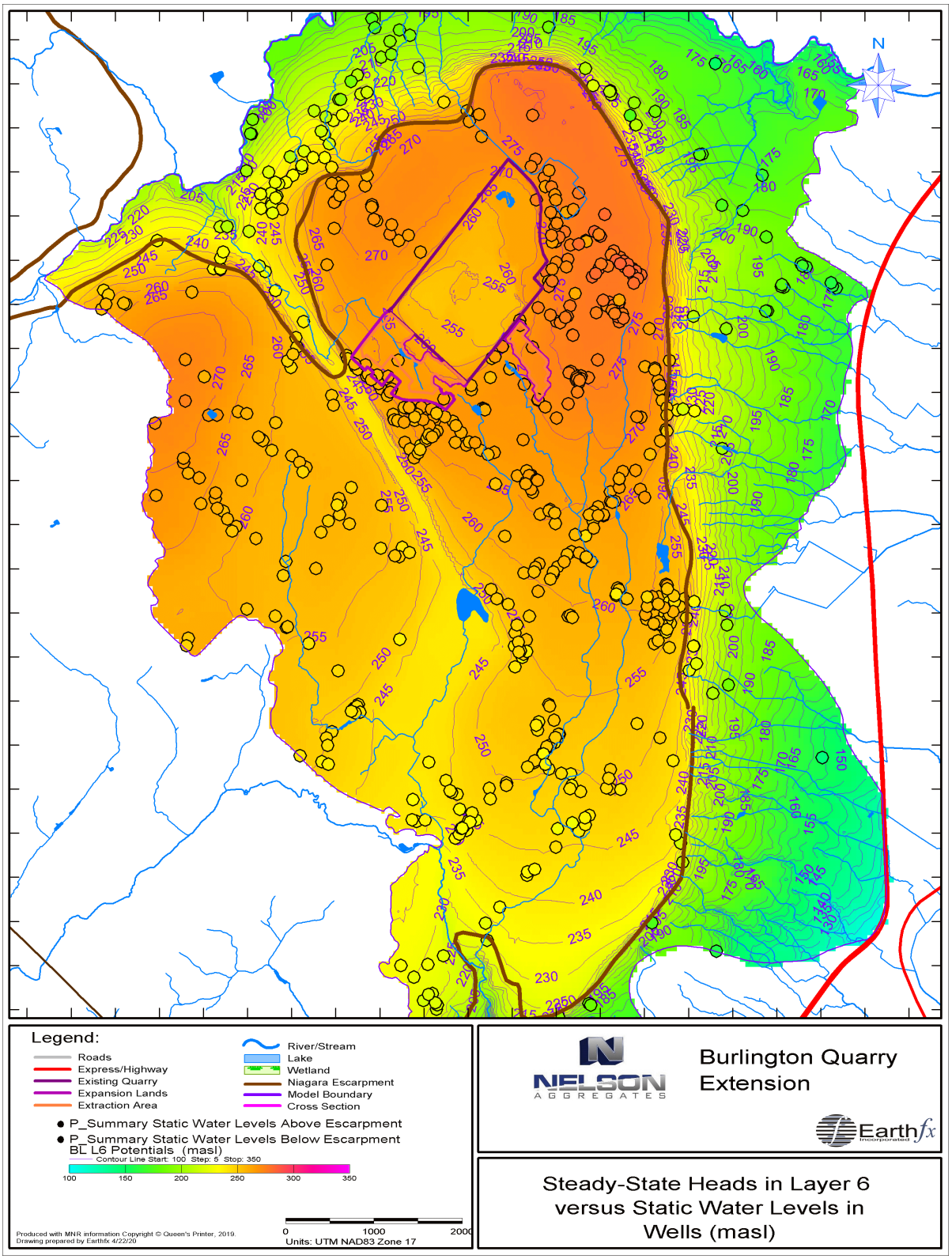

Figure 18.22: Simulated steady state heads in Model Layer 6 (representing the middle fracture zone) versus average water levels in wells (in masl).

19 Appendix E: Integrated GSFLOW Model Calibration

19.1 Calibration Strategy

As noted in the preceding chapters, the overall GSFLOW calibration strategy started with the pre-calibration of the submodels. The PRMS submodel was pre-calibrated to evaluate the submodel's ability to represent the hydrological processes in the study area and to derive reasonable values for many of the model parameters. Process submodels (such as the snowpack model, PET, and precipitation form models) were also tested independently. Similarly, as noted in the preceding appendix, the MODFLOW submodel was pre-calibrated to the average regional groundwater levels.

The final calibration was completed in the fully-integrated in GSFLOW model. A number of GSFLOW simulations were completed and the model parameters were modestly refined. (Note: A 5-year PRMS-only simulation takes 45 minutes to complete, while a 5-year GSFLOW simulation takes between 12 to 14 **days** to complete.) The parameters presented in the preceding two chapters reflect the final integrated calibration parameters.

19.2 Regional Scale Stream Flow Calibration

Figure 19.1 shows the final simulated and observed GSFLOW simulation results at the Aldershot gauge. A Nash-Sutcliffe Efficiency of 0.67 was achieved with the integrated GSFLOW model (a significant improvement over the PRMS-only NSE result of 0.44). An NSE of 0.6 is considered a reasonable value (Chiew and McMahon, 1993).

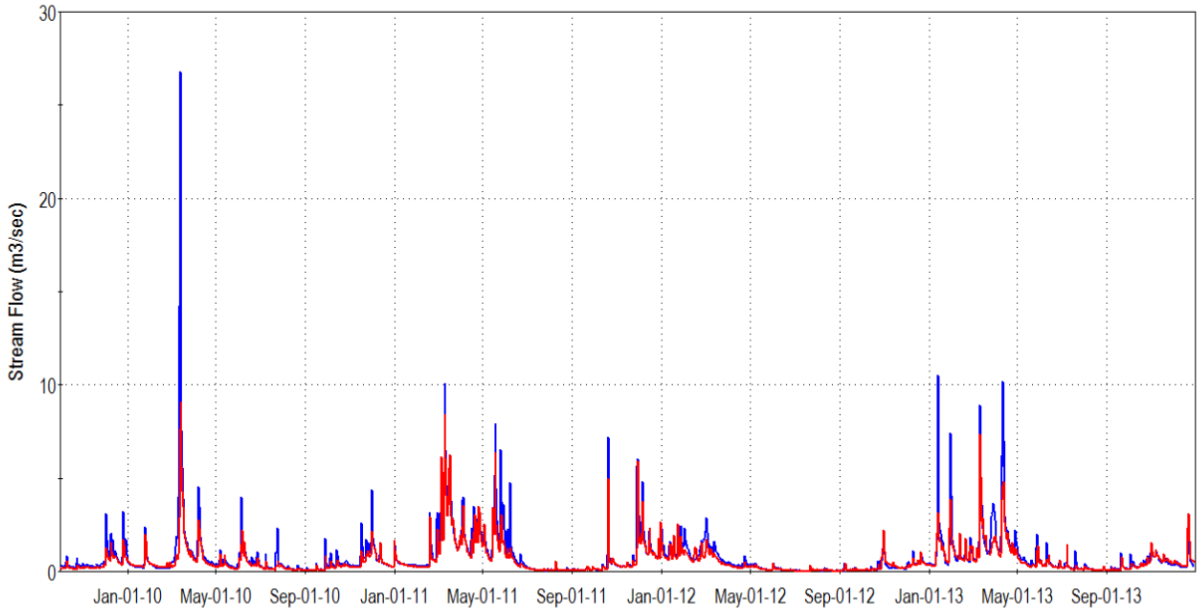

Figure 19.1: Simulated (red) and observed streamflow (blue, in m3s) at the Grindstone Creek near Aldershot gauge.

19.3 Regional Scale Groundwater Calibration

The integrated GSFLOW model was similarly compared to the regional scale water level data. The MECP and local scale water level data sources are discussed in the preceding chapter. While the MODFLOW–only calibration compared observed water levels to a “steady state” simulation, the GSFLOW results compared observed levels to the average of a long-term transient simulation.

Wells with a depth of less than 15 m were used for regional calibration assessment, and compared to water levels simulated in Layer 6, which represents the middle Amabel fracture zone. MECP wells typically have long well screens or open holes and represent a vertically averaged head measurement. This combination of well depth and middle Amabel model layer simulated head provides the most representative comparison between observed and predicted regional levels. (A highly detailed local transient multi-layer assessment is discussed below.)

Average GSFLOW simulated heads in Layer 6 (middle Amabel fracture zone) are shown in Figure 19.2. The average observed water levels are posted on the figure using colour-shaded symbols. Differences between the colour inside the dot and in the surrounding area indicate a deviation from the observations. A visual comparison of the observed and simulated values shows that a good match was achieved although. Comparison with Figure 18.22 shows that the steady-state heads are a reasonable match to the average heads from the long-term transient simulation in this area.

The Mean Error (ME) calibration statistic for the final GSFLOW calibration was -1.32 m. The negative ME indicates that simulated values are slightly higher than the observed values. The GSFLOW ME is an improvement over the MODFLOW steady state ME of -1.86 m. The Mean Absolute Error (MAE) and the Root Mean Squared Error (RMSE) provide a good estimate of the average magnitude of the difference and variance between observed and simulated values. The groundwater submodel had a MAE of 3.33 m and a RMSE of 4.24 m. Intrinsic error in the MECP WWIS data makes it difficult to achieve smaller RMSE values; this is further compounded by the natural local variability in groundwater levels in fractured bedrock.

A comparison of observed and predicted water levels is shown in Figure 19.3. While the negative ME indicates that simulated values are slightly higher than the observed values, the graph indicates that the model is actually lower at the high end (A detailed transient assessment by layer provides much more insight in the following section).

Uniform hydrogeologic properties were used for each of the model layers (as presented in the previous chapter). In other MODFLOW-only simulations, recharge and hydraulic conductivity are at times adjusted to achieve a better localized match using techniques such as pilot point parameter estimation. Local adjustments made with that technique rarely have a physical basis or justification; however, they can artificially improve the calibration statistics. As unsubstantiated local refinements cannot be justified, they have not been used in this simulation. Consistent regional parameters have been used throughout the local scale analysis.

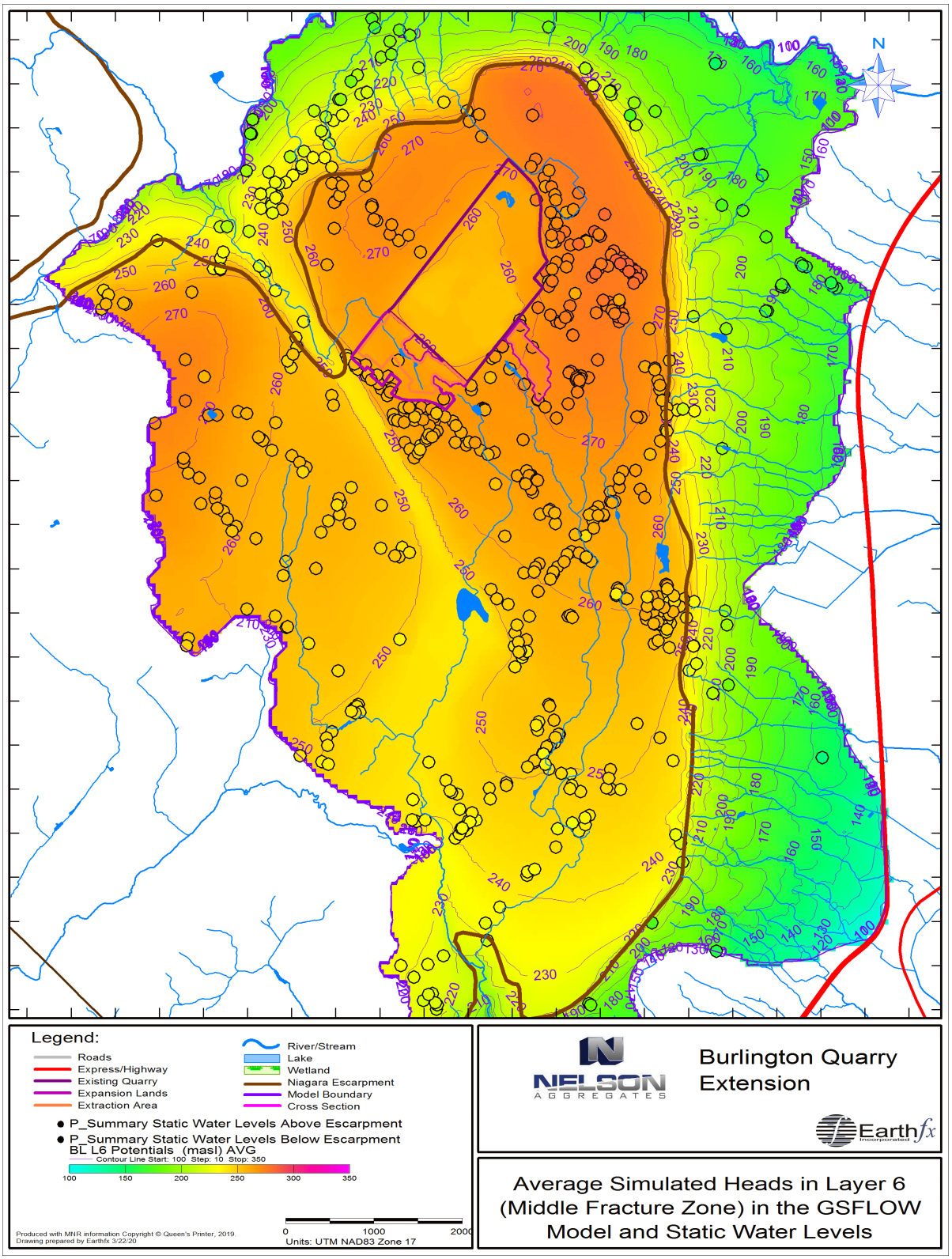

Figure 19.2: Average GSFLOW simulated water levels in Model Layer 6 (representing the middle fracture zone) versus static water levels in wells (in masl).

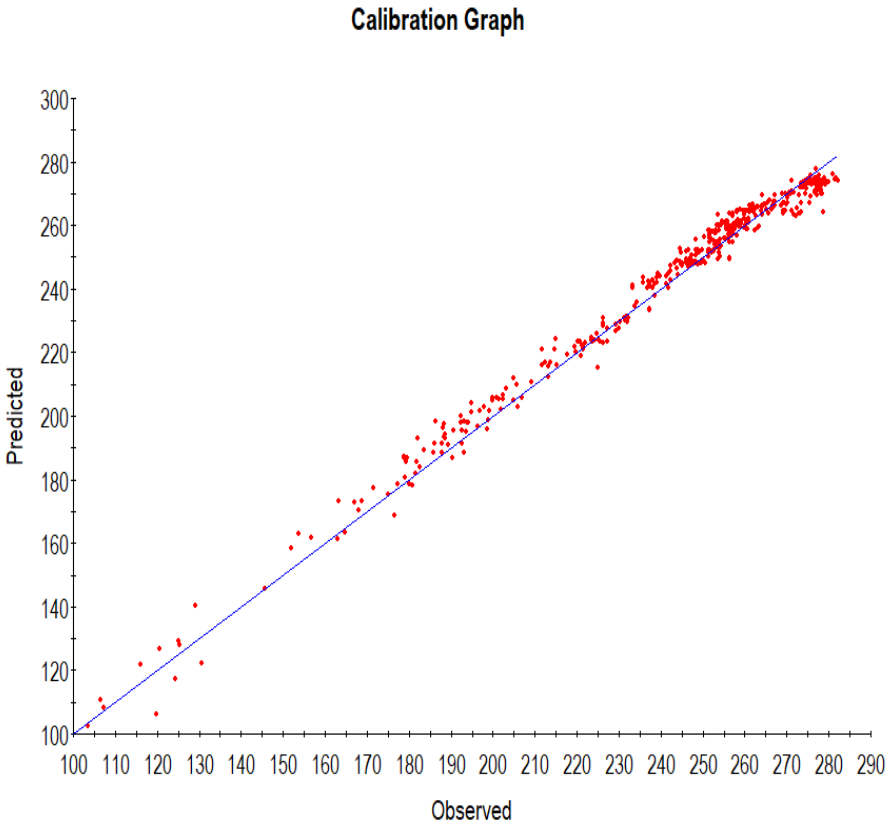

Figure 19.3: Predicted average water level (masl) versus Observed MECP water well measurements

Calibration Statistics Report
Observation Point Parameter: 2441. Shallow Water Levels (Boreholes < 15 m deep) (masl)
Model Result Parameter: 6192. BL L6 Potentials (masl) - Mean
Statistics:(Observed - Predicted) in m

- Number of points: 502
- Mean Error: -1.32842
- Mean Abs. Error: 3.33054
- RMS Error: 4.24226
- R Squared:0.98858
- Min Abs. Difference: 0.00070
- Max Abs. Difference: 13.61465
- Min Model value: 98.20484
- Max Model value: 281.89999
- Min Obs. value: 92.97000
- Max Obs. value: 281.89999

19.4 Local Surface Water Calibration

Spot flow measurements and partial flow records were compared visually against simulated streamflow at these locations and found to match well. Several examples are provided here. Gauge locations are shown in Figure 19.4.

SW10B is an important stream gauge because represents the confluence of flows from two tributaries on either side of the proposed South Lands extension area. Simulated and observed streamflow at SW-10B are presented in Figure 19.5 for WY2017 to WY2019. The observed data includes some data gaps, but the calibration to the new 2019 streamflow data is very good (Figure 19.6).

SW9 monitors the flow through the wetland complex immediately to the east of the South Lands extension area. Simulated and observed streamflow at SW-9 are presented in Figure 19.7 for WY2017 to WY2019. Flow in the stream is intermittent and both the observed and simulated results are very flashy. The observed data also contain gaps. The match to the newly collected 2019 data is excellent (Figure 19.8).

SW29 monitors the watershed west of the South Lands extension area. Both the model and the observations suggest an intermittent, flashy watershed response. Simulated and observed streamflow at SW-29 are presented in Figure 19.9 for WY2017 to WY2019. The model slightly underpredicts the baseflows and overpredicts the peak flows. Uncertainty regarding the diversions of streamflow to the golf course ponds and rates of irrigation may be contributing to the poorer match at this gauge. Comparisons at the other gauges showed a similar pattern with very good matches to the east and west of the quarry and poorer matches to the southwest.

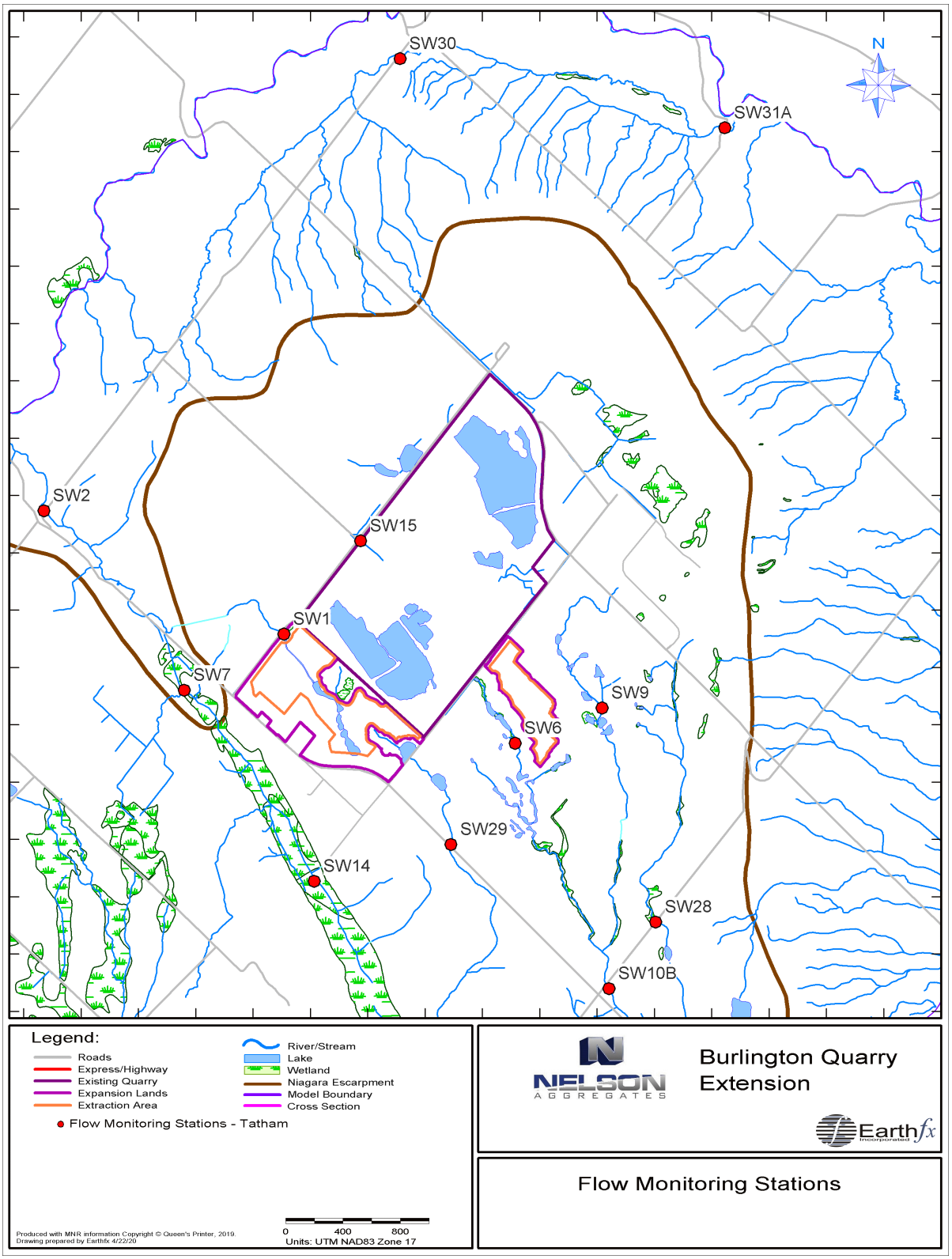

Figure 19.4: Flow monitoring stations used in the local streamflow calibration.

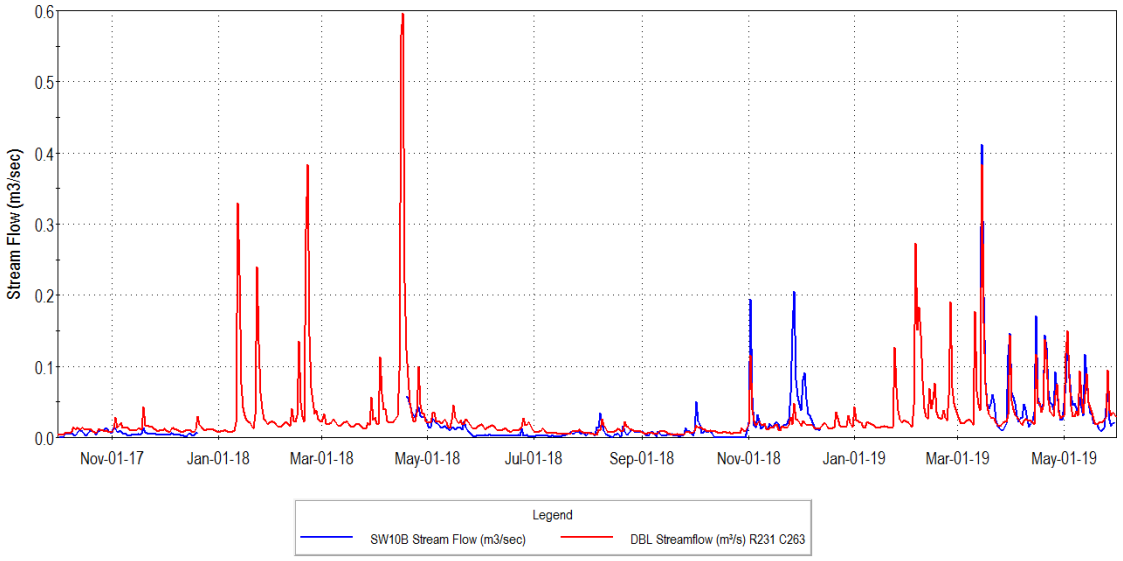

Figure 19.5: Simulated and observed streamflow at SW-10B for WY2017 to WY2019.

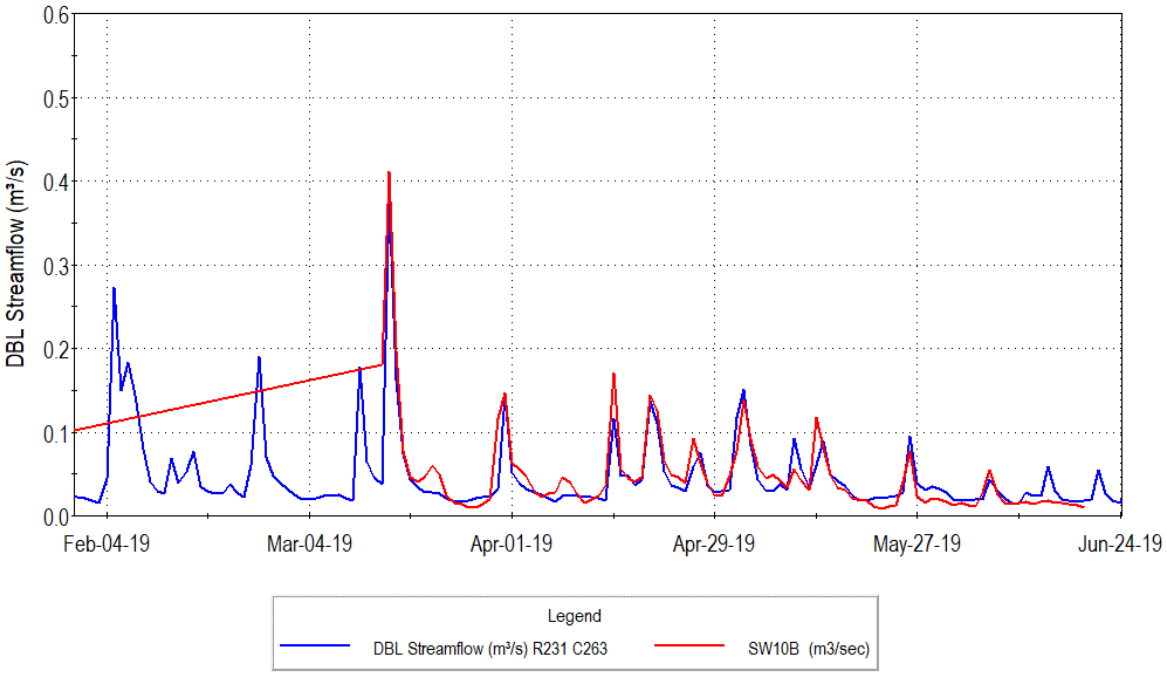

Figure 19.6: SW10B Comparison of observed (red) and simulated (blue) streamflow for 2019.

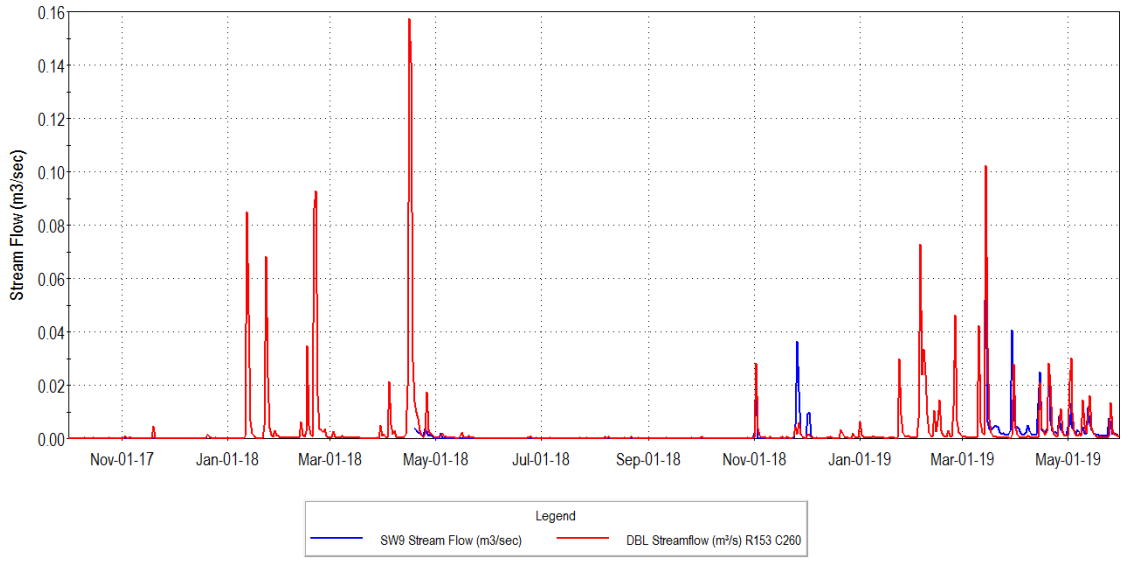

Figure 19.7: Simulated and observed streamflow at SW-09 for WY2017 to WY2019.

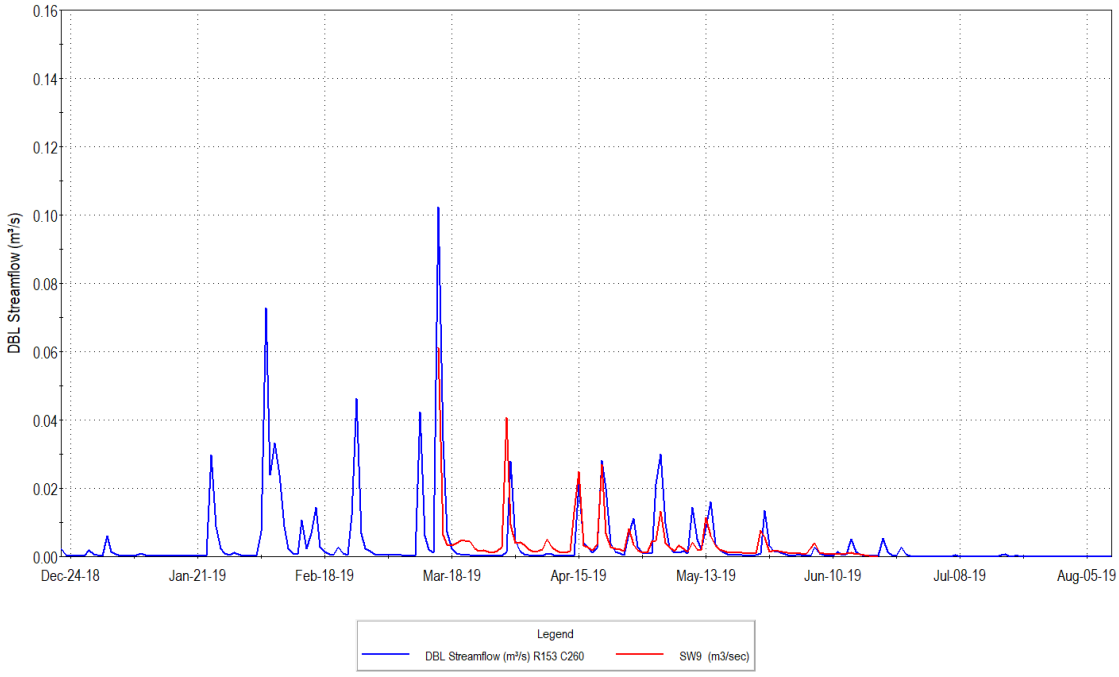

Figure 19.8: Simulated SW9 streamflow in 2019 (blue) very closely matches the observed values.

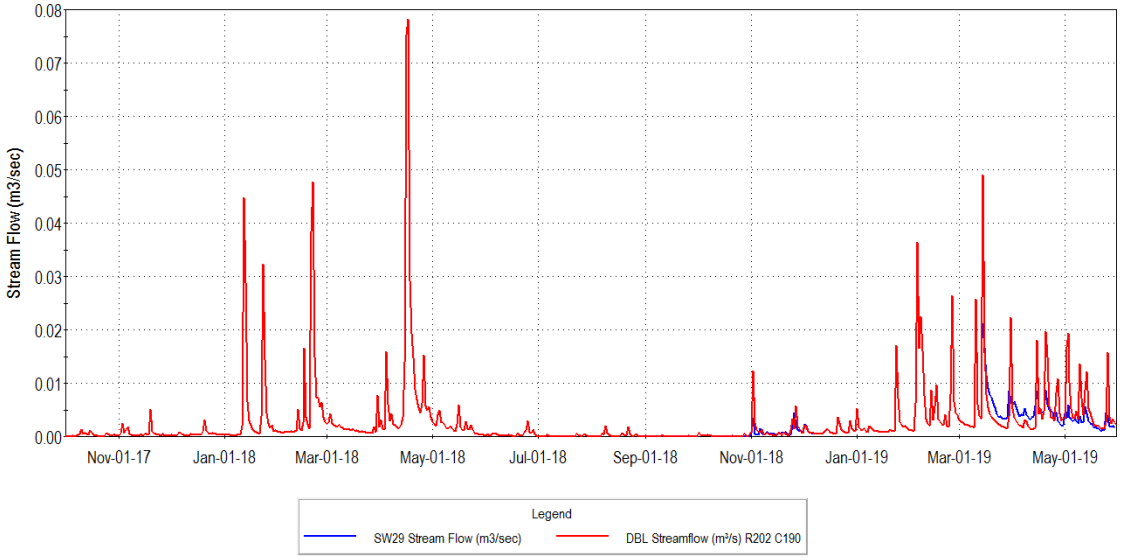

Figure 19.9: Simulated and observed streamflow at SW-29 for WY2017 to WY2019.

19.4.1 SW1: Main Quarry Discharge

As detailed daily historical flows were not available, the north sump was simulated with a set of "generalized operating rules" based on information provided by Nelson and the permit to discharge. The rules define a 7 day per week discharge rate, with an extra stage-dependant discharge rule that kept the internal quarry pond from over-topping a specified level. The decision to use "operating rules" for the simulations was based on the following:

- The rules could be used to simulate operations through periods with data gaps
- The same rules were used through all current and future simulation scenarios. This allows for consistency during the inter-comparison of the future scenarios.

Actual operations were more intermittent, but it is apparent in the data that the rules were followed more closely after January, 2016 (Figure 19.10). Overall, the model appears to be effective at representing the north quarry discharge in recent times.

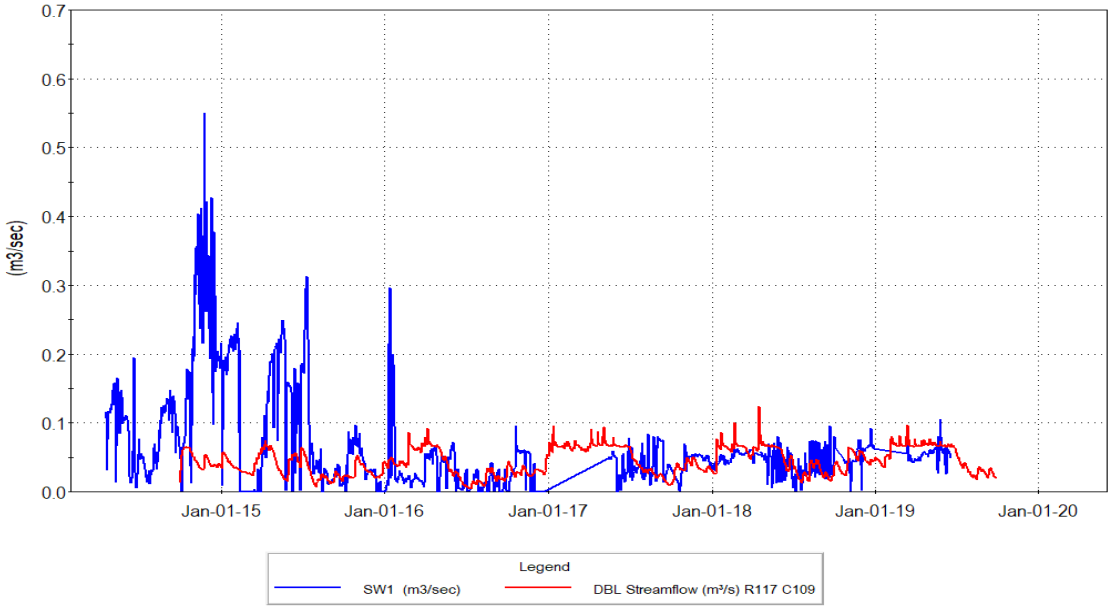

Figure 19.10: Comparison of simulated (red) and observed flows at the North Quarry discharge.

19.4.2 SW6: South Quarry Discharge

The south sump was also simulated with a set of "operating rules" and therefore also may not match the variations in the observed data. The rules define a 5 day per week discharge rate, with an extra stage-dependant discharge rule that kept the internal quarry pond at a specified level.

Actual operations were more intermittent, with spring pumping rates varied on a manual basis. The manual pumping adjustment resulted in higher spring discharge compared to the model simulation (the model included stage dependant winter discharge). The model discharge does not represent the highly variable manual rates in the intermittent historic record (Figure 19.11), but recent operations have been much more consistent with the rules and the model match to the actual flows has become very similar since 2017 (Figure 19.12).

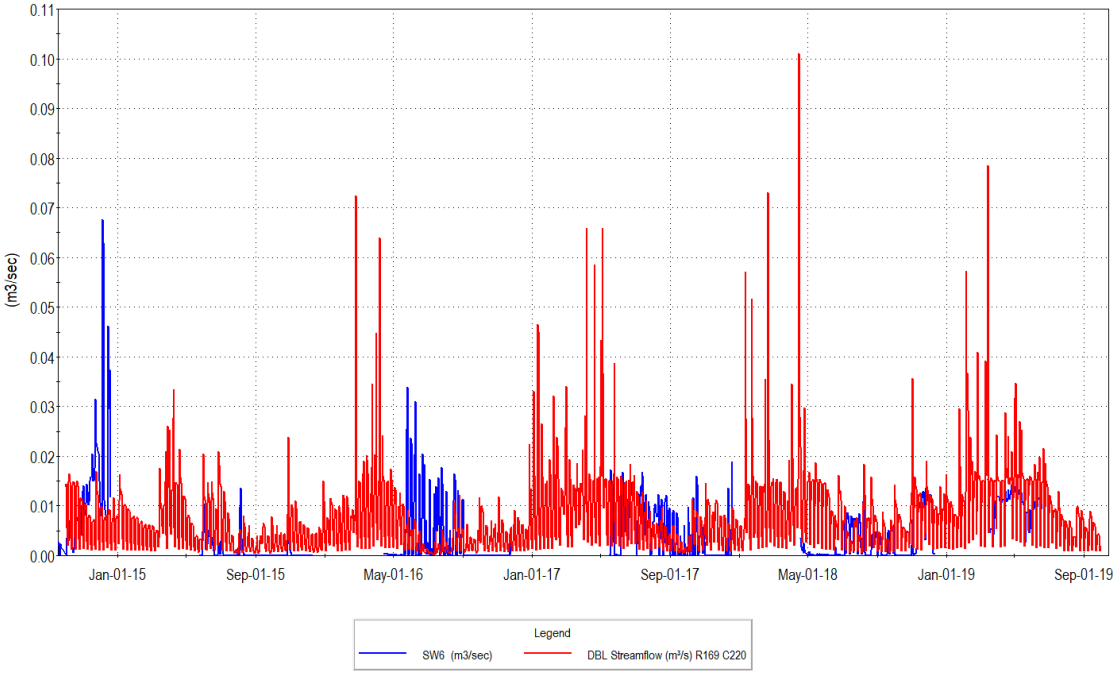

Figure 19.11: Simulated (red) and observed flows at the South Quarry discharge.

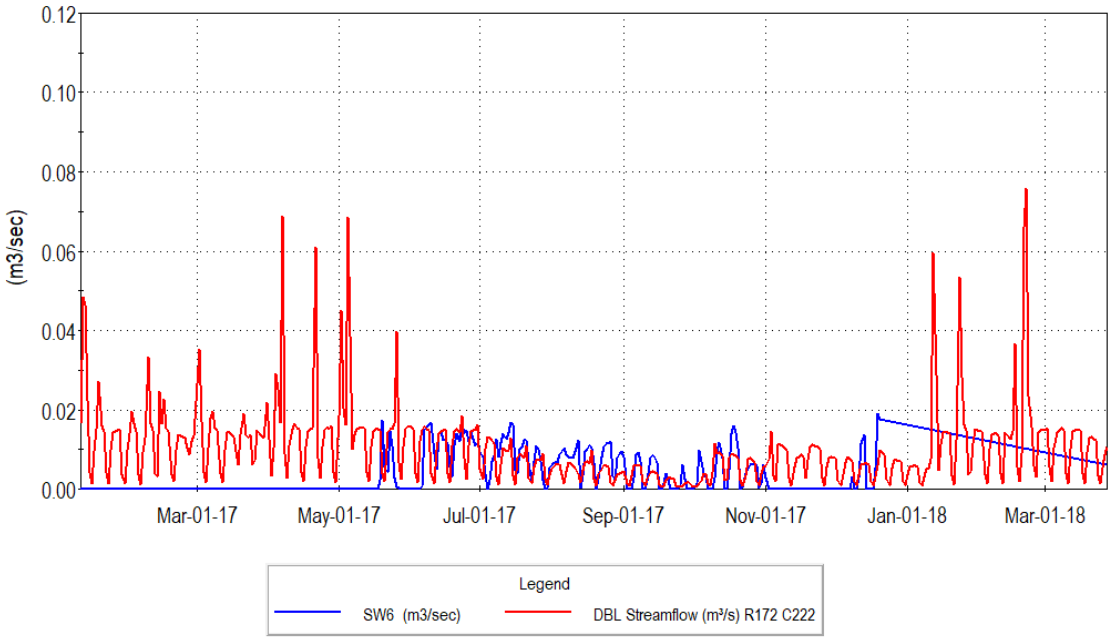

Figure 19.12: Simulated (red) and observed (blue) 2017 South Quarry discharge.

19.4.3 Medad Valley Stream Gauges

The SW2 gauge represents the total streamflow exiting the northern portion of the Medad Valley. The following hydrographs illustrate that the model matches the flow peak timing (Figure 19.13 and Figure 19.14), but under may underestimate the low flows (Figure 19.15). This is likely due to the following reasons:

1. The model does not represent the many constructed in-line and off-line ponds in the valley;
2. The extensive Medad wetlands may have more storage than simulated;
3. The model may overestimate the hydraulic conductivity of the Medad valley infill sediments, as very little borehole information is available in that area. This would result in lower heads in the valley and reduced baseflow.

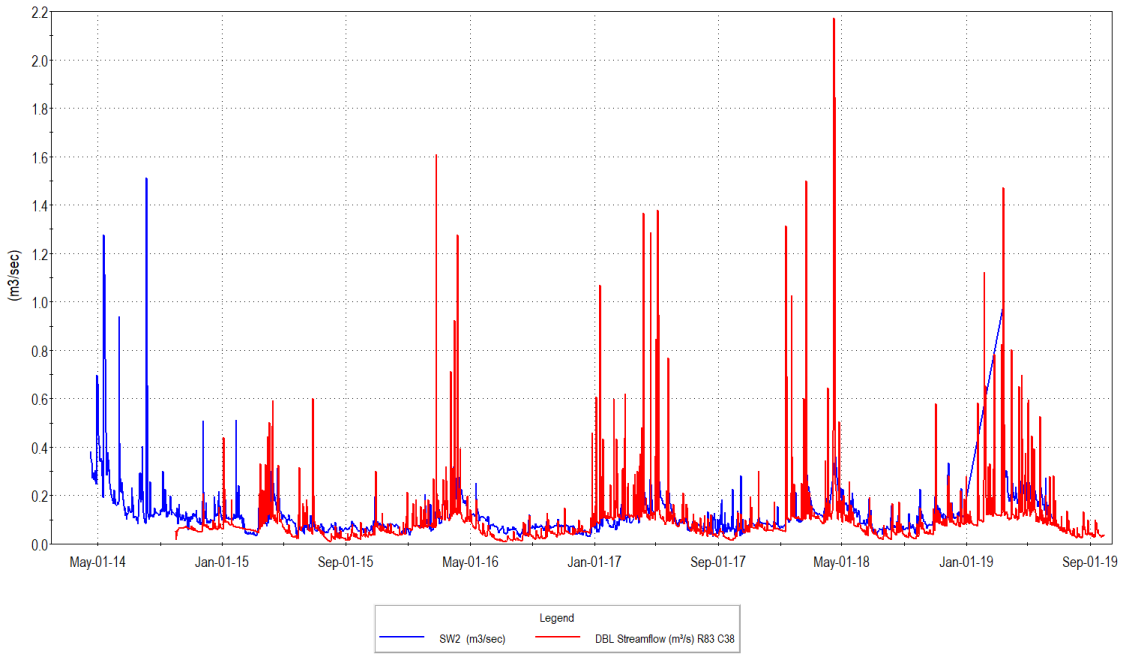

Figure 19.13: Simulated (red) and observed Medad Valley streamflow at SW2.

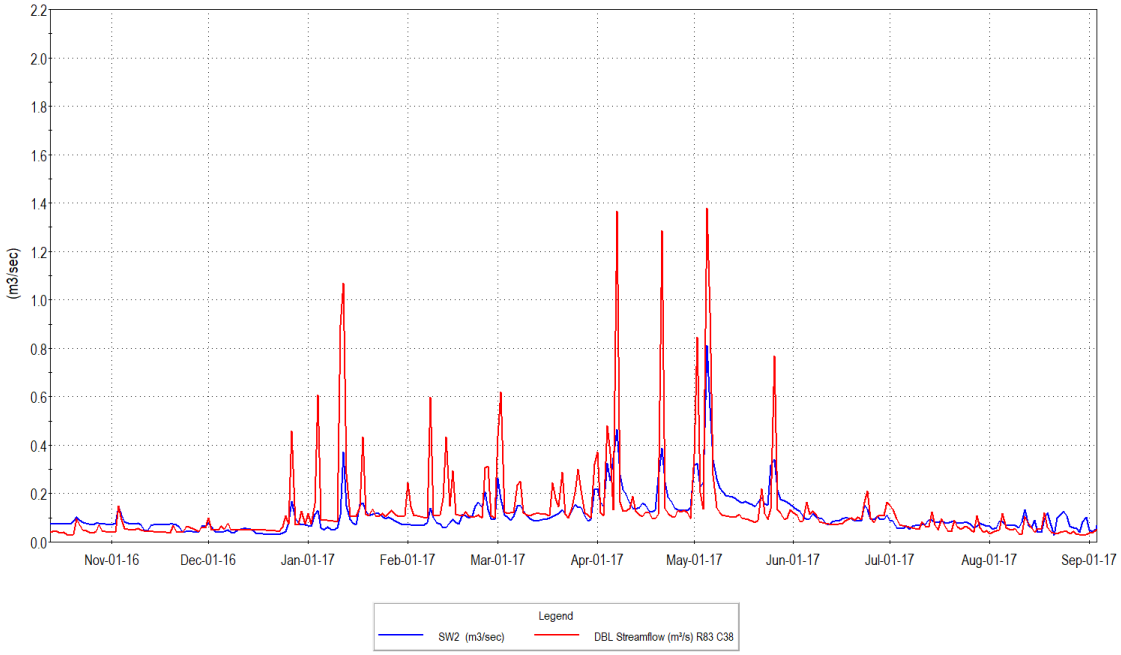

Figure 19.14: Simulated (red) and observed Medad Valley streamflow at SW2 in 2017.

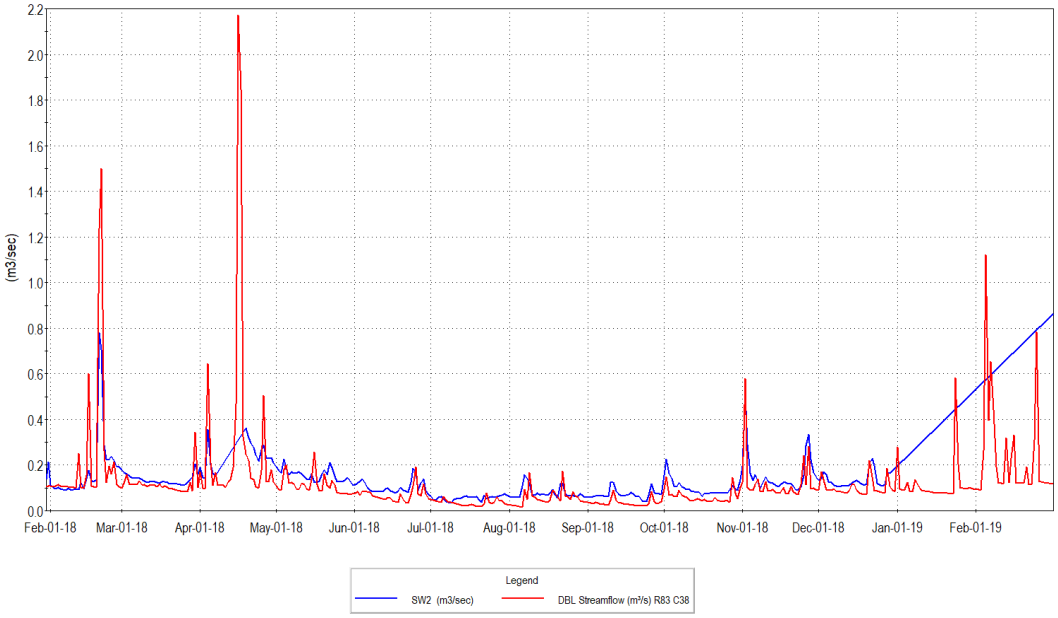

Figure 19.15: Simulated (red) and observed Medad Valley streamflow at SW2 in 2018.

19.5 Local Groundwater Calibration

The overall focus of this assessment is on the prediction of impacts in and around the existing and proposed quarry areas. Nelson maintains an extensive groundwater monitoring network with wells and mini-piezometers. Monthly water level data were collected by Golder starting in 2003 and continuous data were collected in most wells from 2007 to 2013 and starting again in October 2018. Mini-piezometer data were collected by Golder from 2007 to 2013 and new mini-piezometers were installed in wetlands by Tatham Engineering in 2018. Although there are gaps in the data, these data provided transient calibration targets for matching how the groundwater system responded to rainfall events and to seasonal and inter-annual climate variability. Matching these responses increases confidence in the model's ability to predict how water levels will be affected by quarry excavation and seasonal changes in dewatering activities.

Observed and simulated groundwater levels were compared at locations with both continuous (logger) and monthly water level data measurements. Well clusters in the vicinity of the proposed South Extension are presented here, and locations are shown in Figure 19.16. Water levels are shown for WY2010 to WY2014 the period of longest overlap between simulated and observed data.

19.5.1 Calibration Cross Sections

While the following discussion addresses complex transient water level patterns and calibration, a group of four cross sections have been prepared to illustrate the model results through the South Lands extension area. The cross-section locations are shown on Figure 19.17. The cross sections, showing the average simulated water levels, are presented in Figure 19.18 through Figure 19.21.

19.5.2 Calibration and Transient Water Level Overview

A very distinctive pattern of water levels is observed in the transient monitoring in the study area. Near the quarry (less than 100 m), a head difference of as much as 14 m is observed between the shallow (layer 4, weathered bedrock) and deep wells (Layer 8, lower fracture zone). With increasing distance, the heads in the lower aquifers rise, but the upper aquifers exhibit higher seasonal variability as the system is replenished during the spring and drains through the summer. At a distance of more than 800 m from the face, the heads in all layers are relatively the same, with natural seasonal variability of approximately 2 m.

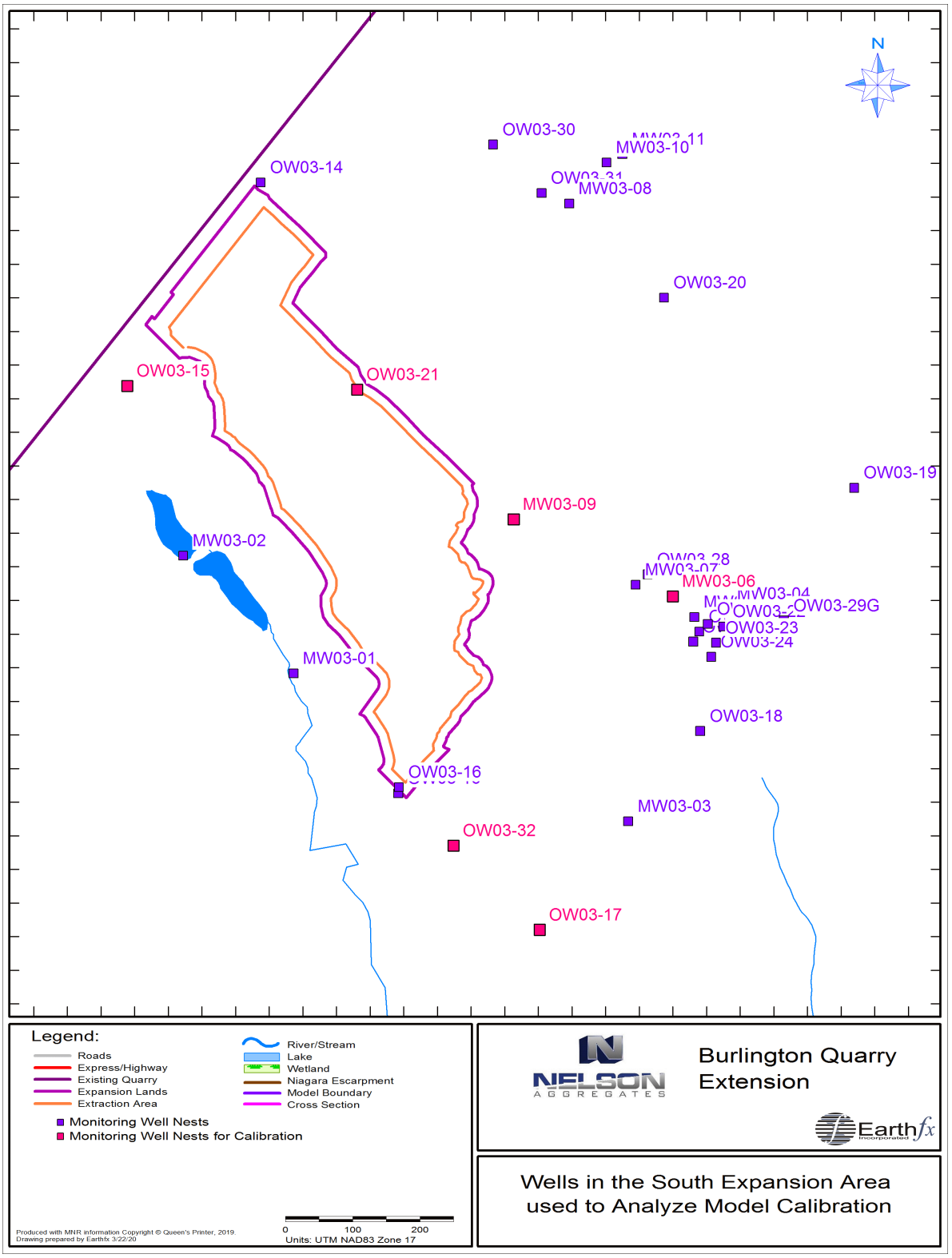

Figure 19.16: Wells in the South Extension area.

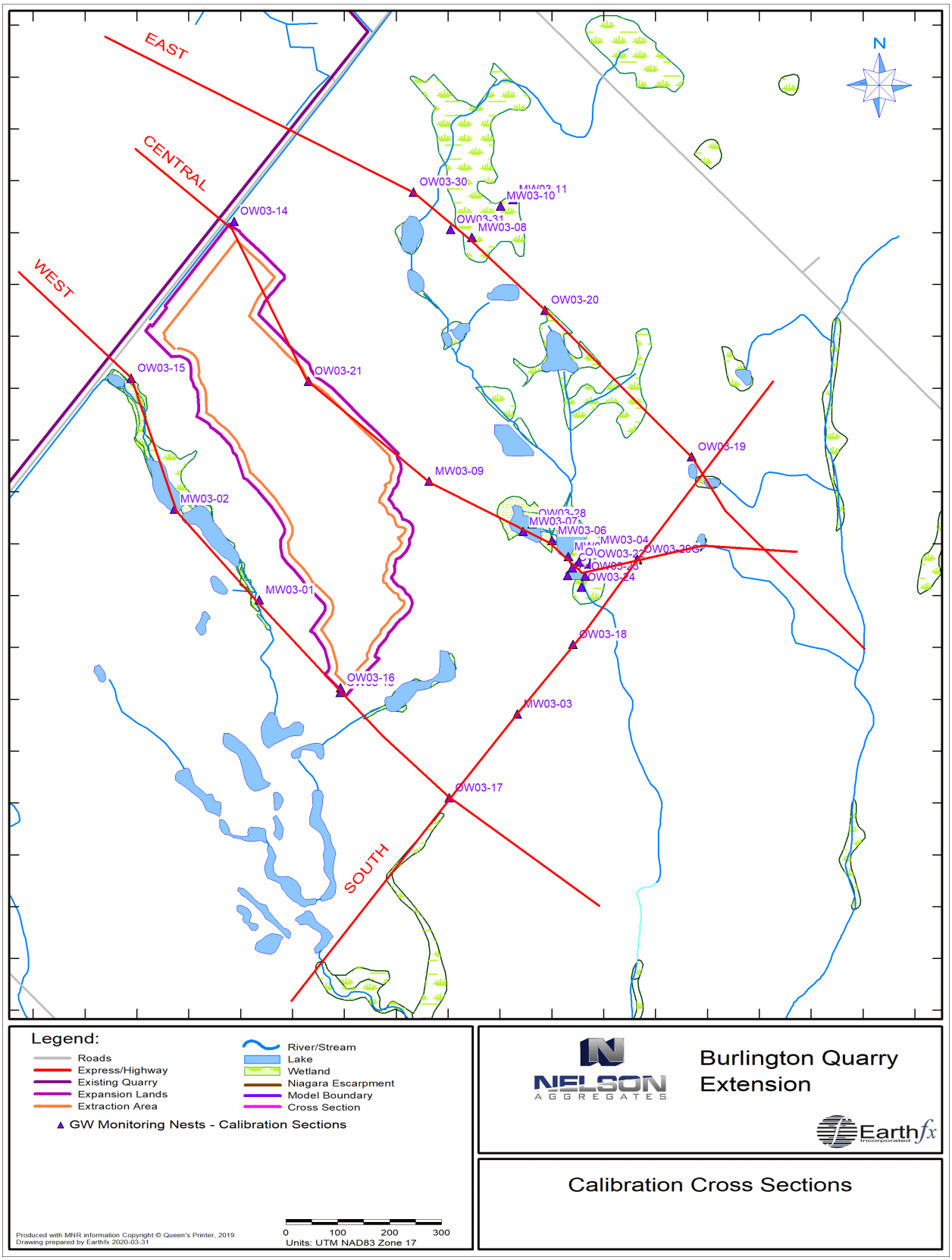

Figure 19.17: Location of calibration cross sections.

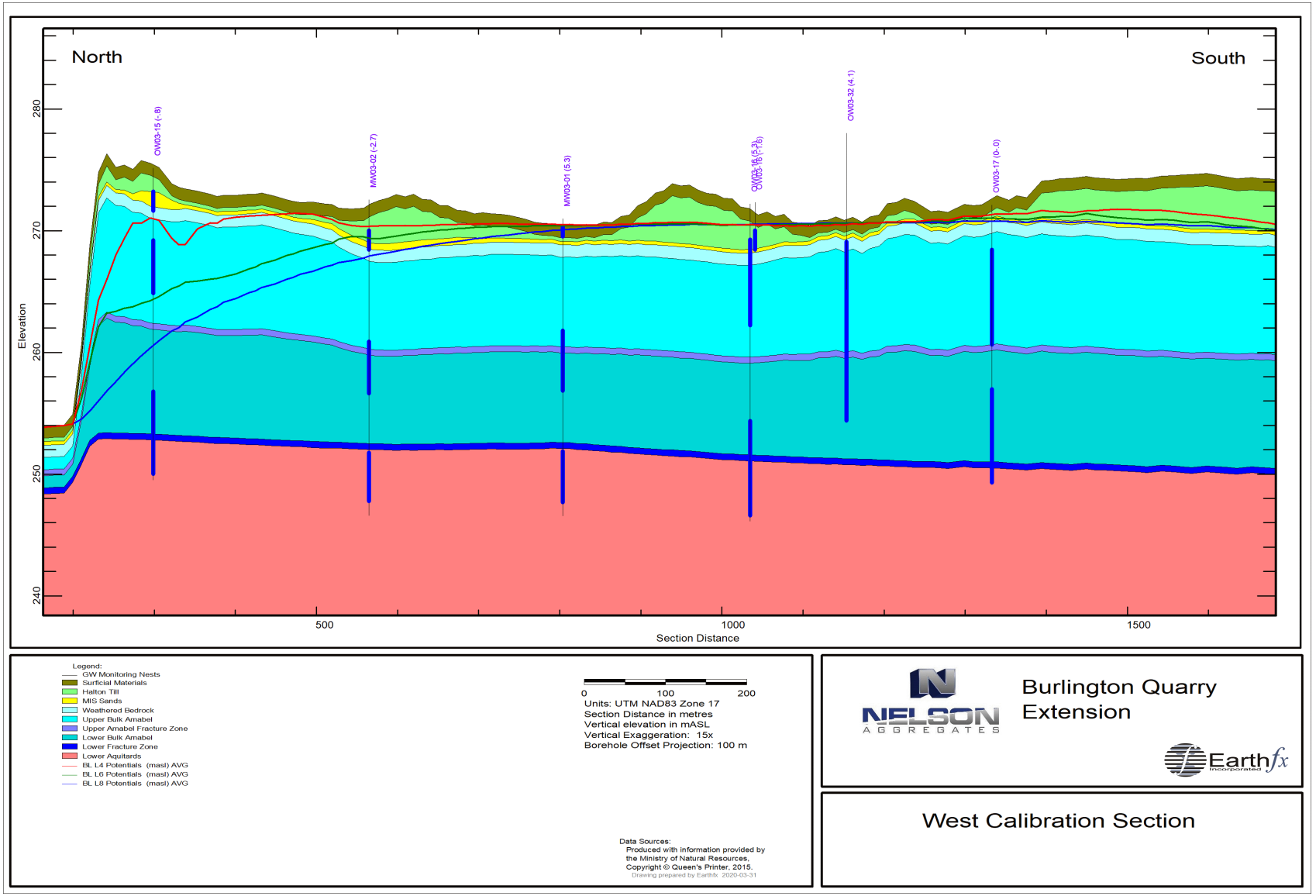

Figure 19.18: West calibration section.

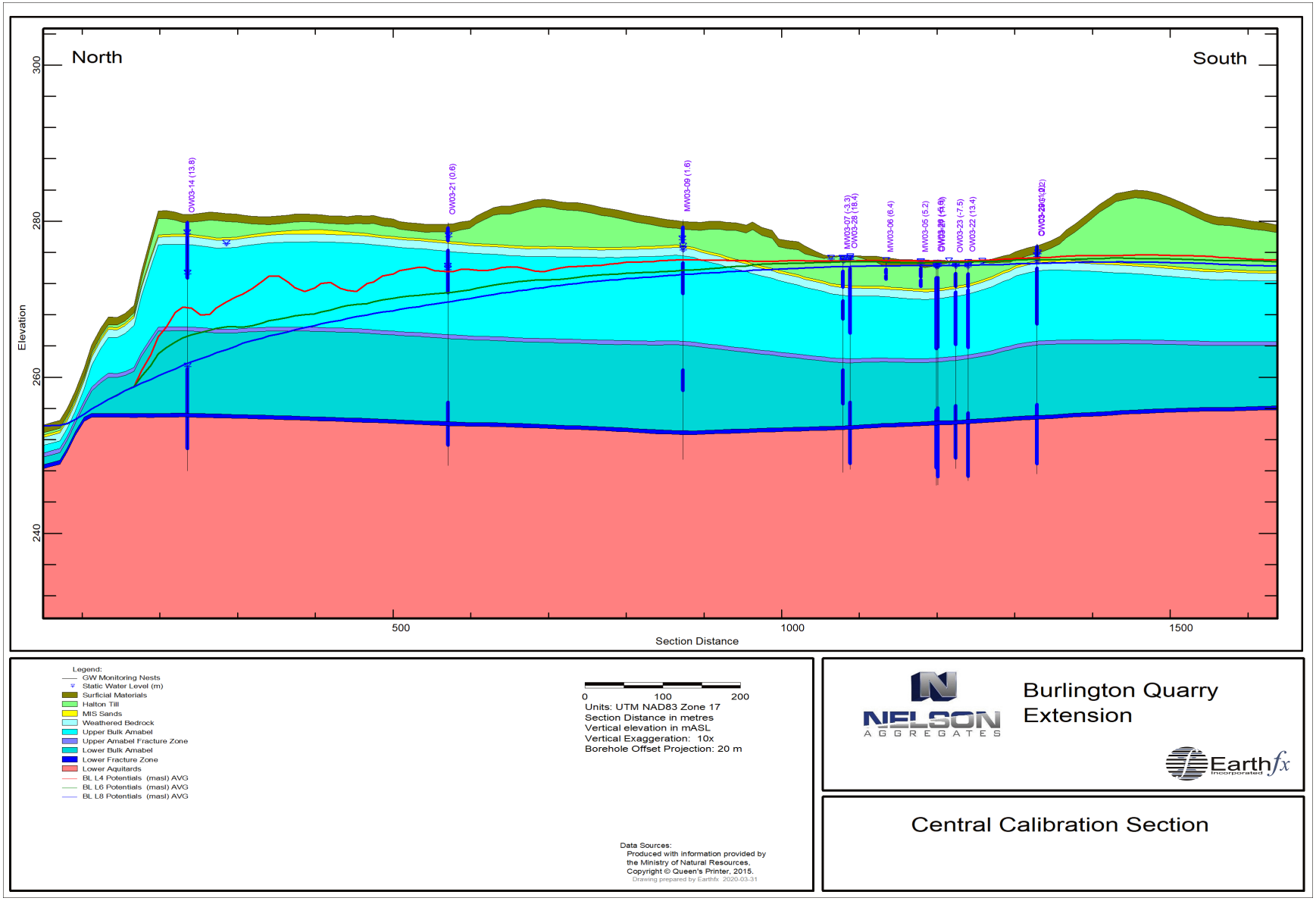

Figure 19.19: Central calibration section.

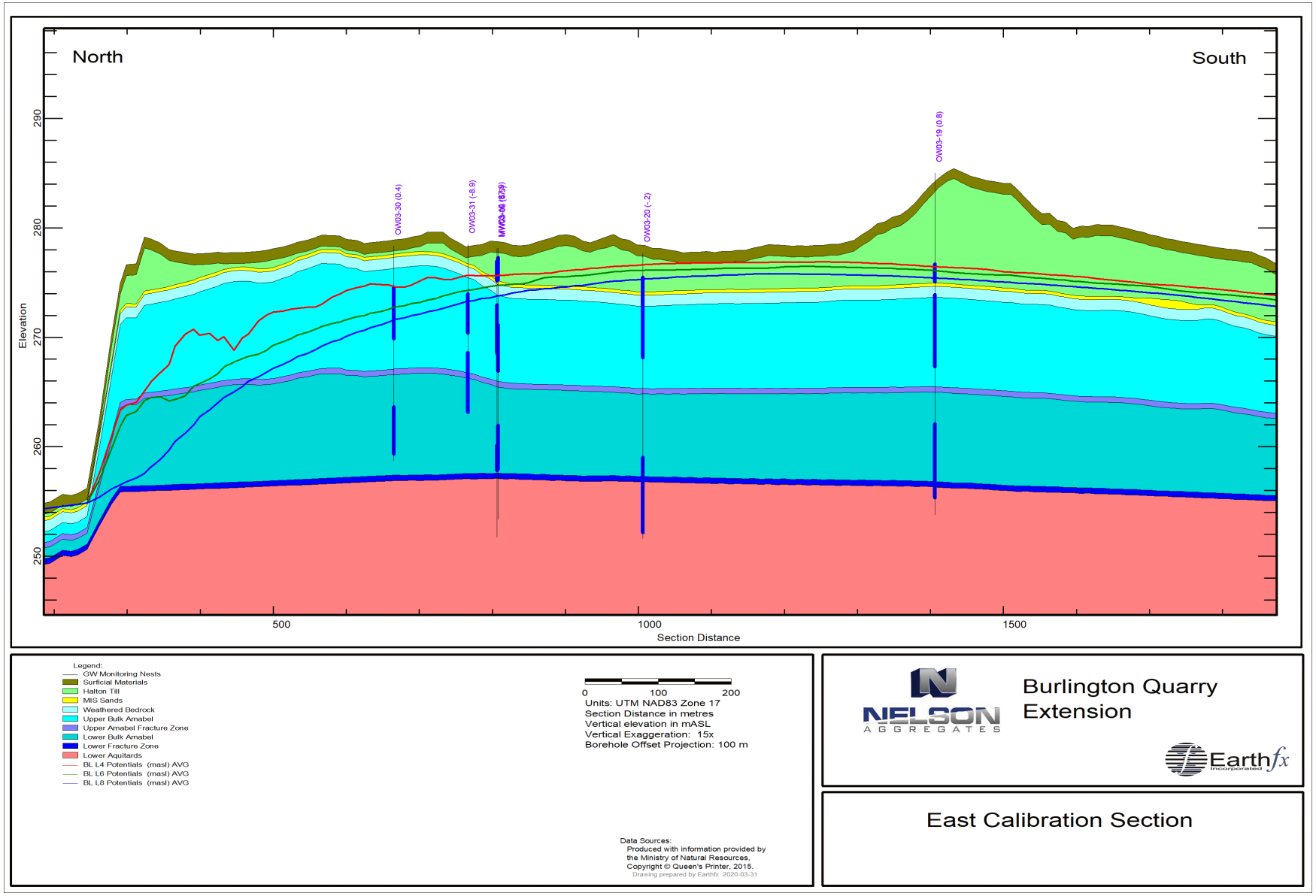

Figure 19.20: East calibration section.

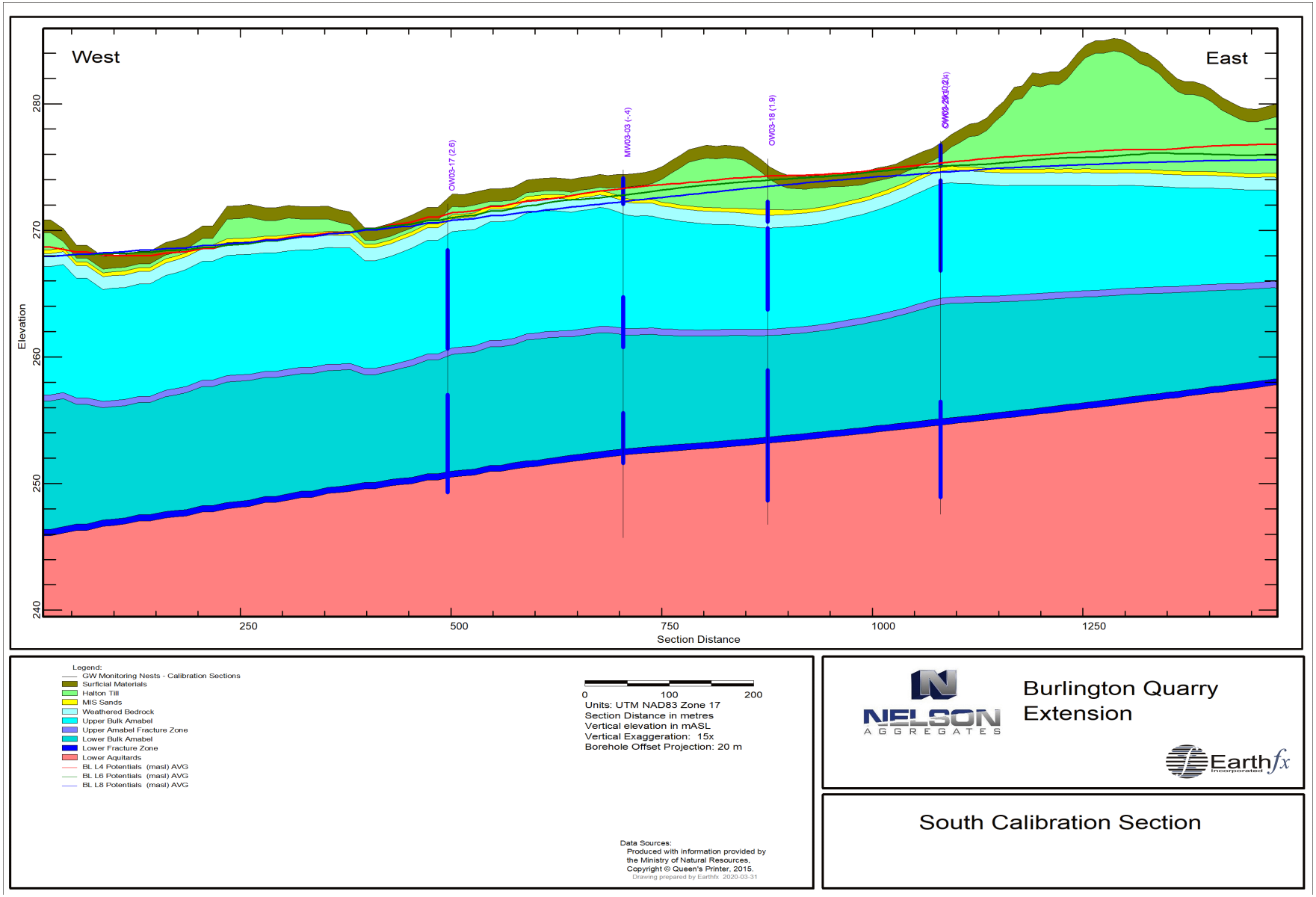

Figure 19.21: South calibration section.

19.5.3 Wells within 100 m of the Quarry Face

Figure 19.22 shows the simulated and observed water levels at the OW03-15 well cluster, the closest to the quarry face (55 m) (Figure 19.18). Simulated water levels are shown for Layers 4 and 8 to represent the upper weathered bedrock and the lower fracture zone aquifer response. A few key aspects of the hydrographs include:

- Shallow water levels are shown in red, while deeper levels are shown in blue.
- Observed manual water levels are shown with symbols and dashed lines
- Observed values from data loggers are shown as thin lines
- Simulated results are shown as thick lines.

Logger data are shown for OW03-15A and 15C, with 15A being the deepest well in the cluster. Water levels in the shallow well (OW03-15C) track about 2 m higher than the simulated heads in Layer 4. The shallow system is influenced by leakage from the south quarry discharge, which occurs nearby, and higher leakage could account for the small difference between the observed and predicted values.

Water levels in the deepest well (OW03-15A) track less than 2 m lower than the simulated heads and the match the seasonal response and change in heads between the shallow and deeper wells match well. Small differences could be related to localized effects of quarry excavation in the immediate vicinity of the quarry face.

Overall, the model predicts the localized impacts very well, particularly given the proximity to the vertical quarry face and effects of south quarry discharge passing immediately by this monitor.

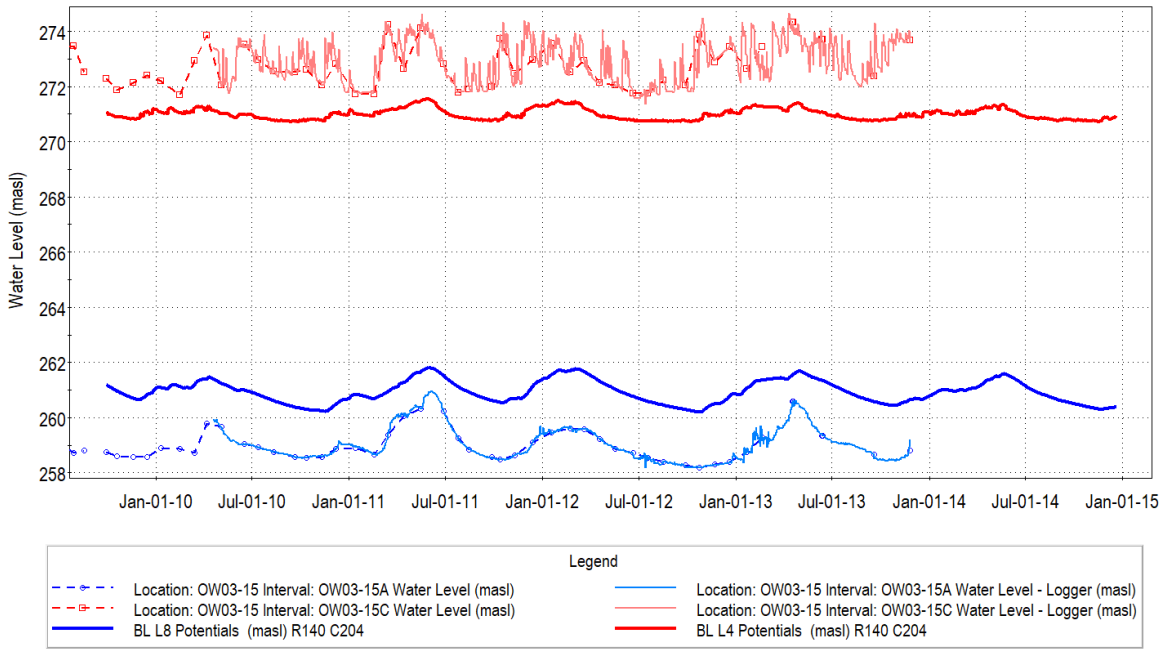

Figure 19.22: Comparison of observed and simulated water levels at monitor OW03-15.

A comparison of observed and predicted water levels at Monitor OW03-14 is shown in Figure 19.23. As previously noted (See Section 3.3.3) the quarry face advanced toward this monitor over the period of monitoring, and water levels dropped over 10 m as the face approached to within 40 m of the monitor

(Figure 19.19). The model does not simulate the movement of the quarry face, but represents the conditions after the progression of the excavation. The simulation should only be compared to the later time data.

The calibration to the lower Layer 8 monitor water levels is excellent, matching both the levels and the seasonal fluctuations in water levels.

It is highly likely that the shallow groundwater monitor at this site is likely not accurately measuring water levels, for the levels remained virtually constant over the entire monitoring period. It is possible that the levels represent residual water trapped at the base of the monitor. The simulated water levels exhibit a seasonally variable water level that indicates seasonal saturation/desaturation patterns. This characteristic pattern is exhibited in the field observations from monitor OW03-21, and is discussed in detail below.

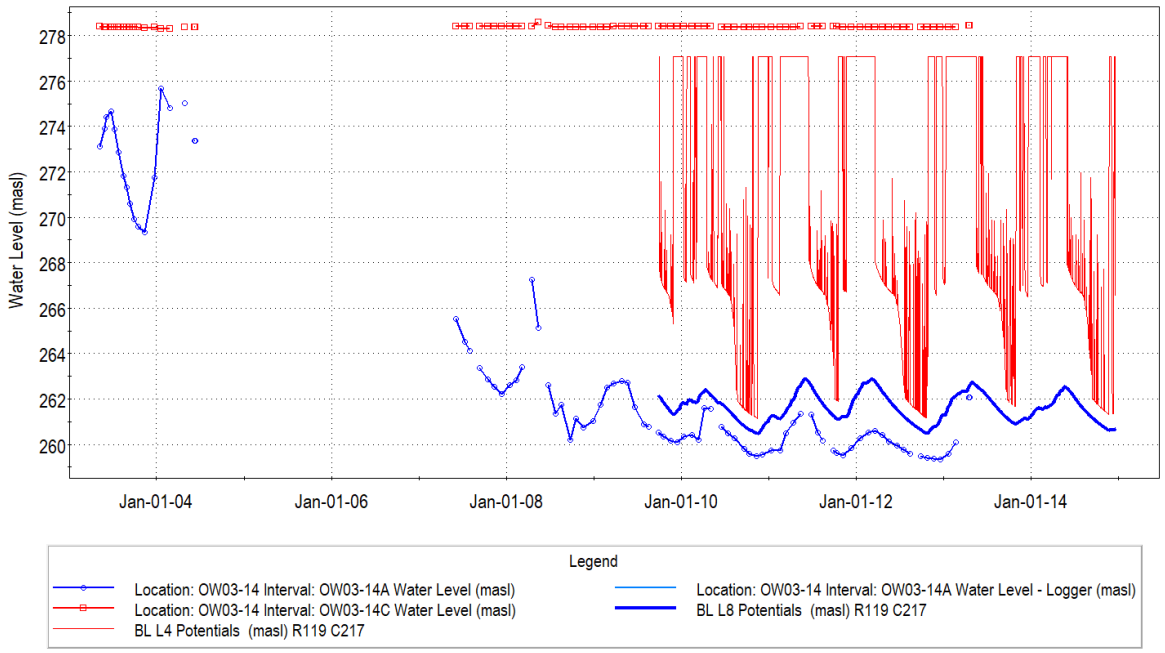

Figure 19.23: Comparison of observed and simulated water levels at monitor OW03-14.

19.5.4 Wells between 100 m and 800 m of the Quarry Face

Figure 19.24 shows the simulated and observed monthly water levels at the OW03-21 well cluster, located 350 m from the quarry face (Figure 19.19). This monitor exhibits a water level response that is typical of wells at this distance that are only partially influenced by the quarry. The manual measurements from the intermediate level monitor, OW03-21B (in light green), show a seasonal variation of more than 5 m, and the shallow monitor (in red) is frequently dry, as indicated by the constant water level. This wide variation in water level indicates that the shallow and middle aquifer systems are replenished by spring recharge, but then they drain to the lower system in the late spring and summer. The model simulates this highly complex pattern exceptionally well, as illustrated by comparing the light green manual measurements to the dark green simulated results. The calibration to the water levels in the deep system is also excellent.

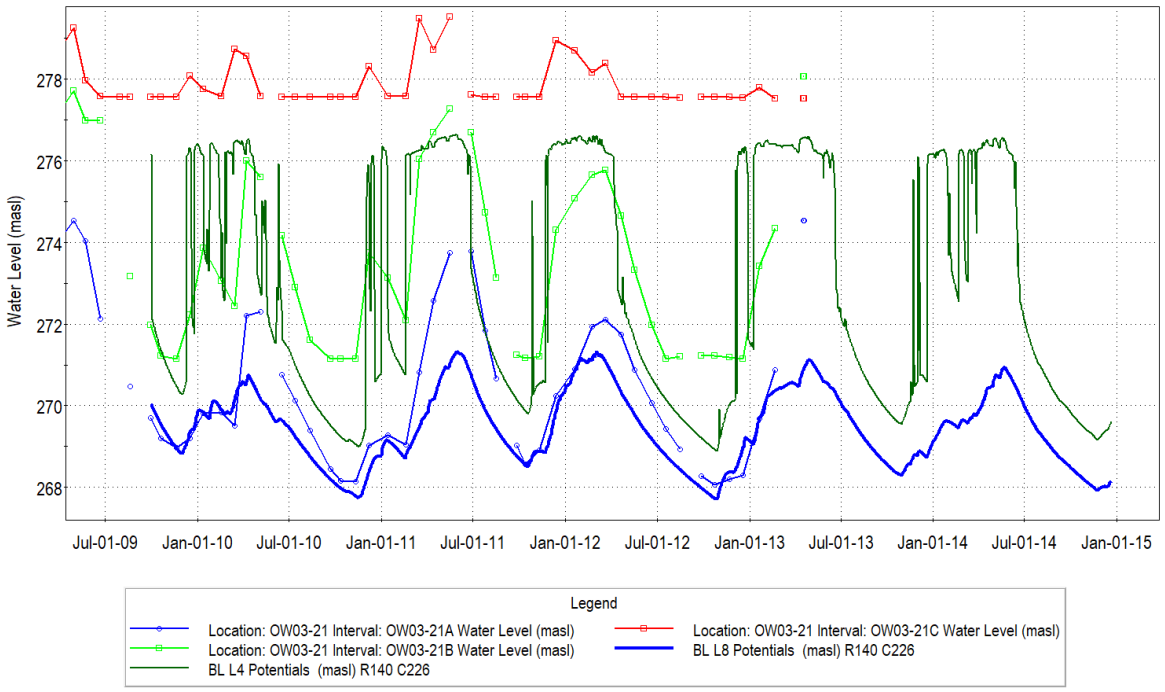

Figure 19.24: Comparison of observed and simulated water levels at monitor OW03-21.

A similar pattern can be observed at monitor MW03-09, which is located 650 m from the quarry face (Figure 19.19). Note that the deep monitor, MW03-09A, is completed in the middle Amabel, and not the deep fracture zone, so MW03-09A and MW03-09B behave in a similar manner. This monitor is less influenced by the quarry but the seasonal fill and drainage pattern to the lower system is evident. The same pattern is again exhibited at monitors OW03-30 and OW-03-31, located 300 m and 400 m from the quarry face (Figure 19.20).

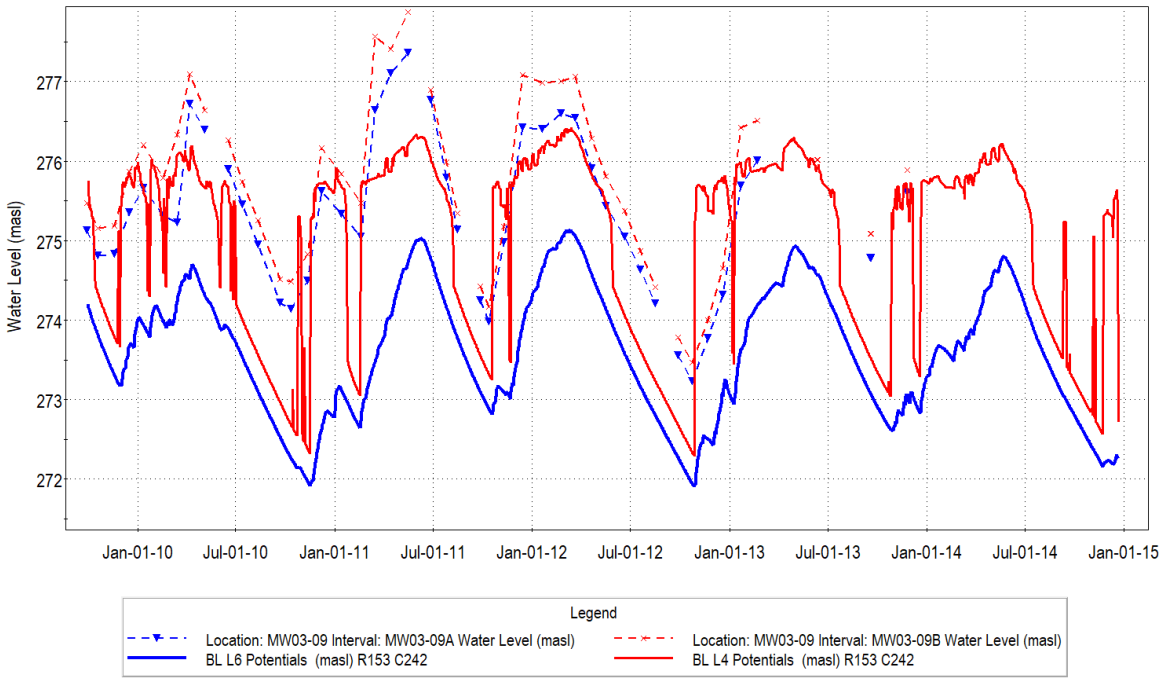

Figure 19.25: Comparison of observed and simulated water levels at monitor MW03-09 (Note: deep monitor is above layer 8).

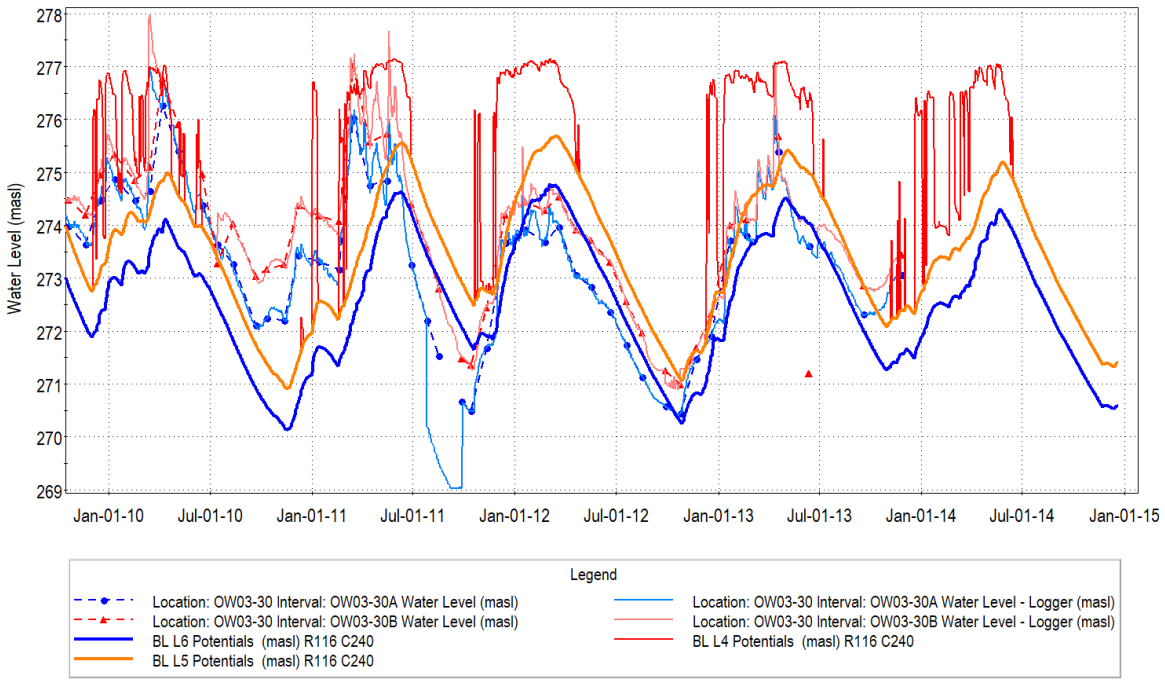

Figure 19.26: Comparison of observed and simulated water levels at monitor OW03-30 (Note: deep monitor is in layer 7).

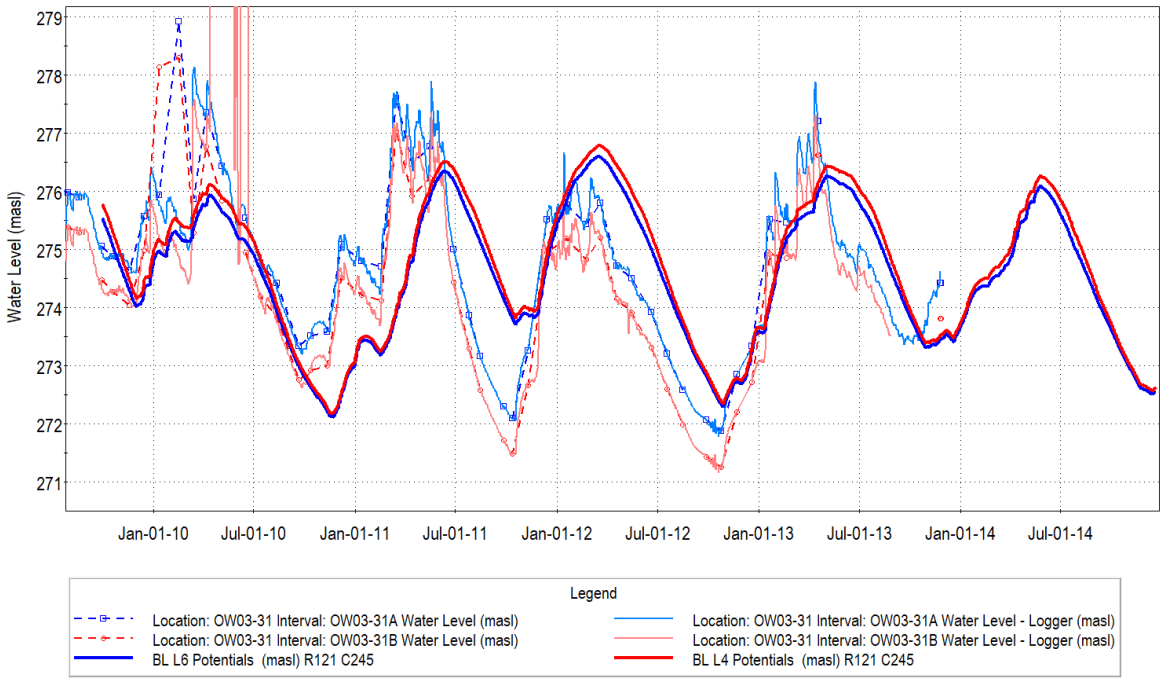

Figure 19.27: Comparison of observed and simulated water levels at monitor OW03-31 (Note: deep monitor in layer 6, shallow monitor in Layer 4-5).

The monitors on the west side of the proposed P12 extension, including OW03-15, exhibit a slightly more complex pattern, largely due to the influence of the quarry discharge and leakage from the stream that flows past these monitors (Figure 19.18). The effects of differential leakage can be seen between monitors MW03-02 (Figure 19.28) and MW03-01 (Figure 19.29). The simulated deep water levels at monitor MW03-02 (Figure 19.28) is somewhat higher than the observed values. One possible explanation is that the model simulation was completed with regular and continuous south quarry discharge, and simulations suggest considerable stream leakage to depth. The actual south quarry discharge was likely much more variable, with much of the flow passing quickly through the system in the spring (see Section 19.4.2 for a discussion of actual versus simulated south discharge). Intermittent high spring flows would likely not be as effective at recharging the lower system as the continuous flows simulated through the summer months.

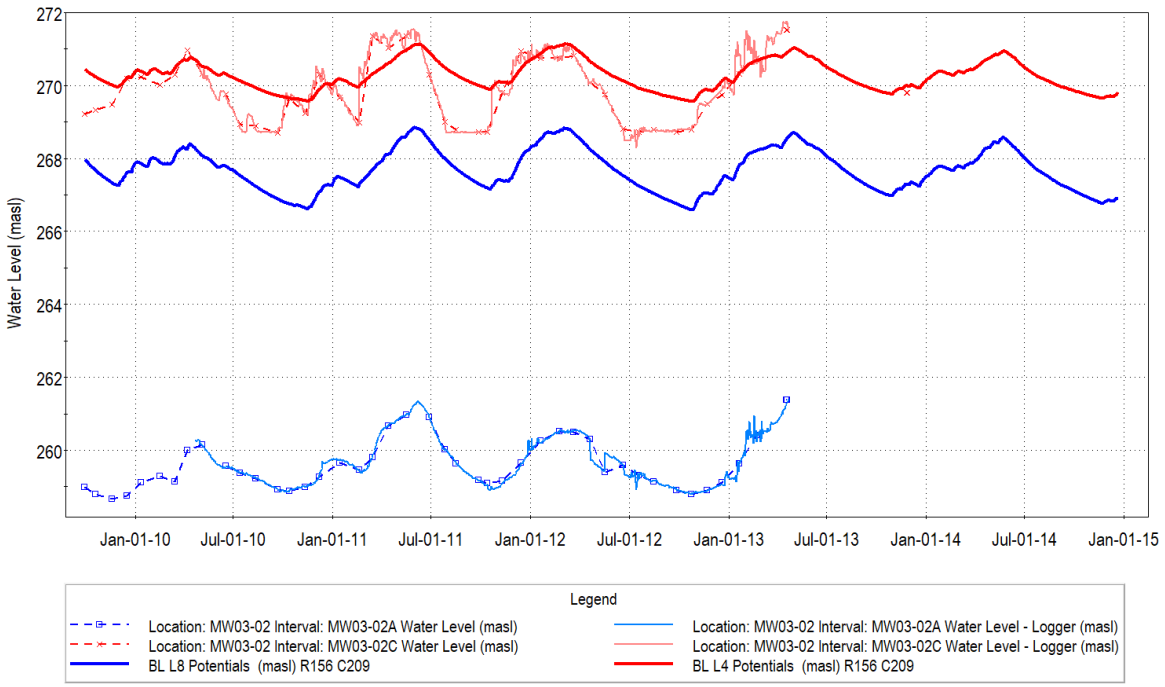

Figure 19.28: Comparison of observed and simulated water levels at monitor MW03-02.

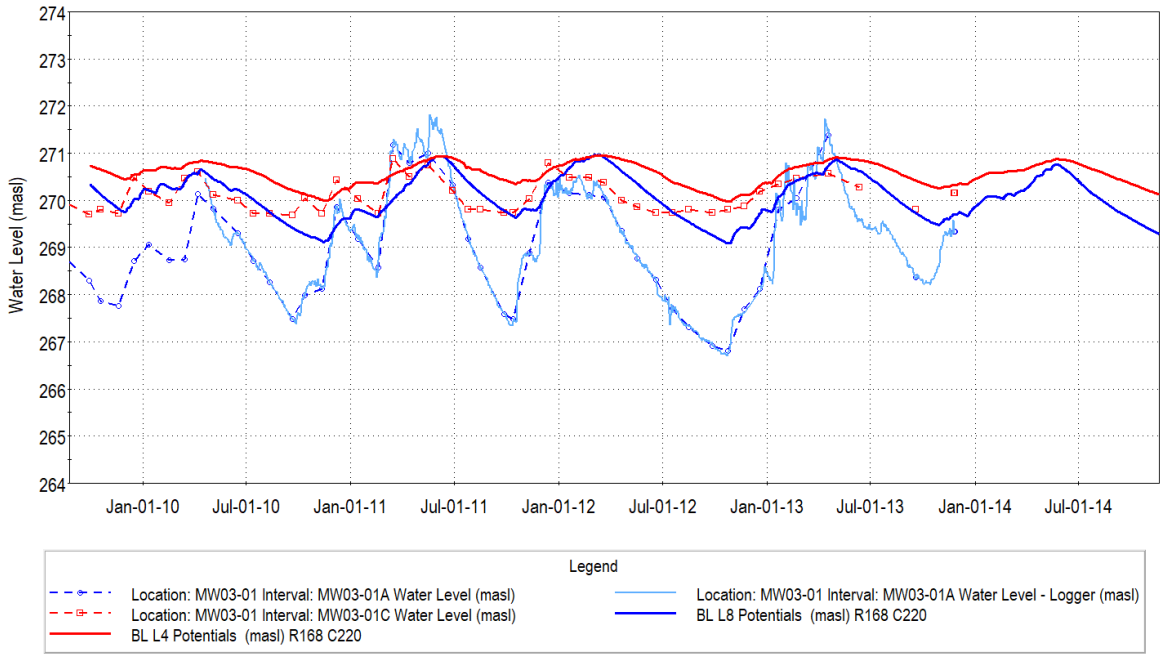

Figure 19.29: Comparison of observed and simulated water levels at monitor MW03-01

19.5.5 Wells greater than 800 m from the Quarry Face

Figure 19.30 compares simulated and observed heads at the MW03-17 well cluster, located about 1100 m from the quarry face (Figure 19.18 and Figure 19.21). Observed heads at this distance show almost no difference (Figure 19.21), and the long well screens at this location may serve to equilibrate heads. The simulated heads are about 1 m lower, but show similar magnitude and seasonal response.

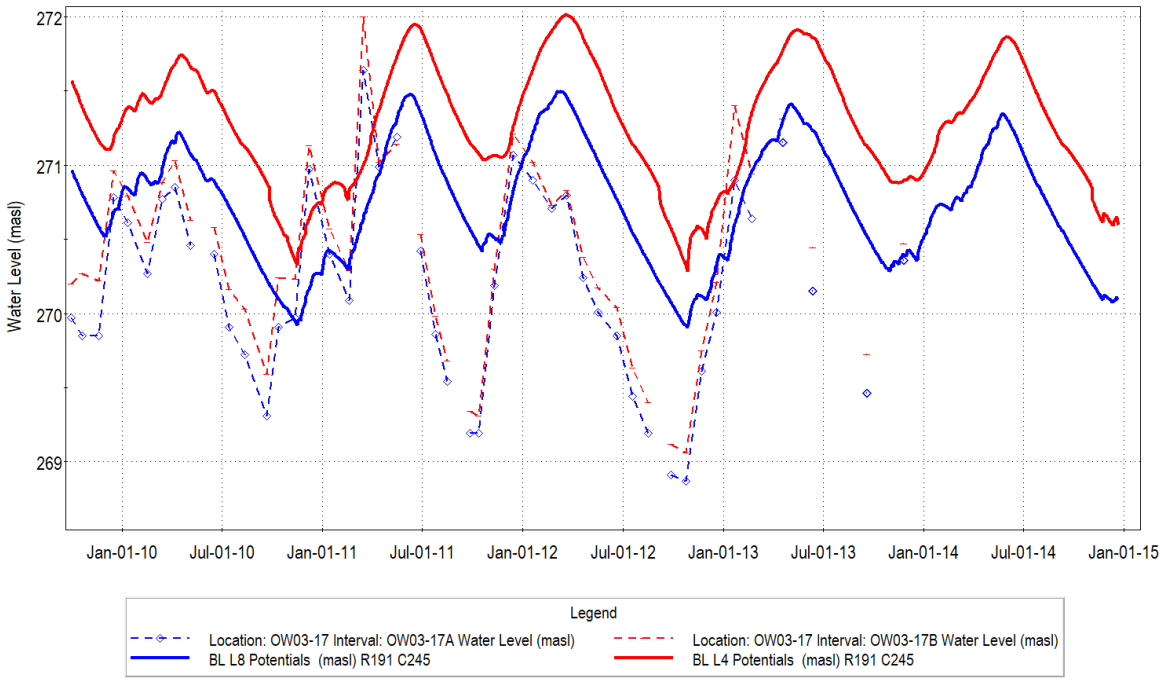

Figure 19.30: Comparison of observed and simulated water levels at monitor OW03-17.

A very similar pattern in both the observations and the model response is shown in at the OW03-18 well cluster shown in Figure 19.31. This well is also about 1100 m from the quarry face. The shallow and deep measurements are very similar, and there is no lag in the timing of the system response. The model predicts a slightly higher separation between heads, but, as noted earlier, the model represents the heads in the layer, while the observations are from long well screens that represent a more blended sample. The magnitude and timing of the model response is excellent.

The model simulation of the response in OW03-29 is excellent, and this well is located near a cluster of wetlands also about 1100 m from the quarry face (Figure 19.32). The monitoring data does suggest a difference in heads between the shallow and deep system, as predicted by the model.

Finally, the observed heads and model simulation results at OW03-19 are shown in Figure 19.33. This well is the furthest from the quarry face, and exhibits the same pattern as the other monitors at this distance.

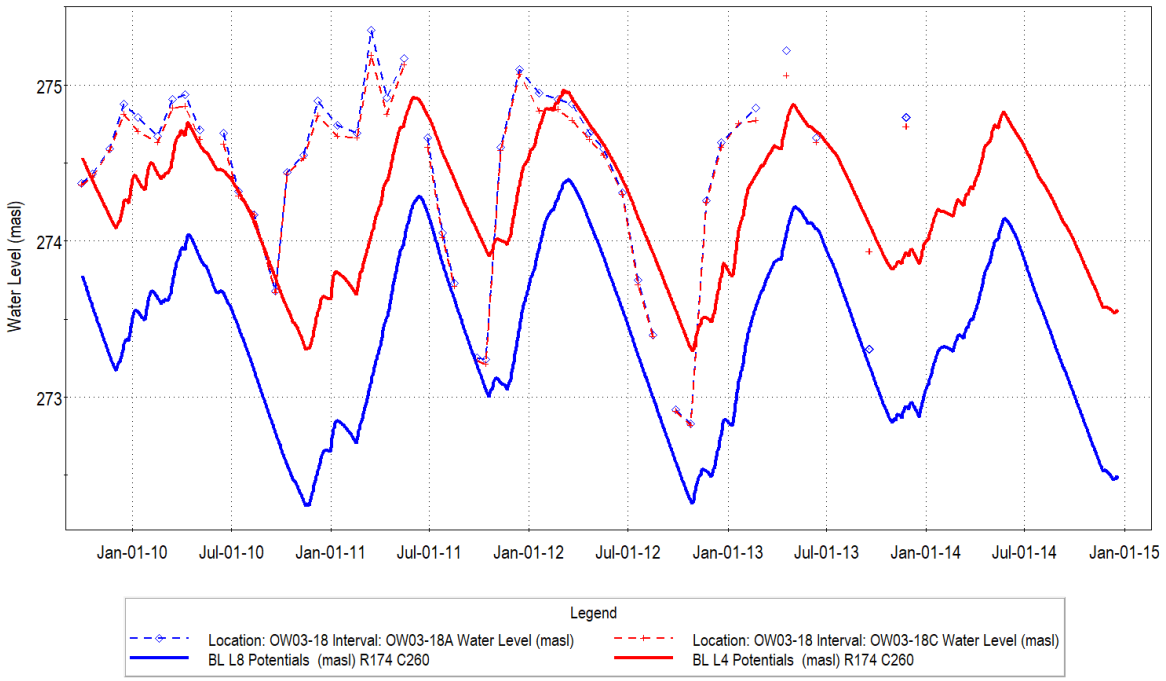

Figure 19.31: Comparison of observed and simulated water levels at monitor OW03-18.

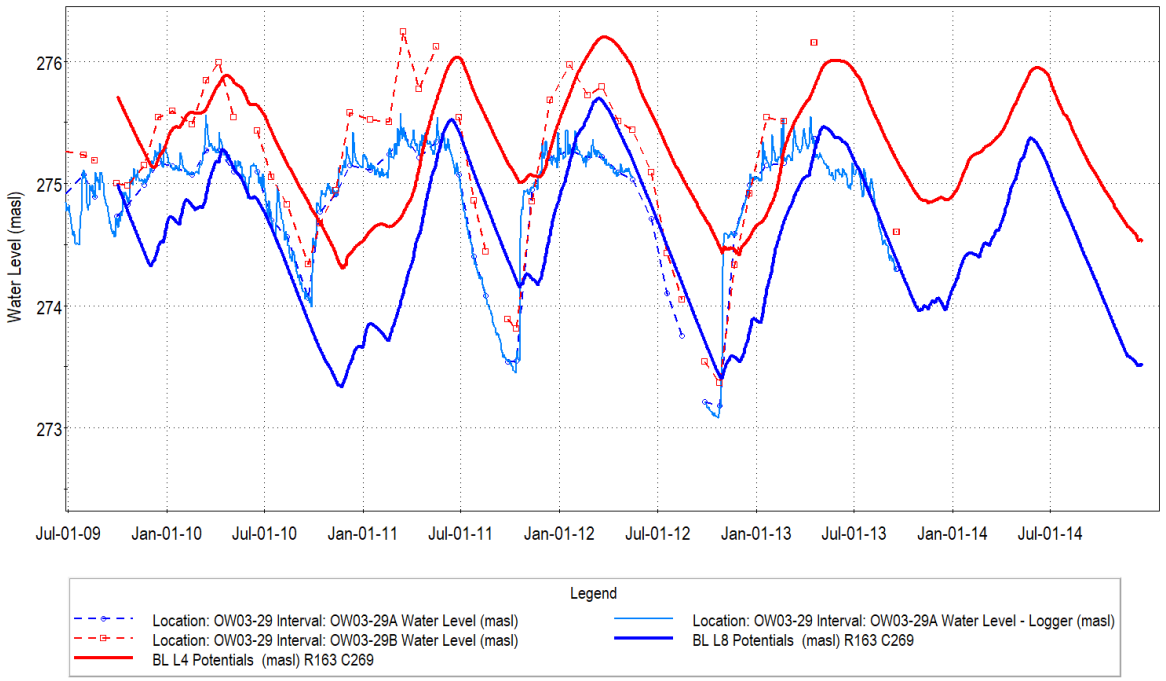

Figure 19.32: Comparison of observed and simulated water levels at monitor OW03-29.

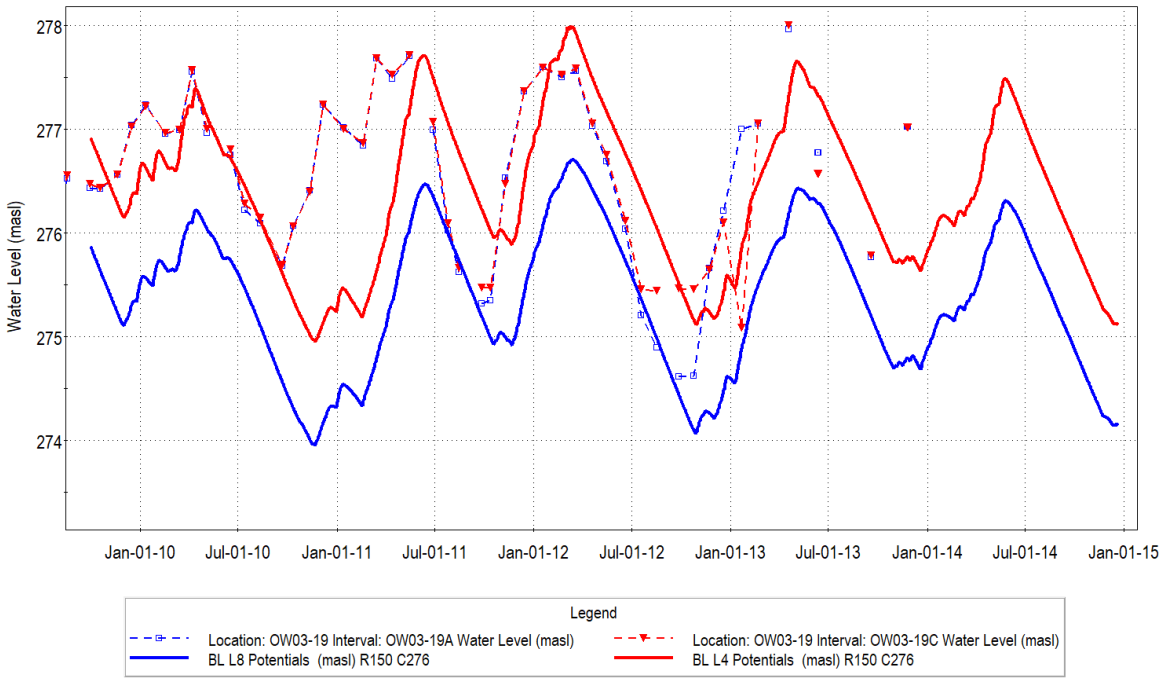

Figure 19.33: Comparison of observed and simulated water levels at monitor OW03-19.

19.5.6 Shallow System Calibration (Mini-piezometers)

The calibration of the model to the shallow water levels observed in the mini-piezometer provides insight into how the shallow system behaves. It is important to again note that a single hydraulic conductivity value was use for the Halton Till across the study area, so no local modifications were completed to match unique calibration problems.

The mini-piezometer and pond staff gauge locations that were used for calibration span the wetland complex to the east of the proposed P12 extension area. The locations discussed in the following sections are shown in Figure 19.34. It should be noted that many of the ponds and staff gauges experience significant periods where the gauge is dry. These are generally observed in the monitoring record as a “flat-line” in the monitoring response. Also note that the ponds are represented in Layer 1, so in some cases the mini-piezometer values are compared to the simulated water levels in Layer 2.

Figure 19.35 shows the observed and simulated water levels at mini-piezometer location GPO03-37, which is located in a northern wetland. The simulated results generally match the observed values, in some cases with a modest temporal lag in response. The mini-piezometer is dry for select periods, as indicated by the flat line portions of the monitoring record, and the simulation illustrates the depth to which local water levels fall during that time.

Figure 19.36 presents the results for MP-17, located just on the edge of a wetland/pond complex. The response is very similar to that observed at GP03-37. Figure 19.37 shows the results MP-13, which is located in a wetter portion of the wetland. The high-resolution data logger results provide a more detailed view of the conditions, but in some cases the data logger does not agree with the manual measurements. Again, the model results are generally very close to the observed values.

The results from three additional mini-piezometers are shown in Figure 19.38 through Figure 19.40. The levels and range of response match the observations very well; however, there is a slight lag in the modelled response. MP6, which is very close to Wetland 13032, illustrates that the model is representing the shallow system well in that area (Figure 19.40).

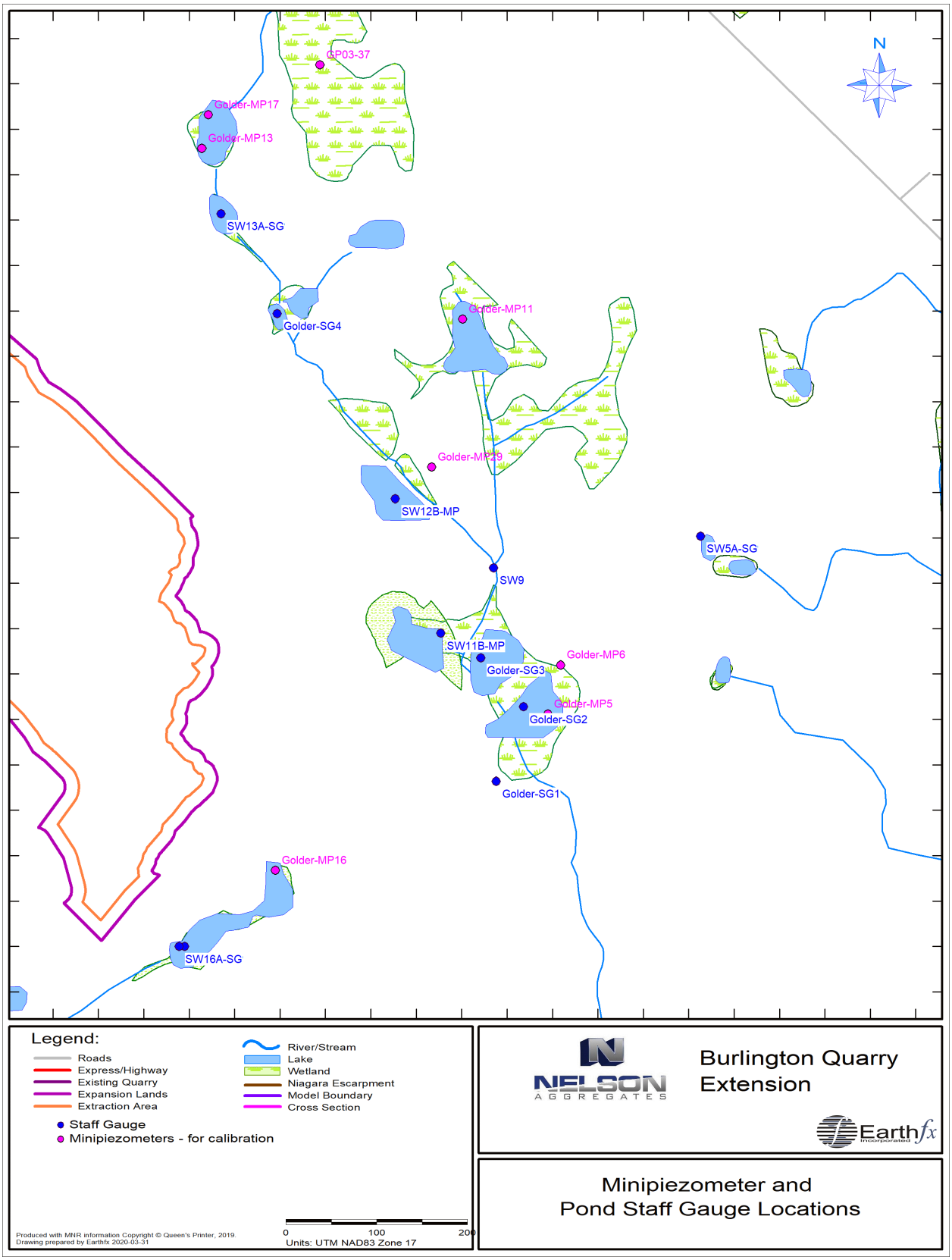

Figure 19.34: Mini-piezometer and pond staff gauge locations.

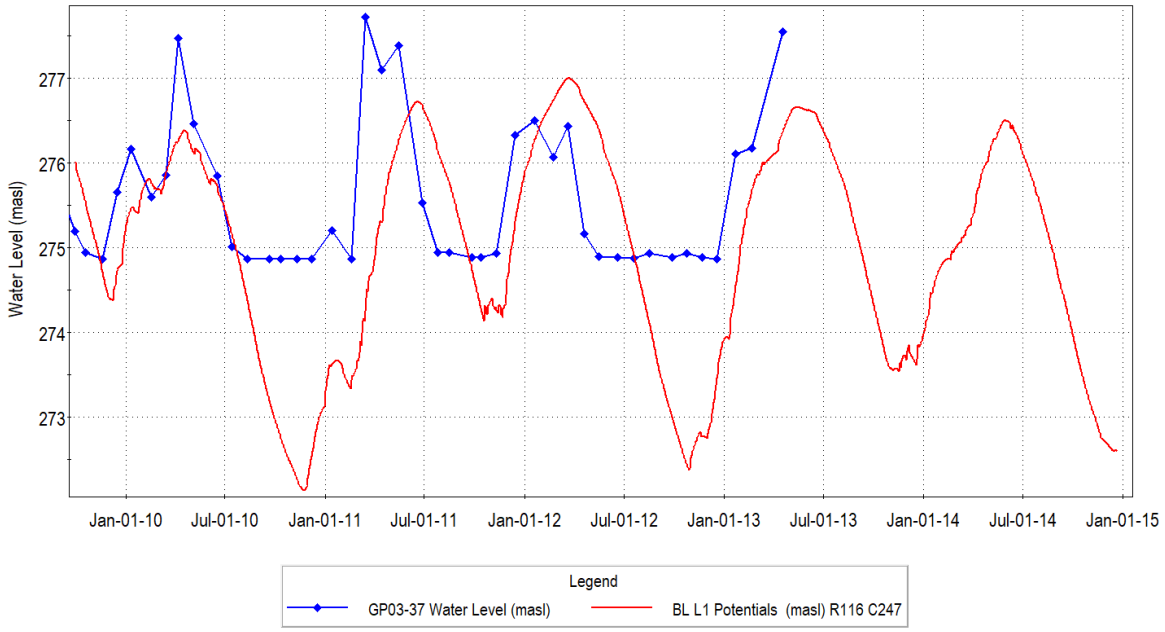

Figure 19.35: Observed and simulated shallow water levels at GP03-37.

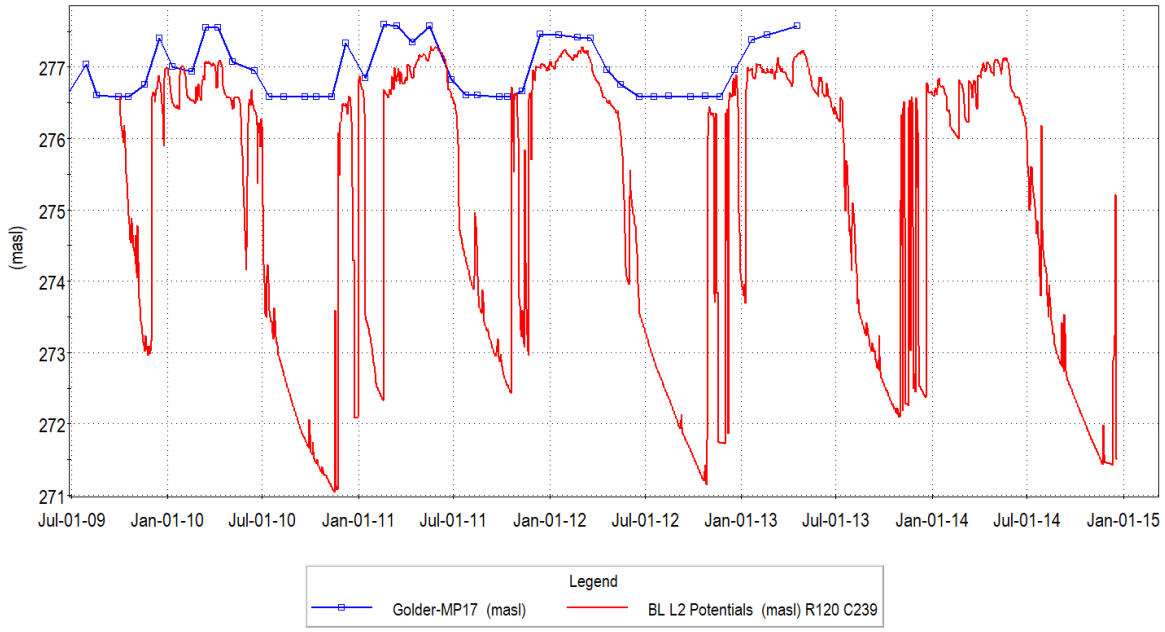

Figure 19.36: Observed and simulated shallow water levels at MP17.

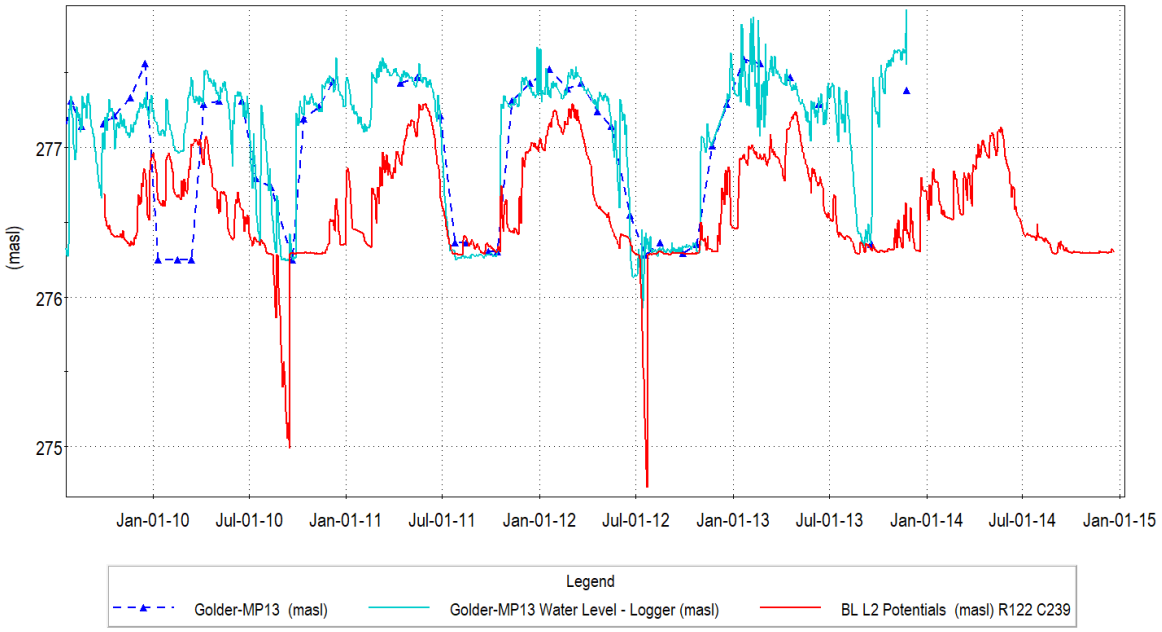

Figure 19.37: Observed and simulated shallow water levels at MP13.

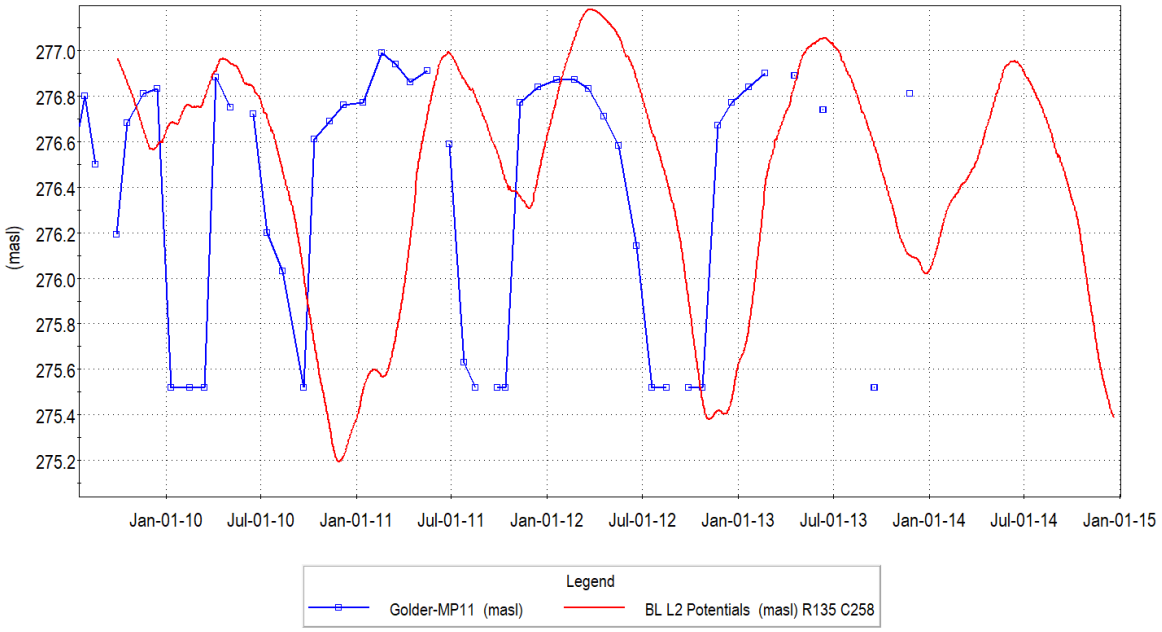

Figure 19.38: Observed and simulated shallow water levels at MP11.

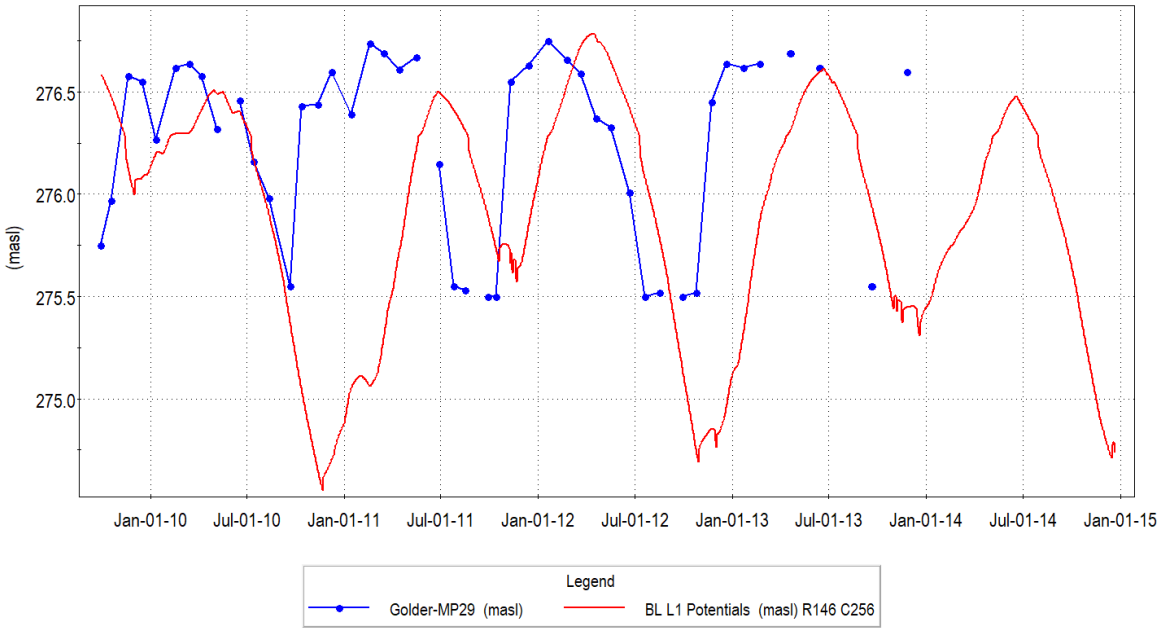

Figure 19.39: Observed and simulated shallow water levels at MP29.

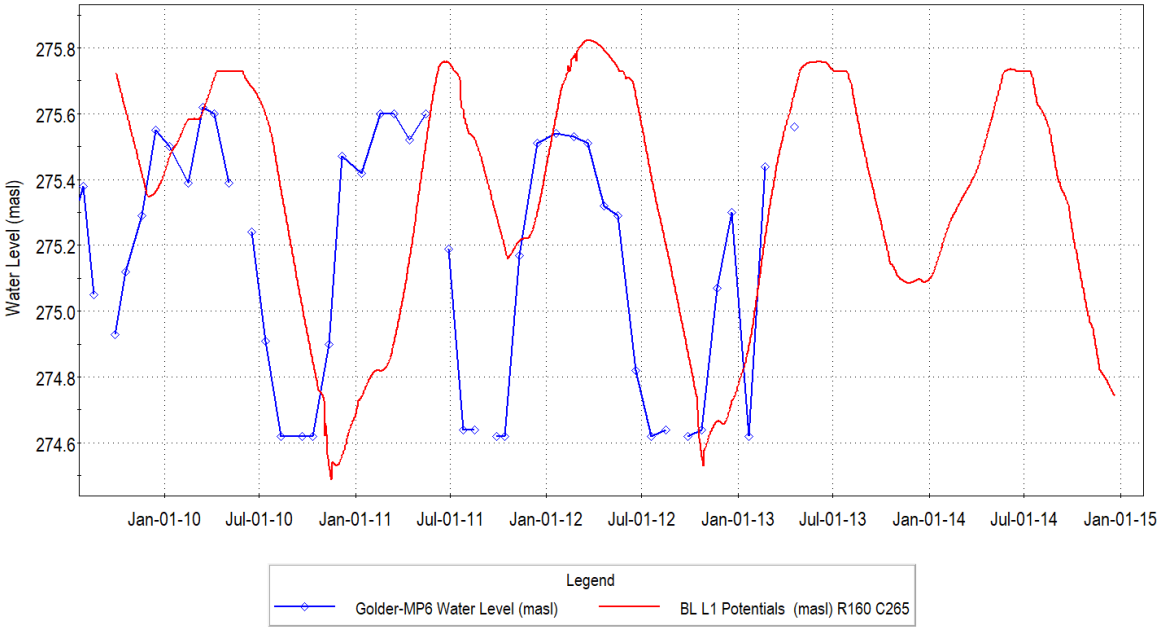

Figure 19.40: Observed and simulated shallow water levels at MP6 (near Pond H).

19.5.7 Groundwater Calibration Conclusions

The comparisons to transient data show excellent calibration matches, particularly considering the uncertain nature of the fractured rock and the inherent simplifications of the numerical model. The model is able to represent the complex effects of the quarry across multiple layers and distances, despite the use of uniform layer properties.

There are also several factors that further complicate obtaining better matches to the local observations. First, the observation wells have relatively long screens and are open to multiple fracture zones. Thus, the heads measured in the observation wells may not correspond exactly to the heads in the horizons represented by the model layers. Also, as noted earlier in Section 18.1.2, the conceptual model of the Amabel aquifer as a set of layers representing fractured and unfractured zones with randomly-distributed vertical fractures was intended to represent the behaviour of the aquifer on a subregional scale and local differences between observed and simulated are to be expected. As well, the quarry was being mined in the vicinity of these wells, although the bulk of the area had been mined out prior to WY2010. The uncertainty and variability in the south quarry discharge rate likely affected the response in nearby wells.

While the model may not always exactly the absolute magnitude of water levels in wells, it is felt that the model is sufficiently well calibrated to assess likely changes in water levels as a result of quarry extension.

The calibration to the shallow mini-piezometers illustrates that the model is representing the shallow flow system well. There is a slight lag in the simulated response, suggesting there might be less storage in the Halton Till, but overall, the calibration is excellent, particularly given the fact that the model uses a single uniform till hydraulic conductivity across the entire study area.

A key goal of this study was to build the integrated model and obtain reasonable parameter values that could be applied consistently across the study area. While reasonable average values were obtained in the calibration, it is understood that local-scale heterogeneity can affect the response of individual wells and well clusters. The model is intended to serve as a framework for assessing likely average change in the area around the quarry and to provide a scientific basis for an adaptive management plan (AMP). The scenarios described in the main report demonstrate that the model is useful for analyzing water level and water budget response to future change in quarry operations.

19.6 Calibration to Surface Water Pond Staff Gauges

The integrated GSFLOW simulation of the shallow wetland ponds demonstrates that the surface water calibration to the small wetlands is excellent. The calibration to the streamflow passing through this wetland chain is shown in Figure 19.8 and illustrates an excellent match to the recent high-quality flow monitoring data.

The calibration to Wetland 11 (numbering shown in Figure 19.49) is shown in Figure 19.41. The field monitoring data only covers the spring and summer period, because the data loggers cannot be frozen. The simulations provide a good match to the pond water levels, even with some uncertainties with in the wetland bathymetry.

The calibration to staff gauge SG3 (part of the large Wetland 17) is shown in Figure 19.42. The model appears to be matching the trends in the manual measurements well.

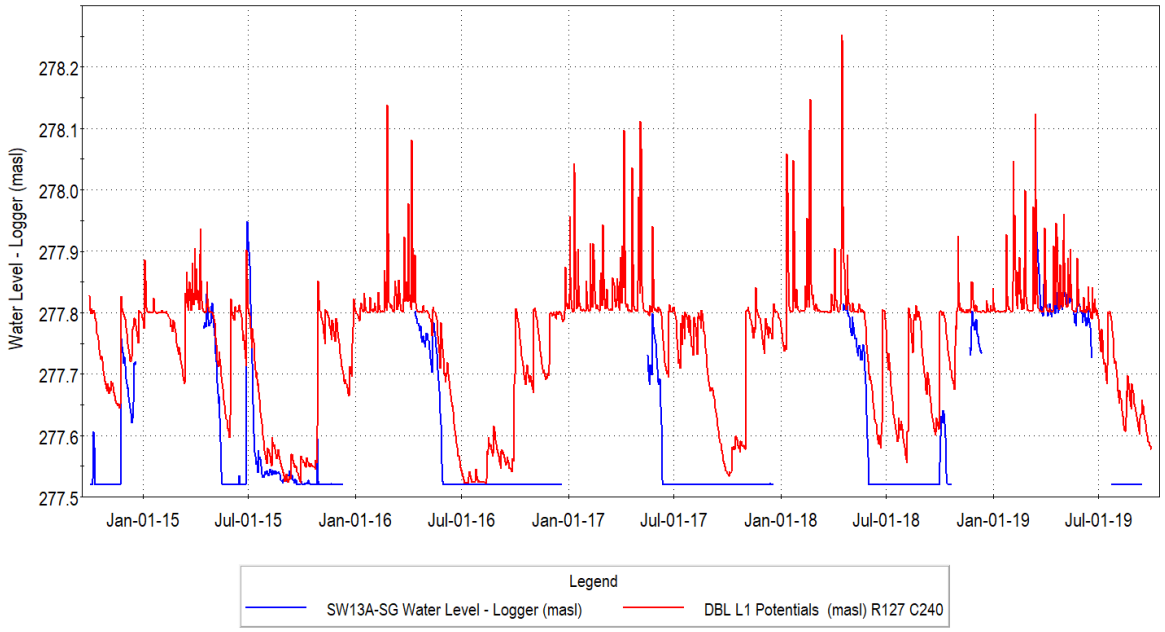

Figure 19.41: Observed and simulated pond elevation at SW13A-SG (Wetland 11).

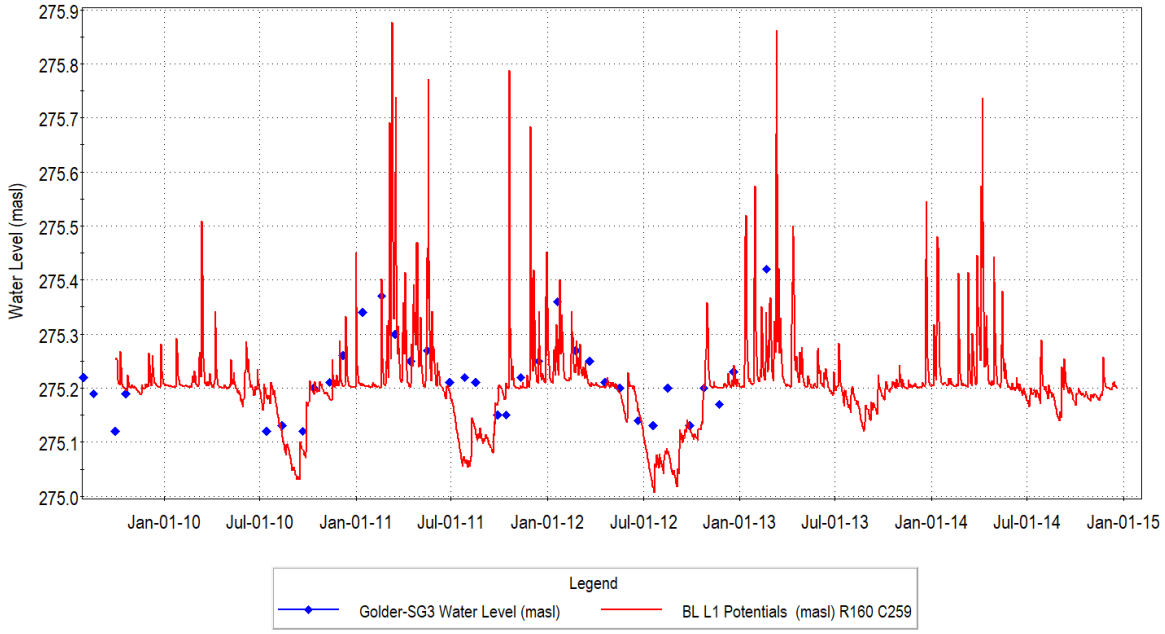

Figure 19.42: Observed and simulated pond elevation at Golder SG-3 (in Wetland 17).

The calibration to Staff Gauge SG2 and Mini-piezometer MP5 is particularly interesting, for it shows both pond and the underlying groundwater level fluctuation (Figure 19.43). These measurements are from the southern portion of Wetland 17, and the pond is immediately south of Stream Gauge SW9 (Figure 19.8). Groundwater levels, shown in blue, indicate that the water levels in the shallow groundwater system are at times above pond levels, and, in the summer recession, below the pond levels. This suggests that the pond both gains and loses groundwater upwelling depending on the time of year. The simulated water levels under the pond match the observed values generally very well, capturing this changing vertical gradient. The surface water calibration to pond levels is also very good (compare red lines). The model matches the trends and range in the pond levels very well, particularly given the size and complexity of the wetland bathymetry in this area.

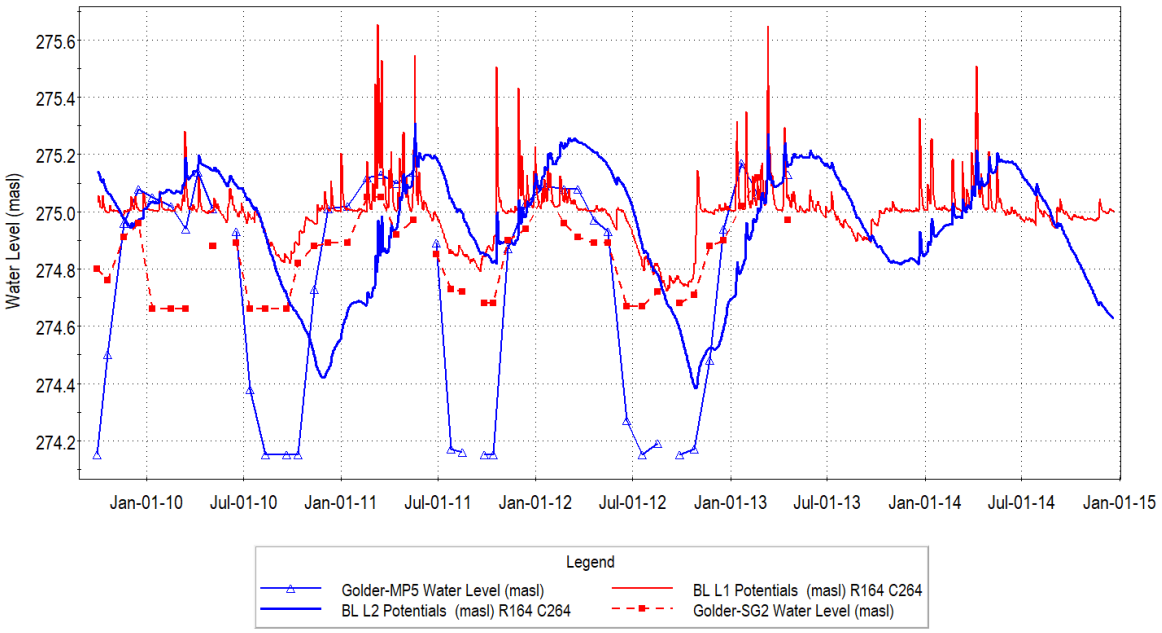

Figure 19.43: Observed and simulated pond and mini-piezometer elevation at Golder SG2 and MP5.

The model calibration to mini-piezometer MP16 (Wetland 20, as shown in Figure 19.49) is shown in Figure 19.44. This elongated wetland is located immediately south of the proposed P12 extension area, and has some topographic relief, ranging from 273.7 masl down to 272 masl near the outlet. MP16 is located near the upper portion of the wetland, while Staff Gauge SW16A-SG is located near the outlet. The water levels in MP16 follow a characteristic pattern: rising through the wet seasons and dropping below the base of the monitor at other times (flat line readings). The simulated water levels match the magnitude and patterns very well, and illustrate where water levels recede to during the dry periods.

The water levels near the outlet of Wetland 20 pond are shown in Figure 19.45. Note that the range of observed water levels is less than 6 cm, compared to the change in topography across the wetland of 1.7 m. The simulated pond levels match the general patterns well, but predict water levels a few centimetres higher than measured. The discrepancy is likely related to uncertainty in the wetland bathymetry – it is very difficult to accurately measure the pond bathymetry to centimeter accuracy due to the thick wetland vegetation. The model likely underestimates the volume of the pond, resulting in higher pond level peaks. While there is uncertainty in the pond bathymetry, the excellent calibration to MP16 suggests the model is representing flow in this area very well.

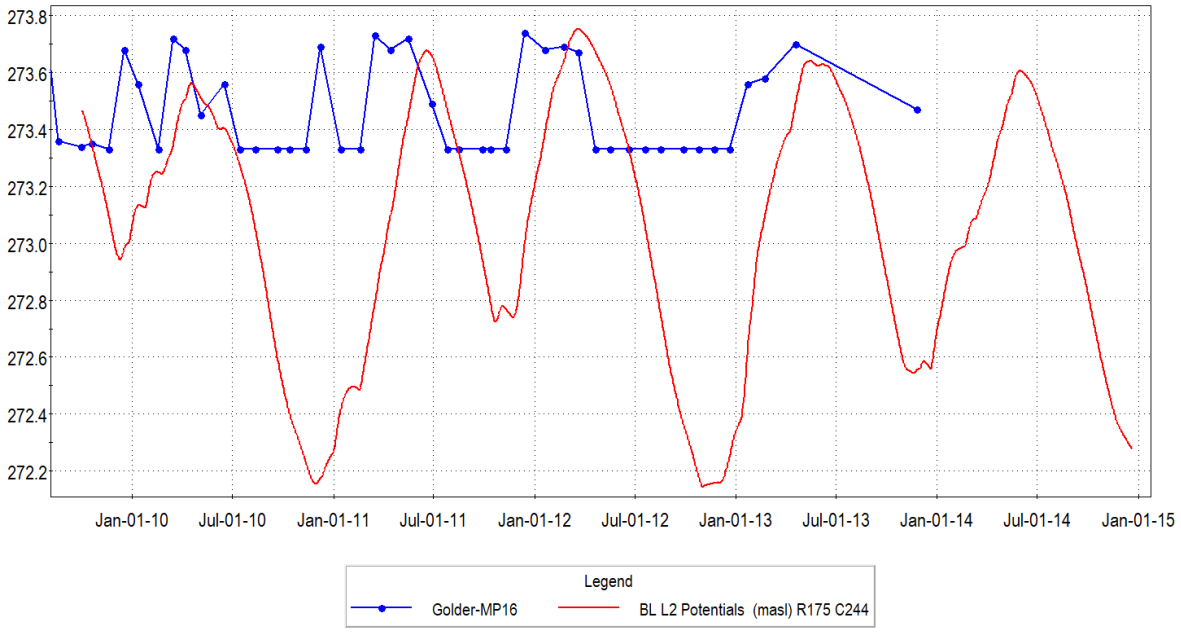

Figure 19.44: Observed and simulated pond elevation at MP16.

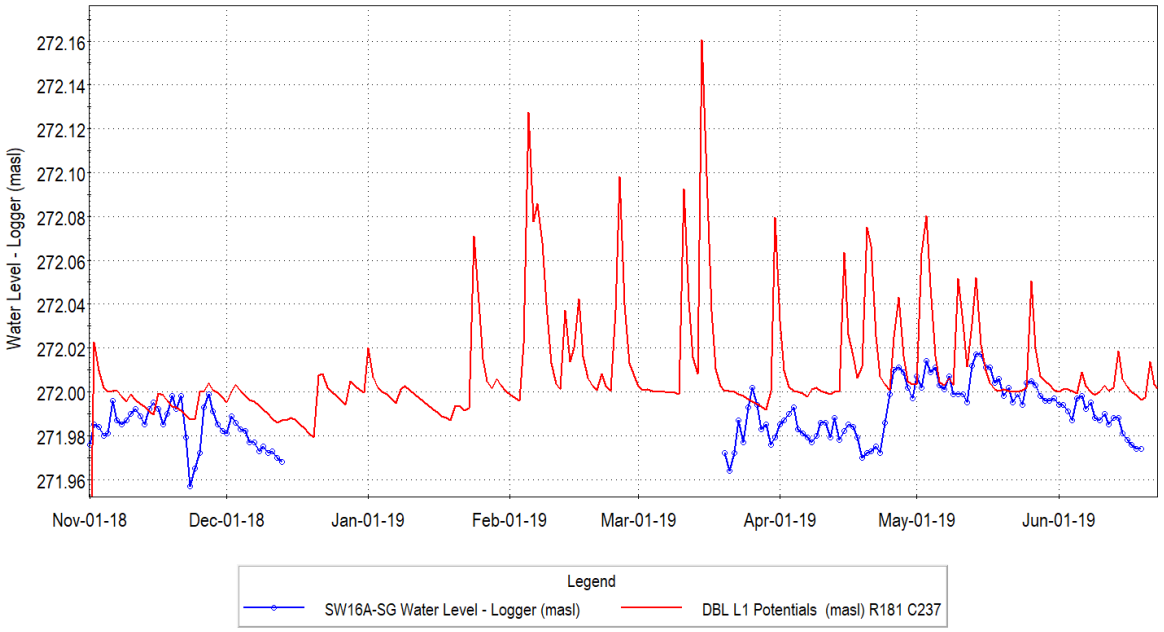

Figure 19.45: Observed and simulated pond elevation at SW16A-SG (note: range of measurements is less than 6 cm).

19.6.1 Wetland Calibration Conclusions

The mini-piezometer and staff gauge model calibration results indicate that the model is representing the wetlands and their interactions with the groundwater system very well. While water levels are easy measure in the field, there is some uncertainty in the wetland pond bathymetry due to the difficulties measuring through thick wetland vegetation. Overall, the calibration is excellent.

19.7 GSFLOW Outputs

Primary GSFLOW model outputs include daily streamflow, groundwater heads, and lake stage. The PRMS submodel also provides daily values for all components of the water budget including precipitation, interception, snowmelt, evapotranspiration, overland runoff, infiltration, and groundwater recharge. The GSFLOW code contains routines to sum many of the daily values over the basin. Earthfx added additional components to the output and aggregated other flow components so that local (cell-based) and subcatchment-based water balances can be readily produced. Average results for key water budget components for the study area were presented in Appendix C.

Additional groundwater submodel outputs include the flows across constant head boundaries; groundwater recharge and groundwater ET; lateral and vertical flows between each cell; well discharge; groundwater discharge to streams and lakes; and groundwater discharge to the soil zone (also referred to as surface leakage). The VL-GSFLOW post-processor takes daily values and aggregates them over time to provide monthly, seasonal, and annual water budgets. Values can also be aggregated spatially to provide water budgets at the subwatershed scale and for particular areas of interest, including individual wetlands.

As an example, Figure 19.46 shows the average March simulated heads in the Layer 4 (weathered bedrock) and simulated streamflow (in m^3/d). Groundwater levels and streamflow are at or near their highs for the year. Figure 19.47 shows the average September simulated heads and streamflow which are at or near their lows for the year. Heads drop between 0 and 1 m in the quarry vicinity and up to 3 m at Mt. Nemo. Many of the lower-order streams have negligible flow.

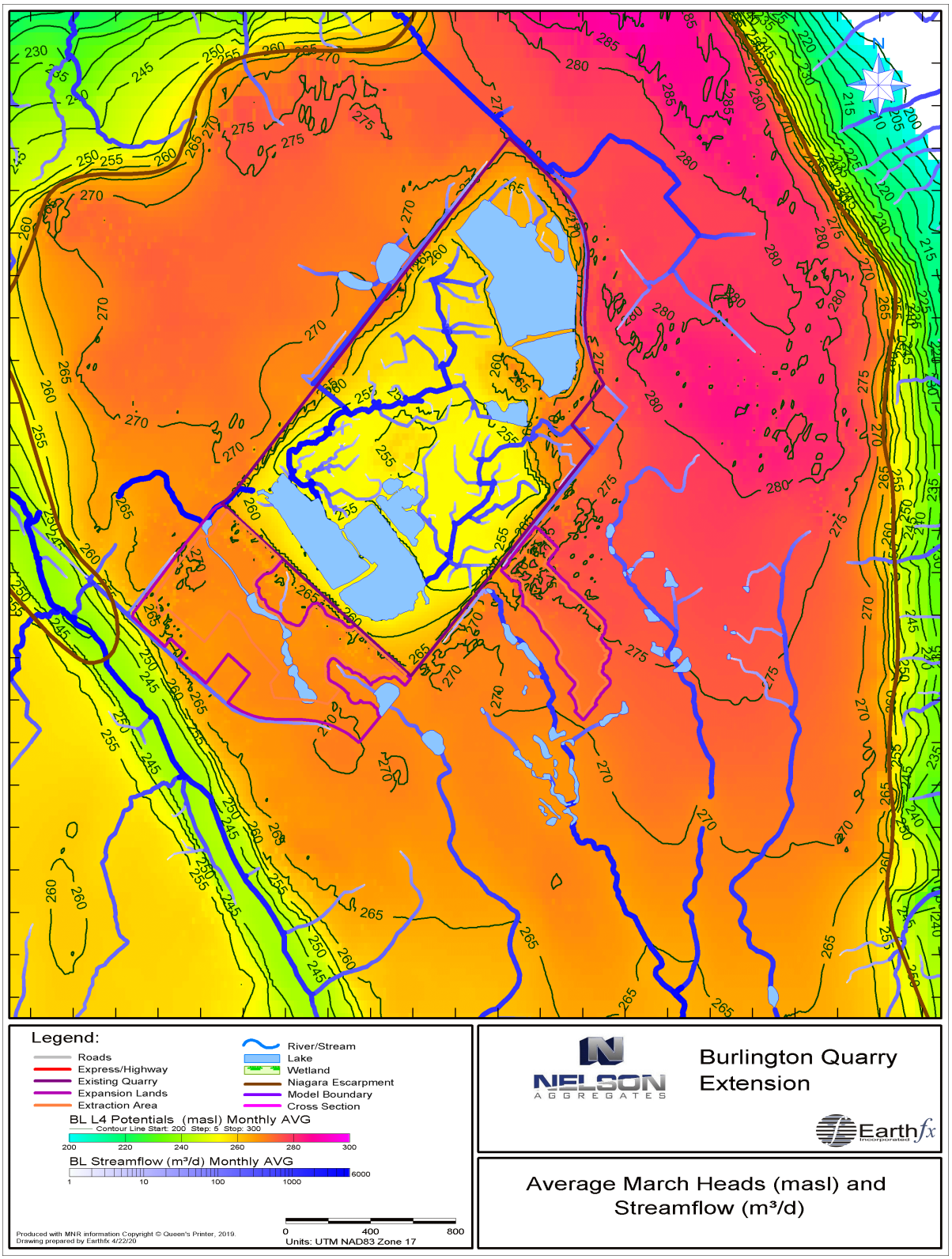

Figure 19.46: Average monthly simulated heads (in masl) and streamflow (in m^3/d) for March.

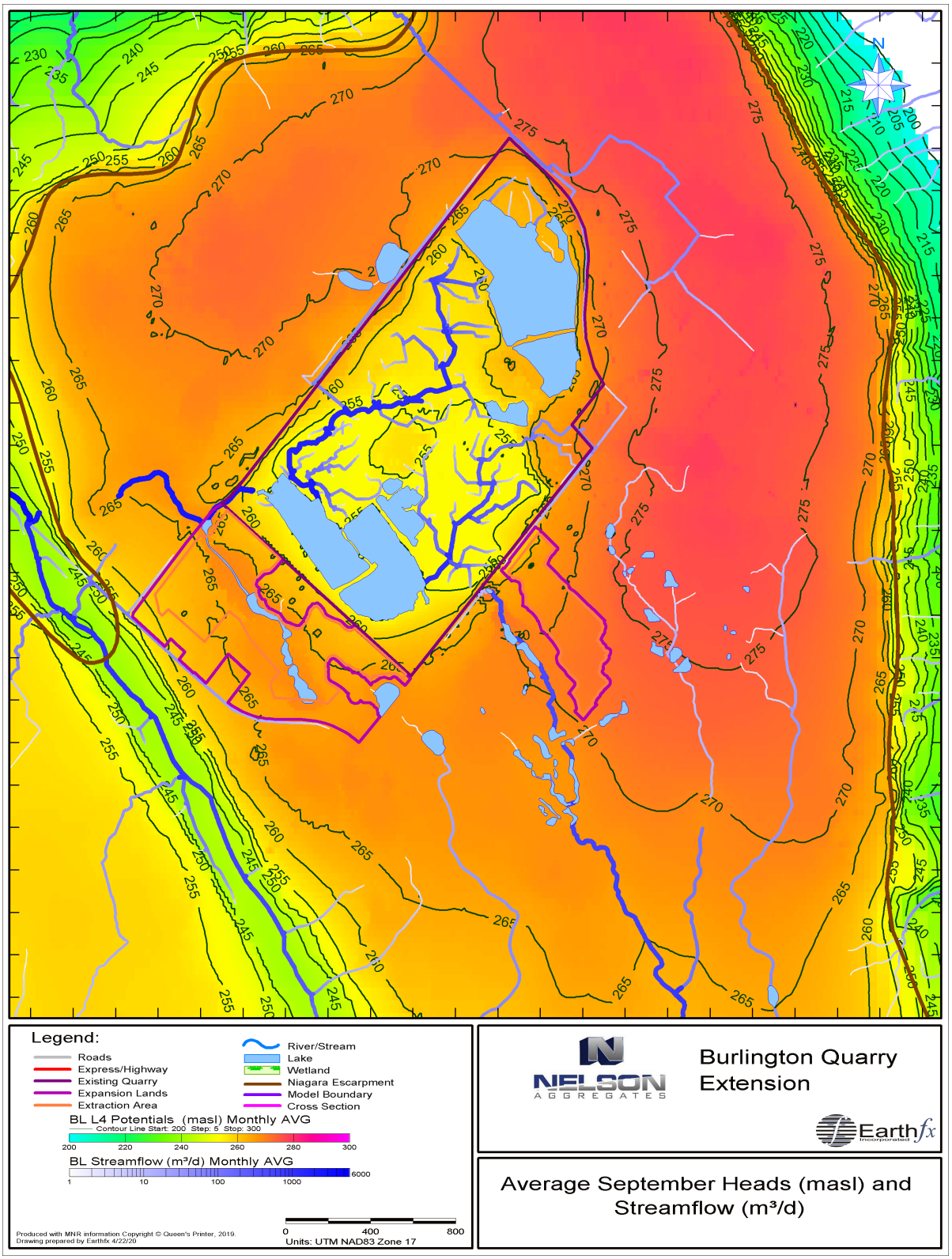

Figure 19.47: Average monthly simulated heads (in masl) and streamflow (in m^3/d) for September.

19.8 Water Budget Assessment

Results from the GSFLOW model were assessed to quantify components of the long-term average water budget under current (baseline) conditions. Model results were saved for each MODFLOW and PRMS cell on a daily basis. The VL-GSFLOW post-processor was used to aggregate these outputs at different time scales and for each subwatershed.

19.8.1 GSFLOW Water Budgets

Daily values for components of the groundwater budget, output by the MODFLOW submodel, were aggregated over the study area to produce simulation period, annual, monthly, and average monthly water budgets. Major water budget components for the surface water system were discussed in Appendix C and include precipitation, AET, Hortonian and Dunnian runoff to streams and lakes, interflow to streams, and lakes, and net groundwater recharge. Major water budget components for the groundwater system include net recharge, surface leakage (i.e., groundwater discharge to the soil zone), groundwater discharge to lakes and streams, and cross-boundary flows.

A water balance for the entire study area for the simulation period is presented in Table 19.1. From a surface water perspective, the principle source of water is precipitation and the dominant loss term is combined evaporation from the canopy and depression storage on impervious areas, and AET from the soil zone (12.8 and 57.4% of precipitation). Combined runoff and interflow to streams and lakes make up the remaining losses. For this basin, groundwater recharge is mostly balanced by groundwater discharge to the soil zone.

Groundwater inflows to the subwatershed area are dominated by recharge but this is balanced by water discharging to the soil zone in riparian areas. Water also moves in and out of the storage reservoir and should balance over the long term, but there is an excess of water “coming out” of storage and going into groundwater in the WY2010-WY2014 simulation period. There is also a significant amount of streamflow loss recharging the aquifer but this is mostly balanced by water discharging directly to the stream channel. Similarly, some lakes contribute to groundwater but this is also mostly balanced by groundwater discharge to lakes, often within the same lake. Other minor terms include groundwater losses to ET and outflow across the model boundaries. The water budget closes within 0.6%.

The daily flows were averaged to create an average monthly water budget (Figure 19.48) that illustrates seasonal trends in the water balance. Water goes into storage during the fall through early spring and comes out of storage during the drier summer months. The rate of recharge also decreases significantly in the late spring and summer as do groundwater discharge to the soil zone and to streams.

Average water budgets were also completed on a smaller scale to analyze inflows and outflows to the 22 wetlands shown in Figure 19.49. The corresponding MNRF wetland ID numbers are shown in Figure 19.50, but note that the wetland areas of the different ID numbers are different. A table correlating the ID numbers is included in Table 19.2. The Earthfx GSFLOW processor was used to compute all flows within each area as well as lateral groundwater flow, streamflow, overland runoff, and interflow crossing the area boundaries. As examples, Figure 19.51 and Figure 19.52 present schematics showing detailed water budgets for wetland areas 9 and 17, respectively. Both areas are net contributors to groundwater and have streams passing through which contribute to the overall water budget. Wetland 17 has 3 ponded areas within it that were treated as shallow lakes with separate water budgets. Changes to the 22 wetland areas were assessed as part of the quarry extension scenario analyses described in the main report.

Table 19.1: Groundwater budget for the GSFLOW model area for WY2010 to WY2014.

GSFLOW Budget Component		Inflows (m^3/d)	Inflows (mm/yr)	% of Precip-itation
PRMS Components	Precipitation	208227	911.0	
	Evaporation from interception	260701	116.8	12.8
	ET from pervious/impervious	119586	523.2	57.4
	Hortonian runoff to lakes	317	1.39	0.15
	Interflow/Dunnian runoff to lakes	1528	6.68	0.73
	Hortonian runoff to streams	10061	44.0	4.8
	Interflow/Dunnian to streams	50164	219.5	24.1
	Groundwater Recharge - Rejected	28159	123.2	13.5
	Groundwater Discharge (PRMS)Rejected Recharge	28249	124.6	-13.7
				99.8
MODFLOW Components	Groundwater recharge to MODFLOW	28155	123.7	13.6
	Groundwater ET	-2817	-12.4	-1.4
	Groundwater discharge to soil zone	-28482	-125.1	-13.7
	Net outflow from groundwater storage	852	3.74	0.4
	Net groundwater boundary outflow	-84.3	-0.62	-0.1
	Groundwater recharge from streams	2885	12.7	1.4
	Groundwater discharge to streams	-2498	-11.0	-1.2
	Groundwater recharge from lakes	2103	9.2	1.01
	Groundwater discharge to lakes	-1229	-5.4	-0.6
				-0.6%

Table 19.2: MNRF Wetland vs Earthfx ID number

Earthfx ID	MNRF Wetland ID Numbers
9	13014
10	13015
11	13016
12	13017, 13018
13	13030
14	13019
15	13021
16	13022
17	13033
18	None
19	13032
20	13036, 13037, 13038, 13039
21	13201
22	13200

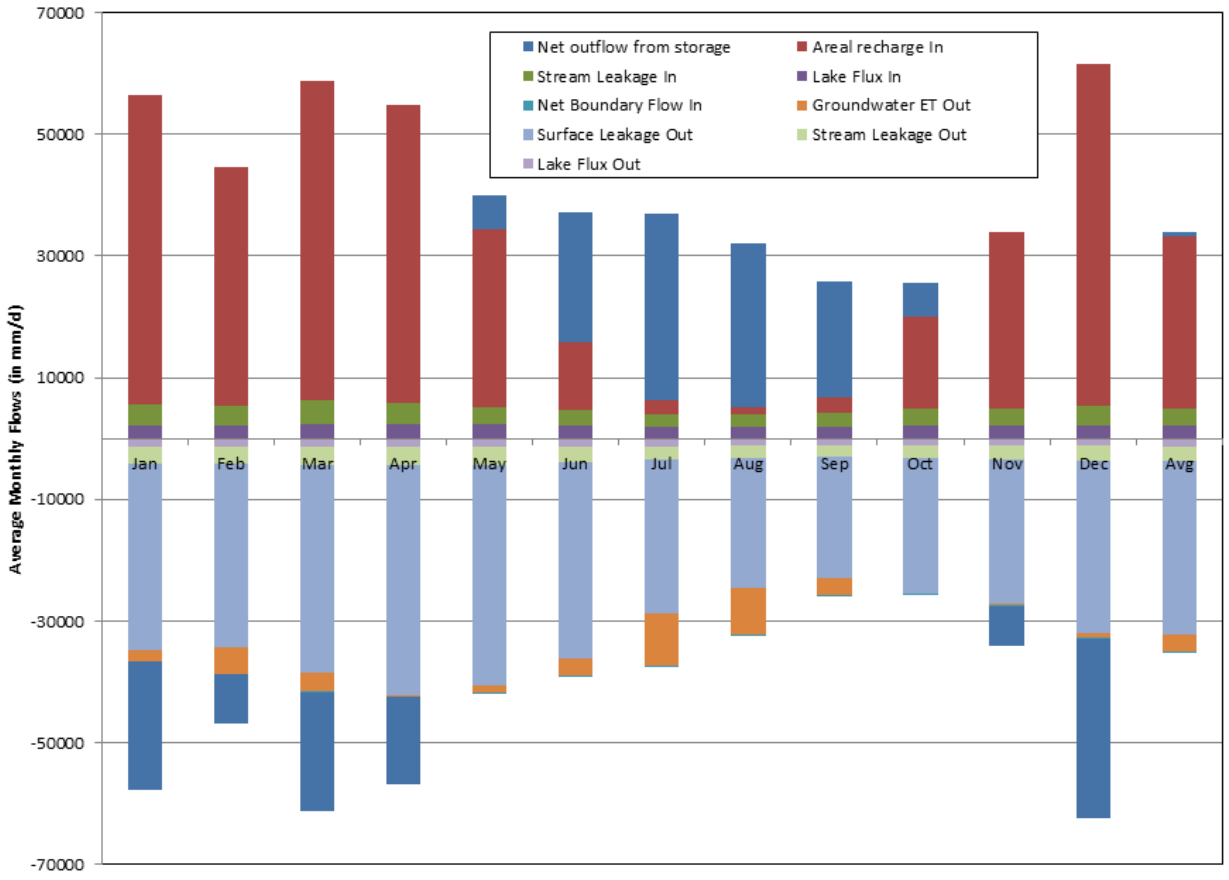

Figure 19.48: Average monthly groundwater budget for the study area (all flows in m^3/d).

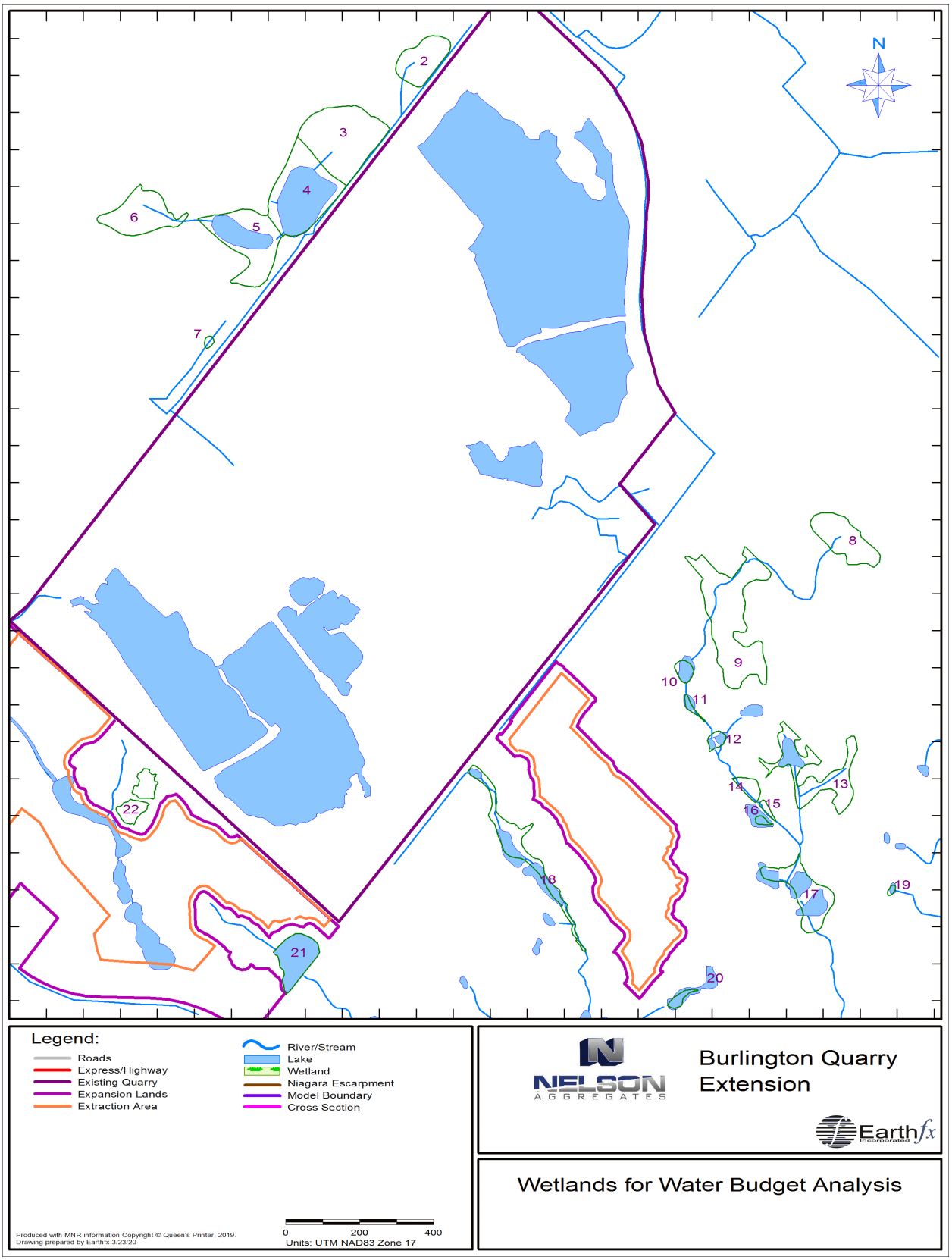

Figure 19.49: Significant wetland features selected for water budget analysis.

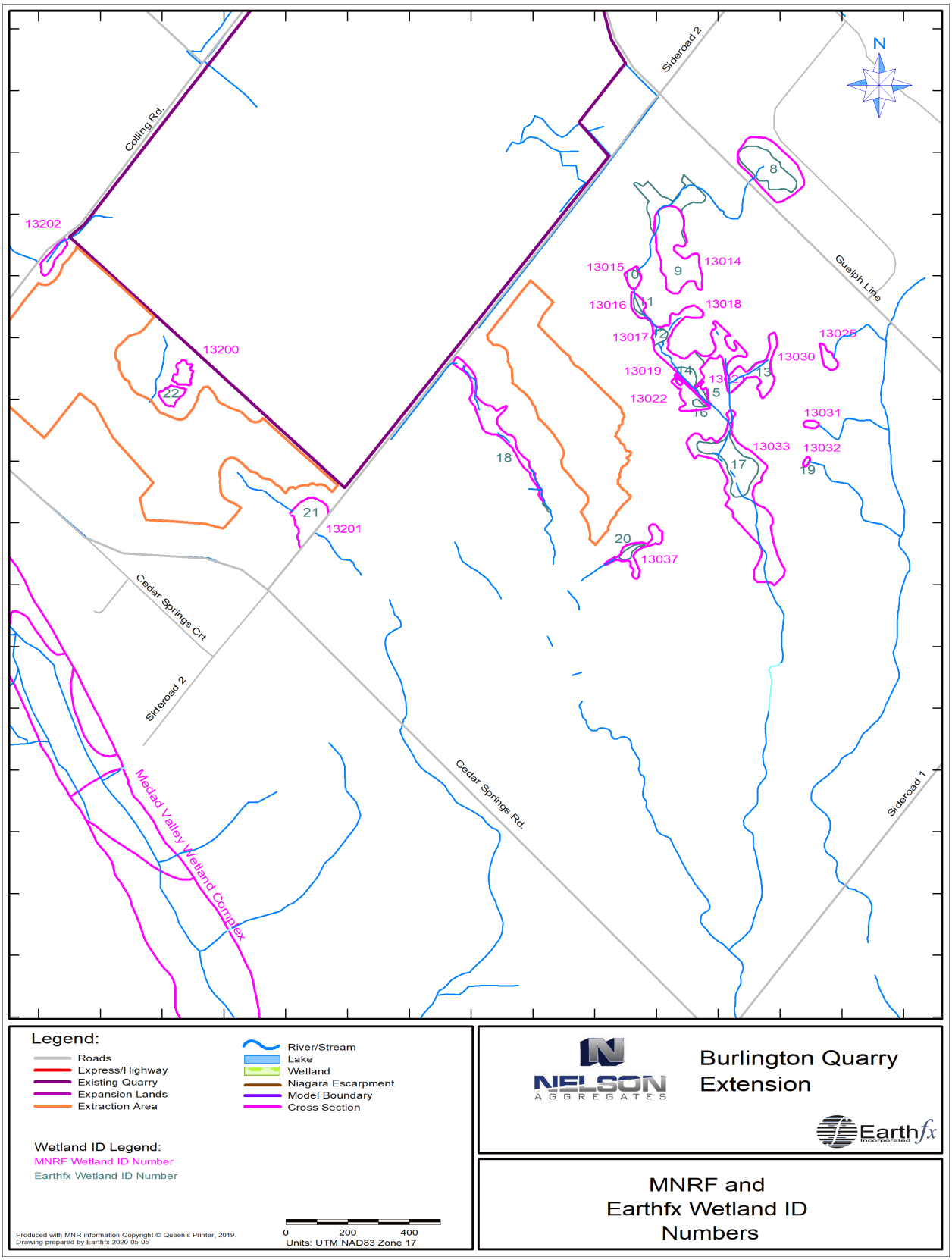

Figure 19.50: MNRF versus Earthfx Wetland ID numbers.

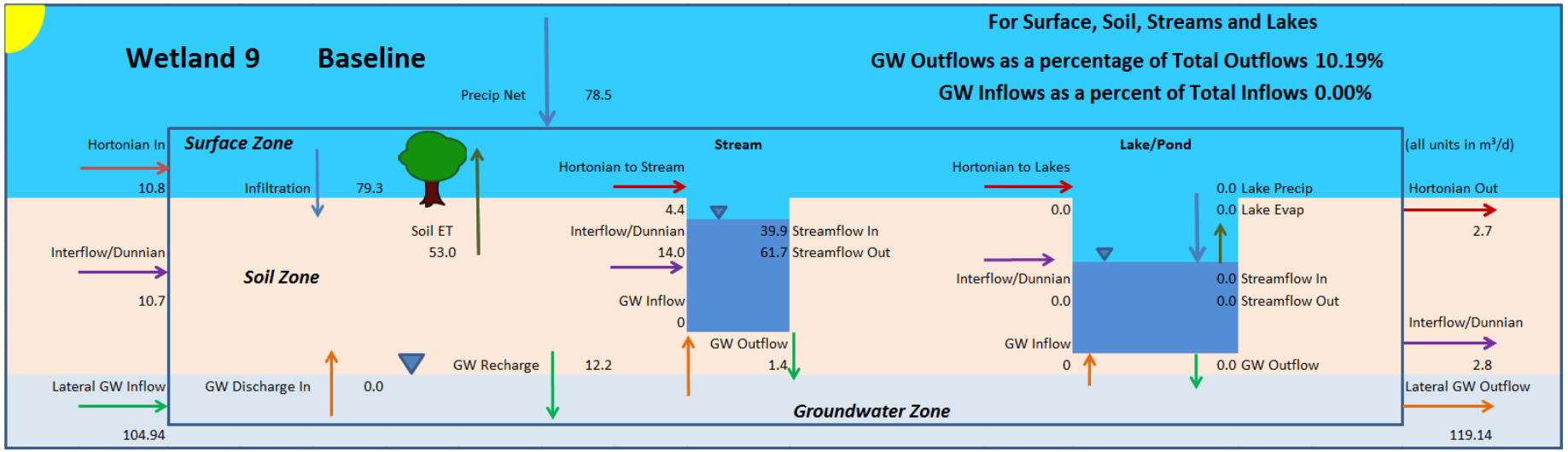

Figure 19.51: Detailed water budget for Wetland 9 averaged over WY2010 to WY2014 under baseline conditions.

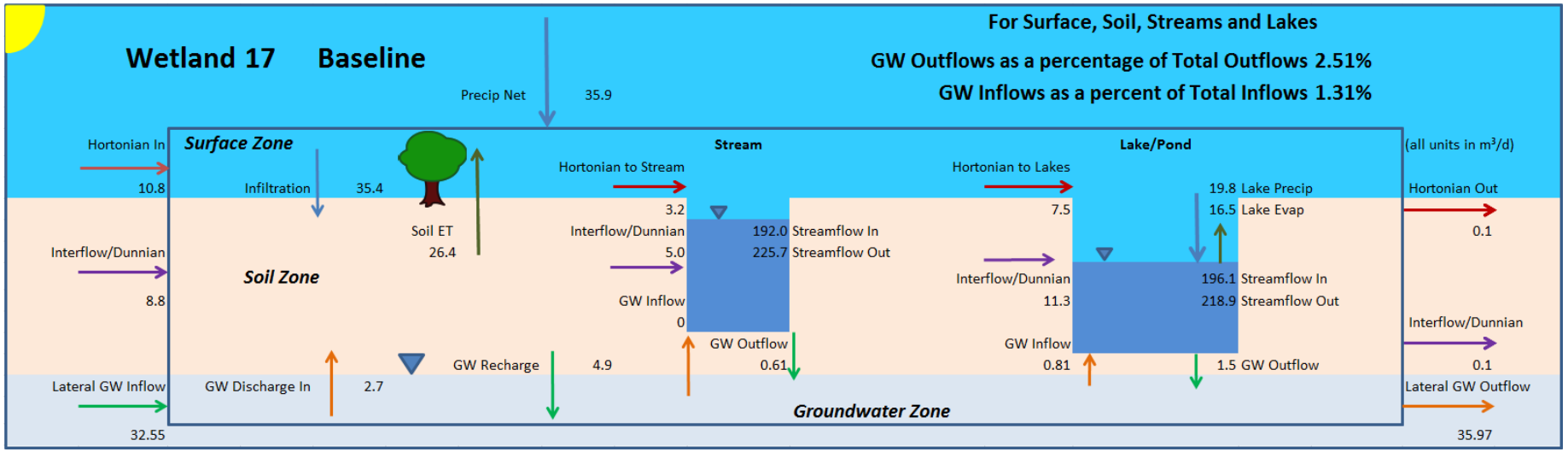

Figure 19.52: Detailed water budget for Wetland 17 averaged over WY2010 to WY2014 under baseline conditions.

20 Appendix F: Curricula Vitae of Report Authors

Dirk Kassenaar, M.Sc., P.Eng.

President, Senior Hydrogeologist

BIOGRAPHY

Dirk Kassenaar, M.Sc., P.Eng. is a senior hydrogeologist and President of Earthfx. Dirk founded Earthfx in 1998 with the goal of integrating environmental simulation and advanced data management. Earthfx is a world leader in the integrated simulation of groundwater and surface water systems, with a particular specialization with the USGS GSFLOW Model. As founder and President, Dirk has technically directed and managed projects for large water management agencies, land developers, mining and oil sand companies and nuclear power stations. In addition to managing projects and operations at Earthfx, Dirk is the key architect of VIEWLOG, overseeing its development into the premier 4-dimensional modeling system interface to the USGS GSFLOW integrated SW/GW model. Dirk has also acted as an expert witness in the fields of geophysics, hydrogeology, and engineering in numerous Canadian and US legal and land development hearings.

EDUCATION

- B.A.Sc. Geological Engineering, University of Waterloo (1986)
- M.Sc. Earth Science, University of Waterloo (1989)

PROFESSIONAL EXPERIENCE

President/ Senior Hydrogeologist, Earthfx Inc. ***1998 - Present***

At Earthfx, Dirk provides senior consulting expertise in geologic and hydrogeologic modeling, geophysical interpretation, hydrogeology, and geological engineering. As President, Mr. Kassenaar is responsible for all aspects of project development, budgeting, technical analysis, and quality control/quality assurance. He is also responsible for product development, code design, and marketing of the VIEWLOG and SiteFX products. Recent projects include:

- Development of a large scale fully integrated GSFLOW model of the City of Toronto and Region of York for water budget analysis, permitting, and drought impact assessment.
- Interpreted the geology in the six-county Southwest Florida Feasibility Study area to create hydrostratigraphic model layers for the new regional simulation model.
- Assessment and optimization of low impact urban design facilities to mitigate the impact of the development of the proposed Town of Seaton.
- Analysis, using a fully integrated GW/SW GSFLOW model, of the interconnection between the Milton wellfield and Kelso Lake reservoir.
- Development of a web interface to the St. John's River WMD VIEWLOG database.
- Development of a comprehensive water management database, geologic and regional scale MODFLOW model of the Oak Ridges Moraine
- Numerical assessment of surface water recharge and groundwater impacts of the proposed Darlington Nuclear Power Station expansion.

Hydrogeologist/ Geophysicist, Gartner Lee Limited 1989 - 1995

As Project Manager and Engineer, Mr. Kassenaar's responsibilities included:

- Managed field investigations, modeling and remediation of a multi-component DNAPL spill in fractured dolostone. Reduced contaminant concentrations in nearby private wells from 1000's of ppb to less than the drinking water limits.
- Designed and assessed over 20 landfill systems and monitoring projects across Canada and the USA. Tasks included modelling of caps and leachate collection systems, geophysical and hydrogeologic assessment of contaminant plumes, and management and analysis of water quality monitoring studies.
- Managed dozens of groundwater modeling projects, including simulations of municipal and hazardous waste landfills, contaminant spills, low-level radioactive waste and ground water supply and WHPA studies.
- Completed water supply capture zone analysis for a major bottled water company.

Logging Scientist, International Ocean Drilling Program Fall 1987

Completed 3 months of downhole geophysical testing using advanced nuclear and geochemical logging probes aboard the research ship JOIDES Resolution. Testing identified significant titanium deposits in gabbros on the flanks of a 6000 m deep submarine canyon in the Southwest Indian Ocean. Results published in Nature v. 333, Issue 6169.

Highwall Geologist and Research Engineer, Syncrude Canada Ltd. 1983 - 1984

Performed daily highwall mapping of oil sand deposits under dragline operations at the Syncrude mine site in Fort McMurray, Alberta. Supervised drilling investigations for ore grade reserve calculations. Promoted to the Research Department in Edmonton to assess the correlations between core measurements and downhole geophysical logs.

SELECT TECHNICAL PAPERS (FULL BIBLIOGRAPHY AVAILABLE ON REQUEST)

Kassenaar, J.D.C. Long-Term Monitoring Network Design with an Integrated Model, abstract presented at Watertech 2017, Banff, AB.

Kassenaar, J.D.C. Integrated Modelling as a Tool for Assessing Groundwater Sustainability under Future Development and Drought in York Region, Ontario, Canada. Proceedings of the Canadian Water Resource Conference, Hamilton, Ontario, June, 2014

Kassenaar, J.D.C., Malott, S., Wexler, E.J., Integrated modelling of Mine and Quarry Impacts, abstract presented at MODFLOW and More, 2019, Golden, CO.

Wexler, E.J., Thompson, P.J., Takeda, M.G.S., Howson, K.N., Cuddy, S.E., Kassenaar, J.D.C., Simulating climate change and extremes with an integrated surface water-groundwater model to assess hydrologic response in the Lake Simcoe watershed. Proceedings of the Canadian Water Resources Conference, Hamilton, Ontario, June, 2014

Kassenaar, D., Wexler, Integrated Surface Water and Groundwater Modeling for Streamflow Restoration and Climate Change Assessment in a Mountain Basin Watershed in Eastern

Washington; paper presented at the CSPG, CSEG, CWLS, GAC, MAC, and IAH Geoconvention 2020, Calgary, AB.

Kassenaar, D., Wexler, E.J., Data Management and Calibration Strategies for Integrated Modelling. in Proceedings of the Watertech Conference, Banff, Alberta, April, 2014

Kassenaar, D., Marchildon, M., Wexler, E.J., Rethinking Recharge. in Proceedings of the Conference "Modflow and More 2013" IGWMC, Golden, CO. May, 2013

Kassenaar, D., Wexler, E.J., Marchildon, M., Thompson, P.J., Integrated Modelling of Groundwater Interaction with Channels, Wetlands and Lakes in GSFLOW. In Proceedings of the Watertech Conference, Banff, Alberta, April, 2013

Li, Q., Unger, A.J., Sudicky, E.A., Kassenaar, J.D., Wexler, E.J., and Shikaze, S., 2008, Simulating the multi-seasonal response of a large-scale watershed with a 3-D physically-based hydrologic model: J. of Hydrology, v. 357, no. 3-4.

Kassenaar, J.D.C., 1988. "Ocean Drilling Program: Plutonic Rocks in Fracture Zones", Leg 118 Shipboard Scientific Party. Nature v. 333, Issue 6169, 12 May, 1988.

E. J. Wexler, M.Sc., M.S.E., P.Eng.

Vice-President and Director of Modelling Services

BIOGRAPHY

E.J. Wexler is Vice-President and Director of Modelling Services at Earth*fx* and has over 35 years of experience in groundwater modelling, contaminant hydrogeology, geostatistical analysis, and model code development. He has taught graduate courses in groundwater at universities in Canada, FL, and NY. He worked as a research hydrologist and groundwater modelling specialist for the USGS in Reston, VA, Long Island, NY, and Miami, FL. Mr. Wexler is a licensed engineer in the Province of Ontario, Canada.

EDUCATION

- B.E. Civil Engineering, City University of New York (1977)
- M.S.E. Civil Engineering, Princeton University (1978)
- M.Sc. Earth Science, University of Waterloo (1988)

PROFESSIONAL EXPERIENCE

Director of Modelling Services, Earthfx Inc. ***2002 - Present***

Mr. Wexler is the Director of Modelling Services at Earth*fx* where he leads a team of surface and groundwater modellers. Mr. Wexler's experience at Earth*fx* includes:

- Directing groundwater flow and contaminant transport studies, with an emphasis on integrated groundwater/surface water modelling using GSFLOW.
- Technical Manager for Source Water Protection studies in southern Ontario. Work included regional groundwater flow and hydrologic modelling for water quality and water quantity risk assessment and wellhead vulnerability assessment.
- Technical Manager for Lake Simcoe Protection Plan studies in southern Ontario. These subwatershed studies assessed regional groundwater flow, delineated ecologically significant groundwater recharge areas, and quantified the impact of land development, drought, and climate change on watershed function.
- Member of Scientific Peer Review team for evaluating the Tampa Bay Water/SWFWMD North Tampa Bay integrated model.
- Conducted integrated GW/SW modelling study for a large-scale development in Ft. Meyers, FL using GSFLOW.
- Developed integrated GW/SW models for the Milton (Kelso and Campbellville) and York /Toronto Tier 3 Source Water Protection Studies
- Developed an integrated GW/SW model for the Little Spokane River watershed in Washington State.
- Developed geostatistical analysis codes (3-D kriging and variogram analysis) for VIEWLOG and advanced water quality and statistical analysis modules for SiteFX.

Hydrogeologist/Hydrologist, Gartner Lee Limited 1990 - 2002

As a senior hydrogeologist at Gartner Lee, Mr. Wexler directed groundwater modelling, groundwater resources management and contaminant hydrogeology studies in Canada, Florida and the Middle East, Selected projects include:

- Development of a groundwater flow and contaminant transport model for a low-level radioactive waste disposal site and evaluation of remedial measures.
- Development of a groundwater flow model for St. Thomas, U.S. Virgin Islands used to investigate the source of volatile organic compounds affecting water supply wells.
- Development of surface water and groundwater models to assess the impact of artificial recharge on the water balance, groundwater flow patterns and salt water intrusion in the arid coastal regions of Northern Oman.
- Co-development of MODNET, a surface water and groundwater model based on the USGS MODFLOW model and the USACE UNET surface water model for SFWMD.

Research Hydrologist, U.S. Geological Survey, Miami, Florida 1986 - 1990

Mr. Wexler developed models for simulating groundwater/surface water interaction. He investigated the effects of density-dependent groundwater flow and solute transport on the feasibility of freshwater storage and recovery in saline aquifers (ASR) at Cape Coral, FL. He developed a coupled, regional-scale/fine-scale flow and transport model for simulating leachate migration at landfills in West Palm Beach, FL. He served as the Groundwater Discipline Specialist and Digital Modelling Specialist and was responsible for technical review and quality control for all surface water and groundwater modelling investigations.

Hydrologist, U.S. Geological Survey, Long Island, New York 1981 - 1985

Mr. Wexler was the Project Chief of a groundwater contaminant transport study at a sanitary landfill site. He investigated the local hydrogeology and studied the physical and geochemical controls on the transport of groundwater solutes. He developed flow and transport models for the study area and simulated long-term contaminant migration.

Research Hydrologist, U.S. Geological Survey, Reston, Virginia 1979 - 1981

Mr. Wexler was responsible for developing and testing finite-element models for simulating groundwater flow, solute transport and parameter estimation. E.J. consulted on field application of these models to sites in Maine, Kansas, and California.

SELECT TECHNICAL PAPERS AND ABSTRACTS (FULL BIBLIOGRAPHY AVAILABLE ON REQUEST)

Century Architects and Engineering Consultants and Earthfx Incorporated, 2004 Study of Integrated Catchment Management, Wadi Ma'awil Catchment, Sultanate Of Oman: Report prepared for the Ministry of Regional Municipalities, Environment and Water Resources, Sultanate of Oman 187 p.

Earthfx Incorporated, 2018, Whitemans Creek Tier Three Local Area Water Budget and Risk Assessment: prepared for the Grand River Conservation Authority, 171 p.

Earthfx Incorporated, 2016, Phase 2 Review of potential cumulative effects to surface water and groundwater from in-situ oil sands operations, focusing on the Mackay River Watershed: prepared for the CEMA – Water Working Group, January 2016, 416 p.

Earthfx Incorporated, 2014, Tier 3 Water Budget and Local Area Risk Assessment for the Region of York Municipal Systems – Risk Assessment Report; prepared for the Regional Municipality of York Transportation and Works Department, March 2014.

Earthfx Incorporated, 2014, Tier 3 Water Budget and Local Area Risk Assessment for the Kelso and Campbellville Groundwater Municipal Systems - Phase 2 Risk Assessment Report: prepared for the Halton Region Conservation Authority, February 2014.

Earthfx Incorporated, 2014, Ecologically Significant Groundwater Recharge Area Delineation in the Central Lake Ontario Conservation Authority Area: prepared for the Central Lake Ontario Conservation Authority, May 2014.

Earthfx Incorporated, 2012, Simulation of Groundwater Flow and Saltwater Movement in the vicinity of the Atlantic Civil Property South Miami-Dade County, FL:

Earthfx Incorporated, 2008, Appendix L: Simulation of groundwater flow in the vicinity of the proposed Southeast Collector trunk sewer -- Southeast Collector Trunk Sewer Environmental Assessment: Prepared for Conestoga-Rovers and Associates, the Regional Municipality of York, and the Regional Municipality of Durham, March 2008

Earthfx Incorporated, 2008, Simulation of groundwater flow in the vicinity of the New Nuclear-Darlington project - New Nuclear-Darlington Geology and Hydrogeology Effects Assessment: Prepared for CH2M Hill Canada Limited and Ontario Power Generation Inc., December 2008.

Earthfx Incorporated, 2008, Surface to Well Advection Time Analysis Wellhead Protection Areas for Municipal Residential Groundwater Systems Located within the Toronto and Region Conservation Authority Watersheds - Caledon East Wells 2, 3, and 4 and Palgrave Wells 2 and 3: prepared for the Regional Municipality of Peel, February 2008.

Earthfx Incorporated, 2008, Addendum Report: Wellhead Protection Area Study and Surface to Well Advection Time Analysis for Palgrave Well 4 located within the Toronto and Region Conservation Authority Watersheds, prepared for the Regional Municipality of Peel, August 2008.

Earthfx Incorporated, Greg Rawl, P.G., and Dean M. Mades (HSW Engineering Inc.), 2012, An integrated surface-water/groundwater modeling analysis of infiltration and stormwater runoff from the Babcock Ranch Community Development, Charlotte and Lee Counties, Florida: Prepared for Babcock Property Holdings, LLC, July 2012.

Kassenaar, J.D.C. and Wexler, E.J., 2006, Groundwater modelling of the Oak Ridges Moraine Area: CAMC/YPDT Technical Report Number 01-06 -- York Peel Durham Toronto (YPDT) - Conservation Authorities Moraine Coalition (CAMC), 265 p.

Quiñones-Aponte, V. and E.J. Wexler, 1995: Preliminary Assessment of Injection, Storage and Recovery of Freshwater in the Lower Hawthorn Aquifer, Cape Coral, FL: USGS Water Resources Investigations Report 94-4121, 102 p.

Swain, E.D. and E.J. Wexler, 1996: A coupled surface water and groundwater flow model (MODBRANCH) for simulation of stream aquifer interaction: USGS Techniques of Water Resources Investigations Book 6, Chapter A6, 125 p.

Thompson, P.J., Wexler, E.J., Takeda, M.G.S., and Kassenaar, D., 2015, Integrated surface water/groundwater modelling to simulate drought and climate change impacts from the reach to the watershed scale: paper presented at the IAH-CNC Conference, Waterloo, Ontario, November 2015.

WEST Consultants Inc. and Earthfx Incorporated, 2018, Integrated Groundwater/Surface Water Model for the Little Spokane Watershed – Water Bank Modeling and Decision Support Tool - Model Development and Application Report:, prepared for Department of Water Resources, Spokane County, 274 p.

WEST Consultants Inc. Earthfx Inc., and Hydrocomp Inc., 2018: Scientific Review of the Integrated Hydrologic Model (IHM) – Final Report prepared for Tampa Bay Water and Southwest Florida Water Management District, February 2018, 508 p.

WEST Consultants Inc. Earthfx Incorporated, and Hydrocomp Incorporated, 2013: Peer Review of the Integrated Northern Tampa Bay Model Application – Final Report prepared for Tampa Bay Water and Southwest Florida Water Management District.

Wexler, E.J., Thompson, P.J., Kassenaar, J.D.C., and Takeda, M.G.S., 2016, Applications of integrated models to watershed and sub-watershed scale analysis -- A Canadian context: XXI International Conference Computational Methods in Water Resources, June 2016, Waterloo, Ontario.

Wexler, E.J., Thompson, P.J., Takeda, M.G.S., Howson, K.N., Cuddy, S.E., and Kassenaar, J.D.C., 2014, Simulating climate change and extremes with an integrated surface water-groundwater model to assess hydrologic response in the Lake Simcoe watershed: Canadian Water Resources Association Conference, Hamilton, ON, June 2014.

Wexler, E.J., Thompson, P.J., Takeda, M.G.S., Malott, S., Shifflett, S.J., and Kassenaar , J.D.C., 2017, Development and application of an irrigation demand module for the USGS GSFLOW Model: 2017 MODFLOW and More conference, Golden CO, May 2017